Catalytic and Stoichiometric Organohalogen Chemistry:

Mechanistic Investigations and Applications

Inaugural-Dissertation

to obtain the academic degree

Doctor rerum naturalium (Dr. rer. nat.)

submitted to the Department of Biology, Chemistry, Pharmacy

of Freie Universität Berlin

by

Sebastian Ponath

2021

Berlin

The present work was carried out under the supervision of Prof. Dr. Mathias Christmann in the period from January 2017 to December 2020 in the Department of Biology, Chemistry, Pharmacy at the Freie Universität Berlin.

1st Reviewer: Prof. Dr. Mathias Christmann
(Institute of Chemistry and Biochemistry, Freie Universität Berlin)

2nd Reviewer: Prof. Dr. Philipp Heretsch
(Institute of Chemistry and Biochemistry, Freie Universität Berlin)

Date of disputation: 17.05.21

I hereby confirm that this work was prepared without the help of third parties and without the use of other than the indicated sources. The thoughts taken from the sources are marked. This thesis has not been submitted to any other examination authority and no doctoral examination has taken place to date.

_____

Sebastian Ponath

Danksagung

Der größte Dank gilt zunächst meinem Doktorvater Herrn Prof. Dr. Mathias Christmann, der mir ein Forschungspraktikum, die Masterarbeit und zuletzt die Promotion in seiner Arbeitsgruppe ermöglicht hat. Vielen Dank für die Unterstützung und das Vertrauen bei diesen interessanten und herausfordernden Fragestellungen. Der gewährte Freiraum bei der eigenen Forschung sowie die Leitung in schwierigen Phasen ist ein zentraler Punkt zum Gelingen dieser Arbeit und meiner eigenen Entwicklung gewesen.

Herrn Prof. Dr. Philipp Heretsch möchte ich für die Übernahme des Zweitgutachtens danken.

Außerdem möchte ich den Kooperationspartnern und Unterstützern danken, die maßgeblich am erfolgreichen Bearbeiten der Projekte beteiligt waren: Stefan Leisering, Dr. Benjamin Schmidt, Patrick Voßnacker, Prof. Dr. Sebastian Hasenstab-Riedel, Chetan Joshi, Prof. Dr. Mathew J. Vetticatt, Amy Bellinghiere, Prof. Dr. Dean J. Tantillo, Dr. Volker Schmidt, Prof. Dr. Christina Thiele, Kim Greis, Maike Lettow und Prof. Dr. Kevin Pagel.

Ein weiterer Dank gilt den Studenten Deniz Meyer, Marvin Busse und Wesley Pietsch, die im Zuge ihrer Bachelorarbeiten und Forschungspraktika an diesen Projekten beteiligt waren.

Der gesamten analytischen Abteilung möchte ich für die Bearbeitung der zahlreichen NMR- und Masseproben sowie für die Einkristallstrukturanalysen danken.

Danke auch an alle, die diese Arbeit Korrektur gelesen haben: Dr. Amel Mekic, Dr. Benjamin Schmidt, Dr. Volker Schmiedel, Stefan Leisering, Merlin Kleoff und Dr. Reinhold Zimmer.

Ein ganz besonderer Dank gilt allen aktuellen und ehemaligen Mitarbeiten der AG Christmann und AG Heretsch, die dafür gesorgt haben, dass man sich bei euch zu Hause fühlt. Danke auch für die fantastischen Momente außerhalb des Labors. Ein besonderer Dank gilt meinen ehemaligen Laborpartnern und Labornachbarn: Dr. Volker Schmiedel, Dr. Tommaso Pecchioli, Merlin Kleoff und Stefan Leisering.

Ein Dankeschön verdienen auch Luise Schefzig und Christiane Groneberg für die synthetisch-praktische Unterstützung und die Betreuung der HPLC und GC-Systeme.

Außerdem möchte ich mich ganz herzlich bei Dr. Reinhold Zimmer für alles was er für die AG Christmann und seine Mitarbeiter getan hat und in Zukunft tun wird bedanken.

Ein weiterer Dank gilt auch meinen ehemaligen Studienkollegen aus Düsseldorf, mit denen mich bis heute eine wertvolle Freundschaft verbindet.

Ich möchte mich auch von Herzen bei denen Bedanken, die außerhalb der Universität dafür gesorgt haben, dass es mir an nichts mangelt. Ein unendlicher Dank gilt meinen Eltern und Großeltern, die mich mein Leben lang unterstützt haben und mir ein festes Fundament gegeben haben. Danke an meine Freunde aus Neuss, Düsseldorf, Berlin und dem Rest der Welt für das Feiern großartiger und das Überwinden nicht so großartiger Momente.

Zum Schluss möchte ich mich noch bei der wichtigsten Person in meinem Leben bedanken. Danke für vier Jahre voller Liebe, Zusammenhalt und Unterstützung.

Zusammenfassung

Organokatalytische α-Chlorierung von Aldehyden

Die direkte organokatalytische α-Chlorierung von Aldehyden wurde im Jahre 2004 von den beiden Arbeitsgruppen um *MacMillan* und *Jørgensen* unabhängig voneinander vorgestellt. Im Anschluss folgten zahlreiche Veröffentlichungen zur Aufklärung des Katalysemechanismus. Die Rolle und Eigenschaften von sogenannten Aminal-Intermediaten wurden seitdem kontrovers diskutiert. Basierend auf Kalorimetrie- und NMR-Experimenten wurde diesen Spezies durch die Arbeitsgruppe um *Blackmond* eine aktive Rolle im Katalysezyklus zugeordnet („on-cycle“). Im Gegensatz zum klassischen „steric-shielding“-Modell, bei dem die C-Cl-Bindungsknüpfung für die Stereoselektivität der Reaktion verantwortlich ist, soll hier das thermodynamische Gleichgewicht zweier diastereomerer Aminal-Intermediate für das Enantiomerenverhältnis der Produkte verantwortlich sein (*Curtin-Hammett*-Paradigma). Erste eigene Forschungsergebnisse konnten dieses Szenario zunächst nicht unterstützen, sodass eine umfassende mechanistische Untersuchung der zuvor erwähnten Reaktion aufgenommen wurde.

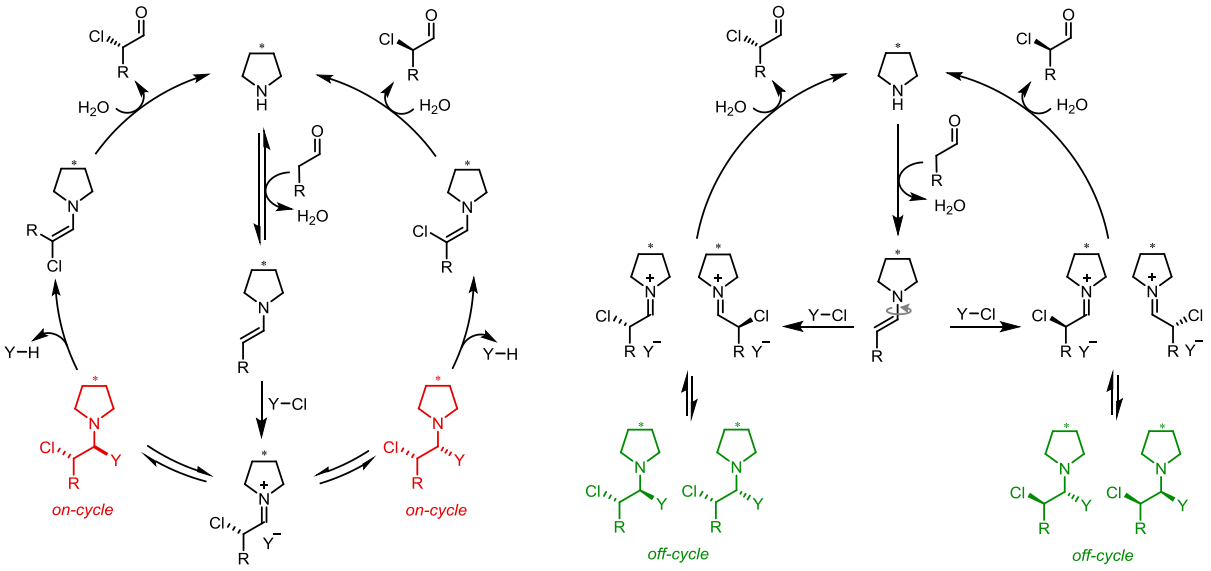

***Curtin-Hammett*-Szenario** **Steric-Shielding-Modell**

Die organokatalytische α-Chlorierung von Aldehyden wurde mit diversen *MacMillan*- und *Jørgensen*-Katalysatoren eingehend untersucht. Die Isolierung und Einkristallstrukturanalyse verschiedenster *MacMillan*-Aminale konnte erstmals die genaue Stereokonfiguration aufklären und damit die in der Literatur vorgenommene Bezeichnung widerlegen. Mit Hilfe einer Kombination aus Zersetzungsexperimenten, NMR-Messungen und DFT-gestützten Berechnungen wurde ein *Curtin-Hammett*-Szenario für diese Spezies zweifelsfrei ausgeschlossen. Stattdessen bilden die Aminale im

Fall der *MacMillan*-Katalysatoren stabile, parasitäre Intermediate, die einen Teil des Katalysators aus dem Katalysezyklus entfernen.

Den Abschluss dieser mechanistischen Studie bildet die gründliche Untersuchung der *Jørgensen*-Aminale, die in der Publikation „Curtin-Hammett Paradigm for Stereocontrol in Organocatalysis by Diarylprolinol Ether Catalysts“ erforscht wurden. Durch eine Modifikation des Reaktionsprozesses wurden erstmals Einkristalle der wesentlich instabileren Aminale erfolgreich für die Strukturanalyse isoliert. Durch eine Kombination aus NMR-Messungen und DFT-basierten Berechnungen konnten die beiden in der Literatur beschriebenen Aminale ausführlich charakterisiert werden. Zur weiteren Aufklärung der absoluten Stereokonfiguration durch Zersetzungs- und Deuterierungsexperimente, gelang es die nachgelagerte Reaktivität genauer zu untersuchen. Neben den *MacMillan*-Aminalen konnte so auch für die *Jørgensen*-Aminale die falsche stereochemische Zuordnung korrigiert werden und ein *Curtin-Hammett*-Szenario ausgeschlossen werden.

Basierend auf einem besseren Verständnis der stabilisierenden Wechselwirkungen innerhalb der Aminale, wurde in weiterführenden Untersuchungen die Bildung dieser parasitären Spezies unterdrückt und die Katalysatorbeladung dadurch deutlich reduziert. Des Weiteren konnte gezeigt werden, dass die organokatalytische α-Chlorierung von Aldehyden Zugang zu synthetisch interessanten chiralen Verbindungen wie Triazolen ermöglicht.

Anwendung neuartiger Polyinterhalogenide

Aufgrund der Instabilität und schlechten Handhabung von reinem BrCl stellt die Synthese und Anwendung stabilisierter Polyinterhalogenide ein interessantes fachübergreifendes Forschungsgebiet dar. In einer aktuellen Veröffentlichung konnte die Arbeitsgruppe *Hasenstab-Riedel* die Synthesen und Charakterisierungen von Verbindungen des Typs $[Y][Cl(BrCl)_x]$ (Y = Kation; x = 1-6) präsentieren.

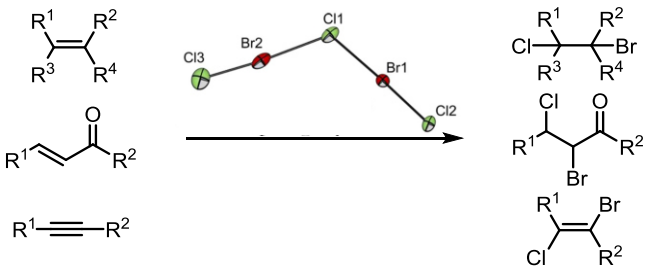

Im zweiten Teil dieser Arbeit wurde die Interhalogenierung von ungesättigten organischen Verbindungen mittels eines neuartigen $[NEt_3Me][Cl(BrCl)_2]$-Komplexes, welcher in der Arbeitsgruppe

Hasenstab-Riedel entwickelt wurde, untersucht. Die gute Atomökonomie in Kombination mit einer hohen Reaktivität bei gleichzeitiger Selektivität konnte anhand verschiedenster Substrate gezeigt werden.

Studien zur Totalsynthese von Hypatulin A und B

Der letzte Teil dieser Arbeit befasst sich mit der Synthese der beiden Naturstoffe Hypatulin A und B. Die beiden polyprenylierten Meroterpene wurden 2016 von der Arbeitsgruppe *Kashiwada* aus den Blättern des Großblumigen Johanniskrautes (*Hypericum patulum*) isoliert und mit Hilfe von 2D-NMR und ECD-Spektroskopie charakterisiert. Die einzigartige hoch-substituierte tri- bzw. bizyklische Struktur und die vier bzw. drei benachbarten quaternären Stereozentren von Hypatulin A und B ließen einen chemisch-synthetischen Zugang zu beiden Naturstoffen erstrebenswert erscheinen. Im Hinblick auf die vielfältige biologische Aktivität verwandter Naturstoffe, sollte die Totalsynthese zusätzlich verschiedenste Derivatisierungsmöglichkeiten eröffnen.

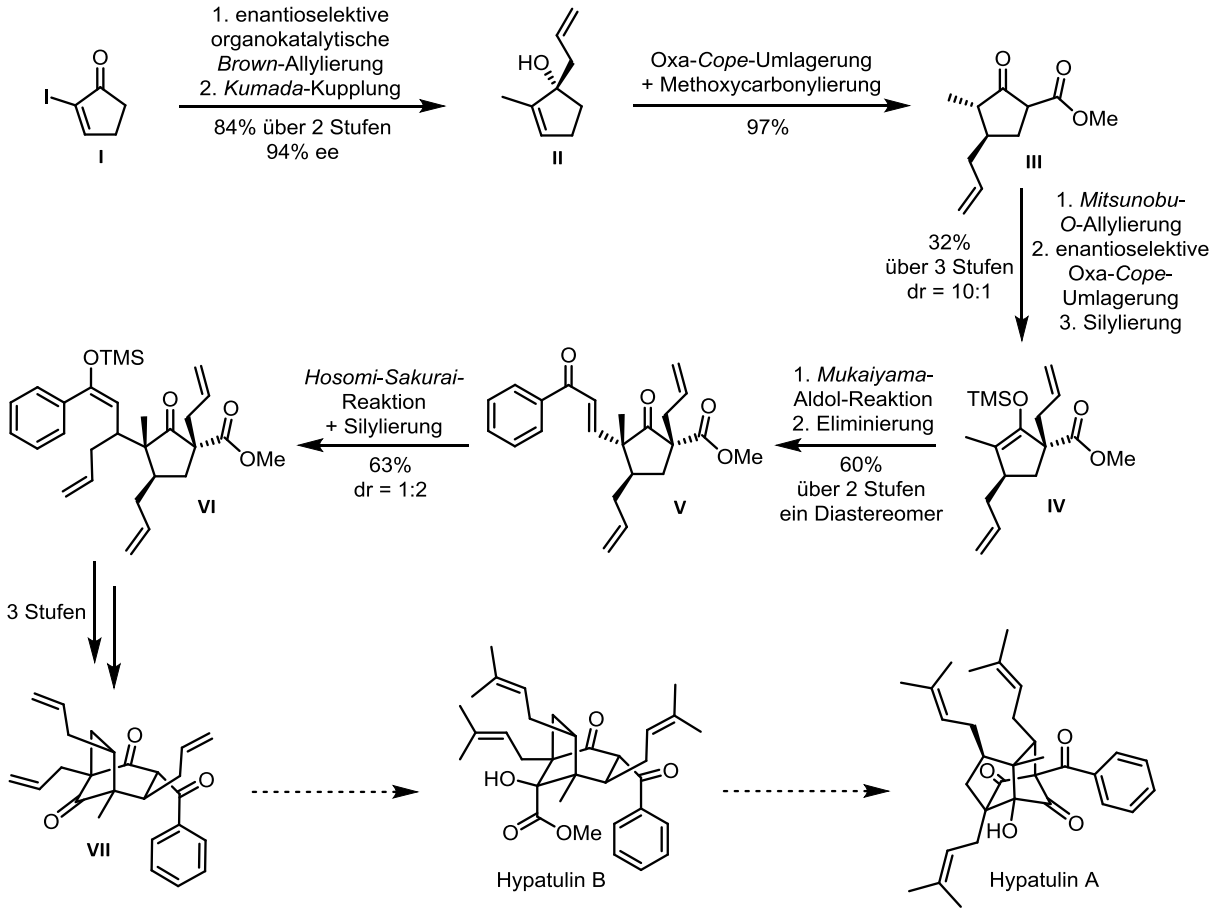

Ausgehend vom iodierten Enon **I** konnte die erste Allylgruppe durch eine organokatalytische *Brown*-Allylierung mit exzellenter Enantioselektivität (94%) eingeführt werden. Eine anschließende Nickel-katalysierte *Kumada*-Reaktion lieferte Alkohol **II** mit einer ausgezeichneten Ausbeute von 84% über zwei Stufen. Die nahezu quantitative Darstellung des β-Ketoesters **III** gelang in einer Eintopf-Reaktion, bei der eine Oxa-*Cope*-Umlagerung mit einer Methoxycarbonylierung kombiniert wurde. Die zweite Allylgruppe wurde durch eine Sequenz bestehend aus einer *Mitsunobu*-artigen *O*-Allylierung und anschließender enantioselektiver Oxa-*Cope*-Umlagerung stereoselektiv eingeführt. Durch eine nachfolgende Silylierung konnte der Silylenolether **IV** mit einer moderaten Ausbeute von 32% über drei Stufen hergestellt werden. Eine intermolekulare *Mukaiyama*-Aldol Reaktion und säurekatalysierte Eliminierung führten mit einer guten Gesamtausbeute von 60% zum Enon **V**. Mit Hilfe der anschließenden *Hosomi-Sakurai*-Reaktion wurde die letzte Allylgruppe zwar mit einer guten Ausbeute (63%) aber schlechten Diastereoselektivität (dr = 1:2) eingeführt. Im weiteren Verlauf gelang es die bizyklische Struktur **VII** nach drei weiteren Schritten aufzubauen.

Abstract

Organocatalytic α-Chlorination of Aldehydes

The organocatalytic α-chlorination of aldehydes was presented independently by the two research groups of *MacMillan* and *Jørgensen* in 2004. Subsequently, numerous publications followed to elucidate the catalytic mechanism. The role and properties of aminal intermediates have been controversially discussed since then. Based on calorimetry and NMR experiments, these species were assigned to play an active role in the catalytic cycle ("on-cycle") by the *Blackmond* group. In contrast to the classical steric-shielding model, in which the C-Cl bond linkage defines the stereoselectivity of the reaction, the thermodynamic equilibrium of two diastereomeric aminal intermediates is supposed to be responsible for the enantiomeric ratio of the products here (*Curtin-Hammett* paradigm). Early results of our own research were unable to support this scenario, so that a comprehensive mechanistic investigation of the aforementioned reaction was commenced.

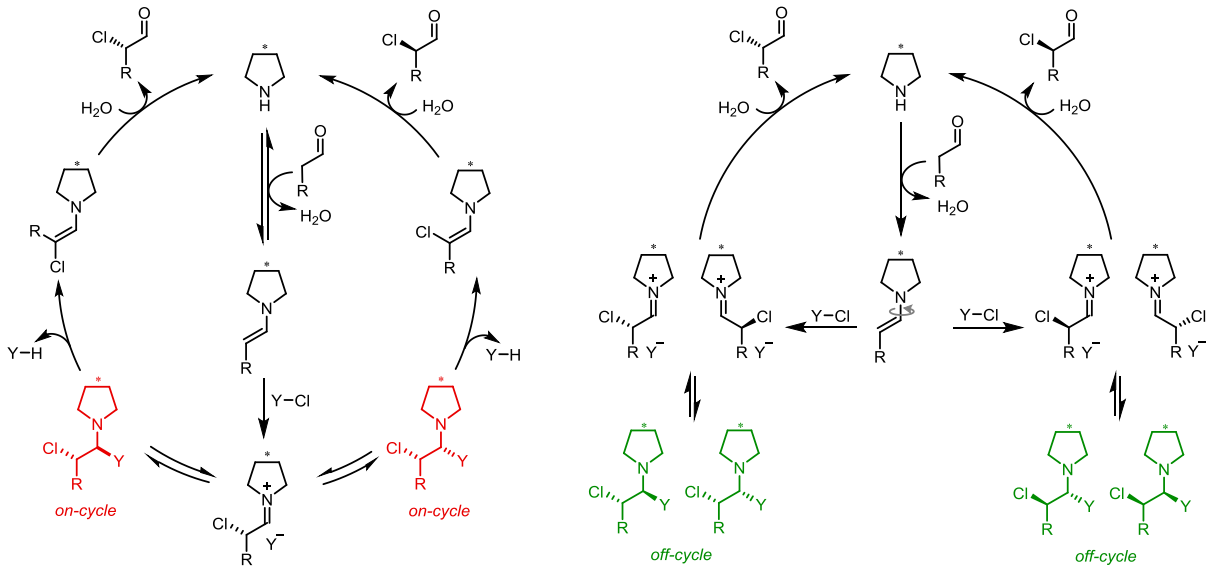

***Curtin-Hammett* Scenario** **Steric-Shielding Model**

The organocatalytic α-chlorination of aldehydes with various *MacMillan* and *Jørgensen* catalysts was investigated in detail. With the isolation and single crystal structure analysis of a wide variety of *MacMillan* aminals we were able to elucidate the exact stereoconfiguration for the first time, thus refuting the assignment made in the literature. Using a combination of decomposition experiments, NMR measurements and DFT-based calculations, the *Curtin-Hammett* scenario could be excluded for these species. Instead, *MacMillan* catalysts form aminals which are stable parasitic intermediates that remove some of the catalyst from the catalytic cycle.

Consequently, the conclusion of this mechanistic study was the thorough investigation of *Jørgensen* aminals, which were considered in the publication "Curtin-Hammett Paradigm for Stereocontrol in Organocatalysis by Diarylprolinol Ether Catalysts". Single crystals of the much more unstable aminals were successfully isolated for structural analysis for the first time by modifying the reaction process. A combination of NMR measurements and DFT-based calculations could be used to further characterize the two aminal species described in the literature. To elucidate the absolute stereoconfiguration and conformation, decomposition and deuterium incorporation experiments allowed the downstream reactivity to be studied in more detail. In addition to the *MacMillan* aminals, the incorrect stereochemical assignment of the aminal species could thus also be corrected for the *Jørgensen* aminals and a *Curtin-Hammett* scenario could be excluded also for this type of catalyst.

Based on the better understanding of the stabilizing interactions within aminals, it was possible to suppress the formation of these parasitic species and significantly reduce the catalyst loading. Furthermore, it could be shown that the organocatalytic α-chlorination of aldehydes can access synthetically interesting chiral compounds such as triazoles.

Application of Novel Polyinterhalides

Due to the instability and dangerous handling of pure BrCl, the synthesis and application of stabilized polyinterhalides represents an interesting interdisciplinary field of research. In a recent publication, the *Hasenstab-Riedel* group successfully completed the syntheses and characterizations of compounds of the type $[Y][Cl(BrCl)_x]$ (Y = cation; x = 1-6).

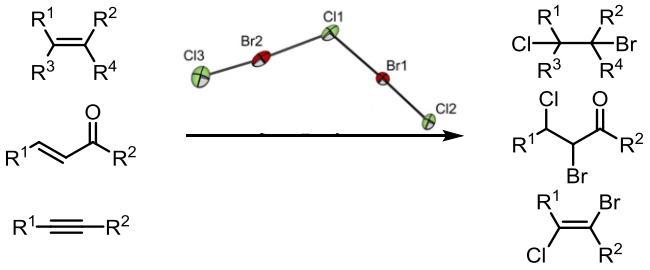

In the second part of this thesis, the interhalogenation of unsaturated organic compounds was investigated using a novel $[NEt_3Me][Cl(BrCl)_2]$ complex developed by the *Hasenstab-Riedel* group. The good atomic economy in combination with a high reactivity and simultaneous selectivity could be demonstrated using a broad substrate scope.

Studies on the Total Synthesis of Hypatulin A and B.

The last part of this thesis deals with studies on the total synthesis of the two natural products hypatulin A and B. The two polyprenylated meroterpenes were isolated from the leaves of goldencup St. John's wort (*Hypericum patulum*) by the *Kashiwada* group in 2016 and characterized by 2D NMR and ECD spectroscopy. The unique highly substituted tri- and bicyclic structures and the four and three adjacent quaternary stereocenters of hypatulin A and B, respectively, suggested that a synthetic approach to both natural products was desirable. In view of the diverse biological activity of related natural products, a total synthesis approach should open up a wide variety of derivatization possibilities.

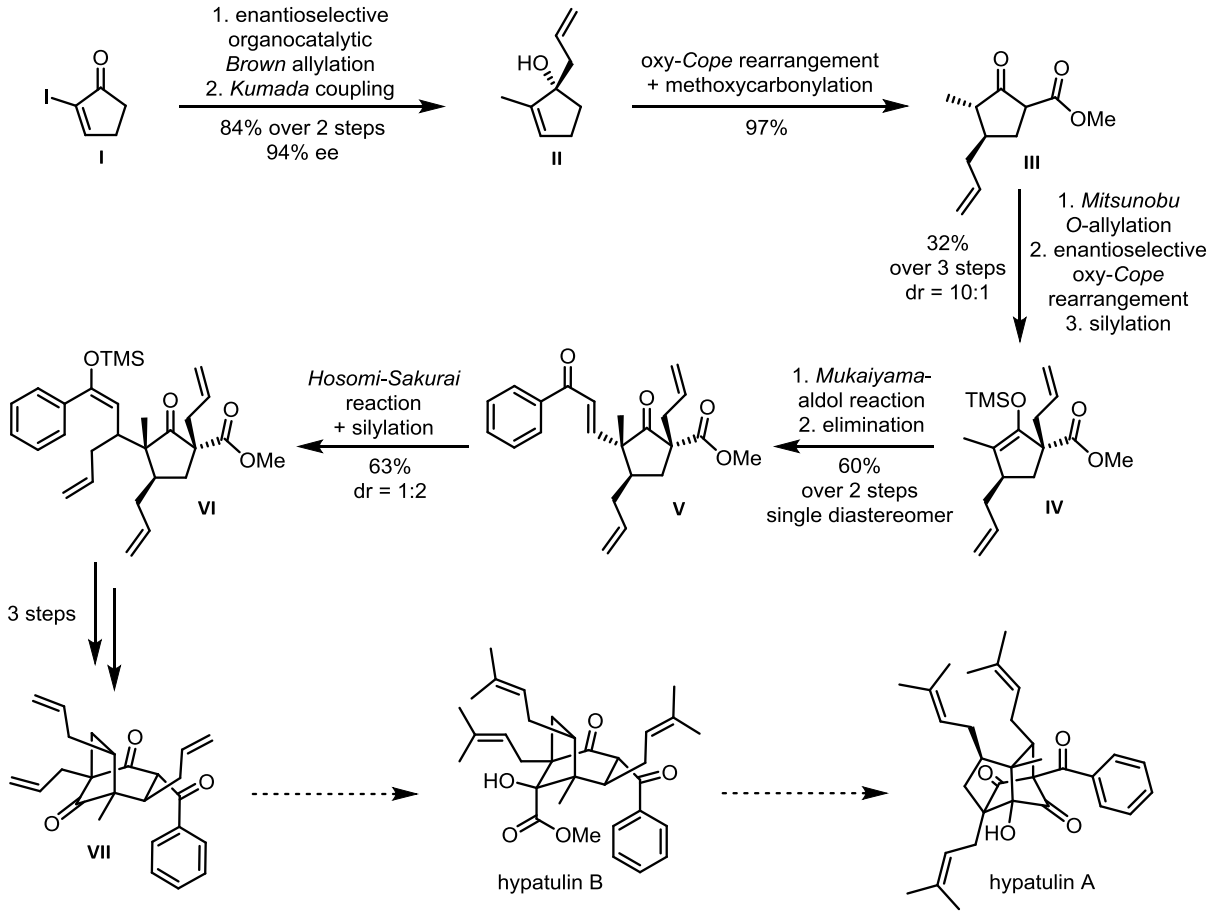

Starting from the commercially available iodinated enone **I**, the first allyl group was introduced by an organocatalytic *Brown* allylation with high enantioselectivity (94%). A subsequent nickel-catalyzed *Kumada* coupling afforded alcohol **II** with an excellent yield of 84% over two steps. Nearly quantitative preparation of β-keto ester **III** was achieved through a one-pot reaction combining an oxy-*Cope* rearrangement with a methoxycarbonylation. The second allyl group could be stereoselectively introduced by a sequence consisting of a *Mitsunobu*-like *O*-allylation followed by an enantioselective oxy-*Cope* rearrangement. Subsequent silylation allowed the preparation of silyl enol ether **IV** with a

satisfactory overall yield of 32% over three steps. An intermolecular *Mukaiyama*-aldol reaction and acid-catalyzed elimination led to the enone **V** with a good yield of 60%. By applying the *Hosomi-Sakurai* reaction, the last allyl group could be introduced with a good yield (63%) but poor diastereoselectivity (dr = 1:2). The construction of the bicyclic structure **VII** could further be realized after three additional steps.

List of Publications:

Ponath, S.; Menger, M.; Grothues, L.; Weber, M.; Lentz, D.; Strohmann, C.; Christmann, M. Mechanistic Studies on the Organocatalytic α-Chlorination of Aldehydes: The Role and Nature of Off-Cycle Intermediates. *Angew. Chem. Int. Ed.* **2018**, *57*, 11683–11687 (DOI:10.1002/anie.201806261); *Angew*. *Chem*. **2018**, *130*, 11857–11861 (DOI:10.1002/ange.201806261).

Ponath, S.; Joshi, C.; Merrill, A. T.; Schmidts, V.; Greis, K.; Lettow, M.; Weber, M.; Steinhauer, S.; Pagel, K.; Thiele, C. M.; Tantillo, D. J.; Vetticatt, M. J.; Christmann, M. On Stereocontrol in Organocatalytic α-Chlorinations of Aldehydes. ChemRxiv. Preprint (https://doi.org/10.26434/chemrxiv.14229875.v1). Submitted to *J. Am. Chem. Soc.* (March 18, 2021).

Schmidt, B.; Ponath, S.; Hannemann, J.; Voßnacker, P.; Sonnenberg, K.; Christmann, M.; Riedel, S. In Situ Synthesis and Applications for Polyinterhalides Based on BrCl. *Chem. Eur. J.* **2020**, *26*, 15183–15189 (doi.org/10.1002/chem.202001267). Highlighted in *ChemistryViews* (November 18, 2020).

Content

1. Mechanistic Studies on the Organocatalytic α-Chlorination of Aldehydes and the Application in Organic Synthesis

1.1. Introduction

1.1.1. Organocatalysis

A catalyst is defined as a substance that accelerates a reaction without undergoing a (net) reaction itself. By opening an alternative reaction pathway, it lowers the activation energy (E_A) without changing the free enthalpy of the reaction (ΔG) (Figure 1).[1]

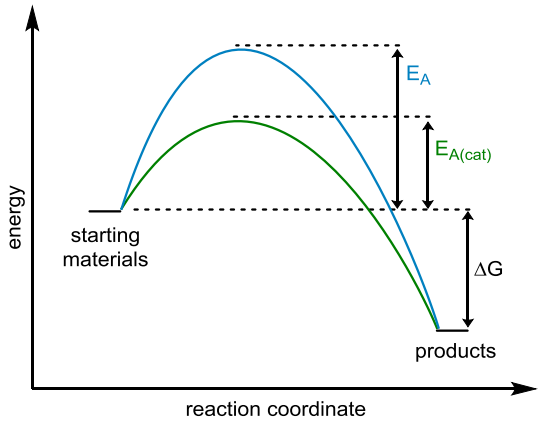

Figure 1: Simplified energy diagram for a catalyzed (green) and non-catalyzed (blue) process.

For catalytic processes, a distinction is made between heterogeneous catalysis, in which the substrate and the catalyst are in different phases, and homogeneous catalysis, in which both substances are in the same phase.[2] Catalytic processes are omnipresent in organisms, play a major role in industry and are therefore extensively researched. Especially heterogeneous catalysis plays a crucial role in our modern society. From the *Haber-Bosch* process, which provides the supply of nitrogen to agriculture, to automotive catalysts, which enable the reduction of toxic emissions, catalysts are a key element of our modern life.[1]

Catalysis can be further divided into subgroups such as biocatalysis, metal catalysis and organocatalysis. By definition, organocatalysis is described as a reaction in which small organic and metal-free molecules serve as catalysts for organic reactions.[3] Within organocatalysis, a distinction is made between covalent and non-covalent interactions. Covalent organocatalysis is represented by the diverse group of amine catalysts[4] (Scheme 1, 1.) or *N*-heterocyclic carbenes[5] (Scheme 1, 2.). In these cases, the substrates and the catalysts give rise to covalently bonded reactive intermediates (enamines, *Breslow* intermediates), which with a suitable reagent lead to formation of the product. Non-covalent organocatalysis is based on activation of the substrate by means of hydrogen bonds

(Scheme 1, 3. and 4.) (chiral *Brønsted* acids[6], urea derivatives[7]) or other electrostatic interactions (Scheme 1, 5.) (halogen bond donors[8]).

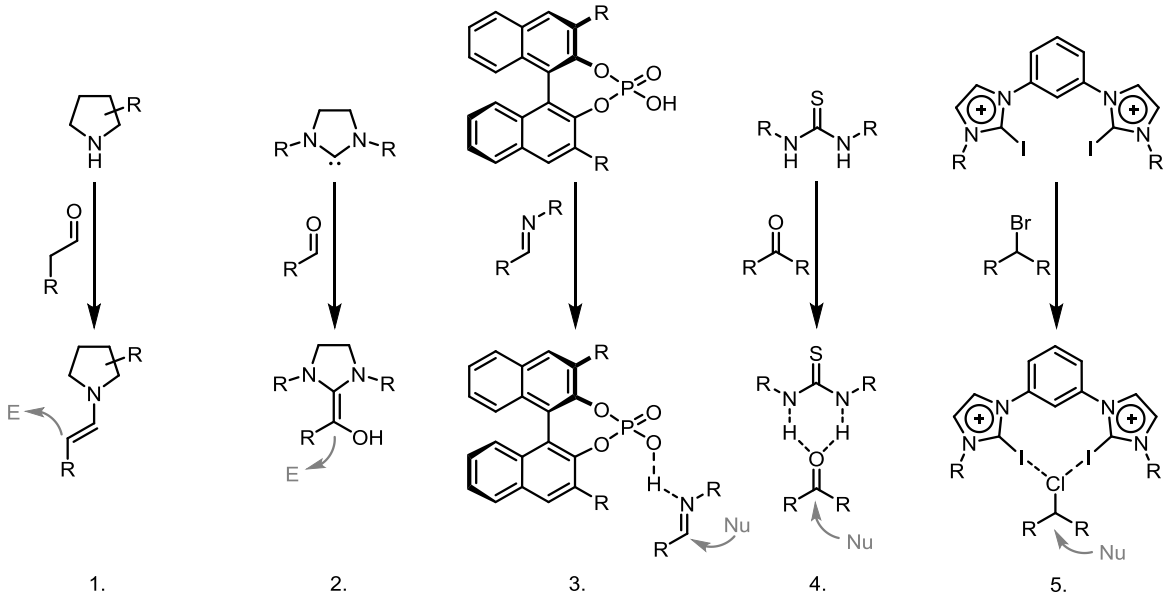

Scheme 1: Different organocatalysts, modes of activation with suitable substrates and possible reactivities (E: electrophile, Nu: nucleophile): 1. Aminocatalysts can form enamines with aldehydes; 2. *N*-Heterocyclic carbenes can form *Breslow* intermediates with aldehydes; 3. Organophosphates can activate imines by hydrogen bonding; 4. Thiourea derivatives can activate ketones by hydrogen bonding; 5. Cationic multidentate halogen bond donors can activate alkyl chlorides by halogen bonding

Although the term “organocatalysis” was coined at the beginning of the new millennium, particularly by *MacMillan*[9], the application of this concept goes back much further historically. The benzoin addition discovered by *Wöhler* and *Liebig* in 1832 can be regarded as the first organocatalytic reaction developed by chemists.[10] Twenty-seven years later, *Liebig* first identified an organic molecule (acetaldehyde) as the catalyst of an organic reaction (oxamide synthesis from dicyan and water).[11] In 1912, *Bredig* and *Fiske* were able to observe a small enantiomeric excess in the addition of hydrogen cyanide to aldehydes by using the diastereomers quinine and quinidine as catalysts.[12] This research marks the first man-made asymmetric organocatalytic reaction. The *Hajos-Parrish-Eder-Sauer-Wiechert* reaction developed in the 1970s can be regarded as another milestone. By using enantiomerically pure proline, it was possible to achieve enantiomeric excesses of >90% for the first time.[13]

Since the introduction of the term "organocatalysis" in 2000, this field of research has seen a tremendous increase in publications every year until 2012. The nearly constant publication numbers since 2012 illustrate that research interest in this topic is undiminished (Figure 2).[14]

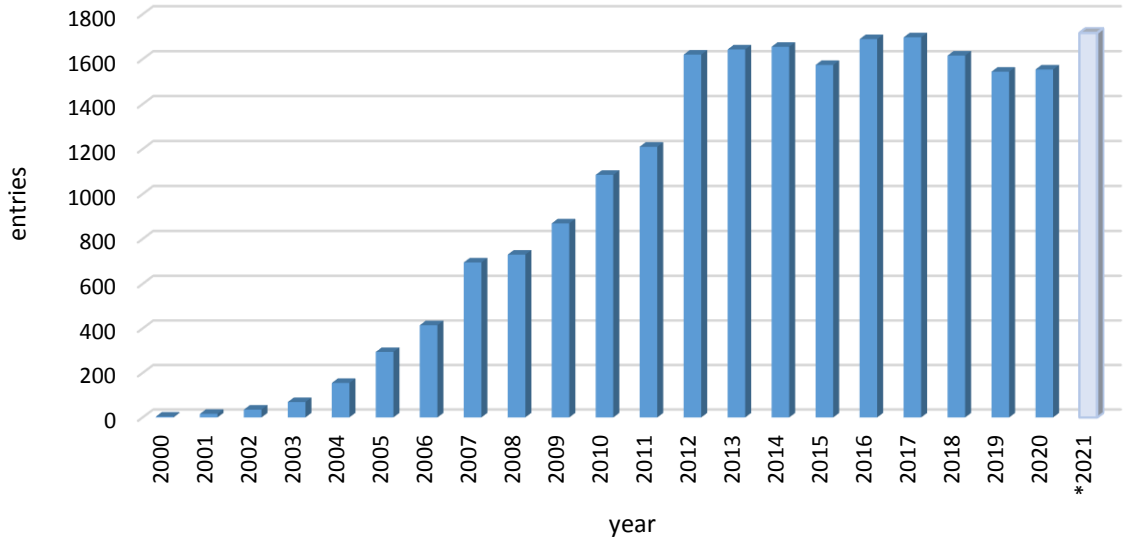

Figure 2: Number of SciFinder entries for the research topic „organocatalysis“ (*: Extrapolation based on 414 entries on March 29, 2021).[14]

1.1.2. Activation of Aldehydes by Secondary Amines

A fascinating subarea of covalent organocatalysis is the activation of aldehydes by secondary amines. A distinction can be made between LUMO, SOMO and HOMO activation.[15]

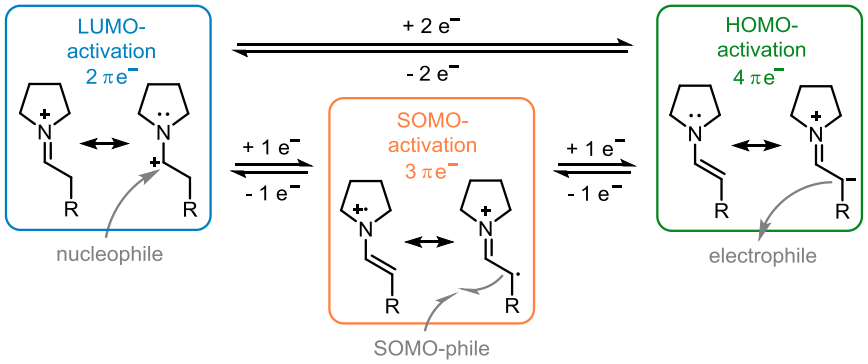

Scheme 2: Different activation modes for aldehydes with secondary amines.

The condensation of a secondary amine with an α-unsubstituted aldehyde generates, after elimination of water, an iminium ion whose LUMO is energetically lowered compared to the carbonyl group. The representation of the resonance structure illustrates the localization of the LUMO at the former carbonyl carbon (blue box). This position is accessible by suitable nucleophiles. At the same time, the acidity of the α-protons increases. The π-system consists of two π-electrons which are part of the C-N

double bond or are present as a free electron pair at the nitrogen atom in a second mesomeric structure.

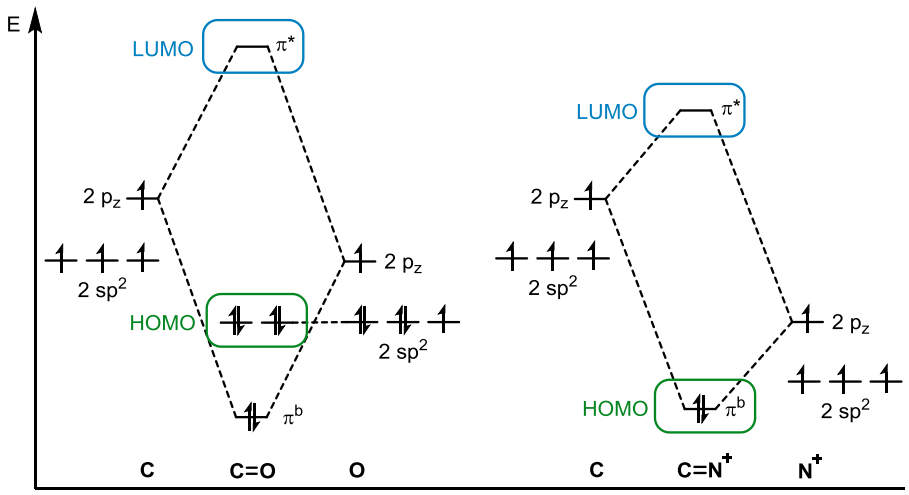

Figure 3: Molecular orbital scheme for the C-O double bond of a carbonyl compound (left) and for the C-N double bond of an iminium ion (right).

Figure 3 illustrates the differences between the C=O carbonyl and the C=N iminium bond by means of a qualitative molecular orbital diagram.[16] The LUMO of the carbonyl bond (left) corresponds to the antibonding π* molecular orbital, which is formed from the linear combination of the two p_z atomic orbitals of the carbon and oxygen atom. The two non-bonding electron pairs of two sp^2 hybrid orbitals of the oxygen atom form the HOMO. The unpaired electron in the third sp^2 hybrid orbital of the oxygen atom would form the σ-bond to the carbon atom in a complete molecular orbital scheme. Compared to the carbonyl bond, the LUMO of the C-N double bond in the iminium ion (Figure 3, right), which results from the same linear combination, is energetically lowered and clearly localized at the carbon atom. The energetic lowering of the LUMO results from the energetically lower atomic orbitals of the positively charged nitrogen. This reflects the increased reactivity toward the HOMO of a nucleophile. The HOMO of the iminium ion is the occupied and binding π-molecular orbital. The three unpaired electrons in the three sp^2 hybrid orbitals of the nitrogen atom would, in a complete molecular orbital scheme, again form the σ-bond to the carbon atom and additionally two more σ-bonds to two (alkyl) substituents.

Examples of LUMO activation include reductive amination[17] (Nu^- = H^-) or activation of carbonyl compounds by *Lewis* or *Brønsted* acids followed by nucleophilic attack at the former carbonyl carbon atom[18]. In addition, iminium catalysis with α,β-unsaturated aldehydes can provide nucleophilic addition at the β-position.[19]

Formal one-electron reduction provides access to SOMO activation with three electrons in the π-system (orange box). The mesomeric structure shows the reactive center of the molecule. In this case, SOMO-philic molecules can react with the α-position of the activated aldehyde. Literature-known examples for the application of SOMO activation are the α-allylation[15] and α-chlorination[20] of aldehydes.

Through another formal one-electron reduction, HOMO activation with four π-electrons in the π-system is accessible (green box). The same activation mode can be achieved by α-deprotonation of the previously mentioned iminium ion. The HOMO, which is localized in the α-position, is energetically higher than the one for the corresponding enol species.[16] Thus, it has a distinct nucleophilic character and is reactive towards electrophiles. HOMO activation, on which enamine catalysis is based, has been and is a subject of versatile research. Applications include aldol reactions and a wide variety of α-functionalizations (α-oxidation, α-chlorination, α-amination, etc.).[4]

Enamine and iminium ion are in direct equilibrium with each other due to protonation/deprotonation (Scheme 2). The equilibrium between iminium ion **3** and enamine **4** can also be interpreted as a simple acid-base equilibrium.[21] The stability of the respective species (enamine and iminium ion) and the available reaction partner (electrophile or nucleophile) define the type of reaction that takes place subsequently. Since the two modes of activation can in principle take place under the same conditions, some organocatalysts can mediate both, nucleophilic and electrophilic reactions. Based on the vinylogy principle[22] functionalizations of α,β-unsaturated aldehydes or conjugated dienals (**1**) in the β-, γ-, δ- and ε-position are accessible (Scheme 3). Due to the cascade-like reaction course, multiple functionalization in one reaction are possible.[23]

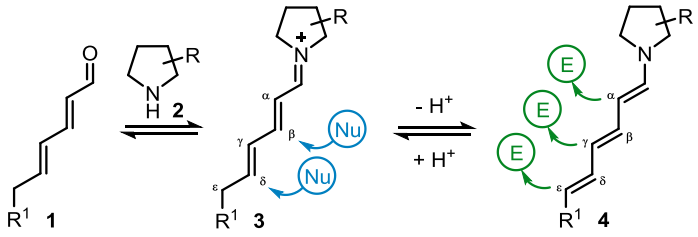

Scheme 3: Reactivities of the polyunsaturated aldehyde **1** and amine catalyst **2** according to the vinylogy principle.

The formation of aminal intermediates in the organocatalytic α-chlorination of aldehydes (Chapter 1.1.4.) is a consequence of a twofold activation. The enamine **6** formed by HOMO activation from aldehyde **5** and catalyst **2** first reacts as a nucleophile with the electrophilic chlorinating reagent NCS (**7**). The resulting α-chloroiminium ion **8** is now LUMO-activated and allows nucleophilic attack of the

succinimide anion (**9**) at the iminium carbon atom, leading to the formation of the aminal **10** (Scheme 4).

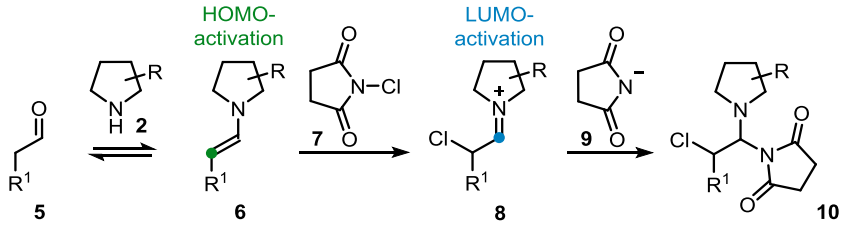

Scheme 4: Aminal formation through the sequence of HOMO and LUMO activation.

1.1.3. Organocatalytic α-Chlorination of Aldehydes

The catalytic cycle shown in Scheme 5 depicts the general and simplified idea of a HOMO-activated, amine-catalyzed reaction of aldehydes with electrophiles. The secondary amine catalyst **2** first condenses with the α-unsubstituted aldehyde **5** to generate the iminium ion **11**. Subsequent deprotonation leads to enamine **6**. This nucleophile can react with an electrophile (E^+) to form the iminium ion **12**. Subsequent hydrolysis releases the α-functionalized aldehyde **13** under regeneration of the catalyst **2**.

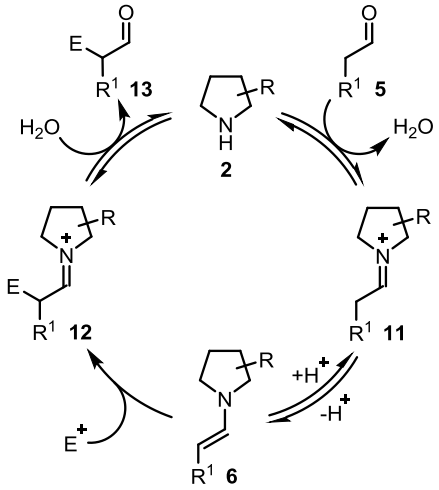

Scheme 5: Simplified catalytic cycle for the amine-catalyzed reaction of aldehydes with electrophiles (E^+).

Based on the HOMO activation, the two research groups of *MacMillan* and *Jørgensen* independently developed the first enantioselective organocatalytic α-chlorination of aldehydes in 2004.[24,25] Previously, other α-functionalizations of aldehydes and ketones had been realized by enamine catalysis.[4]

MacMillan's research group used a combination of imidazolidinone **14** and *Lectka*'s ketone **15** to achieve excellent yields (up to 94%) and enantiomeric excesses (up to 95%) at a temperature of –30 °C (Scheme 6, top). At 4 °C and by using NCS as a chlorinating agent, the enantiomeric excess decreased dramatically (19%).[24]

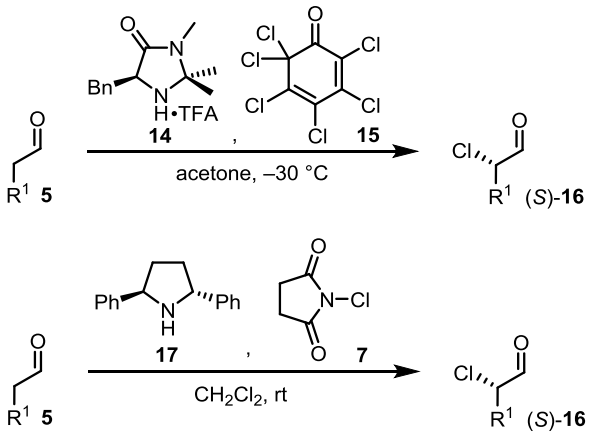

Scheme 6: The first two examples of an enantioselective organocatalytic α-chlorination of aldehydes (top *MacMillan*, bottom *Jørgensen*).

In the course of his doctoral research in the *MacMillan* group, *Brown* observed the racemization of the chiral α-chloroaldehyde over time at room temperature. He also identified significant amounts of dichlorinated aldehyde at this temperature.[26]

Jørgensen and co-workers, on the other hand, used the C_2-symmetric diarylpyrrolidine **17** as a catalyst and NCS as a chlorinating reagent to achieve excellent yields (up to 99%) and enantiomeric excesses (up to 97%) already at room temperature (Scheme 6, bottom). In this example, no racemization could be observed over time.[25]

In 2009, *MacMillan*'s research group developed an α-chlorination protocol based on the SOMO activation mode, using lithium chloride as a low-cost and atom-economical chlorinating reagent (Scheme 7).[20]

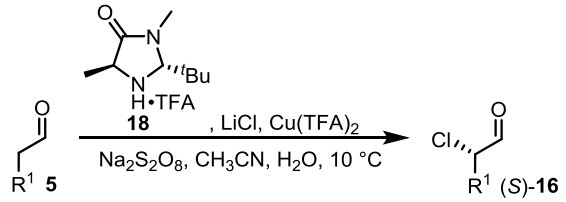

Scheme 7: *MacMillan´*s SOMO chlorination.

The initially employed imidazolidinone catalyst **20** led to unsatisfactory enantioselectivities at room temperature, as in *Brown´*s studies.[20,26] Only the novel design of the pseudo-C_2-symmetric catalyst **18** gave satisfactory results and suppressed the downstream racemization of the product even at elevated temperatures.

MacMillan and *Brown* postulated a downstream mechanism that explains both racemization and dual chlorination of the product (Scheme 8).[20,26] Here, the imidazolidinone catalysts **14** and **19** can re-condense with the chiral α-chloroaldehydes (*R*)-**16** and (*S*)-**16** to form the chloroiminium ions **20a**/**20b** and **21a**/**21b**, which can be in equilibrium with the chloroenamines **22** and **23**, respectively. These chloroenamines can subsequently lead to racemization of the α-stereocenter by non-selective protonation (rac-**16**) or be chlorinated for a second time (**24**). For the pseudo-C_2-symmetric catalyst **18**, downstream racemization or dichlorination was not observed.

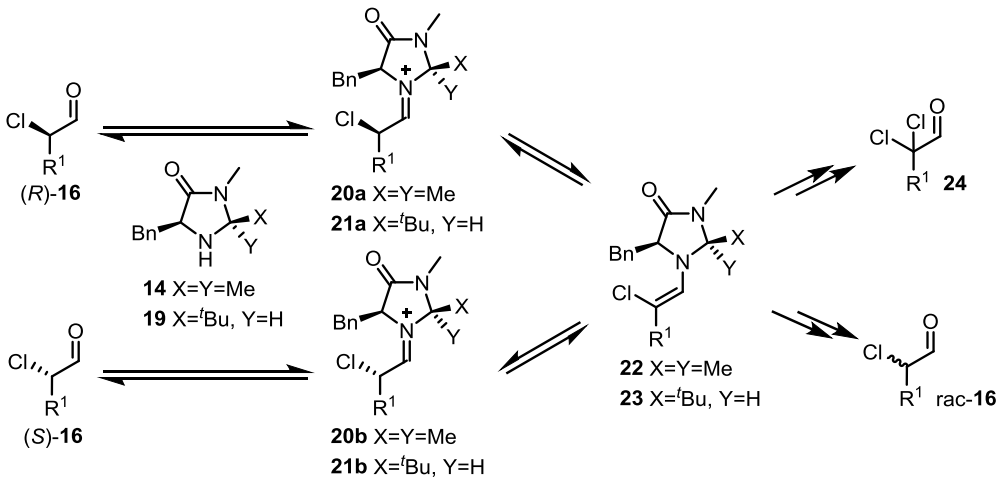

Scheme 8: Postulated mechanism for racemization and dichlorination (X=Y=Me *Brown* dissertation; X=^{t}Bu, Y=H *MacMillan* 2009).

The group of *Jørgensen* showed that two enantiomeric α-halogenated aldehydes have different tendencies to form halo enamines. The authors reason that this phenomenon is due to the different shielding of the two acidic protons of the haloiminium ions (Scheme 9, red). To verify their hypothesis, they condensed a racemic mixture of α-fluoroaldehydes (*R*)-**25** and (*S*)-**25** with a chiral organocatalyst and reacted it with *N*-fluorobenzenesulfonimide as an electrophilic fluorinating reagent. The twofold fluorinated aldehyde **29** was subsequently identified in the reaction mixture. Moreover, the enantiomeric excess of the monofluorinated aldehyde (*S*)-**28** was now 20%. Through this experiment, it was shown that one enantiomer can be preferentially converted to the difluorinated aldehyde **29** via the fluorinated enamine **27**.[27]

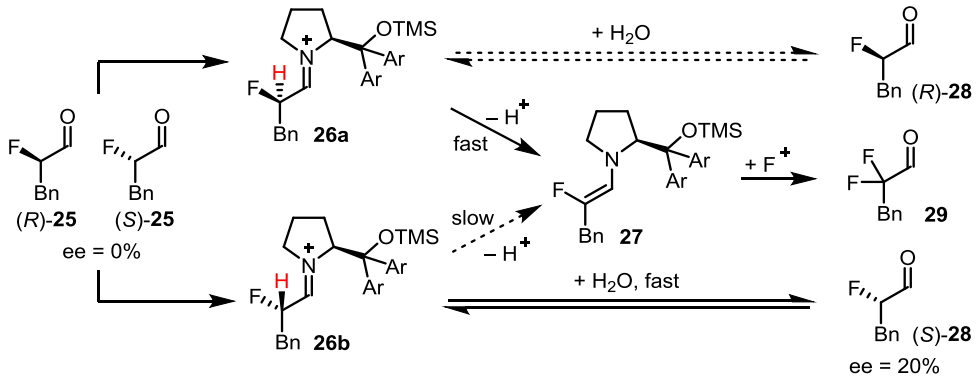

Scheme 9: Kinetic resolution of a racemic α-fluoroaldehyde according to *Jørgensen*.

In another study on the α-chlorination of aldehydes using 2,5-diphenylpyrrolidines as catalysts, the group of *Jørgensen* gained additional insights into the reaction mechanism.[28] Experimental and computational methods led the authors postulate an initial *N*-chlorination of enamine **30**, followed by an [1,3]-sigmatropic shift to form the product, rather than direct chlorination of the nucleophilic enamine carbon (Scheme 10). This hypothesis was investigated by the group of *Metzger*,[29] *Blackmond*,[30] and *Renaud*[31] and was evaluated differently. In addition, the study of *Jørgensen* identified the hydrolysis of the chloroiminium ion **33** as the rate-determining step of the reaction.

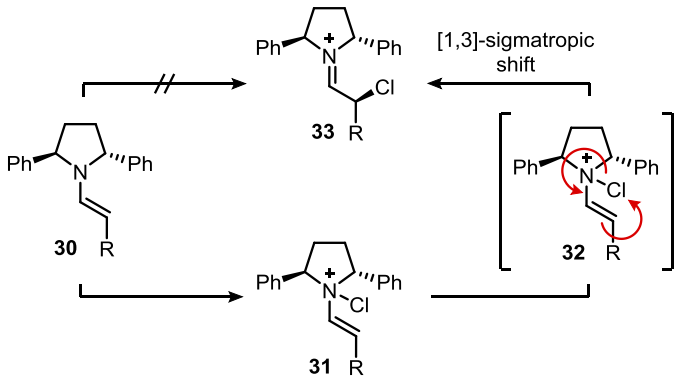

Scheme 10: Excerpt from the reaction mechanism postulated by *Jørgensen*.

Over the course of the last two decades, numerous studies have appeared in which the catalytic properties of various secondary amines have been compared. Of particular interest for organocatalysis is the nucleophilicity of the catalysts and the stability and reactivity of the corresponding enamines. The group of *Mayr* showed that the basicity and nucleophilicity of the imidazolidinone-based *MacMillan* catalysts is significantly lower than that of the pyrrolidine-based catalysts (e.g. *Jørgensen-Hayashi* catalyst). This observation correlates with the nucleophilicity of the corresponding enamines. Again, the enamines of the imidazolidinones show significantly lower nucleophilicity than the pyrrolidine-based enamines.[32]

A crucial factor for the reactivity of enamines is the pyramidalization of the nitrogen atom.[33] A distinct sp^3 hybridization leads to a tetrahedral nitrogen in which the four tetrahedral corners are occupied by the free electron pair and the three bonding partners of the nitrogen. The more planar the nitrogen, the stronger the sp^2 hybridization character. In this borderline case, all bonding partners of the nitrogen lie in a triangular plane and the free electron pair is located in the p orbital, which is perpendicular to it. Figure 4 shows the two boarder cases of hybridization. In an idealized sp^3 hybridized nitrogen, the nonbonding sp^3 orbital carrying the free electron pair points away from the N-C bond axis at a tetrahedral angle of 109.5 °C. The geometric overlap of this orbital with the antibonding π-orbital of the C-C double bond (LUMO) is unfavorable in this case (Figure 4, left). A different picture emerges for an ideal sp^2 hybridization of the nitrogen. Here, the non-bonding p orbital lies in the same plane as the antibonding π orbital of the C-C double bond and the overlap is optimal (Figure 4, right). The more planar the nitrogen and the better the overlap of the nonbonding orbital of the nitrogen with the antibonding π orbital of the C-C double bond, the better the electron donation (n→π*) and the higher the reactivity with electrophiles.[33]

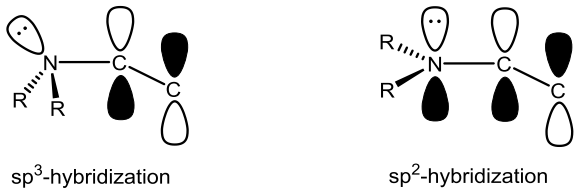

Figure 4: Extreme cases of hybridization at the nitrogen atom and the resulting overlaps with the LUMO of the C-C double bond.

The group of *Vilarrasa* compared the relative stabilities of the enamines formed from the equilibrium between catalyst/aldehyde and enamine. Accordingly, the thermodynamic stability correlates with the subsequent reactivity toward electrophiles.[34]

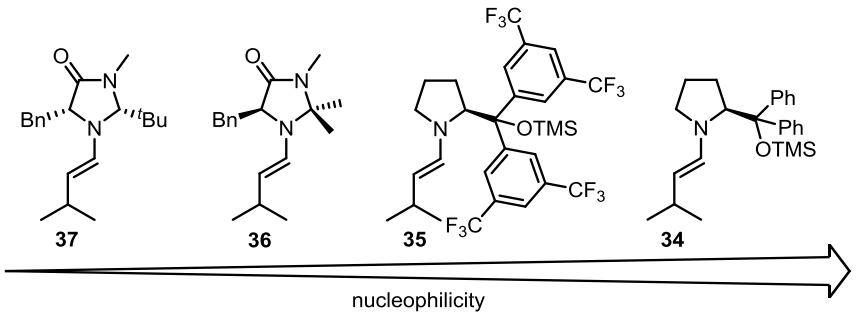

Figure 5: Structure-reactivity relationship of some enamines from the two catalyst classes.

The authors concluded that imidazolidinone enamines such as **36** and **37** posses lower nucleophilicity than pyrrolidine-based enamines such as **34** and **35** (Figure 5). According to the authors, their observation can be rationalized by steric shielding and the electronic structure of the catalysts.

Enamine formation of different catalysts has also been studied by *Wiest*.[21] Figure 6, illustrates that enamine formation proceeds more favorably when using the *Jørgensen-Hayashi* catalyst **38** than with the *MacMillan* imidazolidinones **14** and **19**. These observations are consistent with the previously mentioned publications. The effect of the addition of acid (benzoic acid, TFA) to the reaction mixture is also evident. For example, the addition of benzoic acid dramatically reduces the enamine formation of catalyst **38**. In the case of imidazolidinone **14**, enamine formation is completely suppressed by the addition of TFA.

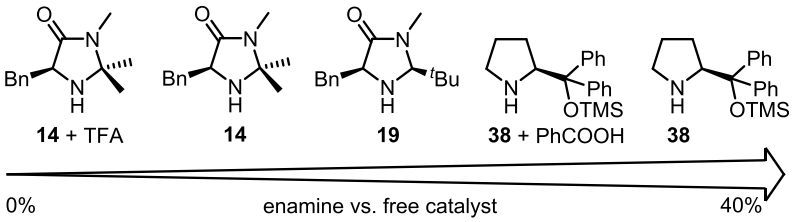

Figure 6: Enamine formation of various catalysts and additives after 30 min according to *Wiest*.

In the context of the conversion of terpene-based starting materials, the organocatalytic α-chlorination of aldehydes was also investigated and applied in the *Christmann* group. The starting point was the desire to make synthetically valuable chiral epoxides accessible by the organocatalytic α-chlorination of aldehydes. SOMO activation according to *MacMillan* initially represented a promising possibility because inexpensive and atom-economical chlorinating agents could be used here. Due to side reactions attributed to the decomposition of radical intermediates,[35] a suitable alternative had to be found. *MacMillan*'s α-chlorination benefits from the simple, inexpensive, and scalable synthesis of imidazolidinone catalysts.[36] However, the quantitative use of *Lectka´*s ketone **15** is expensive[37] and releases pentachlorophenol after conversion, a toxic and probably carcinogenic substance.[38] For the reaction procedure according to *Jørgensen*,[25] the opposite case arises: the synthesis of diphenylpyrrolidine catalyst **17** represents a major disadvantage, especially considering scalability and cost.[39] At the same time, the chlorinating reagent NCS is inexpensive[40] and releases harmless succinimide after conversion. Finally, the combination of catalyst **18** and NCS provided an efficient, inexpensive and scalable system for α-chlorination of aldehydes (Scheme 11).[35]

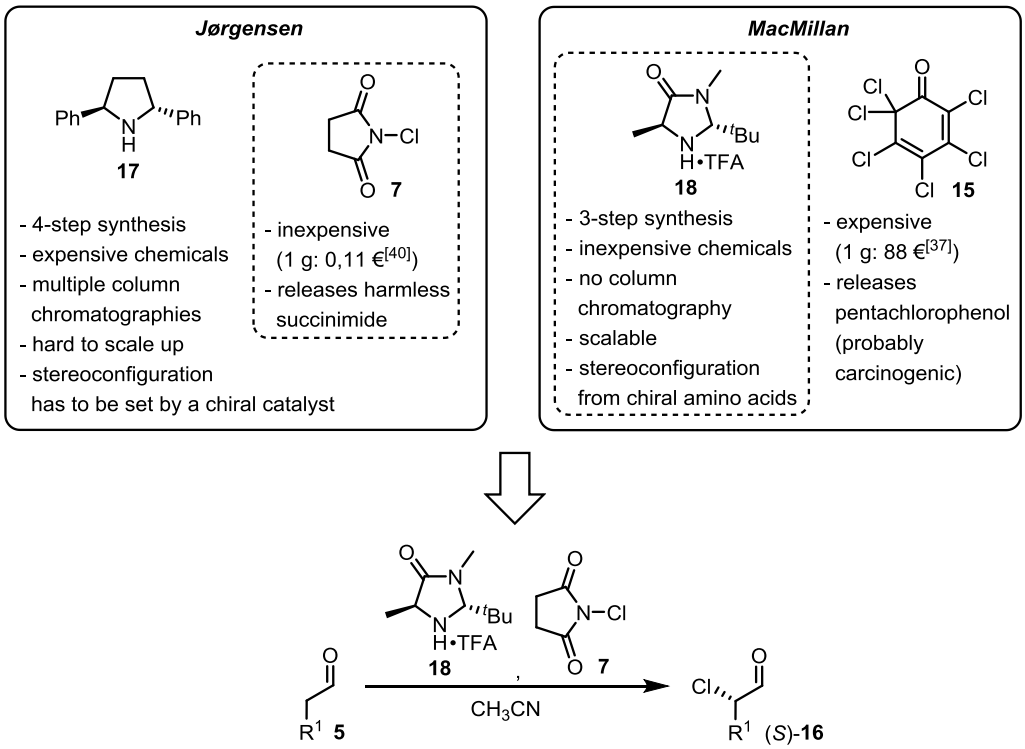

Scheme 11: „*Merged*"-chlorination according to *Christmann*.

1.1.4. Aminal Intermediates

The reaction mechanism was further elucidated by the observation of previously unknown aminal intermediates. These species consist of catalyst, aldehyde and chlorinating reagent and were identified spectroscopically for the first time by the *Jørgensen* group.[28] For this purpose, a previously synthesized enamine **39** was reacted with NCS to generate the aminal **40** (Scheme 12). Interestingly, the authors observed the exclusive formation of one diastereomer (**40a** or **40b**). The unstable nature of the aminal made the isolation impossible, which would have been necessary to elucidate the relative stereoinformation.

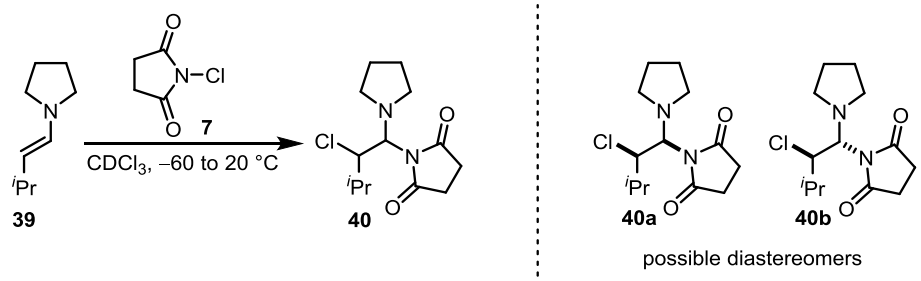

Scheme 12: Aminal synthesis according to *Jørgensen*.

In 2012, the group of *Blackmond* revisited these aminal intermediates in a study on stereocontrol of organocatalytic reactions.[30] The aim was to show that in the organocatalytic α-chlorination of aldehydes, the final stereochemical outcome is not defined by the transition state in which the stereocenter is formed, but by the relative stabilities of two interconverting diastereomeric aminal intermediates. This *Curtin-Hammett* scenario, postulated by the authors should lead to the erosion of the initially near-perfect stereoselectivity of the C-Cl bond formation (**6** to **41**). The remaining anion (Y^-) of the chlorinating agent (Y-Cl) can subsequently form the two equilibrating diastereomeric aminals *syn*-**42** and *anti*-**42** by *syn*- or *anti*-addition to the chiral chloroiminium ion **41**. As a rate-determining step, stereospecific E2 elimination leads to the chloro enamines *E*-**43** or *Z*-**43**. A highly selective protonation and subsequent hydrolysis of the two species generates the two enantiomeric α-chloroaldehydes (*S*)-**16** and (*R*)-**16**, respectively.

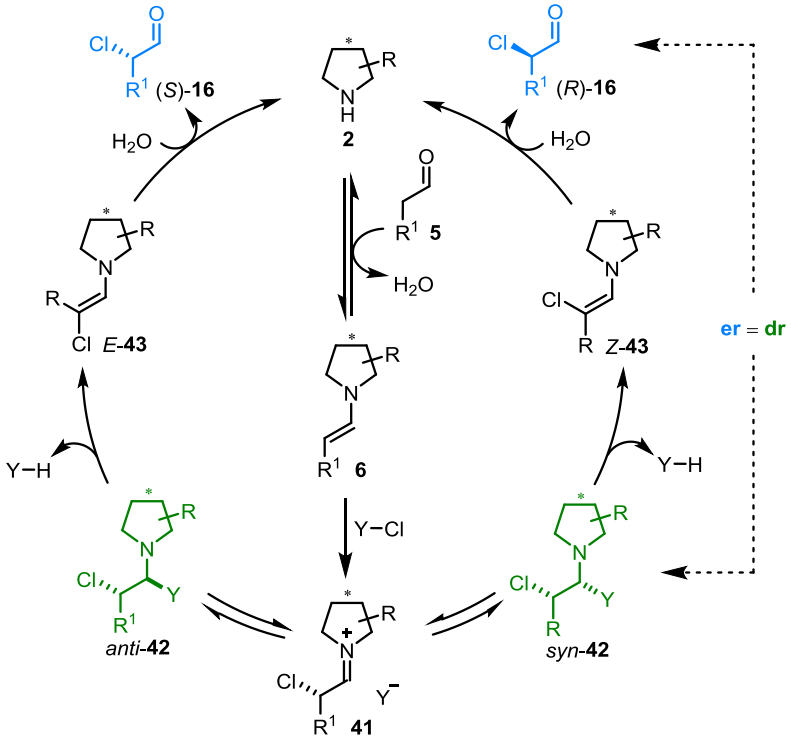

Scheme 13: Catalytic cycle according to *Blackmond*.

The main hint for this new paradigm of stereocontrol was the observation that the diastereomeric ratio of the aminals (Scheme 13, green) was nearly identical to the enantiomeric ratio of the chlorinated products (Scheme 13, blue). The appearance of EXSY-cross-peaks in the NOESY spectrum of the reaction mixture led the authors to postulate the interconversion of the two aminals. All spectroscopic data were taken from ^{1}H NMR spectra of the reaction mixtures. The absolute or relative stereoconfiguration of the aminals could again not be clarified. In the course of their studies the authors used three different chiral pyrrolidine-based catalysts, isovaleraldehyde as the substrate and

NCS and NCP as chlorinating reagents. As a conclusion of their research, they claim “that this concept may apply to related reactions and thus may represent a general phenomenon for amine catalysts lacking an acidic directing proton”.

According to a master thesis prepared in the *Blackmond* group, aminal formation could also be studied using *MacMillan* catalysts **14** and **19**.[21] Under the conditions published by *MacMillan* in 2004[24] (*Lectka*'s ketone **15** as chlorinating reagent), no intermediate (in this case hemiaminal: pentachlorophenol anion) could be identified. Replacing the previously used chlorinating reagent by NCS, two (in analogy to the results previously published by *Blackmond*[30]) diastereomeric aminals were detected (Figure 7). These compounds showed significantly greater stability than the aminals of the *Jørgensen-Hayashi* catalyst and were isolable (the relative and absolute stereoconfiguration of these species could again not be clarified). Importantly, no interconversion of the two diastereomers was observed, not even at elevated temperature. The author concluded that these observations rule out a *Curtin-Hammett* scenario: “In this case they [the two diastereomeric aminals] could not only be detected at room temperature but also be isolated. Even heating did not provide enough energy to equilibrate those diastereomers (no *Curtin-Hammett* scenario).”[21]

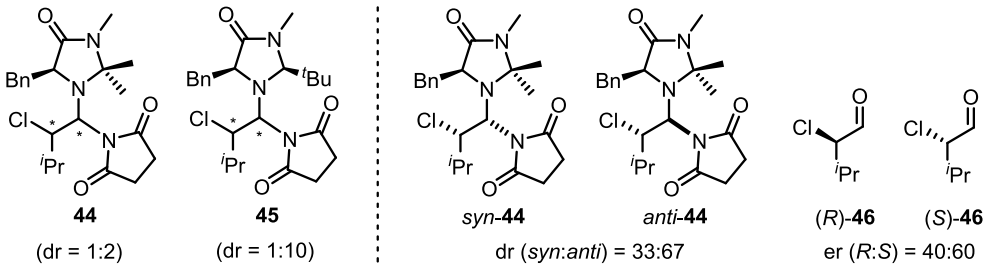

Figure 7: Aminals identified in the aforementioned master thesis and the *syn*- and *anti*-assignment of aminals made by *Blackmond* et al. together with the correlation between the diastereomeric ratio of these aminals and the enantiomeric ratio of the corresponding α-chloroaldehydes (right).

Furthermore, when using *MacMillan* catalyst **19** with TFA, the author observed the decomposition of one diastereomer during the ongoing reaction. In the review article “Explaining Anomalies in Enamine Catalysis: Downstream Species as a New Paradigm for Stereocontrol”[41] *Blackmond et al.* list the results of this master thesis as further evidence for a *Curtin-Hammett* paradigm, despite the author's contrary interpretation.

Further research to elucidate the catalytic mechanism in the *Christmann* group allowed the identification of similar aminal intermediates as observed by *Jørgensen*[28] and *Blackmond*[21,30,41]. These compounds, incorporating the imidazolidinone catalyst **18**, could be isolated and the absolute configuration could be determined by X-ray crystal structure analysis for the first time.[42]

1.1.5. Application in Organic Synthesis

As demonstrated by various groups, α-chloroaldehydes are precursors for numerous compound classes. This concept of "linchpin catalysis", taken up by *MacMillan*, includes the generation of an enantiomerically enriched intermediate by a highly specialized catalytic transformation, which can then be efficiently converted into numerous synthetically valuable building blocks.[20] α-Chlorinated aldehydes are ideal examples for this type of intermediates. They are sufficiently stable compounds, yet possess enough reactivity to undergo further synthetic derivatizations. As presented in Scheme 13, the carbonyl functionality (blue) can be reduced, oxidized or otherwise modified. These transformations can be followed by esterification, etherification and other reactions. Coupled with the good leaving group properties of the chloride atom (red), which enables inter- and intramolecular S_N2 reactions, this opens up access to multiple compounds. Enantiomerically enriched amino acids,[43] epoxides,[35] aziridines[44] or γ-chlorinated *Michael* systems[45] can thus be efficiently constructed in a few steps.

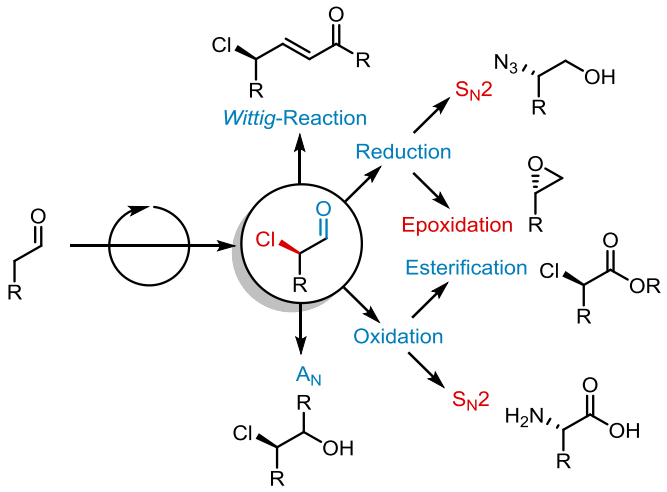

Scheme 13: Possible transformations of α-chloroaldehydes.

By applying these numerous transformations, research groups have further explored the application of chiral α-chloroaldehydes over time, allowing the synthesis of more complex structural elements. The group of *Britton* established the α-chlorine atom as a practical and atom-economical auxiliary in aldol reactions[46] and opened access to heterocycles and their related natural products[47]. *Kokotos* and co-workers developed a one-pot strategy to prepare chiral 2-oxopiperazines, structural motifs in various drugs and natural products.[48]

A more recent example can be found in the *Pihko* group. The synthesis and successful installation of the two stereocenters of (+)–lycoperdic acid was achieved by an organocatalytic *Mukaiyama* aldol and an organocatalytic α-chlorination combined with a *Pinnick* oxidation (Scheme 14).[43]

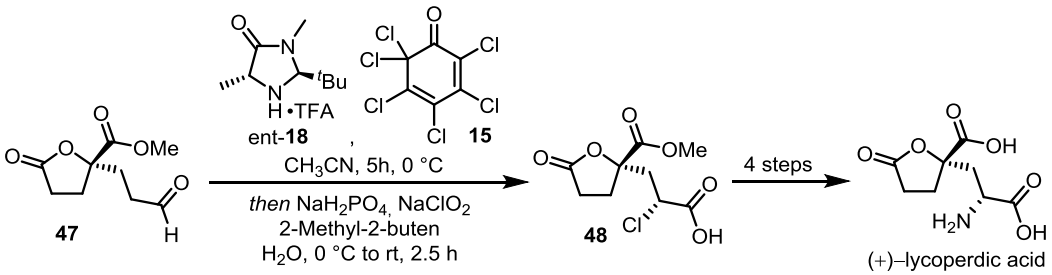

Scheme 14: Part of the synthesis of (+)–lycoperdic acid.

The method developed in the *Christmann* group (chapter 1.1.2; organocatalyst **18** and NCS) found valuable application in the total synthesis of ripostatin B.[49] The aldehyde **49** prepared from geranyl acetate could be efficiently converted to the key intermediate **50** by the previously mentioned method (Scheme 15).

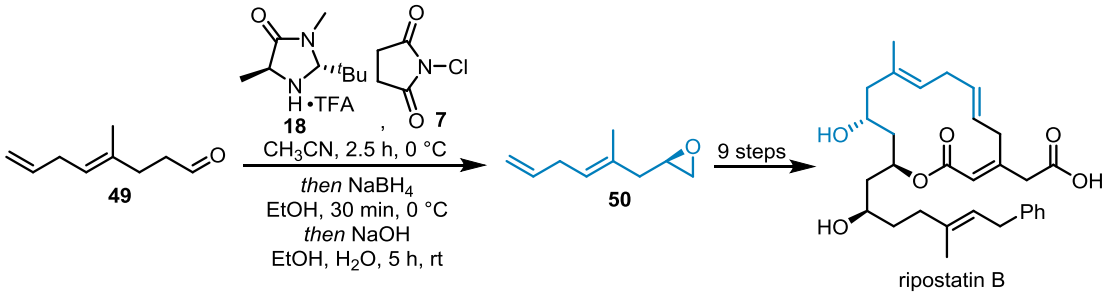

Scheme 15: Part of the total synthesis of ripostatin B.

1.2. Scientific Goal

The combination of imidazolidinone **18** and NCS requires a high catalyst loading to allow for satisfying conversion to the product. Together with the isolation and characterization of the stable aminals, the question arises which role these intermediates play in the catalytic cycle and how to minimize the catalyst loading by better understanding the reaction mechanism. Achieving the isolation and therefor stable nature of these aminals, makes their role in a downstream process as described in the *Curtin-Hammett* scenario[30] seem unrealistic. Instead, it was hypothesized that these aminals are stable parasitic species that accumulate outside the catalytic cycle. Since these aminals remove catalyst from the ongoing reaction and incorporate the product, the first aim was to suppress the formation of these intermediates or to promote their decomposition.

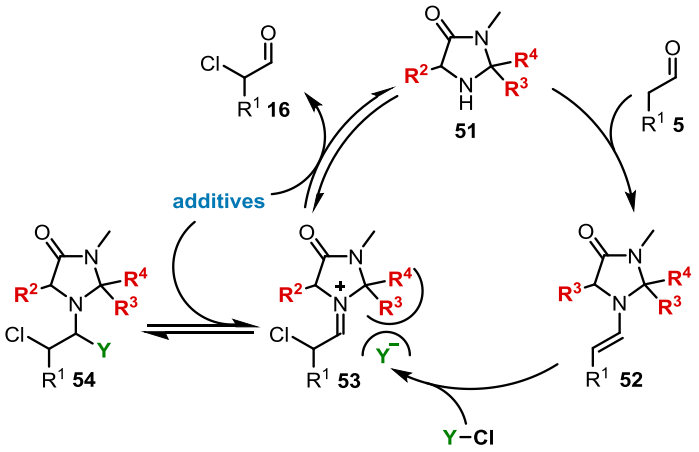

Scheme 16: Simplified catalytic cycle with color-coded modification options.

The catalytic cycle in Scheme 16 reveals various possibilities for modifications of the catalytic system. First, by introducing sterically demanding substituents (**R²**, **R³**, and **R⁴**) on catalyst **51**, the nucleophilic attack of the anion (**Y⁻**) to the chloroiminium ion **53** and hence the formation of the aminal **54** should be prevented. Due to the convenient and flexible synthesis of the imidazolidinone catalysts,[36] the substituent **R²** can be varied by utilizing different amino acids as the starting material. **R³** and **R⁴** can be altered by choosing from a variety of aldehydes (**R³** or **R⁴** = H) or ketones (**R³** and **R⁴** = alkyl, aryl). Another conceptual way to prevent intermediate enrichment is to modify the chlorinating reagent **Y-Cl**. By introducing electron-withdrawing groups, the nucleophilicity of the anion **Y⁻** can be lowered and the leaving group quality increases. Since the chlorinating reagents are used stoichiometrically, a short, inexpensive and scalable synthesis should be envisioned. In addition, the use of additives should be investigated. As mentioned in a previous work on another system,[28] the addition of water and acids can increase the reaction rate. Looking again at the catalytic cycle allows for an explanation of this effect. Water can accelerate the hydrolysis of the chloroiminium ion **53** and thus reduce the

competing formation of the aminal **54**. A *Brønsted* acid could further protonate the anion **Y**$^-$, thus lowering its nucleophilicity. In addition, acidic conditions could facilitate the decomposition of aminal **54** and thus promote the release of the product and catalyst.

The influence of novel imidazolidinone catalysts and additives on the reaction rate should be investigated by time-resolved GC-MS measurements. We intended to observe the accumulation of aminal intermediates when using novel chlorinating reagents by monitoring the course of the reaction with the aid of ^{1}H NMR spectroscopy. A preliminary interpretation of the aminal intermediates should also be made by evaluating the kinetic profile. The decomposition mechanism of the aminals should be elucidated by decomposition and deuterium incorporation experiments. The absolute stereoconfiguration of various intermediates from different catalysts, substrates and chlorinating reagents should be elucidated by single crystal structure analyses. KIE experiments and DFT-based calculation of possible transition states should give a deeper insight into the reaction mechanism. Furthermore, we intended to elucidate the properties of the much more unstable *Blackmond* aminals experimentally by NMR measurements, decomposition and deuterium incorporation experiments, and theoretically by DFT-based calculations.

The evaluation and interpretation of these experiments can subsequently provide further insights into the catalytic mechanism and unambiguous assignment of various aminal species. The results should then be compared to findings from other groups. Of particular interest can be the similarities and variations between different catalyst systems (Ex: *Jørgensen-Hayashi* pyrrolidines and *MacMillan* imidazolidinones).

Based on the better understanding of the stabilizing interactions within aminals, an improved catalytic system should be presented. The applicability should be demonstrated using a wide range of substrates and by synthesizing two chiral regioisomeric bistriazoles. These bistriazoles can be investigated in further studies for their properties as bidentate ligands.

1.3. Publications

1.3.1. Mechanistic Studies on the Organocatalytic α-Chlorination of Aldehydes: The Role and Nature of Off-Cycle Intermediates

Sebastian Ponath, Martina Menger, Lydia Grothues, Manuela Weber, Dieter Lentz, Carsten Strohmann and Mathias Christmann*

Angew. Chem. Int. Ed. **2018**, *57*, 11683–11687.
DOI:10.1002/anie.201806261

Angew. Chem. **2018**, *130*, 11857–11861.
DOI:10.1002/ange.201806261

Abstract:

Herein we report the isolation and characterization of aminal intermediates in the organocatalytic α-chlorination of aldehydes. These species are stable covalent ternary adducts of the substrate, the catalyst and the chlorinating reagent. NMR-assisted kinetic studies and isotopic labeling experiments with the isolated intermediate did not support its involvement in downstream stereoselective processes as proposed by *Blackmond*. By tuning the reactivity of the chlorinating reagent, we were able to suppress the accumulation of rate-limiting off-cycle intermediates. As a result, an efficient and highly enantioselective catalytic system with a broad functional group tolerance was developed.

Author Contribution:

I was first able to develop an optimized catalytic system consisting of an adamantyl-substituted imidazolidinone catalyst and the electron-deficient chlorinating reagent 2-chloro-5-nitroisoindoline-1,3-dione and demonstrate its applicability to a wide range of substrates. Time-dependent ^{1}H NMR measurements to investigate the influence of self-developed chlorinating reagents and the comparison of novel catalysts by time-resolved GC-MS spectroscopy were also carried out by me. Furthermore, the aminal intermediate could be prepared in larger amounts for the first time by an optimized synthesis and workup procedure and subsequent decomposition and deuterium incorporation experiments could be realized. The interpretation of the collected results and the preparation of the manuscript were carried out in collaboration with Prof. Dr. *Mathias Christmann*.

Asymmetric Synthesis

International Edition: DOI: 10.1002/anie.201806261
German Edition: DOI: 10.1002/ange.201806261

Mechanistic Studies on the Organocatalytic α-Chlorination of Aldehydes: The Role and Nature of Off-Cycle Intermediates

*Sebastian Ponath, Martina Menger, Lydia Grothues, Manuela Weber, Dieter Lentz, Carsten Strohmann, and Mathias Christmann**

Abstract: *Herein we report the isolation and characterization of aminal intermediates in the organocatalytic α-chlorination of aldehydes. These species are stable covalent ternary adducts of the substrate, the catalyst and the chlorinating reagent. NMR-assisted kinetic studies and isotopic labeling experiments with the isolated intermediate did not support its involvement in downstream stereoselective processes as proposed by Blackmond. By tuning the reactivity of the chlorinating reagent, we were able to suppress the accumulation of rate-limiting off-cycle intermediates. As a result, an efficient and highly enantioselective catalytic system with a broad functional group tolerance was developed.*

Enantiomerically enriched α-chlorinated aldehydes constitute important chiral building blocks.[1–3] In 2004, MacMillan and Jørgensen reported the first asymmetric organocatalytic α-chlorination of aldehydes via enamine catalysis using imidazolidinones[4] or diarylpyrrolidines[1] as catalysts. Five years later, MacMillan developed a conceptually different SOMO chlorination approach.[2] The group of Britton and others have utilized organocatalytic chlorinations to access chiral heterocycles and natural products.[5]

During a total synthesis campaign, we attempted to convert citronellal as terpene-feedstock into the corresponding 1,2-epoxide by α-chlorination, reduction and base-induced epoxide formation.[6] The application of MacMillan's organo-SOMO methodology[2] led to decomposition which can be attributed to radical intermediates, which react with the electron-rich olefin within the substrate.[7] Expensive chlorinating reagents[4] or catalysts[1] were prohibitive for scale-up. Merging inexpensive *N*-chlorosuccinimide (NCS) **3** and MacMillan's imidazolidinone **2**·TFA resulted in an efficient system that was used in our group[6,8] and by others.[5,9] While yields and enantioselectivities are usually excellent, a relatively high catalyst loading of up to 30 mol% is required to achieve good conversion. Aiming to overcome this obstacle, a detailed investigation of the enamine chlorination was initiated. The mechanism has been discussed controversially by several groups.[10,11] In early studies, the stereochemical outcome was rationalized using a steric shielding model.[12] In contrast, Blackmond, Bures and Armstrong suggested a Curtin–Hammett paradigm where aminals are part of a secondary cycle. In this scenario, the enantioselectivity results from the relative stability and reactivity of intermediates downstream to the primary cycle. They concluded that this mechanistic concept may present a general phenomenon for amine catalysts lacking an acidic directing proton and can be also applied to other enamine-electrophile reactions.[11] In a computational study on related organocatalytic Michael additions of aldehydes and nitroalkenes, Pápai concluded that the reaction rate is dictated by the stability of similar ternary intermediates. The stereoselectivity, however, was rationalized by the attack of the enamine (steric shielding model). The suggestion that the enantioselectivity is determined by the stability of rapidly interconverting intermediates was not supported.[13]

Irrespective whether a downstream cycle is operative, suppressing aminal accumulation was envisioned to be beneficial for the reaction rate. Thus, it was anticipated that tuning the catalyst structure and the counteranion of the Cl^+ source would greatly impact the formation and decomposition of the aminal.

As a model reaction, the chlorination of hydrocinnamaldehyde (**1**) using **2**·TFA as the catalyst and NCS (**3**) as the Cl^+ source was investigated (Figure 1). The substrate was quickly consumed and converted to chloroaldehyde **4**. However, after one hour the catalyst is almost completely caught up in the stable intermediate **5**. It was possible to isolate this intermediate for the first time and unambiguously characterize its structure by *x*-ray crystallography (Figure 2). In order to rule out that the isolated intermediate was a singular example, the reaction was carried out with different (di-)aldehydes and chlorinating reagents. In all cases, stable and isolatable intermediates were observed. The relative configuration corresponds to a formal *syn*-addition of the chlorinating agent to an *E*-enamine double bond.

The optimization began with the synthesis of imidazolidinones **2** and **10**–**13**.[15] Increasing the size of the alkyl groups at C2 and C5 was anticipated to lower the rate of aminal formation and consequently, increase the overall rate of the chlorination reaction. Screening experiments using in situ generated[9] TFA salts of **10**–**13** showed no significant benefit on the reaction rate and the enantioselectivity compared to catalyst **2**. Interestingly, catalyst **13** showed a slightly higher

[*] M. Sc. S. Ponath, M. Sc. M. Menger, M. Sc. L. Grothues, M. Weber, Prof. Dr. D. Lentz, Prof. Dr. M. Christmann
Freie Universität Berlin
Institute of Chemistry and Biochemistry
Takustr. 3, 14195 Berlin (Germany)
E-mail: mathias.christmann@fu-berlin.de
Prof. Dr. C. Strohmann
Technische Universität Dortmund
Faculty of Chemistry and Chemical Biology
Otto-Hahn-Str. 6, 44227 Dortmund (Germany)
Supporting information and the ORCID identification number(s) for the author(s) of this article can be found under: https://doi.org/10.1002/anie.201806261.

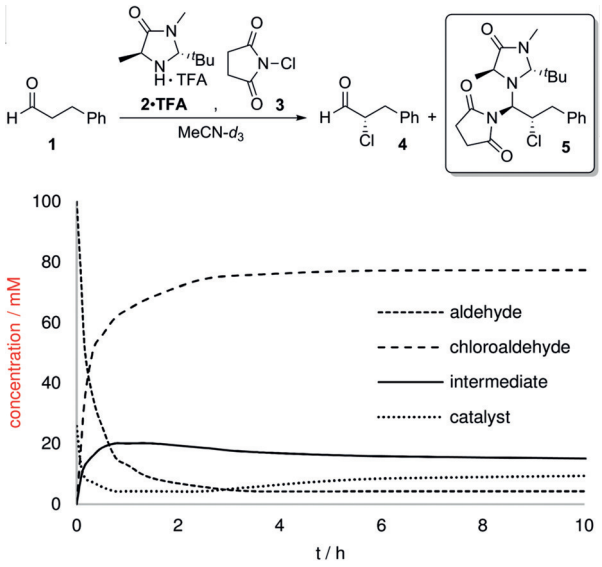

Figure 1. Reaction monitoring by ^{1}H NMR spectroscopy: Hydrocinnamaldehyde **1** (0.1 M) in MeCN-d_3, NCS **3** (1.2 equiv), catalyst **2·TFA** (20 mol%) at 22 °C.

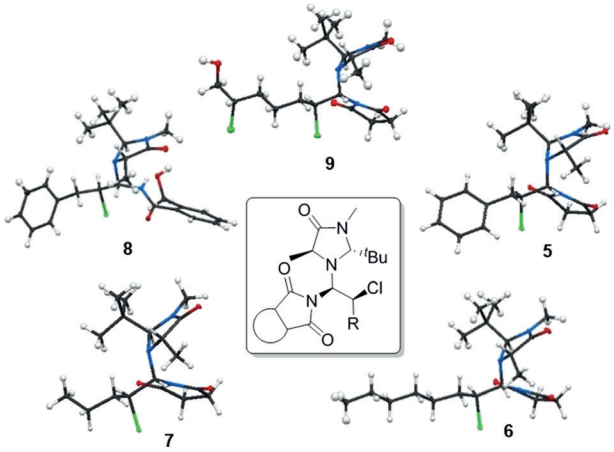

Figure 2. Crystal structures of isolated intermediates: **5** (hydrocinnamaldehyde, NCS, **2**), **6** (octanal, NCS, **2**), **7** (pentanal, NCS, **2**), **8** (hydrocinnamaldehyde, NCP, **2**), phthalimide was cleaved upon workup with $NaBH_4$[14]), **9** (heptanedial, NCS, **2**).

reaction rate, the best enantioselectivity and was convenient to handle as a bench-stable crystalline solid (Figure 3).

We then turned our attention to the modification of the chlorinating reagent. The installation of electron withdrawing groups was anticipated to weaken the N-Cl-bond increasing

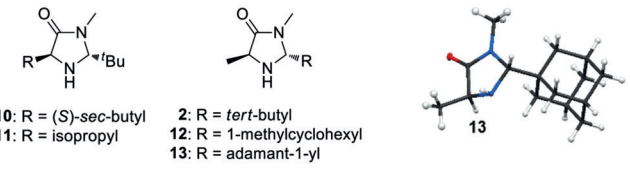

Figure 3. Synthesized imidazolidinone derivatives and crystal structure of catalyst **13**.

the reactivity of the electrophile. More importantly, reducing the nucleophilicity of the nitrogen atom lowers its ability for nucleophilic attack on the iminium ion **14** (k_1). By the same reasoning, the electron-deficient imides would destabilize the intermediates **16** (k_{-1}). Irrespective whether the formation of **16** is inhibited or its decomposition is promoted, both effects would suppress the accumulation of this intermediate as illustrated in Figure 4.

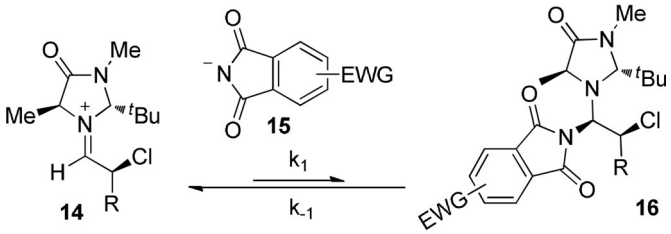

Figure 4. Modified Cl$^+$ source and its effect on enamine formation and decomposition.

To probe that hypothesis, four electronically different chlorinating reagents were synthesized (Figure 5).[16]

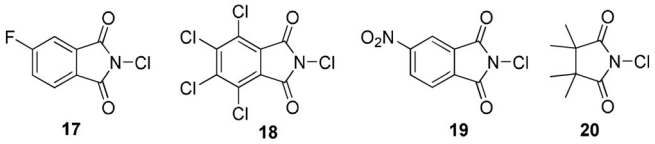

Figure 5. Electronically modified chlorinating reagents.

In analogy to an investigation on the fluorine plus detachment (FPD) of F$^+$-sources,[17] placing electron-withdrawing substituents at the phthalimide was anticipated to increase its reactivity by weakening the N-Cl-bond. In addition, the effect on the accumulation of the aminal intermediates was studied. The tetrachloro- (Cl_4NCP) **18** and the nitrophthalimide (NO_2NCP) derivative **19** afforded the highest reaction rates whereas the fluorophthalimide (FNCP) **17** showed lower reactivity. The tetramethylsuccinimide (Me_4NCS) **20** derivative gave very sluggish conversion. For further investigations, NO_2NCP (**19**) was selected over Cl_4NCP **18** due to higher solubility and its accessibility from inexpensive nitrophthalimide.

In a ^{1}H NMR study, the influence of the Cl$^+$ sources **19** and **20** on aminal formation was studied (Figure 6). As expected, the electron-rich Me_4NCS **20** formed a highly stable aminal intermediate. After 3 h, the aminal concentration reached its maximum with almost all the catalyst and a significant amounts of the product being tied-up in this intermediate. In contrast, using NO_2NCP **19** as the Cl$^+$ source gives rise to an intermediate which reaches its maximum concentration after 30 minutes. Interestingly, the maximum aminal concentration is significantly lower compared to Me_4NCS **20** and quickly drops within the next two hours. As a consequence, the amount of free catalyst is never below 10 mol% and none of the product remains trapped within the aminal intermediate. The rapid decomposition of aminal

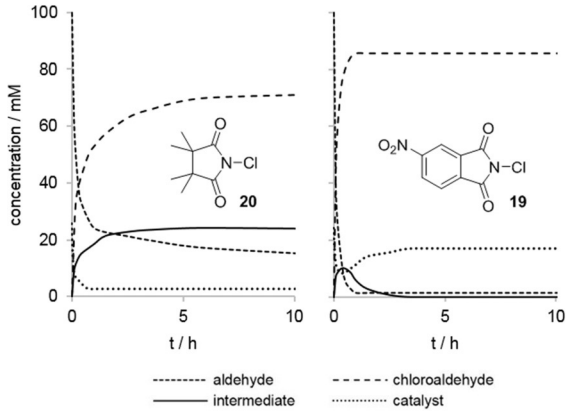

Figure 6. Reaction monitoring by ^{1}H NMR spectroscopy: Hydrocinnamaldehyde **1** (0.1 M) in MeCN-d_3, Me_4NCS (**20**) or NO_2NCP (**19**) (1.2 equiv), **2**·TFA (20 mol%) at 22 °C.

intermediate underscores the excellent leaving group properties of nitrophthalimide anion, which may be attributed to better charge delocalization.

Finally, the effects of acids as additives was investigated. It was found that a 1:1:2 ratio of catalyst:TFA:AcOH gave optimal results, whereas binary acid-catalyst mixtures were inferior. It is conceivable that the acetate ion plays a role beyond a proton source such as forming short-lived adducts with iminium intermediates.

With the ability to follow the concentration of the relevant intermediates **A**, **B** and **C** over time and the isolated aminal in hand, we felt we were in a position to positively contribute to the discussion on the existing conflicting mechanistic proposals (Figure 8). As proposed by Jørgensen[10] and MacMillan,[4] the classical mechanism for chlorination of aldehydes **A** involves condensation with the catalyst **2**·TFA to form enamine **21** as the reactive species. Attack on a Cl^+ source (Y-Cl) from the face opposite to the proximal bulky substituent on *N*-heterocyclic catalyst affords an α-chloroiminium ion **I** in the stereodetermining step. Hydrolysis releases the catalyst **2** alongside formation of α-chloroaldehyde **C**. Jørgensen also noted that the addition of the succinimide anion to the iminium ion intermediate can give rise to aminal intermediates[10] (Figure 7, black).

Upon reinvestigation of the chlorination reaction using the Jørgensen–Hayashi catalyst, Blackmond proposed that the aminal **B** is not only an off-cycle intermediate but instead involved in a secondary stereodetermining catalytic cycle.[18] It was suggested that E2-elimination of succinimide from aminal *syn*-**B** affords *Z*-chloroenamine **23**. Diastereoselective protonation of this intermediate generates an α-chloroiminium ion **I** (or its *Z*-diastereomer)[11] (Figure 7 gray). In their scenario, equilibration of diastereomeric iminium ions **I** prior to hydrolysis is responsible for the stereochemical outcome.

Following the concentrations of **A**, **B** and **C** should allow one to distinguish whether **B** is an off-cycle intermediate or a mandatory intermediate in the pathway toward the product **C**. In the classical mechanism, the aldehyde **A** forms the chloroiminium ion **I,** which upon hydrolysis releases the product **C**. In a non-productive pathway, the chloroiminium

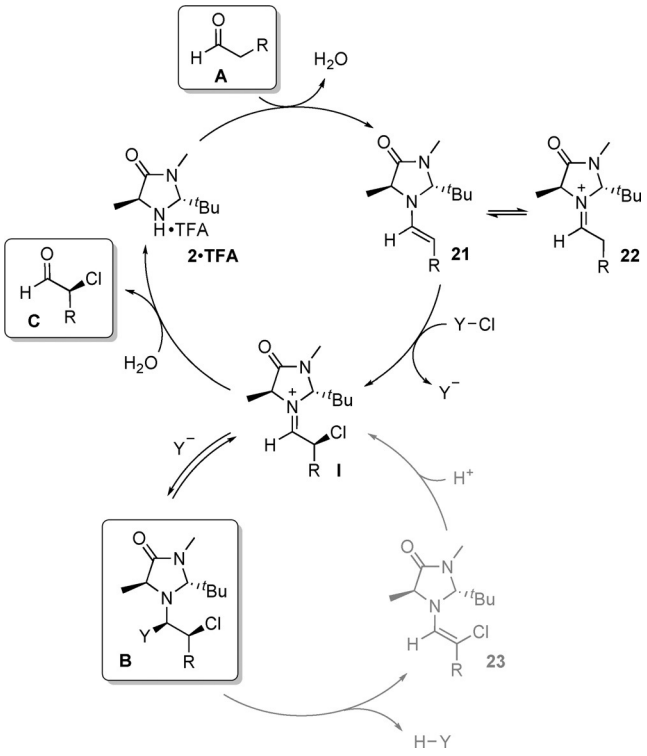

Figure 7. The extended catalytic cycle (black) and downstream pathway in analogy to Blackmond[11] (gray).

ion **I** is in an equilibrium with an off-cycle intermediate **B**. As we have shown above, the stability of **B** strongly depends on the character of the counteranion of the Cl^+ source. In Blackmond's two-cycle mechanism, the chloroiminium ion **I** forms intermediate **B**, which upon elimination of succinimide and protonation forms chloroiminium ion **I** or a diastereomer. Eventually, hydrolysis of **I** affords the product **C**. Assuming that decomposition of **B** is rate-liming, the concentration of **B** would be expected to rise and reach a maximum concentration (c_{max}) before decomposing to the product **C**. Under this premise, the product formation **C** should be delayed and its rate should be maximal at c_{max}(**B**), that is, **C** should have an inflection point at c_{max}(**B**) (see Figure 8b for an idealized kinetic profile). In our observation (Figure 8a), no delay in product formation was observed, that is, the rate was the highest in the beginning and dropped continuously over time. This behavior was observed irrespective whether the inter-

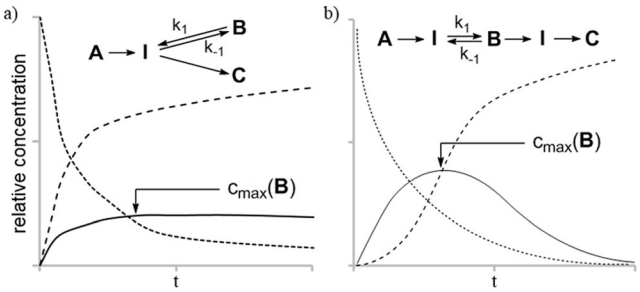

Figure 8. a and b) Experimental observation (a) and idealized kinetic profile with mandatory formation of the intermediate (b); **A**: Substrate, **I**: Iminiumion, **B**: Aminal, **C**: α-Chloroaldehyde.

mediate accumulated (Me_4NCS **20**) or quickly decomposed (NO_2NCP **19**) (Figure 6).

In order to distinguish between the two mechanisms, we subjected the isolated intermediate to the standard reaction conditions using deuterated solvents and acids. If the reaction proceeds through a chloroenamine, one would expect deuteration of the α-position of the aldehyde. Under the standard conditions, the decomposition of the aminal is very slow (see Figure 1). Thus, we did not observe deuterium incorporation. Under more forcing conditions (Figure 9), the aminal **5** was

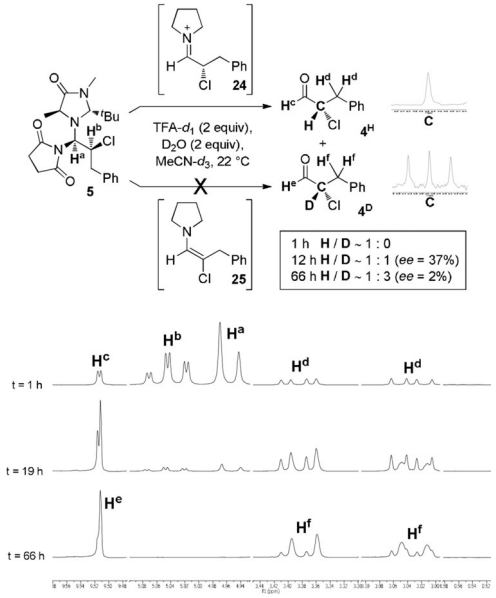

Figure 9. Decomposition process including downstream racemization investigated by ^1H and ^{13}C NMR monitoring.

partially decomposed to the α-chloroaldehyde $\mathbf{4^H}$ after 1 h. Interestingly, no deuteration was observed as seen by ^1H NMR spectroscopy. After 19 h, most of the intermediate was decomposed. At this time, partial deuteration of the α-position was identified by the coupling pattern of the diastereotopic beta protons and the multiplicity of the α-carbon ($\mathbf{4^D}$). This behavior can be explained by a non-selective racemization pathway as evidenced also by the drop of the enantiomeric excess. After 66 h, the chloroaldehyde **4** was nearly racemic. Our experimental results support the classical mechanistic proposal where the enamine chlorination constitutes the stereo-determining step (steric shielding model). We could also show that accumulation of the off-cycle aminal can become rate-limiting and has a negative impact on the reaction rate by removing active catalyst from the catalytic cycle. By tuning the chlorinating reagent with electron withdrawing substituents, we could shift the aminal/iminium equilibrium to the iminium ion (see Figure 4) and increase the overall reaction rate. With an improved catalytic system in hand, we wanted to explore its utility in the chlorination of a diverse set of different aldehydes. Table 1 shows that using 5 mol% of catalyst **13** and 1.2 equiv of NO_2NCP (**19**) were sufficient to achieve excellent enantioselectivities and good to excellent yields.

Table 1: Substrate scope.

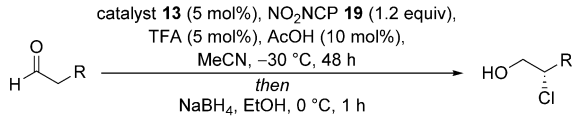

Entry	Product	Yield [%][a]	*ee* [%]
1	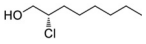	78	97
2[b]	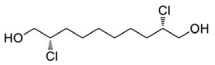	63	>99
3	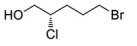	77	98
4	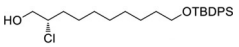	74	96
5	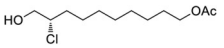	87	96
6	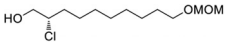	87	96
7	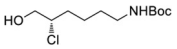	57	96
8	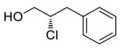	75	98
9	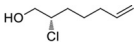	79	97
10[c]	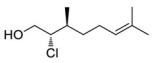	73	97
11	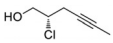	74	98

[a] Isolated yields. [b] 10 mol% of **2**·TFA, 20 mol% of AcOH, 2.4 equiv of NO_2NCP; dr = 95:5. [c] 97% *ee* for the starting material (*S*)-citronellal; Upscaling 5.00 g, 32.4 mmol (*S*)-citronellal, Rondomatic 400®, cryostat; dr = 97:3.

For octanal (entry 1), the reaction proceeds in 78% yield and 97% *ee*. As a result of a Horeau- amplification,[19] decan-1,10-dial is an excellent substrate for bidirectional synthesis[20] and affords the C_2-symmetric dichlorinated alcohol in 63% yield and >99% *ee* along with minor amounts of the *meso* diastereomer (entry 2). Bromides did not interfere with the chlorination as shown for 5-bromopentanal to give the β-chloroalcohol in 77% yield (entry 3). A variety of acid-stable protecting groups such as TBDPS, Ac, and MOM (entries 4–6) were tolerated. In case of the Boc-protected primary amine the yield was slightly lower. Aldehydes bearing aryl-, alkenyl and alkynyl side chains (entries 8–11) gave excellent selectivities (97–98% *ee*) and good yields (73–79%). In case of (*S*)-citronellal (entry 10), we initially encountered a significant drop in the yield. Analysis of side products revealed that the trisubstituted alkene readily reacts with the more electrophilic Cl^+ source NO_2NCP (**19**) compared to NCS (**3**).[21] As a major side product, we were able to isolate the allylic chloride of α-chlorinated citronellal. As only small amounts of (more reactive) enamine compared to the alkene are present in the reaction mixture, we aimed to suppress undesired allylic chlorination by slow addition of the chlorinating agent. It was possible to increase the yield from 29% to 57% by adding NO_2NCP (**19**) over 48 h by hand in small portions. For obvious reasons, an automatic solution for adding the reagent was sought. Using Rondomatic 400®, an automatic fish-feeding device in combination with cryostatic cooling allowed us to achieve an increased yield of 73% and

97% *ee*. Gratifyingly, this reaction could be conveniently carried out on a 5 g-scale (entry 10).

In summary, we have carried out a detailed investigation of the organocatalytic α-chlorination of aldehydes. It was possible to isolate and characterize the off-cycle intermediates for the first time, elucidate their role in the catalytic cycle and to suppress their accumulation. Remarkably, the catalyst loading was reduced from 20–30 mol% [6,8] to 5 mol%. The new catalytic system was applied to a variety of substrates where it demonstrated good functional group tolerance with excellent enantio- and diastereoselectivity. For electron-rich olefins, allylic chlorination could be supressed with a modified reaction procedure capitalizing on the higher reactivity of enamines.

Conflict of interest

The authors declare no conflict of interest.

Keywords: asymmetric synthesis · chlorination · enamine catalysis · organocatalysis · reaction mechanisms

How to cite: *Angew. Chem. Int. Ed.* **2018**, *57*, 11683–11687
Angew. Chem. **2018**, *130*, 11857–11861

[1] N. Halland, A. Braunton, S. Bachmann, M. Marigo, K. A. Jørgensen, *J. Am. Chem. Soc.* **2004**, *126*, 4790.
[2] M. Amatore, T. D. Beeson, S. P. Brown, D. W. C. MacMillan, *Angew. Chem. Int. Ed.* **2009**, *48*, 5121; *Angew. Chem.* **2009**, *121*, 5223.
[3] N. Kaplaneris, C. Spyropoulos, M. G. Kokotou, C. G. Kokotos, *Org. Lett.* **2016**, *18*, 5800.
[4] M. P. Brochu, S. P. Brown, D. W. C. MacMillan, *J. Am. Chem. Soc.* **2004**, *126*, 4108.
[5] a) V. Dhand, J. A. Draper, J. Moore, R. Britton, *Org. Lett.* **2013**, *15*, 1914; b) B. Kang, S. Chang, S. Decker, R. Britton, *Org. Lett.* **2010**, *12*, 1716; c) S. Chang, S. Hur, R. Britton, *Chem. Eur. J.* **2015**, *21*, 16646; d) M. Bergeron-Brlek, T. Teoh, R. Britton, *Org. Lett.* **2013**, *15*, 3554; e) J. A. Draper, R. Britton, *Org. Lett.* **2010**, *12*, 4034; f) M. Bergeron-Brlek, M. Meanwell, R. Britton, *Nat. Commun.* **2015**, *6*, 6903; g) S. D. Halperin, R. Britton, *Org. Biomol. Chem.* **2013**, *11*, 1701.
[6] P. Winter, J. Schwatschek, M. Willot, L. Radtke, T. Olbrisch, A. Schäfer, M. Christmann, *Chem. Commun.* **2011**, *47*, 12200.
[7] T. D. Beeson, A. Mastracchio, J.-B. Hong, K. Ashton, D. W. C. MacMillan, *Science* **2007**, *316*, 582.
[8] a) P. Winter, W. Hiller, M. Christmann, *Angew. Chem. Int. Ed.* **2012**, *51*, 3396; *Angew. Chem.* **2012**, *124*, 3452; b) J. Swatschek, L. Grothues, J. O. Bauer, C. Strohmann, M. Christmann, *J. Org. Chem.* **2014**, *79*, 976.
[9] M. Johannes, M. Brimble, *J. Org. Chem.* **2013**, *78*, 12809.
[10] N. Halland, M. A. Lie, A. Kjærsgaard, M. Marigo, B. Schiøtt, K. A. Jørgensen, *Chem. Eur. J.* **2005**, *11*, 7083.
[11] a) J. Burés, A. Armstrong, D. G. Blackmond, *J. Am. Chem. Soc.* **2012**, *134*, 6741; b) J. Burés, A. Armstrong, D. G. Blackmond, *Chem. Sci.* **2012**, *3*, 1273; c) J. Burés, A. Armstrong, D. G. Blackmond, *Acc. Chem. Res.* **2016**, *49*, 214.
[12] S. Bertelsen, K. A. Jørgensen, *Chem. Soc. Rev.* **2009**, *38*, 2178.
[13] T. Földes, Á. Madarász, Á. Révész, Z. Dobi, S. Varga, A. Hamza, P. R. Nagy, P. Pihko, I. Pápai, *J. Am. Chem. Soc.* **2017**, *139*, 17052.
[14] Z. I. Horii, C. Iwata, Y. Tamura, *J. Org. Chem.* **1961**, *26*, 2273.
[15] T. H. Graham, B. D. Horning, D. W. C. MacMillan, *Org. Synth.* **2011**, *88*, 42.
[16] a) A. Shiri, A. Khoramabadi-zad, *Synthesis* **2009**, 2797; b) D. C. Powers, D. Y. Xiao, M. A. L. Geibel, T. Ritter, *J. Am. Chem. Soc.* **2010**, *132*, 14530.
[17] X.-S. Xue, Y. Wang, M. Li, J.-P. Cheng, *J. Org. Chem.* **2016**, *81*, 4280.
[18] Interestingly, Blackmond et al. observed a strong correlation between the d.r. of the aminal and the e.r. of the chlorinated product (Ref. [11], Table 1). They imply from these data that aminal intermediates are "directly involved in catalyst turnover, rather than existing as parasitic off-cycle reservoirs." We would argue that their observed correlation is in no conflict with an off-cycle intermediate as the product as well the aminal emerge from the same iminium ion.
[19] J. P. Vigneron, M. Dhaenens, A. Horeau, *Tetrahedron* **1973**, *29*, 1055.
[20] a) R. M. de Figueiredo, R. Berner, J. Julis, T. Liu, D. Türp, M. Christmann, *J. Org. Chem.* **2007**, *72*, 640; b) R. M. de Figueiredo, R. Fröhlich, M. Christmann, *Angew. Chem. Int. Ed.* **2008**, *47*, 1450; *Angew. Chem.* **2008**, *120*, 1472.
[21] L. S. Pimenta, E. V. Gusevskaya, E. E. Alberto, *Adv. Synth. Catal.* **2017**, *359*, 2297.

Manuscript received: May 31, 2018
Accepted manuscript online: July 12, 2018
Version of record online: August 3, 2018

1.3.2. On Stereocontrol in Organocatalytic α-Chlorinations of Aldehydes

Sebastian Ponath, Chetan Joshi, Amy T. Merrill, Volker Schmidts, Kim Greis, Maike Lettow, Manuela Weber, Simon Steinhauer, Kevin Pagel, Christina Thiele, Dean J. Tantillo, Mathew J. Vetticatt, Mathias Christmann

ChemRxiv (Preprint) https://doi.org/10.26434/chemrxiv.14229875.v1.

Submitted to *J. Am. Chem. Soc.* (March 18, 2021).

Abstract:

A comprehensive analysis of the organocatalytic α-chlorination of aldehydes with *N*-chloroimides and different catalysts is presented. For this reaction, alternate mechanisms were proposed that differ in the role of resting state intermediates and the rationalization of the observed enantioselectivity. This manuscript aims at resolving these fundamental questions on the basis of rigorous structural characterization of intermediates (configuration and conformation), NMR studies, ion mobility-mass spectrometry, concentration profiles, isotope studies, and DFT calculations.

Author Contribution:

In this publication, the organic synthetic work was performed by me. This includes the synthesis, isolation, and full characterization of the aminals derived from the 1st, 2nd and 3rd generation *MacMillan* catalysts and the *Jørgensen* catalyst. The improved synthesis, characterization and follow-up reactions with the highly unstable *Blackmond* aminals were developed and performed by me. In addition, all synthetic preparations for the NMR and decomposition experiments were prepared, partially performed and evaluated by me. Deuterium incorporation studies, isotope competition experiments, and the KIE experiments planned in consultation with the *Vetticatt* group were also performed by me. The interpretation of the results and the preparation of the manuscript were performed in collaboration with Prof. Dr. *Mathias Christmann* and the other authors.

On Stereocontrol in Organocatalytic α-Chlorinations of Aldehydes

Sebastian Ponath[§‡], Chetan Joshi[‡‡], Amy T. Merrill[†], Volker Schmidts[×], Kim Greis[§#], Maike Lettow[§#], Manuela Weber[§], Simon Steinhauer[§], Kevin Pagel[§#*], Christina Thiele[×*], Dean J. Tantillo[†*], Mathew J. Vetticatt[‡*], Mathias Christmann[§*]

[§]Institute of Chemistry and Biochemistry, Freie Universität Berlin, 14195 Berlin, Germany
[‡]Department of Chemistry, Binghamton University, Binghamton, New York 13902, United States
[†]Department of Chemistry, University of California – Davis, Davis, California 95616, United States
[×]Clemens Schöpf Institute of Organic Chemistry and Biochemistry, Technische Universität Darmstadt, 64287 Darmstadt, Germany
[#]Fritz Haber Institute of the Max Planck Society, 14195 Berlin, Germany

KEYWORDS: Organocatalysis, Chlorination, Reaction Mechanism, Computational Chemistry, Kinetic Isotope Effect

ABSTRACT: A comprehensive analysis of the organocatalytic α-chlorination of aldehydes with *N*-chloroimides and different catalysts is presented. For this reaction, alternate mechanisms were proposed that differ in the role of resting state intermediates and the rationalization of the observed enantioselectivity. This manuscript aims at resolving these fundamental questions on the basis of rigorous structural characterization of intermediates (configuration and conformation), NMR studies, ion mobility-mass spectrometry, concentration profiles, isotope studies, and DFT calculations.

♦ INTRODUCTION

The development of novel concepts to exert stereochemical control over chemical reactions constitutes a fundamental challenge.[1] Toward this goal, catalytic strategies that avoid expensive catalysts, toxic reagents and byproducts are considered among the most desirable. In order to improve on the selectivity and efficiency of a given transformation,[2] it is important to align experimental results with consistent models.

Enantioselective organocatalytic reactions[3] via enamines commence with a condensation of a carbonyl compound and a chiral amine catalyst. In the selectivity-determining step (Scheme 1), the electrophile reacts preferentially with either of the two diastereotopic faces of the most reactive enamine conformer. The relative rates of formation (k_{major}/k_{minor}) of the diastereomeric iminium intermediates **I** (d.r.) and the enantiomeric ratio (e.r.) of the hydrolysis products **P** are usually rationalized by the relative energies of the respective transition states of the enamine-electrophile reaction. In a study on enantioselective fluorinations published in 2005, Jorgensen[4] showed for the first time that processes downstream to the formations of the stereogenic center may result in a product e.r. that is different from the d.r. of the two iminium intermediates (d.r. ≠ e.r.).

In 2012, Blackmond, Bures, and Armstrong[5,6] investigated two reactions catalyzed by Jørgensen-Hayashi diarylprolinol silyl ethers:[7,8] the addition of aldehydes to nitroolefins, and the α-chlorination of isovaleraldehyde. They arrived at the conclusion that "selectivity in these examples is rationalized not by comparison of transition states for formation of the stereogenic center but by the relative stability and reactivity of equilibrated downstream intermediates and in the separate branches of a competitive reaction network".

Scheme 1. Stereopredictive Models

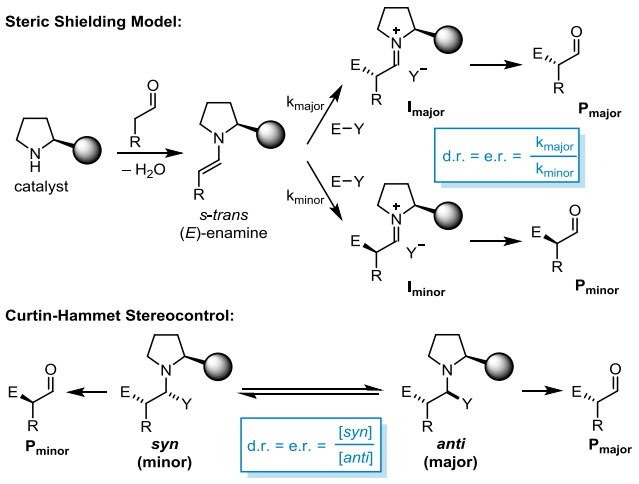

It was further suggested that their concept coined "Curtin-Hammett stereocontrol" may "represent a general phenomenon for amine catalysts lacking an acidic directing proton". This projection is no exaggeration because if true, the design of enantioselective catalysts in these cases

should be augmenting the relative thermodynamic stability of intermediates rather than relative energies of transition states. In the following study, we will validate both models[9] against new experimental data for the α-chlorination of aldehydes with different *N*-chloroimides, catalysts and substrates. To facilitate the reading, we will commence by framing the mechanistic discussion in the historical context.

♦ BACKGROUND

Asymmetric Aldehyde Chlorinations

Over the last years, chiral α-haloaldehydes[10,11] have emerged as important building blocks. The first direct asymmetric α-chlorinations of aldehydes[12] were independently developed by two groups (Scheme 2). In the chlorination of octanal (**1**), MacMillan[13] and co-workers employed 1.2 equiv of Lectka's chloroketone (**2**)[14] at –30 °C in acetone in the presence of 5 mol% of imidazolidinone **3a** (X=Y=Me) to give chloroaldehyde (*S*)-**4** in good yield and high enantiomeric excess.

Scheme 2. α-Chlorination of Aldehydes (2004-2009)

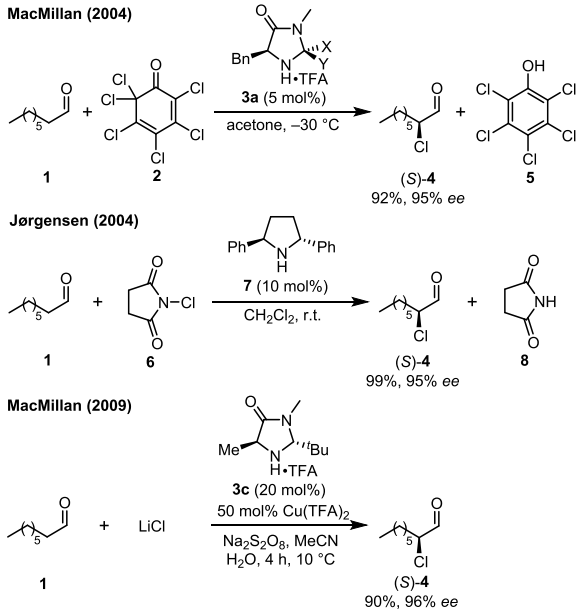

They noted that under these conditions, "product epimerization, formation of 2,2-dichlorooctanal, or octanal aldol dimerization were comprehensively suppressed". As the byproduct, pentachlorophenol (**5**), is a probable human carcinogen, alternative chlorinating agents were considered. Using *N*-chlorosuccinimide (**6**, NCS) as an alternative Cl^+ source at 4 °C, MacMillan observed almost racemic product. By monitoring the chlorination at 23 °C, Brown (MacMillan group) noticed an erosion of the product ee over time.[15] Taken together with the concomitant formation of 2,2-dichlorooctanal, this behavior was ascribed to the reversible formation of a chloroenamine intermediate subsequent to the formation of the stereogenic center. Racemization of the chiral chloroaldehyde can be effected by catalysts **3a** and **3b** (X=^{t}Bu, Y=H) in or without the presence of a chlorinating reagent.[16] It is suppressed effectively at –30 °C. Interestingly, Jørgensen et al. reported that C_2-symmetric (*R*,*R*)-2,5-diphenylpyrrolidine (**7**) (10 mol%) catalyzed the chlorination of aldehydes with NCS (1.3 equiv) at room temperature without noticeable racemization.[17] In order to inhibit chloroenamine formation at room temperature, MacMillan designed imidazolidinone catalyst **3c** with loosely C_2-like symmetry.[18] This catalyst and Lectka's chloroketone constitute a highly effective combination for chlorinations at elevated temperatures[15] and subsequent follow-up transformations.[19] In 2009, MacMillan demonstrated that **3c** can be used for the SOMO chlorination of aldehydes.[18] We started our own investigations in 2011 by initially using the MacMillan's SOMO protocol[20] but later moved to the combination of **3c** (20 mol%) and NCS in acetonitrile[21] due to side reactions[22] of radical intermediates in the SOMO chlorination of terpene aldehydes.

Chlorinations with Jørgensen-Hayashi-type Catalysts

The 2-substituted pyrrolidine scaffold **9** was first employed in enamine chlorinations of isovaleraldehyde **10** by Jørgensen et al. in 2004 (Scheme 3). Using **9a** (20 mol%) in 1,2-dichloroethane afforded (*S*)-2-chloroisovaler-aldehyde **12** with moderate enantioselectivity. (e.r. 82:18).[17] The corresponding diarylprolinol silyl ethers **9b** and **9c** (R=H, X=OTMS) had not been disclosed by that time.[8] In 2012, Blackmond et al. studied the α-chlorination of isovaleraldehyde with NCS in $CDCl_3$ using these two catalysts achieving enantioselectivities in the same ballpark.[6] With the aid of reaction calorimetry, they showed that "a rapid initial rate corresponding to ca. one turnover of the catalyst was followed by a slower zero-order regime, demonstrating that the reaction does not depend on the concentration of either of the two reactants." The observation of two sets of NMR signals at –54 °C featuring EXSY cross peaks led the authors to suggest that those correspond to two interconverting diastereomeric aminals **11** as resting states of the catalytic system. The two species were proposed to be constitutionally "analogous to a species reported by Jørgensen using pyrrolidine" and diastereomeric at C1. Surprisingly, no attempt was reported to directly determine the structure, yet the major species was assigned to be the *anti*-configurated. An inductive reasoning for the structural assignment implies an enamine-NCS reaction occurring with "near perfect facial selectivity" which was derived from the observation of "only two out of four possible diastereomers". In the mechanistic proposal (Scheme 3), stereoselective enamine (**13**)/NCS reaction followed by reversible addition of succinimide to the iminium carbon of the chloroiminium ion affords two aminals **11**, "which equilibrate between one of the two possible *syn* and one of the two possible *anti* diastereomers".[23] Two separate stereospecific E2 eliminations proceeding at identical rates ($k_{syn} \approx k_{anti}$) would provide an *E*-chloroenamine (E-**15**) from the major *anti*-aminal and a *Z*-chloroenamine (Z-**15**) from the minor *syn*-aminal. A stereospecific protonation/hydrolysis which, was not further detailed, would lead to the chloroaldehydes in an enantiomeric ratio identical to the ratio of the observed aminals.[24] The apparent correlation between the ratio of two rapidly equilibrating species (cause) and

the ratio of two product enantiomers (effect) led the authors to formalize a new concept for stereochemical control in organocatalysis entitled the "Curtin-Hammett paradigm".

Scheme 3. On-Cycle Mechanism for Chlorinations with Monosubstituted Pyrrolidine Catalysts

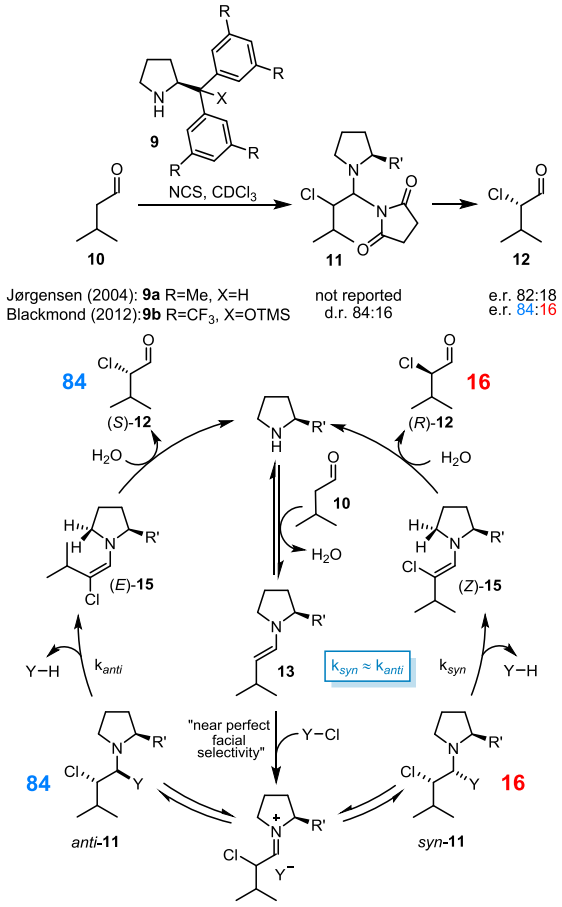

♦ RESULTS AND DISCUSSION

Chlorinations with Imidazolidinone Catalysts

In 2018, our group reported an investigation of the α-chlorination of aldehyde **16** using catalyst **3c**·TFA (20 mol%) with different *N*-chloroimides in acetonitrile.[25] The aim was to improve on the catalytic efficiency and to decrease the catalyst loading. We quickly realized that the main obstacle for good turnover is catalyst accumulation within stable aminals similar to those previously proposed. Gratifyingly, we were able to isolate aminal intermediates **18** in pure form and to obtain several X-ray crystal structures for the first time (Scheme 4). Each of the isolated species was obtained as a single diastereomer with *syn*-configuration. With *N*-chlorophthalimide (NCP) as the chlorinating reagent, opening of the phthalimide moiety was observed to give **18a** upon reductive quenching/work-up. Merging the absolute configuration of the chloroaldehyde product **19** and the aminal **18**, we concluded that both compounds would be derived from iminium ion precursors possessing identical configurations at the chlorine substituted stereogenic center (C2).

Scheme 4. Isolation of Aminal Intermediates Using MacMillan-Type Catalyst 3c

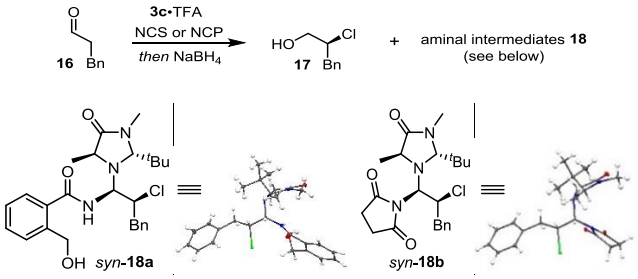

In our mechanistic proposal (Scheme 5), high facial selectivity for the depicted chloroiminium ion **19** was rationalized by the standard steric shielding model. In contrast to the previously discussed on-cycle model, we placed the aminal species *syn*-**18** and *anti*-**18** off the catalytic cycle. As a major consequence of the model, neither kinetic nor thermodynamic ratios of aminal C1 epimers affect the enantiomeric ratio of the chloroaldehyde. Yet, the accumulation of the catalysts within stable aminals is the major negative influence for diminished catalytic efficiency.

Scheme 5. Chlorination Using MacMillan-Type Catalyst 3c with Off-Cycle Aminal Intermediates

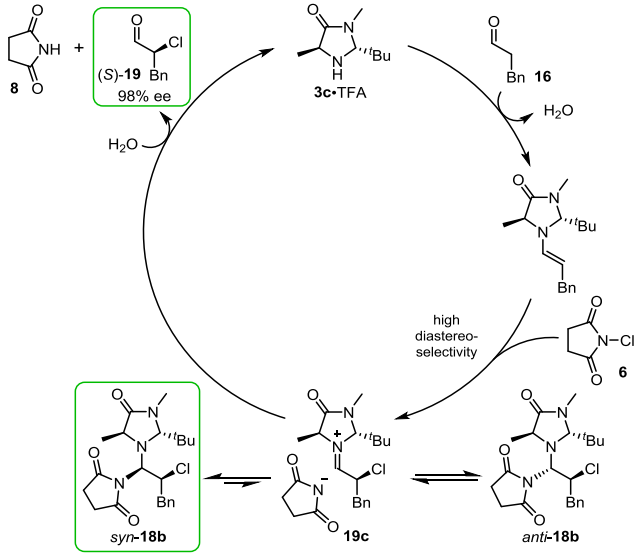

The problem was overcome by using *N*-chloro-4-nitrophthalimide as NCS surrogate. The on-cycle model proposes the stereochemical outcome to be thermodynamically controlled, i.e. the formation of the major enantiomer must proceed through the most stable aminal. In that sense, the on-cycle mechanism predicts a formal inversion of the initially generated stereogenic center for the (2*S*)-*syn*-aminal to give the (2*R*)-chloroaldehyde product under the premise that chlorination and protonation occur with the same sense of stereocontrol imposed by the catalyst. Importantly, due to the C_2-like symmetry of the catalyst, a 180° rotation along the enamine and the chloroenamine C-*N* bond axis does not change the facial shielding significantly. Summarizing the stereochemical considerations, only the off-cycle mechanism aligns the configuration of

the most stable aminal with the observed (*S*)-configuration of the product, whereas the on-cycle model predicts the (*R*)-enantiomer as the major product.

In case of the first and second generation MacMillan catalysts **3a** and **3b**, similar aminals were proposed.[26,27,28] The *syn*/*anti* ratio of respective aminals had been correlated to the enantiomeric ratio, and the *anti*-diastereomer was suggested to lead to the major product enantiomer. It is somewhat puzzling that to the best of our knowledge not a single aminal structure was established directly either by NMR or by X-ray crystallography. Repeating the experiments described for chlorination of isovaleraldehyde using catalysts **3a** and **3b** and NCS as the chlorinating reagent, we have been able to isolate most of the respective stable aminals which are separable chromatographically with no subsequent equilibration being observed. For each of those aminals, single crystals were grown and analyzed.

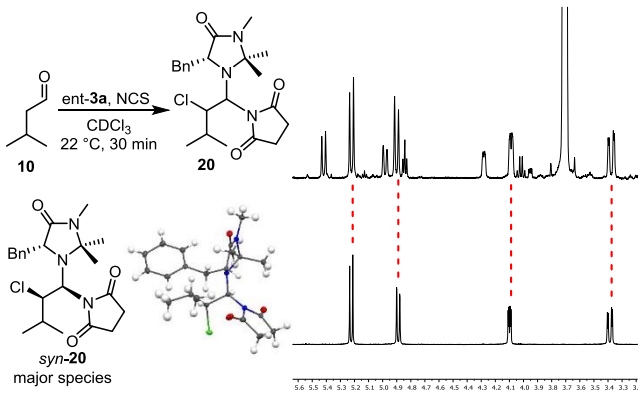

Figure 1. ^{1}H-NMR spectrum of the reaction (in accordance with the literature[28]) (top). Crystal structure and ^{1}H-NMR spectrum of the isolated aminal bearing MacMillan-catalyst **3a** (bottom).

The obtained crystal structures reveal two surprising findings: first, the major aminal diastereomers *syn*-**20** and *syn*-**21** for the imidazolidinone catalysts **3a** and **3b** possess the *syn*- and not *anti*-configuration; second, in case of catalyst **3b**, we also isolated a third aminal, clearly visible in the crude NMR data that was previously overlooked (see SI for details). This third aminal also bears *syn*-configuration and is present in higher concentrations than the minor aminal in Blackmond´s assignment (Figures 1 and 2).

The conformations of the diastereomeric aminals are reflective of steric and stereoelectronic interactions between the catalyst and the chloroaminal substructures and within the chloroaminal substructure itself. In all crystal structures, both *syn*- and *anti*-aminals adopt an antiperiplanar orientation of C1-H and C2-H (Scheme 6). Such an arrangement constitutes the only staggered conformation along the C1-C2 axis where each non-hydrogen substituent (N, Cl, R) possesses only one synclinal interaction with another non-hydrogen substituent. A similar conformational preference in solution is indicated by the observation of large $^3J_{C1\text{-}H,C2\text{-}H}$ coupling constants (10-11 Hz).

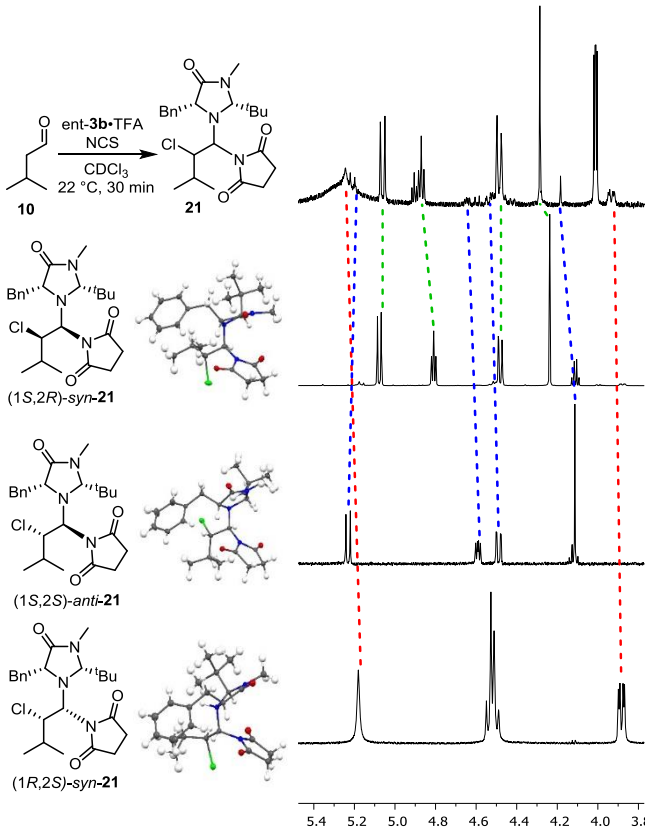

Figure 2. ^{1}H-NMR spectrum of the reaction (in accordance with the literature[27,28]) (top). Crystal structures and ^{1}H-NMR spectra of different isolated aminal diastereoisomers bearing MacMillan-catalyst **3b** (bottom).

The stability of the aminals can be rationalized by a synergistic interplay of anomeric stabilization and gauche effects. In the *syn*-diastereomer, the two best σ→σ* acceptors (C-Cl, C-*N*-imide) are in a gauche orientation whereas in the *anti*-diastereomer, the succinimide and the chlorine substituent are antiperiplanar. As previously noted by others,[29] the catalyst's aminal nitrogen lone pair prefers to be *cis* to the bulkiest substituent (to minimize strain) and *antiperiplanar* to a C-C or a C-X (X = O, N, S) bond (allowing for *n*→σ* stabilization).

Curtin-Hammett conditions refer to situations where each of two rapidly interconverting *conformational isomers* reacts irreversibly to a different product. The Curtin-Hammett principle[30] issues a warning not to relate a conformer ratio directly to the product ratio if the rate of product formation is small relative to the rate of interconversion. Diastereomers must not be treated as individual reactive conformers but as an ensemble of conformations. Diastereomer stability is dominated by the lowest energy conformers but not necessarily by reactive conformations relevant to an ensuing transformation (Scheme 6) let alone the standard free energies ($\Delta\Delta G^{\ddagger}$) of the respective transition states. The "Curtin-Hammett paradigm for stereocontrol" suggests a quantitative relationship between the ratio of two equilibrating diastereomeric aminals and the ratio of their respective E2 elimination products. However, the rel-

ative stability of aminal conformations with C2-H and succinimide in an antiperiplanar orientation (the basis for the stereospecificity of the E2 elimination) is not directly related to the lowest energy conformation. It is also worth noting that the rate of E2 eliminations is expected to be sensitive towards the size of the substituents and other parameters (base, solvent).

Scheme 6. Lowest Energy and Reactive Conformations of *Syn*- and *Anti*-Aminals

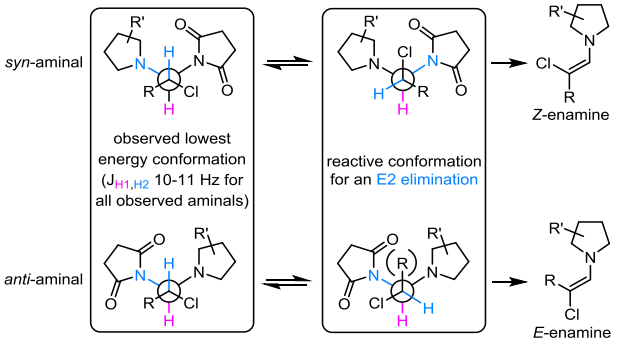

Kinetic Isotope Effects and DFT Calculations

In order to evaluate the first irreversible step in the catalytic cycle, we performed the reaction of **16** and **6** using 20 mol% **3c**·TFA for determination of ^{13}C kinetic isotope effects (KIEs) at natural abundance.[31] By using **6** as a limiting reagent, the reaction was taken to 77% conversion of **16**. The unreacted **16** was re-isolated from the reaction mixture as the corresponding alcohol following a reductive workup (see SI for full experimental details). The ^{13}C isotopic composition of this re-isolated sample was compared to that of a standard sample of reduced **16** (taken from the same batch used for the high conversion reaction) using quantitative NMR methodology. From the relative isotopic composition and the fractional conversion, ^{13}C KIEs for **16** were determined in a standard way.[31] The resulting ^{13}C KIE measurements, from duplicate runs of this experiment, are shown in Figure 3A. There is a normal KIE of ~1.015 on the former carbonyl carbon and unity KIEs on all other carbon atoms of **16**. The qualitative interpretation of the experimental KIEs is that only the carbonyl carbon is involved in the first irreversible step for **16** in the catalytic cycle. There are several steps in the catalytic cycle that involve the carbonyl carbon atom and the exact step that accounts for the experimental KIE is not immediately clear. For the quantitative interpretation of experimental KIEs, we modeled the key steps in the catalytic cycle using B3LYP/6-31+G** with a PCM solvent model for acetonitrile as executed in Gaussian '16.[32,33,34,35] High-level single point energy calculations that include dispersion corrections were performed for all stationary points using B3LYP-D3(BJ)[36]/6-311+G**PCM (acetonitrile). The reported Gibbs free energies were obtained by adding the free energy correction from the optimizations to the high-level single point energy calculations. The free energies were corrected using Grimme's quasi rigid rotor -harmonic oscillator (qRRHO) approach, which raises vibrational frequencies that are below 100 cm^{-1} to 100 cm^{-1}.[37] This approach is routinely utilized and is well-established for evaluating reactivity and selectivity in similar catalytic systems.[38,39] The reaction coordinate diagram for the reaction of **16** and **6** catalyzed by **3c**·TFA leading up to the formation of the chloroiminium ion **Int4** is shown in Figure 3B. The trifluoroacetate counterion of the catalyst salt is included in these calculated structures to either act as a proton shuttle or to stabilize positively charged transition structures/intermediates. The reported free energy barriers ($\Delta G^{\ddagger}$) are computed with respect to the sum of the energies of neutral **3c**, trifluoroacetic acid, **6**, and **16**. The computed free energy profile reveals that the transition structures (TSs) for initial formation of the carbinol amine intermediate **Int 1** (TS1, $\Delta G^{\ddagger}$=10.2 kcal mol^{-1}), loss of water to form the iminium ion **Int2** (TS2, $\Delta G^{\ddagger}$=10.1 kcal mol^{-1}), and deprotonation of **Int2** to form the enamine **Int3** (TS3, $\Delta G^{\ddagger}$=10.4 kcal mol^{-1}) all lie within 0.7 kcal mol^{-1} of each other. The TS for chlorination of **Int3** by **6** (TS4) has a $\Delta G^{\ddagger}$ of 9.3 kcal mol^{-1} and this step is an exergonic process resulting in a α-chloroiminium ion intermediate **Int4** that is 25.1 kcal mol^{-1} below separated starting materials. The experimental ^{13}C KIE determined for **16** reports on TS for the first irreversible step in the catalytic cycle for **16**. Since the $\Delta G^{\ddagger}$ for TS1-TS4 lie within 1.1 kcal mol^{-1} of each other, the prediction of ^{13}C KIEs for the interpretation of our experimental KIE values is complicated – each of these TSs contribute to the observed KIE, with the highest energy transition structure (TS3) contributing the most followed by TS1, TS2, and TS4. Figure 4C shows the predicted ^{13}C KIEs for TS1-4 assuming each to be the sole first irreversible step for **16**. The percentage contribution of each TS (based on relative $\Delta G^{\ddagger}$) to the observed KIEs is also indicated in parentheses. Based on the predicted ^{13}C KIE values for TS1-4, the energy-weighted predicted ^{13}C KIEs for C1 and C2 of **16** are computed (Figure 3C, last row). Comparison of experimental (Figure 3A) and energy-weighted predicted ^{13}C KIEs reveals a good agreement between the two – lending support to the computed reaction coordinate diagram.[40] Next, we computed the steps from the chloroiminium ion intermediate **Int4a** to the final α-chloroaldehyde product **19** (**Int4a** is a complex between the chloroiminium ion-TFA salt and a molecule of water and differs from **Int4** which is a complex between the chloroiminium ion-TFA salt and a molecule of succinimide). In the resulting reaction coordinate diagram (Figure 4A), the reported free energy barriers ($\Delta G^{\ddagger}$) are computed with respect to **Int4a** (the global minimum on this reaction coordinate). The hydrolysis of **Int4a** proceeds via two lower barrier steps – TS6 ($\Delta G^{\ddagger}$=8.8 kcal mol^{-1}) and TS7 ($\Delta G^{\ddagger}$=8.3 kcal mol^{-1}) – to deliver the product aldehyde **19** and regenerate **3c** and trifluoroacetic acid. Based on the observation of *syn*- and *anti*-aminal intermediates in this reaction (Figure 6 and 7), we also computed transition structures for the conversion of **Int4** to *syn*-**18b** (TS5) and *anti*-**18b** (TS5'). The transition structures TS5 and TS5' face a free energy barrier of 11.1 and 8.9 kcal mol^{-1} (relative to **Int4**). The *syn*-aminal *syn*-**18b** was found to be thermodynamically favored over the *anti*-

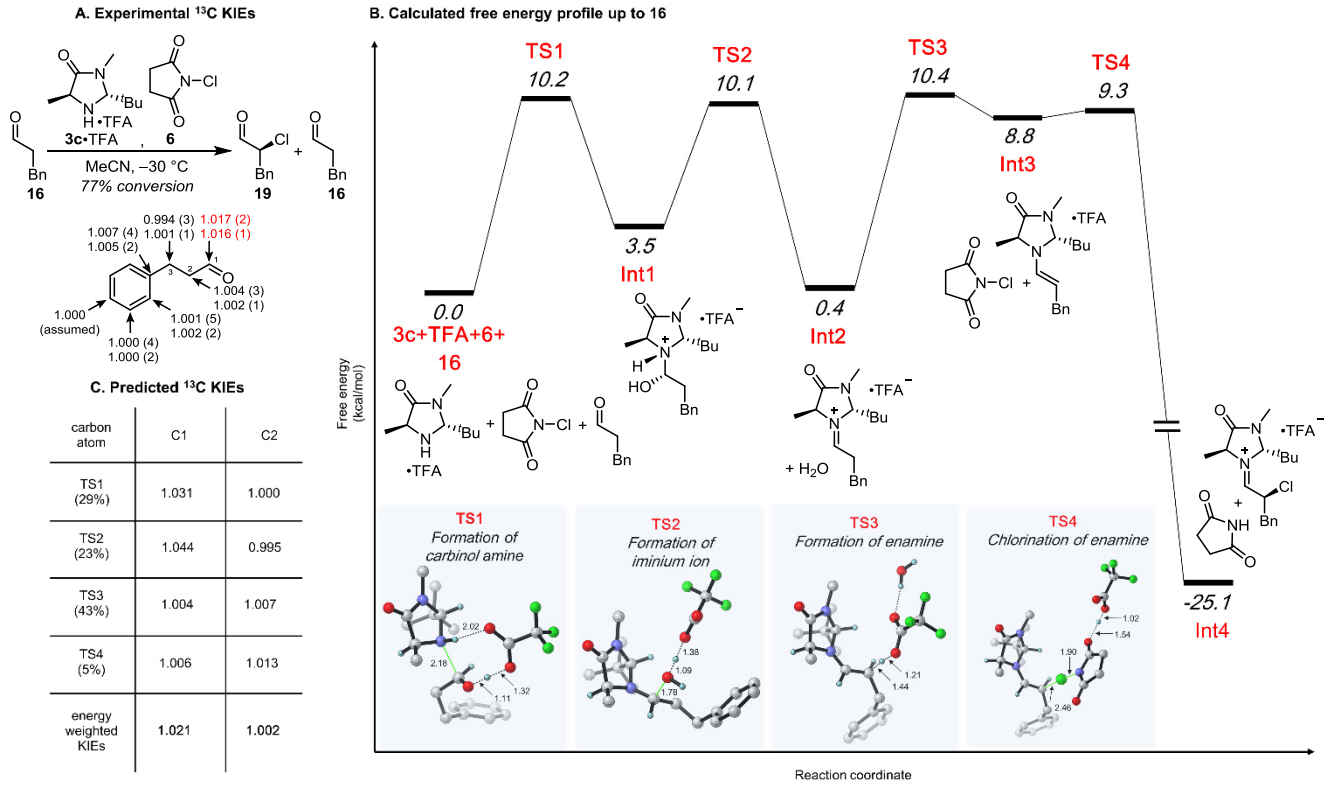

FIGURE 3. Experimental ¹³C KIE studies and supporting DFT calculations. (A) Experimental ¹³C KIEs for the α-chlorination of **16** with the MacMillan Catalyst **3c**·TFA. (B) Reaction coordinate diagram for the reaction of **16** and **6** catalyzed by **3c**•TFA up to the formation of the chloroiminium ion **Int4** calculated at the B3LYP-D3(BJ)/6-311+G** PCM (acetonitrile)//B3LYP/6-31+G** PCM (acetonitrile) level of theory. Some hydrogen atoms have been removed for clarity in the 3D representation of the key transition structures. Key bond-forming and bond-breaking distances are in angstroms (Å). (C) Predicted KIEs at C1 (aldehyde-carbon) and C2 (α-carbon) of **16** for TS1-4 along with energy-weighted predictions for comparison to experimental KIEs.

aminal *anti*-**18b** by 1.7 kcal mol⁻¹. These computed free energies are consistent with the experimental observation of *anti*-**18b** in the initial 5 minutes of the reaction (kinetic aminal) and subsequent accumulation of *syn*-**18b** (thermodynamic aminal) (Figure 7).Our calculations suggest that *syn*-**18b** is a parasitic off-cycle intermediate that has only one path to product **19** – by re-entering the catalytic cycle via TS5 ($\Delta G^{\ddagger}$ =15.3 kcal mol⁻¹) to form **Int4** followed by the previously described hydrolysis via TS6 and TS7. If this pathway is operational for the conversion of *syn*-**18b** to **19**, re-entry of the *syn*-**18b** into the catalytic cycle via TS5 represents the largest change in free energy in the conversion of *syn*-**18b** to **19** (see Supporting Information for a discussion and supporting calculations for the conversion of *anti*-**18b** to **19**). Alternatively, *syn*-**18b** could be an on-cycle intermediate (Curtin-Hammett paradigm[6]) and could undergo an E2-elimination to yield a chloroenamine intermediate. Protonation and subsequent hydrolysis of this chloroenamine intermediate would deliver the product and regenerate the catalyst. In order to evaluate this alternative mechanism, we explored transition state models for the formation of the chloroenamine intermediate utilizing either trifluoroacetate or succinimide anion leaving group as the base that effects the deprotonation with concomitant loss of the succinimide anion. All attempts to locate this TS resulted in an E1-type structure where the succinimide anion is completely dissociated and the base deprotonates a structure resembling a chloroiminium ion (Figure 4A, TS-E1; $\Delta G^{\ddagger}$=28.2 kcal mol⁻¹ with respect to *syn*-**18b**). This is because the incipient carbocation, that forms as the succinimide leaving group departs, is stabilized by the lone pair of electrons on the catalyst nitrogen before deprotonation can occur. Based on this result we hypothesized that disengaging this lone pair from the reaction coordinate by protonation, could result in the identification of an E2-elimination TS.[41] Accordingly, we explored the α-deprotonation of *N*-protonated *syn*-**18b** (with concomitant loss of the succinimide anion) using trifluoroacetate as the base to generate the protonated chloroenamine intermediate. These explorations resulted in the identification of TS-E2 ($\Delta G^{\ddagger}$=50.3 kcal mol⁻¹ with respect to *syn*-**18b**), for the direct conversion of *N*-protonated *syn*-**18b** to the protonated chloroenamine intermediate. Clearly, the barriers for the E2-elimination and E1-elimination pathways are significantly higher than the pathway involving re-entry of *syn*-**18b** into the catalytic cycle as **Int4** (Figure 4D, TS5; $\Delta G^{\ddagger}$=14.2 kcal mol⁻¹ with respect to *syn*-**18b**). In order to gain experimental evidence on the catalytic role of *syn*-**18b**, we envisioned that determination of ¹³C KIEs for the stoichiometric conversion of *syn*-**18b** to product **19** could probe the first irreversible step in the pathway for this reaction (Figure 4B). If the reaction proceeded via turnover-limiting re-entry into the catalytic cycle, a normal ¹³C KIE would be expected only on C1. However, if either the E1- or

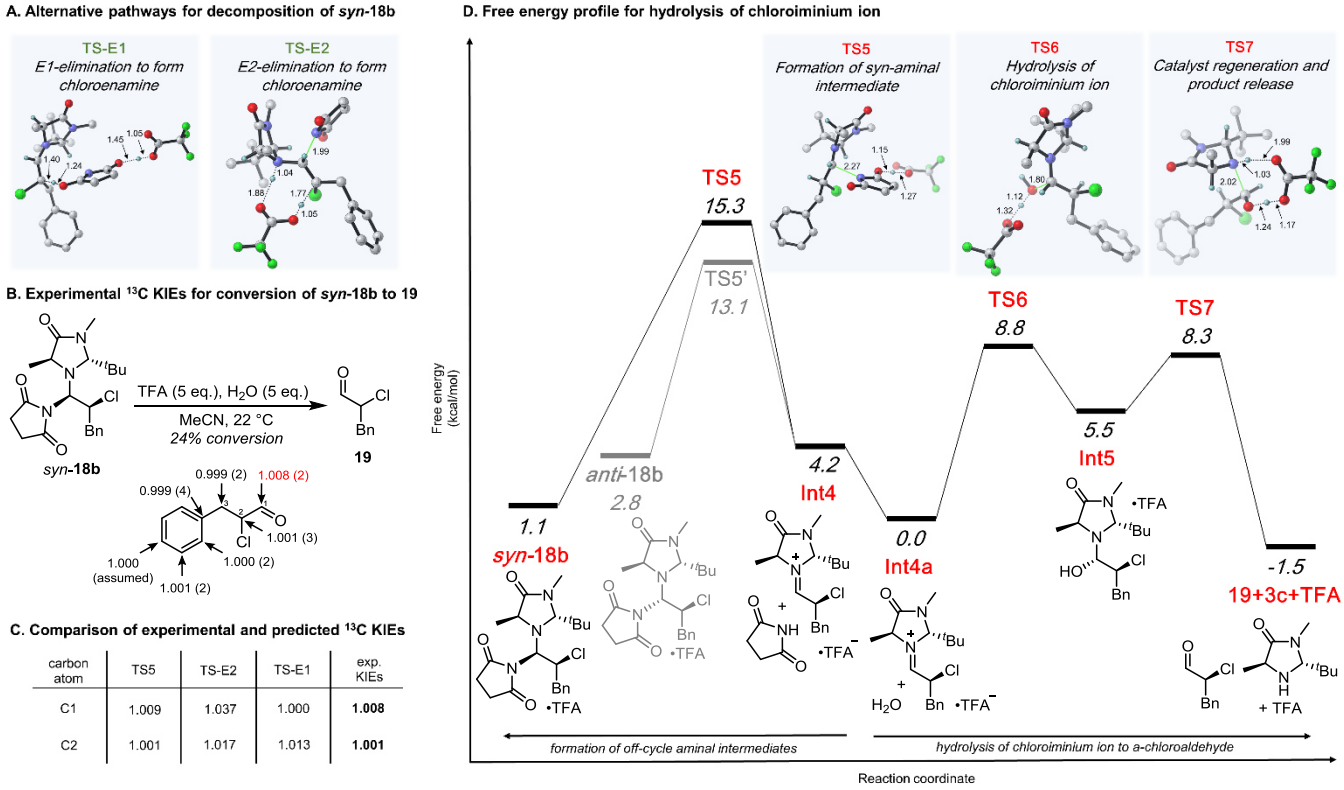

FIGURE 4. Hydrolysis of chloroiminium ion and investigation of the role of experimentally observed aminal intermediates. (A) Calculated transition structures for alternative pathways for re-entry of *syn*-**18b** (as a chloroenamine) into the catalytic cycle. (B) Experimental ^{13}C KIEs determined for the stoichiometric conversion of *syn*-**18b** to **19**. (C) Comparison of experimental ^{13}C KIEs for the conversion of *syn*-**18b** to **19** with the predicted ^{13}C KIE for the rate-determining step in each pathway that converts *syn*-**18b** to **19**. (D) Reaction coordinate diagram for the conversion of the chloroiminium ion **Int4** to the final product **19** calculated at the B3LYP-D3(BJ)/6-311+G** PCM(acetonitrile)// B3LYP/6-31+G** PCM(acetonitrile) level of theory. Also shown is the calculated pathway for the parasitic off-cycle aminal intermediates *syn*-**18b** and *anti*-**18b**. Some hydrogen atoms have been removed for clarity in the 3D representation of the key transition structures. Key bond-forming and bond-breaking distances are in angstroms (Å).

E2-Elimination pathway is operational, a normal ^{13}C KIE would be expected on C2 or both C1 and C2, respectively. The conversion of *syn*-**18b** to **19** was initiated using 5 equivalents each of trifluoroacetic acid and water (Figure 4B). The ^{13}C KIEs were determined by product analysis[42] – by comparison of samples of reduced **19** isolated from 24% and 100% conversion reactions. The key result from this experiment was a 1.008 (2) KIE on C1 and a 1.001 (4) KIE on C2 (Figure 4B) – in qualitative agreement with a mechanism involving turnover-limiting re-entry of *syn*-**18b** into the catalytic cycle. A comparison of this experimental KIE and theoretical KIEs for TS5, TS-E2, and TS-E1 reveals that the experimental values are in excellent agreement with predicted values for TS5 and in poor agreement with those for TS-E2 and TS-E1 (Figure 4C). Thus, evaluation of the reaction energetics and KIEs for the conversion of *syn*-**18b** to **19** supports the role of *syn*-**18b** as a parasitic, off-cycle intermediate that can re-enter the catalytic cycle via turnover-limiting formation of **Int4**. Finally, from the computed reaction coordinate diagram shown in Figure 3B, the chlorination of the enamine intermediate (TS4) is irreversible, and the enantioselectivity-determining step of the reaction. Accordingly, we performed a thorough conformational search for the formation of both *R* and *S* chloroiminium ion via chlorination of the *Si*- and *Re*- faces, respectively, of all possible enamine geometries. The $\Delta\Delta G^{\ddagger}$ between the lowest energy transition structures leading to *R* and *S* chloroiminium ion is 2.9 kcal mol^{-1} (favoring *S*) – a value that is qualitatively consistent with the >90% ee observed for this reaction. The full details of these explorations are included in the Supporting Information. Thus, our experimental KIE results along with a comprehensive DFT analysis of the entire reaction coordinate supports a scenario where the enantioselectivity-determining step is the initial formation of the chloroiminium ion and not any downstream processes.

Deuterium Incorporation Studies

In a deuterium incorporation study, aldehyde **16** was subjected to a chlorination reaction with the MacMillan catalysts **3b** and **3c** and the Jørgensen-Hayashi catalyst **9c** and NCS at two different temperatures. The obtained chloroaldehyde was reduced to alcohol **22** (to avoid racemization) and submitted to NMR measurements. At –30 °C, all catalysts showed little to no incorporation of deuterium. At 20 °C, the MacMillan catalyst **3b** shows significant deuterium incorporation (Figure 5). This observation is in line

with the racemization MacMillan observed for **3b** but not for **3c** (*vide supra*). Our results also rule out the protonation of fleeting chloroenamine intermediates due to the absence of significant deuterium incorporation at low temperature. While the intermediacy of chloroenamine intermediates cannot be studied by these experiments, their presence is not unlikely as chlorination might account for the formation of significant amounts dichloroaldehyde products for catalysts **9c**, **3a**, and **3b**.

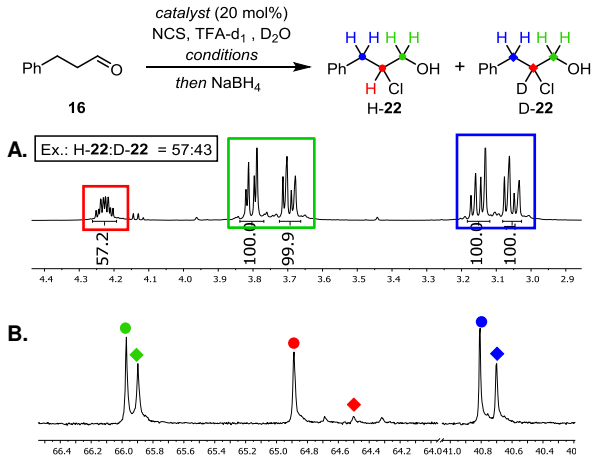

C.

catalyst	solvent	T [°C]	t	H-**22**:D-**22**
3c H•TFA	MeCN	20	18 h	90:10
	MeCN	–30	18 h	100:0
ent-**3b** H•TFA	MeCN	20	18 h	57:34
	MeCN	–30	18 h	95:5
9c	DCM	20	18 h	83:17
	DCM	–30	18 h	89:11
	DCM	20	5 min	97:3[a]

[a]: no TFA-d_1, 12% conversion, 60% ee

Figure 5. Deuterium incorporation of **16** with different catalysts and temperatures with exemplary ^{1}H-NMR (A) and ^{13}C-NMR (B) spectra; C) Quantification of deuterium incorporation under different conditions.

NMR Reaction Progress

We interrogated concentration profiles in order to assess whether the two mechanisms are kinetically distinguishable. Gratifyingly, aldehyde **16** (the substrate), the chloroaldehyde product **19** and the corresponding crystallographically characterized aminal *syn*-**18b** possess separate, non-overlapping NMR resonances (see SI). Monitoring their concentrations over time, it is apparent that the initial rate of chloroaldehyde formation exceeds the build-up of the aminal (Figure 6A). This observation eliminates the possibility of the catalyst being turned over through the thermodynamically most stable aminal. The alternate off-cycle mechanism provides a scenario where the rate of iminium hydrolysis exceeds that of aminal formation. From the iminium ion intermediate, part of the catalyst is diverted into a stable aminal resting state. To identify these subtleties, it is essential to follow individual concentrations over time (NMR spectroscopy) rather than observing a single value for the whole system, for example, the amount of energy released (reaction calorimetry).

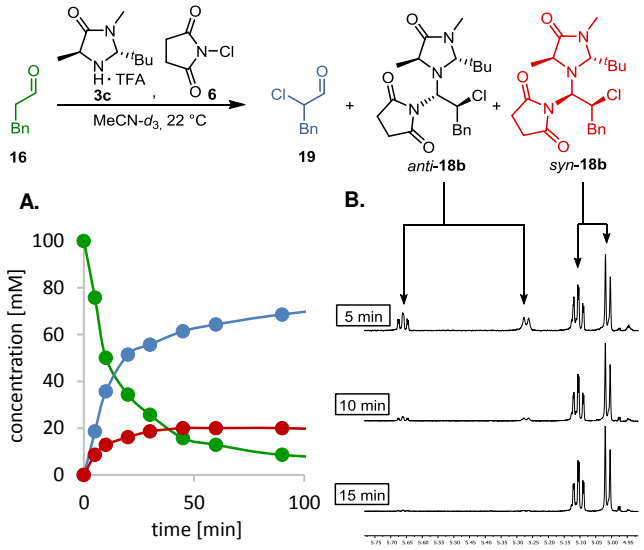

Figure 6. α-Chlorination of aldehyde **16** with catalyst **3c** and NCS (**6**) with concentration/time profile (A) and ^{1}H-NMR spectra with characteristic aminal signals for the first 15 min of the reaction (B).

Caution is due when arguing based on the presence or absence of intermediates in the NMR spectrum. Fleeting species, e.g. enamines[43] and iminium ions,[44] are difficult to observe and reversibly forming aminal diastereomers are certainly no exception. When reanalyzing our data for this reaction, we noted additional, previously overlooked resonances in the NMR spectrum at t = 5 min (Figure 6B) (quickly disappearing thereafter). The possibility of the corresponding species to be the elusive aminal *anti*-**18b** is supported by comparison of the observed and computed ^{1}H chemical shifts (Figure 7).

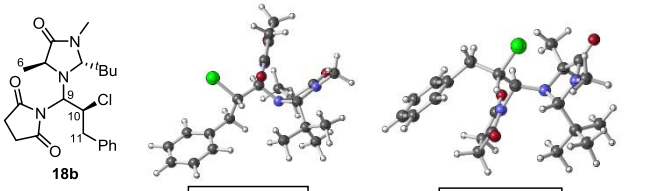

Nuc.#	Calc. δ	Exp. δ	Abs. Dev.	Calc. δ	Exp. δ	Abs. Dev.
H6	1.55	1.47	0.08	1.51	1.50	0.01
H9	4.81	5.01	0.20	5.15	5.27	0.12
H10	5.20	5.10	0.10	5.94	5.66	0.28
H11a	4.09	3.96	0.13	3.47	3.18	0.29
^{t}Bu	1.08	1.10	0.02	0.77	0.91	0.14
MAD			0.11			0.17

Figure 7. Calculated *syn*-**18b** and *anti*-**18b** lowest energy conformations of the aminal **18b** (top). Key ^{1}H chemical shifts calculated at PCM(ACN)-mPW1PW91/6-311+G(2d,p)//PCM (ACN)-B3LYP-D3(BJ)/6-31G+(d,p) level of theory (bottom) (for additional details see SI).

This hypothesis is in line with the calculated reaction path as the thermodynamically more stable aminal *syn*-**18b** accumulates in favor of *anti*-**18b**. While minor *anti*-**18b** will continue to be formed at an (unknown) kinetic ratio, its concentration quickly becomes too small to be observed by NMR as the amount of available catalyst diminishes rapidly into the *syn*-**18b** aminal reservoir. It is worth noting that under Curtin-Hammett conditions, the equilibrium distribution of the equilibrating species and the product distribution must be time-invariant.[45]

The Role of Chloroenamine Intermediates

The DFT calculations for catalyst **3c** demonstrated that chloroenamine formation – either by iminium deprotonation or by E2 elimination from the aminal intermediate – is energetically disfavored compared to the alternative hydrolysis pathway. This assessment is supported by the notable lack of evidence of protonation (no deuterium incorporation) and the absence of dichlorination products. For catalyst **3a**, erosion of the ee was shown upon complete turnover of the substrate in a chlorination reaction.[15] In a direct comparison, MacMillan et al.[18] also showed that in the absence of NCS, catalyst **3b** effects rapid racemization of chloroaldehydes. This result suggests that chloroenamines are accessible even in the absence of chloroaminals, i.e. from the iminium ions by deprotonation. During our efforts to separate aminals from reaction mixtures, we also have been able to characterize the first dichloroaminal **24a** from catalyst **3a**, which we suspect to be derived from the corresponding dichloroiminium intermediate (Scheme 7). In case of the Jørgensen-Hayashi catalyst or unsubstituted pyrrolidine, it was shown that chloroenamine formation is competing[46] with the hydrolysis thus leading to the observation of significant amounts of dichlorination byproduct in both cases. This problem can be overcome by accelerating the hydrolysis step via intramolecular (proline[47]) or intermolecular assistance (2,6-lutidine and H_2O[46]).

Scheme 7. Chloroenamines can Competitively Lead to Racemization and Dichlorination

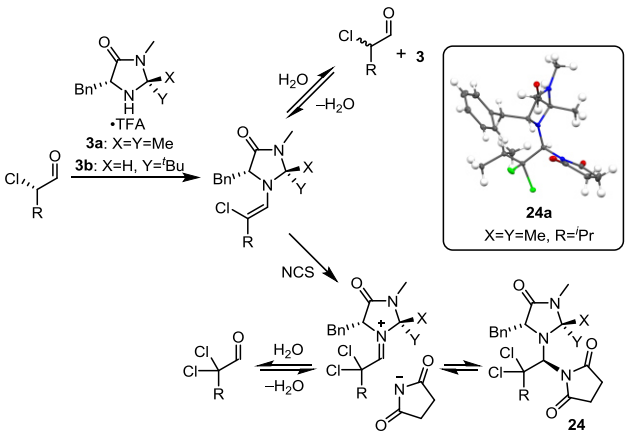

Ion Mobility-Mass Spectrometry Studies

Aminals can be subjected to electrospray ionization followed by collision-induced dissociation. For each aminal, diastereomeric iminium ions can be formed as *E*- and *Z*-isomers. In a feasibility study, we aimed to find out whether iminium ions derived from two isolated C2-epimeric aminals would be separable due their different ion mobilities in a drift gas (He).

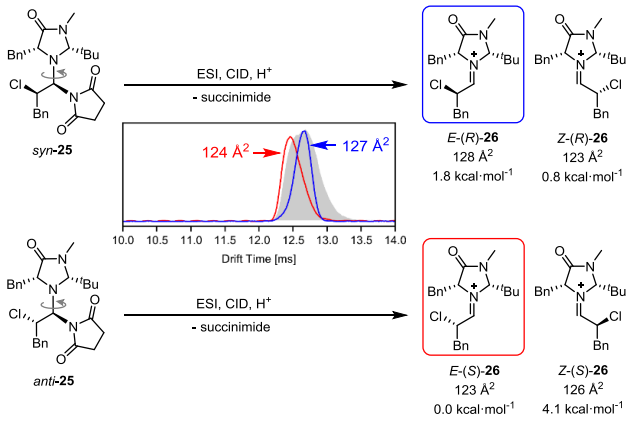

Figure 8. Separate ionization of the diastereomeric aminals *syn*-**25** and *anti*-**25** with arrival time distributions and experimental CCSs of the generated diastereomeric iminium ions (blue and red traces). The trace of the mixture of both diastereomers is depicted in grey. The four possible chloroiminium ions and their calculated CCSs and relative free energies are shown on the right.

Toward this end, instrument-independent collision cross sections (CCSs) were determined by ion mobility–mass spectrometry experiments on a custom-built instrument.[48] The arrival time distributions (ATDs) of the selectively dissociated aminals are represented in Figure 8. The conformational space of the iminium ions **26** was sampled using a genetic algorithm[49] and promising candidate structures were reoptimized at the PBEoD3/6-311+G(d,p) level of theory.[50] Computed CCSs were obtained using the trajectory method.[50] The combined approach was successfully used to make a prediction whether *E*- or *Z*- iminium ions are formed in the decomposition process of the two diastereomeric aminals *syn*-**25** and *anti*-**25**. The ATD traces of the selectively dissociated aminals suggest that the dissociation of each aminal leads to the corresponding *E*-iminium ion. The comparison of the computed and the experimental CCS value suggests the *E*-iminium to be formed for both epimers (see SI for details). Future research will involve spectroscopic investigation (e.g., IR spectroscopy) of the separate iminium ions and following the iminium ion distribution over the course of the reaction.

Aminals with Jørgensen-Hayashi-Type Catalysts

In light of the observations described above for the MacMillan catalysts, we decided to reinvestigate the Jørgensen-Hayashi system for which we have not been able to obtain crystals of sufficient quality. Toward this end, we prepared a reaction mixture using isovaleraldehyde, catalyst **9b** and *N*-chlorophthalimide (NCP) as previously described.[6] In order to obtain cleaner spectra than those reported, we removed all volatile constituents by evaporation. In the ^{1}H-NMR spectrum, **11** showed rather broad resonances at room temperature which split up at around –20 °C and at –54°C two sharp signal sets with a 3:1 ratio were observed.

The presence of EXSY exchange peaks between the two signal groups indicated two rapidly interconverting species. These observations had been previously interpreted as **11** being a mixture of interconverting diastereomers at the aminal carbon with the *anti*-diastereomer as the major and the *syn*-diastereomer as the minor constituent.[6] Interestingly, in both species the large $^3J_{H-H}$ coupling indicates an *antiperiplanar* arrangement of the H-atoms along the C1'-C2' bond. In order to elucidate the structures of the two species from NOE data, we aimed for minimizing exchange contributions to the NOE. This was largely achieved by changing the solvent from $CDCl_3$ to CD_2Cl_2, which allows cooling to –83 °C. We managed to assign most signals of both species and obtained a rather large body of distance data from the NOE of the major species and far less of the minor (see SI). The challenge now is to find out, why two signal sets are obtained and whether we can assign the two signal sets to possible structures of species. It is conceivable that these are interconverting diastereoisomers (*syn* and *anti*) as proposed previously by Blackmond et al.[6] (Scheme 9). An alternative explanation would involve interconverting conformational isomers. For the major species, a comparison of distances with calculated structures allowed the assignment of *syn*-configuration (Figure 9). This is in contrast to what has been claimed previously.[6] The key question now is whether the minor species is a diastereomer or a conformational isomer. For both species, only small difference in the distances were observed indicating a very similar relative orientation of the pyrrolidine ring to the chlorinated substrate; the *antiperiplanar* arrangement of H1' and H2' is conserved (see above). While our recently published pure shift ROE experiment (F1 PSYCHE EASY ROESY[51]) afforded additional distance data, still no safe assignment of the minor species was possible. From the $^3J_{H-H}$ coupling data in the pyrrolidine ring, it is not unlikely that multiple envelope conformations are present. The "averaged" pucker of the pyrrolidine is different for the major and minor species, which we consider unlikely for the *ap* arrangement of H1' and H2' in *syn* vs. *anti*-diastereoisomers. Thus we considered hindered rotation as being a plausible cause. From *J*-coupling analysis (see above and data in the SI) it is quite unlikely, that the pyrrolidine puckers are the reason for the separate signal sets; thus we focused our attention to the orientation of the diarylsilylether group. This hypothesis seems plausible as a structure search in the CCDC data base for Jørgensen-Hayashi catalysts with the pyrrolidine nitrogen bound to stereogenic sp^3 hybridized carbon reveals striking similarities concerning the catalyst structure (see SI).[29,52] Each structure in the database had the pyrrolidine ring in an envelope conformation with the γ-carbon tilted out of plane toward the diarylsilylether moiety and the nitrogen lone pair (*down* conformation). For the orientation of the diarylsilylether group, two distinct conformational minima are observed. In 7/10 crystal structures, the N- and O-substituent at the exocyclic C-C bond of the catalyst possess an *antiperiplanar* (*ap*) relationship whereas in three cases an *exo-synclinal* (*exo-sc*) conformation was adopted.

As NOE data was not entirely conclusive on the nature of the minor species and the process of the two interconverting aminal species **14** at –54 °C, a calculation of the NMR shifts for several conformational isomers and stereoisomers was performed (see SI for details). When the predicted conformers for **14** were separated into the *ap* and *exo-sc* classifications the *ap* chemical shifts corresponded to the major product (mean average deviation (MAD): 1.4 ppm ^{13}C, 0.10 ppm ^1H) and the *exo-sc* chemical shifts were in excellent agreement with the minor product (MAD: 1.5 ppm ^{13}C, 0.13 ppm ^1H) for key chemical shifts (Figure 9).

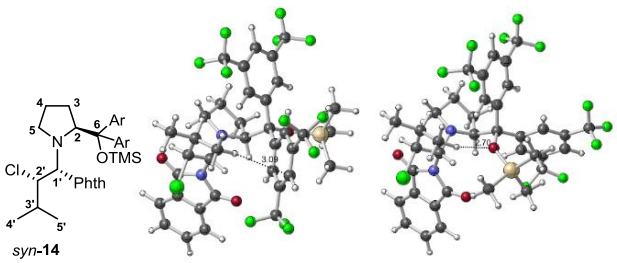

Nuc.#	Calc. δ	Exp. δ	Abs. Dev.	Calc. δ	Exp. δ	Abs. Dev.
C1'	75.2	76.3	1.1	74.6	76.1	1.5
C2	67.9	68.6	0.7	67.1	68.6	1.5
C2'	72.9	65.6	7.3	74.1	66.8	7.3
C3'	32.2	29.3	2.9	32.1	29.0	3.1
C4	25.2	24.3	0.9	25.4	24.1	1.3
C4'	19.9	21.3	1.4	19.7	21.4	1.7
C5	48.4	48.8	0.4	47.9	48.5	0.6
C5'	**12.3**	**12.2**	0.1	**16.2**	**15.7**	0.5
C6	**82.7**	**82.4**	0.3	**84.3**	**84.2**	0.1
MAD			1.4			1.5
H1'	**5.24**	**5.16**	0.08	**6.04**	**5.81**	0.23
H2	**4.80**	**4.60**	0.20	**4.24**	**4.15**	0.09
H2'	5.25	4.98	0.27	5.28	5.05	0.23
H3'	2.39	2.13	0.26	2.67	2.35	0.32
H3a	1.76	1.71	0.05	1.81	1.82	0.01
H3b	**1.80**	**1.71**	0.09	**1.32**	**1.38**	0.06
H4'	1.07	0.95	0.12	1.20	1.06	0.14
H4a	1.18	1.20	0.02	1.25	1.28	0.03
H4b	**0.08**	**0.09**	0.01	**0.63**	**0.63**	0.00
H5'	**0.05**	**-0.01**	0.06	**1.50**	**1.28**	0.22
H5a	3.37	3.29	0.08	3.44	3.27	0.17
H5b	1.97	1.97	0.00	2.16	2.16	0.00
MAD			0.10			0.13

Figure 9. Calculcated *ap* (top left) and *exo-sc* (top right) conformations of the Jørgensen-Hayashi aminal *syn*-**14** (R = $C(3,5\text{-}CF_3\text{-}C_6H_3)_2OTMS$). Bottom: key chemical ^1H and ^{13}C shifts. ^1H and ^{13}C chemical shifts calculated with the mPW1PW91/6-311+G(2d,p) (GIAO; PCM, $CHCl_3$, 219.15 K)//B3LYP-D3(BJ)/6-31G+(d,p) (219.15 K) level of theory (indicative atoms are highlighted in bold).

From the integration of the exchange signals in 1D NOE series a barrier of 12.8(4) kcal mol^{-1} can be determined at –54 °C. Investigation into the rotational barrier from the *ap*

to the *exo-sc* for *syn*-**14** using DFT calculations (see SI for additional details), revealed the barrier of rotation to be ~13.9 kcal mol^{-1}, within the error expected for this method to compare to the experimental 12.8 kcal mol^{-1} barrier between the major and minor products at −54 °C. Further separation of the conformers into *concave* and *convex* pyrrolidine ring puckering, led to worse predicted chemical shifts for both the major and minor products, suggesting an averaging of the ring puckering in the NMR solution (barrier of ~1 kcal mol^{-1} for the major (*ap*) product). The H5' proton shift appears to be diagnostic of *ap* and *exo-sc* conformations with the shift at -0.01 ppm for the major product and at 1.28 ppm for the minor product. In the lowest energy conformer calculated for the *ap* product, a C-H···π interaction can be seen shielding this methyl group proton, which does not occur in the *exo-sc* product (Figure 9).

Additionally, NMR calculations to determine the major and minor products bearing a succinimide (aminal **11**) substituent instead of phthalimide (aminal **14**) found by Blackmond and co workers[6] at −54C were performed. The experimental chemical shifts were compared to the *syn*-**11** *ap* and *exo-sc*, *anti*(C1') *ap* and *exo-sc*, and *anti*(C2')-**11** *ap* calculated chemical shifts. The *syn-ap*-**11** calculated chemical shifts were in good agreement with the major product, while the *syn-exo-sc*-**11** produced some shifts above the expected deviation (<0.3 ppm for ^{1}H shifts and ≤3.1 ppm for ^{13}C shifts – with the exception of 7.3 ppm for C2'-Cl).[53] The *anti* C1' and C2' aminals were found to have greater mean average deviations (MADs) for the ^{1}H and ^{13}C chemical shifts when compared to the minor product chemical shifts than the *syn-exo-sc*-**11** aminal. These results, along with the agreement of *syn-exo-sc*-**14** calculated chemical shifts with the minor product experimental chemical shifts, suggest further analysis of the minor product experimental chemical shifts for **11** at −54 °C may be needed to confirm the chemical shift assignment.

The computationally and NMR spectroscopically derived (2*S*,1'*R*,2'*S*)-configuration and the conformation of the *syn*-aminal **14** share several structural features with the crystallographically determined aminals of the MacMillan catalysts including an *antiperiplanar* orientation of C1'-H and C2'-H and the lone pair of aminal nitrogen from the catalysts being *antiperiplanar* to the imide nitrogen. The stabilization energy of this $n_{N(cat)} \rightarrow \sigma^{*}_{C\text{-}N(imide)}$ interaction (Scheme 8) is predicted to be 16.3 kcal mol^{-1} for the *ap* product and 16.0 kcal mol^{-1} for *exo-sc* product. This interaction is even stronger when the succinimide substituent is present 17.5 (*ap*) and 17.2 (*exo-sc*) kcal mol^{-1}; and it decreases to ~8.0 kcal mol^{-1} in the lowest energy conformer of the *anti*-aminal (see SI for details).[54]

In summary, only the *syn*-diastereomer (2*S*,1'*R*,2'*S*)-**14** allows for an optimal synergistic interplay of stereoelectronic effects and minimized steric interactions.

As additional and independent supporting evidence for the structural assignment, aminal **14** was reduced and the resulting alcohol was converted to the crystalline dinitrobenzoate **15**. After a thorough isolation process only one diastereomer could be isolated. Crystal structure analysis confirmed the *syn*-configuration of aminal **15** (Scheme 8).

Scheme 8. Stereochemical Assignment of Aminal 14

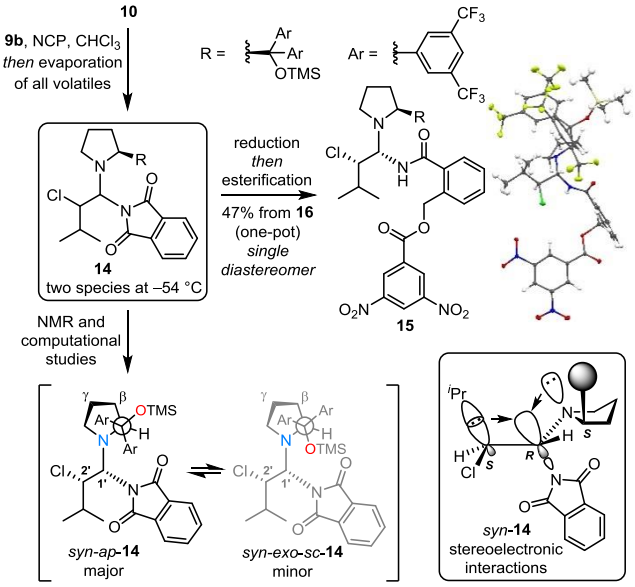

When substituting isovaleraldehyde with propanal, the analogous aminal could be obtained along with the chloroaldehyde being formed in a 57:43 enantiomeric ratio. NMR spectroscopic analysis of the aminal at −54 °C showed the presence two separate sets of sharp signals in a 68:32 ratio. Decomposition of the aminal into the corresponding chloroaldehyde was promoted by addition of 2 equivalents of water and TFA. Determination of the enantiomeric excess revealed high enantiomeric excess for the chloroaldehyde product (1-120 min: 95-93% ee). Additionally, almost no deuterium incorporation was observed when the decomposition of the propanal-derived aminal or aminal **14** was promoted by D_2O with or without TFA-d_1. These observations suggest that only one out of four possible aminal diastereomers is present in sufficient concentration to be detected and isolated. Thus, aminal accumulation solely depends on thermodynamic stability.

♦ CONCLUSION

A comparative analysis of the Curtin-Hammett model for stereocontrol and the steric shielding model showed only the latter to be consistent with experimental evidence. Using crystallography, NMR spectroscopy and computational NMR shift prediction, we have elucidated the configuration and conformation of several aminal intermediates of different catalysts in the organocatalytic α-chlorination of aldehydes. Their relative stability was rationalized by minimizing steric interactions and maximizing stabilizing stereoelectronic effects.

In the case of the Jørgensen-Hayashi catalyst **9b**, the underlying assumption of two equilibrating C1-aminal diastereomers **14** with the *anti*-diastereomer being the major and the *syn*-diastereomer being the minor species[6] was shown to be incorrect. Instead, the two interconverting species, found upon cooling, are proposed to be conformational isomers of the *syn*-diastereomer (Scheme 9). Moreover, the suggested formation of the C2-stereogenic center

by chloroenamine protonation was excluded by the absence of deuterium incorporation under the reaction conditions.

Scheme 9. Structural Revision of Aminal 14

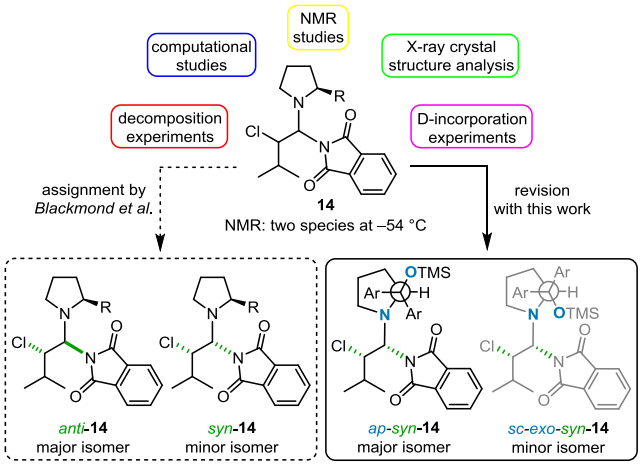

In the case of the MacMillan catalyst **3c**, a combination of ^{13}C KIE studies and DFT calculations demonstrated enamine chlorination not to be the first irreversible step. It also provided complementary evidence to rule out decomposition of the aminal intermediates by an E2 elimination. The calculated transition structures for the enamine chlorination not only correctly predict the stereochemical outcome but also demonstrate that enamine chlorination is faster than (re-)protonation. This in an important finding as it shows that enamine formation in this case is not reversible, i.e. it is not thermodynamically controlled. This observation is supported by the chlorination product lacking significant amounts of deuterium incorporation. With respect to the C1 diastereomeric aminals, DFT calculations predicted the *anti*-aminal as the kinetic and the *syn*-aminal as the thermodynamic intermediate.

Following the concentration/time profile by NMR spectroscopy, we were able to identify the previously overlooked *anti*-aminal being formed within the first 5 minutes of the reaction. It quickly disappears due to accumulation of the catalyst in the *syn*-aminal resting state. The structure of the *anti*-aminal was determined by NMR shift computations and the method was validated against the crystallographically characterized *syn*-aminal diastereomer. These observations rule out a Curtin-Hammett scenario for two reasons. First, Curtin-Hammett conditions require the ratio of the two interconverting intermediates to be time-invariant. Secondly, the dominant conformational minima of the two diastereomeric aminals are unrelated to the reactive conformations for an E2 elimination let alone the respective transition states.

Additionally, we were able to isolate and characterize most of the relevant aminals for the MacMillan catalyst **3a** and **3b** by crystal structure analysis for the first time and to reevaluate the incorrect assignment made in the literature. We also isolated and characterized an intermediate relevant to formation of dihalogenation byproducts. Similar to the fluorination reaction described by Jørgensen, formation of dichlorinated intermediates also could change the initial stereoisomeric ratio of the monochlorination product.

Regarding the iminium intermediates, we have for the first time been able to separate diastereomeric iminium ions in an organocatalytic reaction by ion mobility-mass spectrometry. Future research will involve spectroscopic characterization of the separated iminium ions.

These results highlight the added value of combined computational work and experimentation. They also demonstrate the importance of a careful characterization of reaction intermediates to the understanding of complex reaction networks. Understanding and countering the stabilizing interactions within stable intermediates may provide clues to the design of more efficient catalytic systems.

ASSOCIATED CONTENT

Supporting Information. Experimental procedures, computational details, characterization data of all compounds, NMR spectra, crystallographic data, HPLC and GC traces. This material is available free of charge via the Internet at http://pubs.acs.org.

Accession Codes. 2041073–2041078, 2043370, 2045387 and 2049431 contain supplementary crystallographic data for this paper. These data can be obtained free of charge via www.ccdc.cam.ac.uk/data_request/cif, or by emailing data_request@ccdc.cam.ac.uk, or by contacting The Cambridge Crystallographic Data Centre, 12Union Road, Cambridge CB2 1EZ, UK; fax: +44 1223 336033.

AUTHOR INFORMATION

Corresponding Authors

Mathias Christmann – *Institute of Chemistry and Biochemistry, Freie Universität Berlin, 14195 Berlin, Germany*; ORCiD: 0000-0001-9313-2392; Email: mathias.christmann@fu-berlin.de

Mathew J. Vetticatt – *Department of Chemistry, Binghamton University, Binghamton, New York 13902, United States*; ORCiD: 0000-0001-5709-0885; Email: vetticatt@binghamton.edu

Dean J. Tantillo – *Department of Chemistry, University of California – Davis, Davis, California 95616, United States*; ORCiD: 0000-0002-2992-8844; Email: djtantillo@ucdavis.edu

Christina Thiele – *Clemens Schöpf Institute of Organic Chemistry and Biochemistry, Technische Universität Darmstadt, 64287 Darmstadt, Germany*; ORCiD: 0000-0001-7876-536X; Email: cthiele@thielelab.de

Kevin Pagel – *Institute of Chemistry and Biochemistry, Freie Universität Berlin, 14195 Berlin, Germany; Fritz Haber Institute of the Max Planck Society, 14195 Berlin, Germany*; ORCiD: 0000-0001-8054-4718; Email: kevin.pagel@fu-berlin.de

Authors

Sebastian Ponath – *Institute of Chemistry and Biochemistry, Freie Universität Berlin, 14195 Berlin, Germany*; ORCiD: 0000-0003-2763-0443;

Chetan Joshi – *Department of Chemistry, Binghamton University, Binghamton, New York 13902, United States*;

Amy T. Merrill – *Department of Chemistry, University of California – Davis, Davis, California 95616, United States*; ORCiD: 0000-0003-4801-1721;

Volker Schmidts – *Clemens Schöpf Institute of Organic Chemistry and Biochemistry, Technische Universität Darmstadt, 64287 Darmstadt, Germany*; ORCiD: 0000-0002-7195-312X;

Kim Greis – *Institute of Chemistry and Biochemistry, Freie Universität Berlin, 14195 Berlin, Germany; Fritz Haber Institute of the Max Planck Society, 14195 Berlin, Germany*; ORCiD: 0000-0002-9107-2282;

Maike Lettow – *Institute of Chemistry and Biochemistry, Freie Universität Berlin, 14195 Berlin, Germany; Fritz Haber Institute of the Max Planck Society, 14195 Berlin, Germany*;

Manuela Weber – *Institute of Chemistry and Biochemistry, Freie Universität Berlin, 14195 Berlin, Germany*

Simon Steinhauer– *Institute of Chemistry and Biochemistry, Freie Universität Berlin, 14195 Berlin, Germany*; ORCiD: 0000-0001-7420-1153;

Author Contributions

‡These authors contributed equally.

Notes

The authors declare no competing financial interest.

ACKNOWLEDGMENT

K.G. thanks the Fonds National de la Recherche (FNR), Luxembourg for funding for the project GlycoCat (13549747). C.M.T. thanks the DFG for funding the project TH1115/12-1. D. J. T. is thankful for the support from the US National Science Foundation (CHE-1856416 and the XSEDE program (CHE-030089)). We thank Patrick Voßnacker (FU Berlin) for crystallographic support.

REFERENCES

(1) Carreira, E. M.; Kvaerno, L. Classics in Stereoselective Synthesis; Wiley-VCH, Weinheim, 2009.

(2) Carlson, R.; Carlson, J. E. Design and optimization in organic synthesis, 2nd rev. and enl. ed.; Elsevier, Amsterdam, San Diego, CA, 2005.

(3) List, B.; Maruoka, K. Science of Synthesis, Asymmetric Organocatalysis Vol. 1; Georg Thieme, Stuttgart, New York, 2012.

(4) Marigo, M.; Fielenbach, D.; Braunton, A.; Kjaersgaard, A.; Jørgensen, K. A. Enantioselective Formation of Stereogenic Carbon–Fluorine Centers by a Simple Catalytic Method. *Angew. Chem. Int. Ed.* **2005**, *44*, 3703–3706.

(5) Burés, J.; Armstrong, A.; Blackmond, D. G. The Interplay of Thermodynamics and Kinetics in Dictating Organocatalytic Reactivity and Selectivity. *Pure Appl. Chem.* **2013**, *85*, 1919–1934.

(6) a) Burés, J.; Armstrong, A.; Blackmond, D. G. Curtin–Hammett Paradigm for Stereocontrol in Organocatalysis by Diarylprolinol Ether Catalysts. *J. Am. Chem. Soc.* **2012**, *134*, 6741–6750; b) Burés, J.; Armstrong, A.; Blackmond, D. G. Correction to Curtin–Hammett Paradigm for Stereocontrol in Organocatalysis by Diarylprolinol Ether Catalysts. *J. Am. Chem. Soc.* **2012**, *134*, 14264.

(7) a) Reyes-Rodríguez, G. J.; Rezayee, N. M.; Vidal-Albalat, A.; Jørgensen, K. A. Prevalence of Diarylprolinol Silyl Ethers as Catalysts in Total Synthesis and Patents. *Chem. Rev.* **2019**, *119*, 4221–4260; b) Marigo, M.; Wabnitz, T. C.; Fielenbach, D.; Jørgensen, K. A. Enantioselective Organocatalyzed α Sulfenylation of Aldehydes. *Angew. Chem. Int. Ed.* **2005**, *44*, 794–797.

(8) Hayashi, Y.; Gotoh, H.; Hayashi, T.; Shoji, M. Diphenylprolinol Silyl Ethers as Efficient Organocatalysts for the Asymmetric Michael Reaction of Aldehydes and Nitroalkenes. *Angew. Chem. Int. Ed.* **2005**, *44*, 4212–4215.

(9) Földes, T.; Madarász, Á.; Révész, Á.; Dobi, Z.; Varga, S.; Hamza, A.; Nagy, P. R.; Pihko, P. M.; Pápai, I. Stereocontrol in Diphenylprolinol Silyl Ether Catalyzed Michael Additions: Steric Shielding or Curtin–Hammett Scenario. *J. Am. Chem. Soc.* **2017**, *139*, 17052–17063.

(10) Oestreich, M. Strategies for Catalytic Asymmetric Electrophilic α Halogenation of Carbonyl Compounds. *Angew. Chem. Int. Ed.* **2005**, *44*, 2324–2327.

(11) Britton, R.; Kang, B. α-Haloaldehydes: Versatile Building Blocks for Natural Product Synthesis. *Nat. Prod. Rep.* **2013**, *30*, 227–236.

(12) Shibatomi, K.; Narayama, A. Catalytic Enantioselective α-Chlorination of Carbonyl Compounds. *Asian J. Org. Chem.* **2013**, *2*, 812–823.

(13) Brochu, M. P.; Brown, S. P.; MacMillan, D. W. C. Direct and Enantioselective Organocatalytic α-Chlorination of Aldehydes. *J. Am. Chem. Soc.* **2004**, *126*, 4108–4109.

(14) Wack, H.; Taggi, A. E.; Hafez, A. M.; Drury, W. J.; Lectka, T. Catalytic, Asymmetric α-Halogenation. *J. Am. Chem. Soc.* **2001**, *123*, 1531–1532.

(15) Brown S. P. Iminium and Enamine Activation: Methods for Enantioselective Organocatalysis; California Institute of Technology, Pasadena, California, 2005.

(16) Duan, X.-H.; Mayr, H. Electrophilicities of α-Chlorinating Agents Used in Organocatalysis. *Org. Lett.* **2010**, *12*, 2238–2241.

(17) Halland, N.; Braunton, A.; Bachmann, S.; Marigo, M.; Jørgensen, K. A. Direct Organocatalytic Asymmetric α-Chlorination of Aldehydes. *J. Am. Chem. Soc.* **2004**, *126*, 4790–4791.

(18) Amatore, M.; Beeson, T. D.; Brown, S. P.; MacMillan, D. W. C. Enantioselective Linchpin Catalysis by SOMO Catalysis: An Approach to the Asymmetric α-Chlorination of Aldehydes and Terminal Epoxide Formation. *Angew. Chem. Int. Ed.* **2009**, *48*, 5121–5124.

(19) a) Bourboula, A.; Limnios, D.; Kokotou, M. G.; Mountanea, O. G.; Kokotos, G. Enantioselective Organocatalysis-Based Synthesis of 3-Hydroxy Fatty Acids and Fatty γ-Lactones. *Molecules* **2019**, *24*, 2081; b) Mountanea, O. G.; Limnios, D.; Kokotou, M. G.; Bourboula, A.; Kokotos, G. Asymmetric Synthesis of Saturated Hydroxy Fatty Acids and Fatty Acid Esters of Hydroxy Fatty Acids. *Eur. J. Org. Chem.* **2019**, 2010–2019; c) Kaplaneris, N.; Spyropoulos, C.; Kokotou, M. G.; Kokotos, C. G. Enantioselective Organocatalytic Synthesis of 2-Oxopiperazines from Aldehydes: Identification of the Elusive Epoxy Lactone Intermediate. *Org. Lett.* **2016**, *18*, 5800–5803.

(20) Winter, P.; Vaxelaire, C.; Heinz, C.; Christmann, M. Transforming Terpene Feedstock into Polyketide Architecture. *Chem. Commun.* **2011**, *47*, 394–396.

(21) a) Winter, P.; Swatschek, J.; Willot, M.; Radtke, L.; Olbrisch, T.; Schäfer, A.; Christmann, M. Transforming Terpene-Derived Aldehydes into 1,2-Epoxides via Asymmetric α-Chlorination: Subsequent Epoxide Opening with Carbon Nucleophiles. *Chem. Commun.* **2011**, *47*, 12200–12202; b) Winter, P.; Hiller, W.; Christmann, M. Access to Skipped Polyene Macrolides through Ring-Closing

Metathesis: Total Synthesis of the RNA Polymerase Inhibitor Ripostatin B. *Angew. Chem. Int. Ed.* **2012**, *51*, 3396–3400; c) Swatschek, J.; Grothues, L.; Bauer, J. O.; Strohmann, C.; Christmann, M. A Formal, One-Pot β-Chlorination of Primary Alcohols and Its Utilization in the Transformation of Terpene Feedstock and the Synthesis of a C_2-Symmetrical Terminal Bis-Epoxide. *J. Org. Chem.* **2014**, *79*, 976–983.

(22) Comito, R. J.; Finelli, F. G.; MacMillan, D. W. C. Enantioselective Intramolecular Aldehyde α-Alkylation with Simple Olefins: Direct Access to Homo-Ene Products. *J. Am. Chem. Soc.* **2013**, *135*, 9358–9361.

(23) The succinimide anion/iminium ion pair must be considered inert toward water as direct hydrolysis of the iminium ion (a.k.a. the "classical" pathway) or proton transfer to the succinimide anion would bypass the aminal intermediate.

(24) A publication on organocatalytic selenylations[27] suggested that an exclusive stereospecific reaction of either enamine with water (pKa 14) may "lead selectively and irreversibly" to the two enantiomeric products via iminium ions "being counter-balanced by a hydroxy group [*sic*]".

(25) Ponath, S.; Menger, M.; Grothues, L.; Weber, M.; Lentz, D.; Strohmann, C.; Christmann, M. Mechanistic Studies on the Organocatalytic α-Chlorination of Aldehydes: The Role and Nature of Off-Cycle Intermediates. *Angew. Chem. Int. Ed.* **2018**, *57*, 11683–11687.

(26) Burés, J.; Armstrong, A.; Blackmond, D. G. Explaining Anomalies in Enamine Catalysis: "Downstream Species" as a New Paradigm for Stereocontrol. *Acc. Chem. Res.* **2016**, *49*, 214–222.

(27) a) Burés, J.; Dingwall, P.; Armstrong, A.; Blackmond, D. G. Rationalization of an Unusual Solvent-Induced Inversion of Enantiomeric Excess in Organocatalytic Selenylation of Aldehydes. *Angew. Chem. Int. Ed.* **2014**, *53*, 8700–8704.

(28) Wiest, J. The Role of Charged and Uncharged Intermediates in Organocatalysis, MS Thesis, 2012, Universität Basel (conducted in the Blackmond group at The Scripps Research Institute).

(29) a) Alamillo-Ferrer, C.; Nielsen, C. D.-T.; Salzano, A.; Companyó, X.; Di Sanza, R.; Spivey, A. C.; Rzepa, H. S.; Burés, J. Understanding the Diastereopreference of Intermediates in Aminocatalysis: Application to the Chiral Resolution of Lactols. *J. Org. Chem.* **2021**, *86*, 4326–4335; b) Seebach, D.; Sun, X.; Ebert, M.-O.; Schweizer, W. B.; Purkayastha, N.; Beck, A. K.; Duschmalé, J.; Wennemers, H.; Mukaiyama, T.; Benohoud, M.; Hayashi, Y.; Reiher, M. Stoichiometric Reactions of Enamines Derived from Diphenylprolinol Silyl Ethers with Nitro Olefins and Lessons for the Corresponding Organocatalytic Conversions – a Survey. *Helv. Chim. Acta* **2013**, *96*, 799–852; c) Seebach, D.; Grošelj, U.; Badine, D. M.; Schweizer, W. B.; Beck, A. K. Isolation and X-Ray Structures of Reactive Intermediates of Organocatalysis with Diphenylprolinol Ethers and with Imidazolidinones. *Helv. Chim. Acta* **2008**, *91*, 1999–2034.

(30) a) Seeman, J. I. Effect of Conformational Change on Reactivity in Organic Chemistry. Evaluations, Applications, and Extensions of Curtin-Hammett Winstein-Holness Kinetics. *Chem. Rev.* **1983**, *83*, 83–134; b) Seeman, J. I. The Curtin-Hammett Principle and the Winstein-Holness Equation: New Definition and Recent Extensions to Classical Concepts. *J. Chem. Educ.* **1986**, *63*, 42–48; c) Chakraborty, S.; Saha, C. The Curtin–Hammett Principle. A Qualitative Understanding. *Resonance* **2016**, *21*, 151–171.

(31) Singleton, D. A.; Thomas, A. A. High-Precision Simultaneous Determination of Multiple Small Kinetic Isotope Effects at Natural Abundance. *J. Am. Chem. Soc.* **1995**, *117*, 9357–9358.

(32) a) Becke, A. D. Density-Functional Thermochemistry. III. The Role of Exact Exchange. *J. Chem. Phys.* **1993**, *98*, 5648–5652; b) Stephens, P. J.; Devlin, F. J.; Chabalowski, C. F.; Frisch, M. J. Ab Initio Calculation of Vibrational Absorption and Circular Dichroism Spectra Using Density Functional Force Fields. *J. Phys. Chem.* **1994**, *98*, 11623–11627; c) Lee, C.; Yang, W.; Parr, R. G. Development of the Colle-Salvetti Correlation-Energy Formula into a Functional of the Electron Density. *Phys. Rev. B* **1988**, *37*, 785–789.

(33) Hariharan, P. C.; Pople, J. A. The Influence of Polarization Functions on Molecular Orbital Hydrogenation Energies. *Theoret. Chim. Acta* **1973**, *28*, 213–222.

(34) Tomasi, J.; Mennucci, B.; Cammi, R. Quantum Mechanical Continuum Solvation Models. *Chem. Rev.* **2005**, *105*, 2999–3093.

(35) Frisch, M. J.; Trucks, G. W.; Schlegel, H. B.; Scuseria, G. E.; Robb, M. A.; Cheeseman, J. R.; Scalmani, G.; Barone, V.; Petersson, G. A.; Nakatsuji, H.; Li, X.; Caricato, M.; Marenich, A. V.; Bloino, J.; Janesko, B. G.; Gomperts, R.; Mennucci, B.; Hratchian, H. P.; Ortiz, J. V.; Izmaylov, A. F.; Sonnenberg, J. L.; Williams-Young, D.; Ding, F.; Lipparini, F.; Egidi, F.; Goings, J.; Peng, B.; Petrone, A.; Henderson, T.; Ranasinghe, D.; Zakrzewski, V. G.; Gao, J.; Rega, N.; Zheng, G.; Liang, W.; Hada, M.; Ehara, M.; Toyota, K.; Fukuda, R.; Hasegawa, J.; Ishida, M.; Nakajima, T.; Honda, Y.; Kitao, O.; Nakai, H.; Vreven, T.; Throssell, K.; Montgomery, J. A., Jr.; Peralta, J. E.; Ogliaro, F.; Bearpark, M. J.; Heyd, J. J.; Brothers, E. N.; Kudin, K. N.; Staroverov, V. N.; Keith, T. A.; Kobayashi, R.; Normand, J.; Raghavachari, K.; Rendell, A. P.; Burant, J. C.; Iyengar, S. S.; Tomasi, J.; Cossi, M.; Millam, J. M.; Klene, M.; Adamo, C.; Cammi, R.; Ochterski, J. W.; Martin, R. L.; Morokuma, K.; Farkas, O.; Foresman, J. B.; Fox, D. J. Gaussian 16, Revision C.01; Gaussian, Inc., Wallingford CT, 2016.

(36) a) Grimme, S.; Antony, J.; Ehrlich, S.; Krieg, H. A Consistent and Accurate ab initio Parametrization of Density Functional Dispersion Correction (DFT-D) for the 94 Elements H-Pu. *J. Chem. Phys.* **2010**, *132*, 154104; b) Grimme, S.; Ehrlich, S.; Goerigk, L. Effect of the Damping Function in Dispersion Corrected Density Functional Theory. *J. Comput. Chem.* **2011**, *32*, 1456–1465.

(37) Grimme, S. Supramolecular Binding Thermodynamics by Dispersion-Corrected Density Functional Theory. *Chem. Eur. J.* **2012**, *18*, 9955–9964.

(38) a) Zhu, H.; Clemente, F. R.; Houk, K. N.; Meyer, M. P. Rate Limiting Step Precedes C–C Bond Formation in the Archetypical Proline-Catalyzed Intramolecular Aldol Reaction. *J. Am. Chem. Soc.* **2009**, *131*, 1632–1633; b) Xu, H.; Zuend, S. J.; Woll, M. G.; Tao, Y.; Jacobsen, E. N. Asymmetric Cooperative Catalysis of Strong Brønsted Acid–Promoted Reactions Using Chiral Ureas. *Science* **2010**, *327*, 986–990; c) Klausen, R. S.; Kennedy, C. R.; Hyde, A. M.; Jacobsen, E. N. Chiral Thioureas Promote Enantioselective Pictet–Spengler Cyclization by Stabilizing Every Intermediate and Transition State in the Carboxylic Acid-Catalyzed Reaction. *J. Am. Chem. Soc.* **2017**, *139*, 12299–12309; d) Roytman, V. A.; Karugu, R. W.; Hong, Y.; Hirschi, J. S.; Vetticatt, M. J. ^{13}C Kinetic Isotope Effects as a Quantitative Probe To Distinguish between Enol and Enamine Mechanisms in Aminocatalysis. *Chem. Eur. J.* **2018**, *24*, 8098–8102.

(39) Ashley, M. A.; Hirschi, J. S.; Izzo, J. A.; Vetticatt, M. J. Isotope Effects Reveal the Mechanism of Enamine Formation in L-Proline-Catalyzed α-Amination of Aldehydes *J. Am. Chem. Soc.* **2016**, *138*, 1756–1759.

(40) Considering that there are errors (~0.5 kcal mol^{-1}) associated with the computed energetics of the reaction coordinate, the slight discrepancy between experimental and predicted KIEs for the carbonyl carbon is not significant.

(41) See reference (39) for a similar E2-elimination step in an α-amination reaction catalyzed by L-proline.

(42) a) Frantz, D. E.; Singleton, D. A.; Snyder, J. P. ^{13}C Kinetic Isotope Effects for the Addition of Lithium Dibutylcuprate to Cyclohexenone. Reductive Elimination Is Rate-Determining. *J. Am. Chem. Soc.* **1997**, *119*, 3383–3384; b) Singleton, D. A.; Schulmeier, B. E. Evidence for a Concerted Mechanism in a Palladium Trimethylenemethane Cycloaddition. *J. Am. Chem. Soc.* **1999**, *121*, 9313–9317; c) Frantz, D. E.; Singleton, D. A. Isotope Effects and the Mechanism of Chlorotrimethylsilane-Mediated Addition of Cuprates to Enones. *J. Am. Chem. Soc.* **2000**, *122*, 3288–3295; d) Bandar, J. S.; Sauer, G. S.; Wulff, W. D.; Lambert, T. H.; Vetticatt, M. J. Transition State Analysis of Enantioselective Brønsted Base Catalysis by Chiral Cyclopropenimines. *J. Am. Chem. Soc.* **2014**, *136*, 10700–10707.

(43) a) Schmid, M. B.; Zeitler, K.; Gschwind, R. M. The Elusive Enamine Intermediate in Proline-Catalyzed Aldol Reactions: NMR Detection, Formation Pathway, and Stabilization Trends. *Angew. Chem. Int. Ed.* **2010**, *49*, 4997–5003; b) Schmid, M. B.; Zeitler, K.; Gschwind, R. M. Distinct Conformational Preferences of Prolinol and Prolinol Ether Enamines in Solution Revealed by NMR. *Chem. Sci.* **2011**, *2*, 1793–1803.

(44) Mayr, H.; Ofial, A. R.; Würthwein, E.-U.; Aust, N. C. NMR Spectroscopic Evidence for the Structure of Iminium Ion Pairs. *J. Am. Chem. Soc.* **1997**, *119*, 12727–12733.

(45) Seeman, J. I.; Farone, W. A. Analytical Solution to the Curtin-Hammett/Winstein-Holness Kinetic System. *J. Org. Chem.* **1978**, *43*, 1854–1864.

(46) Jimeno, C.; Cao, L.; Renaud, P. Trichloromethanesulfonyl Chloride: A Chlorinating Reagent for Aldehydes. *J. Org. Chem.* **2016**, *81*, 1251–1255.

(47) Hayes, M. D.; Rodríguez-Alvarado, M.; Brenner-Moyer, S. E. An Organocascade Approach to α,α-Chlorofluoroalcohols. *Tetrahedron Lett.* **2015**, *56*, 4718–4720.

(48) a) Warnke, S.; Helden, G. von; Pagel, K. Analyzing the Higher Order Structure of Proteins with Conformer-Selective Ultraviolet Photodissociation. *Proteomics* **2015**, *15*, 2804–2812; b) Hoffmann, W.; Langenhan, J.; Huhmann, S.; Moschner, J.; Chang, R.; Accorsi, M.; Seo, J.; Rademann, J.; Meijer, G.; Koksch, B.; Bowers, M. T.; Helden, G. von; Pagel, K. An Intrinsic Hydrophobicity Scale for Amino Acids and Its Application to Fluorinated Compounds. *Angew. Chem. Int. Ed.* **2019**, *58*, 8216–8220.

(49) Supady, A.; Blum, V.; Baldauf, C. First-Principles Molecular Structure Search with a Genetic Algorithm. *J. Chem. Inf. Model.* **2015**, *55*, 2338–2348.

(50) a) Adamo, C.; Barone, V. Toward Reliable Density Functional Methods without Adjustable Parameters: The PBEo Model. *J. Chem. Phys.* **1999**, *110*, 6158–6170; b) Mesleh, M. F.; Hunter, J. M.; Shvartsburg; Schatz G. C.; Jarrold, M. F. Structural Information from Ion Mobility Measurements: Effects of the Long-Range Potential. *J. Phys. Chem.* **1996**, *100*, 16082–16086.

(51) a) Ilgen, J.; Kaltschnee, L.; Thiele, C. M. PerfectBASH: Band-Selective Homonuclear Decoupling in Peptides and Peptidomimetics. *Magn. Reson. Chem.* **2018**, *56*, 918–933; b) Ilgen, J.; Nowag, J.; Kaltschnee, L.; Schmidts, V.; Thiele, C. M. Gradient Selected Pure Shift EASY-ROESY Techniques Facilitate the Quantitative Measurement of ^{1}H, ^{1}H-Distance Restraints in Congested Spectral Regions. *J. Magn. Reson.* **2021**, *324*, 106900.

(52) a) Seebach, D.; Sun, X.; Sparr, C.; Ebert, M.-O.; Schweizer, W. B.; Beck, A. K. 1,2-Oxazine *N*-Oxides as Catalyst Resting States in Michael Additions of Aldehydes to Nitro Olefins Organocatalyzed by α,α-Diphenylprolinol Trimethylsilyl Ether. *Helv. Chim. Acta* **2012**, *95*, 1064–1078; b) Cassani, C.; Melchiorre, P. Direct Catalytic Enantioselective Vinylogous Aldol Reaction of α-Branched Enals with Isatins. *Org. Lett.* **2012**, *14*, 5590–5593; c) Weber, A. K.; Schachtner, J.; Fichtler, R.; Leermann, T. M.; Neudörfl, J. M.; von Wangelin, A. J. Modular Synthesis of Cyclic *cis*- and *trans*-1,2-Diamine Derivatives. *Org. Biomol. Chem.* **2014**, *12*, 5267–5277; d) Gurubrahamam, R.; Chen, Y. M.; Huang, W.-Y.; Chan, Y.-T.; Chang, H.-K.; Tsai, M.-K.; Chen, K. Dihydrooxazine *N*-Oxide Intermediates as Resting States in Organocatalytic Kinetic Resolution of Functionalized Nitroallylic Amines with Aldehydes. *Org. Lett.* **2016**, *18*, 3046–3049; e) Boeckman Junior, R. K.; Wang, H.; Rugg, K. W.; Genung, N. E.; Chen, K.; Ryder, T. R. A Scalable Total Synthesis of (–)-Nakadomarin A. *Org. Lett.* **2016**, *18*, 6136–6139.

(53) Lodewyk, M. W.; Siebert, M. R.; Tantillo, D. J. Computational Prediction of ^{1}H and ^{13}C Chemical Shifts: a Useful Tool for Natural Product, Mechanistic, and Synthetic Organic Chemistry. *Chem. Rev.* **2012**, *112*, 1839–1862.

(54) References NBO method: (B3LYP-D3(BJ)/6-31g(d,p), io(3/32=2), 219.15 K, with a Fine grid); a) Foster, J. P.; Weinhold, F. Natural Hybrid Orbitals. *J. Am. Chem. Soc.* **1980**,*102*, 7211–7218; b) Reed, A. E.; Weinhold, F. Natural Bond Orbital Analysis of Near-Hartree–Fock Water Dimer. *J. Chem. Phys.* **1983**, *78*, 4066–4073; c) Reed, A. E.; Weinstock, R. B.; Weinhold, F. Natural Population Analysis. *J. Chem. Phys.* **1985**, *83*, 735–746; d) Reed, A. E.; Weinhold, F. Natural Localized Molecular Orbitals. *J. Chem. Phys.* **1985**, *83*, 1736–1740; e) J. E. Carpenter, Extension of Lewis structure concepts to open-shell and excited-state molecular species, Ph.D. thesis, University of Wisconsin, Madison, WI, 1987; f) Carpenter, J. E.; Weinhold, F. Analysis of the Geometry of the Hydroxymethyl Radical by the "Different Hybrids for Different Spins" Natural Bond Orbital Procedure. *J. Mol. Struct. THEOCHEM* **1988**, *139*, 41–62; g) Reed, A. E.; Curtiss, L. A.; Weinhold, F. Intermolecular Interactions from a Natural Bond Orbital, Donor-Acceptor Viewpoint. *Chem. Rev.* **1988**, *88*, 899–926; h) Weinhold, F. and Carpenter, J. E. in The Structure of Small Molecules and Ions, Naaman, E. R.; Vager, Z. Plenum, 1988, 227–236.

1.4. Summary and Outlook

The two previously mentioned publications made a decisive contribution to the understanding of the reaction mechanism of the organocatalyzed α-chlorination of aldehydes. A better understanding of the stabilizing interactions within stable aminal intermediates was achieved by rigorous characterization and follow-up experiments with these species. Moreover, the synthetic value of this reaction was demonstrated by its application in the synthesis of chiral compounds.

A first mechanistic idea allowed the definition of factors whose modification could have an influence on the reaction mechanism. The modified steric environment of newly designed and synthesized imidazolidinone-based catalysts did not lead to the desired result. The reaction accelerating effect of *Brønsted* acid could be confirmed as expected. Interestingly, the choice and combination of acids plays a crucial role. Thus, a 1:2 mixture of TFA and acetic acid was slightly superior to pure TFA. This observation suggests that acetic acid plays a role beside only being a proton source. However, the most significant effect was obtained by modifying the chlorinating agent. By comparing electron-rich imides such as the tetramethylated analog of NCS (Me_4NCS) and electron-poor derivatives such as nitrated NCP (NO_2NCP), the notion postulated at the outset was confirmed. Electron-deficient chlorinating reagents almost completely suppressed the accumulation of the parasitic intermediates and allowed the reaction to proceed in a much shorter reaction time. On the other hand, electron-rich derivatives provided rapid accumulation of much more stable aminals. ^{1}H NMR studies could proof that the maximum product concentration was significantly lower than with electron-deficient chlorinating reagents. In combination with a slightly modified imidazolidinone catalyst and additives, an improved catalytic system with significantly reduced catalyst loading was presented, showing broad functional group tolerance. In addition, aminal intermediates previously identified only by NMR spectroscopy[28,30] could be isolated and fully characterized. Single crystal structure analysis allowed the relative and absolute stereoconfiguration to be elucidated for the first time. The isolation of this species also allowed decomposition experiments to be carried out, thus defining its role in the catalytic cycle. For this purpose, the intermediate was first exposed to standard reaction conditions. As in the previously performed time-dependent NMR studies, almost no decomposition was observed even with longer reaction times. Only after increasing the equivalents of TFA and water, the aminal decomposes effectively. By using deuterated TFA and deuterated water, the decomposition mechanism could be further studied. Initially, no deuterium incorporation into the α-position could be detected. This finding rules out decomposition via E2 elimination to chloroamine as postulated by *Blackmond*[30] and supports the decomposition mechanism via a chloroiminium ion.

Subsequent intensive scientific discussion with *Burés*, *Armstrong*, and *Blackmond* led to a thorough examination and reflection of all previous research results and motivated us to once again question the interpretation of our own research and to conduct renewed mechanistic studies. In addition to the already studied *MacMillan* aminals, the *Jørgensen* aminals, which were considered in the publication "Curtin-Hammett Paradigm for Stereocontrol in Organocatalysis by Diarylprolinol Ether Catalysis",[30] were comprehensively investigated.

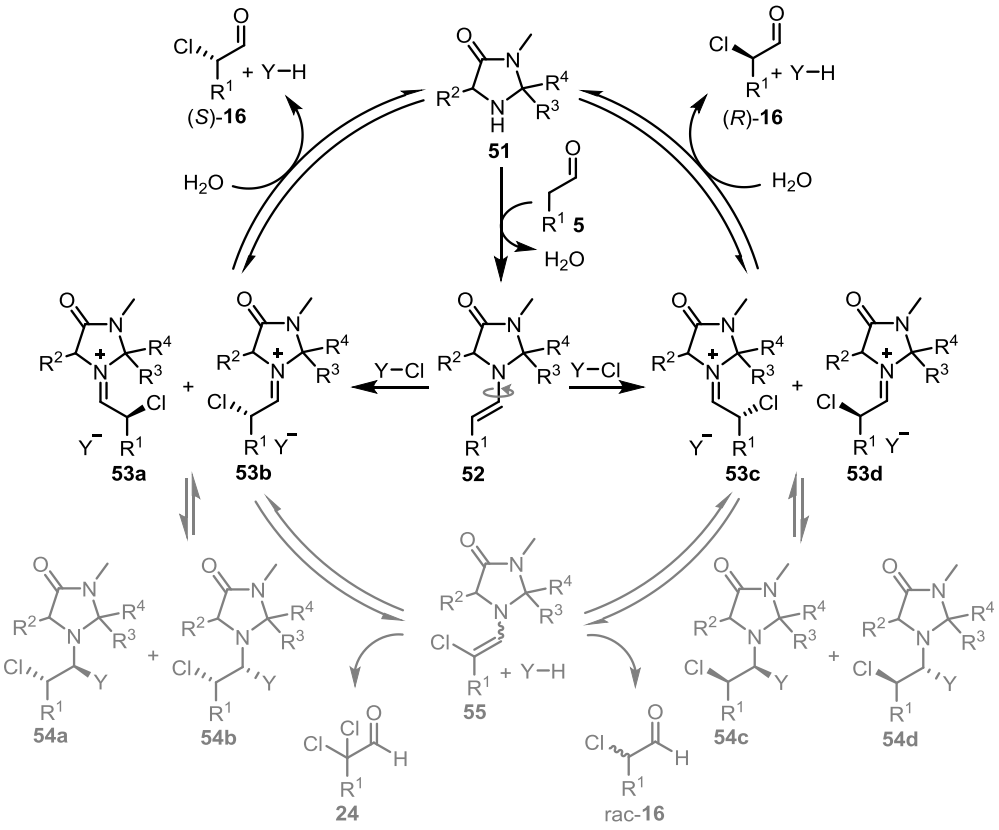

Scheme 17: Final concept of the catalytic cycle for imidazolidinone catalysts.

For the *MacMillan* catalyst **18**, a combination of isotopic competition experiments, calculated and experimental KIE values, and calculated transition states surprisingly demonstrated that the first irreversible step precedes the C-Cl bond formation. The stereoinducing step in this scenario is represented by the nucleophilic attack of the enamine **52** to the electrophilic chlorinating reagent Y-Cl. The rotational preference of the (*E*)-enamine **52** is defined by the choice of catalyst (R^2, R^3 and R^4) and thus by the relative energies of the rotamers. Which rotamer reacts in the subsequent step depends on the energies of the transition states for the C-Cl bond linkage. The four possible diastereomeric chloroiminium ions **53a**-**d** are trifurcation points. First, direct hydrolysis to the desired products (*S*)-**16** and (*R*)-**16** can occur. Here, the accelerating influence of *Brønsted* acids as additives can be particularly emphasized. Depending on the reaction conditions and the type of catalyst, a reverse reaction can take place, which can lead to racemization (rac-**16**) or double chlorination (**24**) of

the aldehyde via the formation of the planar enamine **55**. By addition of the anion of the chlorinating reagent (Y^-), the chloroiminium ions can generate the four diastereomeric aminals **54a**-**d**. Whether and to what extent the formation of the different aminals proceeds can be influenced by the modification of the chlorinating agent (Y-Cl), the structure of the catalyst and additives. Moreover, this reactivity is in direct competition to the hydrolysis of the chloroiminium ions. Consequently, favored hydrolysis can also suppress accumulation of the intermediates. For the entire catalytic cycle to proceed efficiently, all of the processes shown in grey (Scheme 17) should be suppressed. Which of the processes discussed here really proceeds is dependent on the selected reaction conditions. The nature of the catalyst, the chlorinating reagent, additives or the temperature can have an enormous influence on the reaction events and thus, for example, suppress or favor dichlorination, racemization or the formation of one or more diastereomeric aminals.

Numerous aminals with the 1st (**14**), 2nd (**19**) and 3rd (**18**) generation *MacMillan* catalysts could be isolated, the respective diastereomers separated and all compounds fully characterized for the first time. This made it possible to revise the *syn* and *anti* assignment of *MacMillan* aminal diastereomers made in the literature and to characterize additional diastereomers that had previously been overlooked.[21,41] Ion mobility mass spectrometry with aliquots from the reaction mixture and with isolated aminals shed more light on the stereochemical course of the reaction and the decomposition process of the aminals. In combination with the previously mentioned experiments and a comprehensive consideration of the kinetic profile, a *Curtin-Hammett* scenario for the reaction with *MacMillan* catalysts could be ruled out. Most of the corresponding aminals are stable off-cycle intermediates, as anticipated at the beginning of these studies. Interconversion processes, according to the *Curtin-Hammett* scenario could be excluded beyond doubt.

Aminals arising from the *Jørgensen* catalysts showed significantly lower stability than the corresponding *MacMillan* aminals. Decomposition experiments were able to rule out E2 elimination in analogy to the *MacMillan* aminals. In addition, these experiments could show that only one enantiomer of the chloroaldehyde emerges from the two aminal species and not both, as in the *Curtin-Hammett* scenario. *In situ* reduction and functionalization of the formed aminals (**42a**) led to increased stability and made the isolation of the *Jørgensen* aminals possible for the first time. Subsequent X-ray crystal structure analysis revealed a *syn* configuration of the major aminal isomer, in contrast to the *anti* assignment made in the *Curtin-Hammett* scenario. A comparison between the calculated NMR data of a wide range of isomers, which were also calculated, and the experimental NMR data of the two aminal species could refute the *anti* configuration of the major isomer *anti*-**42a** and confirm a *syn* configuration between the chlorine atom and the phthalimide substituent. Additionally, the combination of calculated isomers and NMR-data revealed a *syn* configuration also for the minor

aminal. Interestingly the major and minor species turned out to be rotamers (*ap-syn*-**42a** and *sc-exo-syn*-**42a**) at the bulky substituent of the pyrrolidine catalyst. These findings are summarized in Scheme 18.

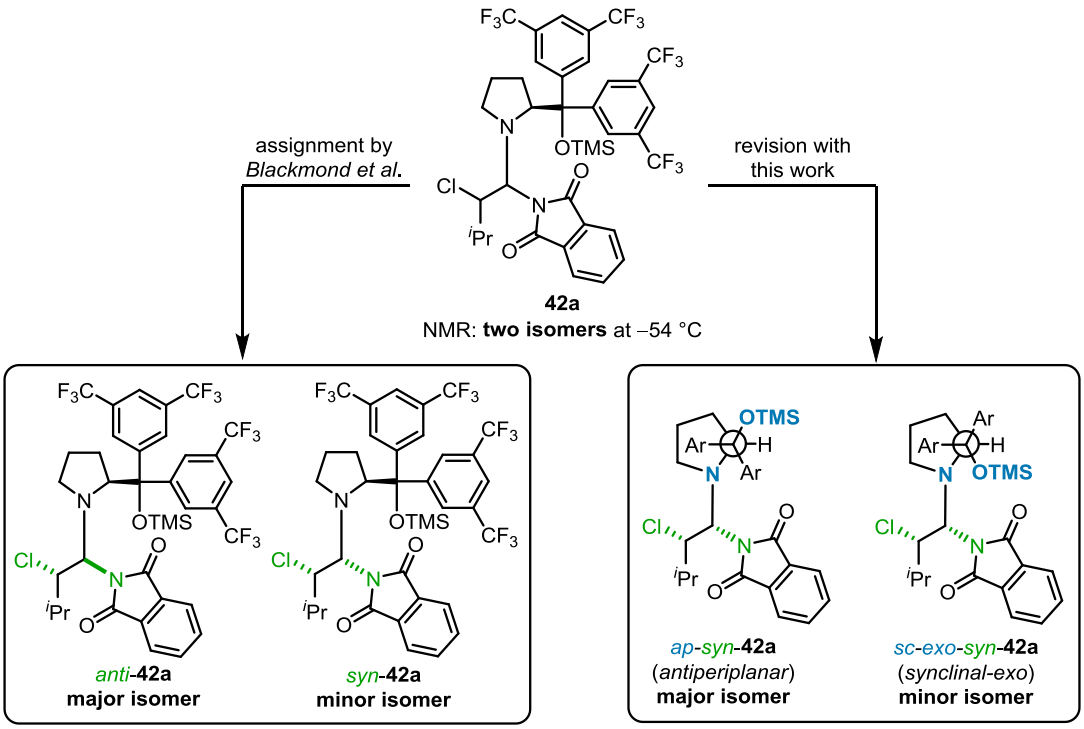

Scheme 18: Assignment of the two aminal species according to *Blackmond*[30,41] and revised structures according to the present work.

The sum and diversity of all experiments and the unambiguous results for both, the *MacMillan* and the *Jørgensen* system, leaves no doubt about the incorrect assignment of numerous aminal intermediates[30,41] and the absence of a *Curtin-Hammett* scenario.

This work shows how powerful a reasonable combination of diverse chemical methods can be. Approved synthetic methods, such as the isolation of intermediates for crystal structure analysis or decomposition experiments, go hand in hand with various modern techniques such as KIE measurements and ion mobility spectrometry. These experimental methods were complemented at various points by DFT-based calculations. The reliability of the interpretation is increased by the combination of the methods and their consistent results. Any misinterpretations thus become much less likely. This approach also promotes exchange between related disciplines and research groups and can be exemplary for the future elucidation of unknown or controversial reaction mechanisms. A deeper understanding of the chemical processes involved can improve manufacturing processes and, in some cases, make them possible in the first place.

1.5. Further Results

The previously developed Cl^+ species and their halogen analogues, were shown to have profitable properties over the traditionally used reagents NXS and NXP (X = Cl, Br, I) in further work by the group of *Christmann* and *Heretsch*. In addition, the applicability of the modified organocatalytic α-chlorination of aldehydes was demonstrated in the synthesis of chiral organic molecules.

Triazoles

Triazoles as structural motifs can be found in numerous products such as drugs, functional materials or agrochemicals.[50] The properties and uses as ligands in coordination chemistry have also been extensively studied.[51] As shown in Scheme 19, two regioisomeric bistriazoles should be synthesized from one common chiral precursor (in the course of the synthesis two different *pseudo*-enantiomeric catalysts (**62** and ent-**18**), which generate the enantiomeric bis-chlorohydrins **57** and ent-**57** were used; the use of one catalyst would generate one common chiral precursor).

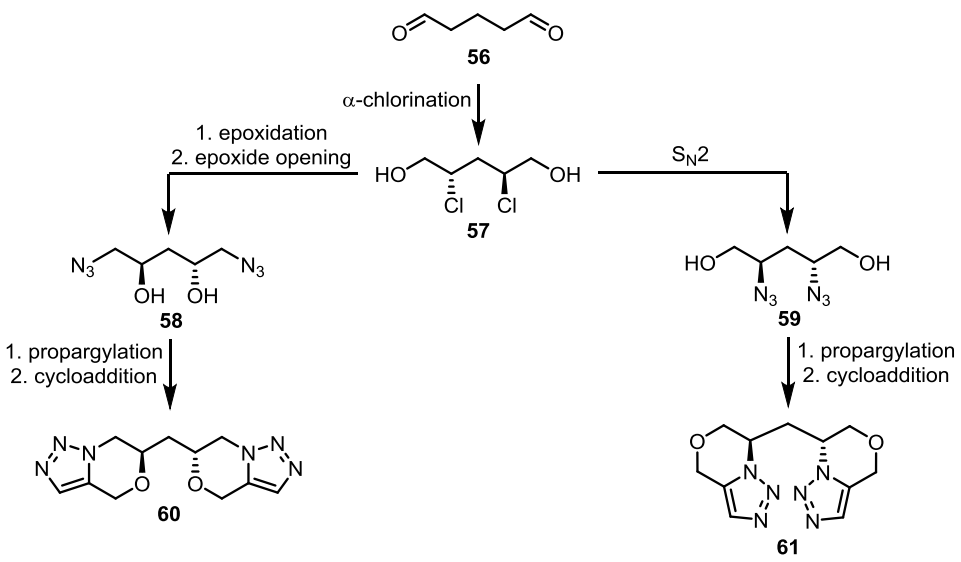

Scheme 19: Synthesis of the two chiral bistriazoles **60** and **61**.

The previously investigated α-chlorination of aldehydes should ensure the correct installation of the two stereocenters and prove its potential as an efficient transformation. The subsequent bifurcation, leading to the regioisomeric bistriazoles **60** and **61**, should be accomplished by direct azide substitution or epoxidation and epoxide opening of the chiral bis-chlorohydrin **57**. Part of the synthetic route to regioisomer **60** was inspired by a publication of *Mekni* and *Baklouti*.[52]

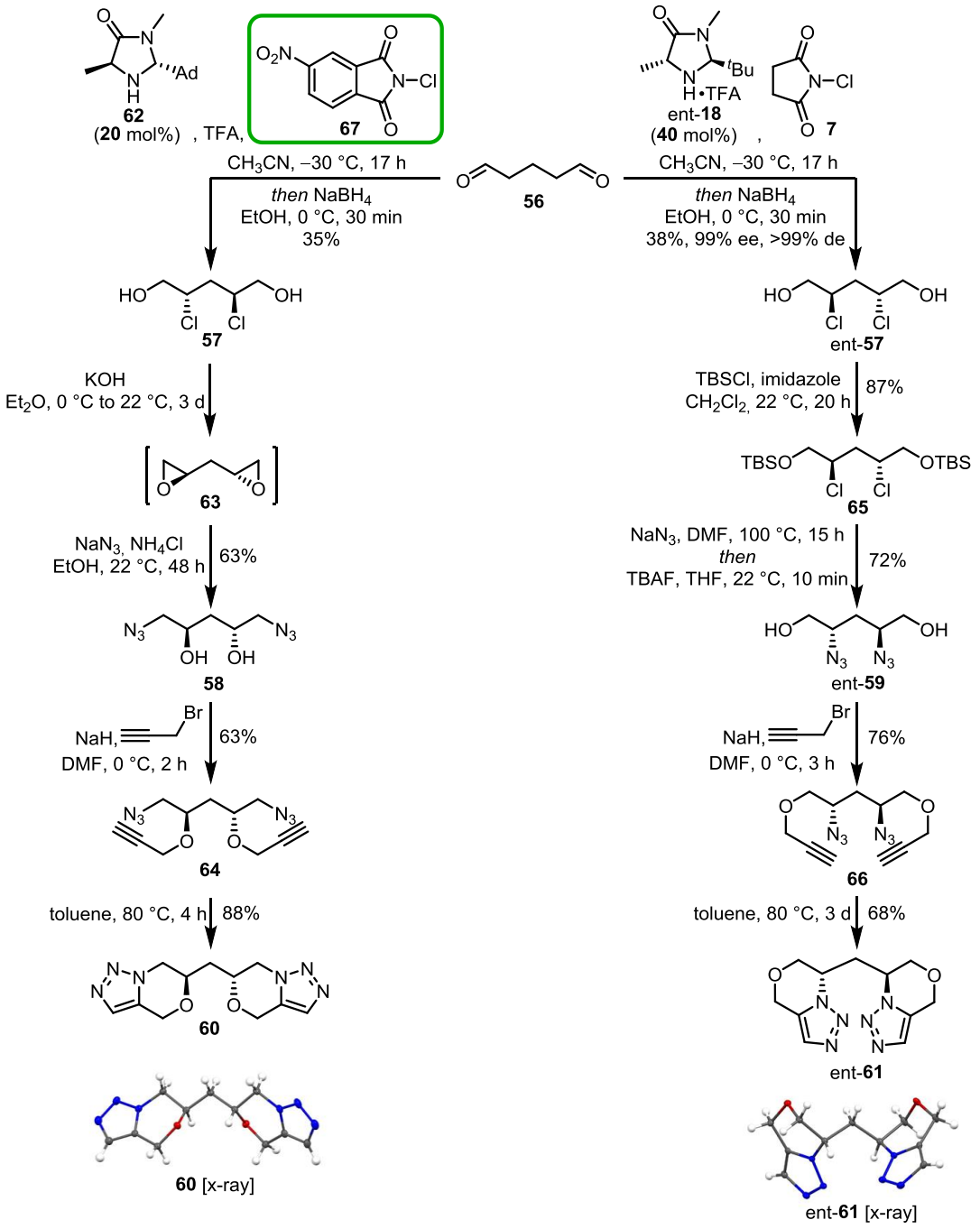

Scheme 20: Synthesis of the two chiral bistriazoles **60** and **61**.

As shown in Scheme 20, the two bistriazoles **60** and ent-**61** could be successfully synthesized in four and five steps, starting from inexpensive glutaraldehyde **56**. In the first step, chiral chlorohydrin ent-**57** was obtained by an organocatalytic α-chlorination of aldehydes followed by reduction in moderate yield of 38% and excellent diastereo- and enantioselectivity. The use of the modified catalytic system consisting of catalyst **62** and the chlorinating reagent NO_2NCP (**67**) allowed a reduction of the catalyst loading from 20 to 10 mol% per functional group with almost identical yield (35%). At this bifurcation point diazide **58** could first be synthesized by twofold inversion of the stereocenters in a one-pot

reaction (epoxidation and epoxide opening) with a yield of 63%. The regioisomeric diazide ent-**59** was accessed by TBS protection of the free alcohols followed by a one-pot azide substitution and deprotection in a good overall yield of 63%. Unfortunately, the direct substitution of chlorohydrin ent-**57** was not possible. It was suspected that the harsh conditions of the azide substitution could lead to ring closure reactions.[53] Subsequent propargylation generated the two regioisomeric propargyl ethers **64** and **66** in 63% and 76% yield, respectively. In the last step, an intramolecular 1,3-dipolar cycloaddition afforded the two regioisomeric bistriazoles **60** and ent-**61** in 88% and 68% yields, respectively. The absolute configuration of the two compounds could be confirmed by single crystal structure analysis.

Both triazoles **60** and ent-**61** can also be precursors for carbenes and offer subsequent coordination to metal-centers (Scheme 21).[54] The presented synthesis enables multiple variations to modify the bistriazoles. The large bite angle (α) of mesionic carbene **68** can in priciple be compressed by two additional substituents (R^1) on the carbon backbone (*Thorpe-Ingold* effect[55]) (Scheme 21, **70**). Using a suitable starting material would be the easiest way to introduce these substituents. The same compressing effect might be achieved by shortening the connection between the oxygen atom and the triazole scaffold (Scheme 21, **69**). Thus the previously performed propargylation of the free alcohols should be substituted by alkynylation of the two hydroxyl groups.[56] In future studies bistriazoles and mesoionic carbenes with different bite angles can be investigated by means of coordination modes to different sized metal centers.

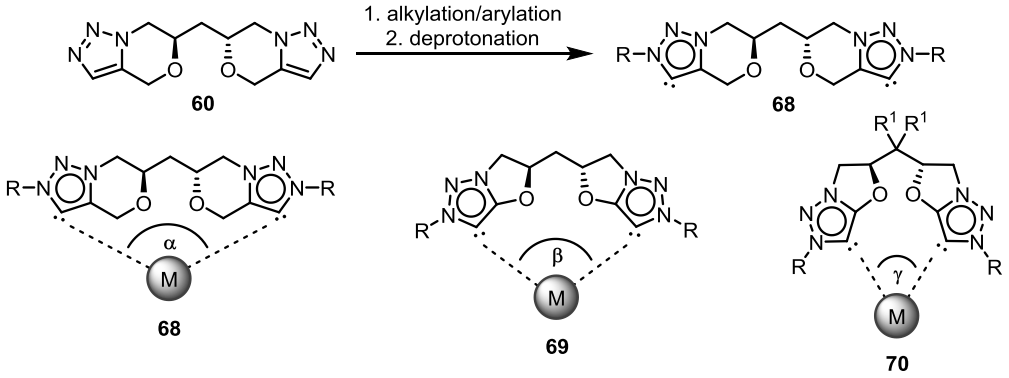

Scheme 21: Possibilities for tuning of the bite angle of mesoionic carbene **68** (α>β>γ).

Allylic Chlorination

The strongly electrophilic chlorinating reagent NO_2NCP (**67**) showed significantly increased reactivity (compared to NCS and NCP) toward unsaturated compounds. For example, in the organocatalytic α-

chlorination of citronellal, it was observed that the electron-rich double bond of this substrate generates the corresponding allyl chloride **72** as a side reaction (Scheme 22, top). In a bachelor thesis supervised by me, it was subsequently shown that numerous olefins react to the corresponding allyl chlorides without further activation.[57] Using the electron-rich aromatic 1,3,5-trimethoxybenzene (**73**) as an internal standard in a ^{1}H NMR kinetic measurement, electrophilic aromatic substitution was observed over time. The three aromatic protons were substituted successively by the chlorine atoms of NO_2NCP in the course of the reaction (Scheme 22, bottom). The corresponding iodine and bromine derivatives of NO_2NCP were also successfully synthesized and a similar reactivity towards olefins was demonstrated.

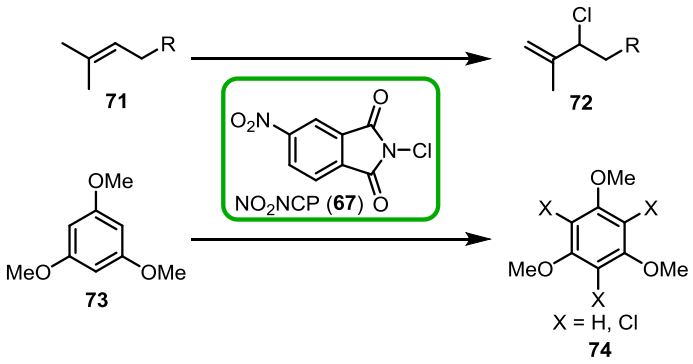

Scheme 22: Allylic chlorination of olefins (top) and S_EAr for electron-rich aromatic compounds (bottom).

Total Synthesis of Dichrocephon A and B

In the course of the first total syntheses of dichrocephon A and B, a chemoselective bromination of the terminal alkyne of compound **75** was envisioned (Scheme 23).[58] With NBS as a brominating reagent, good yields could only be obtained by using stoichiometric amounts of $AgNO_3$. Lowering the catalyst loading to 0.5 equivalents led to a significant drop of the yield and the formation of side products. Only by using NO_2NBP (**77**) it was possible to reduce the amount of silver salt to a catalytic value of 5 mol%. In addition, the yield could be increased from 32% to 91%.[59]

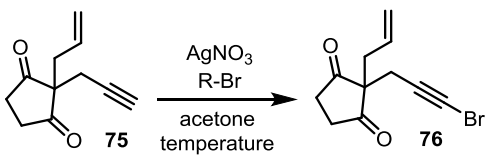

$AgNO_3$ (eq.)	R-Br	temperature	yield
1	NBS	0 °C	79%
0.5	NBS	0 °C	32%
1	NO_2NBP	0 °C	85%
0.05	NO_2NBP	rt	91%

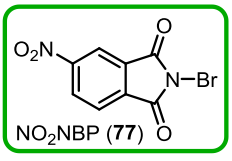

Scheme 23: NO_2NBP as a superior alternative to NBS in the chemoselective bromination of terminal alkynes.

Photocatalytic C-H-Functionalization

In a recent publication by the two groups of *Heretsch* and *Christmann* on the design and use of a self-developed flow system, a regioselective, photocatalytic C-H chlorination of (+)–sclareolide was investigated as a feasibly application (Scheme 24).[60] The commercially available reagents NCS and NCP initially generated yields in the range of 11–24%. The use of NO_2NCP resulted in a further drop of the yield (6%). Good results (41% yield) were finally achieved with the electron-rich chlorine source Me_4NCS (**79**). The beneficial behavior of electron rich chlorinating reagents can be attributed to the more stable N-H bond of the corresponding imides.[61] The superiority of the newly developed chlorinating reagent **79** could also be reproduced on a gram scale.

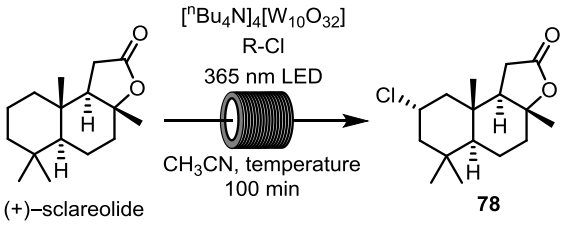

catalyst [mol%]	R-Cl	temperature [°C]	yield [%]
7	NCS	30	24
10	NCP	30	19
10	NO_2NCP	30	6
10	Me_4NCS	0	41

Scheme 24: Photocatalytic C-H-functionalization of (+)–sclareolide.

2. Application of Novel Polyinterhalides in Organic Synthesis

2.1. Introduction

2.1.1. Halogen Bonding

Defined in 2013 by IUPAC,[62] halogen bonding was initially considered to be the interaction between a halogen and a *Lewis* base. In contrast to the traditional nomenclature, the halogens are considered as *Lewis* acidic halogen bridge donors. The *Lewis* bases act as halogen bridge acceptors by providing their electron density. Halogen bridges are not only formed between halogens and *Lewis* bases but also between two halogen species. Halogen bonding can be explained similarly to hydrogen bonding. The main difference, however, is the directional nature of the bond. While hydrogen bonds are non-directional, the halogen bond is formed at a bond angle of 90° or 180°. The reason for the special bonding situation is the σ-hole.[63]

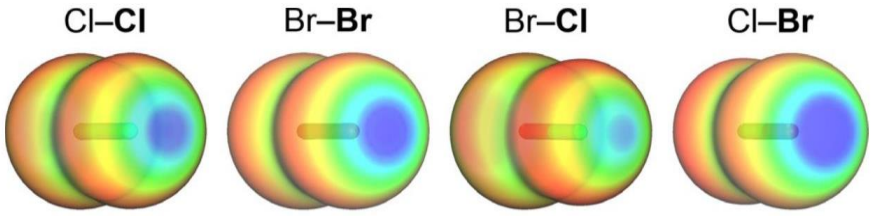

Figure 8: Electrostatic potential of Cl_2, Br_2, and BrCl (red: high electron density, blue: low electron density).[64]

As shown in Figure 8, the electrostatic potential, which reflects the electron distribution in the molecule, is unevenly distributed across the halogen molecules. Rings with areas of larger negative partial charges are formed perpendicular to the bond axis. At the ends, along the bond axis, regions of positive partial charges, the σ-holes, are formed. This anisotropy leads to directional non-covalent halogen bonding with nucleophiles along the bond axis of the halogen species (180°). With electrophiles, interaction occurs perpendicular (90°) to the bond axis. As shown in Figure 8, the intensity of the σ-hole, and thus the electron accepting ability, increases with the atomic radius from chlorine to bromine. While homoatomic dihalogens (Br_2 or Cl_2) show an identical σ-hole at both halogen atoms, interhalogens (BrCl) show a much more pronounced σ-hole at the more electropositive atom.[63] Figure 9 illustrates the different bonding situations between halogen species and nucleophiles or electrophiles and between two halogen species.[65]

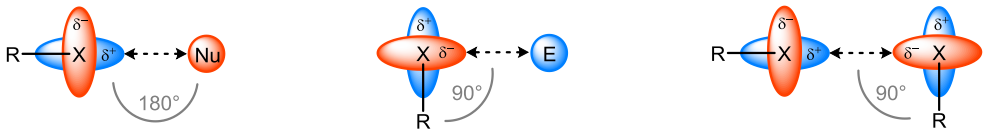

Figure 9: Interaction between halogen and nucleophile (left), between halogen and electrophile (center), and between two halogens (right).

2.1.2. Polyhalides

The importance of halogens and halogenated compounds in the 21st century can hardly be overestimated.[63] Chlorine gas, which comes almost exclusively from the chlorine-alkali electrolysis, is one of the ten most produced inorganic substances worldwide in terms of volume.[66] Chlorine or chlorine-containing compounds play an irreplaceable role in manufacturing processes and end products in most cases. Plastics such as PVC, pharmaceutical products and agrochemicals are just a few examples.[67] The increasing importance of fluorinated products, especially in the field of materials and pharmaceuticals, should also be emphasized here.[68] Beside these substances, which are mostly classified as organohalogen compounds, the interesting class of polyhalogens exists. Polyhalogen compounds can be divided into three categories; neutral (BrCl, IF_7, BrF_3), cationic ($[I_3]^+$, $[Br_3F_8]^+$, $[Br_5]^+$) and anionic ($[Br_9]^-$, $[Br_4]^{2-}$, $[Cl(BrCl)_2]^-$) polyhalogens.[63] A further distinction is made between homoatomic species such as $[I_3]^+$, $[Br_5]^+$ or $[Br_4]^{2-}$ and heteroatomic species (polyinterhalogens) such as $[Br_3F_8]^+$ or $[Cl(BrCl)_2]^-$. The anionic polyinterhalogens will be referred to as polyinterhalides in the following. Among the polyinterhalides, a distinction is made between classical and non-classical species. The former bear an electropositive central atom surrounded by more electronegative halogens ($[IF_6]^-$ or $[ICl_4]^-$). In non-classical polyinterhalides, the central atom is more electronegative than the coordinating diatomic halogen molecules ($[Cl(I_2)_4]^-$ or $[Cl(BrCl)_3]^-$). The distinction is often not clear-cut. For example, the $[IBr_2]^-$ anion can be considered as [Br-I-Br]$^-$ (3-center 4-electron bond analogous to the I^{3-} anion) or as Br^- coordinated by a IBr-molecule (donor-acceptor bond). The choice of the counter cation can influence decisively the structure and geometry of the anion as well as the physical properties of the compound.[63] The structural features of polyinterhalides can be explained by the already mentioned anisotropy of the charge distribution. The exact bonding situation of the non-classical polyinterhalides can be illustrated by the molecular orbital (MO) theory. In Figure 10, the MO scheme for molecular BrCl is shown on the left. It largely corresponds to the MO schemes of the homoatomic dihalogens. The greater electronegativity of chlorine results in the atomic orbitals of chlorine being lower than those of bromine. Unlike homoatomic dihalogens, in this case atomic orbitals of different periods are combined (bromine: 4th period, chlorine: 3rd period). The formation of a non-

classical polyinterhalide such as $[Cl(BrCl)]^-$ (Figure 10, right) occurs via donating a free electron pair of the chloride anion into the LUMO of BrCl. Since this molecular orbital is antibonding, a bond weakening occurs in the BrCl molecule. This phenomenon can be experimentally demonstrated by both single crystal structure analysis and vibrational spectroscopy.[64] Thus, the bonding situation in the polyinterhalide $[Cl(BrCl)]^-$ can be described as a donor-acceptor interaction between Cl^- and BrCl.[63]

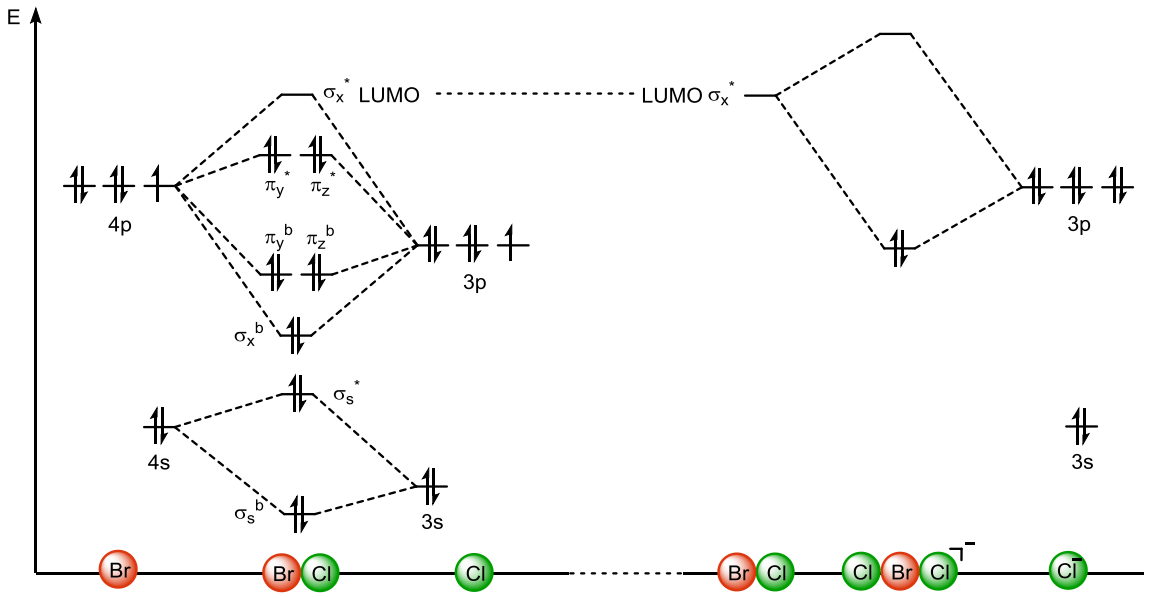

Figure 10: Molecular orbital diagram for the BrCl molecule (left) and for the polyinterhalide $[Cl(BrCl)]^-$ (right).

2.1.3. Polyhalides as Reagents in Organic Chemistry

Due to their better handling (liquid physical state, vapor pressure) and the resulting lower toxic exposure compared to dihalogens, polyhalides found their way into organic synthesis. Nonabromides, for example, are reliable bromination reagents with better selectivities compared to elemental bromine.[69] Analogously, the use of trichlorides is also described.[70] The use of BrCl in organic chemistry is mostly limited to its application as an interhalogenation reagent for unsaturated substrates and not widely used.[71] Despite its high reactivity and perfect atomic economy, its gaseous physical state and high toxicity, degrade BrCl to an inconvenient reagent. Another drawback is the limited storability, which is a result of the equilibrium reaction between BrCl and Br_2/Cl_2.[64] Due to the different vapor pressures, elemental bromine accumulates, which alters the stoichiometry between bromine and chlorine in the compound and decreases the selectivity for the use as a reagent. Thus, dual brominated and chlorinated by-products are generated in the reaction with olefins.

Figure 11: Gaseous BrCl (left)[72] and the ionic liquid $[NEt_3Me][Cl(BrCl)_2]$ (right)[73].

Due to the drawbacks of elementary BrCl, two-component systems with common reagents were established as alternatives.[74] Pioneering work on the enantioselective bromochlorination of olefins is known from the group of *Burns*.[75] Various allylic alcohols (**80**) were converted into the corresponding chiral bromochlorides (**83**) in excellent chemo- and enantioselectivities by using NBS (**81**), chlorotitanium triisopropoxide and the chiral *Schiff* base **82** as the catalyst (Scheme 25).

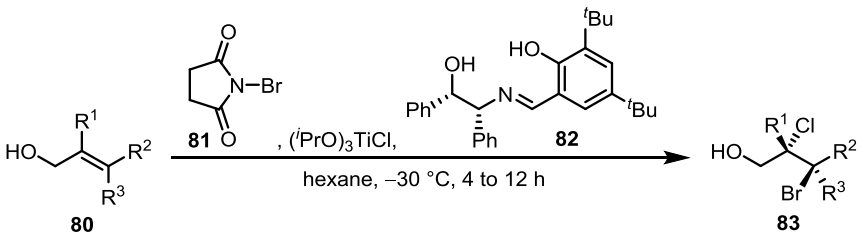

Scheme 25: Chemo- und enantioselective bromochlorination according to *Burns.*

The BrCl molecule has a more distinct σ-hole compared to Br_2 or Cl_2 (Figure 8), which favors the formation of halogen bonds. Therefore, the combination of BrCl with a halogen bond acceptor allows a shift of the equilibrium from Br_2/Cl_2 to BrCl. Based on this concept, the stabilized interhalide $[NEt_4][Cl(BrCl)]$ was first used in the selective bromochlorination of alkenes and dienes in the 1980´s.[71,76] The higher homologues of these interhalides were recently synthesized and characterized in the *Riedel* group.[77]

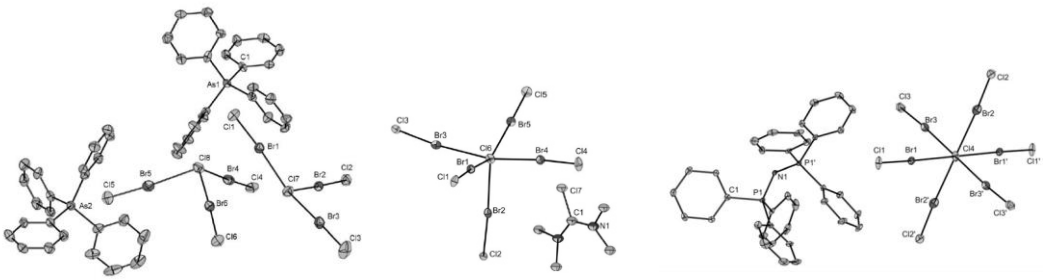

[AsPh$_4$][Cl(BrCl$_3$)] [CClN(Me$_2$)][Cl(BrCl)$_5$] [N(Ph$_3$P)$_2$][Cl(BrCl)$_6$]

Figure 12: A selection of different polyinterhalides synthesized and characterized by the *Riedel* group.[77]

In order to quantify the environmental and economic efficiency of the different interhalogenation reagents the atomic economy factor A will be introduced in the following. Here, the quotient of the molar mass of the reagent and the molar mass of the BrCl equivalents released is formed.

$$A = \frac{M\ ([cation][Cl(BrCl)_x])}{x \cdot M\ (BrCl)}$$

or

$$A = \frac{\sum M\ (reagents)}{M\ (BrCl)}$$

The factor only reflects the atomic economy theoretically possible from the sum formula of the reagent. The reactivity or actually required equivalents are not taken into account here. In the most ideal case, the use of pure BrCl, no by-products are formed and the factor A becomes 1. Consequently, as the value of A increases, the atomic economy of the reagent decreases. Table 1 lists some interhalogenation reagents and the determined atomic economy factor A. Two-component systems such as NBS and HCl·py[75] or the system used by the group of *Burns* for the enantioselective bromochlorination of allylic alcohols[75] are usually significantly inferior to the one-component systems. In the latter, a higher substitution with BrCl molecules (compare entries 2 and 4) and a smaller countercation (compare entries 4 and 5) leads to a better atomic economy factor.

Table 1: Reagents for bromochlorination and the corresponding atomic economy factor A.

entry	reagents	BrCl-equivalents	A
1	BrCl[71]	1	1.0
2	$[NEt_4][Cl(BrCl)]$[71,76]	1	2.4
3	$[NEt_3Me][Cl(BrCl)_2]$[64]	2	1.7
4	$[NEt_4][Cl(BrCl)_3]$[64]	3	1.5
5	$[AsPh_4][Cl(BrCl)_3]$[77]	3	2.2
6	$[NEt_4][Cl(BrCl)_5]$[64]	5	1.3
7	$[(PPh_3)_2N][Cl(BrCl)_6]$[77]	6	1.8
8	NBS, HCl·py[75]	1	2.5
9	NBS, $(^iPrO)_3TiCl$[75]	1	3.8

2.2. Scientific Goal

Polyinterhalides of the type [cation][Cl(BrCl)$_n$] (n = 1–6) developed in the *Riedel* group extend the compound class of non-classical polyinterhalides. In this work, we aimed to test whether the novel compound [NEt$_3$Me][Cl(BrCl)$_2$] (A = 1.7) can mimic or exceed the reactivity of pure BrCl (A = 1.0) or the literature-known polyinterhalide [NEt$_4$][Cl(BrCl)] (A = 2.4). Good atomic economy combined with high stability and cheap and easy synthesis make [NEt$_3$Me][Cl(BrCl)$_2$] a promising interhalogenation reagent. Unsaturated substrates, such as olefins, alkynes or *Michael* systems, are known substrates for bromochlorination and will therefore also be tested in this study. Since regio- and chemoselectivity have a significant influence on the general applicability, unsymmetrical olefins and substrates with additional functional groups will also be interhalogenated in the course of the investigations. In addition, the reaction conditions will be varied to investigate the possible influence of solvent, temperature and reaction time (Scheme 26).

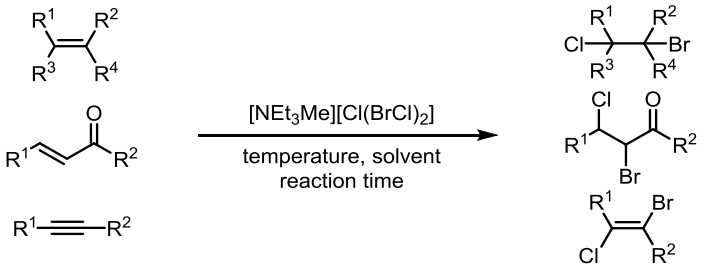

Scheme 26: Work plan for the application of [NEt$_3$Me][Cl(BrCl)$_2$] as an interhalogenation reagent.

2.3. Publication

2.3.1. In Situ Synthesis and Applications for Polyinterhalides based on BrCl

Benjamin Schmidt, Sebastian Ponath, Johannes Hannemann, Patrick Voßnacker, Karsten Sonnenberg, Mathias Christmann, Sebastian Riedel*

Chem. Eur. J. **2020**, *26*, 15183–15189.
doi.org/10.1002/chem.202001267

Highlighted in *ChemistryViews* (November 18, 2020)

Abstract:

The use of neat BrCl in organic and inorganic chemistry is limited due to its gaseous aggregate state and especially its decomposition into Cl_2 and Br_2. The stabilization of BrCl in form of reactive ionic liquids via a novel *in situ* synthesis route shifts this equilibrium drastically to the BrCl side, which leads to safer and easier to handle interhalogenation reagents. Furthermore, the solid state structures of the hitherto unknown $[Cl(BrCl)_2]^-$ and $[Cl(BrCl)_4]^-$ anions were synthesized and characterized by single-crystal X-ray diffraction (XRD), Raman and IR spectroscopy, as well as quantum chemical calculations.

Author Contribution:

Various novel polyinterhalides were synthesized and extensively characterized in the *Riedel* group. My task was to investigate the reaction behavior towards organic molecules. In addition, a comparison with the known reactivity of pure BrCl had to be made and advantages or disadvantages had to be pointed out. For this purpose, I first selected nine suitable unsaturated substrates, six of them were accessible via a one-step synthesis. Subsequently, I was able to find suitable reaction conditions (solvent, concentration, temperature, reaction time) and test the reactivity of $[NEt_3Me][Cl(BrCl)_2]$

towards the nine substrates. The isolation, purification and full characterization of the compounds, some of which were unknown, was also carried out by me. Lastly, I succeeded in preparing single crystals for three interhalogenated compounds. The single crystal structure analysis of a bromochlorinated compound was subsequently carried out by the *Riedel* group.

Full Paper
doi.org/10.1002/chem.202001267

European Chemical Societies Publishing

Polyhalides |*Hot Paper*|

In Situ Synthesis and Applications for Polyinterhalides Based on BrCl

Benjamin Schmidt,[a] Sebastian Ponath,[b] Johannes Hannemann,[a] Patrick Voßnacker,[a] Karsten Sonnenberg,[a] Mathias Christmann,[b] and Sebastian Riedel*[a]

Abstract: The use of neat BrCl in organic and inorganic chemistry is limited due to its gaseous aggregate state and especially its decomposition into Cl_2 and Br_2. The stabilization of BrCl in form of reactive ionic liquids via a novel in situ synthesis route shifts this equilibrium drastically to the BrCl side, which leads to safer and easier-to-handle interhalogenation reagents. Furthermore, the crystalline derivatives of the hitherto unknown $[Cl(BrCl)_2]^-$ and $[Cl(BrCl)_4]^-$ anions were synthesized and characterized by single-crystal X-ray diffraction (XRD), Raman and IR spectroscopy, as well as quantum chemical calculations.

Introduction

After the discovery of attractive interactions between dihalogens and halide anions in 1819,[1] Chattaway and Hoyle carried out first systematic investigations of polybromides and -chlorides in 1923.[2] These reports marked the starting point of the vast chemistry of polyhalogen compounds. In the last years not only our knowledge of the structural diversity of several polyhalogen anions, but also the possible applications of polyhalogen compounds increased continuously.[3] In general, interhalogen anions can be separated into classical interhalides, which possess an electropositive center that is surrounded by more electronegative halogen atoms, for example, $[ICl_4]^-$,[4] $[IF_6]^-$,[5] and nonclassical interhalides. A nonclassical interhalide can be best described as a central halide ion X^-, which is surrounded by dihalogen Y_2 (e.g., $[Cl(I_2)_4]^-$[6]) or interhalogen molecules XY/YZ (e.g., $[Br(IBr)_2{\cdot}2IBr]^-$).[7] Lately first examples of extraordinarily large polyhalogen anions of the lighter halogens such as the octahedrally coordinated monoanions $[Cl_{13}]^-$[8] and $[Cl(BrCl)_6]^-$[9] as well as the highly reactive $[Br_2F_7]^-$ and $[Br_3F_{10}]^-$ anions[10] were reported. Besides the detailed structural investigation of polyhalides, their applications as halogenation reagents,[11] as electrolytes in dye-sensitized solar cells[12] or (redox flow) batteries[13] are well established. Recently further applications as reactive ionic liquids which are able to dissolve noble metals and alloys were reported. These reactive ionic liquids show promise for applications in metal recycling.[14]

The formation of polyhalides can be explained by the concept of halogen bonding. According to this concept, the electrostatic potential of a dihalogen molecule is anisotropic and can be divided into two regions: an area of higher electron density, which forms a belt perpendicular to the molecule's bonding axis, and a region of a more positive electrostatic potential, which is situated on the bonding axis, the so-called σ-hole.[15] While for symmetrical dihalogens such as Br_2 and Cl_2, the σ-hole is symmetrical on both halogen atoms, for diatomic interhalogens such as IBr and BrCl, the σ-hole is more pronounced at the more electropositive halogen atom, see Figure 1. Owing to their polarized bond and pronounced σ-hole, interhalides are expected to form more stable anions and their tendency to form extended polyhalogen networks is lowered.

[a] *B. Schmidt, J. Hannemann, P. Voßnacker, Dr. K. Sonnenberg, Prof. Dr. S. Riedel*
Fachbereich Biologie, Chemie, Pharmazie
Institut für Chemie und Biochemie—Anorganische Chemie
Fabeckstr. 34/36, 14195 Berlin (Germany)
E-mail: s.riedel@fu-berlin.de

[b] *S. Ponath, Prof. Dr. M. Christmann*
Fachbereich Biologie, Chemie, Pharmazie
Institut für Chemie und Biochemie—Organische Chemie
Takustr. 3, 14195 Berlin (Germany)

Supporting information and the ORCID identification number(s) for the author(s) of this article can be found under: https://doi.org/10.1002/chem.202001267.

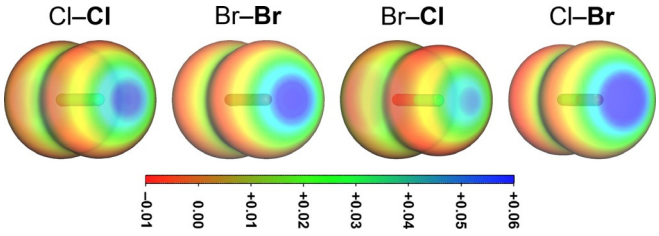

Figure 1. Electrostatic potential in the range of −0.01 au (red) to 0.06 au (blue) for the molecules Cl_2, Br_2 and BrCl (view of the **Cl** or **Br** atom, isosurface value 0.0035 au); calculated at the B3LYP-D3/def2-TZVPP level of theory.

Results and Discussion

Considering the excellent halogen bonding properties, it is surprising that larger nonclassical interhalides based on bromine monochloride (BrCl) have been reported only recently.[9] The interhalide BrCl exists in an equilibrium with Br_2 and Cl_2, see Scheme 1.[16,17] This hampers its use as a reagent due to side reactions. An equilibrium ratio of approximately 60% for BrCl, and 20% for Cl_2 and 20% Br_2 was experimentally determined at room temperature.[16]

This in good agreement with quantum chemical calculations at B3LYP-D3(BJ)/def2-TZVPP[18]-[28] and SCS-MP2/def2-TZVPP[29,30] level of theory. This equilibrium makes the stoichiometric usage of neat BrCl nearly impossible. Due to the different vapor pressures[31] of Br_2, Cl_2 and BrCl, first mainly chlorine boils off a batch of BrCl while bromine is enriched in the remaining liquid. Due to the pronounced σ-hole, the halogen bonding properties of BrCl are enhanced in comparison to Br_2 and Cl_2. Thus, an addition of a halogen bond acceptor, for example, a chloride salt, yielding BrCl based polyinterhalides such as the pentahalide $[Cl(BrCl)_2]^-$, should result in a significant shift of the equilibrium to the BrCl side, see Scheme 2. Our calculations show that the equilibrium is almost entirely located on the side of the BrCl based interhalides (>99.99%, calculated from ΔG°). Therefore, the stabilization of BrCl in form of polyinterhalide compounds provides a convenient BrCl source.

This was partially examined by the use of the trihalide $[Cl(BrCl)]^-$ as efficient bromochlorinating agent.[32–34] Nevertheless, further studies regarding the reactivity of higher polyinterhalides based on BrCl are still necessary.

Herein; we report a new synthetic route for polyinterhalides based on BrCl as well as the preparation and characterization of hitherto unknown BrCl interhalide monoanions, which complete the set of possible coordination numbers. These compounds have been characterized by single crystal X-ray diffraction (XRD), Raman and IR spectroscopy as well as quantum chemical calculations.

A new synthetic approach generates the interhalide BrCl in situ, see Scheme 3. In this approach, a chloride salt was provided in a reaction flask and afterwards elemental chlorine and bromine were condensed onto the salt at −196 °C.

$$2\ BrCl \rightleftharpoons Cl_2 + Br_2$$
$$\Delta G = 5.2\ (5.9)\ kJ\ mol^{-1}$$

Scheme 1. Equilibrium of BrCl with Cl_2 and Br_2 under ambient conditions; ΔG (298.15 K, 0.1 MPa) values were calculated at B3LYP-D3(BJ)/def2-TZVPP and SCS-MP2/def2-TZVPP (*italic*) level of theory.

$$2\ [Cl(BrCl)_2]^- \rightleftharpoons [Cl(Cl_2)_2]^- + [Cl(Br_2)_2]^-$$
$$\Delta G = 65.9\ (78.3)\ kJ\ mol^{-1}$$

Scheme 2. Equilibrium of stabilized BrCl under ambient conditions; ΔG (298.15 K, 0.1 MPa) values were calculated at B3LYP-D3(BJ)/def2-TZVPP and SCS-MP2/def2-TZVPP (*italic*) level of theory.

$$[Cat]Cl + n\ Cl_2 + n\ Br_2 \longrightarrow [Cat][Cl(BrCl)_{2n}]$$

Scheme 3. In situ synthesis of interhalogen compounds based on BrCl.

Condensing Br_2 and Cl_2 as starting materials guarantees the exact stoichiometry compared to the usage of a previously prepared BrCl batch. Warming up to ambient temperature leads to the formation of BrCl, which immediately reacts with the chloride to afford the desired polyinterhalide species. Due to this in situ generation of BrCl the undesired impurities of Br_2 and Cl_2 are minimized and consequently a clean product is obtained. These interhalide compounds offer themselves as an easy-to-handle and safer alternative to neat BrCl for applications in organic and inorganic chemistry.

To demonstrate the advantages of the new synthesis route, a complete set of the possible BrCl interhalides with one to six coordinating BrCl molecules was synthesized and fully characterized, see Figure 2.

To receive the trihalide $[Cl(BrCl)]^-$, 0.5 equivalents of Br_2 and Cl_2 were condensed onto $[NEt_4]Cl$ in dichloromethane (DCM). Slowly cooling the reaction mixture to −24 °C yields single crystals suitable for XRD analysis. The obtained crystal structure of **1** was already published in 1974.[35] The structural motif of the $[Cl(BrCl)]^-$ trihalide was discussed several times in literature.[36] $[NEt_4][Cl(BrCl)]$ contains two crystallographically independent anions in the asymmetric unit. In the following, the structural data of the more symmetrical anion is discussed. The trihalide is almost linear (179.1(1)°) and symmetrical (Cl1–Br1 240.4(1), Cl2–Br1 239.1(1) pm). The bonding situation can be best described as a three-center four-electron (3c–4e) bond and can be compared with other symmetrical trihalides such as $[Br_3]^-$ or $[Cl_3]^-$.[3,37] The 3c-4e bond results in a bond order

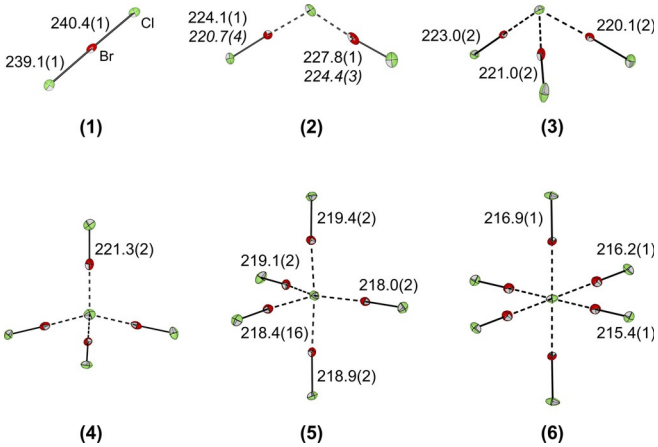

Figure 2. Molecular structures in the solid state of the interhalide salts $[Cat][Cl(BrCl)_n]$ (for $n=1$, 2, 3, 5 $[Cat]^+=[NEt_4]^+$; for $n=4$ $[Cat]^+=[NPr_4]^+$; for $n=6$ $[Cat]^+=[PNP]^+$[9]) with thermal ellipsoids set at 50% probability. The cations and disorders of the anions were omitted for clarity. For the pentahalides (**2**) two different structures, namely $[NEt_4]_2[Cl(BrCl)_2][Cl(BrCl)]$ and$[NEt_4][Cl(BrCl)_2]$ (bond lengths in *italics*), were obtained. For detailed structures, see Figures S1–S5, S38. Bond lengths [pm] of the central chloride to the coordinated BrCl molecules: **2**: 251.7(1), 262.3(1); 259.6(1), 265.5(1); **3**: 266.4(2)–273.0(2); **4**: 278.6(1); **5**: 281.1(2)–298.6(2); **6**: 279.3(1)–291.3(1).

of 0.5, which explains the most elongated BrCl bond in comparison to the larger interhalides.

The addition of 0.85 equivalents of the dihalogens Br_2 and Cl_2 to $[NEt_4]Cl$ in DCM leads to the formation of the hitherto unknown pentahalide $[Cl(BrCl)_2]^-$. The anion possesses a slightly distorted V-shaped structure, see Figure S38. In the crystal structure a partial substitution of the coordinating BrCl molecules by Br_2 is observed. Therefore, a small excess of chlorine (0.85 equiv Br_2, 1.1 equiv Cl_2) was used resulting in crystals of a non-disordered $[Cl(BrCl)_2]^-$ anion and an additional, slightly unsymmetrical $[Cl(BrCl)]^-$, see Figure S2. In contrast to the 3c-4e bond of trihalides, the bonding situation of the higher poly(inter)halides can be best described as a donor–acceptor interaction. The central halide ion acts as Lewis base and donates electron density into the LUMO (σ*) of the Lewis acids, namely the coordinating dihalogen molecules. The charge transfer results in a bond weakening and elongation of the coordinating molecules, which can also be observed experimentally.[3] In case of the non-disordered pentahalide **2** the bond lengths of the coordinating BrCl molecules are elongated by 10.5(2)–14.2(2) pm compared to free BrCl (213.6(1) pm).[38] Adding more equivalents of Br_2 and Cl_2 to the chloride salt, anions with higher coordination numbers can be obtained. Consequently the heptahalide $[Cl(BrCl)_3]^-$ (**3**) crystallized with $[NEt_4]^+$ as the counter ion. The heptahalide was already reported with $[AsPh_4]^+$ as the cation. In the reported structure of $[AsPh_4][Cl(BrCl)_3]$ two crystallographically independent heptahalides, which slightly interact with each other, can be observed in the asymmetric unit.[9] The $[Cl(BrCl)_3]^-$ presented here in $[NEt_4][Cl(BrCl)_3]$ consists of just one discrete anion, which shows no interactions to other halogen atoms and is arranged in a distorted trigonal-pyramidal structure.

Increasing the amount of Br_2 and Cl_2 to 2.5 equivalents and changing the cation to $[NPr_4]^+$ leads to the formation of the nonahalide $[Cl(BrCl)_4]^-$, which is the first reported BrCl based nonahalide, see Figure 3.

The compound crystallizes in the tetragonal space group I_4 and its structure can be best described as a distorted tetrahedron. The obtained polyinterhalide compounds is isostructural to the already published $[NPr_4][Br(Br_2)_4]$ (Figure 3).[39] In comparison to the $[Br(Br_2)_4]^-$, whose intermolecular distances are about 30 pm shorter than the sum of the van der Waals radii (370 pm),[40] the $[Cl(BrCl)_4]^-$ anion is more discrete. The intermolecular distances of **4** are just 10 pm shorter than the sum of the van der Waals radii (360 pm),[40] which again shows the lower tendency of BrCl based interhalides to be stabilized by secondary halogen-halogen interactions. Furthermore, the hypothetical square-planar structure (D_{4h}) has been quantum-chemically investigated at B3LYP-D3(BJ)/def2-TZVPP and SCS-MP2/def2-TZVPP level. Both optimized structures show a transition state for the interconversion of the tetrahedral structure which are 14.6 and 7.2 kJ mol^{-1} higher in energy than the T_d structure.

From a reaction mixture of an excess of Br_2 and Cl_2 (3.5 equiv each) with $[NEt_4]Cl$, single crystals of the undecainterhalide $[NEt_4][Cl(BrCl)_5]$ were obtained (**5**). A similar undecahalide structure was already published earlier with $[CCl(NMe_2)_2]^+$ as the counter ion. With this cation the structural parameter τ ($\tau = (\beta-\alpha)/60°$, β and α are the largest angles in the coordination sphere) was determined to be $\tau = 0.25$, which indicated a rather square-pyramidal arrangement.[9,41] With $[NEt_4]^+$ as the cation, the structural parameter becomes larger ($\tau = 0.38$). This underlines the strong influence of the cation on the structure of the anion. Another reason for the distorted structure of the undecahalide is the bridging between the $[Cl(BrCl)_5]^-$ units, which leads to an octahedral coordination sphere for the central chloride Cl1, see Figure 4.

As mentioned above, the tendency to form extended networks is lowered for BrCl due to its asymmetrical σ-hole in comparison to the symmetrical Br_2. The solid state structure of $[Cl(BrCl)_5]^-$ (**5**) possesses one disordered coordinating dihalogen unit (Br5–Cl6/Br6), which is bridging between two anions, see Figure 4. The interaction of the bromine with the two central chloride ions leads to the formation of a chain.

It was possible to synthesize and crystallize interhalides based on BrCl with tetraalkylammonium as the cation with coordination numbers going from one up to five. The hexa-coordinated tridecainterhalide could not be isolated with tetraalkylammonium cations, even an excess of BrCl leads to the formation of the $[Cl(BrCl)_5]^-$ anion. This underlines the great influ-

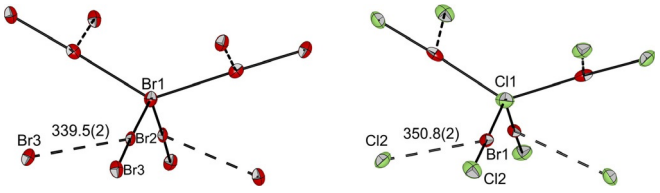

Figure 3. Comparison of the anion structures in the solid state of $[NPr_4][Br(Br_2)_4]^-$ and $[NPr_4][Cl(BrCl)_4]^-$ with thermal ellipsoids set at 50 % probability. Selected bond lengths [pm] and angles [°]: $[Br_9]^-$: Br1–Br2 294.3(1), Br2–Br1-Br2′ 131.2(1), 99.8(1); $[Cl(BrCl)_4]^-$: Cl1–Br1 278.6(1), Br1-Cl1-Br1′ 130.1(1), 100.3(1).

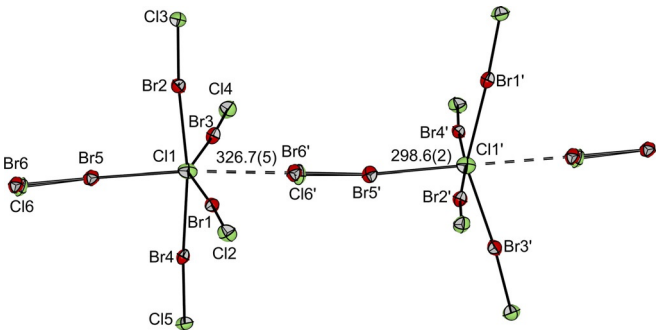

Figure 4. Molecular structures in the solid state of the $[Cl(BrCl)_5]^-$ anions in $[NEt_4][Cl(BrCl)_5]$ with thermal ellipsoids set at 50 % probability. A Br_2/BrCl (Br5-Br6/Br5-Cl6: 60 %/40 % occupation) interacts with two central chloride ions to form a chain (d(Cl1–Br6′) = 326.7(5) pm, d(Cl1–Cl6′) = 340.6(17) pm). Selected bond lengths [pm] and angles [°]: Cl1–Br1 286.4(2), Cl1–Br2 281.6(2), Cl1–Br3 281.4(2), Cl1–Br4 281.1(2), Cl1–Br5 298.6(2), Br1–Cl2 218.0(2), Br2–Cl3 219.4(2), Br3–Cl4 219.1(2), Br4–Cl5 218.9(2), Br5–Cl6 218.4(16), Br5–Br6 231.4(5); Cl1-Br1-Cl2 176.7(1), Cl1-Br2-Cl3 174.9(1), Cl1-Br3-Cl4 175.3(1), Cl1-Br4-Cl5 176.1(1), Cl1-Br5-Cl6 174.8(8), Br3-Cl1-Br1 148.7(1), Br2-Cl1-Br4 171.5(1).

ence of the counter ions size on the obtained anion. Using the large bis(triphenylphosphoranylidene)iminium ($[PNP]^+$) as the cation leads to the formation of the tridecainterhalide, which was already published.[9] In this series of polyinterhalides the Br–Cl bond length of the terminal BrCl molecules is decreasing with the increase of BrCl molecules coordinating to the central atom.

As mentioned before, the $[Cl(BrCl)]^-$ anion exhibits the longest BrCl bond due to the 3c-4e bond. From the pentahalide to the tridecahalide the bonds of the coordinating BrCl molecules are less weakened and therefore less elongated compared to the trihalide and free BrCl (213.6(1) pm).[38] The bonding situation of higher polyinterhalides can be described as donor/acceptor interaction between the central chloride ion, the Lewis base, and the surrounding BrCl molecules, which function as Lewis acids.

The higher the coordination number of the central chloride the less electron density can be donated into each LUMO (σ*) of each coordinating BrCl molecule. This leads to less weakening of the BrCl bond accompanied with shorter bond lengths, see Figure 2. Quantum chemical calculations for the minima structures in the gas phase of the polyinterhalide species (at the B3LYP-D3(BJ)/def2-TZVPP and SCS-MP2/def2-TZVPP level of theory) are in good agreement with the experimental data and verify the described trend, see Figure 5.

Due to their strong Raman scattering, Raman spectroscopy is highly instructive for further analysis of polyinterhalide compounds. Therefore, low temperature Raman spectra of single crystals of each polyinterhalide salt were recorded and compared with quantum chemical calculations, see Figure 6. The trend of decreasing bond weakening of the BrCl units leads to a shift of the BrCl stretching frequencies to higher wavenumbers in the corresponding Raman spectra. Due to the almost inversion-symmetrical structure of trihalides, only the symmetric stretching vibration possesses significant Raman intensity. In the spectrum of $[NEt_4]_2[Cl(BrCl)]_2$, two bands can be observed at 285 and 271 cm^{-1} respectively. These two bands can be explained by two symmetric stretching vibrations of two crystallographically independent $[Cl(BrCl)]^-$ anions, which differ

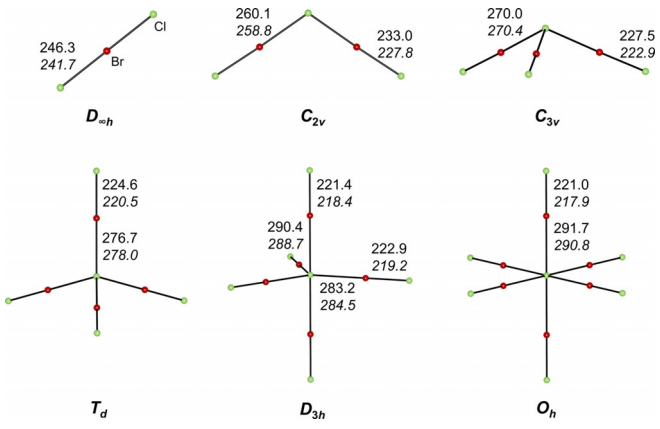

Figure 5. Optimized minima structures of $[Cl(BrCl)_n]^-$ ($n = 1–6$). Calculated bond lengths in pm at the B3LYP-D3(BJ)/def2-TZVPP level (SCS-MP2/def2-TZVPP level in italics) are indicated.

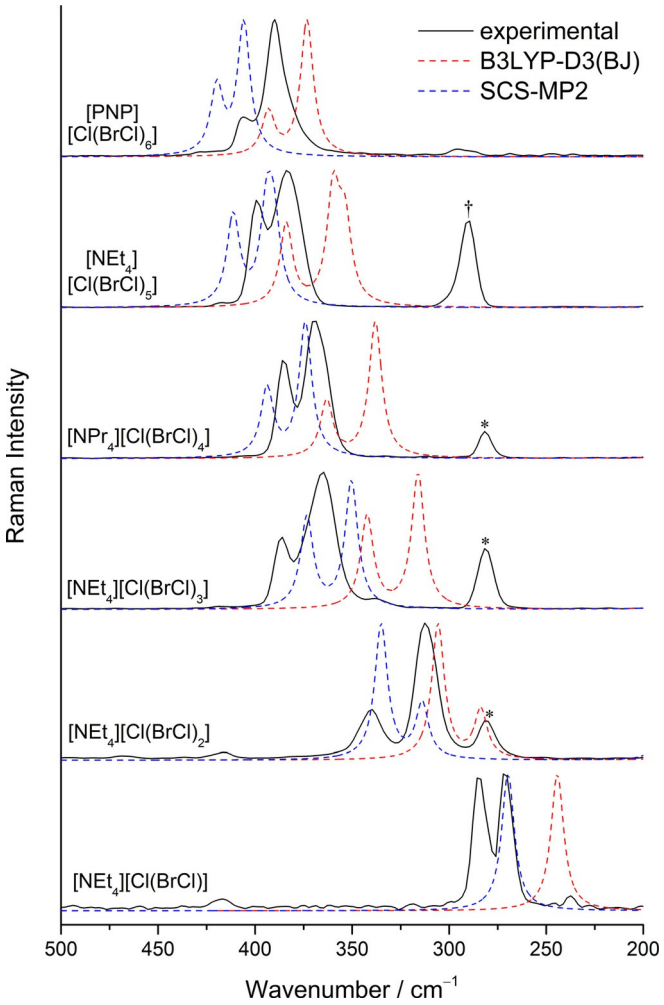

Figure 6. Low temperature Raman spectra of single crystals of the polyinterhalide salts (black) as well as calculated Raman spectra at the SCS-MP2/def2-TZVPP (blue) and B3LYP-D3(BJ)/def2-TZVPP (red) level of theory. The band at 281 cm^{-1} associated with $[Cl(BrCl)]^-$ is indicated by asterisks; the band for the bridging Br_2 molecule is indicated by a dagger.

in bond lengths and angles (241.8(1), 235.7(1) pm, 174.8(1)°; 240.4(1), 239.1(1) pm, 179.1(1)°). These bands are most shifted to lower wavenumbers in comparison to free BrCl (434 cm^{-1})[42] due to the 3c–4e bond in the trihalide. Quantum chemical calculations for the trihalide in $D_{\infty h}$ symmetry at the SCS-MP2/def2-TZVPP level of theory predict one band for the symmetrical stretching vibration at 270 cm^{-1} (A_{1g}), which agrees well with the experimental results.

As described above, the bond weakening decreases with increasing number of coordinating BrCl molecules. The corresponding bands shift to higher wavenumbers and almost reach the frequency of free BrCl. In case of the larger polyinterhalide compounds two major bands in the Br–Cl stretching region can be observed, the symmetric and asymmetric stretch of the coordinating BrCl molecules.

In the spectra of the three and four times coordinated interhalogen compounds, an additional band at 281 cm^{-1} is observed, which can be assigned to a $[Cl(BrCl)]^-$ species, that results from residual mother liquor. The stretching frequency of

the bridging Br_2 molecule in the solid state structure of the undecainterhalide **5** is observed at 290 cm^{-1}. In the Raman spectrum of the pentainterhalide **2**, the intensities of the symmetric and asymmetric stretching modes are inverted with respect to the calculations. This can be explained by interactions in the solid state, as shown by Raman spectra of compound **2** in a DCM solution and in bulk, see Figure S42. All experimental spectra are in good agreement with quantum-chemical calculations, see Figure 6.

Additionally, room-temperature ionic liquids (RT-ILs) containing 1–3 equiv of BrCl were prepared and analyzed by IR spectroscopy (Figure S12). The described trend of bond weakening and shift of vibrational frequencies is also visible in the IR spectra, however Raman spectroscopy is more suited to characterize the polyinterhalide species due to the superior signal to noise ratio.

The usage of poly(inter)halide compounds in organic and inorganic synthesis is growing over the last years.

The bromochlorinating agent $[Cl(BrCl)]^-$ was already reported in the 1980s.[32–34] To demonstrate the reactivity of the polyinterhalide ionic liquid, a variety of substrates including several alkenes, Michael systems and an alkyne was reacted with $[NEt_3Me][Cl(BrCl)_2]$, see Scheme 4 (and Supporting Information, chapters f and g).

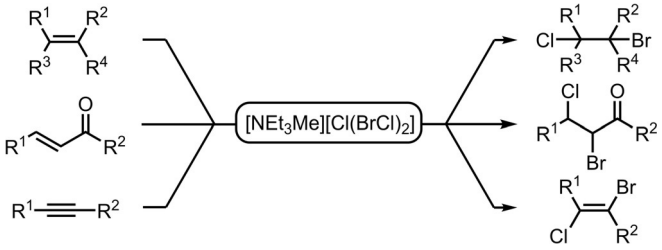

Scheme 4. Interhalogenation of alkenes, Michael systems and alkynes using the reactive ionic liquid based on BrCl (for a detailed substrate scope see Table S4).

The reactions were performed in dichloromethane (DCM) at −78 °C to provide the bromochlorinated product within 60 min reaction time in yields between 71 and 91 %. The interhalogenation of several alkenes and Michael systems was achieved even at low temperatures in very short reaction times and good yields. To investigate the long-term stability of these reactive interhalogenation reagents, Raman spectra of two BrCl based ionic liquids were measured continuously over a period of one year, see Figures S36–37. The prepared ILs ($[NMe_4]Cl$ + 4.5 equiv BrCl, $[NPr_4]Cl$ + 4.5 equiv BrCl) were stored under the exclusion of light in sealed glass ampules. Both ILs are stable against halogenation for at least one year, which proofs that tetraalkylammonium cations ($[NR_4]^+$, R = Me, Et, Pr) are suitable counter ions for these polyinterhalide reagents.

Conclusions

In summary, we have presented a novel in situ synthesis route for BrCl based interhalides. The addition of a halogen bond acceptor, for example, a chloride salt, results in an almost entire shift of the equilibrium to the BrCl side (> 99.99 %). This stabilization of the reactive BrCl provides safer and easy-to-handle polyinterhalide ILs for further applications such as interhalogenation reactions of alkenes, alkynes and Michael systems in organic synthesis. Furthermore, we were able to synthesize via this new route a complete set of the possible BrCl interhalides with coordination numbers of one to six coordinating BrCl molecules, showing that the average Cl–Br distances of the central chloride to the surrounding BrCl molecule correlate well with the coordination number. Within this set, the hitherto unknown V-shaped $[Cl(BrCl)_2]^-$ and the distorted tetrahedral $[Cl(BrCl)_4]^-$ anion were reported for the first time. All structures were characterized by single-crystal X-ray diffraction, single-crystal Raman spectroscopy as well as quantum chemical calculations. Hence, our results not only complete the variety of BrCl based interhalides, they also provide a new syntheses route to stabilize the gaseous BrCl for promising synthetic applications.

Experimental Section

Materials, instruments, and methods: All preparative work was carried out using standard Schlenk techniques. Chlorine (Linde, purity 2.8) was passed through calcium chloride before use to remove traces of water. Bromine (purity > 99 %) was distilled and stored over activated molecular sieve. The $[NR_4]Cl$ salts were obtained from commercial sources, dried for two days at 80 °C at reduced pressure and stored under inert conditions. Dichloromethane was stored over activated 3 Å molecular sieve. Raman spectra were recorded on a Bruker (Karlsruhe, Germany) MultiRAM II equipped with a low-temperature Ge detector (1064 nm, 60 mW, resolution of 4 cm^{-1}). Spectra of single crystals were recorded at −196 °C using the Bruker RamanScope III. ATR-IR spectra of the ILs were recorded with a resolution of 4 cm^{-1} on a Thermo Scientific Nicolet iS50 FT-IR with DTGS-polyethylene detector for the FIR range and for the halogenated alkene on a JASCO FT/IR-4100 spectrometer. NMR spectra were recorded at RT on a JEOL Eclipse + 500 spectrometer. Mass spectroscopy was performed on an Agilent Technologies 6210 ESI-TOF spectrometer. X-ray diffraction data were collected on a Bruker D8 Venture CMOS area detector (Photon 100) diffractometer with MoKα radiation, see Table S1–S2. Deposition numbers 1965314, 1965315, 1965317, 1965318, 1971174, 1984581, and 1984909 contain the supplementary crystallographic data for this paper. These data are provided free of charge by the joint Cambridge Crystallographic Data Centre and Fachinformationszentrum Karlsruhe Access Structures service.

Single crystals were coated with perfluoroether oil at low temperature (−40 °C) and mounted on a 0.2 mm Micromount. The structure was solved with the ShelXT[43] structure solution program using intrinsic phasing and refined with the ShelXL[44] refinement package using least squares on weighted *F2* values for all reflections using OLEX2.[45]

On the one hand, structure optimizations of the polyinterhalide anions were performed at DFT level using the RI-B3LYP hybrid functional with Grimme's dispersion correction D3 and BJ-damping together with the def2-TZVPP basis set.[18]-[28] On the other hand, further optimizations were performed at SCS-MP2 level using the def2-TZVPP basis set.[29,30] All calculations were carried out using the TURBOMOLE V7.3 program.[46] Minima on the potential energy

surface were characterized by harmonic vibrational frequency analyses. Thermochemistry was provided with zero-point vibrational correction, ΔG values were calculated at 298.15 K and 1.0 bar.

[NEt_4][Cl(BrCl)]: Bromine (113 mg, 0.71 mmol, 0.5 equiv), chlorine (50.1 mg, 0.71 mmol, 0.5 equiv) and dichloromethane (0.15 mL) were condensed at −196 °C onto [NEt_4]Cl (234 mg, 1.41 mmol, 1.0 equiv). Thawing to room temperature and slowly cooling to −24 °C resulted in the formation of crystals of [NEt_4][Cl(BrCl)]. Raman (1064 nm, 77 K, 150 mW): 3000(w), 2993(w), 2985(w), 2943(m), 1472(vw), 1457(vw), 1439(vw), 1299(vw), 1124(vw), 1001(vw), 917(vw), 734(vw), 674(w), 417(vw), 285(vs., ν_s Br–Cl), 271(vs., ν_s Br–Cl), 238(vw) cm^{-1}.

[NEt_4]$_2$[Cl(BrCl)$_2$][Cl(BrCl)]: Bromine (225 mg, 1.411, mmol, 0.85 equiv), chlorine (129 mg, 1.82 mmol, 1.1 equiv) and dichloromethane (0.20 mL) were condensed at −196 °C onto [NEt_4]Cl (325 mg, 1.66 mmol, 1.0 equiv). Thawing to room temperature and slowly cooling to −24 °C resulted in the formation of crystals of [NEt_4][Cl(BrCl)$_2$]. Raman (1064 nm, 77 K, 150 mW): $\tilde{\nu}$ = 3013(vw), 2990(w), 2983(w), 2939(w), 1470(vw), 1457(vw), 1300(vw), 1123(vw), 998(vw), 890(vw), 673(vw), 468(vw), 416(w), 340(m, ν_s Br–Cl), 312(vs., ν_{as} Br–Cl), 281(m, ν_s Br–Cl of $[Cl(BrCl)]^-$), 190(w), 158(w), 133(w) cm^{-1}.

[NEt_4][Cl(BrCl)$_3$]: Bromine (363 mg, 2.27 mmol, 1.5 equiv), chlorine (161 mg, 2.27 mmol, 1.5 equiv) and dichloromethane (0.15 mL) were condensed at −196 °C onto [NEt_4]Cl (251 mg, 1.51 mmol, 1.0 equiv). Thawing to room temperature and slowly cooling to −24 °C resulted in the formation of crystals of [NEt_4][Cl(BrCl)$_3$]. Raman (1064 nm, 77 K, 150 mW): $\tilde{\nu}$ = 2992(vw), 2981(vw), 2952(vw), 2938(vw), 1456(vw), 1299(vw), 1120(vw), 1000(vw), 679(vw), 493(vw), 387(m, ν_s Br–Cl), 365(vs., ν_{as} Br–Cl), 281(vs., ν_s Br–Cl of $[Cl(BrCl)]^-$), 177(vw), 137(w) cm^{-1}.

[NPr_4][Cl(BrCl)$_4$]: Bromine (406 mg, 2.54 mmol, 2.5 equiv), chlorine (180 mg, 2.54 mmol, 2.5 equiv) and dichloromethane (0.15 mL) were condensed at −196 °C onto [NPr_4]Cl (225 mg, 1.01 mmol, 1.0 equiv). Thawing to room temperature and slowly cooling to −20 °C resulted in the formation of crystals of [NPr_4][Cl(BrCl)$_4$]. Raman (1064 nm, 77 K, 150 mW): $\tilde{\nu}$ = 2980(vw), 2955(vw), 2939(vw), 2922(vw), 2897(vw), 1457(vw), 1448(vw), 1316(vw), 385(s, ν_s Br–Cl), 369(vs., ν_{as} Br–Cl), 282(w, ν_s Br–Cl of $[Cl(BrCl)]^-$), 170(vw, sh), 153(w, sh), 142(m) cm^{-1}.

[NEt_4][Cl(BrCl)$_5$]: Bromine (834 mg, 5.22 mmol, 5.0 equiv), chlorine (370 mg, 5.22 mmol, 5.0 equiv) and dichloromethane (0.15 mL) were condensed at −196 °C onto [NEt_4]Cl (173 mg, 1.04 mmol, 1.0 equiv). Thawing to room temperature and slowly cooling to −40 °C resulted in the formation of crystals of [NEt_4][Cl(BrCl)$_5$]. Raman (1064 nm, 77 K, 150 mW): $\tilde{\nu}$ = 2987(vw), 2949(vw), 2937(vw), 1456(vw), 1295(vw), 1117(vw), 673(vw), 506(vw), 399(s, ν_s Br–Cl), 383(vs., ν_{as} Br–Cl), 290(vs., ν Br–Br), 154(vw), 138(vw) cm^{-1}.

[PNP][Cl(BrCl)$_6$]: Bromine (618 mg, 3.87 mmol, 7.5 equiv), chlorine (274 mg, 3.87 mmol, 7.5 equiv) and dichloromethane (0.15 mL) were condensed at −196 °C onto [PNP]Cl (296 mg, 0.52 mmol, 1.0 equiv). Thawing to room temperature and slowly cooling to −40 °C resulted in the formation of crystals of [PNP][Cl(BrCl)$_6$]. Raman (1064 nm, 77 K, 150 mW): $\tilde{\nu}$ = 3062(w), 2987(vw), 1590(vw), 1112(vw), 1028(vw) 1001(w) 702(vw), 668(vw), 617(vw), 406(m, ν_s Br–Cl), 390(vs., ν_{as} Br–Cl), 296(vw), 269(vw) cm^{-1}.

Standard procedure of the interhalogenation: The substrate (0.32 mmol, 1.0 equiv) was dissolved in dry DCM (3.2 mL) and cooled to −78 °C. The ionic liquid [NEt_3Me][Cl(BrCl)$_2$] was added (60.4 mg, 0.16 mmol, 0.50 equiv) and the reaction mixture was stirred at −78 °C until thin layer chromatography showed conversion of the substrate (alkenes: < 1 min; alkyne and α,β-unsaturated compounds: 30–60 min). Thereafter water (3.0 mL) was added and the reaction mixture was warmed to RT. The aqueous phase was extracted with DCM (3×5.0 mL), the combined organic phases were dried over $MgSO_4$ and the solvent was removed under reduced pressure. The crude product was purified by column chromatography (SiO_2, *n*-pentane/EtOAc). For a detailed assignment of the ^1H and ^{13}C NMR spectroscopic shifts see Supporting Information (Table S4, Figures S13–S30).

6-Bromo-7-chloro-2,2,3,3,10,10,11,11-octamethyl-4,9-dioxa-3,10-disiladodecane (A): ^1H NMR (500 MHz, RT, $CDCl_3$): δ = 4.48 (ddd, ^3J = 9.2, 5.7, 1.9 Hz, 1H), 4.26 (ddd, ^3J = 8.7, 5.8, 1.9 Hz, 1H), 3.98–3.83 (m, 2H), 3.88–3.76 (m, 2H), 0.90 (s, 18H), 0.10–0.09 (m, 12H); see Figure S13. $^{13}C\{^1H\}$ NMR (126 MHz, RT, $CDCl_3$): δ = 65.2, 64.3, 59.4, 53.9, 25.9 (6×C), 18.4 (2×C), −5.2 (4×C); see Figure S14. ATR-IR: $\tilde{\nu}$ = 2954, 2930, 2858, 1471, 1257, 1096, 839, 777 cm^{-1}. HR-MS (ESI+): *m/z* calcd for $C_{16}H_{37}BrClO_2Si_2+H^+$: 431.1199 $[M+H]^+$; found: 431.1192.

(2-Bromo-3-chloro-3-methylbutoxy)triisopropylsilane (B): ^1H NMR (500 MHz, RT, $CDCl_3$): δ = 4.36 (dd, *J* = 11.2, 3.4 Hz, 1H), 4.18 (dd, *J* = 6.9, 3.5 Hz, 1H), 4.07 (dd, *J* = 11.1, 6.8 Hz, 1H), 1.80 (s, 3H), 1.70 (s, 3H), 1.12–1.07 (m, 21H).; see Figure S15. $^{13}C\{^1H\}$ NMR (126 MHz, RT, $CDCl_3$): δ = 70.6, 66.1, 65.7, 33.2, 29.0, 18.1, 12.1; see Figure S16. ATR-IR: $\tilde{\nu}$ = 2942, 2867, 2190, 1461, 1387, 1123, 1104, 882, 773 cm^{-1}. HR-MS (ESI+): *m/z* calcd for $C_{14}H_{30}BrClOSi+Na^+$: 379.0830 $[M+Na]^+$; found: 379.0829.

(4-Bromo-3-chloro-3-methylbutoxy)triisopropylsilane (C): ^1H NMR (500 MHz, RT, $CDCl_3$): δ = 3.99–3.88 (m, 2H), 3.78 (d, *J* = 10.3 Hz, 1H), 3.67 (d, *J* = 10.3 Hz, 1H), 2.20–2.12 (m, 2H), 1.72 (s, 3H), 1.13–1.02 (m, 21H); see Figure S17. $^{13}C\{^1H\}$ NMR (126 MHz, RT, $CDCl_3$): δ = 70.2, 60.2, 43.7, 43.0, 29.8, 18.2, 12.1; see Figure S18. ATR-IR: $\tilde{\nu}$ = 2943, 2891, 2867, 1737, 1463, 1379, 1217, 1105, 882, 738 cm^{-1}. HR-MS (ESI+): *m/z* calcd for $C_{14}H_{30}BrClOSi+Na^+$: 379.0830 $[M+Na]^+$; found: 379.0840.

(2-Bromo/*chloro*-3-chloro/*bromo*propoxy)triisopropylsilane, regioisomeric ratio = 1:1 (D): ^1H NMR (500 MHz, RT, $CDCl_3$): δ = 4.18–4.13 (m, 1H), 4.12–4.05 (m, 3H), 4.01–3.96 (m, 2H), 3.93 (q, *J* = 4.9 Hz, 1H), 3.88 (dd, *J* = 11.2, 4.9 Hz, 1H), 3.80 (dd, *J* = 10.5, 6.8 Hz, 1H), 3.67 (dd, *J* = 10.5, 4.8 Hz, 1H), 1.15–1.00 (m, 42H); see Figure S19. $^{13}C\{^1H\}$ NMR (126 MHz, RT, $CDCl_3$): δ = 64.8, 64.1, 60.2, 52.3, 45.0, 33.4, 18.1 (2×C), 12.1 (2×C); see Figure S20. ATR-IR: $\tilde{\nu}$ = 2944, 2892, 2867, 1737, 1461, 1380, 1143, 1110, 1069, 1000, 881, 792 cm^{-1}. HR-MS (ESI+): *m/z* calcd for $C_{12}H_{26}BrClOSi+Na^+$: 351.0517 $[M+Na]^+$; found: 351.0520.

2-Bromo-3-chloro-3-methylbutyl-3,5-dinitrobenzoate (E): ^1H NMR (500 MHz, RT, $CDCl_3$): δ = 9.24 (t, *J* = 2.1 Hz, 1H), 9.18 (d, *J* = 2.1 Hz, 2H), 5.13 (dd, *J* = 12.1, 3.2 Hz, 1H), 4.81 (dd, *J* = 12.1, 8.8 Hz, 1H), 4.51 (dd, *J* = 8.8, 3.1 Hz, 1H), 1.87 (s, 3H), 1.78 (s, 3H); see Figure S21. $^{13}C\{^1H\}$ NMR (126 MHz, RT, $CDCl_3$): δ = 162.2, 148.9, 133.4, 129.7, 122.8, 69.0, 68.1, 59.3, 33.2, 28.1; see Figure S22. ATR-IR: $\tilde{\nu}$ = 3098, 2955, 2925, 1735, 1542, 1343, 1274, 1159, 921, 719 cm^{-1}. HR-MS (ESI+): *m/z* calcd for $C_{12}H_{12}BrClN_2O_6+Na^+$: 416.9459 $[M+Na]^+$; found: 416.9463.

3-Bromo-4-chloro-4-phenylbutan-2-one (F): ^1H NMR (500 MHz, RT, $CDCl_3$): δ = 7.44–7.37 (m, 5H), 5.25 (d, *J* = 11.2 Hz, 1H), 4.69 (d, *J* = 11.2 Hz, 1H), 2.48 (s, 3H); see Figure S23. $^{13}C\{^1H\}$ NMR (126 MHz, RT, $CDCl_3$): δ = 198.7, 137.4, 129.6, 128.9, 128.1, 59.9, 53.7, 27.0; see Figure S24. ATR-IR: $\tilde{\nu}$ = 3066, 3032, 2970, 1722, 1455, 1362, 1218, 733 cm^{-1}. HR-MS (ESI+): *m/z* calcd for $C_{10}H_{10}BrClO+Na^+$: 282.9496 $[M+Na]^+$; found: 282.9489; *m/z* calcd for $C_{10}H_{10}BrClO+K^+$: 298.9236 $[M+K]^+$; found: 289.9227.

Ethyl-2-bromo-3-chloro-3-phenylpropanoate (G): ^1H NMR (500 MHz, RT, $CDCl_3$): δ = 7.43–7.36 (m, 5H), 5.27 (d, *J* = 11.3 Hz,

1H), 4.62 (d, $J=11.3$ Hz, 1H), 4.36 (q, $J=7.2$ Hz, 2H), 1.37 (t, $J=7.1$ Hz, 3H); see Figure S25. $^{13}C\{^1H\}$ NMR (126 MHz, RT, $CDCl_3$): $\delta=167.8, 137.2, 129.6, 128.9, 128.1, 62.7, 61.0, 47.7, 14.0$; see Figure S26. ATR-IR: $\tilde{\nu}=3034, 2982, 2936, 1739, 1455, 1266, 1143, 1017, 869, 772\ cm^{-1}$. HR-MS (ESI+): *m/z* calcd for $C_{11}H_{12}BrClO_2+Na^+$: 312.9601 $[M+Na]^+$; found: 312.9604.

2-Bromo-3-chloro-1,3-diphenylpropan-1-one (H): ^1H NMR (500 MHz, RT, $CDCl_3$): $\delta=8.12–8.10$ (m, 2H), 7.68–7.65 (m, 1H), 7.57–7.53 (m, 4H), 7.46–7.40 (m, 3H), 5.61 (s, 2H); see Figure S27. $^{13}C\{^1H\}$ NMR (126 MHz, RT, $CDCl_3$): $\delta=191.3, 137.9, 134.6, 134.3, 129.5, 129.1, 129.0, 128.9, 128.3, 59.9, 47.6$; see Figure S28. ATR-IR: $\tilde{\nu}=3063, 3033, 1685, 1448, 1269, 1229, 976, 776, 731\ cm^{-1}$. HR-MS (ESI+): *m/z* calcd for $C_{15}H_{12}BrClO+Na^+$: 344.9652 $[M+Na]^+$; found: 344.9656; *m/z* calcd for $C_{15}H_{12}BrClO+K^+$: 360.9392 $[M+K]^+$; found: 360.9394.

(*E*)-6-Bromo-7-chloro-2,2,3,3,10,10,11,11-octamethyl-4,9-dioxa-3,10-disiladodec-6-ene (I): ^1H NMR (500 MHz, RT, $CDCl_3$): $\delta=4.55–4.50$ (m, 4H), 0.92–0.91 (m, 18H), 0.12–0.10 (m, 12H); see Figure S29. $^{13}C\{^1H\}$ NMR (126 MHz, RT, $CDCl_3$): $\delta=130.7, 122.4, 66.0, 64.7, 26.0, 18.5, -5.03$; see Figure S30. ATR-IR: $\tilde{\nu}=2953, 2930, 2886, 2858, 1738, 1471, 1363, 1254, 1111, 836, 777\ cm^{-1}$. HR-MS (ESI+): *m/z* calcd for $C_{16}H_{34}BrClO_2Si_2+Na^+$: 451.0861 $[M+Na]^+$; found: 451.0869; *m/z* calcd for $C_{16}H_{34}BrClO_2Si_2+K^+$: 467.0601 $[M+K]^+$; found: 467.0616.

Acknowledgements

We gratefully acknowledge the Zentraleinrichtung für Datenverarbeitung (ZEDAT) of the FU Berlin for computational resources. B.S. thanks the BMBF (project IL-RFB, FKZ: 03SF0526B) for financial support. Open access funding enabled and organized by Projekt DEAL.

Conflict of interest

The authors declare no conflict of interest.

Keywords: bromine monochloride · halogen bonding · halogenation · polyhalides

[1] J. Pelletier, J. B. Caventou, *Ann. Chim. Phys.* **1819**, 142.
[2] F. D. Chattaway, G. Hoyle, *J. Chem. Soc. Trans.* **1923**, *123*, 654.
[3] K. Sonnenberg, L. Mann, F. A. Redeker, B. Schmidt, S. Riedel, *Angew. Chem. Int. Ed.* **2020**, *59*, 5464; *Angew. Chem.* **2020**, *132*, 5506.
[4] R. J. Elema, J. L. de Boer, A. Vos, *Acta Crystallogr. A* **1963**, *16*, 243.
[5] A. R. Mahjoub, K. Seppelt, *Angew. Chem. Int. Ed. Engl.* **1991**, *30*, 323; *Angew. Chem.* **1991**, *103*, 309.
[6] C. Walbaum, M. Richter, U. Sachs, I. Pantenburg, S. Riedel, A.-V. Mudring, G. Meyer, *Angew. Chem. Int. Ed.* **2013**, *52*, 12732; *Angew. Chem.* **2013**, *125*, 12965.
[7] L. Mann, P. Voßnacker, C. Müller, S. Riedel, *Chem. Eur. J.* **2017**, *23*, 244.
[8] K. Sonnenberg, P. Pröhm, N. Schwarze, C. Müller, H. Beckers, S. Riedel, *Angew. Chem. Int. Ed.* **2018**, *57*, 9136; *Angew. Chem.* **2018**, *130*, 9274.
[9] B. Schmidt, K. Sonnenberg, H. Beckers, S. Steinhauer, S. Riedel, *Angew. Chem. Int. Ed.* **2018**, *57*, 9141; *Angew. Chem.* **2018**, *130*, 9279.
[10] S. I. Ivlev, A. J. Karttunen, R. V. Ostvald, F. Kraus, *Chem. Commun.* **2016**, *52*, 12040.
[11] a) T. M. Beck, H. Haller, J. Streuff, S. Riedel, *Synthesis* **2014**, *46*, 740; b) T. Schlama, K. Gabriel, V. Gouverneur, C. Mioskowski, *Angew. Chem. Int. Ed. Engl.* **1997**, *36*, 2342; *Angew. Chem.* **1997**, *109*, 2440.
[12] a) G. Boschloo, A. Hagfeldt, *Acc. Chem. Res.* **2009**, *42*, 1819; b) K. Kakiage, T. Tokutome, S. Iwamoto, T. Kyomen, M. Hanaya, *Chem. Commun.* **2013**, *49*, 179.
[13] a) G. Bauer, J. Drobits, C. Fabjan, H. Mikosch, P. Schuster, *J. Electroanal. Chem.* **1997**, *427*, 123; b) W. Kautek, A. Conradi, C. Fabjan, G. Bauer, *Electrochim. Acta* **2001**, *47*, 815.
[14] a) A. van den Bossche, E. de Witte, W. Dehaen, K. Binnemans, *Green Chem.* **2018**, *20*, 3327; b) X. Li, A. van den Bossche, T. Vander Hoogerstraete, K. Binnemans, *Chem. Commun.* **2018**, *54*, 475; c) X. Li, Z. Li, M. Orefice, K. Binnemans, *ACS Sustainable Chem. Eng.* **2019**, *7*, 2578; d) B. Schmidt, B. Schröder, K. Sonnenberg, S. Steinhauer, S. Riedel, *Angew. Chem. Int. Ed.* **2019**, *58*, 10340; *Angew. Chem.* **2019**, *131*, 10448.
[15] a) G. Cavallo, P. Metrangolo, R. Milani, T. Pilati, A. Priimägi, G. Resnati, G. Terraneo, *Chem. Rev.* **2016**, *116*, 2478; b) T. Clark, M. Hennemann, J. S. Murray, P. Politzer, *J. Mol. Model.* **2007**, *13*, 291.
[16] A. Popov, J. Mannion, *J. Am. Chem. Soc.* **1952**, *74*, 6315.
[17] a) H. Lux, *Ber. Dtsch. Chem. Ges.* **1930**, *63*, 1156; b) N. O. Thiel, J. F. Teichert, *Nachr. Chem.* **2017**, *65*, 772; c) R. E. Buckles, J. W. Long, *J. Am. Chem. Soc.* **1951**, *73*, 998; d) J. F. Mills, J. A. Schneider, *Ind. Eng. Chem. Prod. Res. Dev.* **1973**, *12*, 160.
[18] W. Humphrey, A. Dalke, K. Schulten, *J. Molec. Graphics* **1996**, *14*, 33.
[19] A. D. Becke, *J. Chem. Phys.* **1993**, *98*, 5648.
[20] P. Deglmann, F. Furche, *J. Chem. Phys.* **2002**, *117*, 9535.
[21] P. Deglmann, F. Furche, R. Ahlrichs, *Chem. Phys. Lett.* **2002**, *362*, 511.
[22] P. Deglmann, K. May, F. Furche, R. Ahlrichs, *Chem. Phys. Lett.* **2004**, *384*, 103.
[23] C. Lee, W. Yang, R. G. Parr, *Phys. Rev. B* **1988**, *37*, 785.
[24] S. Grimme, J. Antony, S. Ehrlich, H. Krieg, *J. Chem. Phys.* **2010**, *132*, 154104.
[25] S. Grimme, S. Ehrlich, L. Goerigk, *J. Comput. Chem.* **2011**, *32*, 1456.
[26] A. D. Becke, E. R. Johnson, *J. Chem. Phys.* **2005**, *123*, 154101.
[27] E. R. Johnson, A. D. Becke, *J. Chem. Phys.* **2005**, *123*, 024101.
[28] E. R. Johnson, A. D. Becke, *J. Chem. Phys.* **2006**, *124*, 174104.
[29] S. Grimme, *J. Chem. Phys.* **2003**, *118*, 9095.
[30] F. Weigend, M. Häser, H. Patzelt, R. Ahlrichs, *Chem. Phys. Lett.* **1998**, *294*, 143.
[31] D. R. Stull, *Ind. Eng. Chem.* **1947**, *39*, 540.
[32] T. Negoro, Y. Ikeda, *Bull. Chem. Soc. Jpn.* **1984**, *57*, 2111.
[33] T. Negoro, Y. Ikeda, *Bull. Chem. Soc. Jpn.* **1986**, *59*, 3515.
[34] T. Sotokawa, T. Noda, S. Pi, M. Hirama, *Angew. Chem. Int. Ed.* **2000**, *39*, 3430; *Angew. Chem.* **2000**, *112*, 3572.
[35] W. Gabes, K. Olie, *Cryst. Struct. Comm.* **1974**, *3*, 753.
[36] a) F. Zobi, O. Blacque, G. Steyl, B. Spingler, R. Alberto, *Inorg. Chem.* **2009**, *48*, 4963; b) M. Ghassemzadeh, B. Neumuller, K. Dehnicke, *CCDC 790138: Experimental Crystal Structure Determination*, Cambridge Crystallographic Data Centre, **2014**; c) G. L. Breneman, R. D. Willett, *Acta Crystallogr.* **1967**, *23*, 334.
[37] G. A. Landrum, N. Goldberg, R. Hoffmann, *J. Chem. Soc. Dalton Trans.* **1997**, 3605.
[38] K. P. Huber, G. Herzberg, *Molecular Spectra and Molecular Structure—VI. Constants of Diatomic Molecules*, 2nd ed., Springer, Boston, **1979**.
[39] H. Haller, M. Ellwanger, A. Higelin, S. Riedel, *Angew. Chem. Int. Ed.* **2011**, *50*, 11528; *Angew. Chem.* **2011**, *123*, 11732.
[40] A. Bondi, *J. Phys. Chem.* **1964**, *68*, 441.
[41] A. W. Addison, T. N. Rao, J. Reedijk, J. van Rijn, G. C. Verschoor, *J. Chem. Soc. Dalton Trans.* **1984**, 1349.
[42] H. Stammreich, R. Forneris, Y. Tavares, *Spectrochim. Acta* **1961**, *17*, 1173.
[43] G. M. Sheldrick, *Acta Crystallogr. A* **2008**, *64*, 112.
[44] G. M. Sheldrick, *Acta Crystallogr. Sect. C* **2015**, *71*, 3.
[45] O. V. Dolomanov, L. J. Bourhis, R. J. Gildea, J. A. K. Howard, H. Puschmann, *J. Appl. Crystallogr.* **2009**, *42*, 339.
[46] TURBOMOLE GmbH, TURBOMOLE V7.3. a development of University of Karlsruhe and Forschungszentrum Karlsruhe GmbH, **2018**.

Manuscript received: March 13, 2020
Accepted manuscript online: April 6, 2020
Version of record online: October 22, 2020

2.4. Summary and Outlook

The novel polyinterhalide $[NEt_3Me][Cl(BrCl)_2]$ was successfully established as an atom-economical interhalogenation reagent for a wide variety of unsaturated substrates. The very short reaction times and good yields reflect the high reactivity with simultaneous selectivity towards other functional groups.

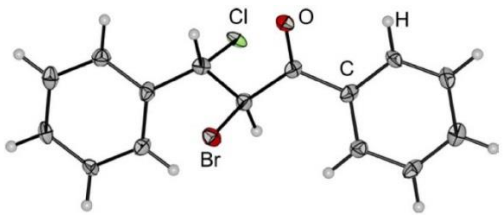

Figure 13: X-ray crystal structure of bromochlorinated (*E*)-chalcon.[64]

The regioselectivity of the reaction with asymmetric olefins (**84**) or 1,4-unsaturated systems (**89**) is a result of the polarization of the two halogen atoms. Together with the *trans*-position of the two halides confirmed by single crystal structure analysis (Figure 13), a reaction mechanism in analogy to the electrophilic bromination of olefins can be postulated.

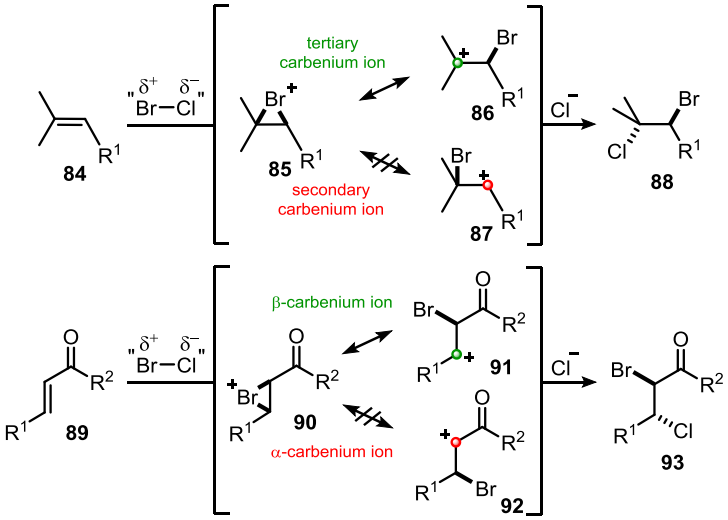

Scheme 27: Explanation of the regioselectivity in the interhalogenation of unsymmetrical olefins (top) and *Michael* systems (bottom).

The positively polarized bromine atom of the polyinterhalide forms a halonium ion with the double bond of an olefin (**84**) or *Michael* system (**89**). By plotting the possible mesomeric boundary formulas, the more stable carbenium ion and thus the most reactive site for the subsequent nucleophilic opening of the halonium ion can be identified. For asymmetric olefins (**84**), the *Markownikov* rule applies and the attack of the chloride will occur at the more highly substituted carbon of the halonium ion **85**. For

Michael systems (**89**), α-carbenium ions (**92**) are energetically less favorable than β-carbenium ions (**93**) due to the electron-withdrawing effects of the carbonyl group. Here, the opening of the halonium ion **90** occurs in the β-position to the carbonyl group (Scheme 27).

The liquid aggregate state and low vapor pressure of the reagent reduce potential risks from exposure, simplify handling, and thus provide a reasonable alternative to pure BrCl. The atomic economy and reactivity of $[NEt_3Me][Cl(BrCl)_2]$ (A = 1.7) is increased compared to the literature known reagent $[NEt_4][Cl(BrCl)]$ (A = 2.4) and the previously mentioned two-component systems (A = 2.5 to 3.8), making it ecologically as well as economically superior. A further increase could be achieved by using the higher coordinated polyinterhalides such as $[NEt_4][Cl(BrCl)_5]$ (A = 1.3).

A direct bromocyanidation would have enormous potential for organic chemistry. For this purpose, the corresponding BrCN analogues, which were also recently developed in the *Riedel* group,[78] can be investigated as reagents. If the polarization and reactivity of these polypseudohalides correspond to the polyinterhalides discussed earlier, bromo-cyanide addition to double bonds would be conceivable. This reactivity with pure BrCN is known so far only for the much more reactive enamines[79] (**96**) and silyl enol ethers[80] (**94**) (Scheme 28).

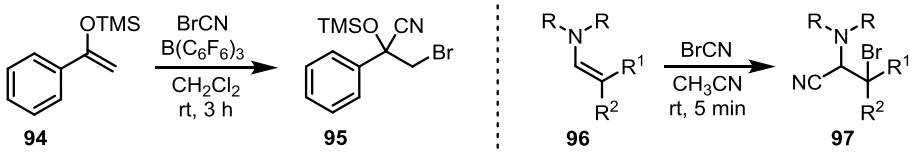

Scheme 28: Literature known reactivities of BrCN with unsaturated substrates.

By weakening the Br-CN bond in the polypseudohalide, its reactivity could be increased and nonactivated alkenes (**98**) could also be accessible as substrates. The β-brominated nitrile **99** thus generated is a valuable synthetic building block due to its numerous downstream transformation possibilities. Base-induced elimination of HBr, for example, can generate α,β-unsaturated nitriles (**100**).[81] These can subsequently be further reduced, esterified or hydrolyzed (**101**) (Scheme 29).

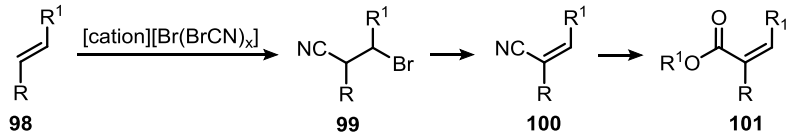

Scheme 29: Bromocyanidation of olefins and possible follow up transformations.

3. Studies on the Total Synthesis of Hypatulin A and B

3.1. Introduction

3.1.1. Natural Products and the Importance for Humanity

Biogenic natural products can be divided into two groups according to their origin.[82]

1. Primary Natural Products

All organisms have a primary or basic metabolism that is responsible for essential processes such as growth or reproduction. The primary natural products produced for this purpose are, for example, proteins, carbohydrates or lipids, which are responsible for energy production or the construction of new cells. Despite the omnipresence of these molecules, the respective structures can vary greatly between different organisms.

2. Secondary Natural Products

The processes of the secondary metabolism, on the other hand, unfold as a continuous response to biotic and abiotic environmental influences and can thus achieve an evolutionary advantage. The secondary metabolism is adaptive and extremely diverse. Thus, it may differ even among several populations of one species. The biosynthesis of defensive secretions or sexual attractants are examples of products emerging from the secondary metabolism. Secondary natural products can be found in the substance classes of terpenes, steroids or alkaloids for example.

Plant metabolism has been used as a rich source of active substances since the dawn of civilization. The use of herbal medicines has been known for 60000 years[83] and the first documented uses of plant-based pharmaceuticals date back almost 5000 years[84]. The importance of natural or nature-derived medicines did not stop in modern times. A milestone in natural product research is the discovery and first synthesis of the analgesic morphine from the opium poppy, whose importance as a cultivated plant in Europe dates back to the Neolithic.[85] In 1804, morphine was isolated for the first time from the opium poppy (*Papaver somniferum*) by the pharmacist's assistant *Sertürner*.[86] *Robinson* finally succeeded in determining the structure in 1925.[86] It took further 27 years before *Gates* was able to carry out the first total synthesis and confirm the structure proposal by *Robinson*.[87] Furthermore, acetylsalicylic acid, which has been on the WHO's list of essential medicines since 1977, is of enormous importance to mankind as an analgesic, anti-inflammatory and antipyretic drug.[88] The use of willow bark and other plants has been known for thousands of years and is partially based on the pharmacological properties of the salicylic acid and its derivatives.[89] The first synthesis of acetylsalicylic acid was achieved in 1897 at the former Farbenfabriken Friedr. Bayer & Co and was

patented in 1899 under the name Aspirin®.[88] Penicillin is another prominent example which confirms the enormous importance of natural substances for human history. The antibiotic effect of the fungus *Penicillium*, described already 1874 by *Billroth*, initiated one of the most important developments in medical history with the discovery of penicillin by *Fleming* in the following century.[90]

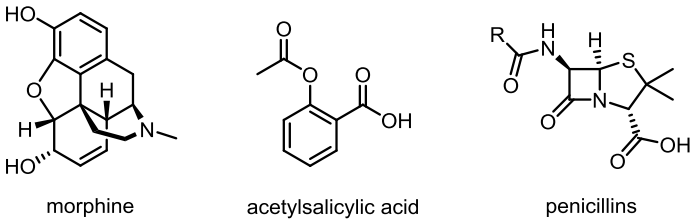

Figure 14: Morphine, acetylsalicylic acid and penicillins as exemplary milestones in natural product research.

In ancient times, preparations from plant or, more rarely, animal materials were mostly used to treat diseases. After it was recognized that defined active ingredients or active ingredient compositions thereof were responsible for the pharmacological activity, the focus shifted to the isolation and later also to the synthetic production of these compounds. Targeted synthetic access to an active ingredient has several advantages over the use of whole plant or animal materials. For one, a more targeted therapy can be achieved by eliminating mixing with useless or even toxic components of the plant or animal. In terms of animal and environmental protection, it is also ethically questionable to exploit enormous quantities of sometimes rare and protected species from the environment and to isolate minute amounts of the active ingredient. Thus, organic synthesis displays an indispensable alternative to provide large quantities of active ingredients.

The synthetic access of active ingredients, can be devided into semisyntheses and total syntheses. Semisyntheses start from an already complex natural substance, which builds up the desired target through further transformations. One of the most prominent examples is the semisynthesis of paclitaxel, which is used to treat cancer. In this process, baccatin III, which is more readily available from the European yew tree (*Taxus baccata*), is converted into paclitaxel in a few steps.[91] The total synthesis of natural products, on the other hand, can be traced back to the simplest commercially available chemicals. The advantage of total synthesis is the ability to generate numerous derivatives that may have higher activity or lower toxicity. Total synthesis is often used to elucidate the structure or structure-activity relationship of newly discovered natural products. Additionally, an academic and industrial interest lies in the development of new efficient synthetic methods to access highly complex structural motifs.

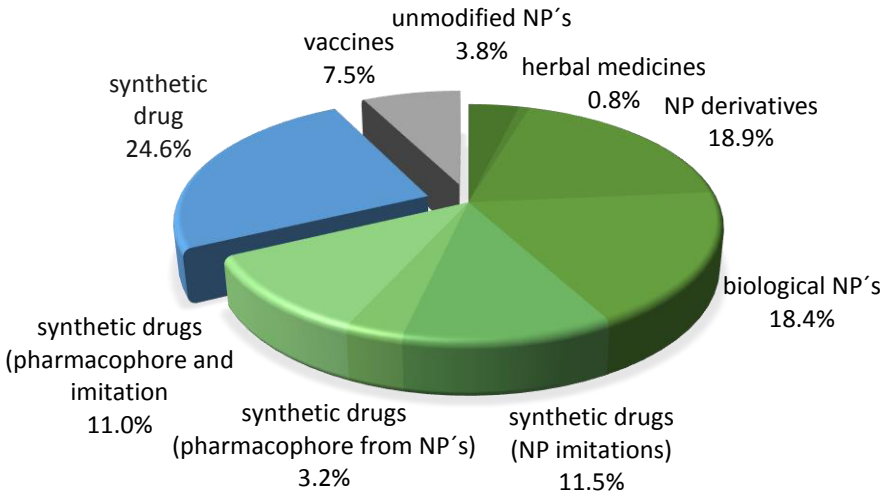

Figure 15: Categorization of all approved drugs (1981-2019)[92] (NP = natural product).

As shown in Figure 15 more than two-thirds of all drugs approved since 1981 have their origin in natural products either as a derivative or imitation of the original structure (presented in different shades of green). Less than 25% of these drugs are not based on any known natural product structure and have a purely synthetic origin (blue). Most of them are products of random screening or modification of already known drugs.[92] Today, drug discovery focuses on circumventing resistance, combating novel pathogens, or treating diseases more effectively. Far less than 10% of the world's biodiversity has been tested for its biological activity to date.[93] Thus, nature as whole can still be seen as an almost inexhaustible source of novel lead structures for the development of new active substances.

3.1.2. The Plant Genus *Hypericum*

With over 500 species, *Hypericum* is the largest plant genus within the plant family *Hypericaceae*. The most famous representative is the St. John's wort (*Hypericum perforatum*) (Figure 16). The distribution of this species, native to Europe, Africa and Western Asia, nowadays covers the entire American continent, East Asia and Australia.[94] Since more than 2000 years St. John's wort enjoyed great popularity as a medicinal plant against a variety of ailments.[94] Already during the *Han* Dynasty (206 B.C. to 220 A.D.), various *Hypericum* species were used in Asia and Europe to treat depression, wounds, burns, diarrhea, and animal bites or stings.[94] *Pliny the Elder* also mentions *Hypericum* in his encyclopedia *Naturalis historia* from 77 A.D.[94] Especially due to the increasing number of depressive disorders, St. John's wort preparations have been experiencing a renaissance as medicinal products since the 1990s.[94]

Figure 16: Inflorescence of St. John´s wort (*Hypericum perforatum*)[95]

In recent decades, numerous pharmacological studies have confirmed the antidepressant, antitumor, antimicrobial, and anti-inflammatory effects of *Hypericum* species.[96] St. John's wort is one of the best-studied medicinal plants to date.[96]

3.1.3. Polyprenylated Acylphloroglucinols

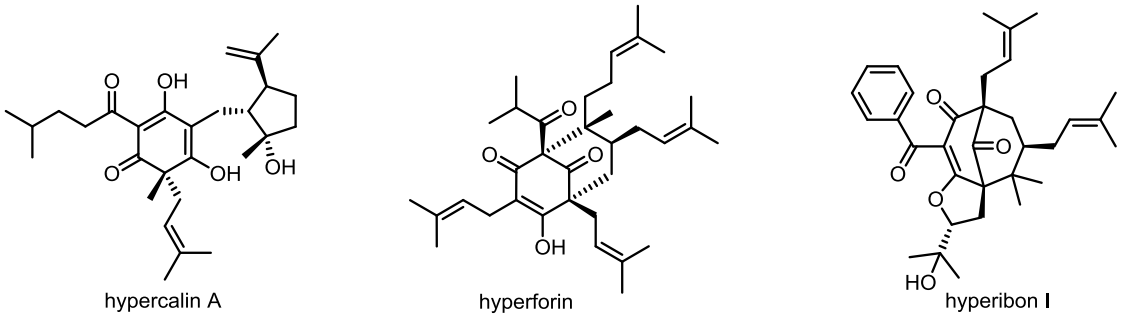

Figure 17: Polyprenylated acylphloroglucinols isolated from *Hypericum*.

In addition to mono- and sesquiterpenes (pinenes, α-humulene, germacrene D), flavonoids (quercitin, biapigenin), naphthodianthrone derivatives (hypericin, pseudohypericin) and other compounds, numerous representatives of the so-called polyprenylated acylphloroglucinols (PAPs) (Figure 17) could be isolated and characterized from the genus *Hypericum*.[97] *Hypericum* is considered to be the main source of the more than 700 known PAPs.[97] This category of natural products belongs to the class of meroterpenes, which means they have a terpenoid structure supplemented by other structural elements (mostly phenol derivatives) (Figure 18).[97] PAPs have innumerable different functions and properties. Cyctotoxic activity against various cancer cell lines is already known for over 50 phloroglucinols.[97] Humolones and lupolones are amaroids that give hops their characteristic flavor profile.[97] Other PAPs exhibit anti-inflammatory properties through inhibition of cyclooxygenases.[97]

Another subgroup is represented by the polycyclic polyprenylated polycyclic acylphloroglucinols (PPAPs). Figure 18 shows the structural features of PPAPs based on hyperforin. The core (red) can be traced back to 1,3,5-trihydroxybenzene (phloroglucinol) and is decorated with a varying number of prenyl residues (green). One additional acyl group (blue), which can be highly variable, can also be found in the molecule. For the hypatulin and hyperibon families these are benzoyl groups, whereas for hyperforin, adhyperforin or hypercalin A, they are a wide variety of acyl groups with branched alkyl chains. In addition, further formal isoprene units (orange) can be added, which enlarge the molecule and increase its complexity.

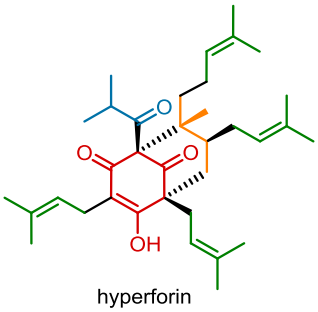

Figure 18: Hyperforin as an example for the structural features of PPAPs.

In analogy to steroids,[98] the basic structure of PPAPs can be altered by rearrangements or oxidations to such an extent that identification becomes difficult. A descriptive example is hypatulon A, which was isolated in 2018 and structurally revised in 2020.

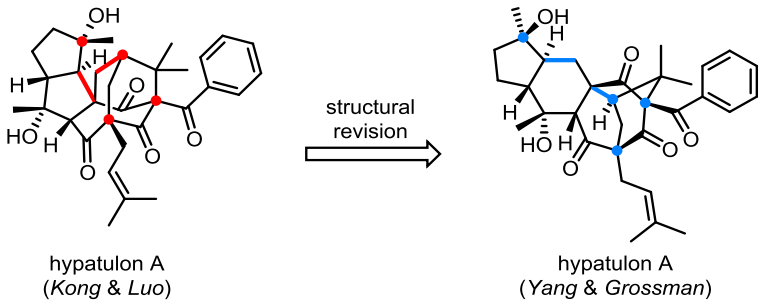

Scheme 30: Proposed structure by *Kong* and *Luo* (left) and the revised structure by *Yang* and *Grossman* (right) for hypatulon A (the deviating connectivities and configurations are highlighted in red and blue).

Luo and *Kong* initially postulated a core structure consisting of two five-membered rings connected to a homoadamantane center.[99] The resulting 5/5/7/6/6-pentacyclic structure was subsequently challenged by *Yang* and *Grossman*. By renewed NMR spectroscopic evaluation and DFT-based calculations, the authors corrected the previously presented structural proposal and postulated a 5/6/6/5/6-pentacyclic core with divergent connectivity (Scheme 30).[100] Due to their often unique structure and biological activity, numerous PPAPs have become the subject of total syntheses.

Hyperforin occupies a central role among the active ingredients in St. John's wort, and most of the pharmacological properties of the plant extracts are closely related to the properties of hyperforin. For example, antibacterial activity against the gram-positive bacteria of the *Staphylococcus aureus* strain, which have already formed resistance to penicillin or methicillin, has been documented.[101] Antitumor properties have been demonstrated both *in vitro* and *in vivo*. Inhibition of cyclooxigenase-1 and 5-lipoxygenase also reduces the formation of proinflammatory eicosanoids. In particular, its effect as a natural antidepressant has been extensively studied. Thus, like synthetic antidepressants, hyperforin increases the concentration of neurotransmitters in the synaptic cleft. In doing so, hyperforin activates ion channels of the TRPC6 type. This leads to a reduction of the Na^+ gradient, which controls the reuptake of neurotransmitters. St. John's wort, and hyperforin in particular, can thus make a contribution to combating the growing numbers of people suffering from depression.[101]

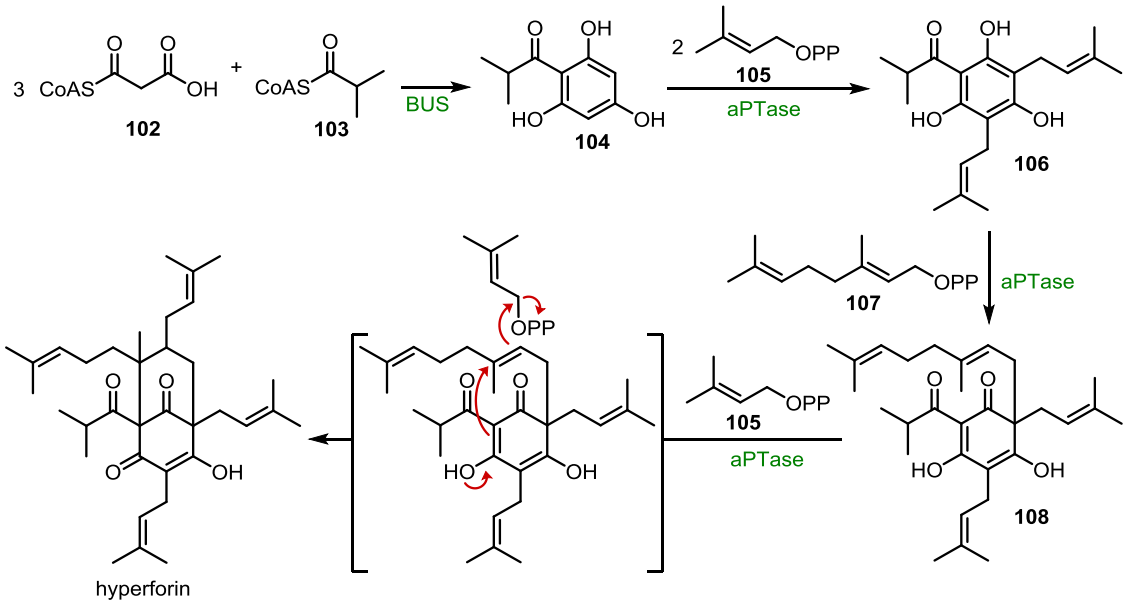

Scheme 31: Biosynthesis of hyperforin according to *Beerhues*.[101]

The intensively discussed biosynthesis of hyperforin was summarized by *Beerhues* in 2006 (Scheme 31).[101] First, the polyketide synthase isobutyrophenone synthase (BUS) catalyzes the condensation of three molecules of malonyl-CoA (**102**) and isobutyryl-CoA (**103**). The resulting phloroisobutyrophenone (**104**) is subsequently functionalized twice with prenyl pyrophosphate (**105**) by aromatic prenyltransferases (aPTases). Further alkylation of the aromatic core of **106** by geranyl pyrophosphate (**107**) generates diketone **108**. Activation of the double bond of the geranyl side chain by prenyl pyrophosphate (**105**) initiates the subsequent ring closure and generates the bicyclic hyperforin.

Due to its exceptionally broad pharmacological spectrum, hyperforin has become the motivation of numerous total syntheses since its isolation in 1975.[102] Pioneering work on the synthesis of the core structure was published 2005 by the research group of *Nicolaou*.[103] In this work, a general approach to medium-sized bridged ring systems, as found in hyperforin, was presented. As a key step, an anullation of cyclic ketones with methacrolein was presented. In another publication by *Mehta* and *Bera* in 2009, both the bicyclic backbone and the four prenyl or homoprenyl residues could be installed.[104] One year later, *Shibasaki* and co-workers succeeded in the synthesis of *ent*-hyperforin in 52 steps.[105] The first enantioselective total synthesis of hyperforin was finally completed in 2013 by the group of *Shair*. An enantiomerically enriched epoxide which was traced back to geraniol determined further stereoselectivities in this 18-step synthesis.[106] In the following years, three additional racemic syntheses were presented by the groups of *Nakada* (2013),[107] *Barriault* (2014),[108] and *Maimone* (2015)[109].

3.1.4. Hypatulin A and B and other Polyprenylated Benzophenones

Another species of the *Hypericum* genus is the goldencup St. John's wort (*Hypericum patulum*). The original distribution area is located in the central Chinese provinces of Guizhou and Sichuan.[110] However, due to its use as a decorative garden plant, this species can now be found almost all over the world.[111] In recent years, goldencup St. John's wort has also proven to be a rich source of biologically active and structurally interesting compounds.

Figure 19: *Hypericum patulum*.[112]

In 2016, *Tanaka* and *Kashiwada* were able to isolate the two meroterpenes hypatulin A and B from the dried leaves of *Hypericum patulum*. 1.48 kg of the starting material was extracted and purified by column chromatography. After separation by HPLC technique, 36.9 mg of hypatulin A and 3.6 mg of hypatulin B were obtained. From the determination of the molecular formula by HRESIMS and the

constitution and relative stereoinformation by 2D NMR spectroscopy (COSY, HSQC, HMBC and NOESY), the authors were able to deduce the structures of hypatulin A and B (Figure 20). The absolute stereoinformation of hypatulin A was confirmed by ECD spectroscopy.[113]

Hypatulin A possesses an unique highly substituted tricyclic octahydro-1,5-methanpentalene core (green). The three linear and flexible prenyl side chains form a strong contrast to the dense and rigid core structure. Together with the four closely spaced quaternary stereocenters, hypatulin A constitutes a challenging target molecule for total synthesis. In hypatulin B, a bicyclo[3.2.1]octane core (green) can be found. Both substances belong to the diverse group of PAPs. Since the acyl group in this case is a benzoyl group, the two hypatulins are assigned to the class of polyprenylated benzophenones (PBPs).

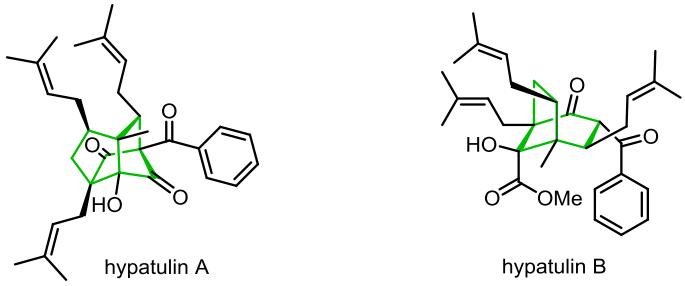

Figure 20: Structural proposal for hypatulin A and B according to *Tanaka* and *Kashiwada*.[113]

For hypatulin A, an antimicrobacterial effect against *Bacillus subtilis* could be demonstrated.[113] Whether the isolated compounds, like their close relatives hyperforin or hypercalin C, possess other interesting pharmacological properties has not been reported and could be the subject of future research. In addition to the two previously mentioned hypatulins, other PBPs, some of them much more complex, could be isolated from *Hypericum patulum*. In 2020, *Tanaka* and *Kashiwada*, who have already identified hypatulin A and B, were able to isolate another member of the PBP family from *Hypericum patulum*.[114] Hypatulin C has an octahydro-1*H*-1,5-methanoindene core decorated by four prenyl residues. No biological activity is known at this time. In the same publication, the authors also report the isolation and characterization of hypelodin B, which has been known since 2014.[115] In the 2020 and 2014 publications, the authors propose a joint biosynthesis of hypatulin C, hypelodin A, and hypelodin B (Scheme 32). The first steps are in analogy to the biosynthesis of hyperforin shown in Scheme 31. Three equivalents of malonyl-CoA (**102**) and benzoyl-CoA (**109**) form benzophenone **110** by condensation. Dual prenylation followed by geranylation generates polyene **111**. Downstream prenylation of the geranyl side chain forms the common cyclization precursor **112**. Addition of the hydroxyl group to the internal double bond (blue) of the geranyl side chain generates hypelodin A. Alternatively, compound **112** can form hypatulin C by a cyclization cascade (green), which can react to

hypelodin B by a further cyclization process. Consideration of the biosyntheses illustrates the common origin of the prenylated acylphloroglucinols and explains the diversity of this distinctly interesting class of compounds.

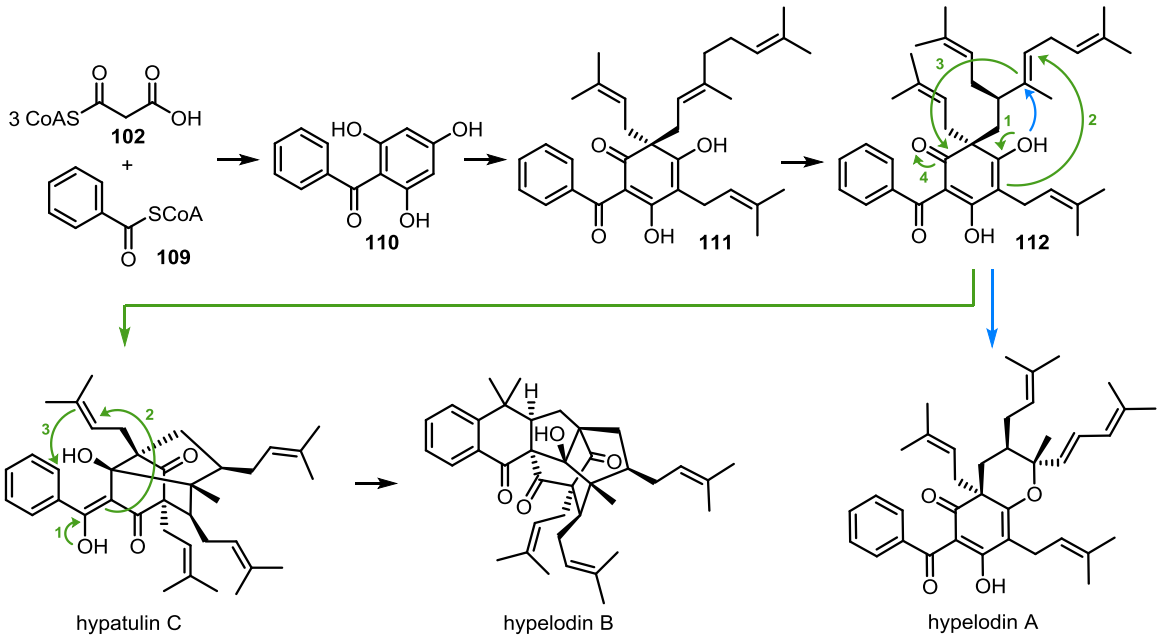

Scheme 32: Proposed biosynthesis of the meroterpenes hypatulin C, hypelodin A and hypelodin B according to *Kashiwada*.[114,115]

3.2. Scientific Goal

The unique structures of hypatulin A and B, the possible common synthetic strategy and the often interesting and versatile pharmacological properties of related PBPs, make the enantioselective total synthesis of the two meroterpenes a precious project. The retrosynthetic analysis of the two natural products is shown in Scheme 33.

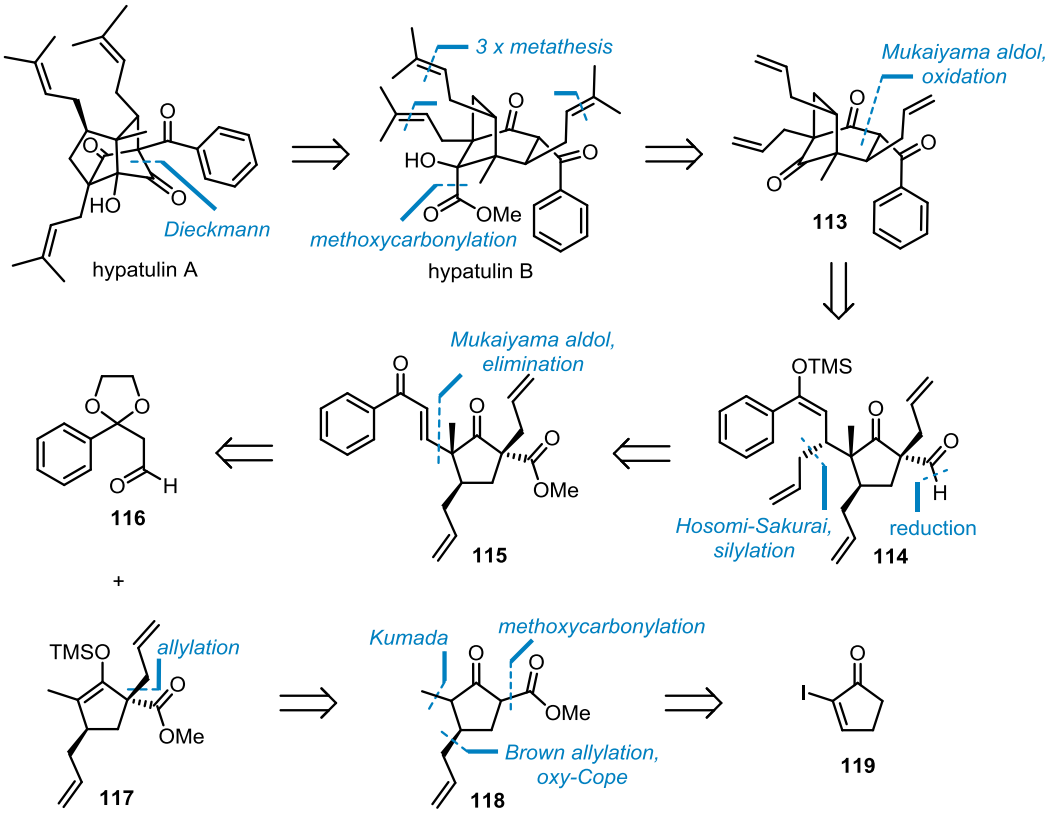

Scheme 33: Retrosynthetic analysis of hypatulin A and hypatulin B.

It was theorized, that Hypatulin A can be accessed by an intramolecular substitution from hypatulin B. The latter can be traced back to triketone **113** by triple olefin metathesis and methoxycarbonylation. Installation of the last allyl group on enone **115** can be realized by a *Hosomi-Sakurai* reaction. The silyl enol ether **114** formed in situ can subsequently set up the second ring system via an intramolecular *Mukaiyama* aldol reaction. Enone **115** can itself also be synthesized from the two fragments **116** and **117** via a *Mukaiyama* aldol reaction followed by elimination. Silyl enol ether **117** can be obtained from β-keto ester **118** via an enantioselective allylation process. The synthesis of the latter β-keto ester can be accessed via an enantioselective *Brown* allylation and oxy-*Cope* rearrangement followed by methoxycarbonylation from the iodinated enone **119**.

As shown in Scheme 34, the common precursor **115** can also be prepared from diketone **120** by double functionalization (allylation, methoxycarbonylation). This diketone **120** can be traced back to aldehyde

116 and silyl enol ether **121** via intermolecular *Mukaiyama* aldol reaction. As before, silyl enol ether **121** can be available from the iodinated enone **119** via an enantioselective *Brown* allylation followed by oxy-*Cope* rearrangement.

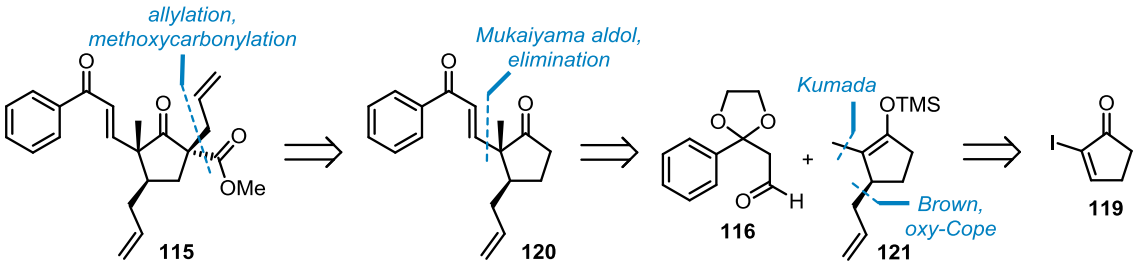

Scheme 34: Alternative retrosynthetic analysis of the common precursor **115**.

3.3. Results

The studies on the total synthesis of hypatulin A and B were planned and carried out in collaboration with *Stefan Leisering*. After initial retrosynthetic considerations and first successful experiments, two different synthetic routes to enone **115** were pursued. In *Leisering's* approach (Scheme 34), the intermolecular *Mukaiyama*-aldol coupling was carried out at an early stage of the synthesis. The second allyl group and the methyl ester on the cyclopentanone scaffold should be installed subsequently. For the synthetic approach detailed in this thesis (Scheme 33), the cyclopentanone scaffold was first fully functionalized before silyl enol ether **117** and aldehyde **116** can generate the common precursor **115**. The execution of both synthetic pathways should reveal which is the most effective route to enone **115**.

Starting from the commercially available enone **119** (due to the high price, the substance was synthesized via a *Baylis-Hillman*-type α-iodination from cyclopent-2-en-1-one[121] on a large scale), the first stereocenter was introduced by an organocatalytic enantioselective *Brown* allylation[116] and alcohol **122** was obtained in excellent yield (88%) and enantioselectivity (94%). Subsequent *Kumada* reaction[117] introduced the methyl group in almost quantitative yield. Unfortunately all attempts to introduce the first allyl group by using 2-methylcyclopent-2-en-1-one as the substrate failed. The iodide substituent on the halogenated enone **119** turned out to be crucial for the reactivity and selectivity of the applied *Brown* allylation. β-Keto ester **118** was synthesized by a self-developed one-pot reaction consisting of an oxy-*Cope* rearrangement[116] and methoxycarbonylation, again in almost quantitative yield (Scheme 35).

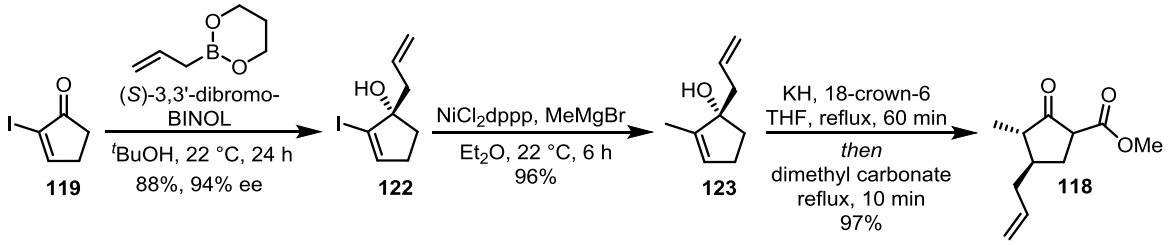

Scheme 35: Introduction of the first stereocenter and follow up synthesis of β-keto ester **118**.

Numerous attempts to introduce the second allyl group in a diastereoselective way via a direct *C*-allylation failed, yielding only the epimer of compound **125a**. An enantioselective version of the *C*-allylation[118] could not efficiently counteract the substrate-induced diastereoselectivity as well. By combining a *Mitsunobu*-like *O*-allylation[119] and subsequent diastereoselective oxy-*Cope* rearrangement[120] of the β-keto ester **118**, the synthesis of the twofold allylated cyclopentenone **125a** was achived in a satisfactory yield of 33% over two steps and a good diastereoselectivity of 10:1

(Scheme 36). The moderate yield of the *O*-allylation is due to the competitive *C*-allylation, a problem known in the literature.[119]

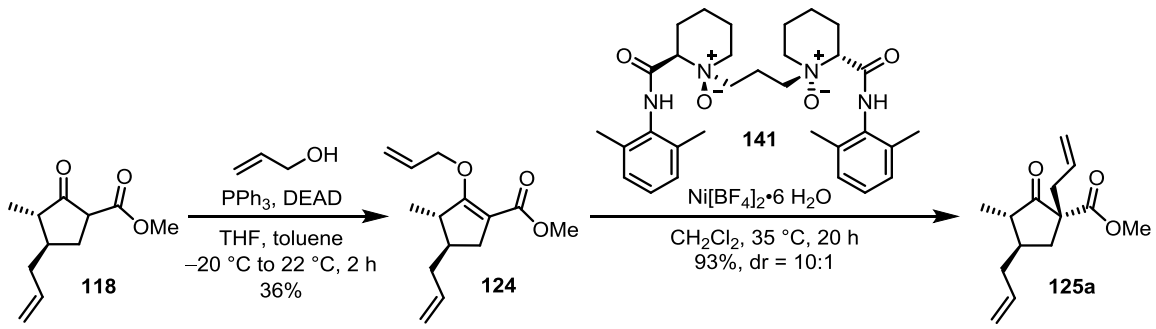

Scheme 36: Stereoselective installation of the second allyl group.

The configuration of the newly generated quaternary stereocenter was confirmed first by ring closing metathesis and later by single crystal structure analysis.[121] Scheme 37 shows that only the desired epimer of the β-keto ester **125a**/**b** is able to undergo a ring closing metathesis due to the *cis*-position of both allyl groups. The good yield of 68% for the metathesis product **126** suggests that the major isomer of the two β-keto esters must be compound **125a**.

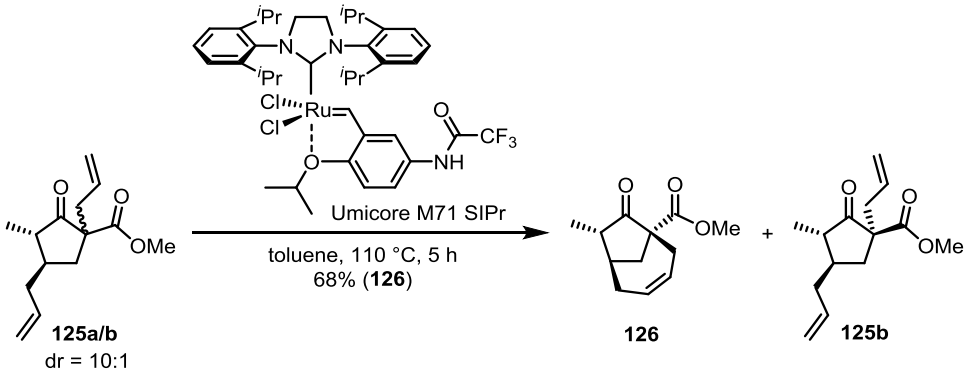

Scheme 37: Verification of the second stereocenter by ring closing metathesis.

In order to achieve near quantitative yields of silyl enol ether **117**, the use of potassium hydride as a base was essential. Other bases such as lithium diisopropylamide, potassium hexamethyldisilazide or triethylamine failed to generate complete conversion. The subsequent *Mukaiyama* aldol reaction of silyl enol ether **117** and literature known aldehyde **116** gave a mixture of ketone **127** and acetal **128** in a good overall yield of 60% (Scheme 38).

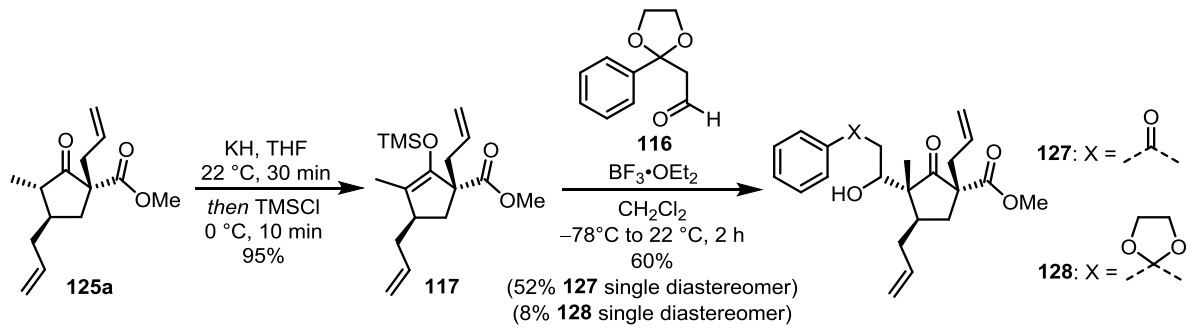

Scheme 38: *Mukaiyama* aldol reaction of the two fragments **117** and **116**.

Ketone **127** and acetal **128** were initially separated by column chromatography for characterization. For the synthetic route, separation was not necessary, since both compounds led quantitatively to the same enone **115** under acidic conditions (Scheme 39).

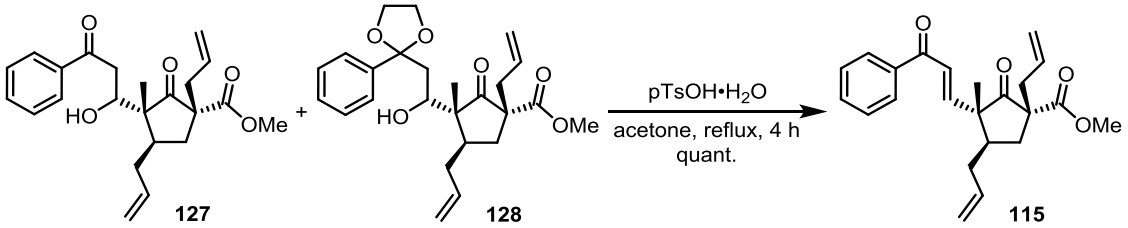

Scheme 39: Acid-catalyzed elimination of the two aldol products **127** und **128**.

The diastereoselective introduction of the third allyl group proved to be challenging. Classic copper-catalyzed conditions invariably afforded the 1,2-adduct.[121] Screening of a wide variety of *Lewis* acids (titanium tetrachloride, boron trifluoride diethyl etherate, ferric(III) chloride, iodine, indium, indium(III) chloride) finally led to the application and optimization of an indium(III)-catalyzed *Hosomi-Sakurai* reaction[122] with a good yield of almost 60%. Subsequently, the addition of triethylamine to the reaction mixture also made the two corresponding silyl enol ethers **130a** and **130b** accessible (Scheme 40). The poor diastereoselectivity could not be improved even by intensive optimization experiments. The column chromatographic separation and assignment of the two diastereomeric species was carried out at a later stage of the synthesis.[121]

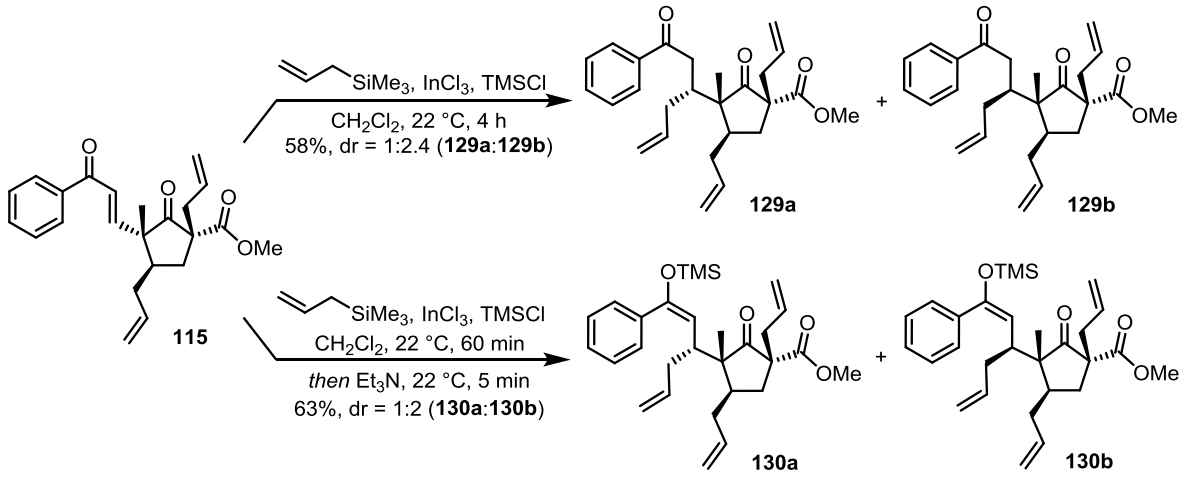

Scheme 40: *Hosomi-Sakurai* reaction of enone **115**.

All attempts to build up the six-membered ring of the hypatulin scaffold under basic conditions via a *Dieckmann*-type ring closure failed. Here, only the decarboxylation product **131** could be identified. It was speculated that the keto group adjacent to the ester functionality enabled decarboxylation. Therefore, reduction of the cyclopentanone scaffold converted the ketone to a secondary alcohol and the aldol precursor **132** was obtained. Analysis of the reaction products after a subsequent intramolecular aldol reaction indicated only the existence of the aldol condensation product **134** (Scheme 41).

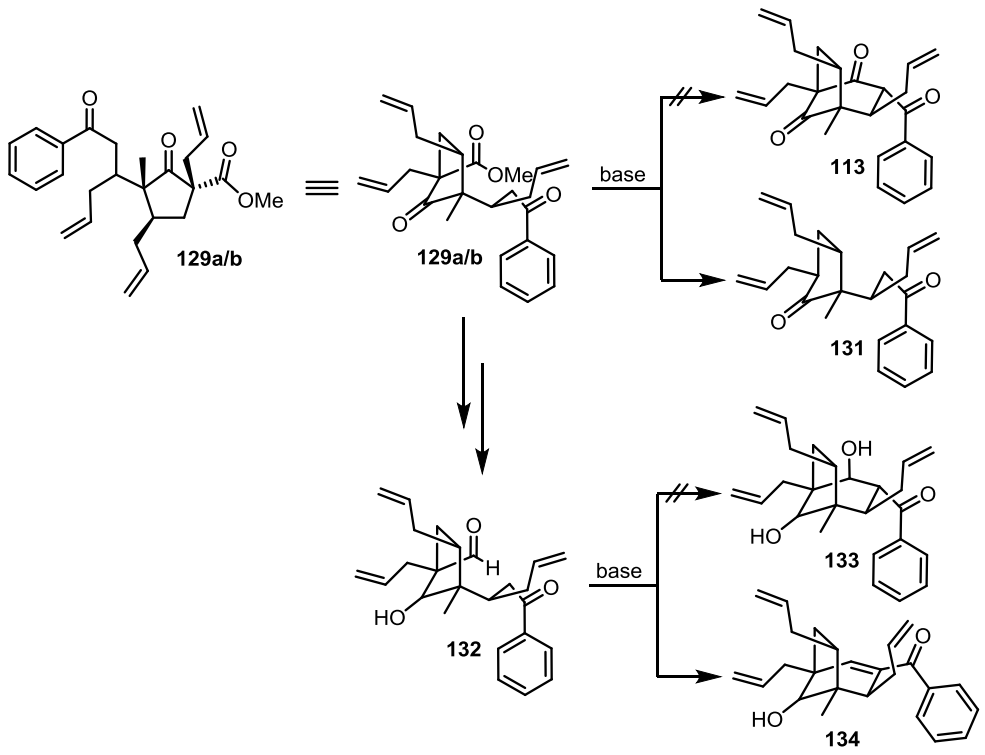

Scheme 41: First attempts to build the bicyclic scaffold of hypatulin B.

*Leisering´*s alternative synthetic route to enone **115** involved a late stage introduction of the allyl and ester group. Initial experiments clarified that the order of functionalization was crucial for the stereoselective arrangement of the two functional groups. It was also observed that the allylation carried out first performed significantly worse than the subsequent methoxycarbonylation. A twofold functionalization that could be carried out as a one-pot reaction seemed favourable at this point. This reaction was carried out and optimized by me. The use of HMPA as an additive was essential here, allowing the allylation to proceed much more efficiently and enone **115** to be obtained as a single diastereomer with a satisfactory yield of 54% (Scheme 42).

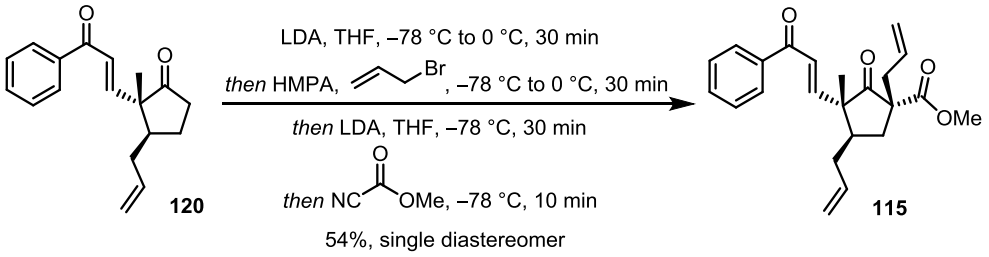

Scheme 42: One-pot procedure for the twofold functionalization of enon **120**.

3.4. Summary and Outlook

In the previously discussed studies on the total synthesis of hypatulin A and B, three of five (hypatulin B) or six (hypatulin A) stereocenters were correctly installed. Moreover, all functional groups, except for the ester functionality in hypatulin B, were successfully introduced. As a result, a nine-step synthesis of silyl enol ether **130a**/**b** can be presented. *Leisering* could further show that after two more steps the assembly of the carbocyclic backbone of hypatulin B can already be accomplished.[121]

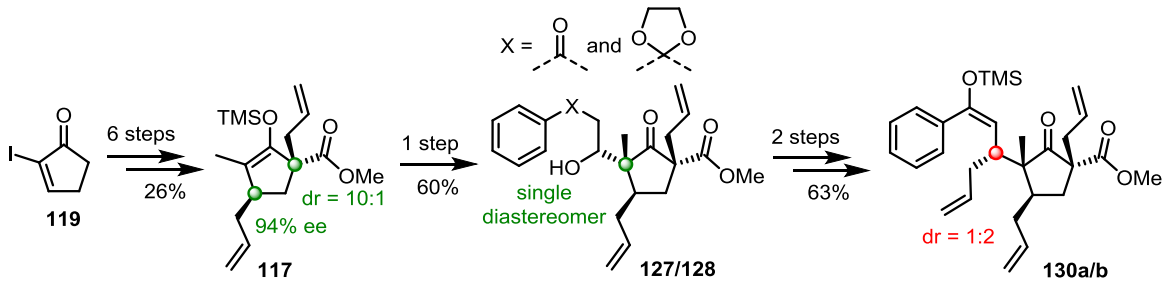

Scheme 43: Summarized synthesis of silyl enol ether **130a**/**b**.

A summarized presentation of the synthetic approach towards silyl enol ether **130** is shown in Scheme 43. Starting from commercially available enone **119**, the stereoselective synthesis of silyl enol ether **117** succeeded in six steps with a total yield of 26%. Five steps proceeded in ≥88% yield. The introduction of the first stereocenter by combining an organocatalytic *Brown* allylation with a one-pot oxy-*Cope* rearrangement/methoxycarbonylation should be highlighted here. The second stereocenter could also be introduced in a highly selective fashion by a combination of two reactions (*Mitsunobu*-like *O*-allylation and diastereoselective oxy-*Cope* rearrangement). The subsequent intermolecular *Mukaiyama*-aldol reaction succeeded in both the efficient coupling of the two fragments **116** and **117** and the correct installation of the third stereocenter. The introduction of the last allyl group could be realized under *Hosomi-Sakurai* conditions with good yields but insufficient diastereoselectivity.

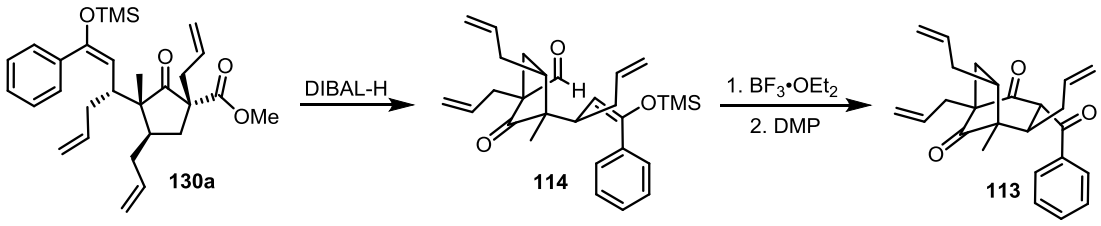

Scheme 44: Continued synthesis by *Leisering*.[121]

In the further process, *Leisering* succeeded in building up the carbocyclic backbone of hypatulin B via an intramolecular *Mukaiyama*-aldol reaction (Scheme 44). Subsequent attempts to introduce the ester functionality failed either due to the lack of reactivity or the wrong stereoselectivity of the reaction.[121]

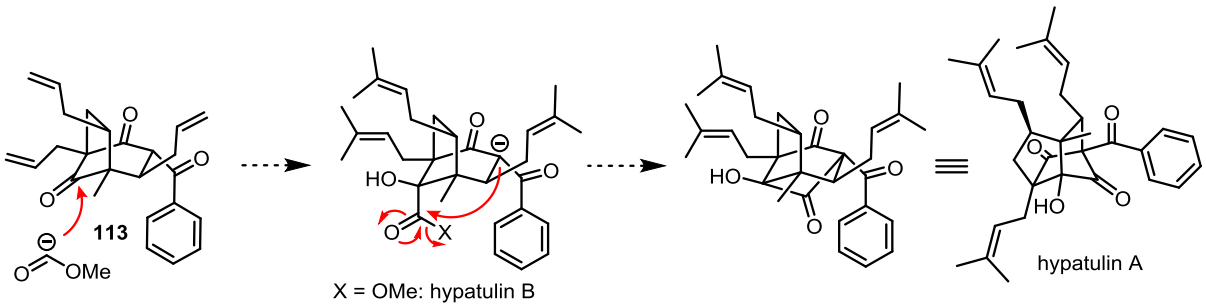

Scheme 45: Required transformations to arrive at the natural products hypatulin A and B.

In order to complete the synthesis of hypatulin B, a way should first be found to introduce the last allyl group and the ester group of hypatulin B stereoselectively. A metathesis should convert the three terminal alkenes into prenyl groups and complete the total synthesis of hypatulin B. Similar examples of late-stage prenylations are numerous in the literature[107,108,123] and should work as expected here. Finally, the conversion of hypatulin B to hypatulin A could be realized by an intramolecular nucleophilic substitution (Scheme 45).

After successful completion of the synthesis, it would first be useful to verify the postulated structures of the two meroterpenes by comparing the spectroscopic data and, if possible, by single crystal structure analysis.

Since the family of polyprenylated acylphloroglucinols represents numerous candidates with highly interesting pharmacological properties, these two new representatives should also be subjected to extended pharmacological tests. The total synthesis approach can enable a wide variety of derivatizations in the further course of the development.

4. References

[1] Brown, T. L.; LeMay, H. E.; Bursten, B. E. *Chemie Studieren kompakt*; Pearson, München, 2011.

[2] Atkins, P. W.; de Paula, J. *Physikalische Chemie*; Wiley-VCH, Weinheim, 2006.

[3] List, B. *Chem*. *Rev*. **2007**, *107*, 5413–5415.

[4] a) Erkkilä, A.; Majander, I.; Pihko, P. M. *Chem*. *Rev*. **2007**, *107*, 5416–5470; b) Mukherjee, S.; Yang, J. W.; Hoffmann, S.; List, B. *Chem*. *Rev*. **2007**, *107*, 5471–5569.

[5] Barik, S.; Biju, A. T. *Chem*. *Commun*. **2020**, *56*, 15484–15495.

[6] Rowland, G. B.; Zhang, H.; Rowland, E. B.; Chennamadhavuni, S.; Wang, Y.; Antillan, J. C. *J. Am. Chem. Soc.* **2005**, *127*, 15696–15697.

[7] Fuerst, D. E.; Jacobson, E. N. *J. Am. Chem. Soc.* **2005**, *127*, 8964–8965.

[8] Jungbauer, S. H.; Huber, S. M. *J. Am. Chem. Soc.* **2015**, *137*, 12110–12120.

[9] MacMillan, D. W. C. *Nature* **2008**, *455*, 304–308.

[10] Wöhler, F.; Liebig, J. *Ann*. *Pharm*. **1832**, *3*, 249–282.

[11] Liebig, J. *Liebigs Ann*. **1860**, *113*, 246–247.

[12] Bredig, G.; Fiske, P. S. *Biochem*. *Z*. **1912**, *46*, 7–23.

[13] a) Hajos, Z. G.; Parrish, D. R. *J. Org*. *Chem*. **1974**, *39*, 1615–1621; b) Eder, U.; Sauer, G.; Wiechert, R. *Angew*. *Chem*. *Int*. *Ed*. *Engl*. **1971**, *10*, 496–497.

[14] SciFinder-entries on the research topic organocatalysis (“containg” or “containing the concept”) from the years 2000 to 2020.

[15] Beeson, T. B.; Mastracchio, A.; Hong, J.-B.; Ashton, K.; MacMillan, D. W. C. *Science* **2007**, *316*, 582–585.

[16] Schalley, C. A.; Leisering, S. *Tutorium Reaktivität und Synthese. Mechanismen synthetisch wichtiger Reaktionen der Organischen Chemie*; Springer Spektrum, Berlin, 2017.

[17] Tajbakhsh, M.; Hosseinzadeh, R.; Alinezhad, H.; Ghahari, S.; Heydari, A.; Khaksar, S. *Synthesis* **2011**, 490–496.

[18] a) Hosomi, A.; Sakurai, H. *Tetrahedron Lett*. **1976**, *17*, 1295–1298; b) Fischer, E.; Speier, A. *Ber*. *Dtsch*. *Chem*. *Ges*. **1895**, *28*, 3252–3258.

[19] Brandau, S.; Landa, A.; Franzén, J.; Marigo, M.; Jørgensen, K. A. *Angew*. *Chem*. *Int*. *Ed*. **2006**, *45*, 4305–4309.

[20] Amatore, M.; Beeson, T. D.; Brown, S. P.; MacMillan, D. W. C. *Angew*. *Chem*. *Int*. *Ed*. **2009**, *48*, 5223–5226.

[21] Wiest, J. *The Role of Charged and Uncharged Intermediates in Organocatalysis*, Master thesis, The Scripps Research Institute, La Jolla, **2012**.

[22] Fuson, R. C. *Chem*. *Rev*. **1935**, *16*, 1–27.

[23] Hepburn, H. B.; Dell´Amico, L.; Melchiorre, P. *Chem*. *Rec*. **2016**, 16, 1787–1806.

[24] Brochu, M. P.; Brown, S. P.; MacMillan, D. W. C. *J. Am. Chem. Soc.* **2004**, *126*, 4108–4109.

[25] Halland, N.; Braunton, A.; Bachmann, S.; Marigo, M.; Jørgensen, K. A. *J. Am. Chem. Soc.* **2004**, *126*, 4790–4791.

[26] Brown, S. P. *Iminium and Enamine Activation: Methods for Enantioselective Organocatalysis, Dissertation*, California Institute of Technology, Pasadena, **2005**.

[27] Marigo, M.; Fielenbach, D.; Braunton, A., Kjærsgaard, A., Jørgensen, K. A. *Angew*. *Chem*. *Int*. *Ed*. **2005**, *44*, 3703–3706.

[28] Halland, N.; Lie, M. A., Kjærsgaard, A., Marigo, M.; Schiøtt, B.; Jørgensen, K. A. *Chem*. *Eur*. *J*. **2005**, *11*, 7083–7090.

[29] Marquez, C. A., Fabbretti, F.; Metzger, J. O. *Angew*. *Chem*. *Int*. *Ed*. **2007**, *46*, 6915–6917.

[30] Burés, J.; Armstrong, A.; Blackmond, D. G. *J. Am. Chem. Soc.* **2012**, *134*, 6741–6750.

[31] Jimeno, C.; Cao, L.; Renaud, P. *J. Org*. *Chem*. **2016**, *81*, 1251–1255.

[32] a) An, F.; Maji, B.; Min, E.; Ofial, A. R.; Mayr, H. *J. Am. Chem. Soc.* **2020**, *142*, 1526–1547; b) Lakhdar, S.; Maji, B.; Mayr, H. *Angew*. *Chem*. *Int*. *Ed*. **2012**, *51*, 5739 –5742.

[33] Schnitzer, T.; Möhler, J. S.; Wennemers, H. *Chem*. *Sci*. **2020**, *11*, 1943–1947.

[34] Carneros, H.; Sánchez, D.; Vilarrasa, J. *Org*. *Lett*. **2014**, *16*, 2900–2903.
[35] Winter, P.; Swatschek, J.; Willot, M.; Radtke, L.; Olbrisch, T.; Schäfer, A.; Christmann, M. *Chem*. *Commun*. **2011**, *47*, 12200–12202.
[36] Graham, T. H.; Horning, B. D.; MacMillan, D. W. C. *Org*. *Synth*. **2011**, *88*, 42–53.
[37] https://abcr.com/de_de/catalogsearch/advanced/result/?cas=21306-21-8 (10.02.21)
[38] https://www.umweltbundesamt.de/sites/default/files/medien/377/dokumente/pcpmono.pdf (10.02.2021)
[39] Reed, C. W.; Lindsley, C. W. *Tetrahedron Lett*. **2019**, *60*, 151104–151108.
[40] https://abcr.com/de_de/catalogsearch/advanced/result/?cas=128-09-6+ (10.02.21)
[41] Burés, J.; Armstrong, A.; Blackmond, D. G. *Acc*. *Chem*. *Res*. **2016**, *49*, 214–222.
[42] Grothues, L. *Studien zur Totalsynthese von Caylobolid A*, Master thesis, Freie Universität Berlin, Berlin, **2013**.
[43] Kortet, S.; Claraz, A.; Pihko, P. M. *Org*. *Lett*. **2020**, *22*, 3010–3013.
[44] Fadeyi, O. O.; Schulte, M. L.; Lindsley, C. W. *Org*. *Lett*. **2010**, *12*, 3276–3278.
[45] Shemet, A.; Sarlah, D.; Carreira, E. M. *Org*. *Lett*. **2015**, *17*, 1878–1881.
[46] Halperin, S. D.; Britton, R. *Org*. *Biomol*. *Chem*. **2013**, *11*, 1702–1705.
[47] a) Dhand, V.; Draper, J. A.; Moore, J.; Britton, R. *Org*. *Lett*. **2013**, *15*, 1914–1917; b) Chang, S.; Hur, S.; Britton, R.; *Chem*. *Eur*. *J*. **2015**, *21*, 16646–16653; c) Bergeron-Brlek, M.; Teoh, T.; Britton, R. *Org*. *Lett*. **2013**, *15*, 3554–3557; d) Draper, J. A.; Britton, R. *Org*. *Lett*. **2010**, *12*, 4034–4037; e) Bergeron-Brlek, M.; Meanwell, M.; Britton, R. *Nat*. *Commun*. **2015**, *6*, 6903.
[48] Kaplaneris, N.; Spyropoulos, C.; Kokotou, M. G.; Kokotos, C. G. *Org*. *Lett*. **2016**, *18*, 5800–5803.
[49] Winter, P.; Hiller, W.; Christmann, M. *Angew*. *Chem*. *Int*. *Ed*. **2012**, *51*, 3396–3400.
[50] a) Huo, J.; Hu, H.; Zhang, M.; Hu, X.; Chen, M.; Chen, D.; Liu, J.; Xiao, G.; Wang, Y.; Wen, Z. *RSC Adv*. **2017**, *7*, 2281–2287; b) Dheer, D.; Singh, V.; Shankar, R. *Bioorg*. *Chem*. **2017**, *71*, 30–54; c) Sahu, A.; Sahu, P.; Agrawal, R. *Curr*. *Chem*. *Biol*. **2020**, *14*, 71–87; d) Dai, Z.-C.; Chen, Y.-F.; Zhang, M.; Li, S.-K.; Yang, T.-T.; Shen, L.; Wang, J.-X.; Qian, S.-S.; Zhu, H.-L.; Ye, Y.-H. *Org*. *Biomol*. *Chem*. **2015**, *13*, 477–486.
[51] Schweinfurth, D.; Hettmanczyk, L.; Suntrup, L.; Sarkar, B. *Z*. *Anorg*. *Allg*. *Chem*. **2017**, *643*, 554–584.
[52] Mekni, N. H.; Baklouti, A. *Heterocycles* **2012**, *85*, 1727–1733.
[53] Kang, B.; Chang, S.; Decker, S.; Britton, R. *Org*. *Lett*. **2010**, *12*, 1716–1719.
[54] Klenk, S.; Suntrup, L.; Sarkar, B. *Nachr*. *Chem*. **2018**, *66*, 717–721.
[55] Jung, M. E.; Piizzi, G. *Chem*. *Rev*. **2005**, *105*, 1735–1766.
[56] Hashmi, A. S. K.; Rudolph, M.; Bats, J. W.; Frey, W.; Rominger, F.; Oeser, T. *Chem*. *Eur*. *J*. **2008**, *14*, 6672–6678.
[57] Meyer, D. F. *Studien zur Alkenhalogenierung durch 5-Nitroisoindolin-1,3-dionderivate*, Bachelor thesis, Freie Universität Berlin, Berlin, **2018**.
[58] Schmiedel, V. M.; Hong, Y. J.; Lentz, D.; Tantillo, D. J.; Christmann, M. *Angew*. *Chem*. *Int*. *Ed*. **2018**, *57*, 2419–2422.
[59] Schmiedel, V. M. *Strained Terpenes as Targets: Total Synthesis of the Dichrocephone Sesquiterpenes and Studies towards Xenicane Diterpenes, Dissertation*, Freie Universität Berlin, Berlin, **2018**.
[60] Kleoff, M.; Schwan, J.; Christmann, M.; Heretsch, P. *Org*. *Lett*. **2021**, *23*, 2370–2374.
[61] Tierney, M. M.; Crespi, S.; Ravelli, D.; Alexanian, E. J. *J*. *Org*. *Chem*. **2019**, *84*, 12983–12991.
[62] Desiraju, G. R.; Ho, P. S.; Kloo, L.; Legon, A. C.; Marquardt, R.; Metrangolo, P.; Politzer, P.; Resnati, G.; Rissanen, K. *Pure Appl*. *Chem*. **2013**, *85*, 1711–1713.
[63] Sonnenberg, K.; Mann, L.; Redeker, F. A.; Schmidt, B.; Riedel, S. *Angew*. *Chem*. *Int*. *Ed*. **2020**, *59*, 5464–5493.
[64] Schmidt, B.; Ponath, S.; Hannemann, J.; Voßnacker, P.; Sonnenberg, K.; Christmann, M.; Riedel, S. *Chem. Eur. J.* **2020**, *26*, 15183–15189. Permission granted for reproduction in print

and electronic format for the purpose of this dissertation; Copyright: **2020** Wiley-VCH Verlag GmbH & Co. KGaA, Weinheim; license number: 4963700864814
[65] Halli, J.; Manolikakes, G. *Nachr*. *Chem*. **2016**, *64*, 131–134.
[66] Janiak, C. *Nichtmetallchemie-Grundlagen und Anwendungen*; Shaker Verlag, Aachen, 2007.
[67] a) Jayaraj, R.; Megha, P.; Sreedev, P. *Interdiscip*. *Toxicol*. **2016**, *9*, 90–100; b) https://www.icis.com/explore/resources/news/2009/10/12/9253580/chlorine-plays-key-role-in-manufacture-of-drugs/ (11.02.21); c) Naumann, K. *Pest Manag*. *Sci*. **2000**, *56*, 3–12; d) Fang, W.-Y.; Ravindar, L.; Rakesh, K. P.; Manukumar, H. M.; Shantharam, C. S.; Alharbi, S.; Qin, H.-L. *Eur*. *J. Med*. *Chem*. **2019**, *173*, 117–153.
[68] a) Ragni, R.; Punzi, A.; Babudri, F.; Farinola, G. M. *Eur*. *J. Org*. *Chem*. **2018**, 3500–3519; b) Berger, R.; Resnati, G.; Metrangolo, P.; Weber, E.; Hulliger, J. *Chem*. *Soc*. *Rev*. **2011**, *40*, 3496–3508; c) Liu, Y.; Jiang, L.; Wang, H.; Wang, H.; Jiao, W.; Chen, G.; Zhang, P.; Hui, D.; Jian, X. *Nanotechnol*. *Rev*. **2019**, *8*, 573–586; d) Wang, J.; Sánchez-Roselló, M.; Acenã, J. L.; del Pozo, C.; Sorochinsky, A. E.; Fustero, S.; Soloshonok, V. A.; Liu, H. *Chem*. *Rev*. **2014**, *114*, 2432–2506; e) Zhou, Y.; Wang, J.; Gu, Z.; Wang, S.; Zhu, W.; Acenã, J. L.; Soloshonok, V. A.; Izawa, K.; Liu, H. *Chem*. *Rev*. **2016**, *116*, 422–518.
[69] Beck, T. M.; Haller, H.; Streuff, J.; Riedel, S. *Synthesis*, **2014**, *46*, 740–747.
[70] Schlama, T.; Gabriel, K.; Gouverneur, V.; Mioskowski, C. *Angew*. *Chem*. *Int*. *Ed*. *Engl*. **1997**, *36*, 2342–2344.
[71] a) Negoro, T.; Ikeda, Y. *Bull*. *Chem*. *Soc*. *Jpn*. **1986**, *59*, 2547–2551; b) Shellhamer, D. F.; Allen, J. L.; Allen, R. D.; Bostic, M. J.; Miller, E. A.; O'Neill, C. M.; Powers, B. J.; Price, E. A.; Probst, J. W.; Heasley, V. L. *J*. *Fluor*. *Chem*. **2000**, *106*, 103–112; c) Shellhamer, D. F.; Davenport, K. J.; Forberg, H. K.; Herrick, M. P.; Jones, R. N.; Rodriguez, S. J.; Sanabria, S.; Trager, N. N.; Weiss, R. J.; Heasley, V. L.; Boatz, J. A. *J*. *Org*. *Chem*. **2008**, *73*, 4532–4538.
[72] http://woelen.homescience.net/science/index.html (12.02.21); copyright by W. Oelen; creative commons license: https://creativecommons.org/licenses/by-sa/3.0/deed.en
[73] with kind permission of Benjamin Schmidt (12.02.21)
[74] a) Reimann, H.; Oliveto, E. P.; Neri, R.; Eisler, M.; Perlman, P. *J. Am. Chem. Soc.* **1960**, *82*, 2308–2311; b) Iwata, C.; Akiyama, T.; Miyashita, K. *Chem*. *Pharm*. *Bull*. **1988**, *36*, 2878–2886; c) Miyashita, K.; Yoneda, K.; Akiyama, T.; Koga, Y.; Tanaka, M.; Yoneyama, T.; Iwata, C. *Chem*. *Pharm*. *Bull*. **1993**, *41*, 465–470.
[75] Hu, D. X.; Seidl, F. J.; Bucher, C.; Burns, N. Z. *J. Am. Chem. Soc.* **2015**, *137*, 3795–3798.
[76] Negoro, T.; Ikeda, Y. *Bull*. *Chem*. *Soc*. *Jpn*. **1984**, *57*, 2111–2115.
[77] Schmidt, B.; Sonnenberg, K.; Beckers, H.; Steinhauer, S.; Riedel, S. *Angew*. *Chem*. *Int*. *Ed*. **2018**, *57*, 9141–9145. Permission granted for reproduction in print and electronic format for the purpose of this dissertation; Copyright: **2021** Wiley-VCH Verlag GmbH & Co. KGaA, Weinheim; license number: 5012440886952
[78] Schmidt, B.; Schröder, B.; Sonnenberg, K.; Steinhauer, S.; Riedel, S. *Angew*. *Chem*. *Int*. *Ed*. **2019**, *58*, 10340–10344.
[79] De Kimpe, N.; Verhk, R.; De Buyck, L.; Schamu, N. *Chem*. *Ber*. **1983**, *116*, 3846–3857.
[80] Nagata, T.; Matsubara, H.; Kiyokawa, K.; Minakata, S. *Org*. *Lett*. **2017**, *19*, 4672–4675.
[81] Matsumoto, T.; Masu, H.; Yamaguchi, K.; Takeda, K. *Org*. *Lett*. **2004**, *6*, 4367–4369.
[82] Martins, A.; Vieira, H.; Gaspar, H.; Santos, S. *Mar*. *Drugs* **2014**, *12*, 1066–1101.
[83] Solecki, R. S. *Science* **1975**, *190*, 880–881.
[84] Hassan, H. M. A. *Chimia* **2015**, *69*, 622–623.
[85] Bakels, C. C. *Der Mohn, die Linearbandkeramik und das Mittelmeergebiet.* Archäologisches Korrespondenzblatt 12, **1982**, 11–13.
[86] Brook, K.; Bennett, J.; Desai, S. P. *J*. *Anesth*. *Hist*. **2017**, *3*, 50–55.
[87] Gates, M.; Tschudi, G. *J*. *Am. Chem. Soc.* **1956**, *78*, 1380–1393.
[88] https://www.bayer.com/de/produkte/aspirin (15.02.21)
[89] Schmid, B.; Kötter, I.; Heide, L. *Eur*. *J*. *Clin*. *Pharmacol*. **2001**, *57*, 387–391.

[90] a) Fleming, A. *Br*. *J*. *Exp*. *Pathol*. **1929**, 10, 226–236; b) Favara, D. M. *Am*. *Surg*. **2014**, *80*, 1192–1195.
[91] a) Gennari, C.; Vulpetti, A.; Donghi, M.; Mongelli, N.; Vanotti, E. *Angew*. *Chem*. *Int*. *Ed*. *Engl*. **1996**, *35*, 1723–1725; b) Ojimam, I.; Habus, I.; Zhao, M.; Zucco, M.; Park, Y. H.; Sun, C. M.; Brigaud, T. *Tetrahedron* **1992**, *48*, 6985–7012.
[92] Newman, D. J.; Cragg, G. M. *J*. *Nat*. *Prod*. **2020**, *83*, 770–803.
[93] Dias, D. A.; Urban, S.; Roessner, U. *Metabolites* **2012**, *2*, 303–336.
[94] a) Greeson, J. M.; Sanford, B.; Monti, D. A. *Psychopharmacology* **2001**, *153*, 402–414; b) Dauncey, E. A.; Irving, J. T. W.; Allkin, R. *J*. *Pharm*. *Pharmacol*. **2019**, *71*, 4–14; c) Silva, A. R.; Taofiq, O.; Ferreira, I. C. F. R.; Barros, L. *Ind*. *Crops Prod*. **2021**, *159*, 113053; d) Istikoglou, C. I.; Mavreas, V.; Geroulanos, G. *Psychiatriki* **2010**, *21*, 332–338; e) Zhang, R.; Ji, Y.; Zhang, X.; Kennelly, E. J.; Long, C. *J*. *Ethnopharmacol*. **2020**, *254*, 112686; f) Galeotti, N. *J*. *Ethnopharmacol*. **2017**, *200*, 136–146.
[95] Pixabay free license (18.02.21)
[96] a) Wurglics, M.; Schubert-Zsilavecz, M. *Clin*. *Pharmacokinet*. **2006**, *45*, 449–468; b) Caccia, S. *Curr*. *Pharm*. *Anal*. **2006**, *2*, 59–68; c) Nohrstedt, A.; Butterwerck, V. *Pharamacopsychiat*. **1997**, *30*, 129–134; d) Pirbalouti, A. G.; Fatahi-Vanani, M.; Craker, L.; Shirmardi, H. *Pharm*. *Biol*. **2014**, *52*, 175–181.
[97] a) Ciochina, R.; Grossman, R. B. *Chem*. *Rev*. **2006**, *106*, 3963–3986; b) Yang, X.-W.; Grossman, R. B.; Xu, G. *Chem*. *Rev*. **2018**, *118*, 3508–3558; c) Decosterd, L. A.; Stoeckli-Evans, H.; Chapuis, J. C.; Sordat, B.; Hostettmann, K. *Helv*. *Chim*. *Acta* **1989**, *72*, 1833–1845; d) Orth, H. C. J.; Rentel, C.; Schmidt, P. C. *J*. *Pharm*. *Pharmacol*. **1999**, *51*, 193–200; e) Matsuhisa, M.; Shikishima, Y.; Takaishi, Y.; Honda, G.; Ito, M.; Takeda, Y.; Shibata, H.; Higuti, T.; Kodzhimatov, O. K.; Ashurmetov, O. *J*. *Nat*. *Prod*. **2002**, *65*, 290–294.
[98] Duecker, F. L.; Reuß, F.; Heretsch, P. *Org*. *Biomol*. *Chem*. **2019**, *17*, 1624–1633.
[99] Liu, Y.-Y.; Ao, Z.; Xue, G.-M.; Wang, X.-B.; Luo, J.-G.; Kong, L.-Y. *Org. Lett.* **2018**, *20*, 7953–7956.
[100] Yang, X.-W.; Grossman, R. B. *Org. Lett.* **2020**, *22*, 760–763.
[101] Beerhues, L. *Phytochemistry* **2006**, *67*, 2201–2207.
[102] Bystrov, N. S.; Chernov, B. K.; Dobrynin, V. N.; Kolosov, M. N. *Tetrahedron Lett*. **1975**, *16*, 2791–2794.
[103] Nicolaou, K. C.; Carenzi, G. E. A.; Jeso, V. *Angew*. *Chem*. *Int*. *Ed*. **2005**, *44*, 3895–3899.
[104] Mehta, G.; Bera, M. K. *Tetrahedron Lett*. **2009**, *50*, 3519–3522.
[105] Shimizu, Y.; Shi, S.-L.; Usuda, H.; Kanai, M.; Shibasaki, M. *Angew*. *Chem*. *Int*. *Ed*. **2010**, *49*, 1103–1106.
[106] Sparling, B. A.; Moebius, D. C.; Shair, M. D. *J. Am. Chem. Soc.* **2013**, *135*, 644–647.
[107] Uwamori, M.; Nakada, M. *Tetrahedron Lett*. **2013**, *54*, 2022–2025.
[108] Bellavance, G.; Barriault, L. *Angew*. *Chem*. *Int*. *Ed*. **2014**, *53*, 6701–6704.
[109] Ting, C. P.; Maimone, T. J. *J. Am. Chem. Soc.* **2015**, *137*, 10516–10519.
[110] http://www.plantsoftheworldonline.org/taxon/urn:lsid:ipni.org:names:927423-1 (15.02.20)
[111] https://npgsweb.ars-grin.gov/gringlobal/taxon/taxonomydetail?id=19598 (15.02.20)
[112] Pixabay free license (18.02.21)
[113] Tanaka, N.; Yano, Y.; Tatano, Y.; Kashiwada, Y. *Org. Lett.* **2016**, *18*, 5360–5363.
[114] Tanaka, N.; Niwa, K.; Yano, Y.; Kashiwada, Y. *J*. *Nat*. *Med*. **2020**, *74*, 264–268.
[115] Hashida, C.; Tanaka, N.; Kawazoe, K.; Murakami, K.; Sun H.-D.; Takaishi, Y.; Kashiwada, Y. *J*. *Nat*. *Med*. **2014**, *68*, 737–742.
[116] a) Barnett, D. S.; Moquist, P. N.; Schaus, S. E. *Angew*. *Chem*. *Int*. *Ed*. **2009**, *48*, 8679–8682; b) Taber, D. F.; Gerstenhaber, D. A., Berry, J. F. *J*. *Org*. *Chem*. **2011**, *76*, 7614–7617.
[117] Taber, D. F.; Berry, J. F. *J*. *Org*. *Chem*. **2013**, *78*, 8437–8441.
[118] Yoshida, M. *J*. *Org*. *Chem*. **2017**, *82*, 12821–12826.
[119] Uyeda, C.; Rötheli, A. R.; Jacobsen, E. N. *Angew*. *Chem*. *Int*. *Ed*. **2010**, *49*, 9753–9756.

[120] Liu, Y.; Hu, H.; Zheng, H.; Xia, Y.; Liu, X.; Lin, L.; Feng, X. *Angew*. *Chem*. *Int*. *Ed*. **2014**, *53*, 11579–11582.
[121] Leisering, S. unpublished results
[122] Lee, P. H.; Lee, K.; Sung, S.-Y.; Chang, S. *J. Org. Chem.* **2001**, *66*, 8646–8649.
[123] Lindermayr, K.; Plietker, B. *Angew*. *Chem*. *Int*. *Ed*. **2013**, *52*, 12183–12186.
[124] Brown, H. C.; Racherla, U. S.; Pellechia, P. J. *J*. *Org*. *Chem*. **1990**, *55*, 1868–1874.
[125] Kim, J. G.; Waltz, K. M.; Garcia, I. F.; Kwiatkowski, D.; Walsh, P. J. *J. Am. Chem. Soc.* **2004**, *126*, 12580–12585.
[126] Vorberg, R.; Trapp, N.; Zimmerli, D.; Wagner, B.; Fischer, H.; Kratochwil, N. A.; Kansy, M.; Carreira, E. M.; Müller, K. *ChemMedChem* **2016**, *11*, 2216–2239.
[127] Zheng, J.; Lin, L.; Kuang, Y.; Zhao, J.; Liu, X.; Feng, X. *Chem*. *Commun*. **2014**, *50*, 994–996.
[128] Ueki, T.; Doe, M.; Tanaka, R.; Morimoto, Y.; Yoshihara, K.; Kinoshita, T. *J*. *Heterocyclic Chem*. **2001**, *38*, 165–172.
[129] Davis, F. A.; Zhang, H.; Lee, S. H. *Org*. *Lett*. **2001**, *3*, 759–762.

5. Appendix

5.1. Abbreviations

Å	Ångström
Ac	acetyl
A_N	nukleophilic addition
ap	antiperiplanar
aq.	aqueous
Ar	aryl
BINOL	1,1'-bi-2-naphthol
Bn	benzyl
Boc	*tert*-butyloxycarbonyl
2,2'-bpy	2,2'-bipyridine
BTEABr	benzyltriethylammonium bromide
c_{max}	maximum concentration
COSY	correlated spectroscopy (NMR)
d	doublet, day
δ	chemical shift
de	diastereomeric excess
DEAD	diethyl azodicarboxylate
DFT	density functional theory
DIBAL-H	diisobutylaluminium hydride
DIPEA	diisopropylethylamine
4-DMAP	4-dimethylaminopyridine
DME	1,2-dimethoxyethane
DMF	dimethylformamide
DMP	*Dess-Martin* periodinane
DMSO	dimethyl sulfoxide
dr	diastereomeric ratio
dppp	1,3-bis(diphenylphosphino)propane
ECD	electronic circular dichroism
ee	enantiomeric excess
equiv.	equivalents
er	enantiomeric ratio
ESI	electron spray ionization

Et	ethyl
EWG	electron withdrawing group
EXSY	exchange spectroscopy (NMR)
GC	gas chromatography
h	hour
HMBC	heteronuclear multiple bond correlation
HMPA	hexamethylphosphoramide
HMQC	heteronuclear multiple-quantum correlation
HOMO	highest occupied molecular orbital
HPLC	high performance liquid chromatography
HR	high resolution
HWE	*Horner-Wadsworth-Emmons*(-reaction)
Hz	Hertz
^{i}Pr	isopropyl
IR	infrared
J	coupling constant
k	reaction rate constant
KH	potassium hydride
KIE	kinetic isotope effect
LDA	lithium diisopropylamide
LUMO	lowest unoccupied molecular orbital
m	multiplet
M	molar mass
mCPBA	meta-chloroperoxybenzoic acid
Me	methyl
Me_4NCS	1-chloro-3,3,4,4-tetramethylpyrrolidine-2,5-dione
min	minute
MOM	methoxymethyl ether
MS	mass spectrometry
mp	melting point
NFSI	*N*-fluorobenzenesulfonimide
NMI	1-methylimidazole
NMR	nuclear magnetic resonance
NO_2NXP	2-halo-5-nitroisoindoline-1,3-dione (X = Cl, Br, I)
NOE	nuclear *Overhauser* effect

NXS	*N*-halosuccinimide (X = Cl, Br, I)
NXP	*N*-halophthalimide (X = Cl, Br, I)
p	pentet
PAP	polyprenylated acylphloroglucinols
PBP	polyprenylated benzophenones
PCP	pentachlorophenol
Ph	phenyl
pK_A	negative decadic logarithm of the acid constant
PPAP	polycyclic polyprenylated acylphloroglucinols
ppm	parts per million
q	quartet
rt	room temperature
R_f	retarding front or relate to front
s	singulet
sc	synclinal
S_EAr	electrophilic aromatic substitution
SDS	stereodetermining step
S_N2	nucleophilic substitution of 2nd kinetic order
SOMO	single occupied molecular orbital
t	triplet
^{t}Bu	*tert*-butyl
TBAF	tetrabutylammonium fluoride
TBDPS	*tert*-butyldiphenylsilyl
TBS	*tert*-butyldimethylsilyl
TCCA	trichloroisocyanuric acid
TEMPO	(2,2,6,6-tetramethylpiperidin-1-yl)oxyl
Tf	triflyl
TFA	trifluoroacetic acid
THF	tetrahydrofuran
TLC	thin layer chromatography
TLS	turnover limiting step
TMS	trimethylsilyl
UV	ultraviolet
$\tilde{\nu}$	wavenumber

5.2. Supporting Information: Mechanistic Studies on the Organocatalytic α-Chlorination of Aldehydes: The Role and Nature of Off-Cycle Intermediates

Angewandte Chemie
Eine Zeitschrift der Gesellschaft Deutscher Chemiker

Supporting Information

Mechanistic Studies on the Organocatalytic α-Chlorination of Aldehydes: The Role and Nature of Off-Cycle Intermediates

*Sebastian Ponath, Martina Menger, Lydia Grothues, Manuela Weber, Dieter Lentz, Carsten Strohmann, and Mathias Christmann**

anie_201806261_sm_miscellaneous_information.pdf

Author Contributions

M. Weber, Dieter Lentz, Prof. Dr. Carsten Strohmann: X-ray crystal structure analysis.

SUPPORTING INFORMATION

Table of Contents

SUPPORTING INFORMATION

1. GENERAL INFORMATION

Anhydrous solvents were provided by purification with MBraun SPS-800 solvent system using solvents of HPLC grade purchased from Fischer Scientific. Triethylamine was distilled from calcium hydride and stored under argon over KOH. Solvents for extraction, crystallization and flash column chromatography were purchased in technical grade and distilled under reduced pressure prior to use. Unless otherwise indicated, all starting materials and reagents were purchased from commercial distributors and used without further purification.

Products were purified by flash column chromatography on silica gel 60 M (0.040-0.063 mm, 230-400 mesh, Macherey-Nagel). TLC-analyses was performed on silica gel coated aluminum plates ALUGRAM® Xtra SIL G/UV_{254} purchased from Macherey-Nagel. Products were detected by UV light at 254 nm and by using staining reagents based on $KMnO_4$, Anisaldeyde, Molybdophosphoric acid and Ceriumsulfate.

^{1}HNMR and ^{13}CNMR spectral data were recorded on Bruker (AC 500, AVIII 700) and JEOL (ECX 400, Eclipse 500) spectrometers. The chemical shifts (δ) are listed in parts per million (ppm) and are reported relative to the corresponding residual solvent signal ($CDCl_3$: δ_H = 7.26 ppm, δ_C = 77.16 ppm, $DMSOd_6$: δ_H = 2.50 ppm, δ_C = 39.52 ppm, CD_3OD: δ_H = 3.31 ppm, δ_C = 49.00 ppm, CD_3CN: δ_H = 1.94 ppm, δ_C = 118.26, $DMFd_7$: δ_H = 8.03 ppm, δ_C = 163.15 ppm). Integrals are in accordance with assignments; coupling constants (*J*) are given in Hz. Multiplicity is indicated as follows: s (singlet), d (doublet), t (triplet), q (quartet), m (multiplet), dd (doublet of doublet), etc. ^{13}CNMR spectra are ^{1}H-broadband decoupled. For detailed peak assignments 2D spectra were measured (COSY, HMQC, HMBC). IR spectra were measured with a Jasco spectrometer (FT/IR-4100) equipped with an ATR unit. High resolution mass spectra were measured with an Agilent 6210 ESI-TOF (10 µL/min, 1.0 bar, 4 kV) instrument. Melting points were determined by digital melting point apparatus (Stuart SMP30) and are uncorrected. Optical rotations values were determined with a Jasco P-2000 polarimeter at the temperatures given. Diastereomeric ratios were determined by ^{1}HNMR. Enantiomeric ratios were determined by chiral HPLC (Agilent Series 1200 with DAD) or by GC (Agilent 7890B) on a chiral column. The specific conditions are given in each case.

2. EXPERIMENTAL PROCEDURES AND COMPOUND CHARACTERIZATION

2.1. ORGANOCATALYSTS

All imidazolidinone derivatives were synthesized following a procedure described by Graham et al.[1]

1-Methylcyclohexane-1-carbaldehyde S1

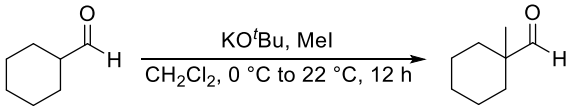

Aldehyde **S1** was synthesized according to a literature-known procedure.[2] KO^{t}Bu (6.50 g, 57.9 mmol, 1.3 equiv) was added slowly to an ice-cooled solution of cyclohexanecarbaldehyde (5.00 g, 44.6 mmol, 1.0 equiv) in anhydrous CH_2Cl_2 (170 mL). Methyliodid (8.50 mL, 134 mmol, 3.0 equiv) was added dropwise and the reaction mixture was stirred at 0 °C for 30 min. After stirring at room temperature over night the organic phase was washed with H_2O (2 x 50 mL) and brine (50 mL), dried over Na_2SO_4 and the solvent was removed under reduced pressure. The crude product was purified by column chromatography (SiO_2, pentane/EtOAc, 100:1) and aldehyde **S1** (2.45 g, 19.3 mmol, 43%) was obtained as a colorless oil.

^{1}HNMR ($CDCl_3$, 400 MHz) δ = 9.36 (s, 1H), 1.82 – 1.72 (m, 2 H), 1.55 – 1.14 (m, 8 H), 0.95 (s, 3H) ppm.

Spectroscopic data were in accordance with published data.[2]

Adamantane-1-carbaldehyde S2

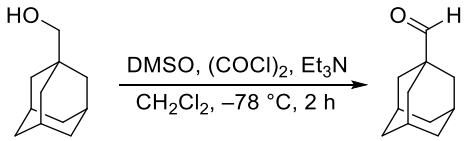

Aldehyde **S2** was synthesized according to a literature-known procedure.[3] Oxalylchloride (6.70 mL, 76.8 mmol, 1.3 equiv) was added dropwise to a solution of anhydrous DMSO (10.3 mL, 145 mmol, 2.5 equiv) in anhydrous CH_2Cl_2 (150 mL) at –78 °C and stirred for 15 min at the same temperature. A solution of 1-adamantanemethanol (9.67 g, 58.0 mol, 1.0 equiv) in anhydrous CH_2Cl_2 (75 mL) was added dropwise and the reaction mixture was stirred for 60 min at –78 °C. The resulting mixture was then treated with anhydrous Et_3N (40.5 mL, 290 mmol, 5.0 equiv) and stirring was continued for 30 min at room temperature. Aqueous KH_2PO_4 (20 wt%, 25 mL) and water (150 mL) were added subsequently and stirring was continued for additional 15 min at room temperature. The mixture was diluted with Et_2O (400 mL), the layers were separated and the organic layer was washed with ice-cooled aqueous KH_2PO_4 (10 w%, 3 x 150 mL), brine (100 mL) and dried over Na_2SO_4. The solvent was removed under reduced pressure and the crude product was purified by column chromatography (CH_2Cl_2). Aldehyde **S2** (8.60 g, 52.4 mmol, 90%) was obtained as a colorless solid.

^{1}HNMR ($CDCl_3$, 400 MHz) δ = 9.31 (s, 1H), 2.06 (p, *J* = 3.0 Hz, 3H), 1.81 – 1.65 (m, 12H) ppm.

Spectroscopic data were in accordance with published data.[3]

SUPPORTING INFORMATION

Methyl L-alaninate hydrochloride S3

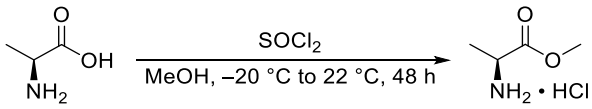

Ester **S3** was synthesized according to a literature-known procedure.[4] L-Alanine (10.0 g, 112 mmol, 1.0 equiv) was suspended in methanol (100 mL) and cooled down to –20 °C. After thionylchloride (8.60 mL, 118 mmol, 1.1 equiv) was added dropwise, the reaction mixture was stirred for 60 min at 0 °C and 48 h at room temperature. The solvent was removed under reduced pressure, the participating solid was filtered off and washed with Et_2O. After the product was dried under vacuum, ester **S3** (15.7 g, quant.) was received as a colorless solid.

^{1}HNMR (DMSO-d_6, 400 MHz) δ = 8.67 (s, 3H), 4.05 (q, *J* = 7.2 Hz, 1H), 3.73 (s, 3H), 1.42 (d, *J* = 7.2 Hz, 3H) ppm.

Spectroscopic data were in accordance with published data.[4]

Methyl L-valinate hydrochloride S4

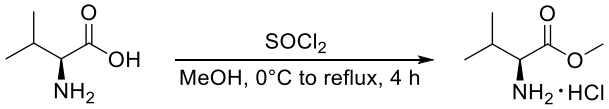

Ester **S4** was synthesized based on a literature-known procedure.[4] L-Valine (2.00 g, 17.1 mmol, 1.0 equiv) was suspended in MeOH (10 mL) and cooled down to 0 °C. $SOCl_2$ (2.50 mL, 34.1 mmol, 2.0 equiv) was added dropwise and the suspension was stirred for 10 min at 0°C before the ice-bath was removed and the reaction mixture was refluxed for 4 h. The solvent was removed under reduced pressure and the residue was dissolved in minimal amount of MeOH. Et_2O was added and the crude product was recrystallized in the freezer overnight. The product was then filtered through a sintered funnel and washed with cold Et_2O (10 mL) and dried under vacuum. The procedure was repeated and ester **S4** (2.61 g, 15.5 mmol, 90%) was obtained as a colorless solid.

^{1}HNMR ($CDCl_3$, 500 MHz): δ = 8.85 (s, 3H), 3.95 (d, *J* = 3.9 Hz, 1H), 3.81 (s, 3H), 2.46 (pd, *J* = 6.9, 4.4 Hz, 1H), 1.14 (t, *J* = 7.3 Hz, 6H) ppm.

Methyl L-isoleucinate hydrochloride S5

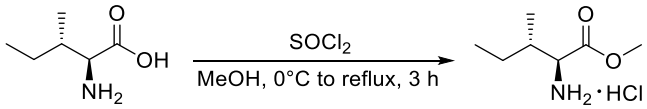

Ester **S5** was synthesized based on a literature-known procedure.[4] L-Isoleucin (2.00 g, 15.3 mmol, 1.0 equiv) was suspended in MeOH (10 mL) and cooled down to 0 °C. $SOCl_2$ (2.20 mL, 30.5 mmol, 2.0 equiv) was slowly added and the solution was stirred for 10 min at 0 °C before the ice-bath was removed and the reaction mixture was refluxed for 4 h. The solvent was removed under reduced pressure and the obtained solid was dissolved in a minimal amount of MeOH. Et_2O was added and recrystallization was performed overnight in the freezer. The crystalline solid was filtered off and the filtrate was concentrated again, treated with MeOH and Et_2O and recrystallized again. Ester **S5** (2.50 g, 13.8 mmol, 90%) was obtained as colorless solid.

^{1}H-NMR ($CDCl_3$, 500 MHz): δ = 8.79 (s, 3H), 4.09 – 4.00 (m, 1H), 3.80 (s, 3H), 2.27 – 2.11 (m, 1H), 1.55 (ddd, *J* = 13.1, 7.4, 5.6 Hz, 1H), 1.44 (ddd, *J* = 13.8, 8.9, 7.3 Hz, 1H), 1.10 (d, *J* = 7.0 Hz, 3H), 0.96 (t, *J* = 7.4 Hz, 3H) ppm.

(*S*)-2-Amino-*N*-methylpropanamide hydrochloride S6

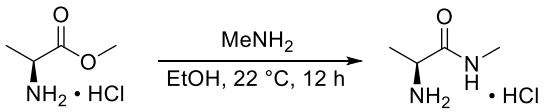

Ester **S3** (15.7 g, 113 mmol, 1.0 equiv) was added to a solution of methylamine in ethanol (33 wt%, 44.8 mL, 338 mmol, 3.0 equiv). The reaction mixture was stirred for 12 h at room temperature. The solvent was removed under reduced pressure and toluene (20 mL) was added to the white precipitate, stirred for 10 min and removed again. The procedure was repeated five times and the solid was dried at 50 °C overnight, receiving amide **S6** (14.8 g, 107 mmol, 95%, 10% $MeNH_2$·HCl) as a colorless solid.

^{1}HNMR (CD_3OD, 400 MHz) δ = 3.90 (q, *J* = 7.0 Hz, 1H), 2.79 (s, 3H), 1.48 (d, *J* = 7.0 Hz, 3H) ppm.

Spectroscopic data were in accordance with published data.[1]

(*S*)-2-Amino-*N*,3-dimethylbutanamide hydrochloride S7

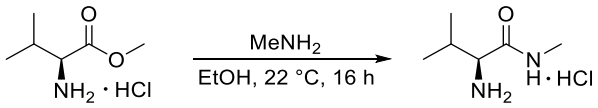

Ester **S4** (2.57 g, 15.3 mmol, 1.0 equiv) was added to a solution of methylamine in ethanol (33 wt%, 5.70 mL, 46.0 mmol, 3.0 equiv). The reaction mixture was stirred for 16 h at room temperature and then concentrated under reduced pressure. The solid was suspended in toluene and concentrated again. The procedure was repeated four times and amide **S7** (1.64 g, 9.84 mmol, 64%) was obtained as a colorless solid.

^{1}HNMR (D_2O, 500 MHz): δ = 3.65 (d, *J* = 4.0 Hz, 1H), 2.58 (s, 3H), 2.04 – 1.86 (m, 1H), 1.53 – 1.36 (m, 1H), 1.32 – 1.17 (m, 1H), 0.99 (d, *J* = 7.0 Hz, 3H), 0.92 (t, *J* = 7.4 Hz, 3H) ppm.

(2*S*,3*S*)-2-Amino-*N*,3-dimethylpentanamide S8

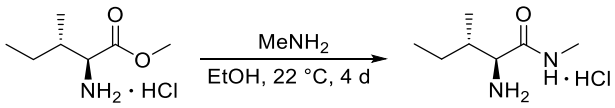

Ester **S5** (2.50 g, 13.8 mmol, 1.0 equiv) was added to a solution of methylamine in ethanol (33 wt%, 5.11 mL, 41.3 mmol, 3.0 equiv) and the suspension was stirred for 4 d at room temperature. The reaction mixture was concentrated under reduced pressure, the solid was suspended in toluene and concentrated again. The procedure was repeated four times and amide **S8** (564 mg, 3.12 mmol, 23%) was obtained as a colorless solid.

^{1}HNMR (D_2O, 400 MHz): δ = 3.35 (d, *J* = 6.4 Hz, 1H), 2.74 (s, 3H), 2.57 (s, 2H), 1.78 – 1.67 (m, 1H), 1.52 – 1.39 (m, 1H), 1.22 – 1.10 (m, 1H), 0.93 – 0.85 (m, 6H) ppm.

(*S*)-*N*-Methyl-2-(((1-methylcyclohexyl)methylene)amino)propanamide S9

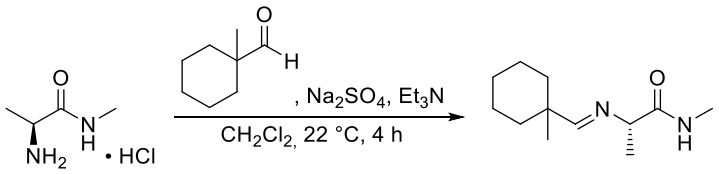

Triethylamine (5.00 mL, 36.1 mmol, 1.5 equiv) and aldehyde **S1** (3.04 g, 24.1 mmol, 1.0 equiv) were added subsequently to a suspension of amide **S3** (5.00 g, 36.1 mmol, 1.5 equiv) and $MgSO_4$ (2.30 g) in CH_2Cl_2 (11 mL). The reaction mixture was stirred for 4 h at room temperature and then diluted with toluene (15 mL). The solids were filtered off and washed with toluene. The filtrate was concentrated under reduced pressure and the solids were filtered off again. The solvent was completely removed under reduced pressure and imin **S9** (4.02 g, 19.1 mmol, 79%) was obtained as a colorless oil. The product was used without further purification.

^{1}HNMR ($CDCl_3$, 400 MHz) δ = 7.45 (s, 1H), 3.69 (q, *J* = 7.0 Hz, 1H), 2.84 (d, *J* = 5.0 Hz, 3H), 1.75 – 1.39 (m, 10H), 1.32 (d, *J* = 7.1 Hz, 3H), 1.00 (s, 3H) ppm.

(2*S*)-(2-Adamantan-1-ylmethylene)amino-*N*-methylpropanamide S10

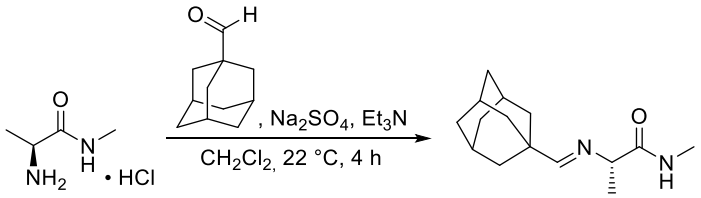

Triethylamine (1.50 mL, 10.8 mmol, 2.7 equiv) and aldehyde **S2** (0.649 g, 3.95 mmol, 1.0 equiv) were added subsequently to a suspension of amide **S3** (1.00 g, 7.22 mmol, 1.8 equiv) and $MgSO_4$ (1.00 g) in CH_2Cl_2 (5 mL). The reaction mixture was stirred for 4 h at room temperature and then diluted with toluene (15 mL). The Solids were filtered off and washed with toluene. The filtrate was concentrated under reduced pressure and the solids were filtered off again. The solvent was completely removed under reduced pressure and imin **S10** (889 mg, 3.58 mmol, 91%) was obtained as pale yellow oil. The product was used without further purification.

^{1}HNMR ($CDCl_3$, 400 MHz,) δ = 7.35 (s, 1H), 3.64 (q, *J* = 7.0 Hz, 1H), 2.83 (d, *J* = 5.0 Hz, 3H), 2.04 (p, *J* = 3.6 Hz, 3H), 1.80 – 1.62 (m, 12H, H-7), 1.30 (d, *J* = 7.0 Hz, 3H) ppm.

(*S*)-2-((2,2-Dimethylpropylidene)amino)-*N*,3-dimethylbutanamide S11

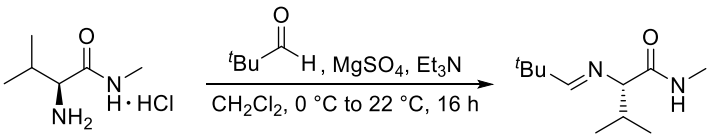

Amide **S4** (1.64 g, 9.84 mmol, 1.0 equiv) and $MgSO_4$ (1.90 g) were suspended in CH_2Cl_2 (15 mL) at 0 °C. Et_3N (1.64 mL, 11.8 mmol, 1.2 equiv) and pivaldehyde (1.18 mL, 10.8 mmol, 1.1 equiv) were added subsequently. The suspension was warmed to room temperature and stirred for 11 h. Additional $MgSO_4$ (0.20 g) and pivaldehyde (1.18 mL, 10.8 mmol, 1.10 equiv) were added and stirring was continued for 5 h. The reaction mixture was treated with Et_2O to induce precipitation. The solids were filtered off and the filtrate was concentrated under reduced pressure. Imine **S11** (1.90 g, 9.58 mmol, 97%) was obtained as colorless oil and was used without further purification.

^{1}HNMR ($CDCl_3$, 500 MHz): δ = 7.41 (s, 1H), 6.70 (s, 1H), 3.36 (d, *J* = 3.9 Hz, 1H), 2.83 (d, *J* = 5.0 Hz, 3H), 2.38 – 2.04 (m, 1H), 1.08 (s, 9H), 0.81 (t, *J* = 6.9, 6.3 Hz, 6H) ppm.

(2*S*,3*R*)-2-((2,2-dimethylpropylidene)amino)-*N*,3-dimethylpentanamide S12

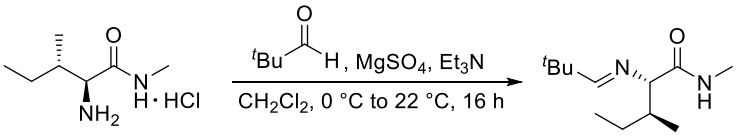

Amide **S5** (700 mg, 4.85 mmol, 1.0 equiv) and $MgSO_4$ (0.90 g) were suspended in CH_2Cl_2 (6 mL) at 0 °C. Et_3N (0.81 mL, 5.82 mmol, 1.2 equiv) and pivaldehyde (0.58 mL, 5.34 mmol, 1.1 equiv) were added subsequently and the suspension was warmed to room temperature for 11 h. Additional $MgSO_4$ (0.50 g) and pivaldehyde (0.58 mL, 5.34 mmol, 1.1 equiv) were added and stirring was continued for 5 h. Et_2O was added to induce precipitation. The solids were filtered off and the filtrate was concentrated under reduced pressure. Imine **S12** (990 mg, 4.66 mmol, 96%) was obtained as colorless oil and was used without further purification.

^{1}HNMR ($CDCl_3$, 700 MHz): δ = 7.42 (s, 1H), 6.70 (s, 1H), 3.43 (d, *J* = 4.0 Hz, 1H), 2.83 (d, *J* = 5.0 Hz, 3H), 1.98 – 1.92 (m, 1H), 1.52 – 1.44 (m, 1H), 1.08 (s, 9H), 0.84 (t, *J* = 7.5 Hz, 3H), 0.80 (d, *J* = 6.9 Hz, 3H) ppm.

(2*R*,5*S*)-3,5-Dimethyl-2-(1-methylcyclohexyl)imidazolidin-4-one hydrochloride S13

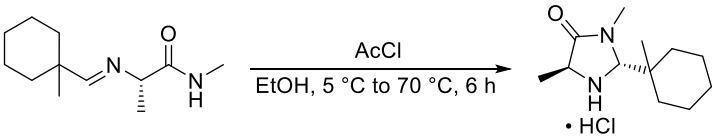

Acetylchloride (1.50 mL, 21.0 mmol, 1.1 equiv) was added dropwise to anhydrous ethanol (10 mL) at 0 °C. Imin **S9** (4.01 g, 19.1 mmol, 1.0 equiv) was added and the solution was stirred for 1 h at 0 °C, 1 h at 70 °C and finally 4 h at room temperature. The solids were filtered off and washed with a small portion of cold ethanol. The filtrate was concentrated under reduced pressure and the precipitate was filtered off again. After drying under vacuum hydrochloride **S13** (2.62 g, 10.6 mmol, 56%, single diastereoisomer) was obtained as a colorless solid. *Trans*-isomerism was confirmed by NOE-spectroscopy.

^{1}HNMR (CD_3OD, 400 MHz) δ = 4.76 (s, 1H), 4.26 (q, *J* = 7.1 Hz, 1H), 3.07 (s, 3H), 1.72 – 1.65 (m, 4H), 1.60 – 1.48 (m, 4H), 1.56 (d, *J* = 7.1 Hz, 3H), 1.43 (td, *J* = 12.2, 3.9 Hz, 1H), 1.31 (td, *J* = 10.0, 8.4, 3.3 Hz, 1H), 1.11 (s, 3H) ppm.

(2*R*,5*S*)-2-(Adamantan-1-yl)-3,5-dimethylimidazolidin-4-one S14

Acetylchloride (0.34 mL, 3.95 mmol, 1.1 equiv) was added dropwise to anhydrous ethanol (5 mL) at 0 °C. Imin **S10** (889 mg, 3.59 mmol, 1.0 equiv) was added and the solution was stirred for 1 h at 0 °C, 1 h at 70 °C and finally 4 h at room temperature. The precipitate was filtered off and washed with a small portion of cold ethanol. The filtrate was concentrated under reduced pressure and the solids were filtered off again. After drying under vacuum hydrochloride **S14** was obtained as a colorless solid (d.r. 1:0.7, *trans*:*cis*). Subsequently the product was stirred in EtOH for 5 h at 70 °C to shift the thermodynamic equilibrium to 10:1 ratio of *trans*:*cis* isomers as indicated by TLC.[1] After removal of all solvents under reduced pressure hydrochloride S14 was obtained as a colorless solid (553 mg, 1.94 mmol, 54%, d.r. 10:1, *trans*:*cis*).

^{1}HNMR (CD_3OD, 500 MHz) δ = 4.56 (s, 2H), 4.25 (q, *J* = 7.0 Hz, 1H), 4.11 (q, *J* = 7.2 Hz, 1H), 3.08 (s, 3H), 3.07 (s, 3H), 2.13 – 2.08 (m, 6H), 1.91 – 1.66 (m, 24H), 1.59 (d, *J* = 7.2 Hz, 3H), 1.55 (d, *J* = 7.1 Hz, 3H) ppm.

(2*R*,5*S*)-2-(*tert*-Butyl)-5-isopropyl-3-methylimidazolidin-4-one hydrochloride S15

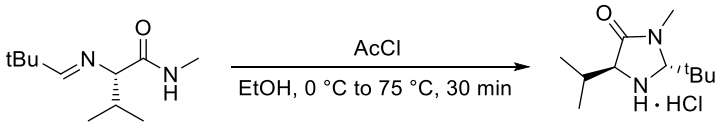

AcCl (0.72 mL, 10.0 mmol, 1.1 equiv) was added dropwise to anhydrous EtOH (5 mL) at 0 °C. The solution was stirred for 15 min and a solution of imin **S11** (1.80 g, 9.12 mmol, 1.0 equiv) in EtOH (1 mL) was added. The reaction mixture was stirred for 15 min at 0 °C and 30 min at 75 °C. After cooing to room temperature, the solution was concentrated under reduced pressure and the mixture was crystallized in the freezer overnight. After filtration hydrochloride **S15** (1.00 g, 4.26 mmol, 47%, single diastereoisomer) was obtained as a colorless solid.

^{1}HNMR (CD_3OD, 700 MHz): δ 4.84 (s. 1H), 4.10 (d, *J* = 4.3 Hz, 1H), 3.06 (s, 3H), 2.38 – 2.32 (m, 1H), 1.17 – 1.15 (s, 12H), 1.12 (d, *J* = 7.0 Hz, 3H) ppm.

(2*R*,5*S*)-5-((*S*)-*sec*-Butyl)-2-(*tert*-butyl)-3-methylimidazolidin-4-one hydrochloride S16

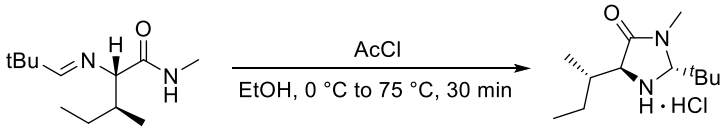

AcCl (0.36 mL, 5.08 mmol, 1.1 equiv) was added dropwise to anhydrous EtOH (2 mL) at 0 °C. The solution was stirred for 15 min at the same temperature and a solution of imin **S12** (989 mg, 4.61 mmol, 1.0 equiv) in EtOH (1 mL) was added. The reaction mixture was stirred for 15 min at 0 °C and 30 min at 75 °C. After cooling to room temperature, the solution was concentrated under reduced pressure and the mixture was crystallized in the freezer overnight. After filtration hydrochloride **S16** was obtained as a colorless solid (417 mg, 1.68 mmol, 36%, single diastereoisomer).

^{1}HNMR (CD_3OD, 700 MHz): δ 4.84 (s, 1H), 4.15 (d, *J* = 3.7 Hz, 1H), 3.05 (s, 3H), 2.07 – 2.03 (m, 1H), 1.61 – 1.55 (m, 1H), 1.53 – 1.46 (m, 1H), 1.16 (s, 9H), 1.09 (d, *J* = 6.9 Hz, 3H), 1.00 (t, *J* = 7.4 Hz, 3H) ppm.

(2*R*,5*S*)-3,5-Dimethyl-2-(1-methylcyclohexyl)imidazolidin-4-one 12

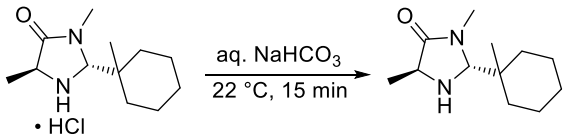

Aqueous saturated $NaHCO_3$-solution (2 mL) was added dropwise to hydrochloride **S13** (210 mg, 851 µmol) and the reaction mixture was stirred for 15 min at room temperature. The free base was extracted with CH_2Cl_2 (3 x 50 mL), the combined organic phases were washed with brine, dried over Na_2SO_4 and the solvent was removed under reduced pressure. Imidazolidinone **12** (172 mg, 817 µmol, 96%, single diastereoisomer) was obtained as a colorless oil.

R_f = 0.4 (EtOAc)

$[\alpha]_D^{23}$ = +17.9° (*c* = 0.80, $CHCl_3$)

^{1}HNMR ($CDCl_3$, 700 MHz) δ = 4.07 (s, 1H), 3.59 (q, *J* = 6.8 Hz, 1H), 2.96 (s, 3H), 1.85 (s, 1H), 1.66 – 1.59 (m, 1H), 1.60 – 1.52 (m, 2H), 1.48 – 1.35 (m, 5H), 1.28 (d, *J* = 6.8 Hz, 3H), 1.28 – 1.23 (m, 1H), 1.17 (m, 1H), 0.91 (s, 3H) ppm.

^{13}CNMR ($CDCl_3$, 176 MHz) δ = 177.2, 83.9, 54.4, 41.0, 34.2, 34.0, 32.2, 26.1, 21.7, 21.6, 18.8, 17.9 ppm.

IR (ATR): $\tilde{\nu}$ = 3313, 2967, 2920, 2857, 1683, 1396, 745 cm^{-1}.

HRMS (ESI, pos. mode): *m*/*z* calculated for $C_{12}H_{23}N_2O$ $[M+H]^+$: 211.1805, found 211.1795; *m*/*z* calculated for $C_{12}H_{22}N_2NaO$ $[M+Na]^+$: 233.1624, found 233.1613.

(2*R*,5*S*)-2-(Adamantan-1-yl)-3,5-dimethylimidazolidin-4-one 13

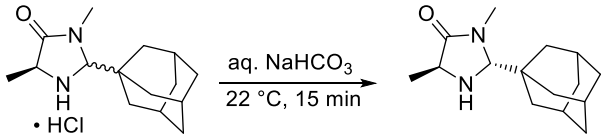

Aqueous saturated $NaHCO_3$-solution (5 mL) was added dropwise to hydrochloride **S14** (553 mg, 1.94 mmol) and the reaction mixture was stirred for 15 min at room temperature. The free base was extracted with CH_2Cl_2 (3 x 80 mL), the combined organic phases were washed with brine, dried over Na_2SO_4 and the solvent was removed under reduced pressure. The free base of compound **S14** was obtained as a white solid (459 mg, 1.85 mmol, 96%). After column chromatography (SiO_2, Et_2O), the *trans*-isomer **13** (169 mg, 680 µmol, 37%) was obtained as a colorless solid. *Trans*-isomerism was confirmed by NOE-spectroscopy.

mp = 115 - 117 °C

R_f(*trans*) = 0.2 (Et_2O) **R_f(*cis*)** = 0.1 (Et_2O)

$[\alpha]_D^{22}$ = +21.7° (*c* = 0.80, $CHCl_3$)

^{1}HNMR ($CDCl_3$, 700 MHz) δ = 3.84 (s, 1H), 3.55 (q, *J* = 6.9 Hz, 1H), 2.97 (s, 3H), 2.01 (p, *J* = 3.2 Hz, 3H), 1.75 – 1.53 (m, 12H), 1.28 (d, *J* = 6.8 Hz, 3H) ppm.

^{13}CNMR ($CDCl_3$, 176 MHz) δ = 177.2, 83.7, 54.5, 40.3, 38.2, 37.1, 32.5, 28.2, 18.6 ppm.

IR (ATR): $\tilde{\nu}$ = 3402, 3285, 2897, 2846, 2362, 1669, 766 cm^{-1}.

HRMS (ESI, pos. mode): *m*/*z* calculated for $C_{15}H_{25}N_2O$ $[M+H]^+$: 249.1962, found 249.1967; *m*/*z* calculated for $C_{15}H_{24}N_2NaO$ $[M+Na]^+$: 271.1781, found 271.1766.

(2*R*,5*S*)-2-(*tert*-Butyl)-5-isopropyl-3-methylimidazolidin-4-one trifluoroacetate 11•TFA

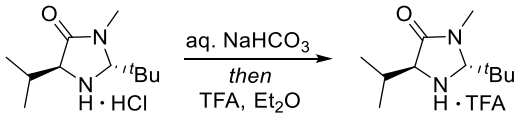

Hydrochloride **S15** (1.13 g, 5.67 mmol, 1.0 equiv) was treated with aqueous saturated $NaHCO_3$-solution (5 mL). The mixture was extracted with CH_2Cl_2 (3 x 15 mL) and the combined organic phases were concentrated under reduced pressure. The obtained oil was dissolved in Et_2O (1 mL) and TFA (440 µL, 5.67 mmol, 1.0 equiv) was added dropwise. The mixture was crystallized in the freezer overnight and imidazolidinone **11•TFA** (1.61 g, 5.15 mmol, 91%, single diastereoisomer) was obtained as a colorless solid.

^{1}HNMR ($CDCl_3$, 700 MHz) δ = 4.72 (d, *J* = 1.1 Hz, 1H), 4.00 (d, *J* = 4.4 Hz, 1H), 3.04 (d, *J* = 0.7 Hz, 3H), 2.28 (heptd, *J* = 6.9, 4.2 Hz, 1H), 1.13 – 1.11 (m, 12H), 1.06 (d, *J* = 7.0 Hz, 3H) ppm.

^{13}CNMR ($CDCl_3$, 176 MHz) δ =170.9, 82.8, 63.8, 37.8, 31.8, 31.1, 25.1, 18.1, 17.5 ppm.

(2*R*,5*S*)-5-((*S*)-*sec*-Butyl)-2-(*tert*-butyl)-3-methylimidazolidin-4-one trifluoroacetate 10•TFA

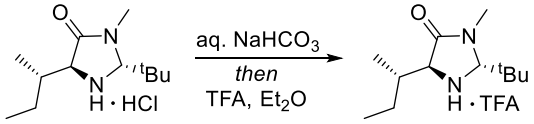

Hydrochloride **S16** (335 mg, 1.58 mmol, 1.0 equiv) was treated with aqueous saturated $NaHCO_3$-solution (2 mL). The mixture was extracted with CH_2Cl_2 (3 x 15 mL) and the combined organic phases were concentrated under reduced pressure. The obtained oil was dissolved in Et_2O (1 mL) and TFA (120 µL, 1.58 mmol, 1.0 equiv) was added dropwise. The mixture was crystallized in the freezer overnight and imidazolidinone **10•TFA** (457 mg, 1.46 mmol, 92%, single diastereoisomer) was obtained as a colorless solid.

^{1}HNMR ($CDCl_3$, 500 MHz) δ = 4.72 (d, *J* = 1.0 Hz, 1H), 4.04 (d, *J* = 3.6 Hz, 1H), 3.03 (s, 3H), 2.07 – 1.88 (m, 1H), 1.57 – 1.50 (m, 1H), 1.46 – 1.39 (m, 1H), 1.12 (s, 9H), 1.06 (d, *J* = 6.9 Hz, 3H), 0.98 (t, *J* = 7.4 Hz, 3H) ppm.

^{13}CNMR ($CDCl_3$, 126 MHz) δ = 170.8, 82.8, 62.9, 38.1, 37.7, 31.7, 25.7, 25.1, 14.6, 12.0 ppm.

2.2. CHLORINATING REAGENTS

The following N-chlorinations were performed based on a literature-known procedure.[6]

3,3,4,4-Tetramethylpyrrolidine-2,5-dione S17

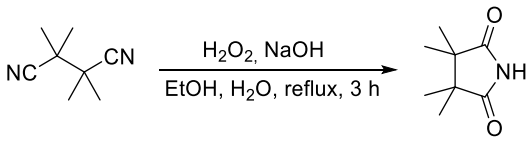

Imid **S17** was synthesized according to a literature-known procedure.[5] A solution of H_2O_2 in water (30 w%, 11.8 mL, 106 mmol, 2.9 equiv) was added to a solution of 2,2,3,3-tetramethylsuccinonitrile (5.00 g, 36.7 mmol, 1.0 equiv) in ethanol (25 mL) at 0 °C and stirred for 3 h under reflux. The reaction mixture was cooled to room temperature and quenched with hydrochloric acid (1 M). The product was extracted with toluene (3 x 100 mL), dried over Na_2SO_4 and the solvent was removed under reduced pressure. Imid **S17** (1.65 g, 10.6 mmol, 29%) was obtained as a colorless solid and was used without further purification.

^{1}HNMR ($CDCl_3$, 400 MHz) δ = 8.57 (s, 1H), 1.18 (s, 12H) ppm.

Spectroscopic data were in accordance with published data.[5]

1-Chloro-3,3,4,4-tetramethylpyrrolidine-2,5-dione 20

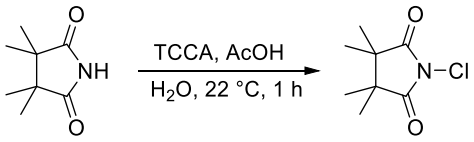

Trichloroisocyanuric acid (725 mg, 3.12 mmol, 0.33 equiv) was added to a suspension of imide **S17** (1.47 g, 9.45 mmol, 1.0 equiv), acetic acid (3.20 mL, 56.0 mmol, 5.9 equiv) and water (20 mL) and the reaction mixture was stirred for 1 h at room temperature. The product was extracted with $CHCl_3$ (3 x 50 mL), the combined organic phases were dried over Na_2SO_4 and the solvent was removed under reduced pressure. Compound **20** (1.63 g, 8.62 mmol, 91%) was obtained as a colorless solid and was used without further purification.

mp: 82 – 84 °C

R_f = 0.8 (pentane:EtOAc = 5:1)

^{1}HNMR ($CDCl_3$, 400 MHz) δ = 1.24 (s, 12H) ppm.

^{13}CNMR ($CDCl_3$, 126 MHz) δ = 177.7, 48.0, 21.8 ppm.

IR (ATR): $\tilde{\nu}$ = 2978, 1743, 1722, 1396, 1382 cm^{-1}.

HRMS (ESI, pos. mode): *m*/*z* calculated for $C_8H_{13}ClNO_2$ $[M+H]^+$: 190.0630, found 190.0626.

1-Chloro-5-nitroisoindoline-1,3-dione 19

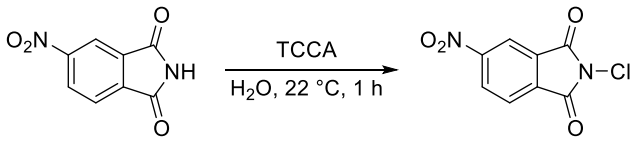

Trichloroisocyanuric acid (121 mg, 521 µmol, 0.33 equiv) was added to a suspension of 4-nitrophthalimide (300 mg, 1.56 mmol, 1.0 equiv) in water (10 mL) and the reaction mixture was stirred for 1 h at room temperature. The solid was filtered off and dried at 50 °C over night. Compound **19** (339 mg, 1.50 mmol, 96%) was obtained as a colorless solid and was used without further purification.

^{1}HNMR (CD_3CN, 500 MHz) δ = 8.63 (dd, *J* = 8.2, 2.0 Hz, 1H), 8.60 (dd, *J* = 2.0, 0.6 Hz, 1H), 8.10 (dd, *J* = 8.2, 0.7 Hz, 1H) ppm.

Spectroscopic data were in accordance with published data.[7]

5-Fluoroisoindoline-1,3-dione S18

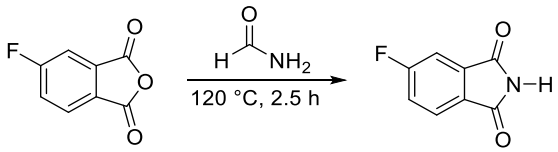

Formamide (15.0 mL, 377 mmol, 12.5 equiv) was added to 5-Fluoroisobenzofuran-1,3-dione (5.00 g, 30.0 mmol, 1.0 equiv) at room temperature and the suspension was stirred for 2.5 h at 120 °C (caution: CO evolution!). After cooling to room temperature, the reaction mixture was poured into water (120 mL). The solids were filtered off, washed with water and dried at 50 °C overnight. Imid **S18** (3.10 g, 18.8 mmol, 63%) was obtained as a colorless solid and was used without further purification.

^{1}HNMR ($DMFd_7$, 500 MHz) δ = 11.43 (s, 1H), 7.98 – 7.95 (m, 1H), 7.75 – 7.66 (m, 2H) ppm.

Spectroscopic data were in accordance with published data.[8]

2-Chloro-5-fluoroisoindoline-1,3-dione 17

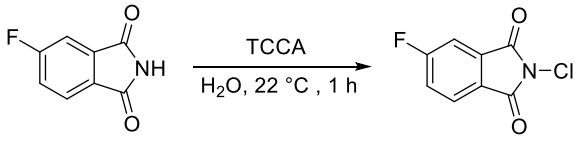

Trichloroisocyanuric acid (1.44 g, 6.19 mmol, 0.33 equiv) was added to a suspension of imide **S18** (3.10 g, 18.7 mmol, 1.00 equiv) in water (200 mL) and the reaction mixture was stirred for 1 h at room temperature. The solids were filtered off and purified by recrystallization ($CHCl_3$, reflux). Compound **17** (3.00 g, 15.0 mmol, 80%) was obtained as a colorless solid.

mp: 155 – 156 °C

^{1}HNMR ($CDCl_3$, 500 MHz) δ = 7.92 (dd, *J* = 8.3, 4.5 Hz, 1H), 7.59 (dd, *J* = 6.8, 2.3 Hz, 1H), 7.45 (td, *J* = 8.6, 2.3 Hz, 1H) ppm.

^{13}CNMR ($CDCl_3$, 126 MHz) δ = 166.7 (d, *J* = 259.6 Hz), 162.4, 162.2 (d, *J* = 2.9 Hz), 133.9 (d, *J* = 9.7 Hz), 127.0 (d, *J* = 3.2 Hz), 126.7 (d, *J* = 9.7 Hz), 121.9 (d, *J* = 23.8 Hz), 112.1 (d, *J* = 25.3 Hz) ppm.

IR (ATR): $\tilde{\nu}$ = 3079, 1785, 1729, 1481, 1224, 1168 cm^{-1}.

HRMS (ESI, pos. mode): *m*/*z* calculated for $C_8H_3ClFNNaO_2$ $[M+Na]^+$: 221.9728, found 221.9732.

4,5,6,7-Tetrachloroisoindoline-1,3-dione S19

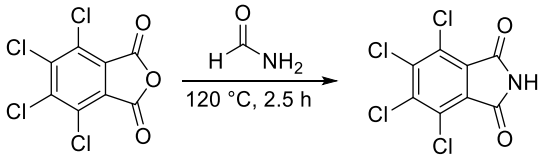

Formamide (8.70 mL, 219 mmol, 12.5 equiv) was added to 4,5,6,7-Tetrachloroisobenzofuran-1,3-dione (5.00 g, 17.5 mmol, 1.0 equiv) at room temperature and the suspension was stirred for 2.5 h at 120 °C (caution: CO evolution!). After cooling to room temperature the reaction mixture was poured into water (120 mL). The solids were filtered off, washed with water and dried at 50 °C over night. Imid **S19** (4.71 g, 16.5 mmol, 94%) was obtained as a colorless solid and was used without further purification.

^{1}HNMR ($DMFd_7$, 500 MHz) δ = 11.93 (s, 1H) ppm.

^{13}CNMR ($DMFd_7$, 126 MHz) δ = 164.8, 138.8, 129.7, 128.8 ppm.

HRMS (ESI, pos. mode): *m*/*z* calculated for $C_8H_2Cl_4NO_2$ $[M+H]^+$: 283,8834, found 283,8841

Anal. Calcd. for $C_8HCl_4NO_2$ (284.90): C 33.73, H 0.35, N 4.92; found: C 33.75, H 0.36, N 4.98.

2,4,5,6,7-Pentachloroisoindoline-1,3-dione 18

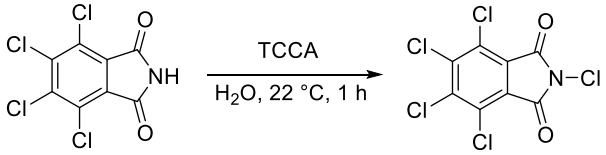

Trichloroisocyanuric acid (869 mg, 3.74 mmol, 0.33 equiv) was added to a suspension of imide **S19** (3.00 g, 10.5 mmol, 1.0 equiv) in water (110 mL) and the reaction mixture was stirred for 1 h at room temperature. The solids were filtered off, dried and compound **18** (3.02 g, 9.46 mmol, 90%) was obtained as a colorless solid.

^{13}CNMR ($DMFd_7$, 126 MHz) δ = 160.0, 139.5, 129.1, 128.5 ppm.

IR (ATR): $\tilde{\nu}$ = 1746, 1038 cm^{-1}.

HRMS (ESI, pos. mode): *m*/*z* calculated for $C_8HCl_5NO_2$ $[M+H]^+$: 317.8445 found 317.8453.

Anal. Calcd. for $C_8Cl_5NO_2$ (319.34): C 30.03, H 0.00, N 4.39; found: C 30.23, H 0.00, N 4.44.

2.3. OFF-CYCLE INTERMEDIATES

1-((1*R*,2*S*)-1-((2*R*,5*S*)-2-(*tert*-Butyl)-3,5-dimethyl-4-oxoimidazolidin-1-yl)-2-chloro-3-phenylpropyl)pyrrolidine-2,5-dione 5

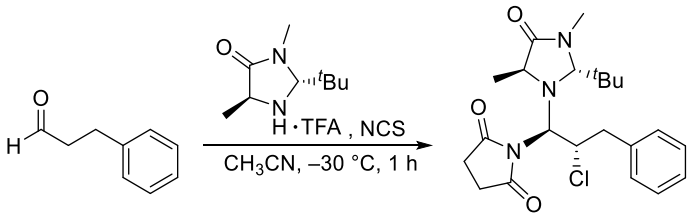

Catalyst **2•TFA** (4.24 g, 14.9 mmol, 20 mol%) and *N*-chlorosuccinimide (11.9 g, 89.4 mmol, 1.2 equiv) were added subsequently to a solution of hydrocinnamic aldehyde (10.0 g, 74.5 mmol, 1.0 equiv) in CH_3CN (250 mL) at –30 °C. After stirring for 1 h, silica was added to the reaction mixture, the solvent was removed under reduced pressure and the crude product was purified by column chromatography (SiO_2, pentane/EtOAc, 5:1 to 1:10). Parasitic intermediate **5** (2.84 g, 6.76 mmol, 9%) was obtained as a white solid.

$\mathbf{R_f}$ = 0.4 (pentane:EtOAc = 1:5)

^{1}HNMR ($CDCl_3$, 700 MHz) δ = 7.36 – 7.25 (m, 5H), 5.02 (d, *J* = 10.7, 1H), 4.98 (s, 1H), 4.97 (td, *J* = 10.4, 2.2 Hz, 1H), 3.96 (q, *J* = 7.5 Hz, 1H), 3.92 – 3.86 (m, 2H), 2.88 (s, 3H), 2.80 (dd, J = 14.9, 10.3 Hz, 1H), 2.76 – 2.58 (m, 4H), 1.45 (d, J = 7.4 Hz, 3H), 1.10 (s, 9H) ppm.

^{13}CNMR ($CDCl_3$, 176 MHz) δ = 179.5, 176.7, 175.6, 137.1, 129.4, 128.5, 127.1, 84.8, 71.5, 60.5, 58.3, 38.6, 31.8, 28.1, 28.0, 11.6 ppm.

IR (ATR): $\tilde{\nu}$ = 3031, 2957, 2871, 1778, 1708, 1455, 1432, 1396, 1375, 1252, 1201, 816, 751, 701 cm^{-1}.

HRMS (ESI, pos. mode): *m*/*z* calculated for $C_{22}H_{30}ClN_3NaO_3$ $[M+Na]^+$: 442.1868, found 442.1880.

The following three off-cycle intermediates **6**, **7** and **8** were synthesized according to the procedure described above.

1-((1*R*,2*S*)-1-((2*R*,5*S*)-2-(*tert*-Butyl)-3,5-dimethyl-4-oxoimidazolidin-1-yl)-2-chlorooctyl)pyrrolidine-2,5-dione 6

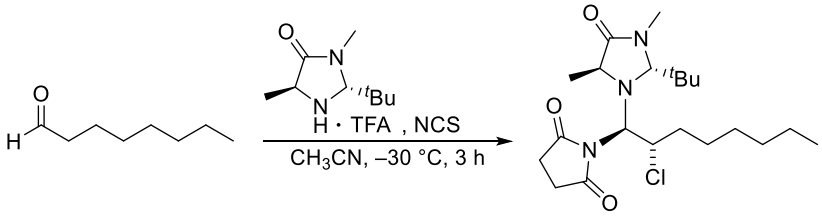

Yield: 120 mg, 330 µmol, 18%

$\mathbf{R_f}$ = 0.4 (pentane:EtOAc = 1:6)

^{1}HNMR ($CDCl_3$, 700 MHz) δ = 4.97 (s, 1H), 4.90 (d, *J* = 10.7 Hz, 1H), 4.59 (td, *J* = 10.4, 1.7 Hz, 1H), 3.89 (q, *J* = 7.5 Hz, 1H), 2.84 (s, 3H), 2.74 – 2.54 (m, 4H), 2.41 (tdd, *J* = 11.4, 4.7, 2.1 Hz, 1H), 1.72 – 1.63 (m, 1H), 1.62 – 1.51 (m, 1H), 1.39 (d, *J* = 7.5 Hz, 3H), 1.38 – 1.25 (m, 7H), 0.99, (s, 9H), 0.88 (t, J = 7.0 Hz, 3H) ppm.

^{13}CNMR ($CDCl_3$, 176 MHz) δ = 179.5, 176.8, 175.7, 84.7, 71.6, 61.0, 58.1, 38.5, 36.3, 31.8, 31.8, 29.1, 28.1, 28.0, 27.8, 26.6, 22.7, 14.2, 11.5 ppm.

IR: $\tilde{\nu}$ = 2950, 2870, 1780, 1710, 1680, 1480, 1440, 1400, 1370, 1340, 1260, 1170, 1150, 790 cm^{-1}.

HRMS (ESI, pos. mode): *m*/*z* calculated for $C_{17}H_{28}ClN_3O_3$ $[M+H]^+$: 414. 2577, found: 414.2524; *m*/*z* calculated for $C_{17}H_{27}ClN_3NaO_3$ $[M+Na]^+$: 436.2409, found: 436.2343.

1-((1*R*,2*S*)-1-((2*R*,5*S*)-2-(*tert*-butyl)-3,5-dimethyl-4-oxoimidazolidin-1-yl)-2-chloropentyl)pyrrolidine-2,5-dione 7

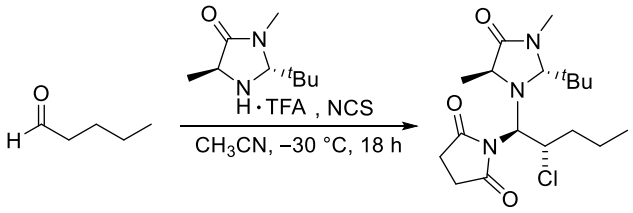

Yield: 72.1 mg, 194 mmol, 10%

R_f = 0.4 (pentane:EtOAc = 1:6)

^{1}HNMR ($CDCl_3$, 500 MHz) δ = 4.96 (s, 1H), 4.90 (d, *J* = 10.7 Hz, 1H), 4.60 (td, *J* = 10.4, 1.9 Hz, 1H), 3.89 (q, *J* = 7.4 Hz, 1H), 2.84 (s, 3H), 2.74 – 2.54 (m, 4H), 2.39 (dd, *J* = 3.9, 1.7 Hz, 3H), 1.80 – 1.65 (m, 1H), 1.62 – 1.51 (m, 1H), 1.46 – 1.41 (m, 1H), 1.39 (d, *J* = 7.5 Hz, 3H), 0.99 (s, 9H), 0.95 (t, *J* = 7.4 Hz, 3H) ppm.

^{13}CNMR ($CDCl_3$, 176 MHz) δ = 179.5, 176.8, 175.7, 84.7, 71.6, 60.6, 58.1, 38.5, 38.2, 31.7, 28.1, 28.0, 27.7, 20.0, 13.8, 11.4 ppm.

IR: $\tilde{\nu}$ = 2960, 2930, 2870, 1780, 1710, 1460, 1440, 1400, 1370, 1350, 1280, 1250, 1200, 1150, 820 cm^{-1}.

HRMS (ESI, pos. mode): *m*/*z* calculated for $C_{18}H_{30}ClN_3O_3$ $[M+H]^+$: 372.2049, found: 372.2066.

2-((1*R*,2*S*)-1-((2*R*,5*S*)-2-(*tert*-butyl)-3,5-dimethyl-4-oxoimidazolidin-1-yl)-2-chloro-3-phenylpropyl)isoindoline-1,3-dione 8

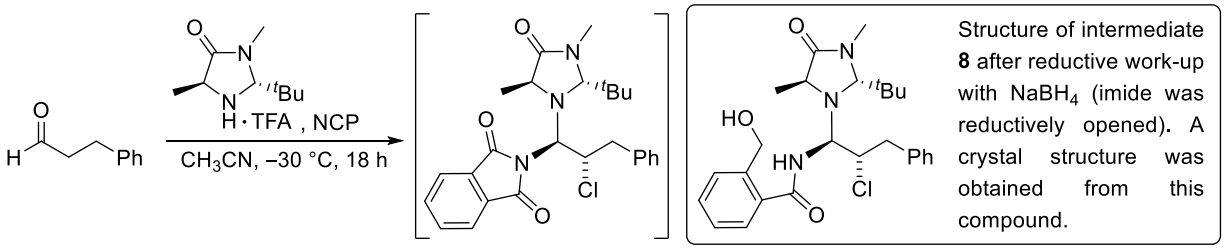

Structure of intermediate **8** after reductive work-up with $NaBH_4$ (imide was reductively opened). A crystal structure was obtained from this compound.

Yield: 99.0 mg, 234 µmol, 16%

R_f = 0.7 (pentane:EtOAc = 1:6)

^{1}HNMR (CD_2Cl_2, 700 MHz) δ = 7.89 – 7.81 (m, 2H), 7.81 – 7.73 (m, 2H), 7.36 – 7.25 (m, 4H), 7.36 – 7.25 (m, 4H), 5.19 (d, *J* = 10.7 Hz, 1H), 5.09 (td, *J* = 10.7, 2.3 Hz, 1H), 4.88 (s, 1H), 4.04 – 3.95 (m, 2H), 2.84 (dd, *J* = 14.7, 10.7 Hz, 1H), 2.67 (d, *J* = 0.7 Hz, 3H), 1.55 (d, *J* = 7.4 Hz, 3H), 1.13 (s, 9H) ppm.

^{13}CNMR (CD_2Cl_2, 176 MHz) δ = 175.03, 170.4, 168.3, 137.4, 134.7, 134.6, 131.4, 130.8, 129.3, 128.4, 126.8, 123.9, 123.5, 84.7, 70.9, 61.7, 58.4, 41.9, 38.5, 31.5, 27.5, 11.4 ppm.

IR: $\tilde{\nu}$ = 2950, 2870, 1780, 1710, 1680, 1480, 1470, 1400, 1370, 1340, 1260, 1170, 1150, 1060, 720 cm^{-1}.

HRMS (ESI, pos. mode): *m*/*z* calculated for $C_{26}H_{30}ClN_3O_3$ $[M+H]^+$: 468.2049 found: 468.2020; *m*/*z* calculated for $C_{26}H_{29}ClN_3NaO_3$ $[M+Na]^+$: 490.1868, found: 490.1853.

1-((1*R*,2*S*,6*S*)-1-((2*R*,5*S*)-2-(*tert*-Butyl)-3,5-dimethyl-4-oxoimidazolidin-1-yl)-2,6-dichloro-7-hydroxyheptyl)pyrrolidine-2,5-dione 9

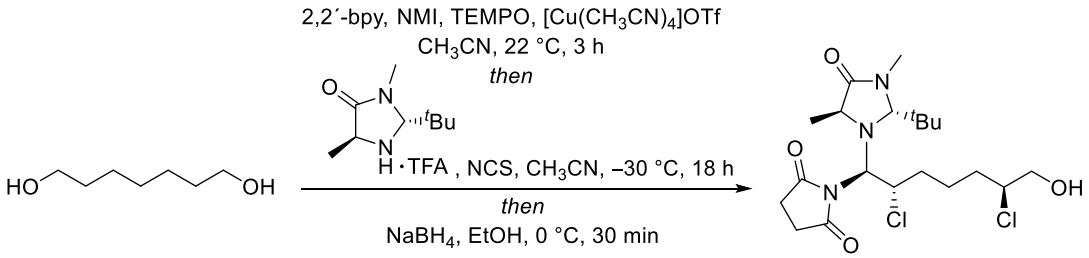

1,7-Heptanediol (5.00 g, 37.8 mmol, 1.0 equiv) was dissolved in CH_3CN (380 mL). $[Cu(CH_3CN)]OTf$ (1.07 g, 2.84 mmol, 7.5 mol%), 2,2´-bpy (443 mg, 2.84 mmol, 7.5 mol%), TEMPO (443 mg, 2.84 mmol, 7.5 mol%) and NMI (450 µL, 5.67 mmol, 15 mol%) were added subsequently at room temperature and stirring was continued for 3 h under oxygen atmosphere. Catalyst **2•TFA** (4.32 g, 15.1 mmol, 40 mol%), *N*-chlorosuccinimide (12.6 g, 94.5 mmol, 2.5 equiv) and CH_3CN (380 mL) were added and the reaction mixture was stirred for 18 h at –30 °C. $NaBH_4$ (7.15 g, 189 mmol, 5.0 equiv) and EtOH (380 mL) were added and stirring was continued for 30 min at 0 °C. The reaction mixture was quenched with aqueous saturated NH_4Cl-solution, concentrated under reduced pressure and the aqueous phase was extracted with EtOAc (3 x 200 mL). After removal of all solvents under reduced pressure, the crude product was purified by column chromatography (SiO_2, pentane:Et_2O = 1:5). Intermediate **9** (587 mg, 1.30 mmol, 3%) was obtained as a colorless solid.

R_f = 0.4 (EtOAc)

mp: 116 °C

^{1}HNMR ($CDCl_3$, 500 MHz) δ = 4.98 (s, 1H), 4.91 (d, *J* = 10.7 Hz, 1H), 4.60 – 4.67 (m, 1H), 4.06 – 3.99 (m, 1H), 3.90 (q, *J* = 7.4 Hz, 1H), 3.79 (dd, *J* = 12.0, 4.0 Hz, 1H), 3.69 (dd, *J* = 12.0, 4.0 Hz, 1H), 2.86 (s, 3H), 2.76 – 2.58 (m, 4H), 2.48 – 2.40 (m, 1H), 1.89 – 1.73 (m, 3H), 1.72 – 1.60 (m, 2H), 1.40 (d, *J* = 7.5 Hz, 3H), 1.00 (s, 9H) ppm.

^{13}CNMR ($CDCl_3$, 125 MHz) δ = 179.4, 176.6, 175.5, 84.5, 71.3, 66.9, 64.5, 60.2, 57.9, 38.4, 35.6, 33.9, 31.6, 28.0, 27.9, 27.6, 23.6, 11.3 ppm.

IR: $\tilde{\nu}$ = 3388, 2945, 1709, 1672, 1338, 1144, 1033, 776, 680, 627, 581 cm^{-1}.

HRMS (ESI, pos. mode): *m*/*z* calculated for $C_{20}H_{33}Cl_2N_3O_4$ $[M+H]^+$: 450.1921 found: 450.1921; *m*/*z* calculated for $C_{20}H_{32}Cl_2N_3NaO_4$ $[M+Na]^+$: 472.1740, found: 472.1736.

2.4. SYNTHESIS OF SUBSTRATES

The following aerobic oxidations were performed according to a literature-know procedure.[9]

Decanedial S20

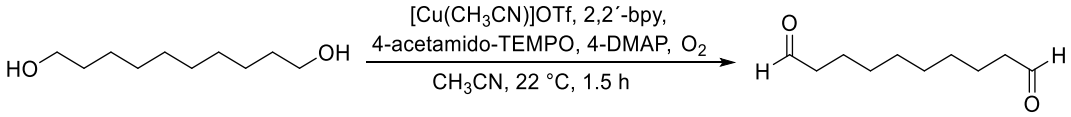

Decane-1,10-diol (2.00 g, 11.5 mmol, 1.0 equiv) was dissolved in CH_3CN (30 mL). [Cu(CH_3CN)]OTf (433 mg, 1.15 mmol, 10 mol%), 2,2´-bpy (180 mg, 1.15 mmol, 10 mol%), 4-acetamido-TEMPO (245 mg, 1.15 mmol, 10 mol%) and 4-DMAP (281 mg, 2.30 mmol, 20 mol%) were added subsequently at room temperature and stirring was continued for 1.5 h under oxygen atmosphere. The reaction mixture was quenched with water and the aqueous phase was extracted with EtOAc (3 x 50 mL). The combined organic phases were dried over Na_2SO_4 and the solvent was removed under reduced pressure. The crude product was purified by column chromatography (SiO_2, pentane/EtOAc 8:1) yielding dialdehyde **S20** (1.51 g, 8.86 mmol, 77%) as a colorless solid.

^{1}HNMR ($CDCl_3$, 400 MHz) δ = 9.76 (t, *J* = 1.7 Hz, 2H), 2.42 (td, *J* = 7.3, 1.8 Hz, 4H), 1.62 (p, *J* = 7.2 Hz, 4H), 1.35 – 1.28 (m, 8H) ppm.

Spectroscopic data were in accordance with published data.[10]

5-Bromopentanal S21

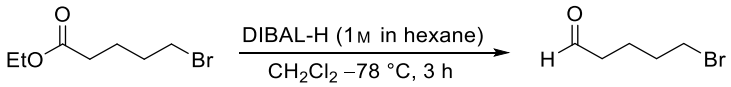

Aldehyde **S21** was synthesized according to literature-known procedure.[11] DIBAL-H (1 M in hexane, 11.0 mL, 11.0 mmol, 1.1 equiv) was added dropwise to a –78°C cooled solution of ethyl-5-bromopentanoate (2.09 g, 10.0 mmol, 1.0 equiv) in anhydrous CH_2Cl_2 (20 mL) under argon-atmosphere and the reaction mixture was stirred for 3 h at the same temperature. The reaction was quenched with Et_2O and brine, the phases were separated and the aqueous phase was extracted with Et_2O (3 x 20 mL). The combined organic phases were dried over Na_2SO_4 and the solvent was removed under reduced pressure. After purification by column chromatography (SiO_2, pentane/Et_2O 20:1), aldehyde **S21** (1.24 g, 7.51 mmol, 75%) was obtained as a colorless oil.

^{1}HNMR ($CDCl_3$, 400 MHz) δ 9.78 (t, *J* = 1.5 Hz, 1H), 3.41 (t, *J* = 6.5 Hz, 2H), 2.49 (td, *J* = 7.1, 1.5 Hz, 2H), 1.94 – 1.85 (m, 2H), 1.84 – 1.75 (m, 2H) ppm.

10-((*tert*-Butyldiphenylsilyl)oxy)decan-1-ol S22

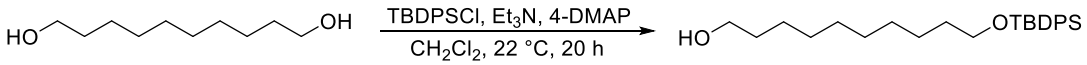

Alcohol **S22** was synthesized according to a literature-known procedure.[12] 1,10-Decanediol (3.00 g, 17.2 mmol, 1.0 equiv), Et_3N (1.20 mL, 8.61 mmol, 0.5 equiv) and 4-DMAP (69.6 mg, 570 µmol, 3 mol%) were dissolved in CH_2Cl_2 (250 mL). TBDPSCl (1.47 mL, 5.68 mmol, 0.3 equiv) was added dropwise and stirring was continued for 20 h at room temperature. The reaction mixture was concentrated under reduced pressure, diluted with hexane and the solids were filtered off. The crude product was purified by column chromatography (SiO_2, pentane/EtOAc 10:1 to 5:1) and alcohol **S22** (1.25 g, 3.02 mmol, 53%) was obtained as a colorless oil.

^{1}HNMR ($CDCl_3$, 400 MHz) δ 7.70 – 7.63 (m, 4H), 7.45 – 7.32 (m, 6H), 3.69 – 3.60 (m, 4H), 1.62 – 1.50 (m, 4H), 1.39 – 1.22 (m, 13H), 1.05 (s, 9H) ppm.

Spectroscopic data were in accordance with published data.[12]

10-((*tert*-Butyldiphenylsilyl)oxy)decanal S23

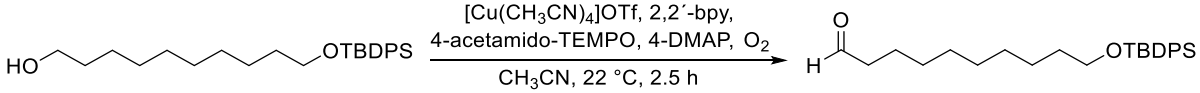

Alcohol **S22** (1.24 g, 3.01 mmol, 1.0 equiv) was dissolved in CH_3CN (30 mL). $[Cu(CH_3CN)_4]OTf$ (56.5 mg, 150 µmol, 5 mol%), 2,2´-bpy (23.0 mg, 150 µmol, 5 mol%), 4-acetamido-TEMPO (32.0 mg, 150 µmol, 5 mol%) and 4-DMAP (37.0 mg, 300 µmol, 10 mol%) were added subsequently at room temperature and stirring was continued for 2.5 h under oxygen atmosphere. The reaction mixture was quenched with water and the aqueous phase was extracted with Et_2O (3 x 50 mL). The combined organic phases were dried over Na_2SO_4, the solvent was removed under reduced pressure and the crude product was purified by column chromatography (SiO_2, pentane/Et_2O 20:1). Aldehyde **S23** (1.10 g, 2.67 mmol, 89%) was obtained as a colorless oil.

^{1}HNMR ($CDCl_3$, 400 MHz) δ = 9.76 (t, *J* = 1.7 Hz, 1H), 7.70 – 7.64 (m, 4H), 7.45 – 7.34 (m, 6H), 3.65 (t, *J* = 6.5 Hz, 3H), 2.41 (td, *J* = 7.3, 1.9 Hz, 2H), 1.72 – 1.46 (m, 4H), 1.43 – 1.19 (m, 10H), 1.05 (s, 9H) ppm.

Spectroscopic data were in accordance with published data.[13]

10-Hydroxydecylacetate S24

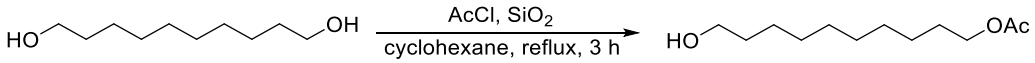

Alcohol **S24** was synthesized according to a literature-known procedure.[14] 1,10-Decanediol (3.00 g, 17.2 mmol, 1.0 equiv) was dissolved in Et_2O (100 mL), silica (50 g) was added and the solvent was removed again under reduced pressure. Cyclohexane (80 mL) and AcCl (3.07 mL, 43.0 mmol, 2.5 equiv) were added and the reaction mixture was stirred for 3 h under reflux and then cooled to room temperature. The solvent was removed under reduced pressure and the silica-adsorbent was washed with EtOAc. After removal of all solvents under reduced pressure, the crude product was purified by column chromatography (SiO_2, pentane/EtOAc 20:1 to 3:1). The alcohol **S24** (701 mg, 3.24 mmol, 19%) was obtained as a white solid. Undesired diprotected alcohol (2.32 g, 8.98 mmol, 52%) was obtained as a colorless oil.

^{1}HNMR ($CDCl_3$, 400 MHz) δ = 4.05 (t, *J* = 6.8 Hz, 2H), 3.64 (t, *J* = 6.6 Hz, 2H), 2.04 (s, 3H), 1.66 – 1.51 (m, 4H), 1.40 – 1.25 (m, 13H) ppm.

Spectroscopic data were in accordance with published data.[15]

10-Oxodecylacetate S25

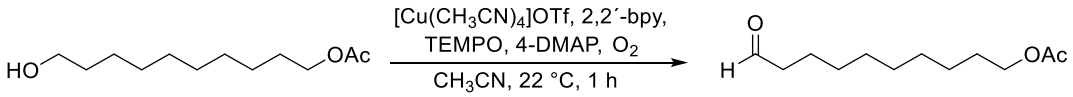

Alcohol **S24** (700 mg, 3.22 mmol, 1.0 equiv) was dissolved in CH_3CN (15 mL). $Cu(CH_3CN)_4OTf$ (60.7 mg, 161 µmol, 5 mol%), 2,2-bpy (25.1 mg, 161 µmol, 5 mol%), TEMPO (25.2 mg, 161 µmol, 5 mol%) and 4-DMAP (39.3 mg, 322 µmol, 10 mol%) were added subsequently at room temperature and stirring was continued for 1 h under oxygen atmosphere. The reaction mixture was quenched with water and the aqueous phase was extracted with EtOAc (3 x 50 mL). The combined organic phases were dried over Na_2SO_4, the solvent was removed under reduced pressure and the crude product was purified by column chromatography (SiO_2, pentane/EtOAc 20:1 to 15:1) yielding aldehyde **S25** (557 mg, 2.60 mmol, 81%) as a colorless oil.

^{1}HNMR ($CDCl_3$, 400 MHz) δ = 9.76 (t, *J* = 1.8 Hz, 1H), 4.05 (t, *J* = 6.8 Hz, 2H), 2.42 (td, *J* = 7.3, 1.8 Hz, 2H), 2.04 (s, 3H), 1.72 – 1.51 (m, 4H), 1.40 – 1.24 (m, 10H) ppm.

Spectroscopic data were in accordance with published data.[16]

10-(Methoxymethoxy)decan-1-ol S26

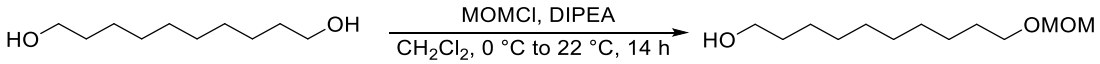

Alcohol **S26** was synthesized according to literature-known procedure.[17] DIPEA (8.78 mL, 51.6 mmol, 3.0 equiv) and MOMCl (1.31 mL, 17.2 mmol, 1.0 equiv) were added subsequently to an ice-cold solution of 1,10-decanediol (3.00 g, 17.2 mmol, 1.0 equiv) in CH_2Cl_2 (100 mL). The reaction mixture was stirred for 14 h at room temperature and finally poured into aqueous HCl (0.5 M). The phases were separated and the aqueous phase was extracted with EtOAc (3 x 100 mL). The combined organic phases were washed with brine and dried over Na_2SO_4. The solvent was removed under reduced pressure and the crude product was purified by column chromatography (SiO_2, pentane/EtOAc 20:1 to 2:1) yielding alcohol **S26** (1.62 g, 7.44 mmol, 43%) as a colorless oil.

^{1}HNMR ($CDCl_3$, 400 MHz) δ = 4.62 (s, 2H), 3.63 (t, *J* = 6.7 Hz, 2H), 3.51 (t, *J* = 6.6 Hz, 2H), 3.36 (s, 3H), 1.64 – 1.50 (m, 4H), 1.42 – 1.22 (m, 13H) ppm.

Spectroscopic data were in accordance with published data.[17]

10-(Methoxymethoxy)decanal S27

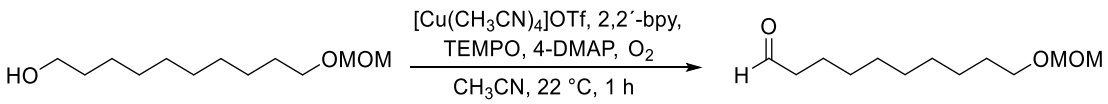

Alcohol **S26** (1.62 g, 7.42 mmol, 1.0 equiv) was dissolved in CH_3CN (20 mL). $[Cu(CH_3CN)_4]OTf$ (140 mg, 371 µmol, 5 mol%), 2,2´-bpy (57.9 mg, 371 µmol, 5 mol%), TEMPO (58.0 mg, 371 µmol, 5 mol%) and 4-DMAP (90.1 mg, 742 µmol, 10 mol%) were added subsequently at room temperature and stirring was continued for 1 h under oxygen atmosphere. The reaction mixture was quenched with water and the aqueous phase was extracted with EtOAc (3 x 50 mL). The combined organic phases were dried over Na_2SO_4, solvent was removed under reduced pressure and the crude product was purified by column chromatography (SiO_2, pentane/EtOAc 20:1 to 15:1) yielding aldehyde **S27** (1.32 g, 6.12 mmol, 83%) as a colorless oil.

R_f = 0.4 (pentane:EtOAc = 1:5)

^{1}HNMR ($CDCl_3$, 500 MHz) δ = 9.74 (t, *J* = 1.8 Hz, 1H), 4.60 (s, 2H), 3.50 (t, *J* = 6.6 Hz, 2H), 3.34 (s, 3H), 2.40 (td, *J* = 7.4, 1.8 Hz, 2H), 1.64 – 1.52 (m, 4H), 1.39 – 1.23 (m, 10H) ppm.

^{13}CNMR ($CDCl_3$, 126 MHz) δ = 203.0, 96.5, 68.0, 55.2, 44.0, 29.8, 29.5 (2C), 29.4, 29.3, 26.3, 22.2 ppm.

IR (ATR): $\tilde{\nu}$ = 2926, 2855, 1725, 1464, 1146, 1110, 721 cm^{-1}.

HRMS (ESI, pos. mode): *m*/*z* calculated for $C_{12}H_{24}NaO_3$ $[M+Na]^+$: 239.1617, found 239.1625.

***tert*-Butyl-(6-hydroxyhexyl)carbamate S28**

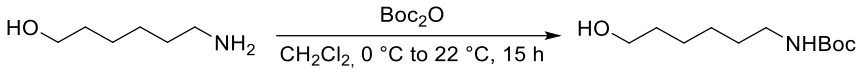

Alcohol **S28** was synthesized according to literature-known procedure.[18] Boc_2O (4.10 g, 18.8 mmol, 1.1 equiv) was added to an ice-cold solution of 6-aminohexan-1-ol (2.00 g, 17.1 mmol, 1.0 equiv) in CH_2Cl_2 (17 mL) and the reaction mixture was stirred for 15 h at room temperature. After the solvent was removed under reduced pressure, the crude product was dissolved in EtOAc. The organic phase was washed with saturated aqueous citric acid, $NaHCO_3$-solution and brine. The organic phase was dried over Na_2SO_4 and the solvent was removed under reduced pressure. The protected amine **S28** (3.72 g, 17.1 mmol, quant.) was obtained as a yellowish oil and was used without further purification.

^{1}HNMR ($CDCl_3$, 400 MHz) δ = 4.51 (s, 1H), 3.63 (t, *J* = 6.5 Hz, 2H), 3.11 (t, *J* = 7.0 Hz, 2H), 1.61 – 1.54 (m, 2H), 1.52 (s, 1H), 1.51 – 1.45 (m, 2H), 1.44 (s, 9H), 1.42 – 1.29 (m, 4H) ppm.

Spectroscopic data were in accordance with published data.[18]

***tert*-Butyl(6-oxohexyl)carbamate S29**

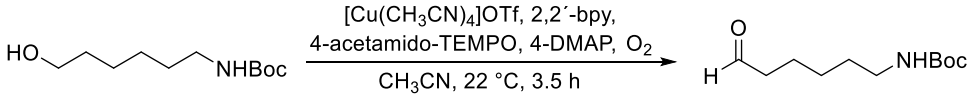

Alcohol **S28** (3.93 g, 18.1 mmol, 1.0 equiv) was dissolved in CH_3CN (100 mL). $[Cu(CH_3CN)_4]OTf$ (341 mg, 905 µmol, 5 mol%), 2,2´-bpy (141 mg, 905 µmol, 5 mol%), 4-acetamido-TEMPO (193 mg, 905 µmol, 5 mol%) and 4-DMAP (221 mg, 1.81 mmol, 10 mol%) were added subsequently at room temperature and stirring was continued for 3.5 h under oxygen atmosphere. The reaction mixture was quenched with water and the aqueous phase was extracted with DCM (3 x 50 mL). The combined organic phases were dried over Na_2SO_4, the solvent was removed under reduced pressure and the crude product was purified by column chromatography (SiO_2, pentane/EtOAc 5:1), yielding aldehyde **S29** (1.30 g, 6.04 mmol, 33%) as a colorless oil.

^{1}HNMR ($CDCl_3$, 400 MHz) δ = 9.76 (t, *J* = 1.7 Hz, 1H), 4.53 (s, 1H), 3.11 (q, *J* = 6.7 Hz, 2H), 2.44 (td, *J* = 7.3, 1.7 Hz, 2H), 1.65 (p, *J* = 7.4 Hz, 2H), 1.54 – 1.45 (m, 2H), 1.44 (s, 8H), 1.40 – 1.30 (m, 2H) ppm.

Spectroscopic data were in accordance with published data.[18]

4-Bromobutanal S30

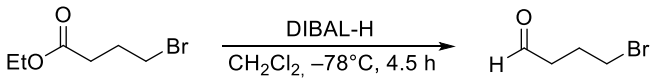

Aldehyde **S30** was synthesized according to a literature-known procedure.[19] DIBAL-H (1 M in hexane, 110 mL, 110 mmol, 1.1 equiv) was added dropwise to a –78 °C cooled solution of ethyl 4-bromobutanoate (19.5 g, 100 mmol, 1.0 equiv) in CH_2Cl_2 (180 mL) over 2 h. The solution was stirred for additional 2.5 h at the same temperature and then quenched with aqueous HCl (10 wt%). The aqueous phase was extracted with CH_2Cl_2 (3 x 100 mL) and the combined organic phases were washed with saturated aqueous $NaHCO_3$-solution and brine. The organic phase was dried over $MgSO_4$, the solvent was removed under reduced pressure and the crude product **S30** was used without further purification.

^{1}HNMR ($CDCl_3$, 400 MHz) δ = 9.82 (t, *J* = 0.8 Hz, 1H), 3.46 (t, *J* = 6.4 Hz, 2H), 2.68 (t, *J* = 7.0 Hz, 2H), 2.18 (p, *J* = 6.6 Hz, 2H) ppm.

Spectroscopic data were in accordance with published data.[19]

2-(3-Bromopropyl)-1,3-dioxolane S31

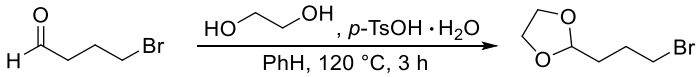

Acetal **S31** was synthesized according to a literature-known procedure.[20] The crude aldehyde **S30** was dissolved in benzene (100 mL), ethylene glycol (22.6 mL, 400 mmol, 4.0 equiv) and *p*-TsOH•H_2O (1.17 g, 6.15 mmol, 6 mol%) were added at room temperature and the reaction mixture was stirred for 3 h at 120 °C using a Dean-Stark-trap to remove water. The reaction mixture was cooled to room temperature, washed with saturated aqueous $NaHCO_3$-solution and brine and the organic phase was dried over $MgSO_4$. The solvent was removed under reduced pressure and the crude product was purified by distillation (4 mbar, 90 °C). Acetal **S31** (16.5 g, 84.6 mmol, 85% over two steps) was obtained as a colorless oil.

^{1}HNMR ($CDCl_3$, 400 MHz) δ = 4.90 (t, *J* = 4.5 Hz, 1H), 4.02 – 3.80 (m, 4H), 3.46 (t, *J* = 6.8 Hz, 2H), 2.07 – 1.93 (m, 2H), 1.88 – 1.78 (m, 2H) ppm.

Spectroscopic data were in accordance with published data.[20]

2-(Hex-5-en-1-yl)-1,3-dioxolane S32

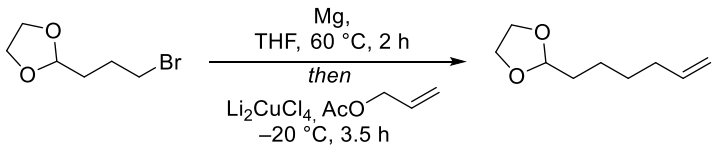

A solution of acetal **S32** (28.4 g, 146 mmol, 1.5 equiv) in anhydrous THF (150 mL) was added to a mixture of manganese cuttings (5.46 g, 225 mmol, 2.3 equiv), one iodine-crystal and THF (50 mL) under argon atmosphere at room temperature. The mixture was stirred for 2 h at 60 °C. The Grignard-reagent was cooled to 0 °C and diluted with anhydrous THF (100 mL). Li_2CuCl_4 (0.1 M in THF, 40 mL, 4.00 mmol, 0.04 equiv) was added to a solution of allyl acetate (10.0 g, 99.9 mmol, 1.0 equiv) in anhydrous THF (500 mL) and the mixture was cooled to –20 °C. The Grignard-reagent was added dropwise over 2 h and stirring was continued for 30 min at the same temperature and additional 1 h at room temperature. The reaction mixture was quenched with saturated aqueous NH_4Cl-solution and extracted with Et_2O (2 x 200 mL). The combined organic phases were dried over $MgSO_4$, the solvent was removed under reduced pressure and the crude product was purified by column chromatography (SiO_2, pentane/Et_2O 1:0 to 20:1) yielding alkene **S32** (13.7 g, 87.7 mmol, 88%) as a colorless oil.

^{1}HNMR ($CDCl_3$, 400 MHz) δ = 5.80 (ddt, *J* = 16.9, 10.1, 6.7 Hz, 1H), 5.04 – 4.96 (m, 1H), 4.96 – 4.91 (m, 1H), 4.84 (t, *J* = 4.8 Hz, 1H), 4.01 – 3.80 (m, 4H), 2.15 – 1.97 (m, 2H), 1.71 – 1.60 (m, 2H), 1.50 – 1.38 (m, 4H) ppm.

Spectroscopic data were in accordance with published data.[21]

Hept-6-enal S33

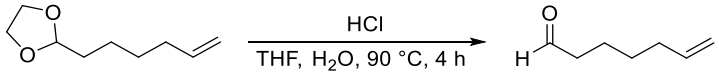

Aqueous HCl (3 M, 66.8 mL, 192 mmol, 6.0 equiv) was added to solution of acetal **S32** (5.00 g, 32.0 mmol, 1.0 equiv) in THF (115 mL) and water (75 mL). The reaction mixture was stirred for 4 h at 90 °C and then cooled to room temperature. The aqueous phase was extracted with pentane (3 x 150 mL), the combined organic phases were washed with saturated aqueous $NaHCO_3$-solution and dried over $MgSO_4$. The solvent was removed under reduced pressure and the crude product was purified by column chromatography (SiO_2, pentane/Et_2O 1:0 to 18:1) yielding aldehyde **S33** (2.28 g, 20.3 mmol, 64%) as a colorless oil.

^{1}HNMR ($CDCl_3$, 400 MHz) δ = 9.77 (t, *J* = 1.8 Hz, 1H), 5.79 (ddt, *J* = 16.9, 10.1, 6.7 Hz, 1H), 5.05 – 4.98 (m, 1H), 4.98 – 4.94 (m, 1H), 2.44 (td, *J* = 7.3, 1.8 Hz, 2H), 2.08 (q, *J* = 7.2 Hz, 2H), 1.72 – 1.59 (m, 2H), 1.52 – 1.39 (m, 2H) ppm.

Spectroscopic data were in accordance with published data.[22]

(*S*)-3,7-Dimethyloct-6-enal S34

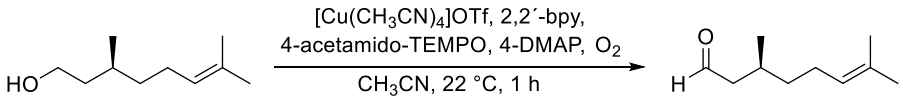

(*S*)-Citronellol (10.0 g, 64.0 mmol, 1.0 equiv) was dissolved in CH_3CN (400 mL). $[Cu(CH_3CN)_4]OTf$ (1.21 g, 3.20 mmol, 5 mol%), 2,2´-bpy (500 mg, 3.20 mmol, 5 mol%), 4-acetamido-TEMPO (683 mg, 3.20 mmol, 5 mol%) and 4-DMAP (782 mg, 6.40 mmol, 10 mol%) were added subsequently at room temperature and stirring was continued for 1 h under oxygen atmosphere. The reaction mixture was quenched with water and the aqueous phase was extracted with EtOAc (3 x 100 mL). The combined organic phases were dried over Na_2SO_4, the solvent was removed under reduced pressure and the crude product was purified by column chromatography (SiO_2, pentane/EtOAc 60:1) yielding aldehyde **S34** (8.33 g, 54.0 mmol, 84%) as a colorless oil.

^{1}HNMR ($CDCl_3$, 400 MHz) δ = 9.75 (t, *J* = 2.4 Hz, 1H), 5.11 – 5.05 (m, 1H), 2.40 (ddd, *J* = 16.0, 5.6, 2.0 Hz, 1H), 2.23 (ddd, *J* = 16.1, 8.0, 2.7 Hz, 1H), 2.14 – 1.90 (m, 3H), 1.68 (s, 3H), 1.60 (s, 3H), 1.41 – 1.20 (m, 2H), 0.97 (d, *J* = 6.7 Hz, 3H) ppm.

Spectroscopic data were in accordance with published data.[23]

Hex-4-yn-1-ol S35

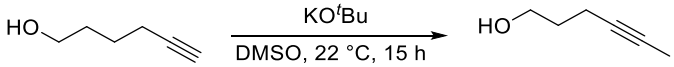

Alcohol **S35** was synthesized according to literature-known procedure.[24] KO^{t}Bu (5.03 g, 44.8 mmol, 2.0 equiv) was added to a solution of hex-5-yn-1-ol (2.20 g, 22.4 mmol, 1.0 equiv) in anhydrous DMSO (65 mL) and the reaction mixture was stirred for 12 h at room temperature. After addition of aqueous HCl (2 M, 20 mL), the aqueous phase was extracted with Et_2O (5 x 30 mL), dried over Na_2SO_4 and the solvent was removed under reduced pressure. The crude product was purified by column chromatography (SiO_2, pentane/Et_2O 3:1) yielding alcohol **S35** (1.84 g, 18.7 mmol, 84%) as a colorless oil.

^{1}HNMR ($CDCl_3$, 400 MHz) δ = 3.74 (td, *J* = 6.1, 0.9 Hz, 2H), 2.28 – 2.20 (m, 2H), 1.76 (td, *J* = 2.6, 0.9 Hz, 3H), 1.75 – 1.68 (m, 2H), 1.67 (s, 1H) ppm.

Spectroscopic data were in accordance with published data.[24]

Hex-4-ynal S36

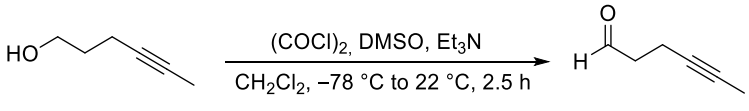

Aldehyde **S36** was synthesized according to literature-known procedure.[24] Anhydrous DMSO (2.90 mL, 41.1 mmol, 2.2 equiv) was dissolved in anhydrous DCM (330 mL) under argon atmosphere and cooled down to –78 °C. $(COCl)_2$ (1.80 mL, 20.6 mmol, 1.1 equiv) was added dropwise and stirring was continued for 20 min. A solution of alcohol **S35** (1.84 g, 18.7 mmol, 1.0 equiv) in anhydrous DCM (18 ml) was added and stirring was continued for 30 min. After the addition of anhydrous Et_3N (12.7 mL, 91.6 mmol, 4.9 equiv) and stirring for 2 h at room temperature, the reaction was quenched with water. The aqueous phase was extracted with CH_2Cl_2 (3 x 80 mL) and the combined organic phases were dried over Na_2SO_4. The solvent was removed under reduced pressure and after column chromatography (SiO_2, pentane/Et_2O 20:1) aldehyde **S36** (889 mg, 9.25 mmol, 50%) was obtained as colorless oil.

^{1}HNMR ($CDCl_3$, 400 MHz) δ = 9.78 (td, *J* = 1.4, 0.5 Hz, 1H), 2.66 – 2.57 (m, 2H), 2.48 – 2.41 (m, 2H), 1.75 (td, *J* = 2.6, 0.5 Hz, 3H) ppm.

Spectroscopic data were in accordance with published data.[24]

2.5. SUBSTRATE SCOPE

The following procedure was applied for all α-chlorination experiments. The subsequent reduction to β-chloro-alcohols was applied due to more comfortable purification, stable stereoinformation and higher boiling points compared to α-chloro-aldehydes. The catalyst was used as a free base, due to the fact that it was not possible to synthesize the TFA-salt.[25]

α-Chlorination with Subsequent Reduction

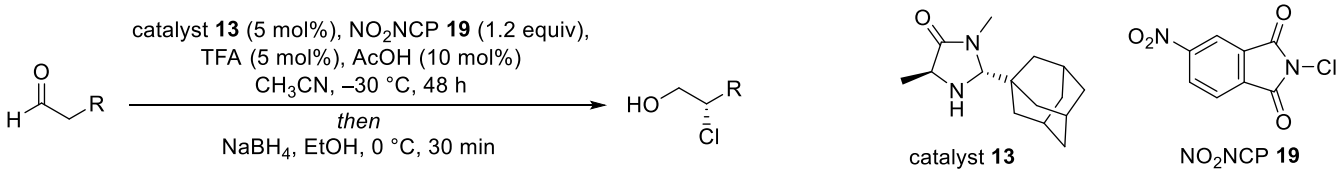

Catalyst **13** (4.67 mg, 18.8 µmol, 5 mol%), TFA (1.40 µL, 18.8 µmol, 5 mol%), AcOH (2.20 µL, 37.6 µmol, 10 mol%) and Cl^+-source **19** (103 mg, 456 µmol, 1.2 equiv) were added subsequently to a –30 °C cooled solution of corresponding aldehyde (376 µmol, 1.0 equiv) in CH_3CN (1.5 mL) and the reaction mixture was stirred for 48 h at the same temperature. $NaBH_4$ (35.6 mg, 940 µmol, 2.5 equiv) and EtOH (0.5 mL) were added and stirring was continued for 30 min at 0 °C. The reaction was quenched with aqueous saturated NH_4Cl-solution and the aqueous phase was extracted with CH_2Cl_2 (3 x 5 mL). The combined organic phases were dried over Na_2SO_4, the solvent was removed under reduced pressure and the crude product was purified by column chromatography.

Entry	Product	Yield [%][a]	*ee* [%]
1	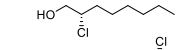	78	97
2[b]	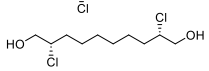	63	>99
3	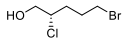	77	98
4	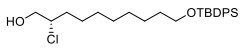	74	96
5	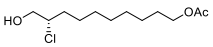	87	96
6	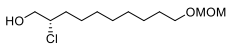	87	96
7	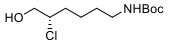	57	96
8	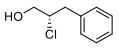	75	98
9	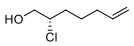	79	97
10[c]	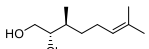	73	97
11	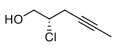	74	98

[a] isolated yields. [b] 10 mol% of catalyst and TFA, 20 mol% of AcOH, 2.4 equiv of NO_2NCP; dr = 95:5. [c] 97% *ee* for the starting material (*S*)-citronellal; Upscaling 5.00 g, 32.4 mmol (*S*)-citronellal, Rondomatic 400®, cryostat; dr = 97:3.

α-Chlorination of (*S*)-Citronellal with Subsequent Reduction

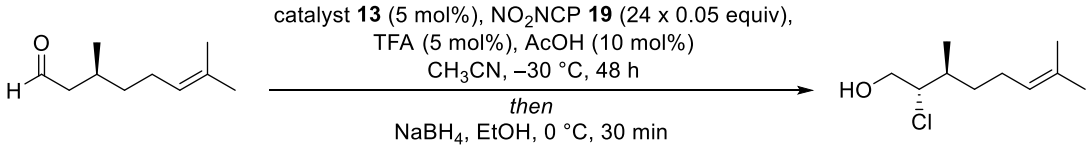

Catalyst **13** (402 mg, 162 µmol, 5 mol%), TFA (125 µL, 162 µmol, 5 mol%) and AcOH (186 µL, 324 µmol, 10 mol%) were added subsequently to a –30 °C (cryostat) cooled solution of (*S*)-citronellal (5.00 g, 32.4 mmol, 1.0 equiv, 97% *ee*) in CH_3CN (130 mL). Cl^+-source **19** (8.81 g, 38.9 mmol, 1.2 equiv) was distributed equally (24 x 367 mg, 24 x 5 mol%) to the white reservoirs of the fish-feeding device Rondomatic 400®. The timer was adjusted so that every 2 hours one reservoir adds the Cl^+-source to the reaction mixture. After 48 h stirring at –30 °C, $NaBH_4$ (3.07 g, 81.0 mmol, 2.5 equiv) and EtOH (45 mL) were added and stirring was continued for 30 min at 0 °C. The reaction was quenched with aqueous saturated NH_4Cl-solution and the aqueous phase was extracted with CH_2Cl_2 (3 x 150 mL). The combined organic phases were dried over Na_2SO_4 and the solvent was removed under reduced pressure. After purification by column chromatography (SiO_2, pentane/Et_2O 10:1), alcohol **S46** (4.51 g, 23.7 mmol, 73%, 97% *ee*, d.r. 97:3) was obtained as a colorless oil.

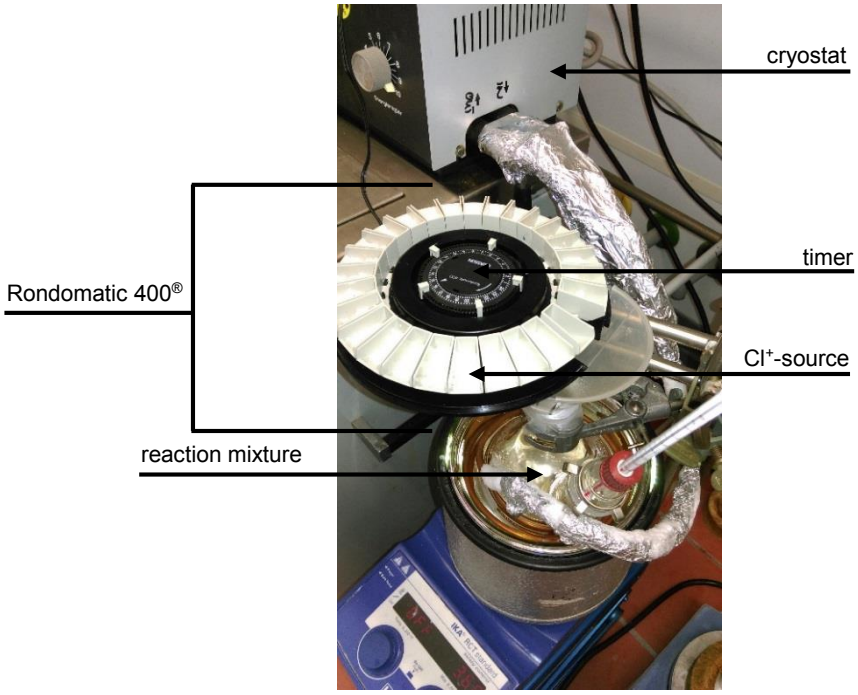

Substrate Scope

(*S*)-2-Chlorooctan-1-ol S37

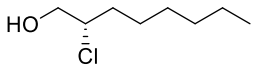

Spectroscopic data were in accordance with published data.[26]

(2*S*,9*S*)-2,9-Dichlorodecane-1,10-diol S38

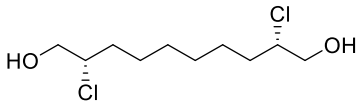

R_f = 0.3 (pentane/EtOAc 2:1)

$[\alpha]_D^{25}$ = –23.6° (*c* = 1.00, $CHCl_3$)

^{1}HNMR ($CDCl_3$, 400 MHz) δ = 4.02 (dddd, *J* = 8.5, 6.8, 5.0, 3.8 Hz, 2H), 3.79 (ddd, *J* = 12.0, 3.8, 0.8 Hz, 2H), 3.67 (ddd, *J* = 12.0, 7.1, 0.8 Hz, 2H), 1.93 (s, 2H), 1.84 – 1.63 (m, 4H), 1.61 – 1.48 (m, 2H), 1.47 – 1.38 (m, 2H), 1.38 – 1.27 (m, 4H) ppm.

^{13}CNMR ($CDCl_3$, 126 MHz) δ = 67.2, 65.4, 34.3, 29.0, 26.3 ppm.

IR (ATR): $\tilde{\nu}$ = 3353, 1459, 1047, 730, 679 cm^{-1}.

HRMS (ESI, pos. mode): *m*/*z* calculated for $C_{10}H_{20}Cl_2NaO_2$ $[M+Na]^+$: 265.0692, found 265.0703.

(*S*)-5-Bromo-2-chloropentan-1-ol S39

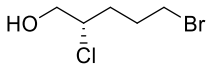

R_f = 0.3 (pentane/Et_2O 3:1)

$[\alpha]_D^{25}$ = –24.9° (*c* = 1.00, $CHCl_3$)

^{1}HNMR ($CDCl_3$, 500 MHz) δ = 4.07 – 3.97 (m, 1H), 3.80 (dd, *J* = 12.0, 4.0 Hz, 1H), 3.70 (dd, *J* = 12.0, 6.7 Hz, 1H), 3.44 (t, *J* = 6.4 Hz, 2H), 2.19 – 2.10 (m, 1H), 2.05 – 1.95 (m, 3H), 1.89 – 1.79 (m, 1H) ppm.

^{13}CNMR ($CDCl_3$, 126 MHz) δ = 67.1, 64.0, 32.9, 32.8, 29.5 ppm.

IR (ATR): $\tilde{\nu}$ = 3366, 1453, 766, 733, 680, 661 cm^{-1}.

HRMS (ESI, pos. mode): *m*/*z* calculated for $C_5H_{10}BrClNaO$ $[M+Na]^+$: 222.9492, found 222.9496.

(*S*)-10-((*tert*-Butyldiphenylsilyl)oxy)-2-chlorodecan-1-ol S40

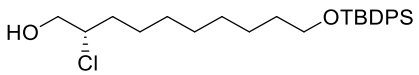

R_f = 0.3 (pentane/EtOAc 10:1)

$[\alpha]_D^{25}$ = –9.7° (*c* = 1.00, $CHCl_3$)

^{1}HNMR ($CDCl_3$, 500 MHz) δ = 7.71 – 7.65 (m, 4H), 7.45 – 7.36 (m, 6H), 4.03 (dddd, *J* = 8.6, 7.0, 5.0, 3.7 Hz, 1H), 3.79 (dd, *J* = 12.0, 3.7 Hz, 1H), 3.69 – 3.64 (m, 3H), 1.99 (s, 1H), 1.81 – 1.66 (m, 2H), 1.61 – 1.48 (m, 3H), 1.46 – 1.28 (m, 9H), 1.06 (s, 9H) ppm.

^{13}CNMR ($CDCl_3$, 126 MHz) δ = 135.7, 134.3, 129.6, 127.7, 67.2, 65.6, 64.1, 34.4, 32.7, 29.5, 29.4, 29.2, 27.0, 26.5, 25.9, 19.4 ppm.

IR (ATR): $\tilde{\nu}$ = 3399, 3015, 2929, 2856, 1463, 1110, 823, 754, 701 cm^{-1}.

HRMS (ESI, pos. mode): *m*/*z* calculated for $C_{26}H_{39}ClNaO_2Si$ $[M+Na]^+$: 469.2292, found 469.2290.

(*S*)-9-Chloro-10-hydroxydecylacetate S41

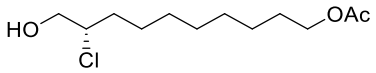

R_f = 0.3 (pentane/EtOAc 5:1)

$[\alpha]_D^{25}$ = –18.7° (*c* = 1.00, $CHCl_3$)

^{1}HNMR ($CDCl_3$, 500 MHz) δ = 4.05 (t, *J* = 6.8 Hz, 2H), 4.03 – 3.99 (m, 1H), 3.78 (dd, *J* = 12.0, 3.8 Hz, 1H), 3.66 (dd, *J* = 12.0, 7.1 Hz, 1H), 2.04 (s, 3H), 1.80 – 1.66 (m, 2H), 1.66 – 1.56 (m, 2H), 1.57 – 1.48 (m, 1H), 1.46 – 1.38 (m, 1H), 1.37 – 1.26 (m, 8H) ppm.

^{13}CNMR ($CDCl_3$, 126 MHz) δ = 171.4, 67.2, 65.5, 64.7, 34.4, 29.4, 29.2, 29.1, 28.7, 26.4, 26.0, 21.2 ppm.

IR (ATR): $\tilde{\nu}$ = 3437, 2927, 2856, 1737, 1719, 1038, 725, 676 cm^{-1}.

HRMS (ESI, pos. mode): *m*/*z* calculated for $C_{12}H_{23}ClNaO_3$ $[M+Na]^+$: 273.1192, found 273.1205.

(*S*)-2-Chloro-10-(methoxymethoxy)decan-1-ol S42

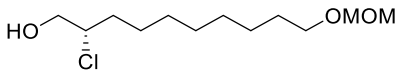

R_f = 0.3 (pentane/EtOAc 5:1)

$[\alpha]_D^{25}$ = –18.8° (*c* = 1.00, $CHCl_3$)

^{1}HNMR ($CDCl_3$, 500 MHz) δ = 4.62 (s, 2H), 4.02 (dddd, *J* = 8.7, 7.1, 5.0, 3.7 Hz, 1H), 3.78 (dd, *J* = 12.0, 3.6 Hz, 1H), 3.66 (dd, *J* = 12.0, 7.1 Hz, 1H), 3.51 (t, *J* = 6.6 Hz, 2H), 3.36 (s, 3H), 2.03 (s, 1H), 1.82 – 1.65 (m, 2H), 1.63 – 1.54 (m, 2H), 1.55 – 1.47 (m, 1H), 1.46 – 1.23 (m, 9H) ppm.

^{13}CNMR ($CDCl_3$, 126 MHz) δ = 96.6, 68.0, 67.2, 65.6, 55.3, 34.4, 29.9, 29.5, 29.4, 29.2, 26.5, 26.3 ppm.

IR (ATR): $\tilde{\nu}$ = 3424, 1465, 1146, 1110, 1041, 725, 674 cm^{-1}.

HRMS (ESI, pos. mode): *m*/*z* calculated for $C_{12}H_{25}ClNaO_3$ $[M+Na]^+$: 275.1392, found 275.1398.

***tert*-Butyl-(*S*)-(5-chloro-6-hydroxyhexyl)carbamate S43**

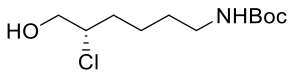

R_f = 0.3 (pentane/Et_2O 1:2)

$[\alpha]_D^{25}$ = –15.3° (*c* = 1.00, $CHCl_3$)

^{1}HNMR ($CDCl_3$, 400 MHz) δ = 4.56 (s, 1H), 4.09 – 3.96 (m, 1H), 3.77 (dd, *J* = 12.0, 4.2 Hz, 1H), 3.67 (dd, *J* = 12.0, 6.7 Hz, 1H), 3.14 (q, *J* = 6.1 Hz, 2H), 1.87 – 1.69 (m, 2H), 1.62 – 1.47 (m, 3H), 1.44 (s, 9H) ppm.

^{13}CNMR ($CDCl_3$, 126 MHz) δ = 156.3, 79.4, 66.7, 64.6, 40.2, 33.7, 29.7, 28.5, 23.3 ppm.

IR (ATR): $\tilde{\nu}$ = 3341, 2934, 1769, 1684, 1455, 731, 682 cm^{-1}.

HRMS (ESI, pos. mode): *m*/*z* calculated for $C_{11}H_{23}ClNO_3$ $[M+H]^+$: 252.1373, found 2521364; *m*/*z* calculated for $C_{11}H_{22}ClNNaO_3$ $[M+Na]^+$: 274.1192, found 274.1194.

(*S*)-2-Chloro-3-phenylpropan-1-ol S44

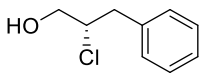

Spectroscopic data were in accordance with published data.[26]

(*S*)-2-Chlorohept-6-en-1-ol S45

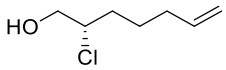

R_f = 0.5 (pentane/EtOAc 5:1)

$[\alpha]_D^{25}$ = –25.4° (*c* = 1.00, $CHCl_3$)

^{1}HNMR ($CDCl_3$, 400 MHz) δ = 5.78 (ddt, *J* = 17.0, 10.1, 6.6 Hz, 1H), 5.02 (dd, *J* = 17.3, 1.7 Hz, 1H), 4.97 (dd, *J* = 10.2, 1.1 Hz, 1H), 4.07 – 3.96 (m, 1H), 3.78 (dd, *J* = 12.0, 3.8 Hz, 1H), 3.66 (dd, *J* = 12.0, 7.0 Hz, 1H), 2.17 (s, 1H), 2.08 (dddd, *J* = 12.3, 7.6, 6.2, 1.2 Hz, 2H), 1.88 – 1.58 (m, 3H), 1.58 – 1.43 (m, 1H) ppm.

^{13}CNMR ($CDCl_3$, 126 MHz) δ = 138.1, 115.3, 67.1, 65.2, 33.7, 33.2, 25.6 ppm.

IR (ATR): $\tilde{\nu}$ = 3356, 3078, 1641, 1458, 993, 733, 678 cm^{-1}.

HRMS (ESI, pos. mode): *m*/*z* calculated for $C_7H_{13}ClNaO_3$ $[M+Na]^+$: 171.0592, found 171.0596.

(2*S*,3*S*)-2-Chloro-3,7-dimethyloct-6-en-1-ol S46

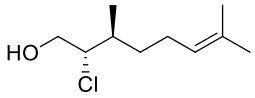

Spectroscopic data were in accordance with published data.[27]

(*S*)-2-Chlorohex-4-yn-1-ol S47

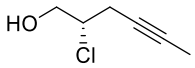

R_f = 0.4 (pentane/Et_2O 2:1)

$[\alpha]_D^{25}$ = +8.2° (*c* = 1.00, $CHCl_3$)

^{1}HNMR ($CDCl_3$, 500 MHz) δ = 4.12 – 4.01 (m, 1H), 3.90 (dd, *J* = 12.1, 4.1 Hz, 1H), 3.80 (dd, *J* = 12.0, 6.1 Hz, 1H), 2.66 (q, *J* = 2.2 Hz, 1H), 2.65 (q, *J* = 2.5, 2.1 Hz, 1H), 2.12 (s, 1H), 1.78 (t, *J* = 2.6 Hz, 3H) ppm.

^{13}CNMR ($CDCl_3$, 126 MHz) δ = 78.9, 74.0, 65.7, 61.3, 24.9, 3.5 ppm.

IR (ATR): $\tilde{\nu}$ = 3365, 2952, 2921, 2851, 1457, 814, 673 cm^{-1}.

HRMS (ESI, pos. mode): *m*/*z* calculated for $C_6H_{10}ClO$ $[M+H]^+$: 133.0373, found 133.0370.

3. Mechanistic Studies

3.1. GCMS Kinetic Experiments

Catalysts

Catalyst **2**,**12** or **13** (570 µmol, 10 mol%), TFA (42.0 µL, 570 µmol, 10 mol%) and *N*-chlorosuccinimide (1.00 g, 7.34 mmol, 1.2 equiv) were added subsequently to a –30 °C cooled solution of hydrocinnamic aldehyde (765 mg, 5.70 mmol, 1.0 equiv) in CH_3CN (23 mL) and the reaction mixture was stirred at the same temperature. Samples (1 mL) were taken from the reaction mixture after defined points of time and purified by a short silica-pad (pentane/EtOAc 5:1). GCMS-measurements indicated the conversion.

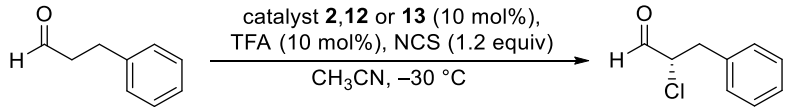

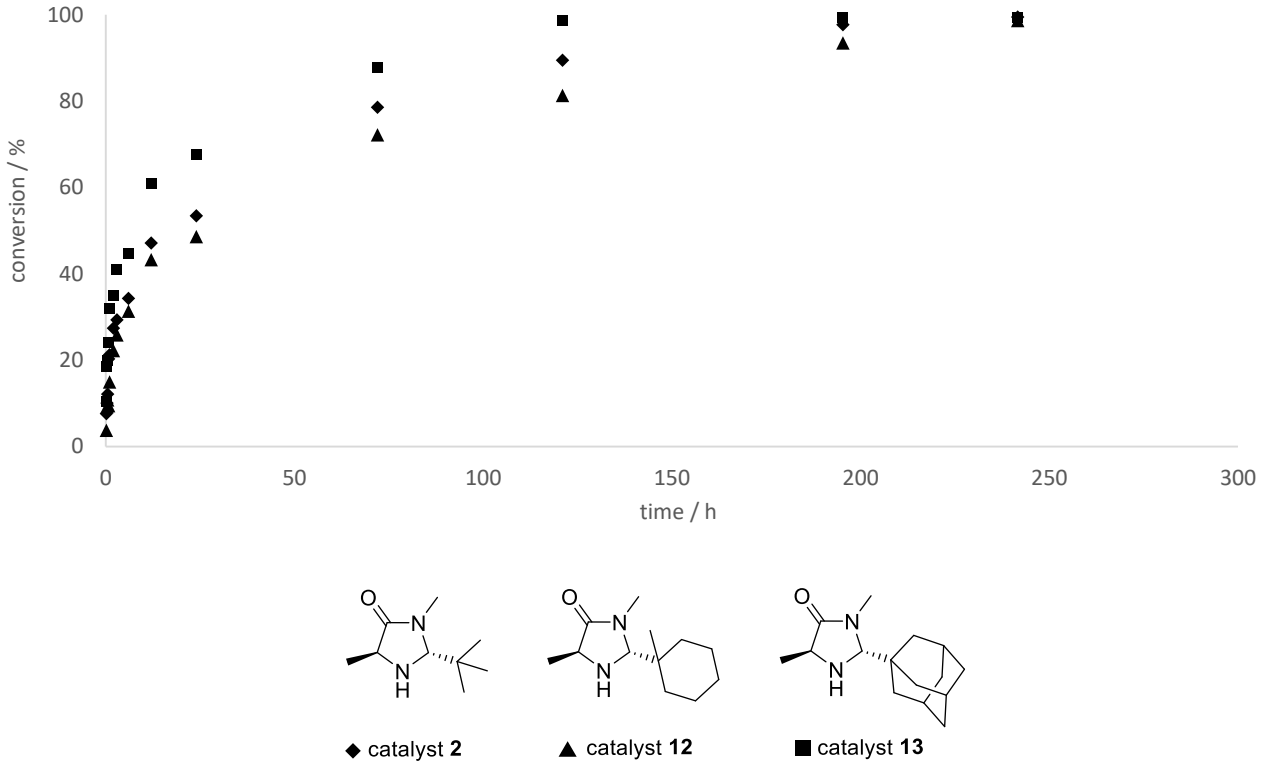

SUPPORTING INFORMATION

Chlorinating reagents I

Catalyst **2** (142 mg, 570 µmol, 10 mol%), TFA (42.0 µL, 570 µmol, 10 mol%) and chlorinating reagents NCS **3**, Me_4NCS **20**, *N*-chlorophthalimide or NO_2NCP **19** (7.34 mmol, 1.2 equiv) were added subsequently to a –30 °C cooled solution of hydrocinnamic aldehyde (765 mg, 5.70 mmol, 1.0 equiv) in CH_3CN (23 mL) and the reaction mixture was stirred at the same temperature. Samples (1 mL) were taken from the reaction mixture after defined points of time and purified by a short silica-pad (pentane/EtOAc 5:1). GCMS-measurements indicated the conversion.

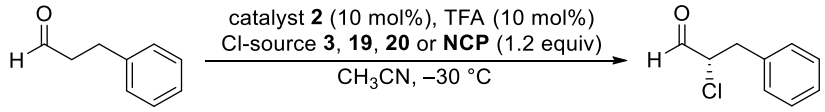

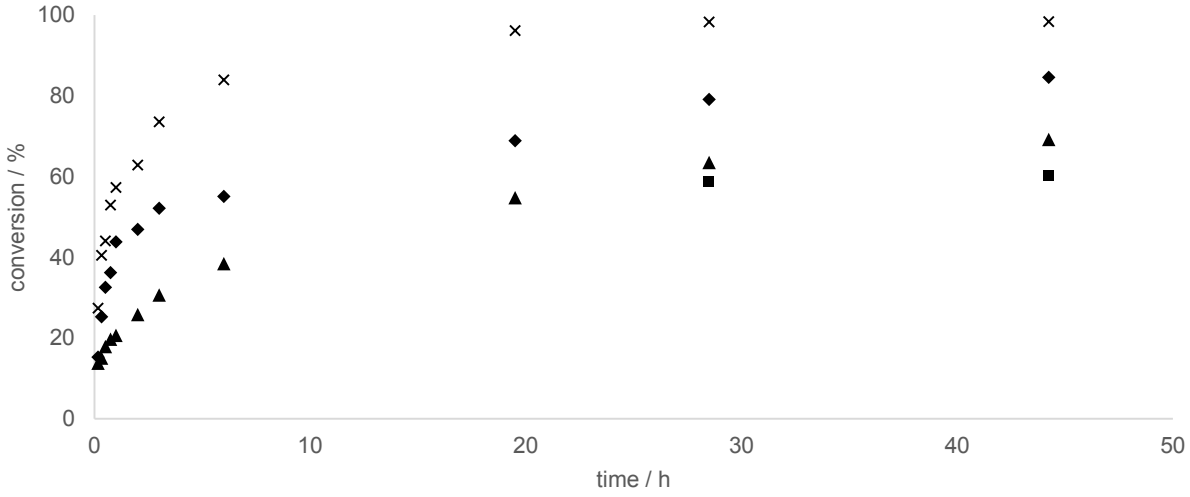

* for Me_4NCS: Overlap of α-chloroaldehyde-signal and Me_4NCS-signal at the first measurement points

SUPPORTING INFORMATION

Additives

Catalyst **2** (71.0 mg, 285 µmol, 5 mol%), **A**: AcOH (51.0 µL, 855 µmol, 15 mol%) or **B**: TFA (63.0 µL, 855 µmol, 15 mol%) or **C**: TFA (21.0 µL, 285 µmol, 5 mol%) and AcOH (34.0 µL, 570 µmol, 10 mol%) and chlorinating reagent **19** (1.66 g, 7.34 mmol, 1.2 equiv) were added subsequently to a –30 °C cooled solution of hydrocinnamic aldehyde (765 mg, 5.70 mmol, 1.0 equiv) in CH_3CN (23 mL) and the reaction mixture was stirred at the same temperature. Samples (1 mL) were taken from the reaction mixture after defined points of time and purified by a silica-pad (pentane/EtOAc 5:1). GCMS-measurements indicated the conversion.

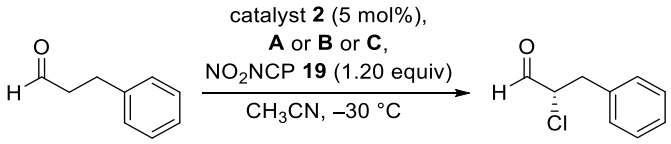

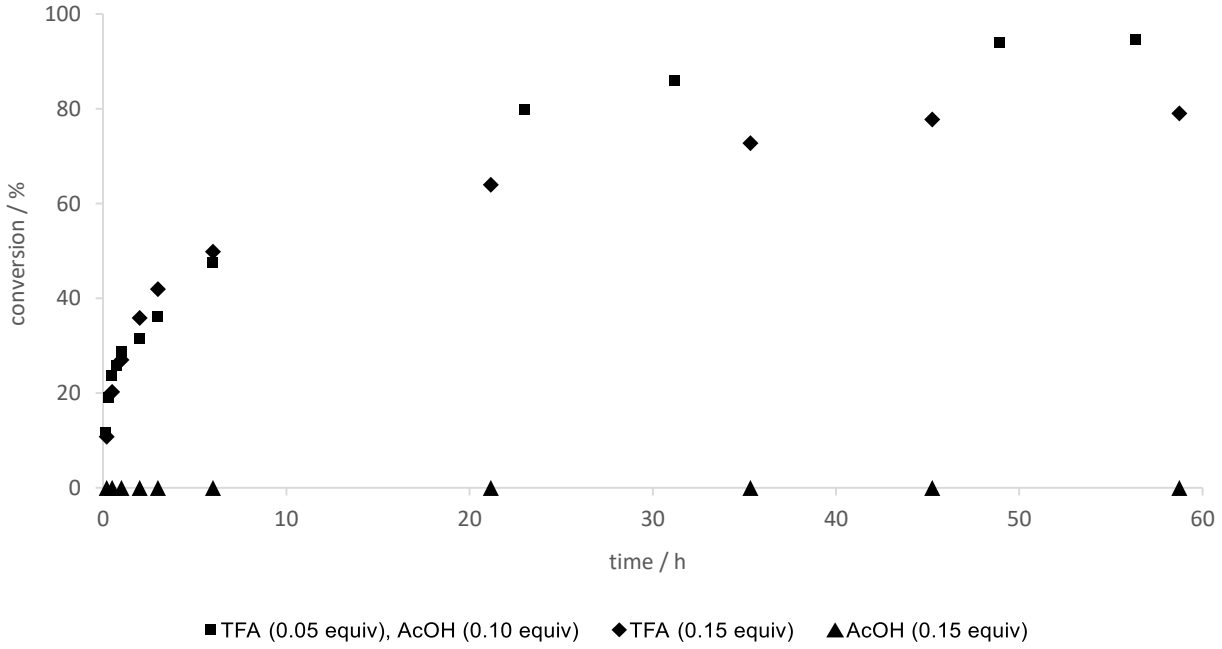

SUPPORTING INFORMATION

Chlorinating reagents II

Catalyst **13** (71.0 mg, 285 µmol, 5 mol%), TFA (21.0 µL, 285 µmol, 5 mol%) and chlorinating reagent **17**, **18** or **19** (7.34 mmol, 1.2 equiv) were added subsequently to a –30 °C cooled solution of hydrocinnamic aldehyde (765 mg, 5.70 mmol, 1.0 equiv) in CH_3CN (23 mL) and the reaction mixture was stirred at the same temperature. Samples (1 mL) were taken from the reaction mixture after defined points of time and purified by a short silica-pad (pentane/EtOAc 5:1). GCMS-measurements indicated the conversion.

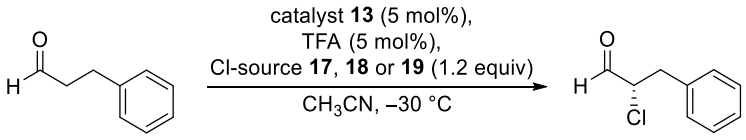

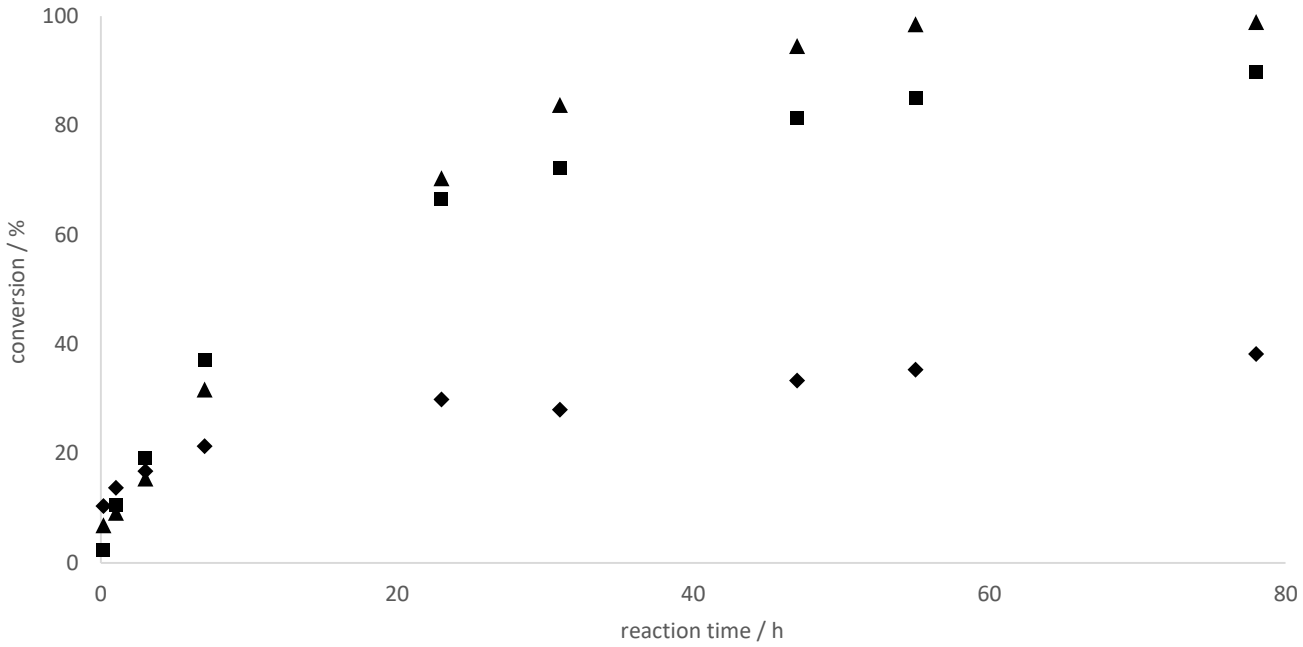

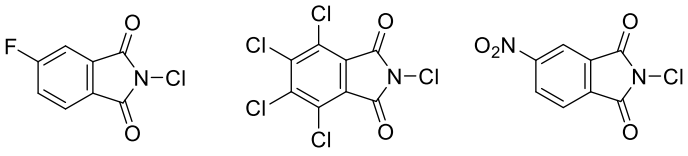

◆FNCP **17** ▲Cl_4NCP **18** ■NO_2NCP **19**

3.2. ^{1}HNMR-Kinetic Experiments

Parasitic Intermediates

Catalyst **2•TFA** (5.70 mg, 20.0 µmol, 20 mol%) was added to a solution of hydrocinnamic aldehyde (13.4 mg, 100 µmol, 1.0 equiv) in MeCN-d_3 (1 mL) and the solution was stirred for 5 min. Chlorinating reagent **3**, **19** or **20** (120 µmol, 1.2 equiv) was added subsequently and ^{1}HNMR-spectra were recorded every five minutes. Integration of proton-signals for starting material, product, free catalyst and parasitic intermediate was calculated with MeCN-d_3-signal as reference (I = 1).

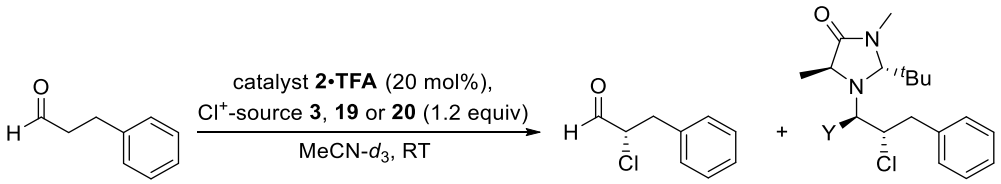

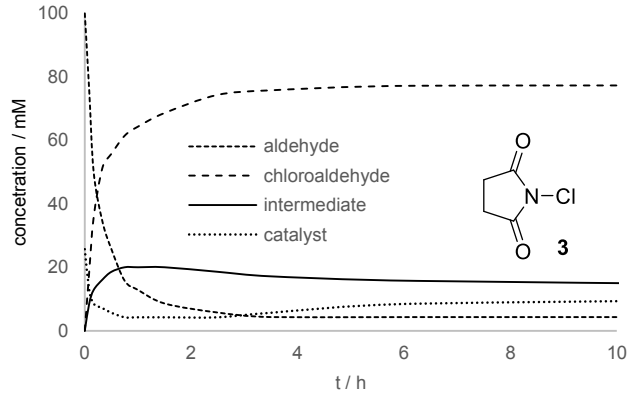

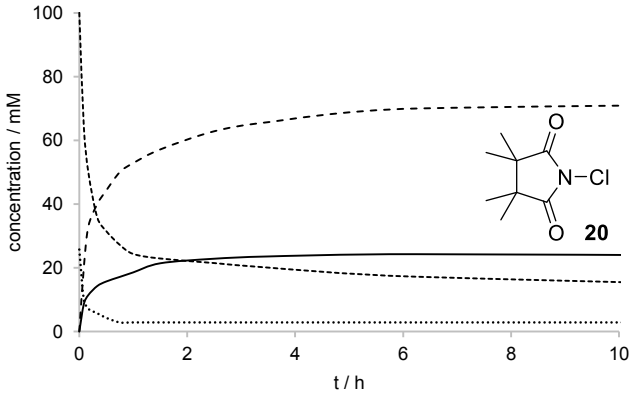

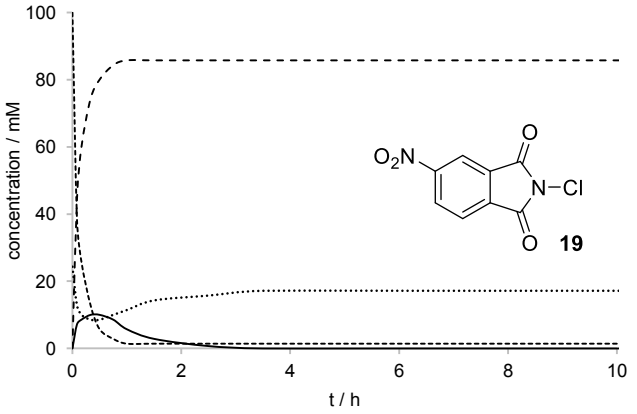

SUPPORTING INFORMATION

Decomposition / Racemization

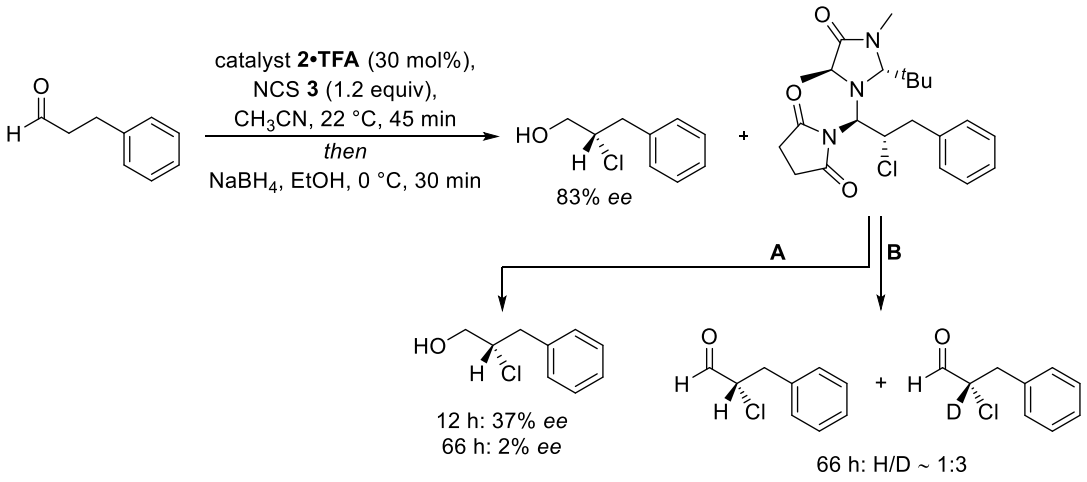

Catalyst **2•TFA** (4.24 g, 14.9 mmol, 30 mol%) and NCS (11.9 g, 89.4 mmol, 1.2 equiv) were added subsequently to a solution of hydrocinnamic aldehyde (10.0 g, 74.5 mmol, 1.0 equiv) in CH_3CN (250 mL) and the reaction mixture was stirred for 45 min at room temperature. After cooling to 0 °C, $NaBH_4$ (7.05 g, 186 mmol, 2.5 equiv) and EtOH (80 mL) were added and stirring was continued for 30 min at the same temperature. The reaction was quenched with saturated aqueous NH_4Cl-solution and the aqueous phase was extracted with EtOAc (3 x 100 mL). The combined organic phases were dried over Na_2SO_4, the solvent was removed under reduced pressure and the crude product was purified by column chromatography (SiO_2, pentane/EtOAc 5:1 to 1:10) yielding parasitic intermediate **5** as a colorless solid (2.84 g, 6.76 mmol, 9%) and β-chloroalcohol **S44** as a colorless oil (83% *ee*).

A: Parasitic intermediate **5** (2.41 g, 5.73 mmol, 1.0 equiv) was dissolved in CH_3CN (70 mL). Water (0.21 mL, 11.5 mmol, 2.0 equiv) and TFA (0.88 mL, 11.5 mmol, 2.0 equiv) were added and the reaction mixture was stirred for 12 h (or 66 h) at room temperature. After cooling to 0 °C, $NaBH_4$ (1.08 g, 28.7 mmol, 5.0 equiv) and EtOH (15 mL) were added and stirring was continued for 30 min at the same temperature. The reaction was quenched with saturated aqueous NH_4Cl-solution and the aqueous phase was extracted with EtOAc (3 x 50 mL). The combined organic phases were dried over Na_2SO_4, the solvent was removed under reduced pressure and the crude product was purified by column chromatography (SiO_2, pentane/EtOAc 5:1) yielding β-chloroalcohol **S44** as a colorless oil (12 h: 37% *ee*; 66 h: 2% *ee*).

B: Parasitic intermediate **5** (210 mg, 500 µmol, 1.0 equiv) was dissolved in CD_3CN (6 mL). D_2O (18.1 µL, 1.00 mmol, 2.0 equiv) and $TFAd_1$ (77.0 µL, 1.00 mmol, 2.0 equiv) were added and the reaction mixture was stirred at room temperature. ^{1}HNMR-spectra were recorded after defined points of time to follow the decomposition and deuteration process. ^{13}C-NMR was recorded after 66 h reaction time and follow up reduction with $NaBH_4$ in EtOH and purification by column chromatography (SiO_2, pentane/EtOAc 5:1).

SUPPORTING INFORMATION

B:

H-NMR:

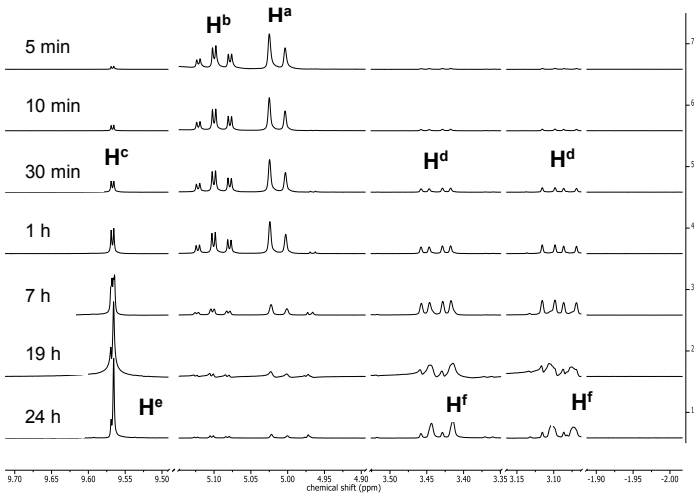

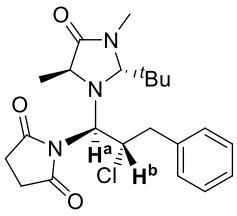

Ha: d
Hb: dt

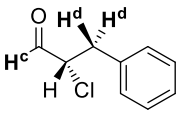

Hc: d
Hd: dd

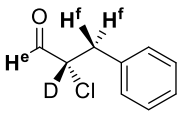

He: s
Hf: d

^{13}C-NMR:

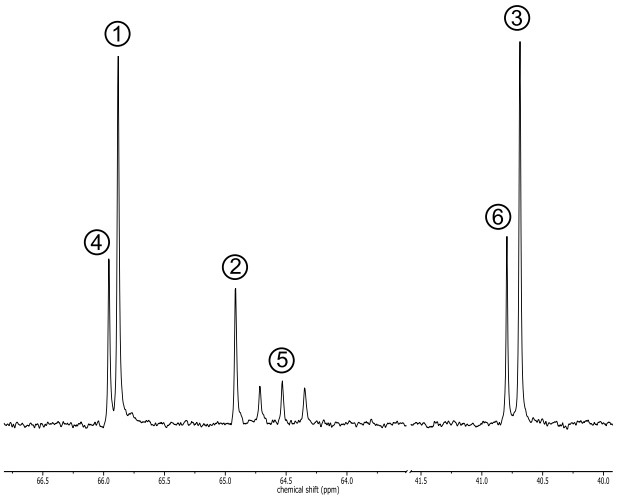

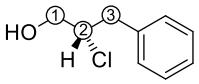

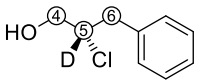

4. ^{1}HNMR AND ^{13}CNMR SPECTRA

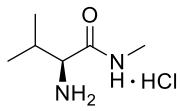

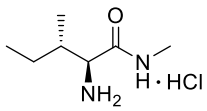

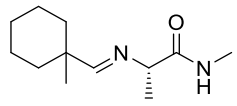
O
N
N
H

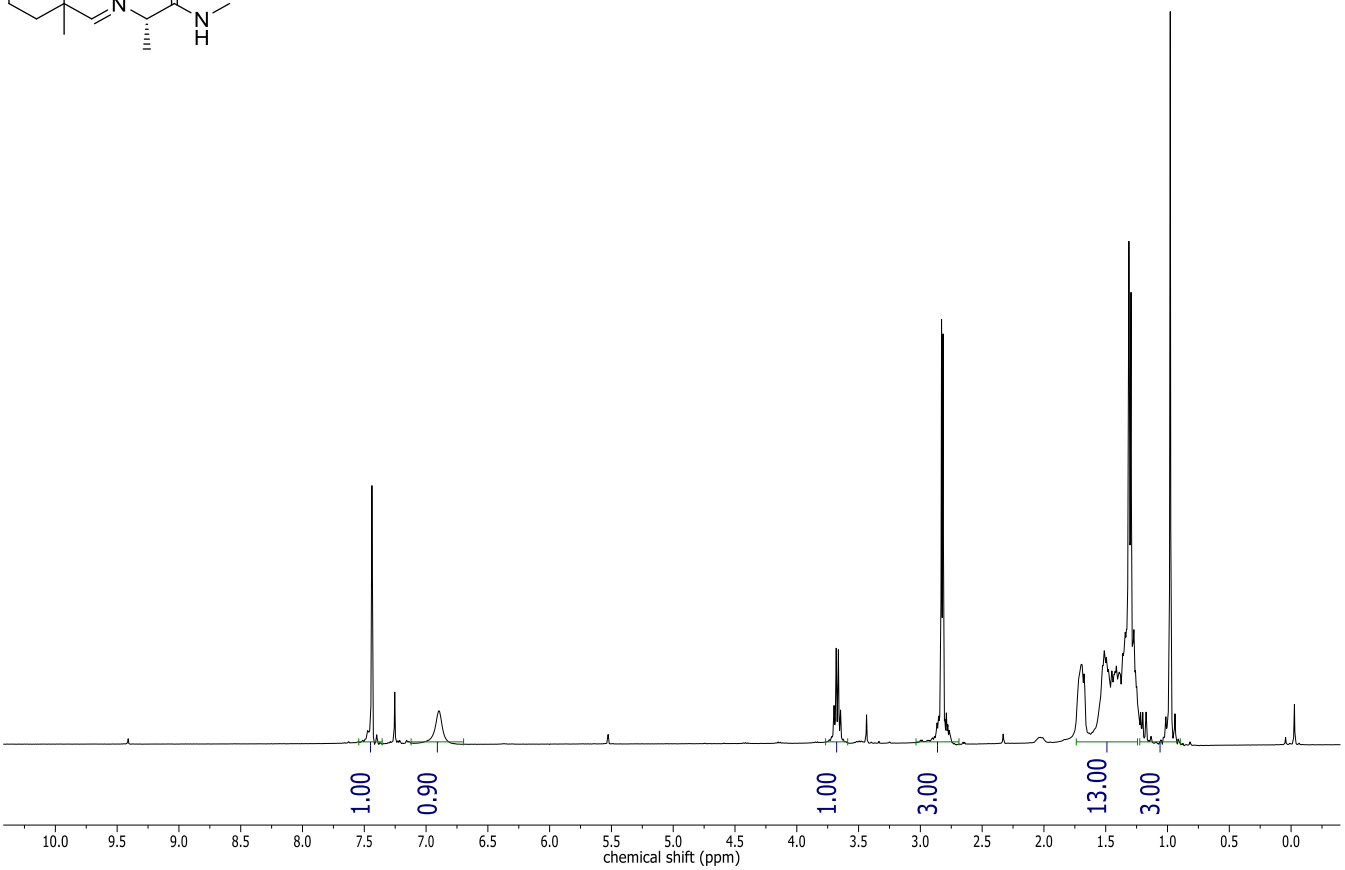
1.00
0.90
1.00
3.00
13.00
3.00
10.0 9.5 9.0 8.5 8.0 7.5 7.0 6.5 6.0 5.5 5.0 4.5 4.0 3.5 3.0 2.5 2.0 1.5 1.0 0.5 0.0
chemical shift (ppm)

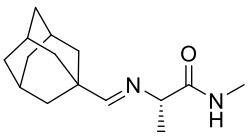
O
N
N
H

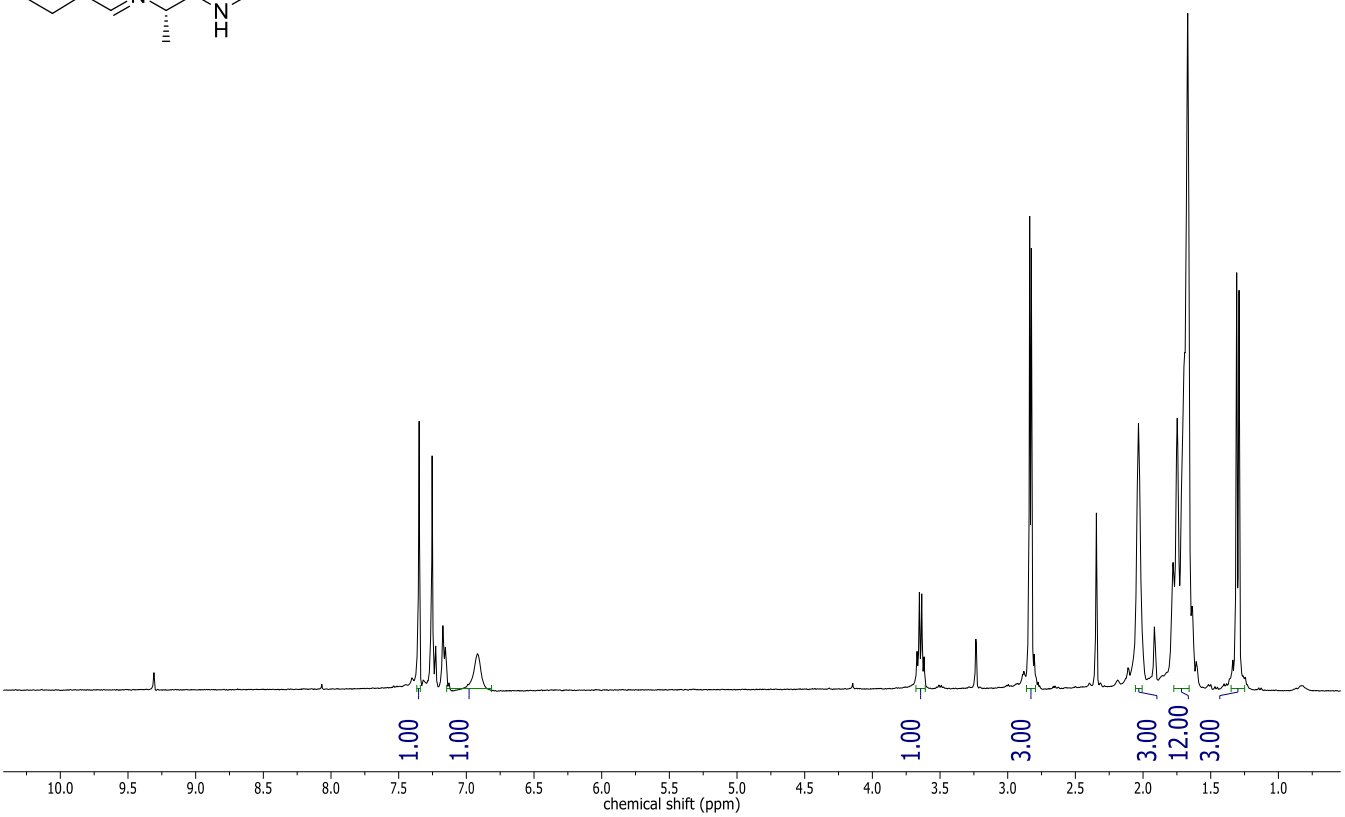
1.00
1.00
1.00
3.00
3.00
12.00
3.00
10.0 9.5 9.0 8.5 8.0 7.5 7.0 6.5 6.0 5.5 5.0 4.5 4.0 3.5 3.0 2.5 2.0 1.5 1.0
chemical shift (ppm)

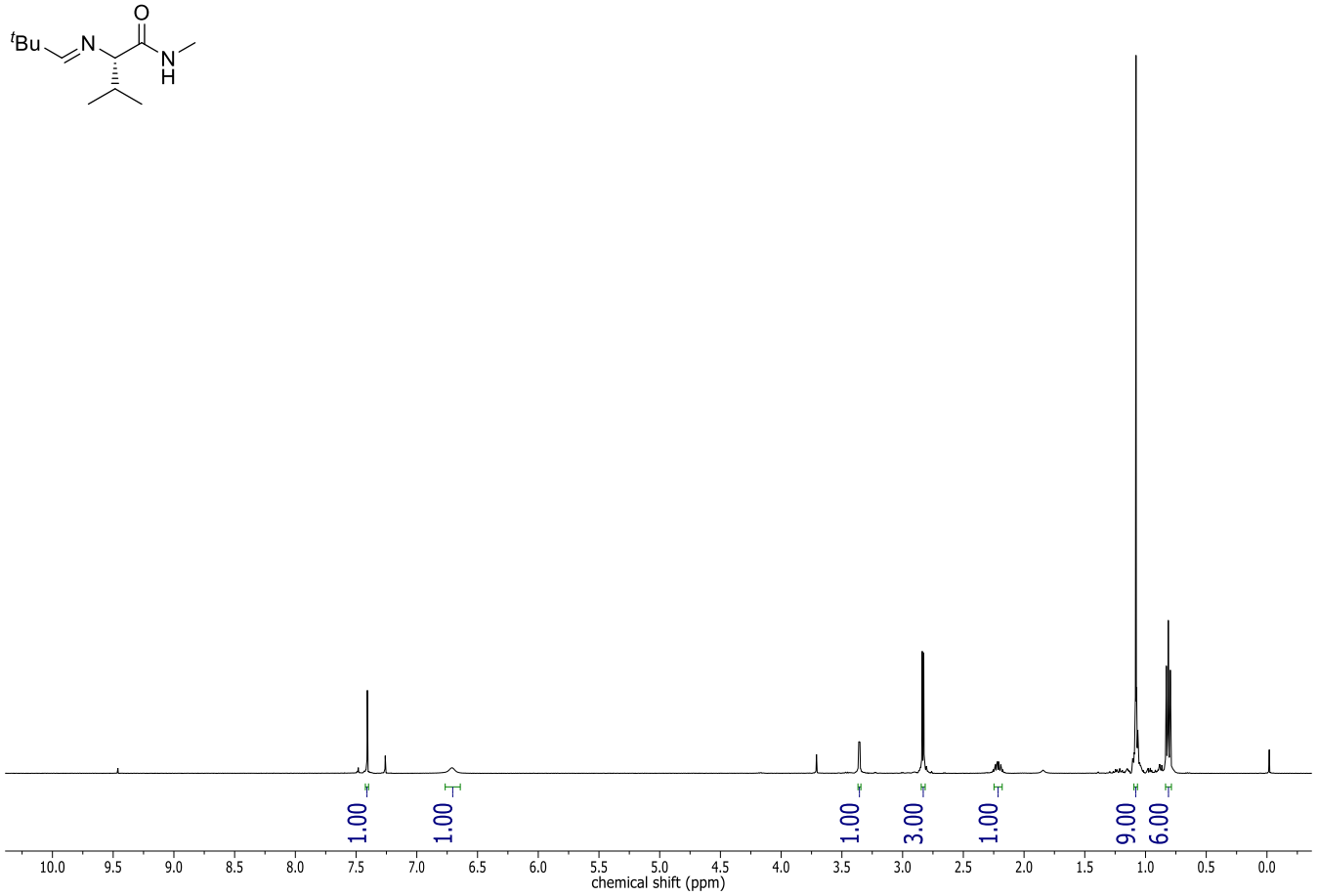
1.00
1.00
1.00
3.00
1.00
9.00
6.00
chemical shift (ppm)

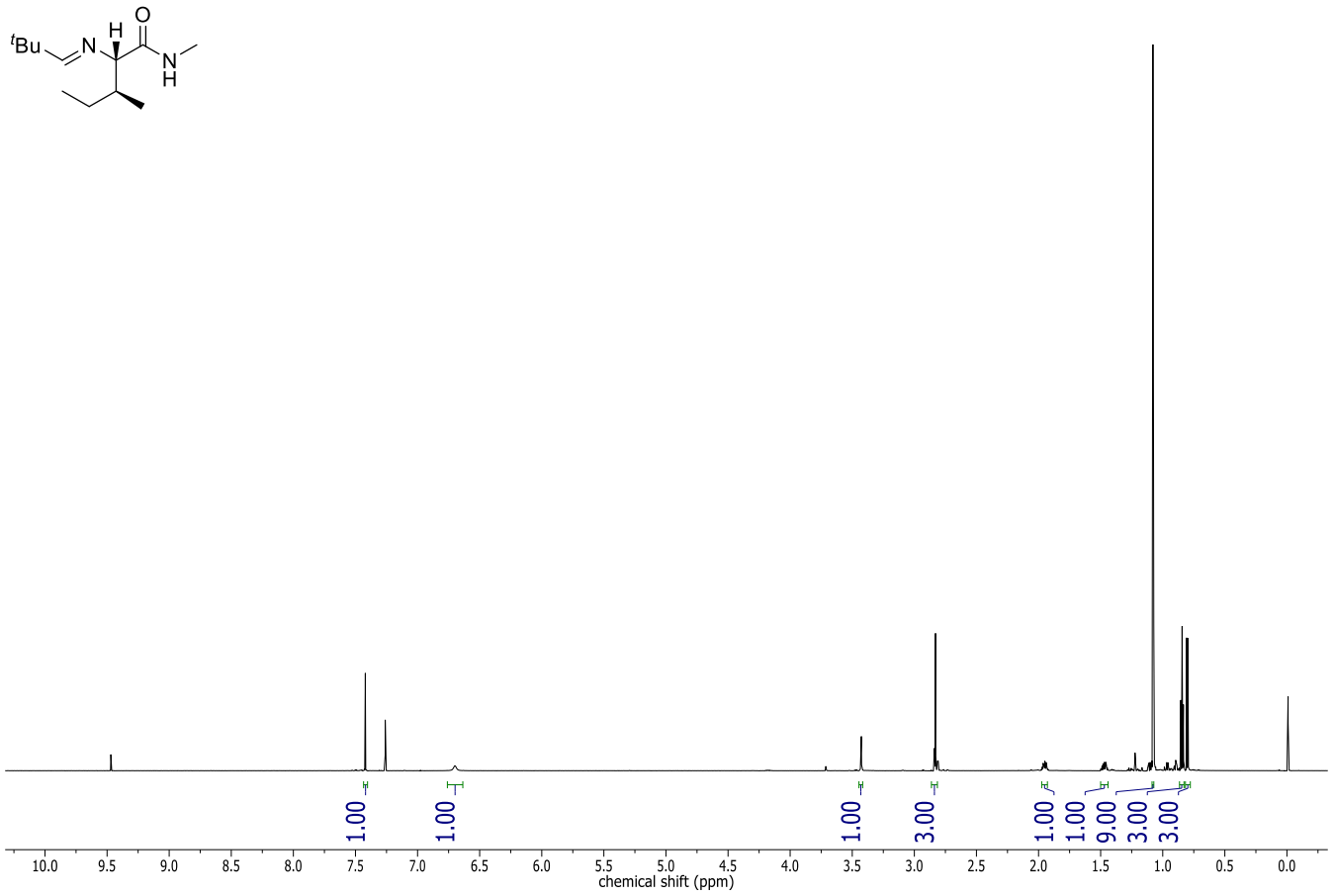
1.00
1.00
1.00
3.00
1.00
1.00
9.00
3.00
3.00
chemical shift (ppm)

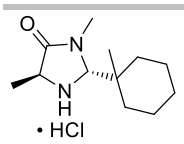
O
N
N
H
• HCl

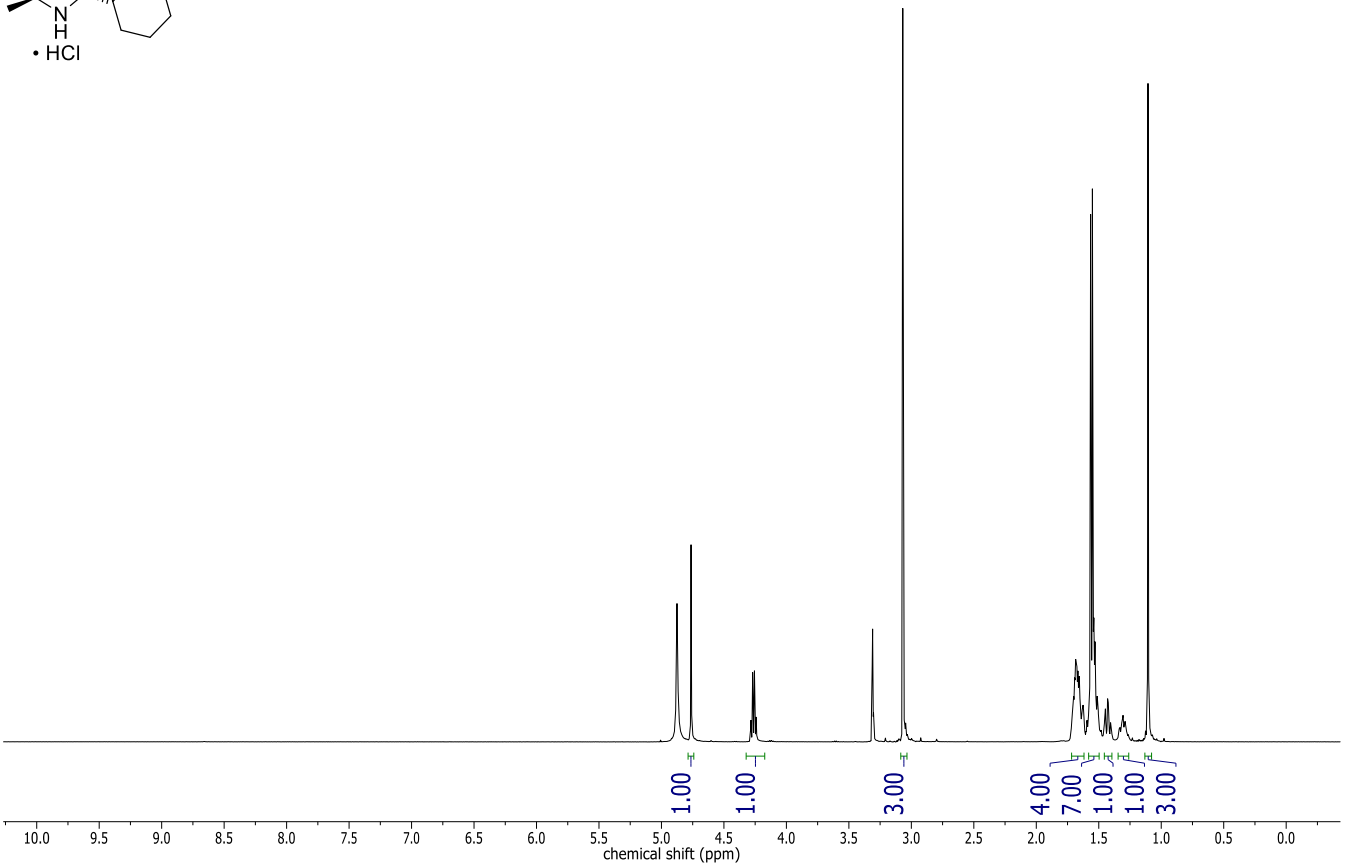
1.00
1.00
3.00
4.00
7.00
1.00
1.00
3.00
10.0 9.5 9.0 8.5 8.0 7.5 7.0 6.5 6.0 5.5 5.0 4.5 4.0 3.5 3.0 2.5 2.0 1.5 1.0 0.5 0.0
chemical shift (ppm)

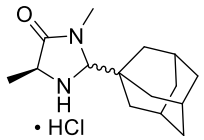
O
N
N
H
• HCl

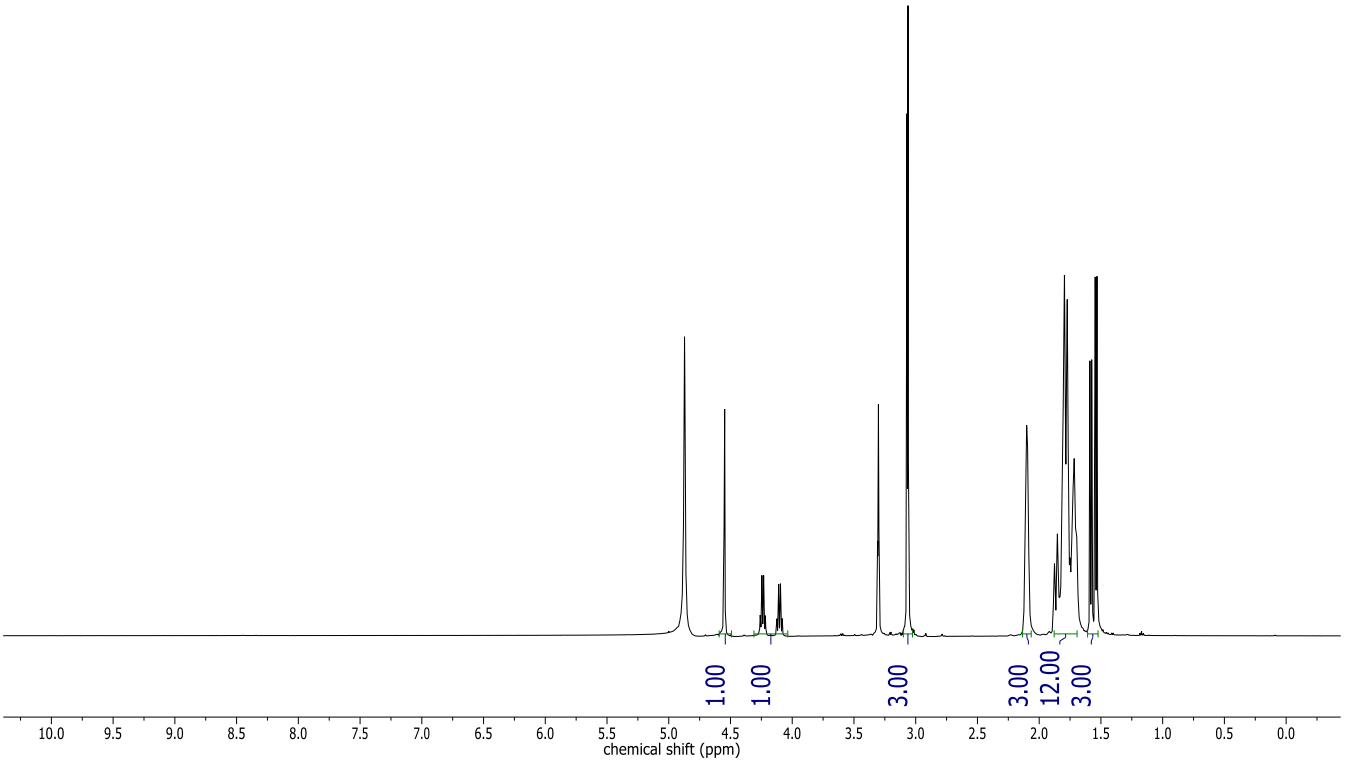
1.00
1.00
3.00
3.00
12.00
3.00
10.0 9.5 9.0 8.5 8.0 7.5 7.0 6.5 6.0 5.5 5.0 4.5 4.0 3.5 3.0 2.5 2.0 1.5 1.0 0.5 0.0
chemical shift (ppm)

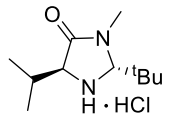
O
N
tBu
N
H · HCl

1.00
1.00
3.00
1.00
9.00
3.00
3.00
10.0 9.5 9.0 8.5 8.0 7.5 7.0 6.5 6.0 5.5 5.0 4.5 4.0 3.5 3.0 2.5 2.0 1.5 1.0 0.5 0.0
chemical shift (ppm)

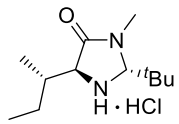
O
N
tBu
N
H · HCl

1.00
1.00
3.00
1.00
1.00
1.00
9.00
3.00
3.00
10.0 9.5 9.0 8.5 8.0 7.5 7.0 6.5 6.0 5.5 5.0 4.5 4.0 3.5 3.0 2.5 2.0 1.5 1.0 0.5 0.0
chemical shift (ppm)

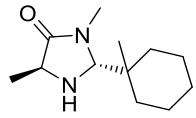

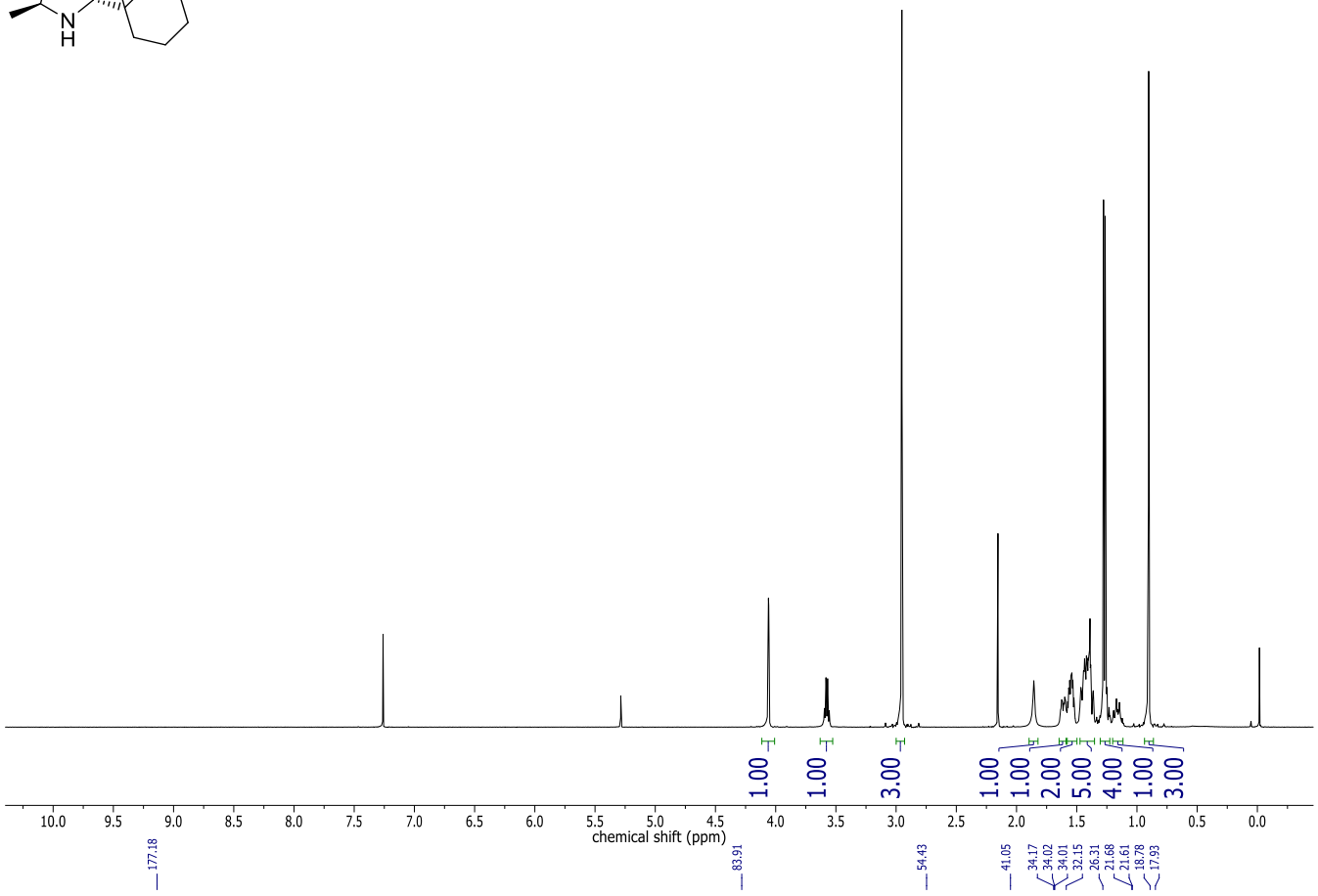
1.00
1.00
3.00
1.00
1.00
2.00
5.00
4.00
1.00
3.00
chemical shift (ppm)
177.18
83.91
54.43
41.05
34.17
34.02
34.01
32.15
26.31
21.68
21.61
18.78
17.93

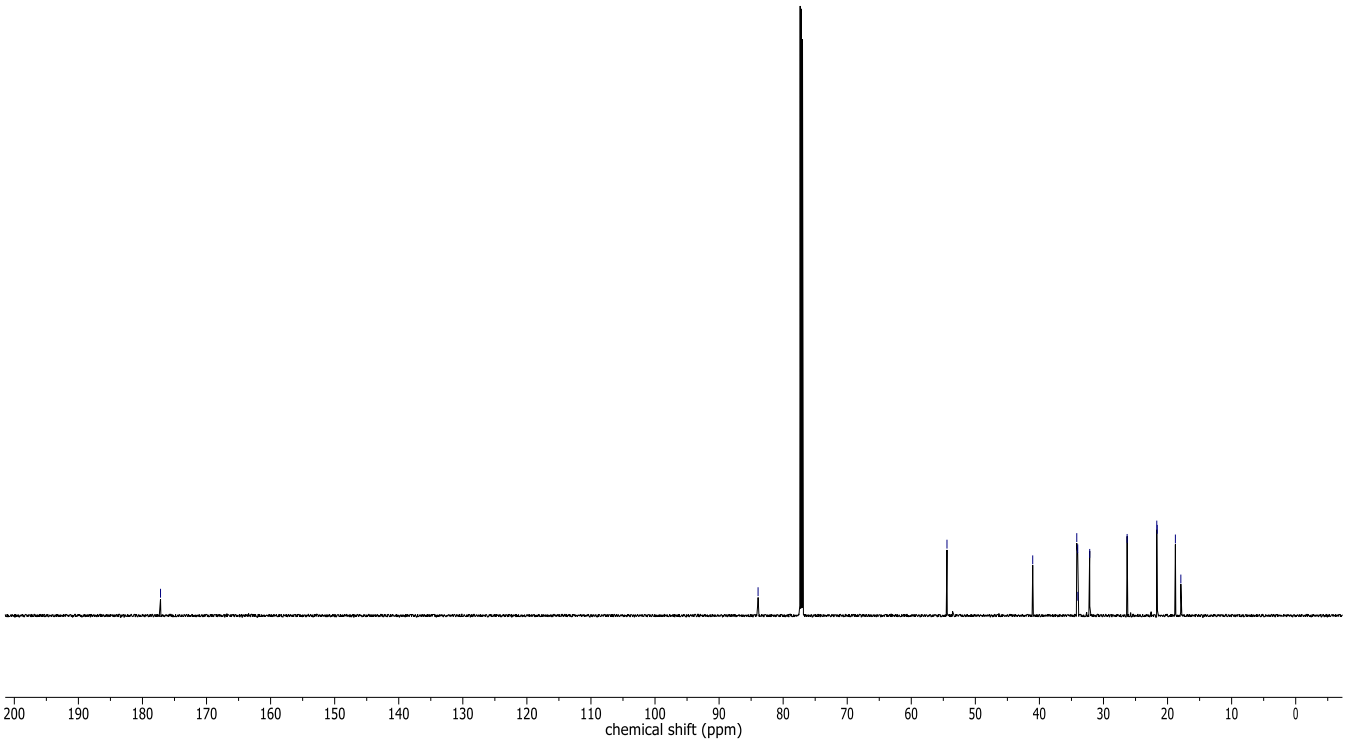
chemical shift (ppm)

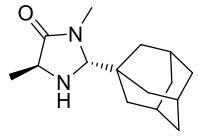
O
N
N
H

1.00
1.00
3.00
3.00
12.00
3.00
chemical shift (ppm)
177.20
83.72
54.53
40.34
38.15
37.06
32.50
28.18
18.57

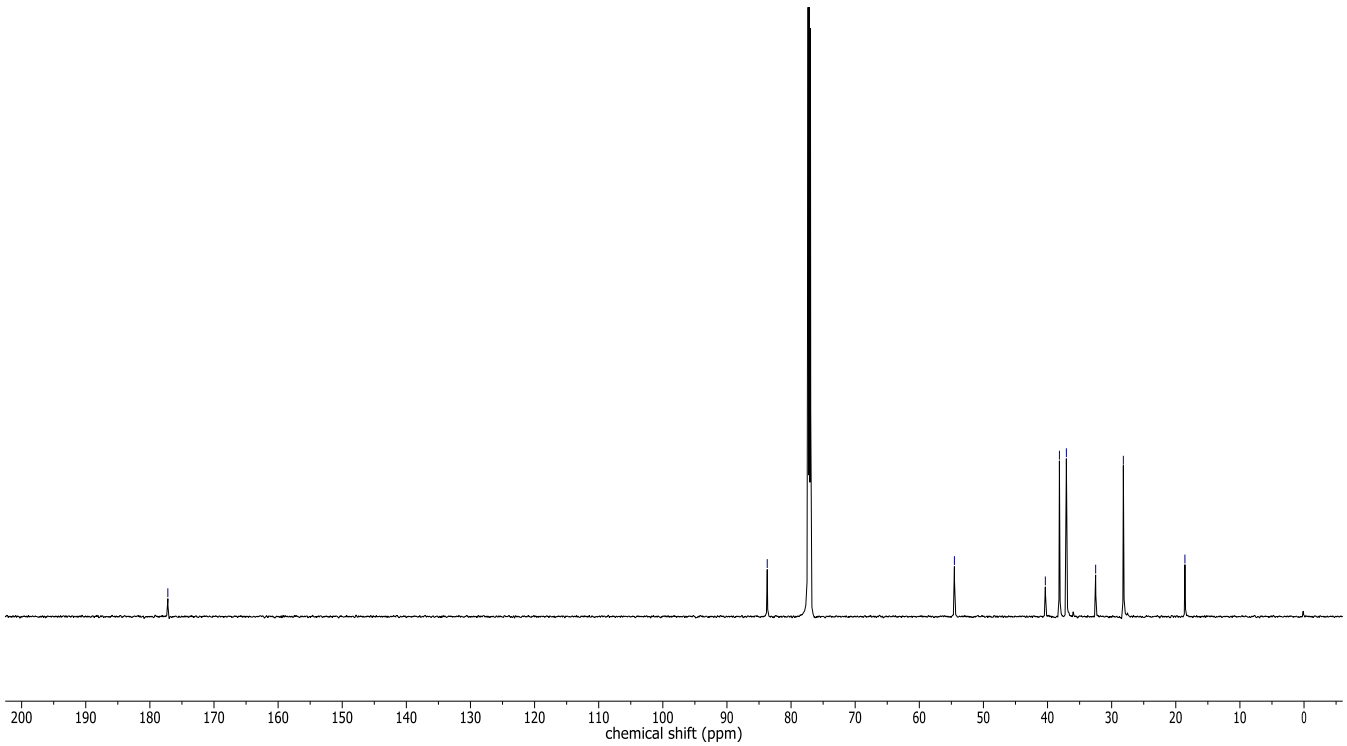
chemical shift (ppm)

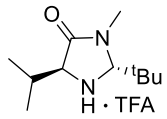
O
N
tBu
N
H · TFA

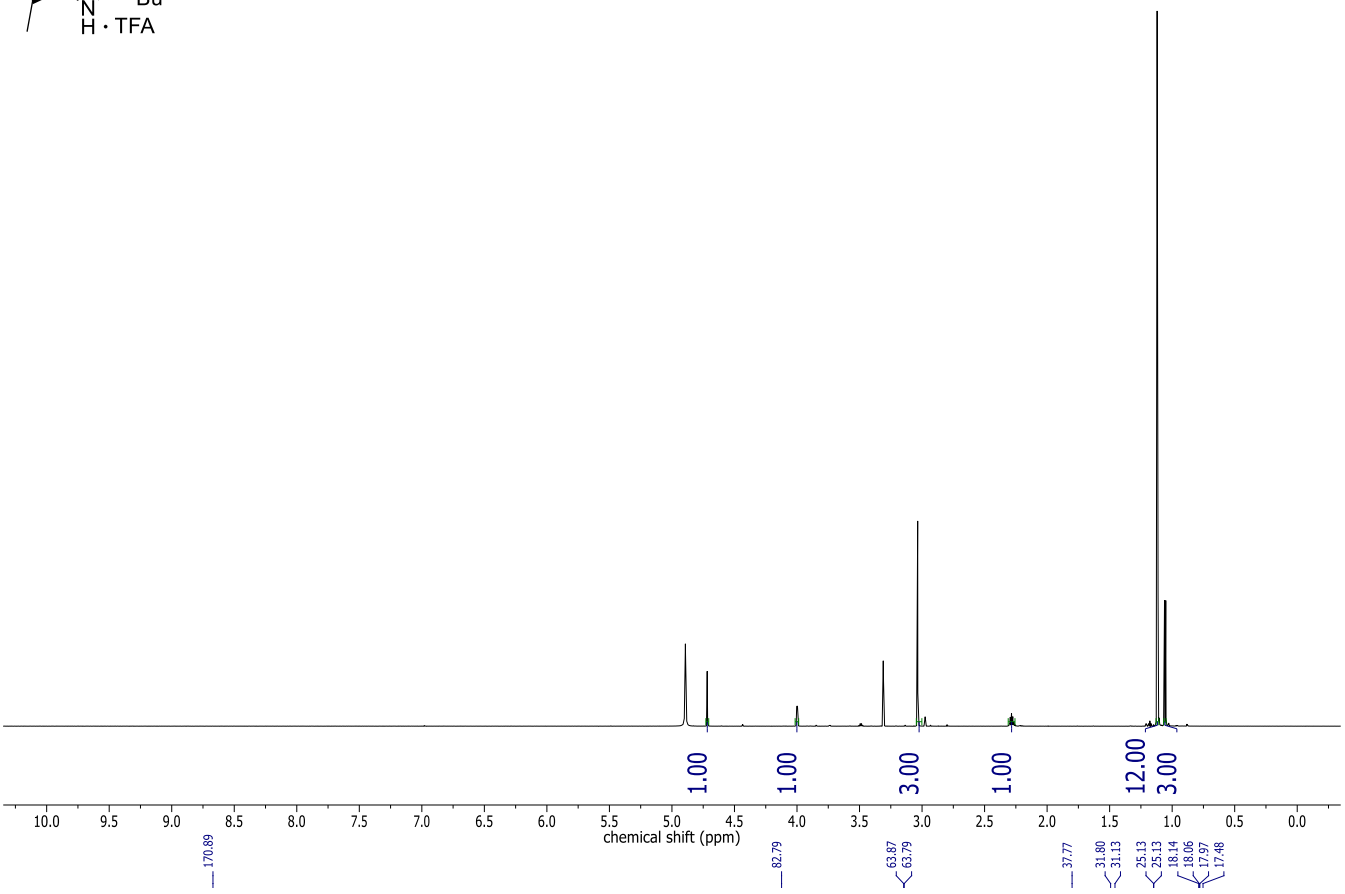
1.00
1.00
3.00
1.00
12.00
3.00
10.0 9.5 9.0 8.5 8.0 7.5 7.0 6.5 6.0 5.5 5.0 4.5 4.0 3.5 3.0 2.5 2.0 1.5 1.0 0.5 0.0
chemical shift (ppm)

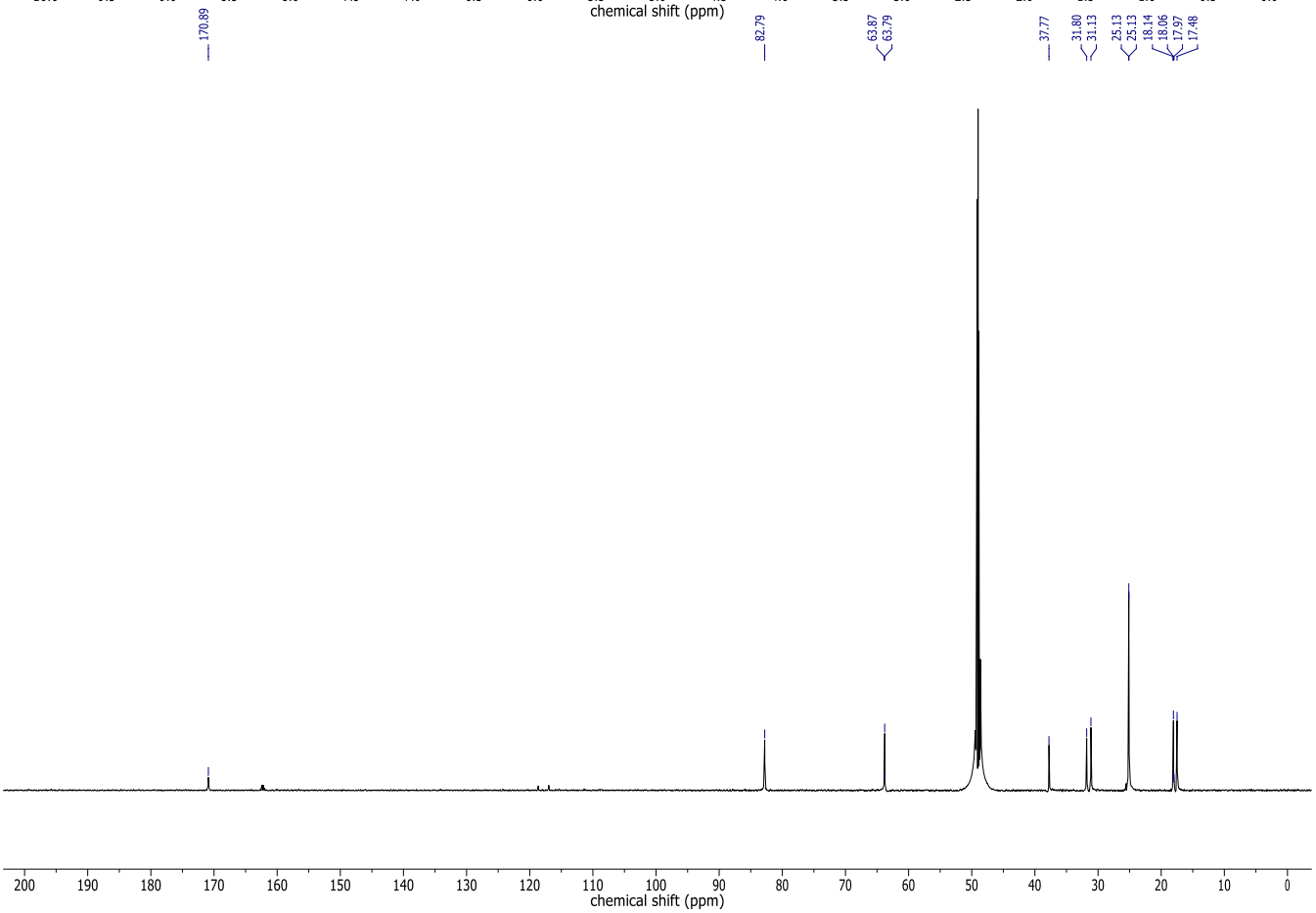
170.89
82.79
63.87
63.79
37.77
31.80
31.13
25.13
25.13
18.14
18.06
17.97
17.48
200 190 180 170 160 150 140 130 120 110 100 90 80 70 60 50 40 30 20 10 0
chemical shift (ppm)

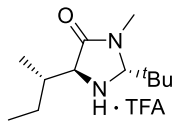
O
N
tBu
N
H · TFA

1.00
1.00
3.00
1.00
1.00
1.00
9.00
3.00
3.00
10.0 9.5 9.0 8.5 8.0 7.5 7.0 6.5 6.0 5.5 5.0 4.5 4.0 3.5 3.0 2.5 2.0 1.5 1.0 0.5 0.0
chemical shift (ppm)

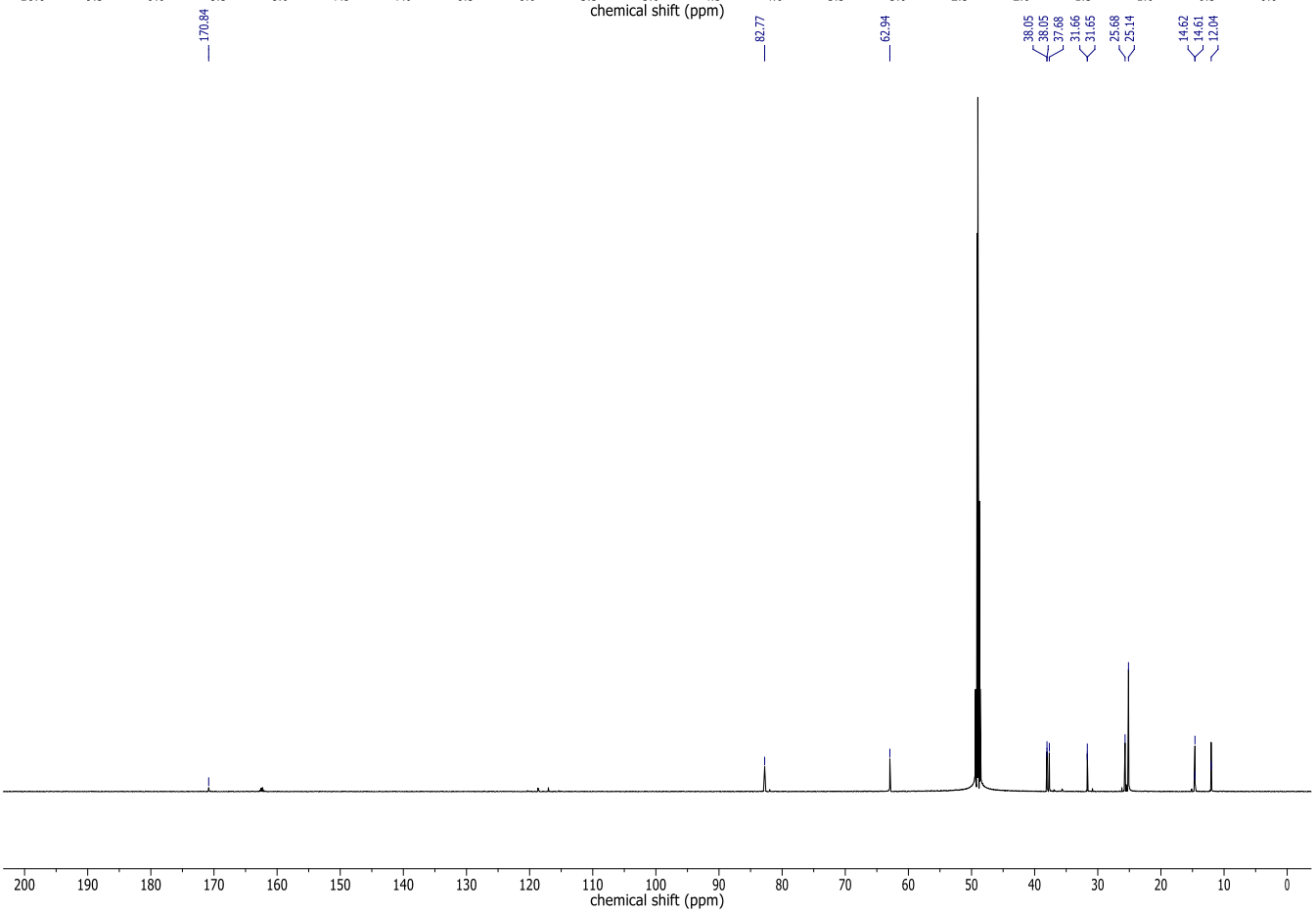
170.84
82.77
62.94
38.05
38.05
37.68
31.66
31.65
25.68
25.14
14.62
14.61
12.04
200 190 180 170 160 150 140 130 120 110 100 90 80 70 60 50 40 30 20 10 0
chemical shift (ppm)

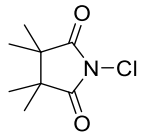
O
N–Cl
O

12.00
10.0 9.5 9.0 8.5 8.0 7.5 7.0 6.5 6.0 5.5 5.0 4.5 4.0 3.5 3.0 2.5 2.0 1.5 1.0 0.5 0.0
f1 (ppm)

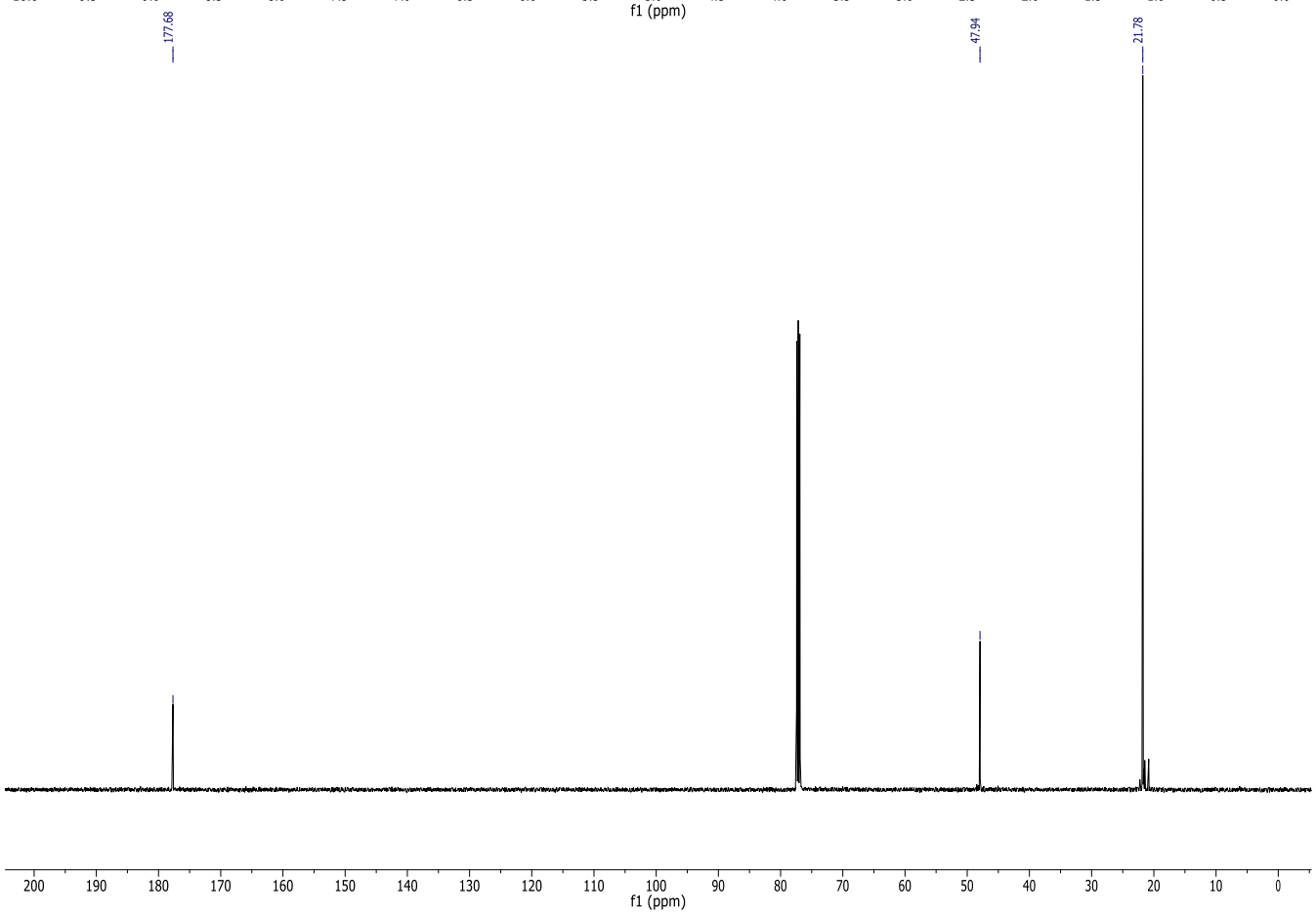
177.68
47.94
21.78
200 190 180 170 160 150 140 130 120 110 100 90 80 70 60 50 40 30 20 10 0
f1 (ppm)

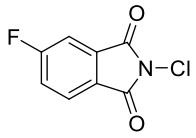
F
O
N–Cl
O

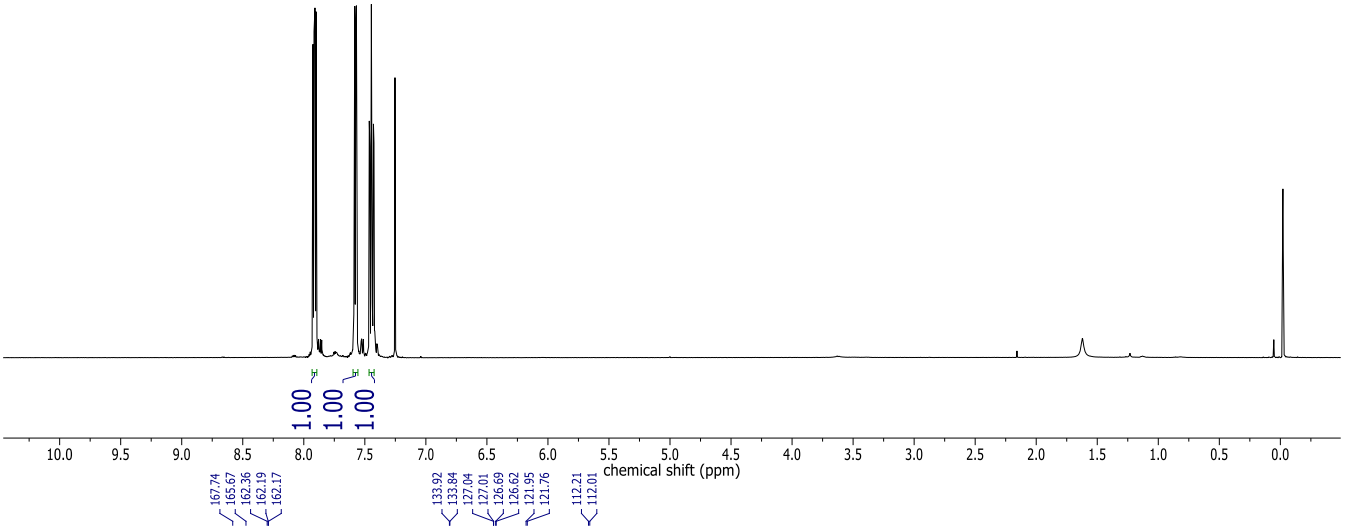
1.00
1.00
1.00
10.0
9.5
9.0
8.5
8.0
7.5
7.0
6.5
6.0
5.5
5.0
4.5
4.0
3.5
3.0
2.5
2.0
1.5
1.0
0.5
0.0
chemical shift (ppm)
167.74
165.67
162.36
162.19
162.17
133.92
133.84
127.04
127.01
126.69
126.62
121.95
121.76
112.21
112.01

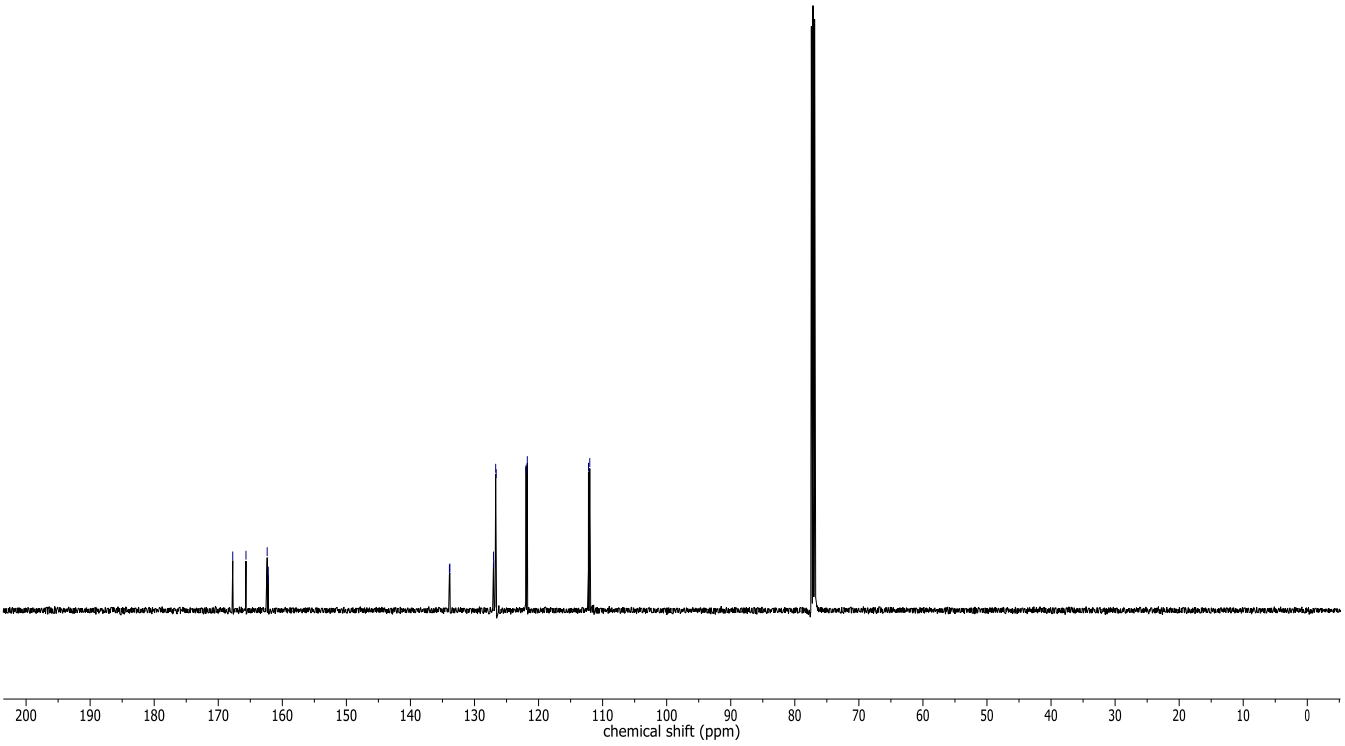
200
190
180
170
160
150
140
130
120
110
100
90
80
70
60
50
40
30
20
10
0
chemical shift (ppm)

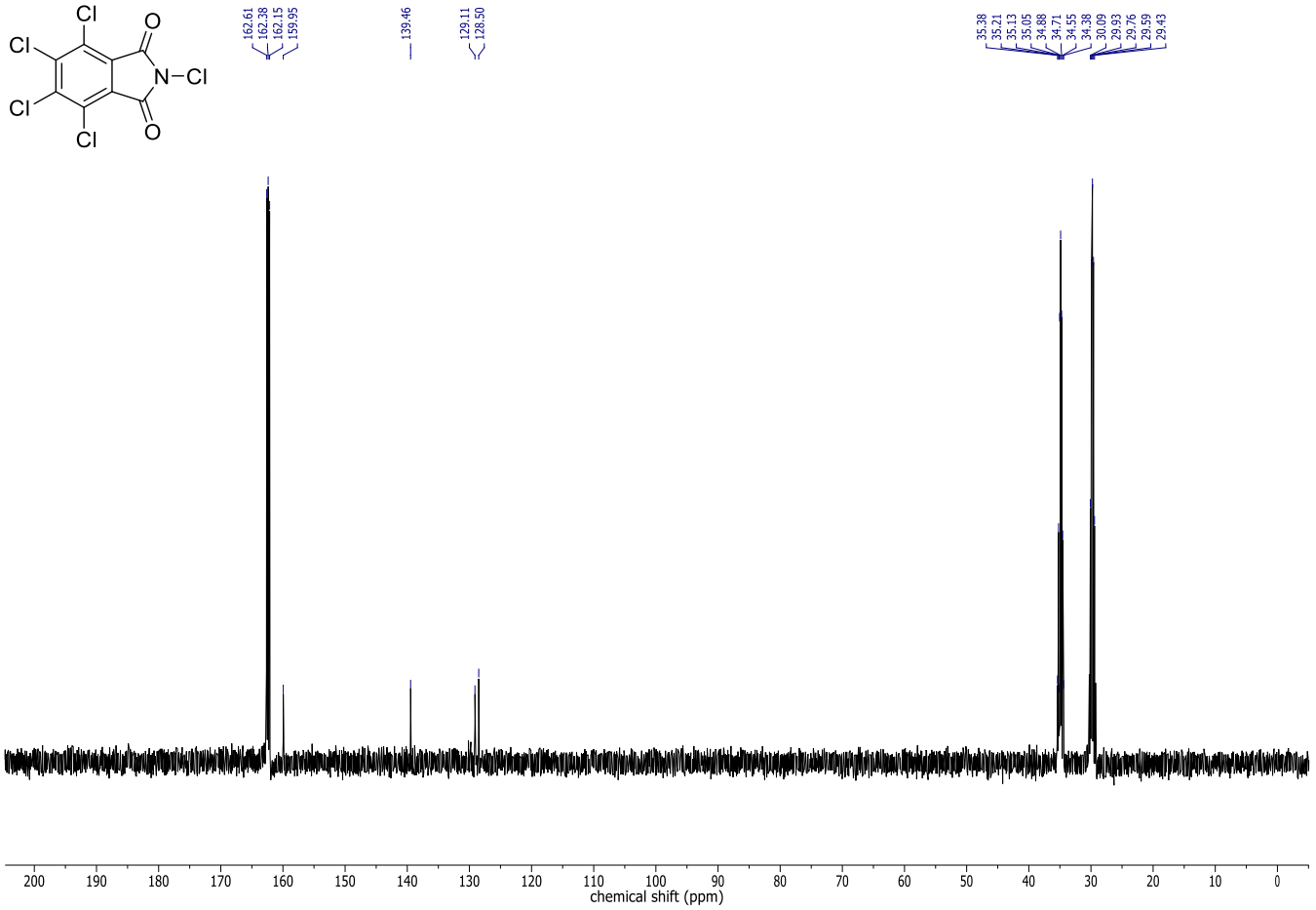
Cl
Cl
Cl
Cl
O
O
N–Cl
162.61
162.38
162.15
159.95
139.46
129.11
128.50
35.38
35.21
35.13
35.05
34.88
34.71
34.55
34.38
30.09
29.93
29.76
29.59
29.43
200
190
180
170
160
150
140
130
120
110
100
90
80
70
60
50
40
30
20
10
0
chemical shift (ppm)

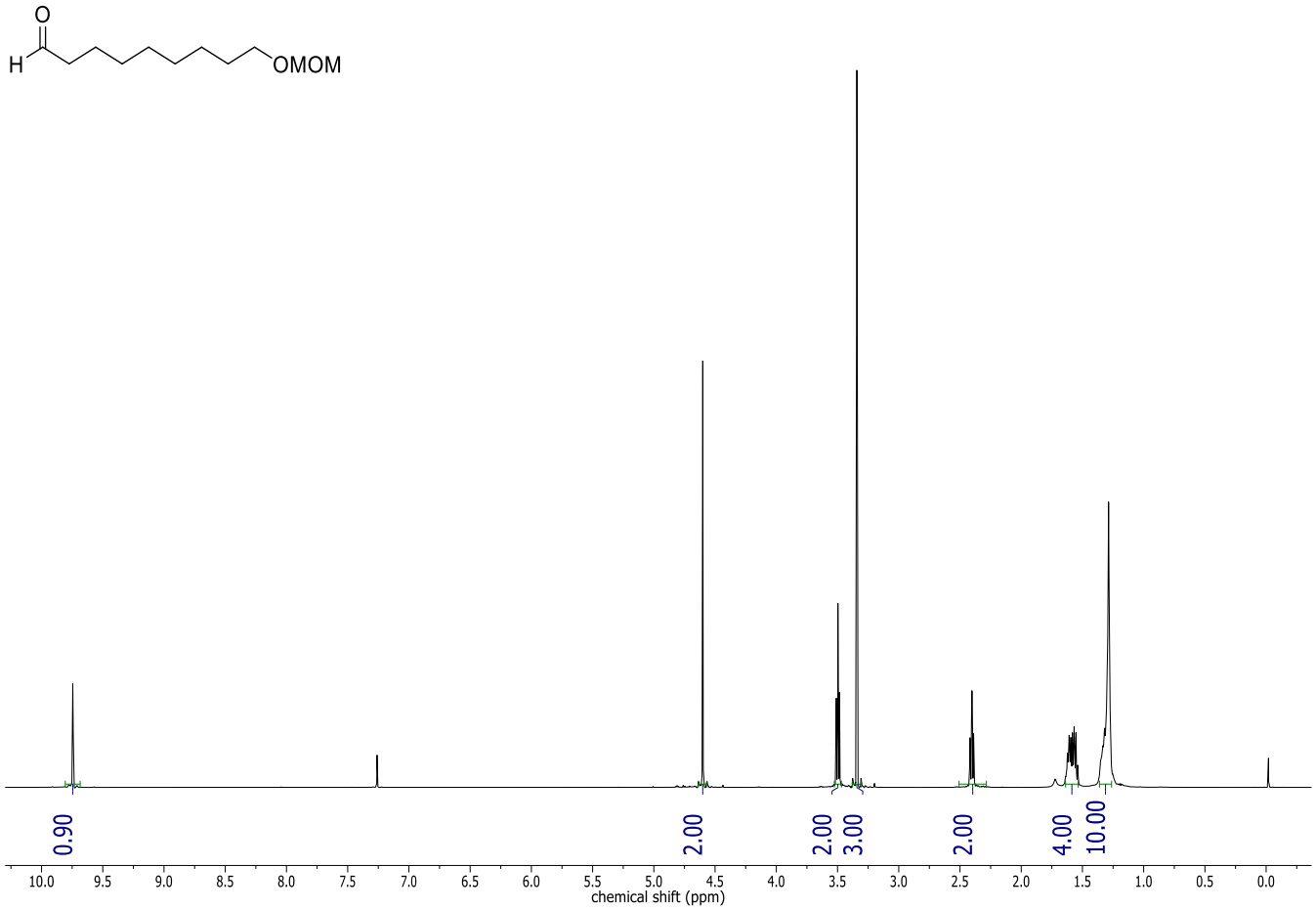
O
H
OMOM
0.90
2.00
2.00
3.00
2.00
4.00
10.00
chemical shift (ppm)

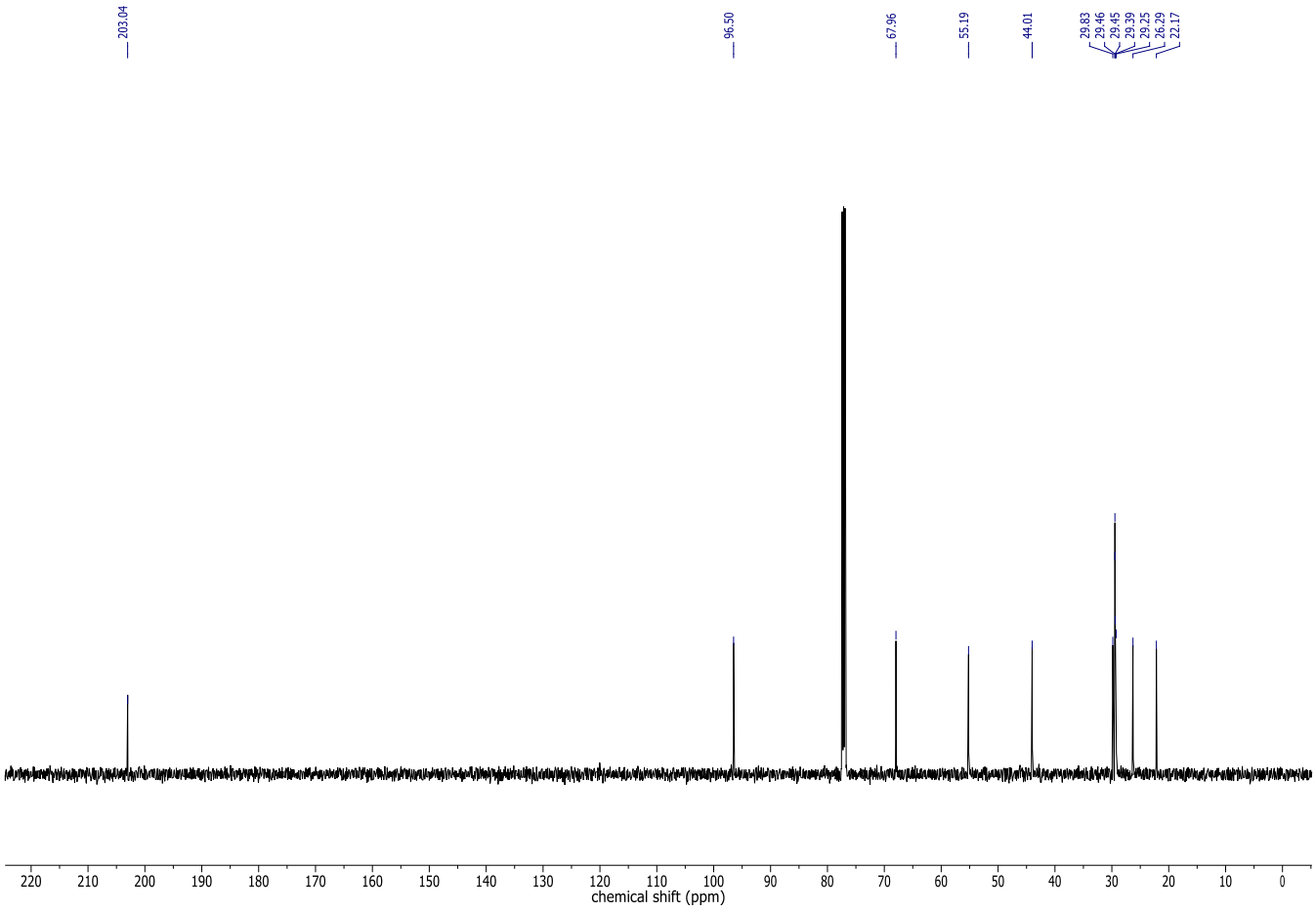
203.04
96.50
67.96
55.19
44.01
29.83
29.46
29.45
29.39
29.25
26.29
22.17
chemical shift (ppm)

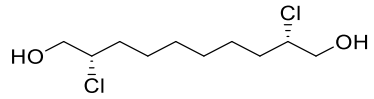
Cl
HO
OH
Cl

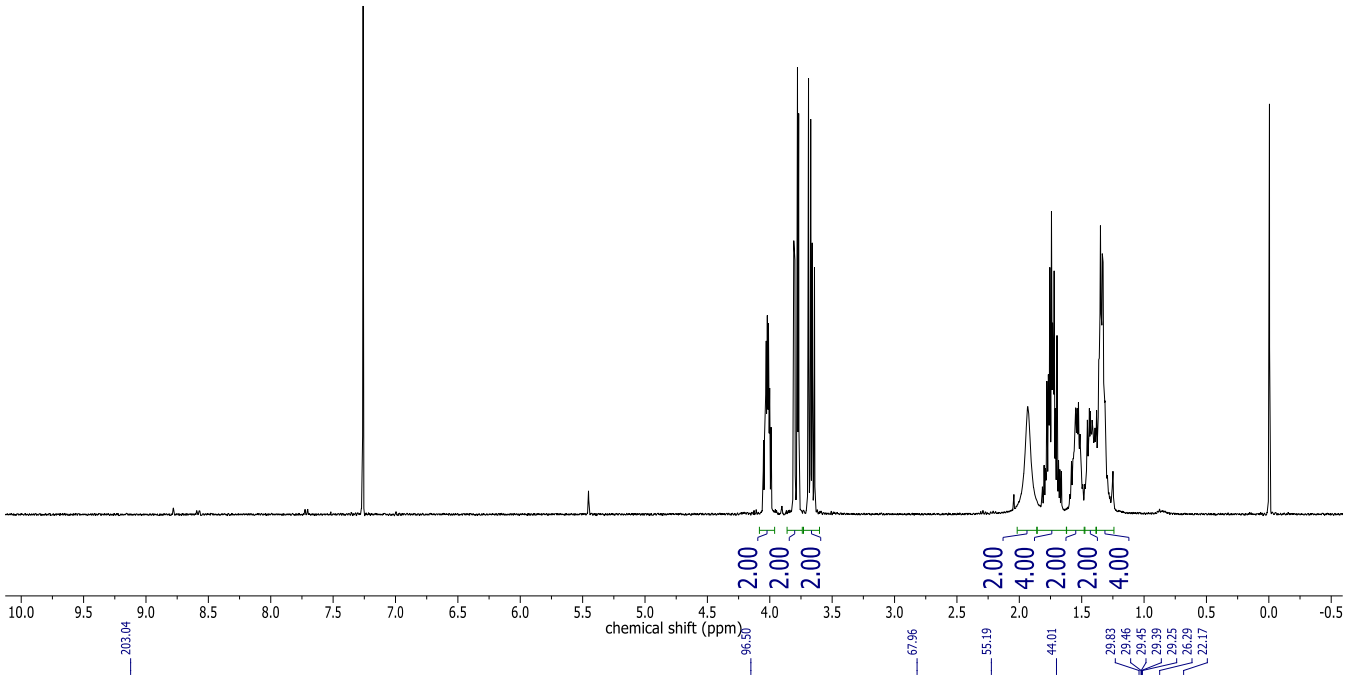
2.00
2.00
2.00
2.00
4.00
2.00
2.00
4.00
10.0 9.5 9.0 8.5 8.0 7.5 7.0 6.5 6.0 5.5 5.0 4.5 4.0 3.5 3.0 2.5 2.0 1.5 1.0 0.5 0.0 -0.5
chemical shift (ppm)
203.04
96.30
67.96
55.19
44.01
29.83
29.46
29.45
29.39
29.25
26.29
22.17

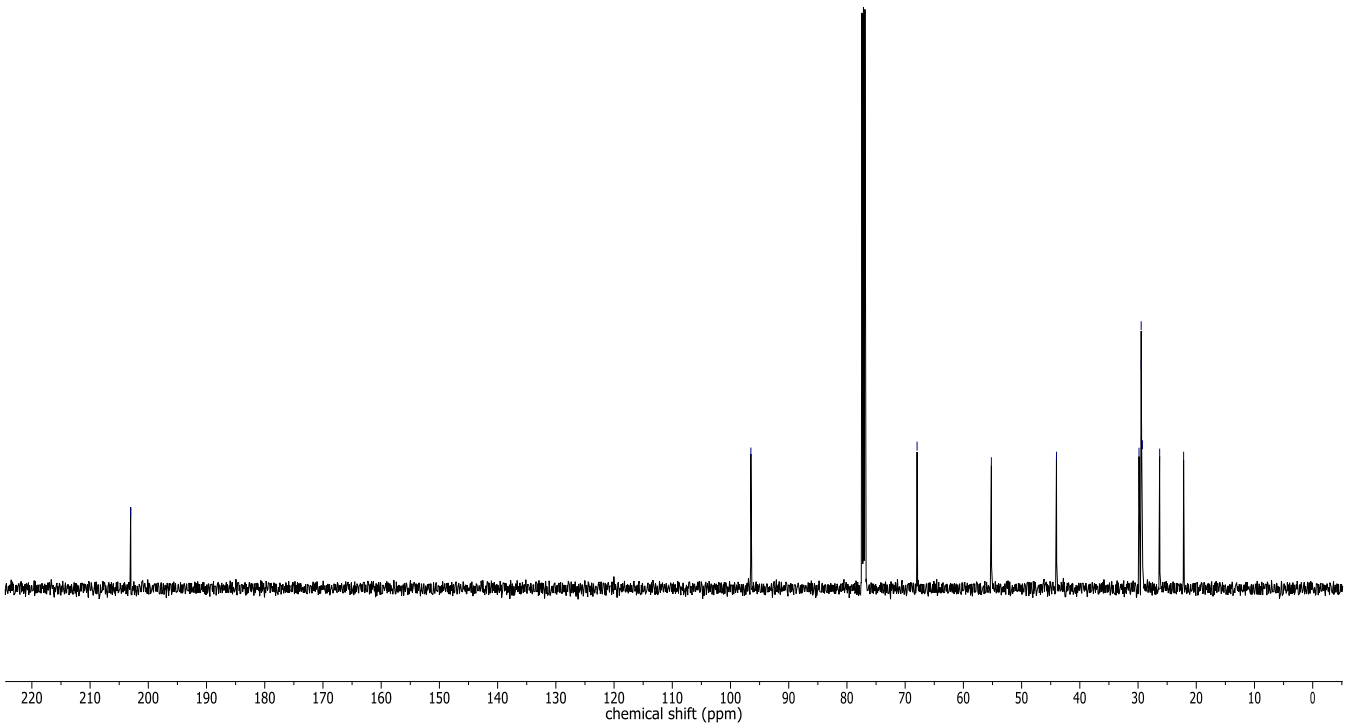
220 210 200 190 180 170 160 150 140 130 120 110 100 90 80 70 60 50 40 30 20 10 0
chemical shift (ppm)

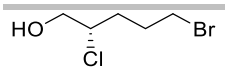
HO
Cl
Br

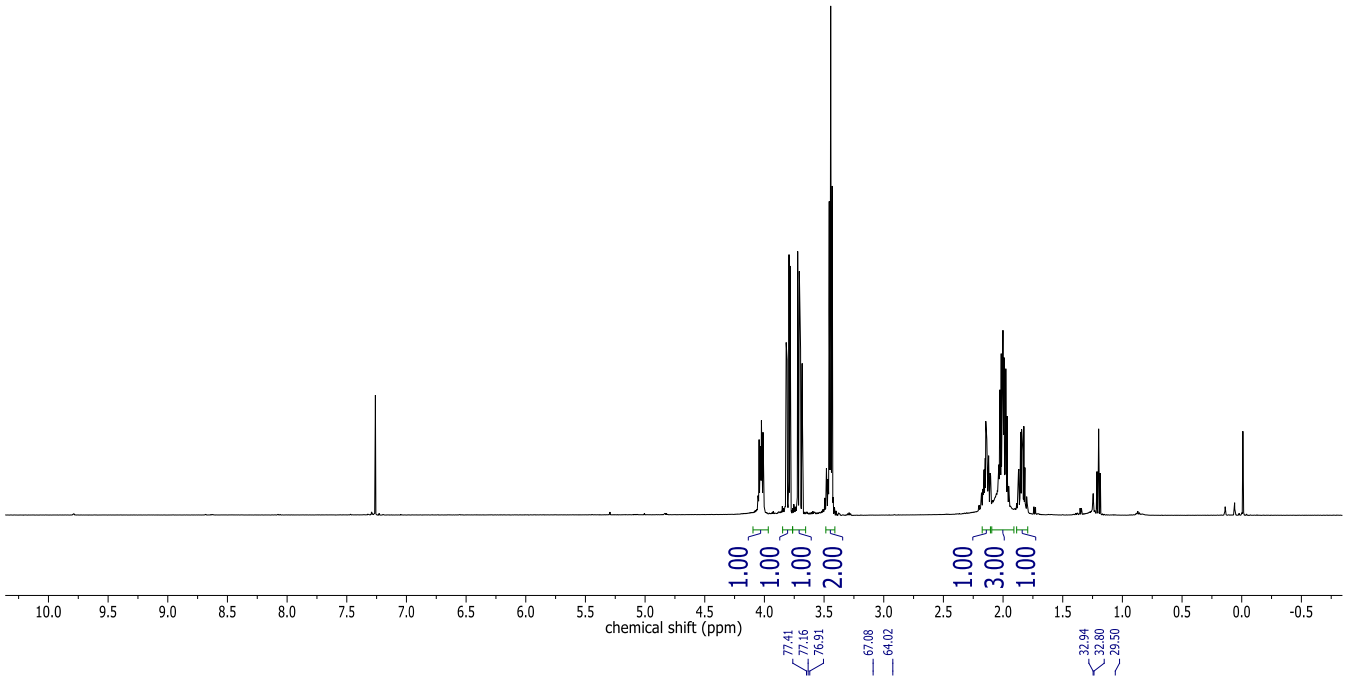
1.00
1.00
1.00
2.00
1.00
3.00
1.00
10.0
9.5
9.0
8.5
8.0
7.5
7.0
6.5
6.0
5.5
5.0
4.5
4.0
3.5
3.0
2.5
2.0
1.5
1.0
0.5
0.0
-0.5
chemical shift (ppm)
77.41
77.16
76.91
67.08
64.02
32.94
32.80
29.50

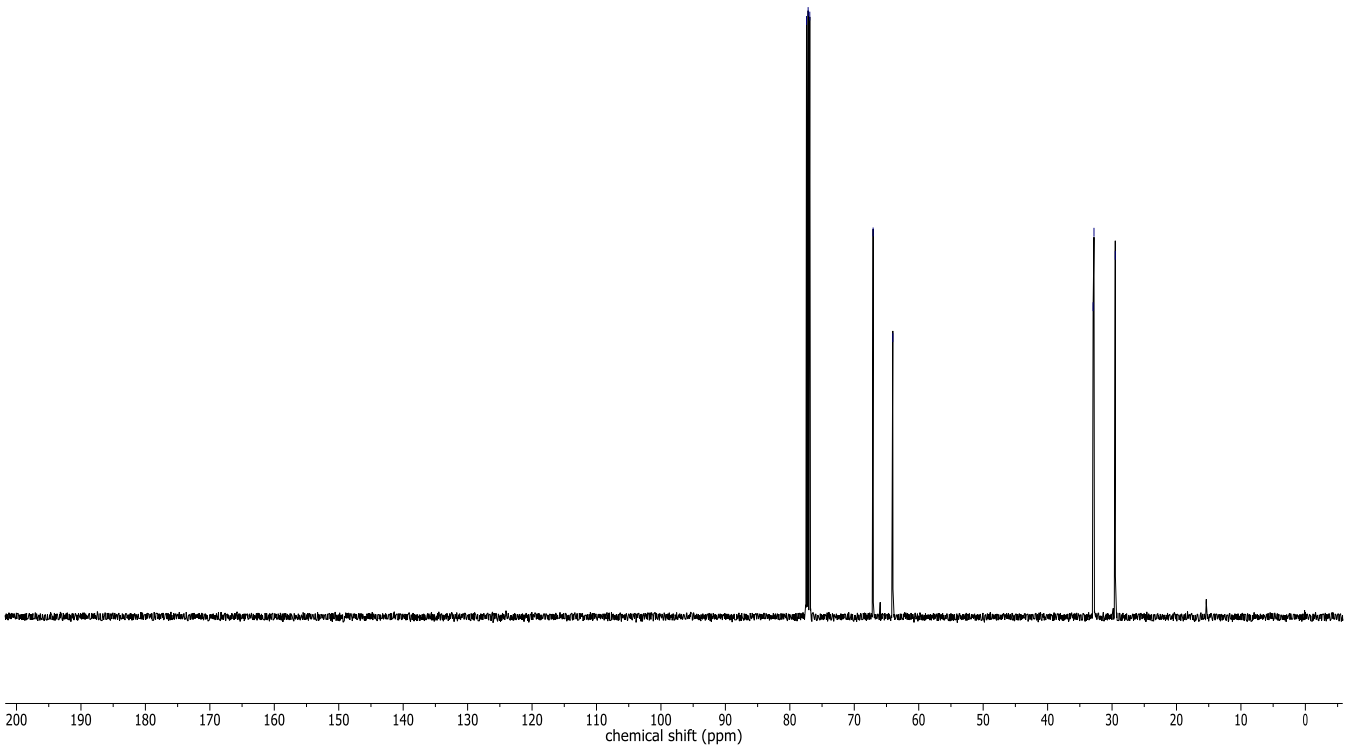
200
190
180
170
160
150
140
130
120
110
100
90
80
70
60
50
40
30
20
10
0
chemical shift (ppm)

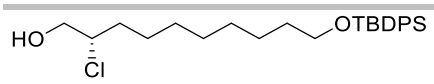
HO
OTBDPS
Cl

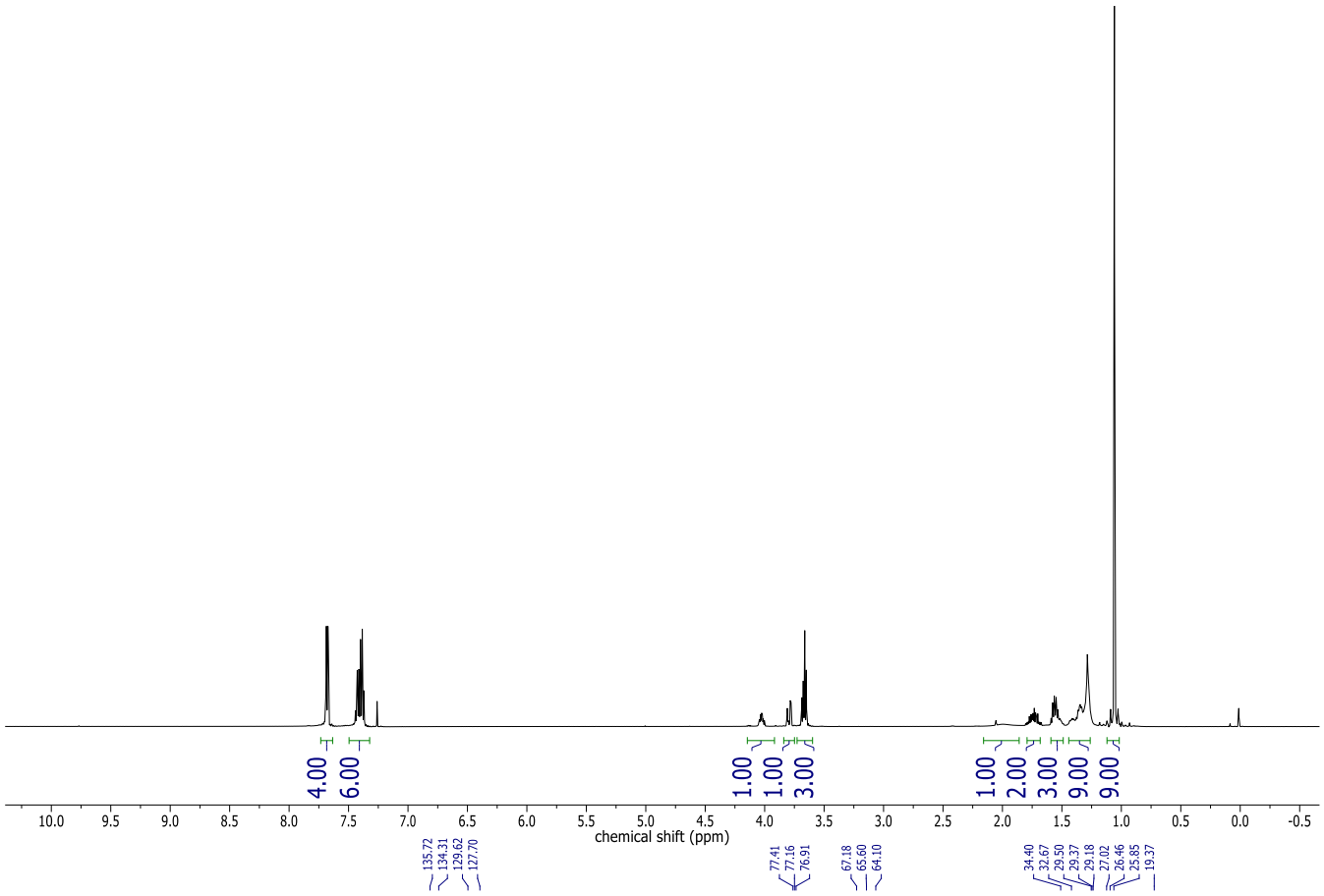
4.00
6.00
1.00
1.00
3.00
1.00
2.00
3.00
9.00
9.00
chemical shift (ppm)
135.72
134.31
129.62
127.70
77.41
77.16
76.91
67.18
65.60
64.10
34.40
32.67
29.50
29.37
29.18
27.02
26.46
25.85
19.37

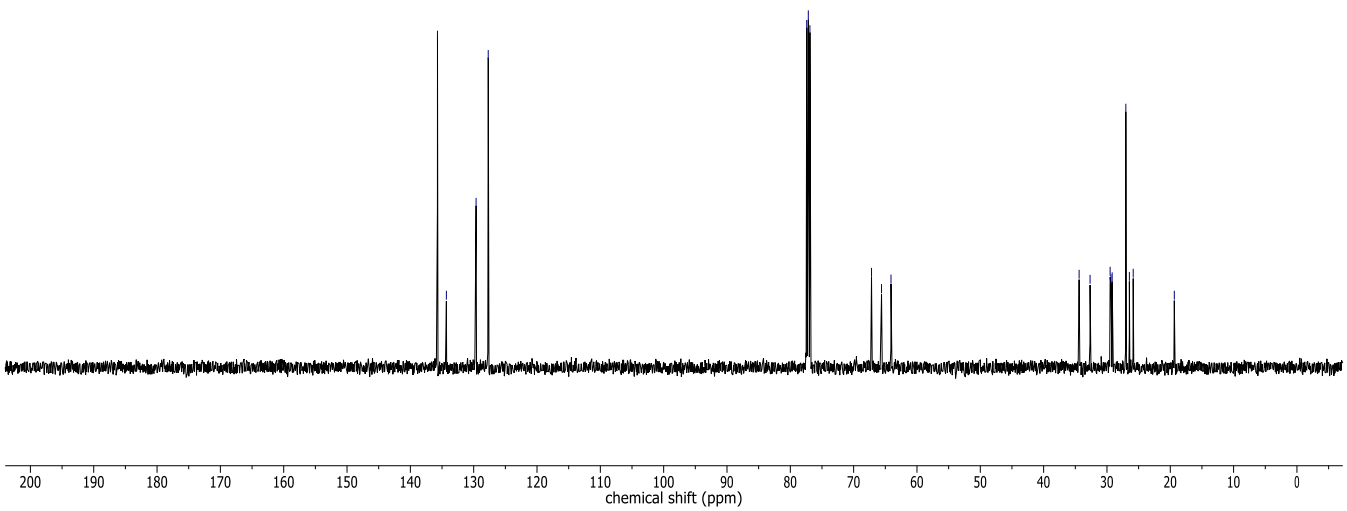
chemical shift (ppm)

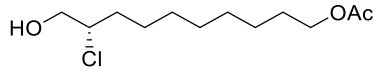
HO
OAc
Cl

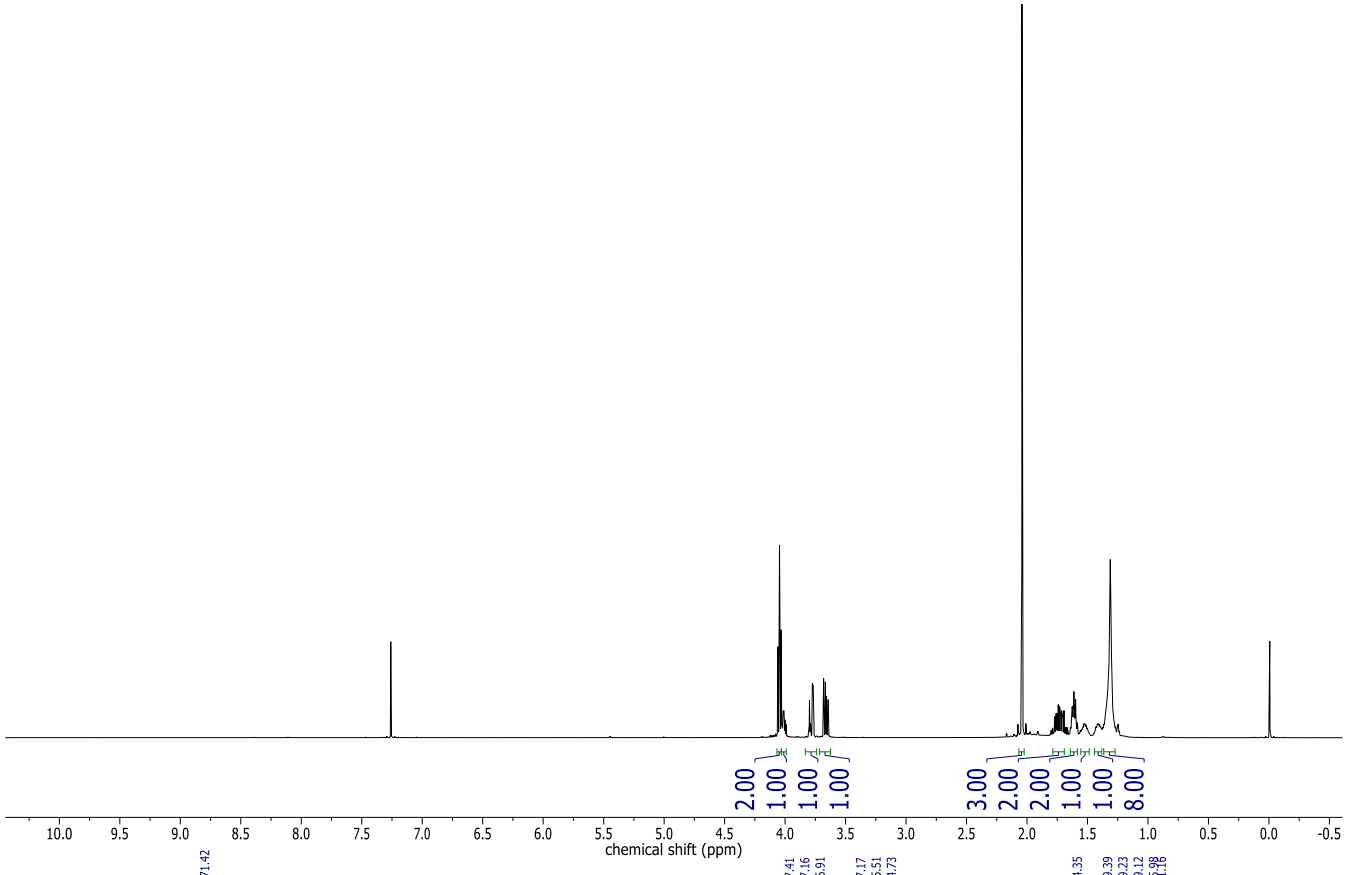
2.00
1.00
1.00
1.00
3.00
2.00
2.00
1.00
1.00
8.00
chemical shift (ppm)

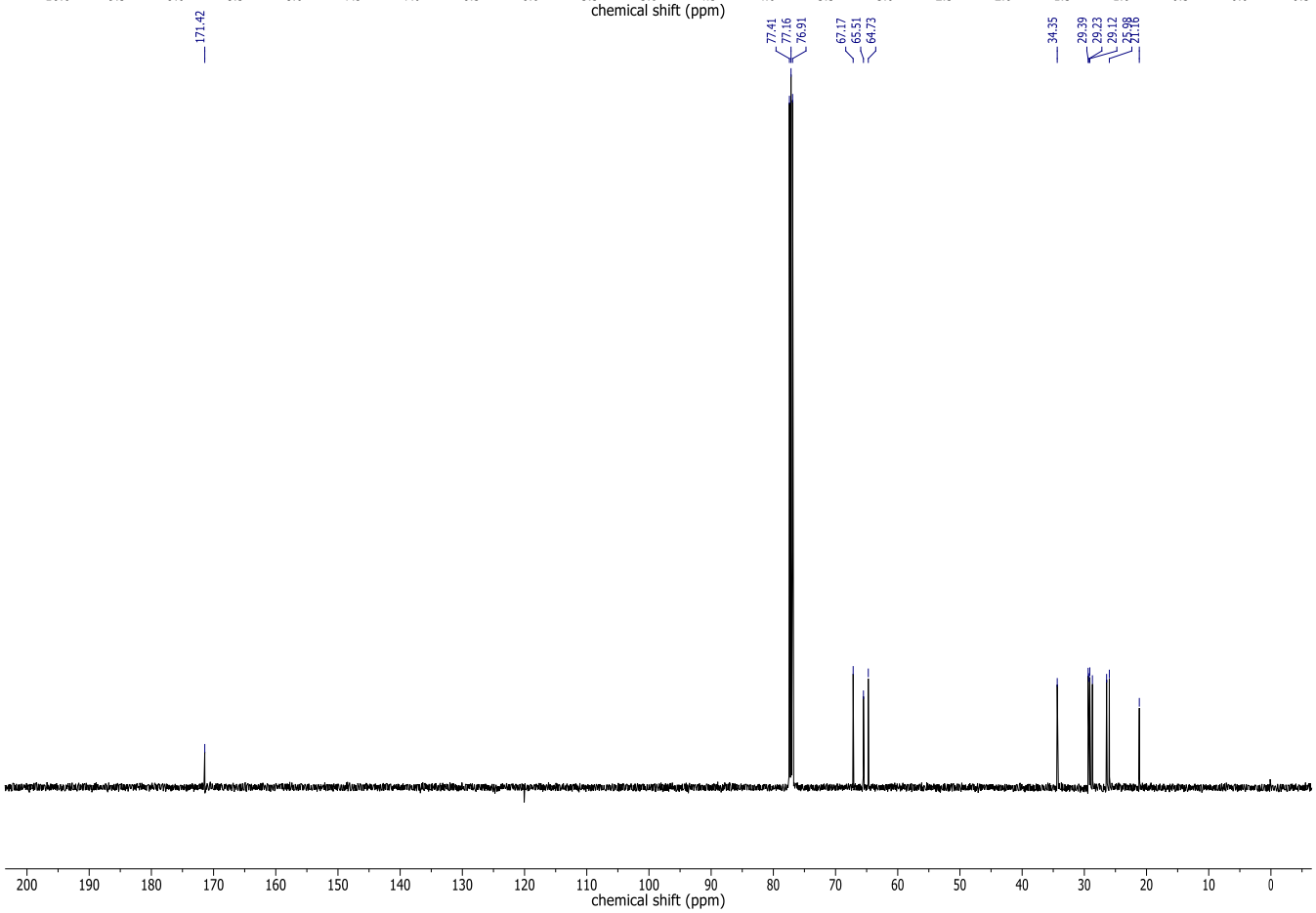
171.42
77.41
77.16
76.91
67.17
65.51
64.73
34.35
29.39
29.23
29.12
25.98
21.18
chemical shift (ppm)

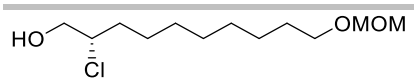
HO
OMOM
Cl

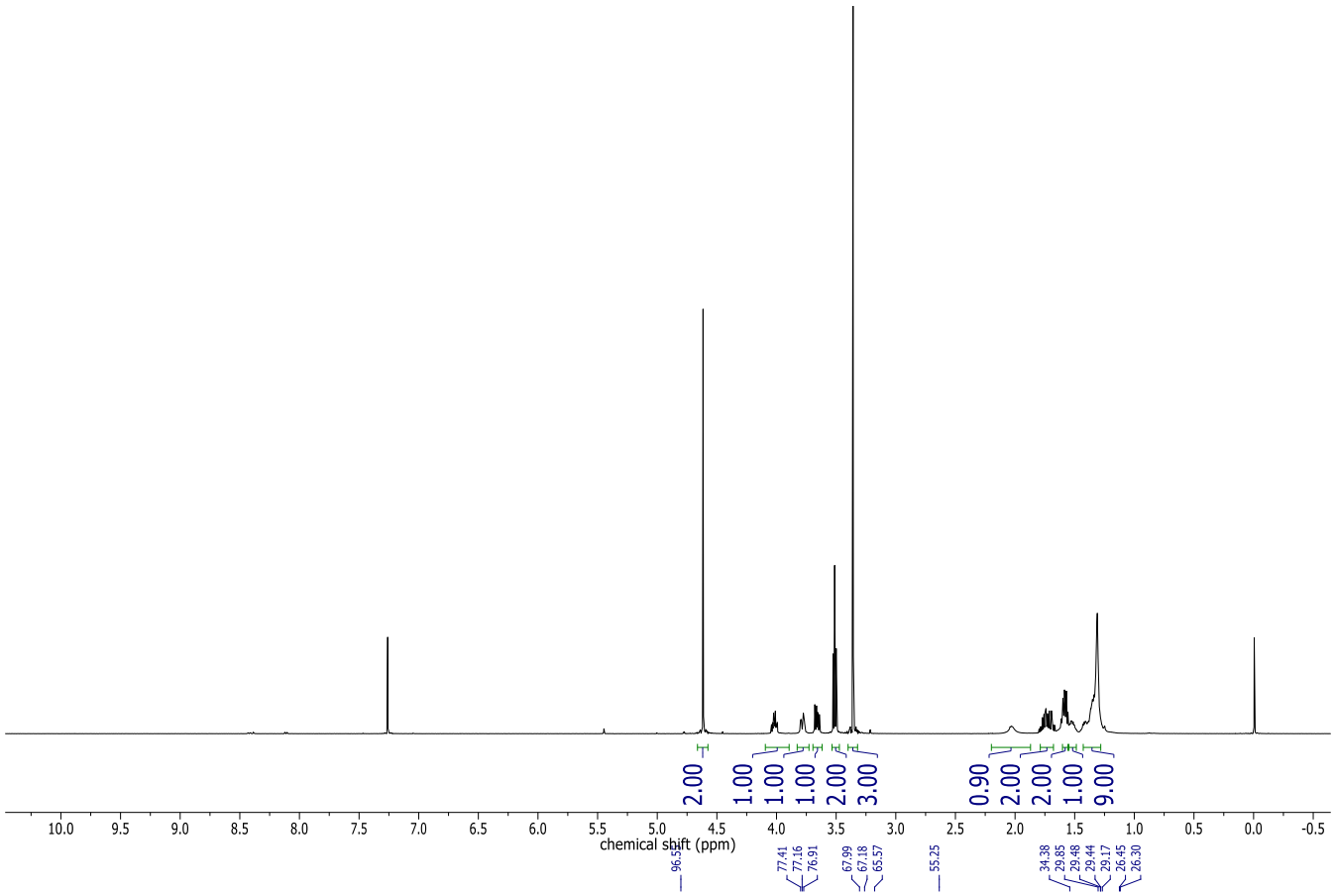
2.00
1.00
1.00
1.00
2.00
3.00
0.90
2.00
2.00
1.00
9.00
chemical shift (ppm)
96.52
77.41
77.16
76.91
67.99
67.18
65.57
55.25
34.38
29.85
29.48
29.44
29.17
26.45
26.30

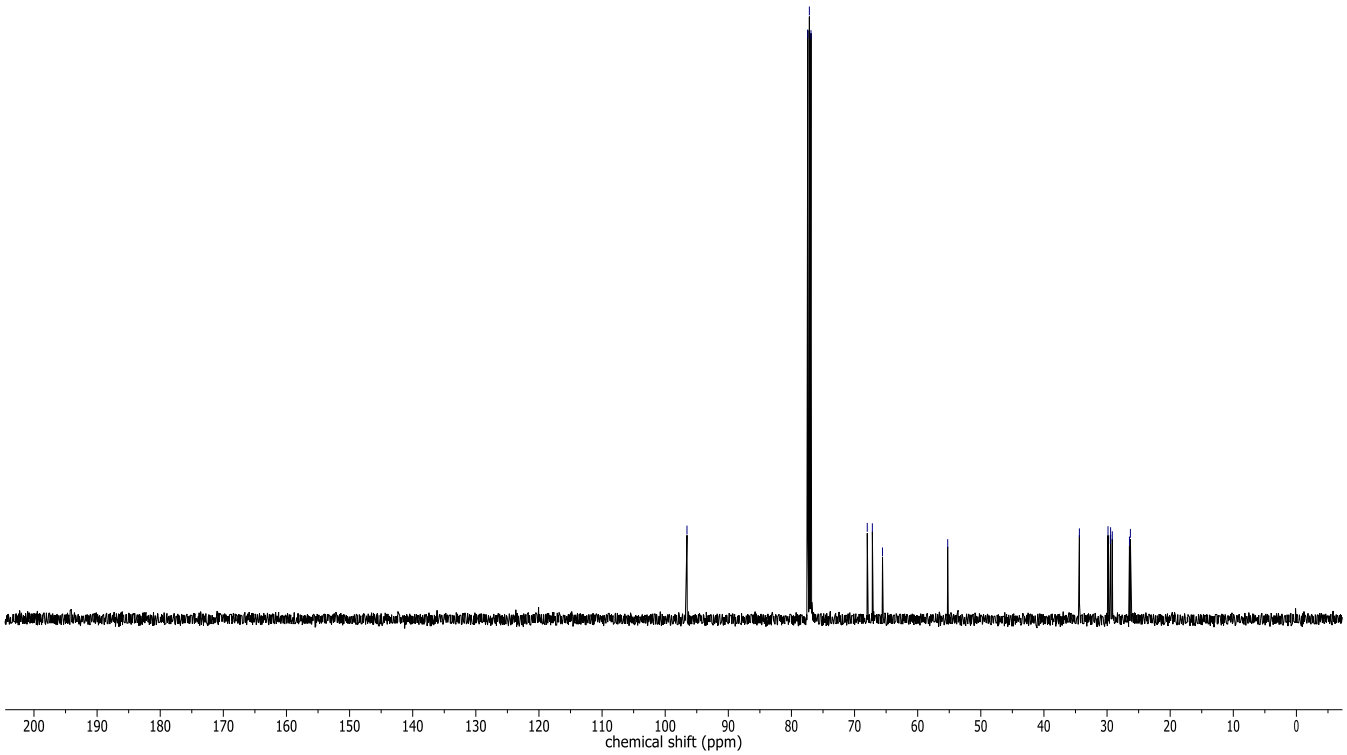
chemical shift (ppm)

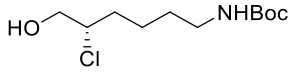
HO
NHBoc
Cl

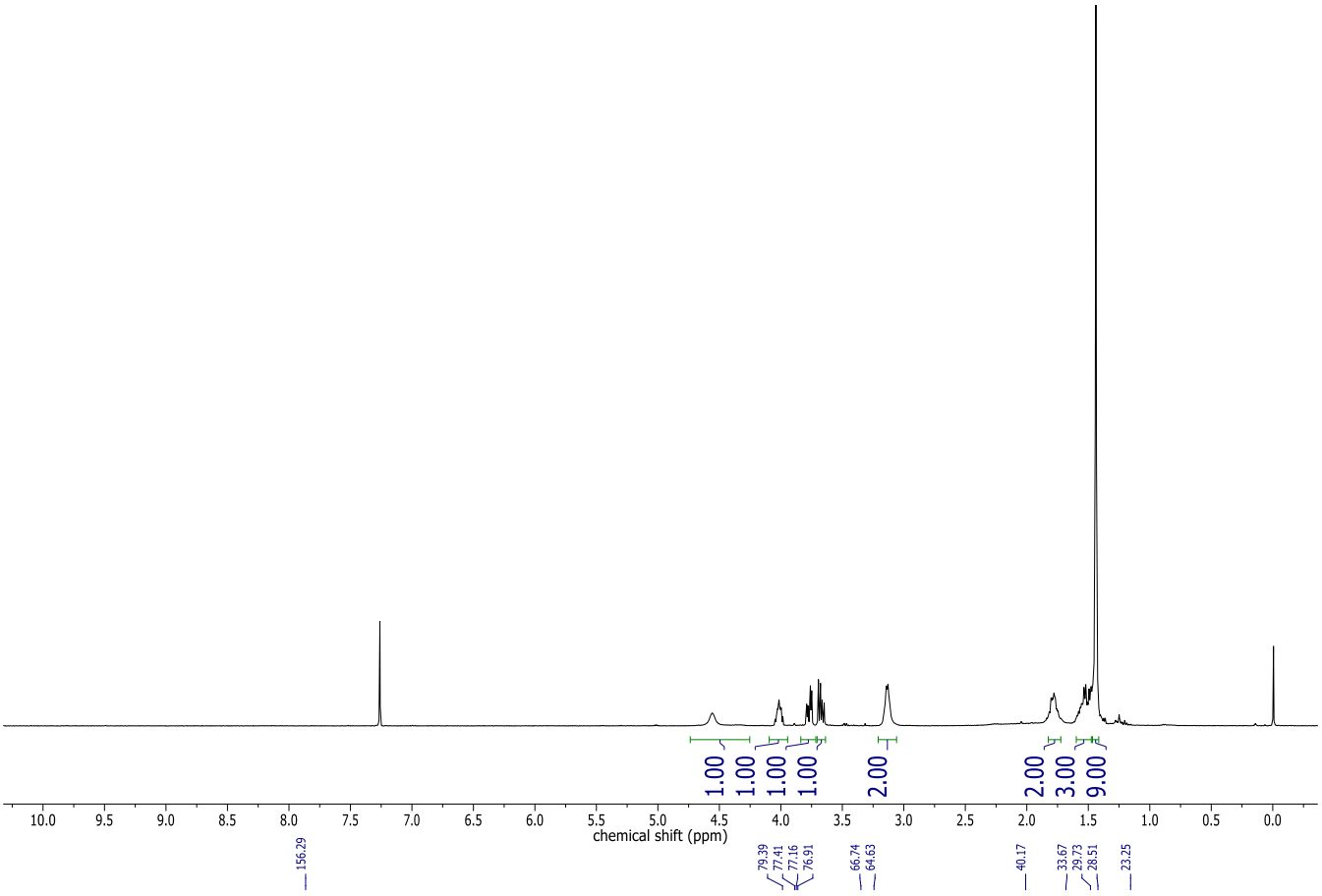
1.00
1.00
1.00
1.00
2.00
2.00
3.00
9.00
chemical shift (ppm)
156.29
79.39
77.41
77.16
76.91
66.74
64.63
40.17
33.67
29.73
28.51
23.25

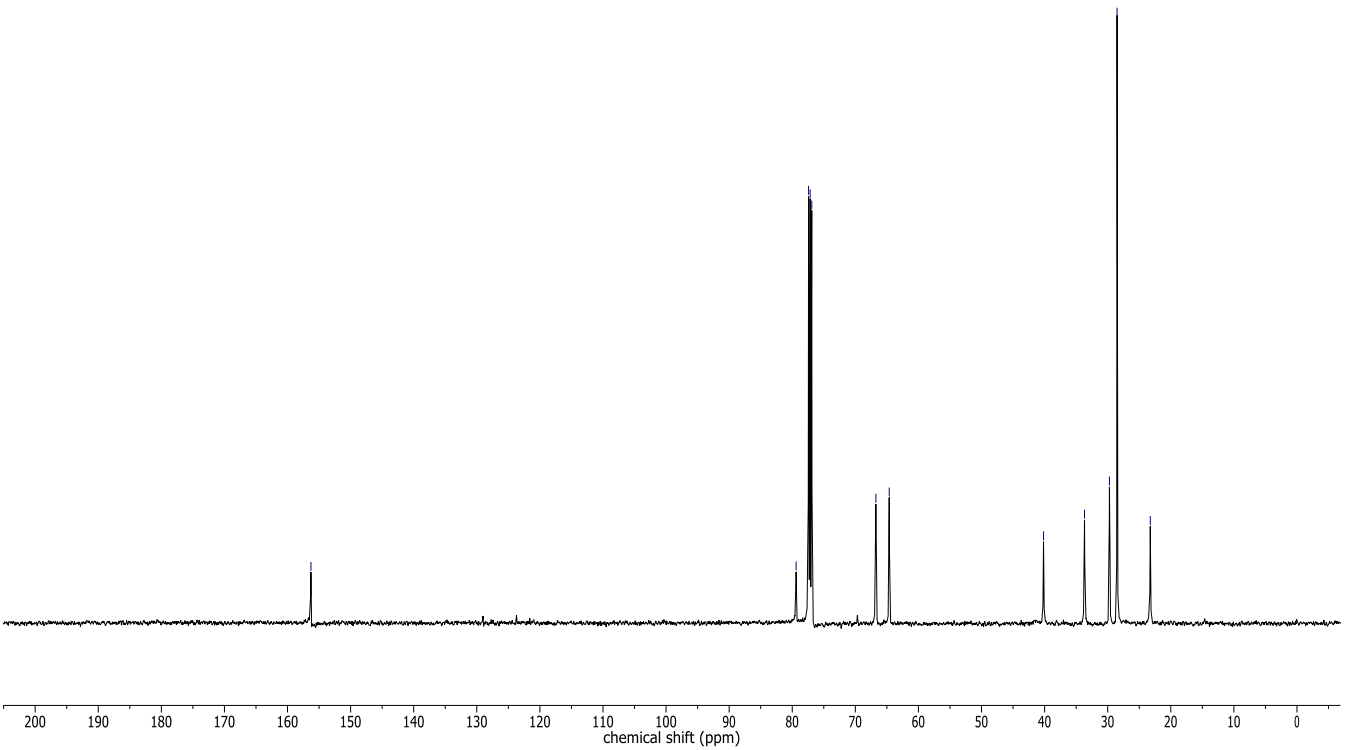
chemical shift (ppm)

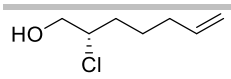
HO
Cl

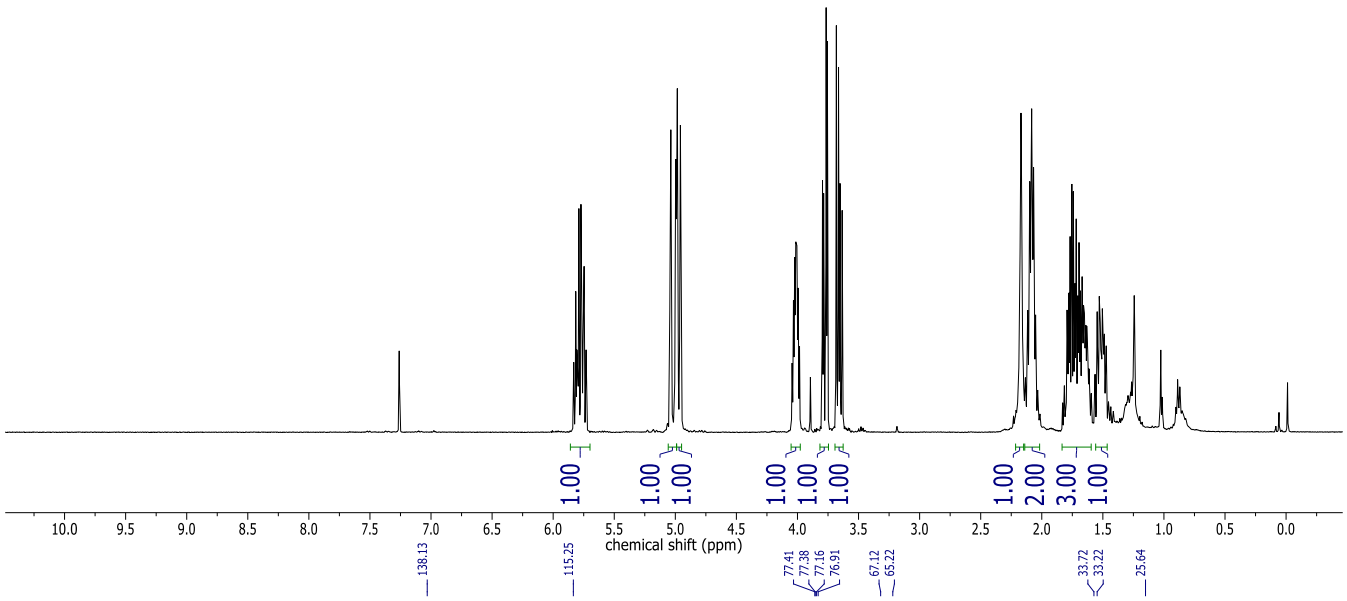
1.00
1.00
1.00
1.00
1.00
1.00
1.00
2.00
3.00
1.00
chemical shift (ppm)
138.13
115.25
77.41
77.38
77.16
76.91
67.12
65.22
33.72
33.22
25.64

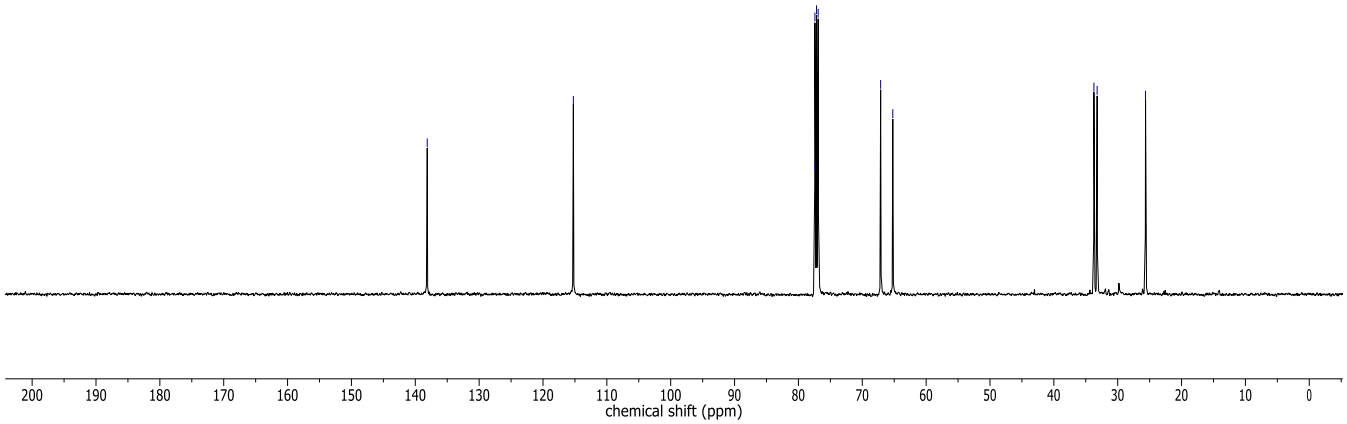
chemical shift (ppm)

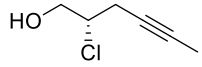
HO
Cl

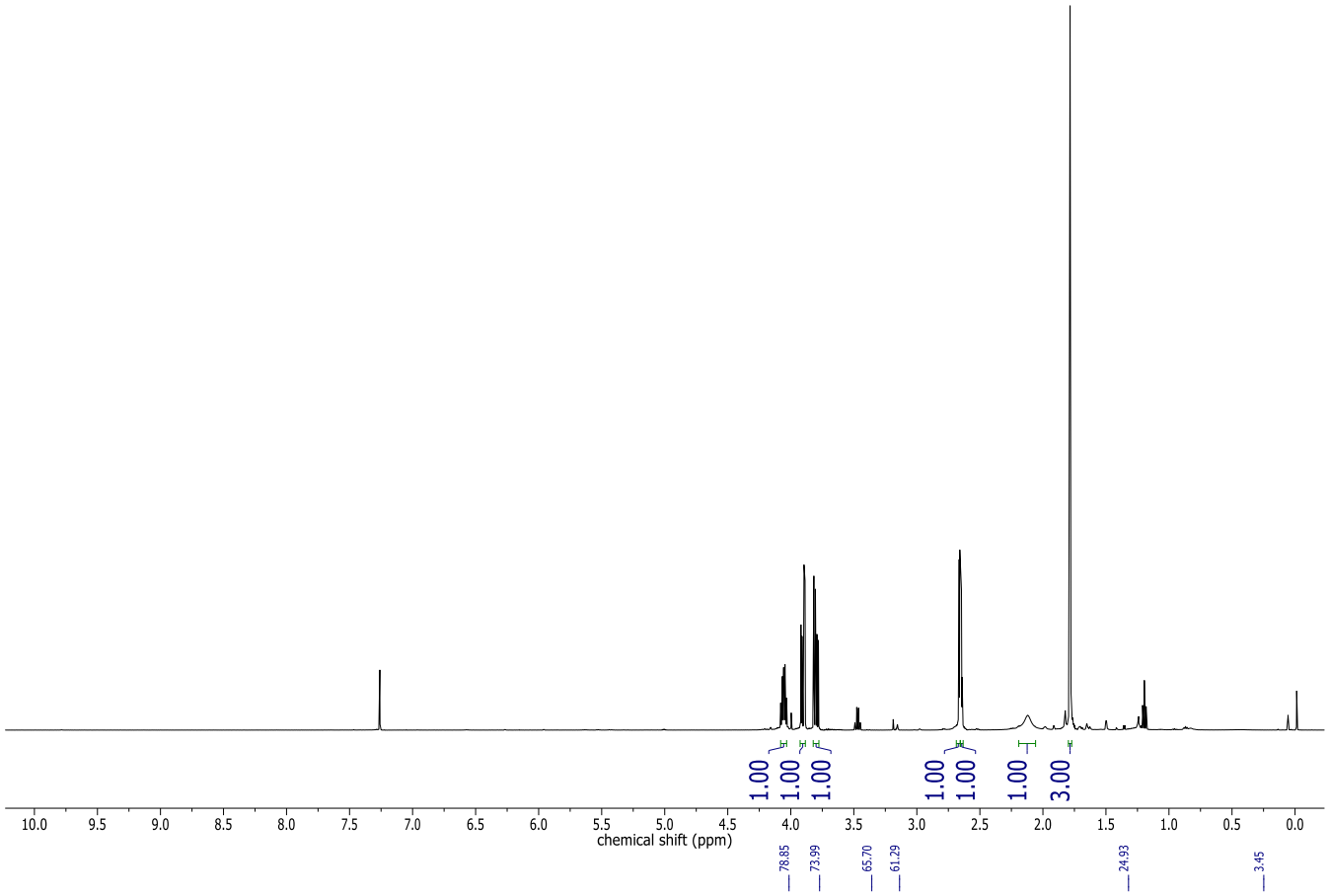
1.00
1.00
1.00
1.00
1.00
1.00
3.00
chemical shift (ppm)
78.85
73.99
65.70
61.29
24.93
3.45

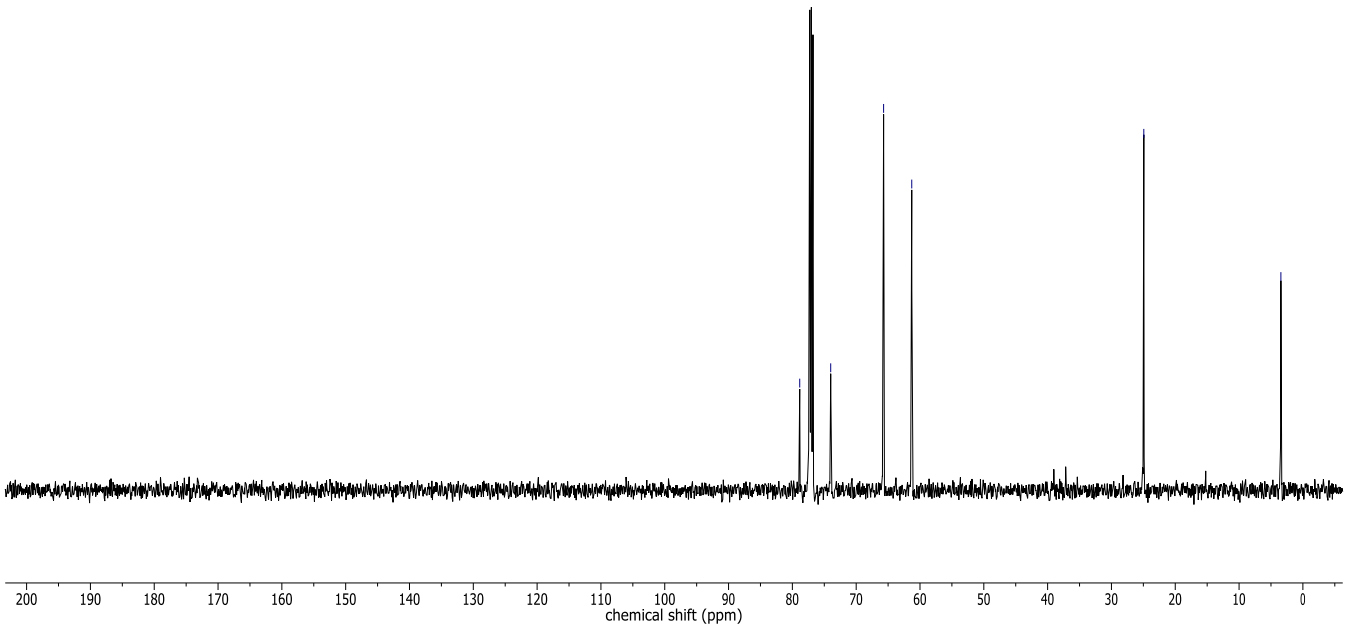
chemical shift (ppm)

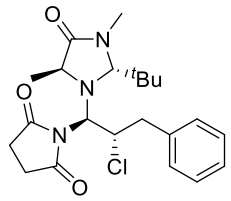
O
N
tBu
O
N
N
Cl
O

5.00
1.00
2.00
1.00
1.00
3.00
1.00
4.00
3.00
9.00
chemical shift (ppm)
179.49
176.66
175.58
137.10
129.41
128.54
127.08
84.81
71.52
60.48
58.32
38.60
31.79
28.07
28.03
11.55

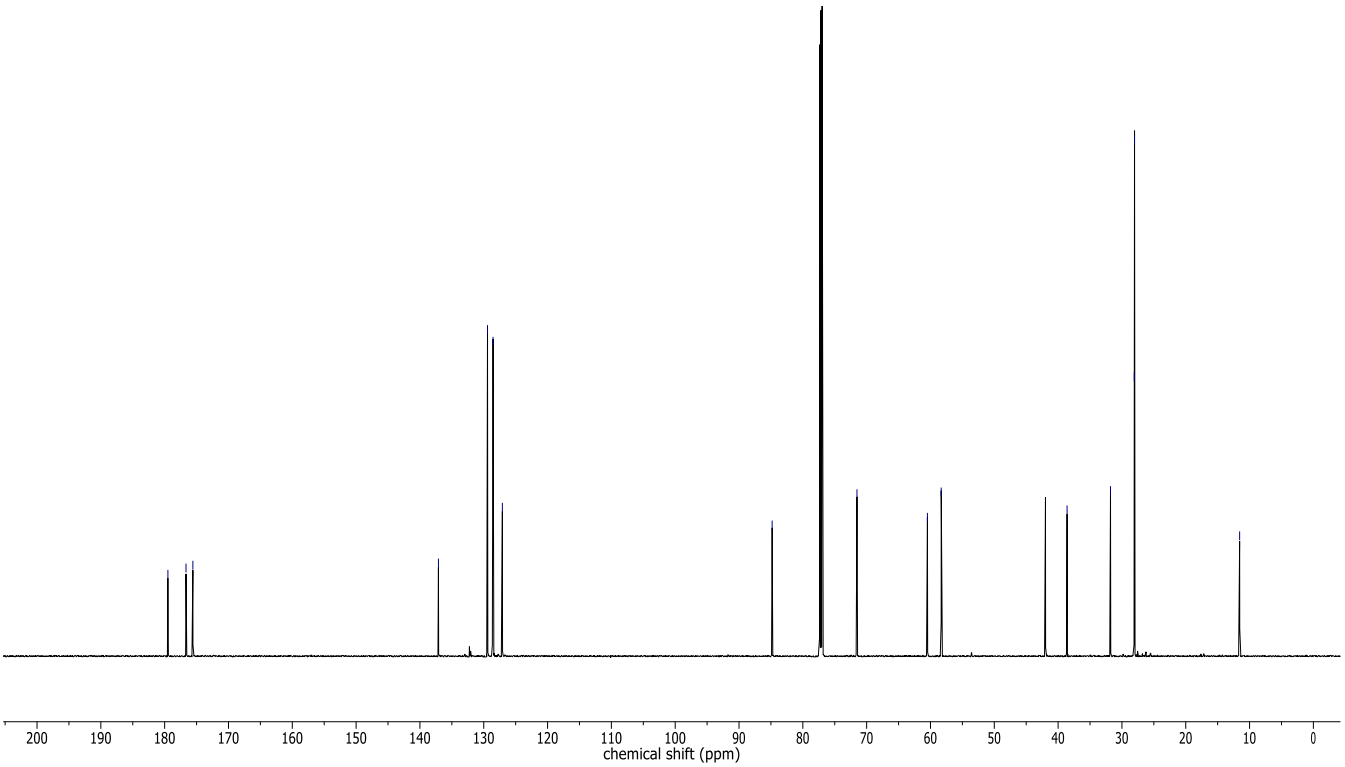
chemical shift (ppm)

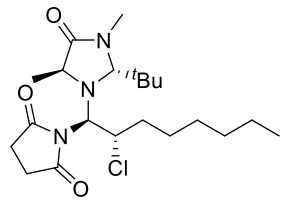
O
N
tBu
O
N
N
Cl
O

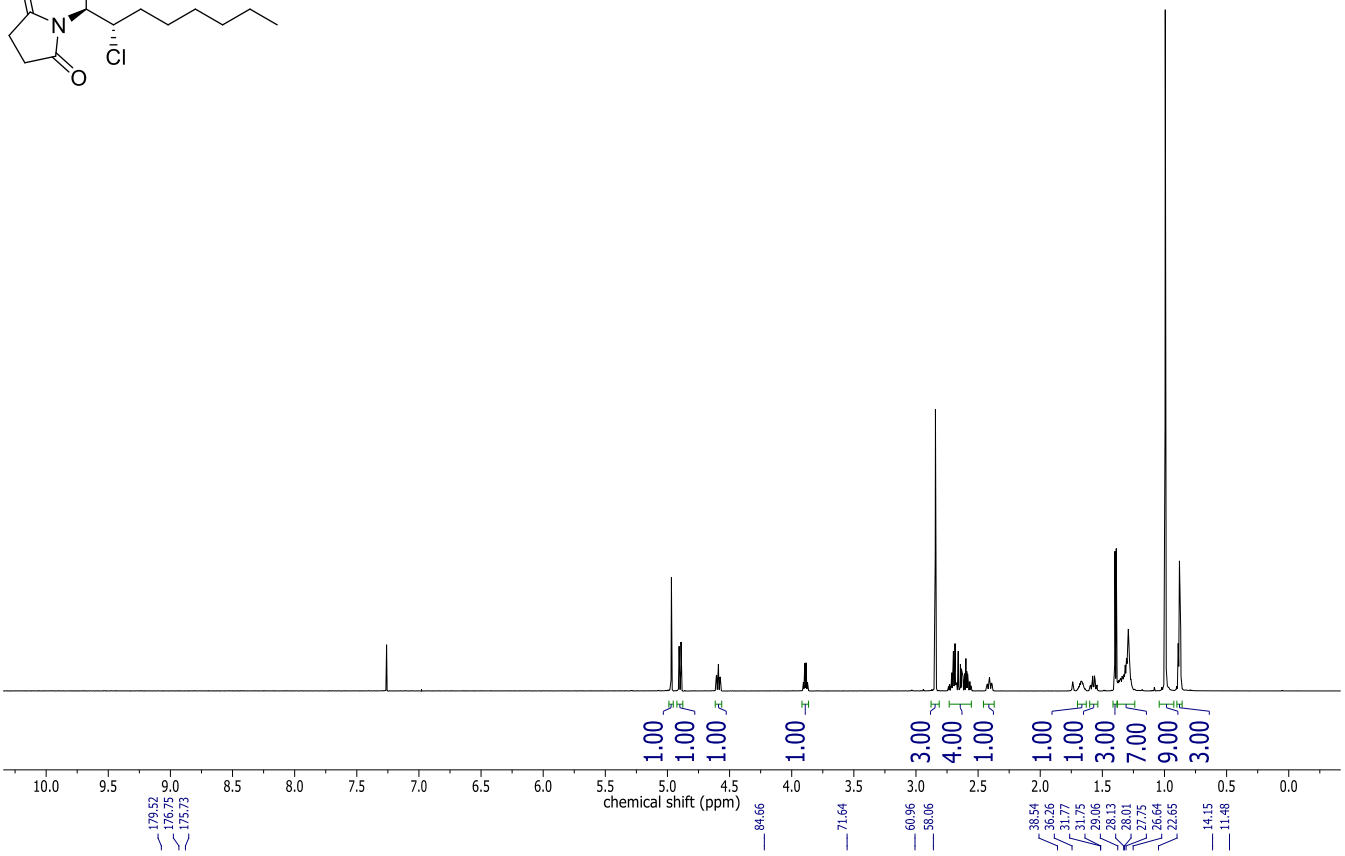
1.00
1.00
1.00
1.00
3.00
4.00
1.00
1.00
1.00
3.00
7.00
9.00
3.00
chemical shift (ppm)

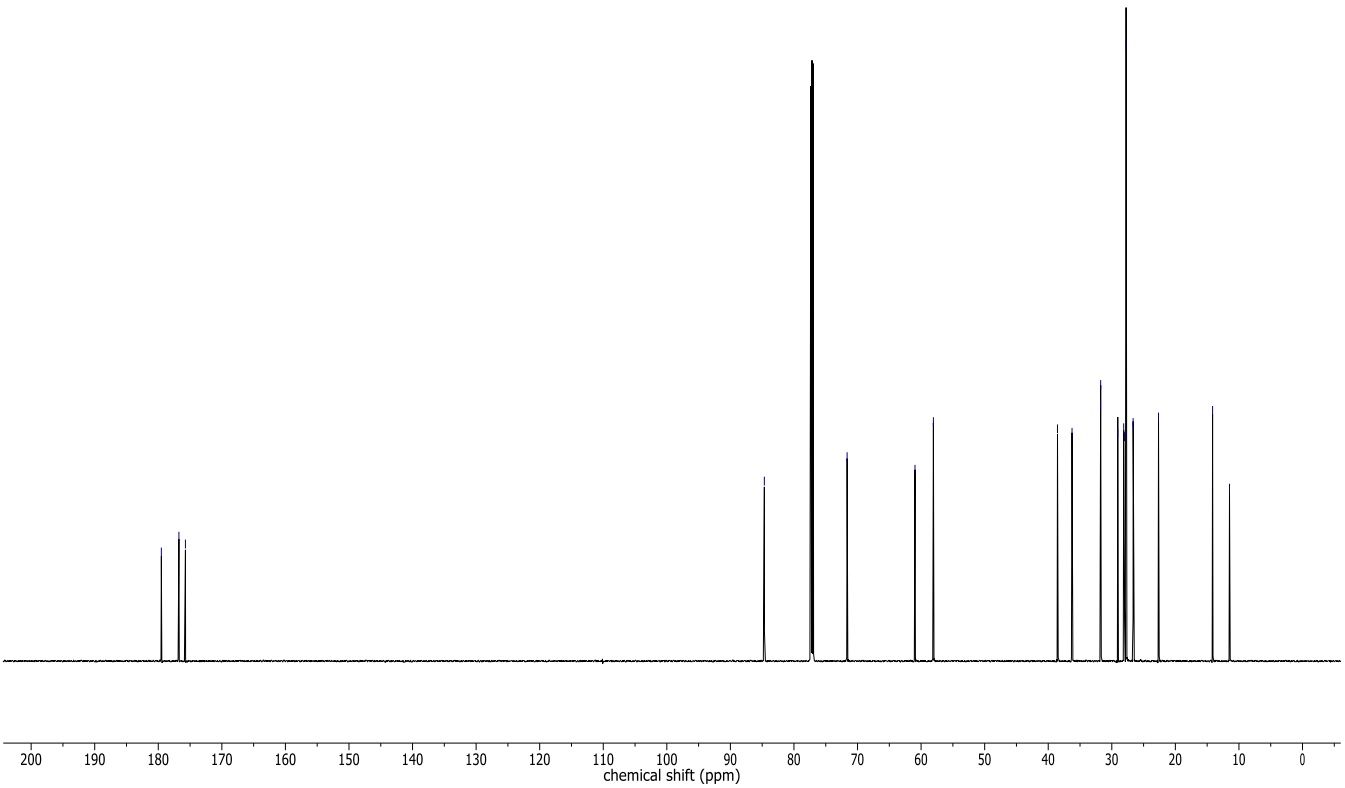
chemical shift (ppm)

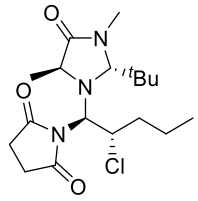
O
N
tBu
O
N
N
Cl
O

1.00
1.00
1.00
1.00
3.00
4.00
1.00
1.00
1.00
1.00
3.00
9.00
3.00
f1 (ppm)

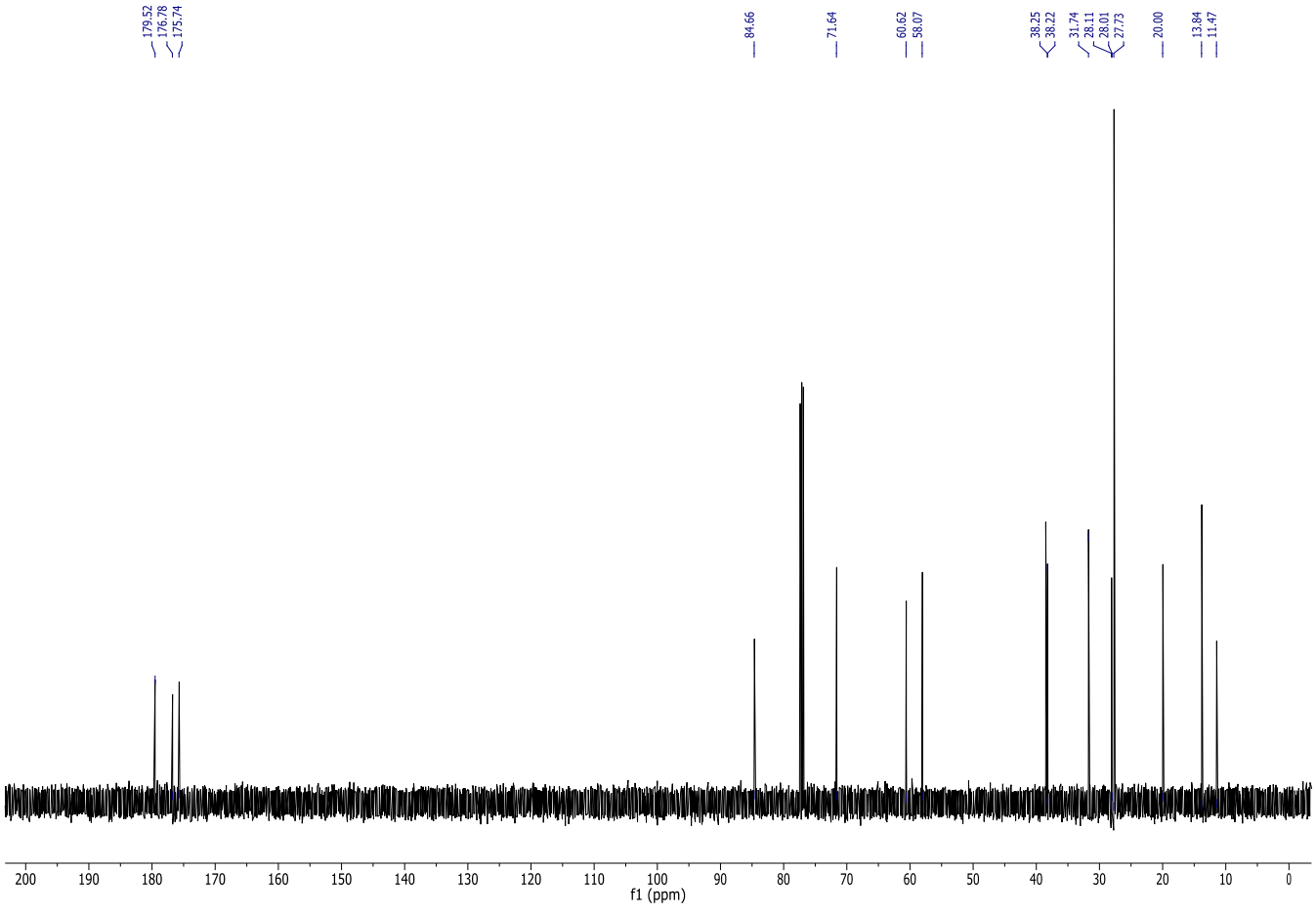
179.52
176.78
175.74
84.66
71.64
60.62
58.07
38.25
38.22
31.74
28.11
28.01
27.73
20.00
13.84
11.47
f1 (ppm)

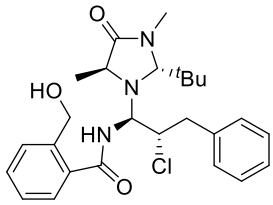
O
N
HO
N
tBu
HN
Cl
O

2.00
2.00
5.00
1.00
1.00
1.00
2.00
1.00
3.00
3.00
9.00
chemical shift (ppm)

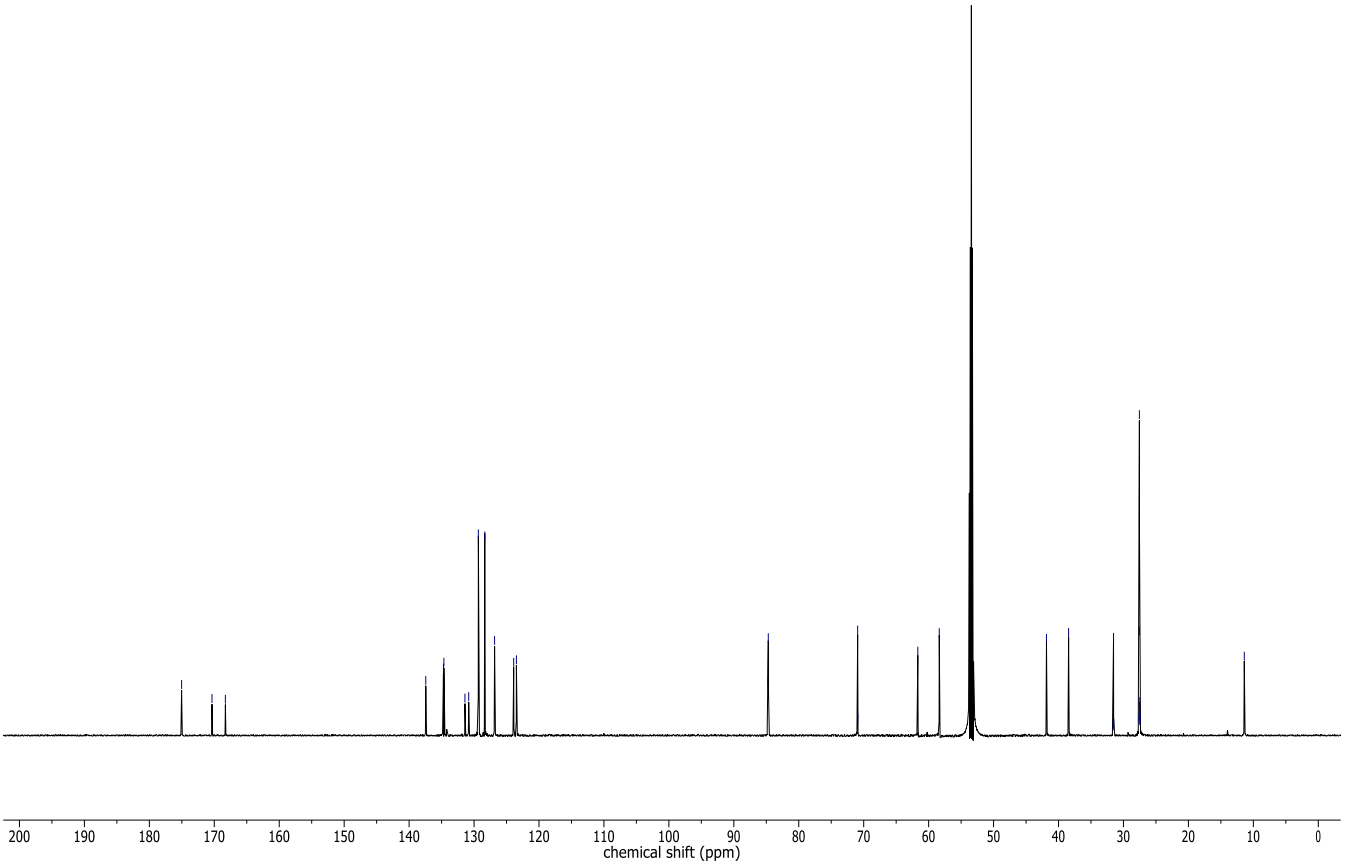
chemical shift (ppm)

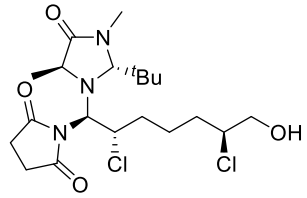
O
N
tBu
O
N
N
OH
Cl
Cl
O

1.00
1.00
1.00
1.00
1.00
1.00
1.00
3.00
4.00
1.00
3.00
2.00
3.00
9.00
chemical shift (ppm)
179.53
176.75
175.70
84.70
71.44
67.05
64.70
64.69
60.38
60.38
58.09
38.54
35.80
34.02
31.80
28.13
28.02
27.76
23.75
11.48

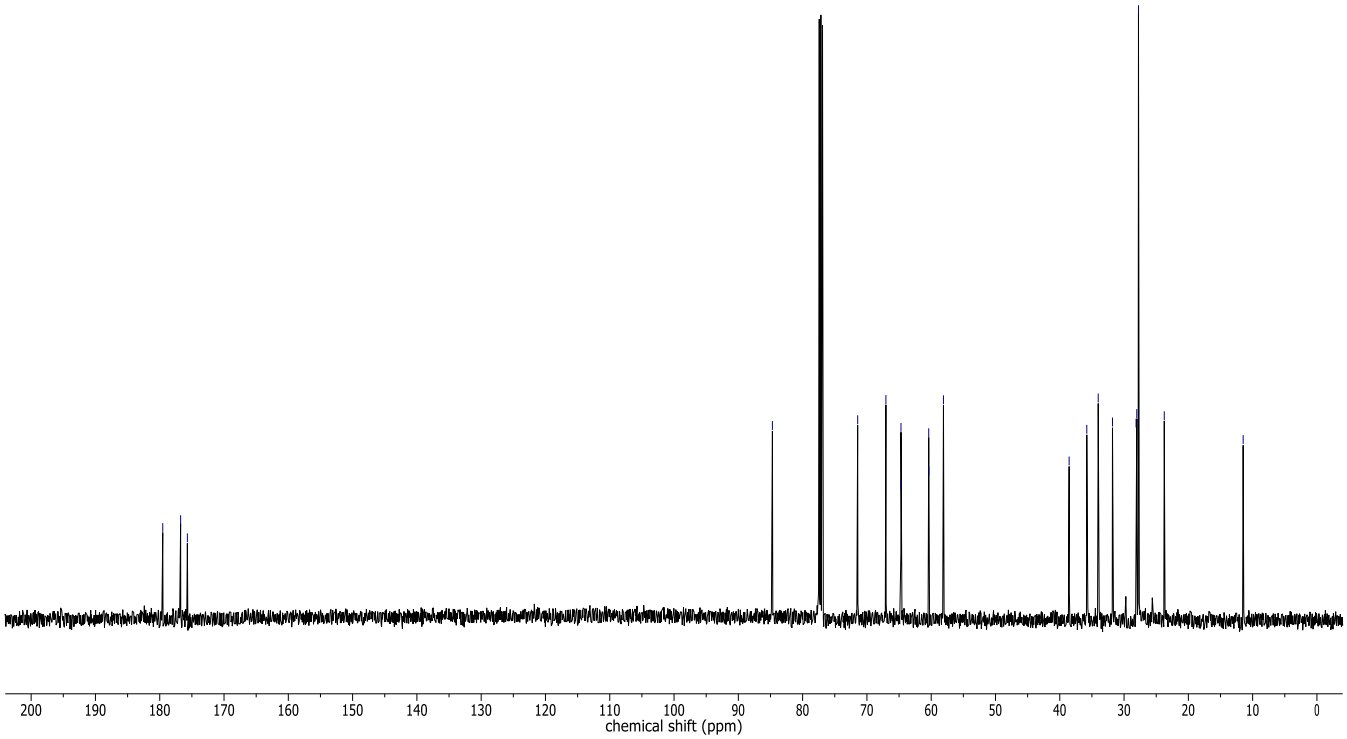
chemical shift (ppm)

5. HPLC /GC SPECTRA

2-Chlorooctan-1-ol

GC: Column: Hydrodex ß-6TBDAc; isotherm 110°C; flow 1,1ml; split 50:1; 2µl; FID 200°C

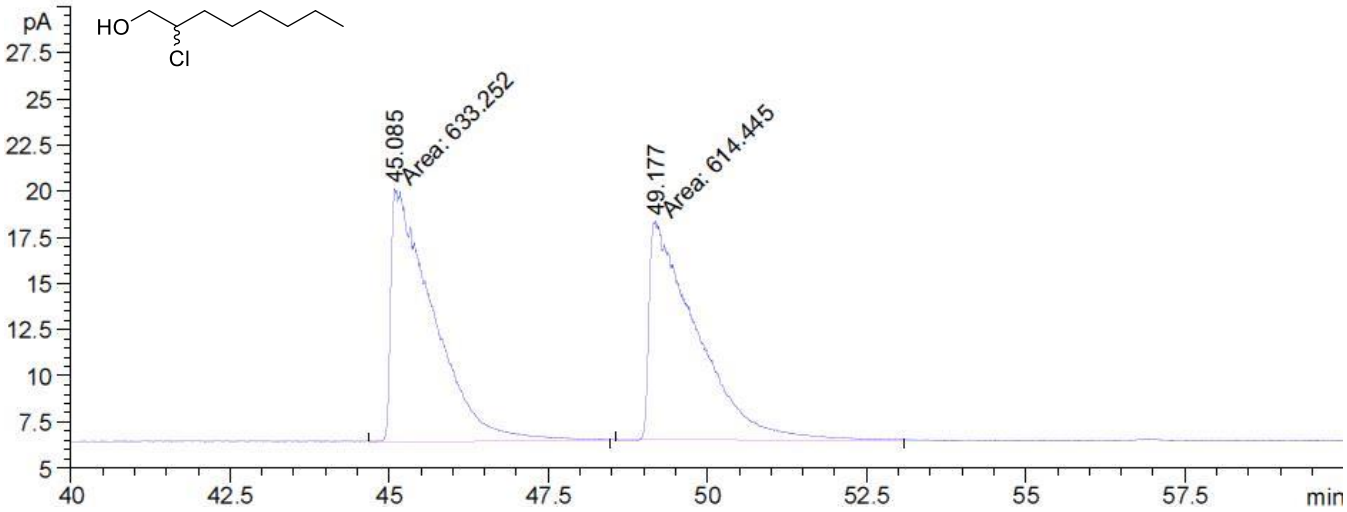

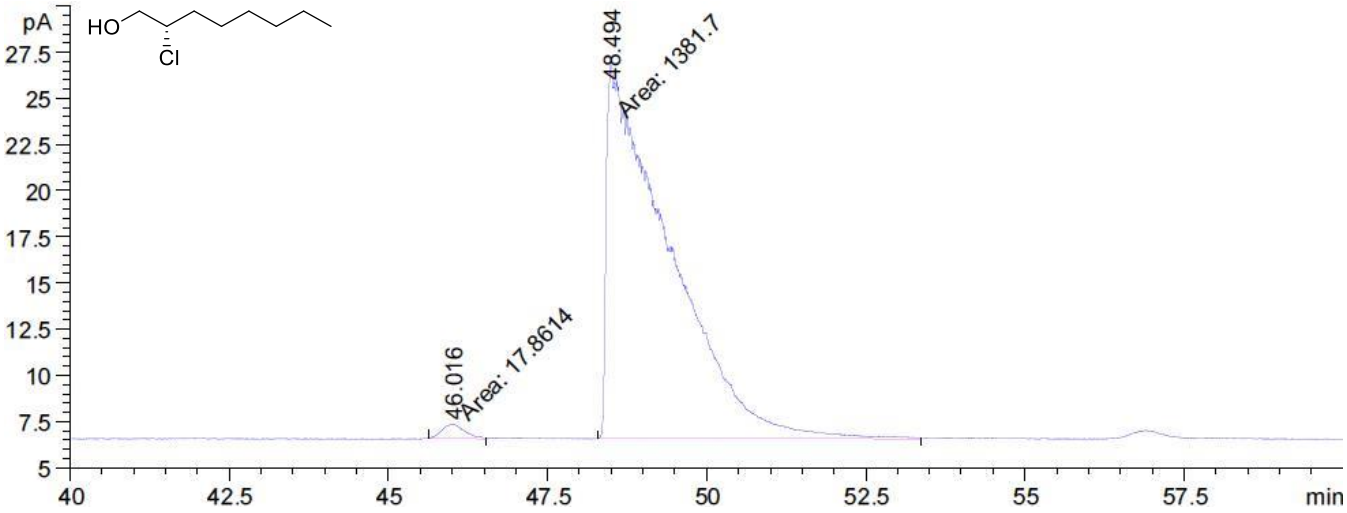

Peak #	RetTime [min]	Type	Width [min]	Area [pA*s]	Height [pA]	Area %
1	46.016	MM	0.3961	17.86141	7.51646e-1	1.27621
2	48.494	MM	1.1142	1381.70081	20.66835	98.72379

SUPPORTING INFORMATION

2,9-Dichlorodecane-1,10-diol

[measured for the di-(3-nitrobenzoate)-derivative]

HPLC: 0,8 ml/min, 20 % ethanol/hexane, 36 bar, Chiralpak IC

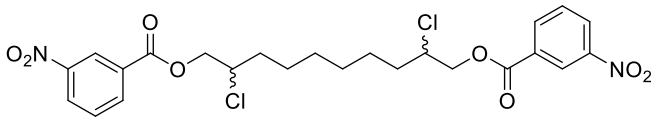

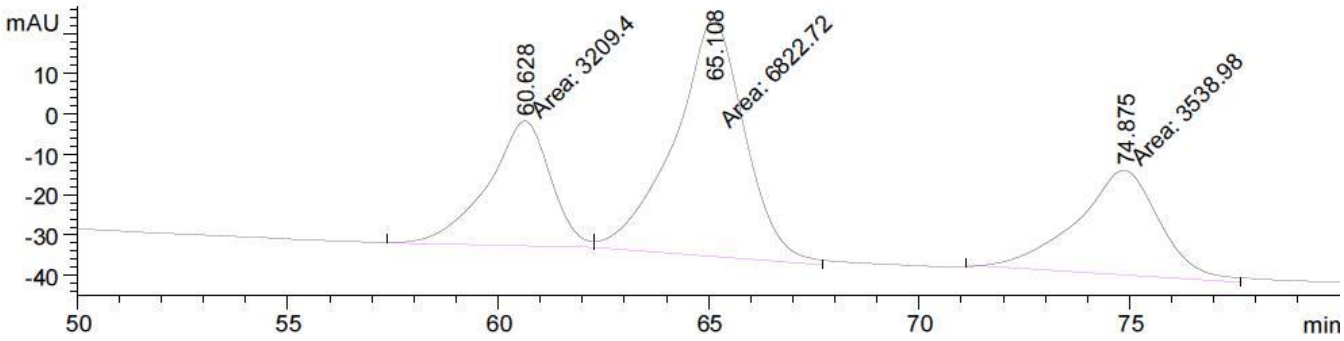

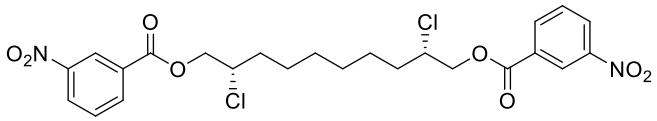

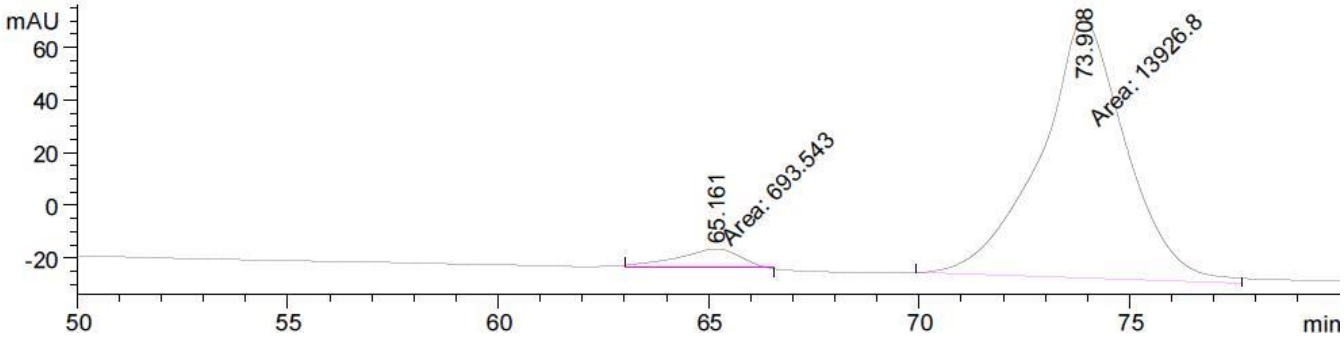

Peak #	RetTime [min]	Type	Width [min]	Area [mAU*s]	Height [mAU]	Area %
1	65.161	MM	1.6901	693.54321	6.83933	4.7437
2	73.908	MM	2.3574	1.39268e4	98.46339	95.2563

5-Bromo-2-chloropentan-1-ol

GC: Hydrodex-ß-6TBDAc, 170°C 1,1 ml/min He ; FID300°, Split 50:1

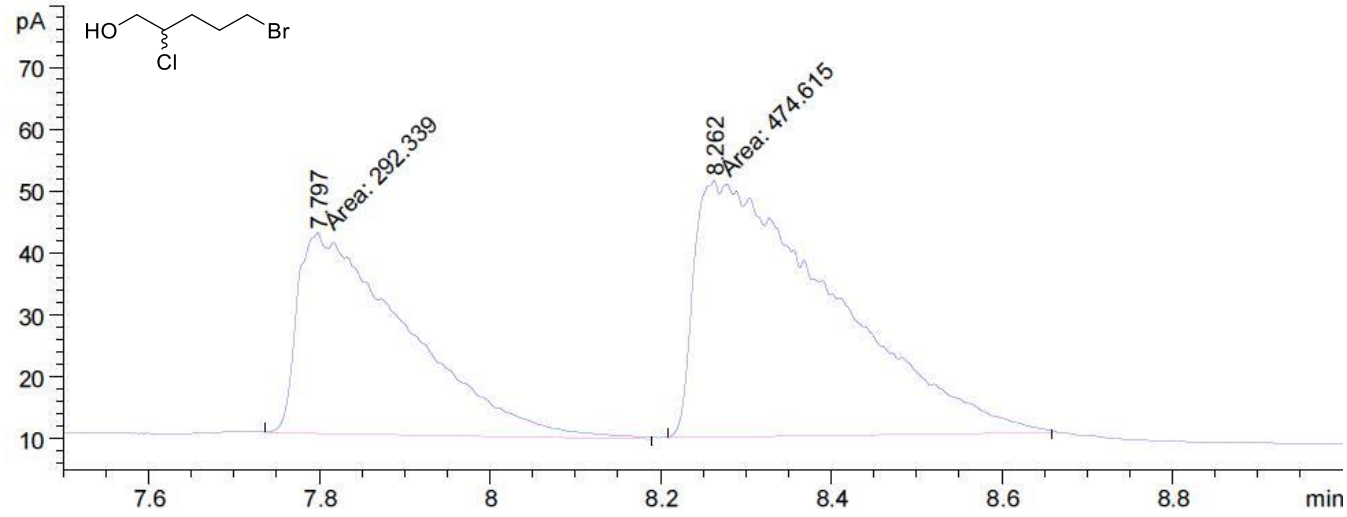

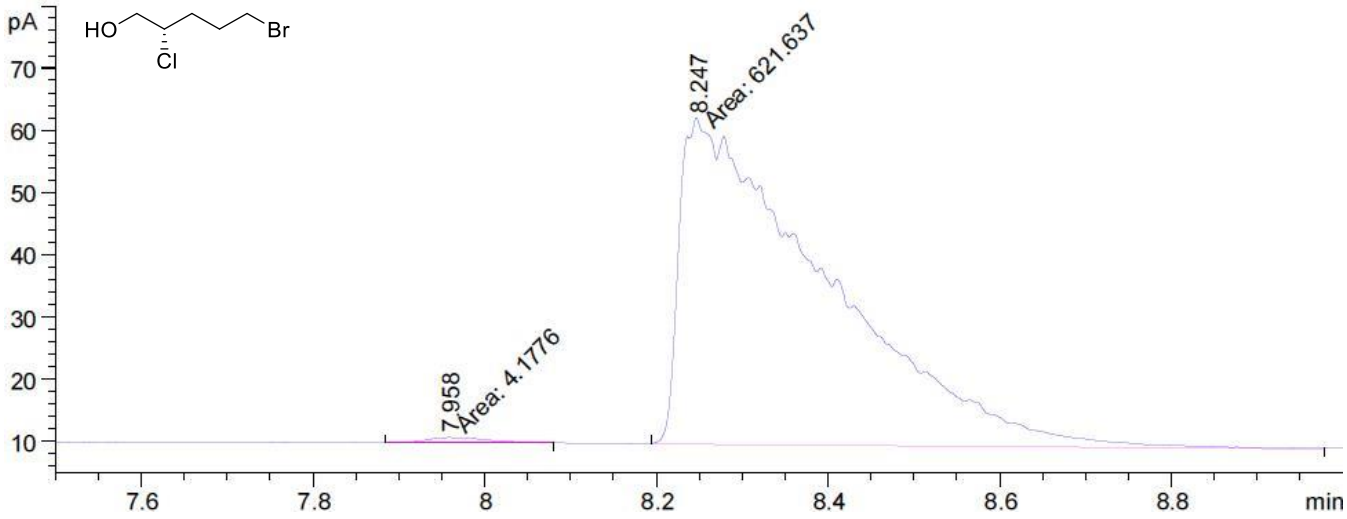

Peak #	RetTime [min]	Type	Width [min]	Area [pA*s]	Height [pA]	Area %
1	7.958	MM	0.0818	4.17760	8.50743e-1	0.66755
2	8.247	MM	0.1977	621.63721	52.39968	99.33245

SUPPORTING INFORMATION

10-((*tert*-Butyldiphenylsilyl)oxy)-2-chlorodecan-1-ol

[measured for the di-(3-nitrobenzoate)-derivative]

HPLC: 0,8 ml/min, 2 % ethyl acetate/hexane, 28 bar, Chiralpak IA

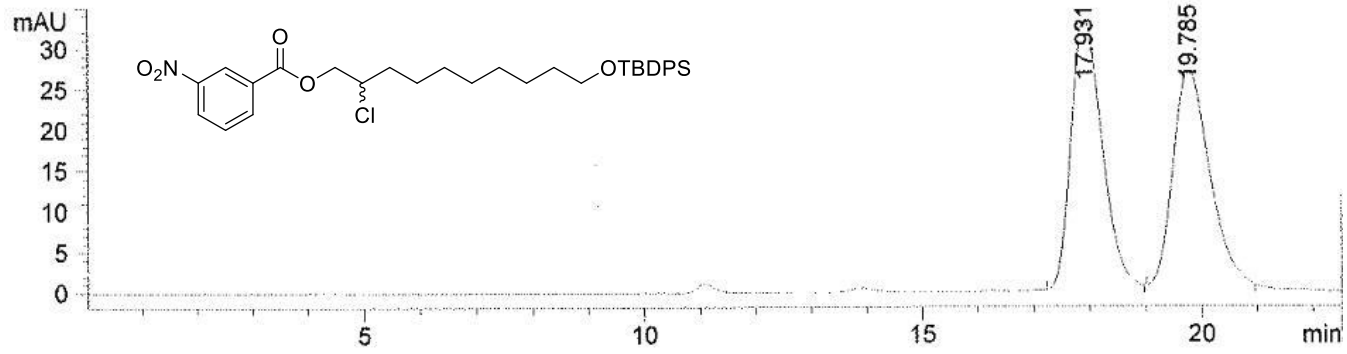

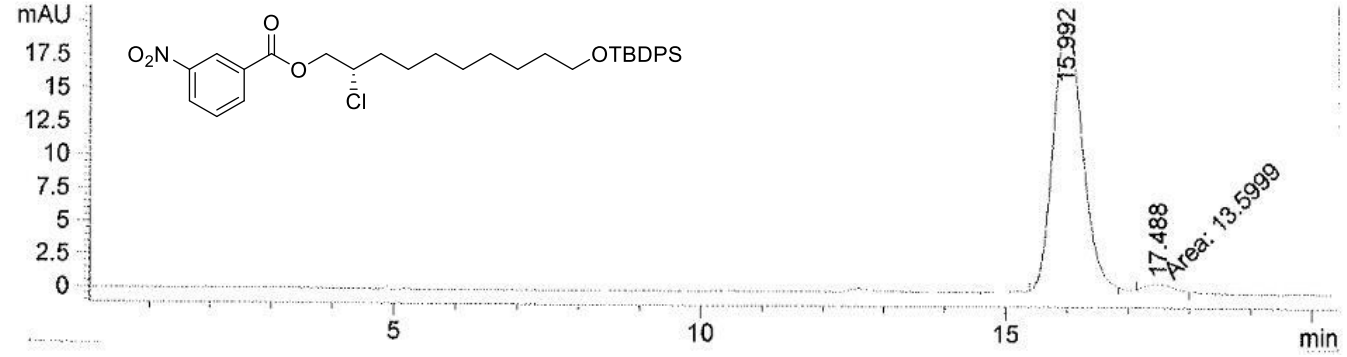

Peak #	RetTime [min]	Type	Width [min]	Area [mAU*s]	Height [mAU]	Area %
1	15.992	BB	0.5122	666.73358	20.24400	98.0010
2	17.488	MM	0.4768	13.59995	4.75433e-1	1.9990

SUPPORTING INFORMATION

9-Chloro-10-hydroxydecylacetate

GC: Hydrodex-ß-6TBDAc, 160°C 1,1 ml/min He ; FID200°, Split 50:1; 2µl

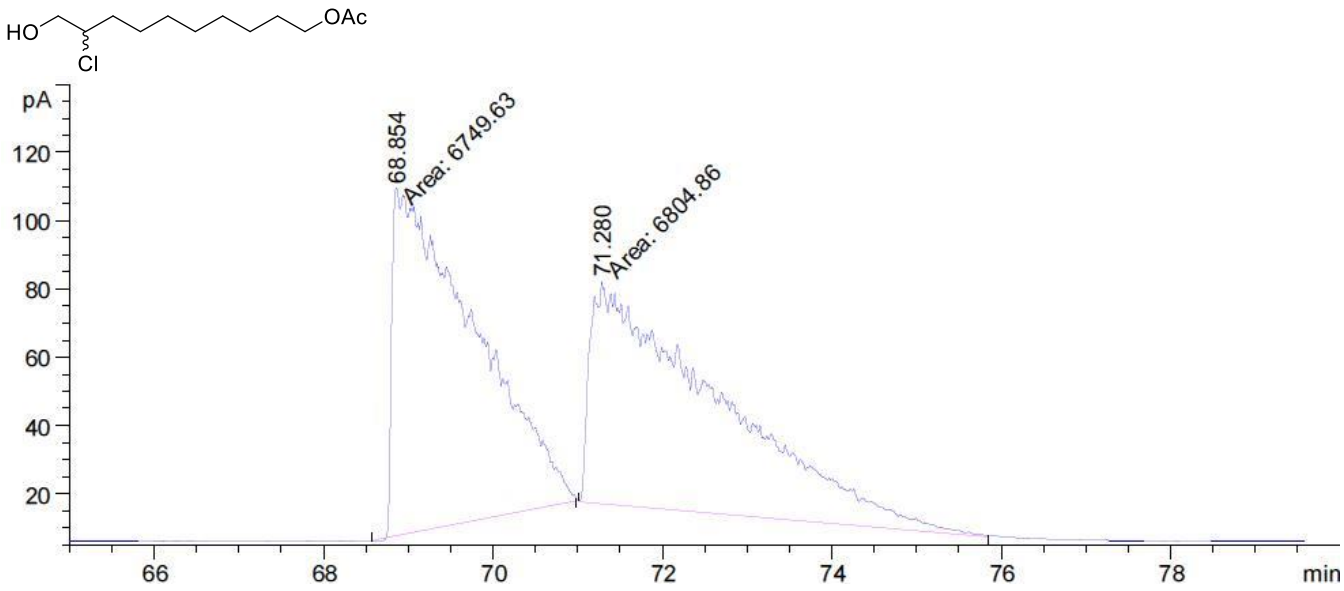

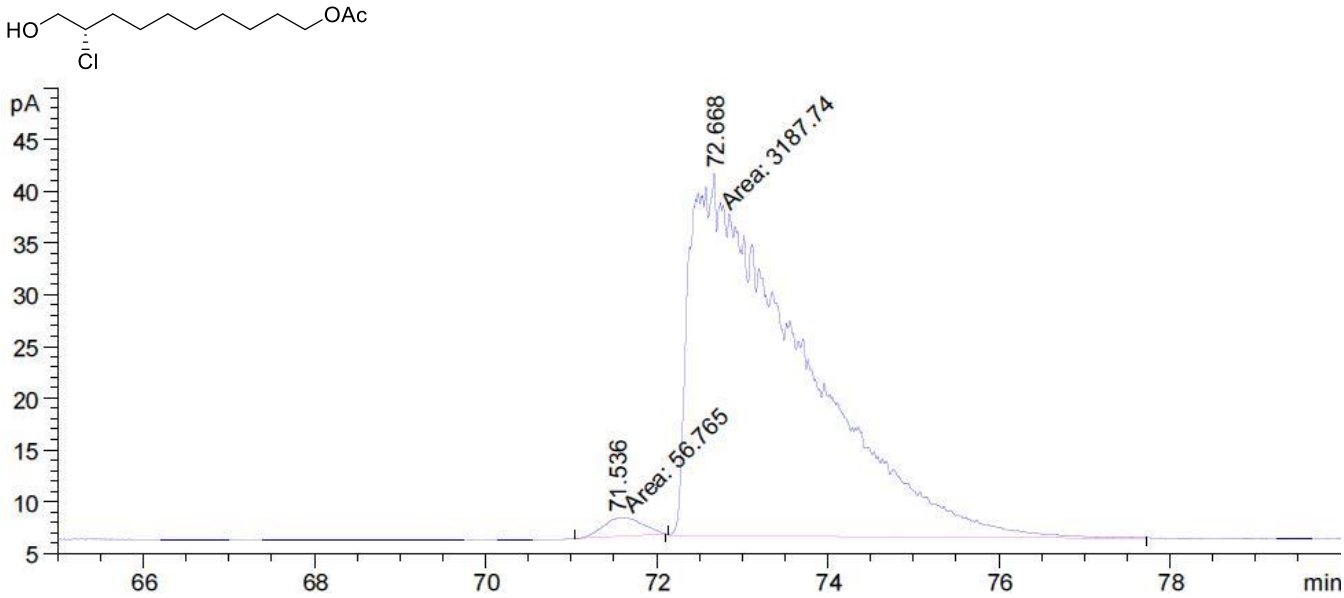

Peak #	RetTime [min]	Type	Width [min]	Area [pA*s]	Height [pA]	Area %
1	71.536	MM	0.5212	56.76500	1.81531	1.74957
2	72.668	MM	1.5169	3187.74097	35.02524	98.25043

SUPPORTING INFORMATION

2-Chloro-10-(methoxymethoxy)decan-1-ol

GC: Hydrodex-ß-6TBDAc, 155°C, 1,1 ml/min, He, FID200°, Split 50:1, 2µl

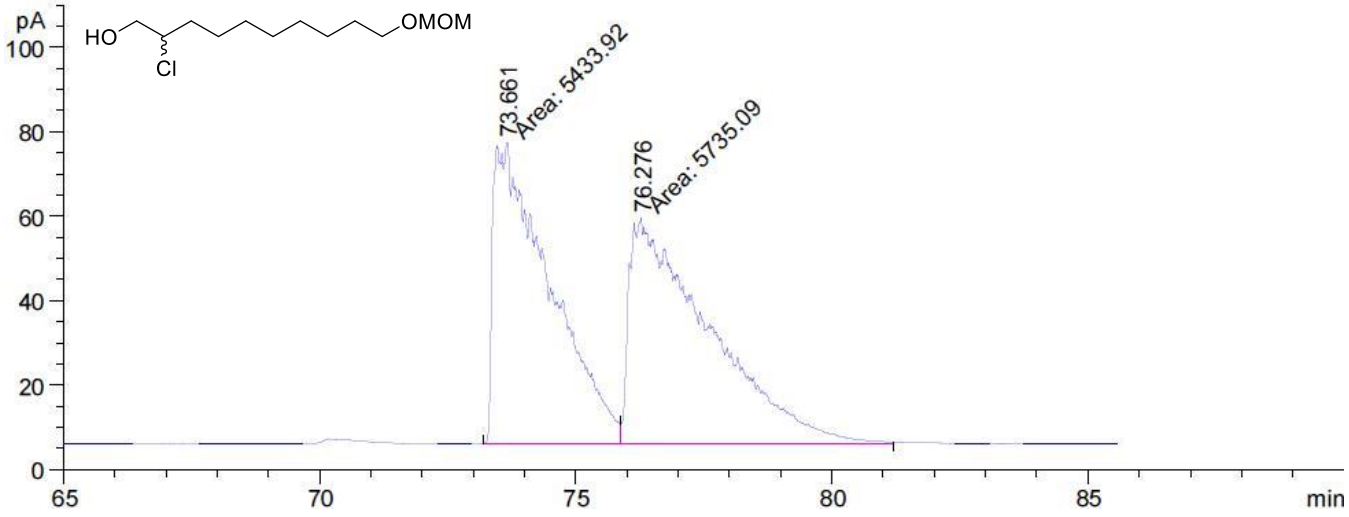

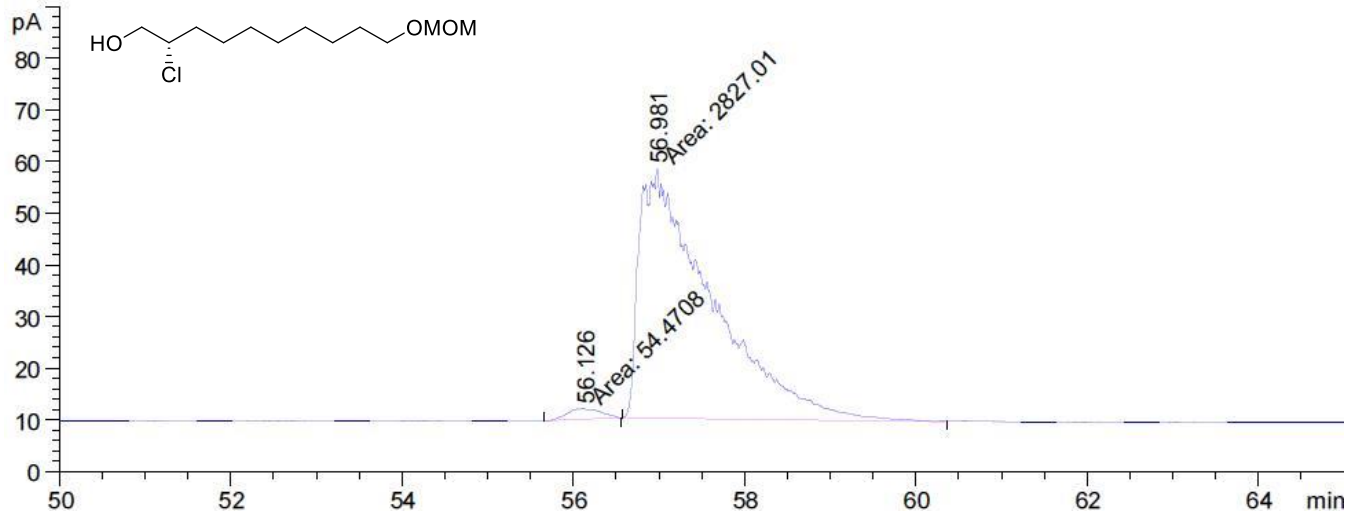

Peak #	RetTime [min]	Type	Width [min]	Area [pA*s]	Height [pA]	Area %
1	56.126	MM	0.4422	54.47081	2.05319	1.89038
2	56.981	MM	0.9768	2827.00879	48.23423	98.10962

SUPPORTING INFORMATION

***tert*-Butyl(5-chloro-6-hydroxyhexyl)carbamate**

GC: Hydrodex-ß-6TBDAc, 180°C 1,1 ml/min He, FID300°, Split 50:1

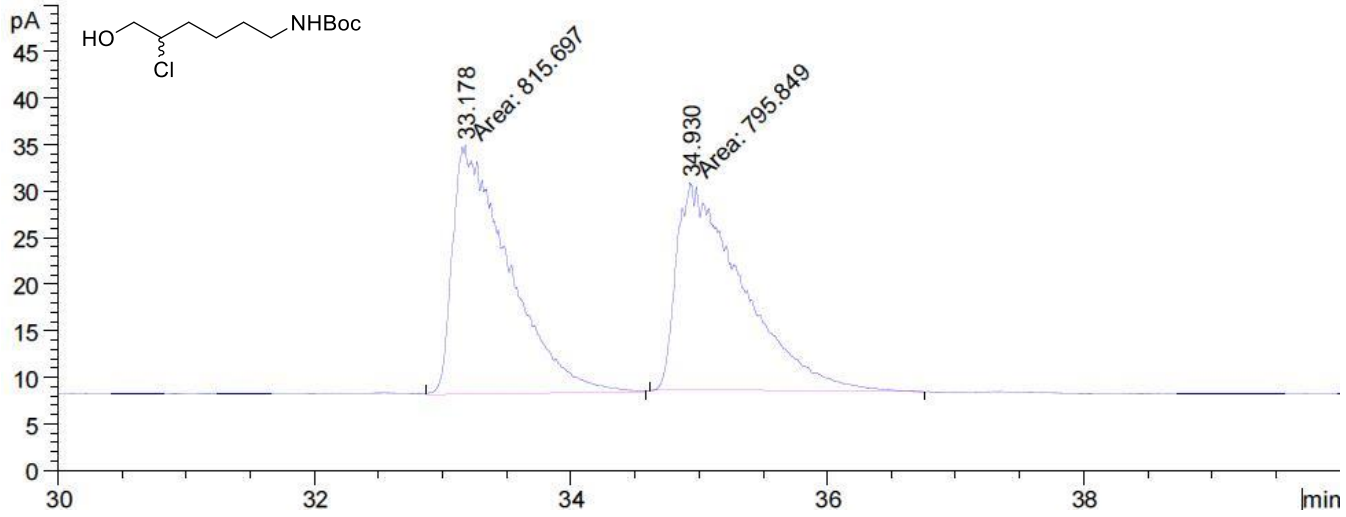

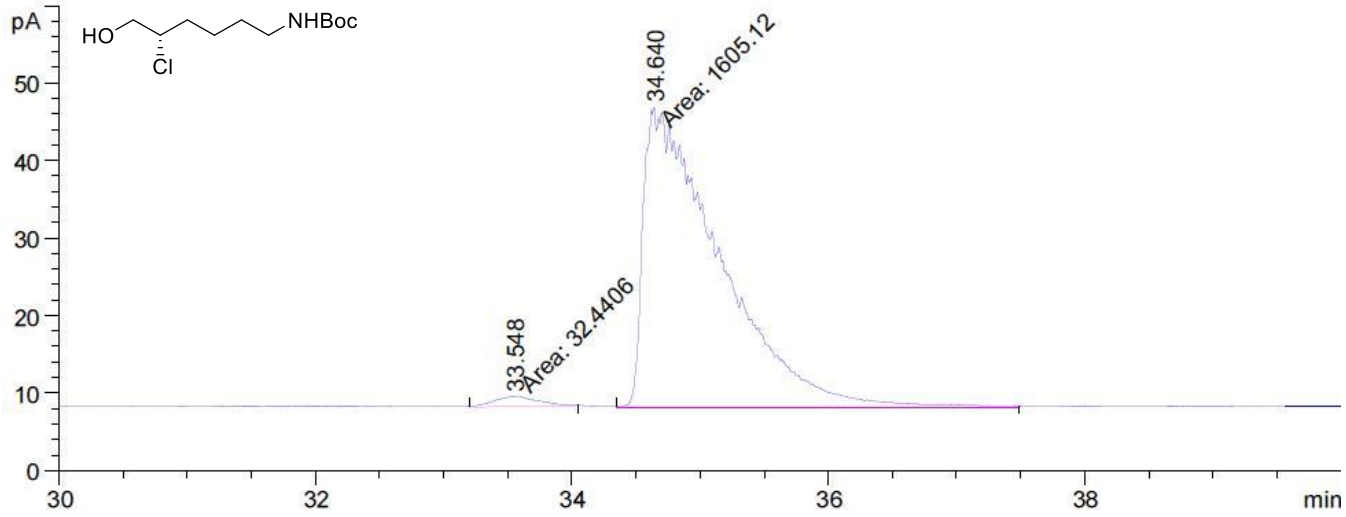

Peak #	RetTime [min]	Type	Width [min]	Area [pA*s]	Height [pA]	Area %
1	33.548	MM	0.3988	32.44061	1.35589	1.98103
2	34.640	MM	0.6910	1605.11829	38.71623	98.01897

2-Chloro-3-phenylpropan-1-ol

HPLC: 5% ethanol/hexane, Chiralpak IA, 0,8 ml/min, 29 bar

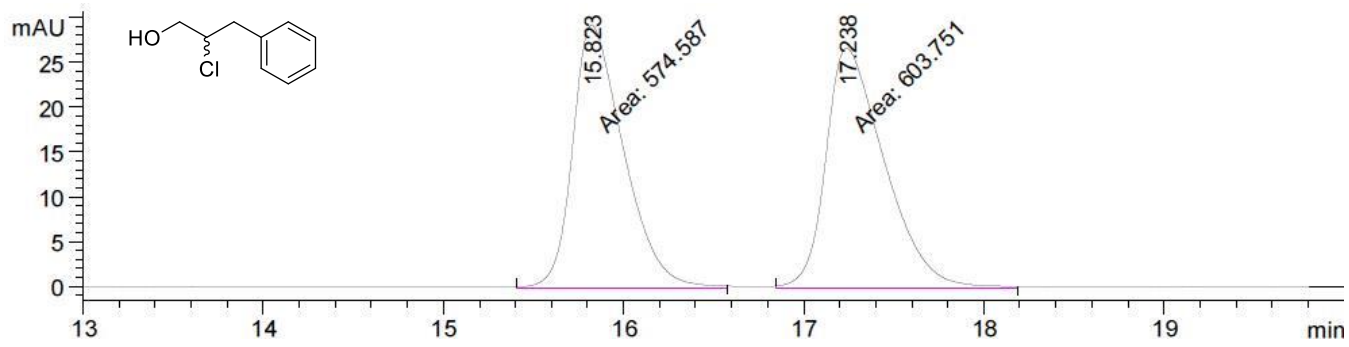

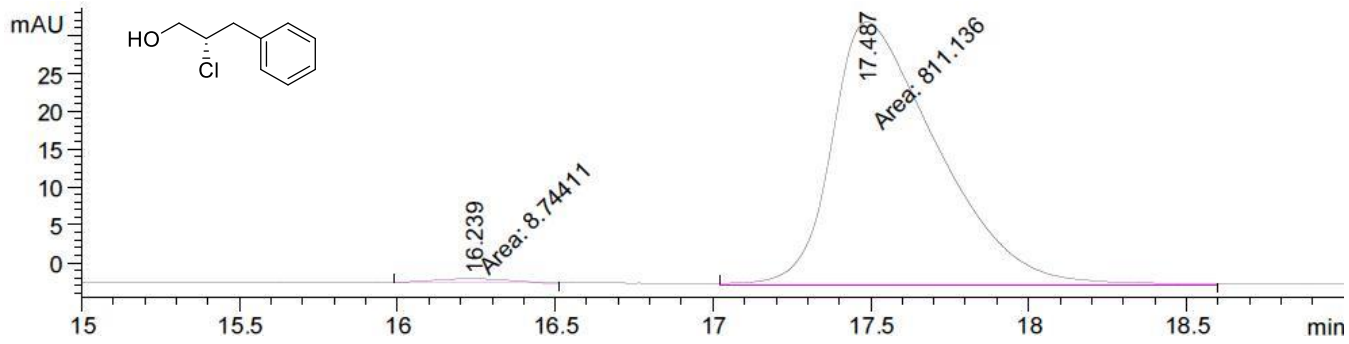

Peak #	RetTime [min]	Type	Width [min]	Area [mAU*s]	Height [mAU]	Area %
1	16.239	MM	0.2825	8.74411	5.15958e-1	1.0665
2	17.487	MM	0.3897	811.13605	34.69317	98.9335

2-Chlorohept-6-en-1-ol

GC: Hydrodex-ß-6TBDAc,100°C, 1,1 ml/min He, FID300°, Split 50:1, 2µl

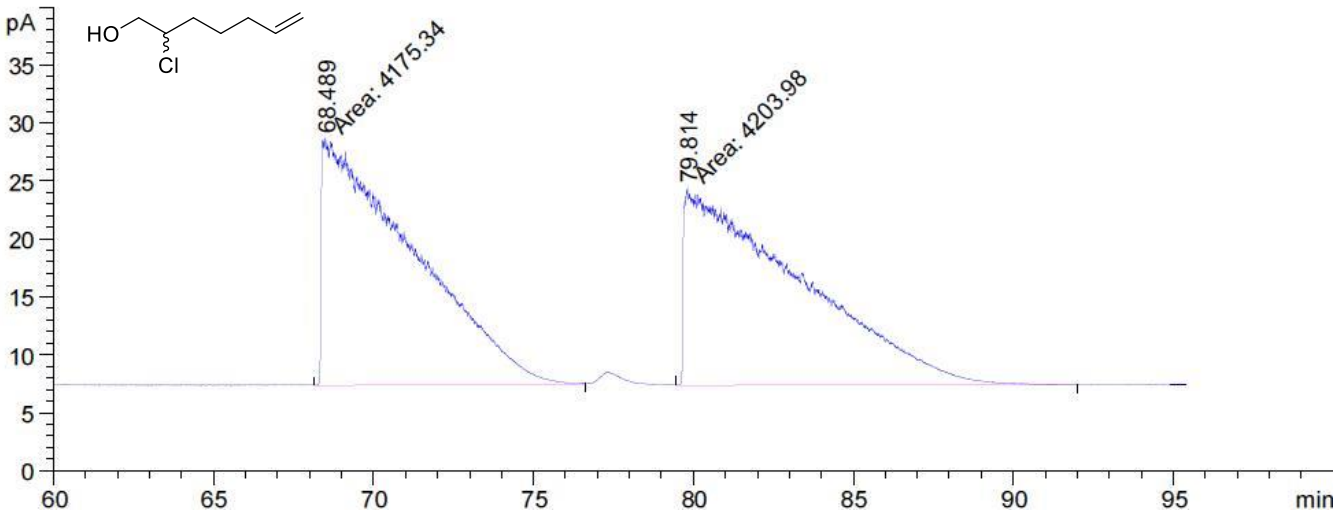

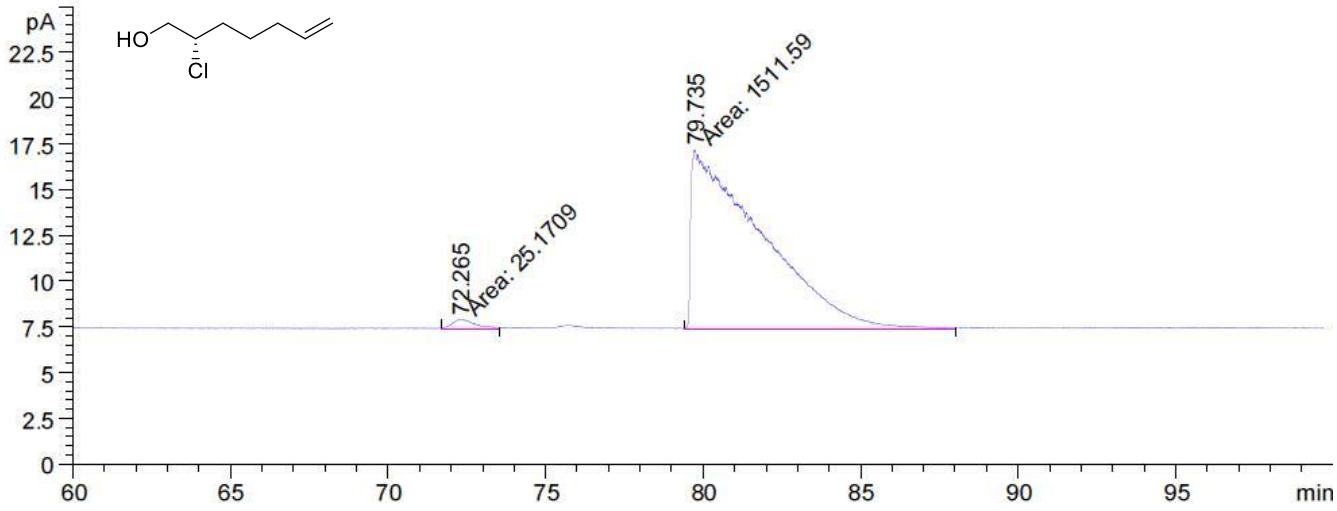

Peak #	RetTime [min]	Type	Width [min]	Area [pA*s]	Height [pA]	Area %
1	72.265	MM	0.8663	25.17089	4.84287e-1	1.63792
2	79.735	MM	2.5801	1511.59119	9.76456	98.36208

SUPPORTING INFORMATION

2-Chloro-3,7-dimethyloct-6-en-1-ol

GC: Hydrodex-ß-TBDA, isotherm 180°C, 0,6 ml/min He, FID200°, Split 50:1, 2µl

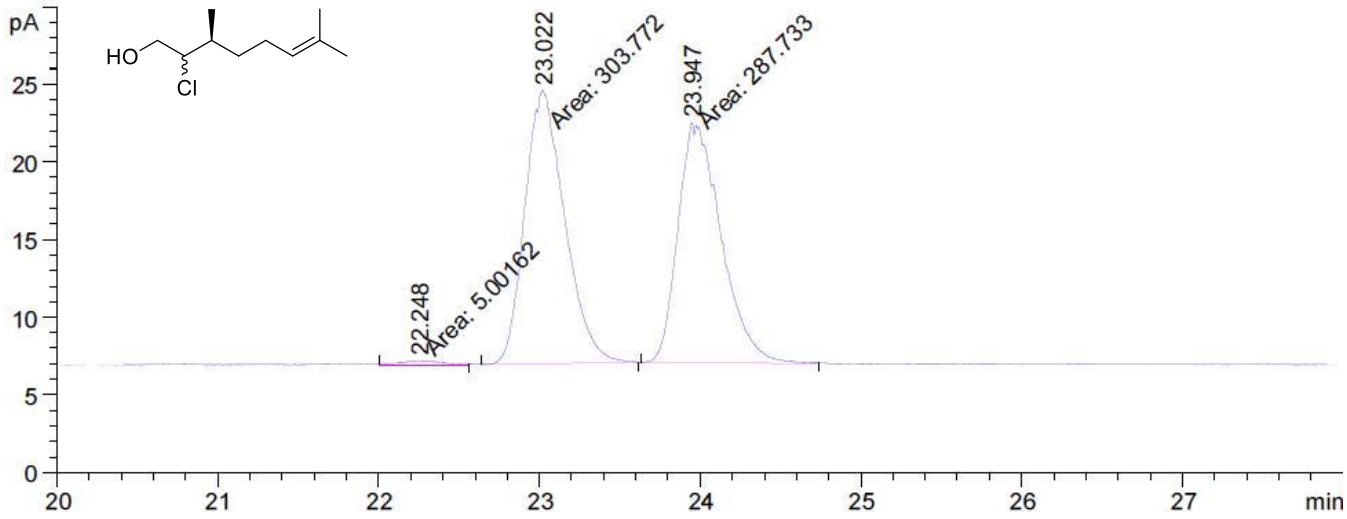

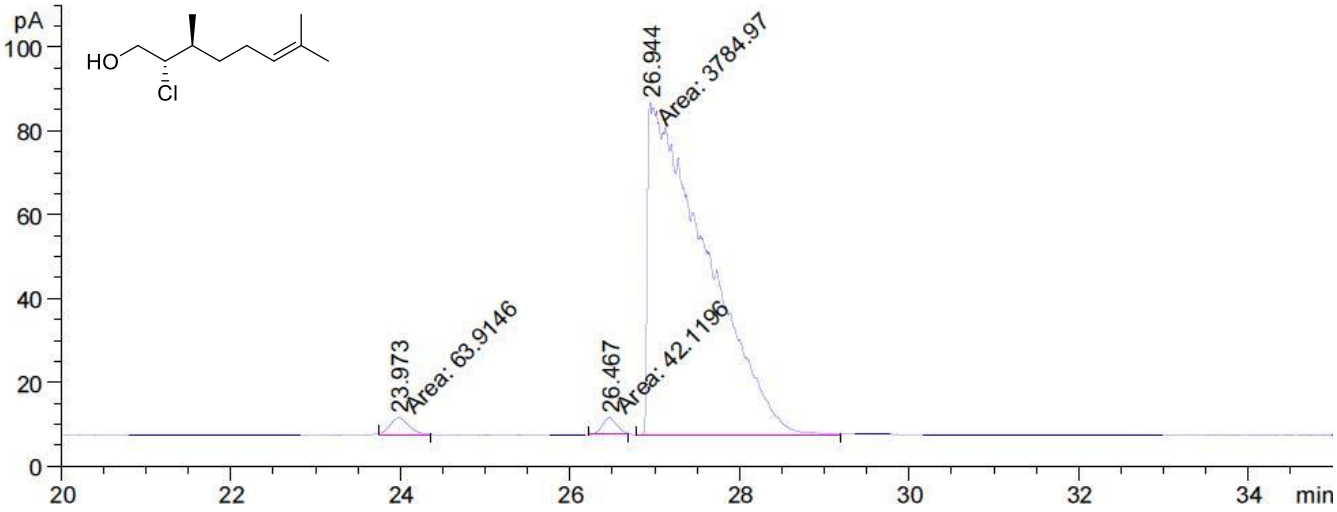

Peak #	RetTime [min]	Type	Width [min]	Area [pA*s]	Height [pA]	Area %
1	23.973	MM	0.2614	63.91455	4.07456	1.64263
2	26.467	MM	0.1815	42.11958	3.86717	1.08249
3	26.944	MM	0.7951	3784.96606	79.33694	97.27489

2-Chlorohex-4-yn-1-ol

GC: Hydrodex-ß-6TBDAc, Tempgrad 50-180°C mit 5°C/min, 1,1 ml/min, He, FID300°, Split 50:1

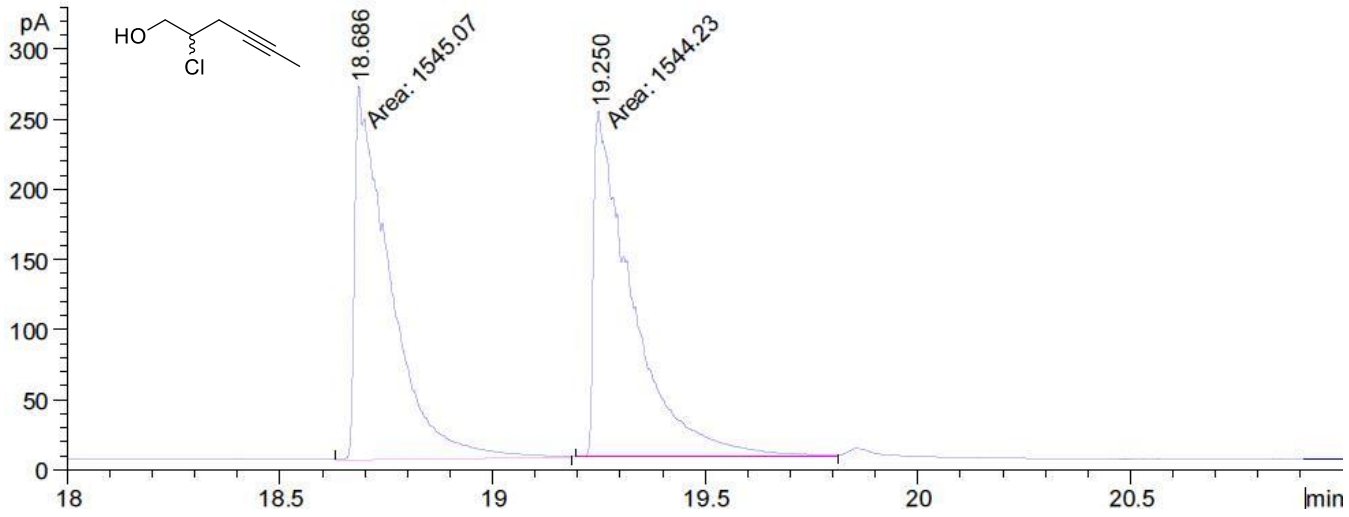

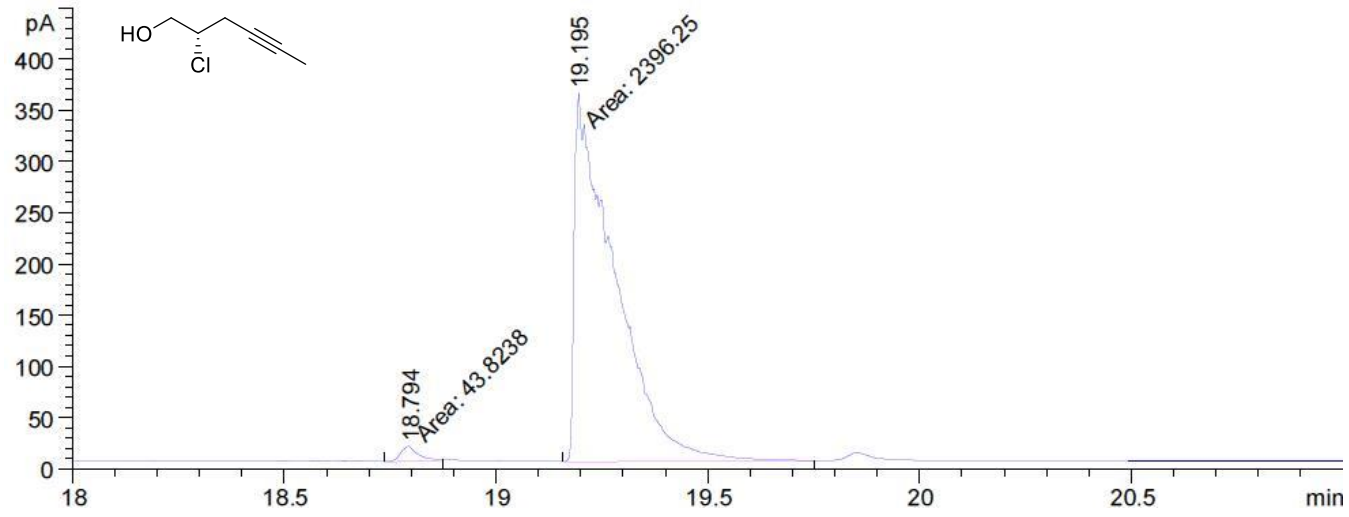

Peak #	RetTime [min]	Type	Width [min]	Area [pA*s]	Height [pA]	Area %
1	18.794	MM	0.0491	43.82376	14.88727	1.79600
2	19.195	MM	0.1111	2396.24756	359.33508	98.20400

6. CRYSTALLOGRAPHIC DATA

Intermediate 5:

ORTEP-structure with 20% probability level:

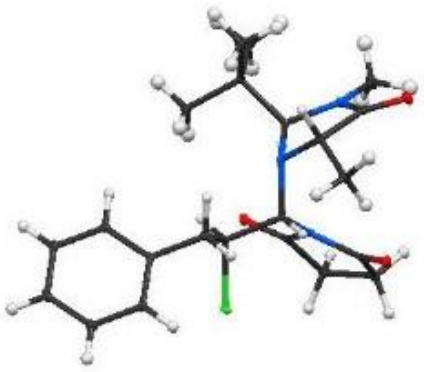

Crystal system	monoclinic
Space group	P 2 1
Cell a [Å]	10.0695(2)
Cell b [Å]	8.8228(2)
Cell c [Å]	12.1525(2)
Cell α [°]	90
Cell β [°]	93.107
Cell γ [°]	90
Volume [$Å^3$]	1078.06(4)
Z	2
Temperature [K]	100
AbsCorr	Multi-Scan
Absorption coefficient [mm^{-1}]	0.205
Nref	4406
R (reflections)	0.0288
wR2 (reflections)	0.0647
GooF	1.045

Intermediate 6:

ORTEP-structure with 20% probability level:

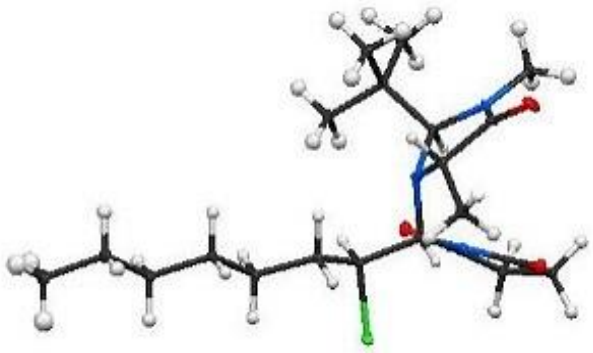

Crystal system	monoclinic
Space group	P 2 1
Cell a [Å]	10.1613(5)
Cell b [Å]	8.8290(3)
Cell c [Å]	13.3188(6)
Cell α [°]	90
Cell β [°]	108.294
Cell γ [°]	90
Volume [$Å^3$]	1134.49(9)
Z	2
Temperature [K]	100
AbsCorr	Multi-Scan
Absorption coefficient [mm^{-1}]	0.194
Nref	4621
R (reflections)	0.0303
wR2 (reflections)	0.0675
GooF	1.067

Intermediate 7:

ORTEP-structure with 20% probability level:

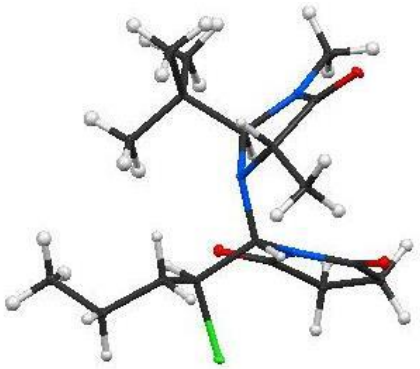

Crystal system	monoclinic
Space group	P 2 1
Cell a [Å]	9.8217(2)
Cell b [Å]	8.9668(1)
Cell c [Å]	11.1680(2)
Cell α [°]	90
Cell β [°]	107.207
Cell γ [°]	90
Volume [$Å^3$]	939.54(3)
Z	2
Temperature [K]	100
AbsCorr	Multi-Scan
Absorption coefficient [mm^{-1}]	0.226
Nref	3845
R (reflections)	0.0263
wR2 (reflections)	0.0616
GooF	1.044

Intermediate 8:

ORTEP-structure with 20% probability level:

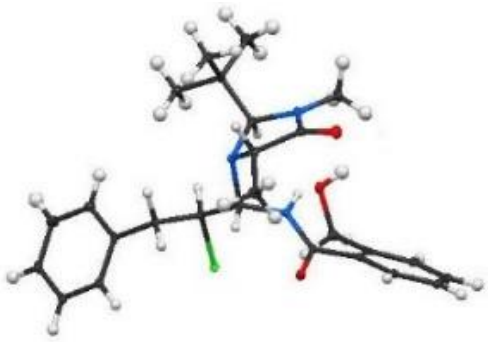

Crystal system	monoclinic
Space group	P 2 1
Cell a [Å]	10.6107(2)
Cell b [Å]	28.3703(6)
Cell c [Å]	12.8872(3)
Cell α [°]	90
Cell β [°]	91.688
Cell γ [°]	90
Volume [$Å^3$]	3877.73(14)
Z	6
Temperature [K]	100
AbsCorr	Multi-Scan
Absorption coefficient [mm^{-1}]	0.179
Nref	15923
R (reflections)	0.0357
wR2 (reflections)	0.0739
GooF	1.028

Intermediate 9:

ORTEP-structure with 20% probability level:

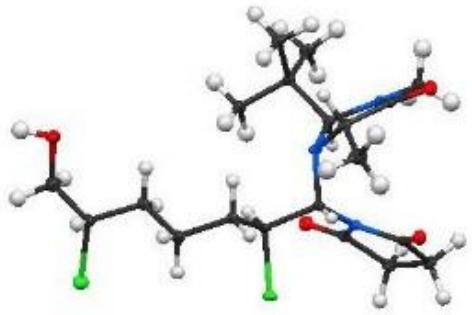

Crystal system	orthorhombic
Space group	P 2_1 2_1 2_1
Cell a [Å]	10.0393(9)
Cell b [Å]	12.5148(9)
Cell c [Å]	18.3306(13)
Cell α [°]	90
Cell β [°]	90
Cell γ [°]	90
Volume [$Å^3$]	2303.1(3)
Z	4
Temperature [K]	173(2)
AbsCorr	**?**
Absorption coefficient [mm^{-1}]	0.312
N_{ref}	4532
R (reflections)	0.0443
wR2 (reflections)	0.1209
GooF	1.000

Catalyst 13:

ORTEP-structure with 20% probability level:

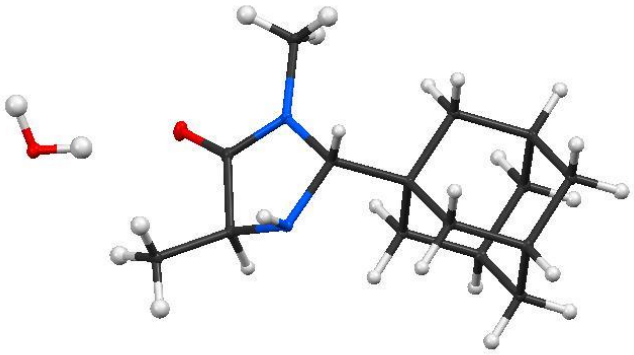

Crystal system	trigonal
Space group	P 3_2 2 1
Cell a [Å]	6.7315(2)
Cell b [Å]	6.7315(2)
Cell c [Å]	52.4761(14)
Cell α [°]	90
Cell β [°]	90
Cell γ [°]	120
Volume [$Å^3$]	2059.28(13)
Z	6
Temperature [K]	100
AbsCorr	Multi-Scan
Absorption coefficient [mm^{-1}]	0.631
N_{ref}	2972
R (reflections)	0.0363
wR2 (reflections)	0.0886
GooF	1.136

References

[1] T. H. Graham, B. D. Horning, D. W. C. MacMillan, *Org. Synth.* **2011**, *88*, 42-53.
[2] J. M. Allen, T. H. Lambert, *J. Am. Chem. Soc.* **2011**, *133*, 1260-1262.
[3] D. J. Augeri et al., *J. Med. Chem.*, **2005**, *48*, 5025-5037.
[4] T. Rehm, V. Stepanenko, X. Zhang, F. Würthner, F. Gröhn, K. Klein, C. Schmuck, *Org. Lett.* **2008**, *10*, 1469-1472.
[5] D. C. Powers, D. Y. Xiao, M. A. L. Geibel, T. Ritter, *J. Am. Chem. Soc.* **2010**, *132*, 14530-14536.
[6] A. Shiri, A. Khoramabadi-zad, *Synthesis* **2009**, *16*, 2797-2801.
[7] R. Yousefi, D. C. Whitehead, J. M. Mueller, R. J. Staples, B. Borhan, *Org. Lett.* **2011**, *13*, 608-611.
[8] X. Yu, K. Chen, S. Guo, P. Shi, C. Song, J. Zhu, *Org. Lett* **2017**, *19*, 5348-5351.
[9] J. M. Hoover, S. S. Stahl, *J. Am. Chem. Soc.* **2011**, *133*, 16901-16910
[10] L. Guillonneau, D. Tadddei, C. J. Moody, *Org. Lett.* **2008**, *10*, 4505-4508.
[11] X. Wang et al., *ACS Med. Chem. Lett.* **2016**, *7*, 1044-1049.
[12] J. M. Tinsley, W. R. Roush, *J. Am. Chem. Soc.* **2005**, *127*, 10818-10819.
[13] A. Yamamoto et al., *Chem Biol Drug Des* **2015**, *86*, 1304-1322.
[14] H. Ogawa, M. Amano, T. Chihara, *Chem. Commun*. **1998**, *0*, 495-496.
[15] H. Tan, J. Li, J. Luo, X. Xie, Y. Zhong, Q. Fu, *Eur. Polym. J.* **2005**, *41*, 1893-1900.
[16] M. Gaydou, T. Moragas, F. Juliá-Hernández, R. Martin, *J. Am. Chem. Soc.* **2017**, *139*, 12161-12164.
[17] H. Kikuchi, K. Sasaki, J. Sekiya, Y. Maeda, A. Amagai, Y. Kubohara, Y. Oshima, *Bioorg. Med. Chem.* **2004**, *12*, 3203-3214.
[18] B. F. Fisher, S. H. Gellman, *J. Am. Chem. Soc.* **2016**, *138*, 10766-10769.
[19] S. Rajkumar, K. Shankland, G. D. Brown, A. J. A. Cobb, *Chem. Sci.* **2012**, *3*, 584-588.
[20] P. D. Brown, A. C. Willis, M. S. Sherburn, A. L. Lawrence, *Angew. Chem. Int. Ed.* **2013**, *52*, 13273-13275.
[21] V. B. Phapale, E. Buñuel, M. Garcías-Iglesias, D. J. Cárdenas, *Angew. Chem. Int. Ed.* **2007**, *46*, 8790-8795.
[22] M. Rosillo, E. Arnáiz, D. Abdi, J. Blanco-Urgoiti, G. Domínguez, J. Pérez-Castells, *Eur. J. Org. Chem.* **2008**, *23*, 3917-3927.
[23] M. Benohoud, S. Tuokko, P. M. Pihko, *Chem. Eur. J.* **2011**, *17*, 8404-8413.
[24] S. Hötling, B. Haberlag, M. Tamm, J. Collatz, P. Mack, J. L. M. Steidle, M. Vences, S. Schulz, *Chem. Eur. J.* **2014**, *20*, 3183-3191.
[25] M. Johannes, M. A. Brimble, *J. Org. Chem*. **2013**, *78*, 12809-12813.
[26] M. Amatore, T. D. Beeson, S. P. Brown, D. W. C. MacMillan, *Angew. Chem.* **2009**, *121*, 5223-5226.
[27] J. Swatschek, L. Grothues, J. O. Bauer, C. Strohmann, M. Christmann, *J. Org. Chem*. **2014**, *79*, 976-983.

5.3. Supporting Information: On Stereocontrol in Organocatalytic α-Chlorinations of Aldehydes

Supporting Information

On Stereocontrol in Organocatalytic α-Chlorinations of Aldehydes

Sebastian Ponath[§‡], Chetan Joshi[‡‡], Amy T. Merrill[†], Volker Schmidts[×], Kim Greis[§#], Maike Lettow[§#], Manuela Weber[§], Simon Steinhauer[§], Kevin Pagel[§#*], Christina Thiele[×*], Dean J. Tantillo[†*], Mathew J. Vetticatt[‡*], Mathias Christmann[§*]

[§]Institute of Chemistry and Biochemistry, Freie Universität Berlin, 14195 Berlin, Germany
[‡]Department of Chemistry, Binghamton University, Binghamton, New York 13902, United States
[†]Department of Chemistry, University of California – Davis, Davis, California 95616, United States
[×]Clemens Schöpf Institute of Organic Chemistry and Biochemistry, Technische Universität Darmstadt, 64287 Darmstadt, Germany
[#]Fritz Haber Institute of the Max Planck Society, 14195 Berlin, Germany

TABLE OF CONTENTS

1. GENERAL INFORMATION

Anhydrous solvents were provided by purification with MBraun SPS-800 solvent system using solvents of HPLC grade purchased from Fischer Scientific. Solvents for extraction, crystallization and flash column chromatography were purchased in technical grade and distilled under reduced pressure prior to use. Unless otherwise indicated, all starting materials and reagents were purchased from commercial distributors and used without further purification. Products were purified by flash column chromatography on silica gel 60 M (0.040-0.063 mm, 230-400 mesh, Macherey-Nagel). TLC-analysis was performed on silica gel coated aluminum plates ALUGRAM® Xtra SIL G/UV_{254} purchased from Macherey-Nagel. Products were detected by UV light at 254 nm and by using staining reagents based on $KMnO_4$, anisaldehyde, molybdophosphoric acid and cerium sulfate. ^{1}H-NMR and ^{13}C-NMR spectral data were recorded on Bruker (AC 500, AVIII 700) and JEOL (ECX 400, Eclipse 500, ECZ 600) spectrometers. The chemical shifts (δ) are listed in parts per million (ppm) and are reported relative to the corresponding residual solvent signal ($CDCl_3$: δ_H = 7.26 ppm, δ_C = 77.16 ppm, CD_2Cl_2: δ_H = 5.32 ppm, δ_C = 53.84 ppm, $DMSOd_6$: δ_H = 2.50 ppm, δ_C = 39.52 ppm, CD_3OD: δ_H = 3.31 ppm, δ_C = 49.00 ppm, CD_3CN: δ_H = 1.94 ppm, δ_C = 118.26, $DMFd_7$: δ_H = 8.03 ppm, δ_C = 163.15 ppm, C_6D_6: δ_H = 7.16 ppm, δ_C = 128.06 ppm). Integrals are in accordance with assignments; coupling constants (*J*) are given in Hz. Multiplicity is indicated as follows: s (singlet), d (doublet), t (triplet), q (quartet), m (multiplet), dd (doublet of doublet), etc. ^{13}CNMR spectra are ^{1}H-broadband decoupled. For detailed peak assignments 2D spectra were measured (COSY, HMQC, HMBC). IR spectra were measured with a Jasco spectrometer (FT/IR-4100) equipped with an ATR unit. High resolution mass spectra were measured with an Agilent 6210 ESI-TOF (10 µL/min, 1.0 bar, 4 kV) instrument. Melting points were determined by digital melting point apparatus (Stuart SMP30) and are uncorrected. Optical rotations values were determined with a Jasco P-2000 polarimeter at the temperatures given. Diastereomeric ratios were determined by ^{1}HNMR. Enantiomeric ratios were determined by chiral HPLC (Agilent Series 1200 with DAD) or by GC (Agilent 7890B) on a chiral column. The specific conditions are given in each case.

NMR Methods for NOE and J-Coupling Analysis

NMR spectra for ^{1}H-^{1}H NOE and *J*-coupling analysis were recorded on a Bruker AVIII 600 MHz spectrometer equipped with a 5 mm triple-resonance broadband inverse probe (^{1}H/^{31}P-BB-^{2}H) with z-gradient (0.494 $T \cdot m^{-1}$maximum gradient strength). Sample temperature was regulated between 190 K and 300 K using a liquid nitrogen evaporator. Experiments were recorded and analyzed with TopSpin 3.5pl7. Assignment spectra at 190 K were recorded using the standard library sequences for HSQC,[1] HMBC[2] and EASY-ROESY[3]. Selective 1D NOE measurements supplemented with a Thrippleton-Keeler filter[4] to suppress unwanted zero-quantum contributions of *J*-coupled nuclei were performed using the standard library *selnogpzs* sequence with a spectral width of 12 ppm and 65536 complex points with 32 scans. Sufficient relaxation was ensured by setting the recovery delay to 15 s, which is larger than $5*T_1$ for every signal as determined by an inversion recovery experiment. The carrier frequency offset was set to 4.7 ppm and the selective pulse offset to the respective signal. The RSnob[5] shape was used for the selective pulse with bandwidths of 15, 25 or 50 Hz, depending on the required selectivity. A mixing time series of 8 independent time points was acquired between 50 and 400 ms in 50 ms steps for each

selected resonance. Spectra were processed by zero-filling once and apodization with exponential broadening with 0.1 Hz. Manual phase correction and automatic baseline correction were applied for each spectrum before integrating the series using the *intser* command. Additionally, a 2D gradient-selected F1-PSYCHE-EASY-ROESY[6] was acquired with spectral widths of 12 ppm in both dimensions and 4096 and 512 complex points, respectively, with 8 scans. The recovery delay was not sufficient for full relaxation to equilibrium. PSYCHE[7] homonuclear decoupling in the indirect dimension was applied with a 30 ms element consisting of two low power chirp pulses with 25° flip angle, 10 kHz sweep width and 15 ms durations each. The pair of spin-locks were set to a tilt angle of 45° and an RF field of 6500 Hz. Gradient strengths were set to the values given in the original publication. The spectrum was processed by zero-filling once in the indirect dimension and applying a 90° shifted squared sine bell apodization. While the quantification may show larger deviations due to the insufficient recovery delay, volume integrals were nevertheless collected for all diagonal peaks, where they were sufficiently resolved by the PSYCHE homodecoupling, and all associated cross-peaks. Integrals were normalized using the PANIC[8] approach: within each spectrum, the cross-peak integrals were divided by the integrals of the selected peak for the 1D spectra or the corresponding diagonal peak at the same chemical shift in F1 for the 2D spectrum. The normalized peak integrals are subjected to a linear fit versus the mixing time. The slope of this fit gives the cross-relaxation rate for NOE cross-peaks or the exchange rate for cross-peaks generated by chemical exchange. The fit usually shows (very) high correlation coefficients (Pearson R > 0.9), with only two exceptions: in some spectra the very last mixing time data point (400 ms) apparently no longer fulfilled the initial rate approximation and had to be excluded from the fitting process to achieve a sufficiently high correlation coefficient. Secondly, for the NOE from the neighboring nuclei 1' and 2' in the aminal part, the fit showed larger deviations resulting in lower apparent cross-relaxation rates, presumably due to insufficient suppression of *J*-coupling contributions and/or strong-coupling effects between these two nuclei.[9] The individual cross-relaxation rates σ_{IS} were converted to NOE derived distances r_{IS} by internal calibration with the cross-relaxation rate of the diastereotopic proton pair H5a/b (denoted $"ref"$, set to 1.76 Å) using equation (1). For methyl groups, the three internuclear distances to individual protons were averaged using "r^{-3} averaging" as described in equation (2).[10,11] Conformational averaging for different conformers was performed using "r^{-6} averaging" using equation (3),[10] where p_i are the individual conformer populations of the M total conformations. Uncertainties were estimated by Gaussian error propagation.[11] In cases where both protons could be selected individually by the selective pulse, the NOE derived distances were averaged and the larger value between the deviations of the individual NOE distances to the average distance or the individual estimated uncertainties are used as an error estimate for the NOE distance. While in some cases the error from Gaussian error propagation is as low as 0.01 A, we assume a reasonable estimate to be at least 0.1 Å in 1D NOE spectra and 0.4 Å in the semiquantitative PSYCHE-EASY ROESY spectra.

$$r_{IS} = r_{ref}\left(\sigma_{ref}/\sigma_{IS}\right)^{-1/6} \quad (1)$$

$$r_{IS,ave}^{Methyl} = \left(\sum_{i=1}^{3} \frac{1}{3} \times r_{IS,i}^{-3}\right)^{-1/3} \quad (2)$$

$$r_{IS,ave} = \left(\sum_{i=1}^{M} \mathrm{p}_i \times r_{IS,i}^{-6}\right)^{-1/6} \quad (3)$$

J-coupling constants were determined either by lineshape analysis in the 1D spectrum or by a 2D (non-pure-shift) version of the PSYCHEDELIC[12] experiment with spectral widths of 7211 Hz and 50 Hz over 16384 and 128 complex points with 16 scans. As for the 1D sel. NOE, the carrier frequency offset was set to 4.7 ppm and the selective pulse offset to the respective signal. The RSnob shape was used for the selective pulse with bandwidths of 15, 25 or 50 Hz, depending on the required selectivity. Spectra were processed by zero-filling to 512 points and apodization with exponential broadening with 1 Hz. Manual phase correction was applied before tilting the spectrum with a shear transformation (45°). Coupling constants were extracted from the peak maxima along the column with the highest sensitivity of the multiplet.

Computational NMR Methods

The NMR chemical shifts for *syn*-**11**, iminium ion derived from *syn*-**11,** *anti(C1')*-**11**, *anti(C2')*-**11**, and *syn*-**14** were calculated using the GIAO method with PCM(chloroform)-mPW1PW91/6-311+G(2d,p)// B3LYP-D3(BJ)/6-31G+(d,p)[13] at 219.15 K using *Gaussian16*[14] Revision C.01. Conformational searching was performed using Grimme's CREST tool in xTB, using version 2.9 (*syn*-**11**; *anti(C1')*-**11**; *anti(C2')*-**11**; *syn*-**14**) and version 2.10.2 (iminium ion derived from *syn*-**11**) with the gfn-ff method and chloroform as the solvent (force constant of 1.0).[15,16] Conformers generated from CREST were optimized with B3LYP-D3(BJ)/3-21 and then any conformers within 5 kcal mol^{-1} from the lowest free energy conformer were reoptimized with B3LYP-D3(BJ)/6-31G+(d,p). If more than 100 conformers were generated from CREST, only the conformers within 5 kcal mol^{-1} from the conformer search were used for DFT optimization. Any conformers within 3 kcal mol^{-1} of the lowest energy conformer at this level of theory were reoptimized with the same level of theory at the lower. Unique conformers from this third optimization were used for the NMR calculations. The scaling factors used to convert the isotropics from the NMR calculations to chemical shifts were a slope = -1.0719, intercept = 31.8733 for ^{1}H shifts and slope = -1.0420, intercept = 186.3567 for ^{13}C shifts.[17,18] The NMR chemical shifts were calculated by averaging the conformer chemical shifts with weights, or percentages, for each conformer determined by minimizing the deviation between the experimental and theoretical shifts using the excel solver function. The barrier of rotation between *syn*-**14** *ap* and *exo-sc* was calculated with optimizing using modredundant and the PCM(chloroform-B3LYP/3-21G (219.15 K) level of theory using *Gaussian16*, Revision C.01 for the 11, 2, 33, 56 atom dihedral angle with 36 steps of 10°. The j-coupling values (Hz) were calculated using the fermi contact (FC) values from reoptimizing relevant conformers from the NMR calculations with B3LYP/6-31G(d) and then calculating coupling using B3LYP/6-31G(d,p) nmr=(FCOnly,Atoms=H,MixedH). The FC values were scaled to j-coupling constants (Hz) values were scaled by 0.9155 as recommended on CHESHIRE.[17,18] The NMR calculations for **18b** were performed using the GIAO method with PCM(acetonitrile)-mPW1PW91/6-311+G(2d,p) from the lowest energy conformer from the mechanistic calculations (Section #) using *Gaussian16*, Revision C.01. The scaling factors used were slope= -1.0681 and intercept=31.7773 for ^{1}H shifts and slope= -1.0502 and intercept=186.9263 for ^{13}C shifts.[17,18] The NBO calculations[19] were performed with B3LYP-D3(BJ)/6-31G+(d,p) with the keywords: pop=(full,nbo) int=finegrid, iop(3/32=2), scf=tight, temperature=219.15 with *Gaussian16*, Revision A.03. Molecular images were generated using CylView.[20] The optimized

geometries for **11** and **14** are deposited in ioChem-BD (doi:10.19061/iochem-bd-6-83; http://dx.doi.org/10.19061/iochem-bd-6-83).[21]

2. CHLORINATIONS WITH MACMILLAN-TYPE CATALYSTS

2.1. Aminals Derived from 1st, 2nd and 3rd Generation MacMillan Catalysts

Motivated by the isolation and X-ray crystal structure analysis of several aminals derived from the 3rd generation MacMillan catalyst **3c**,[22] we aimed at extending the structure determination to the 1st and 2nd generation MacMillan catalysts **3a** and **3b**. The ^{1}H-NMR spectra of the isolated and crystallographically characterized aminals were compared to the NMR spectra recorded during the reactions and our stereochemical assignments were compared to those reported in the literature.[23,24]

Aminals Derived from Isovaleraldehyde, NCS and the 1st Generation MacMillan Catalyst *ent*-3a (NMR Experiment)

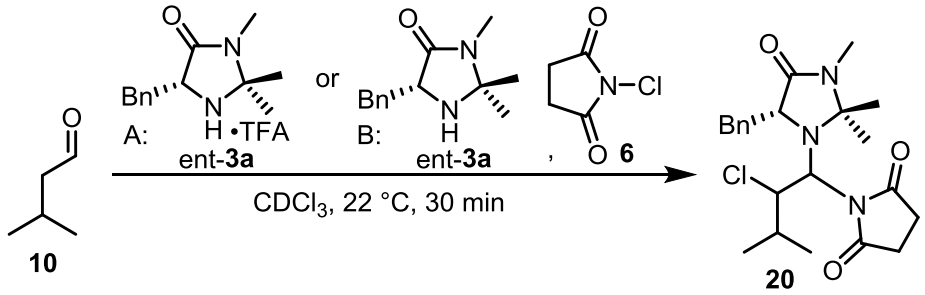

The TFA-salt of catalyst *ent*-**3a** (6.64 mg, 20.0 µmol, 20 mol%) or catalyst *ent*-**3a** as the free base (4.36 mg, 20.0 µmol, 20 mol% or 21.8 mg, 100 µmol, 100 mol%) and NCS (16.0 mg, 120 µmol, 1.2 equiv) were added successively to an NMR-tube containing a solution of isovaleraldehyde (10.8 µL, 100 µmol, 1.0 equiv) in $CDCl_3$ (0.70 mL) at 22 °C. ^{1}H-NMR spectra were recorded after 30 min. The ratio of aminal diastereoisomers is 20:1 for the TFA-salt of the catalyst and 2:1 for the free base. The diastereomeric ratios and the ^{1}H-NMR spectrum for the reaction with the free base of the catalyst is in agreement with the literature.[25]

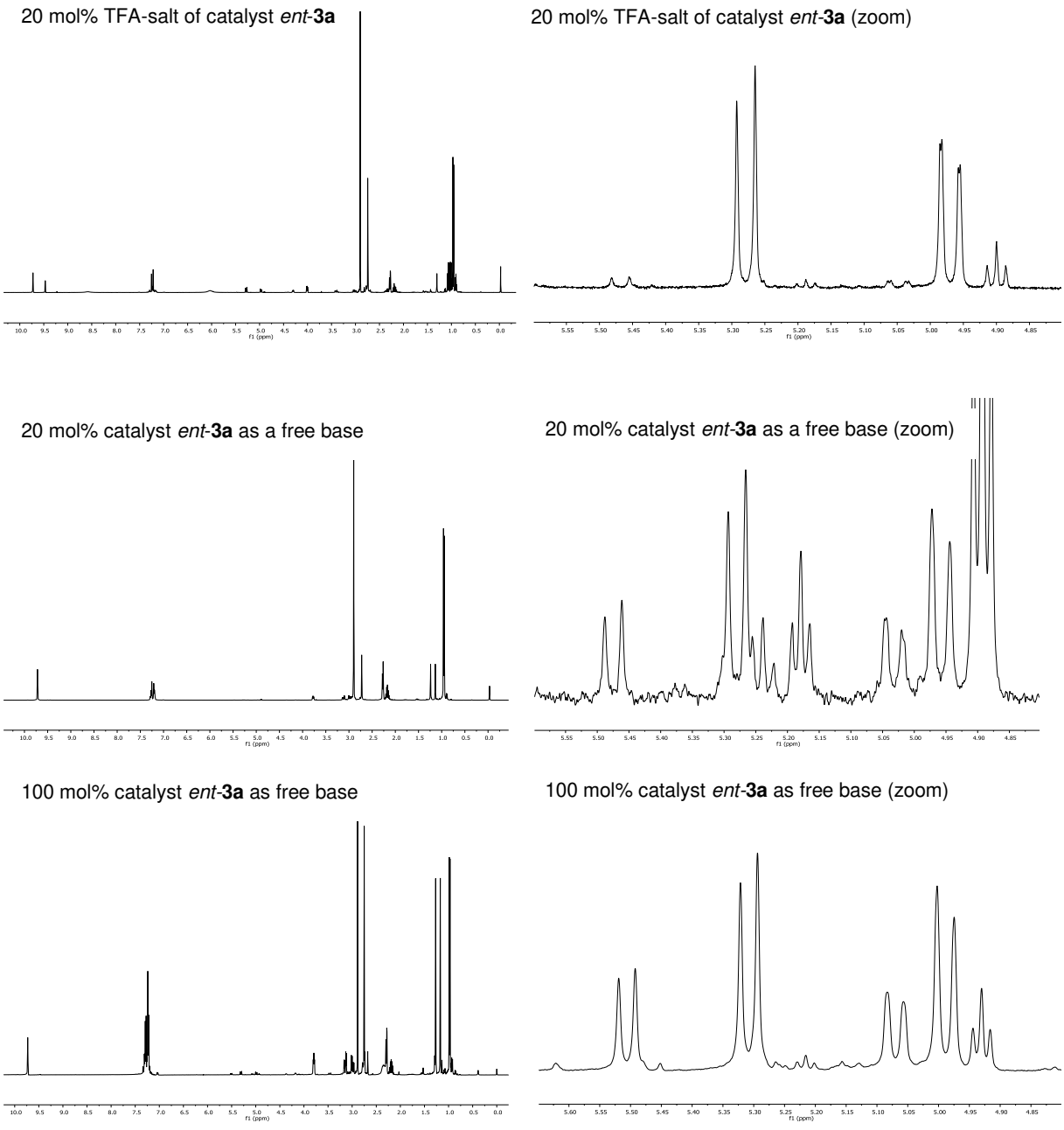

Figure SI-1. ^{1}H-NMR spectra of the α-chlorination reaction (isovaleraldehyde, NCS, catalyst *ent*-**3a** or *ent*-**3a**•TFA) after 30 min.

1-((1*S*,2*R*)-1-((*R*)-5-benzyl-2,2,3-trimethyl-4-oxoimidazolidin-1-yl)-2-chloro-3-methylbutyl)-pyrrolidine-2,5-dione (*syn*-20)

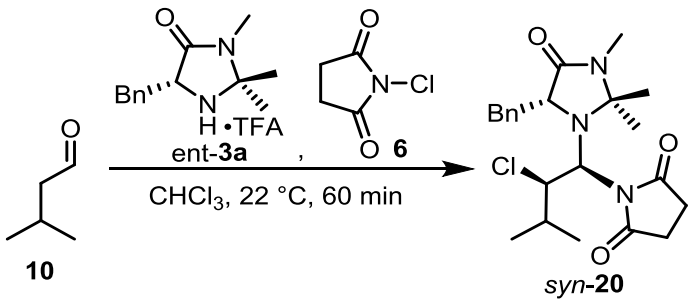

The TFA-salt of catalyst *ent*-**3a** (0.770 g, 2.32 mmol, 20 mol%) and NCS (1.55 g, 11.6 mmol, 1.0 equiv) were added successively to a solution of isovaleraldehyde (1.25 mL, 11.6 mmol, 1.0 equiv) in $CHCl_3$ (46 mL). The reaction was stirred for 60 min and quenched with aqueous saturated $NaHCO_3$ (50 mL). The layers were separated and the aqueous phase was extracted with CH_2Cl_2 (3x50 mL). The combined organic phases were dried over $NaSO_4$, the solvent was removed under reduced pressure and the crude product was purified by column chromatography (SiO_2, pentane/Et_2O/EtOAc, 1:1:1 to 0:1:1 to 0:0:1). Aminal *syn*-**20** was obtained as a colorless solid (0.664 g, 1.58 mmol, 68%). The absolute configuration was determined by X-ray crystal structure analysis.

The ^{1}H-NMR-spectrum of the major species is consistent with that reported literature, which was tentatively assigned the *syn*-coniguration.[23,25]

mp = 107 °C

$[\alpha]_D^{26}$ = –40.8° (*c* = 1.00, dichloromethane)

^{1}H-NMR ($CDCl_3$, 600 MHz) δ = 7.26 – 7.13 (m, 5H), 5.29 (d, *J* = 11.0 Hz, 1H), 4.96 (d, *J* = 11.2 Hz, 1H), 4.17 (dd, *J* = 7.0, 3.0 Hz, 1H), 3.46 (dd, *J* = 14.8, 2.9 Hz, 1H), 3.06 (dd, *J* = 14.8, 7.1 Hz, 1H), 2.78 – 2.71 (m, 7H), 2.34 (hept, *J* = 6.1 Hz, 1H), 1.26 (s, 3H), 1.10 (s, 3H), 0.95 (d, *J* = 6.8 Hz, 3H), 0.91 (d, *J* = 6.5 Hz, 3H) ppm.

^{13}C-NMR ($CDCl_3$, 151 MHz) δ = 179.4, 177.6, 170.8, 137.7, 129.8, 128.1, 126.4, 79.9, 67.9, 67.3, 60.7, 39.7, 28.6, 28.4, 27.8, 27.1, 25.4, 23.1, 21.4, 15.1 ppm.

IR (ATR): $\tilde{\nu}$ = 2969, 2930, 1773, 1704, 1364, 1291, 1173, 911, 818, 728 cm^{-1}.

HRMS (ESI, pos. mode): *m*/*z* calculated for $C_{22}H_{31}ClN_3O_3$ $[M+H]^+$: 420.2049, found 420.2044; *m*/*z* calculated for $C_{22}H_{30}ClN_3NaO_3$ $[M+Na]^+$: 442.1868, found 442.1865; *m*/*z* calculated for $C_{22}H_{30}ClKN_3O_3$ $[M+K]^+$: 458.1608, found 458.1598.

1-((*S*)-1-((*R*)-5-benzyl-2,2,3-trimethyl-4-oxoimidazolidin-1-yl)-2,2-dichloro-3-methylbutyl)-pyrrolidine-2,5-dione (24a)

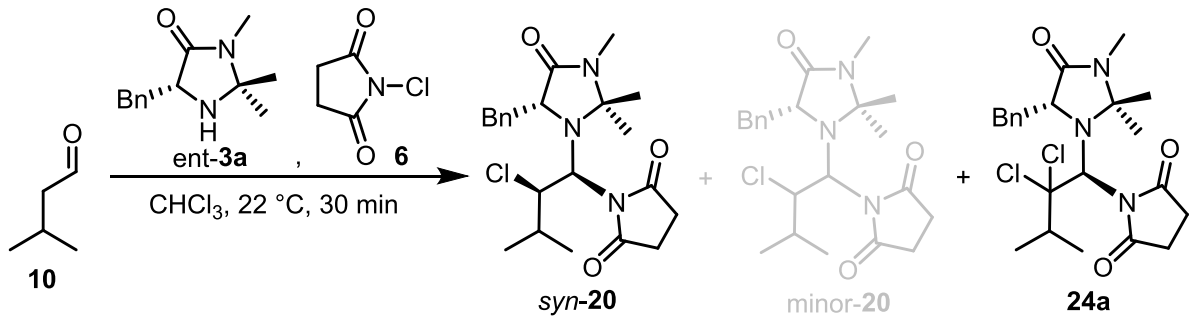

Catalyst *ent*-**3a** (2.23 g, 10.2 mmol, 100 mol%) and NCS (1.64 g, 12.3 mmol, 1.2 equiv) were added successively to a solution of isovaleraldehyde (1.10 mL, 10.2 mmol, 1.0 equiv) in $CHCl_3$ (20 mL) and the reaction was stirred for 30 min at 22 °C. The solvent was removed under reduced pressure and the crude product was purified by column chromatography (SiO_2, EtOAc). Aminal *syn*-**20** was obtained as a colorless solid (1.94 g, 4.62 mmol, 45%). The ^{1}H-NMR spectrum of a mixed fraction showed the existence of the diastereomeric aminal minor-**20**. After a second chromatographic separation attempt (SiO_2, Et_2O then EtOAc), aminal minor-**20** was not detectable anymore. Gratifyingly, a previously unknown dichloroaminal **24a** (96.0 mg, 0.211 mmol, 2%) could be obtained as a colorless solid. The absolute configuration was confirmed by X-ray crystal structure analysis.

The ^{1}H-NMR-spectrum of aminal *syn*-**20** is in accordance with the previous experiment.

Aminal 24a:

mp = 116 °C

$[\alpha]_D^{26}$ = –53.9° (*c* = 0.85, dichloromethane)

^{1}H-NMR ($CDCl_3$, 600 MHz) δ = 7.31 – 7.15 (m, 5H), 6.01 (s, 1H), 5.74 (dd, *J* = 8.0, 2.7 Hz, 1H), 3.54 – 3.45 (m, 1H), 3.05 (dd, *J* = 14.4, 7.9 Hz, 1H), 2.96 (dt, *J* = 13.2, 6.4 Hz, 1H), 2.87 – 2.70 (m, 4H), 2.70 (s, 3H), 1.34 (d, *J* = 6.6 Hz, 3H), 1.31 (s, 3H), 1.22 (d, *J* = 6.3 Hz, 3H), 1.02 (s, 3H) ppm.

^{13}C-NMR ($CDCl_3$, 151 MHz) δ = 178.1, 176.8, 172.1, 138.3, 129.7, 128.2, 126.5, 101.0, 80.6, 73.5, 62.2, 41.3, 39.5, 28.6, 28.2, 28.1, 25.4, 24.7, 19.2, 18.7 ppm.

IR (ATR): $\tilde{\nu}$ = 3058, 2978, 1777, 1710, 1431, 1398, 1309, 1266, 1181, 1141, 947, 818, 768, 732 cm^{-1}.

HRMS (ESI, pos. mode): *m*/*z* calculated for $C_{22}H_{30}Cl_2N_3O_3$ $[M+H]^+$: 454.1659, found 454.1666; *m*/*z* calculated for $C_{22}H_{29}Cl_2N_3NaO_3$ $[M+Na]^+$: 476.1478, found 476.1489; *m*/*z* calculated for $C_{22}H_{29}Cl_2KN_3O_3$ $[M+K]^+$: 492.1218, found 492.1231.

Assignment of Aminal Diastereoisomers Derived from the 1st Generation MacMillan Catalyst

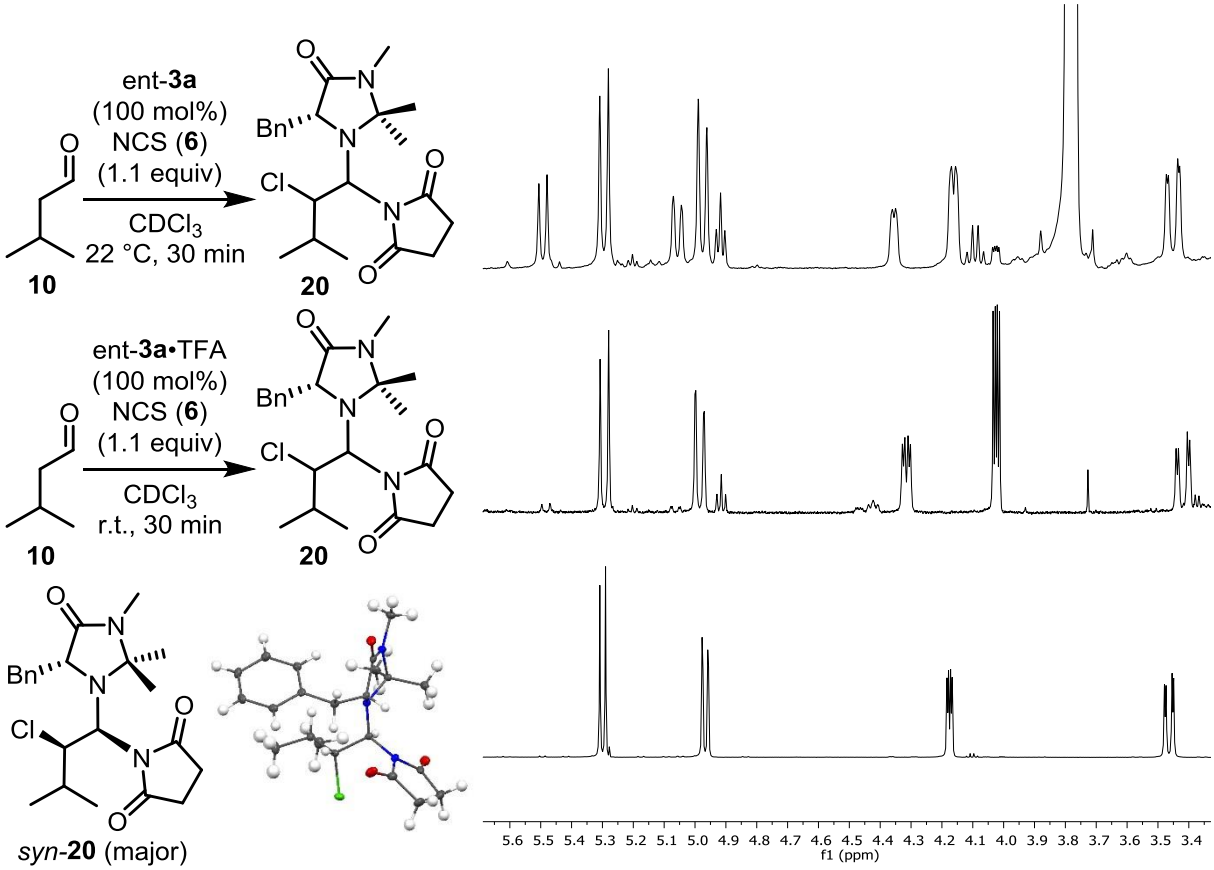

Figure SI-2. ^{1}H-NMR spectrum of the reaction with 100 mol% *ent*-**3a** after 30 min (according to Blackmond et al.[23,25] (top). ^{1}H-NMR spectrum of the reaction with 100 mol% *ent*-**3a**•TFA after 30 min (middle). Crystal structure and ^{1}H-NMR spectrum of the isolated aminal *syn*-**20** (bottom).

In their publication "Explaining Anomalies in Enamine Catalysis: "Downstream Species" as a New Paradigm for Stereocontrol"[23] the authors correlated species described as "major" and "minor" for the 1st generation MacMillan catalyst to the major and minor product enantiomer. According to their model, the major diastereoisomer of the corresponding aminal was suggested to possess the *anti*-configuration whereas the minor diastereoisomer was suggested to possess the *syn*-configuration. We were able to isolate and characterize the major species by X-ray analysis and determined it to possess the *syn*-configuration. Moreover, the authors correlated the enantiomeric ratio of the product (α-chloroaldehyde) to the diastereomeric ratio of the aminals.[23] The e.r.-value of the α-chloroaldehyde (40:60) was cited from the original MacMillan publication[26] and the d.r.-value (33:67) of the aminal refers to experiments done by the authors[25]. These two values however are not directly comparable, since MacMillan and co-workers used the TFA-salt and Blackmond and co-workers used the free base of the catalyst to generate a 33:67 ratio of diastereomers. The different diastereomeric ratios of the aminals are a consequence of the presence or absence of TFA as apparent in the ^{1}H-HNMR spectra shown above. Therefore, a correlation between enantiomeric ratio of the product and diastereomeric ratio of the aminal incorrectly compares two different situations.

Aminals Derived from Isovaleraldehyde, NCS and the 2nd Generation MacMillan Catalyst *ent*-3b (NMR Experiment)

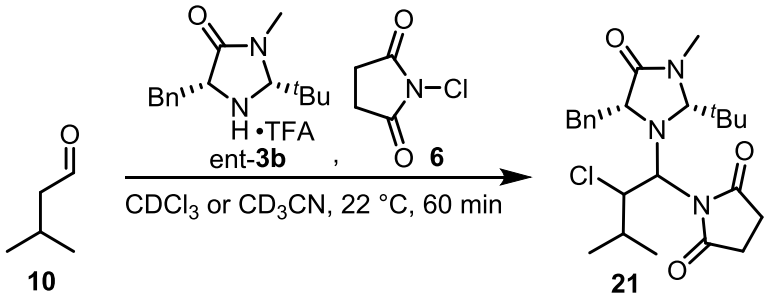

The TFA-salt of catalyst *ent*-**3b** (7.20 mg, 20.0 µmol, 20 mol%) and NCS (13.3 mg, 100 µmol, 1.0 equiv) were added successively to an NMR-tube containing a solution of isovaleraldehyde (10.8 µL, 100 µmol, 1.0 equiv) in $CDCl_3$ or CD_3CN (0.70 mL) at 22 °C. ^{1}H-NMR spectra were recorded after 60 min. The diastereomeric ratio is approximately 9:1:4 in $CDCl_3$ and 3:2 in CD_3CN. The ^{1}H-NMR spectrum ($CDCl_3$) is in accordance with that the literature.[24,25]

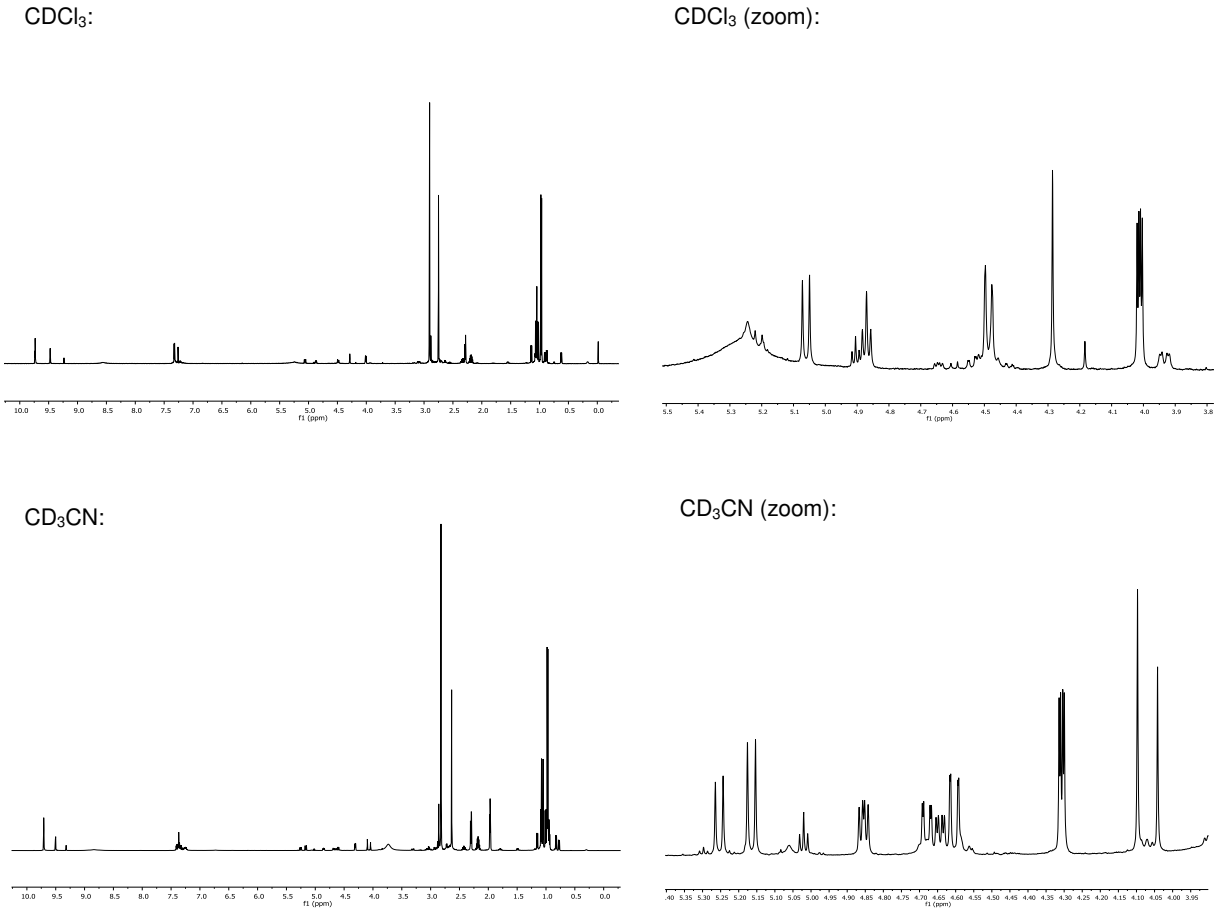

Figure SI-3. ^{1}H-NMR spectra of the α-chlorination reaction (isovaleraldehyde, NCS, catalyst *ent*-**3b**•TFA) in different solvents after 60 min.

1-((1*S*,2*R*)-1-((2*R*,5*R*)-5-benzyl-2-(tert-butyl)-3-methyl-4-oxoimidazolidin-1-yl)-2-chloro-3-methyl-butyl)pyrrolidine-2,5-dione ((1*S*,2*R*)-*syn*-21),
1-((1*S*,2*S*)-1-((2*R*,5*R*)-5-benzyl-2-(*tert*-butyl)-3-methyl-4-oxoimidazolidin-1-yl)-2-chloro-3-methyl-butyl)pyrrolidine-2,5-dione ((1*S*,2*S*)-*anti*-21),
1-((1*R*,2*S*)-1-((2*R*,5*R*)-5-benzyl-2-(tert-butyl)-3-methyl-4-oxoimidazolidin-1-yl)-2-chloro-3-methyl-butyl)pyrrolidine-2,5-dione ((1*R*,2*S*)-*syn*-21)

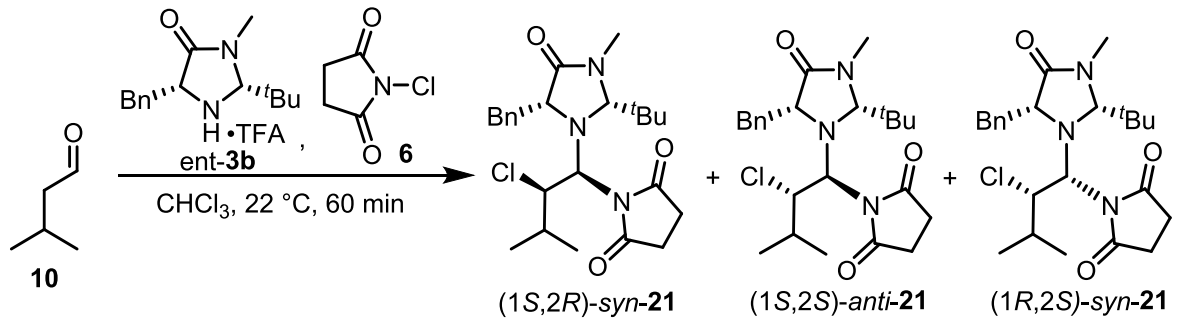

The TFA-salt of catalyst *ent*-**3b** (1.26 g, 3.48 mmol, 20 mol%) and NCS (2.33 g, 17.4 mmol, 1.0 equiv) were added successively to a solution of isovaleraldehyde (1.88 mL, 17.4 mmol, 1.0 equiv) in $CHCl_3$ (70 mL). The reaction was stirred for 60 min and quenched with aqueous saturated $NaHCO_3$ (50 mL). The aqueous phase was extracted with dichloromethane (3x50 mL), the combined organic phases were dried over $NaSO_4$, the solvent was removed under reduced pressure and the crude product was purified by column chromatography (SiO_2, pentane/Et_2O/EtOAc, 1:1:1 to 0:1:1 to 0:0:1). Pure aminal (1*S*,2*R*)-*syn*-**21** was obtained as a colorless solid (0.807 g, 1.80 mmol, 52%). Separation of another fraction from the column chromatography by chiral HPLC enabled further separation of aminal (1*S*,2*R*)-*syn*-**21** (0.339 g, 0.757 mmol, 22%), (1*S*,2*S*)-*anti*-**21** (93.0 mg, 0.208 mmol, 6%) and (1*R*,2*S*)-*syn*-**21** (0.271 g, 0.605 mmol, 17%). The absolute configuration of the three aminals was confirmed by X-ray crystal structure analysis.

Aminal (1*S*,2*R*)-*syn*-21:

The spectroscopic data (^{1}H- and ^{13}C-NMR) are in accordance with the major aminal from the literature.[24,25]

mp = 104 °C

$[\alpha]_D^{26}$ = –32.1° (*c* = 1.00, dichloromethane)

^{1}H-NMR ($CDCl_3$, 600 MHz) δ = 7.37 – 7.31 (m, 4H), 7.24 – 7.20 (m, 1H), 5.08 (d, *J* = 11.1 Hz, 1H), 4.81 (t, 1H), 4.48 (dd, *J* = 11.2, 1.0 Hz, 1H), 4.24 (s, 1H), 3.12 (dd, *J* = 14.9, 6.5 Hz, 1H), 2.88 (s, 3H), 2.85 (dd, *J* = 14.6, 6.9 Hz, 1H), 2.75 – 2.65 (m, 4H), 2.36 (h, *J* = 7.2, 6.6 Hz, 1H), 1.04 (s, 9H), 0.88 (d, *J* = 6.5 Hz, 3H), 0.61 (d, *J* = 6.7 Hz, 3H) ppm.

^{13}C-NMR ($CDCl_3$, 151 MHz) δ = 179.6, 179.2, 173.9, 138.6, 129.3, 128.8, 126.8, 88.5, 76.7, 65.4, 61.8,

41.1, 37.0, 31.7, 29.1, 28.2, 27.9, 26.9, 21.2, 15.8 ppm.

IR (ATR): $\tilde{\nu}$ = 2959, 2924, 2871, 1774, 1702, 1456, 1328, 1172, 1136, 820, 751 cm^{-1}.

HRMS (ESI, pos. mode): *m*/*z* calculated for $C_{24}H_{35}ClN_3O_3$ $[M+H]^+$: 448.2362, found 448.2373; *m*/*z* calculated for $C_{24}H_{34}ClN_3NaO_3$ $[M+Na]^+$: 470.2181, found 470.2188; *m*/*z* calculated for $C_{24}H_{34}ClKN_3O_3$ $[M+K]^+$: 486.1921, found 486.1930.

Aminal (1*S*,2*S*)-*anti*-21:

The spectroscopic data (^{1}H- and ^{13}C-NMR) are in accordance with the minor aminal from the literature.[24,25]

mp = 86 °C

$[\alpha]_D^{26}$ = –6.5° (*c* = 0.40, dichloromethane)

^{1}H-NMR ($CDCl_3$, 500 MHz) δ = 7.43 – 7.40 (m, 2H), 7.33 – 7.29 (m, 2H), 7.23 – 7.19 (m, 1H), 5.23 (d, *J* = 10.8 Hz, 1H), 4.59 (dd, *J* = 7.2, 4.6 Hz, 1H), 4.49 (dd, *J* = 10.8, 2.0 Hz, 1H), 4.11 (s, 1H), 3.23 (dd, *J* = 14.5, 4.5 Hz, 1H), 3.12 (dd, *J* = 14.4, 7.3 Hz, 1H), 2.88 (s, 3H), 2.78 – 2.53 (m, 4H), 1.61 – 1.49 (m, 1H), 1.08 (s, 9H), 0.89 (d, *J* = 6.6 Hz, 3H), 0.76 (d, *J* = 6.6 Hz, 3H) ppm.

^{13}C-NMR ($CDCl_3$, 151 MHz) δ = 179.6, 178.9, 174.1, 139.4, 129.6, 128.4, 126.4, 86.2, 75.4, 66.2, 61.7, 41.2, 38.2, 31.9, 29.8, 28.6, 28.0, 26.3, 21.3, 14.6 ppm.

IR (ATR): $\tilde{\nu}$ = 2964, 2925, 2874, 1772, 1701, 1455, 1364, 1317, 1153, 819, 753, 720 cm^{-1}.

HRMS (ESI, pos. mode): *m*/*z* calculated for $C_{24}H_{35}ClN_3O_3$ $[M+H]^+$: 448.2362, found 448.2352; *m*/*z* calculated for $C_{24}H_{34}ClN_3NaO_3$ $[M+Na]^+$: 470.2181, found 470.2163; *m*/*z* calculated for $C_{24}H_{34}ClKN_3O_3$ $[M+K]^+$: 486.1921, found 486.1904.

Aminal (1*R*,2*S*)-*syn*-21:

mp = 136 °C

$[\alpha]_D^{26}$ = –13.1° (*c* = 1.00, dichloromethane)

^{1}H-NMR ($CDCl_3$, 600 MHz) δ = 7.35 – 7.31 (m, 4H), 7.24 – 7.19 (m, 1H), 5.17 (s, 7H), 4.50 (s, 1H), 4.50 (dd, *J* = 18.0 Hz, 11.4 Hz, 1H), 3.87 (dd, *J* = 11.2, 2.9 Hz, 1H), 3.20 (dd, *J* = 13.9, 3.3 Hz, 1H), 2.90 (s, 3H), 2.81 (dd, *J* = 13.8, 11.6 Hz, 1H), 2.78 – 2.53 (m, 4H), 2.10 (h, *J* = 11.8, 6.5, 6.1 Hz, 1H), 1.04 (s, 9H), 0.88 (d, *J* = 6.8 Hz, 3H), 0.16 (s, 3H) ppm.

^{13}C-NMR ($CDCl_3$, 151 MHz) δ = 179.7, 178.6, 173.9, 138.3, 129.6, 129.1, 127.0, 85.9, 77.4, 67.4, 65.6, 38.6, 37.2, 32.2, 29.7, 28.3, 28.1, 28.0, 20.8, 14.8 ppm.

IR (ATR): $\tilde{\nu}$ = 2964, 2927, 2827, 1776, 1704, 1456, 1329, 1216, 1175, 1091, 908, 750, 735 cm^{-1}.

HRMS (ESI, pos. mode): *m*/*z* calculated for $C_{24}H_{35}ClN_3O_3$ $[M+H]^+$: 448.2362, found 448.2362; *m*/*z* calculated for $C_{24}H_{34}ClN_3NaO_3$ $[M+Na]^+$: 470.2181, found 470.2172; *m*/*z* calculated for $C_{24}H_{34}ClKN_3O_3$ $[M+K]^+$: 486.1921, found 486.1911.

Assignment of Aminal Diastereoisomers Derived from the 2nd Generation MacMillan Catalyst (Isovaleraldehyde as the Substrate)

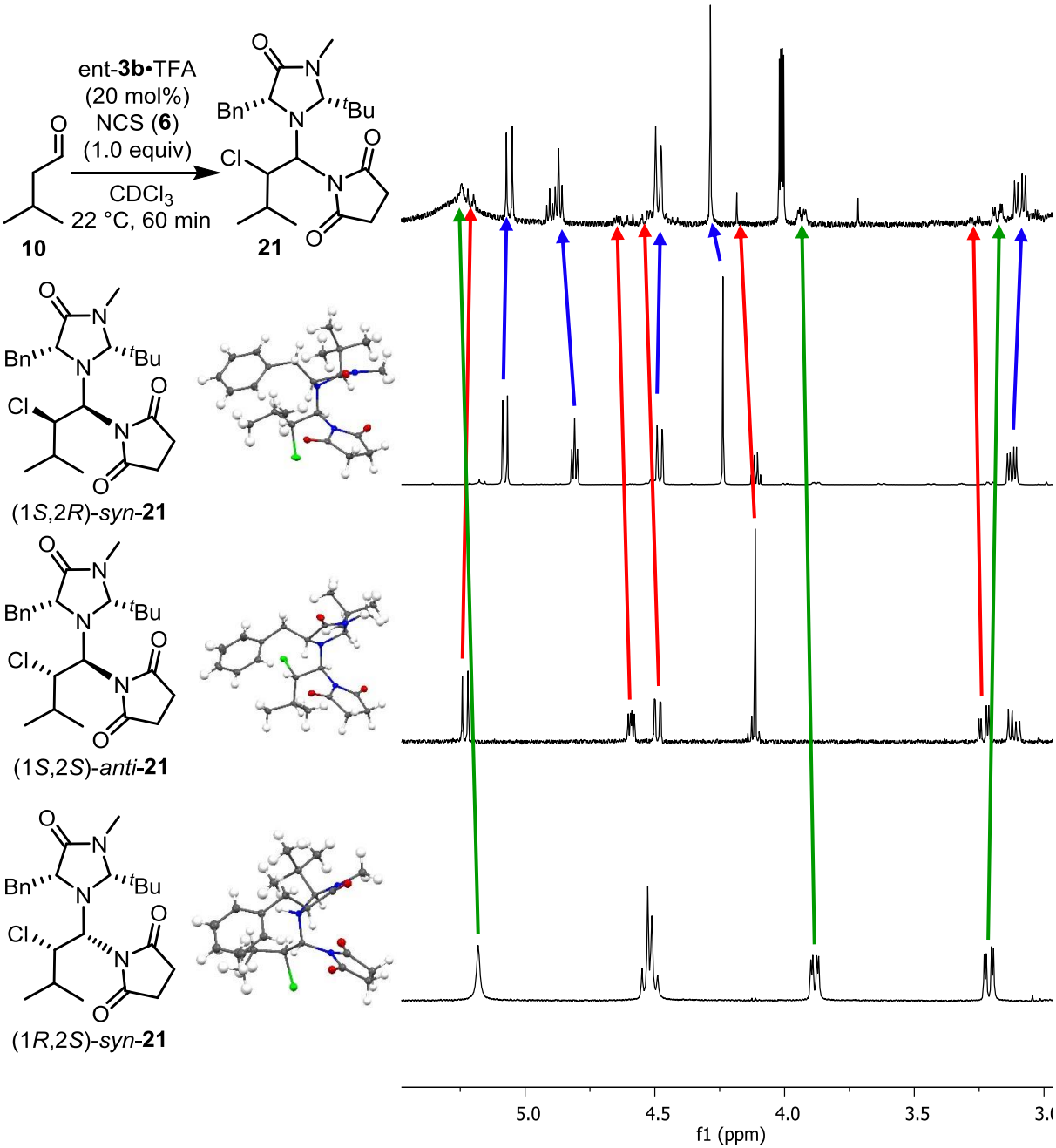

Figure SI-4. ^{1}H-NMR spectrum of the reaction with 20 mol% *ent*-**3b**•TFA after 60 min (according to Blackmond et al.[24,25] (top). Crystal structures and ^{1}H-NMR spectra of the isolated diastereomeric aminals **21** (below).

In their publication "Rationalization of an Unusual Solvent-Induced Inversion of Enantiomeric Excess in Organocatalytic Selenylation of Aldehydes"[24,25] the authors discussed two aminal diastereomers for the 2nd generation MacMillan catalyst but overlooked a third aminal diastereomer (1*R*,2*S*)-*syn*-**21**) indicated by the green arrows. Their rationale is based on the existence of only two out of four possible aminal

species. Isolation and subsequent X-ray crystal structure analysis reveals *syn*-configuration for the major aminal (1*S*,2*R*)-*syn*-**21** and *anti*-configuration for minor aminal (1*S*,2*S*)-*anti*-**21**. The third, previously overlooked aminal (1*R*,2*S*)-*syn*-**21** also has the *syn*-configuration. It is actually present in higher concentration than the species which was named “minor”.

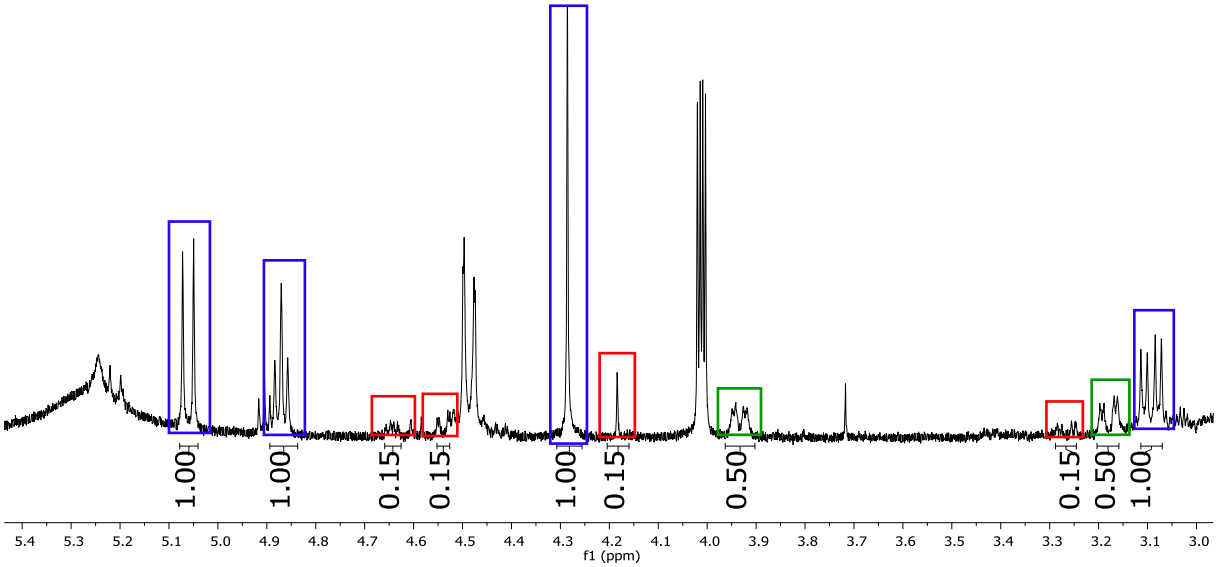

Figure SI-5. ^{1}H-NMR spectrum of the reaction with 20 mol% *ent*-**3b**•TFA after 60 min with integrated signals (blue: major aminal (1*S*,2*R*)-*syn*-**21**; red: minor aminal (1*S*,2*S*)-*anti*-**21**; green: previously overlooked aminal (1*R*,2*S*)-*syn*-**21** (according to Blackmond et al.[24,25]

Since the quality of the crystallographic data for aminal (1*S*,2*R*)-*syn*-**21** was not optimal and to confirm the previous results and conclusions, the same experiments and isolation procedures were repeated using hydrocinnamic aldehyde instead of isovaleraldehyde.

Aminals Derived from Hydrocinnamic Aldehyde, NCS and the 2nd Generation MacMillan Catalyst *ent*-3b (NMR experiment)

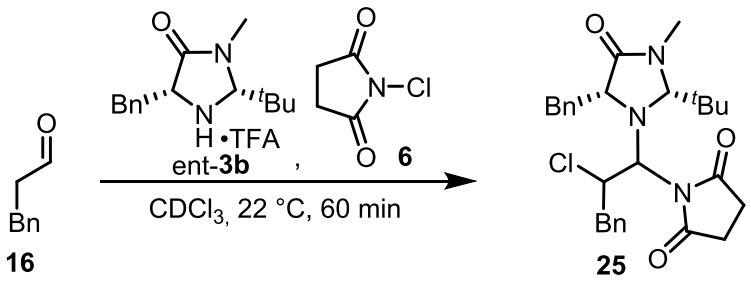

The TFA-salt of catalyst *ent*-**3b** (7.20 mg, 20.0 µmol, 20 mol%) and NCS (13.3 mg, 100 µmol, 1.0 equiv) were added successively to an NMR-tube containing a solution of hydrocinnamic aldehyde (13.4 µL, 100 µmol, 1.0 equiv) in $CDCl_3$ (0.70 mL) at 22 °C. The ^{1}H-NMR spectrum was recorded after 60 min. The diastereomeric ratio is approximately 5:1:3.

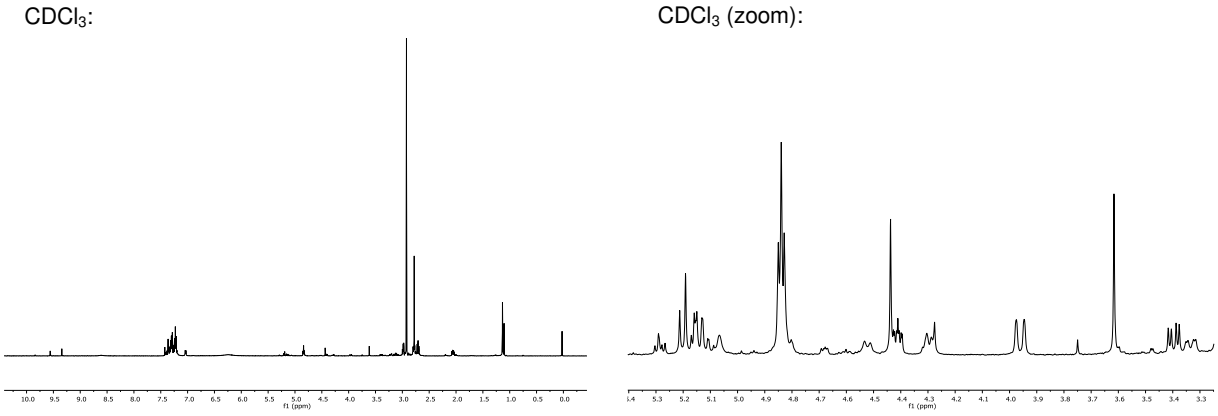

Figure SI-6. ^{1}H-NMR spectra of the α-chlorination reaction (hydrocinnamic aldehyde, NCS, catalyst *ent*-**3b**•TFA) after 60 min.

1-((1*S*,2*R*)-1-((2*R*,5*R*)-5-benzyl-2-(tert-butyl)-3-methyl-4-oxoimidazolidin-1-yl)-2-chloro-3-phenylpropyl)pyrrolidine-2,5-dione ((1*S*,2*R*)-*syn*-25),
1-((1*S*,2*S*)-1-((2*R*,5*R*)-5-benzyl-2-(tert-butyl)-3-methyl-4-oxoimidazolidin-1-yl)-2-chloro-3-phenylpropyl)pyrrolidine-2,5-dione ((1*S*,2*S*)-*anti*-25) ,
1-((1*R*,2*S*)-1-((2*R*,5*R*)-5-benzyl-2-(tert-butyl)-3-methyl-4-oxoimidazolidin-1-yl)-2-chloro-3-phenylpropyl)pyrrolidine-2,5-dione ((1*R*,2*S*)-*syn*-25)

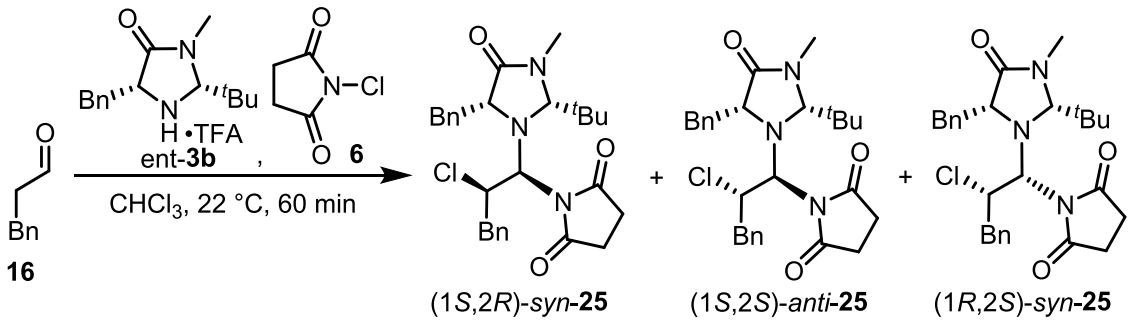

The TFA-salt of catalyst *ent*-**3b** (0.837 g, 2.32 mmol, 20 mol%) and NCS (1.55 g, 11.6 mmol, 1.0 equiv) were added successively to a solution of hydrocinnamic aldehyde (1.54 mL, 11.6 mmol, 1.0 equiv) in $CHCl_3$ (46 mL). The reaction was stirred for 60 min and quenched with aqueous saturated $NaHCO_3$ (50 mL). The aqueous phase was extracted with dichloromethane (3x50 mL), the combined organic phases were dried over $NaSO_4$, the solvent was removed under reduced pressure and the crude product was purified by column chromatography (SiO_2, pentane/Et_2O/EtOAc, 1:1:1 to 0:1:1 to 0:0:1). Aminal (1*S*,2*R*)-*syn*-**25** was obtained as a colorless solid (0.381 g, 0.768 mmol, 33%). Separation of another fraction from the column chromatography by chiral HPLC enabled further separation of aminal (1*S*,2*S*)-*anti*-**25** (57.0 mg, 0.115 mmol, 5%) and aminal (1*R*,2*S*)-*syn*-**25** (0.137 g, 0.272 mmol, 12%). The absolute configuration of the three aminals was determined by X-ray crystal structure analysis.

Aminal (1*S*,2*R*)-*syn*-25:

mp = 158 °C

$[\alpha]_D^{26}$ = –1.96° (*c* = 1.00, dichloromethane)

^{1}H-NMR ($CDCl_3$, 600 MHz) δ = 7.39 – 7.36 (m, 2H), 7.33 – 7.28 (m, 2H), 7.26 – 7.18 (m, 4H), 7.00 – 6.97 (m, 2H), 5.18 (d, *J* = 10.7 Hz, 1H), 5.08 (td, *J* = 10.8, 1.9 Hz, 1H), 4.75 (dd, *J* = 7.6, 5.7 Hz, 1H), 4.33 (s, 1H), 3.93 (dd, *J* = 14.7, 1.4 Hz, 1H), 3.18 – 3.09 (m, 2H), 2.88 (s, 3H), 2.77 – 2.70 (m, 5H), 1.09 (s, 9H) ppm.

^{13}C-NMR ($CDCl_3$, 151 MHz) δ = 179.5, 173.4, 138.1, 137.0, 129.4, 129.1, 128.8, 128.5, 127.0, 126.8, 87.8, 79.1, 61.2, 59.6, 42.3, 41.6, 37.7, 31.9, 29.7, 28.1, 26.7 ppm.

IR (ATR): $\tilde{\nu}$ = 2957, 2925, 1774, 1702, 1455, 1328, 1253, 1148, 1061, 749 cm^{-1}.

HRMS (ESI, pos. mode): *m*/*z* calculated for $C_{28}H_{35}ClN_3O_3$ $[M+H]^+$: 496.2362, found 496.2350; *m*/*z* calculated for $C_{28}H_{34}ClN_3NaO_3$ $[M+Na]^+$: 518.2181, found 518.2160; *m*/*z* calculated for $C_{28}H_{34}ClKN_3O_3$ $[M+K]^+$: 534.1921, found 534.1899.

Aminal (1*S*,2*S*)-*anti*-25:

mp = 150 °C

$[\alpha]_D^{26}$ = –18.43° (*c* = 0.45, dichloromethane)

^{1}H-NMR ($CDCl_3$, 700 MHz) δ = 7.41 – 7.38 (m, 2H), 7.32 – 7.24 (m, 5H), 7.24 – 7.19 (m, 1H), 7.03 – 7.01 (m, 2H), 5.29 (d, *J* = 10.5 Hz, 1H), 4.75 (td, *J* = 10.2, 3.1 Hz, 1H), 4.62 (dd, *J* = 6.7, 4.8 Hz, 1H), 4.19 (s, 1H), 3.20 – 3.13 (m, 2H), 2.92 (s, 3H), 2.85 (dd, *J* = 14.3, 3.1 Hz, 1H), 2.76 – 2.66 (m, 4H), 2.64 (dd, *J* = 14.3, 10.0 Hz, 1H), 1.11 (s, 9H) ppm.

^{13}C-NMR ($CDCl_3$, 151 MHz) δ = 179.2, 174.1, 139.3, 136.6, 129.5, 129.1, 128.5, 128.4, 127.1, 126.4, 86.2, 76.9, 61.8, 60.3, 41.2, 41.0, 38.2, 31.9, 29.8, 28.3, 26.3 ppm.

IR (ATR): $\tilde{\nu}$ = 2955, 2925, 1772, 1702, 1455, 1363, 1255, 1156, 1079, 794, 750 cm^{-1}.

HRMS (ESI, pos. mode): *m*/*z* calculated for $C_{28}H_{35}ClN_3O_3$ $[M+H]^+$: 496.2362, found 496.2381; *m*/*z* calculated for $C_{28}H_{34}ClN_3NaO_3$ $[M+Na]^+$: 518.2181, found 518.2191; *m*/*z* calculated for $C_{28}H_{34}ClKN_3O_3$ $[M+K]^+$: 534.1921, found 534.1935.

Aminal (1*R*,2*S*)-*syn*-25:

mp = 178 °C

$[\alpha]_D^{26}$ = –55.64° (*c* = 1.45, dichloromethane)

^{1}H-NMR ($CDCl_3$, 700 MHz) δ = 7.45 – 7.39 (m, 4H), 7.33 – 7.19 (m, 4H), 7.06 – 7.03 (m, 2H), 4.98 (s, 1H), 4.85 (t, *J* = 11.0 Hz, 1H), 4.54 (d, *J* = 10.0 Hz, 1H), 4.24 (dd, *J* = 11.6, 4.3 Hz, 1H), 3.35 (dd, *J* = 14.1, 4.2 Hz, 1H), 3.23 (d, *J* = 15.9 Hz, 1H), 2.96 (s, 3H), 2.88 (dd, *J* = 14.1, 11.5 Hz, 1H), 2.85 – 2.58 (m, 4H), 1.72 (s, 1H), 1.10 (s, 9H) ppm.

^{13}C-NMR ($CDCl_3$, 176 MHz) δ = 179.3, 178.2, 173.5, 138.2, 137.2, 129.8, 128.9, 128.7, 128.5, 126.9, 126.8, 86.2, 80.3, 67.2, 58.9, 41.0, 38.6, 37.2, 32.2, 28.1, 28.0, 27.8 ppm.

IR (ATR): $\tilde{\nu}$ = 3030, 2958, 1705, 1329, 1254, 1161, 1094, 740 cm^{-1}.

HRMS (ESI, pos. mode): *m*/*z* calculated for $C_{28}H_{34}ClN_3NaO_3$ $[M+Na]^+$: 518.2181, found 518.2184; *m*/*z* calculated for $C_{28}H_{34}ClKN_3O_3$ $[M+K]^+$: 534.1921, found 534.1920.

Assignment of Aminal Diastereoisomers Derived from the 2nd Generation MacMillan Catalyst (Hydrocinnamic Aldehyde as the Substrate)

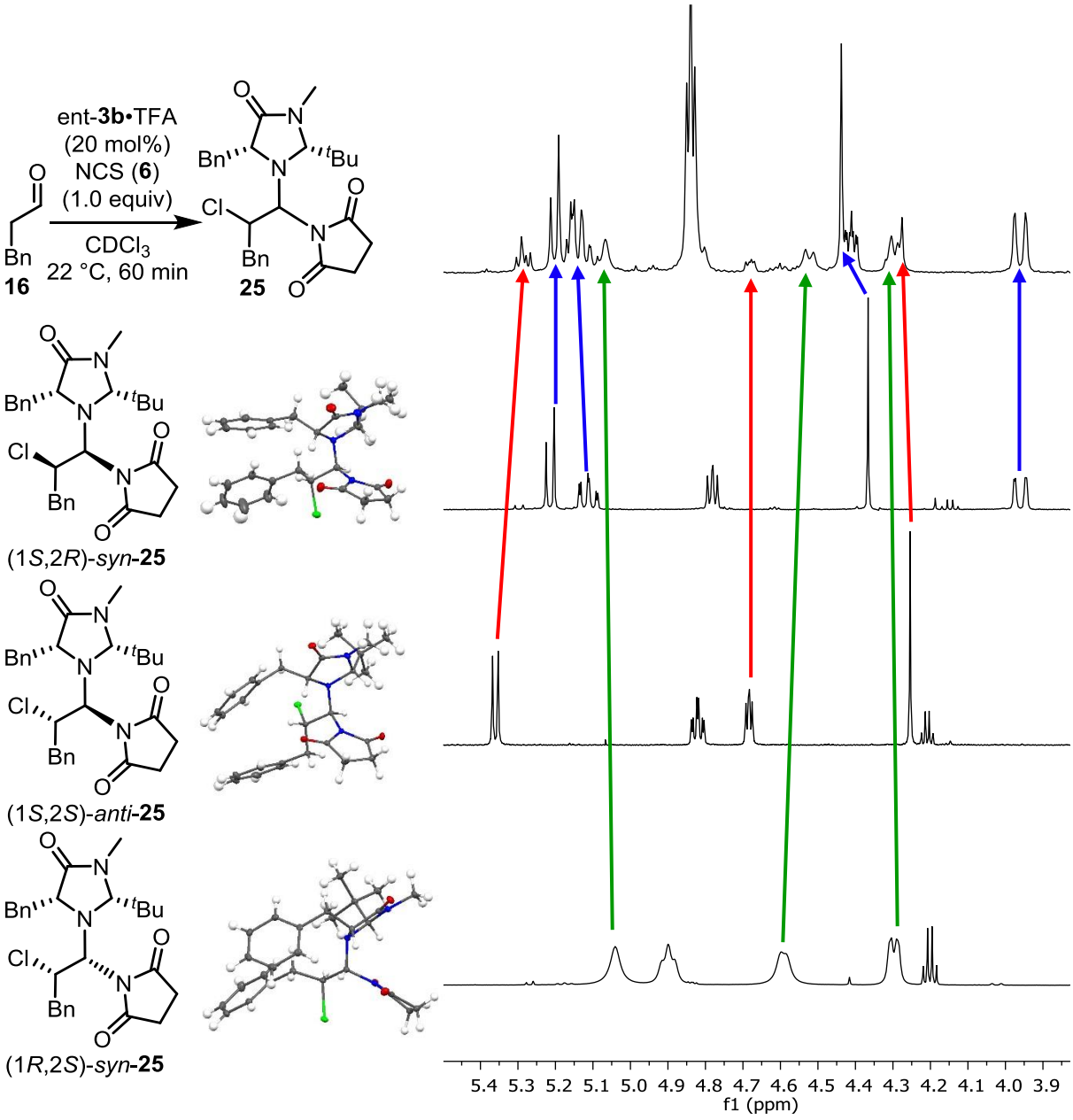

Figure SI-7. ^{1}H-NMR spectrum of the reaction with 20 mol% *ent*-**3b**•TFA after 60 min (top). Crystal structures and ^{1}H-NMR spectra of the isolated diastereomeric aminals **21** (below).

As expected, three diastereomeric species can be detected in the ^{1}H-NMR spectrum. All of them could be isolated and fully characterized. The absolute configurations of the three aminals were determined by X-ray crystal structure analysis and are in accordance with the previous experiment (isovaleraldehyde as the substrate).

Decomposition of Aminal *syn*-18b (Derived from 3rd Generation MacMillan Catalyst)

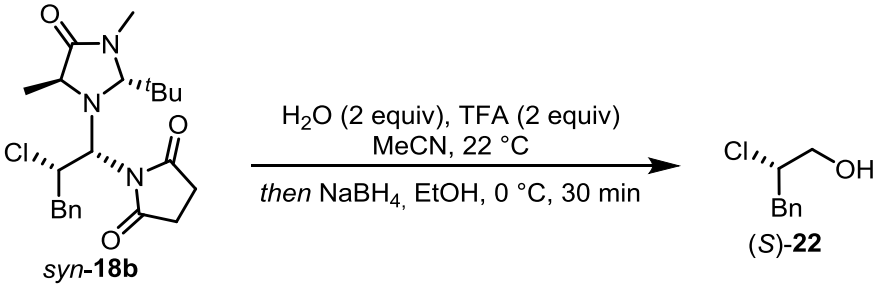

Aminal *syn*-**18b** was synthesized according to the literature procedure.[22] H_2O (85.8 µL, 4.76 mmol, 2.0 equiv) and TFA (364 µL, 4.76 mmol, 2.0 equiv) were added to a solution of aminal *syn*-**18b** (1.00 g, 2.38 mmol, 1.0 equiv) in MeCN (30 mL) at 22 °C. Aliquots (6 mL) were taken from the reaction mixture after defined points of time (5 min, 10 min, 60 min) and added to a solution of $NaBH_4$ (75.1 mg, 1.98 mmol, 5.0 equiv) in EtOH (2.0 mL). After 30 min the reactions were quenched by the addition of aqueous saturated NH_4Cl.The aqueous phase was extracted with EtOAc (3x5 mL), the combined organic phases were dried over Na_2SO_4 and the solvent was removed under reduced pressure. The crude products were purified by column chromatography (SiO_2, pentane/EtOAc 10:1 to 5:1) and the enantiomeric excess was determined by chiral HPLC. The absolute configuration was determined by comparison of the optical rotation with the literature.

The ^{1}H-NMR spectrum is in accordance with the literature.[22]

^{1}H-NMR ($CDCl_3$, 400 MHz) δ = 7.35 – 7.30 (m, 2H), 7.29 – 7.22 (m, 3H), 4.26 – 4.20 (m, 1H), 3.81 (ddd, *J* = 12.1, 7.2, 3.6 Hz, 1H), 3.69 (dt, *J* = 12.1, 6.1 Hz, 1H), 3.14 (dd, *J* = 14.0, 7.0 Hz, 1H), 3.06 (dd, *J* = 14.0, 7.4 Hz, 1H), 2.03 (t, *J* = 6.7 Hz, 1H) ppm.

1. aliquot (5 min): 95% ee
2. aliquot (10 min): 95% ee
3. aliquot (60 min): 94% ee

Sample: $[\alpha]_D^{24}$ = –11.4° (*c* = 1.00, dichloromethane)
(*S*)-2-chloro-3-phenylpropan-1-ol (95% ee): $[\alpha]_D^{24}$ = –13.8° (*c* = 1.00, dichloromethane)
(*R*)-2-chloro-3-phenylpropan-1-ol (93% ee): $[\alpha]_D^{24}$ = +14.0° (*c* = 1.00, dichloromethane)
(*S*)-2-chloro-3-phenylpropan-1-ol (95% ee): $[\alpha]_D$ = –21.7° (*c* = 1.00, $CHCl_3$)[27]

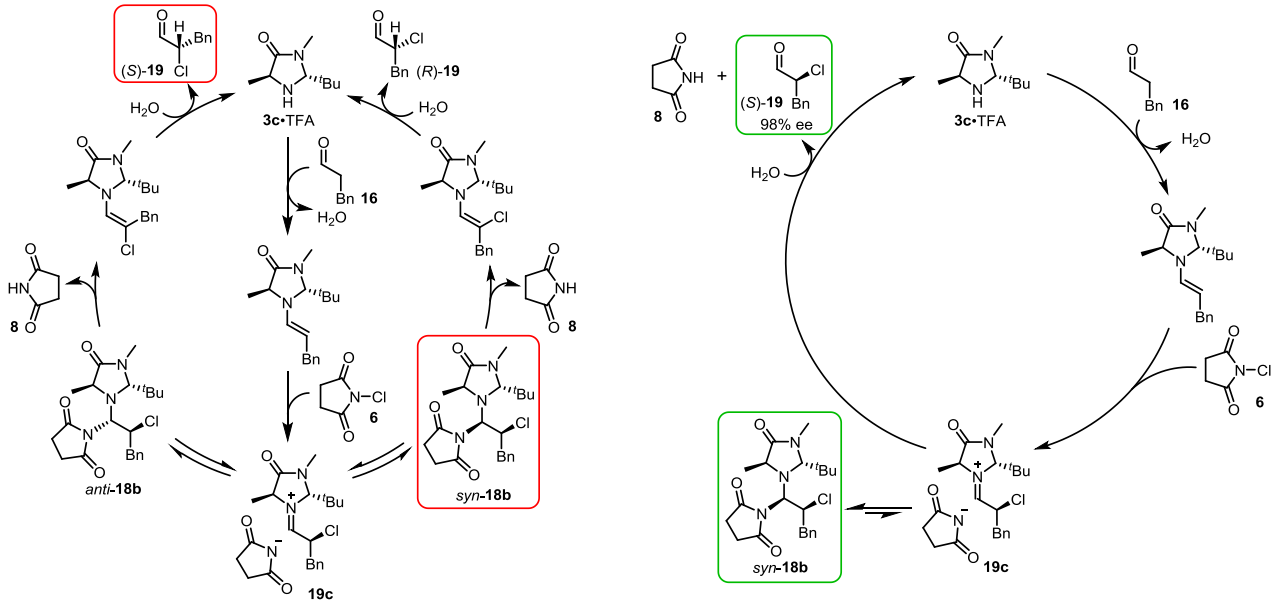

Figure SI-8. Only the off-cycle mechanism (right) can rationalize the observed enenatioselectivity ((*S*)-chloroaldehyde) of the α-chlorination reaction and the decomposition pathway. The on-cycle mechanism[28] (left) predicts the formation of the wrong enantiomer of the chloroaldeyhde ((*R*)-chloroaldehyde).

As observed for most of the aminals derived from the 1st and 2nd generation MacMillan catalyst, aminal *syn*-**18b** is bench-stable and can be isolated and characterized.[22] According to the catalytic cycle of the on-cycle scenario[28] aminal *syn*-**18b** should generate the (*R*)-enantiomer of the chloroaldehyde product. Decomposition under acidic conditions (TFA and water are also present in the catalytic reaction) clearly shows that aminal *syn*-**18b** was converted almost exclusively (95% ee) to the (*S*)-chloroaldehyde product. This experimental outcome is in accordance with our proposed decomposition pathway via a chloroiminium ion.

(*S*)-2-chloro-3-phenylpropan-1-ol ((*S*)-22)

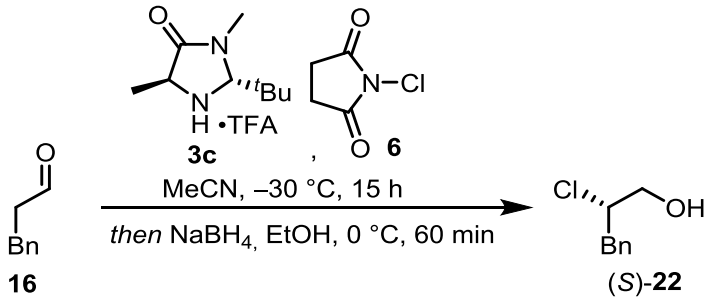

Hydrocinnamic aldehyde (0.266 mL, 2.00 mmol, 1.0 equiv) was dissolved in MeCN (8.0 mL) and cooled to –30 °C. Catalyst **3c** (0.114 g, 0.400 mmol, 20 mol%) and NCS (0.320 g, 2.40 mmol, 1.2 equiv) were added subsequently and the reaction mixture was stirred for 15 h at the same temperature. After the reaction was warmed to 0 °C, MeOH (3.0 mL) and $NaBH_4$ (0.189 g, 5.00 mmol, 2.5 equiv) were added and the mixture was stirred for 60 min at the same temperature. The reaction was quenched with aqueous saturated NH_4Cl (10 mL), the aqueous phase was extracted with dichloromethane (3x15 mL) and the combined organic phases were dried over $NaSO_4$. The solvent was removed under reduced pressure and the crude product was purified by column chromatography (Silica, pentane/EtOAc 10:1). Pure chloroalcohol (*S*)-**22** (0.248 g, 1.45 mmol, 73%, 95% ee) was obtained as a colorless oil.

^{1}H-NMR is in accordance with the literature.[22]

$[\alpha]_D^{24}$ = –13.8° (*c* = 1.00, dichloromethane)

^{1}H-NMR ($CDCl_3$, 400 MHz) δ = 7.35 – 7.30 (m, 2H), 7.29 – 7.22 (m, 3H), 4.26 – 4.20 (m, 1H), 3.81 (ddd, *J* = 12.1, 7.2, 3.6 Hz, 1H), 3.69 (dt, *J* = 12.1, 6.1 Hz, 1H), 3.14 (dd, *J* = 14.0, 7.0 Hz, 1H), 3.06 (dd, *J* = 14.0, 7.4 Hz, 1H), 2.03 (t, *J* = 6.7 Hz, 1H) ppm.

(*R*)-2-chloro-3-phenylpropan-1-ol ((*R*)-22)

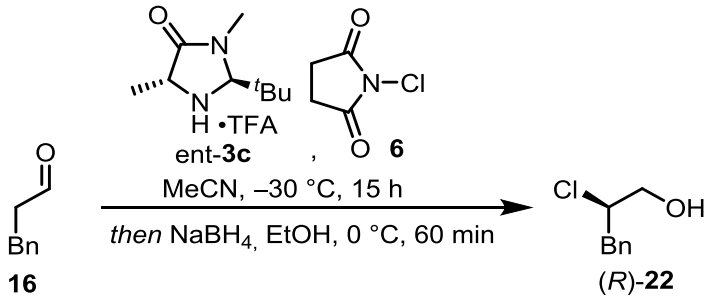

Hydrocinnamic aldehyde (0.266 mL, 2.00 mmol, 1.0 equiv) was dissolved in MeCN (8.0 mL) and cooled to –30 °C. Catalyst *ent*-**3c** (0.114 g, 0.400 mmol, 20 mol%) and NCS (0.320 g, 2.40 mmol, 1.2 equiv) were added subsequently and the reaction mixture was stirred for 15 h at the same temperature. After the reaction was warmed to 0 °C, MeOH (3.0 mL) and $NaBH_4$ (0.189 g, 5.00 mmol, 2.5 equiv) were added and the mixture was stirred for 60 min at the same temperature. The reaction was quenched with aqueous saturated NH_4Cl (10 mL), the aqueous phase was extracted with dichloromethane (3x15 mL) and the combined organic phases were dried over $NaSO_4$. The solvent was removed under reduced pressure and the crude product was purified by column chromatography (Silica, pentane/EtOAc 10:1). Pure chloroalcohol (*R*)-**22** (0.229 g, 1.34 mmol, 67%, 93% ee) was obtained as a colorless oil.

^{1}H-NMR is in accordance with the literature.[22]

$[\alpha]_D^{24}$ = +14.0° (*c* = 1.00, dichloromethane)

^{1}H-NMR ($CDCl_3$, 400 MHz) δ = 7.35 – 7.30 (m, 2H), 7.29 – 7.22 (m, 3H), 4.26 – 4.20 (m, 1H), 3.81 (ddd, *J* = 12.1, 7.2, 3.6 Hz, 1H), 3.69 (dt, *J* = 12.1, 6.1 Hz, 1H), 3.14 (dd, *J* = 14.0, 7.0 Hz, 1H), 3.06 (dd, *J* = 14.0, 7.4 Hz, 1H), 2.03 (t, *J* = 6.7 Hz, 1H) ppm.

2.2. NMR reaction progress (3rd generation MacMillan catalyst)

^{1}H-NMR reaction progress

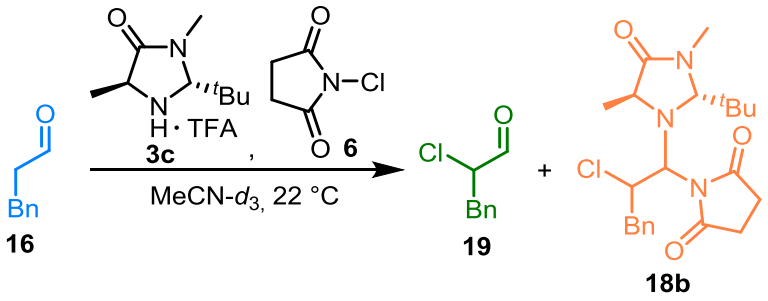

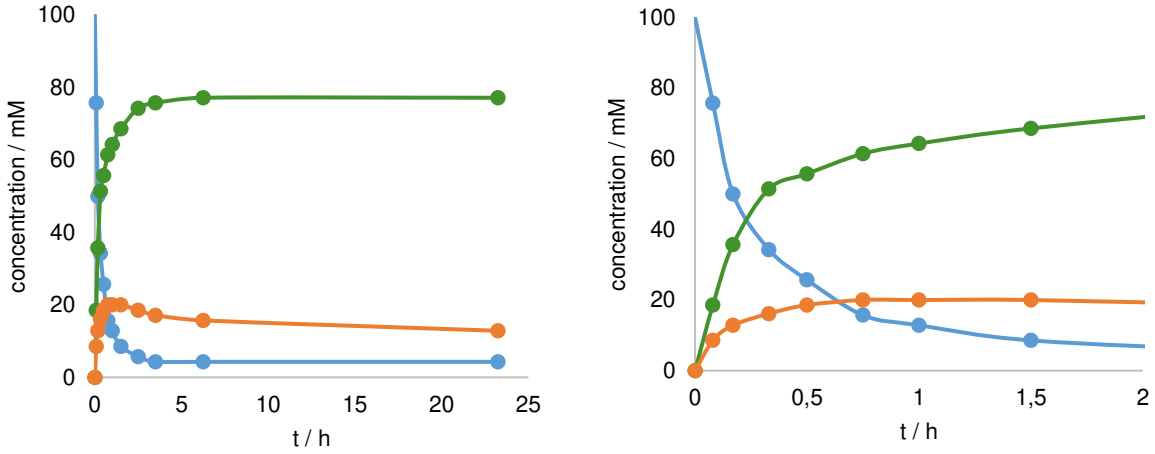

Figure SI-9. ^{1}H-NMR reaction progress of the α-chlorination reaction (hydrocinnamic aldehyde, NCS, catalyst **3c**•TFA) according to our previous publication.[22]

Table SI-1. Experimental data of the reaction progress analysis.[22]

t [min]	t [h]	aldehyde		Cl-aldehyde		aminal	
0	0	0,7	100,03	0	0	0	0
5	0,08	0,53	75,74	0,13	18,58	0,06	8,57
10	0,17	0,35	50,02	0,25	35,73	0,09	12,86
20	0,33	0,24	34,3	0,36	51,44	0,11	16,15
30	0,5	0,18	25,72	0,39	55,73	0,13	18,58
45	0,75	0,11	15,72	0,43	61,45	0,14	20,01
60	1	0,09	12,86	0,45	64,31	0,14	20,01
90	1,5	0,06	8,57	0,48	68,59	0,14	20,01
150	2,5	0,04	5,72	0,52	74,31	0,13	18,58
210	3,5	0,03	4,29	0,53	75,74	0,12	17,15
375	6,25	0,03	4,29	0,54	77,17	0,11	15,72
1395	23,25	0,03	4,29	0,54	77,17	0,09	12,86

We interrogated concentration profiles in order to assess whether the two mechanisms (steric shielding model and Curtin-Hammett scenario) are kinetically distinguishable. Gratifyingly, aldehyde **16**, the

chloroaldehyde product **19** and the corresponding crystallographically characterized aminal *syn*-**18b** possess separate, non-overlapping NMR resonances. By monitoring their concentrations over time[22] it is apparent that the initial rate of chloroaldehyde formation exceeds the build-up of the aminal. This observation eliminates the possibility of the catalyst being turned over through the thermodynamically most stable aminal (Curtin-Hammett scenario). The alternate off-cycle mechanism provides a scenario where the rate of iminium hydrolysis exceeds that of aminal formation. From the iminium ion intermediate, part of the catalyst is diverted into a stable aminal resting state. To further illustrate the absence of an on-cycle-mechanism, the first three ^{1}H-NMR-spectra of the previously considered reaction are shown below. The aminal concentration at no point exceeds the product concentration, not even in the initial phase (5 min) of the reaction. This observation strongly supports an off-cycle-scenario, in which the product can be formed without going through the aminal intermediate. When reanalyzing our data for this reaction, we noted additional, previously overlooked resonances in the NMR spectrum at t = 5 min (quickly disappearing thereafter). The possibility of the corresponding species to be the elusive aminal *anti*-**18b** is supported by comparison of the observed and computed ^{1}H chemical shifts.

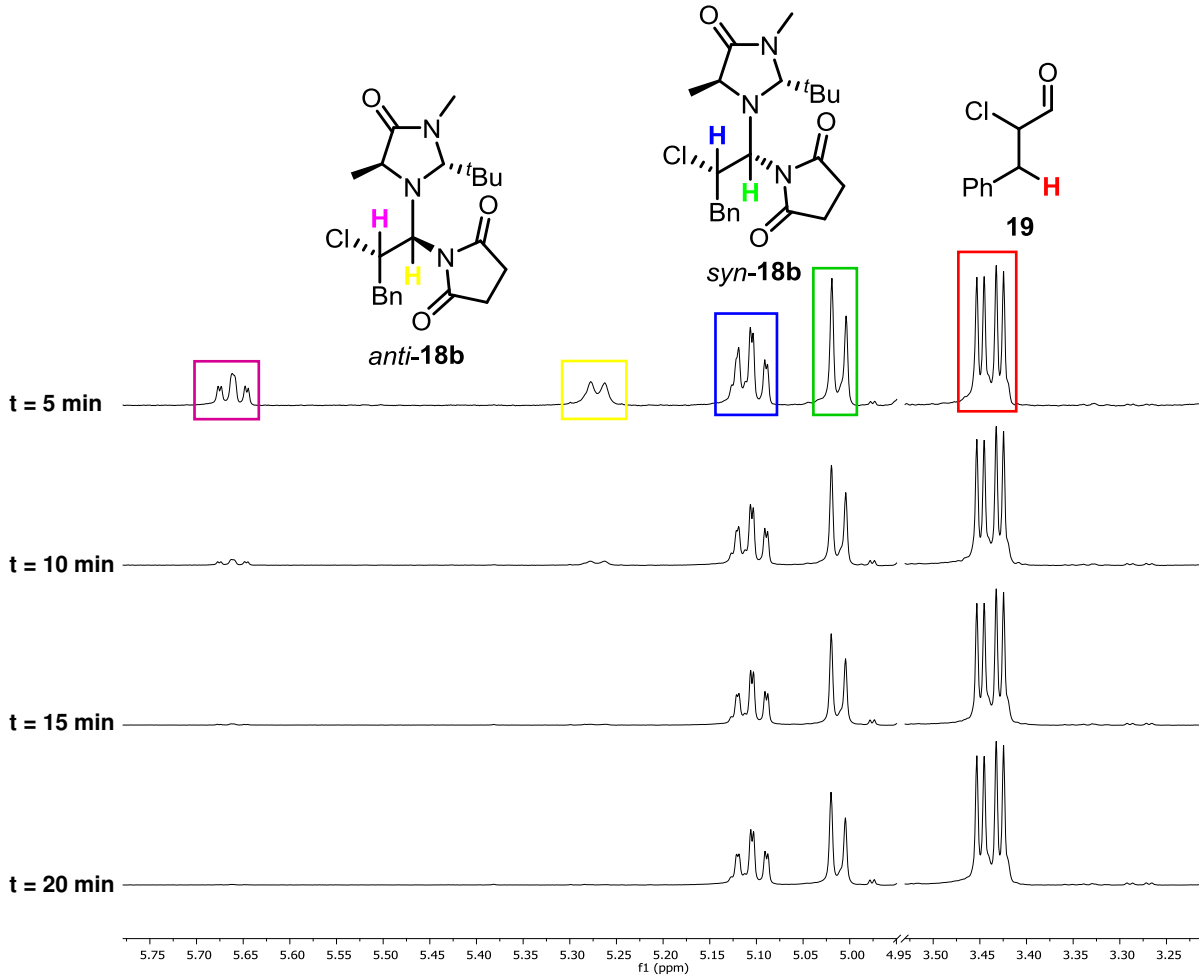

Figure SI-10. ^{1}H-NMR spectra of the initial phase of the α-chlorination reaction (hydrocinnamic aldehyde, NCS, catalyst **3c**•TFA).

NMR Calculations for *syn*-18b and *anti*-18b

^{1}H and ^{13}C NMR calculations were performed to compare to the major and minor sppecies at t = 5 min. The key ^{1}H chemical shifts for *syn*-**18b** and *anti*-**18b** were in good agreement (< 0.3 ppm absolute deviation between experimental and calculated chemical shifts)[17,18] with the experimental shifts for the major and minor products.

Table SI-2. Calculated ^{13}C NMR δ's for *syn*-**18b**.

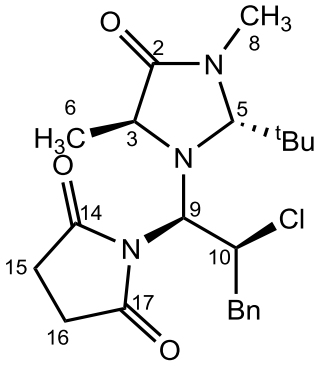

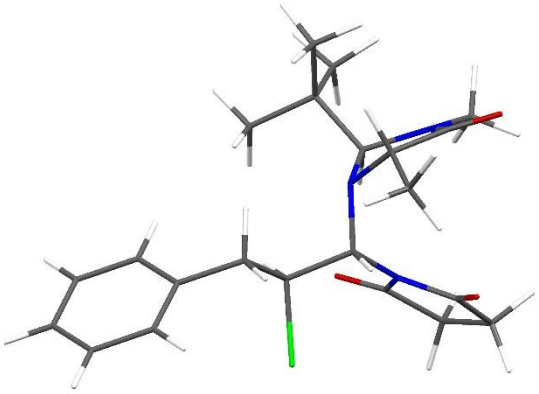

Exp. #	Comp #	Comp. Isotropic	Comp. δ
C5	1	98.9366	83.8
C2	2	3.6610	174.5
C3	3	123.1277	60.7
C4	7	153.8751	31.5
C1'	11	113.1924	70.2
C2'	13	111.3355	72.0
C3'	14	142.8361	42.0
C4'	17	175.0080	11.3
C5'	22	143.6420	41.2
	26	-4.5320	182.3
	27	-2.1380	180.0
C5"	28	155.0907	30.3
C2"	29	155.6905	29.7
C6	34	158.5958	27.0
	38	156.9911	28.5
	42	163.1739	22.6
	49	41.0137	138.9
	50	50.0409	130.3
	51	53.6789	126.9
	52	52.7727	127.7
	54	52.5161	128.0
	56	54.4196	126.2

Table SI-3. Comparison of calculated and experimental ^{1}H NMR δ's for *syn*-**18b**.

Exp. C#	Comp. C#	Comp. H#	Comp. Isotropic	Comp. δ	Avg. Comp. δ	Exp. δ	Abs. Dev.
8	7	8	28.57	3.00			
8	7	9	29.26	2.36			
8	7	10	29.12	2.49			
9	11	12	26.64	4.81	4.81	5.01	0.20
11	14	15	29.18	2.43	2.43		
10	13	16	26.22	5.20	5.20	5.10	0.10
6	17	18	30.32	1.37			
6	17	19	30.54	1.16			
6	17	20	29.51	2.13	1.55	1.47	0.08
3	3	21	27.65	3.87			
5	1	23	27.27	4.22			
15	28	30	28.99	2.61			
16	29	31	28.98	2.62			
tBu	34	35	30.82	0.89			
tBu	34	36	30.65	1.05			
tBu	34	37	30.79	0.93			
tBu	38	39	30.29	1.39			
tBu	38	40	30.02	1.64			
tBu	38	41	30.58	1.12			
tBu	42	43	30.76	0.95			
tBu	42	H32	26.54	0.80			
tBu	42	45	30.75	0.96	1.08	1.10	0.02
16	29	46	29.03	2.57			
15	28	47	28.96	2.64			
11	14	48	27.41	4.09	4.09	3.96	0.13
	50	53	24.03	7.25			
	51	55	23.81	7.46			
	52	57	23.95	7.33			
	54	58	23.92	7.36			
	56	59	23.99	7.29			
						MAD	0.11

Table SI-4. Calculated ^{13}C NMR δ's for *anti*-**18b**

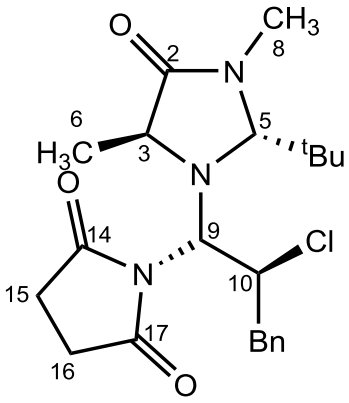

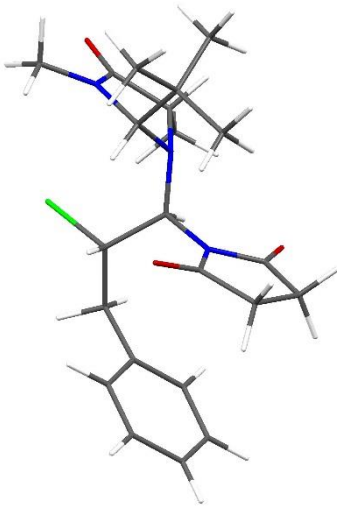

Exp. #	Comp #	Comp. Isotropic	Comp. δ
C5	C	97.8311	84.8
C2	C	2.7976	175.3
C3	C	121.5410	62.3
C4	C	152.4037	32.9
C1'	C	112.1019	71.2
C2'	C	116.7850	66.8
C3'	C	137.7947	46.8
C4'	C	173.1138	13.2
C5'	C	141.3341	43.4
	C	-0.9819	178.9
	C	-3.1036	180.9
C5''	C	155.3086	30.1
C2''	C	156.1731	29.3
C6	C	158.5219	27.0
	C	159.5979	26.0
	C	162.7703	23.0
	C	41.9613	138.0
	C	50.8312	129.6
	C	52.3459	128.1
	C	52.4331	128.1
	C	52.4293	128.1
	C	53.9564	126.6

Table SI-5. Comparison of calculated and experimental ^{1}H NMR δ's for *anti*-**18b**.

Exp. C#	Comp. C#	Comp. H#	Comp. Isotropic	Comp. δ	Avg. Comp. δ	Exp. δ	Abs. Dev.
8	7	8	28.48	3.09			
8	7	9	29.02	2.58			
8	7	10	28.98	2.62			
9	11	12	26.27	5.15	5.15	5.27	0.12
11	14	15	28.67	2.91			
11	14	16	28.07	3.47	3.47	3.18	0.29
10	13	17	25.43	5.94	5.94	5.66	0.28
6	18	19	30.11	1.56			
6	18	20	30.13	1.54			
6	18	21	30.26	1.42	1.51	1.50	0.01
3	3	22	27.68	3.83	3.83	3.91	0.08
5	1	24	27.05	4.42	4.42	4.46	0.04
15	29	31	29.62	2.02			
16	30	32	29.70	1.94			
tBu	35	36	30.98	0.75			
tBu	35	37	30.64	1.06			
tBu	35	38	30.79	0.92			
tBu	39	40	30.88	0.84			
tBu	39	41	31.10	0.63			
tBu	39	42	31.21	0.53			
tBu	43	44	26.54	0.86			
tBu	43	45	31.17	0.57			
tBu	43	46	30.97	0.75	0.77	0.91	0.14
16	30	47	30.59	1.11			
15	29	48	29.30	2.32			
	50	53	24.02	7.26			
	51	55	24.26	7.04			
	52	57	23.95	7.33			
	54	58	24.08	7.21			
	56	59	24.07	7.21			
						MAD	0.14

2.3. KIEs and DFT Calculations (3rd Generation MacMillan Catalyst)

KIE-experiment (1)

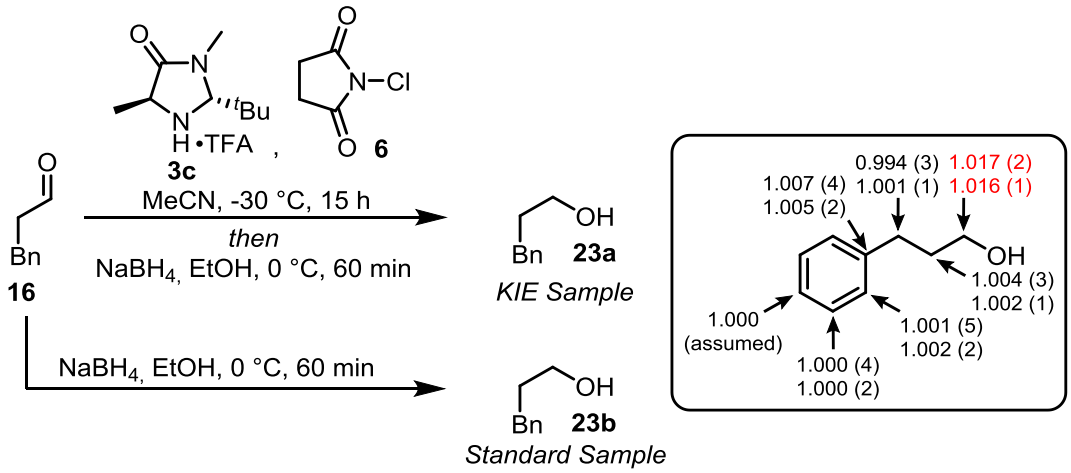

KIE Sample (KIE1&2): Distilled hydrocinnamic aldehyde (1.61 g, 12.0 mmol, 1.0 equiv) was dissolved in MeCN (40 mL) in a 50 mL graduated flask and cooled to –30°C. Catalyst **3c** (0.682 g, 2.40 mmol, 20 mol%) and NCS (1.20 g, 9.00 mmol, 0.75 equiv) were added successively, the volume was adjusted to 50 mL by adding MeCN and the solution was stirred for 15 hours at –30 °C. EtOH (15 mL) and $NaBH_4$ (1.13 g, 30.0 mmol, 2.5 equiv) were added successively and the reaction mixture was stirred for 1 hour at 0 °C. The reaction was quenched with aqueous saturated NH_4Cl (30 mL), extracted with EtOAc (6x50 mL) and dried over Na_2SO_4. The combined organic phases were transferred into a 500 mL graduated flask and the volume was adjusted to 500 mL by adding EtOAc. 10.0 mL were removed from the graduated flask and the solvent was removed under reduced pressure. The crude mixture was taken up with 2 x 0.50 mL $MeCNd_3$ and transferred into an NMR-tube containing 10.0 mg of the internal standard (1,3,5-trimethoxybenzene). The solvent of the remaining organic phase was removed under reduced pressure and the reduced starting material was purified by column chromatography (Silica, 10:1 to 5:1 pentane/EtOAc).

Standard Sample (STD1&2): $NaBH_4$ (0.284 g, 7.50 mmol, 2.5 equiv) was added to a solution of distilled hydrocinnamic aldehyde (from the same batch as in the KIE-experiment) (0.403 g, 3.00 mmol, 1.0 equiv) in EtOH (3.5 mL) at 0 °C. The reaction mixture was stirred for 60 min at 0 °C and subsequently quenched with aqueous saturated NH_4Cl (5 mL). The aqueous phase was extracted with EtOAc (6x5 mL), the combined organic phases were dried over Na_2SO_4 and the solvent was removed under reduced pressure. The crude product was purified by column chromatography (Silica, 10:1 to 5:1 pentane/EtOAc).

This experiment was done in duplicate.

KIE1: m = 0.349 g (2.56 mmol, 21%)
KIE2: m = 0.189 g (1.39 mmol, 12%)

STD1: m = 0.387 g (2.84 mmol, 95%)
STD2: m = 0.378 g (2.78 mmol, 93%)

^{1}H-NMR spectra are in accordance with the literature.[29]

^{1}H-NMR ($CDCl_3$, 400 MHz) δ = 7.32 – 7.27 (m, 2H), 7.23 – 7.17 (m, 3H), 3.68 (t, *J* = 6.4 Hz, 2H), 2.76 – 2.67 (m, 2H), 2.00 – 1.80 (m, 2H), 1.41 – 1.34 (s, 1H) ppm.

Calculation of the conversion:
Mass (internal standard): m_{is} = 0.010 g
Amount of substance (internal standard): n_{is} = 0.060 mmol
^{1}H-NMR integration (internal standard): I_{is} = 3.00 H
Integration (reduced starting material (3.52 ppm)): I_{rsm} = 1.85 H : 2 = 0.93 H
Integration (reduced starting material (1.78 ppm)): I_{rsm} = 1.85 H : 2 = 0.93 H
Amount of substance (reduced starting material): n_{sm} = 0.060 mmol * 0.93 * 50 = 2.767 mmol
Amount of substance (starting material): n_{sm} = 12.00 mmol – (12.00 mmol/50) = 11.76 mmol
(1/50 of the volume was removed before reductive work-up for H-NMR-analysis!)
Conversion: 2.767 mmol / 11.76 mmol – 1) * (-100) = 77%

KIE1 = 77% conversion
KIE2 = 77% conversion

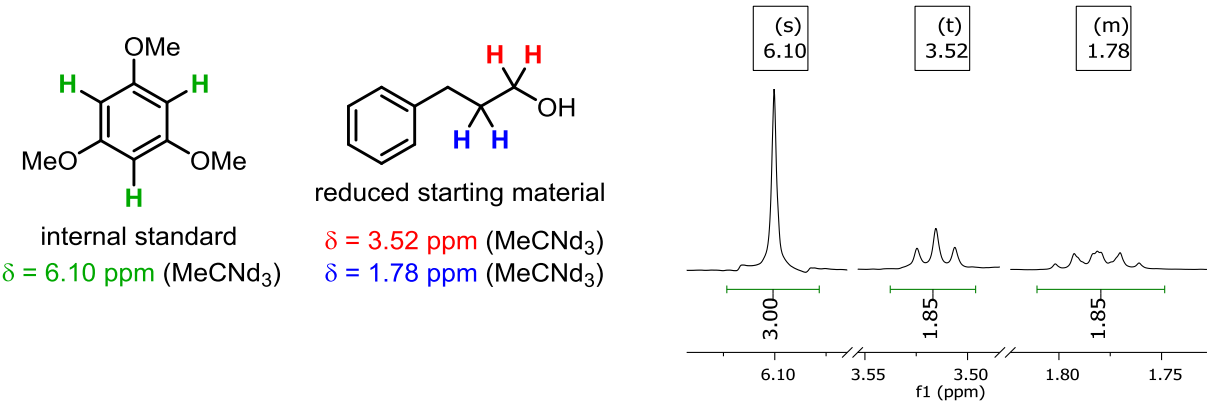

Figure SI-11. Cutout from the ^{1}H-NMR spectrum of the quenched reaction (for determination of the conversion).

Experimental ^{13}C KIEs for the system were determined from analysis of starting material 3-phenylpropanal using NMR methodology at natural abundance. Two independent reactions of starting aldehyde were taken to 77±2 conversion. The unreacted 3-phenylpropanal was reduced *in situ* to 3-phenylpropanol and reisolated for NMR analysis. The reisolated samples KIE1 and KIE2 were compared to two separate standard samples STD1 and STD2, respectively. The standard samples were prepared by reducing 3-phenylpropanal taken from the same batch used for the KIE experiments. Experimental ^{13}C KIEs were measured from relative isotopic composition of the two samples and fractional conversion in a standard way. The isotope effects were then averaged, and a 95% confidence range (C) was calculated using standard method.

$$C = \frac{t_{p,v} S}{\sqrt{n}}$$

S is the standard deviation, **n** is the number of measurements, and $\mathbf{t_{p,v}}$ is distribution function corresponding to confidence level **n**-1.

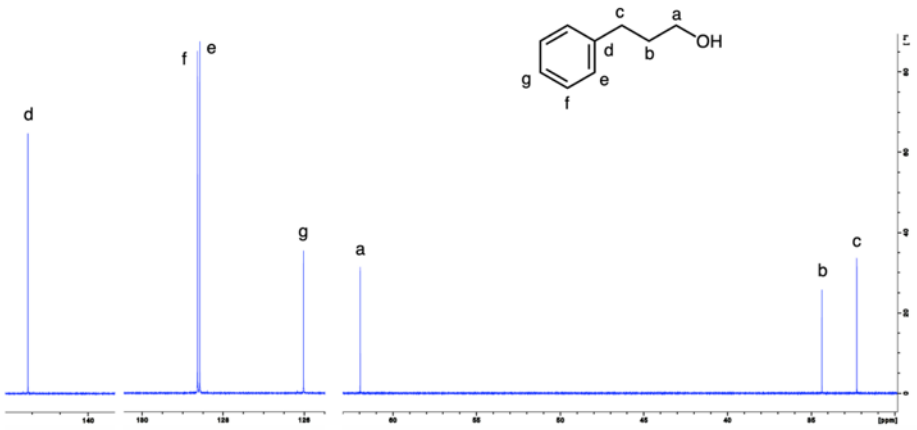

Figure SI-12. ^{13}C-NMR spectrum of the reduced and reisolated starting material (3-phenylpropanol).

STD1/KIE1

The sample for determination of ^{13}C KIEs was prepared from 160 mg of the reisolated sample KIE1, which was quantitatively transferred to a new 5 mm NMR tube using HPLC grade deuterated chloroform ($CDCl_3$) to a height of 5 cm. Likewise, 160 mg of standard sample STD1 was also prepared quantitatively in a 5 mm NMR tube using HPLC grade deuterated chloroform ($CDCl_3$) to a height of 5 cm. For quantitative measurement, ^{13}C spectra were recorded at 150 MHz using inverse gated decoupling with an acquisition time of 10 s, delay time 36 s (5 times T1 of slowest relaxing peak) and 128 transients for acquiring 6 fids for both the samples. A constant integration area was defined for each individual peak which is equal to 10 times the peak-widths at half-height for each peak. The para carbon of 3-phenylpropanol was taken as the standard carbon which was set to an integration value of 1000.0000. All the integrals for STD1 and KIE1 are listed in the tables below.

STD2/KIE2

Similar to the procedure described above, samples for KIE2 and STD2 were each prepared using 268 mg. For quantitative measurement, ^{13}C spectra were recorded at 150 MHz using inverse gated decoupling with an acquisition time of 10 s, delay time 30 s (5 times T1 of slowest relaxing peak) and 128 transients for acquiring 6 fids for both the samples. The spectra were processed as described for the above sample. All the integrals for STD2 and KIE2 are listed in the tables below.

Table SI-6. Standard Sample (STD1 160mg/$CDCl_3$).

peak	fid1	fid2	fid3	fid4	fid5	fid6	average	stddev	cuts=10 X avg hh
1	1000.9305	1003.0809	1002.0465	1009.6958	996.4917	1006.0323	1003.0463	4.5072	1.5,1.5
2	2025.1360	2035.2550	2018.4216	2036.3256	2025.5118	2036.9713	2029.6036	7.6570	2,2
3	2072.8509	2068.8465	2075.8805	2064.7618	2080.6641	2067.4642	2071.7447	5.8884	2,2
4	1000.0000	1000.0000	1000.0000	1000.0000	1000.0000	1000.0000	1000.0000	0.0000	2,2
5	1025.5784	1026.0890	1024.6846	1025.4123	1027.1945	1023.1769	1025.3560	1.3542	3.5,3.5
6	1041.1890	1042.1708	1038.5628	1038.6082	1040.9270	1040.9304	1040.3980	1.4767	4,4
7	996.7377	999.2351	996.4748	1000.5757	996.1794	1000.3555	998.2597	2.0267	3,3

Table SI-7. Reaction taken to 77% conversion (KIE1 160mg/$CDCl_3$).

peak	fid1	fid2	fid3	fid4	fid5	fid6	average	stddev	**KIE**	**95% conf**
1	1013.6563	1013.2420	1013.8523	1014.0950	1013.5953	1012.7271	1013.5280	0.4839	**1.007**	**0.004**
2	2024.8861	2037.0148	2029.6127	2040.8483	2026.1498	2044.3620	2033.8123	8.0881	**1.001**	**0.005**
3	2076.6163	2074.6922	2075.3353	2057.5687	2074.9792	2062.1561	2070.2246	8.1830	**1.000**	**0.004**
4	1000.0000	1000.0000	1000.0000	1000.0000	1000.0000	1000.0000	1000.0000	0.0000	**1.000**	**0.000**
5	1050.1213	1052.8462	1055.0797	1047.5008	1052.0531	1050.8890	1051.4150	2.5751	**1.017**	**0.002**
6	1044.5877	1050.5003	1049.9389	1044.8451	1042.4711	1047.6090	1046.6587	3.2104	**1.004**	**0.003**
7	992.6145	992.3526	990.7697	985.5134	992.9584	985.9063	990.0192	3.4235	**0.994**	**0.003**

Table SI-8. Standard Sample (STD2 268mg/$CDCl_3$).

peak	fid1	fid2	fid3	fid4	fid5	fid6	average	stddev	cuts=10 X avg hh
1	1013.1913	1015.2475	1017.2836	1012.6850	1014.4221	1016.6279	1014.9096	1.8353	2.5,2.5
2	2057.1301	2050.2951	2057.6368	2052.1572	2051.3216	2060.7208	2054.8769	4.1923	4,4
3	2100.1524	2100.3305	2098.9928	2101.5752	2103.3006	2091.8123	2099.3606	3.9776	4,4
4	1000.0000	1000.0000	1000.0000	1000.0000	1000.0000	1000.0000	1000.0000	0.0000	4,4
5	1015.9678	1014.7441	1015.3965	1015.7316	1014.9892	1014.8254	1015.2758	0.5038	5,5
6	1032.2505	1032.3731	1034.0529	1031.8139	1032.2724	1031.1377	1032.3168	0.9661	6,6
7	988.9633	988.2676	989.7361	987.9015	989.4858	988.0125	988.7278	0.7814	4,4

Table SI-9. Reaction taken to 77% conversion (KIE2 268mg/$CDCl_3$).

peak	fid1	fid2	fid3	fid4	fid5	fid6	average	stddev	**KIE**	**95% conf**
1	1022.9126	1022.9606	1021.5724	1024.8493	1020.9465	1021.8850	1022.5211	1.3821	**1.005**	**0.002**
2	2060.4713	2063.4748	2057.1022	2056.2644	2063.5671	2060.5035	2060.2306	3.0759	**1.002**	**0.002**
3	2102.8840	2094.4883	2099.5798	2104.5966	2095.5660	2096.5294	2098.9407	4.1225	**1.000**	**0.002**
4	1000.0000	1000.0000	1000.0000	1000.0000	1000.0000	1000.0000	1000.0000	0.0000	**1.000**	**0.000**
5	1037.2121	1038.4920	1038.6580	1040.5217	1039.7760	1038.1707	1038.8051	1.1789	**1.016**	**0.001**
6	1035.0012	1035.9482	1036.6547	1035.4925	1036.0883	1034.6687	1035.6423	0.7347	**1.002**	**0.001**
7	991.4310	989.5594	988.8080	992.5506	991.0334	989.8827	990.5442	1.3765	**1.001**	**0.001**

KIE-experiment (2)

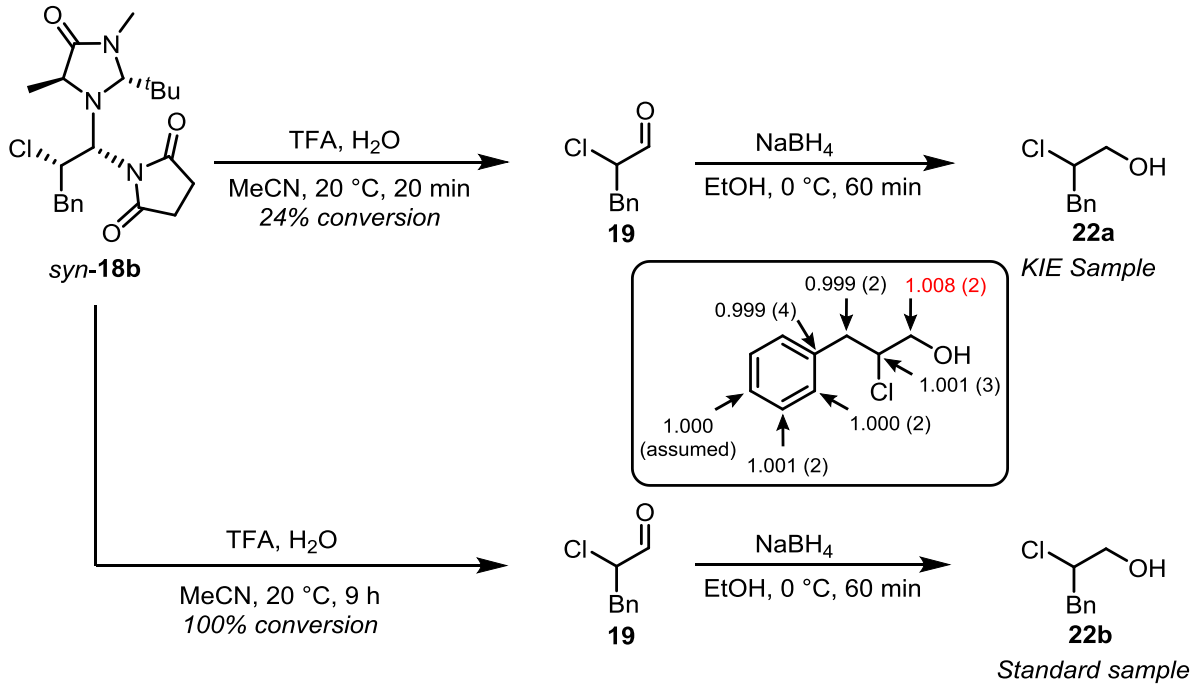

KIE-Sample: Aminal *syn*-**18b** was synthesized according to the literature procedure.[22] The exact time (20 min) and suitable conditions (equivalents of H_2O and TFA, concentration) for 20-30% conversion were defined by a previously performed kinetic ^{1}H-NMR-experiment using 1,3,5-trimethoxybenzene as an internal standard. Aminal *syn*-**18b** (3.36 g, 8.00 mmol, 1.0 equiv) was dissolved in MeCN (200 mL), H_2O (0.722 mL, 40.0 mmol, 5.0 equiv) and TFA (3.06 mL, 40.0 mmol, 5.0 equiv) were added subsequently and the solution was stirred for 20 min at 20 °C. After quenching with saturated aqueous $NaHCO_3$ (200 mL), the aqueous phase was extracted with EtOAc (3x200 mL) three times. The combined organic phases were dried over $NaSO_4$ and the exact volume of the organic phase was adjusted to 1200 ml. 12 mL were taken from the solution and added to flask containing 1,3,5-trimethoxybenzene (6.73 mg, 40.0 µmol) as an internal standard. The solvents were removed under reduced pressure and the residue was taken up by 1.0 mL of $MeCNd_3$. 24% conversion was calculated from the ^{1}H-NMR spectra. The solvents from the combined organic phases were removed under reduced pressure and the product was obtained after column chromatography (5:1 pentane/EtOAc). The pure α-chloro aldehyde (0.434 g, 2.57 mmol, 1.0 equiv) was dissolved in EtOH (20.0 mL) and cooled to 0 °C. $NaBH_4$ (0.243 g, 6.43 mmol, 2.5 equiv) was added and the reaction mixture was stirred for 60 min at the same temperature. After quenching with saturated aqueous NH_4Cl, the aqueous phase was extracted with EtOAc (3x20 mL). The combined organic phases were dried over $NaSO_4$ and the solvents were removed under reduced pressure. The pure β-chloroalcohol (0.350 g, 2.05 mmol, 80%) was obtained after column chromatography (5:1 pentane/EtOAc).

Standard Sample: Aminal *syn*-**18b** (from the same batch as KIE-experiment) (0.840 mg, 2.00 mmol, 1.0 equiv) was dissolved in MeCN (50 mL), H_2O (0.180 mL) and TFA (0.765 mL) were added subsequently and the solution was stirred at 20 °C until TLC showed complete conversion of the aminal (9 h). After quenching with saturated aqueous $NaHCO_3$ (40 mL), the aqueous phase was extracted with

EtOAc (3x50 mL). The combined organic phases were dried over $NaSO_4$ and the solvents were removed under reduced pressure. ^{1}H-NMR of the crude sample confirmed complete conversion of the aminal. The product was obtained after column chromatography (5:1 pentane/EtOAc). The pure α-chloro aldehyde (0.301 g, 1.79 mmol, 1.0 equiv) was dissolved in EtOH (15 mL) and cooled to 0 °C. $NaBH_4$ (0.169 g, 4.46 mmol, 2.5 equiv) was added and the reaction mixture was stirred for 60 min at the same temperature. After quenching with saturated aqueous NH_4Cl (10 mL), the aqueous phase was extracted with EtOAc (3x20 mL). The combined organic phases were dried over $NaSO_4$ and the solvents were removed under reduced pressure. The pure β-chloro alcohol (0.240 g, 1.41 mmol, 79%) was obtained after column chromatography (5:1 pentane/EtOAc).

^{1}H-NMRs are in accordance with the literature.[22]

Product KIEs were performed by isolating the product 2-chloro-3-phenylpropanal from a reaction of *syn*-aminal (*syn*-**18b**) taken to 24% conversion and reduced insitu to 2-chloro-3-phenylpropanol. The standard sample was prepared by isolating the product taken to 100% conversion and reduced in situ Experimental ^{13}C KIEs were measured from changes in relative isotopic composition and fractional conversion.

STD/KIE

Similar to the procedure described for determination of ^{13}C KIEs for 3-phenylpropananol, low conversion and 100% conversion samples of 2-chloro-3-phenylpropanol were each prepared using 231 mg. For quantitative measurement, ^{13}C spectra were recorded at 150 MHz using inverse gated decoupling with an acquisition time of 10 s, delay time 30 s (5 times T1 of slowest relaxing peak) and 128 transients for acquiring 6 fids for both the samples. The spectra were processed as described for the previous samples. A representative spectrum along with integration for both samples are shown in the table below. This experiment was not performed in duplicate due the challenges associated with synthesizing a larger quantities of *syn*-**18b** required for the experiment.

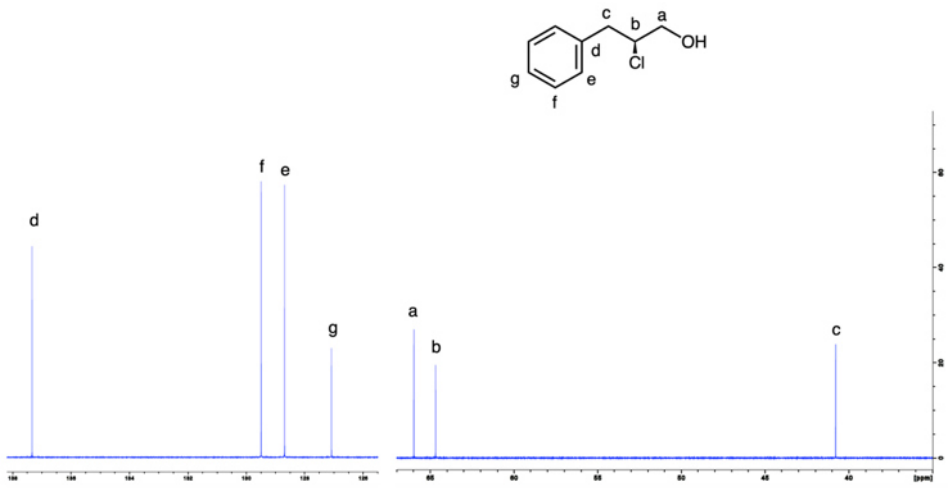

Figure SI-13. ^{13}C-NMR spectrum of the reduced decomposition product of *syn*-**18b** (2-chloro-3-phenylpropanol).

Table SI-10. Standard Sample (STD 231mg/$CDCl_3$).

peak	fid1	fid2	fid3	fid4	fid5	fid6	average	stddev	cuts=10 X avg hh
1	1026.0648	1026.8439	1026.4918	1024.7271	1028.6749	1025.2016	1026.3340	1.3930	2,2
2	2002.9656	2004.9762	2001.9009	2000.6530	2004.8393	2002.2518	2002.9311	1.7051	2.5,2.5
3	1999.7604	2000.0493	2000.2890	1998.7059	1999.6764	1997.1237	1999.2675	1.1812	2.5,2.5
4	1000.0000	1000.0000	1000.0000	1000.0000	1000.0000	1000.0000	1000.0000	0.0000	3,3
5	994.7805	991.0943	994.3898	995.1336	991.5581	992.6222	993.2631	1.7374	3,3
6	1046.7547	1043.5144	1045.1485	1037.3534	1045.1662	1045.3339	1043.8785	3.3577	10,10
7	997.2385	998.3051	1000.9168	999.3783	998.0785	996.2951	998.3687	1.6234	4,4

Table SI-11. Reaction taken to 24% conversion (KIE 231mg/$CDCl_3$).

peak	fid1	fid2	fid3	fid4	fid5	fid6	average	stddev	**KIE**	**95% conf**
1	1021.2407	1023.3972	1024.4986	1027.7109	1033.4467	1030.6276	1026.8203	4.6355	**0.999**	**0.004**
2	1997.0448	2001.1775	2004.2681	2004.6367	2011.8553	2003.1204	2003.6838	4.8723	**1.000**	**0.002**
3	1994.1101	1997.2838	1999.9637	1994.5238	2005.8038	1998.4097	1998.3492	4.2877	**1.001**	**0.002**
4	1000.0000	1000.0000	1000.0000	1000.0000	1000.0000	1000.0000	1000.0000	0.0000	**1.000**	**0.000**
5	984.5027	985.8564	986.8568	986.6361	988.6683	987.7684	986.7148	1.4548	**1.008**	**0.002**
6	1043.8129	1042.6836	1040.2764	1043.1687	1045.8196	1043.1081	1043.1449	1.7913	**1.001**	**0.003**
7	997.5046	998.9728	1000.1525	999.9749	1002.1993	998.2256	999.5050	1.6626	**0.999**	**0.002**

Theoretical Studies

General Information:

All the DFT calculations presented in the manuscript were performed using B3LYP/6-31+G**PCM (solvent = acetonitrile) level of theory as implemented in Gaussian16. All the starting materials and intermediates were verified as true minima (no imaginary frequencies) whereas all the transition states for the system were characterized by one imaginary frequency. Single point energy calculations were performed separately using B3LYP functional with Grimme's dispersion correction with Becke-Johnson damping (D3-BJ) and a triple-ζ basis set (6-311+G**) and a PCM solvent model for acetonitrile was also applied to all single point geometry optimizations. Gibbs free energies were estimated at reaction temperature 243 K and were corrected using Grimme's quasi-RRHO approach. Each intermediate along the reaction coordinate were located by performing Paton's quick reaction coordinate (QRC) procedure from the respective transition states. A thorough conformation search was done for all the optimized transition state and intermediate geometries to identify the lowest energy geometry for each stationary point. Cartesian coordinates of all computed starting materials, intermediates, and transition states are included in the section below. The lowest energy conformation for each transition state reported in the manuscript is highlighted in red. The higher energy conformations for each transition state are also included along with their relative energies.

Exploring the origins of enantioselectivity:

From the computed reaction coordinate diagram shown in Figure 3 of the manuscript, the chlorination of the enamine intermediate (TS4) is irreversible, and the enantioselectivity-determining step of the reaction. Accordingly, we modeled the approach of NCS (**6**) to either face of the two possible (*E*)-enamine intermediates. After a thorough conformational search, the lowest-energy TS for each distinct approach was identified. The approach of **6** from the *Re*-face of enamine that is *syn*-to the *t*-butyl group of the catalyst **3c** was found to be the lowest-energy TS leading to the formation of the (*S*)-enantiomer of **19** (TS4-S1). In contrast, the TS for the approach of **6** to the *Si*-face of the enamine that is *anti* to the *t*-butyl group of **3c** (TS4-R1) was identified as the lowest energy TS for the formation of the (*R*)-enantiomer of 19. The $\Delta\Delta G^{\ddagger}$ between these two TSs is 2.9 kcal mol^{-1} favoring TS4-S1 – a value that is qualitatively consistent with the >90% ee observed for this reaction.

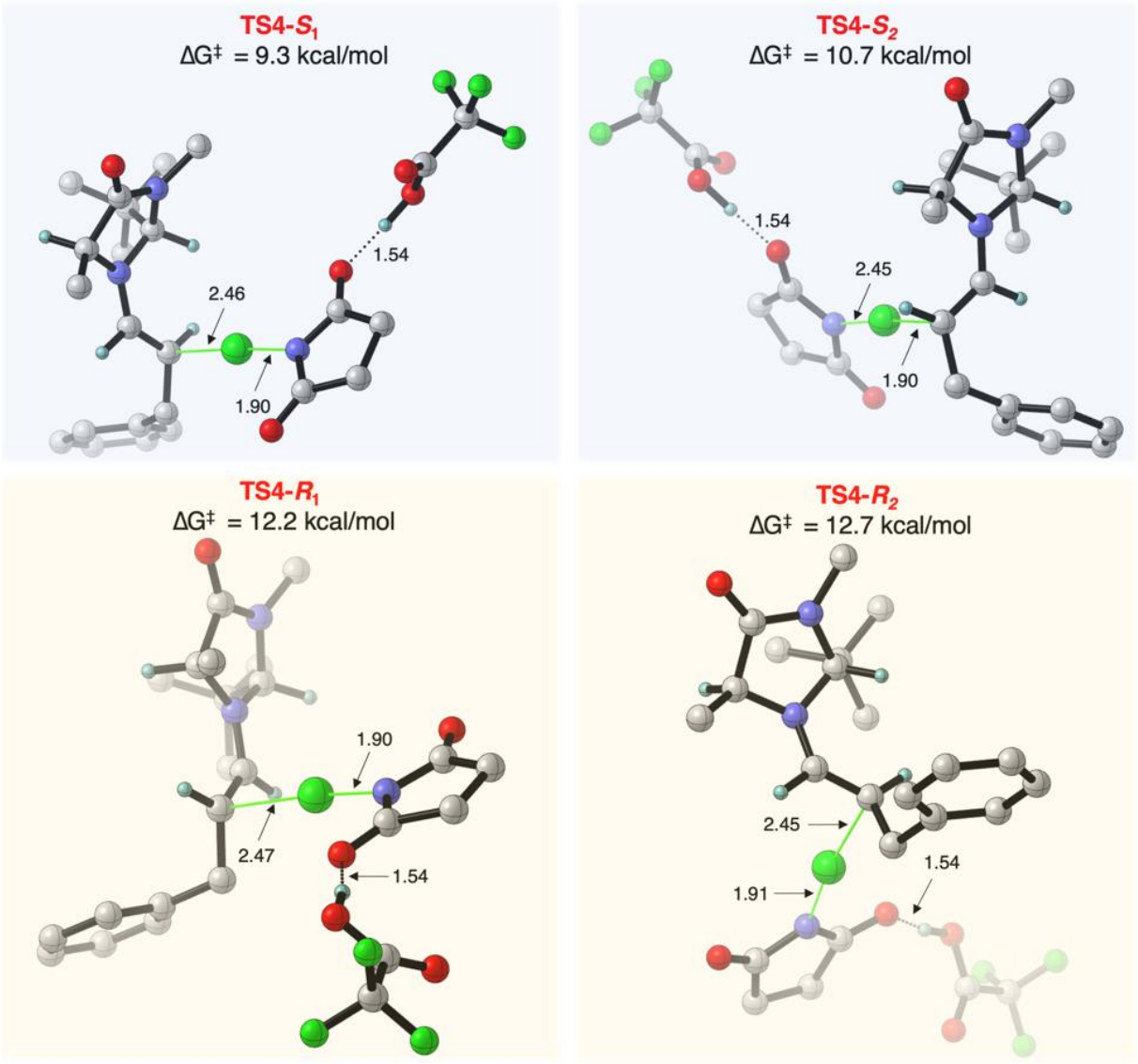

Figure SI-14. Lowest energy transition states for the front and back approach of **6** to the two distinct (*E*)-enamine intermediates calculated at the B3LYP-D3(BJ)/6-311+G** PCM(acetonitrile)// B3LYP/6-31+G** PCM(acetonitrile) level of theory. Some hydrogen atoms have been removed for clarity in the 3D representation of the key transition structures. Key bond-forming and bond-breaking distances are in angstroms (Å).

Computed pathways for the formation of all diastereomers of the aminal intermediate:

In the manuscript, we have described the formation of *syn*-**18b** and *anti*-**18b** from the *Z*-chloroiminium ion (**Int4**). We have also computed the formation of diastereomeric aminals (*syn*-**18b´** and *anti*-**18b´**) from the *E*-chloroiminium ion with the same *S*-configuration at the α-carbon (**Int4´**). The reaction coordinate diagram for the formation of all four aminal diastereomers from the respective enamine intermediates (**Int3** and **Int3´**) is shown in the Figure below. It is important to note that even though **Int4´** is lower in energy that **Int4**, the barrier for its formation from **Int3´** is 1.4 kcal mol^{-1} higher in energy than the barrier for formation of **Int4** from **Int3** (see Figure below). If **Int4´** forms, then it faces only a 6.2 kcal mol^{-1} barrier to form *anti*-**18b´** via $TS_{syn\text{-}\mathbf{18b}'}$.In contrast, formation of *syn*-**18b´** from **Int4´** faces a much higher barrier of 17.2 kcal mol^{-1} via $TS_{anti\text{-}\mathbf{18b}'}$.

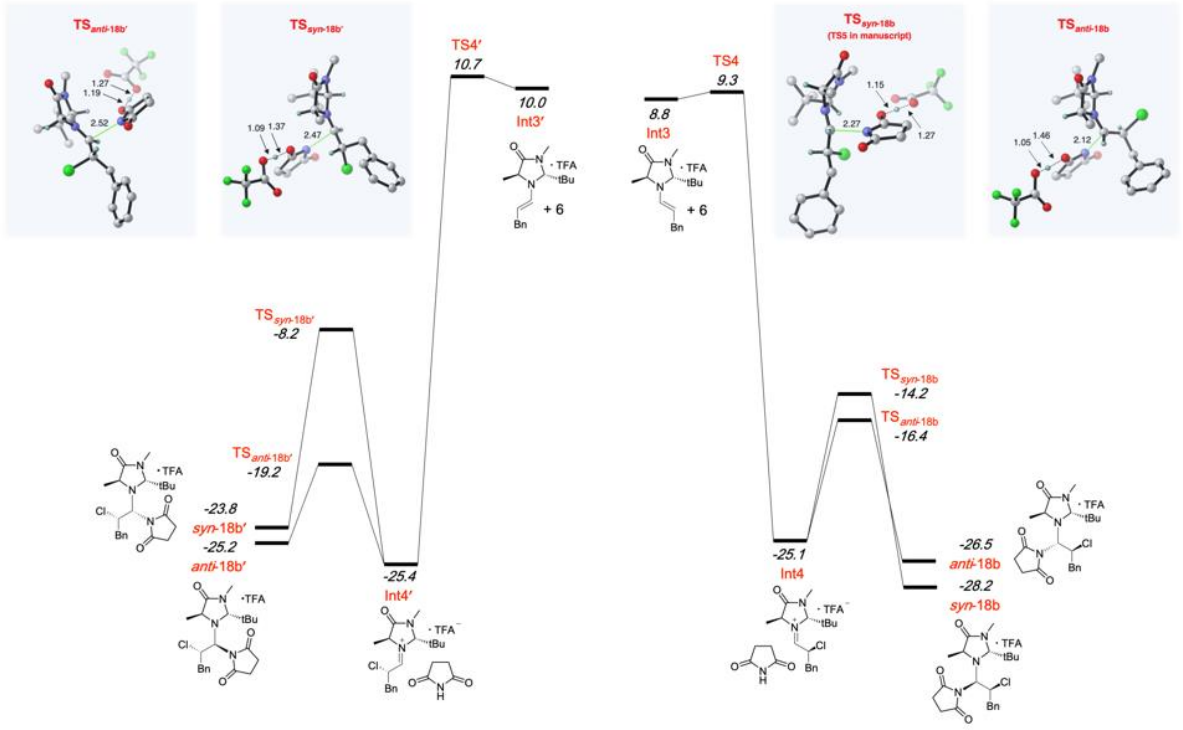

Figure SI-15. Reaction coordinate diagram for the formation of diastereomeric aminals from the respective enamines calculated at the B3LYP-D3(BJ)/6-311+G** PCM(acetonitrile)// B3LYP/6-31+G** PCM(acetonitrile) level of theory. Some hydrogen atoms have been removed for clarity in the 3D representation of the key transition structures. Key bond-forming and bond-breaking distances are in angstroms (Å).

In the manuscript, we show the pathway that converts **Int4** to *syn*-**18b** and *anti*-**18b** via TS5 and TS5´. These transition structures are $TS_{syn\text{-}\mathbf{18b}}$ and $TS_{anti\text{-}\mathbf{18b}}$ respectively in the Figure above. We implied that *syn*-**18b** and *anti*-**18b** re-entered the catalytic cycle as the *Z*-chloroiminium ion (**Int4**) via these same transition states (principle of microscopic reversibility). However, there is a possibility of a C-N bond-rotation event that converts *syn*-**18b** to *syn*-**18b´** and *anti*-**18b** to *anti*-**18b´** and subsequent re-entry of these intermediates into the catalytic cycle as the *E*-chloroiminium intermediate (**Int4´**) via $TS_{syn\text{-}\mathbf{18b}'}$ and $TS_{anti\text{-}\mathbf{18b}'}$. This possibility is unlikely for the *syn*-aminal since $TS_{syn\text{-}\mathbf{18b}'}$ is significantly higher in energy that $TS_{syn\text{-}\mathbf{18b}}$. On the other hand, such a pathway is more than likely for the *anti*-aminal since $TS_{anti\text{-}\mathbf{18b}'}$ is lower in energy that $TS_{anti\text{-}\mathbf{18b}}$. We computed the reaction coordinate for the conversion of *anti*-**18b´** to the 2-chloroaldehyde product via the three sequential transition states $TS_{anti\text{-}\mathbf{18b}'}$. TS6´, and TS7 corresponding to re-entry into the catalytic cycle as the *E*-chloroiminium, hydrolysis, and catalyst regeneration and product release (Figure below). Incidentally, the highest energy barrier for this reaction pathway is re-entry into the catalytic cycle via $TS_{anti\text{-}\mathbf{18b}'}$, which is identical to the relative energetics of the corresponding transition states in the conversion of *syn*-**18b** to the product **19** described in Figure 4 of the manuscript.

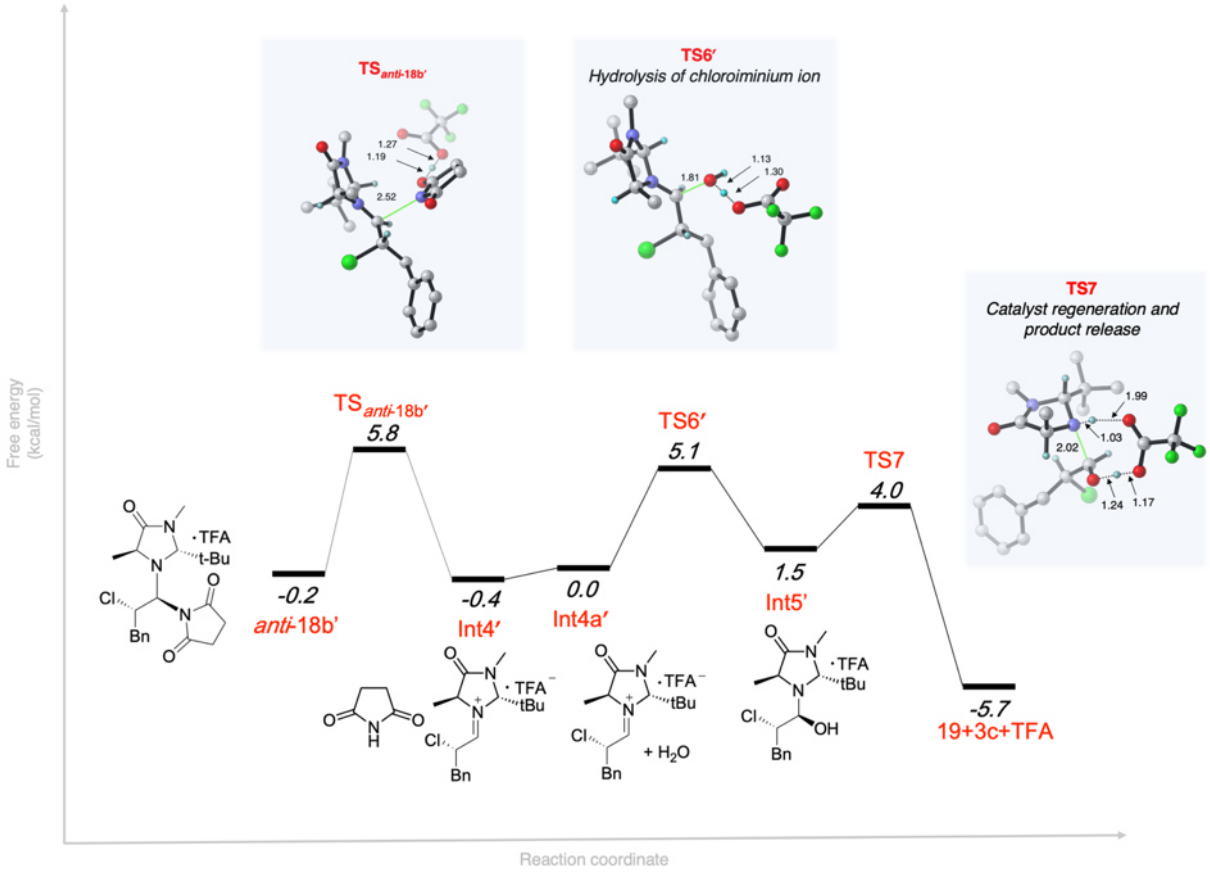

Figure SI-16. Reaction coordinate diagram for the conversion of *anti*-**18b´** to **19** calculated at the B3LYP-D3(BJ)/6-311+G** PCM(acetonitrile)// B3LYP/6-31+G** PCM(acetonitrile) level of theory. Some hydrogen atoms have been removed for clarity in the 3D representation of the key transition structures. Key bond-forming and bond-breaking distances are in angstroms (Å).

Table SI-12. Coordinates and energies of computed structures.

Starting Materials

3-Phenylpropanal (sm.log)
Free Energy = -424.09683
Zero-point Energy = -424.07017
Potential Energy = -424.23595
Single-Point Energy B3LYP-D3(BJ)/6-311+G** PCM = -424.35584
Free Energy B3LYP-D3(BJ)/6-311+G** PCM (extrapolated free energy from qRRHO) = -424.21671
Charge = 0 Multiplicity = 1

C	-3.3413160	-0.0005570	0.5403040
H	-3.9288280	-0.0002450	1.4807970
C	-1.8491150	-0.0005340	0.7243600
H	-1.6071760	0.8704580	1.3516390
H	-1.6070840	-0.8719850	1.3509560
C	-1.0313240	0.0000370	-0.5758450
H	-1.3069810	-0.8785130	-1.1687130
H	-1.3071090	0.8790120	-1.1680190
C	0.4615430	0.0000500	-0.3184150
C	1.1687220	1.2054270	-0.1841310
C	1.1688060	-1.2053300	-0.1845390
C	2.5419580	1.2082530	0.0802440
H	0.6406430	2.1499560	-0.2924210
C	2.5420360	-1.2081510	0.0798330
H	0.6407890	-2.1498560	-0.2931560
C	3.2340200	0.0000540	0.2141230
H	3.0706490	2.1524890	0.1765460
H	3.0707990	-2.1523810	0.1758140
H	4.3012090	0.0000500	0.4160980
O	-3.9173610	0.0006900	-0.5356430

Catalyst (cat.log)
Free Energy = -538.35806
Zero-point Energy = -538.32923
Potential Energy = -538.59681
Single-Point Energy B3LYP-D3(BJ)/6-311+G** PCM = -538.76234
Free Energy B3LYP-D3(BJ)/6-311+G** PCM (extrapolated free energy from qRRHO) = -538.52359
Charge = 0 Multiplicity = 1

C	-0.4544180	-0.1166990	-0.6994830
N	0.4266560	1.0008460	-0.2914750
C	1.5852240	0.5777350	0.2652530
O	2.4887570	1.3031530	0.7022350
C	1.5745020	-0.9521890	0.2523210
N	0.4181660	-1.3045010	-0.5947510
H	0.7590160	-1.5344140	-1.5245490
C	2.8849960	-1.5589870	-0.2398010
H	3.7062150	-1.2645140	0.4186440
H	2.8194820	-2.6512640	-0.2414640
H	3.1204180	-1.2213170	-1.2554950
H	1.3979930	-1.2887160	1.2835090
C	0.1807200	2.4085020	-0.5718670
H	-0.2985190	2.9212640	0.2681390
H	-0.4580440	2.4993570	-1.4525720
H	1.1386980	2.8949920	-0.7695520
H	-0.7422380	0.0344340	-1.7475790
C	-1.7730610	-0.2694120	0.1258260
C	-2.6574980	0.9869790	-0.0160930
H	-2.8146340	1.2546050	-1.0678020
H	-3.6416030	0.7942700	0.4248400
H	-2.2356580	1.8533340	0.4996520
C	-2.5421370	-1.4694220	-0.4650670
H	-2.7842300	-1.3035630	-1.5222530
H	-3.4853780	-1.6125740	0.0733430
H	-1.9560190	-2.3888790	-0.3889400
C	-1.4809210	-0.5254740	1.6153320
H	-0.9261150	-1.4578230	1.7573130
H	-2.4212300	-0.6094630	2.1713200
H	-0.9064070	0.2944330	2.0606280

Trifluoroacetic acid (tfa.log)
Free Energy = -526.81566
Zero-point Energy = -526.79175
Potential Energy = -526.83013
Single-Point Energy B3LYP-D3(BJ)/6-311+G** PCM = -526.98128
Free Energy B3LYP-D3(BJ)/6-311+G** PCM (extrapolated free energy from qRRHO) = -526.96680
Charge = 0 Multiplicity = 1

C	0.9502640	-0.1544060	-0.0000050
C	-0.5942250	0.0015770	0.0000060
O	1.4971790	-1.2288920	-0.0000170
O	1.5236480	1.0442750	-0.0000080
H	2.4938330	0.9458880	-0.0000090
F	-1.0055400	0.6793790	1.0919440
F	-1.1885270	-1.1982590	-0.0002140
F	-1.0055640	0.6797710	-1.0917070

Water (h2o.log)
Free Energy = -76.43466
Zero-point Energy = -76.42090
Potential Energy = -76.44210
Single-Point Energy B3LYP-D3(BJ)/6-311+G** PCM = -76.46677
Free Energy B3LYP-D3(BJ)/6-311+G** PCM (extrapolated free energy from qRRHO) = -76.45933
Charge = 0 Multiplicity = 1

O	-0.0000000	-0.0000000	0.1177180
H	-0.0000000	0.7669030	-0.4708720
H	-0.0000000	-0.7669030	-0.4708720

N-chlorosuccinimide (suc.log)
Free Energy = -820.19336
Zero-point Energy = -820.16822
Potential Energy = -820.24947
Single-Point Energy B3LYP-D3(BJ)/6-311+G** PCM = -820.38399
Free Energy B3LYP-D3(BJ)/6-311+G** PCM (extrapolated free energy from qRRHO) = -820.32788
Charge = 0 Multiplicity = 1

C	-0.4323230	1.1871590	0.0000130
C	-1.8907470	0.7700950	0.0001270
C	-1.8907470	-0.7700950	0.0000880
C	-0.4323230	-1.1871590	-0.0000720
N	0.3190470	-0.0000000	-0.0000370
H	-2.3726500	1.1995430	0.8824860
H	-2.3728100	-1.1995470	-0.8821820
H	-2.3726010	-1.1995720	0.8824610
H	-2.3727600	1.1995770	-0.8821560
O	0.0417140	-2.3036950	-0.0001500
O	0.0417140	2.3036950	0.0001580
Cl	2.0274650	-0.0000000	-0.0000790

Succinimide (suc-h.log)
Free Energy = -360.63967
Zero-point Energy = -360.61626
Potential Energy = -360.70798
Single-Point Energy B3LYP-D3(BJ)/6-311+G** PCM = -360.81019

Free Energy B3LYP-D3(BJ)/6-311+G** PCM (extrapolated free energy from qRRHO) = -360.74188
Charge = 0 Multiplicity = 1

C	-1.1670680	0.2088320	-0.0006280
C	-0.7696220	-1.2596600	0.0000790
C	0.7696220	-1.2596600	0.0000120
C	1.1670680	0.2088320	-0.0005610
N	0.0000000	0.9594370	-0.0000830
H	-1.2020090	-1.7408940	0.8816570
H	1.2020600	-1.7415660	-0.8811660
H	1.2020730	-1.7409440	0.8815300
H	-1.2021240	-1.7416150	-0.8810400
O	2.2926660	0.6803470	0.0002360
O	-2.2926660	0.6803470	0.0004760
H	0.0000000	1.9733530	0.0004920

Intermediates

Int1.log
Potential Energy = -1489.67565
Zero-point Energy = -1489.19554
Free Energy = -1489.23816
Single-Point Energy B3LYP-D3(BJ)/6-311+G** PCM = -1490.13898
Free Energy B3LYP-D3(BJ)/6-311+G** PCM (extrapolated free energy from qRRHO) = -1489.70148
Charge = 0 Multiplicity = 1

C	1.9462360	-0.4304000	1.7290860
H	2.3898140	-1.2580300	1.1725630
H	1.5830110	-0.8318660	2.6796860
C	3.0381520	0.6197670	2.0485670
C	0.7674580	0.1622330	0.9633750
O	0.1653840	1.1293300	1.7475260
H	-0.4028390	1.7375180	1.1951310
H	1.0625910	0.5568670	-0.0119310
O	-1.5240140	2.6278790	0.3369240
C	-2.4769980	1.8901530	-0.0099700
C	-3.7216940	2.6623270	-0.5525430
F	-3.3819940	3.4704220	-1.5886500
F	-4.7076170	1.8510100	-0.9891620
F	-4.2547680	3.4549600	0.4131970
O	-2.5666420	0.6405150	0.0248780
H	3.7589450	0.1333660	2.7145960
C	3.7702050	1.1735960	0.8414430
C	4.8448520	0.4704380	0.2722390
C	3.3971740	2.3983560	0.2656780
C	5.5209050	0.9699360	-0.8443490
H	5.1592610	-0.4733240	0.7121220
C	4.0697700	2.9020450	-0.8528430
H	2.5785320	2.9661620	0.7006990
C	5.1334150	2.1882660	-1.4129520
H	6.3523320	0.4120300	-1.2660380
H	3.7655930	3.8529270	-1.2813190
H	5.6596190	2.5796740	-2.2787650
H	2.5813280	1.4368810	2.6134460
N	-0.3493590	-0.8927940	0.6102410
C	-0.6980180	-1.9453390	1.6396240
C	-0.4468280	-1.5868290	-0.7713480
C	-1.6725010	-2.8154890	0.8395450
H	0.2008640	-2.5205480	1.8718850
H	-0.7990720	-0.8075150	-1.4532840
O	-2.4718120	-3.6122840	1.3238100
N	-1.5482370	-2.5083160	-0.4756630
C	-2.5552190	-2.9395790	-1.4468020
H	-2.3812470	-3.9641360	-1.7847900
H	-3.5363920	-2.8905320	-0.9699830
H	-2.5382840	-2.2690890	-2.3056680
C	0.8043460	-2.2703720	-1.4179650
C	0.3191370	-2.8959460	-2.7521310
H	-0.3477650	-3.7452600	-2.5959650
H	-0.1862780	-2.1628410	-3.3899950
H	1.1906660	-3.2640160	-3.3007970
C	1.8810950	-1.2287830	-1.7922360
H	1.4532620	-0.3969480	-2.3629220
H	2.4164870	-0.8211430	-0.9355300
H	2.6304770	-1.7093760	-2.4282470
C	1.4031990	-3.3998650	-0.5580700
H	0.6525450	-4.1562520	-0.3089970
H	2.1948060	-3.8999530	-1.1244980
H	1.8539350	-3.0415460	0.3699470
C	-1.3324190	-1.3964190	2.9124170
H	-0.6244830	-0.8030320	3.4910270
H	-2.2053760	-0.7788260	2.6859920
H	-1.6578290	-2.2470480	3.5158720
H	-1.1988590	-0.2659730	0.5455450

Int2.log
Potential Energy = -1489.67471
Zero-point Energy = -1489.20052
Free Energy = -1489.24669
Single-Point Energy B3LYP-D3(BJ)/6-311+G** PCM = -1490.13451
Free Energy B3LYP-D3(BJ)/6-311+G** PCM (extrapolated free energy from qRRHO) = -1489.70649
Charge = 0 Multiplicity = 1

C	-0.9076670	-1.4510240	-0.3872190
C	-0.7053740	-2.8638920	1.5019160
C	0.7227300	-2.6529040	0.9841170
N	0.5181550	-1.4692480	0.0906370
N	-1.5554800	-2.1514540	0.7253680
O	-1.0033980	-3.5500940	2.4755070
C	-2.9582150	-1.9579010	1.0920940
H	-3.5989610	-2.7370730	0.6714540
H	-3.0323810	-1.9934810	2.1804440
H	-3.2843840	-0.9790670	0.7399530
C	1.3809230	-0.5192300	-0.0314960
C	1.2192450	0.7867870	-0.7149230
C	2.4250840	1.1515040	-1.6268150
H	2.4994840	0.4246100	-2.4409870
H	2.1759710	2.1138820	-2.0854520
C	1.7463740	-2.4673650	2.0931350
H	1.6535160	-3.3229180	2.7662070
H	2.7672300	-2.4599330	1.7041890
H	1.5515820	-1.5515990	2.6568910
H	0.9956780	-3.5047370	0.3536320
C	-1.1152890	-2.1068240	-1.7988310
H	-1.2533120	-0.4145590	-0.3978180
C	-2.6229500	-2.0259360	-2.1323180
H	-2.7730020	-2.3302500	-3.1725630
H	-3.2195590	-2.6943650	-1.5080200
H	-3.0105980	-1.0074450	-2.0241620
C	-0.3458890	-1.3109870	-2.8717890
H	-0.6860510	-0.2724570	-2.9338690
H	0.7353230	-1.3221330	-2.7055950
H	-0.5233210	-1.7697240	-3.8490820
C	-0.6677540	-3.5802940	-1.8427280
H	-1.1401380	-4.1777900	-1.0567630
H	-0.9632340	-4.0144800	-2.8027090
H	0.4190780	-3.6853190	-1.7664190
H	1.1649890	1.5129720	0.1086330
H	0.2856240	0.8612390	-1.2682000
C	3.7537620	1.2537760	-0.9029550
C	4.0146940	2.3280740	-0.0361460
C	4.7496640	0.2823880	-1.0826630
C	5.2355070	2.4255990	0.6357360
H	3.2608890	3.0982630	0.1094100

C	5.9742900	0.3767590	-0.4120960
H	4.5694440	-0.5514930	-1.7568160
C	6.2199550	1.4481700	0.4506480
H	5.4200860	3.2658580	1.2988600
H	6.7333200	-0.3846850	-0.5667840
H	7.1700720	1.5245520	0.9711210
H	2.3367140	-0.6964060	0.4541960
O	0.2055980	0.6727320	2.5360000
H	-0.5650500	1.0245000	2.0250470
H	0.3612240	1.3062950	3.2479440
O	-1.8272060	1.3783850	0.8585520
C	-2.4962880	2.4448910	0.9188010
C	-3.5454270	2.5697760	-0.2410770
O	-2.4417150	3.3874580	1.7255190
F	-4.3615340	3.6413520	-0.1226540
F	-4.3489880	1.4744090	-0.3167630
F	-2.9249700	2.6827500	-1.4496620

Int3.log
Potential Energy = -2233.46906
Zero-point Energy = -2232.93826
Free Energy = -2232.98928
Single-Point Energy B3LYP-D3(BJ)/6-311+G** PCM = -2234.04146
Free Energy B3LYP-D3(BJ)/6-311+G** PCM (extrapolated free energy from qRRHO) = -2233.56168
Charge = 0 Multiplicity = 1

C	-1.1664720	2.4657730	-0.1544700
C	-0.8513740	2.2752420	2.1757360
C	-2.3119350	1.9105080	1.9023010
N	-2.3392020	1.7958790	0.4289940
N	-0.2484460	2.5334850	0.9948030
O	-0.3144210	2.3101580	3.2878670
C	1.1866930	2.7691910	0.9011040
H	1.6843780	2.1758760	1.6709860
H	1.5438040	2.4572960	-0.0813760
H	1.4423890	3.8218890	1.0576150
C	-2.9811220	0.7477450	-0.2013560
H	-3.7572350	0.3006010	0.4096050
C	-2.7937670	0.2608730	-1.4531300
C	-3.6703920	-0.7961890	-2.1066510
H	-3.0300030	-1.6017840	-2.4904950
H	-2.0634830	0.7088280	-2.1199590
C	-2.7364480	0.6738020	2.6927140
H	-2.5204360	0.8572640	3.7484130
H	-3.8080210	0.4825230	2.5981590
H	-2.1859090	-0.2162640	2.3742630
H	-2.9320000	2.7584290	2.2277080
C	-1.4940740	3.8573210	-0.8060200
H	-0.7157310	1.8236720	-0.9210120
Cl	-0.6328290	-1.4406910	-0.4240500
N	0.6830970	-2.5138660	-0.0345290
C	0.4805070	-3.7822890	0.5498390
C	2.0047690	-2.1910920	-0.2610340
C	1.8549980	-4.3933150	0.7470550
C	2.8523010	-3.3582650	0.1963350
H	1.9936620	-4.5954540	1.8126050
H	3.4239780	-3.7275400	-0.6600470
O	2.3748020	-1.1276540	-0.7528730
O	-0.6062310	-4.2424560	0.8226390
C	-0.2292940	4.4427310	-1.4710590
H	-0.5034150	5.3241060	-2.0605060
H	0.5191650	4.7617330	-0.7420670
H	0.2379380	3.7224030	-2.1528340
C	-2.5584360	3.6566090	-1.9043720
H	-2.1929380	3.0079730	-2.7075700
H	-3.4771210	3.2217720	-1.5022470
H	-2.8069850	4.6255750	-2.3503730
C	-2.0324260	4.8503100	0.2406480
H	-1.3193820	5.0112630	1.0559370
H	-2.2170010	5.8205370	-0.2325960
H	-2.9796260	4.5072470	0.6686220
H	3.5687840	-2.9985350	0.9397540
H	1.8919410	-5.3503410	0.2203270
H	3.8924930	-0.6320820	-0.9117720
O	4.8011550	-0.2227150	-1.0884920
C	5.6235100	-0.4107390	-0.0808380
O	5.4112800	-0.9962000	0.9590350
C	7.0013900	0.2419270	-0.3793350
F	6.8699910	1.5709780	-0.5864840
F	7.5587580	-0.2956490	-1.4872250
F	7.8512910	0.0625310	0.6426210
H	-4.1410040	-0.3493710	-2.9941210
C	-4.7545800	-1.3986480	-1.2351620
C	-6.0382910	-0.8318760	-1.1939430
C	-4.5036130	-2.5347980	-0.4500470
C	-7.0428470	-1.3805660	-0.3904470
H	-6.2535360	0.0446210	-1.8007330
C	-5.5043350	-3.0882180	0.3552080
H	-3.5175480	-2.9913900	-0.4718620
C	-6.7784160	-2.5119950	0.3884050
H	-8.0306510	-0.9282820	-0.3769950
H	-5.2898060	-3.9706590	0.9516830
H	-7.5578880	-2.9427040	1.0103600

Int4.log
Potential Energy = -2233.52559
Zero-point Energy = -2232.99216
Free Energy = -2233.04199
Single-Point Energy B3LYP-D3(BJ)/6-311+G** PCM = -2234.09921
Free Energy B3LYP-D3(BJ)/6-311+G** PCM (extrapolated free energy from qRRHO) = -2233.61562
Charge = 0 Multiplicity = 1

C	0.9402390	2.2301840	0.5755130
C	0.5027330	4.1457900	-0.7397400
C	1.9868650	3.8132210	-0.9631080
N	2.0249080	2.4045230	-0.4527940
N	-0.0284770	3.2119810	0.0836410
O	-0.0837880	5.0894640	-1.2598720
C	-1.4705080	3.1036440	0.3140480
H	-1.9822690	3.4779800	-0.5743480
H	-1.7275290	2.0537610	0.4670710
H	-1.7870090	3.6961130	1.1761920
C	2.7454050	1.4817430	-0.9874700
H	3.4500860	1.8019600	-1.7499830
C	2.6813470	0.0069470	-0.7343940
C	4.0810820	-0.5922070	-0.5054300
H	4.7390100	-0.2847360	-1.3239030
H	4.4684180	-0.1297800	0.4103860
H	1.9639690	-0.2813880	0.0330220
C	2.4441960	4.0079270	-2.3990230
H	2.2023740	5.0366690	-2.6757610
H	3.5239480	3.8811440	-2.5036970
H	1.9227810	3.3364590	-3.0864960
H	2.5907930	4.4261560	-0.2877630
C	1.4341060	2.4492160	2.0519330
H	0.5295620	1.2191770	0.4936670
Cl	1.9440840	-0.5927850	-2.3085880
C	0.2090740	2.2460370	2.9736820
H	0.5486150	2.2349770	4.0137550
H	-0.5172130	3.0558250	2.8760750
H	-0.2924930	1.2945410	2.7735490
C	2.4841840	1.3786940	2.4044470
H	2.0792960	0.3693310	2.2897890
H	3.3947320	1.4774860	1.8050190

H	2.7812480	1.4993960	3.4504460
C	2.0232770	3.8502860	2.2981650
H	1.3376190	4.6469180	1.9929090
H	2.2057970	3.9736950	3.3700080
H	2.9847450	3.9922280	1.7947840
N	-4.6968210	-0.5822140	-0.5044950
C	-5.1131530	-1.1676640	-1.6866090
C	-5.7182360	0.0131040	0.2131920
C	-6.6157670	-0.9585470	-1.8197010
C	-7.0173420	-0.1761770	-0.5586030
H	-7.1030100	-1.9345370	-1.8984060
H	-7.7299820	-0.7113950	0.0752450
H	-7.4467460	0.8059610	-0.7755470
H	-6.8168200	-0.4171750	-2.7484660
O	-5.5737010	0.5869480	1.2843430
O	-4.3766780	-1.7480110	-2.4727230
C	4.0952020	-2.1008840	-0.3592940
C	4.5129340	-2.9137850	-1.4226040
C	3.7082090	-2.7091430	0.8446030
C	4.5360160	-4.3057020	-1.2904990
H	4.8249520	-2.4566540	-2.3575660
C	3.7275560	-4.0998270	0.9784350
H	3.3966170	-2.0960600	1.6859870
C	4.1406900	-4.9026520	-0.0900150
H	4.8642030	-4.9201600	-2.1237840
H	3.4261290	-4.5544150	1.9175990
H	4.1590860	-5.9834430	0.0147770
H	-3.7112260	-0.5937930	-0.1843440
O	0.0996000	-0.9122890	0.9713150
C	-1.1159290	-1.1300350	0.7838390
O	-1.9890280	-0.4009980	0.2577920
C	-1.5906120	-2.5334120	1.2983540
F	-0.9371750	-3.5386520	0.6568490
F	-2.9146170	-2.7571000	1.1266560
F	-1.3378790	-2.6842920	2.6260660
H	-5.2204640	1.6237170	-1.3413180
H	-5.4755720	-0.0730440	-0.9462230
H	-5.1512320	1.1046410	0.3452410
C	-2.6791020	1.9586820	-0.6596500
H	-2.9102910	2.3953910	0.3175530
H	-1.5939840	1.8966420	-0.7758730
H	-3.0406400	2.6604550	-1.4168920
C	-3.1018020	0.0942390	-2.2904840
H	-3.5533630	-0.8857840	-2.4731620
H	-3.5448580	0.7933110	-3.0060820
H	-2.0316130	0.0402470	-2.5099730
H	-1.5386970	1.4502730	1.7886430
C	0.6941620	2.7826230	0.7489030
C	0.0575970	4.0321350	0.8053310
C	1.4137910	2.4405040	-0.4062140
C	0.1303800	4.9182230	-0.2723730
H	-0.4925490	4.3154130	1.6991690
C	1.4861780	3.3258760	-1.4865580
H	1.9268520	1.4844260	-0.4538080
C	0.8434730	4.5656320	-1.4234280
H	-0.3638680	5.8834290	-0.2113780
H	2.0507550	3.0486270	-2.3720580
H	0.9033330	5.2549600	-2.2605080
Cl	-0.7270040	-0.0834880	3.4123120
H	0.5305050	-0.5953730	0.6739480
O	0.6578420	-0.6755290	-2.7444460
H	1.5411640	-0.7915010	-2.3165700
O	3.1296830	-1.0929550	-1.6112530
C	3.3478300	-1.0444570	-0.3760050
C	4.8433580	-1.3228350	0.0009640
O	2.5720920	-0.8066350	0.5724530
F	5.2605550	-2.5262780	-0.4752800
F	5.6662370	-0.3807570	-0.5359510
F	5.0757760	-1.3294200	1.3330070
H	0.6851830	0.1942080	-3.1631330

Int4a.log
Potential Energy = -1949.26126
Zero-point Energy = -1948.79604
Free Energy = -1948.84194
Single-Point Energy B3LYP-D3(BJ)/6-311+G** PCM = -1949.75917
Free Energy B3LYP-D3(BJ)/6-311+G** PCM (extrapolated free energy from qRRHO) = -1949.33986
Charge = 0 Multiplicity = 1

C	-2.9040680	-0.4194010	0.2350550
C	-2.6325550	-2.6725610	-0.4206930
C	-1.2574720	-2.0274910	-0.6080670
N	-1.4376240	-0.7549740	0.1673800
N	-3.4767610	-1.7587520	0.1195280
O	-2.8985910	-3.8425840	-0.6762100
C	-4.7923660	-2.1362520	0.6348710
H	-5.5494840	-2.1479020	-0.1532200
H	-4.7169250	-3.1372150	1.0635260
H	-5.0911810	-1.4325230	1.4123930
C	-0.4784210	-0.1969400	0.8226760
C	-0.6089920	0.8921270	1.8509710
C	0.6110340	1.8250560	1.9247100
H	0.5205620	2.3889040	2.8568570
H	1.5157700	1.2140160	1.9877750
C	-0.1269740	-2.9228550	-0.1213980
H	-0.2065090	-3.8660360	-0.6668420
H	0.8500250	-2.4865910	-0.3300750
H	-0.2131470	-3.1336140	0.9484260
H	-1.0885910	-1.7528200	-1.6541730
C	-3.3771390	0.6021360	-0.8629000
H	-3.1201270	-0.0123440	1.2258540
C	-4.8976800	0.8140910	-0.6800610

syn-18b (*syn*-aminal).log
Potential Energy = -2233.52383
Zero-point Energy = -2232.98813
Free Energy = -2233.03620
Single-Point Energy B3LYP-D3(BJ)/6-311+G** PCM = -2234.10822
Free Energy B3LYP-D3(BJ)/6-311+G** PCM (extrapolated free energy from qRRHO) = -2233.62060
Charge = 0 Multiplicity = 1

C	-0.4491690	-1.7975970	1.1574570
C	-1.5239110	-3.7805250	0.4830270
C	-2.5342340	-2.6316080	0.3980450
N	-1.6701200	-1.4104740	0.4124130
N	-0.3499070	-3.2517390	0.8952080
O	-1.7378290	-4.9712520	0.2287250
C	0.8717840	-4.0428360	0.9685090
H	0.8645170	-4.7706060	0.1536310
H	1.7374070	-3.3879500	0.8578660
H	0.9563130	-4.5866740	1.9145590
C	-1.5216920	-0.6556080	-0.8301570
H	-2.3139000	-0.9715680	-1.5076500
C	-1.7364110	0.8661820	-0.5967830
C	-3.1391240	1.1523050	-0.0449680
H	-3.8827000	0.7665050	-0.7502160
H	-0.9583350	1.2858360	0.0367750
C	-3.5586120	-2.7996610	-0.7177210
H	-4.1242620	-3.7111330	-0.5079500
H	-4.2673270	-1.9664040	-0.7298210
H	-3.1033820	-2.9052280	-1.7037040
H	-3.0927780	-2.6355340	1.3413190
C	-0.4513420	-1.4065050	2.6785170
H	0.4236440	-1.3086810	0.7267240

Cl	-1.5383760	1.7378200	-2.2092710
N	-0.2798400	-0.9287740	-1.6166500
C	0.9561520	-0.3321510	-1.4665370
C	-0.3161310	-1.7563270	-2.7650000
C	1.8883350	-0.7973030	-2.5603030
C	1.0667240	-1.7992320	-3.3776140
H	2.1970110	0.0771420	-3.1414570
H	1.4467220	-2.8227150	-3.3067670
O	-1.3207750	-2.3135010	-3.1599950
O	1.2308430	0.4576540	-0.5585490
C	0.8860890	-1.8467700	3.3155760
H	0.9605100	-1.4320220	4.3261300
H	0.9654550	-2.9328430	3.4048180
H	1.7485210	-1.4826930	2.7453810
C	-0.5447920	0.1280410	2.7809370
H	0.2601080	0.6199700	2.2235140
H	-1.5031820	0.4900370	2.4026260
H	-0.4622630	0.4359540	3.8284710
C	-1.6105730	-2.0368110	3.4719460
H	-1.6252030	-3.1278980	3.3781310
H	-1.4941480	-1.8017190	4.5355030
H	-2.5804130	-1.6415740	3.1558010
H	0.9936730	-1.5477370	-4.4382980
H	2.7876280	-1.2198940	-2.1045250
H	-3.2356830	0.5615430	0.8719940
C	-3.4281280	2.6117000	0.2486430
C	-4.4150020	3.2993150	-0.4719660
C	-2.7375500	3.3006700	1.2588490
C	-4.7041960	4.6401400	-0.1970360
H	-4.9626210	2.7818060	-1.2553470
C	-3.0199140	4.6410840	1.5344820
H	-1.9755200	2.7890740	1.8406390
C	-4.0054240	5.3167740	0.8065030
H	-5.4734770	5.1529660	-0.7673900
H	-2.4742500	5.1552840	2.3205740
H	-4.2273670	6.3578550	1.0221380
H	2.6555720	1.1278530	-0.3040150
O	3.4957000	1.6485780	-0.0774810
C	4.5546770	0.8726600	-0.0322030
C	5.8198960	1.7052090	0.3140990
F	6.0443260	2.6500860	-0.6263830
F	6.9074390	0.9232660	0.3850580
F	5.6764600	2.3319390	1.5027410
O	4.6161190	-0.3226640	-0.2250980
H	-1.5075070	1.4056490	0.9815060
C	0.7798260	-2.5898450	-1.9130310
H	1.1464220	-3.4635690	-2.4574550
H	-0.2158730	-2.8261270	-1.5296960
H	0.7045620	-1.7555190	-2.6169870
H	1.7989960	-3.1750510	-0.1239160
C	3.3730440	-0.6330290	1.7646110
H	2.7947160	0.6585110	0.1191560
C	4.8176950	-0.1036950	1.8969710
H	5.1080340	-0.1055460	2.9527070
H	5.5372040	-0.7273040	1.3614860
H	4.9106770	0.9260690	1.5335750
C	2.4938300	0.1870880	2.7312480
H	2.5490060	1.2587960	2.5051630
H	1.4432880	-0.1105950	2.7060870
H	2.8493720	0.0509060	3.7577440
C	3.3463780	-2.1192400	2.1630480
H	3.9600680	-2.7275570	1.4899480
H	3.7492100	-2.2399940	3.1741220
H	2.3292020	-2.5227180	2.1622510
H	0.9591250	1.5815620	0.6189800
C	-1.1448710	3.2569880	-0.0296560
C	-0.6636340	4.0147090	1.0501740
C	-1.6670460	3.9325440	-1.1415380
C	-0.6924050	5.4113320	1.0140520
H	-0.2700580	3.5110630	1.9300370
C	-1.7014550	5.3304200	-1.1804510
H	-2.0501870	3.3611940	-1.9828680
C	-1.2113670	6.0745520	-0.1034320
H	-0.3169830	5.9802880	1.8598650
H	-2.1112780	5.8351730	-2.0506910
H	-1.2378360	7.1599870	-0.1311740
Cl	1.0022510	1.5561170	-1.7515770
H	-0.3244410	-0.8018520	-0.8102060
O	-0.4673670	-0.7159980	1.2419540
H	-2.0000610	-1.1423450	1.1659450
H	0.0218740	-1.4334340	1.6737380
O	-2.9808750	-1.4074570	1.2305400
C	-3.4575800	-1.8027600	0.0724130
C	-4.9484380	-2.2165940	0.2141020
O	-2.8808970	-1.8647910	-0.9923350
F	-5.0818620	-3.2388260	1.0887070
F	-5.6949440	-1.1853330	0.6677750
F	-5.4548690	-2.6094800	-0.9641920

Int5.log
Potential Energy = -1949.26139
Zero-point Energy = -1948.79334
Free Energy = -1948.83756
Single-Point Energy B3LYP-D3(BJ)/6-311+G** PCM = -1949.75481
Free Energy B3LYP-D3(BJ)/6-311+G** PCM (extrapolated free energy from qRRHO) = -1949.33098
Charge = 0 Multiplicity = 1

C	2.8479570	-0.4198890	0.2974400
C	3.1788680	-2.0851900	-1.3420500
C	1.7708930	-2.2976070	-0.7866200
N	1.5497880	-1.0639370	0.0043330
N	3.7174470	-1.0041560	-0.7385140
O	3.7192410	-2.7693720	-2.2175730
C	4.9482250	-0.3944440	-1.2321830
H	5.8410300	-0.8700730	-0.8165410
H	4.9758230	-0.4998760	-2.3191860
H	4.9574550	0.6650230	-0.9739010
C	0.2907740	-0.4074070	-0.0013390
C	0.2888550	1.1310430	-0.1127780
C	-1.1139280	1.7421000	0.0170570
H	-1.7602340	1.3272430	-0.7631280

product.log (*S*-(19))
Potential Energy = -883.82667
Zero-point Energy = -883.66972
Free Energy = -883.69775
Single-Point Energy B3LYP-D3(BJ)/6-311+G** PCM = -883.98063
Free Energy B3LYP-D3(BJ)/6-311+G** PCM (extrapolated free energy from qRRHO) = -883.85171
Charge = 0 Multiplicity = 1

C	1.5543360	-0.1401000	-0.2522360
C	0.5788650	-0.8150130	0.7258110
H	1.3676790	-0.4306580	-1.2862890
Cl	3.2770780	-0.6606210	0.1189520
H	0.7501140	-1.8944180	0.6703410
C	1.5643120	1.3750860	-0.1387350
H	1.8473870	1.7745930	0.8535280
O	1.2837260	2.1117370	-1.0628590
H	0.8173130	-0.4989870	1.7465030
C	-0.8671920	-0.4916620	0.3938040
C	-1.5760040	0.4711890	1.1273470
C	-1.5186940	-1.1475590	-0.6630480
C	-2.9044020	0.7751410	0.8117550
H	-1.0912900	0.9815950	1.9557640

C	-2.8451130	-0.8455530	-0.9812380
H	-0.9884110	-1.9045210	-1.2357550
C	-3.5419630	0.1187320	-0.2446900
H	-3.4389460	1.5206960	1.3931920
H	-3.3349500	-1.3653710	-1.7995070
H	-4.5739020	0.3521650	-0.4897160

anti-18b.log
Potential Energy = -2233.51758
Zero-point Energy = -2232.98167
Free Energy = -2233.02959
Single-Point Energy B3LYP-D3(BJ)/6-311+G** PCM = -2234.10584
Free Energy B3LYP-D3(BJ)/6-311+G** PCM (extrapolated free energy from qRRHO) = -2233.61785
Charge = 0 Multiplicity = 1

C	2.9544110	-1.3243090	-0.1002390
C	2.6737200	-1.0248020	-2.4146860
C	1.2861080	-0.9717320	-1.7662800
N	1.5980950	-0.7775800	-0.3211500
N	3.5820770	-1.2046860	-1.4325050
O	2.9203350	-0.9234620	-3.6224130
C	5.0134190	-1.1134380	-1.6842030
H	5.1836440	-0.3621570	-2.4593090
H	5.5253020	-0.8071010	-0.7707000
H	5.4351900	-2.0639150	-2.0263420
C	1.1601280	0.4374230	0.3404310
H	0.3598170	0.8508330	-0.2698600
C	2.1727410	1.5931060	0.6006320
C	1.5711680	2.8738550	1.2239240
H	2.9882220	1.2656280	1.2385760
C	0.3481590	0.0148920	-2.4544380
H	0.2497460	-0.3008260	-3.4963020
H	-0.6456830	-0.0052230	-2.0011390
H	0.7316020	1.0374070	-2.4508190
H	0.8403080	-1.9676590	-1.8862410
C	2.9920850	-2.7955900	0.4603130
H	3.5033230	-0.6969110	0.6093060
Cl	2.9889070	2.0185560	-0.9878270
N	0.4561460	0.1057430	1.6282660
C	-0.8689050	-0.2899060	1.6061870
C	1.0027610	0.0243020	2.9227410
C	-1.3205100	-0.6577570	3.0003200
C	-0.0875620	-0.4183520	3.8791330
H	-2.1800740	-0.0388340	3.2724590
H	0.2508230	-1.3118100	4.4098930
O	2.1594890	0.2819190	3.2006630
O	-1.5423060	-0.3195560	0.5749050
C	4.4627100	-3.2144140	0.6854470
H	4.4913280	-4.1686520	1.2217670
H	5.0041870	-3.3548050	-0.2529580
H	5.0057940	-2.4792860	1.2909420
C	2.2740340	-2.8443600	1.8201050
H	2.7394210	-2.1719470	2.5471310
H	1.2181620	-2.5809810	1.7167860
H	2.3244460	-3.8599290	2.2264840
C	2.3239680	-3.8080880	-0.4893400
H	2.7638430	-3.7836250	-1.4915270
H	2.4608660	-4.8210290	-0.0954640
H	1.2471240	-3.6338460	-0.5724800
H	-0.2359960	0.3689890	4.6234600
H	-1.6550560	-1.6994000	2.9974680
H	1.2757670	2.6240190	2.2471820
H	2.3980390	3.5847990	1.3163060
C	0.4065630	3.5349510	0.5084340
C	0.6201740	4.4235060	-0.5591730
C	-0.9140560	3.3119760	0.9288940
C	-0.4534840	5.0446110	-1.2028800
H	1.6335620	4.6367890	-0.8838850
C	-1.9919960	3.9311240	0.2883140
H	-1.1052070	2.6642240	1.7796120
C	-1.7651810	4.7961960	-0.7853020
H	-0.2640870	5.7284080	-2.0254310
H	-3.0042010	3.7429140	0.6345360
H	-2.5995260	5.2811400	-1.2835530
H	-3.0867530	-0.7157070	0.4958220
O	-4.0733650	-0.9489840	0.4995030
C	-4.5537260	-1.1134290	-0.7126060
O	-3.9714420	-1.0230510	-1.7711010
C	-6.0670080	-1.4618580	-0.6463300
F	-6.2729370	-2.5907890	0.0682100
F	-6.5734600	-1.6497260	-1.8741570
F	-6.7646690	-0.4665610	-0.0540270

Int3′.log
Potential Energy = -2233.46721
Zero-point Energy = -2232.93678
Free Energy = -2232.98830
Single-Point Energy B3LYP-D3(BJ)/6-311+G** PCM = -2234.03863
Free Energy B3LYP-D3(BJ)/6-311+G** PCM (extrapolated free energy from qRRHO) = -2233.55972
Charge = 0 Multiplicity = 1

C	-2.6266560	2.4503800	0.7784270
C	-1.5223420	3.9157680	-0.7036390
C	-1.4995120	2.5479870	-1.3843830
N	-2.3190760	1.7439350	-0.4755820
N	-2.2467700	3.8256180	0.4340010
O	-1.0229690	4.9494330	-1.1588150
C	-2.6800680	5.0203450	1.1497690
H	-2.8929100	5.8029220	0.4180380
H	-3.5873750	4.7972780	1.7119570
H	-1.9141910	5.3914730	1.8372380
C	-2.8890640	0.5278930	-0.7748120
H	-3.7156960	0.2693140	-0.1181140
C	-2.5480320	-0.3347000	-1.7643380
C	-3.3463400	-1.5718740	-2.1430910
H	-2.6565380	-2.4200540	-2.2465020
H	-0.4627090	2.1815710	-1.4321660
C	-1.8870200	1.8911850	2.0517060
H	-3.7091810	2.4089470	0.9711340
H	-1.7300520	-0.0962950	-2.4377340
Cl	-0.2363270	-1.6516930	-0.4739190
N	1.1471420	-2.5417150	0.0763850
C	1.0363910	-3.7776350	0.7502140
C	2.4420110	-2.1007200	-0.1074630
C	2.4506000	-4.2249380	1.0669680
C	3.3713980	-3.1349220	0.4890930
H	2.6145650	-5.2083090	0.6189150
H	4.0294480	-3.5060380	-0.3019760
H	4.0006990	-2.6479780	1.2388360
H	2.5447700	-4.3343510	2.1507180
O	2.7320410	-1.0465780	-0.6668220
O	-0.0138360	-4.3256460	1.0012080
C	-2.0489010	2.7048910	-2.8121990
H	-1.9815400	1.7816430	-3.3867170
H	-3.0954690	3.0247850	-2.7883540
H	-1.4596170	3.4710050	-3.3225100
C	-2.2691950	2.7253540	3.2945580
H	-1.8821820	2.2333710	4.1930320
H	-1.8471390	3.7320160	3.2716330
H	-3.3566490	2.8076790	3.4083120
C	-0.3611380	1.9234840	1.8549500
H	0.0052410	2.9433680	1.6973150
H	0.1375190	1.5274920	2.7461530
H	-0.0552940	1.3089460	1.0025880

C	-2.3435480	0.4409220	2.3163490
H	-3.4336810	0.3733900	2.4148440
H	-2.0249580	-0.2464270	1.5305160
H	-1.9061550	0.0909070	3.2574030
H	-3.7735670	-1.4198290	-3.1449540
C	-4.4630630	-1.9580020	-1.1934430
C	-4.2095650	-2.7655950	-0.0733220
C	-5.7776370	-1.5172080	-1.4116650
C	-5.2380530	-3.1213360	0.8046880
H	-3.1989240	-3.1217310	0.1094840
C	-6.8105050	-1.8690560	-0.5363640
H	-5.9948610	-0.8965530	-2.2779170
C	-6.5434660	-2.6727920	0.5765620
H	-5.0208980	-3.7518150	1.6625460
H	-7.8216360	-1.5197980	-0.7265350
H	-7.3442960	-2.9510480	1.2556610
H	4.2053280	-0.4257260	-0.8220110
O	5.0824190	0.0408130	-1.0131430
C	5.8752080	0.0342720	0.0349300
C	7.2094610	0.7594330	-0.2931800
O	5.6676980	-0.4490210	1.1269470
F	8.0263500	0.7706310	0.7706260
F	6.9854230	2.0395260	-0.6632370
F	7.8535440	0.1423900	-1.3090260

syn-18b′.log
Potential Energy = -2233.51380
Zero-point Energy = -2232.97812
Free Energy = -2233.02594
Single-Point Energy B3LYP-D3(BJ)/6-311+G** PCM = -2234.10139
Free Energy B3LYP-D3(BJ)/6-311+G** PCM (extrapolated free energy from qRRHO) = -2233.61352
Charge = 0 Multiplicity = 1

C	-1.8564840	1.5162690	0.5390720
C	-1.0558940	2.6485280	-1.3582430
C	-0.1829640	1.4019620	-1.2095780
N	-0.9067160	0.6342080	-0.1733550
N	-2.0258090	2.6159430	-0.4207840
O	-0.9212940	3.5198530	-2.2252900
C	-3.1410830	3.5545640	-0.4437960
H	-3.4066970	3.7491130	-1.4854550
H	-3.9969730	3.1142900	0.0687400
H	-2.8902920	4.5085310	0.0301960
C	-1.0612310	-0.7812760	-0.0359600
H	-1.8517260	-0.9152110	0.7038930
C	-1.5783720	-1.5790380	-1.2979850
C	-2.8512570	-2.4065590	-1.0185230
H	-3.0719650	-2.9743660	-1.9274720
H	-2.6487100	-3.1254320	-0.2211320
H	0.7991750	1.7077950	-0.8262900
C	-1.3904810	2.0009280	1.9626020
H	-2.8191090	1.0018620	0.6615780
H	-1.7776430	-0.8680320	-2.0928030
Cl	-0.3275230	-2.7195670	-2.0195620
N	0.0848200	-1.4904980	0.6317360
C	1.4339680	-1.3187860	0.4183320
C	-0.1690210	-2.4815330	1.6010800
C	2.2146990	-2.2500960	1.3207470
C	1.1506810	-3.0198380	2.1098960
H	2.8814030	-1.6518450	1.9479080
H	1.2054580	-2.8544120	3.1894060
H	1.1792360	-4.0995380	1.9408560
H	2.8423160	-2.8932250	0.6971150
O	-1.2894440	-2.8115390	1.9446560
O	1.9138040	-0.5184570	-0.3868330
C	0.0511510	0.7837330	-2.5922080
H	0.6112370	-0.1475030	-2.5244570
H	-0.8787650	0.6189110	-3.1435800
H	0.6483590	1.4966790	-3.1666690
C	-2.4786610	2.8953560	2.5975720
H	-2.2209090	3.0933550	3.6432880
H	-2.5698340	3.8628330	2.0997370
H	-3.4604050	2.4073440	2.5879680
C	-0.0648890	2.7789510	1.8839380
H	-0.1531690	3.6705170	1.2544100
H	0.2311490	3.1102370	2.8851610
H	0.7420380	2.1532840	1.4901630
C	-1.2053860	0.7767440	2.8805530
H	-2.1085340	0.1571530	2.9235220
H	-0.3682180	0.1546080	2.5592900
H	-0.9889660	1.1118390	3.9001410
C	-4.0529870	-1.5514520	-0.6573110
C	-4.5709550	-1.5493350	0.6468020
C	-4.6867750	-0.7619670	-1.6317890
C	-5.6921380	-0.7773260	0.9717230
H	-4.0977860	-2.1612420	1.4099460
C	-5.8037200	0.0125290	-1.3099850
H	-4.3115380	-0.7612590	-2.6524120
C	-6.3102680	0.0075480	-0.0051020
H	-6.0808200	-0.7928670	1.9859130
H	-6.2821950	0.6137970	-2.0777230
H	-7.1812400	0.6063630	0.2446450
H	3.4502220	-0.2769000	-0.6037500
O	4.4160170	-0.0882660	-0.8688960
C	5.1693500	0.1863350	0.1700780
O	4.8473470	0.2370470	1.3382510
C	6.6331210	0.4522780	-0.2786510
F	7.1571450	-0.6422470	-0.8755220
F	7.4107460	0.7653100	0.7688980
F	6.6924280	1.4722900	-1.1630920

anti-18b′.log
Potential Energy = -2233.51605
Zero-point Energy = -2232.98059
Free Energy = -2233.02877
Single-Point Energy B3LYP-D3(BJ)/6-311+G** PCM = -2234.10308
Free Energy B3LYP-D3(BJ)/6-311+G** PCM (extrapolated free energy from qRRHO) = -2233.61580
Charge = 0 Multiplicity = 1

C	0.9018130	-1.7271780	-0.9590970
C	2.4756080	-3.2785000	-0.1497600
C	3.0426390	-1.8960290	0.1790040
N	1.9167800	-1.0052690	-0.1549570
N	1.2443790	-3.1291900	-0.6785010
O	3.0338980	-4.3558530	0.0873170
C	0.3585820	-4.2708350	-0.8738650
H	0.4963440	-4.9633590	-0.0401170
H	-0.6762420	-3.9277280	-0.8893740
H	0.5722030	-4.8069730	-1.8036170
C	1.5887340	0.2349000	0.4577310
H	0.8024540	0.6880210	-0.1443410
C	2.7428850	1.2705370	0.5925640
C	2.2931770	2.7013300	0.9653110
H	3.8953800	-1.6988840	-0.4877090
C	0.8984730	-1.3844450	-2.4960980
H	-0.0999910	-1.5210680	-0.5714640
H	3.4602480	0.9458330	1.3377040
Cl	3.7155140	1.3128120	-0.9603400
N	0.8896240	0.1186550	1.8360340
C	-0.4775180	-0.0786710	1.8911410
C	1.4383610	0.2043890	3.1366820
C	-0.9379850	-0.2106690	3.3231400
C	0.3393300	-0.0530850	4.1501510
H	-1.4254750	-1.1817840	3.4484310

H	0.5984260	-0.9502620	4.7198330
H	0.3062870	0.7840970	4.8517100
H	-1.6868140	0.5603480	3.5259430
O	2.5997200	0.4617410	3.3900420
O	-1.1957140	-0.1241950	0.8879040
C	3.5652060	-1.9190910	1.6186660
H	4.0298040	-0.9785590	1.9114540
H	2.7745400	-2.1596200	2.3342630
H	4.3238850	-2.7037970	1.6778550
C	-0.2001170	-2.2026000	-3.2121960
H	-0.3065260	-1.8417970	-4.2407180
H	0.0367120	-3.2670730	-3.2679150
H	-1.1747160	-2.0894060	-2.7227090
C	2.2628350	-1.6837230	-3.1419500
H	2.5285200	-2.7427290	-3.0547750
H	2.2294550	-1.4401900	-4.2096240
H	3.0573670	-1.0849130	-2.6881600
C	0.5531480	0.1073580	-2.6889910
H	-0.3975130	0.3669720	-2.2088240
H	1.3348850	0.7640070	-2.3033150
H	0.4480280	0.3201950	-3.7583010
H	1.8484580	2.6465940	1.9637900
H	3.2072590	3.2922480	1.0751620
C	1.3379770	3.4111440	0.0244960
C	-0.0499260	3.3584040	0.2285570
C	1.8218200	4.1743640	-1.0510960
C	-0.9315460	4.0268550	-0.6267690
H	-0.4502530	2.8041740	1.0727480
C	0.9452390	4.8453150	-1.9079790
H	2.8926520	4.2496740	-1.2140470
C	-0.4362110	4.7700890	-1.7015760
H	-2.0013360	3.9721500	-0.4470400
H	1.3418590	5.4314920	-2.7320840
H	-1.1181100	5.2937830	-2.3651760
H	-2.7786970	-0.3152100	0.9029630
O	-3.7789470	-0.4726670	0.9595420
C	-4.3987220	-0.1648870	-0.1577250
O	-3.9247170	0.2621700	-1.1875490
C	-5.9241100	-0.4246520	-0.0130270
F	-6.1675200	-1.7218550	0.2795830
F	-6.5747430	-0.1260870	-1.1474420
F	-6.4488920	0.3273980	0.9804430

Int4′.log
Potential Energy = -2233.52515
Zero-point Energy = -2232.99167
Free Energy = -2233.04178
Single-Point Energy B3LYP-D3(BJ)/6-311+G** PCM = -2234.09953
Free Energy B3LYP-D3(BJ)/6-311+G** PCM (extrapolated free energy from qRRHO) = -2233.61616
Charge = 0 Multiplicity = 1

C	0.5057100	2.0118400	-0.5734890
C	0.3276840	3.3585180	1.3565140
C	-1.0855050	2.7958810	1.1348800
N	-0.8166260	1.7463180	0.1044920
N	1.1647370	2.8349480	0.4340460
O	0.6298980	4.1230640	2.2678620
C	2.6145810	3.0071770	0.5321140
H	2.8852540	3.0151490	1.5896410
H	3.1158550	2.1749730	0.0372260
H	2.9390320	3.9491610	0.0818730
C	-1.5083000	0.7082520	-0.2162790
H	-1.0354380	0.0051190	-0.9134190
C	-2.8825480	0.3440270	0.2850680
C	-3.3183950	-1.0261410	-0.2557360
H	-1.7141450	3.5636590	0.6713470
C	0.3429650	2.6831150	-1.9874170
H	1.0172930	1.0476930	-0.6744390
H	-2.9127650	0.3481070	1.3739920
Cl	-4.0387350	1.6686030	-0.2374650
N	4.1818220	-1.1429250	0.8940540
C	5.1854980	-0.2369080	0.6041840
C	4.4671940	-1.9680830	1.9676810
C	6.3226990	-0.4512430	1.5935500
C	5.8474520	-1.6016200	2.4963740
H	6.4992380	0.4816390	2.1363920
H	5.7598100	-1.3191690	3.5492430
H	6.4903840	-2.4849620	2.4477020
H	7.2358910	-0.6838740	1.0385110
O	3.7176470	-2.8341710	2.3972670
O	5.1367910	0.5887320	-0.2980960
C	-1.6968020	2.3327890	2.4554620
H	-2.7738770	2.1839050	2.3853990
H	-1.2109470	1.4286240	2.8312870
H	-1.5208150	3.1359420	3.1748650
C	1.7610040	2.8547710	-2.5811740
H	1.6713370	3.1987690	-3.6158120
H	2.3504620	3.5985690	-2.0418160
H	2.3141190	1.9098220	-2.5910260
C	-0.3487320	4.0560700	-1.9052010
H	0.1737970	4.7412470	-1.2304970
H	-0.3536470	4.5155160	-2.8983030
H	-1.3930290	3.9735300	-1.5873380
C	-0.4549220	1.7575590	-2.9283600
H	-0.0329230	0.7485720	-2.9690800
H	-1.5111910	1.6845070	-2.6506810
H	-0.4257660	2.1741260	-3.9396110
H	-2.5049960	-1.7207440	-0.0113130
H	-3.3780880	-0.9798880	-1.3470230
C	-4.6195300	-1.5323630	0.3304670
C	-5.8015790	-1.5146080	-0.4228450
C	-4.6613630	-2.0372810	1.6398420
C	-7.0023260	-1.9818210	0.1212780
H	-5.7830340	-1.1361010	-1.4412540
C	-5.8598210	-2.5017960	2.1875380
H	-3.7509370	-2.0771790	2.2333410
C	-7.0352610	-2.4738830	1.4291480
H	-7.9083690	-1.9622140	-0.4773790
H	-5.8739030	-2.8915890	3.2012100
H	-7.9665830	-2.8384240	1.8525320
O	-0.1177520	-1.6251080	-1.6863120
H	3.2990100	-1.1972780	0.3561010
C	1.0348540	-1.7967120	-1.2376970
O	1.7120970	-1.0605120	-0.4795400
C	1.7065260	-3.1343570	-1.7007020
F	1.0135460	-4.2109070	-1.2423040
F	2.9815280	-3.2776250	-1.2715580
F	1.7351460	-3.2311330	-3.0554200

Int4a′.log
Potential Energy = -1949.25759
Zero-point Energy = -1948.79233
Free Energy = -1948.83881
Single-Point Energy B3LYP-D3(BJ)/6-311+G** PCM = -1949.75178
Free Energy B3LYP-D3(BJ)/6-311+G** PCM (extrapolated free energy from qRRHO) = -1949.33300
Charge = 0 Multiplicity = 1

C	3.3793040	-0.3438340	-0.6281640
C	3.0655760	-1.7154410	1.2670310
C	2.0713280	-0.5588050	1.4469340
N	2.1267590	0.0767900	0.0955720
N	3.7079030	-1.5715620	0.0841130
O	3.2075540	-2.6371710	2.0632940
C	4.5314220	-2.6463780	-0.4699910

H	4.0957420	-3.5999170	-0.1666090
H	4.5296550	-2.5780160	-1.5581430
H	5.5601560	-2.5981440	-0.1046600
C	1.2463370	0.7983050	-0.5085210
H	1.4831790	1.0792040	-1.5273280
C	-0.0153530	1.3863510	0.0716440
C	-0.8112710	2.1515590	-0.9940500
H	-0.1991810	2.9712710	-1.3824930
H	2.4811850	0.1582300	2.1664910
C	4.4970840	0.7601150	-0.6261380
H	3.0958370	-0.5743460	-1.6597580
H	-0.6306090	0.6118450	0.5263510
Cl	0.4814650	2.4992290	1.4445480
C	0.7142870	-1.0725110	1.9225470
H	0.0921170	-0.2741970	2.3267010
H	0.1770710	-1.6039630	1.1334990
H	0.9171910	-1.7758980	2.7336140
C	5.7146760	0.2024240	-1.3989070
H	6.4513870	1.0019410	-1.5196940
H	6.2062700	-0.6138700	-0.8665150
H	5.4385350	-0.1465920	-2.3998790
C	4.9252890	1.1383090	0.8036840
H	5.2627510	0.2666420	1.3727740
H	5.7620170	1.8415450	0.7547120
H	4.1218280	1.6338760	1.3579490
C	4.0029380	2.0184970	-1.3694640
H	3.6566680	1.7884750	-2.3836170
H	3.2070660	2.5427280	-0.8326210
H	4.8347470	2.7229210	-1.4617320
H	-0.9668460	1.4411140	-1.8146340
C	-2.1478430	2.6722430	-0.5071500
C	-2.3787170	4.0488380	-0.3837030
C	-3.1831380	1.7791330	-0.1860950
C	-3.6168370	4.5283550	0.0572630
H	-1.5877290	4.7508080	-0.6342430
C	-4.4186690	2.2564510	0.2584840
H	-3.0231550	0.7078980	-0.2857540
C	-4.6396370	3.6328990	0.3816820
H	-3.7793100	5.5986310	0.1463910
H	-5.2101650	1.5537520	0.5027270
H	-5.6016240	4.0029630	0.7242030
O	0.1323700	-1.0197810	-1.9114570
H	-0.7084270	-1.3127920	-1.4605150
O	-2.0214000	-1.6607310	-0.4697650
C	-2.8574200	-2.4955140	-0.9143120
O	-2.8958700	-3.0930550	-2.0015370
C	-4.0140370	-2.7960410	0.1011900
F	-4.6918040	-1.6631090	0.4324370
F	-3.5308240	-3.3170380	1.2624030
F	-4.9305710	-3.6737670	-0.3663180
H	-0.0882440	-0.9181980	-2.8470760
H	3.7892620	-3.6889490	0.2444790
H	4.0751140	-2.8992690	-1.3256940
H	5.2768250	-2.7614000	-0.0201730
C	0.8585870	0.4326410	-0.4897690
H	1.1289170	0.7414440	-1.5018270
C	-0.1027130	1.5014070	0.0885170
C	-1.0741420	2.0110830	-0.9896530
H	-0.5034910	2.5569490	-1.7480220
H	2.7526370	0.4336970	2.1851800
C	4.3400090	0.4921030	-0.9247020
H	2.7382860	-0.8231920	-1.5436500
H	-0.6570520	1.0883880	0.9294940
Cl	0.8293510	2.9065140	0.7952750
C	0.8714750	-0.5461420	2.3909940
H	0.3586270	0.3833330	2.6444180
H	0.1875730	-1.2113390	1.8614600
H	1.1583290	-1.0288010	3.3289790
C	5.3866790	-0.2467700	-1.7861810
H	6.1276800	0.4709600	-2.1537010
H	5.9280450	-1.0101580	-1.2225320
H	4.9283600	-0.7234670	-2.6607870
C	5.0109370	1.0273390	0.3528200
H	5.3934650	0.2149320	0.9800920
H	5.8600520	1.6656520	0.0857520
H	4.3166790	1.6300500	0.9455750
C	3.7922260	1.6745430	-1.7507400
H	3.3130630	1.3313720	-2.6761220
H	3.0688460	2.2622880	-1.1800780
H	4.6158060	2.3377890	-2.0356930
H	-1.4886810	1.1219530	-1.4780330
C	-2.2063340	2.8713970	-0.4668650
C	-2.2318620	4.2527590	-0.7052430
C	-3.2628110	2.2970000	0.2587190
C	-3.2803140	5.0446410	-0.2249160
H	-1.4262070	4.7128840	-1.2712090
C	-4.3102960	3.0845900	0.7433830
H	-3.2718190	1.2249810	0.4405740
C	-4.3220010	4.4631320	0.5034780
H	-3.2819480	6.1130930	-0.4210960
H	-5.1194000	2.6215280	1.3010730
H	-5.1375710	5.0758540	0.8764310
O	-0.0120260	-0.7576120	-0.6406340
H	-1.4565980	-1.3224630	-0.1375430
O	-2.3365630	-1.7312320	0.1332700
C	-2.6225620	-2.7602200	-0.6360220
O	-1.9677270	-3.2072360	-1.5521230
C	-3.9846380	-3.3826390	-0.2247640
F	-4.9855390	-2.4886020	-0.3857620
F	-3.9724210	-3.7606370	1.0718730
F	-4.2650080	-4.4608080	-0.9709960
H	0.2688110	-1.2766220	-1.4085040

Int5′.log
Potential Energy = -1949.26099
Zero-point Energy = -1948.79335
Free Energy = -1948.83855
Single-Point Energy B3LYP-D3(BJ)/6-311+G** PCM = -1949.75299
Free Energy B3LYP-D3(BJ)/6-311+G** PCM (extrapolated free energy from qRRHO) = -1949.33054
Charge = 0 Multiplicity = 1

C	3.1423700	-0.4627680	-0.5876620
C	2.9921210	-1.5649160	1.4859430
C	2.1576970	-0.2863180	1.6051260
N	2.0736570	0.1905140	0.2039530
N	3.4923300	-1.6309230	0.2328640
O	3.1703980	-2.3979020	2.3809440
C	4.2071650	-2.8073760	-0.2464530

Transition States

Formation of carbinol amine (TS1)

Conformation name	Extrapolated Free energy (kcal/mol)

TS1-lowest	0.0
1	0.9
2	0.1
3	1.5
4	2.3
5	1.4
6	1.5
7	0.5

TS1-lowest.log
Potential Energy = -1489.66362
Zero-point Energy = -1489.18887
Free Energy = -1489.23186
Single-Point Energy B3LYP-D3(BJ)/6-311+G** PCM = -1490.12258
Free Energy B3LYP-D3(BJ)/6-311+G** PCM (extrapolated free energy from qRRHO) = -1489.69083
Nimag = 1 (-162.6618)
Charge = 0 Multiplicity = 1

C	1.8517090	-0.8511400	1.6926950
H	2.0070440	-1.7005300	1.0261210
H	1.4013680	-1.2130030	2.6208840
C	3.2250410	-0.2001630	2.0381640
C	0.9361530	0.1470150	1.0546780
O	0.4214710	1.0438850	1.8105020
H	-0.0740900	1.8766850	1.2616730
H	1.0578790	0.3821560	-0.0013810
O	-0.6648440	2.8873570	0.6484180
C	-1.7764790	2.5928830	0.0968280
C	-2.4661420	3.8293810	-0.5562970
F	-1.7045350	4.3270220	-1.5635700
F	-3.6739420	3.5343710	-1.0747810
F	-2.6448290	4.8269570	0.3433280
O	-2.3375590	1.4956530	0.0125340
H	3.7872370	-0.9518640	2.6022390
C	4.0319780	0.2445030	0.8336160
C	4.7148170	-0.6966460	0.0456070
C	4.1130900	1.5989250	0.4760850
C	5.4509620	-0.2970820	-1.0728450
H	4.6757730	-1.7500000	0.3134110
C	4.8487960	2.0035020	-0.6431880
H	3.6020130	2.3446700	1.0800220
C	5.5186850	1.0561710	-1.4225760
H	5.9752980	-1.0401360	-1.6670750
H	4.9001820	3.0573670	-0.9016440
H	6.0926470	1.3683920	-2.2901460
H	3.0559370	0.6454640	2.7114060
N	-0.8125710	-1.0379910	0.5345580
C	-1.2744170	-1.9646060	1.6063180
C	-1.2471790	-1.6343010	-0.7795250
C	-2.4527290	-2.6943130	0.9517430
H	-0.4871050	-2.6962800	1.8190460
H	-1.5765160	-0.8042420	-1.4129600
O	-3.2962320	-3.3773790	1.5380340
N	-2.4280920	-2.4223760	-0.3733750
C	-3.5480770	-2.7692240	-1.2427410
H	-3.4840610	-3.7987480	-1.6069870
H	-4.4743010	-2.6615600	-0.6736720
H	-3.5688350	-2.0892630	-2.0952580
C	-0.1805590	-2.4460100	-1.5841700
C	-0.8325990	-2.9522400	-2.8928420
H	-1.5888910	-3.7185880	-2.7126240
H	-1.2928600	-2.1352340	-3.4600700
H	-0.0615370	-3.4008130	-3.5269190
C	0.9802190	-1.5134500	-1.9876800
H	0.6135150	-0.5892060	-2.4491230
H	1.6204850	-1.2506450	-1.1449520
H	1.6167270	-2.0179160	-2.7214270
C	0.3584270	-3.6590820	-0.8036040
H	-0.4461780	-4.3447160	-0.5187960
H	1.0597230	-4.2178330	-1.4320280
H	0.8974220	-3.3659480	0.1013920
C	-1.6886230	-1.2641990	2.8982030
H	-0.8400980	-0.7734750	3.3776320
H	-2.4619780	-0.5130660	2.7077140
H	-2.0961040	-2.0077730	3.5874050
H	-1.3774290	-0.1821550	0.6063230

1.log
Potential Energy = -1489.66305
Zero-point Energy = -1489.18786
Free Energy = -1489.23113
Single-Point Energy B3LYP-D3(BJ)/6-311+G** PCM = -1490.12134
Free Energy B3LYP-D3(BJ)/6-311+G** PCM (extrapolated free energy from qRRHO) = -1489.68941
Nimag = 1 (-133.0078)
Charge = 0 Multiplicity = 1

C	1.3952340	-2.0585190	-0.2956850
H	0.6543910	-2.7384950	-0.7173550
H	1.5549830	-2.3234810	0.7525740
C	2.7223600	-2.2428810	-1.0968820
C	0.8997970	-0.6508130	-0.3909580
O	1.3984420	0.2147100	0.4164610
H	1.1683160	1.2481300	0.1533250
H	0.5363960	-0.2916880	-1.3530400
O	0.9013840	2.5506950	-0.1393410
C	-0.3032820	2.9011140	0.0743550
C	-0.5365840	4.4259900	-0.1568090
F	-0.1999490	4.7857890	-1.4207210
F	-1.8194550	4.7914340	0.0351080
F	0.2243440	5.1668250	0.6875980
O	-1.2666370	2.2105270	0.4283730
H	2.8918930	-3.3241100	-1.1457100
N	-1.1276380	-0.7687640	0.3082940
C	-1.3055380	-1.5724850	1.5509810
C	-2.4312110	-0.8364550	-0.4483670
C	-2.8214460	-1.5322140	1.7740390
H	-1.0095870	-2.6095680	1.3581450
H	-2.5984200	0.1555130	-0.8803050
O	-3.4079200	-1.8478030	2.8120990
N	-3.3967640	-1.0496250	0.6482010
C	-4.8041900	-0.6638800	0.6185940
H	-5.4600800	-1.5120210	0.4016090
H	-5.0726100	-0.2620670	1.5982070
H	-4.9529060	0.1066340	-0.1388470
C	-2.5387860	-1.8794290	-1.6086610
C	-3.9394450	-1.7492500	-2.2536400
H	-4.7378150	-2.0848270	-1.5891580
H	-4.1510560	-0.7185810	-2.5600750
H	-3.9800800	-2.3751560	-3.1504490
C	-1.5046070	-1.5463420	-2.7040070
H	-1.5451900	-0.4889660	-2.9901390
H	-0.4842290	-1.7870390	-2.4039890
H	-1.7176530	-2.1381650	-3.5997510
C	-2.3545080	-3.3304070	-1.1269920
H	-3.0841800	-3.5945350	-0.3548720
H	-2.5005830	-4.0171980	-1.9671150
H	-1.3524710	-3.5143660	-0.7299250
C	-0.5396960	-1.0353980	2.7574440
H	0.5391090	-1.1023900	2.6092910

H	-0.7993970	0.0094530	2.9558850
H	-0.8087180	-1.6271620	3.6357470
H	-1.0704100	0.2198650	0.5867710
H	2.5724970	-1.9048860	-2.1277910
C	3.9415430	-1.5664760	-0.5046010
C	4.5174920	-0.4455590	-1.1196000
C	4.5319200	-2.0612450	0.6699130
C	5.6483880	0.1720030	-0.5743510
H	4.0795290	-0.0518050	-2.0335340
C	5.6601160	-1.4472440	1.2192630
H	4.1094150	-2.9371500	1.1568430
C	6.2224610	-0.3258920	0.5986110
H	6.0789280	1.0392140	-1.0670180
H	6.1030400	-1.8465780	2.1273130
H	7.1009810	0.1509690	1.0234210

2.log
Potential Energy = -1489.66496
Zero-point Energy = -1489.19036
Free Energy = -1489.23392
Single-Point Energy B3LYP-D3(BJ)/6-311+G** PCM = -1490.12166
Free Energy B3LYP-D3(BJ)/6-311+G** PCM (extrapolated free energy from qRRHO) = -1489.69061
Nimag = 1 (-159.5359)
Charge = 0 Multiplicity = 1

C	-1.9653850	-0.7125110	0.1104430
H	-2.2411440	0.1988790	-0.4212960
H	-2.1445120	-0.5648650	1.1787030
C	-2.8470350	-1.8908900	-0.4008790
C	-0.5229010	-1.0335570	-0.1203970
O	0.0367360	-1.8601330	0.6826190
H	1.0298210	-2.2281050	0.3435010
H	-0.1213740	-0.9566050	-1.1303810
O	2.2120980	-2.6975850	-0.0244520
C	3.1570820	-1.8426210	0.0234930
C	4.5447200	-2.4646840	-0.3217580
F	4.5342030	-3.0264980	-1.5560110
F	5.5386610	-1.5555300	-0.3030570
F	4.8723890	-3.4403360	0.5616880
O	3.1057220	-0.6393620	0.2981610
H	-2.5724640	-2.7984990	0.1452100
N	0.4916070	0.8218670	0.3783950
C	0.0210830	1.4512440	1.6441730
C	1.0179580	1.9310480	-0.4958790
C	0.8347450	2.7483000	1.7117850
H	-1.0395140	1.7097530	1.5494400
H	1.9127700	1.5458770	-0.9956940
O	0.9590800	3.4734240	2.7019940
N	1.4256300	2.9337000	0.5087110
C	2.4563230	3.9488180	0.3158100
H	2.0310410	4.9303660	0.0868400
H	3.0373150	4.0309630	1.2372090
H	3.1154660	3.6457920	-0.4985480
C	0.0622600	2.4852040	-1.6026320
C	0.8123240	3.5825990	-2.3948410
H	0.9933910	4.4785980	-1.7981010
H	1.7723400	3.2206810	-2.7801410
H	0.2043280	3.8831080	-3.2538160
C	-0.2800470	1.3605290	-2.6019440
H	0.6199480	0.8382900	-2.9466160
H	-0.9699960	0.6257350	-2.1856990
H	-0.7691490	1.7898930	-3.4819870
C	-1.2290100	3.0931700	-1.0243210
H	-1.0129680	3.9051040	-0.3225060
H	-1.8332580	3.5114700	-1.8359840
H	-1.8458440	2.3506050	-0.5110750
C	0.2293250	0.5859890	2.8846950
H	-0.3797080	-0.3185910	2.8485190
H	1.2793060	0.2939310	2.9886820
H	-0.0545900	1.1629750	3.7680840
H	1.3318110	0.2729610	0.6003710
H	-2.6324740	-2.0687120	-1.4604280
C	-4.3223640	-1.6003290	-0.2190490
C	-5.0609430	-0.9706910	-1.2326460
C	-4.9755740	-1.9366720	0.9767510
C	-6.4176120	-0.6818430	-1.0564020
H	-4.5726070	-0.7097480	-2.1685520
C	-6.3319600	-1.6495970	1.1570440
H	-4.4201830	-2.4318310	1.7696800
C	-7.0575310	-1.0197750	0.1404570
H	-6.9738930	-0.1981590	-1.8543470
H	-6.8215800	-1.9217310	2.0878040
H	-8.1120450	-0.7989810	0.2778100

3.log
Potential Energy = -1489.66343
Zero-point Energy = -1489.18829
Free Energy = -1489.23175
Single-Point Energy B3LYP-D3(BJ)/6-311+G** PCM = -1490.12013
Free Energy B3LYP-D3(BJ)/6-311+G** PCM (extrapolated free energy from qRRHO) = -1489.68845
Nimag = 1 (-134.5445)
Charge = 0 Multiplicity = 1

C	0.1158290	1.5392610	1.6073560
C	1.0535020	1.9694490	-0.5663780
N	0.5247230	0.8806700	0.3344090
H	-0.9273680	1.8642190	1.5300780
H	1.9136050	1.5587500	-1.1056700
C	1.0069150	2.7861640	1.6512620
O	1.2218000	3.4885800	2.6418120
N	1.5450560	2.9536430	0.4207820
C	2.6384300	3.8931390	0.1888380
H	3.2476740	3.5395480	-0.6441380
H	2.2774370	4.9002950	-0.0365010
H	3.2526940	3.9387560	1.0909630
C	0.2879640	0.6636660	2.8452930
H	0.1017610	1.2715150	3.7339240
H	-0.4207850	-0.1679470	2.8532270
H	1.3043170	0.2629820	2.9109990
C	0.0664120	2.5514000	-1.6273220
C	-1.2722050	2.9985010	-1.0113870
H	-1.8943810	3.4595720	-1.7854940
H	-1.8380170	2.1618160	-0.5955010
H	-1.1242470	3.7456830	-0.2244040
C	0.7197470	3.7750080	-2.3101550
H	1.7203950	3.5448820	-2.6925890
H	0.1038910	4.0775210	-3.1630600
H	0.7914970	4.6339780	-1.6390470
C	-0.1682280	1.4909240	-2.7222320
H	-0.8412390	1.8946020	-3.4857400
H	0.7736790	1.2247730	-3.2161180
H	-0.6082060	0.5724040	-2.3362380
C	-1.9709030	-0.6179270	-0.0808880
H	-2.1935420	0.0568850	0.7484680
H	-2.2433430	-0.1318410	-1.0198380
C	-2.8099060	-1.9206870	0.0889800
H	-2.5064330	-2.4288810	1.0108070
H	-2.5875930	-2.5941300	-0.7445000
C	-4.2939570	-1.6210990	0.1331700
C	-4.9401730	-1.3711560	1.3534460
C	-5.0480160	-1.5663330	-1.0492530
C	-6.3055840	-1.0725170	1.3926090
H	-4.3725720	-1.4163920	2.2798190
C	-6.4134370	-1.2679730	-1.0144090

H	-4.5646570	-1.7643240	-2.0029570
C	-7.0466970	-1.0189630	0.2076770
H	-6.7896870	-0.8867430	2.3471900
H	-6.9817740	-1.2346870	-1.9396030
H	-8.1080450	-0.7902490	0.2366440
C	-0.5188640	-0.9695350	-0.0842710
O	-0.0044950	-1.4388050	-1.1606430
H	0.9783100	-1.8940480	-1.0063830
H	-0.0781410	-1.2928620	0.8601760
O	2.1835600	-2.4978020	-0.8542280
C	3.0198630	-1.9252290	-0.0855850
C	4.3939740	-2.6617440	-0.0366060
F	4.2445780	-3.9552450	0.3411570
F	5.2596090	-2.0903500	0.8234370
F	4.9828430	-2.6652880	-1.2593220
H	1.3577620	0.3139080	0.5441370
O	2.8862970	-0.9005130	0.5951460

4.log
Potential Energy = -1489.66173
Zero-point Energy = -1489.18580
Free Energy = -1489.22874
Single-Point Energy B3LYP-D3(BJ)/6-311+G** PCM = -1490.12018
Free Energy B3LYP-D3(BJ)/6-311+G** PCM (extrapolated free energy from qRRHO) = -1489.68718
Nimag = 1 (-121.2814)
Charge = 0 Multiplicity = 1

C	-1.9362220	-1.2364370	1.6801090
C	-2.1796150	-1.0106530	-0.7029140
N	-1.2733680	-0.6907640	0.4615470
H	-1.6324250	-2.2789660	1.8237220
H	-2.1490240	-0.1541110	-1.3843020
C	-3.4213220	-1.2158550	1.2978550
O	-4.3713680	-1.3083160	2.0782900
N	-3.5012210	-1.0378190	-0.0417000
C	-4.7660950	-0.7094380	-0.6932850
H	-4.5680000	-0.1213330	-1.5905630
H	-5.3329470	-1.6023130	-0.9704380
H	-5.3681280	-0.1172740	-0.0004970
C	-1.6542950	-0.4426060	2.9523350
H	-2.2940510	-0.8231750	3.7521610
H	-0.6155040	-0.5513770	3.2734460
H	-1.8731220	0.6208580	2.8151330
C	-1.8451250	-2.2889170	-1.5360590
C	-1.6683590	-3.5429540	-0.6599880
H	-1.5115150	-4.4163480	-1.3014640
H	-0.8030050	-3.4674180	0.0023290
H	-2.5580740	-3.7405890	-0.0527110
C	-2.9939460	-2.5542530	-2.5363390
H	-3.2299200	-1.6673810	-3.1348620
H	-2.6871920	-3.3450400	-3.2282410
H	-3.9057640	-2.8922280	-2.0386560
C	-0.5713420	-2.0260140	-2.3645790
H	-0.3424100	-2.9062890	-2.9740740
H	-0.7150750	-1.1784090	-3.0448160
H	0.2985450	-1.8079400	-1.7468610
C	1.3528600	-1.8902930	0.9390880
H	0.6522400	-2.3752630	1.6219580
H	1.4412220	-2.4965700	0.0353980
C	2.7329700	-1.8084870	1.6644330
H	2.6439480	-1.1521750	2.5366990
C	0.8550440	-0.5233020	0.5974070
O	1.2402560	0.0186690	-0.5020880
H	1.0395020	1.0786750	-0.5401520
H	0.6412490	0.1473350	1.4312650
O	0.8261190	2.4459400	-0.6095520
C	-0.2825750	2.8814930	-0.1691350
C	-0.4347940	4.4251500	-0.3373100
F	0.5196980	5.0843330	0.3674700
F	-1.6305060	4.8810610	0.0857210
F	-0.3003110	4.7927030	-1.6357530
H	-1.3240700	0.3360380	0.5288940
O	-1.2156550	2.2637620	0.3625670
C	3.8960150	-1.3657270	0.8005320
C	4.4900060	-0.1076740	0.9767820
C	4.4137930	-2.2163540	-0.1900370
C	5.5676450	0.2963630	0.1811120
H	4.1084510	0.5621850	1.7435190
C	5.4885730	-1.8169100	-0.9881540
H	3.9768520	-3.2016240	-0.3354080
C	6.0691910	-0.5565260	-0.8059420
H	6.0133710	1.2750970	0.3344290
H	5.8757580	-2.4902910	-1.7476500
H	6.9061800	-0.2457170	-1.4243980
H	2.9258150	-2.8152190	2.0510700

5.log
Potential Energy = -1489.66220
Zero-point Energy = -1489.18672
Free Energy = -1489.22968
Single-Point Energy B3LYP-D3(BJ)/6-311+G** PCM = -1490.12110
Free Energy B3LYP-D3(BJ)/6-311+G** PCM (extrapolated free energy from qRRHO) = -1489.68857
Nimag = 1 (-135.1105)
Charge = 0 Multiplicity = 1

C	-0.9506580	-1.5101310	1.4119860
C	-2.5037390	-0.6472750	-0.2115040
N	-1.0486660	-0.6657880	0.1871530
H	-0.7896810	-2.5542920	1.1223230
H	-2.7331220	0.3635400	-0.5648450
C	-2.3502470	-1.3896660	2.0265770
O	-2.6633830	-1.6939950	3.1799850
N	-3.1685550	-0.8520290	1.0923590
C	-4.4998500	-0.3613880	1.4371840
H	-4.7744930	0.4465040	0.7574600
H	-5.2580780	-1.1471120	1.3809760
H	-4.4727980	0.0218490	2.4597300
C	0.1417270	-1.0743970	2.3850460
H	0.0366650	-1.6482310	3.3090040
H	1.1402380	-1.2643080	1.9844590
H	0.0544960	-0.0114280	2.6306490
C	-2.9442430	-1.6476250	-1.3270330
C	-2.5017090	-3.0936030	-1.0359880
H	-2.8917740	-3.7585470	-1.8136380
H	-1.4147910	-3.2018790	-1.0301350
H	-2.8931870	-3.4492130	-0.0769160
C	-4.4854180	-1.6271670	-1.4479910
H	-4.8741780	-0.6094870	-1.5652340
H	-4.7800730	-2.1954390	-2.3359620
H	-4.9737760	-2.0904220	-0.5876100
C	-2.3756420	-1.1673930	-2.6776960
H	-2.6929920	-1.8494600	-3.4732130
H	-2.7520950	-0.1681500	-2.9262840
H	-1.2876400	-1.1201150	-2.6874470
C	1.1096270	-1.9785120	-1.3281990
H	0.9421260	-2.6234780	-0.4630040
H	0.4780020	-2.3180930	-2.1515030
C	2.6018870	-2.0914680	-1.7694210
C	0.7744810	-0.5620810	-0.9875260
O	0.5354070	0.2544600	-1.9458940
H	0.5373670	1.3037050	-1.6310900
H	1.1943880	-0.1456740	-0.0716440
O	0.5660670	2.6142610	-1.2937820
C	0.0367510	2.9356870	-0.1825340

C	0.0843970	4.4720070	0.0824530
F	1.3567100	4.9382530	0.0371050
F	-0.4232090	4.8080860	1.2844310
F	-0.6245640	5.1462430	-0.8580260
H	-0.8638080	0.3040120	0.4774330
O	-0.4892300	2.2145280	0.6743470
H	2.7407200	-3.1237140	-2.1082340
C	3.6090200	-1.7690440	-0.6823450
C	3.8457250	-2.6765800	0.3633890
C	4.3228660	-0.5612880	-0.6925260
C	4.7644570	-2.3824600	1.3741940
H	3.3122710	-3.6241060	0.3832510
C	5.2436250	-0.2624630	0.3178150
H	4.1617100	0.1498480	-1.4989880
C	5.4658750	-1.1716340	1.3557890
H	4.9362440	-3.0993380	2.1721110
H	5.7868860	0.6778320	0.2904900
H	6.1816290	-0.9427710	2.1399240
H	2.7653780	-1.4457030	-2.6375060

6.log
Potential Energy = -1489.66343
Zero-point Energy = -1489.18829
Free Energy = -1489.23176
Single-Point Energy B3LYP-D3(BJ)/6-311+G** PCM = -1490.12013
Free Energy B3LYP-D3(BJ)/6-311+G** PCM (extrapolated free energy from qRRHO) = -1489.68846
Nimag = 1 (-134.5974)
Charge = 0 Multiplicity = 1

C	0.1157540	1.5393690	1.6073830
C	1.0536400	1.9692590	-0.5663350
N	0.5247270	0.8806120	0.3345420
H	-0.9274310	1.8643370	1.5299920
H	1.9137670	1.5584550	-1.1055090
C	1.0068650	2.7862540	1.6512020
O	1.2216510	3.4888220	2.6416660
N	1.5451580	2.9535300	0.4207660
C	2.6385000	3.8930590	0.1887990
H	3.2474980	3.5396860	-0.6444420
H	2.2774610	4.9002850	-0.0361610
H	3.2530230	3.9384170	1.0907630
C	0.2877830	0.6639120	2.8454320
H	0.1015020	1.2718600	3.7339790
H	-0.4209670	-0.1677000	2.8533890
H	1.3041280	0.2632310	2.9112670
C	0.0666680	2.5511730	-1.6274130
C	-1.2719390	2.9984770	-1.0116030
H	-1.8940340	3.4594990	-1.7858040
H	-1.8378420	2.1618930	-0.5956380
H	-1.1239610	3.7457500	-0.2247090
C	0.7201710	3.7746320	-2.3103540
H	1.7207950	3.5443410	-2.6927540
H	0.1043660	4.0771370	-3.1632980
H	0.7920230	4.6336610	-1.6393340
C	-0.1680350	1.4906050	-2.7222190
H	-0.8408670	1.8943270	-3.4858620
H	0.7738800	1.2242030	-3.2159540
H	-0.6082510	0.5722240	-2.3361670
C	-1.9709290	-0.6178790	-0.0807230
H	-2.1935190	0.0570010	0.7485900
H	-2.2433960	-0.1318520	-1.0196970
C	-2.8099620	-1.9206000	0.0892750
H	-2.5065970	-2.4286370	1.0112230
H	-2.5875650	-2.5941880	-0.7440670
C	-4.2940160	-1.6209920	0.1332460
C	-4.9404880	-1.3713760	1.3534510
C	-5.0478240	-1.5658850	-1.0493240
C	-6.3059040	-1.0727200	1.3924020
H	-4.3730880	-1.4168800	2.2799320
C	-6.4132430	-1.2675090	-1.0146910
H	-4.5642650	-1.7636250	-2.0029800
C	-7.0467620	-1.0188240	0.2073290
H	-6.7902070	-0.8872000	2.3469320
H	-6.9813820	-1.2339590	-1.9399980
H	-8.1081110	-0.7900970	0.2361310
C	-0.5188900	-0.9695120	-0.0841700
O	-0.0046290	-1.4388200	-1.1605870
H	0.9782970	-1.8939170	-1.0065410
H	-0.0781190	-1.2928540	0.8602500
O	2.1838700	-2.4973260	-0.8549180
C	3.0197720	-1.9252860	-0.0854450
C	4.3940020	-2.6615880	-0.0367050
F	4.2448790	-3.9542560	0.3441700
F	5.2607060	-2.0883670	0.8210350
F	4.9814230	-2.6679720	-1.2600600
H	1.3576910	0.3138010	0.5444440
O	2.8856000	-0.9014580	0.5965050

7.log
Potential Energy = -1489.66169
Zero-point Energy = -1489.18761
Free Energy = -1489.23092
Single-Point Energy B3LYP-D3(BJ)/6-311+G** PCM = -1490.12078
Free Energy B3LYP-D3(BJ)/6-311+G** PCM (extrapolated free energy from qRRHO) = -1489.69002
Nimag = 1 (-225.2892)
Charge = 0 Multiplicity = 1

C	-1.2272110	1.6296880	1.7244310
C	0.2093770	2.2830240	-0.0051090
C	-0.0097490	0.7165340	1.7547960
H	0.9349330	2.9336880	0.5117010
H	-0.3052540	-0.3203680	1.9252010
C	-0.0322600	-0.9759410	-0.6285860
H	0.5214760	-0.6141840	-1.4939590
O	0.5365800	-1.8271480	0.1386550
N	-1.1067290	2.4547060	0.6437900
C	-1.9444290	3.6440330	0.5351690
H	-2.3907120	3.7290280	-0.4566380
H	-2.7414310	3.5444480	1.2724860
H	-1.3688160	4.5495920	0.7535220
O	-2.1363140	1.6398050	2.5557440
C	-1.5343390	-0.9932450	-0.7322160
H	-1.9199100	0.0267720	-0.7809090
C	-2.2804870	-1.8205580	0.3333950
H	-2.1256540	-1.3865840	1.3251090
H	-1.8623840	-2.8310260	0.3590680
N	0.5157080	0.8691710	0.3759510
C	3.6959380	-1.1549220	0.0828330
C	5.2039670	-1.5382140	-0.0180230
O	3.4047620	0.0100360	0.3679100
H	1.5287650	0.7000970	0.3539300
O	2.9260650	-2.1445230	-0.1550350
H	1.6455390	-1.9312690	-0.0082900
C	0.3494040	2.6362720	-1.5179040
C	0.3498410	4.1772530	-1.6821340
H	0.6386990	4.4264430	-2.7079490
H	-0.6285710	4.6263820	-1.5042260
H	1.0725610	4.6516440	-1.0092660
C	-0.7491520	2.0362820	-2.4146110
H	-0.6541690	2.4481880	-3.4245660
H	-1.7545870	2.2726660	-2.0550440
C	1.7364350	2.1403570	-1.9878610
H	1.9010690	2.4547000	-3.0229800
H	2.5416890	2.5653120	-1.3785330

H	1.8318970	1.0518800	-1.9587410
C	0.9692440	1.1336870	2.8657260
H	0.4784380	1.0320320	3.8375760
H	1.8476810	0.4834370	2.8502160
H	1.3004680	2.1705970	2.7548640
H	-0.6679660	0.9519230	-2.5058830
F	5.5025580	-2.0222100	-1.2490470
F	6.0194600	-0.4907310	0.2105480
F	5.5215480	-2.5021540	0.8816280
C	-3.7668930	-1.8834840	0.0415970
C	-4.6391300	-0.9069140	0.5473950
C	-4.2991390	-2.9063790	-0.7584330
C	-6.0067430	-0.9487310	0.2590680
H	-4.2446260	-0.1122770	1.1762920
C	-5.6661800	-2.9519270	-1.0495990
H	-3.6397390	-3.6765340	-1.1519150
C	-6.5249980	-1.9716000	-0.5420200
H	-6.6665120	-0.1861660	0.6634840
H	-6.0595880	-3.7543950	-1.6673160
H	-7.5876030	-2.0071920	-0.7641970
H	-1.7303650	-1.4267620	-1.7250610

Formation of iminium ion (TS2)

Conformation name	**Extrapolated Free energy (kcal/mol)**
TS2-lowest	0.0
1	2.2
2	2.1
3	1.2
4	0.6
5	0.5
6	0.6
7	1.4
8	1.9
9	4.1
10	1.4
11	1.9
12	1.1
13	1.4
14	1.0
15	-0.4
16	-0.1
17	-0.2
18	1.5
19	1.1
20	1.5
21	5.8
22	6.1
23	7.1
24	4.7
25	7.4
26	5.1

TS2-lowest.log (Enamine 2)
Potential Energy = -1489.66107
Zero-point Energy = -1489.18625
Free Energy = -1489.22898
Single-Point Energy B3LYP-D3(BJ)/6-311+G** PCM = -1490.12306
Free Energy B3LYP-D3(BJ)/6-311+G** PCM (extrapolated free energy from qRRHO) = -1489.69097
Nimag = 1 (-269.9625 cm^{-1})
Charge = 0 Multiplicity = 1

C	-2.1887330	-0.0465630	-0.4475410
C	-2.7481900	-0.1260620	1.8444790
C	-2.5697810	-1.5728380	1.3734760
N	-1.8347970	-1.3904070	0.0881530
N	-2.4932770	0.6877860	0.7939620
O	-3.0679970	0.2296140	2.9811960
C	-2.4508120	2.1389360	0.9339600
H	-3.4414530	2.5905240	0.8241220
H	-2.0710280	2.3770210	1.9296920
H	-1.7767760	2.5548760	0.1848880
C	-0.5887650	-1.9120650	-0.0662850
C	0.0851510	-1.9191980	-1.4268600
C	1.3082870	-2.8621740	-1.5373900
H	1.0196350	-3.8580710	-1.1825680
H	1.5179980	-2.9669310	-2.6075520
C	-1.9418990	-2.4809050	2.4228550
H	-2.5830430	-2.4508140	3.3072180
H	-1.9014060	-3.5178500	2.0782260
H	-0.9425260	-2.1512050	2.7131070
H	-3.5650420	-1.9656920	1.1381160
C	-3.3463480	-0.0415220	-1.5080320
H	-1.3045690	0.4017240	-0.9087200
C	-3.5273770	1.4006170	-2.0344580
H	-4.2194910	1.3912200	-2.8825200
H	-3.9480180	2.0697210	-1.2805420
H	-2.5801040	1.8262400	-2.3846700
C	-2.9527870	-0.9365580	-2.6992030
H	-2.0250170	-0.5983930	-3.1729420
H	-2.8358390	-1.9811100	-2.3962620
H	-3.7413090	-0.8980890	-3.4576200
C	-4.6861930	-0.5387460	-0.9323100
H	-4.9824260	0.0185130	-0.0378730
H	-5.4740820	-0.4007800	-1.6800410
H	-4.6553220	-1.6052750	-0.6898860
H	0.3472340	-0.9044970	-1.7402720
H	-0.6648520	-2.2851630	-2.1325360
C	2.5802210	-2.4220080	-0.8369560
C	3.3477900	-1.3619480	-1.3497680
C	3.0313450	-3.0683030	0.3262110
C	4.5224230	-0.9541730	-0.7148850
H	3.0243870	-0.8554700	-2.2557540
C	4.2083930	-2.6594510	0.9673840
H	2.4677770	-3.9077660	0.7266830
C	4.9562100	-1.6002100	0.4491520
H	5.1016210	-0.1340300	-1.1292890
H	4.5383210	-3.1742420	1.8649700
H	5.8699630	-1.2823890	0.9422360
H	-0.4808910	-2.8478780	0.4729440
O	0.5171030	-0.9860990	0.9686830
H	0.7168780	0.0101890	0.5838690
H	1.3729980	-1.4509040	1.0249260

O	0.8953060	1.2539410	0.0146890
C	1.6225310	2.0897860	0.6466230
C	1.8136060	3.4209040	-0.1497850
O	2.1733030	1.9846670	1.7435760
F	2.5259700	4.3409930	0.5321730
F	0.6211220	3.9909260	-0.4618580
F	2.4663250	3.1983890	-1.3209710

1.log
Potential Energy = -1489.66249
Zero-point Energy = -1489.18824
Free Energy = -1489.23172
Single-Point Energy B3LYP-D3(BJ)/6-311+G** PCM = -1490.11830
Free Energy B3LYP-D3(BJ)/6-311+G** PCM (extrapolated free energy from qRRHO) = -1489.68753
Nimag = 1 (-309.6177 cm^{-1})
Charge = 0 Multiplicity = 1

C	2.9163420	-0.0892340	-0.3998050
C	3.0941390	-2.3930880	0.0742480
C	2.4340840	-1.7323080	1.2886810
N	2.0021580	-0.4196300	0.7273880
N	3.3212000	-1.4310090	-0.8507370
O	3.3681970	-3.5895760	-0.0373540
C	3.8155230	-1.7444070	-2.1865760
H	4.9087010	-1.7654930	-2.2261400
H	3.4399180	-2.7298620	-2.4695140
H	3.4464850	-1.0010640	-2.8951280
C	0.6885600	-0.0846140	0.6966300
C	0.2516700	1.3123210	0.3111540
C	-1.2719890	1.5398080	0.4004290
H	-1.7892110	0.9284120	-0.3444370
H	-1.6227930	1.2106010	1.3853150
C	1.3732150	-2.6012100	1.9507580
H	1.8609770	-3.5253290	2.2701570
H	0.9615480	-2.1191500	2.8416240
H	0.5626630	-2.8657380	1.2693160
H	3.2211080	-1.5386160	2.0255120
C	4.1050930	0.8649880	-0.0247340
H	2.3443270	0.3911040	-1.1987510
C	4.8940600	1.2007950	-1.3105310
H	5.6309560	1.9792970	-1.0890220
H	5.4405250	0.3394880	-1.7014760
H	4.2377730	1.5826090	-2.1010160
C	3.5403810	2.1800430	0.5472630
H	2.8848500	2.6874560	-0.1682940
H	2.9855850	2.0104930	1.4744730
H	4.3669960	2.8607140	0.7746210
C	5.0646310	0.2414890	1.0068460
H	5.4427090	-0.7326880	0.6808710
H	5.9285980	0.9006440	1.1403730
H	4.5920740	0.1272190	1.9869770
H	0.6176640	1.5868750	-0.6833930
H	0.7473270	1.9838980	1.0200450
C	-1.6343500	2.9972760	0.1938430
C	-1.6670560	3.8897400	1.2767530
C	-1.9235370	3.4902750	-1.0878270
C	-1.9765150	5.2396480	1.0851320
H	-1.4551670	3.5239490	2.2787680
C	-2.2327660	4.8398060	-1.2847030
H	-1.9127450	2.8116840	-1.9374520
C	-2.2592710	5.7196580	-0.1979470
H	-2.0014380	5.9134190	1.9369710
H	-2.4575730	5.2012740	-2.2841980
H	-2.5031470	6.7673200	-0.3483300
H	0.1435240	-0.4855490	1.5453420
O	-0.1256740	-1.1394490	-0.5045090
H	-0.2425590	-0.6952790	-1.3596100
H	-1.1104150	-1.5302140	-0.1983810
O	-2.2760230	-2.0600690	0.2166960
C	-3.2632010	-1.8081300	-0.5529800
O	-3.2887880	-1.1654220	-1.6042330
C	-4.5957220	-2.4280770	-0.0264160
F	-4.5002500	-3.7777020	0.0850540
F	-4.9075450	-1.9467770	1.2044070
F	-5.6448950	-2.1683600	-0.8325580

2.log
Potential Energy = -1489.65965
Zero-point Energy = -1489.18505
Free Energy = -1489.22863
Single-Point Energy B3LYP-D3(BJ)/6-311+G** PCM = -1490.11864
Free Energy B3LYP-D3(BJ)/6-311+G** PCM (extrapolated free energy from qRRHO) = -1489.68763
Nimag = 1 (-222.1627 cm^{-1})
Charge = 0 Multiplicity = 1

C	-2.7695910	-0.1669450	0.3649140
C	-1.8990570	-2.3524920	0.1672370
C	-1.8496940	-1.7152730	-1.2252570
N	-1.9970380	-0.2667750	-0.9043290
N	-2.4034680	-1.4329180	1.0237490
O	-1.5444360	-3.4978390	0.4532300
C	-2.4519230	-1.6621950	2.4629530
H	-3.3818170	-2.1494890	2.7712660
H	-1.6152830	-2.3086270	2.7354160
H	-2.3562610	-0.7096780	2.9868740
C	-1.0130300	0.6208940	-1.1885420
C	-1.2980500	2.1089270	-1.1563150
C	-0.1438890	3.0265960	-1.6216880
H	0.3126100	2.6059020	-2.5241690
H	-0.6074980	3.9714640	-1.9280310
C	-0.6510510	-2.1376540	-2.0620440
H	-0.7053200	-3.2226760	-2.1815740
H	-0.6915760	-1.6925980	-3.0603280
H	0.3064380	-1.9016300	-1.5941070
H	-2.7555600	-2.0250490	-1.7576560
C	-4.3134790	0.0589970	0.1957800
H	-2.3682800	0.6613860	0.9553270
C	-4.9335480	0.2671260	1.5963520
H	-5.9781290	0.5756100	1.4872680
H	-4.9262780	-0.6463810	2.1952730
H	-4.4131240	1.0522860	2.1567470
C	-4.5579460	1.3372450	-0.6295750
H	-4.1190150	2.2202950	-0.1536740
H	-4.1556180	1.2461050	-1.6424990
H	-5.6351200	1.5126960	-0.7146350
C	-5.0186590	-1.1239000	-0.4955230
H	-4.8184070	-2.0741660	0.0093590
H	-6.1012630	-0.9619520	-0.4725170
H	-4.7293430	-1.2146290	-1.5467950
H	-1.6711790	2.4188530	-0.1762330
H	-2.1282030	2.2440450	-1.8566190
C	0.9407990	3.3394800	-0.6035480
C	0.6268950	3.9646150	0.6172480
C	2.2893330	3.0576850	-0.8783500
C	1.6288830	4.2899790	1.5356390
H	-0.4065750	4.2099770	0.8488780
C	3.2946180	3.3851860	0.0375430
H	2.5536510	2.5778210	-1.8170590
C	2.9671930	4.0014750	1.2483160
H	1.3641490	4.7734070	2.4714780
H	4.3303380	3.1566640	-0.1961360
H	3.7459980	4.2548510	1.9613430
H	-0.4100740	0.3146890	-2.0377020
O	0.2498020	0.4462580	0.0892450

H	0.6285480	1.3179610	0.3048790
H	1.0869670	-0.1913560	-0.1366250
O	2.1777580	-1.0070040	-0.4604330
C	2.9763500	-1.3174150	0.4831580
O	2.9531000	-1.0028320	1.6750300
C	4.1438700	-2.2311930	-0.0130220
F	3.6741190	-3.3713620	-0.5819850
F	4.8959010	-1.5990060	-0.9524160
F	4.9800720	-2.6000110	0.9797440

3.log
Potential Energy = -1489.66151
Zero-point Energy = -1489.18751
Free Energy = -1489.23110
Single-Point Energy B3LYP-D3(BJ)/6-311+G** PCM = -1490.11948
Free Energy B3LYP-D3(BJ)/6-311+G** PCM (extrapolated free energy from qRRHO) = -1489.68907
Nimag = 1 (-324.0648 cm^{-1})
Charge = 0 Multiplicity = 1

C	3.0112410	-0.4737330	-0.4844450
C	2.6207980	-1.9757880	1.2915410
C	2.0312580	-0.6235450	1.7049870
N	1.9536360	0.0910360	0.3977810
N	3.1374380	-1.8411710	0.0474330
O	2.6222740	-3.0029010	1.9730450
C	3.6489220	-2.9822410	-0.7033290
H	4.7051020	-3.1737100	-0.4916100
H	3.0735890	-3.8660870	-0.4202920
H	3.5261120	-2.8001350	-1.7722060
C	0.7514200	0.4792220	-0.0986660
C	0.6657720	1.3456090	-1.3378940
C	-0.7540190	1.8698410	-1.6509830
H	-0.6964970	2.3740370	-2.6216200
H	-1.4461780	1.0322470	-1.7761580
C	0.7520730	-0.7442590	2.5223790
H	0.9923840	-1.3174110	3.4211090
H	0.3885100	0.2359790	2.8418420
H	-0.0398160	-1.2720120	1.9880260
H	2.7793920	-0.1134720	2.3213340
C	4.3500180	0.3449520	-0.5140560
H	2.6343380	-0.5295950	-1.5098870
C	5.3114770	-0.3167720	-1.5268280
H	6.1850980	0.3271040	-1.6695390
H	5.6766020	-1.2867710	-1.1817280
H	4.8382480	-0.4534000	-2.5058560
C	4.0581100	1.7790190	-0.9973600
H	3.6063460	1.7884280	-1.9951590
H	3.3982810	2.3102380	-0.3054070
H	4.9963450	2.3397690	-1.0570230
C	5.0377360	0.4115470	0.8629530
H	5.2061720	-0.5833960	1.2872790
H	6.0159060	0.8914190	0.7548370
H	4.4629260	1.0084320	1.5773530
H	1.0647980	0.8193970	-2.2111550
H	1.3255260	2.2008780	-1.1661760
C	-1.2977930	2.8358020	-0.6142460
C	-2.2861990	2.4403630	0.3000610
C	-0.8143290	4.1536470	-0.5479490
C	-2.7751350	3.3354720	1.2590260
H	-2.6779170	1.4271490	0.2605910
C	-1.3000650	5.0494080	0.4076540
H	-0.0574450	4.4842950	-1.2556610
C	-2.2832110	4.6419770	1.3169840
H	-3.5416390	3.0100040	1.9567860
H	-0.9166330	6.0654080	0.4389170
H	-2.6637740	5.3381570	2.0587570
H	0.0631210	0.7750910	0.6862780
O	-0.1580410	-0.9898530	-0.5597260
H	-0.0893720	-1.1797920	-1.5090540
H	-1.2276000	-1.0552580	-0.2813260
O	-2.5023720	-1.1546130	0.1139630
C	-3.2453450	-1.8294730	-0.6769120
O	-2.9598880	-2.3687830	-1.7467420
C	-4.7120760	-1.9421230	-0.1535690
F	-4.7555040	-2.5254800	1.0712460
F	-5.2840190	-0.7164070	-0.0326940
F	-5.5003800	-2.6703790	-0.9696810

4.log
Potential Energy = -1489.66303
Zero-point Energy = -1489.18910
Free Energy = -1489.23259
Single-Point Energy B3LYP-D3(BJ)/6-311+G** PCM = -1490.12040
Free Energy B3LYP-D3(BJ)/6-311+G** PCM (extrapolated free energy from qRRHO) = -1489.68996
Nimag = 1 (-326.9458 cm^{-1})
Charge = 0 Multiplicity = 1

C	1.9498940	-0.6852460	0.6724980
C	3.7033260	-0.3305070	-0.8676560
C	2.9514240	-1.5854720	-1.3217480
N	1.6733950	-1.4726930	-0.5610700
N	3.0863740	0.1462170	0.2384880
O	4.6946510	0.1560680	-1.4162020
C	3.4664490	1.4146260	0.8499540
H	4.2667080	1.2922290	1.5859150
H	3.8199250	2.0832420	0.0623780
H	2.5959840	1.8587800	1.3346670
C	0.4915310	-1.3590850	-1.2212330
C	-0.8204140	-1.4594610	-0.4723920
C	-2.0679270	-1.3427020	-1.3729370
H	-2.1503700	-0.3253670	-1.7675130
H	-1.9571730	-2.0170060	-2.2306780
C	2.8615840	-1.7253330	-2.8355860
H	3.8830200	-1.7479590	-3.2230060
H	2.3778890	-2.6635720	-3.1206780
H	2.3396390	-0.8868340	-3.3006720
H	3.4966530	-2.4530430	-0.9340080
C	2.2201560	-1.5479400	1.9550480
H	1.1002040	-0.0287720	0.8800320
C	2.3915150	-0.6000660	3.1636310
H	2.4259030	-1.1912780	4.0842710
H	3.3183670	-0.0241370	3.1137000
H	1.5533230	0.1004770	3.2514750
C	1.0010490	-2.4515790	2.2257070
H	0.0858590	-1.8685330	2.3729280
H	0.8378140	-3.1625740	1.4109210
H	1.1734760	-3.0279490	3.1402830
C	3.4766770	-2.4297430	1.8239170
H	4.3644200	-1.8449620	1.5623190
H	3.6769630	-2.9184760	2.7830100
H	3.3434070	-3.2213810	1.0804460
H	-0.8743300	-0.7274900	0.3377300
H	-0.8170310	-2.4511620	-0.0071680
C	-3.3390300	-1.6853770	-0.6208780
C	-3.7990870	-3.0097650	-0.5543000
C	-4.0698690	-0.6888690	0.0439370
C	-4.9568510	-3.3317150	0.1603620
H	-3.2506110	-3.7945200	-1.0701520
C	-5.2280040	-1.0062500	0.7605160
H	-3.7328940	0.3437730	-0.0035190
C	-5.6751080	-2.3299370	0.8215540
H	-5.2994760	-4.3620190	0.1961250
H	-5.7817580	-0.2199050	1.2656730
H	-6.5765220	-2.5777320	1.3744840

H	0.4935220	-1.9113080	-2.1556880
O	0.4585630	0.2559860	-1.9622620
H	0.1490030	1.0588990	-1.2715310
H	-0.1114070	0.2834180	-2.7479220
O	-0.1404720	1.9824470	-0.3388710
C	-0.8462150	2.9706510	-0.7355600
C	-1.1394870	3.9824360	0.4174190
O	-1.3019890	3.2080180	-1.8544740
F	-1.8582110	5.0462620	0.0058850
F	0.0093440	4.4606090	0.9594990
F	-1.8383140	3.3907220	1.4207500

5.log
Potential Energy = -1489.66201
Zero-point Energy = -1489.18806
Free Energy = -1489.23178
Single-Point Energy B3LYP-D3(BJ)/6-311+G** PCM = -1490.12032
Free Energy B3LYP-D3(BJ)/6-311+G** PCM (extrapolated free energy from qRRHO) = -1489.69009
Nimag = 1 (-338.0783 cm^{-1})
Charge = 0 Multiplicity = 1

C	-0.6678660	2.0195690	0.4497310
C	-0.6493540	2.8554140	-1.7572660
C	0.8029790	2.5509570	-1.3768490
N	0.6328230	1.6693650	-0.1857940
N	-1.4328840	2.5201910	-0.7057340
O	-1.0332190	3.3231880	-2.8315370
C	-2.8888900	2.5535000	-0.7856480
H	-3.2920060	3.5372500	-0.5270820
H	-3.1828790	2.3173560	-1.8104100
H	-3.3072070	1.8058500	-0.1101890
C	1.0733200	0.3840990	-0.2197110
C	1.0737550	-0.4595920	1.0381770
C	1.7316680	-1.8487110	0.8883360
H	1.6081660	-2.3550020	1.8527860
H	1.1824840	-2.4527460	0.1598720
C	1.6373960	2.0202500	-2.5350360
H	1.6280230	2.7798830	-3.3203950
H	2.6778390	1.8645010	-2.2374180
H	1.2324120	1.0964410	-2.9526980
H	1.2565240	3.4883870	-1.0365820
C	-0.5648210	3.0226660	1.6521100
H	-1.1471910	1.1070180	0.8157560
C	-1.9726970	3.2111160	2.2611550
H	-1.8907840	3.7838090	3.1904050
H	-2.6426090	3.7633680	1.5981470
H	-2.4412190	2.2507100	2.5046930
C	0.3498120	2.4227210	2.7379900
H	-0.0271170	1.4613460	3.1028500
H	1.3714210	2.2851260	2.3724480
H	0.3921910	3.1044920	3.5934400
C	-0.0092160	4.3973250	1.2338410
H	-0.5857620	4.8424630	0.4166490
H	-0.0642880	5.0834170	2.0853590
H	1.0414610	4.3385840	0.9343120
H	0.0579940	-0.5823160	1.4230950
H	1.6268180	0.1146490	1.7872030
C	3.2062110	-1.8192050	0.5253400
C	3.6700910	-2.3813670	-0.6734640
C	4.1469920	-1.2428990	1.3965260
C	5.0309630	-2.3617600	-1.0006790
H	2.9643340	-2.8474010	-1.3567630
C	5.5058860	-1.2203430	1.0742960
H	3.8174510	-0.8152050	2.3404280
C	5.9534840	-1.7783740	-0.1288600
H	5.3661560	-2.8038110	-1.9346460
H	6.2155950	-0.7722770	1.7640160
H	7.0100910	-1.7622690	-0.3796240
H	1.9753850	0.2793060	-0.8143100
O	0.0003580	-0.5014050	-1.3285240
H	-0.9032860	-0.9328190	-0.8604480
H	0.4599550	-1.2122210	-1.8032520
O	-2.0262060	-1.3672060	-0.2691220
C	-2.2886720	-2.5991100	-0.4849310
C	-3.5932620	-3.0598410	0.2384820
O	-1.6647700	-3.4237890	-1.1536310
F	-3.4615510	-2.9613780	1.5871270
F	-3.9165290	-4.3392850	-0.0375260
F	-4.6547530	-2.2926230	-0.1157890

6.log
Potential Energy = -1489.66303
Zero-point Energy = -1489.18910
Free Energy = -1489.23259
Single-Point Energy B3LYP-D3(BJ)/6-311+G** PCM = -1490.12040
Free Energy B3LYP-D3(BJ)/6-311+G** PCM (extrapolated free energy from qRRHO) = -1489.68996
Nimag = 1 (-327.0302 cm^{-1})
Charge = 0 Multiplicity = 1

C	1.9497960	-0.6855510	0.6724740
C	3.7032480	-0.3311680	-0.8677400
C	2.9509950	-1.5859030	-1.3218810
N	1.6730390	-1.4728540	-0.5611250
N	3.0864730	0.1456470	0.2384630
O	4.6946800	0.1551780	-1.4162980
C	3.4669310	1.4138960	0.8500180
H	4.2670550	1.2911890	1.5860750
H	3.8207500	2.0824020	0.0625040
H	2.5965680	1.8583490	1.3346420
C	0.4911560	-1.3589270	-1.2212230
C	-0.8207720	-1.4590850	-0.4723180
C	-2.0683000	-1.3420470	-1.3728110
H	-2.1507160	-0.3246080	-1.7671270
H	-1.9575820	-2.0161370	-2.2307270
C	2.8610390	-1.7256130	-2.8357280
H	3.8824490	-1.7484500	-3.2232050
H	2.3771040	-2.6637110	-3.1208790
H	2.3392690	-0.8869490	-3.3007110
H	3.4960260	-2.4536450	-0.9342430
C	2.2198970	-1.5483790	1.9549690
H	1.1002840	-0.0288700	0.8800860
C	2.3914810	-0.6006110	3.1636030
H	2.4257320	-1.1918800	4.0842130
H	3.3184690	-0.0248990	3.1136990
H	1.5534540	0.1001270	3.2514830
C	1.0006030	-2.4517720	2.2256040
H	0.0855480	-1.8685310	2.3728910
H	0.8371860	-3.1626770	1.4107780
H	1.1729320	-3.0282370	3.1401390
C	3.4762280	-2.4304430	1.8237590
H	4.3640890	-1.8458350	1.5621760
H	3.6764310	-2.9192770	2.7828180
H	3.3427750	-3.2220070	1.0802420
H	-0.8745120	-0.7271380	0.3378380
H	-0.8175590	-2.4508040	-0.0071350
C	-3.3394040	-1.6848840	-0.6208270
C	-3.7993220	-3.0093270	-0.5543480
C	-4.0703780	-0.6884940	0.0440130
C	-4.9570830	-3.3314430	0.1602420
H	-3.2507340	-3.7939930	-1.0702170
C	-5.2285120	-1.0060420	0.7605210
H	-3.7335110	0.3441870	-0.0033670
C	-5.6754770	-2.3297800	0.8214600
H	-5.2995990	-4.3617860	0.1959290

H	-5.7823730	-0.2197880	1.2657020
H	-6.5768900	-2.5777040	1.3743350
H	0.4929690	-1.9111120	-2.1557010
O	0.4584900	0.2561280	-1.9621050
H	0.1491980	1.0591180	-1.2712900
H	-0.1115580	0.2837410	-2.7477020
O	-0.1399530	1.9827030	-0.3387040
C	-0.8456320	2.9709460	-0.7354260
C	-1.1386590	3.9828970	0.4174670
O	-1.3015190	3.2082090	-1.8543140
F	-1.8570940	5.0468780	0.0058340
F	0.0102750	4.4608080	0.9595520
F	-1.8376730	3.3914270	1.4208130

7.log
Potential Energy = -1489.66171
Zero-point Energy = -1489.18784
Free Energy = -1489.23117
Single-Point Energy B3LYP-D3(BJ)/6-311+G** PCM = -1490.11933
Free Energy B3LYP-D3(BJ)/6-311+G** PCM (extrapolated free energy from qRRHO) = -1489.68879
Nimag = 1 (-319.4351 cm^{-1})
Charge = 0 Multiplicity = 1

C	1.4178620	-1.2262770	0.6745040
C	3.2013550	-1.5723010	-0.8345990
C	2.0640050	-2.5107840	-1.2536040
N	0.8979530	-1.9239230	-0.5341140
N	2.7712060	-0.8499690	0.2258590
O	4.3059410	-1.4900100	-1.3755540
C	3.5648920	0.2322330	0.7976190
H	4.2719440	-0.1307950	1.5495610
H	4.1295870	0.7062580	-0.0077490
H	2.8999670	0.9677010	1.2518420
C	-0.1909630	-1.4704780	-1.2082150
C	-1.4743980	-1.1403080	-0.4750600
C	-2.6317890	-0.7250630	-1.4075760
H	-2.3741560	0.2059880	-1.9178280
H	-2.7571940	-1.4923420	-2.1808990
C	1.9486850	-2.7019800	-2.7599030
H	2.8989160	-3.1115830	-3.1103500
H	1.1628360	-3.4179270	-3.0130320
H	1.7759640	-1.7720760	-3.3080950
H	2.2687700	-3.4920550	-0.8119550
C	1.3804030	-2.0697370	1.9983800
H	0.8397500	-0.3124340	0.8356320
C	1.8397880	-1.1705070	3.1689520
H	1.6739230	-1.6968970	4.1142580
H	2.9032760	-0.9270210	3.1166300
H	1.2719740	-0.2340450	3.2077080
C	-0.0674410	-2.5158510	2.2810980
H	-0.7459950	-1.6620020	2.3781060
H	-0.4450240	-3.1791610	1.4979110
H	-0.0973210	-3.0677840	3.2259900
C	2.2834150	-3.3167630	1.9373110
H	3.3147590	-3.0669500	1.6687210
H	2.3081080	-3.7925580	2.9230800
H	1.9048270	-4.0614110	1.2306500
H	-1.3083760	-0.3714840	0.2852860
H	-1.7585510	-2.0545680	0.0552120
C	-3.9323980	-0.5528230	-0.6488360
C	-4.7996200	-1.6384110	-0.4495570
C	-4.2884410	0.6936340	-0.1105740
C	-5.9891170	-1.4851710	0.2693720
H	-4.5451730	-2.6102790	-0.8661970
C	-5.4764720	0.8519850	0.6098290
H	-3.6331990	1.5482010	-0.2616560
C	-6.3311560	-0.2381670	0.8027820
H	-6.6491730	-2.3368670	0.4081230
H	-5.7356480	1.8261260	1.0150310
H	-7.2563050	-0.1162320	1.3586400
H	-0.3571540	-2.0162580	-2.1316540
O	0.1084320	0.1041850	-1.9885060
H	0.2524590	0.9417600	-1.2896100
H	0.8689460	0.0654900	-2.5881710
O	0.3481200	1.9180930	-0.3629320
C	0.8361630	3.0291990	-0.7619620
C	0.8725280	4.0962700	0.3781170
O	1.2568120	3.3462410	-1.8747470
F	1.4175210	5.2638690	-0.0187690
F	1.5950590	3.6581350	1.4410990
F	-0.3775910	4.3711270	0.8318970

8.log
Potential Energy = -1489.66281
Zero-point Energy = -1489.18914
Free Energy = -1489.23327
Single-Point Energy B3LYP-D3(BJ)/6-311+G** PCM = -1490.11742
Free Energy B3LYP-D3(BJ)/6-311+G** PCM (extrapolated free energy from qRRHO) = -1489.68788
Nimag = 1 (-301.9079 cm^{-1})
Charge = 0 Multiplicity = 1

C	2.8651430	-0.4922060	0.2683590
C	3.2823360	-2.0585370	-1.4520040
C	1.7835630	-2.1426610	-1.1535730
N	1.5779300	-0.9171800	-0.3408840
N	3.8234450	-1.0974800	-0.6693640
O	3.8825970	-2.7326000	-2.2912850
C	5.1801200	-0.6066500	-0.8983240
H	5.9303530	-1.2211030	-0.3935500
H	5.3793770	-0.6287680	-1.9719730
H	5.2593130	0.4197160	-0.5386430
C	0.4521800	-0.1676890	-0.4155720
C	0.5144400	1.3280920	-0.1898490
C	-0.8298460	2.0490660	-0.4179590
H	-1.2221620	1.7766390	-1.4046890
H	-1.5589180	1.7113870	0.3237270
C	0.9614520	-2.2432030	-2.4351110
H	1.3283750	-3.1053040	-2.9970900
H	-0.0988210	-2.4087300	-2.2287290
H	1.0752260	-1.3528560	-3.0610170
H	1.6031170	-3.0388050	-0.5461120
C	3.0755840	-0.9145040	1.7668060
H	2.9557420	0.5964730	0.2042090
C	4.5216400	-0.5811040	2.1954280
H	4.6168710	-0.7270460	3.2760740
H	5.2567070	-1.2297720	1.7137370
H	4.7813660	0.4616700	1.9811640
C	2.1249780	-0.0987000	2.6672330
H	2.3331210	0.9750300	2.5946070
H	1.0724450	-0.2644210	2.4284140
H	2.2772320	-0.3904230	3.7113740
C	2.8271640	-2.4191090	1.9783460
H	3.4697290	-3.0321390	1.3378280
H	3.0526770	-2.6837850	3.0163370
H	1.7842710	-2.6943710	1.7936140
H	1.2479060	1.7125240	-0.9103610
H	0.8905830	1.5553510	0.8093320
C	-0.6806880	3.5549060	-0.3288660
C	-0.8714320	4.2250700	0.8893230
C	-0.3241780	4.3092340	-1.4578050
C	-0.7071520	5.6109590	0.9797360
H	-1.1561120	3.6586480	1.7728630
C	-0.1591380	5.6949600	-1.3726600
H	-0.1806690	3.8088910	-2.4127010

C	-0.3491440	6.3508060	-0.1517920
H	-0.8632200	6.1114920	1.9312360
H	0.1123790	6.2613220	-2.2591110
H	-0.2246160	7.4276820	-0.0843650
H	-0.1806830	-0.4535230	-1.2494940
O	-0.6818800	-0.6674930	0.8398350
H	-1.7546010	-0.6605710	0.5400490
H	-0.4843870	-1.5977110	1.0390780
O	-3.0468740	-0.6593970	0.2160810
C	-3.5873260	-1.8065140	0.3768880
O	-3.0775040	-2.8587520	0.7652300
C	-5.1054620	-1.8014020	0.0152990
F	-5.7924510	-0.9317990	0.7993650
F	-5.3032540	-1.4207810	-1.2724430
F	-5.6785560	-3.0122900	0.1657040

9.log
Potential Energy = -1489.65736
Zero-point Energy = -1489.18316
Free Energy = -1489.22653
Single-Point Energy B3LYP-D3(BJ)/6-311+G** PCM = -1490.11533
Free Energy B3LYP-D3(BJ)/6-311+G** PCM (extrapolated free energy from qRRHO) = -1489.68449
Nimag = 1 (-259.3944 cm^{-1})
Charge = 0 Multiplicity = 1

C	3.0482640	0.2436420	-0.0441230
C	3.4644160	-1.9819580	-0.7227370
C	1.9581610	-1.8897830	-0.4686920
N	1.7637570	-0.4195740	-0.3912150
N	4.0106260	-0.7612020	-0.5200690
O	4.0670680	-2.9932880	-1.0868310
C	5.3830840	-0.4664820	-0.9244820
H	6.1078560	-0.7529900	-0.1577510
H	5.6030410	-1.0266670	-1.8359390
H	5.4799960	0.6008170	-1.1258950
C	0.6545870	0.1961500	-0.8653320
C	0.7441060	1.6047450	-1.4130420
C	-0.5620650	2.1680300	-2.0237720
H	-0.2627110	2.8253500	-2.8486440
H	-1.1374460	1.3568530	-2.4831300
C	1.1622470	-2.6150730	-1.5496900
H	1.5196910	-3.6468000	-1.5874320
H	0.0942190	-2.6417970	-1.3207940
H	1.3122410	-2.1646520	-2.5355790
H	1.7400970	-2.3533490	0.5019120
C	3.2217230	0.6335620	1.4678860
H	3.1637300	1.1496430	-0.6465170
C	4.6643930	1.1328510	1.7059490
H	4.7353030	1.5542550	2.7136380
H	5.3978000	0.3264100	1.6385020
H	4.9464180	1.9220210	0.9999530
C	2.2699410	1.7978050	1.8117390
H	2.5000130	2.6888600	1.2168060
H	1.2173640	1.5493820	1.6611490
H	2.3932900	2.0675660	2.8653050
C	2.9483320	-0.5590900	2.4026120
H	3.5963100	-1.4113130	2.1734960
H	3.1482290	-0.2650680	3.4378170
H	1.9070620	-0.8933160	2.3579250
H	1.4933000	1.5389680	-2.2124790
H	1.1397260	2.2929000	-0.6649820
C	-1.4565940	2.9656670	-1.0911530
C	-2.7926740	2.5983210	-0.8801170
C	-0.9790790	4.1271470	-0.4616160
C	-3.6279450	3.3597950	-0.0550930
H	-3.1823350	1.7032410	-1.3570420
C	-1.8075600	4.8896910	0.3656200
H	0.0481230	4.4459400	-0.6229630
C	-3.1378290	4.5076540	0.5735390
H	-4.6593140	3.0533660	0.0960450
H	-1.4167570	5.7844800	0.8421830
H	-3.7838090	5.1003250	1.2148030
H	0.0419400	-0.4601420	-1.4746960
O	-0.5507630	0.3432800	0.4279420
H	-1.4788490	-0.1801210	0.1740350
H	-0.1969480	-0.1503970	1.1863850
O	-2.6169520	-0.8721740	-0.1298980
C	-2.7952510	-1.8678820	0.6479280
O	-2.1015080	-2.2544040	1.5918840
C	-4.0937260	-2.6644900	0.3057590
F	-5.1959210	-1.8814690	0.4333880
F	-4.0717520	-3.1167570	-0.9742550
F	-4.2734600	-3.7370440	1.1031990

10.log
Potential Energy = -1489.66178
Zero-point Energy = -1489.18774
Free Energy = -1489.23108
Single-Point Energy B3LYP-D3(BJ)/6-311+G** PCM = -1490.11946
Free Energy B3LYP-D3(BJ)/6-311+G** PCM (extrapolated free energy from qRRHO) = -1489.68876
Nimag = 1 (-331.0284 cm^{-1})
Charge = 0 Multiplicity = 1

C	-3.0935230	-0.3488320	-0.4440750
C	-3.4353370	0.0880690	1.8531470
C	-1.9704560	-0.3317880	1.7100630
N	-1.7811600	-0.2371540	0.2412340
N	-3.9986140	0.1052170	0.6237800
O	-3.9926600	0.3907780	2.9102330
C	-5.3130970	0.7003000	0.3972550
H	-6.1237550	-0.0071230	0.5917340
H	-5.4283200	1.5530220	1.0700100
H	-5.3808180	1.0448490	-0.6350980
C	-0.6228760	0.1871470	-0.3245560
C	-0.6483790	0.9181020	-1.6520460
C	0.7003070	1.5548320	-2.0554010
H	1.4760740	0.7859740	-2.1121260
H	0.5737270	1.9419700	-3.0725200
C	-1.0493420	0.5348470	2.5634580
H	-1.4039160	0.4783670	3.5953500
H	-0.0182080	0.1727570	2.5461480
H	-1.0716450	1.5831040	2.2505800
H	-1.8779540	-1.3746650	2.0399930
C	-3.4402470	-1.7683450	-1.0202260
H	-3.1369780	0.3706210	-1.2673680
C	-4.8988700	-1.7726690	-1.5285930
H	-5.0859850	-2.7040550	-2.0723690
H	-5.6227320	-1.7217910	-0.7121630
H	-5.0929250	-0.9445330	-2.2195930
C	-2.5266940	-2.0665370	-2.2269330
H	-2.6745210	-1.3326270	-3.0277950
H	-1.4682490	-2.0788150	-1.9591180
H	-2.7766530	-3.0508580	-2.6358490
C	-3.2769440	-2.8723860	0.0401850
H	-3.8989550	-2.6854640	0.9217490
H	-3.5877900	-3.8336150	-0.3815400
H	-2.2371570	-2.9808300	0.3632940
H	-1.3978530	1.7134800	-1.5602730
H	-0.9837270	0.2467880	-2.4446040
C	1.1532600	2.6808780	-1.1439030
C	0.5076620	3.9287110	-1.1802430
C	2.2177090	2.5064780	-0.2463700
C	0.9096440	4.9702660	-0.3405600
H	-0.3112810	4.0896750	-1.8778230

C	2.6235850	3.5481440	0.5964410
H	2.7342900	1.5508860	-0.2116250
C	1.9702900	4.7825340	0.5535580
H	0.4002300	5.9286980	-0.3877270
H	3.4513710	3.3932430	1.2828920
H	2.2855660	5.5922270	1.2052960
H	0.0522920	0.6268900	0.4021310
O	0.3785640	-1.1959370	-0.7083210
H	1.4916940	-1.0793800	-0.6182840
H	0.1481330	-1.8915130	-0.0700530
O	2.8048640	-0.9987640	-0.5349500
C	3.2963710	-1.9134310	0.2127620
O	2.7142030	-2.7994270	0.8389160
C	4.8523130	-1.8342660	0.2963420
F	5.4162260	-1.9632080	-0.9313160
F	5.2558390	-0.6397620	0.7987060
F	5.3782050	-2.7958360	1.0807000

11.log
Potential Energy = -1489.66281
Zero-point Energy = -1489.18914
Free Energy = -1489.23327
Single-Point Energy B3LYP-D3(BJ)/6-311+G** PCM = -1490.11742
Free Energy B3LYP-D3(BJ)/6-311+G** PCM (extrapolated free energy from qRRHO) = -1489.68788
Nimag = 1 (-301.8792 cm^{-1})
Charge = 0 Multiplicity = 1

C	2.8650320	-0.4926000	0.2684990
C	3.2821400	-2.0586630	-1.4521230
C	1.7833850	-2.1428240	-1.1536030
N	1.5777950	-0.9174120	-0.3407940
N	3.8233160	-1.0977640	-0.6693210
O	3.8823220	-2.7325890	-2.2915680
C	5.1799130	-0.6067470	-0.8983450
H	5.9302200	-1.2204870	-0.3928220
H	5.3794230	-0.6298170	-1.9719220
H	5.2587010	0.4199890	-0.5396000
C	0.4521560	-0.1677620	-0.4155270
C	0.5145970	1.3279940	-0.1896900
C	-0.8295090	2.0491880	-0.4181810
H	-1.2215310	1.7768950	-1.4050650
H	-1.5588840	1.7115630	0.3232340
C	0.9611760	-2.2433030	-2.4350770
H	1.3280230	-3.1054070	-2.9970990
H	-0.0990860	-2.4087910	-2.2286130
H	1.0749360	-1.3529530	-3.0609820
H	1.6030060	-3.0390030	-0.5461780
C	3.0754270	-0.9150980	1.7668900
H	2.9557030	0.5960790	0.2045220
C	4.5215120	-0.5818620	2.1955300
H	4.6167130	-0.7277570	3.2761860
H	5.2564980	-1.2306500	1.7138800
H	4.7813620	0.4608710	1.9812040
C	2.1248910	-0.0992850	2.6673860
H	2.3332280	0.9744210	2.5949600
H	1.0723500	-0.2647830	2.4284470
H	2.2770100	-0.3912140	3.7114900
C	2.8268500	-2.4196970	1.9782820
H	3.4693120	-3.0327320	1.3376630
H	3.0523870	-2.6845090	3.0162330
H	1.7839120	-2.6948180	1.7935810
H	1.2483430	1.7123780	-0.9099400
H	0.8904580	1.5551180	0.8096290
C	-0.6801390	3.5549980	-0.3289270
C	-0.8711520	4.2251020	0.8892540
C	-0.3231400	4.3093510	-1.4576940
C	-0.7066580	5.6109550	0.9798260
H	-1.1562120	3.6586610	1.7726600
C	-0.1578840	5.6950420	-1.3723910
H	-0.1794120	3.8090570	-2.4125830
C	-0.3481590	6.3508270	-0.1515310
H	-0.8629380	6.1114420	1.9313150
H	0.1140150	6.2614240	-2.2587120
H	-0.2234620	7.4276750	-0.0839810
H	-0.1806920	-0.4534610	-1.2495050
O	-0.6820350	-0.6674720	0.8397780
H	-1.7547380	-0.6604760	0.5399670
H	-0.4845840	-1.5976860	1.0390900
O	-3.0470200	-0.6591170	0.2160180
C	-3.5876450	-1.8061480	0.3768550
O	-3.0779780	-2.8584560	0.7652060
C	-5.1057700	-1.8008050	0.0152200
F	-5.7925650	-0.9306060	0.7987870
F	-5.3033720	-1.4207960	-1.2727390
F	-5.6792060	-3.0114550	0.1662120

12.log
Potential Energy = -1489.66213
Zero-point Energy = -1489.18799
Free Energy = -1489.23136
Single-Point Energy B3LYP-D3(BJ)/6-311+G** PCM = -1490.12005
Free Energy B3LYP-D3(BJ)/6-311+G** PCM (extrapolated free energy from qRRHO) = -1489.68928
Nimag = 1 (-310.6199 cm^{-1})
Charge = 0 Multiplicity = 1

C	-2.8903140	-0.6469700	-0.5149400
C	-3.5303720	0.2473580	1.5773630
C	-2.0718030	-0.1926140	1.7245390
N	-1.6817550	-0.3732850	0.3048840
N	-3.9211430	0.0116440	0.3036690
O	-4.2180760	0.7582360	2.4634720
C	-5.1774820	0.5445240	-0.2171280
H	-6.0245080	-0.1109680	0.0024070
H	-5.3612260	1.5156180	0.2478380
H	-5.0969960	0.6725620	-1.2970750
C	-0.4325170	-0.1293050	-0.1547310
C	-0.1997140	0.2977170	-1.5904420
C	-0.6051660	1.7687080	-1.8551870
H	-0.5117540	1.9254300	-2.9363410
H	-1.6620160	1.9188220	-1.6124340
C	-1.2482260	0.8113380	2.5244550
H	-1.7419920	0.9525250	3.4888950
H	-0.2376370	0.4435080	2.7200380
H	-1.1889590	1.7810280	2.0224820
H	-2.0564450	-1.1568870	2.2491380
C	-3.1846000	-2.1596560	-0.8249230
H	-2.8121110	-0.1163990	-1.4685130
C	-4.5702860	-2.2803770	-1.4970600
H	-4.7052660	-3.3057640	-1.8554980
H	-5.3875350	-2.0677960	-0.8041190
H	-4.6639980	-1.6155160	-2.3630500
C	-2.1352180	-2.6939350	-1.8215670
H	-2.1670500	-2.1409210	-2.7677910
H	-1.1204760	-2.6470900	-1.4219790
H	-2.3563850	-3.7416490	-2.0504030
C	-3.1719450	-3.0235420	0.4496200
H	-3.8857350	-2.6600320	1.1961920
H	-3.4591800	-4.0492840	0.1967430
H	-2.1780630	-3.0680800	0.9046890
H	-0.7318720	-0.3595860	-2.2795040
H	0.8646090	0.1751370	-1.8034990
C	0.2292100	2.8058820	-1.1247520
C	-0.3592080	3.6865100	-0.2052980
C	1.6071190	2.9256540	-1.3730580

C	0.4042320	4.6560070	0.4550500
H	-1.4261420	3.6183430	-0.0076410
C	2.3739190	3.8903270	-0.7150840
H	2.0856110	2.2651630	-2.0921280
C	1.7747410	4.7594910	0.2039770
H	-0.0734160	5.3276820	1.1627580
H	3.4373650	3.9667740	-0.9233380
H	2.3701370	5.5107410	0.7145550
H	0.1660430	0.4259420	0.5600690
O	0.5238830	-1.5994870	-0.1121890
H	1.6233220	-1.4303830	-0.2344690
H	0.4015280	-2.0097130	0.7597120
O	2.9146110	-1.2328350	-0.4405690
C	3.6602130	-1.6752210	0.4992500
O	3.3420540	-2.2408950	1.5456160
C	5.1745690	-1.4220960	0.2180400
F	5.5551520	-1.9580210	-0.9688460
F	5.4422700	-0.0918030	0.1602850
F	5.9734380	-1.9486950	1.1677840

13.log
Potential Energy = -1489.66178
Zero-point Energy = -1489.18774
Free Energy = -1489.23108
Single-Point Energy B3LYP-D3(BJ)/6-311+G** PCM = -1490.11946
Free Energy B3LYP-D3(BJ)/6-311+G** PCM (extrapolated free energy from qRRHO) = -1489.68876
Nimag = 1 (-330.9669 cm^{-1})
Charge = 0 Multiplicity = 1

C	3.0935500	-0.3485140	0.4439820
C	3.4350370	0.0877620	-1.8534080
C	1.9701980	-0.3321370	-1.7100250
N	1.7810920	-0.2371240	-0.2411940
N	3.9984600	0.1053250	-0.6241160
O	3.9922150	0.3901960	-2.9106480
C	5.3129340	0.7005680	-0.3979590
H	6.1236130	-0.0068010	-0.5925510
H	5.4279210	1.5532270	-1.0708370
H	5.3808630	1.0452400	0.6343370
C	0.6228350	0.1871480	0.3246450
C	0.6483910	0.9182950	1.6520230
C	-0.7003040	1.5549860	2.0554170
H	-1.4760150	0.7860850	2.1123190
H	-0.5736450	1.9422630	3.0724730
C	1.0489460	0.5342530	-2.5635230
H	1.4033620	0.4774910	-3.5954540
H	0.0178170	0.1721690	-2.5459580
H	1.0712890	1.5825960	-2.2509380
H	1.8776960	-1.3751040	-2.0396700
C	3.4405120	-1.7678390	1.0204620
H	3.1370350	0.3711650	1.2670760
C	4.8991660	-1.7718040	1.5287470
H	5.0864860	-2.7030730	2.0726530
H	5.6229770	-1.7209130	0.7122740
H	5.0931010	-0.9435290	2.2196150
C	2.5270870	-2.0659030	2.2272980
H	2.6746980	-1.3316710	3.0279030
H	1.4686330	-2.0786520	1.9595300
H	2.7773940	-3.0499960	2.6365520
C	3.2773310	-2.8721640	-0.0396710
H	3.8993130	-2.6853850	-0.9212870
H	3.5883010	-3.8332500	0.3822920
H	2.2375560	-2.9808190	-0.3627420
H	1.3977970	1.7137180	1.5600750
H	0.9838590	0.2471180	2.4446430
C	-1.1534130	2.6808920	1.1438270
C	-0.5079980	3.9288220	1.1800890
C	-2.2178200	2.5062730	0.2462880
C	-0.9101120	4.9702580	0.3403210
H	0.3109050	4.0899520	1.8776790
C	-2.6238290	3.5478180	-0.5966090
H	-2.7342790	1.5506120	0.2116140
C	-1.9707120	4.7823060	-0.5538050
H	-0.4008390	5.9287680	0.3874300
H	-3.4515820	3.3927490	-1.2830610
H	-2.2860930	5.5919050	-1.2056080
H	-0.0524770	0.6266730	-0.4020410
O	-0.3784600	-1.1960140	0.7087670
H	-1.4915860	-1.0794940	0.6188600
H	-0.1481600	-1.8916120	0.0704760
O	-2.8048140	-0.9989940	0.5355310
C	-3.2961330	-1.9135090	-0.2124810
O	-2.7137880	-2.7992780	-0.8387920
C	-4.8520650	-1.8344450	-0.2963200
F	-5.4162050	-1.9631320	0.9312520
F	-5.2555280	-0.6400580	-0.7990310
F	-5.3777820	-2.7962010	-1.0805700

14.log
Potential Energy = -1489.66326
Zero-point Energy = -1489.19008
Free Energy = -1489.23415
Single-Point Energy B3LYP-D3(BJ)/6-311+G** PCM = -1490.11854
Free Energy B3LYP-D3(BJ)/6-311+G** PCM (extrapolated free energy from qRRHO) = -1489.68943
Nimag = 1 (-378.5909 cm^{-1})
Charge = 0 Multiplicity = 1

C	-1.2140390	1.6419790	0.4122200
C	-1.1311840	2.7783480	-1.6503700
C	0.2929720	2.2678690	-1.4011770
N	0.0927420	1.3673840	-0.2403640
N	-1.9330390	2.3470900	-0.6518730
O	-1.4855890	3.4448390	-2.6252990
C	-3.3825270	2.5024470	-0.7158030
H	-3.6915490	2.4169630	-1.7595630
H	-3.8571920	1.7118850	-0.1335370
H	-3.7090070	3.4753160	-0.3367380
C	0.7376550	0.1984100	0.0069190
H	0.4142720	-0.2384160	0.9474100
C	2.2390470	0.0932050	-0.2132410
C	2.8822060	-1.0752030	0.5653970
H	2.6429640	-0.9714090	1.6296360
H	0.9133920	3.1225550	-1.1006470
C	-1.0884940	2.4426890	1.7570580
H	-1.7236560	0.6938000	0.6182570
H	2.4660480	-0.0020980	-1.2762420
C	0.8685670	1.6697130	-2.6876890
H	1.9449780	1.5107920	-2.6188410
H	0.3797040	0.7288190	-2.9486030
H	0.6902630	2.3925720	-3.4878940
C	-2.4921340	2.6364900	2.3725230
H	-2.3915260	3.0619660	3.3761700
H	-3.1120180	3.3226610	1.7916210
H	-3.0265510	1.6844590	2.4696650
C	-0.4265150	3.8151050	1.5376880
H	-0.9891470	4.4303260	0.8280660
H	-0.3857640	4.3601270	2.4864780
H	0.6008590	3.7133940	1.1738620
C	-0.2453970	1.6267110	2.7595710
H	-0.6644440	0.6272710	2.9266460
H	0.7943440	1.5238500	2.4363630
H	-0.2340050	2.1408390	3.7259120
O	0.0955260	-1.0241680	-1.0458000
H	-0.9744650	-1.2758530	-0.7932920

H	0.5955700	-1.8531720	-0.9564000
O	-2.2284180	-1.5161810	-0.5095180
C	-2.4620310	-2.7351820	-0.1957170
O	-1.6834850	-3.6860520	-0.1391460
C	-3.9628220	-2.9706050	0.1607560
F	-4.7781470	-2.5962060	-0.8563290
F	-4.2330790	-4.2618780	0.4355540
F	-4.3217100	-2.2436220	1.2503250
H	2.6802960	1.0367060	0.1266030
H	2.4537860	-2.0296920	0.2368740
C	4.3858750	-1.1204550	0.3826400
C	4.9585980	-1.8301260	-0.6841530
C	5.2361810	-0.4321680	1.2617090
C	6.3440140	-1.8489290	-0.8714710
H	4.3158770	-2.3764520	-1.3704340
C	6.6223440	-0.4480250	1.0783210
H	4.8111160	0.1160900	2.0991310
C	7.1809900	-1.1563670	0.0096060
H	6.7684720	-2.4073610	-1.7010110
H	7.2641170	0.0878220	1.7719890
H	8.2576590	-1.1726550	-0.1323980

15.log
Potential Energy = -1489.66309
Zero-point Energy = -1489.18922
Free Energy = -1489.23270
Single-Point Energy B3LYP-D3(BJ)/6-311+G** PCM = -1490.12199
Free Energy B3LYP-D3(BJ)/6-311+G** PCM (extrapolated free energy from qRRHO) = -1489.69160
Nimag = 1 (-291.0837 cm^{-1})
Charge = 0 Multiplicity = 1

C	2.1556070	-0.1911370	0.4938210
C	3.1404510	-0.4468800	-1.6319580
C	2.2441500	-1.6756080	-1.4392940
N	1.4850200	-1.3090340	-0.2196250
N	3.0018210	0.3686220	-0.5635870
O	3.8449660	-0.2300750	-2.6205610
C	3.5815790	1.7072980	-0.5446020
H	3.5596060	2.1055200	-1.5610400
H	2.9883340	2.3495780	0.1071690
H	4.6192110	1.7009700	-0.1978920
C	0.1821630	-1.5934850	0.0427450
H	-0.1084380	-1.2286910	1.0238170
C	-0.3686470	-2.9797950	-0.2724990
C	-1.5609040	-3.4003240	0.6178160
H	-1.7700770	-4.4514910	0.3881790
H	2.8899910	-2.5376000	-1.2250280
C	2.9336220	-0.6435150	1.7807420
H	1.4079690	0.5559220	0.7833200
H	-0.6474620	-3.0455780	-1.3258080
C	1.4565020	-1.9588390	-2.7208940
H	0.9747990	-2.9365800	-2.6962580
H	0.7046450	-1.1901640	-2.9109610
H	2.1730190	-1.9617300	-3.5462660
C	3.5393910	0.5954480	2.4769580
H	3.9546150	0.2995010	3.4457290
H	4.3516660	1.0434140	1.9007820
H	2.7817180	1.3651770	2.6637170
C	4.0528090	-1.6446460	1.4418700
H	4.7800220	-1.2213970	0.7414350
H	4.5932980	-1.9155800	2.3547500
H	3.6509130	-2.5679810	1.0128400
C	1.9467430	-1.3007670	2.7682660
H	1.1138310	-0.6328720	3.0181780
H	1.5421390	-2.2401770	2.3813600
H	2.4690450	-1.5332510	3.7018100
O	-0.8246620	-0.5498050	-0.9015100
H	-0.7335280	0.5150370	-0.6010890
H	-1.7567970	-0.8126070	-0.7847880
O	-0.5316870	1.7846920	-0.2357640
C	-1.5216060	2.5751040	-0.4059520
O	-2.6434240	2.3394880	-0.8538430
C	-1.1903730	4.0334840	0.0437590
F	-0.1263620	4.5306420	-0.6368080
F	-2.2190680	4.8832440	-0.1496990
F	-0.8760270	4.0789740	1.3643880
H	0.4454870	-3.6946860	-0.1150570
H	-1.2563340	-3.3679930	1.6692480
C	-2.8336290	-2.5919590	0.4391240
C	-3.3330590	-1.7914240	1.4791070
C	-3.5546830	-2.6414200	-0.7683350
C	-4.5160310	-1.0610930	1.3212500
H	-2.7952390	-1.7449470	2.4226270
C	-4.7355350	-1.9107190	-0.9299330
H	-3.1964880	-3.2649860	-1.5839690
C	-5.2205030	-1.1176740	0.1157390
H	-4.8842240	-0.4497580	2.1400150
H	-5.2779110	-1.9654950	-1.8693120
H	-6.1384190	-0.5511000	-0.0088890

16.log
Potential Energy = -1489.66225
Zero-point Energy = -1489.18884
Free Energy = -1489.23238
Single-Point Energy B3LYP-D3(BJ)/6-311+G** PCM = -1490.12098
Free Energy B3LYP-D3(BJ)/6-311+G** PCM (extrapolated free energy from qRRHO) = -1489.69110
Nimag = 1 (-361.3958 cm^{-1})
Charge = 0 Multiplicity = 1

C	-0.2826440	1.6543360	0.6961040
C	-0.8995090	3.4405790	-0.7097270
C	0.3779920	2.8519770	-1.3213680
N	0.5375240	1.5984350	-0.5428510
N	-1.2536260	2.6999010	0.3629430
O	-1.5150200	4.4133860	-1.1517730
C	-2.5320930	2.8961280	1.0384480
H	-3.2771770	3.1764780	0.2910750
H	-2.8353470	1.9645410	1.5172410
H	-2.4815760	3.6883230	1.7911700
C	0.9706560	0.3964840	-1.0047680
H	1.0047860	-0.3424270	-0.2091530
C	2.1690260	0.3238370	-1.9358550
C	2.7779630	-1.0887970	-2.0978680
H	2.0514140	-1.7699070	-2.5557640
H	1.2085250	3.5322920	-1.0915120
C	0.5568170	1.9322650	1.9928570
H	-0.8126530	0.7034360	0.8231740
H	1.9097380	0.7103170	-2.9219130
C	0.2319540	2.7523980	-2.8422250
H	1.1899460	2.5859480	-3.3353690
H	-0.4670100	1.9646570	-3.1303670
H	-0.1576120	3.7123850	-3.1906610
C	-0.3795190	1.9367010	3.2216290
H	0.2231440	1.9764410	4.1347280
H	-1.0455070	2.8021350	3.2360410
H	-0.9906450	1.0280320	3.2689510
C	1.3011930	3.2770640	1.9084530
H	0.6123110	4.1157380	1.7640280
H	1.8456920	3.4549950	2.8416020
H	2.0340490	3.2819000	1.0955160
C	1.5803310	0.7946270	2.1859410
H	1.0936210	-0.1866020	2.2318720
H	2.3323010	0.7758620	1.3924200
H	2.1105770	0.9406900	3.1324170

O	-0.3083620	-0.3211870	-1.9387240
H	-1.1697440	-0.6460000	-1.2950890
H	-0.0031540	-1.1168810	-2.4058980
O	-2.1835330	-0.9729720	-0.5252020
C	-2.5548070	-2.1913150	-0.6495840
O	-2.1030010	-3.0712750	-1.3814970
C	-3.7525770	-2.5382430	0.2887560
F	-4.8305530	-1.7599440	0.0168340
F	-4.1466900	-3.8216880	0.1719090
F	-3.4296860	-2.3340020	1.5913430
H	2.9272210	0.9963820	-1.5195460
H	3.5935570	-0.9950930	-2.8232270
C	3.3096010	-1.7047970	-0.8180420
C	4.4985100	-1.2287430	-0.2398280
C	2.6357160	-2.7594310	-0.1840040
C	4.9960830	-1.7868410	0.9400590
H	5.0436250	-0.4201970	-0.7214500
C	3.1303720	-3.3214240	0.9986330
H	1.7207400	-3.1519260	-0.6212900
C	4.3117330	-2.8358320	1.5650410
H	5.9196060	-1.4076020	1.3683960
H	2.5937520	-4.1387760	1.4719290
H	4.6994320	-3.2722450	2.4809240

17.log
Potential Energy = -1489.66308
Zero-point Energy = -1489.18914
Free Energy = -1489.23251
Single-Point Energy B3LYP-D3(BJ)/6-311+G** PCM = -1490.12191
Free Energy B3LYP-D3(BJ)/6-311+G** PCM (extrapolated free energy from qRRHO) = -1489.69134
Nimag = 1 (-290.5330 cm^{-1})
Charge = 0 Multiplicity = 1

C	-2.1568900	-0.1633950	-0.4805990
C	-3.1344230	-0.4490860	1.6446970
C	-2.2536260	-1.6841930	1.4232750
N	-1.4958600	-1.3026680	0.2073770
N	-2.9920150	0.3852600	0.5915060
O	-3.8309500	-0.2430910	2.6412660
C	-3.5540640	1.7316490	0.6028710
H	-3.5170670	2.1109870	1.6261150
H	-2.9588080	2.3779870	-0.0430040
H	-4.5949270	1.7454270	0.2662690
C	-0.1963520	-1.5942890	-0.0654330
H	0.0930650	-1.2133900	-1.0406880
C	0.3412410	-2.9928870	0.2172890
C	1.5324410	-3.4025630	-0.6798270
H	1.7325220	-4.4604360	-0.4743360
H	-2.9108150	-2.5339660	1.1950660
C	-2.9454820	-0.5822410	-1.7722720
H	-1.4021940	0.5805900	-0.7595430
H	0.6162480	-3.0880700	1.2694500
C	-1.4637100	-2.0023640	2.6952400
H	-0.9939100	-2.9851090	2.6488020
H	-0.7020370	-1.2464950	2.8971370
H	-2.1764580	-2.0136230	3.5237990
C	-3.5514460	0.6746890	-2.4352620
H	-3.9714040	0.4034670	-3.4092270
H	-4.3604090	1.1095650	-1.8445500
H	-2.7933170	1.4476150	-2.6062990
C	-4.0662500	-1.5868360	-1.4493550
H	-4.7860380	-1.1778990	-0.7328760
H	-4.6152380	-1.8326970	-2.3642580
H	-3.6649370	-2.5221250	-1.0464910
C	-1.9671230	-1.2196790	-2.7811420
H	-1.1345880	-0.5479580	-3.0219900
H	-1.5614850	-2.1681740	-2.4180250
H	-2.4964500	-1.4305930	-3.7158570
O	0.8226500	-0.5778080	0.8921830
H	0.7884350	0.4791440	0.5519370
H	1.7453420	-0.8842340	0.8113060
O	0.6542370	1.7266910	0.0968050
C	1.4967400	2.5857890	0.5283260
O	2.4290960	2.4419420	1.3182590
C	1.2460530	4.0035740	-0.0765760
F	0.0117090	4.4655460	0.2503780
F	2.1396660	4.9170010	0.3530950
F	1.3172730	3.9805180	-1.4323260
H	-0.4792030	-3.6958700	0.0403230
H	1.2311190	-3.3428370	-1.7310130
C	2.8101080	-2.6076760	-0.4775100
C	3.3139570	-1.7782580	-1.4924310
C	3.5284730	-2.6947580	0.7294550
C	4.4979300	-1.0553830	-1.3102130
H	2.7783110	-1.7022530	-2.4352150
C	4.7106180	-1.9716680	0.9153560
H	3.1672140	-3.3415280	1.5254610
C	5.1994190	-1.1488100	-0.1051090
H	4.8694260	-0.4209850	-2.1097280
H	5.2507550	-2.0556760	1.8538470
H	6.1182210	-0.5881470	0.0382890

18.log
Potential Energy = -1489.66019
Zero-point Energy = -1489.18653
Free Energy = -1489.22984
Single-Point Energy B3LYP-D3(BJ)/6-311+G** PCM = -1490.11899
Free Energy B3LYP-D3(BJ)/6-311+G** PCM (extrapolated free energy from qRRHO) = -1489.68863
Nimag = 1 (-392.7208 cm^{-1})
Charge = 0 Multiplicity = 1

C	-2.8509660	-0.1189270	0.5924330
C	-2.6438470	-2.2067690	-0.4783960
C	-2.0375180	-1.1791810	-1.4414520
N	-1.9560870	0.0295210	-0.5841970
N	-3.0235780	-1.5726330	0.6533040
O	-2.7410090	-3.4160790	-0.6976450
C	-3.4670080	-2.3088540	1.8319330
H	-2.9247530	-3.2557560	1.8698720
H	-3.2417630	-1.7284480	2.7277280
H	-4.5391600	-2.5247090	1.8030430
C	-0.9581320	0.9485100	-0.5287500
H	-1.2380320	1.7828450	0.1072070
C	-0.2411590	1.3821020	-1.8012260
C	0.2813470	2.8379720	-1.7467280
H	0.6403220	3.0825810	-2.7523730
H	-2.7664470	-0.9980800	-2.2424370
C	-4.1879450	0.6965480	0.4812050
H	-2.3150490	0.2127970	1.4892080
H	0.5802450	0.7007460	-2.0298410
C	-0.7559100	-1.7256030	-2.0692080
H	-0.4122730	-1.1080610	-2.8993880
H	0.0506340	-1.8373430	-1.3422550
H	-0.9942330	-2.7155050	-2.4672690
C	-4.9954720	0.5355290	1.7882740
H	-5.8527880	1.2161530	1.7707930
H	-5.3882320	-0.4755780	1.9148080
H	-4.3931140	0.7855410	2.6692650
C	-5.0404200	0.2283500	-0.7122960
H	-5.2943710	-0.8340920	-0.6402140
H	-5.9795080	0.7908520	-0.7363440
H	-4.5305860	0.4022450	-1.6651410
C	-3.8596250	2.1947980	0.3112590
H	-3.2362160	2.5722230	1.1305520

H	-3.3572470	2.3991400	-0.6385300
H	-4.7894200	2.7724870	0.3178200
O	0.2798580	0.3939260	0.5637880
H	1.0893110	-0.3223170	0.2274600
H	0.7290740	1.1775000	0.9265170
O	2.0134440	-1.1562600	-0.1512960
C	2.9003880	-1.4512960	0.7237960
O	3.0147020	-1.0642580	1.8850630
C	3.9564480	-2.4551270	0.1628790
F	4.5759020	-1.9563490	-0.9368370
F	4.9166570	-2.7512130	1.0613670
F	3.3734420	-3.6255450	-0.2024310
H	-0.9583810	1.3092890	-2.6253360
H	-0.5584990	3.5115010	-1.5427110
C	1.3922950	3.0931200	-0.7464010
C	1.1371610	3.7433820	0.4721430
C	2.7079040	2.6795990	-1.0176280
C	2.1631400	3.9630770	1.4003830
H	0.1324260	4.0961320	0.6921120
C	3.7340510	2.9002250	-0.0963610
H	2.9301420	2.1839760	-1.9595070
C	3.4645330	3.5406980	1.1189860
H	1.9429830	4.4689120	2.3360080
H	4.7444340	2.5749500	-0.3271640
H	4.2626120	3.7122190	1.8351200

19.log
Potential Energy = -1489.66231
Zero-point Energy = -1489.18932
Free Energy = -1489.23334
Single-Point Energy B3LYP-D3(BJ)/6-311+G** PCM = -1490.11822
Free Energy B3LYP-D3(BJ)/6-311+G** PCM (extrapolated free energy from qRRHO) = -1489.68925
Nimag = 1 (-406.5721 cm^{-1})
Charge = 0 Multiplicity = 1

C	3.3139270	-0.2198350	-0.5508950
C	3.3116440	-1.3128700	1.5352840
C	2.1613940	-0.3013600	1.5971430
N	2.0808420	0.1560300	0.1884660
N	3.8669720	-1.2717520	0.3039050
O	3.6449860	-2.0640800	2.4538880
C	4.8512580	-2.2608790	-0.1227090
H	4.6121460	-3.2118290	0.3575500
H	4.7990360	-2.3805760	-1.2056180
H	5.8692250	-1.9769150	0.1596130
C	0.9619750	0.4568180	-0.5132440
H	1.2059120	0.7973830	-1.5147950
C	-0.1620720	1.2556710	0.1228170
C	-1.1301690	1.8498940	-0.9215420
H	2.4749730	0.5353030	2.2348190
C	4.2817570	0.9896640	-0.8092750
H	3.0346820	-0.6548400	-1.5182420
H	-0.7217390	0.6504080	0.8366440
C	0.9258030	-0.9570980	2.2179830
H	0.1621150	-0.2265120	2.4841430
H	0.4926190	-1.7153850	1.5619650
H	1.2508300	-1.4471340	3.1392960
C	5.4973880	0.5099840	-1.6329860
H	6.0940670	1.3766850	-1.9349350
H	6.1538380	-0.1511720	-1.0634890
H	5.1877700	-0.0114320	-2.5461010
C	4.7661260	1.6122820	0.5128420
H	5.2935810	0.8840480	1.1372660
H	5.4620020	2.4305250	0.3009270
H	3.9348200	2.0299920	1.0895990
C	3.5484280	2.0658330	-1.6375930
H	3.1631010	1.6628510	-2.5817430
H	2.7219800	2.5203750	-1.0839790
H	4.2494020	2.8681520	-1.8888570
O	0.1943470	-1.0374940	-1.0350620
H	-0.7945880	-1.3560620	-0.5873080
H	0.0921130	-1.0479800	-2.0001180
O	-1.9023870	-1.7625540	-0.0411190
C	-2.7314960	-2.2767180	-0.8699970
O	-2.6267120	-2.4199370	-2.0874350
C	-4.0363550	-2.7645480	-0.1667290
F	-4.6763540	-1.7350090	0.4443360
F	-4.9097870	-3.3230450	-1.0278180
F	-3.7646610	-3.6900080	0.7875730
H	0.3067010	2.0680490	0.6904850
H	-0.5585780	2.4458360	-1.6425130
H	-1.6045850	1.0366880	-1.4807250
C	-2.1969300	2.7160390	-0.2828200
C	-3.3952750	2.1534620	0.1841940
C	-1.9994630	4.0962640	-0.1225070
C	-4.3687880	2.9473430	0.7980620
H	-3.5687960	1.0870530	0.0637760
C	-2.9705470	4.8943780	0.4903760
H	-1.0806230	4.5510750	-0.4851850
C	-4.1592360	4.3215730	0.9539010
H	-5.2910720	2.4934800	1.1497350
H	-2.8002450	5.9616380	0.6010120
H	-4.9162490	4.9400500	1.4273560

20.log
Potential Energy = -1489.66019
Zero-point Energy = -1489.18653
Free Energy = -1489.22984
Single-Point Energy B3LYP-D3(BJ)/6-311+G** PCM = -1490.11898
Free Energy B3LYP-D3(BJ)/6-311+G** PCM (extrapolated free energy from qRRHO) = -1489.68863
Nimag = 1 (-392.8019 cm^{-1})
Charge = 0 Multiplicity = 1

C	-2.8507190	-0.1190700	0.5924780
C	-2.6436850	-2.2066600	-0.4788590
C	-2.0374180	-1.1788570	-1.4417230
N	-1.9559650	0.0296610	-0.5842120
N	-3.0232760	-1.5727940	0.6530380
O	-2.7408990	-3.4159140	-0.6983950
C	-3.4666120	-2.3092920	1.8315290
H	-2.9243860	-3.2562240	1.8691720
H	-3.2412480	-1.7291200	2.7274460
H	-4.5387750	-2.5251030	1.8027000
C	-0.9580950	0.9487320	-0.5287180
H	-1.2379930	1.7829440	0.1073980
C	-0.2412510	1.3825630	-1.8011850
C	0.2811030	2.8384800	-1.7465260
H	-2.7663700	-0.9975980	-2.2426490
C	-4.1877460	0.6963760	0.4815780
H	-2.3147160	0.2124730	1.4892670
H	0.5802170	0.7013260	-2.0299240
C	-0.7558170	-1.7251380	-2.0696230
H	-0.4121980	-1.1074150	-2.8996760
H	0.0507380	-1.8370280	-1.3427060
H	-0.9941400	-2.7149550	-2.4678960
C	-4.9950700	0.5351100	1.7887430
H	-5.8524140	1.2157060	1.7715050
H	-5.3877750	-0.4760310	1.9151730
H	-4.3925860	0.7850000	2.6696830
C	-5.0403760	0.2283370	-0.7118730
H	-5.2943020	-0.8341190	-0.6399110
H	-5.9794750	0.7908290	-0.7357140
H	-4.5306740	0.4023750	-1.6647630
C	-3.8595200	2.1946680	0.3118340

H	-3.2359860	2.5719790	1.1310840
H	-3.3573180	2.3991990	-0.6380080
H	-4.7893400	2.7723140	0.3186600
O	0.2800350	0.3940950	0.5636610
H	1.0893790	-0.3223020	0.2273510
H	0.7293540	1.1776420	0.9263190
O	2.0133670	-1.1564140	-0.1513330
C	2.9001330	-1.4517050	0.7238570
O	3.0143760	-1.0647750	1.8851660
C	3.9561000	-2.4556610	0.1629850
F	4.5763040	-1.9565150	-0.9361500
F	4.9157370	-2.7525550	1.0618180
F	3.3728840	-3.6256780	-0.2032470
H	-0.9585070	1.3097720	-2.6252680
H	0.6399120	3.0832940	-2.7521810
H	-0.5587830	3.5118880	-1.5422820
C	1.3921650	3.0935810	-0.7463130
C	1.1371530	3.7437010	0.4723320
C	2.7077650	2.6801690	-1.0177570
C	2.1632440	3.9633750	1.4004530
H	0.1324220	4.0963520	0.6924760
C	3.7340220	2.9007730	-0.0966070
H	2.9299090	2.1846550	-1.9597150
C	3.4646260	3.5411130	1.1188370
H	1.9431800	4.4691010	2.3361600
H	4.7443950	2.5755840	-0.3275770
H	4.2627920	3.7126180	1.8348790

21.log
Potential Energy = -1489.65495
Zero-point Energy = -1489.18085
Free Energy = -1489.22400
Single-Point Energy B3LYP-D3(BJ)/6-311+G** PCM = -1490.11262
Free Energy B3LYP-D3(BJ)/6-311+G** PCM (extrapolated free energy from qRRHO) = -1489.68166
Nimag = 1 (-330.9198 cm^{-1})
Charge = 0 Multiplicity = 1

C	2.7836090	-1.4664520	-0.1699070
C	2.8317280	-0.4095240	1.9397200
C	1.5180930	0.0340310	1.2940840
N	1.4377840	-0.8874680	0.1351920
N	3.4491010	-1.2938040	1.1230670
O	3.2286750	-0.0643470	3.0537400
C	4.5380950	-2.1362370	1.6145920
H	4.3367830	-2.3875910	2.6583360
H	4.5798680	-3.0526030	1.0255840
H	5.5060020	-1.6316220	1.5599500
C	0.3589430	-1.1643800	-0.6319060
C	-1.0393860	-1.3671830	-0.0668200
C	-2.0076050	-1.9764890	-1.1038860
H	-2.1126760	-1.2903650	-1.9489430
H	1.6146620	1.0674090	0.9336090
C	3.5715730	-0.8389470	-1.3786910
H	2.6588970	-2.5383010	-0.3656820
H	-0.9366920	-2.0576640	0.7766630
C	0.3978400	-0.0200960	2.3367590
H	-0.5196000	0.4478840	1.9815630
H	0.1861720	-1.0444300	2.6540250
H	0.7446530	0.5423400	3.2073850
C	5.0218340	-1.3756270	-1.3756410
H	5.5233470	-1.0498300	-2.2922130
H	5.6019680	-0.9923310	-0.5341460
H	5.0543380	-2.4703880	-1.3563270
C	3.6211380	0.6971660	-1.2888200
H	4.1283180	1.0246010	-0.3752330
H	4.1822990	1.0995930	-2.1380240
H	2.6303470	1.1612420	-1.2989320
C	2.9446590	-1.2981520	-2.7149060
H	2.9213050	-2.3918080	-2.7841970
H	1.9285150	-0.9381650	-2.8869620
H	3.5519750	-0.9273490	-3.5460430
H	-1.4547220	-0.4369660	0.3238830
H	-1.5736900	-2.9052430	-1.4934650
C	-3.3691640	-2.2678030	-0.5063770
C	-3.6313640	-3.4966490	0.1195550
C	-4.3917060	-1.3070800	-0.5456560
C	-4.8791880	-3.7589440	0.6933070
H	-2.8543300	-4.2569410	0.1527450
C	-5.6412960	-1.5644270	0.0267790
H	-4.2098440	-0.3519110	-1.0324650
C	-5.8890770	-2.7921260	0.6493570
H	-5.0633480	-4.7181660	1.1690310
H	-6.4205880	-0.8087740	-0.0176470
H	-6.8602510	-2.9951380	1.0913610
H	0.6012660	-1.9113420	-1.3836600
O	-0.0150290	0.1494610	-1.7681940
H	-0.5375690	1.0187570	-1.3192900
H	0.8042930	0.4843740	-2.1636460
O	-1.2453960	2.0494480	-0.8454200
C	-0.5612310	3.0081200	-0.3496840
O	0.6580700	3.1025340	-0.2016170
C	-1.4620590	4.1976380	0.1096140
F	-2.1345890	4.7337430	-0.9414170
F	-0.7557170	5.1941050	0.6804630
F	-2.3900360	3.7945780	1.0140680

22.log
Potential Energy = -1489.65593
Zero-point Energy = -1489.18221
Free Energy = -1489.22598
Single-Point Energy B3LYP-D3(BJ)/6-311+G** PCM = -1490.11120
Free Energy B3LYP-D3(BJ)/6-311+G** PCM (extrapolated free energy from qRRHO) = -1489.68125
Nimag = 1 (-297.0900 cm^{-1})
Charge = 0 Multiplicity = 1

C	-3.1260970	-0.3858910	-0.7275710
C	-4.2680010	0.9950400	0.8050760
C	-2.8075580	0.9818010	1.2684260
N	-2.1382050	0.3838820	0.0885860
N	-4.3703010	0.2859820	-0.3408020
O	-5.1837310	1.6050900	1.3595050
C	-5.5566060	0.3890970	-1.1884710
H	-5.9312360	1.4138720	-1.1368390
H	-5.2849590	0.1569180	-2.2184910
H	-6.3522220	-0.2881520	-0.8678870
C	-0.8233600	0.3886520	-0.2167930
C	0.0646570	1.6046270	0.0022760
C	1.4234440	1.4957730	-0.7209620
H	1.9845670	0.6404330	-0.3347100
H	-2.7145650	0.3040990	2.1278460
C	-3.1565350	-1.9461630	-0.5310180
H	-2.9258750	-0.1804110	-1.7858330
H	-0.4799500	2.4654140	-0.3994450
C	-2.3971660	2.3896350	1.7060920
H	-1.4305290	2.4016610	2.2088380
H	-2.3825850	3.0896560	0.8668880
H	-3.1498730	2.7316580	2.4208760
C	-4.4183160	-2.5176040	-1.2163860
H	-4.3649410	-3.6106890	-1.2027230
H	-5.3360330	-2.2301250	-0.6987400
H	-4.4942940	-2.2068600	-2.2644310
C	-3.1790660	-2.3329660	0.9588760
H	-4.0447760	-1.9028280	1.4742120
H	-3.2528140	-3.4215220	1.0532110

H	-2.2664890	-2.0163420	1.4701080
C	-1.9350340	-2.5846600	-1.2275560
H	-1.8760850	-2.2882810	-2.2817160
H	-0.9942840	-2.3362720	-0.7379580
H	-2.0330700	-3.6747520	-1.1992640
H	0.2263430	1.8004290	1.0643410
H	1.2454710	1.3072060	-1.7862130
C	2.2478580	2.7572950	-0.5602150
C	2.1234780	3.8188840	-1.4699490
C	3.1360200	2.9011170	0.5170990
C	2.8625180	4.9946460	-1.3067890
H	1.4469770	3.7224740	-2.3160030
C	3.8768710	4.0750420	0.6849160
H	3.2521410	2.0858370	1.2272960
C	3.7416340	5.1269760	-0.2269660
H	2.7550530	5.8031960	-2.0243970
H	4.5617320	4.1652680	1.5234120
H	4.3189860	6.0382010	-0.1002470
H	-0.6450800	-0.0868260	-1.1784200
O	0.0075320	-0.8582640	0.7478410
H	0.8980800	-1.3655960	0.3286360
H	0.2631080	-0.4924740	1.6097470
O	1.9343400	-2.0331700	-0.1933640
C	2.8591220	-2.3056860	0.6449780
O	2.9319900	-2.0320200	1.8437930
C	4.0318870	-3.1007970	-0.0108690
F	4.5716830	-2.4157700	-1.0509880
F	3.6018870	-4.2932170	-0.4980910
F	5.0316740	-3.3617040	0.8553060

23.log
Potential Energy = -1489.65068
Zero-point Energy = -1489.17631
Free Energy = -1489.21947
Single-Point Energy B3LYP-D3(BJ)/6-311+G** PCM = -1490.11087
Free Energy B3LYP-D3(BJ)/6-311+G** PCM (extrapolated free energy from qRRHO) = -1489.67967
Nimag = 1 (-280.3329 cm^{-1})
Charge = 0 Multiplicity = 1

C	-2.8367730	-1.0145370	-0.0039030
C	-3.3021610	1.0374540	-1.0736320
C	-1.7779870	0.9659920	-0.9746880
N	-1.5783980	-0.4511600	-0.5862440
N	-3.8291050	-0.1125360	-0.5930170
O	-3.9401320	1.9671540	-1.5695950
C	-5.2206470	-0.4720010	-0.8598700
H	-5.4882090	-0.1036580	-1.8527250
H	-5.3234360	-1.5572230	-0.8386020
H	-5.9066610	-0.0334720	-0.1307890
C	-0.4353250	-1.1697490	-0.6385420
C	0.5255010	-1.1174480	-1.8242490
C	1.3345460	-2.4207190	-2.0296550
H	0.6382300	-3.2664550	-2.0643560
H	-1.4311780	1.6165790	-0.1598950
C	-2.9179120	-1.1123690	1.5637870
H	-2.9820920	-2.0205590	-0.4150130
H	-0.0914990	-0.9795820	-2.7150820
C	-1.1550850	1.4530130	-2.2851570
H	-0.0691710	1.5218720	-2.2244550
H	-1.4353510	0.8203450	-3.1312710
H	-1.5457050	2.4571440	-2.4683730
C	-4.3627840	-1.4799310	1.9740780
H	-4.3851810	-1.6898810	3.0479440
H	-5.0645520	-0.6648010	1.7876950
H	-4.7201640	-2.3771690	1.4569670
C	-2.5428170	0.2194330	2.2385010
H	-3.2194860	1.0239730	1.9324030
H	-2.6234450	0.1182900	3.3253520
H	-1.5223850	0.5441370	2.0134470
C	-2.0175650	-2.2617930	2.0702360
H	-2.2913520	-3.2139710	1.6016670
H	-0.9501490	-2.1078990	1.9013720
H	-2.1496540	-2.3754910	3.1503810
H	1.1948190	-0.2569150	-1.7635830
H	1.7768640	-2.3488710	-3.0303640
C	2.4363380	-2.7125590	-1.0298500
C	3.6025590	-1.9304610	-1.0024660
C	2.3334510	-3.7844290	-0.1318550
C	4.6275340	-2.2006240	-0.0928780
H	3.7113350	-1.1030190	-1.6996630
C	3.3576680	-4.0606340	0.7810860
H	1.4458620	-4.4123830	-0.1464980
C	4.5077950	-3.2672710	0.8057480
H	5.5212510	-1.5828350	-0.0883850
H	3.2562840	-4.8959040	1.4684540
H	5.3053180	-3.4797530	1.5118500
H	-0.6012360	-2.1857820	-0.2903450
O	0.6962800	-0.6996370	0.6644390
H	1.2310040	0.2302480	0.4766850
H	0.2061740	-0.5737040	1.4919320
O	1.9715760	1.3650930	0.2466370
C	1.4605470	2.4463410	0.6897930
O	0.3801050	2.6260340	1.2571550
C	2.3818920	3.6828560	0.4418540
F	3.5915430	3.5235160	1.0373710
F	1.8540730	4.8302940	0.9147650
F	2.6111600	3.8650880	-0.8844740

24.log
Potential Energy = -1489.65446
Zero-point Energy = -1489.18064
Free Energy = -1489.22390
Single-Point Energy B3LYP-D3(BJ)/6-311+G** PCM = -1490.11397
Free Energy B3LYP-D3(BJ)/6-311+G** PCM (extrapolated free energy from qRRHO) = -1489.68341
Nimag = 1 (-331.0632 cm^{-1})
Charge = 0 Multiplicity = 1

C	-1.2994360	2.0527380	0.1249970
C	0.1922520	2.8433220	-1.5229660
C	0.6664490	1.4271090	-1.1922750
N	-0.4733880	0.9176870	-0.3920810
N	-0.9388050	3.1039230	-0.8287580
O	0.7219130	3.5980040	-2.3403050
C	-1.7960430	4.2332540	-1.1847940
H	-1.7725200	4.3569070	-2.2698510
H	-2.8182370	4.0249660	-0.8682300
H	-1.4618550	5.1655430	-0.7225060
C	-0.7621490	-0.3661380	-0.0754380
C	-0.6141920	-1.5173730	-1.0583240
C	-1.2642110	-2.8333620	-0.5722210
H	-1.0555090	-3.5879910	-1.3389640
H	1.5637410	1.4775030	-0.5604480
C	-1.0853200	2.4616210	1.6290910
H	-2.3568200	1.7953540	-0.0106120
H	-1.0995030	-1.1962630	-1.9854060
C	1.0215110	0.6983960	-2.4916550
H	1.5259890	-0.2497660	-2.3090410
H	0.1413290	0.5298190	-3.1173900
H	1.7117920	1.3439350	-3.0406620
C	-1.8126650	3.7981080	1.9048970
H	-1.7862490	4.0021310	2.9798610
H	-1.3325900	4.6402150	1.4028240
H	-2.8654400	3.7625450	1.6042230
C	0.4070950	2.6425090	1.9613360

H	0.8552700	3.4354260	1.3534820
H	0.5198080	2.9307150	3.0112210
H	0.9962390	1.7341670	1.8036130
C	-1.7391480	1.4150320	2.5593540
H	-2.8072620	1.3061400	2.3397690
H	-1.2932830	0.4202020	2.5068690
H	-1.6470040	1.7455200	3.5983170
H	0.4339740	-1.7070820	-1.2919060
H	-0.7701410	-3.1682720	0.3436180
C	-2.7616660	-2.7494530	-0.3448290
C	-3.3007540	-2.7797560	0.9503120
C	-3.6462660	-2.6382860	-1.4314000
C	-4.6826160	-2.6969620	1.1580750
H	-2.6346600	-2.8759290	1.8041780
C	-5.0260180	-2.5548330	-1.2293890
H	-3.2525680	-2.6256840	-2.4451390
C	-5.5498420	-2.5823750	0.0685190
H	-5.0780350	-2.7248830	2.1695430
H	-5.6922750	-2.4743300	-2.0837320
H	-6.6226150	-2.5203930	0.2265060
H	-1.6947940	-0.4253770	0.4798020
O	0.2811770	-0.9966660	1.2118330
H	1.3002480	-1.2928230	0.8848590
H	0.3886920	-0.3283220	1.9057670
O	2.5031790	-1.7423490	0.5202240
C	3.4411210	-0.8742810	0.5336810
O	3.3886960	0.3276600	0.7976980
C	4.8231340	-1.4953040	0.1565360
F	5.1943600	-2.4409000	1.0578550
F	5.8100150	-0.5778200	0.1122150
F	4.7803460	-2.0970830	-1.0591070

25.log
Potential Energy = -1489.65026
Zero-point Energy = -1489.17613
Free Energy = -1489.21937
Single-Point Energy B3LYP-D3(BJ)/6-311+G** PCM = -1490.11007
Free Energy B3LYP-D3(BJ)/6-311+G** PCM (extrapolated free energy from qRRHO) = -1489.67919
Nimag = 1 (-236.1868 cm^{-1})
Charge = 0 Multiplicity = 1

C	2.9655790	-0.7450410	0.6106690
C	4.4321080	0.7061370	-0.5284450
C	3.0214750	1.2467400	-0.7881910
N	2.2396610	0.5069990	0.2333050
N	4.3451060	-0.3543190	0.3043430
O	5.4741260	1.1958540	-0.9670610
C	5.5249760	-0.8816780	0.9865860
H	6.2083350	-0.0527500	1.1832920
H	5.2227530	-1.3319140	1.9329440
H	6.0493770	-1.6299140	0.3871820
C	1.0213930	0.8014080	0.7349330
C	0.6384340	2.2166790	1.1385650
C	-0.7581190	2.3781870	1.7796020
H	-0.9990470	1.4958420	2.3824200
H	2.6999500	0.9250300	-1.7875580
C	2.5065830	-2.0757000	-0.0899820
H	2.8711870	-0.8794080	1.6944240
H	1.3939700	2.4908450	1.8840140
C	3.0390790	2.7757330	-0.7580580
H	2.1183460	3.2047510	-1.1544030
H	3.2286320	3.1668860	0.2443520
H	3.8591140	3.0930490	-1.4074760
C	3.5745190	-3.1690130	0.1368200
H	3.1849640	-4.1250250	-0.2269840
H	4.4973810	-2.9632810	-0.4101870
H	3.8161000	-3.2970830	1.1977950
C	2.3024020	-1.8859650	-1.6041390
H	3.2211330	-1.5486300	-2.0963400
H	2.0246950	-2.8432810	-2.0575520
H	1.5021840	-1.1720600	-1.8164090
C	1.2006860	-2.5729550	0.5630510
H	1.3201040	-2.6972810	1.6459840
H	0.3511680	-1.9158500	0.3818990
H	0.9364670	-3.5508610	0.1473550
H	0.7586960	2.9180310	0.3154440
H	-0.6806330	3.2116740	2.4885040
C	-1.9123610	2.6769210	0.8344640
C	-1.8218470	3.6928950	-0.1331350
C	-3.1279210	1.9855930	0.9553580
C	-2.9075200	3.9985270	-0.9601450
H	-0.9043430	4.2661790	-0.2380510
C	-4.2173290	2.2914820	0.1341800
H	-3.2201130	1.1959480	1.6954270
C	-4.1105810	3.2981950	-0.8298360
H	-2.8131800	4.7880780	-1.7002090
H	-5.1463430	1.7396710	0.2458090
H	-4.9543790	3.5348540	-1.4712570
H	0.7140450	0.0686800	1.4776190
O	-0.2215510	0.3850130	-0.4906190
H	-1.0233320	-0.2825890	-0.1737430
H	-0.6430620	1.1944170	-0.8252770
O	-1.9813860	-1.1609470	0.2652910
C	-2.8160470	-1.5887280	-0.5979480
O	-2.9087590	-1.3359580	-1.8008490
C	-3.8506340	-2.5778900	0.0297410
F	-4.5566410	-1.9857090	1.0279140
F	-3.2326250	-3.6610840	0.5688000
F	-4.7458720	-3.0391650	-0.8679560

26.log
Potential Energy = -1489.65542
Zero-point Energy = -1489.18140
Free Energy = -1489.22461
Single-Point Energy B3LYP-D3(BJ)/6-311+G** PCM = -1490.11360
Free Energy B3LYP-D3(BJ)/6-311+G** PCM (extrapolated free energy from qRRHO) = -1489.68278
Nimag = 1 (-305.1265 cm^{-1})
Charge = 0 Multiplicity = 1

C	-2.6594770	0.3627560	0.7733560
C	-4.2758100	0.6552950	-0.9180470
C	-2.9187240	0.7163630	-1.6264930
N	-2.0180240	0.2048410	-0.5669730
N	-4.0744490	0.3832110	0.3901150
O	-5.3714230	0.7754100	-1.4692310
C	-5.1728560	-0.0572890	1.2477360
H	-5.8521990	-0.6717240	0.6526200
H	-4.7727950	-0.6541940	2.0677310
H	-5.7363230	0.7834110	1.6602630
C	-0.7497720	-0.2450180	-0.6933940
C	-0.3046190	-1.1100200	-1.8639070
C	1.0543550	-1.8112140	-1.6392890
H	1.2926120	-2.3376640	-2.5702210
H	-2.6781050	1.7664330	-1.8410500
C	-2.2165580	1.5991840	1.6391320
H	-2.4633750	-0.5465570	1.3538520
H	-1.0767310	-1.8729200	-2.0028390
C	-2.9992220	-0.0479650	-2.9501080
H	-2.1170780	0.1050020	-3.5712920
H	-3.1557290	-1.1182510	-2.7938280
H	-3.8625940	0.3461160	-3.4922410
C	-3.1864350	1.7557790	2.8321240
H	-2.7961280	2.5229440	3.5081950
H	-4.1818440	2.0760540	2.5167870

H	-3.2822160	0.8292750	3.4093380
C	-2.2211810	2.9010920	0.8176270
H	-3.2116520	3.1098630	0.3987350
H	-1.9582510	3.7440050	1.4654940
H	-1.4909580	2.8661740	0.0052040
C	-0.8116650	1.3472940	2.2284900
H	-0.7741660	0.4008310	2.7808910
H	-0.0319930	1.3428750	1.4680130
H	-0.5675670	2.1481350	2.9340290
H	-0.2604760	-0.5338740	-2.7905720
H	1.8409050	-1.0662890	-1.4918430
C	1.0622470	-2.7980890	-0.4864730
C	1.7394660	-2.5098690	0.7085210
C	0.3852410	-4.0252420	-0.5913620
C	1.7364740	-3.4194550	1.7728040
H	2.2762180	-1.5693480	0.8030810
C	0.3797110	-4.9350850	0.4686850
H	-0.1355890	-4.2746670	-1.5130770
C	1.0555220	-4.6340440	1.6571740
H	2.2687020	-3.1777590	2.6886140
H	-0.1460100	-5.8802560	0.3657520
H	1.0541170	-5.3419200	2.4809890
H	-0.3713680	-0.6084600	0.2589350
O	0.3567640	1.1356330	-0.8083270
H	1.3936680	1.0421710	-0.4225650
H	0.4171990	1.4379030	-1.7289230
O	2.6218020	0.9658580	0.0944950
C	3.5103800	1.5887680	-0.5808790
O	3.3906440	2.2229370	-1.6297590
C	4.9240020	1.4909890	0.0741950
F	5.3135130	0.1986330	0.2164190
F	4.9291690	2.0486450	1.3122650
F	5.8749020	2.1163020	-0.6485550

Formation of enamine (TS3)

Conformation name	Extrapolated Free energy (kcal/mol)
TS3-lowest	0.0
1	1.2
2	0.5
3	1.3
4	0.9
5	1.6
6	1.3
7	3.2
8	2.3
9	2.6
10	2.7
11	2.2
12	3.4
13	3.1
14	2.7
15	2.4
16	2.1
17	3.2
18	2.4
19	2.0
20	1.8
21	1.7
22	2.1
23	1.6
24	1.8

TS3-lowest.log (Enamine 2)
Potential Energy = -1489.65579
Zero-point Energy = -1489.18747
Free Energy = -1489.23284
Single-Point Energy B3LYP-D3(BJ)/6-311+G** PCM = -1490.11344
Free Energy B3LYP-D3(BJ)/6-311+G** PCM (extrapolated free energy from qRRHO) = -1489.69048
Nimag = 1 (-1187.7406 cm^{-1})
Charge = 0 Multiplicity = 1

C	-0.1574210	1.7542590	0.3996040
C	-1.3320550	2.8990120	-1.3018630
C	-0.0728660	2.3291580	-1.9627140
N	0.3945820	1.3747860	-0.9257660
N	-1.3482980	2.5141450	-0.0053190
O	-2.1909620	3.5738310	-1.8717520
C	-2.5095980	2.7435460	0.8492150
H	-3.4076800	2.6833550	0.2311380
H	-2.5520570	1.9734170	1.6201480
H	-2.4800390	3.7289410	1.3230100
C	0.9173820	0.1811110	-1.2147440
C	1.0484730	-0.9477280	-0.4019030
C	2.0034900	-2.0666860	-0.8350700
C	-0.3612370	1.7340590	-3.3362680
H	-0.8513680	2.5040260	-3.9369780
H	0.5563790	1.4420260	-3.8522550
H	-1.0291510	0.8702780	-3.2690510
H	0.6564210	3.1414950	-2.0677920
C	0.8500190	2.5471490	1.3056370
H	-0.4803160	0.8499870	0.9236530
C	0.1647760	2.8799520	2.6495070
H	0.9083580	3.2918250	3.3393230
H	-0.6254200	3.6261000	2.5408500
H	-0.2626970	1.9869650	3.1191230
C	2.0777410	1.6630800	1.6045950
H	1.7997300	0.7555850	2.1505320
H	2.6091810	1.3720320	0.6946270
H	2.7778460	2.2222560	2.2336280
C	1.3197570	3.8521460	0.6356490
H	0.4798250	4.4979330	0.3599250
H	1.9483690	4.4130820	1.3346460
H	1.9221090	3.6566850	-0.2570300
H	1.1981000	0.0736060	-2.2594320
H	-0.2430860	-1.5221250	-0.6572260
H	0.9706550	-0.8154030	0.6754280
O	-1.2610430	-2.1561810	-0.8289860
C	-2.1793160	-1.9079390	0.0354620
O	-2.1485280	-1.1296760	0.9854510
C	-3.4663560	-2.7467530	-0.2311360
F	-3.2025320	-4.0721870	-0.1611240
F	-3.9644160	-2.4934630	-1.4633050
F	-4.4354460	-2.4761230	0.6638120
H	2.0067640	-2.1345120	-1.9293480

H	-3.3245770	-0.6518550	2.3728570
O	-3.7938960	-0.2767860	3.1423840
H	-4.6103530	-0.7864980	3.2209610
H	1.6142110	-3.0216520	-0.4643030
C	3.4264910	-1.8885320	-0.3310520
C	3.8032040	-2.3726340	0.9313230
C	4.3901070	-1.2223570	-1.1040280
C	5.1026130	-2.1879600	1.4141390
H	3.0738010	-2.9012680	1.5407440
C	5.6915520	-1.0370630	-0.6271110
H	4.1234540	-0.8496190	-2.0902350
C	6.0522300	-1.5176850	0.6361200
H	5.3737700	-2.5720210	2.3936740
H	6.4236190	-0.5228690	-1.2437360
H	7.0632140	-1.3766510	1.0073250

1.log
Potential Energy = -1489.65425
Zero-point Energy = -1489.18574
Free Energy = -1489.23052
Single-Point Energy B3LYP-D3(BJ)/6-311+G** PCM = -1490.11230
Free Energy B3LYP-D3(BJ)/6-311+G** PCM (extrapolated free energy from qRRHO) = -1489.68857
Nimag = 1 (-1184.5882 cm^{-1})
Charge = 0 Multiplicity = 1

C	-2.1995800	-0.6142750	-0.4140810
C	-3.4781750	0.5370270	1.2061690
C	-2.8341940	-0.6468350	1.9347400
N	-1.8205050	-1.0833510	0.9425240
N	-3.0595710	0.5293860	-0.0801630
O	-4.2314890	1.3644400	1.7217140
C	-3.3525130	1.6336070	-0.9893400
H	-3.3871960	2.5567040	-0.4072410
H	-2.5618400	1.7096650	-1.7366250
H	-4.3152640	1.5046960	-1.4922570
C	-0.6069380	-1.5251660	1.2804200
C	0.5526290	-1.6020410	0.5059200
C	1.6791980	-2.5287680	0.9839770
H	1.4273160	-3.5651560	0.7201920
C	-2.2972410	-0.2578130	3.3076120
H	-3.1153710	0.1997900	3.8690340
H	-1.9532280	-1.1292130	3.8696260
H	-1.4818030	0.4673640	3.2303670
H	-3.5932910	-1.4296960	2.0529520
C	-2.8859690	-1.7169040	-1.2967570
H	-1.3077780	-0.2440420	-0.9279140
C	-3.2253200	-1.1160230	-2.6789220
H	-3.5546830	-1.9171600	-3.3483390
H	-4.0339460	-0.3835950	-2.6273720
H	-2.3530190	-0.6383740	-3.1388900
C	-1.9048080	-2.8871840	-1.5153570
H	-1.0018530	-2.5661840	-2.0450560
H	-1.6078170	-3.3580270	-0.5741590
H	-2.3907230	-3.6521010	-2.1296240
C	-4.1729800	-2.2557400	-0.6442030
H	-4.8895580	-1.4569750	-0.4274680
H	-4.6610040	-2.9566130	-1.3290760
H	-3.9619670	-2.8004870	0.2813860
H	-0.5165410	-1.7812550	2.3332640
H	0.9957340	-0.2431380	0.7622300
H	0.4493110	-1.5427120	-0.5756870
O	1.4463780	0.8603840	0.9428050
C	1.1773420	1.6969510	0.0050670
O	0.5343670	1.5143820	-1.0258470
C	1.7812050	3.1046700	0.2954000
F	1.5002420	3.9828990	-0.6860850
F	3.1271700	3.0404060	0.4148750
F	1.2916850	3.6117670	1.4507760
H	1.7401610	-2.4923760	2.0777460
C	3.0371140	-2.1980740	0.3922060
C	3.3270960	-2.5122570	-0.9455620
C	4.0327890	-1.5781210	1.1609950
C	4.5724690	-2.2072000	-1.5021060
H	2.5740990	-3.0056270	-1.5558950
C	5.2824270	-1.2739950	0.6104170
H	3.8293970	-1.3310590	2.2000380
C	5.5559970	-1.5855960	-0.7247450
H	4.7765900	-2.4597910	-2.5389170
H	6.0401870	-0.7957930	1.2248990
H	6.5257800	-1.3512600	-1.1541790
H	0.0036500	2.5699450	-2.4867800
O	-0.3829370	2.9644340	-3.2918480
H	0.0394720	3.8278970	-3.3845810

2.log
Potential Energy = -1489.65426
Zero-point Energy = -1489.18578
Free Energy = -1489.23079
Single-Point Energy B3LYP-D3(BJ)/6-311+G** PCM = -1490.11317
Free Energy B3LYP-D3(BJ)/6-311+G** PCM (extrapolated free energy from qRRHO) = -1489.68969
Nimag = 1 (-1170.4086 cm^{-1})
Charge = 0 Multiplicity = 1

C	-1.5988630	-1.4802660	-0.2662370
C	-1.7836370	-1.7350240	2.0758960
C	-0.3720050	-2.2012210	1.7061200
N	-0.2510530	-1.6934900	0.3168800
N	-2.4033040	-1.3087550	0.9516200
O	-2.2573110	-1.7322150	3.2134500
C	-3.6980110	-0.6359000	0.9967630
H	-3.7573780	-0.0682040	1.9275360
H	-3.7817870	0.0489080	0.1521650
H	-4.5293050	-1.3463230	0.9705110
C	0.8802550	-1.1854430	-0.1809500
C	1.0555300	-0.3468300	-1.2815550
C	2.4390800	-0.1990160	-1.9391710
H	2.5383100	-0.9548380	-2.7286760
C	0.6785340	-1.7010260	2.6912290
H	0.3745280	-2.0142270	3.6929540
H	1.6607990	-2.1344970	2.4896790
H	0.7556540	-0.6098940	2.6777190
H	-0.3654850	-3.2981280	1.6988690
C	-2.0743790	-2.6428560	-1.2084850
H	-1.6036170	-0.5396510	-0.8245750
C	-3.4764480	-2.3024900	-1.7605670
H	-3.7427830	-3.0262650	-2.5375250
H	-4.2503870	-2.3528850	-0.9914560
H	-3.5024000	-1.3054150	-2.2142700
C	-1.1088140	-2.7634690	-2.4056260
H	-1.0921020	-1.8485710	-3.0070710
H	-0.0869160	-2.9914860	-2.0901740
H	-1.4445820	-3.5772920	-3.0563730
C	-2.1306790	-3.9934270	-0.4700780
H	-2.7714200	-3.9500120	0.4165280
H	-2.5459530	-4.7552810	-1.1376450
H	-1.1349860	-4.3337370	-0.1689310
H	1.7576570	-1.4101130	0.4187240
H	0.8364150	0.9176020	-0.6076940
H	0.2386470	-0.2719870	-1.9965740
O	0.7219440	2.0371430	-0.1840330
C	-0.4606350	2.5268470	-0.3105380
O	-1.4587960	2.0051850	-0.7997700
C	-0.5494690	3.9742770	0.2619370
F	-1.7831550	4.4943590	0.1182180

F	0.3189740	4.7990000	-0.3669700
F	-0.2483990	3.9912360	1.5809470
H	-3.2350130	2.5415230	-1.1201900
O	-4.1777790	2.6414080	-1.3526460
H	-4.4031180	3.5536130	-1.1296900
H	2.4659490	0.7732520	-2.4452820
C	3.6276570	-0.3076260	-1.0029900
C	4.0272370	0.7830460	-0.2129840
C	4.3564480	-1.5030680	-0.9045150
C	5.1210860	0.6809850	0.6511350
H	3.4792150	1.7193280	-0.2779700
C	5.4518440	-1.6104470	-0.0406480
H	4.0674760	-2.3561010	-1.5140360
C	5.8373280	-0.5176950	0.7413890
H	5.4167070	1.5381540	1.2496550
H	6.0036030	-2.5445160	0.0171640
H	6.6891610	-0.5968570	1.4106160

3.log
Potential Energy = -1489.65556
Zero-point Energy = -1489.18711
Free Energy = -1489.23272
Single-Point Energy B3LYP-D3(BJ)/6-311+G** PCM = -1490.11126
Free Energy B3LYP-D3(BJ)/6-311+G** PCM (extrapolated free energy from qRRHO) = -1489.68842
Nimag = 1 (-1179.1869 cm^{-1})
Charge = 0 Multiplicity = 1

C	-1.2013630	-1.7339540	0.7129140
C	-1.1177050	-3.6126720	-0.7172050
C	-1.6616950	-2.4566270	-1.5624440
N	-1.3552170	-1.2910960	-0.6945270
N	-0.8414180	-3.1449970	0.5223580
O	-0.9435410	-4.7650760	-1.1149070
C	-0.1351030	-3.9562770	1.5092570
H	0.5758460	-4.5970220	0.9837740
H	0.4067080	-3.3027000	2.1939280
H	-0.8177720	-4.5904200	2.0819360
C	-0.9329980	-0.1174070	-1.1696340
C	-0.2532820	0.9110000	-0.5113590
C	-0.2219150	2.3048410	-1.1502730
C	-1.0529080	-2.4260030	-2.9596460
H	-1.2217150	-3.4032960	-3.4182280
H	-1.5298130	-1.6738430	-3.5924480
H	0.0247330	-2.2407850	-2.9261350
H	-2.7487850	-2.5748150	-1.6452470
C	-2.4738460	-1.4916820	1.6004530
H	-0.3529830	-1.2099080	1.1640930
C	-2.1918740	-1.9937660	3.0338400
H	-3.0137570	-1.6880500	3.6889990
H	-2.1218890	-3.0824990	3.0879670
H	-1.2690660	-1.5650560	3.4407560
C	-2.7673400	0.0204600	1.6744130
H	-1.9411110	0.5713910	2.1355860
H	-2.9653120	0.4522930	0.6898340
H	-3.6556430	0.1834210	2.2930590
C	-3.7100840	-2.2192170	1.0393240
H	-3.5369620	-3.2939580	0.9237300
H	-4.5485540	-2.0954220	1.7321010
H	-4.0222660	-1.8058470	0.0752090
H	-1.0795080	-0.0068720	-2.2411350
H	1.0767140	0.4409540	-0.7566020
H	-0.2609710	0.9172030	0.5766600
O	2.2264260	0.1224080	-0.9825350
C	3.0862490	0.5276060	-0.1172970
O	2.9027490	1.1998250	0.8937020
C	4.5306140	0.0664240	-0.4823350
F	4.9194450	0.5939970	-1.6669020
F	4.6013680	-1.2800490	-0.5923490
F	5.4288530	0.4466250	0.4465890
H	-0.1868390	2.1993680	-2.2411350
H	4.0005810	1.8736770	2.2649270
O	4.4322160	2.2804310	3.0406110
H	5.3759960	2.1094750	2.9279480
H	0.7070710	2.8039420	-0.8531760
C	-1.3978130	3.1862780	-0.7620130
C	-1.3167730	4.0402370	0.3482670
C	-2.5955710	3.1549750	-1.4933140
C	-2.4043920	4.8351340	0.7251110
H	-0.3934630	4.0857480	0.9210760
C	-3.6849090	3.9487960	-1.1224510
H	-2.6763060	2.5079940	-2.3638220
C	-3.5937260	4.7913580	-0.0090850
H	-2.3200960	5.4908600	1.5873210
H	-4.6013250	3.9133450	-1.7050760
H	-4.4382700	5.4105850	0.2791300

4.log
Potential Energy = -1489.65510
Zero-point Energy = -1489.18668
Free Energy = -1489.23265
Single-Point Energy B3LYP-D3(BJ)/6-311+G** PCM = -1490.11153
Free Energy B3LYP-D3(BJ)/6-311+G** PCM (extrapolated free energy from qRRHO) = -1489.68908
Nimag = 1 (-1209.0288 cm^{-1})
Charge = 0 Multiplicity = 1

C	-0.9401270	2.0526560	-0.5268090
C	0.3886130	3.3236300	0.9566900
C	-0.1653610	2.1532730	1.7752950
N	-0.6769740	1.2637380	0.7014760
N	-0.0408920	3.1954900	-0.3204950
O	1.1181890	4.2148540	1.3922600
C	0.4607460	4.0539170	-1.3893150
H	1.5006310	4.3046510	-1.1704420
H	0.4111530	3.5177530	-2.3378700
H	-0.1111640	4.9825910	-1.4708000
C	-0.5576810	-0.0644260	0.7360230
C	-0.6176540	-0.9867070	-0.3126710
C	-0.8340940	-2.4685790	0.0174670
C	0.8810920	1.5455200	2.7018550
H	1.2888760	2.3510730	3.3173300
H	0.4434890	0.8020010	3.3721690
H	1.7001700	1.0868330	2.1405010
H	-1.0062910	2.5233950	2.3739360
C	-2.4505060	2.4295700	-0.7319600
H	-0.5972790	1.4852250	-1.3977260
C	-2.5941270	3.2355070	-2.0418900
H	-3.6570160	3.3640340	-2.2698150
H	-2.1555060	4.2330780	-1.9673410
H	-2.1347720	2.7161540	-2.8905860
C	-3.2877350	1.1416900	-0.8691740
H	-2.9851030	0.5511160	-1.7400470
H	-3.2210720	0.5085460	0.0195050
H	-4.3398170	1.4112360	-1.0063200
C	-2.9965140	3.2634160	0.4424360
H	-2.4052730	4.1687730	0.6133830
H	-4.0205180	3.5784390	0.2177970
H	-3.0314100	2.6843880	1.3704840
H	-0.2922000	-0.4491670	1.7171800
H	0.7609080	-0.9484930	-0.6953280
H	-1.0675190	-0.6669840	-1.2511800
O	1.8543190	-0.9981530	-1.2297570
C	2.8279000	-1.2106700	-0.4182040
O	2.7911430	-1.3840490	0.7972820
C	4.2004500	-1.2363090	-1.1579500

F	4.4275660	-0.0685590	-1.8028250
F	4.2344690	-2.2258170	-2.0808260
F	5.2254450	-1.4375190	-0.3075860
H	-0.3339620	-2.7017070	0.9648200
H	4.0669490	-1.7398580	2.1323530
O	4.5993070	-1.9299470	2.9286040
H	5.5119000	-1.9916970	2.6188180
H	-0.3431410	-3.0744070	-0.7521910
C	-2.2973650	-2.8718430	0.0994090
C	-2.9636860	-3.3814290	-1.0251860
C	-3.0204420	-2.7271390	1.2939810
C	-4.3174380	-3.7288100	-0.9634140
H	-2.4177470	-3.5104260	-1.9569190
C	-4.3726400	-3.0748770	1.3620920
H	-2.5212060	-2.3434240	2.1807630
C	-5.0275300	-3.5753780	0.2312850
H	-4.8139590	-4.1229270	-1.8458230
H	-4.9127270	-2.9597100	2.2978010
H	-6.0777180	-3.8477680	0.2829440

5.log
Potential Energy = -1489.65358
Zero-point Energy = -1489.18548
Free Energy = -1489.23092
Single-Point Energy B3LYP-D3(BJ)/6-311+G** PCM = -1490.11057
Free Energy B3LYP-D3(BJ)/6-311+G** PCM (extrapolated free energy from qRRHO) = -1489.68791
Nimag = 1 (-1208.5109 cm^{-1})
Charge = 0 Multiplicity = 1

C	2.6466040	-0.5250640	0.4019880
C	3.3606550	1.6515210	-0.1760490
C	2.7555660	1.0484840	-1.4476990
N	2.0503180	-0.1376920	-0.8993410
N	3.2403340	0.7493020	0.8258790
O	3.8541620	2.7760040	-0.0857880
C	3.5661360	1.0879320	2.2079230
H	3.3127000	2.1366560	2.3757060
H	2.9791580	0.4629220	2.8820140
H	4.6294250	0.9482480	2.4229530
C	0.8606200	-0.5510580	-1.3398560
C	-0.0850030	-1.3609590	-0.7055630
C	-1.1580860	-2.0310920	-1.5761540
C	1.8902880	2.0440840	-2.2113750
H	2.4952720	2.9336360	-2.4031370
H	1.5706340	1.6435820	-3.1763530
H	1.0094930	2.3402460	-1.6345660
H	3.5788240	0.7177540	-2.0923950
C	3.6552830	-1.7248420	0.3069510
H	1.8468100	-0.7924290	1.0997210
C	4.1965910	-2.0394660	1.7190120
H	4.7731760	-2.9692460	1.6841490
H	4.8625570	-1.2585520	2.0929220
H	3.3856460	-2.1803970	2.4424440
C	2.9181730	-2.9767230	-0.2117060
H	2.1142980	-3.2838540	0.4653760
H	2.4948590	-2.8233030	-1.2082370
H	3.6269650	-3.8083510	-0.2773490
C	4.8341910	-1.4082730	-0.6323510
H	5.3660330	-0.4998610	-0.3317860
H	5.5527520	-2.2335250	-0.6024260
H	4.5084720	-1.2992130	-1.6714550
H	0.5769180	-0.1147290	-2.2942460
H	-0.7389700	-0.3002460	0.0276730
H	0.2432760	-1.9630230	0.1400670
O	-1.2720400	0.4581520	0.8094550
C	-1.8548260	1.4630760	0.2602010
O	-1.9631050	1.7302610	-0.9338530
C	-2.4757780	2.4211640	1.3221250
F	-3.0968640	3.4703300	0.7494000
F	-1.5220830	2.9118860	2.1479190
F	-3.3856630	1.7754960	2.0874320
H	-0.7173080	-2.8986870	-2.0854220
H	-2.7476650	3.1240580	-1.9224880
O	-3.0984820	3.7665430	-2.5688070
H	-3.5406980	4.4449160	-2.0426240
H	-1.4736610	-1.3348060	-2.3614100
C	-2.3730850	-2.4961390	-0.7947500
C	-3.5707040	-1.7659690	-0.8116920
C	-2.3223130	-3.6756730	-0.0344230
C	-4.6857870	-2.1961930	-0.0847890
H	-3.6318470	-0.8536740	-1.3996440
C	-3.4325700	-4.1084960	0.6964580
H	-1.4081950	-4.2648400	-0.0195860
C	-4.6199200	-3.3686740	0.6739840
H	-5.6045530	-1.6170080	-0.1143090
H	-3.3727360	-5.0250770	1.2767480
H	-5.4851860	-3.7053970	1.2376660

6.log
Potential Energy = -1489.65300
Zero-point Energy = -1489.18458
Free Energy = -1489.22976
Single-Point Energy B3LYP-D3(BJ)/6-311+G** PCM = -1490.11164
Free Energy B3LYP-D3(BJ)/6-311+G** PCM (extrapolated free energy from qRRHO) = -1489.68841
Nimag = 1 (-1198.2314 cm^{-1})
Charge = 0 Multiplicity = 1

C	2.5755320	-0.0615980	-0.4401340
C	2.5823060	-0.8704600	1.7793790
C	1.8836520	0.4918310	1.8222040
N	1.6324170	0.7357860	0.3795060
N	2.9083000	-1.1449010	0.4943020
O	2.7925320	-1.5954730	2.7524560
C	3.4317050	-2.4473690	0.0951840
H	2.9830380	-3.2097220	0.7351620
H	3.1613740	-2.6436850	-0.9432460
H	4.5191650	-2.5018640	0.1997920
C	0.5132950	1.2980290	-0.0841380
C	-0.0159840	1.2633960	-1.3744860
C	-1.0547490	2.3101680	-1.8198400
C	0.6521150	0.4886020	2.7203270
H	0.9568410	0.1219480	3.7036830
H	0.2475330	1.4953280	2.8504650
H	-0.1271290	-0.1683870	2.3250560
H	2.6029210	1.2302530	2.1969850
C	3.8098330	0.7519600	-0.9716350
H	2.0401580	-0.4841930	-1.2962760
C	4.6903240	-0.1781060	-1.8354380
H	5.4610180	0.4176240	-2.3348740
H	5.2023890	-0.9378730	-1.2407930
H	4.1058620	-0.6815810	-2.6139780
C	3.3202150	1.9096010	-1.8659370
H	2.7811740	1.5435330	-2.7459020
H	2.6719290	2.6035370	-1.3238490
H	4.1859750	2.4753890	-2.2248070
C	4.6540470	1.3291760	0.1801290
H	4.9909690	0.5508800	0.8722520
H	5.5467240	1.8112040	-0.2311200
H	4.1058260	2.0897200	0.7446590
H	-0.0795590	1.7820470	0.6864200
H	-0.7688430	0.0245730	-1.3136820
H	0.6509580	0.9698890	-2.1832680
O	-1.3948820	-0.9665530	-1.5856480
C	-1.7484070	-1.6950090	-0.5863680

O	-1.5497760	-1.5113070	0.6107590
C	-2.5317150	-2.9604770	-1.0529520
F	-1.7830670	-3.7141670	-1.8908920
F	-3.6610960	-2.6144870	-1.7133190
F	-2.8896800	-3.7400040	-0.0146300
H	-1.6203560	1.8835390	-2.6561200
H	-2.1175570	-2.3933680	2.1851710
O	-2.3454370	-2.7237410	3.0750140
H	-2.8619960	-3.5259600	2.9261710
H	-0.5254420	3.1826190	-2.2241360
C	-2.0226710	2.7752800	-0.7491230
C	-1.7779160	3.9511220	-0.0223270
C	-3.1860560	2.0440580	-0.4591550
C	-2.6645170	4.3829570	0.9698560
H	-0.8881120	4.5375090	-0.2396400
C	-4.0754670	2.4711180	0.5310110
H	-3.4010790	1.1376880	-1.0191470
C	-3.8166270	3.6424410	1.2509200
H	-2.4567320	5.2976690	1.5179280
H	-4.9720530	1.8928420	0.7359320
H	-4.5084220	3.9768370	2.0185700

7.log
Potential Energy = -1489.65094
Zero-point Energy = -1489.18265
Free Energy = -1489.22755
Single-Point Energy B3LYP-D3(BJ)/6-311+G** PCM = -1490.10884
Free Energy B3LYP-D3(BJ)/6-311+G** PCM (extrapolated free energy from qRRHO) = -1489.68545
Nimag = 1 (-1148.9197 cm^{-1})
Charge = 0 Multiplicity = 1

C	2.8422840	0.0222060	0.7162370
C	4.7535410	0.4491740	-0.6002260
C	3.5987170	0.2055680	-1.5792960
N	2.4243840	0.3170220	-0.6760040
N	4.2637490	0.3942470	0.6594600
O	5.9212320	0.6778020	-0.9188760
C	5.0768560	0.7372370	1.8211630
H	5.7753310	1.5245400	1.5309220
H	4.4308060	1.1045510	2.6198360
H	5.6510860	-0.1188510	2.1876020
C	1.3234260	1.0017670	-1.0022530
C	0.1863610	1.2912790	-0.2452910
C	-0.6028700	2.5532530	-0.6462910
H	-0.6765920	2.6006750	-1.7389510
C	3.6370330	1.1633880	-2.7637400
H	4.6136580	1.0562370	-3.2415710
H	2.8737240	0.9207550	-3.5068710
H	3.5215230	2.2051120	-2.4497760
H	3.6737870	-0.8230900	-1.9510580
C	2.5748010	-1.4488440	1.1951550
H	2.3147110	0.7086670	1.3866550
C	2.9421890	-1.5591440	2.6920130
H	2.6179500	-2.5335440	3.0710170
H	4.0180340	-1.4858640	2.8658610
H	2.4413090	-0.7889960	3.2895160
C	1.0763340	-1.7679250	1.0437300
H	0.4503260	-1.0903650	1.6318300
H	0.7566220	-1.7199660	-0.0002470
H	0.8849280	-2.7841750	1.4026040
C	3.3919460	-2.4793760	0.3927300
H	4.4660740	-2.2723040	0.4274220
H	3.2358050	-3.4750160	0.8202500
H	3.0761540	-2.5252290	-0.6540480
H	1.3092880	1.3237100	-2.0404650
H	-0.6742560	0.2125650	-0.7324520
H	-0.0357570	3.4409800	-0.3354630
C	-1.9917630	2.6410960	-0.0428930
C	-3.1391380	2.4397270	-0.8237520
C	-2.1571980	2.9447590	1.3182950
C	-4.4172890	2.5311090	-0.2618940
H	-3.0328730	2.2112770	-1.8812810
C	-3.4312060	3.0343810	1.8855480
H	-1.2812450	3.1194040	1.9388850
C	-4.5677730	2.8266600	1.0960940
H	-5.2927390	2.3734770	-0.8857830
H	-3.5367240	3.2712400	2.9406080
H	-5.5590060	2.8989660	1.5342720
H	0.2242210	1.0976300	0.8266450
O	-1.4139080	-0.5805730	-1.2306070
C	-2.2596010	-1.1566930	-0.4496740
O	-2.4032180	-1.0307770	0.7612160
C	-3.1801650	-2.1393420	-1.2363710
F	-2.4529820	-3.1242980	-1.8146040
F	-4.0905400	-2.7237740	-0.4341880
F	-3.8529650	-1.4981810	-2.2193480
H	-3.5178250	-1.8093330	2.0648750
O	-4.0032980	-2.1377200	2.8457500
H	-4.7222410	-2.6771930	2.4926620

8.log
Potential Energy = -1489.65382
Zero-point Energy = -1489.18543
Free Energy = -1489.23089
Single-Point Energy B3LYP-D3(BJ)/6-311+G** PCM = -1490.10971
Free Energy B3LYP-D3(BJ)/6-311+G** PCM (extrapolated free energy from qRRHO) = -1489.68677
Nimag = 1 (-1155.2441 cm^{-1})
Charge = 0 Multiplicity = 1

C	2.0155920	-1.1994680	0.7191720
C	3.9205020	-1.5198830	-0.6376280
C	2.7184950	-1.4563950	-1.5873390
N	1.6721310	-0.8987490	-0.6924380
N	3.4781120	-1.3184850	0.6248120
O	5.0899840	-1.7008210	-0.9792260
C	4.3965730	-1.1458380	1.7456710
H	5.2838310	-0.6201650	1.3869230
H	3.9132600	-0.5492520	2.5203160
H	4.7083920	-2.1040890	2.1711670
C	0.8281670	0.0637500	-1.0752860
C	-0.1395070	0.7476050	-0.3367150
C	-0.5812380	2.1346820	-0.8285620
H	-1.6087310	2.3129490	-0.4933410
C	3.0231210	-0.6614760	-2.8511080
H	3.8985240	-1.1150490	-3.3218030
H	2.1989430	-0.7061030	-3.5670860
H	3.2561200	0.3840090	-2.6291640
H	2.4473790	-2.4809550	-1.8678260
C	1.2989120	-2.4590000	1.3228660
H	1.7632380	-0.3266120	1.3303650
C	1.7131220	-2.6074920	2.8039190
H	1.1006830	-3.3850410	3.2713580
H	2.7576210	-2.9058080	2.9180610
H	1.5534070	-1.6798060	3.3650630
C	-0.2270850	-2.2535660	1.2714460
H	-0.5393840	-1.3734680	1.8430290
H	-0.5916600	-2.1525950	0.2464170
H	-0.7226360	-3.1236040	1.7138420
C	1.6579480	-3.7499180	0.5627120
H	2.7386800	-3.9198530	0.5266680
H	1.2084430	-4.6069790	1.0743330
H	1.2673450	-3.7427690	-0.4595490
H	0.8769210	0.2825280	-2.1387240
H	-1.3099290	-0.0159080	-0.7043150

H	-0.6000400	2.1404930	-1.9247410
C	0.3041390	3.2640330	-0.3282580
C	0.0548430	3.8708200	0.9125790
C	1.4006310	3.7122480	-1.0810850
C	0.8826100	4.8901480	1.3938500
H	-0.7962310	3.5446270	1.5059090
C	2.2301240	4.7326210	-0.6056040
H	1.6054480	3.2636160	-2.0503440
C	1.9751450	5.3243380	0.6361130
H	0.6708970	5.3477120	2.3563010
H	3.0708760	5.0679430	-1.2066140
H	2.6172200	6.1183730	1.0061990
H	-0.1246400	0.6369480	0.7472690
O	-2.3198040	-0.5629090	-1.0544830
C	-3.3533630	-0.3299340	-0.3242540
O	-3.4474100	0.3880210	0.6664760
C	-4.6035270	-1.1086410	-0.8346910
F	-4.3978880	-2.4452180	-0.7653970
F	-5.7004560	-0.8263920	-0.1086870
F	-4.8755300	-0.8041130	-2.1246060
H	-4.8319060	0.8289030	1.8819560
O	-5.4731140	1.1096570	2.5622250
H	-4.9873710	1.7187150	3.1331980

9.log
Potential Energy = -1489.65129
Zero-point Energy = -1489.18284
Free Energy = -1489.22819
Single-Point Energy B3LYP-D3(BJ)/6-311+G** PCM = -1490.10949
Free Energy B3LYP-D3(BJ)/6-311+G** PCM (extrapolated free energy from qRRHO) = -1489.68639
Nimag = 1 (-1151.9620 cm^{-1})
Charge = 0 Multiplicity = 1

C	2.4854800	-1.1826820	0.4863830
C	4.3367050	-0.0291300	-0.4153150
C	3.0962660	0.5068580	-1.1393590
N	2.0078240	0.0067150	-0.2605160
N	3.9336460	-0.9257030	0.5139370
O	5.4975780	0.3203630	-0.6344670
C	4.8588640	-1.4953200	1.4881700
H	5.5984990	-0.7348560	1.7468600
H	4.3090470	-1.7823280	2.3854100
H	5.3835930	-2.3698690	1.0925990
C	0.9766440	0.7711920	0.1179670
C	-0.0654470	0.4835860	0.9985280
C	-0.8098080	1.6321840	1.7121070
H	-0.3292650	1.8005460	2.6837060
C	3.1592200	2.0142460	-1.3526810
H	4.0825690	2.2311410	-1.8949660
H	2.3239710	2.3730850	-1.9588770
H	3.1818440	2.5603510	-0.4051120
H	3.0290650	0.0129700	-2.1159190
C	2.0848770	-2.5666320	-0.1362290
H	2.0904780	-1.1313600	1.5065390
C	2.5967460	-3.6964470	0.7849830
H	2.1857650	-4.6518030	0.4435840
H	3.6850160	-3.7878800	0.7694050
H	2.2753600	-3.5509690	1.8226100
C	0.5498850	-2.6679440	-0.2099230
H	0.0885030	-2.5918480	0.7801310
H	0.1212700	-1.8985820	-0.8563270
H	0.2720460	-3.6417370	-0.6257170
C	2.6689790	-2.7586720	-1.5488580
H	3.7576030	-2.6451500	-1.5636850
H	2.4403180	-3.7701230	-1.8996940
H	2.2314310	-2.0605560	-2.2691840
H	0.9318610	1.7242390	-0.4001670
H	-1.0747930	0.0294610	0.0625280
H	-1.8277070	1.2895270	1.9323850
C	-0.8723130	2.9519740	0.9665600
C	0.0084740	3.9965150	1.2891820
C	-1.8113900	3.1661440	-0.0558050
C	-0.0430110	5.2189640	0.6112940
H	0.7381970	3.8531990	2.0826680
C	-1.8668480	4.3860070	-0.7364650
H	-2.5061740	2.3735610	-0.3190860
C	-0.9817190	5.4175230	-0.4056710
H	0.6460360	6.0145210	0.8806630
H	-2.6045660	4.5318410	-1.5205800
H	-1.0265490	6.3667510	-0.9316820
H	0.0295870	-0.4082780	1.6179600
O	-1.9742050	-0.2999010	-0.6577600
C	-2.9233130	-0.9549510	-0.0854320
O	-3.0418730	-1.2569540	1.0977330
C	-4.0249200	-1.3754920	-1.1045700
F	-5.0171130	-2.0648450	-0.5129250
F	-4.5754650	-0.2896970	-1.6963250
F	-3.5085960	-2.1557010	-2.0823600
H	-4.3186440	-2.1996040	2.1345320
O	-4.9114780	-2.6681500	2.7522020
H	-4.4944810	-2.5815630	3.6191120

10.log
Potential Energy = -1489.65071
Zero-point Energy = -1489.18202
Free Energy = -1489.22688
Single-Point Energy B3LYP-D3(BJ)/6-311+G** PCM = -1490.10994
Free Energy B3LYP-D3(BJ)/6-311+G** PCM (extrapolated free energy from qRRHO) = -1489.68610
Nimag = 1 (-1179.5848 cm^{-1})
Charge = 0 Multiplicity = 1

C	-2.7589840	-0.3587960	-0.6907580
C	-3.8148220	0.7923480	1.0785090
C	-2.3273100	0.7110010	1.4399430
N	-1.7320350	0.3222720	0.1355180
N	-3.9887320	0.2309490	-0.1399210
O	-4.6921740	1.3035980	1.7761100
C	-5.2662060	0.2923320	-0.8420980
H	-5.7482810	1.2407210	-0.5964490
H	-5.0916720	0.2447170	-1.9178960
H	-5.9347380	-0.5227240	-0.5496270
C	-0.6312020	0.9005670	-0.3575370
C	-0.0070480	0.7113550	-1.5894580
C	0.8679780	1.8313230	-2.1939570
H	0.2273250	2.4699930	-2.8150730
C	-1.8127000	2.0021810	2.0638380
H	-2.4382510	2.2197170	2.9327800
H	-0.7816990	1.9011880	2.4110460
H	-1.8821280	2.8460500	1.3713080
H	-2.1931240	-0.1073940	2.1569460
C	-2.7184160	-1.9275920	-0.6502060
H	-2.6366330	-0.0334930	-1.7292190
C	-3.7805410	-2.4804460	-1.6265860
H	-3.6527180	-3.5635190	-1.7206380
H	-4.8009250	-2.3038980	-1.2793800
H	-3.6751440	-2.0474620	-2.6278150
C	-1.3350210	-2.4138930	-1.1209570
H	-1.1144950	-2.0921290	-2.1438900
H	-0.5397770	-2.0609760	-0.4608550
H	-1.3137030	-3.5083200	-1.1100990
C	-2.9893270	-2.4790760	0.7626590
H	-3.9409500	-2.1223530	1.1692460
H	-3.0400170	-3.5718320	0.7201580
H	-2.1881950	-2.2202670	1.4616340

H	-0.1351210	1.5590380	0.3485940
H	1.0108490	-0.2724590	-1.2412030
H	1.5874750	1.3654770	-2.8767210
C	1.6142800	2.7053130	-1.2041690
C	1.0547400	3.9099280	-0.7483710
C	2.8833730	2.3396570	-0.7275730
C	1.7371930	4.7224720	0.1625190
H	0.0782000	4.2175630	-1.1153160
C	3.5700830	3.1483780	0.1831250
H	3.3407130	1.4190240	-1.0795430
C	2.9980760	4.3426690	0.6332800
H	1.2866120	5.6519350	0.4991610
H	4.5530950	2.8484220	0.5353010
H	3.5317340	4.9734400	1.3382860
H	-0.5530880	0.1499450	-2.3480810
O	1.9359010	-1.0332650	-1.2343550
C	2.2550580	-1.4810050	-0.0708910
O	1.7196790	-1.2568950	1.0103110
C	3.4910510	-2.4285550	-0.1400090
F	3.8324900	-2.8941330	1.0765410
F	3.2378720	-3.4967520	-0.9310370
F	4.5671260	-1.7870760	-0.6503830
H	2.0375450	-1.7874030	2.7911810
O	2.0736810	-1.9703710	3.7493960
H	2.8368770	-2.5493950	3.8713870

11.log
Potential Energy = -1489.65354
Zero-point Energy = -1489.18515
Free Energy = -1489.23091
Single-Point Energy B3LYP-D3(BJ)/6-311+G** PCM = -1490.10954
Free Energy B3LYP-D3(BJ)/6-311+G** PCM (extrapolated free energy from qRRHO) = -1489.68691
Nimag = 1 (-1180.7665 cm^{-1})
Charge = 0 Multiplicity = 1

C	-1.9986950	-1.4229600	-0.5600410
C	-2.9907190	-1.9988850	1.5034270
C	-1.5235830	-1.6723660	1.8053490
N	-1.1155190	-0.9892290	0.5506270
N	-3.2109190	-1.7951420	0.1843860
O	-3.8255450	-2.3630350	2.3326280
C	-4.5515340	-1.8510430	-0.3898370
H	-5.2587920	-1.4629030	0.3460060
H	-4.5873120	-1.2309390	-1.2861550
H	-4.8439630	-2.8729440	-0.6479760
C	-0.3808400	0.1262000	0.5392600
C	0.0110900	0.9264010	-0.5355630
C	0.3609330	2.3966680	-0.2576890
H	1.0847410	2.7338360	-1.0079470
C	-1.3618610	-0.8754080	3.0939770
H	-1.8366910	-1.4460860	3.8955930
H	-0.3104390	-0.7404870	3.3587130
H	-1.8497430	0.1017300	3.0326730
H	-0.9743410	-2.6164650	1.8991720
C	-1.4161310	-2.5653590	-1.4652340
H	-2.2142410	-0.5532980	-1.1897520
C	-2.4284820	-2.8758640	-2.5903300
H	-1.9633190	-3.5517900	-3.3148350
H	-3.3283200	-3.3701570	-2.2174650
H	-2.7277240	-1.9696360	-3.1292480
C	-0.1071530	-2.0833310	-2.1190510
H	-0.2650940	-1.1972040	-2.7425660
H	0.6617720	-1.8548820	-1.3774810
H	0.2841040	-2.8740270	-2.7671430
C	-1.1345830	-3.8516980	-0.6658170
H	-2.0241580	-4.2132160	-0.1403020
H	-0.8169860	-4.6419980	-1.3535430
H	-0.3276490	-3.7115790	0.0600480
H	0.0193970	0.3909400	1.5139290
H	1.3427960	0.4085420	-0.7573400
H	0.8593640	2.4699380	0.7156010
C	-0.8442260	3.3220970	-0.2869700
C	-1.2564990	3.9198040	-1.4879320
C	-1.5834430	3.5856930	0.8768730
C	-2.3805130	4.7511550	-1.5291190
H	-0.6905990	3.7358270	-2.3983020
C	-2.7063880	4.4179660	0.8418210
H	-1.2760680	3.1412540	1.8206310
C	-3.1108820	5.0024570	-0.3632280
H	-2.6812470	5.2054550	-2.4691580
H	-3.2613830	4.6132620	1.7552400
H	-3.9818360	5.6508160	-0.3917710
H	-0.4611820	0.7500280	-1.5018810
O	2.4597270	0.1193330	-1.1005300
C	3.3036730	0.0773210	-0.1305810
O	3.1156770	0.3106820	1.0600200
C	4.7245460	-0.3363490	-0.6210950
F	5.6135470	-0.3677410	0.3899550
F	4.7029600	-1.5658520	-1.1859170
F	5.1899690	0.5315540	-1.5487610
H	4.1783810	0.2740210	2.6138850
O	4.5877200	0.2900150	3.5001150
H	5.5284430	0.1299500	3.3516050

12.log
Potential Energy = -1489.65137
Zero-point Energy = -1489.18299
Free Energy = -1489.22808
Single-Point Energy B3LYP-D3(BJ)/6-311+G** PCM = -1490.10840
Free Energy B3LYP-D3(BJ)/6-311+G** PCM (extrapolated free energy from qRRHO) = -1489.68511
Nimag = 1 (-1166.0594 cm^{-1})
Charge = 0 Multiplicity = 1

C	-2.9115690	-0.6317250	0.3494180
C	-4.3509180	0.5274750	-1.1199090
C	-2.9918330	1.2327820	-1.1976470
N	-2.1067990	0.2275280	-0.5543430
N	-4.2352880	-0.5303100	-0.2843120
O	-5.3639510	0.8609110	-1.7361660
C	-5.3015500	-1.5164980	-0.1384630
H	-5.8053890	-1.6238900	-1.1012210
H	-4.8708180	-2.4757370	0.1517000
H	-6.0407480	-1.2139810	0.6086870
C	-0.9156210	-0.1136550	-1.0555320
C	-0.0069710	-1.0788470	-0.6198500
C	0.9657450	-1.6566590	-1.6635130
H	1.3420290	-0.8448860	-2.2958210
C	-2.6329830	1.6416840	-2.6207510
H	-3.4462910	2.2661130	-2.9978850
H	-1.7149760	2.2334420	-2.6532510
H	-2.5311830	0.7755820	-3.2812790
H	-3.0342260	2.1304740	-0.5700120
C	-2.8828860	-0.2179230	1.8628610
H	-2.5470610	-1.6606430	0.2615100
C	-3.7530750	-1.2077460	2.6689900
H	-3.6080600	-1.0236710	3.7382090
H	-4.8190950	-1.0907110	2.4618330
H	-3.4725890	-2.2488400	2.4728700
C	-1.4387390	-0.3115960	2.3905150
H	-1.0379240	-1.3269490	2.3020420
H	-0.7659730	0.3746430	1.8716430
H	-1.4252990	-0.0464620	3.4525950
C	-3.4073250	1.2137750	2.0822960
H	-4.4162130	1.3486690	1.6794230

H	-3.4533350	1.4211310	3.1562150
H	-2.7452560	1.9626110	1.6366580
H	-0.5968480	0.5151310	-1.8824950
H	0.8530900	-0.1932880	0.1615880
H	0.4157490	-2.3390650	-2.3257060
C	2.1356530	-2.4125160	-1.0610830
C	3.4415020	-1.9057940	-1.1302570
C	1.9348210	-3.6509960	-0.4292470
C	4.5175750	-2.6097510	-0.5784630
H	3.6190050	-0.9527230	-1.6220200
C	3.0052690	-4.3567300	0.1266590
H	0.9329860	-4.0710440	-0.3773250
C	4.3027370	-3.8371720	0.0547560
H	5.5212090	-2.1990080	-0.6453050
H	2.8278300	-5.3135720	0.6098170
H	5.1363860	-4.3859070	0.4833670
H	-0.3441190	-1.7908280	0.1331640
O	1.6059750	0.4143070	0.8691060
C	2.1943510	1.3948080	0.2802730
O	2.1139580	1.7435190	-0.8943030
C	3.1006330	2.1963690	1.2630770
F	3.7558630	3.1939200	0.6389200
F	2.3632140	2.7488510	2.2548090
F	4.0259960	1.3959550	1.8389250
H	2.8809260	3.1120330	-1.9350250
O	3.1853600	3.7640610	-2.5948840
H	3.8755110	4.2742460	-2.1521010

13.log
Potential Energy = -1489.65086
Zero-point Energy = -1489.18293
Free Energy = -1489.22874
Single-Point Energy B3LYP-D3(BJ)/6-311+G** PCM = -1490.10774
Free Energy B3LYP-D3(BJ)/6-311+G** PCM (extrapolated free energy from qRRHO) = -1489.68561
Nimag = 1 (-1175.9065 cm^{-1})
Charge = 0 Multiplicity = 1

C	3.1581390	0.1724770	0.5004580
C	3.5154660	0.2860960	-1.8270180
C	2.2784190	-0.6004070	-1.6528610
N	2.0049990	-0.4450310	-0.2086340
N	3.8882160	0.7665370	-0.6187210
O	4.0362650	0.5664360	-2.9068380
C	4.8688790	1.8417140	-0.4988340
H	4.7315320	2.5272330	-1.3375850
H	4.7037810	2.3783530	0.4357680
H	5.8955290	1.4658310	-0.5227510
C	0.8881240	-0.7751150	0.4431770
C	-0.2731740	-1.3896950	-0.0270410
C	-1.1851510	-2.0624460	1.0145110
H	-1.2872280	-1.4066490	1.8860450
C	1.1787180	-0.1133400	-2.6040410
H	1.6179480	-0.0394500	-3.6018600
H	0.3368370	-0.8020330	-2.6560120
H	0.8128600	0.8738770	-2.3097760
H	2.5342680	-1.6433430	-1.8802860
C	4.0056060	-0.8463920	1.3508500
H	2.7876950	0.9630440	1.1634930
C	5.1660180	-0.0862630	2.0323680
H	5.6730430	-0.7580290	2.7319410
H	5.9150540	0.2608740	1.3182650
H	4.8054210	0.7755950	2.6054340
C	3.1384750	-1.4649640	2.4679050
H	2.6686790	-0.6984620	3.0951850
H	2.3596010	-2.1264210	2.0782020
H	3.7763410	-2.0722660	3.1175780
C	4.5732480	-1.9728130	0.4679170
H	5.2126350	-1.5834100	-0.3305720
H	5.1831360	-2.6452560	1.0795920
H	3.7773240	-2.5742570	0.0167630
H	0.8859250	-0.4469210	1.4800640
H	-0.2079830	-1.9186370	-0.9769720
O	-1.7001040	0.6919240	-0.8465450
C	-2.0014860	1.5818530	0.0315960
O	-1.7059610	1.6152910	1.2228240
C	-2.8508900	2.7346980	-0.5848550
F	-3.1895910	3.6552730	0.3382010
F	-3.9948660	2.2600870	-1.1284240
F	-2.1653690	3.3698150	-1.5638460
H	-0.7058630	-2.9849950	1.3699630
C	-2.5627730	-2.4132600	0.4836910
C	-3.7035170	-1.7110910	0.8990480
C	-2.7252570	-3.4635030	-0.4349340
C	-4.9712510	-2.0412720	0.4073260
H	-3.5999560	-0.8998180	1.6152010
C	-3.9885510	-3.7955610	-0.9318570
H	-1.8563660	-4.0312910	-0.7598600
C	-5.1180130	-3.0837440	-0.5122480
H	-5.8416070	-1.4851390	0.7444670
H	-4.0919040	-4.6124420	-1.6407170
H	-6.1011390	-3.3424780	-0.8947770
H	-1.0171690	-0.1940660	-0.4210170
H	-2.0238650	2.8047190	2.6442980
O	-2.0921160	3.3226880	3.4691490
H	-2.6994580	4.0461860	3.2683520

14.log
Potential Energy = -1489.65001
Zero-point Energy = -1489.18150
Free Energy = -1489.22641
Single-Point Energy B3LYP-D3(BJ)/6-311+G** PCM = -1490.10979
Free Energy B3LYP-D3(BJ)/6-311+G** PCM (extrapolated free energy from qRRHO) = -1489.68619
Nimag = 1 (-1181.5008 cm^{-1})
Charge = 0 Multiplicity = 1

C	-2.5365300	-0.2219870	0.5204660
C	-2.7903430	-2.2793990	-0.5991670
C	-1.8958920	-1.4328110	-1.5102460
N	-1.6189180	-0.2630750	-0.6498550
N	-3.0134180	-1.6041490	0.5510910
O	-3.1779470	-3.4202880	-0.8531750
C	-3.6127270	-2.2568250	1.7114510
H	-3.2481560	-3.2852330	1.7539450
H	-3.3118830	-1.7303320	2.6174470
H	-4.7045430	-2.2785830	1.6524870
C	-0.6701210	0.6620720	-0.8177660
C	0.2527520	0.8052780	-1.8527310
C	0.9477330	2.1634850	-2.0881440
C	-0.6823000	-2.2739100	-1.9242820
H	-1.0605860	-3.2165720	-2.3269990
H	-0.0833720	-1.7939930	-2.6965740
H	-0.0489940	-2.4947150	-1.0612800
H	-2.4580340	-1.1243430	-2.4010120
C	-3.6864450	0.8470010	0.3991310
H	-1.9517060	-0.0101240	1.4232960
C	-4.5518410	0.8002460	1.6789450
H	-5.2600640	1.6345140	1.6638200
H	-5.1370340	-0.1180220	1.7551850
H	-3.9429220	0.9012130	2.5846880
C	-3.0883670	2.2650360	0.2954620
H	-2.4065530	2.4852740	1.1247910
H	-2.5578770	2.4269500	-0.6467190
H	-3.9000000	2.9982100	0.3356200
C	-4.5705430	0.5795320	-0.8327950

H	-5.0350620	-0.4108190	-0.7960450
H	-5.3762200	1.3195910	-0.8724480
H	-4.0033880	0.6651800	-1.7654330
H	-0.5908840	1.3505630	0.0198940
H	0.0320640	0.2837130	-2.7837320
O	2.3857980	-0.6233270	-1.2537900
C	2.5273830	-1.2151880	-0.1193870
O	1.7372680	-1.2786640	0.8171780
C	3.9149150	-1.9174490	-0.0096120
F	4.0629130	-2.5501850	1.1682760
F	4.9211740	-1.0194210	-0.1232540
F	4.0732890	-2.8348180	-0.9917210
H	0.3177690	2.7681300	-2.7528230
H	1.3580620	-0.0278140	-1.3872180
H	1.7881650	-2.0258960	2.5606280
O	1.7228000	-2.3694170	3.4717770
H	0.8725030	-2.0525560	3.8025590
H	1.8743710	1.9706590	-2.6410320
C	1.2702530	2.9761800	-0.8486670
C	0.4357430	4.0298190	-0.4441030
C	2.4173290	2.7065150	-0.0836510
C	0.7296530	4.7868150	0.6952190
H	-0.4485600	4.2658870	-1.0310320
C	2.7154330	3.4590390	1.0556660
H	3.0868860	1.9073110	-0.3891920
C	1.8703550	4.5016920	1.4511420
H	0.0707420	5.5997530	0.9871190
H	3.6103550	3.2357670	1.6297530
H	2.1028990	5.0893900	2.3344470

15.log
Potential Energy = -1489.65263
Zero-point Energy = -1489.18455
Free Energy = -1489.23051
Single-Point Energy B3LYP-D3(BJ)/6-311+G** PCM = -1490.10882
Free Energy B3LYP-D3(BJ)/6-311+G** PCM (extrapolated free energy from qRRHO) = -1489.68670
Nimag = 1 (-1202.9716 cm^{-1})
Charge = 0 Multiplicity = 1

C	-1.6477470	-1.9980930	0.6194240
C	-1.5440690	-2.9808100	-1.5207660
C	-1.1989170	-1.5043720	-1.7393170
N	-1.0784370	-1.0195600	-0.3473450
N	-1.6758590	-3.2122820	-0.1948260
O	-1.6167740	-3.8274110	-2.4116610
C	-1.7362100	-4.5714110	0.3360410
H	-1.0787190	-5.2042590	-0.2636530
H	-1.3906640	-4.5707290	1.3700960
H	-2.7479080	-4.9841570	0.2940910
C	-0.5088200	0.1132940	0.0675460
C	0.0591230	1.1499880	-0.6763660
C	0.2753980	2.5085160	0.0076170
C	0.0675770	-1.4136910	-2.5995180
H	-0.0864130	-2.0499220	-3.4744350
H	0.2640120	-0.4014730	-2.9494860
H	0.9414500	-1.7787600	-2.0531320
H	-2.0321000	-1.0000220	-2.2450000
C	-3.0497850	-1.5806580	1.1995300
H	-0.9461080	-2.1266870	1.4519030
C	-3.5427320	-2.6834720	2.1635280
H	-4.4432040	-2.3335580	2.6777880
H	-3.8061300	-3.6060790	1.6428630
H	-2.7952810	-2.9170850	2.9303050
C	-2.9207840	-0.2763970	2.0134990
H	-2.1557190	-0.3553940	2.7948500
H	-2.6946130	0.5898970	1.3862130
H	-3.8743550	-0.0698900	2.5093940
C	-4.0819640	-1.3785300	0.0751310
H	-4.2182560	-2.2858750	-0.5217900
H	-5.0529010	-1.1229480	0.5113230
H	-3.7986880	-0.5588090	-0.5930630
H	-0.4252090	0.1794490	1.1498550
H	-0.2109090	1.2156640	-1.7294310
O	2.5863500	0.4708880	-1.0042180
C	3.2817210	0.2139730	0.0464920
O	2.9166190	0.1741690	1.2180810
C	4.7730010	-0.0736520	-0.3067530
F	5.5043800	-0.3453040	0.7910350
F	5.3390590	0.9899850	-0.9226320
F	4.8785840	-1.1333300	-1.1415330
H	1.4213470	0.6886840	-0.7775840
H	3.7448250	-0.2009390	2.8652140
O	4.0202790	-0.3792480	3.7848260
H	4.9764060	-0.5094480	3.7460940
H	1.1353630	3.0013500	-0.4610710
H	0.5439410	2.3465540	1.0573820
C	-0.9251220	3.4363380	-0.0748040
C	-1.7871760	3.6057020	1.0190760
C	-1.2042340	4.1392230	-1.2582050
C	-2.9024720	4.4461650	0.9329610
H	-1.5810690	3.0816780	1.9492740
C	-2.3181840	4.9783410	-1.3502850
H	-0.5414010	4.0319190	-2.1138170
C	-3.1736740	5.1337950	-0.2537940
H	-3.5546970	4.5659850	1.7936350
H	-2.5147010	5.5146270	-2.2745610
H	-4.0377890	5.7882730	-0.3223260

16.log
Potential Energy = -1489.65301
Zero-point Energy = -1489.18503
Free Energy = -1489.23095
Single-Point Energy B3LYP-D3(BJ)/6-311+G** PCM = -1490.10925
Free Energy B3LYP-D3(BJ)/6-311+G** PCM (extrapolated free energy from qRRHO) = -1489.68719
Nimag = 1 (-1172.7140 cm^{-1})
Charge = 0 Multiplicity = 1

C	2.7467140	-1.4089580	-0.5812360
C	2.2282760	-2.6018590	1.3847600
C	1.3111580	-1.3749960	1.4057380
N	1.5485490	-0.8050750	0.0623380
N	2.9130310	-2.6217610	0.2184620
O	2.2728250	-3.4640330	2.2624080
C	3.6603010	-3.8033780	-0.2030700
H	3.1141790	-4.6900790	0.1253740
H	3.7399670	-3.8113470	-1.2904720
H	4.6628910	-3.8327530	0.2325360
C	0.8014310	0.0994820	-0.5742460
C	-0.3325000	0.7844350	-0.1323790
C	-0.7647770	2.0513040	-0.8857710
C	-0.1221780	-1.8347780	1.7008640
H	-0.0848900	-2.4682010	2.5903910
H	-0.7938440	-1.0032030	1.9081480
H	-0.5245570	-2.4230830	0.8716640
H	1.6462040	-0.6739300	2.1806860
C	4.0088790	-0.4688450	-0.5926550
H	2.4983420	-1.6776940	-1.6147750
C	5.1774240	-1.2060590	-1.2852130
H	6.0106220	-0.5095100	-1.4206910
H	5.5513650	-2.0450740	-0.6955870
H	4.8929620	-1.5762240	-2.2768980
C	3.7156450	0.8058630	-1.4108110
H	3.3641380	0.5712940	-2.4224200
H	2.9835220	1.4572400	-0.9261970

H	4.6390560	1.3846600	-1.5120210
C	4.4217750	-0.0712890	0.8362470
H	4.6590340	-0.9451870	1.4511770
H	5.3176530	0.5565050	0.7969020
H	3.6396790	0.5078590	1.3378110
H	1.1041490	0.2539710	-1.6078820
H	-0.5065050	0.8205400	0.9418460
O	-2.2573070	-0.8261510	-0.9604750
C	-3.3787680	-0.6749780	-0.3487510
O	-3.6511320	0.0798590	0.5797690
C	-4.4804890	-1.6124700	-0.9299230
F	-5.6542160	-1.4649790	-0.2864090
F	-4.1172150	-2.9116420	-0.8265820
F	-4.6965110	-1.3512420	-2.2400250
H	-1.3590980	-0.1347660	-0.5563110
H	-5.1986510	0.4475830	1.5903740
O	-5.9097640	0.7447770	2.1896000
H	-6.6845520	0.2217600	1.9470980
H	-1.8535210	2.1503630	-0.8049120
H	-0.5397480	1.9350180	-1.9520050
C	-0.1185730	3.3242110	-0.3649290
C	0.9631540	3.9155410	-1.0346590
C	-0.5872910	3.9321410	0.8110600
C	1.5673730	5.0767970	-0.5406400
H	1.3327340	3.4684010	-1.9543300
C	0.0140080	5.0910450	1.3099190
H	-1.4328640	3.4967700	1.3385220
C	1.0962700	5.6675950	0.6357120
H	2.4014730	5.5204150	-1.0773130
H	-0.3656890	5.5466030	2.2202990
H	1.5624070	6.5702450	1.0200060

17.log
Potential Energy = -1489.65085
Zero-point Energy = -1489.18269
Free Energy = -1489.22774
Single-Point Energy B3LYP-D3(BJ)/6-311+G** PCM = -1490.10845
Free Energy B3LYP-D3(BJ)/6-311+G** PCM (extrapolated free energy from qRRHO) = -1489.68534
Nimag = 1 (-1147.5580 cm^{-1})
Charge = 0 Multiplicity = 1

C	3.5330880	-0.0058360	-0.6121920
C	3.4042920	-1.5510720	1.1651460
C	2.1670000	-0.6633110	1.3167540
N	2.2241460	0.1414470	0.0799990
N	4.0498390	-1.2170440	0.0238690
O	3.7104130	-2.4712070	1.9238290
C	5.1040350	-2.0645950	-0.5259480
H	4.8407930	-3.1070850	-0.3355250
H	5.1746210	-1.9016020	-1.6015570
H	6.0753850	-1.8629230	-0.0657820
C	1.2585060	0.9189690	-0.4153500
C	0.0040750	1.2295390	0.1121410
C	-0.6801900	2.5016600	-0.4236840
C	0.9332060	-1.5621560	1.4679520
H	1.1250150	-2.2492410	2.2956640
H	0.0286770	-1.0010850	1.6963530
H	0.7676990	-2.1500800	0.5604580
H	2.2724200	-0.0173880	2.1977250
C	4.4785010	1.2459160	-0.4658250
H	3.3556690	-0.1930250	-1.6780840
C	5.7923350	0.9737280	-1.2332010
H	6.3946020	1.8873520	-1.2489600
H	6.3982160	0.1964190	-0.7642530
H	5.6017480	0.6868780	-2.2737480
C	3.8264460	2.4937150	-1.0988310
H	3.5283040	2.3192670	-2.1392990
H	2.9560810	2.8446560	-0.5375970
H	4.5539830	3.3113290	-1.1007910
C	4.7922550	1.5349320	1.0136060
H	5.2878460	0.6886500	1.4994620
H	5.4654890	2.3952220	1.0838360
H	3.8877510	1.7816020	1.5793250
H	1.4895410	1.3101230	-1.4036240
H	-0.1485480	1.0481110	1.1755110
O	-1.4300380	-0.6631700	-1.0719940
C	-2.3365110	-1.2559980	-0.3768570
O	-2.5887900	-1.1418700	0.8178750
C	-3.1760540	-2.2354290	-1.2525860
F	-4.1224150	-2.8660820	-0.5312930
F	-2.3887130	-3.1834410	-1.8120140
F	-3.7984220	-1.5765010	-2.2571310
H	-0.7708910	0.1444240	-0.4946570
H	-3.8375050	-1.9224240	1.9959970
O	-4.4098770	-2.2485250	2.7164970
H	-5.0593930	-2.8207520	2.2883490
H	-0.5701560	2.5419800	-1.5134300
H	-0.1608390	3.3833920	-0.0241830
C	-2.1495040	2.6107280	-0.0619800
C	-2.5352880	2.9603150	1.2423960
C	-3.1538180	2.3761690	-1.0123710
C	-3.8849800	3.0631050	1.5902130
H	-1.7723600	3.1599900	1.9914110
C	-4.5065700	2.4805500	-0.6706840
H	-2.8759570	2.1113390	-2.0294260
C	-4.8770540	2.8222580	0.6332900
H	-4.1615510	3.3356670	2.6049140
H	-5.2682750	2.2969790	-1.4234110
H	-5.9266050	2.9046680	0.9005920

18.log
Potential Energy = -1489.65101
Zero-point Energy = -1489.18265
Free Energy = -1489.22799
Single-Point Energy B3LYP-D3(BJ)/6-311+G** PCM = -1490.10962
Free Energy B3LYP-D3(BJ)/6-311+G** PCM (extrapolated free energy from qRRHO) = -1489.68661
Nimag = 1 (-1145.3557 cm^{-1})
Charge = 0 Multiplicity = 1

C	2.9284020	-0.6227170	-0.5075450
C	2.4269210	-2.8838830	-0.0762700
C	1.4389360	-2.0810820	0.7765820
N	1.6736970	-0.7070710	0.2856970
N	3.1434740	-2.0300050	-0.8420370
O	2.4995460	-4.1128390	-0.1041030
C	3.9804540	-2.5097040	-1.9377680
H	3.4810840	-3.3610450	-2.4049940
H	4.1019960	-1.7147530	-2.6740070
H	4.9657030	-2.8335980	-1.5906550
C	0.8937840	0.3642590	0.4615460
C	-0.2865120	0.4885830	1.1923340
C	-0.7905420	1.8840990	1.6132300
C	0.0290370	-2.6454760	0.5645950
H	0.0834520	-3.7260330	0.7174250
H	-0.6933700	-2.2420490	1.2725750
H	-0.3207610	-2.4557640	-0.4537480
H	1.7156860	-2.1589890	1.8359690
C	4.1301280	0.0426600	0.2618280
H	2.7338670	-0.0492330	-1.4216430
C	5.3622200	0.0828790	-0.6703710
H	6.1533210	0.6711770	-0.1951020
H	5.7717050	-0.9100460	-0.8654490
H	5.1292920	0.5580950	-1.6301820
C	3.7827100	1.4984200	0.6356070

H	3.4802720	2.0858580	-0.2387410
H	2.9930110	1.5599790	1.3893220
H	4.6694120	1.9785320	1.0613000
C	4.4757440	-0.7393270	1.5424020
H	4.7486190	-1.7772760	1.3274420
H	5.3317870	-0.2698510	2.0375410
H	3.6451020	-0.7366630	2.2556900
H	1.2203950	1.2292670	-0.1105590
H	-0.4853820	-0.2745320	1.9435090
O	-2.1475700	-0.1737230	-0.5689700
C	-3.2174630	-0.6481130	-0.0319240
O	-3.4540700	-0.8523000	1.1541860
C	-4.3009240	-0.9726300	-1.1043310
F	-5.4102680	-1.4974430	-0.5507090
F	-3.8363080	-1.8607380	-2.0124930
F	-4.6661800	0.1449470	-1.7742330
H	-1.2748400	0.0895040	0.2006730
H	-4.9363650	-1.4951300	2.1339430
O	-5.6087120	-1.8020590	2.7713870
H	-6.3958150	-1.9892780	2.2440210
H	-0.3687510	2.1264900	2.5965570
H	-1.8755290	1.8170680	1.7592370
C	-0.4847630	3.0235380	0.6592280
C	-1.1996940	3.1800660	-0.5405920
C	0.5147630	3.9605460	0.9632300
C	-0.9207920	4.2383410	-1.4097210
H	-1.9816000	2.4696720	-0.7943370
C	0.7970490	5.0224450	0.0968520
H	1.0739410	3.8618930	1.8905010
C	0.0799520	5.1642710	-1.0943480
H	-1.4888440	4.3430680	-2.3299320
H	1.5728900	5.7376260	0.3554740
H	0.2943360	5.9889720	-1.7679140

19.log
Potential Energy = -1489.65248
Zero-point Energy = -1489.184748
Free Energy = -1489.230437
Single-Point Energy B3LYP-D3(BJ)/6-311+G** PCM = -1490.10942
Free Energy B3LYP-D3(BJ)/6-311+G** PCM (extrapolated free energy from qRRHO) = -1489.68737
Nimag = 1 (-1194.8229 cm^{-1})
Charge = 0 Multiplicity = 1

C	3.3290180	-0.4374140	-0.7853580
C	3.7998740	-0.8514930	1.4893910
C	2.2832100	-1.0154950	1.3573420
N	2.1046080	-0.9445340	-0.1091280
N	4.3290320	-0.6286650	0.2646700
O	4.4339170	-0.9725760	2.5378790
C	5.7696060	-0.7047330	0.0370570
H	6.1791340	-1.4843560	0.6827380
H	5.9569840	-0.9641930	-1.0052260
H	6.2722180	0.2379580	0.2700630
C	1.0419450	-1.3527420	-0.8052030
C	-0.2632970	-1.5834680	-0.3641930
C	-1.1584210	-2.5001910	-1.2114380
H	-0.8606560	-3.5442980	-1.0462600
C	1.8626750	-2.3372490	2.0126510
H	2.2952770	-2.3600540	3.0156310
H	0.7823730	-2.4338250	2.1097870
H	2.2468150	-3.1908140	1.4465170
H	1.7801820	-0.1737750	1.8488090
C	3.2083580	1.0413240	-1.3057600
H	3.5590160	-1.0900420	-1.6366510
C	4.5476790	1.4637040	-1.9502730
H	4.4199160	2.4363970	-2.4354830
H	5.3490080	1.5717350	-1.2168880
H	4.8716140	0.7526620	-2.7189110
C	2.1212790	1.1239120	-2.3981660
H	2.3037450	0.4082760	-3.2086100
H	1.1150970	0.9619690	-2.0048320
H	2.1336740	2.1260280	-2.8383360
C	2.8610200	2.0074270	-0.1587120
H	3.6205520	1.9918120	0.6296240
H	2.8072350	3.0305360	-0.5442800
H	1.8889870	1.7746090	0.2874730
H	1.2261200	-1.4323290	-1.8754600
H	-0.7575650	-0.2480010	-0.5696920
H	-0.9865860	-2.2923730	-2.2741610
C	-2.6379740	-2.3679820	-0.9015290
C	-3.1790780	-2.9646770	0.2488140
C	-3.4984210	-1.6554380	-1.7494050
C	-4.5389380	-2.8450290	0.5491760
H	-2.5315460	-3.5330510	0.9126310
C	-4.8609500	-1.5355370	-1.4557710
H	-3.0998220	-1.1909560	-2.6478390
C	-5.3857730	-2.1283570	-0.3034210
H	-4.9373820	-3.3152100	1.4439160
H	-5.5103990	-0.9813800	-2.1277770
H	-6.4435640	-2.0372650	-0.0740790
H	-0.4343380	-1.6416050	0.7084240
O	-1.2453100	0.8441770	-0.7666890
C	-1.7486280	1.4142180	0.2694390
O	-1.7922430	1.0099340	1.4279260
C	-2.3652030	2.8028730	-0.0827890
F	-2.8931950	3.4070510	0.9992720
F	-1.4287740	3.6335620	-0.5977400
F	-3.3499670	2.6784230	-1.0024370
H	-2.4531100	1.6864460	3.0531970
O	-2.7320370	1.9060100	3.9629180
H	-3.2235370	2.7338800	3.8876480

20.log
Potential Energy = -1489.65454
Zero-point Energy = -1489.18650
Free Energy = -1489.23215
Single-Point Energy B3LYP-D3(BJ)/6-311+G** PCM = -1490.11007
Free Energy B3LYP-D3(BJ)/6-311+G** PCM (extrapolated free energy from qRRHO) = -1489.68768
Nimag = 1 (-1183.6187 cm^{-1})
Charge = 0 Multiplicity = 1

C	-2.9257910	-0.9239940	-0.5253150
C	-3.4250940	-0.5082010	1.7427910
C	-1.9775470	-0.0440860	1.5588550
N	-1.8195760	-0.1439780	0.0922040
N	-3.9222500	-0.8919610	0.5447350
O	-4.0486040	-0.4696020	2.8037360
C	-5.3523870	-1.1213400	0.3570240
H	-5.8993600	-0.4113640	0.9808170
H	-5.6103230	-0.9554100	-0.6892040
H	-5.6468730	-2.1343760	0.6443720
C	-0.8697680	0.4262290	-0.6504850
C	0.3727240	0.9285460	-0.2551350
C	1.0929990	1.9297090	-1.1652190
H	0.8878470	1.6766900	-2.2122650
C	-1.8233010	1.3640750	2.1469820
H	-2.2313180	1.3442510	3.1603170
H	-0.7840460	1.6833350	2.2078790
H	-2.3851920	2.0941950	1.5574330
H	-1.3018420	-0.7425730	2.0681240
C	-2.5118000	-2.3701720	-0.9836760
H	-3.3021370	-0.3742730	-1.3968320
C	-3.7506360	-3.0942270	-1.5570030
H	-3.4355740	-4.0418430	-2.0047750

H	-4.4895200	-3.3300600	-0.7887960
H	-4.2389510	-2.5059420	-2.3423540
C	-1.4622180	-2.2827610	-2.1120950
H	-1.8097850	-1.6586580	-2.9439480
H	-0.4991990	-1.9019940	-1.7642480
H	-1.2818520	-3.2865630	-2.5095410
C	-1.9371650	-3.1824440	0.1911070
H	-2.6570050	-3.2782410	1.0104040
H	-1.6885620	-4.1930240	-0.1484080
H	-1.0185440	-2.7343450	0.5830640
H	-1.0822350	0.4077290	-1.7179480
H	1.1427890	-0.2591250	-0.4392820
H	2.1729430	1.8193630	-1.0182480
C	0.7059620	3.3767720	-0.9065650
C	-0.3606050	3.9742820	-1.5960260
C	1.3971160	4.1422870	0.0451230
C	-0.7316270	5.2975220	-1.3381580
H	-0.9028560	3.4024160	-2.3455920
C	1.0285380	5.4654770	0.3087290
H	2.2328640	3.6998310	0.5821570
C	-0.0390110	6.0479650	-0.3819260
H	-1.5570160	5.7428600	-1.8867350
H	1.5779320	6.0411900	1.0484570
H	-0.3245970	7.0765910	-0.1816080
H	0.5478320	1.0719170	0.8089590
O	1.8602080	-1.2264300	-0.5984020
C	2.9891400	-1.1721880	0.0142410
O	3.4442570	-0.2686480	0.7096940
C	3.8280130	-2.4672480	-0.2107690
F	5.0138130	-2.4137880	0.4258370
F	3.1684760	-3.5577910	0.2439940
F	4.0788560	-2.6606880	-1.5264190
H	5.0382740	-0.0077060	1.6766790
O	5.8013080	0.2679330	2.2199670
H	6.4462000	-0.4461300	2.1370100

21.log
Potential Energy = -1489.65274
Zero-point Energy = -1489.18458
Free Energy = -1489.23013
Single-Point Energy B3LYP-D3(BJ)/6-311+G** PCM = -1490.11031
Free Energy B3LYP-D3(BJ)/6-311+G** PCM (extrapolated free energy from qRRHO) = -1489.68769
Nimag = 1 (-1176.9071 cm^{-1})
Charge = 0 Multiplicity = 1

C	2.9590250	-0.0971970	0.3830970
C	3.5438430	-1.8075490	-1.1324680
C	2.0946440	-1.4478880	-1.4719530
N	1.8828100	-0.2504280	-0.6316800
N	3.9952780	-0.9666350	-0.1740900
O	4.2045710	-2.6805620	-1.6961160
C	5.4146110	-0.8931800	0.1613460
H	5.9918900	-1.0551800	-0.7512780
H	5.6412440	0.0958690	0.5603480
H	5.7035140	-1.6523640	0.8933840
C	0.9180770	0.6629160	-0.7678990
C	-0.2995430	0.5486050	-1.4396420
C	-1.0670050	1.8013290	-1.8956300
H	-2.1244650	1.5275160	-1.9879860
C	1.9764400	-1.2259490	-2.9855080
H	2.4280340	-2.0884910	-3.4812960
H	0.9433390	-1.1477070	-3.3209930
H	2.5178140	-0.3251350	-3.2888870
H	1.4320640	-2.2640920	-1.1575740
C	2.5201100	-0.4686920	1.8468030
H	3.3056950	0.9436330	0.3757360
C	3.7240520	-0.2880950	2.7986440
H	3.3838880	-0.4050440	3.8323720
H	4.5056590	-1.0313400	2.6300990
H	4.1674440	0.7103810	2.7092390
C	1.4066020	0.4895840	2.3194520
H	1.7067860	1.5399750	2.2290220
H	0.4685380	0.3443380	1.7789650
H	1.1981610	0.2992980	3.3770270
C	2.0141890	-1.9205420	1.9239130
H	2.7816650	-2.6360660	1.6117190
H	1.7414320	-2.1598290	2.9567420
H	1.1226420	-2.0723450	1.3071390
H	1.0962770	1.5741250	-0.2011910
H	-1.0838020	0.0137790	-0.3639200
H	-0.7333170	2.0703260	-2.9057760
C	-0.9388130	3.0158560	-0.9958160
C	-1.7187110	3.1407010	0.1656970
C	-0.0375510	4.0464190	-1.3056870
C	-1.5999930	4.2604740	0.9938270
H	-2.4274210	2.3573990	0.4209550
C	0.0858470	5.1687710	-0.4796390
H	0.5686840	3.9724480	-2.2055300
C	-0.6954920	5.2789950	0.6744450
H	-2.2171140	4.3396780	1.8844640
H	0.7874070	5.9561340	-0.7406880
H	-0.6049750	6.1510170	1.3156390
H	-0.4232870	-0.2970180	-2.1127070
O	-1.8046220	-0.4504170	0.4903130
C	-2.8346120	-1.0800060	0.0466230
O	-3.1973540	-1.2392030	-1.1151350
C	-3.6800730	-1.6875380	1.2073340
F	-4.7648510	-2.3408200	0.7484330
F	-2.9493890	-2.5661320	1.9318880
F	-4.1112940	-0.7210830	2.0505600
H	-4.6252940	-2.1398300	-1.9507730
O	-5.2978760	-2.5613080	-2.5192880
H	-5.9209500	-2.9798680	-1.9116150

22.log
Potential Energy = -1489.65177
Zero-point Energy = -1489.18389
Free Energy = -1489.22932
Single-Point Energy B3LYP-D3(BJ)/6-311+G** PCM = -1490.10954
Free Energy B3LYP-D3(BJ)/6-311+G** PCM (extrapolated free energy from qRRHO) = -1489.68709
Nimag = 1 (-1199.7506 cm^{-1})
Charge = 0 Multiplicity = 1

C	-3.2328400	0.0939410	0.8033320
C	-4.1367980	-1.3447230	-0.8332130
C	-2.6256020	-1.5903040	-0.8726920
N	-2.1704560	-0.8228460	0.3066430
N	-4.4185080	-0.4799010	0.1677420
O	-4.9613830	-1.9039320	-1.5564820
C	-5.7897330	-0.2816580	0.6315090
H	-6.3169310	-1.2358700	0.5671330
H	-5.7754100	0.0526190	1.6690380
H	-6.3257380	0.4526260	0.0244110
C	-0.9962430	-0.9366710	0.9302350
C	0.1895020	-1.5169620	0.4733690
C	1.2250000	-1.9657100	1.5160260
H	0.8453880	-2.8518640	2.0423140
C	-2.3633260	-3.1012640	-0.8276880
H	-2.9989080	-3.5670860	-1.5845460
H	-1.3293160	-3.3570420	-1.0537430
H	-2.6261410	-3.5127660	0.1511070
H	-2.2091040	-1.1626350	-1.7933930
C	-2.9816880	1.6080110	0.4629230
H	-3.3107240	-0.0115790	1.8923280

C	-4.2024920	2.4413900	0.9124630
H	-3.9645620	3.5050930	0.8134910
H	-5.0857370	2.2491270	0.3001570
H	-4.4577990	2.2581530	1.9623160
C	-1.7576950	2.1208450	1.2496160
H	-1.8720470	1.9566020	2.3276560
H	-0.8203120	1.6625240	0.9276800
H	-1.6552200	3.1988920	1.0907820
C	-2.7521460	1.8084010	-1.0461170
H	-3.6049710	1.4569010	-1.6361000
H	-2.6231140	2.8743770	-1.2590640
H	-1.8504320	1.2938130	-1.3926350
H	-0.9670120	-0.4371920	1.8971960
H	0.7494440	-0.3636470	-0.1957210
H	1.3456240	-1.1811680	2.2715680
C	2.5775170	-2.3082450	0.9188360
C	2.7514540	-3.4980970	0.1927180
C	3.6826140	-1.4601490	1.0811370
C	3.9906800	-3.8267770	-0.3635130
H	1.9112720	-4.1773320	0.0674550
C	4.9264360	-1.7860830	0.5290280
H	3.5685050	-0.5369730	1.6427610
C	5.0844850	-2.9698550	-0.1974130
H	4.1037690	-4.7530320	-0.9200340
H	5.7700660	-1.1158190	0.6689550
H	6.0494960	-3.2251110	-0.6257140
H	0.1312060	-2.1503850	-0.4094110
O	1.2672250	0.4377030	-0.9368700
C	1.8656010	1.4175680	-0.3583950
O	1.9489950	1.6670710	0.8407940
C	2.5403330	2.3697870	-1.3920500
F	3.1817980	3.3895770	-0.7895560
F	3.4454170	1.7065500	-2.1473460
F	1.6208760	2.9033250	-2.2298550
H	2.7540260	3.0254720	1.8655230
O	3.1079470	3.6511020	2.5263520
H	3.5819860	4.3212370	2.0175850

23.log
Potential Energy = -1489.65395
Zero-point Energy = -1489.18594
Free Energy = -1489.23165
Single-Point Energy B3LYP-D3(BJ)/6-311+G** PCM = -1490.11023
Free Energy B3LYP-D3(BJ)/6-311+G** PCM (extrapolated free energy from qRRHO) = -1489.68794
Nimag = 1 (-1207.5758 cm^{-1})
Charge = 0 Multiplicity = 1

C	1.8357380	-2.0017510	0.8069500
C	3.2612390	-2.0519450	-1.0725350
C	2.2607000	-0.9287750	-1.3583270
N	1.5467820	-0.8322580	-0.0669380
N	3.0381570	-2.5376380	0.1700720
O	4.1659360	-2.4004230	-1.8313980
C	4.0096400	-3.4084200	0.8274000
H	5.0120070	-3.0892190	0.5342750
H	3.9036990	-3.3161270	1.9085440
H	3.8814260	-4.4557790	0.5413710
C	0.7797000	0.1768180	0.3472300
C	0.1721890	1.1854340	-0.4060800
C	-0.2569870	2.4800870	0.2935070
H	-0.5978740	2.2447300	1.3079380
C	3.0304950	0.3285560	-1.7830760
H	3.7138460	0.0413340	-2.5857520
H	2.3781730	1.1146490	-2.1601280
H	3.6168730	0.7242930	-0.9488370
H	1.5749790	-1.2407980	-2.1559810
C	0.6485920	-3.0269580	0.9167230
H	2.0809830	-1.6398470	1.8128040
C	1.0963080	-4.2328330	1.7727860
H	0.2301740	-4.8719230	1.9704280
H	1.8431550	-4.8478760	1.2670460
H	1.5007870	-3.9180670	2.7415800
C	-0.5478230	-2.3681120	1.6347250
H	-0.2621040	-1.9583780	2.6106780
H	-1.0091300	-1.5727170	1.0450830
H	-1.3204850	-3.1233410	1.8092100
C	0.2088970	-3.5183310	-0.4743260
H	1.0307040	-4.0013540	-1.0127850
H	-0.5923850	-4.2563180	-0.3665310
H	-0.1799250	-2.7005760	-1.0894290
H	0.5450150	0.1393070	1.4095230
H	-1.0702970	0.5419070	-0.6942430
H	-1.1198020	2.8973920	-0.2373520
C	0.8403300	3.5303950	0.3516550
C	1.7404400	3.5764970	1.4277690
C	0.9900860	4.4666540	-0.6829350
C	2.7656900	4.5262920	1.4669640
H	1.6363380	2.8672810	2.2457060
C	2.0155690	5.4172760	-0.6501140
H	0.2960660	4.4535340	-1.5201680
C	2.9086120	5.4497000	0.4256110
H	3.4486110	4.5480270	2.3117550
H	2.1127730	6.1340650	-1.4608280
H	3.7034340	6.1893830	0.4553360
H	0.5011930	1.3137340	-1.4357250
O	-2.1161300	0.1271370	-1.1587260
C	-3.1228480	0.1635420	-0.3599430
O	-3.1623690	0.5298190	0.8112390
C	-4.4234860	-0.3493360	-1.0504420
F	-5.4862640	-0.2910900	-0.2250280
F	-4.7162360	0.3880460	-2.1463440
F	-4.2846830	-1.6355170	-1.4483620
H	-4.4922510	0.6113850	2.1394900
O	-5.0632820	0.7021580	2.9263090
H	-5.9476390	0.4493480	2.6320100

24.log
Potential Energy = -1489.65274
Zero-point Energy = -1489.18457
Free Energy = -1489.23008
Single-Point Energy B3LYP-D3(BJ)/6-311+G** PCM = -1490.11033
Free Energy B3LYP-D3(BJ)/6-311+G** PCM (extrapolated free energy from qRRHO) = -1489.68767
Nimag = 1 (-1177.1316 cm^{-1})
Charge = 0 Multiplicity = 1

C	2.9618060	-0.0865770	0.3642210
C	3.5449600	-1.7715100	-1.1802500
C	2.0928870	-1.4117810	-1.5070080
N	1.8814780	-0.2275070	-0.6481950
N	3.9980810	-0.9442650	-0.2108650
O	4.2059500	-2.6331860	-1.7607690
C	5.4188520	-0.8710010	0.1186110
H	5.9921740	-1.0148280	-0.7995470
H	5.6436580	0.1118480	0.5335870
H	5.7143450	-1.6416300	0.8358910
C	0.9113860	0.6828860	-0.7642310
C	-0.3093480	0.5737050	-1.4313550
C	-1.0876200	1.8297760	-1.8583990
H	-2.1435150	1.5499780	-1.9493270
C	1.9657300	-1.1686240	-3.0165530
H	2.4194020	-2.0215190	-3.5269350
H	0.9305020	-1.0912490	-3.3456550
H	2.5007360	-0.2606640	-3.3097000
H	1.4346260	-2.2346490	-1.2009180

C	2.5303060	-0.4820040	1.8238860
H	3.3055510	0.9552160	0.3713500
C	3.7388810	-0.3174100	2.7727180
H	3.4037430	-0.4525860	3.8058660
H	4.5199460	-1.0572290	2.5874240
H	4.1813320	0.6827240	2.6987670
C	1.4195950	0.4687400	2.3178670
H	1.7197490	1.5203380	2.2425140
H	0.4785630	0.3324030	1.7802980
H	1.2167910	0.2615880	3.3733670
C	2.0243950	-1.9348380	1.8796590
H	2.7898190	-2.6452050	1.5510070
H	1.7577890	-2.1912940	2.9099760
H	1.1291080	-2.0760200	1.2658340
H	1.0875040	1.5852070	-0.1828920
H	-1.0797110	0.0076730	-0.3615410
H	-0.7617680	2.1204570	-2.8651090
C	-0.9618600	3.0275200	-0.9361170
C	-1.7374220	3.1261560	0.2308040
C	-0.0672400	4.0685930	-1.2298300
C	-1.6211380	4.2305440	1.0796890
H	-2.4416990	2.3349760	0.4738190
C	0.0537570	5.1756310	-0.3830470
H	0.5355870	4.0150360	-2.1334130
C	-0.7232930	5.2597220	0.7761290
H	-2.2350250	4.2895290	1.9741130
H	0.7500840	5.9715370	-0.6319190
H	-0.6346890	6.1198750	1.4334130
H	-0.4309980	-0.2590190	-2.1208050
O	-1.7743690	-0.5028890	0.4879370
C	-2.8387380	-1.0749220	0.0475940
O	-3.2737010	-1.1113690	-1.0996330
C	-3.6117900	-1.8066920	1.1868750
F	-4.7825030	-2.3121880	0.7532730
F	-2.8787870	-2.8345850	1.6769500
F	-3.8828750	-0.9718060	2.2152340
H	-4.7583180	-1.9102490	-1.9397790
O	-5.4641260	-2.2646170	-2.5137660
H	-6.0593720	-2.7436240	-1.9230980

Chlorination of enamine (TS4)

(*S*)-TS-front

Conformation name	Extrapolated Free energy (kcal/mol)
TS4-Sf-lowest	**0.0**
1	0.5
2	1.0
3	0.2
4	1.4
5	0.6
6	0.6
7	0.9

TS-Sf-lowest.log

Potential Energy = -2233.46980
Zero-point Energy = -2232.93920
Free Energy = -2232.98976
Single-Point Energy B3LYP-D3(BJ)/6-311+G** PCM = -2234.04089
Free Energy B3LYP-D3(BJ)/6-311+G** PCM (extrapolated free energy from qRRHO) = -2233.56086
Nimag = 1 (-171.2674 cm^{-1})
Charge = 0 Multiplicity = 1

C	1.4362000	-2.0260730	0.1852510
C	0.6589640	-2.5454550	2.3535050
C	1.9872400	-1.8056210	2.5386940
N	2.2158010	-1.2590210	1.1802660
N	0.3820540	-2.6041080	1.0309380
O	-0.0429360	-2.9908790	3.2634590
C	-0.9020110	-3.0898600	0.5364720
H	-1.6744240	-2.8186980	1.2590040
H	-1.1237620	-2.6181050	-0.4216270
H	-0.9089440	-4.1766620	0.4121940
C	2.6962700	-0.0165110	0.9672230
H	3.1743400	0.4192710	1.8393750
C	2.6298390	0.7631100	-0.1734300
C	3.4840250	2.0109890	-0.3095340
H	3.7139220	2.4055100	0.6867900
H	2.9099480	2.7835200	-0.8322730
H	2.2665530	0.3375310	-1.1023570
C	1.9217000	-0.7861010	3.6715830
H	1.5900990	-1.3082500	4.5724590
H	2.9013980	-0.3496510	3.8798890
H	1.2096700	0.0145820	3.4518760
H	2.7596910	-2.5493130	2.7731390
C	2.2850320	-3.0774390	-0.6150130
H	0.9755380	-1.3327920	-0.5265310
Cl	0.4689130	1.7273330	0.4829900
N	-1.2008020	2.5821520	0.7876870
C	-1.3399020	3.7131330	1.5954140
C	-2.3732320	2.1463290	0.2431010
C	-2.8144340	4.0976710	1.6004990
C	-3.4990880	3.0598870	0.6961410
H	-3.1780470	4.0783990	2.6314920
H	-3.9716900	3.5004970	-0.1866800
O	-2.4718490	1.1604460	-0.4986300
O	-0.4271040	4.2681930	2.1794700
C	1.3752820	-3.8038310	-1.6299300
H	1.9936850	-4.4149550	-2.2952100
H	0.6614060	-4.4734930	-1.1450620
H	0.8183980	-3.0962140	-2.2546980
C	3.3899880	-2.3456000	-1.4034120
H	2.9707990	-1.6475540	-2.1357420
H	4.0669580	-1.7934900	-0.7462370
H	3.9855440	-3.0805060	-1.9546820
C	2.9351940	-4.1129440	0.3214480
H	2.1929360	-4.6324590	0.9360870
H	3.4537290	-4.8694300	-0.2764430
H	3.6781470	-3.6526550	0.9803000
H	-4.2550230	2.4590660	1.2094640
H	-2.9121420	5.1228650	1.2333920
C	4.7781290	1.7606790	-1.0718350
C	4.8343980	1.9359080	-2.4627700
C	5.9369270	1.3332880	-0.4050200
C	6.0135370	1.6837950	-3.1717770
H	3.9493190	2.2762250	-2.9952770
C	7.1187870	1.0828490	-1.1084250
H	5.9164780	1.1995340	0.6740020
C	7.1605770	1.2552410	-2.4963600
H	6.0367420	1.8274260	-4.2484800
H	8.0066210	0.7579240	-0.5730110
H	8.0785510	1.0629090	-3.0441750

H	-3.7921740	0.5960690	-1.0643750
O	-4.5875760	0.1596840	-1.5413600
C	-5.5791260	-0.0979560	-0.7233580
O	-5.6488720	0.1226780	0.4677200
C	-6.7532220	-0.7683980	-1.4897840
F	-6.3628880	-1.9411010	-2.0385400
F	-7.1952980	0.0269540	-2.4897950
F	-7.7868040	-1.0179020	-0.6713350

1.log
Potential Energy = -2233.46971
Zero-point Energy = -2232.93890
Free Energy = -2232.98921
Single-Point Energy B3LYP-D3(BJ)/6-311+G** PCM = -2234.04053
Free Energy B3LYP-D3(BJ)/6-311+G** PCM (extrapolated free energy from qRRHO) = -2233.56003
Nimag = 1 (-171.7683 cm^{-1})
Charge = 0 Multiplicity = 1

C	-3.6684520	-1.2846770	0.0439140
C	-3.1339440	-2.8612820	-1.6305480
C	-2.9388380	-1.4799660	-2.2628740
N	-2.9850500	-0.5982410	-1.0729360
N	-3.4985410	-2.6935340	-0.3390530
O	-2.9658140	-3.9391640	-2.2042870
C	-3.5938430	-3.8190540	0.5844800
H	-2.8382370	-4.5570070	0.3076520
H	-3.4027260	-3.4714640	1.6004680
H	-4.5767530	-4.2978240	0.5472560
C	-2.1605030	0.4586480	-0.9178040
H	-1.6905320	0.7812090	-1.8419910
C	-1.8223210	1.1420680	0.2357150
C	-1.1164920	2.4843520	0.1620650
H	-0.5429530	2.5430960	-0.7700860
H	-0.3958140	2.5566160	0.9835840
H	-2.3425670	0.9332850	1.1640620
C	-1.6676740	-1.4089620	-3.1034460
H	-1.7067390	-2.2170420	-3.8380570
H	-1.5959210	-0.4648870	-3.6487410
H	-0.7717180	-1.5398480	-2.4898910
H	-3.8036920	-1.2774690	-2.9078000
C	-5.1603820	-0.8375750	0.2497230
H	-3.1164690	-1.1035410	0.9725750
Cl	0.0755730	-0.3545370	0.6944540
N	1.5740650	-1.3810250	1.2446500
C	2.8640780	-0.9720530	1.0693310
C	1.4567550	-2.6250500	1.8692570
C	3.7991320	-2.0318770	1.6256780
C	2.8650860	-3.1361220	2.1468190
H	4.4705540	-2.3625960	0.8284330
H	2.9681890	-3.3202260	3.2195200
O	0.4034320	-3.1768090	2.1303680
O	3.1889180	0.0976490	0.5386820
C	-5.7570470	-1.5887310	1.4602600
H	-6.7360890	-1.1625780	1.7019930
H	-5.9074070	-2.6518710	1.2595060
H	-5.1250830	-1.4892690	2.3501780
C	-5.2029910	0.6726930	0.5585660
H	-4.6681250	0.9126690	1.4833470
H	-4.7788860	1.2703530	-0.2525180
H	-6.2443400	0.9830880	0.6925900
C	-6.0149210	-1.1202460	-1.0000870
H	-5.9872710	-2.1767110	-1.2857080
H	-7.0588290	-0.8634470	-0.7928520
H	-5.6943830	-0.5164430	-1.8548300
H	2.9983050	-4.0915050	1.6318550
H	4.4150930	-1.5815920	2.4096780
C	-2.0765920	3.6631450	0.2459770
C	-2.3922390	4.2428020	1.4840310
C	-2.6791270	4.1853430	-0.9091200
C	-3.2919500	5.3105240	1.5690170
H	-1.9269620	3.8583670	2.3887120
C	-3.5765370	5.2542600	-0.8301860
H	-2.4407000	3.7553670	-1.8790830
C	-3.8883170	5.8197040	0.4111580
H	-3.5216100	5.7466870	2.5372550
H	-4.0280650	5.6476450	-1.7367530
H	-4.5839200	6.6515250	0.4742240
H	4.6400180	0.5562630	0.2808210
O	5.5511380	0.9935370	0.1096450
C	6.3794550	0.1925400	-0.5153900
O	6.1896900	-0.9479880	-0.8835480
C	7.7403280	0.9030150	-0.7578160
F	8.2996620	1.2878020	0.4115320
F	8.6064930	0.0914900	-1.3837460
F	7.5783660	2.0081600	-1.5198910

2.log
Potential Energy = -2233.46737
Zero-point Energy = -2232.93698
Free Energy = -2232.98725
Single-Point Energy B3LYP-D3(BJ)/6-311+G** PCM = -2234.03933
Free Energy B3LYP-D3(BJ)/6-311+G** PCM (extrapolated free energy from qRRHO) = -2233.55921
Nimag = 1 (-167.5942 cm^{-1})
Charge = 0 Multiplicity = 1

C	-3.7582770	-1.2903020	0.0612160
C	-2.6282090	-3.3491590	-0.1830060
C	-2.4951300	-2.6227220	-1.5246840
N	-2.9446640	-1.2565110	-1.1712110
N	-3.3054780	-2.5488370	0.6713530
O	-2.1764780	-4.4674510	0.0727590
C	-3.4510990	-2.8829010	2.0839360
H	-2.5559740	-3.4194740	2.4049950
H	-3.5495660	-1.9654210	2.6655410
H	-4.3215950	-3.5197630	2.2672320
C	-2.3370910	-0.1428660	-1.6402840
H	-1.7237270	-0.3211680	-2.5186430
C	-2.3848910	1.1471720	-1.1532920
C	-1.9172930	2.3062050	-2.0198820
H	-1.0772150	1.9837600	-2.6448560
H	-3.0629580	1.4002420	-0.3459600
C	-1.0892480	-2.7408880	-2.1053500
H	-0.8380130	-3.8029610	-2.1613090
H	-1.0345800	-2.3312140	-3.1168600
H	-0.3491290	-2.2411590	-1.4740110
H	-3.2074580	-3.0775090	-2.2256660
C	-5.3056810	-1.2061500	-0.1958200
H	-3.4660920	-0.4595990	0.7127990
Cl	-0.4588620	0.6652590	0.3627440
N	0.9475810	0.4923970	1.6026870
C	2.2560700	0.3560530	1.2366210
C	0.7472150	0.5238770	2.9855990
C	3.1122930	0.2815920	2.4885040
C	2.1095970	0.3747720	3.6503370
H	3.6829460	-0.6508850	2.4712050
H	2.2796910	1.2358750	4.3020250
O	-0.3349360	0.6474210	3.5288400
O	2.6484770	0.3065740	0.0646700
C	-6.0507950	-1.2070520	1.1569640
H	-7.1097410	-0.9876390	0.9863340
H	-5.9976320	-2.1741710	1.6619650
H	-5.6596430	-0.4399380	1.8350970
C	-5.6311700	0.1173390	-0.9181900
H	-5.3589230	0.9877870	-0.3121200

H	-5.1226210	0.1933590	-1.8831280
H	-6.7089750	0.1708090	-1.1031470
C	-5.8019640	-2.3836980	-1.0555470
H	-5.5617200	-3.3511810	-0.6030570
H	-6.8909000	-2.3288760	-1.1554380
H	-5.3799250	-2.3536320	-2.0649510
H	2.0959750	-0.5195130	4.2794210
H	3.8300110	1.1073040	2.4710170
H	4.1144480	0.0888980	-0.3798640
O	5.0452210	0.0058580	-0.7987800
C	5.7380100	-0.9802450	-0.2824840
O	5.4095180	-1.7524050	0.5938620
C	7.1364070	-1.0694720	-0.9546840
F	7.8324010	0.0756200	-0.7733370
F	7.8575600	-2.0780460	-0.4416560
F	7.0203220	-1.2743060	-2.2859970
H	-2.7323200	2.5690050	-2.7113840
C	-1.5332080	3.5590400	-1.2531360
C	-2.5125380	4.3185530	-0.5928070
C	-0.2029150	3.9987030	-1.2017000
C	-2.1704710	5.4771020	0.1103750
H	-3.5533530	4.0055340	-0.6331790
C	0.1445290	5.1604160	-0.5036630
H	0.5685970	3.4268470	-1.7107320
C	-0.8382740	5.9026070	0.1578690
H	-2.9437210	6.0502890	0.6143400
H	1.1815390	5.4836250	-0.4778760
H	-0.5709840	6.8047820	0.7005110

3.log
Potential Energy = -2233.46751
Zero-point Energy = -2232.93690
Free Energy = -2232.98708
Single-Point Energy B3LYP-D3(BJ)/6-311+G** PCM = -2234.04096
Free Energy B3LYP-D3(BJ)/6-311+G** PCM (extrapolated free energy from qRRHO) = -2233.56052
Nimag = 1 (-185.2852 cm^{-1})
Charge = 0 Multiplicity = 1

C	4.1883060	-0.5942920	-0.1173580
C	3.8784760	-1.1507810	2.1561150
C	3.5007990	0.3270880	2.0199240
N	3.4264230	0.4820260	0.5489490
N	4.2126800	-1.6218250	0.9332250
O	3.8595620	-1.7994760	3.2042620
C	4.4555190	-3.0407760	0.6963100
H	3.8036710	-3.6175260	1.3556340
H	4.2203530	-3.2799180	-0.3415020
H	5.4930890	-3.3193510	0.9031320
C	2.4785970	1.2282170	-0.0587720
H	1.9863450	1.9304810	0.6053870
C	2.0566760	1.1885710	-1.3731780
C	1.2203700	2.2940210	-2.0057160
H	0.4867730	1.8314010	-2.6764420
H	2.5954070	0.5796870	-2.0904700
C	2.2315120	0.6678470	2.7949610
H	2.3769340	0.3546660	3.8317380
H	2.0346480	1.7424710	2.7949010
H	1.3612070	0.1425800	2.3912820
H	4.3312890	0.9264020	2.4154520
C	5.6058360	-0.1469850	-0.6275030
H	3.6122030	-0.9752390	-0.9676110
Cl	0.4071210	-0.5897190	-0.9327190
N	-0.9070010	-1.9556400	-0.8533110
C	-2.2433120	-1.6950980	-0.7623890
C	-0.6000060	-3.3169400	-0.9140380
C	-3.0036540	-3.0101370	-0.7489200
C	-1.9118680	-4.0888190	-0.8398800
H	-3.5998200	-3.0634710	0.1662620
H	-1.9996480	-4.7199460	-1.7282390
O	0.5243860	-3.7740500	-1.0084380
O	-2.7276790	-0.5578660	-0.7031980
C	6.2962370	-1.3349560	-1.3328370
H	7.2102860	-0.9823460	-1.8215390
H	6.5858410	-2.1234850	-0.6346910
H	5.6569620	-1.7745910	-2.1069850
C	5.4443760	0.9896650	-1.6577550
H	4.8757600	0.6644600	-2.5353570
H	4.9501010	1.8653290	-1.2285500
H	6.4341220	1.3023110	-2.0062140
C	6.4934980	0.3465150	0.5305170
H	6.6114410	-0.4136630	1.3094850
H	7.4919800	0.5832970	0.1489380
H	6.0942190	1.2578310	0.9865380
H	-1.8823840	-4.7468080	0.0329320
H	-3.6966200	-3.0244700	-1.5953440
H	-4.2322830	-0.2478210	-0.5574580
O	-5.2041920	0.0770120	-0.5262050
C	-5.8759540	-0.4537370	0.4665300
O	-5.4869730	-1.2437450	1.3013030
C	-7.3421750	0.0618870	0.4648040
F	-7.9755770	-0.2992870	-0.6745780
F	-8.0339860	-0.4394450	1.4995160
F	-7.3840980	1.4102930	0.5488230
H	1.8847310	2.8838230	-2.6526390
C	0.5110260	3.2357420	-1.0511320
C	-0.7552280	2.9240800	-0.5300640
C	1.1077490	4.4489580	-0.6731060
C	-1.4041060	3.7996080	0.3463260
H	-1.2357390	1.9911900	-0.8111460
C	0.4626350	5.3270830	0.2037950
H	2.0842520	4.7111390	-1.0737000
C	-0.7972250	5.0041030	0.7174190
H	-2.3855250	3.5424920	0.7351010
H	0.9412330	6.2624820	0.4799900
H	-1.3029920	5.6856610	1.3953180

4.log
Potential Energy = -2233.46733
Zero-point Energy = -2232.93678
Free Energy = -2232.98692
Single-Point Energy B3LYP-D3(BJ)/6-311+G** PCM = -2234.03906
Free Energy B3LYP-D3(BJ)/6-311+G** PCM (extrapolated free energy from qRRHO) = -2233.55865
Nimag = 1 (-169.1557 cm^{-1})
Charge = 0 Multiplicity = 1

C	2.3315200	-2.1027860	-0.5619230
C	2.2387070	-3.1470730	1.5532530
C	3.4184580	-2.1721090	1.6073580
N	3.2012690	-1.3704900	0.3811250
N	1.6461990	-3.0365800	0.3426470
O	1.8832200	-3.8897320	2.4709260
C	0.3886080	-3.7106670	0.0388320
H	-0.2096270	-3.7521820	0.9513070
H	-0.1521440	-3.1446890	-0.7206940
H	0.5468520	-4.7322810	-0.3192110
C	3.3978360	-0.0330410	0.3386070
H	4.0277540	0.3384410	1.1416030
C	2.9031380	0.8916660	-0.5581840
C	3.5209430	2.2783460	-0.6446620
H	3.8577810	2.5942750	0.3488150
H	2.3507570	0.5614480	-1.4309200
C	3.4557230	-1.3954720	2.9205180
H	3.4479790	-2.1198850	3.7387680

H	4.3660680	-0.7982920	3.0116430
H	2.5848790	-0.7421020	3.0251070
H	4.3438680	-2.7552940	1.5121720
C	3.1112390	-2.7874540	-1.7416700
H	1.5905280	-1.4153090	-0.9841910
Cl	0.8819810	1.1958520	0.8787330
N	-0.7154320	1.5425790	1.8148560
C	-0.7413320	2.1682860	3.0645770
C	-1.9517230	1.2320780	1.3259730
C	-2.2000130	2.2936200	3.4854020
C	-3.0026220	1.6687260	2.3322340
H	-2.3370770	1.7745770	4.4378270
H	-3.6857230	2.3722520	1.8477680
O	-2.1506510	0.6838830	0.2353700
O	0.2428160	2.5350500	3.6794220
C	2.1056600	-3.4793470	-2.6880620
H	2.6293470	-3.8139260	-3.5894260
H	1.6448130	-4.3602730	-2.2355380
H	1.3095770	-2.7950880	-3.0034620
C	3.8631590	-1.7103630	-2.5503470
H	3.1758280	-0.9850530	-2.9982170
H	4.5877260	-1.1685180	-1.9364530
H	4.4106430	-2.1912080	-3.3675700
C	4.1241330	-3.8249230	-1.2222470
H	3.6443560	-4.5946060	-0.6090940
H	4.5980510	-4.3287180	-2.0709270
H	4.9198960	-3.3549130	-0.6359400
H	-3.5867580	0.7948250	2.6344040
H	-2.4289170	3.3504560	3.6472890
H	-3.5447110	0.3194480	-0.3362230
O	-4.4265390	0.1355780	-0.8220400
C	-5.0199380	-0.9518760	-0.3915060
O	-4.6506440	-1.7218310	0.4697350
C	-6.3572960	-1.1735390	-1.1521000
F	-6.1470400	-1.2793560	-2.4833810
F	-7.2027030	-0.1372190	-0.9503450
F	-6.9699500	-2.2937630	-0.7392860
H	4.4248440	2.2131120	-1.2693980
C	2.6165400	3.3422430	-1.2410680
C	2.2649410	3.2989250	-2.5999490
C	2.1291660	4.4002870	-0.4608750
C	1.4388470	4.2773500	-3.1602500
H	2.6449680	2.4969470	-3.2286620
C	1.3061900	5.3853520	-1.0176290
H	2.3941980	4.4540990	0.5918820
C	0.9551470	5.3255670	-2.3694860
H	1.1789060	4.2250070	-4.2138720
H	0.9407340	6.1971300	-0.3947480
H	0.3161190	6.0889550	-2.8038810

5.log
Potential Energy = -2233.46755
Zero-point Energy = -2232.93690
Free Energy = -2232.98702
Single-Point Energy B3LYP-D3(BJ)/6-311+G** PCM = -2234.04042
Free Energy B3LYP-D3(BJ)/6-311+G** PCM (extrapolated free energy from qRRHO) = -2233.55989
Nimag = 1 (-182.4978 cm^{-1})
Charge = 0 Multiplicity = 1

C	-1.8954910	2.4654130	-0.1473520
C	-2.4465080	2.5194600	2.1477600
C	-3.5036680	1.6414560	1.4713940
N	-2.8977740	1.4181920	0.1383960
N	-1.5567540	2.9171320	1.2097250
O	-2.4091360	2.7967130	3.3483490
C	-0.3303870	3.6235060	1.5637370
H	0.0054000	3.2645020	2.5387600
H	0.4374120	3.4127050	0.8181500
H	-0.4830430	4.7050210	1.6259610
C	-2.9475610	0.2264450	-0.4958300
H	-3.7074990	-0.4422300	-0.1061660
C	-2.1558650	-0.2368410	-1.5282260
C	-2.5159530	-1.4591580	-2.3634370
H	-1.5925380	-2.0026160	-2.5950300
H	-1.4638300	0.4394710	-2.0172750
C	-3.8159240	0.3894130	2.2849650
H	-4.1003920	0.7056680	3.2915570
H	-4.6538630	-0.1688090	1.8609110
H	-2.9457300	-0.2687580	2.3598130
H	-4.4206340	2.2361940	1.3673570
C	-2.4134340	3.5981870	-1.1048680
H	-1.0081520	2.0064930	-0.5963350
Cl	-0.4156240	-1.0628910	0.0157620
N	1.0554580	-1.7356210	1.0069190
C	0.9047710	-2.4619160	2.1912860
C	2.3545090	-1.5605350	0.6291690
C	2.2983210	-2.8256120	2.6888120
C	3.2602340	-2.2352950	1.6447800
H	2.4348770	-2.4029780	3.6879930
H	3.8599570	-2.9935780	1.1326680
O	2.7085210	-0.9459070	-0.3851650
O	-0.1622890	-2.7376270	2.7079140
C	-1.2736110	4.6067590	-1.3674340
H	-1.5810860	5.3021900	-2.1550980
H	-1.0328160	5.2032460	-0.4845970
H	-0.3600180	4.1056060	-1.7073690
C	-2.8213270	2.9776600	-2.4569360
H	-1.9720750	2.5003080	-2.9570790
H	-3.6188800	2.2382250	-2.3448110
H	-3.1892620	3.7681420	-3.1191300
C	-3.6238630	4.3378370	-0.5049710
H	-3.3967220	4.7663760	0.4765180
H	-3.9106920	5.1626800	-1.1652690
H	-4.4932370	3.6800270	-0.4084250
H	3.9490090	-1.4902400	2.0525720
H	2.3683420	-3.9130990	2.7764500
H	4.1768120	-0.6857380	-0.7844390
O	5.1050350	-0.4999680	-1.1778690
C	5.9092430	0.0666600	-0.3113950
O	5.6811260	0.3675700	0.8417500
C	7.2980440	0.3338390	-0.9557670
F	7.1839570	1.1411450	-2.0342400
F	7.8691810	-0.8215910	-1.3651070
F	8.1319770	0.9220430	-0.0844920
C	-3.5280870	-2.4156830	-1.7628530
C	-3.1215700	-3.4830520	-0.9467190
C	-4.8995220	-2.2577460	-2.0189570
C	-4.0581870	-4.3641850	-0.3974220
H	-2.0641620	-3.6262680	-0.7429340
C	-5.8404060	-3.1354730	-1.4711020
H	-5.2329840	-1.4433750	-2.6579670
C	-5.4218870	-4.1923870	-0.6564740
H	-3.7220210	-5.1863310	0.2281730
H	-6.8964730	-2.9966370	-1.6849340
H	-6.1499360	-4.8781210	-0.2328000
H	-2.8999740	-1.0999900	-3.3287060

6.log
Potential Energy = -2233.46970
Zero-point Energy = -2232.93905
Free Energy = -2232.98951
Single-Point Energy B3LYP-D3(BJ)/6-311+G** PCM = -2234.04006
Free Energy B3LYP-D3(BJ)/6-311+G** PCM (extrapolated free energy from qRRHO) = -2233.55987

Nimag = 1 (-169.4774 cm^{-1})
Charge = 0 Multiplicity = 1

C	1.3950860	-2.0067280	0.4283510
C	0.9290820	-2.3898500	2.7111870
C	2.2618500	-1.6362050	2.6642300
N	2.2935500	-1.1746490	1.2565240
N	0.4738700	-2.5331540	1.4457330
O	0.3645460	-2.7796200	3.7352760
C	-0.8556250	-3.0632200	1.1627250
H	-1.5286490	-2.7526120	1.9644640
H	-1.2129920	-2.6583030	0.2151990
H	-0.8587130	-4.1559960	1.1107260
C	2.7184810	0.0565190	0.9028700
H	3.3063360	0.5501230	1.6708350
C	2.4816200	0.7604280	-0.2634450
C	3.2844710	2.0057710	-0.5947880
H	3.6370040	2.4697750	0.3334060
H	2.6297400	2.7341880	-1.0850930
H	1.9986110	0.2738240	-1.1036760
C	2.3453660	-0.5498460	3.7317600
H	2.1455110	-1.0165650	4.6994110
H	3.3410920	-0.1023330	3.7762970
H	1.6036240	0.2366230	3.5655830
H	3.0670280	-2.3628690	2.8329900
C	2.1387220	-3.1044010	-0.4137870
H	0.8332100	-1.3619450	-0.2558050
Cl	0.4146430	1.7537730	0.6256440
N	-1.2047800	2.6239330	1.0939920
C	-1.2435580	3.8560640	1.7510980
C	-2.4366310	2.1137700	0.8043730
C	-2.7082240	4.2312820	1.9409610
C	-3.5001310	3.0757400	1.3068350
H	-2.9037780	4.3526370	3.0098740
H	-4.1211890	3.3884170	0.4624850
O	-2.6252310	1.0372570	0.2243800
O	-0.2647480	4.4910920	2.0984270
C	1.1094350	-3.8821040	-1.2631480
H	1.6400410	-4.5327380	-1.9657880
H	0.4632980	-4.5199400	-0.6558920
H	0.4769630	-3.2073350	-1.8513050
C	3.1315550	-2.4217270	-1.3763380
H	2.6199090	-1.7647560	-2.0874490
H	3.8843410	-1.8356920	-0.8425800
H	3.6547810	-3.1885730	-1.9567520
C	2.9066870	-4.0884670	0.4883160
H	2.2508190	-4.5732620	1.2187170
H	3.3508370	-4.8766900	-0.1281520
H	3.7235670	-3.5940070	1.0231170
H	-4.1462300	2.5512260	2.0165030
H	-2.8897900	5.1955210	1.4586970
C	4.4703020	1.7196880	-1.5059130
C	4.3315710	1.7802630	-2.9008330
C	5.7218490	1.3730790	-0.9735710
C	5.4108830	1.4944170	-3.7433460
H	3.3720330	2.0573410	-3.3312680
C	6.8046510	1.0893940	-1.8111300
H	5.8522220	1.3289230	0.1051290
C	6.6520820	1.1468460	-3.2007470
H	5.2832590	1.5488650	-4.8209370
H	7.7668150	0.8283910	-1.3791320
H	7.4927940	0.9287080	-3.8529590
H	-4.0145400	0.4493170	-0.1154240
O	-4.9256270	0.0070650	-0.2683420
C	-5.1716100	-0.2196350	-1.5363600
O	-4.4712630	0.0226760	-2.4963950
C	-6.5656130	-0.8870050	-1.7031680
F	-7.5419330	-0.1027060	-1.1933220
F	-6.6121780	-2.0742710	-1.0571920
F	-6.8459540	-1.1085250	-2.9966490

7.log
Potential Energy = -2233.46969
Zero-point Energy = -2232.93889
Free Energy = -2232.98902
Single-Point Energy B3LYP-D3(BJ)/6-311+G** PCM = -2234.04007
Free Energy B3LYP-D3(BJ)/6-311+G** PCM (extrapolated free energy from qRRHO) = -2233.55940
Nimag = 1 (-169.2657 cm^{-1})
Charge = 0 Multiplicity = 1

C	1.2996140	-1.9352750	0.6324310
C	0.8454910	-2.0783730	2.9448770
C	2.1951360	-1.3657420	2.8145450
N	2.2263070	-1.0484250	1.3674750
N	0.3752800	-2.3351570	1.7031670
O	0.2806820	-2.3493760	4.0065110
C	-0.9729830	-2.8479740	1.4832690
H	-1.6266920	-2.4412530	2.2575250
H	-1.3292360	-2.5240510	0.5046630
H	-1.0101160	-3.9399670	1.5361330
C	2.6817160	0.1287730	0.8893260
H	3.2897080	0.6797960	1.6005110
C	2.4539930	0.7190740	-0.3400200
C	3.2881840	1.9015090	-0.7995490
H	3.6639790	2.4444070	0.0752150
H	2.6492810	2.5969230	-1.3544130
H	1.9490470	0.1656530	-1.1241720
C	2.3095850	-0.1794730	3.7667990
H	2.1062350	-0.5418190	4.7775200
H	3.3147540	0.2486050	3.7613670
H	1.5837030	0.6021890	3.5251810
H	2.9850590	-2.0900320	3.0515190
C	2.0088670	-3.1294120	-0.1008830
H	0.7466410	-1.3475560	-0.1080210
Cl	0.4247100	1.8592730	0.4627130
N	-1.1594390	2.8222390	0.8609130
C	-1.1525850	4.0630080	1.5028280
C	-2.4072310	2.3762320	0.5347240
C	-2.5999400	4.5201990	1.6374720
C	-3.4327780	3.3983590	0.9952590
H	-2.8236110	4.6718210	2.6969080
H	-4.0150400	3.7306980	0.1310360
O	-2.6347940	1.3061260	-0.0427680
O	-0.1526790	4.6483240	1.8763170
C	0.9518150	-3.9728350	-0.8468940
H	1.4590750	-4.7034140	-1.4852420
H	0.3066790	-4.5312040	-0.1648020
H	0.3197410	-3.3527620	-1.4927350
C	2.9967670	-2.5706830	-1.1449180
H	2.4847250	-1.9812690	-1.9127470
H	3.7692450	-1.9471250	-0.6872610
H	3.4959230	-3.4038300	-1.6502810
C	2.7747850	-4.0279130	0.8882630
H	2.1229010	-4.4179840	1.6766380
H	3.1918250	-4.8867090	0.3523590
H	3.6109430	-3.4969420	1.3539240
H	-4.1229800	2.9165870	1.6937480
H	-2.7122330	5.4838230	1.1332820
C	4.4554320	1.4921780	-1.6874360
C	4.3067090	1.4296120	-3.0812210
C	5.6990190	1.1523810	-1.1324390
C	5.3682110	1.0303350	-3.8999550
H	3.3535240	1.6993330	-3.5300540
C	6.7641040	0.7556540	-1.9464270
H	5.8370820	1.2029250	-0.0549470

C	6.6014540	0.6909150	-3.3346370
H	5.2330320	0.9902140	-4.9772560
H	7.7205390	0.5019090	-1.4977070
H	7.4284850	0.3846710	-3.9686760
H	-4.0399810	0.7948480	-0.4477000
O	-4.9815630	0.4899030	-0.7087540
C	-4.9855200	-0.6646490	-1.3309880
O	-4.0435450	-1.3763150	-1.6081920
C	-6.4377840	-1.0627520	-1.7173610
F	-6.9727660	-0.1576790	-2.5685470
F	-7.2336880	-1.1210980	-0.6262270
F	-6.4684960	-2.2628790	-2.3169850

(*R*)-TS-front

Conformation name	Extrapolated Free energy (kcal/mol)
TS4-Rf-lowest	0.0
1	0.9
2	0.7
3	0.5
4	1.7
5	1.0
6	0.3

TS4-Rf-lowest.log
Potential Energy = -2233.46593
Zero-point Energy = -2232.93534
Free Energy = -2232.98602
Single-Point Energy B3LYP-D3(BJ)/6-311+G** PCM = -2234.03614
Free Energy B3LYP-D3(BJ)/6-311+G** PCM (extrapolated free energy from qRRHO) = -2233.55623
Nimag = 1 (-187.5221 cm^{-1})
Charge = 0 Multiplicity = 1

C	4.4000250	-1.2425990	-0.3594760
C	4.2129450	-2.0664110	1.8393300
C	3.2823380	-0.8511910	1.7804990
N	3.2966190	-0.5371380	0.3392030
N	4.7121860	-2.2984330	0.6045560
O	4.4118610	-2.7583960	2.8391880
C	5.4119630	-3.5398940	0.2888250
H	4.9318380	-4.3547750	0.8348710
H	5.3395200	-3.7323540	-0.7818300
H	6.4660880	-3.5032030	0.5781510
C	2.4552490	0.2707560	-0.3356960
H	2.6290590	0.2687660	-1.4081080
C	1.4126760	1.0519050	0.1282470
C	0.8313370	2.1594600	-0.7365040
H	-0.2476540	2.2259870	-0.5591040
H	1.2584990	1.1601240	1.1962360
Cl	-0.2804220	-0.6748720	-0.3578210
N	-1.7415300	-1.8426890	-0.6698720
C	-3.0299030	-1.5339690	-0.3440030
C	-1.5948840	-3.0997180	-1.2613000
C	-3.9305470	-2.6928160	-0.7353360
C	-2.9787460	-3.7310010	-1.3516370
H	-4.4456250	-3.0559920	0.1588480
H	-2.9678620	-4.6819150	-0.8121960
H	-3.1972920	-3.9473700	-2.4009530
H	-4.6932290	-2.3277820	-1.4288260
O	-0.5371680	-3.5770760	-1.6297210
O	-3.3781910	-0.4715290	0.1866930
C	1.9305190	-1.2417980	2.3917860
H	2.1311490	-1.6632810	3.3799310
H	1.2650980	-0.3889660	2.5171320
H	1.4268290	-1.9971680	1.7839970
H	3.7189960	-0.0231740	2.3553590
C	5.6337740	-0.3312190	-0.7216980
H	4.0126390	-1.6900540	-1.2831520
C	6.7020710	-1.1901250	-1.4357510
H	7.4936410	-0.5365650	-1.8155420
H	7.1738590	-1.9127300	-0.7673170
H	6.2822170	-1.7306060	-2.2919510
C	5.2093590	0.7844970	-1.6996710
H	4.7142980	0.3819690	-2.5912450
H	4.5491620	1.5202220	-1.2336770
H	6.1016010	1.3219240	-2.0363850
C	6.2432420	0.3078930	0.5393680
H	6.5846220	-0.4464230	1.2553320
H	7.1115210	0.9137530	0.2606720
H	5.5305390	0.9698650	1.0418080
H	-4.8350680	-0.0901000	0.5245130
O	-5.7464270	0.2488840	0.8492910
C	-6.6711790	0.1597230	-0.0754620
O	-6.5650670	-0.2636830	-1.2076310
C	-8.0293330	0.6888240	0.4640650
F	-7.9277010	1.9818730	0.8455330
F	-8.9878780	0.6069150	-0.4714170
F	-8.4328190	-0.0265920	1.5383770
H	0.9639280	1.9087710	-1.7946990
C	1.4610620	3.5154190	-0.4492710
C	1.0409270	4.2777710	0.6524450
C	2.4806960	4.0282750	-1.2652020
C	1.6300410	5.5129400	0.9379380
H	0.2432920	3.9033180	1.2899060
C	3.0712420	5.2651350	-0.9857490
H	2.8120050	3.4587940	-2.1300990
C	2.6496010	6.0110580	0.1193690
H	1.2893030	6.0881620	1.7943710
H	3.8561480	5.6461990	-1.6331910
H	3.1057850	6.9723950	0.3371990

1.log
Potential Energy = -2233.46286
Zero-point Energy = -2232.93195
Free Energy = -2232.98172
Single-Point Energy B3LYP-D3(BJ)/6-311+G** PCM = -2234.03590
Free Energy B3LYP-D3(BJ)/6-311+G** PCM (extrapolated free energy from qRRHO) = -2233.55476
Nimag = 1 (-208.1776 cm^{-1})
Charge = 0 Multiplicity = 1

C	-2.5843210	2.0334160	-0.0069720
C	-2.5821120	2.5607910	2.2868460
C	-2.9226860	1.0687680	2.2118540
N	-2.6792770	0.7813400	0.7849360
N	-2.2926970	3.0084830	1.0447690
O	-2.5153950	3.2209110	3.3252550
C	-1.6792330	4.3152890	0.8303970
H	-0.9761600	4.5035220	1.6446230
H	-1.1397020	4.3095740	-0.1170140
H	-2.4189970	5.1208750	0.8192480
C	-2.5630360	-0.4230960	0.1879840
H	-2.3267310	-0.3555180	-0.8693490
C	-2.6692240	-1.6897150	0.7303460
C	-2.8922710	-2.9393700	-0.1178430
H	-3.9416150	-3.2358450	0.0160930
H	-2.2973280	-3.7579180	0.3039740
H	-2.9952970	-1.7976610	1.7587640

Cl	-0.2520810	-1.8798750	1.1905940
N	1.5513880	-2.2587060	1.6481990
C	2.6188000	-1.6692550	1.0362110
C	1.9049880	-3.1703490	2.6453420
C	3.9000400	-2.2080000	1.6505560
C	3.4264490	-3.2051660	2.7207260
H	4.5025060	-2.6702330	0.8633460
H	3.7642430	-4.2286750	2.5370690
H	3.7345250	-2.9305870	3.7332170
H	4.4748000	-1.3725400	2.0602810
O	1.1153750	-3.8083350	3.3175690
O	2.5275850	-0.8339820	0.1278520
C	-2.0603430	0.3214770	3.2367250
H	-2.2023060	0.8174120	4.2002270
H	-2.3512480	-0.7220030	3.3484030
H	-1.0018550	0.3678790	2.9713090
H	-3.9842900	0.9200160	2.4527850
C	-3.8714370	2.3799110	-0.8479500
H	-1.7298120	1.9615550	-0.6907740
C	-3.6289030	3.6975600	-1.6186960
H	-4.4587680	3.8663240	-2.3122130
H	-3.5782470	4.5658450	-0.9591060
H	-2.7076790	3.6564890	-2.2112410
C	-4.1427160	1.2779420	-1.8923940
H	-3.2698630	1.0921420	-2.5288510
H	-4.4473190	0.3336240	-1.4346820
H	-4.9611960	1.5982860	-2.5449750
C	-5.1071610	2.5315110	0.0578000
H	-4.9729910	3.3200200	0.8050030
H	-5.9768250	2.7998270	-0.5507730
H	-5.3463260	1.5966220	0.5748700
C	-2.6136960	-2.8280040	-1.6052570
C	-1.3214530	-3.0148390	-2.1226900
C	-3.6573260	-2.5612420	-2.5055500
C	-1.0783870	-2.9285620	-3.4968680
H	-0.5017090	-3.2334570	-1.4449150
C	-3.4197890	-2.4745670	-3.8810220
H	-4.6676110	-2.4273490	-2.1262930
C	-2.1270880	-2.6566040	-4.3816850
H	-0.0715910	-3.0803170	-3.8759670
H	-4.2439610	-2.2709350	-4.5589300
H	-1.9397790	-2.5938870	-5.4497600
H	3.7252460	-0.1400000	-0.5623340
O	4.4610530	0.2905460	-1.1300920
C	4.9584850	1.3695140	-0.5751840
O	4.6588170	1.8799650	0.4834820
C	6.0608560	1.9834860	-1.4829980
F	5.5526130	2.3384090	-2.6849450
F	6.5979500	3.0775880	-0.9214390
F	7.0569140	1.0960850	-1.7034010

2.log
Potential Energy = -2233.46590
Zero-point Energy = -2232.93524
Free Energy = -2232.98560
Single-Point Energy B3LYP-D3(BJ)/6-311+G** PCM = -2234.03546
Free Energy B3LYP-D3(BJ)/6-311+G** PCM (extrapolated free energy from qRRHO) = -2233.55515
Nimag = 1 (-185.9689 cm^{-1})
Charge = 0 Multiplicity = 1

C	1.1550040	2.5438430	-0.1961330
C	1.1257300	2.5353320	-2.5514090
C	1.9157310	1.2859100	-2.1508830
N	1.7031090	1.2563890	-0.6916680
N	0.6377590	3.1238870	-1.4363430
O	0.9132840	2.8975160	-3.7098390
C	-0.3733170	4.1740460	-1.5130640
H	-1.0466950	3.9435480	-2.3413940
H	-0.9418950	4.1971180	-0.5830920
H	0.0685050	5.1587110	-1.6903890
C	1.9468610	0.2363010	0.1548110
H	1.6268760	0.4394610	1.1728580
C	2.5004900	-1.0065790	-0.0910560
C	3.0186490	-1.8631180	1.0535660
H	2.8174920	-2.9175410	0.8346830
H	2.9203470	-1.2230150	-1.0672810
Cl	0.2988060	-2.0946630	-0.3529930
N	-1.2685800	-3.1352170	-0.5747340
C	-2.5225670	-2.6556310	-0.3303050
C	-1.2456090	-4.4630630	-1.0074390
C	-3.5346300	-3.7533900	-0.6130270
C	-2.6868230	-4.9547350	-1.0628520
H	-4.1110470	-3.9457640	0.2964570
H	-2.7872550	-5.8237760	-0.4070710
H	-2.9076240	-5.2813390	-2.0826450
H	-4.2324250	-3.4033420	-1.3791750
O	-0.2380800	-5.0880710	-1.2836680
O	-2.7642770	-1.5065780	0.0593500
C	1.3813730	0.0923370	-2.9532330
H	1.4027480	0.3750300	-4.0086370
H	1.9912110	-0.8015520	-2.8306620
H	0.3513360	-0.1408250	-2.6730860
H	2.9803720	1.4331080	-2.3783190
C	2.2033630	3.4598250	0.5424720
H	0.3246230	2.3398660	0.4909430
C	1.5043010	4.7616870	0.9956500
H	2.1871170	5.3332990	1.6321030
H	1.2313800	5.4045040	0.1567530
H	0.6025130	4.5544300	1.5832880
C	2.7321820	2.7561120	1.8098590
H	1.9175180	2.4371210	2.4706860
H	3.3560720	1.8893740	1.5779840
H	3.3547070	3.4580500	2.3737410
C	3.3889610	3.8027930	-0.3777710
H	3.0654450	4.3278510	-1.2821160
H	4.0869710	4.4592030	0.1518880
H	3.9434930	2.9063340	-0.6734900
H	-4.1784070	-0.9384690	0.3313930
O	-5.1271040	-0.5877290	0.4899330
C	-5.1431090	0.6237500	0.9918000
O	-4.2037510	1.3355620	1.2774030
C	-6.6082680	1.1002110	1.1996930
F	-7.2758880	0.2675640	2.0297900
F	-6.6469250	2.3322560	1.7303120
F	-7.2760790	1.1316240	0.0240190
H	2.4726570	-1.6196800	1.9716140
C	4.5128930	-1.6862680	1.2851020
C	5.4439310	-2.3632170	0.4811630
C	4.9946960	-0.8372640	2.2928140
C	6.8179160	-2.1887530	0.6707070
H	5.0904430	-3.0355870	-0.2971710
C	6.3685420	-0.6616950	2.4887330
H	4.2900800	-0.3135260	2.9341820
C	7.2856690	-1.3350670	1.6757450
H	7.5218790	-2.7231750	0.0388150
H	6.7206250	-0.0031010	3.2778920
H	8.3528570	-1.2012630	1.8271800

3.log
Potential Energy = -2233.46576
Zero-point Energy = -2232.93514
Free Energy = -2232.98568
Single-Point Energy B3LYP-D3(BJ)/6-311+G** PCM = -2234.03546

Free Energy B3LYP-D3(BJ)/6-311+G** PCM (extrapolated free energy from qRRHO) = -2233.55538
Nimag = 1 (-187.8362 cm^{-1})
Charge = 0 Multiplicity = 1

C	4.4464930	-1.0152420	-0.1966280
C	4.1597430	-1.7940070	2.0074730
C	3.1261750	-0.6768850	1.8335430
N	3.2267720	-0.4036630	0.3875120
N	4.7781540	-2.0094900	0.8247140
O	4.3411700	-2.4359480	3.0433880
C	5.6182820	-3.1836730	0.6097270
H	5.1745910	-4.0273070	1.1427910
H	5.6557330	-3.4108060	-0.4559130
H	6.6357560	-3.0353770	0.9825940
C	2.3687880	0.2953190	-0.3815640
H	2.6300630	0.2784630	-1.4358770
C	1.2201730	0.9818870	-0.0329070
C	0.6052800	1.9941870	-0.9867860
H	-0.4863310	1.9471690	-0.9079840
H	0.9682880	1.1096700	1.0141720
Cl	-0.2551720	-0.9209390	-0.5682280
N	-1.5698980	-2.2390650	-0.9273380
C	-2.9075660	-2.0258560	-0.7632520
C	-1.2532330	-3.5244110	-1.3728410
C	-3.6586610	-3.2952840	-1.1285110
C	-2.5601990	-4.2901470	-1.5383050
H	-4.2395920	-3.6241490	-0.2620530
H	-2.5275460	-5.1819940	-0.9068170
H	-2.6437960	-4.6217270	-2.5768330
H	-4.3638460	-3.0717510	-1.9340400
O	-0.1249520	-3.9303670	-1.5837000
O	-3.3998050	-0.9587480	-0.3762060
C	1.7725230	-1.1780960	2.3527030
H	1.9323270	-1.5507290	3.3675630
H	1.0228890	-0.3894310	2.3967100
H	1.3914470	-1.9946330	1.7349610
H	3.4353170	0.2053850	2.4103920
C	5.6126400	0.0032540	-0.4905470
H	4.1805260	-1.5217010	-1.1326220
C	6.8136650	-0.7654060	-1.0868190
H	7.5669710	-0.0478140	-1.4267920
H	7.2965910	-1.4187340	-0.3577940
H	6.5189470	-1.3688500	-1.9532210
C	5.1654380	1.0444200	-1.5379240
H	4.7891360	0.5703400	-2.4521180
H	4.3997230	1.7224300	-1.1529360
H	6.0262130	1.6593060	-1.8194140
C	6.0506070	0.7332320	0.7922340
H	6.3995240	0.0358240	1.5604050
H	6.8785530	1.4121700	0.5637490
H	5.2387360	1.3368740	1.2107390
H	-4.9137670	-0.7098520	-0.1767190
O	-5.9234920	-0.5798290	-0.0655270
C	-6.2302190	0.5680890	0.4895910
O	-5.4857500	1.4496420	0.8627270
C	-7.7722620	0.6986960	0.6370740
F	-8.2683760	-0.2919220	1.4127230
F	-8.1085570	1.8707090	1.1975300
F	-8.3820570	0.6222920	-0.5674100
H	0.8607640	1.7293050	-2.0187010
C	1.0569840	3.4189250	-0.6979660
C	0.4505920	4.1655720	0.3248260
C	2.0927220	4.0139740	-1.4338960
C	0.8739670	5.4665080	0.6121500
H	-0.3626610	3.7266330	0.8981920
C	2.5179640	5.3165050	-1.1525170
H	2.5666810	3.4566290	-2.2381800
C	1.9113590	6.0468850	-0.1257880
H	0.3901700	6.0281840	1.4064410
H	3.3185940	5.7604550	-1.7376660
H	2.2387390	7.0591250	0.0931640

4.log
Potential Energy = -2233.46324
Zero-point Energy = -2232.93284
Free Energy = -2232.98280
Single-Point Energy B3LYP-D3(BJ)/6-311+G** PCM = -2234.03401
Free Energy B3LYP-D3(BJ)/6-311+G** PCM (extrapolated free energy from qRRHO) = -2233.55357
Nimag = 1 (-191.0590 cm^{-1})
Charge = 0 Multiplicity = 1

C	2.7482410	-2.6180430	-0.2848630
C	3.7041980	-2.3771060	1.8540380
C	3.7316070	-0.9763590	1.2348760
N	2.9300200	-1.1777050	0.0152660
N	3.0525600	-3.2153350	1.0165620
O	4.1449640	-2.6691520	2.9672500
C	2.6345370	-4.5460280	1.4466470
H	2.3305730	-4.4904010	2.4941710
H	1.7867580	-4.8711580	0.8430460
H	3.4412020	-5.2794570	1.3591740
C	2.4100290	-0.2314630	-0.7964080
H	1.7922580	-0.6451400	-1.5884270
C	2.5333960	1.1415800	-0.7538350
C	2.1981110	1.9686980	-1.9878030
H	3.0459210	1.8987310	-2.6865470
H	3.2059760	1.6008030	-0.0377060
Cl	0.3671970	1.3204150	0.5078240
N	-1.2326160	1.6623610	1.4310920
C	-2.4430780	1.1719230	1.0322090
C	-1.2949690	2.4619560	2.5765930
C	-3.5121470	1.6578560	1.9954380
C	-2.7514410	2.5169520	3.0188700
H	-4.2661930	2.2172640	1.4343950
H	-3.0748880	3.5612930	3.0304010
H	-2.8231710	2.1359260	4.0410930
H	-4.0070280	0.7899370	2.4404450
O	-0.3391140	3.0027020	3.1003010
O	-2.6087930	0.4504630	0.0416160
C	3.1886800	0.0258350	2.2613620
H	3.7609780	-0.1083300	3.1826870
H	3.3054960	1.0593670	1.9382250
H	2.1331620	-0.1602640	2.4733150
H	4.7653330	-0.7080560	0.9753490
C	3.6506520	-3.1628360	-1.4573100
H	1.6972870	-2.8034440	-0.5397170
C	3.3711660	-4.6705940	-1.6502170
H	3.8823500	-5.0190010	-2.5532010
H	3.7395720	-5.2737390	-0.8182510
H	2.3013870	-4.8718410	-1.7787070
C	3.2974500	-2.4549470	-2.7828370
H	2.2276710	-2.5249990	-3.0125440
H	3.5882100	-1.4011290	-2.7852250
H	3.8397140	-2.9396470	-3.6009230
C	5.1450860	-2.9500670	-1.1548410
H	5.4510650	-3.4549120	-0.2330110
H	5.7471990	-3.3621590	-1.9711520
H	5.3926390	-1.8870210	-1.0699430
H	-3.9702520	-0.1166810	-0.4368190
O	-4.8293780	-0.4536870	-0.8790290
C	-5.3609860	-1.4665390	-0.2375030
O	-4.9623690	-2.0147840	0.7682570
C	-6.6590940	-1.9359790	-0.9519220
F	-6.3930190	-2.3483900	-2.2120680
F	-7.2323130	-2.9558890	-0.2947760

F	-7.5600310	-0.9308570	-1.0296960
H	1.3387970	1.5301490	-2.5064820
C	1.9380230	3.4407040	-1.7215850
C	2.9676750	4.2724910	-1.2521120
C	0.6805980	4.0116760	-1.9638870
C	2.7439520	5.6322270	-1.0187430
H	3.9560760	3.8557740	-1.0726900
C	0.4522790	5.3734220	-1.7372730
H	-0.1284130	3.3859240	-2.3317980
C	1.4829300	6.1885990	-1.2605400
H	3.5546800	6.2574440	-0.6550540
H	-0.5299680	5.7947640	-1.9327560
H	1.3079480	7.2458350	-1.0832060

5.log
Potential Energy = -2233.46325
Zero-point Energy = -2232.93305
Free Energy = -2232.98350
Single-Point Energy B3LYP-D3(BJ)/6-311+G** PCM = -2234.03446
Free Energy B3LYP-D3(BJ)/6-311+G** PCM (extrapolated free energy from qRRHO) = -2233.55471
Nimag = 1 (-192.4734 cm^{-1})
Charge = 0 Multiplicity = 1

C	3.0240340	-2.4589160	-0.3299190
C	3.9688390	-2.1618410	1.8070340
C	3.8716210	-0.7566610	1.2051170
N	3.0819700	-1.0117790	-0.0125360
N	3.3886730	-3.0434540	0.9616540
O	4.4378100	-2.4280400	2.9151470
C	3.0843850	-4.4085310	1.3793450
H	2.7845240	-4.3890550	2.4293380
H	2.2616990	-4.7952890	0.7773280
H	3.9476070	-5.0724950	1.2785430
C	2.4749780	-0.1047690	-0.8081680
H	1.8917740	-0.5611110	-1.6028200
C	2.4751760	1.2733500	-0.7468860
C	2.0627920	2.0837810	-1.9684920
H	3.1079820	1.7807880	-0.0271300
Cl	0.3100390	1.2414760	0.5219470
N	-1.3102800	1.4304960	1.4563660
C	-2.4990500	0.9403130	0.9970680
C	-1.4094610	2.1007770	2.6795350
C	-3.5938470	1.2956010	1.9873310
C	-2.8673000	2.0434650	3.1172000
H	-4.3412350	1.9096840	1.4759300
H	-3.2317010	3.0630980	3.2672990
H	-2.9223560	1.5263820	4.0792770
H	-4.0891490	0.3765510	2.3120920
O	-0.4782150	2.6218460	3.2642610
O	-2.6306750	0.3131540	-0.0610720
C	3.2513650	0.1824790	2.2472200
H	3.8399840	0.0880160	3.1631390
H	3.2754840	1.2260390	1.9363830
H	2.2177050	-0.0972000	2.4638250
H	4.8765570	-0.3972630	0.9426370
C	3.9615610	-2.9077970	-1.5151870
H	1.9913670	-2.7324860	-0.5800500
C	3.8229110	-4.4335460	-1.7191010
H	4.3586330	-4.7251110	-2.6279600
H	4.2519770	-5.0057860	-0.8943960
H	2.7761220	-4.7339270	-1.8434920
C	3.5299760	-2.2253750	-2.8308700
H	2.4686220	-2.3922540	-3.0496840
H	3.7220630	-1.1491910	-2.8272930
H	4.1053450	-2.6515100	-3.6588790
C	5.4325400	-2.5588480	-1.2243060
H	5.7923800	-3.0389380	-0.3087280
H	6.0628250	-2.9082650	-2.0485600
H	5.5810580	-1.4779210	-1.1341860
H	-3.9517100	-0.3173870	-0.5603260
O	-4.7675720	-0.7318900	-1.0204680
C	-5.4597600	-1.4981270	-0.2126430
O	-5.2480540	-1.7443010	0.9564440
C	-6.6793690	-2.1083080	-0.9580010
F	-6.2781240	-2.8496300	-2.0150780
F	-7.3975520	-2.8991350	-0.1461040
F	-7.4959960	-1.1361550	-1.4232820
H	1.2478990	1.5743570	-2.4940640
H	2.9129550	2.1037150	-2.6676370
C	1.6651750	3.5207770	-1.6813560
C	2.6091430	4.4380000	-1.1913860
C	0.3612160	3.9749810	-1.9247590
C	2.2568990	5.7667840	-0.9388730
H	3.6313940	4.1136210	-1.0108790
C	0.0042170	5.3053420	-1.6788510
H	-0.3827560	3.2817060	-2.3085700
C	0.9505990	6.2059530	-1.1815580
H	3.0028770	6.4595910	-0.5594380
H	-1.0121270	5.6354840	-1.8753660
H	0.6758430	7.2390510	-0.9891160

6.log
Potential Energy = -2233.46284
Zero-point Energy = -2232.93211
Free Energy = -2232.98229
Single-Point Energy B3LYP-D3(BJ)/6-311+G** PCM = -2234.03622
Free Energy B3LYP-D3(BJ)/6-311+G** PCM (extrapolated free energy from qRRHO) = -2233.55567
Nimag = 1 (-207.1104 cm^{-1})
Charge = 0 Multiplicity = 1

C	-4.5370210	0.5806250	-0.2161190
C	-4.3850850	2.6059480	0.9738200
C	-3.3864980	1.6602270	1.6496020
N	-3.3821360	0.5179380	0.7148350
N	-4.9022520	1.9941700	-0.1147890
O	-4.6202250	3.7614740	1.3316000
C	-5.6803100	2.7323980	-1.1046720
H	-5.2479700	3.7299140	-1.2087040
H	-5.6281780	2.2158300	-2.0633490
H	-6.7279420	2.8388700	-0.8087330
C	-2.4974600	-0.4981730	0.6474160
H	-2.6917500	-1.1810390	-0.1737470
C	-1.3936440	-0.7614400	1.4366790
C	-0.7187530	-2.1300910	1.4877250
H	-1.0037260	-2.5934410	2.4421410
H	-1.2208210	-0.1577910	2.3205380
Cl	0.1589790	0.4505080	-0.0441080
N	1.5399860	1.3187960	-1.0215580
C	2.8553220	1.2623780	-0.6647980
C	1.3013350	2.0630690	-2.1789610
C	3.6748750	2.0596600	-1.6648930
C	2.6437190	2.5857550	-2.6765170
H	4.2026970	2.8559760	-1.1317700
H	2.6011800	3.6772480	-2.7231760
H	2.8086910	2.2163120	-3.6923490
H	4.4291990	1.4021720	-2.1059600
O	0.2055080	2.2428460	-2.6785280
O	3.2823120	0.6514370	0.3234370
C	-2.0637210	2.4100310	1.8511180
H	-2.2981080	3.3438340	2.3683290
H	-1.3561540	1.8540120	2.4645940
H	-1.5934290	2.6476090	0.8944320
H	-3.7792060	1.3481860	2.6271320

C	-5.7183460	-0.4026530	0.1332750
H	-4.1895410	0.3620570	-1.2331750
C	-6.8369400	-0.2393130	-0.9208270
H	-7.5930240	-1.0154690	-0.7657680
H	-7.3447550	0.7242160	-0.8484630
H	-6.4516150	-0.3538390	-1.9405890
C	-5.2360490	-1.8662740	0.0698540
H	-4.7749690	-2.1051210	-0.8954000
H	-4.5259800	-2.1077260	0.8645410
H	-6.0967780	-2.5311650	0.1941410
C	-6.2851580	-0.1192610	1.5364320
H	-6.6611270	0.9046980	1.6271940
H	-7.1221630	-0.7959530	1.7369040
H	-5.5356850	-0.2870820	2.3166990
H	4.7672430	0.5084410	0.7098470
O	5.7070170	0.3854460	1.1014800
C	6.5692750	-0.0352380	0.2084280
O	6.3812850	-0.2711270	-0.9669480
C	7.9720400	-0.2146700	0.8532430
F	7.9277630	-1.1092020	1.8660250
F	8.8673960	-0.6510230	-0.0459710
F	8.4241260	0.9558330	1.3575830
H	0.3660390	-1.9820140	1.5428060
C	-1.0388870	-3.1045560	0.3694880
C	-2.0358450	-4.0781700	0.5397390
C	-0.3353370	-3.0796600	-0.8458530
C	-2.3301070	-4.9953520	-0.4741680
H	-2.5823290	-4.1233130	1.4787520
C	-0.6262090	-3.9937440	-1.8630840
H	0.4484200	-2.3428250	-0.9938370
C	-1.6263670	-4.9546880	-1.6816110
H	-3.1032110	-5.7424730	-0.3179390
H	-0.0668930	-3.9590550	-2.7938550
H	-1.8496500	-5.6679510	-2.4697800

(*S*)-TS-back

Conformation name	Extrapolated Free energy (kcal/mol)
TS4-Sb-lowest	0.0
1	1.9
2	2.4
3	1.5

TS4-Sb-lowest.log
Potential Energy = -2233.46543
Zero-point Energy = -2232.93478
Free Energy = -2232.98492
Single-Point Energy B3LYP-D3(BJ)/6-311+G** PCM = -2234.03911
Free Energy B3LYP-D3(BJ)/6-311+G** PCM (extrapolated free energy from qRRHO) = -2233.55860
Nimag = 1 (-192.3533 cm^{-1})
Charge = 0 Multiplicity = 1

C	-2.3955980	2.4865830	0.7785440
C	-1.3161090	3.9298080	-0.7440620
C	-1.2860590	2.5499090	-1.4048870
N	-2.1288780	1.7612910	-0.4884320
N	-2.0238940	3.8527700	0.4051680
O	-0.8334860	4.9563420	-1.2256140
C	-2.4697650	5.0583040	1.0982740
H	-2.7242770	5.8123630	0.3502560
H	-3.3540380	4.8277010	1.6926350
H	-1.6940600	5.4670470	1.7516100
C	-2.6982290	0.5677980	-0.7476880
H	-3.4593230	0.2822410	-0.0271560
C	-2.4136100	-0.3207910	-1.7691190
C	-3.3688660	-1.4401540	-2.1674150
H	-2.7750740	-2.3116890	-2.4663760
H	-0.2561020	2.1688400	-1.4130720
C	-1.6181800	1.9288640	2.0275870
H	-3.4712880	2.4454240	0.9939480
H	-1.7252400	-0.0240820	-2.5508670
Cl	-0.5771380	-1.4955010	-0.6593680
N	0.8929820	-2.5142660	-0.0143360
C	0.7425780	-3.7398220	0.6388080
C	2.1919690	-2.1242340	-0.1612330
C	2.1351470	-4.2464640	0.9949440
C	3.0981290	-3.1802700	0.4479110
H	2.2779830	-5.2318660	0.5435670
H	3.7653410	-3.5609750	-0.3311580
H	3.7209060	-2.7119440	1.2149570
H	2.1967860	-4.3666180	2.0800840
O	2.5456680	-1.0728230	-0.7101840
O	-0.3237020	-4.2799460	0.8701340
C	-1.8059920	2.6823530	-2.8442200
H	-1.6431490	1.7826820	-3.4359480
H	-2.8734920	2.9219470	-2.8496240
H	-1.2611350	3.5017680	-3.3192460
C	-1.9164000	2.8175840	3.2557540
H	-1.5008290	2.3426200	4.1500960
H	-1.4632770	3.8076220	3.1759510
H	-2.9936040	2.9385930	3.4185590
C	-0.1014040	1.9016520	1.7675220
H	0.2899430	2.9004980	1.5479830
H	0.4181270	1.5335870	2.6583270
H	0.1539060	1.2348940	0.9383360
C	-2.1151350	0.5056540	2.3586800
H	-3.2025610	0.4795630	2.4975070
H	-1.8424520	-0.2235510	1.5935280
H	-1.6569250	0.1761380	3.2968280
H	-3.9018680	-1.1174210	-3.0726540
C	-4.3904750	-1.8564790	-1.1262420
C	-4.0747600	-2.8023100	-0.1375760
C	-5.6822120	-1.3067430	-1.1348160
C	-5.0226080	-3.1852910	0.8165080
H	-3.0818570	-3.2424330	-0.1159040
C	-6.6331480	-1.6858910	-0.1817540
H	-5.9475790	-0.5794590	-1.8986480
C	-6.3053450	-2.6274690	0.7987210
H	-4.7601950	-3.9226330	1.5701170
H	-7.6281580	-1.2505360	-0.2093230
H	-7.0428310	-2.9275640	1.5375850
H	3.9990760	-0.5681260	-0.8127540
O	4.9180340	-0.1483500	-0.9877360
C	5.6569310	-0.0982780	0.0937080
C	7.0254430	0.5709370	-0.2147380
O	5.3852560	-0.4903180	1.2095120
F	7.8150200	0.5823730	0.8703240
F	6.8529280	1.8500810	-0.6187910
F	7.6781810	-0.0869450	-1.1987410

1.log
Potential Energy = -2233.46774
Zero-point Energy = -2232.93705
Free Energy = -2232.98699
Single-Point Energy B3LYP-D3(BJ)/6-311+G** PCM = -2234.03861
Free Energy B3LYP-D3(BJ)/6-311+G** PCM (extrapolated free energy from qRRHO) = -2233.55785
Nimag = 1 (-170.9527 cm^{-1})
Charge = 0 Multiplicity = 1

C	-1.8852200	2.5765870	1.2115560
C	-1.6050980	3.4927530	-0.9449790
C	-1.7219820	1.9825740	-1.1607040
N	-2.0737010	1.5139850	0.1919760
N	-1.8021620	3.7677550	0.3640070
O	-1.4330760	4.3241830	-1.8379390
C	-2.0397650	5.1348930	0.8188200
H	-2.6154150	5.6576070	0.0518930
H	-2.6116760	5.1133230	1.7466490
H	-1.1071300	5.6813010	0.9837480
C	-2.5947170	0.3140520	0.5128910
H	-2.9837310	0.2655960	1.5273000
C	-2.6634770	-0.8381500	-0.2506600
C	-3.5960680	-1.9682770	0.1496610
H	-3.1347190	-2.9264490	-0.1113500
H	-3.7266590	-1.9634870	1.2381460
H	-0.7490840	1.5789840	-1.4714650
C	-0.6397750	2.3701280	2.1510190
H	-2.7852940	2.6346200	1.8375400
H	-2.3684890	-0.8105830	-1.2926950
Cl	-0.4914990	-1.7713120	0.3938080
N	1.1433030	-2.6604090	0.7426650
C	1.2343040	-3.7956370	1.5521520
C	2.3398460	-2.2527310	0.2272970
C	2.6986370	-4.2143880	1.5948450
C	3.4309800	-3.1925460	0.7100300
H	2.7816030	-5.2413450	1.2290350
H	3.9168140	-3.6434890	-0.1602910
H	4.1864690	-2.6093790	1.2439530
H	3.0356890	-4.2044890	2.6349580
O	2.4807750	-1.2711490	-0.5123460
O	0.2938900	-4.3296240	2.1110260
C	-2.7691030	1.7212200	-2.2533860
H	-2.7769410	0.6859380	-2.5908060
H	-3.7704130	1.9870800	-1.9020550
H	-2.5189640	2.3535250	-3.1087340
C	-0.5152300	3.5760430	3.1088980
H	0.2554950	3.3609310	3.8557500
H	-0.2184550	4.4914940	2.5936030
H	-1.4506650	3.7656820	3.6478240
C	0.6539950	2.2288520	1.3294870
H	0.8418580	3.1151560	0.7145770
H	1.5077400	2.1098680	2.0045940
H	0.6250290	1.3502440	0.6780460
C	-0.8430240	1.1121050	3.0219520
H	-1.7850350	1.1552800	3.5817080
H	-0.8234560	0.1894140	2.4390320
H	-0.0306970	1.0488280	3.7532240
C	-4.9566250	-1.8776400	-0.5279670
C	-5.9989950	-1.1307930	0.0428020
C	-5.1909250	-2.5242280	-1.7509510
C	-7.2401440	-1.0282070	-0.5922030
H	-5.8401480	-0.6286430	0.9943030
C	-6.4299140	-2.4222110	-2.3922330
H	-4.3982050	-3.1155290	-2.2033820
C	-7.4594630	-1.6724840	-1.8148050
H	-8.0358860	-0.4496980	-0.1310780
H	-6.5913500	-2.9319140	-3.3380830
H	-8.4236650	-1.5950280	-2.3088320
H	3.8312090	-0.7171300	-1.0224150
O	4.6511420	-0.2855950	-1.4591250
C	5.6108760	-0.0562610	-0.5959110
O	5.6263960	-0.2971460	0.5932020
C	6.8261200	0.6091770	-1.3000530
F	6.4792470	1.8029400	-1.8322250
F	7.8319400	0.8172670	-0.4364790
F	7.2913840	-0.1689930	-2.3028370

2.log
Potential Energy = -2233.46485
Zero-point Energy = -2232.93457
Free Energy = -2232.98474
Single-Point Energy B3LYP-D3(BJ)/6-311+G** PCM = -2234.03723
Free Energy B3LYP-D3(BJ)/6-311+G** PCM (extrapolated free energy from qRRHO) = -2233.55711
Nimag = 1 (-171.8028 cm^{-1})
Charge = 0 Multiplicity = 1

C	-2.7058680	3.0154530	0.6276940
C	-1.8811130	3.7965180	-1.4413000
C	-1.9170200	2.2731130	-1.5712490
N	-2.5903330	1.8808380	-0.3214810
N	-2.4226090	4.1501540	-0.2540050
O	-1.4918530	4.5736960	-2.3151280
C	-2.8014910	5.5340440	0.0175810
H	-3.1744500	5.9778370	-0.9081480
H	-3.5909720	5.5517160	0.7690210
H	-1.9556600	6.1303670	0.3706090
C	-3.1477100	0.6794350	-0.0599520
H	-3.7954200	0.6824560	0.8139220
C	-2.9881560	-0.5168990	-0.7311370
C	-3.9937280	-1.6392060	-0.5170510
H	-4.3015620	-1.6611780	0.5344890
H	-4.9005250	-1.4058200	-1.0957840
H	-0.8917990	1.8807690	-1.6040410
C	-1.7561670	2.9254220	1.8793070
H	-3.7422300	3.0792560	0.9854010
H	-2.4203300	-0.5450690	-1.6532300
Cl	-0.9680190	-1.2229210	0.5375410
N	0.5877030	-1.8890280	1.3528590
C	0.5680300	-2.6744550	2.5094870
C	1.8414160	-1.6568590	0.8628440
C	2.0112280	-3.0218040	2.8517570
C	2.8541230	-2.3588540	1.7498760
H	2.1140180	-4.1098580	2.8798160
H	3.4118360	-3.0776490	1.1421560
H	3.5678170	-1.6198360	2.1241040
H	2.2346870	-2.6415540	3.8523500
O	2.0785310	-0.9803870	-0.1447560
O	-0.4373480	-3.0010550	3.1121990
C	-2.6569520	1.9112220	-2.8685320
H	-2.5856000	0.8525200	-3.1133250
H	-3.7133950	2.1878530	-2.8005930
H	-2.1985990	2.4779830	-3.6825020
C	-1.9106450	4.2021860	2.7358800
H	-1.3662340	4.0694240	3.6762110
H	-1.4985940	5.0869160	2.2468490
H	-2.9589220	4.3991320	2.9887990
C	-0.2872460	2.7711010	1.4466650
H	0.0463530	3.6185750	0.8386330
H	0.3554040	2.7285790	2.3322150
H	-0.1288030	1.8492440	0.8791010
C	-2.1694420	1.7293900	2.7631340
H	-3.2287440	1.7814810	3.0421000
H	-1.9799080	0.7671060	2.2844990
H	-1.5855070	1.7499860	3.6890280
C	-3.5179310	-3.0181110	-0.9373960
C	-3.2595130	-3.3032360	-2.2880760
C	-3.3525920	-4.0450890	0.0025000
C	-2.8352680	-4.5740310	-2.6861440
H	-3.3964510	-2.5271430	-3.0375770
C	-2.9330340	-5.3206520	-0.3908330
H	-3.5509050	-3.8454600	1.0524250
C	-2.6698580	-5.5891850	-1.7371680
H	-2.6405460	-4.7731820	-3.7363370
H	-2.8118150	-6.1015390	0.3548520

H	-2.3435480	-6.5784020	-2.0450910
H	3.4846340	-0.5998850	-0.6684180
O	4.3475510	-0.3149500	-1.1398130
C	5.2296730	0.1802760	-0.3057800
O	5.1357230	0.3139860	0.8964810
C	6.5119960	0.6143270	-1.0691440
F	6.2277470	1.5668820	-1.9857080
F	7.4326260	1.1102860	-0.2282180
F	7.0642440	-0.4331310	-1.7217370

3.log
Potential Energy = -2233.46543
Zero-point Energy = -2232.93491
Free Energy = -2232.98531
Single-Point Energy B3LYP-D3(BJ)/6-311+G** PCM = -2234.03863
Free Energy B3LYP-D3(BJ)/6-311+G** PCM (extrapolated free energy from qRRHO) = -2233.55852
Nimag = 1 (-190.9753 cm^{-1})
Charge = 0 Multiplicity = 1

C	-3.7783670	-0.3556430	1.4307710
C	-5.5319040	0.9399670	0.5300570
C	-4.5051520	0.8098680	-0.5974540
N	-3.5493990	-0.1532610	-0.0213310
N	-5.1249230	0.1984310	1.5845880
O	-6.5926070	1.5624790	0.4534660
C	-6.0338280	-0.1106920	2.6850990
H	-7.0376160	-0.2451630	2.2761610
H	-5.7147660	-1.0342610	3.1686120
H	-6.0673800	0.6908200	3.4281010
C	-2.6275470	-0.8701160	-0.6939810
H	-2.2022530	-1.6857150	-0.1159730
C	-2.1528860	-0.6753540	-1.9787980
C	-1.4118530	-1.7614940	-2.7501900
H	-0.6387170	-1.2846260	-3.3636260
H	-4.0239930	1.7817560	-0.7703030
C	-2.6997920	0.3124040	2.3611140
H	-3.7988860	-1.4326750	1.6424910
H	-2.6187670	0.0754620	-2.6051770
Cl	-0.4011950	0.9407510	-1.4227980
N	0.9772170	2.2364860	-1.2374980
C	0.8642230	3.5373580	-1.7327390
C	2.1701300	1.9802970	-0.6268790
C	2.1590610	4.2706300	-1.4038050
C	3.0278930	3.2339150	-0.6726880
H	1.9214550	5.1439270	-0.7902370
H	3.2836630	3.5254180	0.3499950
H	3.9611830	3.0048060	-1.1949460
H	2.6063740	4.6305030	-2.3342530
O	2.4761440	0.8917700	-0.1247690
O	-0.1084200	3.9782560	-2.3174940
C	-5.2299520	0.3521020	-1.8721190
H	-4.6024440	0.4139090	-2.7601200
H	-5.5919560	-0.6746850	-1.7645910
H	-6.0885930	1.0116550	-2.0192300
C	-3.1023040	0.1129540	3.8393230
H	-2.2786010	0.4406840	4.4814040
H	-3.9804640	0.6996030	4.1160260
H	-3.2992310	-0.9403820	4.0697430
C	-2.5681550	1.8168630	2.0633320
H	-3.5159530	2.3440500	2.2147610
H	-1.8323550	2.2628540	2.7405690
H	-2.2260370	1.9974810	1.0397390
C	-1.3360180	-0.3805600	2.1575160
H	-1.4063050	-1.4636370	2.3134640
H	-0.9142000	-0.1963460	1.1678360
H	-0.6227200	0.0103330	2.8903460
H	-2.1220120	-2.2089050	-3.4596270
C	-0.7897640	-2.8703940	-1.9232950
C	0.5001350	-2.7376310	-1.3852320
C	-1.4921620	-4.0621650	-1.6839380
C	1.0703550	-3.7643510	-0.6263500
H	1.0619400	-1.8253880	-1.5642640
C	-0.9266890	-5.0917320	-0.9247800
H	-2.4887120	-4.1871040	-2.1011280
C	0.3581460	-4.9453350	-0.3924520
H	2.0718800	-3.6435580	-0.2230510
H	-1.4865550	-6.0071890	-0.7550620
H	0.8019860	-5.7448710	0.1936970
H	3.8284510	0.5742090	0.5543120
O	4.6564440	0.3192020	1.1008010
C	5.6489640	-0.0924380	0.3491570
C	6.8745280	-0.4633750	1.2304460
O	5.6885440	-0.1951230	-0.8587350
F	7.8968810	-0.9020480	0.4800070
F	6.5590760	-1.4359020	2.1151410
F	7.3038690	0.6090100	1.9340450

(*R*)-TS-back

Conformation name	Extrapolated Free energy (kcal/mol)
TS4-Rb-lowest	0.0
1	0.6
2	0.9
3	1.7

TS4-Rb-lowest.log
Potential Energy = -2233.46612
Zero-point Energy = -2232.93524
Free Energy = -2232.98573
Single-Point Energy B3LYP-D3(BJ)/6-311+G** PCM = -2234.03577
Free Energy B3LYP-D3(BJ)/6-311+G** PCM (extrapolated free energy from qRRHO) = -2233.55538
Nimag = 1 (-203.2629 cm^{-1})
Charge = 0 Multiplicity = 1

C	-3.3008510	-1.1285990	-1.2914060
C	-5.2086170	-2.0593700	-0.2577480
C	-4.1217700	-1.9819430	0.8201900
N	-3.1343610	-1.0759070	0.1821480
N	-4.7156180	-1.5244490	-1.3974470
O	-6.3450400	-2.5092930	-0.0981590
C	-5.5671230	-1.2645690	-2.5540690
H	-6.5544980	-0.9647180	-2.1962530
H	-5.1374910	-0.4550950	-3.1452800
H	-5.6812330	-2.1493110	-3.1868930
C	-2.6007950	-0.0235120	0.8367350
H	-2.8642470	0.0193710	1.8887950
C	-1.7481330	0.9609320	0.3653790
C	-1.6451990	2.2967620	1.0842670
H	-0.6224410	2.6771120	0.9940490
H	-1.8405000	2.1532950	2.1529280
H	-1.4573530	0.9631370	-0.6806990
C	-4.6837830	-1.5467210	2.1688460
H	-5.4704360	-2.2546630	2.4400500
H	-3.9230020	-1.5757000	2.9528070
H	-5.1247410	-0.5465510	2.1268060
H	-3.6774990	-2.9784400	0.9320750
C	-2.3083690	-2.0806760	-2.0456340
H	-3.1822950	-0.1150950	-1.6896070

Cl	0.2191250	-0.0853760	1.3725210
N	1.8748670	-0.6814830	2.1135310
C	3.0460280	-0.6931600	1.4153300
C	2.0030770	-1.1167490	3.4339620
C	4.1566500	-1.2059950	2.3162300
C	3.4657930	-1.4796240	3.6618390
H	4.9438360	-0.4489110	2.3708200
H	3.8555830	-0.8668030	4.4792740
O	1.0907140	-1.1834540	4.2380170
O	3.1564830	-0.3373420	0.2345770
C	-2.6353330	-2.0632550	-3.5552670
H	-1.8480350	-2.5959910	-4.0981740
H	-3.5803090	-2.5611870	-3.7836290
H	-2.6748620	-1.0421860	-3.9515630
C	-2.3905470	-3.5283320	-1.5262170
H	-1.7435840	-4.1691420	-2.1340200
H	-2.0463880	-3.6075500	-0.4904420
H	-3.4062130	-3.9316970	-1.5935060
C	-0.8708420	-1.5589130	-1.8645760
H	-0.7525780	-0.5501000	-2.2757140
H	-0.5699240	-1.5440250	-0.8153560
H	-0.1769230	-2.2137130	-2.4016630
H	3.5248150	-2.5256460	3.9742890
H	4.5919550	-2.1019600	1.8637310
C	-2.6092740	3.3330440	0.5230770
C	-3.9029410	3.4755300	1.0482320
C	-2.2282040	4.1570940	-0.5469370
C	-4.7945890	4.4117340	0.5160230
H	-4.2143040	2.8530440	1.8837550
C	-3.1173850	5.0930340	-1.0849640
H	-1.2261690	4.0680600	-0.9601020
C	-4.4052800	5.2228960	-0.5553700
H	-5.7899050	4.5103920	0.9403690
H	-2.8022950	5.7228770	-1.9122760
H	-5.0961730	5.9518630	-0.9688890
H	4.4803670	-0.2698870	-0.5474300
O	5.2819090	-0.2286310	-1.1867560
C	6.2986220	0.4182710	-0.6714190
O	6.3866630	0.9320900	0.4244020
C	7.4785950	0.4672500	-1.6819120
F	7.1144790	1.1043420	-2.8177230
F	8.5339270	1.1146620	-1.1642670
F	7.8786260	-0.7794740	-2.0194450

1.log
Potential Energy = -2233.46607
Zero-point Energy = -2232.93504
Free Energy = -2232.98523
Single-Point Energy B3LYP-D3(BJ)/6-311+G** PCM = -2234.03525
Free Energy B3LYP-D3(BJ)/6-311+G** PCM (extrapolated free energy from qRRHO) = -2233.55440
Nimag = 1 (-203.4857 cm^{-1})
Charge = 0 Multiplicity = 1

C	-3.2966830	-0.8747570	-1.4396090
C	-5.2671500	-1.8516490	-0.5813030
C	-4.2042890	-1.9768120	0.5157690
N	-3.1623870	-1.0383910	0.0290560
N	-4.7250260	-1.1838230	-1.6244170
O	-6.4252730	-2.2672610	-0.5071230
C	-5.5380460	-0.7245360	-2.7462660
H	-6.5199940	-0.4353080	-2.3655850
H	-5.0623340	0.1411190	-3.2083660
H	-5.6745530	-1.5043010	-3.5009780
C	-2.5964370	-0.1163530	0.8357730
H	-2.8817150	-0.2110850	1.8787430
C	-1.6902180	0.8834270	0.5241440
C	-1.5427480	2.0964180	1.4286310
H	-0.4999200	2.4297500	1.4201340
H	-1.7802110	1.8144610	2.4606280
H	-1.3757580	1.0211110	-0.5059020
C	-4.7808620	-1.7061380	1.9009100
H	-5.6070470	-2.4043450	2.0542780
H	-4.0438440	-1.8818010	2.6883500
H	-5.1730670	-0.6889330	1.9904080
H	-3.8075620	-2.9990700	0.4955700
C	-2.3309450	-1.7569920	-2.3051800
H	-3.1223800	0.1777640	-1.6879310
Cl	0.2107420	-0.3895880	1.3914400
N	1.8272150	-1.1668340	2.0423010
C	3.0253380	-1.0405600	1.4036480
C	1.8928980	-1.9135590	3.2202550
C	4.0916980	-1.7750780	2.1995480
C	3.3384310	-2.3597840	3.4054900
H	4.8749340	-1.0651570	2.4807630
H	3.7022210	-1.9841410	4.3656750
O	0.9467860	-2.1509110	3.9492890
O	3.1887520	-0.4207110	0.3446390
C	-2.6253090	-1.5140430	-3.8020210
H	-1.8485390	-1.9980100	-4.4026560
H	-3.5843130	-1.9345840	-4.1126260
H	-2.6161710	-0.4466820	-4.0507910
C	-2.4859500	-3.2576960	-1.9952190
H	-1.8530390	-3.8360900	-2.6761310
H	-2.1690720	-3.4958380	-0.9751580
H	-3.5159770	-3.6015750	-2.1352250
C	-0.8764960	-1.3311820	-2.0320760
H	-0.7070500	-0.2810140	-2.2953210
H	-0.5965620	-1.4771390	-0.9871390
H	-0.2005620	-1.9347580	-2.6464640
H	3.3667690	-3.4521250	3.4440750
H	4.5488310	-2.5370340	1.5618090
C	-2.4337560	3.2529350	0.9959330
C	-3.7549830	3.3593370	1.4577440
C	-1.9556970	4.2293570	0.1089420
C	-4.5782580	4.4096580	1.0416160
H	-4.1424020	2.6175570	2.1522320
C	-2.7764010	5.2806150	-0.3129460
H	-0.9315970	4.1687790	-0.2519420
C	-4.0919720	5.3738660	0.1517850
H	-5.5963000	4.4773530	1.4150740
H	-2.3863410	6.0274770	-0.9988570
H	-4.7299250	6.1914670	-0.1711260
H	4.5374210	-0.2996810	-0.3961310
O	5.3771070	-0.2739740	-0.9838440
C	6.1586870	0.7410680	-0.7049120
O	5.9988500	1.6111220	0.1249910
C	7.4204920	0.7148700	-1.6125220
F	7.0802630	0.7407870	-2.9205090
F	8.2148870	1.7690000	-1.3704050
F	8.1422950	-0.4089450	-1.3974070

2.log
Potential Energy = -2233.46318
Zero-point Energy = -2232.93256
Free Energy = -2232.98266
Single-Point Energy B3LYP-D3(BJ)/6-311+G** PCM = -2234.03449
Free Energy B3LYP-D3(BJ)/6-311+G** PCM (extrapolated free energy from qRRHO) = -2233.55397
Nimag = 1 (-210.8518 cm^{-1})
Charge = 0 Multiplicity = 1

C	-3.9907910	-1.0164820	-0.9464790
C	-5.9962170	-0.9961520	0.2988210
C	-4.8967050	-0.4768100	1.2316440
N	-3.8000060	-0.1938080	0.2728710

N	-5.4481600	-1.2314190	-0.9144640
O	-7.1820660	-1.1446750	0.6016960
C	-6.2710620	-1.5317320	-2.0820460
H	-7.2012990	-0.9645640	-2.0049490
H	-5.7406850	-1.2308210	-2.9862270
H	-6.5178450	-2.5950880	-2.1486560
C	-3.1225930	0.9763750	0.2865730
H	-3.3782970	1.6223050	1.1205470
C	-2.1483350	1.4337220	-0.5812480
C	-1.8804550	2.9282130	-0.6977060
H	-1.9665750	3.3972020	0.2886820
H	-2.6767860	3.3692440	-1.3159290
H	-1.8572040	0.8248880	-1.4314950
C	-5.3813240	0.6884370	2.0873380
H	-6.2562310	0.3446970	2.6441410
H	-4.6252320	1.0013240	2.8115670
H	-5.6800120	1.5477860	1.4797850
H	-4.5943370	-1.2954310	1.8962330
C	-3.1484230	-2.3382090	-1.0034560
H	-3.7386020	-0.4059480	-1.8205200
Cl	-0.3945840	0.8091800	1.0480730
N	1.0963940	0.4412040	2.1667260
C	2.2361870	-0.1587690	1.7168030
C	1.1354130	0.7803270	3.5209200
C	3.2160670	-0.2890720	2.8699630
C	2.4931070	0.3526750	4.0651710
H	4.1500890	0.2099730	2.5978950
H	3.0069650	1.2356330	4.4553080
O	0.2308090	1.3221250	4.1300980
O	2.4128690	-0.5295290	0.5493110
C	-3.5113930	-3.1202040	-2.2850770
H	-2.8103160	-3.9519850	-2.4074430
H	-4.5162650	-3.5464730	-2.2432580
H	-3.4362230	-2.4924450	-3.1803990
C	-3.3982150	-3.2338310	0.2244330
H	-2.8537900	-4.1760450	0.1036970
H	-3.0394480	-2.7657290	1.1462440
H	-4.4580950	-3.4819180	0.3428780
C	-1.6520550	-1.9807570	-1.0733950
H	-1.4195240	-1.3900360	-1.9667260
H	-1.3223450	-1.4251060	-0.1936990
H	-1.0612600	-2.9009830	-1.1279260
H	2.3380320	-0.3365170	4.8994850
H	3.4407840	-1.3492340	3.0206210
C	-0.5472160	3.2917590	-1.3263400
C	-0.2878870	2.9876050	-2.6727010
C	0.4422450	3.9620320	-0.5933380
C	0.9301090	3.3313990	-3.2657070
H	-1.0468480	2.4831980	-3.2663330
C	1.6614970	4.3129870	-1.1831730
H	0.2587530	4.2103610	0.4487220
C	1.9112960	3.9958640	-2.5214870
H	1.1102180	3.0864770	-4.3087700
H	2.4140640	4.8323390	-0.5963060
H	2.8573500	4.2665490	-2.9813900
H	3.7121550	-1.1494270	-0.0000130
O	4.4927890	-1.6179090	-0.4722120
C	5.6426100	-1.0348500	-0.2361470
O	5.8655410	-0.0605940	0.4520500
C	6.7877000	-1.7725740	-0.9845790
F	6.5838100	-1.7475440	-2.3211420
F	7.9762220	-1.2011600	-0.7363460
F	6.8597750	-3.0678710	-0.6035340

3.log
Potential Energy = -2233.46277
Zero-point Energy = -2232.93196
Free Energy = -2232.98065

Single-Point Energy B3LYP-D3(BJ)/6-311+G** PCM = -2234.03485
Free Energy B3LYP-D3(BJ)/6-311+G** PCM (extrapolated free energy from qRRHO) = -2233.55273
Nimag = 1 (-221.9132 cm^{-1})
Charge = 0 Multiplicity = 1

C	-3.1584530	-2.2484970	-0.4667830
C	-5.2630690	-1.9280350	0.5547800
C	-4.3275320	-0.8621820	1.1349350
N	-3.1880880	-0.9150100	0.1850450
N	-4.5767060	-2.6375010	-0.3690790
O	-6.4464170	-2.0874420	0.8615140
C	-5.2418430	-3.5903310	-1.2524250
H	-6.2349070	-3.2043230	-1.4928770
H	-4.6645720	-3.6958980	-2.1715000
H	-5.3555390	-4.5729650	-0.7858910
C	-2.6773370	0.2028990	-0.3766570
H	-3.1008660	1.1234910	0.0083110
C	-1.6766090	0.3180890	-1.3254730
C	-1.5293870	1.5430730	-2.2238310
H	-1.8807260	1.2486410	-3.2224600
H	-0.4638230	1.7714490	-2.3382760
H	-1.2251020	-0.5828600	-1.7292440
C	-5.0273120	0.4822110	1.2992050
H	-5.8959000	0.3224580	1.9423680
H	-4.3815450	1.2179960	1.7846090
H	-5.3796140	0.8824430	0.3441760
H	-3.9891020	-1.2013830	2.1215450
C	-2.1647990	-3.2869250	0.1615200
H	-2.8972720	-2.1117940	-1.5219750
Cl	0.0097550	0.8107780	0.3758520
N	1.4984790	1.2249670	1.5067340
C	2.7564720	0.7480430	1.2873610
C	1.3965270	2.0466720	2.6305190
C	3.6859910	1.2822890	2.3648960
C	2.7809120	2.1426100	3.2617760
H	4.4899080	1.8502890	1.8878110
H	3.0798050	3.1937480	3.2959630
O	0.3706550	2.5779810	3.0160790
O	3.0641840	-0.0004890	0.3503580
C	-2.3038080	-4.6361870	-0.5777280
H	-1.5031270	-5.3073130	-0.2508840
H	-3.2519570	-5.1342290	-0.3632460
H	-2.2101900	-4.5174710	-1.6633030
C	-2.4291710	-3.5027560	1.6634520
H	-1.7672890	-4.2896840	2.0393980
H	-2.2233800	-2.5987180	2.2447270
H	-3.4584740	-3.8217330	1.8574710
C	-0.7211550	-2.7874760	-0.0316820
H	-0.4717600	-2.6742790	-1.0929130
H	-0.5476010	-1.8340640	0.4702870
H	-0.0243450	-3.5188970	0.3906360
H	2.7234570	1.7801760	4.2917380
H	4.1432450	0.4390180	2.8903300
C	-2.2765520	2.7941960	-1.8016890
C	-1.6607010	3.7816580	-1.0175820
C	-3.6059770	2.9980930	-2.2064230
C	-2.3545550	4.9368080	-0.6420560
H	-0.6304040	3.6466580	-0.7015280
C	-4.3041870	4.1500770	-1.8329200
H	-4.0962450	2.2498570	-2.8249730
C	-3.6796720	5.1243430	-1.0469960
H	-1.8577600	5.6907440	-0.0378680
H	-5.3308330	4.2888080	-2.1600430
H	-4.2183090	6.0223960	-0.7586340
H	4.4771560	-0.5550870	0.0883270
O	5.3606920	-1.0414950	-0.0983450
C	6.2184790	-0.2964520	-0.7523380

O	6.0850070	0.8453300	-1.1397110
C	7.5368390	-1.0820150	-0.9993610
F	7.3024910	-2.2200340	-1.6903770
F	8.4162630	-0.3473280	-1.6977570
F	8.1183410	-1.4248810	0.1729530

Formation of syn-aminal *syn*-18b (TS5)

Conformation name	Extrapolated Free energy (kcal/mol)
TS5-int-lowest	0.0
1	6.0
2	0.4
3	2.5
4	2.9

TS5-int-lowest.log
Potential Energy = -2233.49662
Zero-point Energy = -2232.96689
Free Energy = -2233.01536
Single-Point Energy B3LYP-D3(BJ)/6-311+G** PCM = -2234.07919
Free Energy B3LYP-D3(BJ)/6-311+G** PCM (extrapolated free energy from qRRHO) = -2233.59792
Nimag = 1 (-242.8971 cm^{-1})
Charge = 0 Multiplicity = 1

C	-0.0676900	2.1356700	-0.6441190
C	0.9788090	3.1016740	1.2401920
C	-0.5069930	2.9616280	1.5893770
N	-0.9509820	1.9741380	0.5565620
N	1.1690310	2.5910120	0.0026550
O	1.8373290	3.5880490	1.9750120
C	2.4970760	2.4401650	-0.5832410
H	3.2135170	2.3313810	0.2325880
H	2.5237350	1.5438740	-1.2048540
H	2.7799400	3.3122370	-1.1802000
C	-1.6942840	0.9372200	0.8608640
H	-2.1639830	0.9970090	1.8353970
C	-2.4458780	0.0269650	-0.0963270
C	-3.3817480	-0.9441160	0.6443950
H	-2.7845330	-1.6901020	1.1700190
H	-3.9068770	-0.3570510	1.4072770
H	-3.0491590	0.6961920	-0.7150180
C	-0.7655650	2.6180150	3.0469230
H	-0.2965590	3.4011620	3.6471960
H	-1.8332430	2.6174410	3.2788630
H	-0.3272610	1.6609880	3.3316340
H	-0.9998720	3.9116160	1.3569160
C	-0.6157420	3.1043120	-1.7578170
H	0.0974660	1.1490490	-1.0755460
Cl	-1.4136870	-0.8828310	-1.2879210
C	0.2834820	2.9306420	-3.0045730
H	-0.1396280	3.5043420	-3.8349190
H	1.2995430	3.2964250	-2.8415670
H	0.3395630	1.8825890	-3.3176700
C	-2.0544100	2.7154100	-2.1509580
H	-2.1112020	1.6905540	-2.5296750
H	-2.7515780	2.8350020	-1.3156950
H	-2.3965060	3.3763980	-2.9532310
C	-0.6004470	4.5850190	-1.3291630
H	0.3842370	4.9041600	-0.9752460
H	-0.8561500	5.2076520	-2.1922510
H	-1.3401610	4.8007420	-0.5522300
N	-0.3978570	-0.6315820	1.8649200
C	-0.7766850	-1.1686660	3.0935660
C	0.8306060	-1.0403030	1.5649360
C	0.3165750	-2.0852860	3.6416530
C	1.4286050	-1.9865420	2.5908720
H	-0.0848200	-3.0963210	3.7555430
H	1.6711590	-2.9410090	2.1140590
H	2.3630620	-1.5690780	2.9778770
H	0.6206480	-1.7372640	4.6326570
O	1.4394860	-0.6535150	0.5116560
O	-1.8443010	-0.9175730	3.6424710
H	2.4918950	-1.0858790	0.3430170
O	3.6545720	-1.5644430	0.1757170
C	4.1898400	-1.3628880	-0.9718070
C	5.6122050	-1.9990250	-1.0639670
O	3.7456330	-0.7647180	-1.9484080
F	6.4442030	-1.4802660	-0.1254900
F	5.5650180	-3.3399090	-0.8600690
F	6.1895210	-1.7974740	-2.2649060
C	-4.3991650	-1.6148080	-0.2566480
C	-4.2834460	-2.9728860	-0.5841800
C	-5.4881580	-0.8905870	-0.7674960
C	-5.2268660	-3.5932020	-1.4097180
H	-3.4509800	-3.5495840	-0.1901910
C	-6.4311560	-1.5055800	-1.5950360
H	-5.6072120	0.1594780	-0.5103080
C	-6.3020670	-2.8603420	-1.9201860
H	-5.1209280	-4.6468120	-1.6516680
H	-7.2683870	-0.9299920	-1.9792050
H	-7.0362030	-3.3405350	-2.5605070

1.log
Potential Energy = -2233.48496
Zero-point Energy = -2232.95406
Free Energy = -2233.00229
Single-Point Energy B3LYP-D3(BJ)/6-311+G** PCM = -2234.07105
Free Energy B3LYP-D3(BJ)/6-311+G** PCM (extrapolated free energy from qRRHO) = -2233.58838
Nimag = 1 (-101.8706 cm^{-1})
Charge = 0 Multiplicity = 1

C	-0.0106870	2.4907310	-0.4376370
C	0.2278160	2.9209930	1.8731100
C	-1.2757390	2.9052890	1.5746230
N	-1.2982800	2.1796660	0.2681380
N	0.8815700	2.6473780	0.7203170
O	0.7354740	3.1427780	2.9716370
C	2.3304100	2.4804990	0.6638020
H	2.6648120	2.1164680	1.6368010
H	2.5872920	1.7457870	-0.1006790
H	2.8398480	3.4258870	0.4535010
C	-2.0723070	1.1379720	0.0490340
H	-2.8608890	1.0032940	0.7807140
C	-2.4184770	0.5864320	-1.3307070
C	-3.7019110	-0.2802240	-1.4140390
H	-4.4454720	0.2145910	-0.7783600
H	-4.0542820	-0.1513040	-2.4427020
H	-2.6536750	1.4886440	-1.8984220
C	-2.1385950	2.3733380	2.7040690
H	-1.9397210	2.9993540	3.5772540
H	-3.2024320	2.4597560	2.4686050
H	-1.9108740	1.3404560	2.9632030
H	-1.5808930	3.9353060	1.3617420
C	-0.0410040	3.7264970	-1.4126750
H	0.2870370	1.6048200	-0.9971630
Cl	-1.0450820	-0.1541010	-2.2584830
C	1.2661130	3.6896900	-2.2400150
H	1.2264660	4.4672850	-3.0090340

H	2.1524350	3.8799850	-1.6308330
H	1.3954150	2.7264540	-2.7449950
C	-1.2262820	3.6129790	-2.3913350
H	-1.1699180	2.7030320	-2.9965030
H	-2.1887250	3.6480110	-1.8707510
H	-1.2022700	4.4615950	-3.0819850
C	-0.1316300	5.0793390	-0.6790390
H	0.6424320	5.1894560	0.0860750
H	0.0075460	5.8868170	-1.4047110
H	-1.1098010	5.2357390	-0.2145750
N	-1.1139780	-0.6278450	1.0797740
C	-1.7910530	-1.2411960	2.1367090
C	0.1167650	-1.1198340	1.0117440
C	-0.9380270	-2.3467230	2.7543530
C	0.3922140	-2.2354450	2.0023130
H	-1.4392100	-3.3075140	2.6039190
H	0.6757970	-3.1443340	1.4634900
H	1.2355540	-1.9600270	2.6427460
H	-0.8488910	-2.1842280	3.8315430
O	0.9893500	-0.6705680	0.1905560
O	-2.9060750	-0.9031140	2.5134950
H	1.9902380	-1.1695170	0.2266670
O	3.1535260	-1.7760390	0.2709330
C	4.1032370	-1.2430160	-0.3996990
C	5.4309260	-2.0554690	-0.2715260
O	4.1011350	-0.2270230	-1.0936050
F	5.8339460	-2.1392190	1.0223750
F	5.2755800	-3.3260430	-0.7243680
F	6.4453920	-1.5058180	-0.9691460
C	-3.6811230	-1.7670060	-1.1067940
C	-4.2671320	-2.2631730	0.0661790
C	-3.1858400	-2.6900760	-2.0444480
C	-4.3257870	-3.6380280	0.3166990
H	-4.6750240	-1.5708210	0.7947880
C	-3.2369220	-4.0638180	-1.7956780
H	-2.7678240	-2.3347750	-2.9806610
C	-3.8041910	-4.5439470	-0.6103770
H	-4.7837150	-3.9976820	1.2338120
H	-2.8456240	-4.7583930	-2.5336240
H	-3.8506140	-5.6121940	-0.4191220

2.log
Potential Energy = -2233.49716
Zero-point Energy = -2232.96578
Free Energy = -2233.01358
Single-Point Energy B3LYP-D3(BJ)/6-311+G** PCM = -2234.08080
Free Energy B3LYP-D3(BJ)/6-311+G** PCM (extrapolated free energy from qRRHO) = -2233.59722
Nimag = 1 (-41.5476 cm^{-1})
Charge = 0 Multiplicity = 1

C	-0.2079630	2.0054930	0.0927230
C	0.2336690	1.6796300	2.3910850
C	-1.2249670	1.2658580	2.1687090
N	-1.2420470	1.0896830	0.6819630
N	0.7512260	2.0605390	1.2012560
O	0.8200500	1.6530350	3.4715570
C	2.1754370	2.3338310	1.0310920
H	2.7229610	1.7397450	1.7644590
H	2.4855200	2.0373530	0.0285540
H	2.4084040	3.3900490	1.1919530
C	-1.8114260	0.0648760	0.1111190
H	-2.4566640	-0.5140270	0.7589900
C	-2.0629700	-0.1502940	-1.3692320
C	-3.0049530	-1.3410270	-1.6331140
H	-3.0293390	-1.4901980	-2.7159990
H	-2.5888080	-2.2407270	-1.1767560
H	-2.5363160	0.7594890	-1.7395210
C	-1.6667590	0.0829670	3.0141540
H	-1.4802460	0.3492260	4.0572100
H	-2.7366170	-0.1110050	2.9072590
H	-1.1032980	-0.8209730	2.7804590
H	-1.8605040	2.1276850	2.3968520
C	-0.7439880	3.4084070	-0.3733680
H	0.2493010	1.4936390	-0.7546610
Cl	-0.5614480	-0.3093210	-2.3907240
C	0.4313480	4.1504000	-1.0519320
H	0.0558580	5.0732780	-1.5043210
H	1.2118260	4.4311920	-0.3418930
H	0.8849040	3.5506130	-1.8483690
C	-1.8634140	3.2365380	-1.4183050
H	-1.5253300	2.6644420	-2.2884000
H	-2.7526590	2.7630160	-0.9909670
H	-2.1698940	4.2231180	-1.7789880
C	-1.2760370	4.2663930	0.7906410
H	-0.5454950	4.3652660	1.5992110
H	-1.4928330	5.2734050	0.4209180
H	-2.2098390	3.8708160	1.2017360
N	-0.3852940	-1.8578010	0.4756280
C	-0.8543680	-3.0948900	0.8726380
C	0.9553810	-1.8789870	0.4420200
C	0.2968100	-4.0774160	1.1038010
C	1.5429090	-3.2397990	0.8027220
H	0.1760400	-4.9380370	0.4392860
H	2.1335090	-3.6178540	-0.0377040
H	2.2197850	-3.1354290	1.6562660
H	0.2568890	-4.4483060	2.1321790
O	1.6585160	-0.8705390	0.1495960
O	-2.0475620	-3.3668060	1.0228970
H	2.9908630	-0.9936730	0.0928700
O	4.0898510	-1.1087500	0.0847470
C	4.7145330	-0.3105810	-0.7252880
C	6.2504860	-0.5618770	-0.6743310
O	4.2597940	0.5474750	-1.4631090
F	6.7351370	-0.3715400	0.5760140
F	6.5478190	-1.8329230	-1.0362130
F	6.9179330	0.2634070	-1.4997520
C	-4.4122270	-1.0819270	-1.1209010
C	-5.2650740	-0.1997290	-1.8054900
C	-4.8887090	-1.7204870	0.0342090
C	-6.5609250	0.0432280	-1.3444490
H	-4.9183150	0.2921150	-2.7114300
C	-6.1876820	-1.4791690	0.4962020
H	-4.2376830	-2.4099610	0.5645290
C	-7.0260750	-0.5961730	-0.1894670
H	-7.2083420	0.7247450	-1.8887040
H	-6.5429990	-1.9844700	1.3898350
H	-8.0346600	-0.4104220	0.1681380

3.log
Potential Energy = -2233.49340
Zero-point Energy = -2232.96070
Free Energy = -2233.00849
Single-Point Energy B3LYP-D3(BJ)/6-311+G** PCM = -2234.07881
Free Energy B3LYP-D3(BJ)/6-311+G** PCM (extrapolated free energy from qRRHO) = -2233.59390
Nimag = 1 (-57.5343 cm^{-1})
Charge = 0 Multiplicity = 1

C	-2.9809140	0.1760540	-0.7843200
C	-3.2989800	-2.1426870	-0.4827470
C	-1.8699800	-1.9682390	-1.0069420
N	-1.6479400	-0.5092420	-0.7503780
N	-3.8573470	-0.9199850	-0.3590240
O	-3.8275400	-3.2214260	-0.2130040
C	-5.1434840	-0.7206130	0.2996650

H	-5.9760910	-0.7768430	-0.4076050
H	-5.2682080	-1.5029260	1.0501380
H	-5.1479590	0.2519350	0.7921500
C	-0.5216150	-0.0552300	-0.2599430
H	0.3050640	-0.7521950	-0.3210400
C	-0.0713320	1.3920670	-0.1578110
C	1.3899750	1.5074310	0.3068300
H	1.4623290	1.1963390	1.3496520
H	1.9583230	0.7841620	-0.2888760
H	-0.1485410	1.7952440	-1.1698570
C	-0.8794700	-2.9434100	-0.3907870
H	-1.2629120	-3.9488480	-0.5803230
H	0.1049620	-2.8633470	-0.8552610
H	-0.7879960	-2.8032900	0.6871560
H	-1.8850300	-2.1090050	-2.0930120
C	-3.3769310	0.8029190	-2.1736920
H	-2.9789870	0.9491390	-0.0170180
Cl	-1.1382720	2.4835280	0.8376360
C	-4.6811680	1.6073020	-1.9614660
H	-4.9174350	2.1550960	-2.8789220
H	-5.5358030	0.9651340	-1.7380580
H	-4.5774220	2.3399010	-1.1536000
C	-2.2918980	1.7804250	-2.6652510
H	-2.1121260	2.5873320	-1.9484200
H	-1.3503460	1.2671030	-2.8837390
H	-2.6265730	2.2438700	-3.5984620
C	-3.6136590	-0.2591650	-3.2653480
H	-4.3386570	-1.0174520	-2.9552440
H	-4.0132230	0.2309100	-4.1588330
H	-2.6865920	-0.7580930	-3.5639300
N	-0.4299630	-0.5585310	2.0319830
C	-1.5746620	-0.4464490	2.8024210
C	0.5817410	-1.0257320	2.7925970
C	-1.3034760	-0.8398770	4.2578970
C	0.1735090	-1.2351470	4.2487710
H	-1.9754690	-1.6545110	4.5437740
H	0.3555520	-2.2778450	4.5267570
H	0.8034610	-0.6119770	4.8911750
H	-1.5273090	0.0126010	4.9064390
O	1.7499330	-1.2709540	2.4055770
O	-2.6709330	-0.0850540	2.3761520
H	2.6082350	-1.6864800	1.2727640
O	3.3933050	-2.0690860	0.7136350
C	3.2188310	-2.0144780	-0.5766370
C	4.4425440	-2.6184870	-1.3209350
O	2.2691860	-1.5718540	-1.1957940
F	4.6269260	-3.9120560	-0.9738300
F	4.2770510	-2.5665270	-2.6518330
F	5.5736170	-1.9441730	-1.0147920
C	1.9857420	2.8875180	0.1156510
C	2.2391460	3.7196440	1.2149850
C	2.3117060	3.3537670	-1.1681600
C	2.7961020	4.9904970	1.0386130
H	2.0001380	3.3710030	2.2160900
C	2.8648710	4.6240520	-1.3494130
H	2.1407110	2.7176290	-2.0337330
C	3.1077510	5.4479360	-0.2449210
H	2.9859560	5.6201490	1.9031640
H	3.1122110	4.9666940	-2.3500950
H	3.5410510	6.4341100	-0.3838930

4.log
Potential Energy = -2233.49469
Zero-point Energy = -2232.96320
Free Energy = -2233.01182
Single-Point Energy B3LYP-D3(BJ)/6-311+G** PCM = -2234.07622
Free Energy B3LYP-D3(BJ)/6-311+G** PCM (extrapolated free energy from qRRHO) = -2233.59335
Nimag = 1 (-78.2152 cm^{-1})
Charge = 0 Multiplicity = 1

C	2.3706890	2.0188620	0.0951800
C	0.6256560	3.3962350	-0.7103440
C	0.8831690	2.3336090	-1.7881450
N	1.5994580	1.2984390	-0.9784650
N	1.4503170	3.1413770	0.3324070
O	-0.1945290	4.3080640	-0.7912610
C	1.3869530	3.8940940	1.5809500
H	0.3570050	4.2249200	1.7255840
H	1.6762370	3.2438970	2.4070350
H	2.0360420	4.7748400	1.5585560
C	1.1375770	0.0810020	-0.8797500
H	0.3705870	-0.1890720	-1.5964970
C	1.8168330	-1.0857280	-0.2045950
C	2.8152490	-1.7367740	-1.1991160
H	2.2626690	-2.0503620	-2.0895390
H	2.2895350	-0.8019810	0.7343670
C	-0.3564400	1.8927540	-2.5459530
H	-0.7793650	2.7870270	-3.0102610
H	-0.1019480	1.1926440	-3.3464990
H	-1.1147270	1.4530210	-1.8947970
H	1.6125680	2.7367350	-2.4972620
C	3.8405550	2.4612300	-0.2484910
H	2.3721040	1.3769430	0.9791850
Cl	0.5697870	-2.3397740	0.2310160
N	-0.5894940	0.4465120	0.8170910
C	-1.9213530	0.3539430	0.7114470
C	-0.2397960	0.5121820	2.1491370
C	-2.6362800	0.3916360	2.0576720
C	-1.4758850	0.5033840	3.0513820
H	-3.3242250	1.2424070	2.0872100
H	-1.4120040	-0.3389140	3.7465230
O	0.9246270	0.5651810	2.5576620
O	-2.5211560	0.2413200	-0.3971940
C	4.5116610	2.8644510	1.0871130
H	5.5671190	3.0883630	0.9049010
H	4.0621880	3.7558950	1.5298790
H	4.4638700	2.0532470	1.8214720
C	4.6388140	1.2909290	-0.8458470
H	4.6724730	0.4314740	-0.1699930
H	4.2353030	0.9773960	-1.8129800
H	5.6728600	1.6081920	-1.0115580
C	3.9084720	3.6556150	-1.2216790
H	3.3117820	4.5056110	-0.8790300
H	4.9470500	3.9924840	-1.2956780
H	3.5897860	3.3885940	-2.2335090
H	-1.4966610	1.4204740	3.6475720
H	-3.2335150	-0.5173000	2.1792010
H	3.5190090	-0.9654680	-1.5180200
C	3.5768330	-2.9165840	-0.6248940
C	3.4357690	-4.1903850	-1.1923610
C	4.4555960	-2.7563360	0.4577940
C	4.1540900	-5.2808880	-0.6915740
H	2.7597720	-4.3311500	-2.0314180
C	5.1716810	-3.8440850	0.9634570
H	4.5890230	-1.7786760	0.9134650
C	5.0230670	-5.1113450	0.3896970
H	4.0314930	-6.2600230	-1.1453770
H	5.8470810	-3.7005300	1.8018030
H	5.5805960	-5.9569640	0.7814420
H	-3.8704250	0.1329330	-0.4348510
O	-4.9587500	0.1233960	-0.5683730
C	-5.5384690	-0.9701480	-0.1750460
C	-7.0767990	-0.8933330	-0.4008290
F	-7.6175240	0.1415650	0.2853010

F	-7.6949860	-2.0170480	0.0019000
F	-7.3687020	-0.7101810	-1.7103760
O	-5.0397640	-1.9679260	0.3169070

Formation of anti-aminal *anti*-18b (TS5')

Conformation name	Extrapolated Free energy (kcal/mol)
TS-lowest	0.0
1	3.2
2	0.0

TS5'-lowest.log
Potential Energy = -2233.50047
Zero-point Energy = -2232.96722
Free Energy = -2233.01545
Single-Point Energy B3LYP-D3(BJ)/6-311+G** PCM = -2234.08648
Free Energy B3LYP-D3(BJ)/6-311+G** PCM (extrapolated free energy from qRRHO) = -2233.60146
Nimag = 1 (-94.9987)
Charge = 0 Multiplicity = 1

C	2.9618650	-1.5642330	-0.2622350
C	1.9922820	-2.1236090	-2.3428050
C	0.9290250	-1.3190890	-1.5939730
N	1.7342770	-0.7355930	-0.4815950
N	3.1171150	-2.1622620	-1.5928540
O	1.8550800	-2.6041590	-3.4678160
C	4.3976650	-2.5832650	-2.1588660
H	4.4278680	-2.2777080	-3.2067860
H	5.2085030	-2.0941960	-1.6177920
H	4.5352060	-3.6659710	-2.1067180
C	1.4269200	0.4300670	0.0622570
H	0.6002530	0.9299270	-0.4232240
C	2.4364540	1.3628500	0.7138100
C	1.8746620	2.7225910	1.1774350
H	2.7314510	3.2909240	1.5504360
H	2.9514930	0.8885630	1.5452460
C	0.2614040	-0.3061880	-2.5195270
H	-0.1302860	-0.8552580	-3.3791900
H	-0.5738430	0.1925060	-2.0270040
H	0.9779180	0.4362040	-2.8832910
H	0.1713550	-1.9931910	-1.1814810
C	2.8688980	-2.6071120	0.9084130
H	3.8084330	-0.9000150	-0.0738760
Cl	3.7578040	1.6704260	-0.5487560
N	0.1311670	0.1736090	1.7237170
C	-1.1200310	-0.2409550	1.4214170
C	0.2566440	0.3419070	3.0976380
C	-1.9896290	-0.4076160	2.6582920
C	-1.0521050	-0.0122430	3.8021390
H	-2.8715850	0.2330960	2.5664310
H	-0.8664710	-0.8203380	4.5155240
O	1.2792640	0.7235780	3.6605220
O	-1.5075170	-0.4593300	0.2492970
C	4.0194670	-3.6286020	0.7742980
H	4.0383040	-4.2560540	1.6708830
H	3.8857250	-4.2898350	-0.0849360
H	4.9973250	-3.1416100	0.6949950
C	3.0538370	-1.8693820	2.2474720
H	4.0280560	-1.3682800	2.2919970
H	2.2768980	-1.1286960	2.4307600
H	3.0176200	-2.5901400	3.0707380
C	1.5296000	-3.3659840	0.9012280
H	1.3683380	-3.8975460	-0.0426050
H	1.5326400	-4.1156480	1.6988620
H	0.6819370	-2.6985830	1.0790990
H	-1.3972550	0.8560160	4.3707130
H	-2.3408810	-1.4424970	2.7158300
H	-2.8788490	-0.8574420	-0.0785830
O	-3.8022470	-1.2140170	-0.4229040
C	-4.8026960	-0.4295210	-0.1229830
O	-4.7862480	0.6192520	0.4911390
C	-6.1364630	-1.0142400	-0.6685480
F	-6.0933630	-1.1462850	-2.0142360
F	-7.1779900	-0.2228900	-0.3654010
F	-6.3786850	-2.2378710	-0.1443530
H	1.2427280	2.5180100	2.0426600
C	1.1132750	3.5486910	0.1581350
C	-0.2815680	3.4344780	0.0395100
C	1.7762660	4.4776060	-0.6606930
C	-0.9918290	4.2063230	-0.8854140
H	-0.8207070	2.7476510	0.6857630
C	1.0701840	5.2523220	-1.5850480
H	2.8511330	4.6010890	-0.5685870
C	-0.3167810	5.1158630	-1.7041680
H	-2.0705320	4.1018340	-0.9579460
H	1.6026380	5.9666000	-2.2065540
H	-0.8664000	5.7199450	-2.4201120

1.log
Potential Energy = -2233.49345
Zero-point Energy = -2232.96020
Free Energy = -2233.00817
Single-Point Energy B3LYP-D3(BJ)/6-311+G** PCM = -2234.08163
Free Energy B3LYP-D3(BJ)/6-311+G** PCM (extrapolated free energy from qRRHO) = -2233.59635
Nimag = 1 (-107.7322)
Charge = 0 Multiplicity = 1

C	3.3205930	-1.2017400	0.1074410
C	2.4327860	-2.9175490	-1.2524370
C	1.2917090	-1.9249120	-1.0382270
N	2.0242210	-0.7422980	-0.4913900
N	3.5452170	-2.4323800	-0.6591540
O	2.3546530	-3.9578160	-1.9075160
C	4.8675570	-2.9845730	-0.9476130
H	4.8799230	-3.3257100	-1.9849090
H	5.6190400	-2.2051840	-0.8157470
H	5.1121070	-3.8293630	-0.2991830
C	1.5094600	0.4760500	-0.6021020
H	0.6113970	0.4761210	-1.2046550
C	2.2589560	1.8136230	-0.6744720
C	1.5625820	2.8073060	-1.6416520
H	1.5540310	2.3514190	-2.6371800
H	2.2197340	3.6793160	-1.6991960
H	2.4000360	2.2434650	0.3142060
C	0.5334220	-1.6788290	-2.3395020
H	0.2324680	-2.6523390	-2.7342750
H	-0.3695110	-1.0909650	-2.1710000
H	1.1663980	-1.1862230	-3.0838070
H	0.5996180	-2.3078710	-0.2808330
C	3.3139700	-1.4000550	1.6653620
H	4.1006470	-0.4844200	-0.1430650
Cl	3.9598750	1.6151750	-1.3599130
N	0.2659280	0.9410490	1.0015120
C	-0.9402640	0.3315930	1.0192650
C	0.3380440	1.8862920	2.0164540
C	-1.8226930	0.8315280	2.1526480
C	-0.9563370	1.8987930	2.8270900
H	-2.7588900	1.2159730	1.7380680
H	-0.7262230	1.6805600	3.8738280
O	1.3117720	2.6035410	2.2333650

O	-1.2761550	-0.5495660	0.1932860
C	4.5395620	-2.2451060	2.0774140
H	4.6124560	-2.2471680	3.1696110
H	4.4513270	-3.2847570	1.7530070
H	5.4766430	-1.8329760	1.6879890
C	3.4569240	-0.0188090	2.3319860
H	4.3992650	0.4604100	2.0423880
H	2.6409810	0.6584650	2.0850590
H	3.4656490	-0.1353980	3.4207660
C	2.0407600	-2.1091650	2.1598060
H	1.9201440	-3.0946380	1.6973020
H	2.1081480	-2.2651920	3.2413790
H	1.1433700	-1.5164880	1.9665010
H	-1.3900200	2.9019000	2.7858190
H	-2.0744340	-0.0071490	2.8092560
C	0.1620810	3.2695220	-1.2853190
C	-0.0358470	4.2963680	-0.3484940
C	-0.9577620	2.7359200	-1.9404330
C	-1.3205300	4.7604590	-0.0571770
H	0.8208450	4.7365200	0.1539810
C	-2.2462960	3.1965130	-1.6503740
H	-0.8244970	1.9657150	-2.6961030
C	-2.4316370	4.2086220	-0.7049690
H	-1.4536070	5.5571260	0.6691790
H	-3.1001470	2.7705000	-2.1689850
H	-3.4305420	4.5715810	-0.4813640
H	-2.5894480	-1.2027000	0.1962010
O	-3.4533530	-1.7934380	0.1488990
C	-4.5486990	-1.0980270	-0.0026280
O	-4.6762920	0.1076170	-0.0868010
C	-5.7860980	-2.0376070	-0.0710760
F	-5.6939740	-2.8821210	-1.1242240
F	-6.9246690	-1.3379870	-0.2025550
F	-5.8881130	-2.7891260	1.0491910

2.log
Potential Energy = -2233.50217
Zero-point Energy = -2232.96933
Free Energy = -2233.01848
Single-Point Energy B3LYP-D3(BJ)/6-311+G** PCM = -2234.08509
Free Energy B3LYP-D3(BJ)/6-311+G** PCM (extrapolated free energy from qRRHO) = -2233.60140
Nimag = 1 (-86.7932)
Charge = 0 Multiplicity = 1

C	-1.7531000	2.5492890	0.2229870
C	-0.2696500	3.6869190	-1.2227940
C	0.3534760	2.3092670	-0.9936490
N	-0.7866820	1.5731760	-0.3732690
N	-1.4651000	3.7343240	-0.5918680
O	0.2185850	4.5779720	-1.9173640
C	-2.4355150	4.7907220	-0.8742090
H	-2.3424510	5.0715390	-1.9253260
H	-3.4418870	4.4132860	-0.6898860
H	-2.2684160	5.6781550	-0.2591230
C	-0.9253970	0.2682310	-0.5093920
H	-0.1868970	-0.1840050	-1.1574790
C	-2.2540690	-0.4740520	-0.4555020
C	-2.1089420	-1.9590650	-0.8194550
H	-2.7695420	-0.3400940	0.4921190
C	0.8749770	1.7230060	-2.3025140
H	1.5646280	2.4510920	-2.7363560
H	1.4240190	0.7965130	-2.1320100
H	0.0628060	1.5516990	-3.0152830
H	1.1734650	2.3834140	-0.2718320
C	-1.6081390	2.7752630	1.7702480
H	-2.7702960	2.2128760	0.0098600
Cl	-3.3442240	0.3237000	-1.7222850
N	0.0802780	-0.7760010	1.0758870
C	1.4289140	-0.7764700	1.0010440
C	-0.3354700	-1.5472280	2.1526210
C	2.0717140	-1.5916880	2.1135900
C	0.8690410	-2.1035140	2.9114400
H	2.6783430	-2.3874210	1.6709350
H	0.8416020	-1.7376210	3.9420280
O	-1.5106270	-1.7510880	2.4470670
O	2.0685060	-0.1686570	0.1088180
C	-2.3792820	4.0514230	2.1726960
H	-2.4005090	4.1187520	3.2648620
H	-1.8998250	4.9587710	1.7982320
H	-3.4179740	4.0329470	1.8255530
C	-2.2525720	1.5878220	2.5093860
H	-3.3159600	1.4960650	2.2582350
H	-1.7629070	0.6392860	2.2929180
H	-2.1838070	1.7495750	3.5900360
C	-0.1365920	2.9288620	2.1953700
H	0.3510580	3.7633970	1.6803750
H	-0.0889880	3.1383110	3.2687180
H	0.4371600	2.0162180	2.0116470
H	0.7977470	-3.1942250	2.9474270
H	2.7437650	-0.9506880	2.6922750
H	3.5214700	-0.2174080	0.0043700
O	4.5606300	-0.1250710	-0.1207960
C	5.1531930	-1.2628860	-0.3647370
O	4.6611580	-2.3711290	-0.4512790
C	6.6827310	-1.0533480	-0.5524100
F	6.9327330	-0.2432540	-1.6071630
F	7.3133950	-2.2187690	-0.7699150
F	7.2338110	-0.4817020	0.5428010
H	-1.3897980	-2.3886370	-0.1189740
H	-1.6715780	-2.0317040	-1.8201040
C	-3.4036870	-2.7458750	-0.7619280
C	-3.9852200	-3.2526140	-1.9324060
C	-4.0328480	-2.9990150	0.4679490
C	-5.1728930	-3.9901040	-1.8810080
H	-3.5066700	-3.0700950	-2.8910650
C	-5.2218830	-3.7312940	0.5214840
H	-3.5807200	-2.6276560	1.3834310
C	-5.7967970	-4.2291170	-0.6532520
H	-5.6080870	-4.3755430	-2.7986780
H	-5.6956230	-3.9189770	1.4810140
H	-6.7191920	-4.8011120	-0.6107420

Formation of syn-18b' ($TS_{syn\text{-}18b'}$)

Conformation name	Extrapolated Free energy (kcal/mol)
TS-lowest	0.0
1	1.4

TS-lowest.log
Potential Energy = -2233.49084
Zero-point Energy = -2232.95906
Free Energy = -2233.00727
Single-Point Energy B3LYP-D3(BJ)/6-311+G** PCM = -2234.07235
Free Energy B3LYP-D3(BJ)/6-311+G** PCM (extrapolated free energy from qRRHO) = -2233.58878
Nimag = 1 (-58.6095)
Charge = 0 Multiplicity = 1

C	3.3758330	-1.2079090	-0.6598080
C	2.2233830	-1.2548260	-2.7199250
C	1.1945980	-0.7703580	-1.6951220

N	2.0766130	-0.4323860	-0.5336930
N	3.4199070	-1.4046260	-2.1065300
O	1.9987620	-1.4196840	-3.9164320
C	4.6561960	-1.5404920	-2.8776180
H	4.5565080	-0.9521490	-3.7918840
H	5.4905030	-1.1564650	-2.2899860
H	4.8567750	-2.5793350	-3.1491310
C	1.8576010	0.3433720	0.4912330
H	2.6334280	0.3328340	1.2500660
C	0.9705990	1.5679850	0.5216520
C	1.6926170	2.7073230	-0.2538520
H	2.6649340	2.8820700	0.2163040
H	0.5671310	-1.6032150	-1.3595520
C	3.4792960	-2.5207660	0.1901660
H	4.1831310	-0.5308780	-0.3647720
H	-0.0266880	1.3763210	0.1380870
Cl	0.7416250	2.1101380	2.2421080
N	0.3458150	-0.9495720	1.9479720
C	-0.8834150	-1.2372330	1.5052380
C	0.4088030	-1.1919290	3.3102950
C	-1.8158260	-1.7580470	2.5916780
C	-0.9242390	-1.7354600	3.8361900
H	-2.1734200	-2.7571470	2.3232850
H	-0.7641300	-2.7236810	4.2774500
H	-1.2949130	-1.0781100	4.6281690
H	-2.6915140	-1.1056370	2.6652910
O	1.4046430	-1.0000090	4.0070730
O	-1.2336810	-1.0847430	0.2966370
C	0.2864820	0.2898610	-2.3072060
H	-0.5374900	0.5448310	-1.6436340
H	0.8288170	1.1827370	-2.6211600
H	-0.1413610	-0.1638080	-3.2047130
C	4.7223430	-3.3090410	-0.2819260
H	4.8827140	-4.1474640	0.4025230
H	4.5925920	-3.7250990	-1.2833100
H	5.6308640	-2.6971490	-0.2686770
C	2.2335450	-3.4108810	0.0324270
H	2.0530900	-3.6769900	-1.0146220
H	2.3863960	-4.3450310	0.5821430
H	1.3408200	-2.9308570	0.4409640
C	3.6936990	-2.1587390	1.6742370
H	4.5764080	-1.5210300	1.8041810
H	2.8324110	-1.6663490	2.1260570
H	3.8697450	-3.0778310	2.2425990
H	1.8936980	2.3439270	-1.2653200
C	0.9121700	4.0056700	-0.3178440
C	1.3882170	5.1506510	0.3358320
C	-0.2812630	4.0965470	-1.0514140
C	0.6884660	6.3592960	0.2631730
H	2.3122390	5.0975380	0.9051180
C	-0.9848560	5.3013390	-1.1229720
H	-0.6656380	3.2271210	-1.5776620
C	-0.5021280	6.4374370	-0.4645900
H	1.0738070	7.2360210	0.7755570
H	-1.9058990	5.3530210	-1.6961870
H	-1.0477760	7.3746630	-0.5217350
H	-2.5066280	-1.3861940	-0.1142360
O	-3.4572070	-1.6772830	-0.5552050
C	-4.4428740	-0.8758100	-0.2794600
O	-4.4425340	0.1304530	0.4074990
C	-5.7523160	-1.3528970	-0.9726190
F	-6.0649080	-2.6194650	-0.6119930
F	-5.6187140	-1.3340360	-2.3204680
F	-6.7959300	-0.5679840	-0.6547000

1.log
Potential Energy = -2233.49102
Zero-point Energy = -2232.95979
Free Energy = -2233.00858
Single-Point Energy B3LYP-D3(BJ)/6-311+G** PCM = -2234.07121
Free Energy B3LYP-D3(BJ)/6-311+G** PCM (extrapolated free energy from qRRHO) = -2233.58877
Nimag = 1 (-61.9068)
Charge = 0 Multiplicity = 1

C	-1.8130170	-2.4931970	-1.1402690
C	-3.8246230	-2.7245180	0.0727710
C	-3.0569120	-1.6039910	0.7782400
N	-2.0022920	-1.2892390	-0.2360220
N	-3.1279240	-3.1172680	-1.0187790
O	-4.9254770	-3.1473700	0.4179770
C	-3.7491450	-3.9274280	-2.0669600
H	-4.8054300	-3.6580460	-2.1271030
H	-3.2664680	-3.7124190	-3.0210900
H	-3.6714160	-4.9968830	-1.8588220
C	-1.2660640	-0.2217790	-0.3820060
H	-0.4972460	-0.2971870	-1.1440820
C	-1.6536880	1.1972650	-0.0267710
C	-2.7005070	1.6923450	-1.0645390
H	-2.2633010	1.6063350	-2.0637200
H	-2.5227240	-1.9908450	1.6530020
C	-0.6024710	-3.4291430	-0.7987290
H	-1.6886300	-2.1133340	-2.1586160
H	-2.0067920	1.2936300	0.9955180
Cl	-0.1893940	2.2705920	-0.1457840
N	0.3949080	-0.3482360	1.3969580
C	-0.0490660	-0.2869960	2.7011350
C	1.7258500	-0.1716540	1.3714040
C	1.1111470	-0.0766010	3.6769500
C	2.3343000	0.0029300	2.7590160
H	1.1464170	-0.9117540	4.3827990
H	3.0729720	-0.7840240	2.9403270
H	2.8596970	0.9618190	2.8097700
H	0.9373890	0.8353620	4.2556860
O	2.4012120	-0.1538000	0.3052730
O	-1.2334650	-0.3869600	3.0343500
C	-4.0141380	-0.5180310	1.2549270
H	-3.5054780	0.2183840	1.8738090
H	-4.5554090	-0.0409260	0.4367680
H	-4.7521090	-1.0230550	1.8832440
C	-0.7446210	-4.7294210	-1.6221700
H	0.1681660	-5.3202900	-1.4998680
H	-1.5800690	-5.3449890	-1.2818670
H	-0.8650420	-4.5304850	-2.6926380
C	-0.5534600	-3.7882710	0.6970860
H	-1.4770350	-4.2744720	1.0291170
H	0.2647320	-4.4942600	0.8713890
H	-0.3673120	-2.9082600	1.3176850
C	0.7125190	-2.7477950	-1.2299550
H	0.6913490	-2.4803750	-2.2932380
H	0.9458030	-1.8571090	-0.6471910
H	1.5410920	-3.4489100	-1.0866880
H	-3.5495590	1.0042980	-1.0329590
C	-3.1794360	3.1126060	-0.8350750
C	-2.8914600	4.1155150	-1.7711090
C	-3.9398020	3.4467890	0.2966450
C	-3.3489700	5.4235270	-1.5827210
H	-2.3058790	3.8722950	-2.6535510
C	-4.3948410	4.7534250	0.4903200
H	-4.1864030	2.6863200	1.0325170
C	-4.1002580	5.7470050	-0.4494780
H	-3.1166170	6.1864660	-2.3200240
H	-4.9827210	4.9932890	1.3715000
H	-4.4558900	6.7622370	-0.3003350
H	3.7538890	0.0246360	0.3358730
O	4.8380730	0.1351660	0.3763710

C	5.3811670	0.4974920	-0.7473270
C	6.9262320	0.6188720	-0.5995170
O	4.8478370	0.7308190	-1.8176920
F	7.5060890	1.0015960	-1.7503050
F	7.4742910	-0.5654650	-0.2371360
F	7.2561790	1.5271120	0.3490590

Formation of anti-anti18b' ($TS_{anti\text{-}18b'}$)

TS-lowest.log
Potential Energy = -2233.50709
Zero-point Energy = -2232.97791
Free Energy = -2233.02678
Single-Point Energy B3LYP-D3(BJ)/6-311+G** PCM = -2234.08656
Free Energy B3LYP-D3(BJ)/6-311+G** PCM (extrapolated free energy from qRRHO) = -2233.60624
Nimag = 1 (-494.2657)
Charge = 0 Multiplicity = 1

C	0.7553950	2.0075520	-0.1593370
C	0.2995140	2.8729210	1.9872940
C	-1.0680540	2.4503560	1.4277240
N	-0.6532540	1.6570390	0.2335520
N	1.2637350	2.5507530	1.0957680
O	0.4695730	3.3815280	3.0920910
C	2.6837520	2.6033130	1.4462810
H	2.7816970	2.3576760	2.5055510
H	3.2295660	1.8696990	0.8514970
H	3.1043600	3.5983810	1.2792520
C	-1.2604740	0.6747920	-0.3513370
H	-0.7053660	0.1912140	-1.1459570
C	-2.7142960	0.2818740	-0.2167870
C	-3.0654790	-0.8567410	-1.1849440
H	-1.6004830	3.3397430	1.0742580
C	0.8302640	2.9761920	-1.3923690
H	1.2719540	1.0727950	-0.3981280
H	-2.9483800	0.0030550	0.8081800
Cl	-3.7337960	1.7689450	-0.5820500
N	-0.4735560	-1.4067320	0.8263090
C	0.7597970	-1.8201470	0.5668020
C	-0.9996430	-2.1714740	1.8588800
C	1.2274440	-2.9758000	1.4358890
C	0.0053300	-3.2274680	2.3275200
H	2.1242030	-2.6839770	1.9911980
H	0.2069320	-3.0922170	3.3939080
H	-0.4286110	-4.2232040	2.1982200
H	1.4977250	-3.8292530	0.8066020
O	-2.1255430	-2.0065410	2.3245710
O	1.4776180	-1.2734230	-0.3415940
C	-1.8926690	1.7263430	2.4888510
H	-2.9451290	1.6599210	2.2139220
H	-1.4994630	0.7293090	2.6978530
H	-1.8233980	2.3236400	3.4010400
C	2.3214220	3.2690830	-1.6760050
H	2.4017200	3.8195800	-2.6180780
H	2.7760740	3.8863470	-0.8986310
H	2.9057750	2.3484020	-1.7769920
C	0.0879850	4.2999610	-1.1340690
H	0.4625840	4.8109670	-0.2414560
H	0.2410070	4.9719670	-1.9840850
H	-0.9915810	4.1524690	-1.0304690
C	0.2381520	2.2841240	-2.6378060
H	0.7211940	1.3211860	-2.8387200
H	-0.8423220	2.1299950	-2.5625300
H	0.4048610	2.9218760	-3.5110210
H	-2.3519090	-1.6596160	-0.9676150
H	-2.8820800	-0.5251930	-2.2115970
C	-4.4822070	-1.3758820	-1.0485500
C	-5.4078690	-1.2068570	-2.0871710
C	-4.8855820	-2.0543560	0.1133120
C	-6.7122220	-1.6990960	-1.9701700
H	-5.1080000	-0.6881560	-2.9940340
C	-6.1890880	-2.5430530	0.2336870
H	-4.1749090	-2.2010720	0.9231240
C	-7.1071300	-2.3673020	-0.8079500
H	-7.4158670	-1.5597180	-2.7858850
H	-6.4862490	-3.0664100	1.1381300
H	-8.1191260	-2.7505810	-0.7147530
H	2.6018430	-1.6573800	-0.4675820
O	3.7335270	-2.0611650	-0.6549070
C	4.6670350	-1.1894870	-0.5031280
C	6.0746670	-1.8103610	-0.7591650
O	4.5837530	-0.0031650	-0.2038500
F	6.1826360	-2.2617720	-2.0340160
F	6.3051030	-2.8645830	0.0617720
F	7.0677870	-0.9225030	-0.5616410

1.log
Potential Energy = -2233.50099
Zero-point Energy = -2232.97161
Free Energy = -2233.02034
Single-Point Energy B3LYP-D3(BJ)/6-311+G** PCM = -2234.08469
Free Energy B3LYP-D3(BJ)/6-311+G** PCM (extrapolated free energy from qRRHO) = -2233.60403
Nimag = 1 (-389.2397)
Charge = 0 Multiplicity = 1

C	-1.1561550	1.4775340	-1.2816290
C	-2.7760180	2.9260920	-0.3623500
C	-3.1981720	1.5178010	0.0829510
N	-1.9823030	0.7295480	-0.2737740
N	-1.6173240	2.8439240	-1.0544130
O	-3.3867600	3.9558020	-0.0876860
C	-0.8588390	4.0399240	-1.4172450
H	0.1940090	3.7797770	-1.5269370
H	-1.2213630	4.4824740	-2.3488290
H	-0.9692440	4.7730640	-0.6159710
C	-1.5144300	-0.3538880	0.2667590
H	-0.5661160	-0.6950600	-0.1273800
C	-2.2664960	-1.3156440	1.1566980
C	-1.4431560	-2.5427760	1.5937880
H	-2.1162160	-3.1687290	2.1863620
H	-0.6842880	-2.1566050	2.2798250
N	-0.0491940	0.3793210	2.0910860
C	1.1522630	0.8726510	1.7977880
C	-0.2696240	0.4893950	3.4558820
C	1.9168260	1.3861640	3.0089610
C	0.9317430	1.1303760	4.1556190
H	2.8593000	0.8391060	3.1097970
H	1.3162690	0.4458430	4.9171570
H	0.6108510	2.0431950	4.6658400
H	2.1668220	2.4422680	2.8695210
O	-1.3006160	0.1173000	4.0145120
O	1.6027450	0.9048410	0.6060810
C	-3.6319310	1.5169140	1.5468160
H	-4.2944960	2.3759140	1.6768140
H	-4.1960600	0.6209250	1.8054400
H	-2.7829050	1.6292050	2.2239110
H	-4.0212260	1.1749050	-0.5533780
C	-1.3308770	0.9480280	-2.7492960
H	-0.1075350	1.3812960	-0.9811850
Cl	-3.7820070	-1.8347810	0.2468940
H	-2.6225610	-0.8107010	2.0511680
C	-0.8657360	-0.5201380	-2.8361930
H	0.1588000	-0.6472740	-2.4693360

H	-1.5235940	-1.2040940	-2.2925600
H	-0.8786020	-0.8352290	-3.8838910
C	-0.4182100	1.7885860	-3.6717190
H	-0.7646140	2.8189860	-3.7728600
H	0.6180570	1.8011540	-3.3168370
H	-0.4199180	1.3453900	-4.6720040
C	-2.7884920	1.0570540	-3.2328530
H	-3.1661260	2.0822700	-3.1668380
H	-2.8445530	0.7544890	-4.2830490
H	-3.4576410	0.3975190	-2.6715550
C	-0.7798090	-3.3664270	0.5076590
C	0.5610970	-3.1364440	0.1589370
C	-1.4726610	-4.3979320	-0.1473800
C	1.1875140	-3.8988460	-0.8320700
H	1.1266130	-2.3649470	0.6754580
C	-0.8493880	-5.1624790	-1.1371830
H	-2.5022760	-4.6097840	0.1247920
C	0.4821490	-4.9126170	-1.4859810
H	2.2258620	-3.7049100	-1.0846910
H	-1.4013610	-5.9575810	-1.6301480
H	0.9674970	-5.5094220	-2.2526650
H	2.7458930	1.4011750	0.4130400
O	3.7336280	1.9633310	0.2171470
C	4.7854380	1.3795160	-0.2556840
C	4.6232730	-0.1441130	-0.5601680
F	3.6437630	-0.3552530	-1.4737500
F	5.7529090	-0.6859170	-1.0440570
F	4.2870850	-0.8311490	0.5599900
O	5.8648710	1.9056760	-0.4799020

E2-Mechanism (TS-E2)

Conformation name	Extrapolated Free energy (kcal/mol)
TS-E2	0.0
1	0.9

TS-E2.log
Potential Energy = -2233.42985
Zero-point Energy = -2232.89629
Free Energy = -2232.94300
Single-Point Energy B3LYP-D3(BJ)/6-311+G** PCM = -2234.02725
Free Energy B3LYP-D3(BJ)/6-311+G** PCM (extrapolated free energy from qRRHO) = -2233.54041
Nimag = 1 (-338.6068 cm^{-1})
Charge = 0 Multiplicity = 1

C	-2.2726820	-0.9271960	-0.7481570
C	-3.1142270	-1.2022830	1.4434540
C	-1.6178270	-1.4975780	1.5356850
N	-1.0817470	-0.8216420	0.2523880
N	-3.4090540	-0.8714840	0.1665630
O	-3.9001980	-1.2481600	2.3867650
C	-4.7162290	-0.3178230	-0.1867410
H	-5.0405680	0.3502890	0.6140570
H	-4.6305640	0.2445990	-1.1154850
H	-5.4634790	-1.1059000	-0.3093810
C	-0.4888800	0.5420700	0.4951520
H	-0.4783400	0.7825330	1.5482030
C	0.6685680	0.9533080	-0.1725320
C	1.2007610	2.3320760	0.2112530
H	0.6130110	3.0947730	-0.3191040
H	1.8647630	-0.2221270	0.3789040
C	-0.9881730	-1.1159980	2.8668330
H	-1.4143400	-1.7937190	3.6111600
H	0.0936260	-1.2666010	2.8631620
H	-1.2262470	-0.0953020	3.1691910
H	-1.4609540	-2.5640220	1.3665690
C	-2.2450480	-2.1968370	-1.6700770
H	-2.2403510	-0.0303830	-1.3699270
Cl	0.8090770	0.6159590	-1.9388910
N	-2.0358710	1.7908020	0.3421700
C	-2.5292130	2.4522740	-0.7622140
C	-2.2567880	2.5230590	1.4880050
C	-3.1928190	3.7657990	-0.3470270
C	-3.0390260	3.7962760	1.1766840
H	-2.6849810	4.5931490	-0.8520690
H	-3.9935210	3.7665700	1.7110230
O	-1.8664190	2.1888550	2.6107570
O	-2.4671140	2.0358290	-1.9209940
C	-3.5459110	-2.1541910	-2.5095850
H	-3.4937160	-2.9353800	-3.2734280
H	-4.4351700	-2.3466970	-1.9057710
H	-3.6698140	-1.1959010	-3.0246730
C	-1.0587800	-2.1344200	-2.6532160
H	-1.0862160	-1.2231250	-3.2565110
H	-0.0884820	-2.1877220	-2.1552460
H	-1.1221990	-2.9909290	-3.3317260
C	-2.2061980	-3.5351400	-0.9050420
H	-3.0082540	-3.6123060	-0.1642640
H	-2.3478390	-4.3517440	-1.6195900
H	-1.2433310	-3.7113590	-0.4157050
H	-2.4824810	4.6611420	1.5492080
H	-4.2321450	3.7640100	-0.6874780
H	0.9942020	2.4671940	1.2792650
C	2.6774590	2.5838060	-0.0375620
C	3.1145450	3.1916480	-1.2238080
C	3.6345840	2.2424070	0.9302760
C	4.4732970	3.4370180	-1.4462210
H	2.3859310	3.4785840	-1.9771280
C	4.9935410	2.4871090	0.7140550
H	3.3142480	1.7859200	1.8635970
C	5.4180660	3.0832520	-0.4780510
H	4.7914240	3.9086710	-2.3717270
H	5.7181140	2.2180010	1.4774640
H	6.4734040	3.2770320	-0.6468880
H	-0.2941070	-1.4078670	-0.0853860
O	1.2065520	-2.5374070	-0.0206420
C	2.3055770	-2.1190380	0.3109540
O	2.6543340	-0.8886610	0.5511390
C	3.4997560	-3.0943460	0.4978530
F	3.9810410	-3.0183410	1.7567560
F	4.5020160	-2.7846810	-0.3510950
F	3.1299900	-4.3615970	0.2662250

1.log
Potential Energy = -2233.43162
Zero-point Energy = -2232.89817
Free Energy = -2232.94495
Single-Point Energy B3LYP-D3(BJ)/6-311+G** PCM = -2234.02560
Free Energy B3LYP-D3(BJ)/6-311+G** PCM (extrapolated free energy from qRRHO) = -2233.53893
Nimag = 1 (-323.8199 cm^{-1})
Charge = 0 Multiplicity = 1

C	-0.8868030	-2.2718910	-0.0544120
C	-1.4009180	-1.7870380	2.2002150
C	-0.0587240	-1.1098600	1.9276830
N	-0.0445590	-1.0360190	0.3834360
N	-1.8257100	-2.3735510	1.0575630
O	-1.9851120	-1.7831920	3.2806250
C	-3.1807220	-2.9097540	0.9381560
H	-3.8650170	-2.2519030	1.4779420

H	-3.4642540	-2.9428840	-0.1133960
H	-3.2547290	-3.9143110	1.3623180
C	-0.4393850	0.3142990	-0.1668660
H	-0.6478580	1.0227210	0.6218580
C	0.2701650	0.8605970	-1.2360620
C	-0.0476120	2.2698960	-1.7346830
H	0.7686350	2.5695480	-2.4024650
H	1.9137280	0.9895550	-0.6359380
C	0.1655660	0.1761880	2.7071130
H	0.2582210	-0.1134280	3.7570900
H	1.0959430	0.6677640	2.4149840
H	-0.6737250	0.8670630	2.6229150
H	0.7409650	-1.8109210	2.1713760
C	-0.0535120	-3.5770610	-0.3184400
H	-1.4034650	-1.9871710	-0.9724210
Cl	0.6898770	-0.2082340	-2.6288440
N	-2.4218580	0.1529340	-0.4051890
C	-3.1311150	-0.1712350	-1.5400340
C	-3.1797360	0.9272400	0.4442170
C	-4.5245200	0.4590920	-1.4975550
C	-4.5697120	1.1703790	-0.1411620
H	-4.6301790	1.1392340	-2.3485170
H	-5.3205920	0.7597570	0.5406520
O	-2.7837080	1.3557890	1.5309980
O	-2.7149820	-0.8932980	-2.4485210
C	-1.0788010	-4.6821220	-0.6747450
H	-0.5337260	-5.5660970	-1.0182210
H	-1.6798330	-4.9836770	0.1854410
H	-1.7495410	-4.3729150	-1.4831150
C	0.8763820	-3.4017580	-1.5356530
H	0.3174500	-3.1151450	-2.4302660
H	1.6623820	-2.6621520	-1.3693880
H	1.3697090	-4.3576840	-1.7373180
C	0.7752130	-4.0567500	0.8904120
H	0.1685230	-4.1598620	1.7954040
H	1.1852050	-5.0455430	0.6632180
H	1.6290120	-3.4050090	1.0995250
H	-4.7470330	2.2476460	-0.2110190
H	-5.2774960	-0.3258020	-1.6114860
H	-0.9508390	2.2287600	-2.3588900
C	-0.2337290	3.3376430	-0.6688680
C	0.8354710	3.7614010	0.1383650
C	-1.4745840	3.9723210	-0.5153810
C	0.6626880	4.7784550	1.0805470
H	1.8145630	3.3055870	0.0253010
C	-1.6509090	4.9951240	0.4223590
H	-2.3099170	3.6689680	-1.1408800
C	-0.5827580	5.3992660	1.2270030
H	1.5030520	5.0917500	1.6935320
H	-2.6212980	5.4729630	0.5220490
H	-0.7158720	6.1925150	1.9568080
H	0.9413660	-1.1742460	0.0954950
O	2.8404570	-1.0719010	0.2444320
C	3.4415600	-0.0449040	-0.0284180
O	2.9456650	1.0719020	-0.4808280
C	4.9820090	0.0451330	0.1440610
F	5.3101470	1.0562670	0.9751630
F	5.5761940	0.2736870	-1.0462160
F	5.4783190	-1.0922890	0.6495350

E1-Mechanism (TS-E1)

Conformation name	Extrapolated Free energy (kcal/mol)
TS-E1	0.0

1	2.8
2	1.9
3	1.1

TS-E1.log
Potential Energy = -2233.47717
Zero-point Energy = -2232.94991
Free Energy = -2232.99863
Single-Point Energy B3LYP-D3(BJ)/6-311+G** PCM = -2234.05418
Free Energy B3LYP-D3(BJ)/6-311+G** PCM (extrapolated free energy from qRRHO) = -2233.57563
Nimag = 1 (-1285.1321 cm^{-1})
Charge = 0 Multiplicity = 1

C	1.3689690	-2.0491260	-0.7237330
C	0.2940610	-3.3944340	0.8866180
C	1.7298810	-3.1901280	1.3841540
N	2.1691450	-2.0459990	0.5295190
N	0.1338850	-2.6826180	-0.2520010
O	-0.5550960	-4.0831730	1.4509940
C	-1.1408350	-2.5872250	-0.9523900
H	-1.9280990	-2.8401450	-0.2412560
H	-1.2896690	-1.5642440	-1.3034300
H	-1.1961960	-3.2836280	-1.7947210
C	2.9679790	-1.1028390	0.9976430
H	3.4076700	-1.3738900	1.9513660
C	3.2284560	0.2503300	0.6268280
C	3.2459730	0.8283380	-0.7930200
H	4.1085340	0.4142400	-1.3252960
H	2.1888830	0.8220090	1.3634110
C	1.8005340	-2.9720910	2.8892500
H	1.2788340	-3.8063340	3.3643820
H	2.8293400	-2.9722260	3.2563250
H	1.3064450	-2.0425920	3.1863610
H	2.3164230	-4.0765110	1.1159810
C	2.0504700	-2.7997610	-1.9409670
H	1.1454130	-1.0175760	-0.9971440
Cl	4.6860040	0.8378580	1.5750640
N	-0.2254080	0.8900300	0.5289000
C	0.1632540	1.3678640	1.7152120
C	-1.5733250	1.0696170	0.4316080
C	-0.9562680	1.9254890	2.5727250
C	-2.1792970	1.7175390	1.6731320
H	-1.0049260	1.3787940	3.5192580
H	-2.6806470	2.6498410	1.3962690
O	-2.2267910	0.7360390	-0.5810730
O	1.3718970	1.3753500	2.1200210
C	1.3838910	-2.2876840	-3.2387590
H	1.8557690	-2.7644920	-4.1036080
H	0.3160900	-2.5163670	-3.2805230
H	1.5038430	-1.2045840	-3.3493950
C	3.5585040	-2.4895170	-2.0172610
H	3.7553220	-1.4258320	-2.1634850
H	4.0954050	-2.8256200	-1.1254870
H	3.9839250	-3.0156030	-2.8775160
C	1.8765220	-4.3299780	-1.8482440
H	0.8268810	-4.6314920	-1.8011190
H	2.3110070	-4.7903090	-2.7409590
H	2.3970820	-4.7553420	-0.9848690
H	-2.9353200	1.0530800	2.1014620
H	-0.7544860	2.9742630	2.8100480
H	2.3465750	0.4842140	-1.3074080
C	3.3025620	2.3444030	-0.8993940
C	2.1335940	3.1181160	-0.8448390
C	4.5271610	2.9951650	-1.1112790
C	2.1897600	4.5088590	-0.9763820
H	1.1755760	2.6264670	-0.7058750

C	4.5876810	4.3856470	-1.2435030
H	5.4407550	2.4103080	-1.1739670
C	3.4178190	5.1483580	-1.1728800
H	1.2733060	5.0907430	-0.9331470
H	5.5462390	4.8701520	-1.4062560
H	3.4616830	6.2285110	-1.2784510
H	-3.6659990	0.8996880	-0.6801070
O	-4.6886710	1.0347100	-0.8914340
C	-5.4755860	0.4245080	-0.0474010
C	-6.9665160	0.6578860	-0.4234770
O	-5.1755860	-0.2460590	0.9214110
F	-7.2290440	0.2096930	-1.6725800
F	-7.2728440	1.9756860	-0.3883260
F	-7.7912890	0.0212940	0.4239030

1.log
Potential Energy = -2233.47575
Zero-point Energy = -2232.94890
Free Energy = -2232.99826
Single-Point Energy B3LYP-D3(BJ)/6-311+G** PCM = -2234.04871
Free Energy B3LYP-D3(BJ)/6-311+G** PCM (extrapolated free energy from qRRHO) = -2233.57122
Nimag = 1 (-1295.0076 cm^{-1})
Charge = 0 Multiplicity = 1

C	2.9849450	2.0380300	0.3581050
C	1.0843850	3.4271840	0.4489930
C	1.1370300	2.8444990	-0.9701130
N	2.0778810	1.7007670	-0.7689890
N	2.1058080	2.8931610	1.1611230
O	0.2491830	4.2326480	0.8546230
C	2.3191630	3.1715970	2.5751710
H	1.3661850	3.4870400	3.0015500
H	2.6597170	2.2647160	3.0799680
H	3.0524280	3.9692090	2.7301560
C	1.8723700	0.5214660	-1.3295430
H	1.0939470	0.5508840	-2.0835690
C	2.3221410	-0.7985250	-1.0265770
C	3.7060190	-1.1857200	-0.4870360
H	4.4365310	-1.0610340	-1.2939470
H	1.3645590	-1.1144050	-0.0623030
C	-0.2354590	2.5050250	-1.5299010
H	-0.8563000	3.3989880	-1.4313600
H	-0.1863080	2.2499890	-2.5915130
H	-0.7079870	1.6849930	-0.9828250
H	1.6229840	3.5805750	-1.6205290
C	4.3513130	2.7177300	-0.0657190
H	3.1967710	1.1307240	0.9235510
Cl	1.8623020	-1.9095260	-2.4091090
N	-1.1868470	-0.8494400	-0.3862090
C	-0.6202230	-1.3798330	0.7014370
C	-2.5372430	-0.9004080	-0.2159170
C	-1.5988880	-1.8475150	1.7629530
C	-2.9487630	-1.5247310	1.1146080
H	-1.4465710	-2.9117360	1.9651650
H	-3.5553180	-0.8138680	1.6829020
O	-3.3426740	-0.4740160	-1.0733930
O	0.6370460	-1.5008050	0.8723940
C	5.3550630	2.5054060	1.0909660
H	6.3217570	2.9410740	0.8203490
H	5.0293330	2.9818150	2.0195010
H	5.5159890	1.4408600	1.2930640
C	4.9238930	2.0614100	-1.3379810
H	5.1282960	0.9974930	-1.2009150
H	4.2573420	2.1794560	-2.1971200
H	5.8748730	2.5424270	-1.5868230
C	4.1943650	4.2306370	-0.3248420
H	3.7907840	4.7638430	0.5399310
H	5.1794120	4.6549100	-0.5422380
H	3.5583380	4.4434790	-1.1889970
H	-3.5654720	-2.4098430	0.9307000
H	-1.4176160	-1.3069370	2.6969210
H	3.9792590	-0.4822290	0.3010170
C	3.8400890	-2.5912310	0.0768730
C	4.3698600	-3.6257050	-0.7081860
C	3.4935500	-2.8703920	1.4073900
C	4.5319200	-4.9124370	-0.1854090
H	4.6596230	-3.4232720	-1.7355810
C	3.6550470	-4.1544420	1.9348460
H	3.0924930	-2.0801010	2.0353270
C	4.1722450	-5.1815480	1.1385350
H	4.9432530	-5.7000390	-0.8102900
H	3.3820720	-4.3504800	2.9678910
H	4.3007230	-6.1791630	1.5484130
H	-4.7732380	-0.5065760	-0.8896170
O	-5.8286780	-0.5484920	-0.8972330
C	-6.3819040	0.0987880	0.0911780
C	-7.9319930	-0.0013930	0.0105390
O	-5.8445390	0.7172260	0.9900350
F	-8.3380330	-1.2916890	0.0438180
F	-8.3928150	0.5429590	-1.1395120
F	-8.5192780	0.6407180	1.0335780

2.log
Potential Energy = -2233.47519
Zero-point Energy = -2232.94829
Free Energy = -2232.99732
Single-Point Energy B3LYP-D3(BJ)/6-311+G** PCM = -2234.05049
Free Energy B3LYP-D3(BJ)/6-311+G** PCM (extrapolated free energy from qRRHO) = -2233.57262
Nimag = 1 (-1259.1695 cm^{-1})
Charge = 0 Multiplicity = 1

C	2.0498260	1.8758320	0.4238910
C	0.0898470	2.7268940	-0.5656430
C	0.8114320	1.9101900	-1.6486550
N	1.7480020	1.1008190	-0.8094870
N	0.7880520	2.6055080	0.5892540
O	-0.9474910	3.3645870	-0.7321720
C	0.3496220	3.1930280	1.8484260
H	-0.7335960	3.3119600	1.8036720
H	0.6069940	2.5242600	2.6727260
H	0.8018440	4.1743190	2.0233420
C	1.8763960	-0.2040580	-0.9813270
H	1.4159670	-0.5521190	-1.8990550
C	2.3209290	-1.2435930	-0.1108110
C	3.5172410	-1.2388880	0.8371880
H	3.5758340	-0.2560830	1.3164360
H	1.2678590	-1.3163430	0.7554230
C	-0.1448790	1.1362520	-2.5425030
H	-0.8460440	1.8587240	-2.9672670
H	0.3779460	0.6546450	-3.3728120
H	-0.7121350	0.3914160	-1.9776500
H	1.4055250	2.5981900	-2.2597040
C	3.3291090	2.8029110	0.3525920
H	2.1631080	1.1746830	1.2524840
Cl	2.1894250	-2.8589800	-0.9594130
N	-1.2182530	-1.2356040	0.1639400
C	-0.7657930	-1.4451750	1.4038700
C	-2.5793740	-1.2549920	0.2115160
C	-1.8472490	-1.6338310	2.4514440
C	-3.1244870	-1.5012090	1.6158950
H	-1.7315600	-2.6102200	2.9313360
H	-3.7623090	-0.6640850	1.9141150
O	-3.2939820	-1.0860100	-0.8015390
O	0.4689340	-1.4876430	1.7174500

C	3.7780970	3.0867240	1.8047530
H	4.6862080	3.6972180	1.7931150
H	3.0235260	3.6326600	2.3770220
H	4.0078530	2.1601060	2.3421790
C	4.4782070	2.0918710	-0.3855850
H	4.7763940	1.1614260	0.1015070
H	4.2204150	1.8698280	-1.4251490
H	5.3557850	2.7458250	-0.3933170
C	3.0454220	4.1433240	-0.3569430
H	2.2347530	4.7045810	0.1151190
H	3.9454870	4.7639750	-0.3090640
H	2.8046110	4.0133090	-1.4160480
H	-3.7432990	-2.4035470	1.6188660
H	-1.7465020	-0.8718270	3.2300600
H	3.2983220	-1.9387400	1.6499940
C	4.8820340	-1.5938300	0.2572290
C	5.8415780	-2.1572390	1.1130100
C	5.2379270	-1.3529710	-1.0762240
C	7.1262940	-2.4595460	0.6537150
H	5.5807170	-2.3614580	2.1486140
C	6.5207500	-1.6577430	-1.5418490
H	4.5133680	-0.9327910	-1.7672410
C	7.4711140	-2.2101930	-0.6784170
H	7.8526650	-2.8948380	1.3340110
H	6.7735390	-1.4661550	-2.5807220
H	8.4664980	-2.4495280	-1.0409000
H	-4.7354010	-1.0677030	-0.7406680
O	-5.7880650	-1.1082210	-0.8207020
C	-6.3969050	-0.2008100	-0.1078870
C	-7.9392760	-0.3233670	-0.2666330
O	-5.9120320	0.6510470	0.6120710
F	-8.3746760	-1.5244730	0.1811780
F	-8.3078930	-0.2120650	-1.5631600
F	-8.5813520	0.6308000	0.4271480

3.log
Potential Energy = -2233.47279
Zero-point Energy = -2232.94589
Free Energy = -2232.99537
Single-Point Energy B3LYP-D3(BJ)/6-311+G** PCM = -2234.05134
Free Energy B3LYP-D3(BJ)/6-311+G** PCM (extrapolated free energy from qRRHO) = -2233.57392
Nimag = 1 (-1303.8422 cm^{-1})
Charge = 0 Multiplicity = 1

C	-3.6113070	1.2122550	0.1742270
C	-2.4974060	2.5515250	-1.4138140
C	-1.4539120	2.2071300	-0.3462540
N	-2.1440510	1.1051440	0.3846140
N	-3.6542310	1.9193400	-1.1078660
O	-2.2928160	3.2599570	-2.3986260
C	-4.7942750	1.9124360	-2.0199670
H	-4.4148550	1.8880300	-3.0432730
H	-5.3970870	1.0222020	-1.8384180
H	-5.4176640	2.8032340	-1.9009070
C	-1.4780230	0.1811510	1.0580480
H	-0.4598440	0.4672810	1.3133660
C	-1.7722930	-1.1811050	1.3571830
C	-3.0548830	-1.9764760	1.1340950
H	-2.8220540	-2.9968470	1.4635910
H	-0.7495980	-1.7895450	0.5933580
C	-0.1118010	1.8275950	-0.9616940
H	0.2202980	2.6617790	-1.5844860
H	0.6472090	1.6455580	-0.1992440
H	-0.2042490	0.9373690	-1.5902760
H	-1.3300190	3.0696080	0.3184460
C	-4.3502390	1.9520030	1.3550200
H	-4.0441800	0.2193210	0.0550350
Cl	-1.0783390	-1.5991500	2.9993370
N	1.6605580	-0.9517030	0.6751260
C	1.2855760	-2.0942030	0.0968160
C	3.0132320	-0.8445620	0.5401860
C	2.4142910	-2.8980960	-0.5183470
C	3.6332980	-2.0255890	-0.2011780
H	2.4511140	-3.8932430	-0.0653540
H	4.1631430	-1.6658200	-1.0878040
O	3.6601560	0.1287310	0.9842660
O	0.0791500	-2.5101670	0.0425230
C	-5.8661420	1.9443530	1.0506060
H	-6.4082290	2.3186720	1.9245070
H	-6.1241720	2.5894660	0.2080940
H	-6.2339120	0.9341360	0.8403400
C	-4.1258830	1.1939620	2.6778110
H	-4.5183980	0.1737170	2.6364570
H	-3.0711090	1.1538750	2.9643490
H	-4.6596910	1.7122290	3.4803980
C	-3.8748850	3.4074710	1.5255330
H	-3.9587270	3.9818470	0.5977760
H	-4.5013780	3.9034320	2.2735320
H	-2.8426540	3.4635160	1.8845320
H	4.3674070	-2.5200690	0.4422190
H	2.2332700	-3.0319470	-1.5890970
H	-3.8469440	-1.6359880	1.8107060
C	-3.6161960	-2.0743910	-0.2816020
C	-4.9904930	-2.3338250	-0.4266730
C	-2.8310390	-1.9917020	-1.4414610
C	-5.5640920	-2.5074540	-1.6880920
H	-5.6173290	-2.4003680	0.4591290
C	-3.4053160	-2.1581620	-2.7069680
H	-1.7655090	-1.8051000	-1.3724070
C	-4.7715980	-2.4180150	-2.8371270
H	-6.6283620	-2.7077850	-1.7719370
H	-2.7779990	-2.0859530	-3.5908490
H	-5.2142220	-2.5474250	-3.8202870
H	5.0942590	0.2672730	0.8143140
O	6.1335020	0.4388930	0.8125370
C	6.6477480	0.4860620	-0.3860950
C	8.1788560	0.7499210	-0.3142150
O	6.0891410	0.3512460	-1.4577040
F	8.8076550	-0.2336760	0.3703100
F	8.4414450	1.9186180	0.3145690
F	8.7236720	0.8106880	-1.5401960

Hydrolysis of chloroiminium ion (TS6)

Conformation name	Extrapolated Free energy (kcal/mol)
TS6-lowest	0.0
1	3.7
2	5.6
3	4.5
4	4.0
5	2.6
6	2.0
7	1.6
8	1.1
9	2.2

10 2.6

TS6-lowest.log
Potential Energy = -1949.25117
Zero-point Energy = -1948.78680
Free Energy = -1948.83082
Single-Point Energy B3LYP-D3(BJ)/6-311+G** PCM = -1949.74621
Free Energy B3LYP-D3(BJ)/6-311+G** PCM (extrapolated free energy from qRRHO) = -1949.32585
Nimag = 1 (-334.7303 cm^{-1})
Charge = 0 Multiplicity = 1

C	2.8955910	-0.0482040	0.1680960
C	3.3827080	-1.9184980	-1.1956040
C	1.9931950	-2.1754130	-0.6106640
N	1.6500630	-0.8319040	-0.0725290
N	3.8134410	-0.7085280	-0.7701720
O	3.9865730	-2.6754010	-1.9565940
C	4.9835810	-0.0681420	-1.3674970
H	5.9142360	-0.3904180	-0.8932950
H	5.0215260	-0.3365020	-2.4254350
H	4.8913790	1.0142570	-1.2740780
C	0.3887410	-0.3649380	-0.0606740
C	0.1073720	1.1334310	-0.1578130
C	-1.3636050	1.5186740	0.0527000
H	-1.9841560	0.9700550	-0.6619880
H	-1.6355370	1.1772550	1.0552300
C	1.0347960	-2.7372850	-1.6557870
H	1.4825630	-3.6488260	-2.0586000
H	0.0663930	-2.9980050	-1.2235440
H	0.8823480	-2.0347010	-2.4804220
H	2.0900890	-2.8953500	0.2117130
C	3.4022340	-0.0169090	1.6545150
H	2.7442570	0.9815200	-0.1670940
C	4.8005240	0.6392610	1.7010610
H	5.0824460	0.8027360	2.7458240
H	5.5691920	0.0069530	1.2516840
H	4.8125070	1.6144620	1.2017180
C	2.4570170	0.8579320	2.5045900
H	2.4396960	1.8923230	2.1418340
H	1.4316250	0.4833980	2.5301740
H	2.8194450	0.8834030	3.5370200
C	3.4983560	-1.4298860	2.2579750
H	4.1547930	-2.0786350	1.6690970
H	3.9174040	-1.3691500	3.2671700
H	2.5206820	-1.9141480	2.3442290
H	0.7495260	1.7083960	0.5061280
C	-1.6284650	3.0082380	-0.0467960
C	-1.2175730	3.8732190	0.9799540
C	-2.3010370	3.5493270	-1.1511980
C	-1.4610340	5.2467510	0.8984580
H	-0.7111170	3.4708650	1.8542360
C	-2.5508290	4.9230530	-1.2345340
H	-2.6327820	2.8924230	-1.9507320
C	-2.1285540	5.7765510	-0.2111940
H	-1.1371220	5.9003740	1.7033080
H	-3.0750960	5.3236820	-2.0974100
H	-2.3223280	6.8433720	-0.2739470
Cl	0.6329890	1.6004930	-1.8595830
H	-0.3149590	-0.9651320	-0.6304690
O	-0.3816310	-0.7214830	1.5286200
H	-1.4001990	-1.1730380	1.4189980
H	0.1793360	-1.3944580	1.9462030
O	-2.6177710	-1.6904950	1.3615540
C	-3.0128880	-2.0296770	0.1949010
C	-4.4366550	-2.6675900	0.2143890
O	-2.4311580	-1.9202830	-0.8863440
F	-4.4504550	-3.8032910	0.9579780
F	-5.3480060	-1.8221440	0.7573920
F	-4.8760320	-2.9912920	-1.0179130

1.log
Potential Energy = -1949.24688
Zero-point Energy = -1948.78171
Free Energy = -1948.82596
Single-Point Energy B3LYP-D3(BJ)/6-311+G** PCM = -1949.74093
Free Energy B3LYP-D3(BJ)/6-311+G** PCM (extrapolated free energy from qRRHO) = -1949.32002
Nimag = 1 (-222.3064 cm^{-1})
Charge = 0 Multiplicity = 1

C	3.0208430	-0.1564760	-0.3326480
C	3.1710770	-2.4505080	0.1991190
C	2.3387470	-1.7907600	1.3046420
N	1.9540580	-0.4993170	0.6548990
N	3.4969950	-1.4971020	-0.7045160
O	3.4782950	-3.6414590	0.1470840
C	4.1596550	-1.8173120	-1.9646690
H	5.2488800	-1.8254910	-1.8643290
H	3.8326560	-2.8093020	-2.2825050
H	3.8746640	-1.0841330	-2.7208260
C	0.6660350	-0.1588130	0.5356160
C	0.1764590	1.2384760	0.1499530
C	-1.2988920	1.4475700	0.5316560
H	-1.9314590	0.7816770	-0.0621500
H	-1.3911670	1.1348680	1.5795980
C	1.2203870	-2.6786750	1.8308400
H	1.6858710	-3.5930820	2.2063740
H	0.6935940	-2.2100730	2.6663900
H	0.5058540	-2.9577900	1.0545510
H	3.0121430	-1.5551160	2.1350460
C	4.1332430	0.8105020	0.2084680
H	2.5605610	0.3109390	-1.2034170
C	5.0865100	1.1468360	-0.9614250
H	5.7781930	1.9344450	-0.6468720
H	5.6897250	0.2882190	-1.2650900
H	4.5414120	1.5148480	-1.8378080
C	3.4841760	2.1226040	0.6912930
H	2.9192600	2.6158190	-0.1067560
H	2.8267270	1.9556680	1.5500300
H	4.2667610	2.8169710	1.0124960
C	4.9527010	0.2031550	1.3631570
H	5.3777320	-0.7702360	1.0990350
H	5.7870630	0.8708500	1.6006720
H	4.3591150	0.0950540	2.2758340
H	0.8025100	1.9552700	0.6811980
C	-1.7722000	2.8813410	0.3998400
C	-1.3470770	3.8606940	1.3116490
C	-2.6546460	3.2536400	-0.6237390
C	-1.7839230	5.1827580	1.1956740
H	-0.6768810	3.5889210	2.1239640
C	-3.0964840	4.5755080	-0.7413250
H	-2.9998130	2.5051310	-1.3315270
C	-2.6602420	5.5445530	0.1666020
H	-1.4464960	5.9268450	1.9114150
H	-3.7813710	4.8451910	-1.5400890
H	-3.0035870	6.5710800	0.0776080
H	0.0547610	-0.5798070	1.3258100
O	-0.1160670	-1.2443160	-0.7628840
H	-0.2406990	-0.7564940	-1.5941480
H	-1.0555830	-1.6722160	-0.4765930
O	-2.2140850	-2.3383180	-0.0336620
C	-3.3264630	-1.8800520	-0.4501430
O	-3.5552820	-0.9059090	-1.1729060
C	-4.5429530	-2.7096330	0.0738980
F	-4.4369140	-4.0189620	-0.2694920

F	-4.6195250	-2.6590390	1.4301720
F	-5.7248240	-2.2692010	-0.4055400
Cl	0.4281750	1.6405450	-1.6216870

2.log
Potential Energy = -1949.24102
Zero-point Energy = -1948.77561
Free Energy = -1948.81978
Single-Point Energy B3LYP-D3(BJ)/6-311+G** PCM = -1949.73822
Free Energy B3LYP-D3(BJ)/6-311+G** PCM (extrapolated free energy from qRRHO) = -1949.31697
Nimag = 1 (-192.4248 cm^{-1})
Charge = 0 Multiplicity = 1

C	2.8894970	0.4179300	0.3334400
C	1.9558430	2.4592440	-0.3999840
C	1.7478320	1.4390170	-1.5255110
N	1.9463970	0.1504670	-0.7949480
N	2.5694180	1.8239840	0.6266920
O	1.6198690	3.6430760	-0.4302890
C	2.7918360	2.4695610	1.9160210
H	3.7414650	3.0121030	1.9444520
H	1.9807310	3.1797810	2.0874890
H	2.7844320	1.7167250	2.7058150
C	0.9881180	-0.7810200	-0.7533630
C	1.2649510	-2.2372670	-0.3661630
C	0.2700700	-3.2468120	-0.9773750
H	0.3833770	-3.1507590	-2.0636930
H	0.6469790	-4.2403780	-0.7169870
C	0.4550880	1.6231910	-2.3043350
H	0.4854960	2.6240780	-2.7422440
H	0.3830250	0.9072500	-3.1277170
H	-0.4374990	1.5607890	-1.6797890
H	2.5841280	1.5426380	-2.2243130
C	4.4055310	0.1416630	0.0270390
H	2.5936490	-0.1983500	1.1833380
C	5.1935200	0.3079790	1.3473810
H	6.2282490	-0.0129210	1.1920110
H	5.2235470	1.3459740	1.6862210
H	4.7725200	-0.3062330	2.1510700
C	4.5844710	-1.3108130	-0.4568240
H	4.2292000	-2.0344590	0.2842180
H	4.0734040	-1.4852690	-1.4088790
H	5.6485190	-1.5091650	-0.6190590
C	4.9952690	1.0951550	-1.0304710
H	4.8283590	2.1467100	-0.7775010
H	6.0774120	0.9402260	-1.0881030
H	4.5916740	0.9035200	-2.0291240
H	2.2465620	-2.4731730	-0.7744000
C	-1.1977920	-3.1367630	-0.6131450
C	-1.6901780	-3.6668010	0.5920030
C	-2.1074970	-2.5447310	-1.5034050
C	-3.0496080	-3.5831160	0.9068390
H	-1.0111460	-4.1593760	1.2810550
C	-3.4681320	-2.4641760	-1.1930640
H	-1.7536540	-2.1532530	-2.4538320
C	-3.9428200	-2.9790660	0.0163960
H	-3.4107550	-3.9992230	1.8428030
H	-4.1543180	-2.0031770	-1.8973560
H	-4.9996240	-2.9190220	0.2590010
H	0.3030960	-0.7143960	-1.5913040
O	-0.2605370	-0.2465070	0.5422210
H	-0.6111020	-0.9975070	1.0487370
H	-1.0955650	0.3295850	0.2269110
O	-2.1910560	1.1610540	-0.1716250
C	-3.0805160	1.3804530	0.7112190
O	-3.1585750	0.9743680	1.8743230
C	-4.2183640	2.3154250	0.1853990
F	-3.7302810	3.5353450	-0.1625320
F	-4.8156700	1.7974860	-0.9195600
F	-5.1910690	2.5251690	1.0974720
Cl	1.4641170	-2.5203600	1.4324080

3.log
Potential Energy = -1949.24357
Zero-point Energy = -1948.77902
Free Energy = -1948.82349
Single-Point Energy B3LYP-D3(BJ)/6-311+G** PCM = -1949.73882
Free Energy B3LYP-D3(BJ)/6-311+G** PCM (extrapolated free energy from qRRHO) = -1949.31874
Nimag = 1 (-270.5133 cm^{-1})
Charge = 0 Multiplicity = 1

C	-1.0258770	-1.7574150	-0.5882850
C	-2.5649860	-2.3536380	1.1003070
C	-1.1685940	-2.6872120	1.6360520
N	-0.2976520	-1.9019590	0.7074530
N	-2.4216590	-1.8005640	-0.1259950
O	-3.6259040	-2.5546840	1.6927850
C	-3.5519460	-1.2590890	-0.8716840
H	-4.0326460	-2.0191450	-1.4949580
H	-4.2838410	-0.8824680	-0.1551640
H	-3.2093260	-0.4357180	-1.4991950
C	0.5927710	-1.0273360	1.1904650
C	1.7553820	-0.4376040	0.3920710
C	2.8097950	0.2101550	1.3102420
H	2.4040620	1.1214370	1.7583460
H	2.9964970	-0.4990320	2.1259030
C	-1.0157840	-2.4335390	3.1292590
H	-1.7885120	-3.0167270	3.6359260
H	-0.0464630	-2.7799600	3.4978110
H	-1.1534250	-1.3813000	3.3851330
H	-0.9830910	-3.7495530	1.4444520
C	-0.6641210	-2.8335330	-1.6760540
H	-0.8191030	-0.7689580	-0.9999490
C	-1.3379500	-2.4165650	-3.0040180
H	-0.9894480	-3.0733930	-3.8071530
H	-2.4261660	-2.5016850	-2.9651640
H	-1.0816740	-1.3879640	-3.2810550
C	0.8605180	-2.8579410	-1.9019750
H	1.2405750	-1.8840450	-2.2257070
H	1.3964690	-3.1740110	-1.0018810
H	1.0963460	-3.5787670	-2.6911660
C	-1.1329990	-4.2516540	-1.2965740
H	-2.2003500	-4.2845640	-1.0574080
H	-0.9661320	-4.9233450	-2.1447860
H	-0.5700270	-4.6585360	-0.4511880
H	2.2119870	-1.2757470	-0.1375880
C	4.1206840	0.5205640	0.6156410
C	5.0060650	-0.5147710	0.2764800
C	4.4806480	1.8406750	0.3121540
C	6.2172150	-0.2379420	-0.3625780
H	4.7526000	-1.5438700	0.5202600
C	5.6939210	2.1219210	-0.3244250
H	3.8098290	2.6539250	0.5754930
C	6.5644660	1.0830850	-0.6659500
H	6.8913260	-1.0510600	-0.6158380
H	5.9570950	3.1510770	-0.5509040
H	7.5075280	1.3000350	-1.1589600
H	0.9192290	-1.2943370	2.1892300
O	-0.3467970	0.4513560	1.8041540
H	-1.0017590	0.9784800	1.1236980
O	-1.9211670	1.6449010	0.3228360
C	-1.8718290	2.9096320	0.4609950
O	-1.1483910	3.5917820	1.1927050
C	-2.8964960	3.6489300	-0.4579750

F	-2.6502070	3.3956360	-1.7701490
F	-4.1684320	3.2443360	-0.2071050
F	-2.8691780	4.9887960	-0.3016830
Cl	1.2651020	0.7311390	-0.9157250
H	0.1999970	1.1214450	2.2446370

4.log
Potential Energy = -1949.24205
Zero-point Energy = -1948.77664
Free Energy = -1948.82065
Single-Point Energy B3LYP-D3(BJ)/6-311+G** PCM = -1949.74090
Free Energy B3LYP-D3(BJ)/6-311+G** PCM (extrapolated free energy from qRRHO) = -1949.31950
Nimag = 1 (-226.1030 cm^{-1})
Charge = 0 Multiplicity = 1

C	-2.1799620	-0.6944740	-0.3179740
C	-2.5365210	-0.4004970	1.9976650
C	-1.7824220	-1.7241620	1.8336030
N	-1.2595600	-1.5969300	0.4384980
N	-2.6916310	0.1501390	0.7717890
O	-2.9246590	0.0731650	3.0661610
C	-3.2666740	1.4778340	0.5873060
H	-4.3567080	1.4420440	0.5000260
H	-3.0063060	2.0846810	1.4559160
H	-2.8420720	1.9345710	-0.3068840
C	0.0427710	-1.7568460	0.1799630
C	0.6106880	-1.9775460	-1.2232280
C	1.9645790	-2.7226070	-1.2262990
H	1.7540690	-3.7192350	-0.8207040
H	2.2324720	-2.8685850	-2.2768030
C	-0.7716530	-1.9837110	2.9421950
H	-1.3144500	-1.9404370	3.8895360
H	-0.3316500	-2.9810220	2.8592980
H	0.0203850	-1.2328760	2.9613130
H	-2.5213550	-2.5326060	1.8394900
C	-3.2971000	-1.4262030	-1.1489710
H	-1.5880560	-0.0798430	-0.9986840
C	-4.0350890	-0.3656330	-1.9990490
H	-4.7220800	-0.8700230	-2.6857140
H	-4.6300380	0.3185530	-1.3905490
H	-3.3375500	0.2258420	-2.6022630
C	-2.6576400	-2.4435440	-2.1139820
H	-1.9538970	-1.9651610	-2.8032430
H	-2.1500020	-3.2492310	-1.5746600
H	-3.4419810	-2.9051150	-2.7219140
C	-4.3197010	-2.1607290	-0.2605380
H	-4.7681310	-1.4999480	0.4875970
H	-5.1309950	-2.5425520	-0.8885100
H	-3.8776180	-3.0218100	0.2495580
H	-0.0993260	-2.6187570	-1.7431020
C	3.1313380	-2.1151880	-0.4709920
C	3.9040900	-1.0804490	-1.0276980
C	3.4904780	-2.6104200	0.7943260
C	4.9901790	-0.5448970	-0.3291480
H	3.6603590	-0.6985030	-2.0140380
C	4.5778110	-2.0772280	1.4933770
H	2.9246100	-3.4290910	1.2319000
C	5.3290210	-1.0398070	0.9342990
H	5.5742850	0.2540050	-0.7760850
H	4.8383330	-2.4765860	2.4689980
H	6.1750980	-0.6252430	1.4739980
H	0.5262590	-2.3999200	0.9056910
O	0.9643160	-0.2601940	0.8207230
H	0.6103050	0.7067270	0.5360940
O	0.1151090	2.0083910	0.2583510
C	1.0082980	2.9068060	0.1521450
O	2.2356470	2.8181320	0.2591870
C	0.4007380	4.3131030	-0.1614240
F	-0.3109920	4.2967090	-1.3192720
F	-0.4489270	4.7140430	0.8205070
F	1.3379890	5.2760880	-0.2891350
Cl	0.6801800	-0.4717460	-2.2509480
H	1.9059950	-0.3029650	0.5801070

5.log
Potential Energy = -1949.24618
Zero-point Energy = -1948.78104
Free Energy = -1948.82472
Single-Point Energy B3LYP-D3(BJ)/6-311+G** PCM = -1949.74322
Free Energy B3LYP-D3(BJ)/6-311+G** PCM (extrapolated free energy from qRRHO) = -1949.32175
Nimag = 1 (-261.7286 cm^{-1})
Charge = 0 Multiplicity = 1

C	2.9130930	-0.0045410	-0.0920550
C	3.3528360	2.3167710	0.0171920
C	1.8725980	2.1869440	-0.3446230
N	1.6263550	0.7482990	-0.0568310
N	3.8649320	1.0768240	0.1937540
O	3.9603010	3.3781240	0.1616750
C	5.1741910	0.8773790	0.8121020
H	5.9855310	0.9279140	0.0815060
H	5.3272350	1.6613040	1.5568300
H	5.1966090	-0.0955330	1.3039560
C	0.4398440	0.3006290	0.3898440
C	0.3506340	-0.9335190	1.2841040
C	-1.0789220	-1.4551230	1.5609090
H	-1.1249700	-1.7122400	2.6226890
H	-1.8014300	-0.6489030	1.4104100
C	1.0145490	3.1766990	0.4371680
H	1.3990460	4.1788810	0.2336520
H	-0.0321160	3.1456320	0.1275200
H	1.0752710	2.9964620	1.5145210
H	1.7561740	2.3802580	-1.4183320
C	3.2042930	-0.7875680	-1.4225410
H	2.9403480	-0.7143830	0.7397360
C	4.6610840	-1.3023960	-1.4017620
H	4.8111240	-1.9806740	-2.2474530
H	5.3863890	-0.4919740	-1.5012500
H	4.8851950	-1.8630110	-0.4876340
C	2.2824660	-2.0218270	-1.5058310
H	2.4637610	-2.7092110	-0.6715170
H	1.2207910	-1.7672840	-1.5166500
H	2.4932970	-2.5696860	-2.4294300
C	3.0131610	0.0998790	-2.6659650
H	3.6448250	0.9932310	-2.6282170
H	3.2938820	-0.4617060	-3.5623170
H	1.9740190	0.4174260	-2.7991630
H	0.9896640	-1.7379410	0.9288470
C	-1.4712070	-2.6872470	0.7607090
C	-2.5808210	-2.6721500	-0.0951540
C	-0.7622570	-3.8893330	0.9177100
C	-2.9690720	-3.8255940	-0.7848010
H	-3.1415990	-1.7518920	-0.2297660
C	-1.1430430	-5.0419480	0.2257180
H	0.0884920	-3.9334050	1.5939550
C	-2.2495100	-5.0137030	-0.6300660
H	-3.8321780	-3.7925870	-1.4436540
H	-0.5814350	-5.9618350	0.3613150
H	-2.5491100	-5.9094480	-1.1662420
Cl	1.1214350	-0.3854150	2.8696480
H	-0.2478580	1.0856020	0.6917810
O	-0.5755970	-0.2415570	-0.9932330
H	-1.5668580	0.2344320	-0.9924020
H	-0.1198490	0.0683590	-1.7921080

O	-2.8076090	0.7835340	-1.0505970
C	-3.0748940	1.6554160	-0.1587290
C	-4.4958080	2.2745060	-0.3404560
O	-2.3806380	2.0434650	0.7848240
F	-4.6188110	2.8718620	-1.5529300
F	-5.4578980	1.3198830	-0.2651350
F	-4.7820250	3.2038370	0.5930370

6.log
Potential Energy = -1949.24682
Zero-point Energy = -1948.78252
Free Energy = -1948.82707
Single-Point Energy B3LYP-D3(BJ)/6-311+G** PCM = -1949.74236
Free Energy B3LYP-D3(BJ)/6-311+G** PCM (extrapolated free energy from qRRHO) = -1949.32261
Nimag = 1 (-303.8552 cm^{-1})
Charge = 0 Multiplicity = 1

C	-2.9405970	0.4737770	0.2440760
C	-2.8819030	0.9851190	-2.0648600
C	-1.4254360	0.9857490	-1.5957550
N	-1.5491580	0.3158870	-0.2733930
N	-3.6717200	0.6514360	-1.0177150
O	-3.2600850	1.2129770	-3.2138920
C	-5.0774910	0.2991690	-1.2102990
H	-5.7249970	1.1795660	-1.2077020
H	-5.1781350	-0.2040870	-2.1742520
H	-5.3925340	-0.3782380	-0.4161100
C	-0.5742100	-0.4546230	0.2289240
C	-0.8674160	-1.5843140	1.2128260
C	0.3627620	-2.3397080	1.7580610
H	0.9676050	-1.5992500	2.2889220
H	-0.0200850	-3.0316920	2.5136000
C	-0.5054750	0.3051960	-2.6035740
H	-0.6446610	0.8041970	-3.5654110
H	0.5470140	0.4054010	-2.3282680
H	-0.7523290	-0.7532820	-2.7267160
H	-1.0999440	2.0241290	-1.4574770
C	-3.1550860	1.6315330	1.2849350
H	-3.2615610	-0.4656410	0.7011370
C	-4.6705490	1.8369850	1.5075120
H	-4.8163350	2.5326570	2.3395840
H	-5.1606000	2.2685560	0.6322180
H	-5.1775210	0.9019580	1.7689590
C	-2.5486170	1.2230880	2.6441360
H	-3.0248730	0.3157780	3.0333130
H	-1.4705930	1.0531990	2.6074490
H	-2.7213780	2.0205290	3.3731920
C	-2.5458800	2.9619800	0.8069530
H	-2.9685190	3.2786060	-0.1519560
H	-2.7652420	3.7475590	1.5364070
H	-1.4571490	2.9156740	0.7026590
H	-1.4478900	-1.2163930	2.0561320
C	1.2161230	-3.1035780	0.7618300
C	0.9597080	-4.4603290	0.5037550
C	2.2972220	-2.4934280	0.1056830
C	1.7448200	-5.1815540	-0.3993050
H	0.1425850	-4.9573620	1.0184440
C	3.0834560	-3.2121020	-0.8014060
H	2.5473840	-1.4572380	0.3112530
C	2.8078370	-4.5573710	-1.0602520
H	1.5295440	-6.2305130	-0.5817590
H	3.9160800	-2.7204000	-1.2963160
H	3.4208790	-5.1169240	-1.7607500
Cl	-1.9853350	-2.7594940	0.3438450
H	0.1990080	-0.6979050	-0.4906090
O	0.5248390	0.5406790	1.2881700
H	1.5629640	0.6852280	0.9160610
H	0.1557160	1.4394350	1.2851160
O	2.8104600	0.9215060	0.5067550
C	3.0177190	2.1739100	0.3503520
C	4.4692900	2.4793060	-0.1331610
O	2.2419550	3.1146800	0.5252570
F	5.3907580	1.9894600	0.7336870
F	4.7106760	1.9067380	-1.3402620
F	4.7049420	3.7999160	-0.2631600

7.log
Potential Energy = -1949.24800
Zero-point Energy = -1948.78443
Free Energy = -1948.82873
Single-Point Energy B3LYP-D3(BJ)/6-311+G** PCM = -1949.74262
Free Energy B3LYP-D3(BJ)/6-311+G** PCM (extrapolated free energy from qRRHO) = -1949.32334
Nimag = 1 (-448.0910 cm^{-1})
Charge = 0 Multiplicity = 1

C	2.9079170	-0.0286740	0.1623210
C	3.3687160	-1.9005530	-1.2049060
C	1.9605740	-2.1174130	-0.6485620
N	1.6475950	-0.7660510	-0.1228810
N	3.8233570	-0.7026090	-0.7696180
O	3.9663290	-2.6700060	-1.9588610
C	5.0104370	-0.0825980	-1.3544190
H	5.9320870	-0.4294580	-0.8800600
H	5.0477990	-0.3393980	-2.4153630
H	4.9415650	1.0005520	-1.2489830
C	0.3890350	-0.3032600	-0.0596060
C	0.0963090	1.1970090	-0.1365290
C	-1.3923660	1.5545160	-0.0024100
H	-1.9542800	1.0247860	-0.7770780
H	-1.7395460	1.1681400	0.9602490
C	1.0114650	-2.6471080	-1.7197060
H	1.4448690	-3.5658120	-2.1221630
H	0.0274360	-2.8872250	-1.3117190
H	0.8946040	-1.9323700	-2.5399460
H	2.0109550	-2.8390500	0.1763870
C	3.3937610	-0.0476440	1.6584360
H	2.7976700	1.0128120	-0.1543490
C	4.8425050	0.4841860	1.7301580
H	5.1257640	0.6063630	2.7802100
H	5.5565040	-0.2077990	1.2785590
H	4.9468800	1.4615210	1.2462040
C	2.5185520	0.9010700	2.5011440
H	2.5288260	1.9229800	2.1054120
H	1.4846640	0.5600320	2.5722860
H	2.9047510	0.9426080	3.5240590
C	3.3483450	-1.4642510	2.2594310
H	3.9659480	-2.1658700	1.6890880
H	3.7427710	-1.4403870	3.2804280
H	2.3260380	-1.8503080	2.3077100
H	0.6960140	1.7668180	0.5718530
C	-1.6765610	3.0426860	-0.0620890
C	-1.3082810	3.8813120	1.0018030
C	-2.3275110	3.6067870	-1.1677540
C	-1.5735050	5.2523810	0.9563390
H	-0.8173510	3.4608110	1.8763840
C	-2.5989850	4.9781270	-1.2151830
H	-2.6249200	2.9701040	-1.9966220
C	-2.2199510	5.8056510	-0.1543780
H	-1.2824920	5.8856990	1.7894470
H	-3.1058840	5.3970480	-2.0797100
H	-2.4304160	6.8705560	-0.1893160
Cl	0.6923570	1.7302100	-1.7946690
H	-0.3206270	-0.8911660	-0.6348510
O	-0.3374150	-0.8133460	1.4866310

H	-1.3709470	-1.2809390	1.3952960
H	-0.3429530	-0.1420810	2.1864500
O	-2.5296390	-1.8511860	1.3516070
C	-2.9676010	-2.1039460	0.1762180
C	-4.3733550	-2.7790850	0.2050100
O	-2.4373600	-1.8859350	-0.9134890
F	-4.3432900	-3.9443670	0.8988200
F	-5.2876460	-1.9769450	0.8065240
F	-4.8362640	-3.0590540	-1.0289010

8.log
Potential Energy = -1949.24828
Zero-point Energy = -1948.78306
Free Energy = -1948.82687
Single-Point Energy B3LYP-D3(BJ)/6-311+G** PCM = -1949.74551
Free Energy B3LYP-D3(BJ)/6-311+G** PCM (extrapolated free energy from qRRHO) = -1949.32411
Nimag = 1 (-221.1495 cm^{-1})
Charge = 0 Multiplicity = 1

C	-2.7520840	0.0407560	0.3317730
C	-2.9423950	2.2811700	-0.3972320
C	-1.4443950	1.9729000	-0.3778850
N	-1.4544570	0.4930800	-0.2443250
N	-3.6196960	1.1606140	-0.0575620
O	-3.4430200	3.3602300	-0.7171940
C	-5.0618980	1.0528570	-0.2684670
H	-5.6321140	1.4602920	0.5702050
H	-5.3217270	1.6122140	-1.1698030
H	-5.3300520	0.0048340	-0.4058150
C	-0.4720850	-0.2775020	-0.7309370
C	-0.7578620	-1.6950240	-1.2367380
C	0.4531090	-2.4765850	-1.7917240
H	0.0428870	-3.2423630	-2.4561450
H	1.0544420	-1.8089630	-2.4161450
C	-0.7551050	2.5157850	-1.6273950
H	-0.9575430	3.5883630	-1.6775630
H	0.3275260	2.3783790	-1.5911680
H	-1.1503060	2.0475530	-2.5339390
H	-0.9969290	2.4292640	0.5137080
C	-2.7456920	-0.2620930	1.8744650
H	-3.0883120	-0.8563390	-0.1961120
C	-4.2010170	-0.4210900	2.3676120
H	-4.1873680	-0.7766740	3.4026310
H	-4.7476110	0.5244970	2.3553730
H	-4.7582880	-1.1561430	1.7763100
C	-2.0200030	-1.5982810	2.1338040
H	-2.4996190	-2.4236640	1.5936160
H	-0.9654180	-1.5541270	1.8595070
H	-2.0726690	-1.8367890	3.2010590
C	-2.0666010	0.8640110	2.6750150
H	-2.5543730	1.8305890	2.5096810
H	-2.1369080	0.6438640	3.7451400
H	-1.0056180	0.9555210	2.4266350
H	-1.2996630	-2.2840890	-0.4990710
C	1.3315240	-3.1674400	-0.7607330
C	2.6907980	-2.8338140	-0.6410010
C	0.8166880	-4.1916750	0.0536830
C	3.5134090	-3.4975110	0.2777680
H	3.1107070	-2.0575950	-1.2754600
C	1.6352660	-4.8520130	0.9711460
H	-0.2266410	-4.4827500	-0.0364080
C	2.9867260	-4.5052530	1.0876980
H	4.5617920	-3.2254820	0.3538620
H	1.2204940	-5.6409720	1.5913840
H	3.6221890	-5.0209210	1.8012160
Cl	-1.9373770	-1.4656400	-2.6332270
H	0.2284320	0.2620050	-1.3607740
O	0.6984830	-0.5791320	0.6048750
H	1.3553260	0.2774960	0.7299370
H	1.2797140	-1.3447370	0.4289420
O	2.2248110	1.3233300	0.9756600
C	2.8150090	1.7834240	-0.0560900
C	3.8855480	2.8628690	0.3018100
O	2.6474090	1.4987070	-1.2453620
F	3.3212480	3.9195310	0.9417010
F	4.8367240	2.3577130	1.1285530
F	4.5205880	3.3492800	-0.7842530

9.log
Potential Energy = -1949.24741
Zero-point Energy = -1948.78399
Free Energy = -1948.82843
Single-Point Energy B3LYP-D3(BJ)/6-311+G** PCM = -1949.74140
Free Energy B3LYP-D3(BJ)/6-311+G** PCM (extrapolated free energy from qRRHO) = -1949.32242
Nimag = 1 (-442.2547 cm^{-1})
Charge = 0 Multiplicity = 1

C	2.7191600	-0.2041100	0.7638350
C	4.5393150	-0.4094500	-0.7304020
C	3.2870380	-0.7790120	-1.5292260
N	2.2186010	-0.2645920	-0.6368800
N	4.1609790	-0.0529110	0.5187420
O	5.6902090	-0.4035680	-1.1688430
C	5.0897000	0.6031930	1.4366960
H	5.6944710	-0.1171470	1.9936510
H	5.7578550	1.2418880	0.8548840
H	4.5282460	1.2174800	2.1412870
C	1.0497860	0.1802760	-1.1105650
C	0.2225040	1.2251810	-0.3623110
C	-1.0819220	1.6098090	-1.0771300
H	-0.8377930	2.0020550	-2.0691950
H	-1.6548270	0.6911020	-1.2229420
C	3.3176910	-0.1930320	-2.9368540
H	4.2447510	-0.5220110	-3.4121450
H	2.4869260	-0.5555120	-3.5472160
H	3.3087010	0.9007960	-2.9208440
H	3.2213820	-1.8718660	-1.5968500
C	2.3445550	-1.4249090	1.6782770
H	2.3495210	0.7092380	1.2379090
C	3.1501070	-1.3364480	2.9932920
H	2.7791680	-2.0952670	3.6893110
H	4.2142740	-1.5282020	2.8390160
H	3.0365970	-0.3612300	3.4798250
C	0.8489760	-1.3486350	2.0427710
H	0.6065240	-0.4077350	2.5507890
H	0.2035610	-1.4609390	1.1715990
H	0.6011230	-2.1622770	2.7317340
C	2.6415290	-2.7723860	0.9956000
H	3.6954250	-2.8610240	0.7113130
H	2.4233130	-3.5885240	1.6919460
H	2.0195340	-2.9207890	0.1081810
H	0.0328310	0.9272360	0.6675390
C	-1.9341110	2.6037630	-0.3125270
C	-2.6262310	2.2044080	0.8420910
C	-2.0637910	3.9292710	-0.7492050
C	-3.4185540	3.1122510	1.5495010
H	-2.5550530	1.1745880	1.1833240
C	-2.8597340	4.8396890	-0.0461910
H	-1.5403700	4.2519990	-1.6451920
C	-3.5370750	4.4345100	1.1074780
H	-3.9487220	2.7853240	2.4394210
H	-2.9493680	5.8625250	-0.4007170
H	-4.1561360	5.1398330	1.6542000
Cl	1.2926670	2.7199000	-0.2376770

H	1.0602780	0.3494780	-2.1816800
O	-0.0940980	-1.2212090	-1.2173520
H	-1.0842360	-1.3713070	-0.6763750
H	-0.2685590	-1.4000370	-2.1554150
O	-2.1971090	-1.5884870	-0.0599540
C	-3.0439210	-2.2483560	-0.7601000
C	-4.3666850	-2.5177610	0.0216830
O	-2.9413380	-2.6622300	-1.9133620
F	-4.1281640	-3.1660360	1.1887880
F	-4.9941230	-1.3541380	0.3297630
F	-5.2369520	-3.2677160	-0.6823350

10.log
Potential Energy = -1949.24591
Zero-point Energy = -1948.78201
Free Energy = -1948.82618
Single-Point Energy B3LYP-D3(BJ)/6-311+G** PCM = -1949.74144
Free Energy B3LYP-D3(BJ)/6-311+G** PCM (extrapolated free energy from qRRHO) = -1949.32170
Nimag = 1 (-480.8318 cm^{-1})
Charge = 0 Multiplicity = 1

C	-2.7588980	-0.9998410	-0.4688040
C	-4.0750940	-0.1463160	1.3005930
C	-2.6173310	0.0506980	1.7218570
N	-1.9155980	-0.1633540	0.4306890
N	-4.0944050	-0.6870590	0.0607950
O	-5.0595890	0.1724430	1.9684750
C	-5.3263020	-0.7439100	-0.7235560
H	-5.9172790	-1.6347300	-0.4958340
H	-5.9250670	0.1395320	-0.4916000
H	-5.0789990	-0.7420730	-1.7854880
C	-0.7534060	0.4303280	0.1428800
C	-0.3340510	0.7367420	-1.2920280
C	1.0309720	1.4347470	-1.4615320
H	1.8008310	0.7012580	-1.2102090
H	1.1360220	1.6355690	-2.5315880
C	-2.3968440	1.4096950	2.3784540
H	-3.1045950	1.4961120	3.2062730
H	-1.3902680	1.5062580	2.7925700
H	-2.5824350	2.2299890	1.6789670
H	-2.3461140	-0.7414290	2.4307560
C	-2.4185860	-2.5334610	-0.4988370
H	-2.6899590	-0.6104470	-1.4880270
C	-3.5427690	-3.2837490	-1.2469370
H	-3.2338690	-4.3221150	-1.4024100
H	-4.4758340	-3.3026860	-0.6793140
H	-3.7410070	-2.8493240	-2.2330470
C	-1.1094210	-2.7527310	-1.2842360
H	-1.1871640	-2.3644030	-2.3069480
H	-0.2531070	-2.2940500	-0.7885340
H	-0.9086340	-3.8262950	-1.3597700
C	-2.2787080	-3.1220070	0.9166820
H	-3.1879310	-2.9757700	1.5094400
H	-2.1066150	-4.2009600	0.8469300
H	-1.4303620	-2.6873880	1.4528750
H	-0.3497050	-0.1607460	-1.9075220
C	1.2595780	2.7116390	-0.6742950
C	0.9303120	3.9625380	-1.2214220
C	1.8394010	2.6762270	0.6045850
C	1.1538880	5.1411760	-0.5044240
H	0.5029750	4.0149090	-2.2183490
C	2.0635900	3.8533130	1.3256700
H	2.1336010	1.7237870	1.0362520
C	1.7172220	5.0902570	0.7746930
H	0.8937810	6.0981570	-0.9476660
H	2.5156070	3.8019530	2.3120030
H	1.8942790	6.0059040	1.3312770
Cl	-1.6559370	1.8111550	-1.9963600
H	-0.4911890	1.2201740	0.8369330
O	0.5996500	-0.6804320	0.6471830
H	1.6280550	-0.9291430	0.2162200
H	0.6982530	-0.6068590	1.6091220
O	2.7653220	-1.2725730	-0.2645030
C	3.6354640	-1.5504090	0.6354870
C	5.0010960	-1.9778990	0.0144600
O	3.5215070	-1.5211930	1.8589030
F	4.8612370	-3.0838800	-0.7590820
F	5.5096920	-0.9981260	-0.7740550
F	5.9270600	-2.2591190	0.9518270

Hydrolysis of chloroiminium ion (TS6')

Conformation name	Extrapolated Free energy (kcal/mol)
TS6'-lowest	0.0
1	0.3
2	0.4
3	1.3
4	1.4
5	7.8

TS6′-lowest.log
Potential Energy = -1949.24993
Zero-point Energy = -1948.78615
Free Energy = -1948.83066
Single-Point Energy B3LYP-D3(BJ)/6-311+G** PCM = -1949.74410
Free Energy B3LYP-D3(BJ)/6-311+G** PCM (extrapolated free energy from qRRHO) = -1949.32483
Nimag = 1 (-394.5465 cm^{-1})
Charge = 0 Multiplicity = 1

C	3.3143630	-0.3728650	-0.6322180
C	3.2125240	-1.5659510	1.3980330
C	2.1441210	-0.4717540	1.5097160
N	2.0901440	0.0360690	0.1147710
N	3.7866740	-1.4968120	0.1760890
O	3.4749480	-2.3887490	2.2755060
C	4.6968430	-2.5351590	-0.2987110
H	4.3712660	-3.4922370	0.1136690
H	4.6585420	-2.5796420	-1.3876470
H	5.7273660	-2.3525940	0.0185900
C	1.0189370	0.4459970	-0.5736820
H	1.2718860	0.7991990	-1.5674850
C	-0.1277950	1.2342110	0.0631440
C	-1.0601490	1.8436440	-0.9957120
H	-0.4865610	2.5379880	-1.6176840
H	2.5302590	0.3220860	2.1602310
C	4.3516930	0.7887180	-0.8216370
H	3.0173970	-0.7425430	-1.6204870
H	-0.6905590	0.6171060	0.7587660
Cl	0.5938430	2.5687080	1.0954060
C	0.8632590	-1.0367110	2.1229130
H	0.1755740	-0.2500000	2.4352360
H	0.3536080	-1.7290030	1.4495120
H	1.1564220	-1.5885800	3.0194560
C	5.5659580	0.2606790	-1.6174770
H	6.2166290	1.1010970	-1.8788510
H	6.1665320	-0.4462110	-1.0413150
H	5.2607990	-0.2232420	-2.5523080
C	4.8261780	1.3480660	0.5320460

H	5.2812280	0.5723990	1.1564280
H	5.5830090	2.1208340	0.3634240
H	4.0048160	1.8103470	1.0881120
C	3.7060300	1.9234310	-1.6448980
H	3.3310080	1.5645590	-2.6108170
H	2.8895930	2.4124660	-1.1067240
H	4.4590870	2.6897270	-1.8535900
H	-1.3835220	1.0220180	-1.6440890
C	-2.2810110	2.5367470	-0.4243860
C	-2.4289480	3.9267900	-0.5240990
C	-3.2947930	1.7937010	0.2017410
C	-3.5604550	4.5649000	-0.0048560
H	-1.6555240	4.5148890	-1.0110050
C	-4.4239530	2.4285480	0.7251000
H	-3.2042640	0.7128080	0.2755500
C	-4.5603050	3.8175490	0.6237400
H	-3.6583100	5.6431720	-0.0922200
H	-5.1991690	1.8385410	1.2055730
H	-5.4396750	4.3108730	1.0273950
O	0.1195270	-1.0138210	-1.1678240
H	-0.8530080	-1.3550020	-0.7044250
O	-1.9392930	-1.7639340	-0.1166430
C	-2.7419960	-2.4054470	-0.8816290
O	-2.6442510	-2.6474990	-2.0831510
C	-3.9949680	-2.9254450	-0.1102420
F	-4.6747740	-1.9043110	0.4697490
F	-3.6378220	-3.7824230	0.8797350
F	-4.8601210	-3.5780190	-0.9112280
H	-0.0036890	-0.9769930	-2.1299370

1.log
Potential Energy = -1949.24780
Zero-point Energy = -1948.78402
Free Energy = -1948.82865
Single-Point Energy B3LYP-D3(BJ)/6-311+G** PCM = -1949.74365
Free Energy B3LYP-D3(BJ)/6-311+G** PCM (extrapolated free energy from qRRHO) = -1949.32449
Nimag = 1 (-416.3740 cm^{-1})
Charge = 0 Multiplicity = 1

C	2.4085910	-1.2682910	-0.7753590
C	1.8237410	-3.2259470	0.3986370
C	1.2459380	-2.0655920	1.2177850
N	1.4125200	-0.9247690	0.2801390
N	2.4051040	-2.7299470	-0.7161690
O	1.7384640	-4.4161160	0.7023400
C	2.8645740	-3.6046480	-1.7910630
H	2.1963810	-4.4666190	-1.8416930
H	2.8290250	-3.0639740	-2.7375090
H	3.8830810	-3.9640470	-1.6195730
C	0.5769410	0.1005620	0.0743890
H	0.9545620	0.8094490	-0.6546790
C	-0.2127310	0.7610050	1.2045720
C	-0.9287320	2.0704680	0.8090080
H	1.8917130	-1.9038330	2.0891530
C	3.8117260	-0.6019720	-0.5577460
H	2.0172360	-0.9492180	-1.7480330
H	-0.9588090	0.0779200	1.6012990
Cl	0.9299800	1.0520030	2.6117440
C	-0.1633820	-2.4072350	1.7013250
H	-0.5072360	-1.7259000	2.4803630
H	-0.8850210	-2.4303240	0.8820730
H	-0.1146250	-3.4070020	2.1399310
C	4.7518600	-1.0109970	-1.7134930
H	5.6766170	-0.4293010	-1.6469010
H	5.0296730	-2.0662390	-1.6717690
H	4.3042430	-0.8080960	-2.6931860
C	4.4340590	-1.0219860	0.7863570
H	4.5459410	-2.1085090	0.8615360
H	5.4315960	-0.5811980	0.8813120
H	3.8387140	-0.6700930	1.6345050
C	3.6599670	0.9330980	-0.5938750
H	3.1972880	1.2756090	-1.5270450
H	3.0769270	1.3115530	0.2497090
H	4.6508060	1.3942090	-0.5342400
H	-1.7321960	1.7871540	0.1223100
O	-0.7977950	-0.4820210	-0.9598230
H	-1.8548720	-0.5849260	-0.5641110
O	-3.0320940	-0.7513090	-0.0518260
C	-4.0045460	-0.5508810	-0.8613790
O	-3.9757840	-0.2134940	-2.0432090
C	-5.3884060	-0.7935710	-0.1824690
F	-5.5467530	-0.0064180	0.9110420
F	-5.5093480	-2.0812240	0.2295730
F	-6.4206280	-0.5399710	-1.0108070
H	-0.8313520	-0.0053840	-1.8040330
H	-1.4169280	2.4377180	1.7162530
C	-0.0911210	3.1701530	0.1854960
C	0.6317820	4.0736720	0.9823320
C	-0.0507990	3.3328760	-1.2086140
C	1.3907520	5.0926430	0.4009740
H	0.5936090	3.9848550	2.0635570
C	0.7083190	4.3509880	-1.7945860
H	-0.6349420	2.6733620	-1.8454350
C	1.4362050	5.2317290	-0.9902930
H	1.9402540	5.7822620	1.0352860
H	0.7217940	4.4588310	-2.8752310
H	2.0232990	6.0262750	-1.4413900

2.log
Potential Energy = -1949.24751
Zero-point Energy = -1948.78376
Free Energy = -1948.82843
Single-Point Energy B3LYP-D3(BJ)/6-311+G** PCM = -1949.74337
Free Energy B3LYP-D3(BJ)/6-311+G** PCM (extrapolated free energy from qRRHO) = -1949.32429
Nimag = 1 (-381.0451 cm^{-1})
Charge = 0 Multiplicity = 1

C	2.1176430	0.9731310	0.9323700
C	3.4741420	2.0704710	-0.6512730
C	2.9562280	0.8109220	-1.3558230
N	1.9210180	0.3366280	-0.4023190
N	2.9276180	2.1399490	0.5825520
O	4.2364400	2.8965920	-1.1538200
C	3.0703450	3.3316330	1.4140100
H	3.0879320	4.2058710	0.7602430
H	2.2190100	3.4043340	2.0916260
H	3.9953030	3.3154590	1.9972570
C	0.7416970	-0.2323160	-0.6831590
H	0.1823960	-0.4968330	0.2072320
C	0.5574570	-1.2317880	-1.8265640
C	-0.8068230	-1.9555910	-1.8325960
H	3.7680970	0.0749140	-1.3947380
C	2.7642150	0.0179260	1.9960390
H	1.1456450	1.3114200	1.3091390
H	0.6866500	-0.7441760	-2.7898130
Cl	1.9304330	-2.4460640	-1.7602710
C	2.5255170	1.1497470	-2.7833510
H	2.3578600	0.2582720	-3.3884890
H	1.6393100	1.7885790	-2.8021460
H	3.3488950	1.7037600	-3.2407800
C	2.8857650	0.7670830	3.3416990
H	3.1938830	0.0610490	4.1192120
H	3.6341220	1.5616770	3.3117140
H	1.9288480	1.2024210	3.6514610

C	4.1547340	-0.4674320	1.5473760
H	4.8409920	0.3671710	1.3711880
H	4.5932000	-1.0945110	2.3302940
H	4.0970220	-1.0729800	0.6376220
C	1.8448630	-1.2012690	2.2172750
H	0.8329100	-0.9017060	2.5138630
H	1.7800110	-1.8371080	1.3305330
H	2.2515150	-1.8160040	3.0263570
O	-0.4240640	1.0640550	-1.1678400
H	-1.3944220	1.1637050	-0.6054160
O	-2.4852520	1.3041200	0.0985040
C	-3.4636540	1.8039220	-0.5592290
O	-3.5125610	2.1476670	-1.7392100
C	-4.7409190	1.9649360	0.3227800
F	-4.4989300	2.7514960	1.4015840
F	-5.1652690	0.7632210	0.7903610
F	-5.7687720	2.5168910	-0.3517550
H	-0.6113200	1.1205340	-2.1184720
H	-0.8072130	-2.5990920	-2.7167870
H	-1.5667080	-1.1875120	-2.0094260
C	-1.1782820	-2.7640980	-0.6040710
C	-0.8047380	-4.1135170	-0.4930050
C	-1.9363070	-2.1921560	0.4308100
C	-1.1599170	-4.8648680	0.6303010
H	-0.2399070	-4.5810580	-1.2939400
C	-2.2918850	-2.9421510	1.5568060
H	-2.2669770	-1.1596110	0.3535120
C	-1.9016110	-4.2798590	1.6620490
H	-0.8636500	-5.9078640	0.6957260
H	-2.8805280	-2.4814500	2.3449550
H	-2.1812770	-4.8644930	2.5336140
H	5.2399470	1.7751040	1.6291370
H	3.7522360	2.5072980	2.2639070
C	4.4444030	-0.8464710	1.5957800
H	5.2366540	-0.6865240	0.8573910
H	4.9266770	-1.0509980	2.5569970
H	3.8794650	-1.7412670	1.3166680
C	2.4311140	0.0924170	2.7750980
H	1.7368080	0.9340000	2.8839650
H	1.8610780	-0.8094060	2.5362400
H	2.8980780	-0.0711340	3.7513340
H	-1.9589970	-0.4443490	0.2944510
C	-2.5315700	-2.5088740	0.3309370
C	-2.8320240	-3.4774470	1.2985700
C	-3.1798050	-2.5759020	-0.9126460
C	-3.7518720	-4.4961720	1.0292500
H	-2.3452260	-3.4346460	2.2691480
C	-4.0964180	-3.5941250	-1.1868480
H	-2.9739220	-1.8228230	-1.6697920
C	-4.3846090	-4.5591210	-0.2155260
H	-3.9730550	-5.2373160	1.7918800
H	-4.5899390	-3.6293290	-2.1537930
H	-5.0997860	-5.3489190	-0.4259280
O	-0.1375420	0.8610760	-1.0069230
H	-0.8752150	1.5495950	-0.5174920
O	-1.6760590	2.3684370	0.1231140
C	-2.6199060	2.8650380	-0.5837380
O	-2.8859150	2.6809300	-1.7707570
C	-3.5270410	3.8269470	0.2462300
F	-2.8055420	4.8386050	0.7916730
F	-4.1287280	3.1676830	1.2695740
F	-4.5028620	4.3877000	-0.4954100
H	-0.5446520	0.4745950	-1.7986640

3.log
Potential Energy = -1949.249631
Zero-point Energy = -1948.78593
Free Energy = -1948.83085
Single-Point Energy B3LYP-D3(BJ)/6-311+G** PCM = -1949.74168
Free Energy B3LYP-D3(BJ)/6-311+G** PCM (extrapolated free energy from qRRHO) = -1949.32290
Nimag = 1 (-355.7261 cm^{-1})
Charge = 0 Multiplicity = 1

C	2.8627180	0.7576730	0.3601370
C	3.8037000	0.0081630	-1.6670530
C	2.7100560	-1.0092370	-1.3209250
N	2.0088240	-0.3272390	-0.2044480
N	3.8004560	0.9902260	-0.7381290
O	4.5361930	-0.0533380	-2.6546330
C	4.5912050	2.2056460	-0.9097940
H	4.6401110	2.4349030	-1.9760520
H	4.1066910	3.0299970	-0.3852160
H	5.6108690	2.0876690	-0.5326430
C	0.7004050	-0.3313200	0.0729530
H	0.4616890	0.2365400	0.9654660
C	-0.1886180	-1.5667240	-0.0999830
C	-1.5379380	-1.4018820	0.6188140
H	-1.3566120	-1.3227040	1.6950990
H	3.1884440	-1.9183920	-0.9377380
C	3.5293970	0.3842840	1.7306160
H	2.2464590	1.6527940	0.5023330
H	-0.3403050	-1.8010320	-1.1514950
Cl	0.6995020	-3.0251330	0.5694680
C	1.9031250	-1.3628170	-2.5700510
H	1.2499090	-2.2215080	-2.4123140
H	1.3230290	-0.5128180	-2.9379180
H	2.6213360	-1.6373650	-3.3464710
C	4.3518600	1.5902680	2.2369190
H	4.6934270	1.3895980	3.2572090

4.log
Potential Energy = -1949.247187
Zero-point Energy = -1948.78263
Free Energy = -1948.82673
Single-Point Energy B3LYP-D3(BJ)/6-311+G** PCM = -1949.74308
Free Energy B3LYP-D3(BJ)/6-311+G** PCM (extrapolated free energy from qRRHO) = -1949.32262
Nimag = 1 (-310.9690 cm^{-1})
Charge = 0 Multiplicity = 1

C	-2.6986250	0.4657670	-0.8877210
C	-2.3567930	2.3382520	0.5025160
C	-1.9179440	1.1233180	1.3285200
N	-1.8854940	0.0566510	0.2936240
N	-2.7302300	1.9200200	-0.7280910
O	-2.3435540	3.5045270	0.8973940
C	-3.0111670	2.8663030	-1.8036490
H	-2.3672810	3.7377620	-1.6700490
H	-2.7911020	2.3991840	-2.7643800
H	-4.0527940	3.1994440	-1.7950520
C	-1.0165880	-0.9531120	0.1518680
H	-1.2934790	-1.6204180	-0.6568350
C	-0.3934530	-1.6937070	1.3412590
C	0.1620690	-3.0917230	0.9846510
H	-2.7164440	0.8886570	2.0424190
C	-4.1054930	-0.2248560	-0.9574270
H	-2.1412680	0.2183090	-1.7980030
H	0.3652930	-1.0850420	1.8282190
Cl	-1.6958140	-1.9515560	2.6134520
C	-0.6400660	1.4293320	2.1056200
H	-0.4217640	0.6610240	2.8482080
H	0.2235440	1.5722240	1.4542250
H	-0.8154470	2.3643390	2.6439920
C	-4.8367240	0.2469510	-2.2338950
H	-5.7522400	-0.3392810	-2.3614890

H	-5.1299580	1.2975840	-2.1819800
H	-4.2237180	0.1011380	-3.1306690
C	-4.9624010	0.1039090	0.2786890
H	-5.1086150	1.1822290	0.3983170
H	-5.9517270	-0.3520770	0.1698240
H	-4.5182570	-0.2946700	1.1959600
C	-3.9206450	-1.7540110	-1.0571620
H	-3.2945270	-2.0348170	-1.9126130
H	-3.4882100	-2.1780730	-0.1466490
H	-4.8973400	-2.2265950	-1.2007150
O	0.4309350	-0.3485620	-0.7378910
H	1.2179940	0.3012090	-0.2936140
O	2.1562380	1.0911600	0.2196490
C	3.0262320	1.5476110	-0.5988100
O	3.1461220	1.3530810	-1.8077530
C	4.0566810	2.4835630	0.1095810
F	3.4408090	3.5552600	0.6715820
F	4.9918920	2.9606690	-0.7365390
F	4.7115850	1.8323100	1.1046640
H	0.8826560	-1.0953540	-1.1693810
H	0.3844720	-3.5827400	1.9360120
H	-0.6347650	-3.6703770	0.5071440
C	1.4110940	-3.1102730	0.1225150
C	1.3509910	-3.4956290	-1.2267300
C	2.6605230	-2.7755120	0.6706840
C	2.5090760	-3.5321820	-2.0136230
H	0.3982110	-3.7857520	-1.6625820
C	3.8161080	-2.8123630	-0.1120960
H	2.7304780	-2.4903420	1.7173200
C	3.7437330	-3.1882240	-1.4585270
H	2.4423780	-3.8348650	-3.0543210
H	4.7735190	-2.5515570	0.3291730
H	4.6431540	-3.2176770	-2.0660220

5.log
Potential Energy = -1949.23941
Zero-point Energy = -1948.77437
Free Energy = -1948.81900
Single-Point Energy B3LYP-D3(BJ)/6-311+G** PCM = -1949.73291
Free Energy B3LYP-D3(BJ)/6-311+G** PCM (extrapolated free energy from qRRHO) = -1949.31249
Nimag = 1 (-186.9810 cm^{-1})
Charge = 0 Multiplicity = 1

C	3.1181100	0.5354530	-0.8234870
C	4.3992260	-0.8366830	0.6059300
C	2.9543720	-1.0417580	1.0668240
N	2.1941190	-0.3111330	0.0165670
N	4.4048120	-0.0854250	-0.5166800
O	5.3819840	-1.3696430	1.1200890
C	5.5626730	-0.0867920	-1.4112300
H	5.9905320	-1.0916980	-1.4185320
H	5.2380640	0.1737550	-2.4185060
H	6.3335550	0.6171530	-1.0898670
C	0.8743770	-0.2896400	-0.1859570
C	-0.0494010	-1.4899800	0.0760330
C	-1.3163060	-1.4094250	-0.7931530
H	-1.8953630	-0.5245470	-0.5159560
H	2.7905050	-0.5683310	2.0415960
C	3.0905050	2.0882560	-0.5626190
H	2.8709100	0.3548470	-1.8761930
H	0.5065240	-2.3946070	-0.1675040
Cl	-0.5043900	-1.6974070	1.8415520
C	2.7336070	-2.5584810	1.1697460
H	1.7889200	-2.8167410	1.6422850
H	2.8050570	-3.0347130	0.1874920
H	3.5367650	-2.9532980	1.7965040
C	4.3162510	2.7349400	-1.2494700
H	4.2180430	3.8228320	-1.1852220
H	5.2551630	2.4649230	-0.7624950
H	4.3811060	2.4757380	-2.3119040
C	3.1442450	2.4075990	0.9423250
H	4.0432050	1.9888800	1.4079520
H	3.1818600	3.4927590	1.0836440
H	2.2630820	2.0339960	1.4678440
C	1.8400570	2.7166820	-1.2158340
H	1.7784070	2.4597640	-2.2800030
H	0.9109700	2.4288540	-0.7287550
H	1.9097270	3.8068810	-1.1463480
H	-0.9679460	-1.2561510	-1.8226710
C	-2.1835550	-2.6506700	-0.7443110
C	-3.4143510	-2.6407240	-0.0734770
C	-1.7749140	-3.8312320	-1.3847630
C	-4.2168030	-3.7856200	-0.0350460
H	-3.7481260	-1.7323880	0.4206310
C	-2.5722810	-4.9778990	-1.3458280
H	-0.8312320	-3.8540450	-1.9249910
C	-3.7967520	-4.9583730	-0.6690570
H	-5.1682380	-3.7589660	0.4882400
H	-2.2415790	-5.8820340	-1.8487940
H	-4.4193510	-5.8478220	-0.6414460
H	0.6121250	0.2142600	-1.1111280
O	0.0749520	1.0253110	0.8481290
H	-0.8164190	1.4617730	0.4348660
H	-0.1720190	0.6380890	1.7055100
O	-1.9303770	2.0646620	-0.1663760
C	-2.8245870	2.4913420	0.6348910
C	-4.0053950	3.1889250	-0.1142660
O	-2.8748540	2.4261550	1.8656720
F	-4.6102350	2.3366770	-0.9824610
F	-3.5695330	4.2517870	-0.8393840
F	-4.9602590	3.6454570	0.7223510

Catalyst regeneration and product release (TS7)

Conformation name	Extrapolated Free energy (kcal/mol)
TS7-lowest	0.0
1	3.6
2	3.6
3	4.5
4	2.3
5	5.3
6	3.8
7	5.6
8	1.1
9	0.7
10	1.6

TS7-lowest.log
Potential Energy = -1949.25101
Zero-point Energy = -1948.78659
Free Energy = -1948.83046
Single-Point Energy B3LYP-D3(BJ)/6-311+G** PCM = -1949.74709
Free Energy B3LYP-D3(BJ)/6-311+G** PCM (extrapolated free energy from qRRHO) = -1949.32653
Nimag = 1 (-492.3687 cm^{-1})

Charge = 0 Multiplicity = 1

C	1.0639590	1.7565980	-1.7950990
C	-0.2708930	2.3394820	0.0328890
C	-0.1808220	0.8788080	-1.8252270
H	-0.9995880	3.0098360	-0.4502400
H	0.0659700	-0.1538370	-2.0768710
C	-0.1489250	-0.8124890	0.4540330
H	-0.6715330	-0.5341840	1.3706490
O	-0.6908270	-1.6602060	-0.3341430
N	1.0289200	2.5007140	-0.6487910
C	1.9203040	3.6473820	-0.4984670
H	2.3730770	3.6700700	0.4930590
H	2.7081110	3.5396320	-1.2441460
H	1.3868740	4.5863310	-0.6790740
O	1.9286660	1.7983340	-2.6690720
C	1.3778500	-0.8602110	0.5916570
H	1.7864850	0.1287560	0.7839120
C	2.1135610	-1.5683490	-0.5498780
H	1.8706510	-1.0305140	-1.4725620
H	1.7078280	-2.5763580	-0.6604390
N	-0.6271330	0.9464870	-0.4067470
C	-3.8247910	-1.0629700	-0.2117750
C	-5.3295320	-1.4568300	-0.1564260
O	-3.5182530	0.1205400	-0.3345990
H	-1.6437700	0.8025400	-0.3472500
O	-3.0553030	-2.0889970	-0.1176320
H	-1.9104120	-1.8428750	-0.2039220
C	-0.3851580	2.6589670	1.5545680
C	-0.3428680	4.1973580	1.7431830
H	-0.6213520	4.4353270	2.7742350
H	0.6471800	4.6218070	1.5700880
H	-1.0544310	4.7031880	1.0816820
C	0.7004860	2.0169540	2.4374130
H	0.6293040	2.4311810	3.4481500
H	1.7109970	2.2210180	2.0719910
C	-1.7832970	2.1937080	2.0250640
H	-1.9293570	2.4928870	3.0671670
H	-2.5810110	2.6541600	1.4320100
H	-1.9110970	1.1090200	1.9795190
C	-1.2108860	1.3949030	-2.8426400
H	-0.7744940	1.3495420	-3.8439080
H	-2.1022840	0.7631120	-2.8231080
H	-1.5090980	2.4285260	-2.6452470
H	0.5802510	0.9365340	2.5342450
Cl	1.6440390	-1.7747320	2.1772690
F	-5.6133560	-2.1331630	0.9811550
F	-6.1342890	-0.3805610	-0.2026320
F	-5.6549450	-2.2581010	-1.1988180
C	3.6209790	-1.6130600	-0.3902230
C	4.3981510	-0.4602750	-0.5857570
C	4.2701170	-2.8116730	-0.0623630
C	5.7876570	-0.5018580	-0.4426900
H	3.9181180	0.4742910	-0.8648520
C	5.6608930	-2.8581950	0.0785730
H	3.6842230	-3.7152580	0.0830470
C	6.4240590	-1.7019910	-0.1081280
H	6.3725040	0.3998660	-0.6003930
H	6.1453790	-3.7968230	0.3320110
H	7.5042880	-1.7362130	-0.0005890

1.log
Potential Energy = -1949.24594
Zero-point Energy = -1948.78197
Free Energy = -1948.82590
Single-Point Energy B3LYP-D3(BJ)/6-311+G** PCM = -1949.74085
Free Energy B3LYP-D3(BJ)/6-311+G** PCM (extrapolated free energy from qRRHO) = -1949.32081

Nimag = 1 (-506.0454 cm^{-1})
Charge = 0 Multiplicity = 1

C	-0.4872840	2.5446190	1.7234570
C	1.0762730	2.2660040	0.0038530
C	0.1217160	1.1589380	1.8817700
H	2.0289420	2.5006800	0.5057360
H	-0.6537840	0.4297950	2.1172460
C	-0.3080020	-0.6205850	-0.3207610
H	0.0157800	-0.3655960	-1.3310290
O	0.2235360	-1.6211500	0.2839970
N	0.0248150	3.1081160	0.5952660
C	-0.1561850	4.5334570	0.3445280
H	-0.5049350	4.7192850	-0.6718900
H	-0.9123850	4.8860940	1.0460720
H	0.7734970	5.0846920	0.5186860
O	-1.2706190	3.0666710	2.5170300
C	-1.8077000	-0.5146900	-0.0544560
H	-1.9958980	-0.5702960	1.0177990
C	-2.5096700	-1.7012040	-0.7606600
H	-1.9825670	-2.6038020	-0.4352370
H	-2.3657290	-1.6077240	-1.8417360
N	0.6829530	0.8962630	0.5233480
C	3.3518350	-1.7996570	0.1976880
C	4.7337570	-2.4920670	0.0195940
O	3.2919670	-0.7046010	0.7510930
H	1.5453660	0.3433990	0.6139270
O	2.3902640	-2.5034540	-0.2885910
H	1.3345030	-2.0376040	-0.0569430
C	1.3892290	2.3986890	-1.5201030
C	2.1495840	3.7304700	-1.7535410
H	2.5334120	3.7429820	-2.7782020
H	1.5172560	4.6112730	-1.6358790
H	3.0057910	3.8286690	-1.0772270
C	0.1587540	2.3583410	-2.4432950
H	0.4815200	2.5520000	-3.4716370
H	-0.5838910	3.1148360	-2.1785410
C	2.3704160	1.2675120	-1.9059270
H	2.7017290	1.4180130	-2.9375620
H	3.2588010	1.2674330	-1.2662390
H	1.9177530	0.2743840	-1.8586530
C	1.1699940	1.1363750	3.0050450
H	0.6849770	1.3973950	3.9492260
H	1.5986200	0.1356160	3.0988020
H	1.9797150	1.8497220	2.8256400
H	-0.3442650	1.3908570	-2.4340150
Cl	-2.5273120	1.0581990	-0.6082370
F	4.9879130	-2.7377960	-1.2873290
F	5.7401080	-1.7382280	0.4961600
F	4.7655200	-3.6790310	0.6708520
C	-3.9838620	-1.8268520	-0.4351590
C	-4.9621170	-1.5094110	-1.3875890
C	-4.3968780	-2.2813720	0.8275070
C	-6.3222590	-1.6359250	-1.0863690
H	-4.6588070	-1.1625290	-2.3717580
C	-5.7544120	-2.4055210	1.1335800
H	-3.6531530	-2.5471540	1.5751160
C	-6.7225150	-2.0817910	0.1764440
H	-7.0658010	-1.3867800	-1.8380340
H	-6.0555300	-2.7606740	2.1149610
H	-7.7780640	-2.1811940	0.4120840

2.log
Potential Energy = -1949.24440
Zero-point Energy = -1948.77977
Free Energy = -1948.82337
Single-Point Energy B3LYP-D3(BJ)/6-311+G** PCM = -1949.74179

Free Energy B3LYP-D3(BJ)/6-311+G** PCM (extrapolated free energy from qRRHO) = -1949.32076
Nimag = 1 (-500.3399 cm^{-1})
Charge = 0 Multiplicity = 1

C	-0.8663320	-3.3403780	-1.0437420
C	0.1349870	-2.2737740	0.7848040
C	0.0726130	-2.2784330	-1.5966060
H	1.1083300	-2.7843610	0.8642510
H	-0.4068830	-1.7442420	-2.4170640
C	-0.5309800	0.4263900	-0.8299190
H	-0.6076720	0.7018920	0.2214320
O	0.3927900	0.9424720	-1.5579610
N	-0.8614910	-3.2485480	0.3141580
C	-1.4395300	-4.3188200	1.1191670
H	-2.1163530	-3.9268540	1.8792780
H	-2.0048500	-4.9573890	0.4401760
H	-0.6572060	-4.9156670	1.5988190
O	-1.4793790	-4.1637100	-1.7236550
C	-1.8457870	0.2817290	-1.5893160
H	-1.6606870	-0.2223320	-2.5377240
C	-2.4340900	1.6802750	-1.9203900
H	-1.7038590	2.1616400	-2.5782890
N	0.2591420	-1.3694190	-0.4270920
C	3.2919530	0.9235950	-0.3629900
C	4.6795040	1.5161040	0.0172690
O	3.1314240	-0.2941950	-0.3527040
H	1.2187860	-0.9997250	-0.4347920
O	2.4357760	1.8405000	-0.6506470
H	1.4179440	1.3968250	-1.0379920
C	-0.0714030	-1.5933200	2.1748960
C	0.2341610	-2.6327520	3.2851260
H	0.2761220	-2.1169310	4.2492800
H	-0.5282130	-3.4081260	3.3681820
H	1.2032110	-3.1182130	3.1259630
C	-1.4775050	-1.0136570	2.4092600
H	-1.5420420	-0.6454520	3.4385090
H	-2.2614450	-1.7625930	2.2731410
C	0.9907020	-0.4793760	2.3255830
H	0.9377040	-0.0696060	3.3384800
H	2.0035710	-0.8662160	2.1744670
H	0.8402230	0.3548980	1.6367140
C	1.3762340	-2.9035110	-2.1170710
H	1.1393990	-3.5907750	-2.9334300
H	2.0399660	-2.1242610	-2.4995920
H	1.9030450	-3.4628020	-1.3383970
H	-1.7070370	-0.1784240	1.7470680
Cl	-3.0731040	-0.7399810	-0.7219070
F	4.5757030	2.3354400	1.0905160
F	5.5710690	0.5565600	0.3212620
F	5.1912580	2.2443810	-1.0029040
C	-2.7517330	2.5878710	-0.7477990
C	-1.7878690	3.4787270	-0.2477660
C	-4.0240040	2.5784060	-0.1546740
C	-2.0800710	4.3225810	0.8279310
H	-0.8046500	3.5205300	-0.7088580
C	-4.3202500	3.4215570	0.9204500
H	-4.7893930	1.9112540	-0.5404580
C	-3.3473510	4.2939930	1.4182720
H	-1.3209400	5.0057370	1.1980010
H	-5.3116830	3.4004510	1.3638640
H	-3.5775460	4.9518970	2.2512240
H	-3.3352780	1.5030900	-2.5143420

3.log
Potential Energy = -1949.24375
Zero-point Energy = -1948.77976
Free Energy = -1948.82349

Single-Point Energy B3LYP-D3(BJ)/6-311+G** PCM = -1949.73962
Free Energy B3LYP-D3(BJ)/6-311+G** PCM (extrapolated free energy from qRRHO) = -1949.31936
Nimag = 1 (-491.2565 cm^{-1})
Charge = 0 Multiplicity = 1

C	-2.9135440	-1.3243350	1.6240160
C	-2.7165180	0.3464560	-0.0061310
C	-1.5584750	-0.6610650	1.8181770
H	-3.0123460	1.2622580	0.5311450
H	-0.7946290	-1.4194170	1.9938590
C	0.3072860	-0.8350170	-0.3847590
H	0.0295450	-0.4679820	-1.3725930
O	1.2410800	-0.2502170	0.2727870
N	-3.5042300	-0.7755950	0.5279240
C	-4.9217240	-1.0039940	0.2715990
H	-5.0955640	-1.3314330	-0.7543060
H	-5.2455610	-1.7918750	0.9518780
H	-5.5064080	-0.1002540	0.4707210
O	-3.3963840	-2.1761480	2.3710240
C	0.3229550	-2.3443950	-0.2038150
H	0.4770870	-2.5887190	0.8472130
C	1.4623590	-2.9673970	-1.0634920
H	1.3414410	-2.6386670	-2.1004660
N	-1.3308390	0.0080390	0.5041160
C	1.1362100	2.8807350	0.3133440
C	1.7070240	4.3254860	0.2055460
O	0.0590520	2.7050300	0.8843280
H	-0.8367290	0.8977750	0.6546250
O	1.9006950	2.0111520	-0.2358670
H	1.5293940	0.8459250	-0.0214940
C	-2.8524760	0.7074530	-1.5194080
C	-4.2254630	1.3917940	-1.7485770
H	-4.2442720	1.8166920	-2.7568770
H	-5.0664190	0.7013110	-1.6748990
H	-4.3899070	2.2113220	-1.0403820
C	-2.7252820	-0.4890280	-2.4784950
H	-2.9249660	-0.1488720	-3.5000450
H	-3.4390000	-1.2831040	-2.2452890
C	-1.7807510	1.7696260	-1.8571260
H	-1.9345630	2.1196520	-2.8821190
H	-1.8501170	2.6373220	-1.1932740
H	-0.7605240	1.3831940	-1.8021930
C	-1.5784650	0.3017130	3.0157010
H	-1.8072840	-0.2628600	3.9234000
H	-0.5998020	0.7727300	3.1358970
H	-2.3328990	1.0852880	2.8982320
H	-1.7293500	-0.9334010	-2.4695590
Cl	-1.2391730	-3.1337400	-0.6890370
F	1.9087570	4.6735640	-1.0881790
F	0.8836570	5.2413600	0.7479860
F	2.8998330	4.4217190	0.8417020
H	1.2858470	-4.0470800	-1.0490460
C	2.8696280	-2.6839530	-0.5774840
C	3.7244290	-1.8391360	-1.2988820
C	3.3560990	-3.2970990	0.5879760
C	5.0322920	-1.6031090	-0.8635670
H	3.3662940	-1.3622310	-2.2076680
C	4.6602230	-3.0600070	1.0291120
H	2.7145450	-3.9703430	1.1517030
C	5.5030420	-2.2099880	0.3043560
H	5.6805030	-0.9464180	-1.4366750
H	5.0199460	-3.5433250	1.9329340
H	6.5183240	-2.0277820	0.6443020

4.log
Potential Energy = -1949.24967
Zero-point Energy = -1948.78455

Free Energy = -1948.82828
Single-Point Energy B3LYP-D3(BJ)/6-311+G** PCM = -1949.74430
Free Energy B3LYP-D3(BJ)/6-311+G** PCM (extrapolated free energy from qRRHO) = -1949.32292
Nimag = 1 (-353.0256 cm^{-1})
Charge = 0 Multiplicity = 1

C	-0.2350390	-0.9723700	-0.4731210
H	0.2935820	-0.8131030	-1.4123540
O	0.2216980	-1.8435150	0.3476350
C	-1.7506830	-0.8167670	-0.5376460
H	-2.0272890	0.1872770	-0.8486700
C	3.3816840	-1.6531910	0.1521120
C	4.8358420	-2.1969680	0.0250670
O	3.2168810	-0.4504010	0.3742200
O	2.5021340	-2.5672250	-0.0025820
H	1.3090400	-2.1661570	0.1625800
Cl	-2.2184270	-1.8774470	-1.9747610
F	5.0444000	-2.7332470	-1.2023480
F	5.7603500	-1.2361920	0.2088820
F	5.0728320	-3.1701410	0.9373090
N	0.5324180	0.7975310	0.2406800
C	0.0159300	1.3490050	1.5325950
C	1.0426340	1.9752410	-0.5712650
C	0.7963720	2.6615130	1.6762370
H	-1.0495820	1.5780350	1.4350350
H	1.9510520	1.6344390	-1.0782280
H	1.4031120	0.2953860	0.4699680
O	0.8855720	3.3338550	2.7043540
N	1.4170040	2.9151410	0.5002810
C	2.4701980	3.9234210	0.4010910
H	2.0662880	4.9260310	0.2369350
H	3.0346960	3.9261560	1.3361890
H	3.1387930	3.6675780	-0.4214420
C	0.2577120	0.4368700	2.7342540
H	-0.2783420	-0.5081200	2.6415730
H	1.3237060	0.2183860	2.8500810
H	-0.0867590	0.9486180	3.6358290
C	0.0963690	2.5869260	-1.6552420
C	0.8102440	3.8055770	-2.2890420
H	0.2223310	4.1564840	-3.1425820
H	0.9019770	4.6417260	-1.5935280
H	1.8079910	3.5470000	-2.6602580
C	-0.1310850	1.5674030	-2.7909960
H	0.8187070	1.1775740	-3.1745990
H	-0.7545250	0.7230620	-2.4974360
H	-0.6447510	2.0592970	-3.6226550
C	-1.2472690	3.0649950	-1.0753030
H	-1.1027240	3.8107250	-0.2871030
H	-1.8414810	3.5334950	-1.8661660
H	-1.8463880	2.2479260	-0.6653510
C	-2.5054800	-1.2508130	0.7213050
H	-2.2202970	-2.2755280	0.9692800
H	-2.1439760	-0.6165010	1.5376080
C	-4.0137050	-1.1259060	0.6260050
C	-4.8151100	-2.2661800	0.4722390
C	-4.6394830	0.1278300	0.7092090
C	-6.2070920	-2.1580260	0.3921580
H	-4.3477990	-3.2455750	0.4160790
C	-6.0300020	0.2406550	0.6265370
H	-4.0406690	1.0240090	0.8503240
C	-6.8189220	-0.9032910	0.4661150
H	-6.8107490	-3.0533350	0.2744080
H	-6.4959470	1.2194250	0.6952560
H	-7.8999140	-0.8174260	0.4059730

5.log
Potential Energy = -1949.24583
Zero-point Energy = -1948.77984
Free Energy = -1948.82356
Single-Point Energy B3LYP-D3(BJ)/6-311+G** PCM = -1949.74041
Free Energy B3LYP-D3(BJ)/6-311+G** PCM (extrapolated free energy from qRRHO) = -1949.31813
Nimag = 1 (-182.7738 cm^{-1})
Charge = 0 Multiplicity = 1

C	-0.4263140	-0.7666210	-0.3001490
H	-0.1255300	-1.2251390	0.6439450
O	0.1220020	-1.2109160	-1.3699740
C	-1.8984960	-0.3937960	-0.3160830
C	-2.7102910	-1.6160730	0.1901840
H	-2.5565940	-2.4493500	-0.5016470
H	-2.2782530	-1.9106530	1.1541600
C	2.8965280	-2.1112280	0.0191990
C	4.2033880	-2.9515910	0.1476470
O	2.6878930	-1.2268180	0.8598960
O	2.1852890	-2.4569360	-0.9776660
H	1.0624870	-1.7597240	-1.1754870
F	3.9265770	-4.2750010	0.2407800
F	4.9308560	-2.6154520	1.2301380
F	4.9942070	-2.7804980	-0.9410210
C	-4.1893320	-1.3418860	0.3715860
C	-4.6460630	-0.5921910	1.4669770
C	-5.1286550	-1.8428010	-0.5404020
C	-6.0092050	-0.3388760	1.6398060
H	-3.9350620	-0.2105470	2.1958700
C	-6.4942100	-1.5944760	-0.3682010
H	-4.7913190	-2.4317410	-1.3888610
C	-6.9381580	-0.8390000	0.7208460
H	-6.3454120	0.2411870	2.4943420
H	-7.2080740	-1.9921320	-1.0837600
H	-7.9982860	-0.6460270	0.8564180
H	-2.0835440	0.4603930	0.3344050
Cl	-2.4707480	0.1024800	-1.9629800
N	0.6753100	0.8485570	0.3522160
C	0.1436060	1.5363480	1.5679230
C	1.5201210	1.8712290	-0.3914650
C	1.2012360	2.6162770	1.8311170
H	-0.8032990	2.0281410	1.3229480
H	2.3824010	1.3345900	-0.8001050
O	1.3406770	3.2448820	2.8810260
C	3.2489280	3.4391950	0.7564580
H	3.1224210	4.5014770	0.5328920
H	3.6800150	3.3421340	1.7551900
H	3.9300390	3.0003910	0.0262380
N	1.9803960	2.7143930	0.7292800
H	1.3849230	0.1774860	0.6825000
C	-0.0396580	0.6226470	2.7770100
H	-0.2687100	1.2430330	3.6466330
H	-0.8660220	-0.0787480	2.6432760
H	0.8726410	0.0578670	2.9922280
C	0.8503490	2.6557080	-1.5622020
C	1.7749790	3.8222520	-1.9818640
H	1.8091280	4.6145370	-1.2304290
H	2.7974890	3.4853980	-2.1843380
H	1.3869270	4.2632560	-2.9053790
C	-0.5182660	3.2450140	-1.1753870
H	-0.9087330	3.8363640	-2.0100240
H	-1.2574830	2.4715340	-0.9579620
H	-0.4388520	3.9145330	-0.3122080
C	0.7257160	1.7159240	-2.7785460
H	0.1230170	0.8337230	-2.5719470
H	0.2615610	2.2544860	-3.6112950
H	1.7160200	1.3812530	-3.1094650

6.log

Potential Energy = -1949.24520
Zero-point Energy = -1948.77947
Free Energy = -1948.82349
Single-Point Energy B3LYP-D3(BJ)/6-311+G** PCM = -1949.74218
Free Energy B3LYP-D3(BJ)/6-311+G** PCM (extrapolated free energy from qRRHO) = -1949.32047
Nimag = 1 (-184.3497 cm^{-1})
Charge = 0 Multiplicity = 1

C	0.7139820	-0.3444080	-1.0328300
H	1.1607050	0.2641110	-0.2446750
O	0.1745010	0.2686700	-2.0208860
C	1.4989440	-1.6141770	-1.2925640
C	2.9902150	-1.2552330	-1.5667990
H	3.0289940	-0.5430540	-2.3963320
C	-0.6336890	2.9344980	-0.3845530
C	-0.9798820	4.4469490	-0.2338760
O	-0.6765710	2.2228750	0.6273310
O	-0.3415570	2.6140260	-1.5810210
H	-0.0640200	1.3257380	-1.7972240
F	0.0446560	5.2271940	-0.6564210
F	-1.2498430	4.7920110	1.0396640
F	-2.0661670	4.7687800	-0.9797120
H	1.4341980	-2.2911070	-0.4413460
Cl	0.8724320	-2.5388000	-2.7241510
N	-0.7753960	-0.7079250	0.3613030
C	-0.3565940	-1.4767910	1.5731260
C	-2.2759000	-0.9105740	0.2128410
C	-1.6422120	-1.5178300	2.4088140
H	-0.0907440	-2.4984460	1.2829840
H	-2.6930430	0.0426090	-0.1274340
O	-1.7137200	-1.8106420	3.6032280
C	-3.9657770	-0.7583660	2.1843450
H	-4.6202530	-1.6258140	2.3016600
H	-3.8033360	-0.3091940	3.1666070
H	-4.4518140	-0.0317080	1.5320780
N	-2.6666820	-1.1186880	1.6205320
H	-0.7146040	0.2892960	0.6143910
C	0.7886630	-0.8343910	2.3516020
H	0.9252720	-1.3859120	3.2847560
H	1.7311070	-0.8691160	1.8017790
H	0.5613410	0.2066040	2.6014610
C	-2.7668450	-2.0239320	-0.7639550
C	-4.2795100	-2.2596000	-0.5445260
H	-4.4880200	-2.7492250	0.4095530
H	-4.8540150	-1.3283180	-0.5947840
H	-4.6509950	-2.9161530	-1.3375730
C	-2.0387140	-3.3626440	-0.5453170
H	-2.4605280	-4.1201490	-1.2140120
H	-0.9721060	-3.2962140	-0.7673530
H	-2.1670220	-3.7266290	0.4797440
C	-2.5925200	-1.5232120	-2.2121600
H	-1.5607420	-1.2760240	-2.4537310
H	-2.9271890	-2.2972810	-2.9106310
H	-3.2055440	-0.6308350	-2.3860990
H	3.4633260	-2.1792750	-1.9095500
C	3.7394860	-0.7181530	-0.3622390
C	3.9569610	0.6583600	-0.1975490
C	4.2510010	-1.6005490	0.6031610
C	4.6575450	1.1436880	0.9112190
H	3.5867250	1.3561650	-0.9444200
C	4.9516490	-1.1186370	1.7118450
H	4.1078470	-2.6716250	0.4827900
C	5.1543470	0.2563400	1.8703780
H	4.8183770	2.2121130	1.0208060
H	5.3425990	-1.8158260	2.4470770
H	5.7007660	0.6318370	2.7304190

7.log
Potential Energy = -1949.24378
Zero-point Energy = -1948.77757
Free Energy = -1948.82128
Single-Point Energy B3LYP-D3(BJ)/6-311+G** PCM = -1949.74017
Free Energy B3LYP-D3(BJ)/6-311+G** PCM (extrapolated free energy from qRRHO) = -1949.31767
Nimag = 1 (-166.7933 cm^{-1})
Charge = 0 Multiplicity = 1

C	0.6752510	-0.6500430	0.1739330
H	0.7524660	0.0164450	1.0346350
O	0.9418270	-0.1531300	-0.9781810
C	1.1078590	-2.0690590	0.4975860
C	2.3932850	-2.0672730	1.3750050
C	0.0470380	2.8675910	-0.2387100
C	0.0695870	4.4207630	-0.3729760
O	-0.7258530	2.3668250	0.5899550
O	0.8548910	2.2926090	-1.0342230
H	0.8842690	0.9437210	-0.9913280
F	1.3206460	4.9104360	-0.1958450
F	-0.7312860	5.0307070	0.5219870
F	-0.3409940	4.8012930	-1.6089070
H	0.3316210	-2.5759320	1.0695100
Cl	1.3425340	-3.0769260	-0.9922950
N	-1.3491250	-0.4953750	0.4685840
C	-1.8539370	-1.0804500	1.7477600
C	-2.5180530	-0.5038380	-0.5044690
C	-3.3533010	-0.7598440	1.6943160
H	-1.7295270	-2.1680070	1.7252370
H	-2.4501200	0.4170960	-1.0922010
O	-4.1298460	-0.7960150	2.6492880
C	-4.9220910	0.2719630	0.1123960
H	-5.7045770	-0.4461960	-0.1447110
H	-5.2440850	0.8398520	0.9877850
H	-4.7758300	0.9545830	-0.7260550
N	-3.6538350	-0.3809090	0.4302040
H	-1.2112200	0.5124210	0.6410390
C	-1.1978270	-0.5060550	3.0005800
H	-1.7371390	-0.8768600	3.8752000
H	-0.1550470	-0.8163270	3.0967720
H	-1.2433390	0.5872650	3.0089200
C	-2.6246200	-1.6975640	-1.5042260
C	-4.0150670	-1.6651450	-2.1803630
H	-4.8168420	-1.9379010	-1.4901590
H	-4.2406760	-0.6838090	-2.6114720
H	-4.0253310	-2.3922660	-2.9983330
C	-2.4588090	-3.0654050	-0.8176430
H	-2.6088240	-3.8622280	-1.5533240
H	-1.4600760	-3.2017980	-0.3981150
H	-3.2006050	-3.2115760	-0.0252960
C	-1.5739780	-1.5058000	-2.6169670
H	-0.5546100	-1.4746180	-2.2369860
H	-1.6426040	-2.3325370	-3.3316150
H	-1.7602350	-0.5751660	-3.1660400
H	2.6130250	-3.1168820	1.5899040
H	2.1166040	-1.6063460	2.3302920
C	3.6184810	-1.3754110	0.8116440
C	4.5142710	-2.0620070	-0.0234000
C	3.8999310	-0.0398910	1.1401470
C	5.6476800	-1.4238870	-0.5347400
H	4.3274120	-3.1027050	-0.2701960
C	5.0325510	0.6017180	0.6302610
H	3.2379930	0.5029280	1.8104190
C	5.9082880	-0.0879690	-0.2131530
H	6.3293840	-1.9723900	-1.1783560
H	5.2322290	1.6351730	0.8980480
H	6.7906450	0.4071950	-0.6077890

8.log
Potential Energy = -1949.25022
Zero-point Energy = -1948.785715
Free Energy = -1948.82956
Single-Point Energy B3LYP-D3(BJ)/6-311+G** PCM = -1949.74546
Free Energy B3LYP-D3(BJ)/6-311+G** PCM (extrapolated free energy from qRRHO) = -1949.32480
Nimag = 1 (-381.4409 cm^{-1})
Charge = 0 Multiplicity = 1

C	0.5113790	2.3894900	-1.8330060
C	-0.4357110	2.3747420	0.3008610
C	-0.6177670	1.3674950	-1.8331020
H	-1.3019540	3.0344680	0.1323670
H	-0.3165630	0.4604450	-2.3572620
C	0.0135680	-0.7607400	-0.0582360
H	-0.2790290	-0.7283410	0.9957960
O	-0.6626630	-1.4858070	-0.8595100
N	0.6742930	2.8427850	-0.5521700
C	1.4759140	4.0371800	-0.3040440
H	2.1263050	3.9047380	0.5610270
H	2.0932140	4.1968150	-1.1882330
H	0.8404300	4.9161070	-0.1525930
O	1.1352120	2.7640380	-2.8243990
C	1.5321930	-0.6995040	-0.2302080
C	2.1565290	-1.8598560	0.5839970
H	1.7599960	-2.8040380	0.1989230
H	1.7952040	-1.7565330	1.6146950
N	-0.7604260	1.0723340	-0.3779680
C	-3.7217120	-1.2779530	0.0419550
C	-5.1433020	-1.8425490	0.3269950
O	-3.5313730	-0.0668710	0.0939920
H	-1.7289560	0.8000970	-0.1671330
O	-2.8798140	-2.2149840	-0.2291290
H	-1.8270460	-1.8326380	-0.4976910
C	-0.2551260	2.3478960	1.8483900
C	-0.2880900	3.8034570	2.3814370
H	-0.3667560	3.7788920	3.4725630
H	0.6112580	4.3697100	2.1353440
H	-1.1552770	4.3519990	1.9982040
C	1.0352580	1.6651210	2.3352760
H	1.1591830	1.8498380	3.4069570
H	1.9266570	2.0474040	1.8300860
C	-1.4854310	1.6292560	2.4498420
H	-1.4337880	1.6793220	3.5414850
H	-2.4207920	2.1067920	2.1382750
H	-1.5390050	0.5723350	2.1762990
C	-1.8877010	1.9295770	-2.4907840
H	-1.6726950	2.1645640	-3.5366070
H	-2.6853540	1.1829690	-2.4606870
H	-2.2425030	2.8415650	-2.0013210
H	1.0019670	0.5816810	2.2071570
F	-5.1180430	-2.7243360	1.3535200
F	-6.0148630	-0.8697530	0.6450270
F	-5.6288670	-2.4922470	-0.7571310
C	3.6720180	-1.8899080	0.5857330
C	4.4092590	-1.0116910	1.3957050
C	4.3679640	-2.8097270	-0.2119970
C	5.8065070	-1.0424910	1.3971830
H	3.8929710	-0.3038610	2.0388660
C	5.7659000	-2.8458850	-0.2108090
H	3.8126000	-3.5032080	-0.8373770
C	6.4900080	-1.9595810	0.5918470
H	6.3594900	-0.3564130	2.0323220
H	6.2863720	-3.5667080	-0.8348330
H	7.5757400	-1.9867970	0.5952690
H	1.9227920	0.2586540	0.1060780
Cl	2.0213880	-0.8309190	-1.9799760

9.log
Potential Energy = -1949.24902
Zero-point Energy = -1948.78464
Free Energy = -1948.82845
Single-Point Energy B3LYP-D3(BJ)/6-311+G** PCM = -1949.74601
Free Energy B3LYP-D3(BJ)/6-311+G** PCM (extrapolated free energy from qRRHO) = -1949.32543
Nimag = 1 (-453.2927 cm^{-1})
Charge = 0 Multiplicity = 1

C	-1.5214730	-3.1195530	-0.6560270
C	-0.9135380	-1.9030380	1.2401530
C	-0.1401490	-2.5299160	-0.9057060
H	-0.2814690	-2.6478690	1.7503390
H	-0.0684390	-2.1323290	-1.9177700
C	-0.2336920	0.3209230	-0.9920280
H	-0.0678050	0.9114280	-0.0871150
O	0.7256320	0.1814740	-1.8224700
N	-1.9887090	-2.6209230	0.5286920
C	-3.1491770	-3.2365470	1.1645650
H	-3.8366170	-2.4826820	1.5493730
H	-3.6593330	-3.8219990	0.3994970
H	-2.8466500	-3.9045870	1.9778390
O	-2.0903700	-3.9353910	-1.3798080
C	-1.6428670	0.5025530	-1.5429140
C	-1.8489010	1.9765280	-1.9908940
H	-1.0795060	2.2187940	-2.7299450
N	-0.1069820	-1.4030850	0.0718620
C	3.4071860	0.0397090	-0.0875220
C	4.8992390	0.3590610	0.2179620
O	2.8002070	-0.7472720	0.6335900
H	0.8606840	-1.2303830	0.3725520
O	2.9812490	0.6778560	-1.1208000
H	1.8798750	0.4297330	-1.4135200
C	-1.2841830	-0.8729790	2.3479150
C	-1.7747320	-1.6417540	3.6019530
H	-1.8411050	-0.9429930	4.4414470
H	-2.7629850	-2.0851370	3.4726690
H	-1.0759220	-2.4362570	3.8855230
C	-2.3525200	0.1539910	1.9361310
H	-2.6803740	0.7086260	2.8211590
H	-3.2370520	-0.3158910	1.4963470
C	0.0130740	-0.1390610	2.7604700
H	-0.2015190	0.5235850	3.6041690
H	0.7894230	-0.8430810	3.0791410
H	0.4262610	0.4804700	1.9602840
C	0.9654620	-3.5774620	-0.7004850
H	0.8229600	-4.3892160	-1.4188470
H	1.9450190	-3.1264290	-0.8775440
H	0.9543080	-4.0056420	0.3062650
H	-1.9680260	0.8924480	1.2312620
F	5.0901550	1.6891950	0.3787820
F	5.3261610	-0.2526700	1.3365710
F	5.6939620	-0.0465170	-0.8012280
H	-2.3895060	0.2158170	-0.8063690
Cl	-1.9580920	-0.5586410	-2.9935230
H	-2.8147910	2.0092790	-2.5023940
C	-1.8410400	2.9932100	-0.8638980
C	-0.6785860	3.7114480	-0.5435760
C	-3.0125590	3.2529960	-0.1351290
C	-0.6817280	4.6549510	0.4884900
H	0.2330870	3.5407570	-1.1105550
C	-3.0199280	4.1959990	0.8960860
H	-3.9269210	2.7183010	-0.3806250
C	-1.8524550	4.8981170	1.2131800
H	0.2270990	5.2027360	0.7201450

H	-3.9367790	4.3856130	1.4467150
H	-1.8573700	5.6334180	2.0124100

H	-4.9786820	-1.4443730	1.6915200
H	-4.4453950	-4.7689110	-0.9905780
H	-5.9474310	-3.1367670	0.1415870

10.log
Potential Energy = -1949.24828
Zero-point Energy = -1948.78385
Free Energy = -1948.82750
Single-Point Energy B3LYP-D3(BJ)/6-311+G** PCM = -1949.74475
Free Energy B3LYP-D3(BJ)/6-311+G** PCM (extrapolated free energy from qRRHO) = -1949.32397
Nimag = 1 (-533.9049 cm^{-1})
Charge = 0 Multiplicity = 1

C	3.1105990	-0.5891380	-1.5764200
C	2.7654150	0.5519640	0.4332690
C	1.8510890	0.2519050	-1.7318080
H	3.2081330	1.5316230	0.1907390
H	1.0685650	-0.3165230	-2.2351290
C	-0.1719290	-0.6699280	0.0412660
H	-0.2702150	-0.2611160	1.0504640
O	-0.9765110	-0.2706630	-0.8637940
N	3.5296740	-0.4917140	-0.2777750
C	4.8716910	-0.9379430	0.0842810
H	4.8628760	-1.5075260	1.0139780
H	5.2222060	-1.5831640	-0.7214070
H	5.5569860	-0.0893320	0.1824370
O	3.6680490	-1.2123160	-2.4783790
C	0.2732070	-2.1292750	0.0491580
C	-0.5983710	-2.9795080	1.0136650
N	1.4601320	0.4828650	-0.3113630
C	-1.5114290	2.8287570	-0.3068340
C	-2.3983320	4.1040390	-0.2070370
O	-0.2932690	2.9341030	-0.1821090
H	0.9598380	1.3768130	-0.2222830
O	-2.2112050	1.7714220	-0.5165380
H	-1.5742250	0.7824280	-0.6540990
C	2.6998910	0.5178630	1.9902780
C	4.0708280	0.9658520	2.5595340
H	3.9677790	1.1392610	3.6350500
H	4.8542960	0.2183640	2.4270180
H	4.4084910	1.9024080	2.1028020
C	2.3334040	-0.8523000	2.5883890
H	2.4828780	-0.8241270	3.6723240
H	2.9519870	-1.6622170	2.1916370
C	1.6677230	1.5777290	2.4403850
H	1.6666220	1.6379900	3.5327380
H	1.9171260	2.5710430	2.0519490
H	0.6475580	1.3407670	2.1277560
C	2.1282840	1.5362320	-2.5289570
H	2.4625090	1.2662080	-3.5342340
H	1.2130440	2.1272610	-2.6151630
H	2.9024710	2.1550150	-2.0655210
H	1.2852660	-1.1081850	2.4251080
F	-3.2878190	3.9949990	0.8085400
F	-1.6677240	5.2123430	0.0088790
F	-3.1036250	4.2935450	-1.3472090
H	1.3058380	-2.2023560	0.3833770
Cl	0.2691760	-2.8510260	-1.6231840
H	-0.1841790	-3.9916060	0.9862640
H	-0.4090340	-2.5950440	2.0225660
C	-2.0920220	-3.0177510	0.7597090
C	-2.9518120	-2.1143220	1.4040930
C	-2.6522870	-3.9769510	-0.0984570
C	-4.3313490	-2.1522970	1.1819960
H	-2.5437270	-1.3789350	2.0931600
C	-4.0313360	-4.0183000	-0.3234290
H	-2.0066350	-4.6990220	-0.5893570
C	-4.8755280	-3.1031200	0.3132650

2.4. Ion Mobility-Mass Spectrometry with Aminals (2nd Generation MacMillan Catalyst)

Diastereomeric aminals were dissolved in acetonitrile to yield pure and 1:1 mixed solutions. Arrival time distributions (ATDs) and mass spectra of iminium ions were recorded on a home-built drift-tube ion mobility instrument which is described in detail elsewhere.[30,31] Briefly, iminium ions in the gas phase were generated by nanoelectrospray ionization followed by in-source fragmentation of intact aminal precursors. Subsequently, the ions are injected to the drift tube (161.2 cm) using helium at ca. 4.00 mbar as drift gas. Drift times were recorded at 14 different drift voltages from 2300 to 1000 V in 100 V steps. After transfer of the ions for mbar pressure to high vacuum, the ions are selected by their mass-to-charge ratio in a quadrupole mass filter. The ATDs are record using an electron multiplier detector which is on axis to the drift tube. For mass spectral analysis, the ions are pulsed off-axis to a Wiley-McLaren time-of-flight mass analyser. From the drift times, the instrument-independent collision cross sections (CCSs) can be derived using the Mason-Schamp equation.[32,33] Arrival time distributions (ATDs) of iminium ions generated from both diastereomeric aminals and their mixture are shown below.

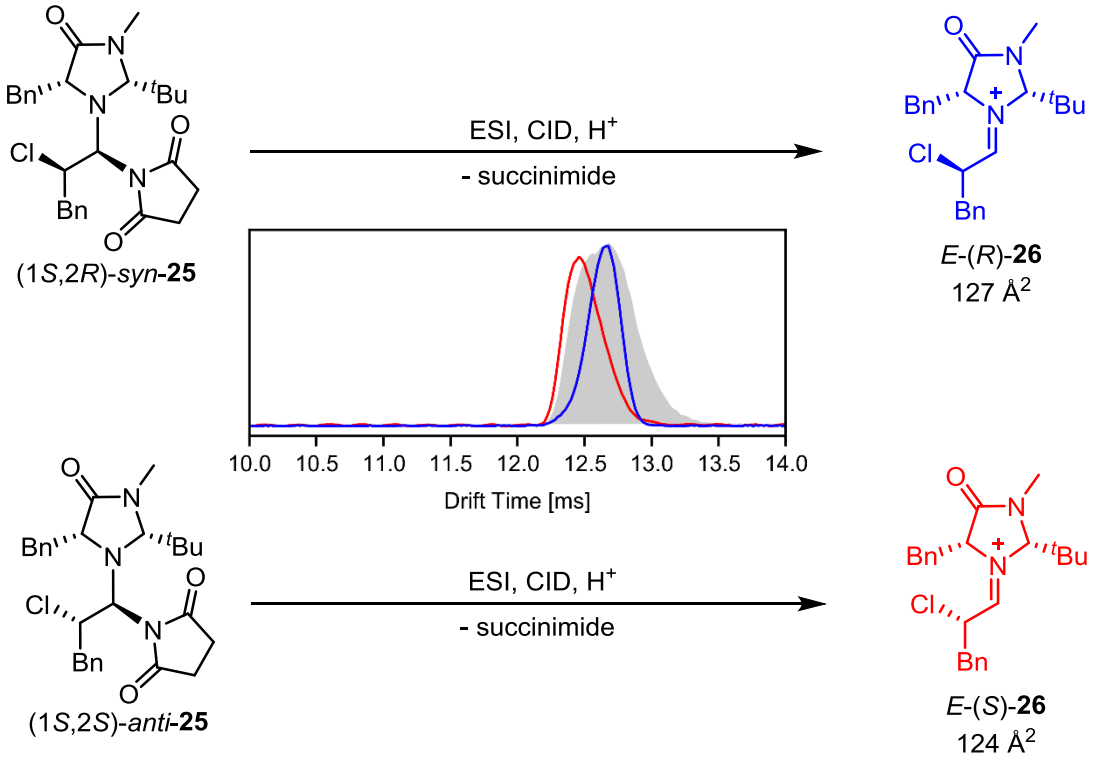

Figure SI-17. Ionization of aminals *syn*-**25** and *anti*-**25** and arrival time distributions of diastereomeric *E*-(*R*)- (blue trace) and *E*-(*S*)-iminium ions (red trace). The trace of the mixture of both diastereomers is depicted in light grey.

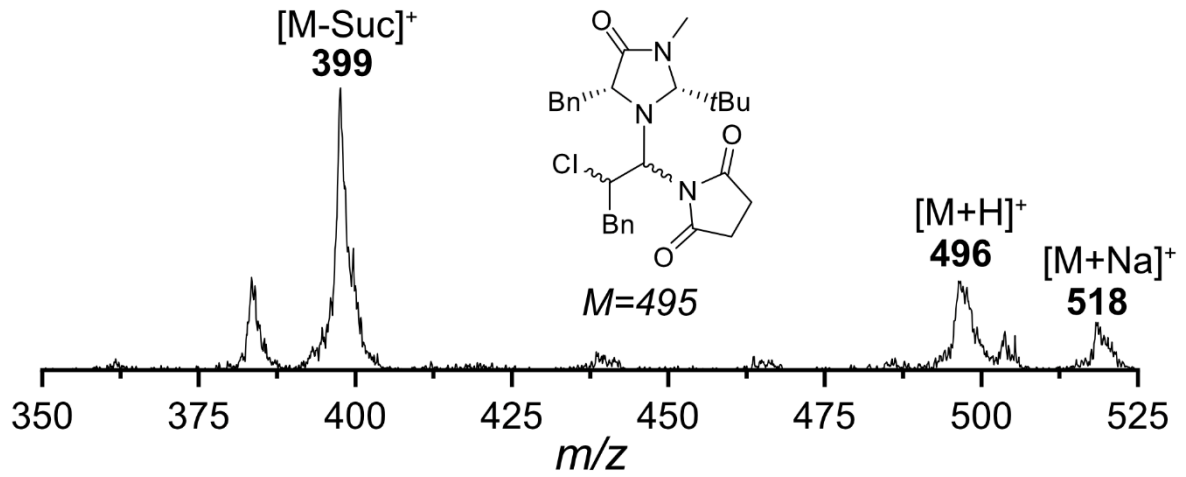

Figure SI-18. Mass spectra of iminium ions (*m/z* = 399) generated from aminal precursor ions $[M+H]^+$ (*m/z* = 496) and $[M+Na]^+$ (*m/z* = 518).

Computational Methods

For each iminium ion (*E*-(*R*), *E*-(*S*), *Z*-(*R*) and *Z*-(*S*)) the conformational space was sampled by using a genetic algorithm (GA) FAFOOM.[34] In this case, all rotatable bonds were sampled, generating a pool of starting structures, which are automatically optimized with FHI-aims[35] (version 171221) at the dispersion corrected density functional PBE+vdW^{TS} [36,37] level of theory using *light* basis set settings. For each type of isomers, ten GA runs were performed that yielded ca. 120 structures for each candidate. From that pool of structures, a certain number of distinct low-energy structures for each isomer were reoptimized, frequencies and Merz-Singh-Kollman[38] charges calculated at the hybrid-DFT level PBE0+D3/6-311+G(d,p)[39] using default settings in Gaussian 16, Revision A.03.[14] The reoptimized structures and computed Merz-Singh-Kollman were used as input to compute theoretical CCS values using the trajectory method using the software hpccs.[40] The calculation was carried out in helium as drift gas at 298.15 K. Default settings were used except for the number of points in velocity integration (60) and the number of points in Monte Carlo integrations of impact parameters and orientation (750). Computed energies plus zero-point vibrational energy, free energies at 298.15 K and computed CCSs are shown in Table SI-13. 3D-structures of each lowest-energy isomer are shown below and their xyz-coordinates can be found at the end of this chapter.

Table SI-13. List of conformations reoptimized at PBE0+D3/6-311+G(d,p) level of theory. Energies (ΔE, including zero-point-vibrational energy), free energies (ΔF) at 298.15 K and collision cross sections calculated with the trajectory method (CCS™) in He are assigned to each structure. The lowest-energy conformers for each isomer are labelled with an asterisk (*).

ID	ΔE(PBE0+D3) [kcal mol^{-1}]	ΔF(PBE0+D3) [kcal mol^{-1}]	CCS™ [Å^2]
trans_S/conf_00*	0.0	0.0	123
trans_S/conf_01	1.4	0.5	124
trans_S/conf_02	3.6	3.8	125
trans_S/conf_03	3.7	2.8	127
trans_S/conf_04	5.9	4.5	129
trans_S/conf_05	6.6	5.1	129
trans_R/conf_00*	2.4	1.8	128
trans_R/conf_01	2.4	2.1	125
trans_R/conf_02	4.4	5.3	123
trans_R/conf_03	5.3	4.4	131
trans_R/conf_04	5.5	5.1	127
cis_S/conf_00*	4.5	4.1	126
cis_S/conf_01	5.7	5.2	128
cis_S/conf_02	6.2	4.9	133
cis_S/conf_03	7.9	8.3	123
cis_S/conf_04	7.1	7.1	123
cis_R/conf_00*	1.4	0.8	123
cis_R/conf_01	5.0	4.2	124
cis_R/conf_02	6.0	6.0	123
cis_R/conf_03	7.9	6.6	133

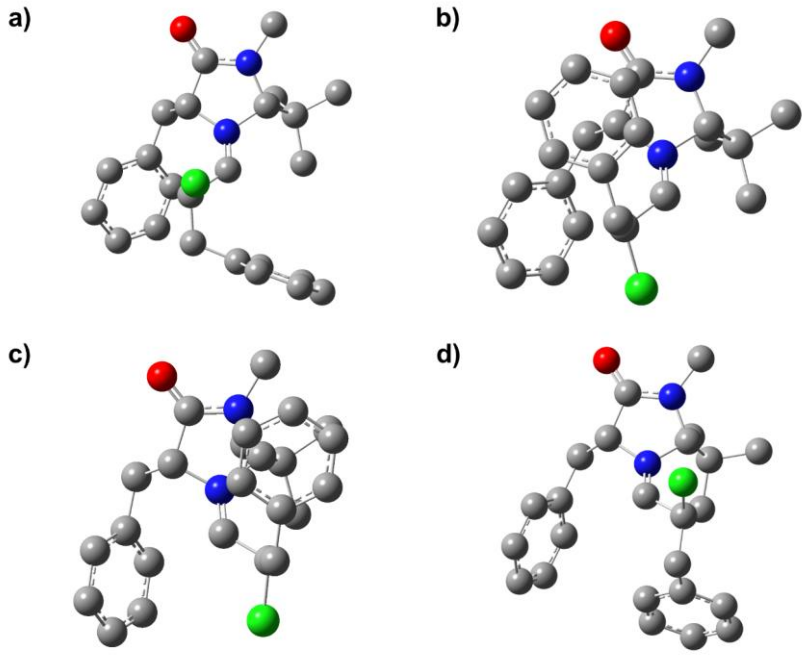

Figure SI-19. Computed lowest-energy structures for four distinct iminium ions: (a) *E*-(*R*), (b) *E*-(*S*), (c) *Z*-(*R*) and (d) *Z*-(*S*). Hydrogens are omitted for clarity.

Table SI-14. xyz-Coordinates of reoptimized structures

MacMillan_Catalyst/trans_R/conf_00

Charge=+1, Multiplicity=+1

C	1.84003	0.99505	0.73778
C	1.87689	-1.39314	0.16100
C	3.20941	0.38309	0.98485
C	0.57872	2.65319	-0.74446
H	1.49436	-2.20115	0.79753
N	1.02636	-0.19435	0.46042
N	3.15318	-0.93582	0.65539
O	4.16256	0.98874	1.40093
C	4.27626	-1.81150	0.92437
H	4.90108	-1.31845	1.66978
H	3.91977	-2.76549	1.31794
H	4.88011	-1.98828	0.03147
C	1.83570	-1.89411	-1.30880
C	2.49158	-3.28176	-1.33395
H	2.35714	-3.72038	-2.32549
H	3.56365	-3.24543	-1.14025
H	2.03039	-3.96123	-0.61011
C	0.38475	-2.05627	-1.76311
H	0.37340	-2.48931	-2.76622
H	-0.18391	-2.73604	-1.11920
H	-0.14883	-1.10394	-1.82123
C	2.57569	-0.96109	-2.26105
H	3.58578	-0.73216	-1.91160
H	2.66458	-1.43742	-3.24034
H	2.03820	-0.02259	-2.41211
C	-0.22548	-0.31614	0.71021
C	-1.10207	0.71089	1.32873
H	-0.65278	1.69874	1.36399
C	-2.50843	0.78235	0.73921
H	-2.44310	1.46510	-0.11296
H	-3.14719	1.26456	1.48379
C	-3.06516	-0.54151	0.29415
C	-3.00226	-0.89306	-1.05507
C	-3.60588	-1.45076	1.20434
C	-3.45602	-2.13359	-1.48830
H	-2.61068	-0.17809	-1.77407
C	-4.05726	-2.69272	0.77274
H	-3.68457	-1.18389	2.25304
C	-3.97868	-3.03872	-0.57213
H	-3.41420	-2.38775	-2.54213
H	-4.48313	-3.38799	1.48800
H	-4.34081	-4.00463	-0.90682
Cl	-1.08994	0.08438	3.03342
C	-0.14099	2.19010	-1.84663
C	-1.35629	2.77053	-2.19751
H	0.26865	1.39488	-2.46276
C	0.05139	3.70581	0.00806

C	-1.87497	3.81130	-1.43714
H	-1.89064	2.41892	-3.07390
C	-1.16902	4.27651	-0.33069
H	0.61337	4.09914	0.85154
H	-1.55961	5.10148	0.25517
H	-2.81795	4.27042	-1.71287
H	-0.67395	-1.29503	0.55978
C	1.90178	2.04431	-0.38138
H	2.59058	2.80653	-0.00499
H	2.37666	1.60581	-1.25992
H	1.48721	1.44767	1.66739

MacMillan_Catalyst/trans_S/conf_00

Charge=+1, Multiplicity=+1

C	0.41962	0.36877	-0.95798
C	2.26889	-0.46636	0.43457
C	1.75472	0.95658	-1.38065
C	-1.58113	-0.95126	-1.78399
H	2.54054	-0.09008	1.42983
N	0.78370	-0.30263	0.30796
N	2.72979	0.44849	-0.57849
O	1.89818	1.74227	-2.28135
C	4.07297	0.99252	-0.62465
H	4.00882	1.98443	-1.07374
H	4.47731	1.07097	0.38653
H	4.74258	0.38337	-1.23482
C	2.75948	-1.93583	0.33659
C	4.26519	-1.93514	0.63010
H	4.60753	-2.96758	0.73142
H	4.84539	-1.48000	-0.17267
H	4.50010	-1.41973	1.56710
C	2.07124	-2.78487	1.40757
H	2.49767	-3.79052	1.39031
H	2.23377	-2.38976	2.41690
H	0.99628	-2.89864	1.23752
C	2.50604	-2.53977	-1.03969
H	2.87715	-1.89740	-1.84304
H	3.02445	-3.49834	-1.11770
H	1.44427	-2.73809	-1.20398
C	0.03497	-0.48273	1.33093
C	-1.42521	-0.23976	1.45397
Cl	-2.05801	-1.67239	2.32485
C	-1.67126	1.05380	2.24405
H	-1.20116	0.98452	3.22939
H	-2.75031	1.13186	2.39888
C	-1.13248	2.21497	1.45425
C	0.16780	2.67500	1.66643
C	-1.88680	2.77205	0.42037
C	0.71763	3.64794	0.83910
H	0.75041	2.27996	2.49572
C	-1.34045	3.74922	-0.40351

H	-2.90621	2.43351	0.25816
C	-0.03189	4.17713	-0.20557
H	1.72786	4.00178	1.01519
H	-1.93580	4.17772	-1.20245
H	0.39883	4.92880	-0.85710
H	-1.92421	-0.20674	0.48701
C	-2.65040	-0.06158	-1.91293
C	-3.93919	-0.45584	-1.57791
H	-2.46984	0.94368	-2.28394
C	-1.83037	-2.24765	-1.33786
C	-4.17575	-1.74859	-1.11739
H	-4.76423	0.23956	-1.69048
C	-3.12159	-2.64579	-1.00697
H	-1.01228	-2.95798	-1.25564
H	-3.30273	-3.65772	-0.66190
H	-5.18254	-2.05794	-0.85962
H	0.53429	-0.81742	2.23759
C	-0.18458	-0.48871	-2.07474
H	-0.17113	0.17170	-2.94792
H	0.47112	-1.32801	-2.30641
H	-0.25628	1.19090	-0.71267

MacMillan_Catalyst/cis_R/conf_00

Charge=+1, Multiplicity=+1

C	-0.34914	-1.21055	-1.23991
C	1.11752	-0.83267	0.69123
C	0.93105	-2.01645	-1.34987
C	-2.82433	-1.11879	-0.96727
H	1.76623	0.03044	0.87372
N	-0.06297	-0.34109	-0.08195
N	1.72474	-1.69737	-0.29445
O	1.19576	-2.76155	-2.25902
C	3.10152	-2.14299	-0.24262
H	3.43423	-2.30245	-1.26897
H	3.71710	-1.37308	0.22477
H	3.20982	-3.08369	0.30241
C	0.77712	-1.51543	2.05075
C	2.10648	-1.73471	2.78532
H	1.89847	-2.06654	3.80540
H	2.72409	-2.50062	2.31632
H	2.68989	-0.81060	2.85272
C	-0.09652	-0.61756	2.92789
H	-0.35338	-1.16520	3.83791
H	0.42715	0.28720	3.25018
H	-1.04017	-0.33622	2.45209
C	0.07471	-2.85627	1.85754
H	0.59086	-3.49816	1.13934
H	0.04556	-3.38732	2.81195
H	-0.96092	-2.72838	1.53568
C	-0.63263	0.80074	0.03160
C	-0.23846	1.91779	0.92622

Cl	-1.73447	2.52456	1.68834
C	0.45283	2.99433	0.07400
H	-0.22503	3.33234	-0.71488
H	0.64435	3.84757	0.72992
C	1.72832	2.43297	-0.49593
C	2.88929	2.39682	0.27825
C	1.74938	1.86739	-1.77134
C	4.04439	1.79708	-0.21002
H	2.89522	2.85834	1.26239
C	2.90079	1.25969	-2.25898
H	0.86418	1.92465	-2.40077
C	4.04882	1.21951	-1.47571
H	4.94623	1.79319	0.39295
H	2.90654	0.83126	-3.25550
H	4.95200	0.75798	-1.85993
H	0.42086	1.59985	1.72827
C	-3.38150	-0.93287	0.29765
C	-3.31429	-0.36597	-2.03715
C	-4.40352	-0.00920	0.49455
H	-3.02461	-1.52475	1.13584
C	-4.87400	0.74421	-0.57268
H	-4.83216	0.11883	1.48248
C	-4.33170	0.55958	-1.84172
H	-2.90648	-0.51564	-3.03379
H	-5.67011	1.46473	-0.42179
H	-4.71125	1.12989	-2.68268
H	-1.43727	1.00664	-0.67398
C	-1.64331	-2.02644	-1.15713
H	-0.40159	-0.56442	-2.11959
H	-1.69932	-2.57349	-2.10282
H	-1.58009	-2.76935	-0.36249

MacMillan_Catalyst/cis_S/conf_00

Charge=+1, Multiplicity=+1

C	1.65003	1.56613	0.30206
C	2.05068	-0.80711	-0.09756
C	3.12435	1.28632	0.03486
C	-0.46934	2.75200	-0.42391
H	2.09183	-1.63748	0.61480
N	1.10968	0.20172	0.45798
N	3.28487	-0.06258	-0.04360
O	3.97689	2.13246	-0.03395
C	4.58765	-0.68646	-0.10740
H	5.32400	0.07464	0.15167
H	4.64246	-1.50711	0.61275
H	4.81662	-1.06621	-1.10607
C	1.66566	-1.36577	-1.51148
C	2.21408	-2.79569	-1.57549
H	2.00231	-3.23023	-2.55523
H	3.29639	-2.83265	-1.42703
H	1.74550	-3.43717	-0.82166

C	0.15098	-1.40508	-1.70647
H	-0.06810	-1.84675	-2.68126
H	-0.36403	-2.02089	-0.96558
H	-0.29958	-0.40930	-1.69125
C	2.28422	-0.53333	-2.63445
H	3.37386	-0.50438	-2.59051
H	2.00620	-0.97594	-3.59393
H	1.92347	0.49698	-2.64169
C	0.11389	-0.04810	1.22494
C	-0.27294	-1.37833	1.77425
H	0.10325	-2.21290	1.18635
C	-1.76381	-1.51922	2.03905
H	-1.90885	-2.40227	2.66538
H	-2.11789	-0.65394	2.60766
C	-2.49464	-1.66161	0.73224
C	-2.92618	-0.53673	0.03142
C	-2.68352	-2.92686	0.17552
C	-3.52849	-0.67704	-1.21363
H	-2.81286	0.45570	0.46037
C	-3.28785	-3.06649	-1.06687
H	-2.36762	-3.81008	0.72431
C	-3.70636	-1.93919	-1.76645
H	-3.87035	0.20274	-1.74667
H	-3.44123	-4.05519	-1.48542
H	-4.18490	-2.04696	-2.73370
Cl	0.67223	-1.36424	3.31884
C	-0.83474	3.30457	0.80724
C	-1.46090	2.52739	-1.37630
C	-2.16157	3.61141	1.08146
H	-0.07663	3.53330	1.55265
C	-3.14247	3.38945	0.11886
H	-2.42739	4.04767	2.03831
C	-2.78617	2.85855	-1.11368
H	-1.19158	2.11277	-2.34349
H	-4.17578	3.64511	0.32570
H	-3.54109	2.70762	-1.87794
H	-0.42278	0.81888	1.60795
C	0.96808	2.43933	-0.74439
H	1.58953	2.05194	1.27860
H	1.56995	3.35430	-0.78664
H	1.03645	1.97745	-1.73064

The combined approach (comparison of experimental and calculated CCSs) was successfully used to make a prediction whether *E*- or *Z*- iminium ions are formed in the decomposition process of the two diastereomeric aminals (1*S*,2*R*)-*syn*-**25** and (1*S*,2*S*)-*anti*-**25**. The ATD traces of the selectively dissociated aminals suggest that the dissociation of each aminal leads to the corresponding *E*-iminium ion. The comparison of the computed and the experimental CCS value suggests the *E*-iminium to be formed for both epimers.

3. CHLORINATIONS WITH THE JØRGENSEN-HAYASHI-TYPE CATALYST

3.1. Aminals Derived from Isovaleraldehyde

3.1.1. Synthesis and Derivatization

2-(1-((*S*)-2-(bis(3,5-bis(trifluoromethyl)phenyl)((trimethylsilyl)oxy)methyl)pyrrolidin-1-yl)-2-chloro-3-methylbutyl)isoindoline-1,3-dione (14)

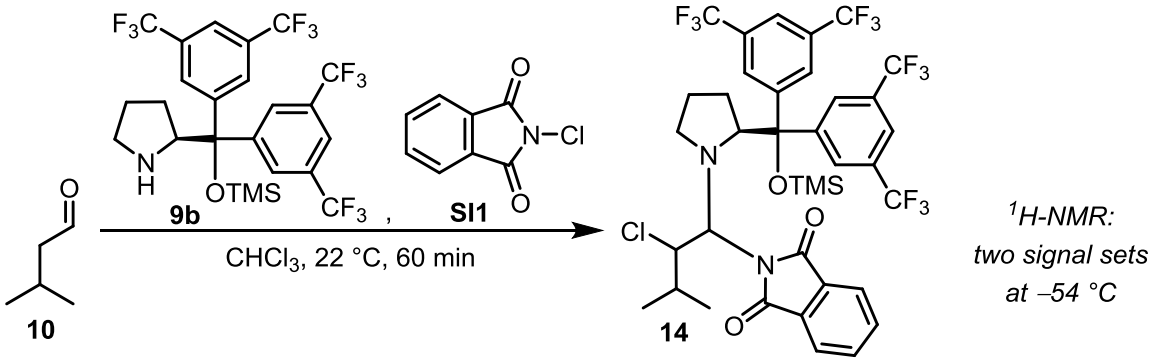

Catalysts **9b** (0.896 g, 1.50 mmol, 50 mol%) and NCP (0.272 g, 1.50 mmol, 0.5 equiv) were added successively to a solution of isovaleraldehyde (0.323 mL, 3.00 mmol, 1.0 equiv) in $CHCl_3$ (14 mL) at 22 °C. After 60 min the solvent and unreacted isovaleraldehyde were removed under reduced pressure. The crude product was dissolved in pentane (5 mL) and the precipitating solids were filtered off. Pentane was removed under reduced pressure and the product was obtained as a foamy off-white solid (1.04 g, 1.23 mmol, 82%). Attempts to further purify the product by column chromatography (Silica, Alox) resulted in decomposition. ^{1}H-NMR-spectra were recorded at 22 °C and –54 °C. Both spectra and the ratio of the two signal sets at –54 °C (80:20) are in accordance with the spectra from the literature.[28] (The aromatic signals were left out)

mp = 56 °C

IR (ATR): $\tilde{\nu}$ = 3017, 2970, 1738, 1366, 1278, 1217, 1135, 907, 842, 733 cm^{-1}.

HRMS (ESI, pos. mode): *m*/*z* calculated for $C_{37}H_{35}ClF_{12}N_2NaO_3Si$ $[M+Na]^+$: 869.1806, found 869.1766.

major species:

^{1}H-NMR ($CDCl_3$, 600 MHz, –54 °C) δ = 5.16 (d, *J* = 10.3 Hz, 1H), 4.99 (d, *J* = 10.5 Hz, 1H), 4.60 (dd, *J* = 7.3, 4.8 Hz, 1H), 3.29 (dt, *J* = 11.7, 7.9 Hz, 1H), 2.16 – 2.10 (m, 1H), 1.97 (dt, *J* = 11.3, 7.3 Hz, 1H), 1.73 – 1.68 (m, 2H), 1.19 (dq, *J* = 13.1, 6.6 Hz, 1H), 0.95 (d, *J* = 6.7 Hz, 3H), 0.14 – 0.05 (m, 1H), -0.07 (d, *J* = 6.5 Hz, 3H), -0.22 (s, 9H) ppm.

^{13}C-NMR ($CDCl_3$, 151 MHz, –54 °C) δ = 171.2, 170.3, 84.0, 76.1, 68.5, 65.4, 48.6, 29.1, 27.5, 24.0, 21.2, 12.0, 1.6 ppm.

minor species:

^{1}H-NMR ($CDCl_3$, 600 MHz, –54 °C) δ = 5.81 (d, *J* = 10.7 Hz, 1H), 5.05 (d, *J* = 10.8 Hz, 1H), 4.14 (dd, *J* = 9.9, 4.0 Hz, 1H), 3.27 – 3.22 (m, 1H), 2.39 – 2.32 (m, 1H), 2.19 – 2.16 (m, 1H), 1.87 – 1.80 (m, 2H), 1.42 – 1.35 (m, 1H), 1.28 (d, *J* = 6.6 Hz, 3H), 1.06 (d, *J* = 6.9 Hz, 3H), 0.62 (dp, *J* = 14.7, 7.5 Hz, 1H), -0.21 (s, 9H) ppm.

^{13}C-NMR ($CDCl_3$, 151 MHz, –54 °C) δ = 170.7, 170.8, 82.2, 75.9, 68.7, 66.5, 48.2, 29.2, 28.8, 23.9, 21.3, 15.5, 1.8 ppm.

The combination of aldehyde, Jørgensen-Hayashi-type catalyst **9b**, and NCP generates the corresponding aminal species almost quantitatively. The conversion of the aldehyde to the α-chloroaldehyde is always below 5%. The low conversion in combination with the high volatility of chloroaldehyde **12** and alcohol **SI5** makes the isolation and purification difficult. To overcome these problems, *in-situ* reduced chloroaldehyde **12** was directly converted into the non-volatile 3,5-dinitrobenzoylester **SI2**.

Enantiomeric Excess (Isovaleraldehyde, catalyst 9b and NCS)

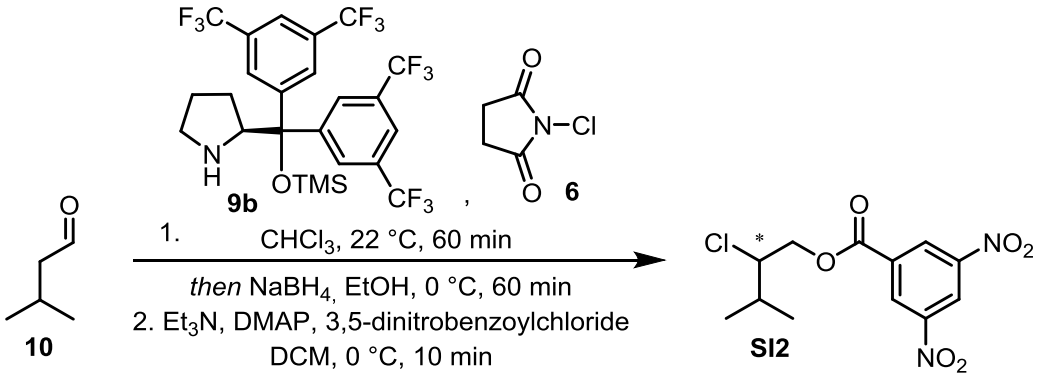

Isovaleraldehyde (0.215 mL, 2.00 mmol, 1.0 equiv) was dissolved in $CHCl_3$ (4.0 mL) at 22 °C. Catalyst **9b** (0.120 g, 0.200 mmol, 10 mol%) and NCS (0.293 g, 2.20 mmol, 1.1 equiv) were added subsequently and the reaction mixture was stirred for 60 min at the same temperature. After the reaction was cooled to 0 °C, MeOH (1.3 mL) and $NaBH_4$ (0.189 g, 5.00 mmol, 2.5 equiv) were added and the mixture was stirred for 60 min at the same temperature. The reaction was quenched with aqueous saturated NH_4Cl (5 mL), the aqueous phase was extracted with dichloromethane (3x5 mL) and the combined organic phases were dried over $NaSO_4$. The solvent was removed under reduced pressure (product is volatile!) and the crude product was redissolved in dichloromethane (4 mL). The solution was cooled to 0 °C and DMAP (12.2 mg, 0.100 mmol, 0.05 equiv) and 3,5-dinitrobenzoylchloride (0.300 g, 1.30 mmol, 0.7 equiv) were added subsequently. Et_3N (0.236 mL, 1.70 mmol, 0.9 equiv) was added dropwise and the reaction mixture was stirred for 10 min at 0 °C. The reaction was quenched with aqueous saturated $NaHCO_3$ (5 mL), the aqueous phase was extracted with dichloromethane (3x5 mL) and the combined organic phases were dried over $NaSO_4$. The solvent was removed under reduced pressure and the crude product was purified by column chromatography (Silica, pentane/EtOAc 10:1). Ester **SI2** (0.013 g, 41.0 µmol, 2%, 49% ee for the (*S*)-enantiomer) was obtained as a colorless solid.

^{1}H-NMR ($CDCl_3$, 600 MHz) δ = 9.24 (t, *J* = 2.2 Hz, 1H), 9.16 (d, *J* = 2.1 Hz, 2H), 4.66 (dd, *J* = 11.7, 4.7 Hz, 1H), 4.61 (dd, *J* = 11.7, 7.9 Hz, 1H), 4.18 (dt, *J* = 7.9, 4.6 Hz, 1H), 2.17 (heptd, *J* = 6.8, 4.7 Hz, 1H), 1.13 (d, *J* = 6.8 Hz, 3H), 1.09 (d, *J* = 6.7 Hz, 3H) ppm.

^{13}C-NMR ($CDCl_3$, 151 MHz) δ = 162.3, 148.9, 133.5, 129.7, 122.8, 68.5, 65.0, 31.7, 20.0, 17.5 ppm.

(*S*)-2-chloro-3-methylbutyl-3,5-dinitrobenzoate ((*S*)-SI2)

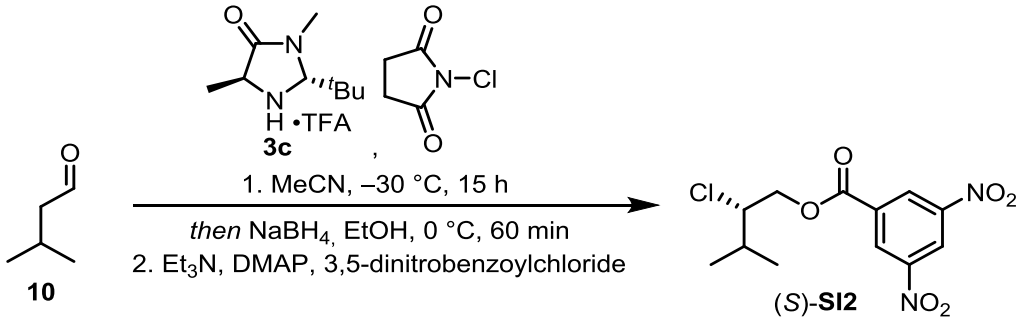

Isovaleraldehyde (0.108 mL, 1.00 mmol, 1.0 equiv) was dissolved in MeCN (4.0 mL) and cooled to –30 °C. Catalyst **3c** (56.9 mg, 0.200 mmol, 20 mol%) and NCS (0.147 g, 1.10 mmol, 1.1 equiv) were added subsequently and the reaction mixture was stirred for 15 h at the same temperature. After the reaction was warmed to 0 °C, MeOH (1.3 mL) and $NaBH_4$ (94.6 mg, 2.50 mmol, 2.5 equiv) were added and the mixture was stirred for 60 min at the same temperature. The reaction was quenched with aqueous saturated NH_4Cl (10 mL), the aqueous phase was extracted with dichloromethane (3x10 mL) and the combined organic phases were dried over $NaSO_4$. The solvent was removed under reduced pressure (product is volatile!) and the crude product was redissolved in dichloromethane (4 mL). The solution was cooled to 0 °C and DMAP (12.2 mg, 0.100 mmol, 0.1 equiv) and 3,5-dinitrobenzoylchloride (0.300 g, 1.30 mmol, 1.3 equiv) were added subsequently. Et_3N (0.237 mL, 1.70 mmol, 1.7 equiv) was added dropwise and the reaction mixture was stirred for 10 min at 0 °C. The reaction was quenched with aqueous saturated $NaHCO_3$ (10 mL), the aqueous phase was extracted with dichloromethane (3x10 mL) and the combined organic phases were dried over $NaSO_4$. The solvent was removed under reduced pressure and the crude product was purified by column chromatography (Silica, pentane/EtOAc 10:1). Ester (*S*)-**SI2** (0.108 g, 0.341 mmol, 34%, 96% ee) was obtained as colorless solid.

The ^{1}H-NMR spectrum is in accordance with the previous experiment.

(*R*)-2-chloro-3-methylbutyl-3,5-dinitrobenzoate ((*R*)-SI2)

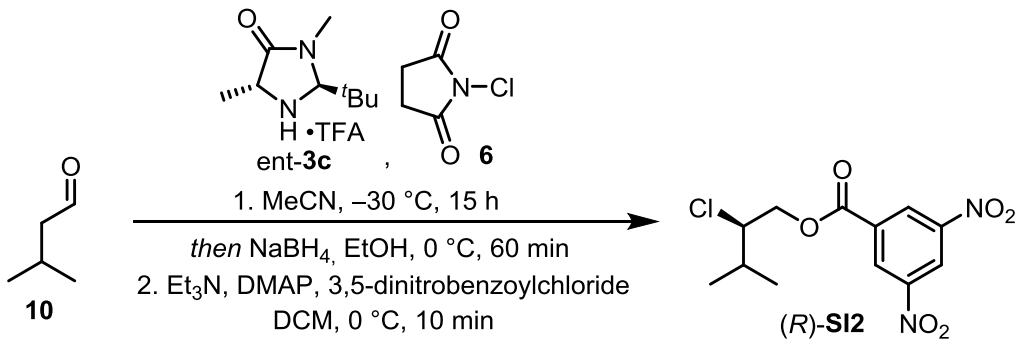

Isovaleraldehyde (0.108 mL, 1.00 mmol, 1.0 equiv) was dissolved in MeCN (4.0 mL) and cooled to –30 °C. Catalyst *ent*-**3c** (56.9 mg, 0.200 mmol, 20 mol%) and NCS (0.147 g, 1.10 mmol, 1.1 equiv) were added subsequently and the reaction mixture was stirred for 15 h at the same temperature. After the reaction was warmed to 0 °C, MeOH (1.3 mL) and $NaBH_4$ (94.6 mg, 2.50 mmol, 2.5 equiv) were added and the mixture was stirred for 60 min at the same temperature. The reaction was quenched with aqueous saturated NH_4Cl (10 mL), the aqueous phase was extracted with dichloromethane (3x10 mL) and the combined organic phases were dried over $NaSO_4$. The solvent was removed under reduced pressure (product is volatile!) and the crude product was redissolved in dichloromethane (4 mL). The solution was cooled to 0 °C and DMAP (12.2 mg, 0.100 mmol, 0.1 equiv) and 3,5-dinitrobenzoylchloride (0.300 g, 1.30 mmol, 1.3 equiv) were added subsequently. Et_3N (0.237 mL, 1.70 mmol, 1.7 equiv) was added dropwise and the reaction mixture was stirred for 10 min at 0 °C. The reaction was quenched with aqueous saturated $NaHCO_3$ (10 mL), the aqueous phase was extracted with dichloromethane (3x10 mL) and the combined organic phases were dried over $NaSO_4$. The solvent was removed under reduced pressure and the crude product was purified by column chromatography (Silica, pentane/EtOAc 10:1). Ester (*R*)**-SI2** (97.0 mg, 0.306 mmol, 31%, 95% ee) was obtained as colorless solid.

Spectroscopic data are in accordance with the previous experiment.

In contrast to most of the aminals derived from the MacMillan-type catalysts, all attempts to purify or crystallize aminal **14** failed and led to decomposition. The reduction of *N*-alkylphthalimides to amides is literature known[22,41] and was anticipated to increase the stability of aminal **14** and enabled subsequent purification and crystallization.

***N*-((1*S*,2*S*)-1-((*S*)-2-(bis(3,5-bis(trifluoromethyl)phenyl)((trimethylsilyl)oxy)methyl)pyrrolidin-1-yl)-2-chloro-3-methylbutyl)-2-(hydroxymethyl)benzamide (SI3),**
2-((1*R*,2*S*)-1-((*S*)-2-(bis(3,5-bis(trifluoromethyl)phenyl)((trimethylsilyl)oxy)methyl)pyrrolidin-1-yl)-2-chloro-3-methylbutyl)-3-hydroxyisoindolin-1-one (SI4)

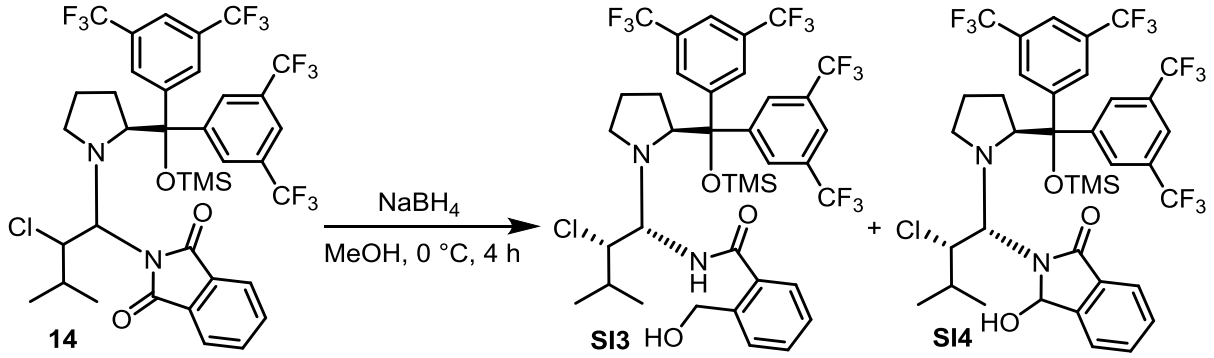

one signal set
at –60 °C and 22 °C

$NaBH_4$ (67.0 mg, 1.77 mmol, 3.0 equiv) was added to a solution of aminal **14** (0.500 g, 0.590 mmol, 1.0 equiv) in dry MeOH (7.0 mL) at 0 °C. After 4 h at 0 °C the reaction was quenched by the addition of aqueous saturated $NaHCO_3$ (5 mL). The aqueous phase was extracted with dichloromethane (3x5 mL), the combined organic phases were dried over Na_2SO_4 and the solvent was removed under reduced pressure. After purification by column chromatography (SiO_2, pentane/EtOAc 20:1 to 5:1) amide **SI3** (0.122 g, 0.143 mmol, 24%) was obtained as an off-white foamy solid. The absolute configuration was determined by x-ray crystal structure analysis of the 3,5-dinitrobenzoyl-derivative. Hemiaminal **SI4** (94.0 mg, 0.111 mmol, 19%) was obtained as a pale yellow oil. The substance appears as a defined spot on the TLC. ^{1}H-NMR of the hemiaminal **SI4** shows extremely broadened signals for every hydrogen atom. A tentative structure proposal is based on the molecular mass and was supported by a further reduction process.

Amide SI3:

mp = 76 °C

$[\alpha]_D^{26}$ = –99.8° (*c* = 3.00, dichloromethane)

^{1}H-NMR ($CDCl_3$, 400 MHz) δ = 8.31 (s, 2H), 8.06 (s, 2H), 7.94 (s, 2H), 7.62 (dd, *J* = 7.6, 1.6 Hz, 1H), 7.54 – 7.38 (m, 3H), 7.03 (d, *J* = 8.9 Hz, 1H), 5.29 (s, 1H), 4.95 – 4.86 (m, 1H), 4.72 (dd, *J* = 12.1, 5.9 Hz, 1H), 4.63 (dd, *J* = 12.2, 6.2 Hz, 1H), 4.24 (t, *J* = 6.1 Hz, 1H), 3.76 (d, *J* = 7.4 Hz, 1H), 2.61 (dd, *J* =

9.8, 7.8 Hz, 1H), 2.31 (t, *J* = 8.6 Hz, 1H), 2.09 – 1.98 (m, 1H), 1.86 – 1.73 (m, 2H), 1.35 (s, 1H), 0.91 (d, *J* = 6.6 Hz, 3H), 0.30 (s, 3H), 0.07 – -0.10 (m, 1H), -0.12 (s, 9H) ppm.

^{13}C-NMR ($CDCl_3$, 176 MHz) δ = 171.3, 145.6, 144.4, 140.4, 135.6, 132.5 – 131.9 (m), 131.9, 131.3, 131.2 – 130.7 (m), 130.5, 129.5, 128.5, 127.9, 123.4 (2xq, *J* = 273.0, 47.6 Hz), 122.3, 121.7, 83.1, 71.6, 70.5, 68.9, 64.9, 47.2, 31.2, 28.1, 24.2, 20.5, 14.4, 1.7 ppm.

IR (ATR): $\tilde{\nu}$ = 3276, 2968, 2924, 1734, 1636, 1541, 1372, 1278, 1173, 1136, 910, 844, 712 cm^{-1}.

HRMS (ESI, pos. mode): *m*/*z* calculated for $C_{37}H_{40}ClF_{12}N_2O_3Si$ $[M+H]^+$: 851.2300, found 851,2320; *m*/*z* calculated for $C_{37}H_{39}ClF_{12}N_2NaO_3Si$ $[M+Na]^+$: 873.2119, found 873.2157; *m*/*z* calculated for $C_{37}H_{39}ClF_{12}KN_2O_3Si$ $[M+K]^+$: 889.1859, found 889.1889.

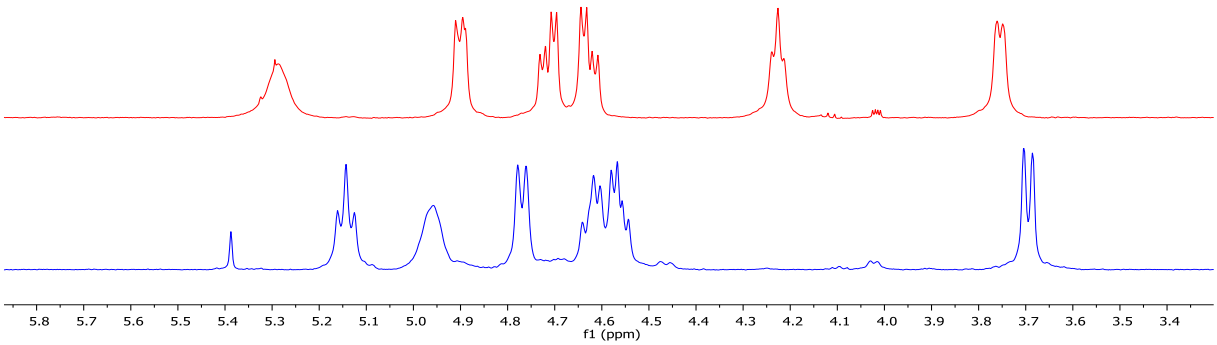

Figure SI-20. ^{1}H-NMR spectra of amide **SI3** at 23 °C (red spectrum) and –60 °C (blue spectrum). We noted the absence of a second set of signals at –60 °C.

Hemiaminal SI4:

HRMS (ESI, pos. mode): *m*/*z* calculated for $C_{37}H_{37}ClF_{12}N_2NaO_3Si$ $[M+Na]^+$: 871.1962, found 871.2005; *m*/*z* calculated for $C_{37}H_{37}ClF_{12}KN_2O_3Si$ $[M+K]^+$: 887.1702, found 887.1733.

***N*-((1*S*,2*S*)-1-((*S*)-2-(bis(3,5-bis(trifluoromethyl)phenyl)((trimethylsilyl)oxy)methyl)pyrrolidin-1-yl)-2-chloro-3-methylbutyl)-2-(hydroxymethyl)benzamide (SI3) (reduction of SI4)**

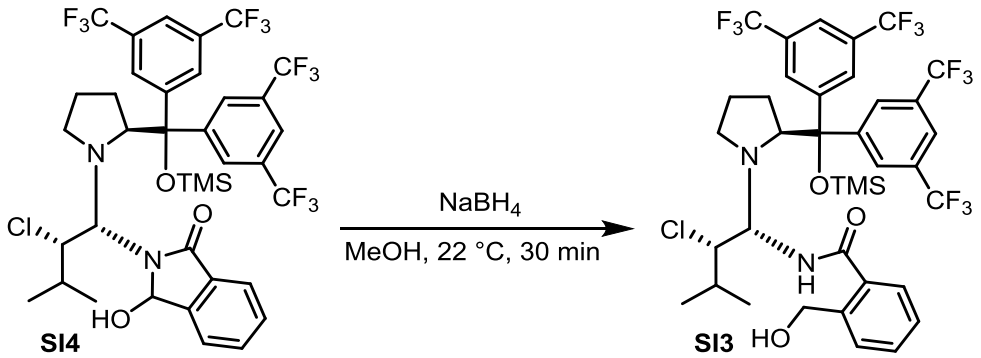

$NaBH_4$ (13.4 mg, 0.353 mmol, 5.0 equiv) was added to a solution of hemiaminal **SI4** (60 mg, 70.7 µmol, 1.0 equiv) in dry MeOH (0.8 mL) at 22 °C. After 30 min the reaction was quenched by the addition of aqueous saturated $NaHCO_3$ (1 mL). The aqueous phase was extracted with dichloromethane (3x1 mL), the combined organic phases were dried over Na_2SO_4 and the solvent was removed under reduced pressure. After purification by column chromatography (SiO_2, pentane/EtOAc 10:1 to 5:1) amide **SI3** (36.0 mg, 42.3 µmol, 60%) was obtained as an off-white foamy solid.

The spectroscopic data are in accordance with the previously isolated amide **SI3**.

After the reduction of aminal **14** isolation and purification without notable decomposition was possible. Unfortunately, all attempts to isolate single crystals for X-ray crystal structure analysis failed. The esterification of the primary alcohol in amide **SI3** with 3,5-dinitrobenzoyl chloride was anticipated to positively impact the crystallization behavior.

2-(((1*S*,2*S*)-1-((*S*)-2-(bis(3,5-bis(trifluoromethyl)phenyl)((trimethylsilyl)oxy)methyl)pyrrolidin-1-yl)-2-chloro-3-methylbutyl)carbamoyl)benzyl 3,5-dinitrobenzoate (15)

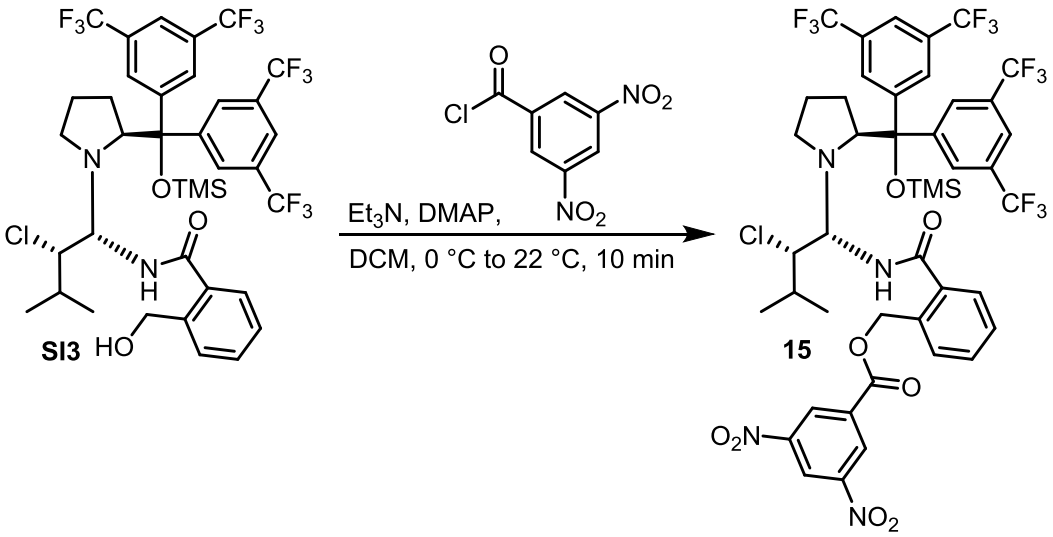

3,5-Dinitrobenzoylchlorid (16.5 mg, 71.5 µmol, 1.3 equiv) and DMAP (1.00 mg, 8.25 µmol, 0.15 equiv) were added to an ice-cold solution of alcohol **SI3** (46.8 mg, 55.0 µmol, 1.0 equiv) in dichloromethane (0.30 mL). Et_3N (13.0 µL, 93.5 µmol, 1.7 equiv) was added slowly and the solution was warmed to 22 °C over 10 min. The reaction was quenched with aqueous saturated $NaHCO_3$ (0.5 mL), the aqueous phase was extracted with dichloromethane (3x0.5 mL) and the combined organic phases were dried over Na_2SO_4. The solvent was removed under reduced pressure and the crude product was purified by column chromatography (SiO_2, pentane/EtOAc 6:1). Ester **15** (39.0 mg, 37.3 µmol, 68%) was obtained as an off-white foamy solid. The absolute configuration was determined by X-ray crystal structure analysis.

mp = 151 °C

$[\alpha]_D^{26}$ = –53.9° (*c* = 2.00, dichloromethane)

^{1}H-NMR ($CDCl_3$, 700 MHz) δ = 9.22 (t, *J* = 2.1 Hz, 1H), 9.17 (d, *J* = 2.2 Hz, 2H), 8.30 (s, 2H), 8.07 (s, 2H), 7.93 (d, *J* = 6.8 Hz, 2H), 7.61 (ddd, *J* = 7.7, 6.4, 1.3 Hz, 2H), 7.53 (td, *J* = 7.6, 1.4 Hz, 1H), 7.47 (td, *J* = 7.5, 1.3 Hz, 1H), 6.94 (d, *J* = 9.0 Hz, 1H), 5.85 (d, *J* = 12.8 Hz, 1H), 5.75 (d, *J* = 13.1 Hz, 1H), 5.33 (s, 1H), 4.98 (d, *J* = 9.4 Hz, 1H), 3.79 (s, 1H), 2.67 (td, *J* = 9.6, 7.3 Hz, 1H), 2.33 (ddd, *J* = 9.9, 7.9, 2.7 Hz, 1H), 2.08 (s, 1H), 1.93 – 1.86 (m, 1H), 1.85 – 1.79 (m, 1H), 1.40 (dddd, *J* = 12.5, 10.1, 7.0, 2.7 Hz, 1H), 0.91 (d, *J* = 6.6 Hz, 3H), 0.32 (s, 3H), 0.02 (s, 1H), -0.12 (s, 9H) ppm.

^{13}C-NMR ($CDCl_3$, 176 MHz) δ = 169.9, 162.8, 148.8, 145.6, 144.5, 136.1, 133.9, 133.7, 132.0 (q, *J* = 33.5, 33.0 Hz), 131.2, 131.1 – 130.7 (m), 130.6, 130.2, 129.7, 129.6, 129.3, 127.5, 123.4 (qd, *J* = 273.0, 40.2 Hz), 122.7, 122.2, 121.7, 83.2, 71.7, 70.8, 68.8, 66.2, 47.1, 31.0, 28.2, 24.2, 20.7, 1.7 ppm.

IR (ATR): $\tilde{\nu}$ = 3353, 3106, 2964, 1736, 1666, 1629, 1548, 1463, 1371, 1345, 1276, 1171, 1133, 910, 843, 722 cm^{-1}.

HRMS (ESI, pos. mode): *m*/*z* calculated for $C_{44}H_{41}ClF_{12}N_4NaO_8Si$ $[M+Na]^+$: 1067.2083, found 1067.2087; *m*/*z* calculated for $C_{44}H_{41}ClF_{12}KN_4O_8Si$ $[M+K]^+$: 1083.1823, found 1083.1816.

To avoid the oversight and potential loss of possible additional stereoisomers during the numerous purifications, an optimized synthesis protocol with a subsequent thorough isolation and purification process was developed.

2-(((1*S*,2*S*)-1-((*S*)-2-(bis(3,5-bis(trifluoromethyl)phenyl)((trimethylsilyl)oxy)methyl)pyrrolidin-1-yl)-2-chloro-3-methylbutyl)carbamoyl)benzyl 3,5-dinitrobenzoate (15) (optimized procedure)

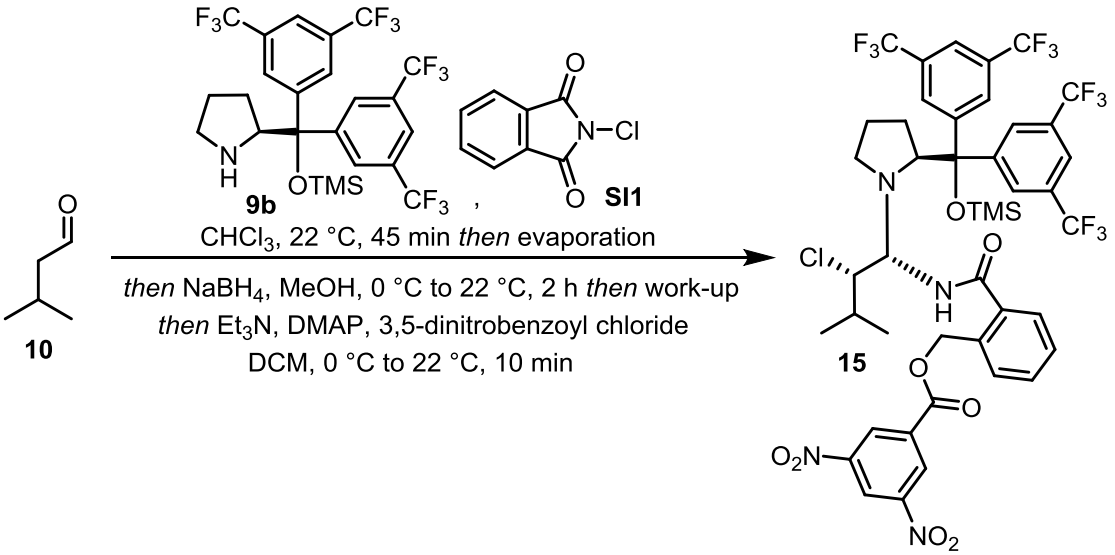

Catalyst **9b** (2.39 g, 4.00 mmol, 50 mol%) and NCP (0.726 g, 4.00 mmol, 0.5 equiv) were added successively to a solution of isovaleraldehyde (0.861 mL, 8.00 mmol, 1.0 equiv) in $CHCl_3$ (36 mL) at 22 °C. After 45 min the solvent and unreacted isovaleraldehyde were removed under reduced pressure. The crude product was dissolved in dry MeOH (40 mL) and cooled to 0 °C. $NaBH_4$ (1.34 g, 35.4 mmol, 10.0 equiv) was added in portions and the reaction was stirred for 2 h at 22 °C. The reaction was quenched with aqueous saturated $NaHCO_3$ (20 mL), the aqueous phase was extracted with dichloromethane (3x20 **mL**) and the combined organic phases were dried over Na_2SO_4. The solvent was removed under reduced pressure and the crude product was dissolved again in dichloromethane (14 mL). The reaction mixture was cooled to 0 °C and 3,5-dinitrobenzoyl chloride (1.02 g, 4.41 mmol, 1.3 equiv) and DMAP (41.5 mg, 0.340 mmol, 10 mol%) were added successively. Et_3N (0.804 mL, 5.77 mmol, 1.7 equiv) was added dropwise and the reaction mixture was stirred for 10 min at 22 °C. The reaction was quenched with aqueous saturated $NaHCO_3$ (15 mL), the aqueous phase was extracted with dichloromethane (3x20 mL) and the combined organic phases were dried over Na_2SO_4. The solvent was removed under reduced pressure and the crude product was purified by column chromatography (SiO_2, pentane/EtOAc 10:1 to 0:1). Ester **15** (1.96 g, 1.87 mmol, 47% over 3 steps, single diastereomer) was obtained as an off-white foamy solid. The spectroscopic data are in accordance with the previously isolated ester **15**.

After a thorough analysis of all fractions from the column chromatographic, only a single diastereomer could be detected and isolated. This of course does not exclude the presence of additional, labile diastereomers, but it is the best we could do.

***N*-((1*S*,2*S*)-1-((*S*)-2-(bis(3,5-bis(trifluoromethyl)phenyl)((trimethylsilyl)oxy)methyl)pyrrolidin-1-yl)-2-chloro-3-methylbutyl)-2-(hydroxymethyl)benzamide (SI3) (ester hydrolysis)**

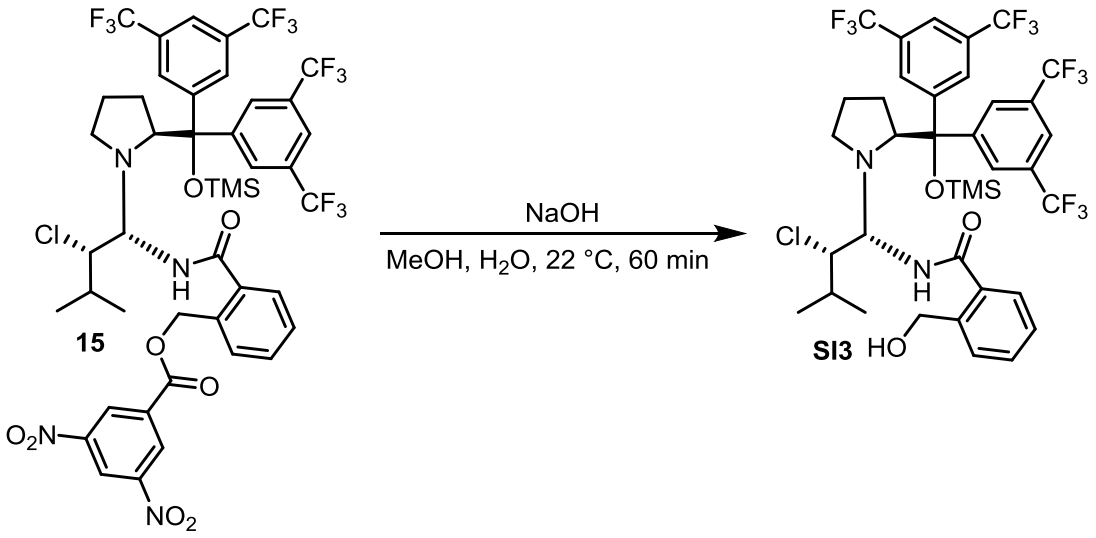

Three drops of aqueous NaOH (1 M) were added to a solution of ester **15** (0.140 g, 0.134 mmol, 1.0 equiv) in MeOH (0.5 mL) at 22 °C and the reaction was stirred for 60 min at the same temperature. H_2O (1 mL) was added, the aqueous phase was extracted with dichloromethane (3x1 mL), the combined organic phases were dried over Na_2SO_4 and the solvent was removed under reduced pressure. After column chromatography (SiO_2, pentane/EtOAc 10:1 to 5:1) pure alcohol **SI3** (62.0 mg, 72.8 µmol, 54%) was obtained as an off-white foamy solid.

The spectroscopic data are in accordance with the previously synthesized alcohol **SI3**.

3.1.2. Structural Analysis

NOE and *J*-Coupling Analysis of Aminal 14

To extend the characterization data above, a full assignment of all NMR resonances of the aminal **14** was attempted in $CDCl_3$ at 219 K (see Table SI-15). At this temperature there is still severe overlap of the two species in the NMR spectra, particularly in the aromatic region, where most of the signals are additionally split by the ^{19}F *J*-couplings (see Figures SI-21 to SI-22). Subsequently, aminal **14** was dissolved in CD_2Cl_2, showing almost the exact same chemical shifts and coupling patterns (see Table SI-16), indicating that no major structural change is observed in this solvent. The solvent change however allows to further cool down to 190 K, at which most resonances for the major species could be assigned. For the minor species, however, some aromatic signals (particularly quaternary carbons) remain unassigned as they could not be resolved.

Table SI-15. Assignment of aminal **14** in $CDCl_3$ at 219 K, shifts relative to $CHCl_3$ at 7.26 ppm.

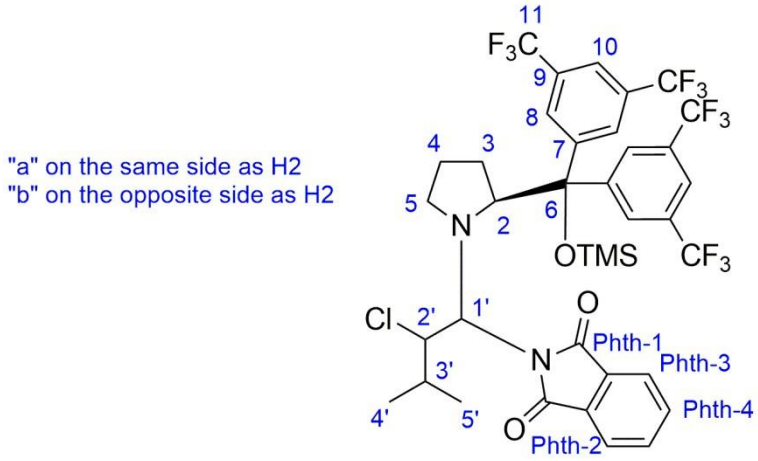

	Major (80%)		Minor (20%)	
Position	$\delta\ ^{13}C\ (ppm)$	$\delta\ ^{1}H\ (ppm)$	$\delta\ ^{13}C\ (ppm)$	$\delta\ ^{1}H\ (ppm)$
2	68.6	4.60	68.6	4.15
3a	27.7	1.71[1]	29.0	1.82
3b	27.7	1.71[1]	29.0	1.38
4a	24.3	1.20	24.1	1.28
4b	24.3	0.09	24.1	0.63
5a	48.8	3.29	48.5	3.27
5b	48.8	1.97	48.5	2.16
6	82.4		84.2	
OTMS	1.7	-0.16	1.9	-0.15
1'	76.3	5.16	76.1	5.81
2'	65.6	4.98	66.8	5.05
3'	29.3	2.13	29.0	2.35
4'	21.3	0.95	21.4	1.06
5'	12.2	-0.01	15.7	1.28
Phth-1[2]	170.5/171.4		170.8/170.9	

[1] diastereotopic protons strongly coupled
[2] hindered rotation around C1'-N-bond, no assignment Pth-1 vs Pth-1' etc.

Table SI-16. Assignment of aminal **14** in CD_2Cl_2 at 190 K, shifts relative to $CHDCl_2$ @ 5.35 ppm.

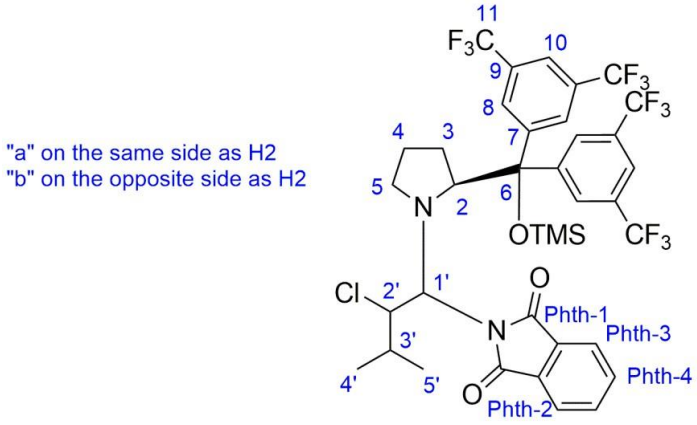

	Major (78%)			Minor (22%)		
Position	$\delta\ ^{13}C\ (ppm)$	$\delta\ ^{1}H\ (ppm)$	$J\ (Hz)$	$\delta\ ^{13}C\ (ppm)$	$\delta\ ^{1}H\ (ppm)$	$J\ (Hz)$
2	68.3	4.56	$^{3}J_{2,3a/b}$ = 7.6, 4.7	67.5	4.13	$^{3}J_{2,3a/b}$ = 9.8, 2.4
3a	27.5	1.68[1]	[1]	28.7	1.82	?
3b	27.5	1.68[1]	[1]	28.7	1.38	?
4a	24.1	1.15	$^{3}J_{4a,5a}$ = 8.0	23.6	1.24	$^{2}J_{4a,4b}$ = 11.8
4b	24.1	0.05	$^{3}J_{4b,5a}$ = 6.7	23.6	0.36	$^{2}J_{4a,4b}$ = 11.8, $^{3}J_{4b,5a}$ = 9.3, $^{3}J_{4b,5b}$ = 6.7
5a	48.8	3.24	$^{2}J_{5a,5b}$ = 11.1, $^{3}J_{4b,5a}$ = 6.7, $^{3}J_{4a,5a}$ = 8.0	48.2	3.12	$^{2}J_{5a,5b}$ = 9.8, $^{3}J_{4b,5a}$ = 9.3
5b	48.8	1.94	$^{2}J_{5a,5b}$ = 11.1	48.2	2.29	$^{2}J_{5a,5b}$ = 9.8, $^{3}J_{4b,5b}$ = 6.7
6	82.2			84.3		
7A[2]	145.6			145.5		
7B[2]	143.9			?		
8A[2]	130.4/131.4	9.37/7.36		?	?	
8B[2]	128.5/130.0	8.20/7.68		129.2/132.1	8.02/7.49	
10A[2]	122.7	8.02		?	?	
10B[2]	122.1	7.98		?	?	
11A[2]	123.9/124.4			?		
11B[2]	124.4/124.6			?		
OTMS	1.3	-0.24		1.7	-0.21	
1'	75.9	5.15	$^{3}J_{1',2'}$ = 10.3	75.4	5.81	$^{3}J_{1',2'}$ = 10.9
2'	65.8	5.02	$^{3}J_{1',2'}$ = 10.3, $^{3}J_{2',3'}$ < 1.0	67.0	5.07	$^{3}J_{1',2'}$ = 10.9, $^{3}J_{2',3'}$ < 1.0
3'	29.3	2.14	$^{3}J_{2',3'}$ < 1.0	29.3	2.38	$^{3}J_{2',3'}$ < 1.0
4'	21.2	0.93		21.3	1.03	
5'	12.0	-0.08		15.7	1.27	
Phth-1[3]	170.2/171.7			170.9/171.0		
Phth-2[3]	131.5/?			?		

[1] diastereotopic protons strongly coupled
[2] hindered rotation around C2-C6-bond, no assignment of diastereotopic aromatic rings A vs B, NOE contacts hint at ring B being atop the pyrrolidine
[3] hindered rotation around C1'-N-bond, no assignment Pth-1 vs Pth-1' etc.
[?] obfuscated by overlap / not determined

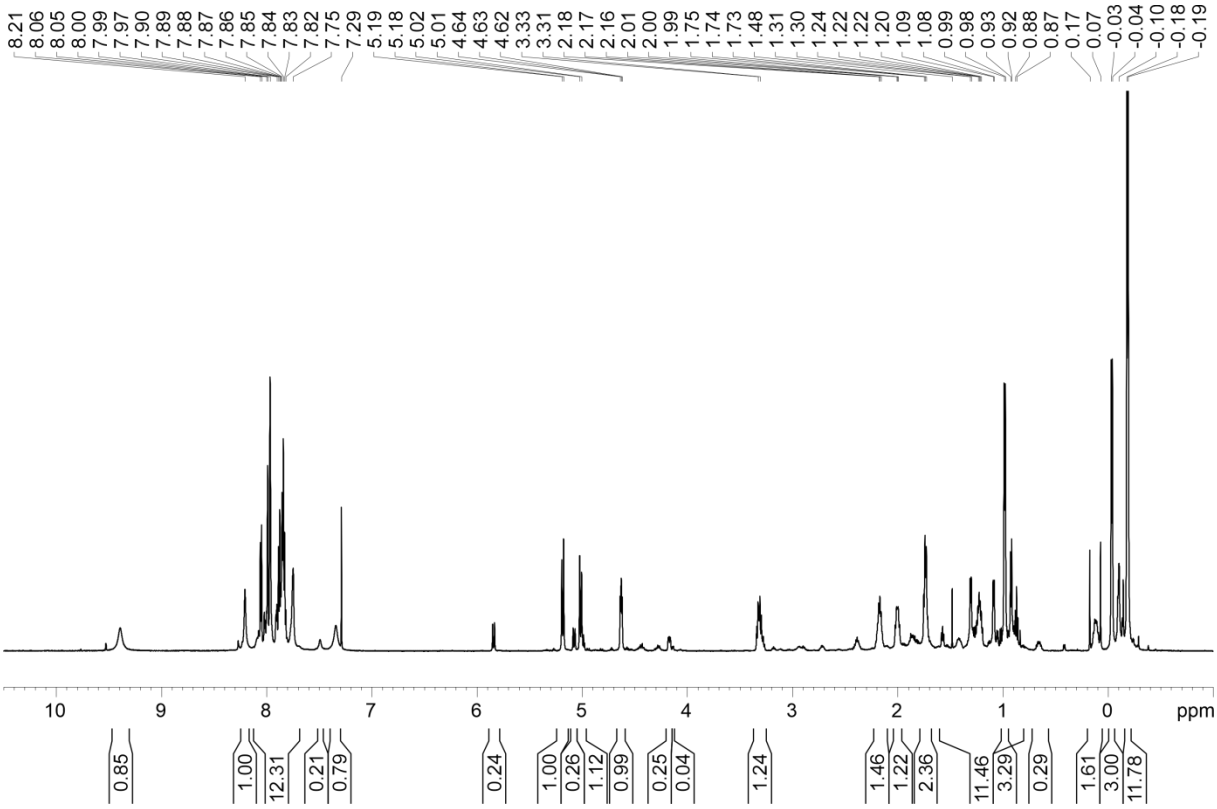

Figure SI-21. ^{1}H Spectrum of aminal **14** in $CDCl_3$ at 219 K.

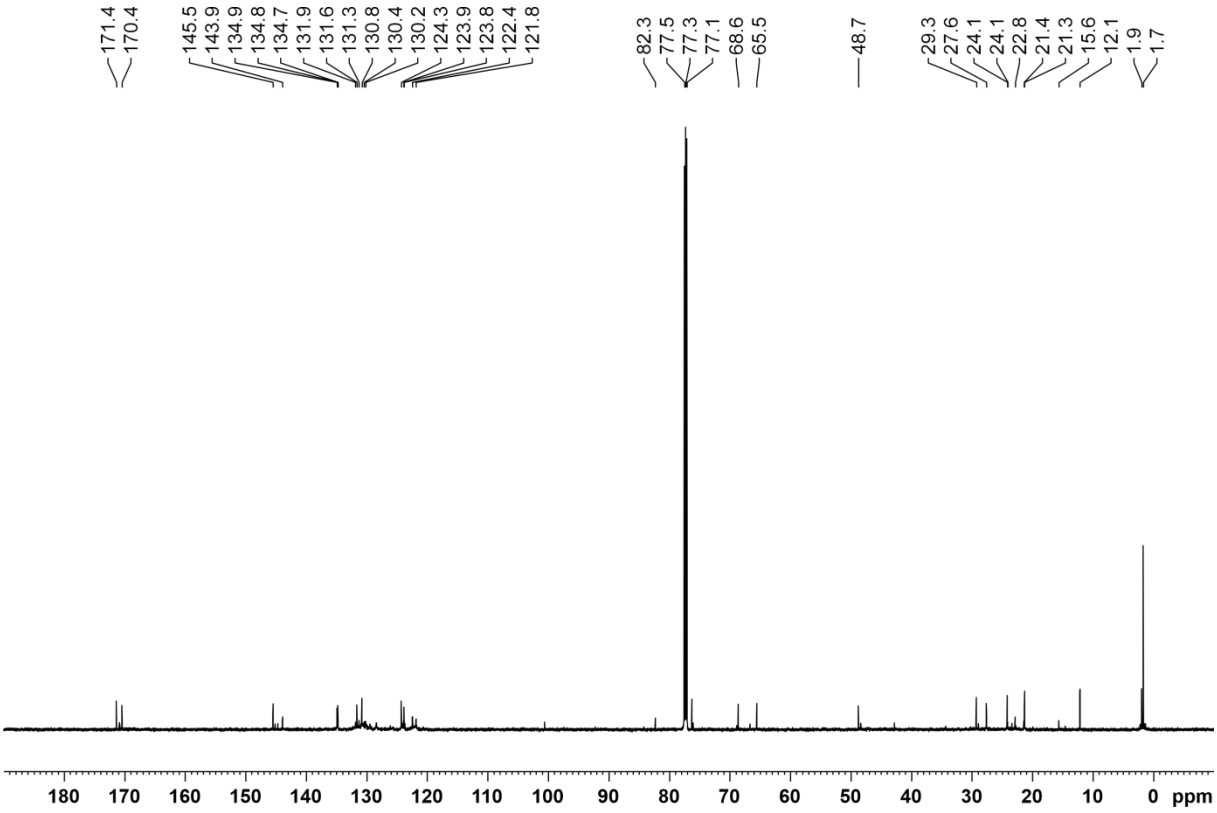

Figure SI-22. $\{^{1}H\}^{13}C$ Spectrum of aminal **14** in $CDCl_3$ at 219 K.

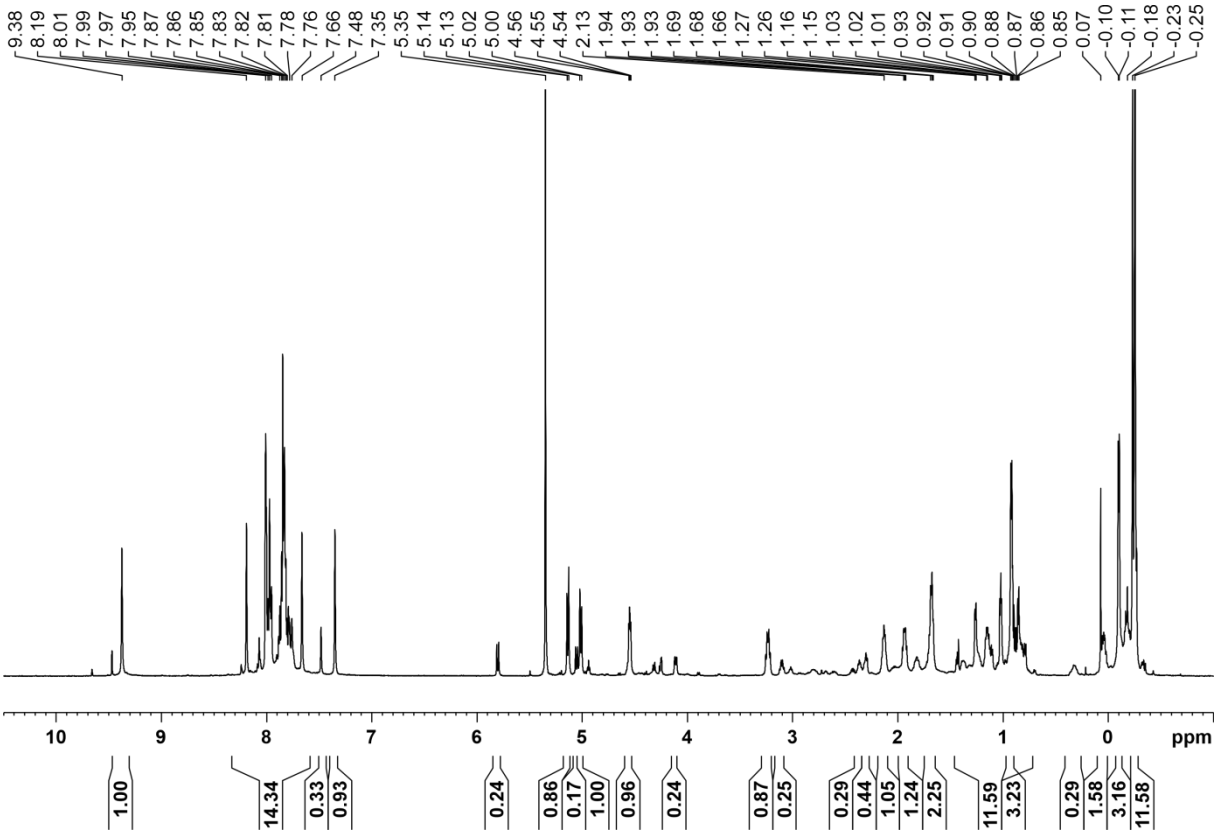

Figure SI-23. ^{1}H Spectrum of aminal **14** in CD_2Cl_2 at 190 K.

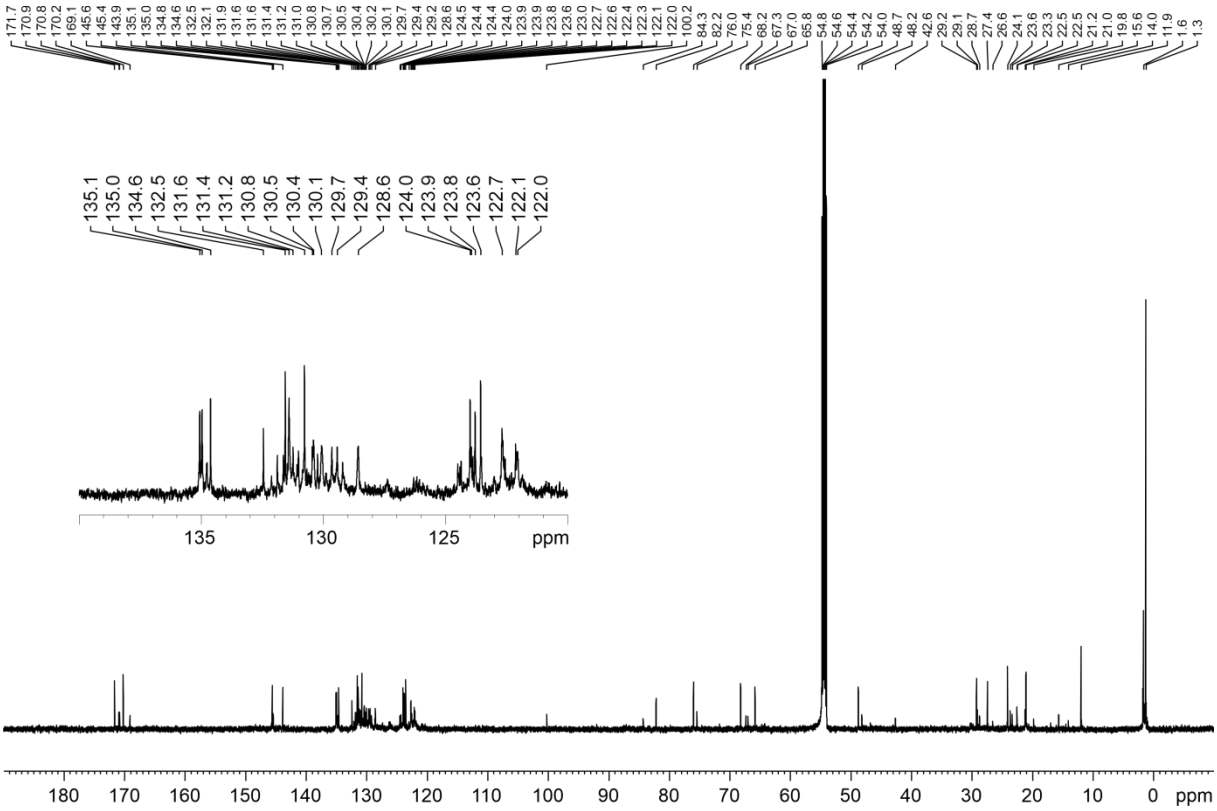

Figure SI-24. $\{^{1}H\}^{13}C$ Spectrum of aminal **14** in CD_2Cl_2 at 190 K.

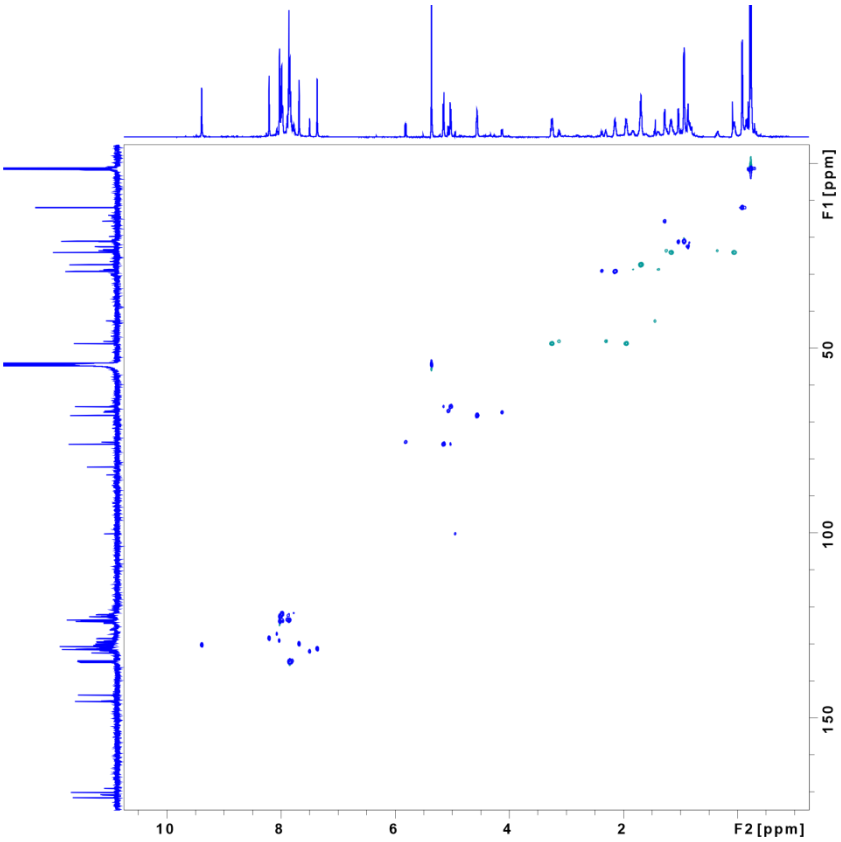

Figure SI-25. ^{1}H-^{13}C HSQC Spectrum of aminal **14** in CD_2Cl_2 at 190 K.

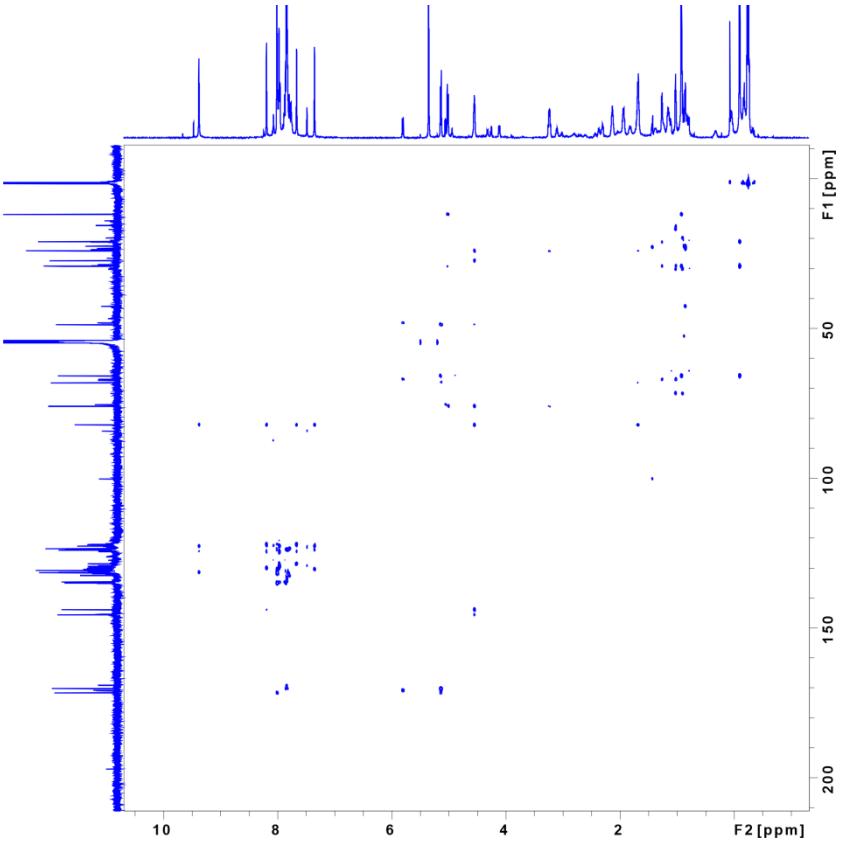

Figure SI-26. ^{1}H-^{13}C HMBC Spectrum of aminal **14** in CD_2Cl_2 at 190 K.

The experimental ^{13}C chemical shifts of major and minor species are fairly similar, while the observed ^{1}H chemical shifts as well as some – but notably not all – *J*-couplings show more marked differences between the two signal sets. The aminal proton H1' as well as the pyrrolidine proton H2 show the largest deviations in chemical shift between the major and the minor species, accompanied by a large difference for the resonance of the methyl group 5'. The *J*-couplings in the aminal part indicate an *anti-periplanar* arrangement of the protons H1' and H2' for both major and minor species. While not all *J*-couplings along the pyrrolidine ring could be determined experimentally, the observed values apparently differ between the major and minor species, possibly indicating a difference in the (average) ring pucker.

From the EASY-ROESY spectra, the interconversion between the major and minor species is evident (see Figure SI-27). While the NOE/ROE contacts have the opposite phase to the diagonal, the cross-peaks generated by chemical exchange have the same phase. These exchange peaks become even more prevalent at higher temperatures (219 K and 240 K, not shown here). Based on the exchange rate determined by the PANIC analysis, we estimate an energy difference for interconversion at 190 K of $\Delta G^{\ddagger} \approx 12.4$ kcal mol^{-1}. The distinction between chemical exchange and NOE is not immediately obvious in the 1D NOE spectra, as the compound is in the slow motion regime, i.e. both effects show signals with the same phase as the selected (diagonal) signal. A representative mixing time series of selective 1D NOE spectra showing this behavior is given in Figure SI-28.

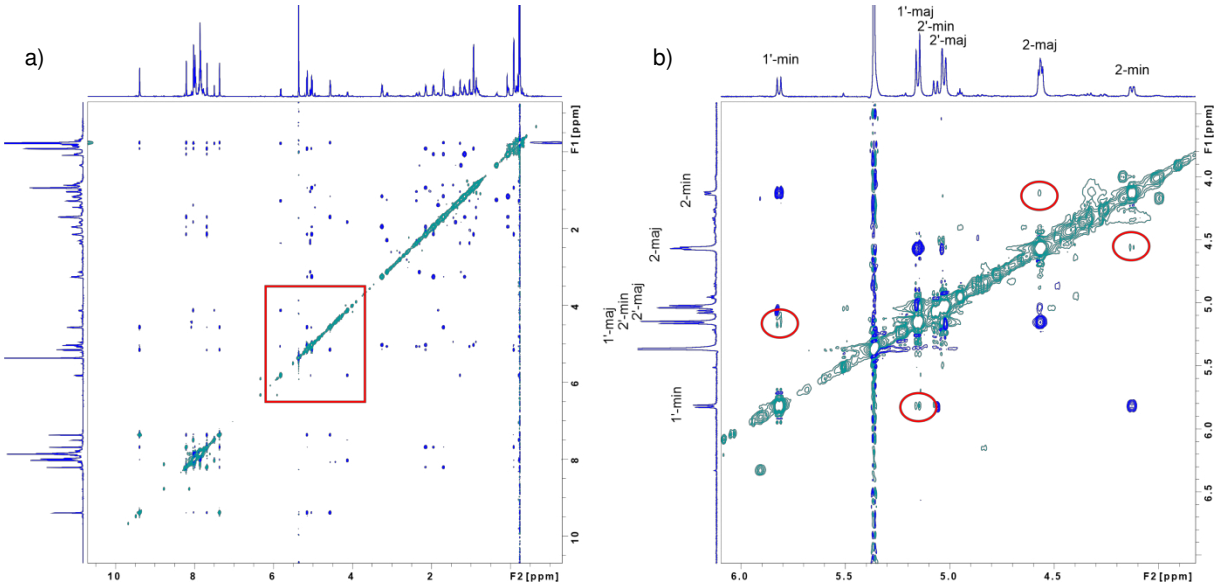

Figure SI-27. EASY-ROESY of aminal **14** in CD_2Cl_2 at 190 K. Diagonal peaks and signals generated by chemical exchange are colored green, while NOE/ROE cross-peaks are colored blue. a) full spectrum. b) zoom into the spectral region between 6 and 4 ppm. The highlighted signals show the interconversion of the major and minor species (negative phase, green cross-peaks) vs. the positive, blue cross-peaks for the NOE/ROE contacts.

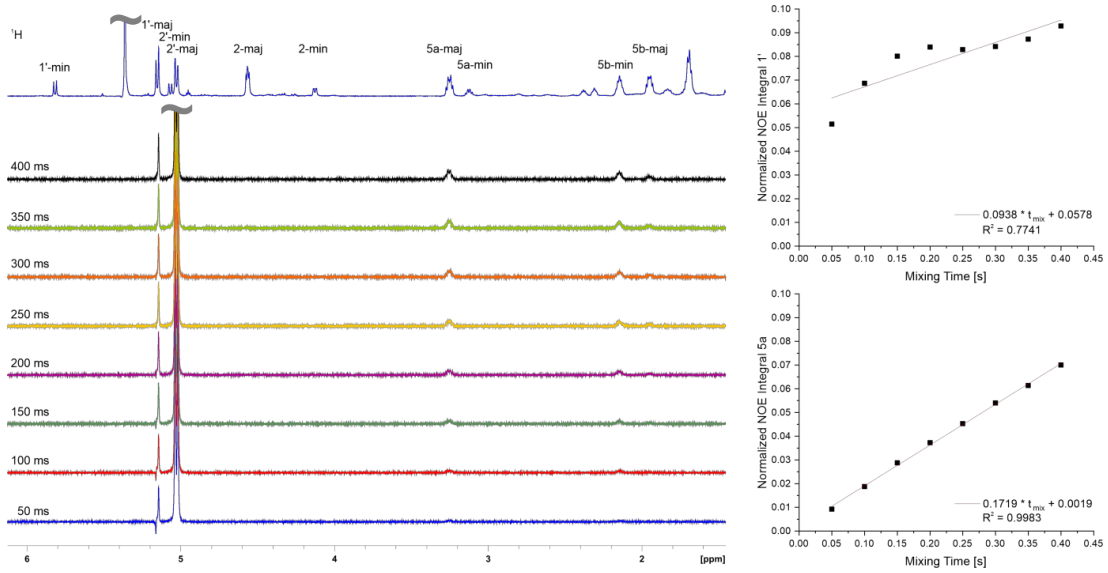

Figure SI-28. a) Example of a selective 1D NOE mixing time series of aminal **14** in CD_2Cl_2 at 190 K, with the signal H2'-major selected. The mixing time is indicated with each spectrum. The NOE spectra are scaled to match the intensity of the selected signal for display purposes. The blue spectrum at the very top shows the corresponding part of the 1D ^{1}H NMR spectrum. Note the distorted line shape of the H1'-major signal at 5.15 ppm which never reaches the expected doublet lineshape due to insufficient zero-quantum suppression. This leads to a larger error on the distance extracted from this peak (see below). All other signals show the expected undistorted linear build-up of the NOE cross-peak intensities with increasing mixing time. b) Selected PANIC plots for the normalized NOE integrals for the NOEs H2'-major -> H1'-major (top panel) and H2'-major -> H5a-major. As expected from the lineshapes, the linear fit of the normalized integrals is fairly bad for the first NOE (H2'-major -> H1'-major) due to the *J*-coupling contributions, while the latter example shows the high-confidence linear fit ($R^2 > 0.99$) observed for all other NOE contacts. The slope of the linear fit to the PANIC plot is used as cross-relaxation rate σ. Note that some "relayed" cross peaks are visible, which originate from magnetization transfer between the two species caused by chemical exchange and subsequent NOE (or vice versa).

The NOE derived distances calculated from the cross-relaxation rates by internal calibration with the cross-relaxation rate of the diastereotopic proton pair H5a/b are collected in Table SI-17. In cases where both signals could be selected with the selective pulse in the 1D NOE spectra, the distances corresponding to the individual cross-relaxation rates are averaged. While the set of distances for the minor species is smaller, the observed distances show very similar values for both species. Particularly the close distances from the protons H1' and H2' of the aminal to the pyrrolidine protons H2 and H5b indicate a similar geometry of both major and minor species with respect to the relative arrangement of the Cl and phthalimide substituents with respect to the pyrrolidine ring. The particularly interesting distance between the protons H1' and H2' in the aminal is difficult to address with these measurements. We used a variant of the 1D NOE pulse sequence already including a Thrippleton-Keeler element[4] to suppress unwanted contributions by *J*-coupling of the two neighboring nuclei, however, the applied filter element was apparently not able to fully suppress these effects in the case of these two protons. Over the course of the mixing time series, the shape of the multiplet of the H2' signal changes over time (see

Figure SI-28, the mixing time series for the H1'-minor -> H2'-minor NOE shows the same effect but to a lesser extent), indicating *J*-coupling evolution alongside the desired NOE build-up. This effect results in an apparent oscillation in the normalized intensities of the PANIC plot (noted already by Kolmer *et al.*[9] for such cases) and finally gives a reduced apparent NOE derived distance (see Table SI-17). Correcting for these effects would require extensive numerical simulations, which we did not undertake. We estimate the true experimental value for the H1'-H2' NOE distance to be around 2.9 Å, consistent with the *anti*-periplanar arrangement derived from the large (>10 Hz) $^3J_{HH}$ couplings.

Table SI-17. Experimental NOE derived distances for aminal **14** in $CDCl_3$ at 219 K and CD_2Cl_2 at 190 K.

		Quantitative 1D selective NOE				Semi-quantitative 2D F1-PSYCHE-EASY-ROESY	
		$CDCl_3$ @ 219K		CD_2Cl_2 @ 190K		CD_2Cl_2 @ 190K	
Nucleus 1	Nucleus 2	Major (Å)	Minor (Å)	Major (Å)	Minor (Å)	Major (Å)	Minor (Å)
1'	2	2.30	2.44	2.21 (2)	2.30 (3)	2.38	2.14
1'	5a	3.10		3.08 (6)		2.29	
1'	2'	2.58[1]	2.67[1]	2.39 (27)[1]	2.79 (5)[1]		
1'	3'			2.79 (4)		2.44	
1‘	5‘					2.43	2.47
2'	2			3.56 (9)			
2'	5a	2.16	2.16	2.15 (6)	2.21 (3)	1.98	1.98
2'	5b	2.22		2.53 (7)			
2'	3'			2.22 (6)		2.22	2.01
2'	4'			3.03 (3)		2.72	2.74
3'	5a			2.72 (5)			
3'	5b			2.41 (3)		2.28	
3'	4'			2.90 (3)		2.61	2.35
3‘	5‘					2.50	2.47
4‘	5‘					3.05	
5'	5a			3.47 (5)			
5'	5b			3.28 (4)			
2	5a			3.17 (10)			
4a	4b					1.85	1.85
4a	5a					2.46	
4b	5b					2.31	
5a	5b	1.76[2]	1.77	1.76[2]	1.83 (1)	1.76[2]	1.83

[1] insufficient zero-quantum suppression. Oscillation observed in PANIC fit.

[2] fixed reference distance.

Using the optimized geometries from the DFT calculations of chemical shifts enables the comparison of experimental distances to expected ones for different relative configurations of C1' and C2' as well as different conformations of the pyrrolidine ring and the bulky ligand. The *syn* geometries use the phthalimide substituent, while the *anti* geometries are taken from the corresponding succinimide calculations below. The values in Table SI-18 show an overall better agreement of experimental and calculated values for the *syn* arrangement of Cl and imide substituents at C2' and C1', respectively. Applying ensemble averaging with the populations used below in the calculation of chemical shifts improves the agreement with the experimental data slightly (see Table SI-19). From the geometry optimizations, particularly short distances are expected for H1'-H2, H2'-H5a and H3'-H5b for the *syn* diastereoisomers, while the latter distance is expected to be much larger in the *anti* diastereoisomers. Distances expected to be larger than 3 Å from the DFT calculations are apparently underestimated by the experimental methods, which might be taken as indication for conformational flexibility (see below). Also distances involving the methyl groups 4' and 5' are underestimated. Interestingly, the experimental value for the H2'-H2 NOE distance is much shorter as compared to the expected value from the calculated ensembles. While this one particular value is well reproduced in the *anti(S,S)/sc-exo* geometry, several others (notably the short H3'-H5b distance) show much larger deviations from the experimental values. The observed deviations of NOEs involving methyl groups are a notorious issue in NOE analysis. The internal averaging of the internuclear interactions of the three methyl protons and another proton of interest are coupled to the overall tumbling of the molecule as well as any internal averaging related to conformational flexibility of the entire molecule. Furthermore the averaging depends on the angle the bond vectors (C-Me axis for the methyl group) of the two interacting partner take with respect to each other.[10,42] The approximations taken herein, namely equal weighting of the three methyl proton distances (usually called "slow tumbling" or "r^{-3} averaging", equation (2)) without considering corrections to angular contributions in addition to the "r^{-6} averaging" of several geometries to form a conformer ensemble may not be applicable to the case here. Ignoring the methyl groups in the distance comparisons improves the agreement of experimental and calculated distances significantly, to ~0.4 Å RMSD for the favored *syn* models vs up to 1.0 Å for the disfavored *anti* models of the major species. Thus the NOE data indicate that the major species is the *syn*-configured aminal. As the RMSD values are the root mean squared deviations normalized to the number of observations, they are expected to be larger for the major species, where four times the number of NOEs are experimentally observed than for the minor species. Thus the smaller value of the RMSD for the minor species does not indicate a better fit to any of the structures and no discrimination between structures is possible as all RMSD values for the minor species are (almost) within experimental error (at least 0.1 Å). The experimental NOE data therefore suggests that the major species is the *syn* diastereoisomer and not any of the *anti* models. With the reduced dataset for the minor species, however, no discrimination between the two configurations is possible based on NOEs alone. The NOEs indicate that the conformation of the pyrrolidine ring with respect to the rest of the compound (rotation around N-C1' bond) is unchanged. Thus this can be excluded as a reason for the second signal set.[43] As the large ^3J coupling between H1' and H2' indicates that the antiperiplanar arrangement prevails, and the average ring-pucker is different in the two signal sets, we consider it unlikely that the minor signal set would be due to the *anti*-diastereoisomer but consider a different conformation (*sc-exo*, see below and main text) more likely.

Furthermore, quite distinct chemical shifts are observed. Thus we conducted calculations of the chemical shifts (see below).

Table SI-18. Comparison of experimentally derived NOE distances from quantitative 1D selective NOE spectra (CD_2Cl_2, 190 K) with the internuclear distances of different structure models of aminal **14**. For the calculated geometries, the first row specifies the arrangement of the Cl and imide substituents at C2' and C1', while the second row specifies the orientation of the bulky ligand at C2. The last column shows a potential geometry where the pyrrolidine ring is rotated 180° relative to the aminal.

		Experimental		Calculated					
				syn(R,S)	*syn(R,S)*	*anti(R,R)*	*anti(S,S)*	*anti(S,S)*	*syn(R,S)*
				ap	*sc-exo*	*ap*	*ap*	*sc-exo*	*sc-exo*
Nucleus 1	Nucleus 2	Major (Å)	Minor (Å)	(Å)	(Å)	(Å)	(Å)	(Å)	(Å)
H1'	H2	2.21 (2)	2.30 (3)	2.40	2.51	2.38	2.47	2.45	3.62
H1'	H5a	3.08 (6)		3.62	3.71	3.67	3.70	3.71	2.60
H1'	H2'	2.39 (27)[1]	2.79 (5)[1]	3.04	3.06	3.05	3.06	3.07	3.04
H1'	H3'	2.79 (4)		3.18	3.09	3.17	3.12	3.11	3.08
H2'	H2	3.56 (9)		4.55	4.43	4.57	3.89	3.80	2.89
H2'	H5a	2.15 (6)	2.21 (3)	2.42	2.57	2.64	2.16	2.20	4.48
H2'	H5b	2.53 (7)		2.78	2.54	2.52	3.12	3.08	4.67
H2'	H3'	2.22 (6)		2.45	2.49	2.44	2.43	2.44	2.49
H2'	H4'	3.03 (3)		2.89	2.87	3.97	2.92	2.91	2.92
H3'	H5a	2.72 (5)		3.34	3.51	4.18	4.39	4.46	3.15
H3'	H5b	2.41 (3)		2.26	2.21	4.76	4.69	4.70	4.27
H3'	H4'	2.90 (3)		2.61	2.63	2.64	2.61	2.61	2.62
H5'	H5a	3.47 (5)		5.32	5.50	5.51	5.61	5.61	3.20
H5'	H5b	3.28 (4)		4.64	4.64	5.34	6.11	6.12	4.19
H2	H5a	3.17 (10)		3.65	3.38	3.61	3.44	3.32	2.99
H5a	H5b	1.76[2]	1.83 (1)	1.76	1.77	1.76	1.77	1.77	1.79
RMSD vs major (Å)				0.71	0.74	1.10	1.18	1.18	1.06
RMSD vs major (Å) /without 5'				0.45	0.45	0.89	0.83	0.84	1.10
RMSD vs minor (Å)				0.18	0.25	0.26	0.17	0.16	1.32

[1] insufficient zero-quantum suppression. Oscillation observed in PANIC fit.

[2] fixed reference distance.

Table SI-19. Comparison of experimentally derived NOE distances from quantitative 1D selective NOE spectra (CD_2Cl_2, 190 K) with the internuclear distances of different averaged ensemble structure models of aminal **14**. For the calculated ensembles, the first row specifies the arrangement of the Cl and imide substituents at C2' and C1', while the second row specifies the orientation of the bulky ligand at C2.

		Experimental		Calculated averaged ensemble				
				syn(R,S)	*syn(R,S)*	*anti(R,R)*	*anti(S,S)*	*anti(S,S)*
				ap	*sc-exo*	*ap*	*ap*	*sc-exo*
Nucleus 1	Nucleus 2	Major (Å)	Minor (Å)	(Å)	(Å)	(Å)	(Å)	(Å)
H1'	H2	2.21 (2)	2.30 (3)	2.38	2.48	2.33	2.47	2.45
H1'	H5a	3.08 (6)		3.62	3.68	3.64	3.58	3.71
H1'	H2'	2.39 (27)[1]	2.79 (5)[1]	3.04	3.06	3.04	3.06	3.07
H1'	H3'	2.79 (4)		3.19	3.12	3.21	3.17	3.11
H2'	H2	3.56 (9)		4.54	4.43	4.56	3.79	3.80
H2'	H5a	2.15 (6)	2.21 (3)	2.29	2.27	2.35	2.16	2.20
H2'	H5b	2.53 (7)		2.96	2.79	2.73	3.32	3.08
H2'	H3'	2.22 (6)		2.44	2.48	2.44	2.43	2.44
H2'	H4'	3.03 (3)		2.89	2.88	3.98	2.94	2.91
H3'	H5a	2.72 (5)		3.04	2.99	3.99	4.20	4.46
H3'	H5b	2.41 (3)		2.38	2.35	4.97	4.88	4.70
H3'	H4'	2.90 (3)		2.61	2.62	2.64	2.61	2.61
H5'	H5a	3.47 (5)		5.15	5.17	5.23	5.58	5.61
H5'	H5b	3.28 (4)		4.73	4.72	5.63	6.20	6.12
H2	H5a	3.17 (10)		3.74	3.55	3.76	3.58	3.32
H5a	H5b	1.76[2]	1.83 (1)	1.77	1.77	1.76	1.77	1.77
RMSD vs major (Å)				0.69	0.67	1.12	1.20	1.18
RMSD vs major (Å) /without 5'				0.43	0.40	0.91	0.85	0.84
RMSD vs minor (Å)				0.14	0.17	0.15	0.16	0.16

[1] insufficient zero-quantum suppression. Oscillation observed in PANIC fit.

[2] fixed reference distance.

Computational NMR Analysis of Aminals 11 (Succinimide Substituent) and 14 (Phthalimide Substituent)

The calculated ^{1}H and ^{13}C chemical shifts for the *syn*, *anti*(C1‘), and *anti*(C2‘) isomers of **11** were compared to Blackmond and coworkers experimental shifts (‡)[28] (Tables SI-20–SI29). The weights, or percentages, for the conformers used in the calculations can be found in Table SI-40. The *syn*-**11** diastereomer resulted in the lowest MAD of the ^{1}H and ^{13}C chemical shifts compared to their major product at –54°C. The calculated chemical shifts for the *anti*(C1‘) and *anti*(C2‘) isomers were compared to the minor product at –54°C, but did not result in good agreement with the experimental shifts. Continuation of the search for the minor product at –54°C, led to the separation of the calculated *ap* and *exo-sc* rotational conformer chemical shifts for *syn*-**14**. When the calculated chemical shifts were separated by this rotational classification, the *ap* and *exo-sc* weighted chemical shifts were in good agreement with major and minor chemical shifts respectively at –54°C (Tables SI-30–SI-33). Using the same classification of the *ap* and *exo-sc* conformers for the succinimide version of the aminal (*syn*-**11**) the weighted *ap* conformers were in good agreement with major product chemical shifts (mean average deviations (MADs): 1.7 ppm for ^{13}C; 0.16 ppm for ^{1}H), while not all the *exo-sc* conformer chemical shifts were in good agreement with the minor product chemical shifts, such as the C(5‘)H shift predicted to be 1.51 ppm, but which was reported to occur at -0.13 ppm. Given the similarities between the calculated lowest energy conformers between the phthalimide (*syn*-**14**) and succinimide (*syn*-**11**) substituent aminals, and the good agreement between the *exo-sc* chemical shifts, further investigation may be needed to confirm all of the experimental minor product chemical shifts.

For NMR calculations with this level of theory: PCM(chloroform)-mPW1PW91/6-311+G(2d,p)//B3LYP-D3(BJ)/6-31G+(d,p) expected absolute deviation for the ^{1}H chemical shifts is < 0.3 ppm and < 7-8 ppm for ^{13}C chemical shifts[17,18] and are highlighted in red in the tables below. The C2‘ ^{13}C shift deviations for both major and minor products when compared to the *ap* and *exo-sc* calculated chemical shifts are around this upper limit of deviation. This is expected for carbons bonded to halogens due to relativistic effects.[44] The ^{1}H shifts for the H2‘ carbon also had deviations ~0.3 ppm as well, suggesting minor variations in conformers or solvent interactions may be affecting this chemical shift.[45] Chemical shifts that differ in the major and minor products are indicated (*).Chemical shift assignments which could be switched are assigned to minimize the mean average deviation (MAD and indicated (**).
The *J*-couplings for the *syn*-**14** *ap* and *exo-sc* rotamers were also calculated for the pyrrolidine ring and compared to the calculated experimental *J*-couplings which were generally within ~0.5 Hz of the experimental values (Tables SI-34–SI-37). Additionally, the theoretical chemical shifts for the iminium ion that forms from *syn*-**11** were calculated to compare to unassigned peaks in the *syn*-**11** spectra; however, no iminium ion peaks were able to be determined with this comparison (Tables SI-38 & SI-39). The barrier of rotation for the *syn*-**14** *ap* and *exo-sc* rotamers was also calculated and found to be 13.9 kcal mol^{-1} at –54°C with implicit chloroform when rotating the -OTMS group from the *ap* orientation towards the *exo-sc* orientation, similar to the experimental value of 12.8 kcal mol^{-1} (Figure SI-29).

Table SI-20. Comparison of calculated and experiment major ^{13}C NMR δ's for *syn*-**11** (*ap*) at –54°C

Exp. C#	Comp. C#	Comp. Isotropic	Comp. δ	Avg. Comp. δ	Syn. δ‡	Abs. Dev.
C5	C1	135.6845	48.6		48.4	0.2
C2	C2	116.4527	67.1		67.8	0.7
C3	C3	156.9831	28.2		27.3	0.9
C4	C4	159.9259	25.4		23.8	1.6
*C1'	C12	107.0240	76.1		76.5	0.4
*C2'	C14	111.0191	72.3		64.3	8.0
C3'	C16	152.8208	32.2		28.7	3.5
*C4'	C18	165.6695	19.9		20.8	0.9
*C5'	C22	173.5483	12.3		11.7	0.6
	C27	154.8925	30.2			
	C28	155.4406	29.7			
**C5''	C34	-2.2923	181.0		179.5	1.5
**C2''	C36	-3.8047	182.5		180.9	1.6
*C6	C38	100.1433	82.7		81.9	0.8
	C39	34.6347	145.6			
	C40	50.0127	130.8			
	C41	48.8364	132.0			
	C42	50.6022	130.3			
	C44	51.8776	129.1			
	C46	59.7108	121.5			
	C48	33.1497	147.0			
	C49	48.2190	132.6			
	C50	46.7355	134.0			
	C51	48.3657	132.4			
	C53	49.2026	131.6			
	C55	58.2757	122.9			
	C57	52.3549	128.6			
	C58	52.4529	128.5			
	C59	51.8145	129.1			
	C60	51.9597	129.0			
	C62	184.8693	1.4			
	C66	186.5223	-0.2			
*OTMS	C70	185.8696	0.5	0.6	1.3	0.7
					MAD:	1.7

Table SI-21. Comparison of calculated and experimental major ^{1}H NMR δ's for *syn*-**11** (*ap*) at –54°C.

Exp. #	Comp. C#	Comp. H#	Comp. Isotropic	Comp. δ	Avg. Comp. δ	Exp. δ‡	Abs. Dev.
C(5)H	1	H5	28.22	3.41	3.41	3.20	0.21
C(5)H	1	H6	29.88	1.86	1.86	1.85	0.01
*C(2)H	2	H7	26.77	4.76	4.76	4.48	0.28
C(3)H	3	H8	29.94	1.80			
C(4)H	4	H9	31.64	0.21	0.21	0.13	0.08
C(4)H	4	H10	30.57	1.21	1.21	1.15	0.06
*C(1')H	12	H13	26.35	5.16	5.16	5.00	0.16
*C(2')H	14	H15	26.29	5.21	5.21	4.90	0.31
C(3')H	16	H17	29.39	2.32	2.32	2.05	0.27
	18	H19	30.65	1.14			
	18	H20	30.74	1.06			
**C(4')H	18	H21	30.86	0.95	1.05	0.91	0.14
	22	H23	31.39	0.45			
	22	H24	31.83	0.04			
**C(5')H	22	H25	32.15	-0.26	0.08	-0.13	0.21
	27	H29	29.07	2.62			
**C(3"/C4")H	27	H30	28.98	2.70	2.66	2.77	0.11
	28	H31	28.89	2.78			
**C(3"/C4")H	28	H32	28.89	2.79	2.79	2.94	0.15
	40	H43	22.84	8.43			
	41	H32	26.54	7.74			
	46	H47	23.36	7.94			
	49	H52	21.22	9.94			
	50	H54	46.39	-13.55			
	55	H56	23.35	7.95			
	62	H63	31.37	0.47			
	62	H64	31.43	0.41			
	62	H65	31.66	0.20			
	66	H67	32.17	-0.28			
	66	H68	32.39	-0.48			
	66	H69	32.83	-0.90			
	70	H71	31.85	0.02			
	70	H72	31.80	0.07			
*OTMS	70	H73	32.03	-0.14	-0.07	-0.26	0.19
C(3)H	3	H87	29.86	1.88	1.84	1.72	0.12
						MAD	0.16

Table SI-22. Comparison of calculated and experimental minor ^{13}C NMR δ's for *syn*-**11** (*exo-sc*) at –54°C.

Exp. C#	Comp. C#	Comp. Isotropic	Comp. δ	Avg. Comp. δ	Syn. δ‡	Abs. Dev.
C5	C1	136.4713	47.9		48.4	0.5
C2	C2	117.7784	65.8		70.7	4.9
C3	C3	156.1918	28.9		27.3	1.6
C4	C4	160.7078	24.6		23.8	0.8
*C1'	C12	107.8337	75.4		76.5	1.1
*C2'	C14	109.9297	73.3		65.4	7.9
C3'	C16	153.0082	32.0		28.7	3.3
*C4'	C18	165.8347	19.7		20.8	1.1
*C5'	C22	169.4198	16.3		11.7	4.6
	C27	155.0574	30.0			
	C28	155.2203	29.9			
**C5''	C34	-2.7958	181.5		179	2.5
**C2''	C36	-2.1768	180.9		180.1	0.8
*C6	C38	98.5761	84.2		83.7	0.5
	C39	34.5114	145.7			
	C40	46.9006	133.8			
	C41	49.8154	131.0			
	C42	49.4106	131.4			
	C44	49.4941	131.3			
	C46	57.4787	123.7			
	C48	33.6336	146.6			
	C49	51.1595	129.7			
	C50	47.3518	133.4			
	C51	51.6159	129.3			
	C53	51.1792	129.7			
	C55	59.7931	121.5			
	C57	52.2149	128.7			
	C58	51.6628	129.3			
	C59	52.2399	128.7			
	C60	52.5823	128.4			
	C62	185.8896	0.4			
	C66	184.4579	1.8			
*OTMS	C70	184.2350	2.0	1.4	1.5	0.1
					MAD:	2.3

Table SI-23. Comparison of calculated and experimental minor ^{1}H NMR δ's for *syn*-**11** (*exo-sc*) at –54°C.

Exp. C#	Comp. C#	Comp. H#	Comp. Isotropic	Comp. δ	Avg. Comp. δ	Exp. δ‡	Abs. Dev.
C(5)H	1	H5	28.34	3.29	3.29	3.2	0.09
C(5)H	1	H6	29.45	2.26	2.26	1.85	0.41
*C(2)H	2	H7	27.34	4.23	4.23	4.08	0.15
C(3)H	3	H8	29.88	1.86			
C(4)H	4	H9	31.73	0.13	0.13	0.13	0.00
C(4)H	4	H10	30.61	1.18	1.18	1.15	0.03
*C(1')H	12	H13	25.50	5.95	5.95	5.66	0.29
*C(2')H	14	H15	26.24	5.25	5.25	4.95	0.30
C(3')H	16	H17	29.06	2.62	2.62	2.05	0.57
	18	H19	30.56	1.23			
	18	H20	30.75	1.05			
**C(4')H	18	H21	30.52	1.26	1.18	0.91	0.27
	22	H23	30.28	1.49			
	22	H24	30.50	1.28			
**C(5')H	22	H25	29.97	1.77	1.51	-0.13	1.64
	27	H29	29.02	2.66			
**C(3"/C4")H	27	H30	28.98	2.70	2.68	2.77	0.09
	28	H31	28.85	2.82			
**C(3"/C4")H	28	H32	28.94	2.74	2.78	2.94	0.16
	40	H43	23.70	7.63			
	41	H32	26.54	8.05			
	46	H47	23.33	7.97			
	49	H52	24.19	7.17			
	50	H54	44.85	-12.10			
	55	H56	23.36	7.94			
	62	H63	31.59	0.27			
	62	H64	33.66	-1.67			
	62	H65	32.31	-0.40			
	66	H67	31.11	0.71			
	66	H68	31.89	-0.02			
	66	H69	31.69	0.17			
	70	H71	31.64	0.22			
	70	H72	31.75	0.12			
*OTMS	70	H73	31.85	0.02	-0.06	-0.29	0.23
C(3)H	3	H87	30.40	1.38	1.62	1.72	0.10
						MAD	0.31

Table SI-24. Comparison of calculated and experimental minor ^{13}C NMR δ's for *anti(C1')*-**11** (*ap*) at –54°C.

Exp. C#	Comp. C#	Comp. Isotropic	Comp. δ	Avg. Comp. δ	Syn. δ‡	Abs. Dev.
C5	C1	135.9947	48.3		48.4	0.1
C2	C2	115.7302	67.8		70.7	2.9
C3	C3	157.0734	28.1		27.3	0.8
C4	C4	160.2338	25.1		23.8	1.3
*C1'	C12	114.5331	68.9		76.5	7.6
*C2'	C14	108.4440	74.8		65.4	9.4
C3'	C16	151.6796	33.3		28.7	4.6
*C4'	C18	165.9822	19.6		20.8	1.2
*C5'	C22	171.6763	14.1		11.7	2.4
	C27	155.5999	29.5			
	C28	155.5434	29.6			
**C5''	C34	-1.1724	180.0		179	1.0
**C2''	C36	0.6840	178.2		180.1	1.9
*C6	C38	100.5030	82.4		83.7	1.3
	C39	36.4178	143.9			
	C40	48.3516	132.4			
	C41	49.8264	131.0			
	C42	54.0621	127.0			
	C44	51.5846	129.3			
	C46	60.4671	120.8			
	C48	34.4201	145.8			
	C49	50.9172	130.0			
	C50	46.9404	133.8			
	C51	49.8517	131.0			
	C53	48.0804	132.7			
	C55	56.4885	124.6			
	C57	51.7504	129.2			
	C58	52.3672	128.6			
	C59	51.8414	129.1			
	C60	51.3528	129.6			
	C62	185.8755	0.5			
	C66	184.8698	1.4			
*OTMS	C70	186.2035	0.1	0.7	1.5	0.8
					MAD:	2.7

Table SI-25. Comparison of calculated and experimental minor ^{1}H NMR δ's for *anti(C1')*-**11** (*ap*) at –54°C.

Exp. #	Comp. C#	Comp. H#	Comp. Isotropic	Comp. δ	Avg. Comp. δ	Exp. δ‡	Abs. Dev.
C(5)H	1	H5	28.45	3.19	3.19	3.2	0.01
C(5)H	1	H6	29.84	1.90	1.90	1.85	0.05
*C(2)H	2	H7	26.12	5.37	5.37	4.08	1.29
C(3)H	3	H8	29.64	2.09			
C(4)H	4	H9	31.73	0.13	0.13	0.13	0.00
C(4)H	4	H10	30.34	1.43	1.43	1.15	0.28
*C(1')H	12	H13	26.40	5.10	5.10	5.66	0.56
*C(2')H	14	H15	25.93	5.54	5.54	4.95	0.59
C(3')H	16	H17	30.19	1.57	1.57	2.05	0.48
	18	H19	30.78	1.02			
	18	H20	30.64	1.15			
**C(4')H	18	H21	30.86	0.94	1.04	0.91	0.13
	22	H23	31.16	0.67			
	22	H24	31.15	0.67			
**C(5')H	22	H25	30.59	1.19	0.85	-0.13	0.98
	27	H29	29.28	2.42			
**C(3"/C4")H	27	H30	29.05	2.63	2.52	2.77	0.25
	28	H31	29.31	2.39			
**C(3"/C4")H	28	H32	28.94	2.74	2.57	2.94	0.37
	40	H43	23.98	7.36			
	41	H32	26.54	8.40			
	46	H47	23.40	7.91			
	49	H52	22.52	8.73			
	50	H54	24.02	7.32			
	55	H56	23.34	7.96			
	62	H63	32.02	-0.13			
	62	H64	31.85	0.02			
	62	H65	32.28	-0.38			
	66	H67	31.80	0.07			
	66	H68	31.33	0.51			
	66	H69	31.44	0.41			
	70	H71	32.57	-0.65			
	70	H72	31.91	-0.04			
*OTMS	70	H73	32.21	-0.31	-0.06	-0.29	0.23
C(3)H	3	H87	29.91	1.83	1.96	1.72	0.24
						MAD	0.39

Table SI-26. Comparison of calculated and experimental minor ^{13}C NMR δ's for *anti(C1')*-**11** (*exo-sc*) at –54°C.

Exp. C#	Comp. C#	Comp. Isotropic	Comp. δ	Avg. Comp. δ	Syn. δ‡	Abs. Dev.
C5	C1	135.4575	48.8		48.4	0.4
C2	C2	110.9980	72.3		70.7	1.6
C3	C3	156.3759	28.8		27.3	1.5
C4	C4	160.0842	25.2		23.8	1.4
*C1'	C12	113.3557	70.1		76.5	6.4
*C2'	C14	109.9617	73.3		65.4	7.9‡
C3'	C16	151.9450	33.0		28.7	4.3
*C4'	C18	165.7677	19.8		20.8	1.0
*C5'	C22	171.3154	14.4		11.7	2.7
	C27	155.0763	30.0			
	C28	154.6013	30.5			
**C5''	C34	-2.1163	180.9		179	1.9
**C2''	C36	-0.3893	179.2		180.1	0.9
*C6	C38	96.1129	86.6		83.7	2.9
	C39	33.8334	146.4			
	C40	48.5481	132.3			
	C41	48.0533	132.7			
	C42	49.9668	130.9			
	C44	48.8141	132.0			
	C46	58.6709	122.5			
	C48	34.4047	145.8			
	C49	51.4280	129.5			
	C50	46.5023	134.2			
	C51	51.3556	129.6			
	C53	52.2943	128.7			
	C55	59.7534	121.5			
	C57	52.1849	128.8			
	C58	51.1248	129.8			
	C59	52.2953	128.7			
	C60	52.5062	128.5			
	C62	185.1263	1.2			
	C66	185.3374	1.0			
*OTMS	C70	186.3819	0.0	0.7	1.5	0.8
					MAD:	2.6

Table SI-27. Comparison of calculated and experimental minor ^{1}H NMR δ's for *anti(C1')*-**11** (*exo-sc*) at –54°C.

Exp. #	Comp. C#	Comp. H#	Comp. Isotropic	Comp. δ	Avg. Comp. δ	Exp. δ‡	Abs. Dev.
C(5)H	1	H5	28.55	3.10	3.10	3.2	0.10
C(5)H	1	H6	29.35	2.35	2.35	1.85	0.50
*C(2)H	2	H7	26.17	5.32	5.32	4.08	1.24
C(3)H	3	H8	29.54	2.17			
C(4)H	4	H9	31.20	0.63	0.63	0.13	0.50
C(4)H	4	H10	30.44	1.33	1.33	1.15	0.18
*C(1')H	12	H13	25.27	6.16	6.16	5.66	0.50
*C(2')H	14	H15	25.69	5.77	5.77	4.95	0.82
C(3')H	16	H17	30.11	1.64	1.64	2.05	0.41
	18	H19	30.82	0.99			
	18	H20	30.90	0.91			
**C(4')H	18	H21	30.49	1.29	1.06	0.91	0.15
	22	H23	30.62	1.17			
	22	H24	30.63	1.16			
**C(5')H	22	H25	31.08	0.74	1.03	-0.13	1.16
	27	H29	29.21	2.48			
**C(3"/C4")H	27	H30	29.12	2.57	2.52	2.77	0.25
	28	H31	29.04	2.64			
**C(3"/C4")H	28	H32	28.60	3.05	2.85	2.94	0.09
	40	H43	23.64	7.68			
	41	H32	26.54	8.23			
	46	H47	23.34	7.96			
	49	H52	23.93	7.41			
	50	H54	22.55	8.70			
	55	H56	23.42	7.89			
	62	H63	30.13	1.63			
	62	H64	31.48	0.37			
	62	H65	32.00	-0.12			
	66	H67	31.55	0.31			
	66	H68	32.05	-0.17			
	66	H69	32.11	-0.22			
	70	H71	32.58	-0.66			
	70	H72	32.48	-0.56			
*OTMS	70	H73	33.84	-1.84	-0.14	-0.29	0.15
C(3)H	3	H87	30.32	1.45	1.81	1.72	0.09
						MAD	0.44

Table SI-28. Comparison of calculated and experimental minor ^{13}C NMR δ's for *anti(C2')*-**11** (*ap*) at –54°C.

Exp. C#	Comp. C#	Comp. Isotropic	Comp. δ	Avg. Comp. δ	Syn. δ‡	Abs. Dev.
C5	C1	136.9004	47.5		48.4	0.9
C2	C2	115.5457	68.0		70.7	2.7
C3	C3	156.5798	28.6		27.3	1.3
C4	C4	160.0619	25.2		23.8	1.4
C1'	C12	108.9728	74.3		76.5	2.2
C2'	C14	108.1558	75.0		65.4	9.6‡
C3'	C16	152.3606	32.6		28.7	3.9
C4'	C18	171.9968	13.8		20.8	7.0
C5'	C22	165.6509	19.9		11.7	8.2
	C27	155.1158	30.0			
	C28	154.7914	30.3			
C5''	C34	-2.7252	181.5		179	2.5
C2''	C36	-2.8807	181.6		180.1	1.5
C6	C38	100.0367	82.8		83.7	0.9
	C39	35.3661	144.9			
	C40	49.8824	131.0			
	C41	46.8657	133.9			
	C42	51.2183	129.7			
	C44	51.2936	129.6			
	C46	60.2623	121.0			
	C48	33.8848	146.3			
	C49	47.5167	133.2			
	C50	48.6472	132.2			
	C51	49.5448	131.3			
	C53	49.3588	131.5			
	C55	57.4194	123.7			
	C57	52.2395	128.7			
	C58	52.1519	128.8			
	C59	51.9835	129.0			
	C60	51.7189	129.2			
	C62	185.5768	0.7			
	C66	185.4877	0.8			
	C70	185.4005	0.9	0.8	1.5	0.7
					MAD:	3.3

Table SI-29. Comparison of calculated and experimental minor ^{1}H NMR δ's for *anti(C2')*-**11** (*ap*) at –54°C.

Exp. #	Comp. C#	Comp. H#	Comp. Isotropic	Comp. δ	Avg. Comp. δ	Exp. δ‡	Abs. Dev.
C(5)H	1	H5	28.44	3.21	3.21	3.2	0.01
C(5)H	1	H6	29.52	2.20	2.20	1.85	0.35
*C(2)H	2	H7	26.72	4.80	4.80	4.08	0.72
C(3)H	3	H8	29.93	1.81			
C(4)H	4	H9	31.73	0.13	0.13	0.13	0.00
C(4)H	4	H10	30.66	1.14	1.14	1.15	0.01
*C(1')H	12	H13	26.37	5.13	5.13	5.66	0.53
*C(2')H	14	H15	26.69	4.83	4.83	4.95	0.12
C(3')H	16	H17	30.02	1.73	1.73	2.05	0.32
	18	H19	31.16	0.66			
	18	H20	31.07	0.75			
**C(4')H	18	H21	31.18	0.64	0.68	0.91	0.23
	22	H23	30.82	0.98			
	22	H24	30.79	1.01			
**C(5')H	22	H25	30.91	0.90	0.97	-0.13	1.10
	27	H29	29.06	2.63			
**C(3"/C4")H	27	H30	29.11	2.58	2.60	2.77	0.17
	28	H31	28.87	2.80			
**C(3"/C4")H	28	H32	28.93	2.75	2.78	2.94	0.16
	40	H43	22.83	8.43			
	41	H32	26.54	8.77			
	46	H47	23.36	7.94			
	49	H52	23.34	7.96			
	50	H54	22.36	8.87			
	55	H56	23.38	7.92			
	62	H63	31.97	-0.09			
	62	H64	32.08	-0.19			
	62	H65	32.12	-0.23			
	66	H67	31.50	0.34			
	66	H68	31.47	0.37			
	66	H69	31.42	0.43			
	70	H71	32.37	-0.47			
	70	H72	32.35	-0.44			
*OTMS	70	H73	32.07	-0.18	-0.05	-0.29	0.24
C(3)H	3	H87	30.06	1.69	1.75	1.72	0.03
						MAD	0.28

Table SI-30. Comparison of calculated and experimental major ^{13}C NMR δ's for *syn*-**14** (*ap*) at –54°C.

Exp. C#	Comp. C#	Comp. Isotropic	Comp. δ	Avg. Comp. δ	Syn. δ	Abs. Dev.
C5	C1	135.9388	48.4		48.8	0.4
C1'	C12	107.9988	75.2		76.3	1.1
C2'	C14	110.3959	72.9		65.6	7.3‡
C3'	C16	152.7793	32.2		29.3	2.9
C4'	C18	165.6499	19.9		21.3	1.4
C2	C2	115.6540	67.9		68.6	0.7
C5'	C22	173.5018	12.3		12.2	0.1
	C27	49.2818	131.5			
C2"/C5"	C29	6.8274	172.3		171.4	0.9
C3	C3	156.9539	28.2		27.7	0.5
C2"/C5"	C31	8.1297	171.0		170.5	0.5
C6	C33	100.1346	82.7		82.4	0.3
	C34	35.4051	144.9			
	C35	49.7620	131.1			
	C36	48.7174	132.1			
	C37	50.5989	130.3			
	C39	51.8300	129.1			
C4	C4	160.0826	25.2		24.3	0.9
	C41	59.6637	121.6			
	C43	33.8341	146.4			
	C44	46.4848	134.2			
	C45	48.1872	132.6			
	C46	48.4947	132.3			
	C48	49.1247	131.7			
	C50	58.0782	123.1			
	C52	52.3296	128.6			
	C53	52.3279	128.6			
	C54	51.7803	129.2			
	C55	51.8710	129.1			
OTMS	C57	185.6073	0.7			
OTMS	C61	185.5508	0.8			
OTMS	C65	185.6881	0.6	0.7	1.7	1.0
	C83	49.9831	130.9			
	C84	57.2058	123.9			
	C85	57.5833	123.6			
	C86	45.7889	134.9			
	C88	45.6369	135.0			
					MAD:	1.4

Table SI-31. Comparison of calculated and experimental major ^{1}H NMR δ's for *syn*-**14** (*ap*) at –54°C.

Exp. C#	Comp. C#	Comp. H#	Comp. Isotropic	Comp. δ	Avg. Comp. δ	Exp. δ	Abs. Dev.
C4a	C4	H10	30.61	1.18	1.18	1.20	0.02
C1'	C12	H13	26.26	5.24	5.24	5.16	0.08
C2'	C14	H15	26.24	5.25	5.25	4.98	0.27
C3'	C16	H17	29.31	2.39	2.39	2.13	0.26
C4'	C18	H19	30.70	1.09			
C4'	C18	H20	30.75	1.05			
C4'	C18	H21	30.74	1.06	1.07	0.95	0.12
C5'	C22	H23	31.34	0.50			
C5'	C22	H24	32.43	-0.52			
C5'	C22	H25	31.69	0.17	0.05	-0.01	0.06
	C35	H38	22.87	8.40			
	C36	H40	23.44	7.87			
	C41	H42	23.34	7.97			
	C44	H47	22.28	8.95			
	C45	H49	22.75	8.52			
C5a	C1	H5	28.26	3.37	3.37	3.29	0.08
	C50	H51	23.30	8.00			
OTMS	C57	H58	31.77	0.10			
OTMS	C57	H59	31.98	-0.10			
C5b	C1	H6	29.76	1.97	1.97	1.97	0.00
OTMS	C57	H32	26.54	-0.05			
OTMS	C61	H62	31.54	0.31			
OTMS	C61	H63	31.20	0.63			
OTMS	C61	H64	31.83	0.04			
OTMS	C65	H66	32.09	-0.20			
OTMS	C65	H67	32.15	-0.26			
OTMS	C65	H68	33.17	-1.21	-0.08	-0.16	0.08
C2	C2	H7	26.73	4.80	4.80	4.60	0.20
C3a	C3	H8	29.99	1.76	1.76	1.71	0.05
C3b	C3	H82	29.94	1.80	1.80	1.71	0.09
	C84	H87	23.36	7.94			
	C85	H89	23.50	7.81			
C4b	C4	H9	31.79	0.08	0.08	0.09	0.01
	C86	H90	23.53	7.79			
	C88	H91	23.55	7.76			
						MAD	0.10

Table SI-32. Comparison of calculated and experimental minor ^{13}C NMR δ's for *syn*-**14** (*exo-sc*) at –54°C.

Exp. C#	Comp. C#	Comp. Isotropic	Comp. δ	Avg. Comp. δ	Syn. δ	Abs. Dev.
C5	C1	136.4232	47.9		48.5	0.6
C1'	C12	108.6580	74.6		76.1	1.5
C2'	C14	109.1710	74.1		66.8	7.3
C3'	C16	152.8625	32.1		29.0	3.1
C4'	C18	165.8239	19.7		21.4	1.7
C2	C2	116.4201	67.1		68.6	1.5
C5'	C22	169.4610	16.2		15.7	0.5
	C27	48.8475	132.0			
C2"/C5"	C29	8.3013	170.9		170.8	0.1
C3	C3	155.8692	29.3		29.0	0.3
C2"/C5"	C31	7.8370	171.3		170.9	0.4
C6	C33	98.5273	84.3		84.2	0.1
	C34	34.5708	145.7			
	C35	47.0622	133.7			
	C36	49.5313	131.3			
	C37	49.5707	131.3			
	C39	49.6703	131.2			
C4	C4	159.8652	25.4		24.1	1.3
	C41	57.9075	123.3			
	C43	34.3743	145.9			
	C44	50.9557	129.9			
	C45	46.9211	133.8			
	C46	51.8629	129.1			
	C48	50.8591	130.0			
	C50	59.5760	121.7			
	C52	52.2178	128.7			
	C53	51.6846	129.2			
	C54	52.3688	128.6			
	C55	52.5147	128.4			
OTMS	C57	184.1522	2.1			
OTMS	C61	184.4262	1.9			
OTMS	C65	185.9906	0.4	1.4	1.9	0.5
	C83	49.5982	131.2			
	C84	57.5751	123.6			
	C85	57.9324	123.2			
	C86	46.5484	134.2			
	C88	46.3394	134.4			
					MAD:	1.5

Table SI-33. Comparison of calculated and experimental minor ^{1}H NMR δ's for *syn*-**14** (*exo-sc*) at –54°C.

Exp. C#	Comp. C#	Comp. H#	Comp. Isotropic	Comp. δ	Avg. Comp. δ	Exp. δ	Abs. Dev.
C4a	C4	H10	30.53	1.25	1.25	1.28	0.03
C1'	C12	H13	25.39	6.04	6.04	5.81	0.23
C2'	C14	H15	26.21	5.28	5.28	5.05	0.23
C3'	C16	H17	29.01	2.67	2.67	2.35	0.32
C4'	C18	H19	30.54	1.25			
C4'	C18	H20	30.64	1.15			
C4'	C18	H21	30.59	1.20	1.20	1.06	0.14
C5'	C22	H23	30.41	1.37			
C5'	C22	H24	30.21	1.55			
C5'	C22	H25	30.17	1.59	1.50	1.28	0.22
	C35	H38	23.52	7.80			
	C36	H40	23.29	8.00			
	C41	H42	23.37	7.94			
	C44	H47	24.09	7.27			
	C45	H49	22.31	8.92			
C5a	C1	H5	28.18	3.44	3.44	3.27	0.17
	C50	H51	23.33	7.97			
OTMS	C57	H58	31.59	0.26			
OTMS	C57	H59	31.09	0.73			
C5b	C1	H6	29.56	2.16	2.16	2.16	0.00
OTMS	C57	H60	26.54	0.43			
OTMS	C61	H62	31.71	0.15			
OTMS	C61	H63	31.76	0.10			
OTMS	C61	H64	31.73	0.13			
OTMS	C65	H66	31.56	0.30			
OTMS	C65	H67	33.86	-1.85			
OTMS	C65	H68	32.27	-0.37	-0.01	-0.15	0.14
C2	C2	H7	27.33	4.24	4.24	4.15	0.09
C3a	C3	H8	29.94	1.81	1.81	1.82	0.01
C3b	C3	H82	30.46	1.32	1.32	1.38	0.06
	C84	H87	23.43	7.88			
	C85	H89	23.46	7.85			
C4b	C4	H9	31.20	0.63	0.63	0.63	0.00
	C86	H90	23.52	7.80			
	C88	H91	23.53	7.79			
						MAD	0.13

Table SI-34. Comparison of the experimental *J*-couplings for the *syn*-**14** major product to the calculated *ap* conformers averaged according to Table SI-31.

Scaling Factor:		0.9155			
		Comp. FC	**Comp. FC**	**Syn.**	
Exp. H#	**Comp. H#**	***J* (Hz)**	***J* (Hz) Scaled**	***J*-coupling**	**Abs. Dev.**
5a-5b	5-6	-11.93	-10.92		
5a-4b	5-9	6.87	6.29		
5a-4a	5-10	8.95	8.19		
5b-4a	6-10	8.67	7.94		
5b-4b	6-9	6.27	5.74		
4a-4b	9-10	-13.68	-12.52		
4a-3b	10-82	5.56	5.09		
2-3a	8-7	9.56	8.75	7.6	1.15
3a-3b	8-82	-14.93	-13.67		
2-3b	82-7	3.49	3.19	4.7	1.51
1'-2'	13-15	10.72	9.81	10.3	0.49
2'-3'	15-17	1.89	1.73	1.0	0.73

Table SI-35. Calculated *J*-couplings for the relevant *syn*-**14** *ap* conformers.

	Weight of Conformer:	0.1393	0.3362	0.0028	0.4677	0.0540
Exp. H#	**Comp. H#**	**4**	**58**	**8**	**17**	**46**
5a-5b	5-6	-11.03	-13.22	-11.06	-11.13	-13.19
5a-4b	5-9	10.93	0.58	10.96	10.89	0.56
5a-4a	5-10	9.34	8.31	9.30	9.36	8.22
5b-4a	6-10	10.47	5.87	10.43	10.46	5.78
5b-4b	6-9	1.42	13.84	1.40	1.43	13.85
4a-4b	9-10	-13.94	-13.26	-13.93	-13.95	-13.22
4a-3b	10-82	0.58	13.35	0.58	0.57	13.41
2-3a	8-7	9.70	9.41	9.73	9.67	9.18
3a-3b	8-82	-14.32	-15.15	-14.48	-14.92	-15.34
2'-3b	82-7	0.69	7.80	0.70	0.73	7.90
1'-2'	13-15	10.79	10.51	10.82	10.87	10.55
2'-3'	15-17	1.94	1.84	1.96	1.92	1.84

Table SI-36. Comparison of the experimental *J*-couplings for the *syn*-**14** minor product to the calculated *exo-sc* conformers averaged according to Table SI-33.

Scaling Factor:		0.9155			
		Comp. FC	**Comp. FC**	**Syn.**	
Exp. H#	**Comp. H#**	**J (Hz)**	**J (Hz) Scaled**	**J-coupling**	**Abs. Dev.**
5a-5b	5-6	-11.31	-10.35		
5a-4b	5-9	6.45	5.90		
5a-4a	5-10	7.99	7.32		
5b-4a	6-10	7.19	6.59		
5b-4b	6-9	7.24	6.63		
4a-4b	9-10	-13.41	-12.28		
4a-3b	10-82	7.24	6.63		
2-3a	7-8	9.84	9.00	9.8	0.80
3a-3b	8-82	-14.55	-13.32		
2-3b	82-7	5.73	5.25	2.4	2.85
1'-2'	13-15	11.40	10.44	10.9	0.46
2'-3'	15-17	1.37	1.25	1	0.25

Table SI-37. Calculated *J*-couplings for the relevant *syn*-**14** *exo-sc* conformers.

	Weight of Conformer:	0.4860	0.4150	0.0990
Exp. H#	**Comp. H#**	**33**	**62**	**21**
5a-5b	5-6	-10.08	-12.57	-12.06
5a-4b	5-9	12.68	0.56	0.53
5a-4a	5-10	7.57	8.31	8.74
5b-4a	6-10	8.93	5.53	5.68
5b-4b	6-9	0.64	13.53	13.32
4a-4b	9-10	-13.67	-13.18	-13.07
4a-3b	10-82	0.57	13.38	14.29
2-3a	8-7	11.19	8.94	6.96
3a-3b	8-82	-14.75	-14.53	-13.62
2'-3b	82-7	1.12	9.64	12.02
1'-2'	13-15	11.63	11.29	10.79
2'-3'	15-17	1.27	1.32	2.03

Table SI-38. Calculated ^{13}C NMR δ's for the *syn*-**11** iminium ion.

Exp. #	Comp #	Comp. Isotropic	Comp. δ	Avg. Comp. δ
C5	C1	127.0736	56.9	
C2	C2	100.6921	82.2	
C3	C3	154.3676	30.7	
C4	C4	157.6886	27.5	
C1'	C12	4.3992	174.6	
C2'	C14	114.4977	69.0	
C3'	C16	146.7122	38.0	
C4'	C18	161.9306	23.4	
C5'	C22	165.5088	20.0	
	C27	98.2156	84.6	
	C28	39.8560	140.6	
C5"	C34	22.8471	156.9	
C2"	C36	22.5460	157.2	
C6	C38	48.7216	132.1	
	C39	49.0893	131.7	
	C40	46.4822	134.2	
	C41	22.8941	156.9	
	C42	46.4378	134.3	
	C44	55.6195	125.5	
	C46	51.8209	129.1	
	C48	52.1416	128.8	
	C49	52.1917	128.8	
	C50	205.2978	-18.2	
	C51	181.5245	4.6	
	C53	31.8869	148.2	
	C55	180.5291	5.6	
	C57	30.8771	149.2	
	C58	30.7102	149.4	
	C59	181.3023	4.9	
	C60	31.8039	148.3	
	C62	31.1726	148.9	
	C66	240.5816	-52.0	
	C70	227.3965	-39.4	19.2

Table SI-39. Calculated ^{1}H NMR δ's for the *syn*-**11** iminium ion.

Exp. #	Comp. C #	Comp #	Comp. Isotropic	Comp. δ	Avg. Comp. δ
C(5)H	1	H5	27.1258	4.43	4.43
C(5)H	1	H6	28.2451	3.38	3.38
C(2)H	2	H7	25.7323	5.73	5.73
C(3)H	3	H8	28.3500	3.29	
C(4)H	4	H9	29.8048	1.93	1.93
C(4)H	4	H10	29.0370	2.65	2.65
C(1')H	12	H13	22.0869	9.13	9.13
C(2')H	14	H15	26.5460	4.97	4.97
C(3')H	16	H17	28.5227	3.13	3.13
	18	H19	29.6889	2.04	
	18	H20	29.6119	2.11	
C(4' or 5')H	18	H21	29.6133	2.11	2.09
	22	H23	29.9158	1.83	
	22	H24	29.5853	2.13	
C(4' or 5')H	22	H25	29.7018	2.03	2.00
	27	H29	47.6406	-14.71	
C(3"/C4")H	27	H30	48.4402	-15.46	-15.08
	28	H31	45.5225	-12.73	
C(3"/C4")H	28	H32	22.8399	8.43	-2.15
	40	H43	22.7776	8.49	
	41	H32	26.5383	8.70	
	46	H47	51.9737	-18.75	
	49	H52	31.0776	0.74	
	50	H54	30.9380	0.87	
	55	H56	30.7511	1.05	
	62	H52	31.0776	0.74	
	62	H53	31.8869	-0.01	
	62	H54	30.9380	0.87	
	66	H56	30.7511	1.05	
	66	H57	30.8771	0.93	
	66	H58	30.7102	1.09	
	70	H60	31.8039	0.06	
	70	H61	31.2639	0.57	
OTMS	70	H62	31.1726	0.65	0.66
C(3)H	3	H76	28.8069	2.86	3.07

Table SI-40. Weighted Averaging for the Calculated NMR and NBO calculations for *syn*-**11**, *anti(C1')*-**11**, *anti(C2')*-**11**, and *syn*-**14**

syn-**11** (*ap*) at –54°C

Filename	Computed Energy (H)	Conformer Weight
crest_confs_1_h_2_nmr_2.log	-3561.5159	0.4707
crest_confs_8_h_2_nmr_2.log	-3561.5156	0.1656
crest_confs_5_h_2_nmr_2.log	-3561.5153	0.0668
crest_confs_7_h_2_nmr.log	-3561.5153	0.1344
crest_confs_21_h_7_nmr_2.log	-3561.5145	0.1625

syn-**11** (*exo-sc*) at –54°C

Filename	Computed Energy (H)	Conformer Weight
crest_confs_11_h_2_nmr_2.log	-3561.5131	0.8337
crest_confs_12_h_6_nmr_8.log	-3561.5130	0.1663

anti(C1')-**11** (*ap*) at –54°C

Filename	Computed Energy (H)	Conformer Weight
crest_confs_2_h_5_nmr_2.log	-3561.5137	0.0994
crest_confs_3_h_3_nmr_2.log	-3561.5133	0.4934
crest_confs_39_h_2_nmr.log	-3561.5114	0.1949
crest_confs_7_h_4_nmr_2.log	-3561.5113	0.1826
crest_confs_10_h_5_nmr.log	-3561.5101	0.0105
crest_confs_18_h_2_nmr.log	-3561.5101	0.0099
crest_confs_12_h_5_nmr.log	-3561.5094	0.0093

anti(C1')-**11** (*exo-sc*) at –54°C

Filename	Computed Energy (H)	Conformer Weight
crest_confs_44_h_4_nmr.log	-3561.5098	1

anti(C2')-**11** (*ap*) at –54°C

Filename	Computed Energy (H)	Conformer Weight
crest_confs_55_h_3_low.log	-3561.5143	0.2927
crest_confs_23_h_2_low.log	-3561.5134	0.1472
crest_confs_6_h_3_low.log	-3561.5133	0.0620
crest_confs_7_h_3_low.log	-3561.5129	0.3022
crest_confs_9_h_3_low.log	-3561.5128	0.1959

syn-**14** (*ap*) at –54°C

Filename	Computed Energy (H)	Conformer Weight
crest_confs_8_h_2_low.log	-3713.9415	0.0028
crest_confs_4_h_2_low.log	-3713.9408	0.1393
crest_confs_58_h_2_low.log	-3713.9398	0.3362
crest_confs_17_h_3_low.log	-3713.9389	0.4677
crest_confs_46_h_4_low.log	-3713.9379	0.0540

syn-**14** (*exo-sc*) at –54°C

Filename	Computed Energy (H)	Conformer Weight
crest_confs_33_h_2_low.log	-3713.9381	0.4860
crest_confs_21_h_2_low.log	-3713.9380	0.0990
crest_confs_62_h_3_low.log	-3713.9375	0.4150

DFT NBO Analysis for 11 and 14

NBO analysis was performed assess the $n_{N(cat)}$-$\sigma^*_{C\text{-}N(imide)}$ interaction differences between the *ap* and *exc-sc* conformers for **11** and **14**, and between the *syn* and *anti* (C1')-**11** diastereomers The *syn* interactions were higher in energy when compared to the *anti*-conformers for **11**, with a minor difference in the weighted energies between the *ap* and *exo-sc* products (0.31 kcal mol^{-1}). The phthalimide aminal had a similar difference in energies between the two rotational isomers (0.30 kcal mol^{-1}).

Table SI-41. DFT NBO Analysis

***syn*-11 (*ap*) Interaction:**	**LP(1)N11-BD*(1)C12-N33**	
Conformer	**E2 Stabilization Energy (kcal mol^{-1})**	**Conformer Weight**
1	17.91	0.4707
5	17.09	0.0668
7	17.74	0.1344
8	17.08	0.1656
21	16.92	0.1625
Weighted Energy:	17.53	

***syn*-11 (*exo-sc*) Interaction:**	**LP(1)N11-BD*(1)C12-N33**	
Conformer	**E2 Stabilization Energy (kcal mol^{-1})**	**Conformer Weight**
11	17.19	0.8337
12	17.36	0.1663
Weighted Energy:	17.22	

***anti(C1')*-11 Interaction:**	**LP(1)N11-BD*(1)C12-N33**	
Conformer	**E2 Stabilization Energy (kcal mol^{-1})**	**Orientation of OTMS**
crest_confs_2_h_5_nmr_2.log	7.95	Ap
crest_confs_3_h_3_nmr_2.log	7.68	Ap
crest_confs_39_h_2_nmr.log	7.84	Ap
crest_confs_7_h_4_nmr_2.log	7.51	Ap
crest_confs_10_h_5_nmr.log	8.51	Ap
crest_confs_18_h_2_nmr.log	8.42	Ap
crest_confs_44_h_4_nmr.log	7.48	Exo-sc
crest_confs_12_h_5_nmr.log	15.91	Ap

***syn*-14 (*ap*) Interaction:**	**LP(1)N11-BD*(1)C12-N28**	
Conformer	**E2 Stabilization Energy (kcal mol^{-1})**	**Conformer Weight**
crest_confs_8_h_2_low.log	16.65	0.0028
crest_confs_4_h_2_low.log	16.65	0.1393
crest_confs_58_h_2_low.log	15.99	0.3362
crest_confs_17_h_3_low.log	16.48	0.4677
crest_confs_46_h_4_low.log	15.86	0.0540
Weighted Energy:	16.31	

***syn*-14 (*exo-sc*) Interaction:**	**LP(1)N11-BD*(1)C12-N28**	
Conformer	**E2 Stabilization Energy (kcal mol^{-1})**	**Conformer Weight**
crest_confs_33_h_2_low.log	15.97	0.4860
crest_confs_21_h_2_low.log	15.52	0.0990
crest_confs_62_h_3_low.log	16.17	0.4150
Weighted Energy:	16.01	

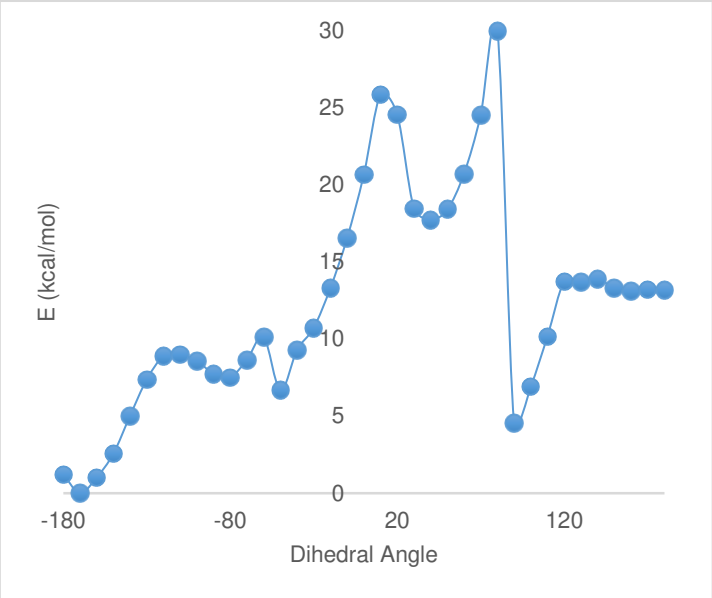

Frame	Diheral Angle	Relative (kcal mol^{-1})	Energy
1	-180	1.24	
2	-170	0.00	
3	-160	1.02	
4	-150	2.57	
5	-140	5.03	
6	-130	7.38	
7	-120	8.88	
8	-110	8.98	
9	-100	8.58	
10	-90	7.75	
11	-80	7.52	
12	-70	8.65	
13	-60	10.12	
14	-50	6.68	
15	-40	9.28	
16	-30	10.73	
17	-20	13.31	
18	-10	16.54	
19	0	20.66	
20	10	25.84	
21	20	24.55	
22	30	18.48	
23	40	17.73	
24	50	18.40	

25	60	20.71
26	70	24.51
27	80	29.97
28	90	4.55
29	100	6.92
30	110	10.18
31	120	13.73
32	130	13.70
33	140	13.90
34	150	13.30
35	160	13.09
36	170	13.19
37	180	13.16

Figure SI-29. Dihedral angle scan to calculate the *ap* to *exo-sc* rotational barrier for *syn*-**14**.

Structure Search in the CCDC Data Base

A structure search in the CCDC data base for Jørgensen-Hayashi catalysts **9b** and **9c** with the pyrrolidine nitrogen bound to a stereogenic sp^3 hybridized carbon reveals striking similarities concerning the catalyst structure. Each structure in the database had the pyrrolidine ring in an envelope conformation with the γ-carbon tilted out of plane toward the diarylsilylether moiety and the nitrogen lone pair (down conformation). For the orientation of the diarylsilylether group, two distinct conformational minima can be observed. In 7/10 crystal structures, the N- and O-substituent at the exocyclic C-C bond of the catalyst possess an antiperiplanar (*ap*) relationship whereas in three cases an exo-synclinal (*exo-sc*) conformation was adopted.

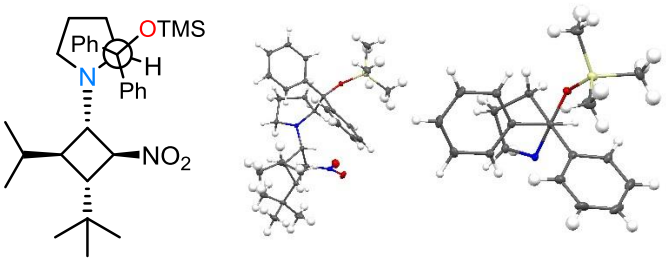

Figure SI-30. 883666[46,47] (*ap*)

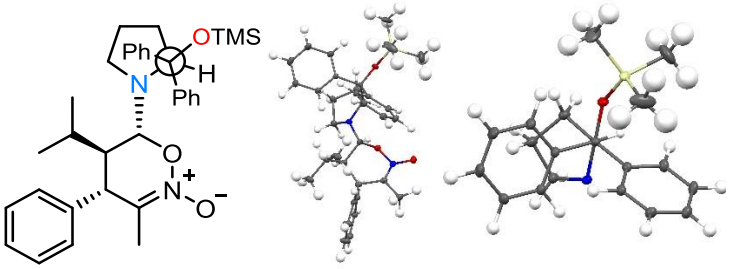

Figure SI-31. 883667[46,47] (*ap*)

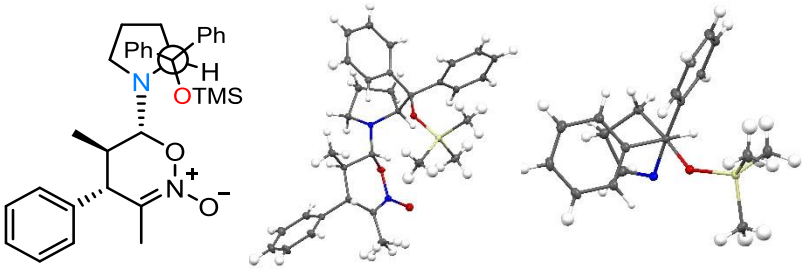

Figure SI-32. 883668[46,47] (*sc-exo*)

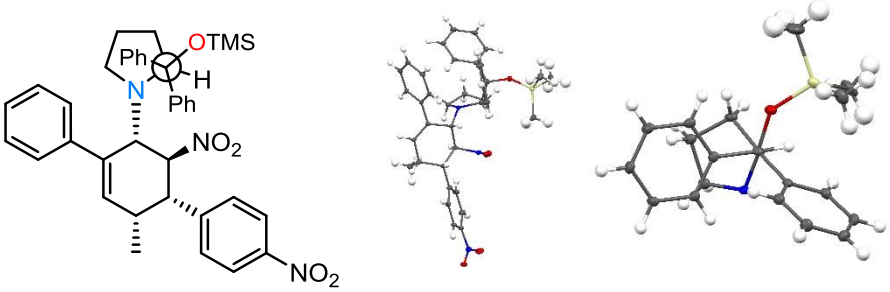

Figure SI-33. 885695[48] (*ap*)

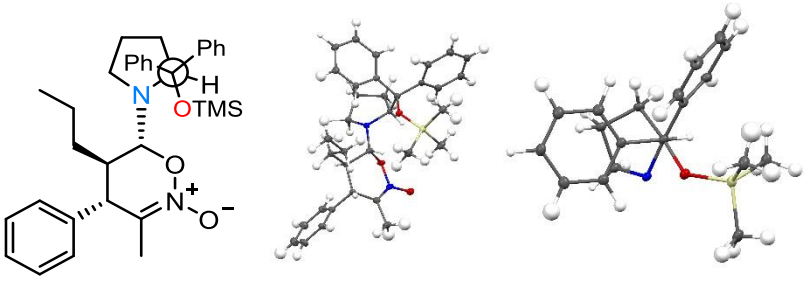

Figure SI-34. 919662[47] (*sc-exo*)

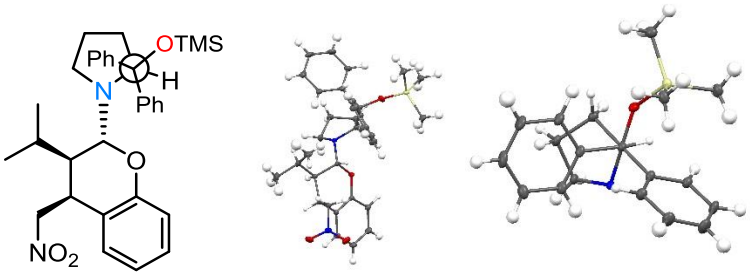

Figure SI-35. 919664[47] (*ap*)

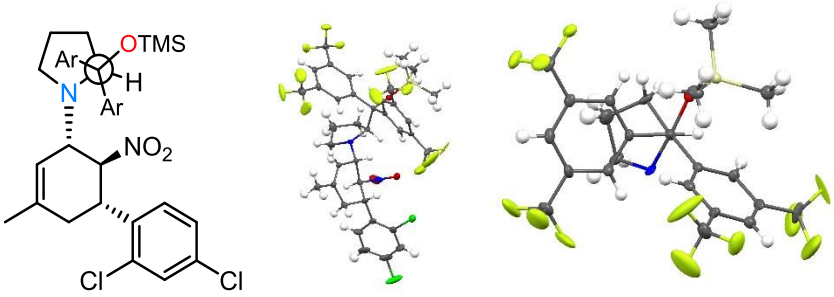

Figure SI-36. 973119[49] (*ap*)

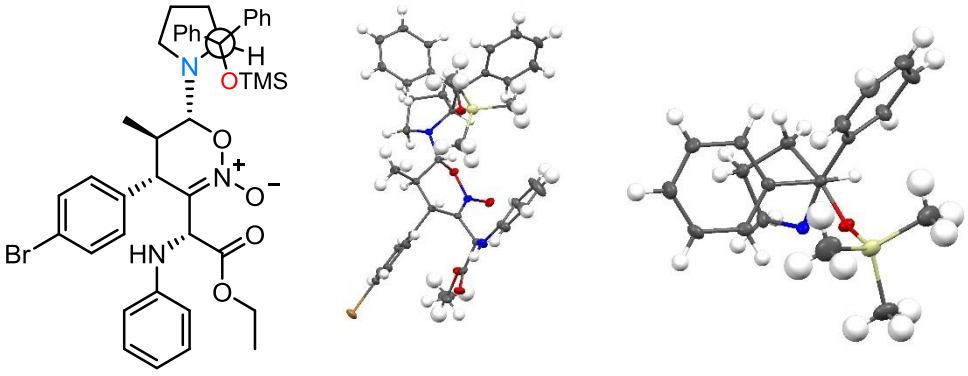

Figure SI-37. 1434063[50] (*sc-exo*)

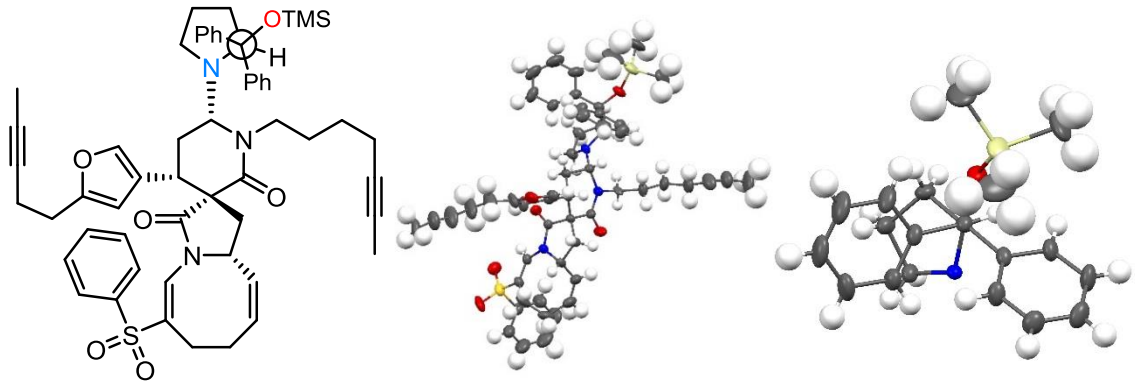

Figure SI-38. 1521504[51] (*ap*)

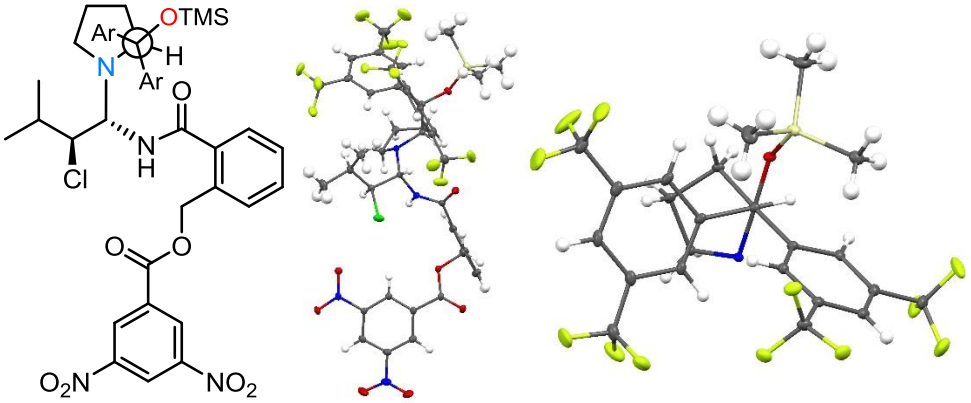

Figure SI-39. 2045387 (*ap*)
(This work)

3.1.3. Decomposition and Deuterium Incorporation Studies

Decomposition and deuterium incorporation experiments were envisioned to shed more light on the decomposition mechanism of aminal **14** and should allow the distinction between E2-elimination (via chloroenamine)[28] and hydrolysis via chloroiminium ion.

Decomposition of Aminal 14 (1)

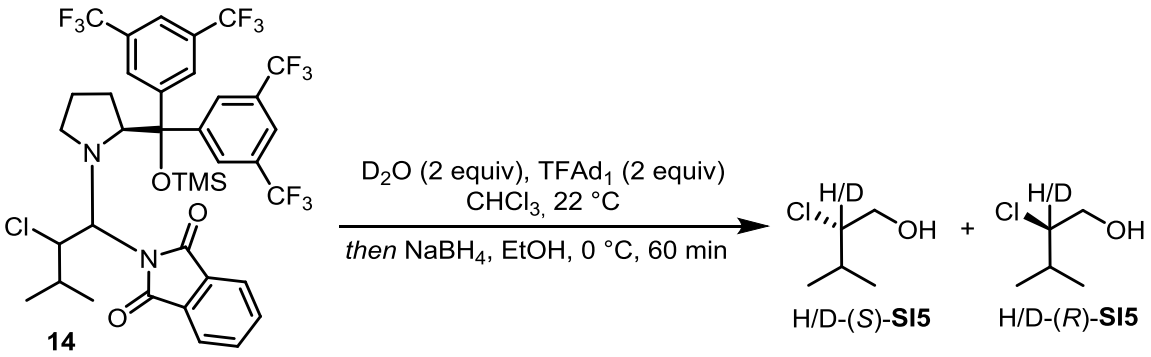

D_2O (36.1 µL, 2.00 mmol, 2.0 equiv) and $TFAd_1$ (154 µL, 2.00 mmol, 2.0 equiv) were added subsequently to a solution of aminal **14** (0.847 g, 1.00 mmol, 1.0 equiv) in $CHCl_3$ (50 mL) at 22 °C. Aliquots (5 mL) were taken from the reaction mixture after defined points of time (10 min, 30 min, 60 min, 2 h, 4 h, 22 h, 70 h) and added to a solution of $NaBH_4$ (18.9 mg, 500 µmol, 5.0 equiv) in EtOH (2.0 mL). After 30 min the reactions were quenched with aqueous saturated NH_4Cl.The aqueous phase was extracted with EtOAc (3x5 mL), the combined organic phases were dried over Na_2SO_4 and the solvent was removed under reduced pressure. The crude products were purified by column chromatography (SiO_2, pentane/EtOAc 10:1). Deuterium incorporation was quantified by ^{1}H-NMR spectra analysis and the enantiomeric excess was determined by chiral GC.

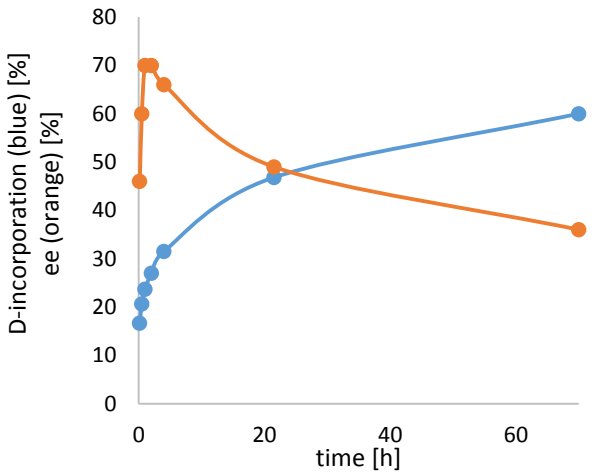

t [min]	t [h]	integration 3.93 ppm	integration 3.81 ppm	deuterium incorp. [%]	ee [%]
10	0,2	1,00	1,20	16,67	46
30	0,5	1,00	1,26	20,63	60
60	1,0	1,00	1,31	23,66	70
120	2,0	1,00	1,37	27,01	70
240	4,0	1,00	1,46	31,51	66
1290	21,5	1,00	1,88	46,81	49
4200	70,0	1,00	2,50	60,00	36

Figure SI-40. Monitoring of the decomposition of aminal **14** with deuterium incorporation and ee over time.

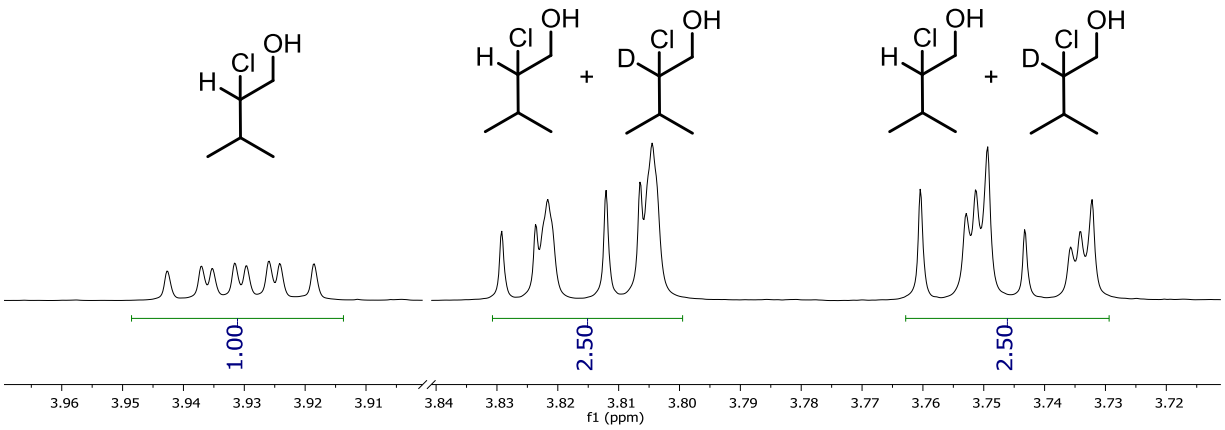

Figure SI-41. Exemplary ^{1}H-NMR spectrum of a reduced sample (70 h).

When synthesizing aminal **14** it was not possible to remove all chloroaldehyde residues under reduced pressure. At the beginning of the decomposition experiment, these residues are present in higher concentrations than the chloroaldehydes formed by the decomposition of the aminal. As a consequence, the ee of the first sample (t = 10 min; ee = 46%) corresponds roughly with the ee of the products formed from the α-chlorination reaction (ee = 49% with NCS). Over time, the proportion of chloroaldehyde originating from the decomposition of the aminal increases compared to the chloroaldehyde originating from the α-chlorination reaction. Since the aminal decomposes exclusively to the (*S*)-chloroaldehyde (see decomposition with the aminal **SI6** derived from propanal), the ee increases over time. The acid-catalyzed (TFA-d_1) racemization of the chloroaldehydes subsequently leads to a continuous decrease of the ee over time. A comparison with the decomposition experiment of the propanal-derived aminal (aminal could be obtained without chloroaldehyde impurities) helps to rationalize this experiment.

Decomposition of Aminal 14 (2)

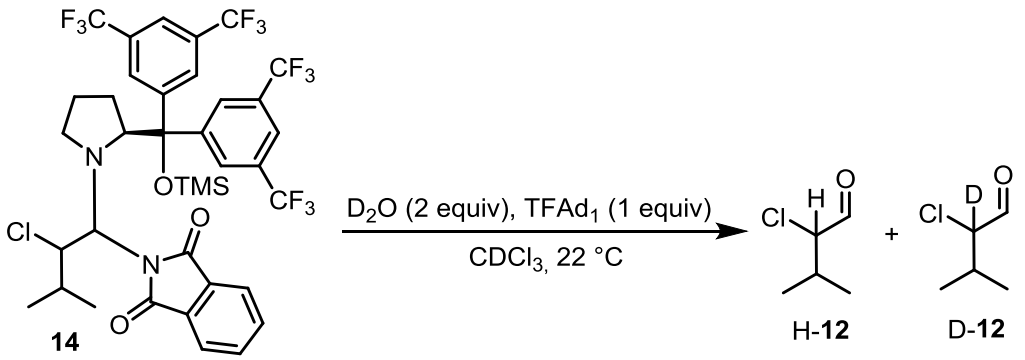

0.60 mL of a stock solution ($CDCl_3$ (6.0 mL), D_2O (4.73 µL) and $TFAd_1$ (9.11 µL)) was added to a NMR-tube containing aminal **14** (10.0 mg, 11.8 µmol, 1.0 equiv). The NMR-tube was tightly sealed and ^{1}H-NMR spectra were recorded every 5 min over a period of 10 h. Two additional spectra were recorded after 24 h and 43 h. Conversion was quantified by ^{1}H-NMR spectra analysis with $CDCl_3$ as the internal standard. Deuterium incorporation was qualitatively evaluated by ^{1}H-NMR spectroscopy.

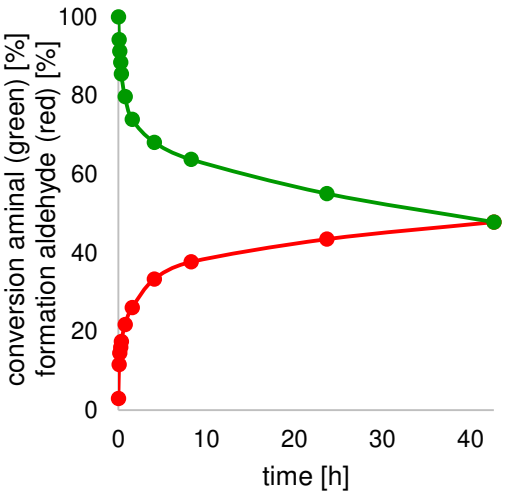

time [min]	time [h]	integration aldehyde 9.52 ppm	conversion aldehyde [%]	integration aminal 5.03 ppm	conversion aminal [%]
0	0,0	0,02	3	0,69	100
5	0,1	0,08	12	0,65	94
10	0,2	0,1	14	0,63	91
15	0,3	0,11	16	0,61	88
20	0,3	0,12	17	0,59	85
45	0,8	0,15	22	0,55	80
95	1,6	0,18	26	0,51	74
245	4,1	0,23	33	0,47	68
495	8,3	0,26	38	0,44	64
1420	23,7	0,3	43	0,38	55
2560	42,7	0,33	48	0,33	48

Figure SI-42. Monitoring of the decomposition of aminal **14**.

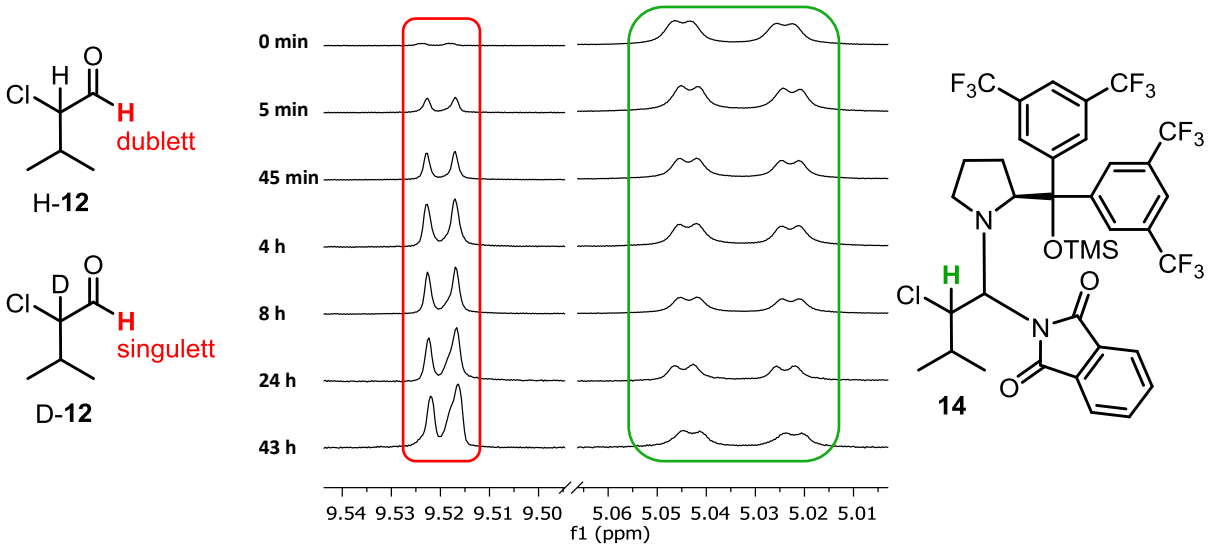

Figure SI-43. ^{1}H-NMR spectra of the ongoing decomposition reaction (2 equiv of D_2O, 1 equiv of $TFAd_1$) of aminal **14** allows a qualitative evaluation of the deuterium incorporation into the α-chloroaldehydes.

The analysis of the aldehyde-H signals in the ^{1}H-NMR spectra allows a qualitative evaluation of the deuterium incorporation into the α-chloroaldehydes. Almost no deuterium incorporation was observed during the first hours. Downstream incorporation of deuterium into the chloroaldehyde can be explained by acid-catalyzed enolization or enamine formation (doublet at 9.52 ppm (α-H-chloroaldehyde) -> singlet at 9.52 ppm (α-D-chloroaldehyde)).

Decomposition of Aminal 14 (3)

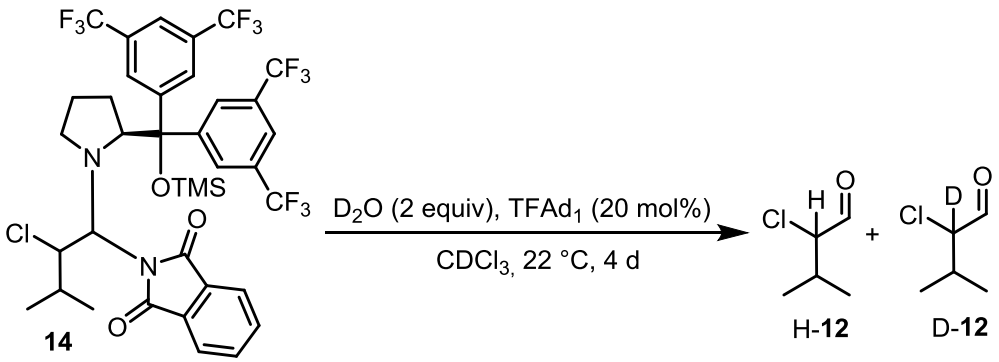

0.60 mL of a stock solution ($CDCl_3$ (6.0 mL), D_2O (4.73 µL) and $TFAd_1$ (1.82 µL)) was added to a NMR-tube containing aminal **14** (10.0 mg, 11.8 µmol, 1.0 equiv). The NMR-tube was tightly sealed and ^{1}H-NMR spectra were recorded over a period of 4 days. Deuterium incorporation and conversion was qualitatively evaluated by ^{1}H-NMR spectroscopy.

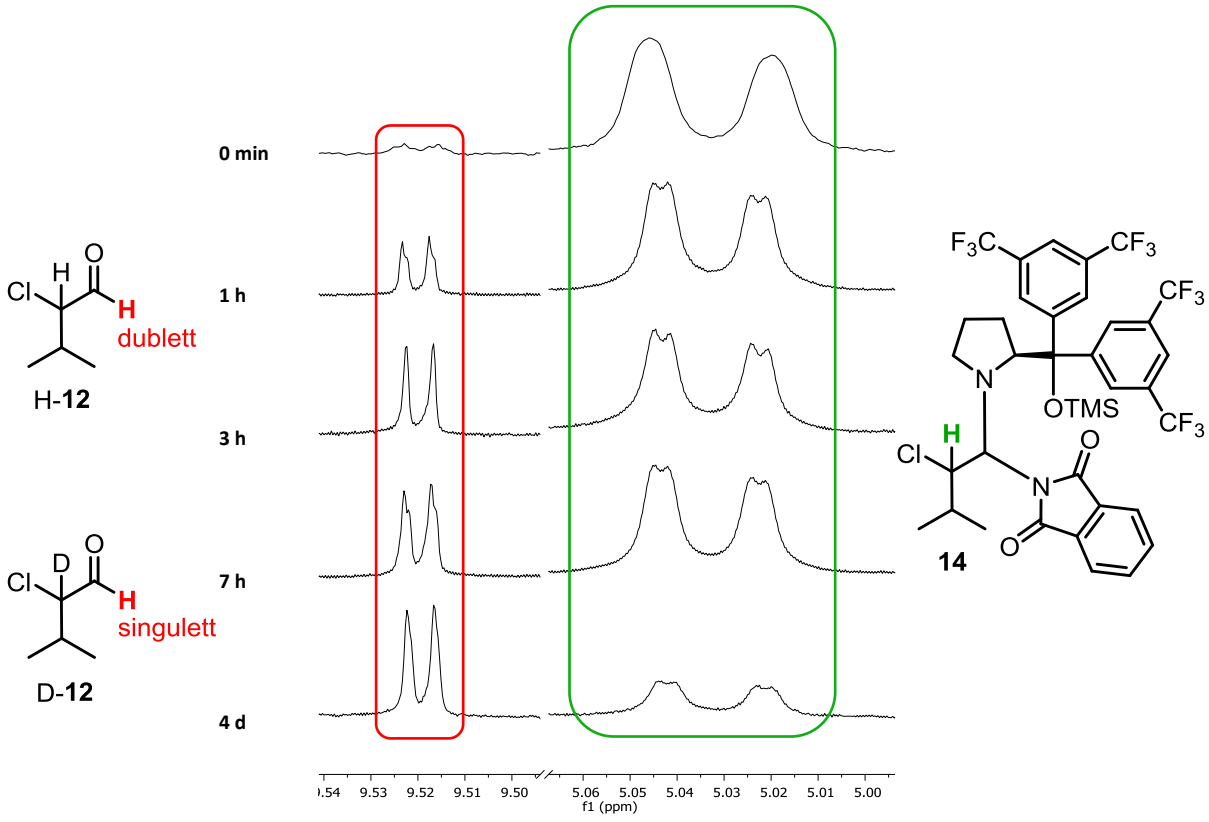

Figure SI-44. ^{1}H-NMR spectra of the ongoing decomposition reaction (2 equiv of D_2O, 20 mol% of $TFAd_1$) of aminal **14** allows a qualitative evaluation of the deuterium incorporation into the α-chloroaldehydes.

Lowering the amount of TFA-d_1 (from to 2 equiv to 20 mol%) leads to a slower decomposition of aminal **14**. Deuterium incorporation into the α-position of the aldehyde can be almost completely suppressed when using 20 mol% TFA-d_1 (clean doublet for the aldehyde-proton).

Decomposition of Aminal 14 (4)

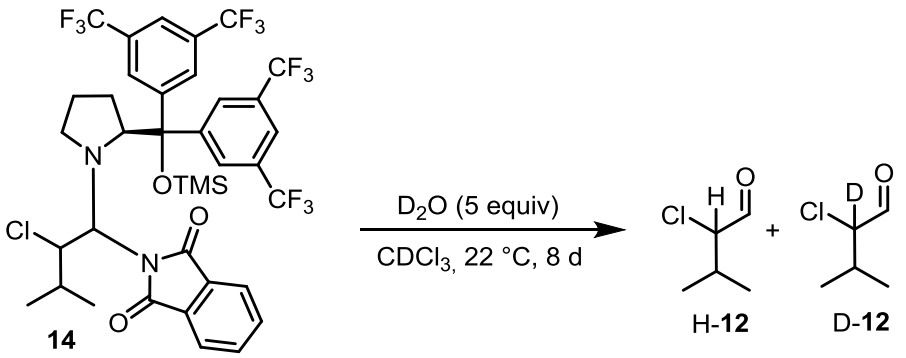

0.60 mL of a stock solution ($CDCl_3$ (6.0 mL), D_2O (11.8 µL)) was added to a NMR-tube containing aminal **14** (10.0 mg, 11.8 µmol, 1.0 equiv). The NMR-tube was tightly sealed and ^{1}H-NMR spectra were recorded over a period of 8 days. Deuterium incorporation and conversion was qualitatively and quantitatively evaluated by ^{1}H-NMR spectroscopy.

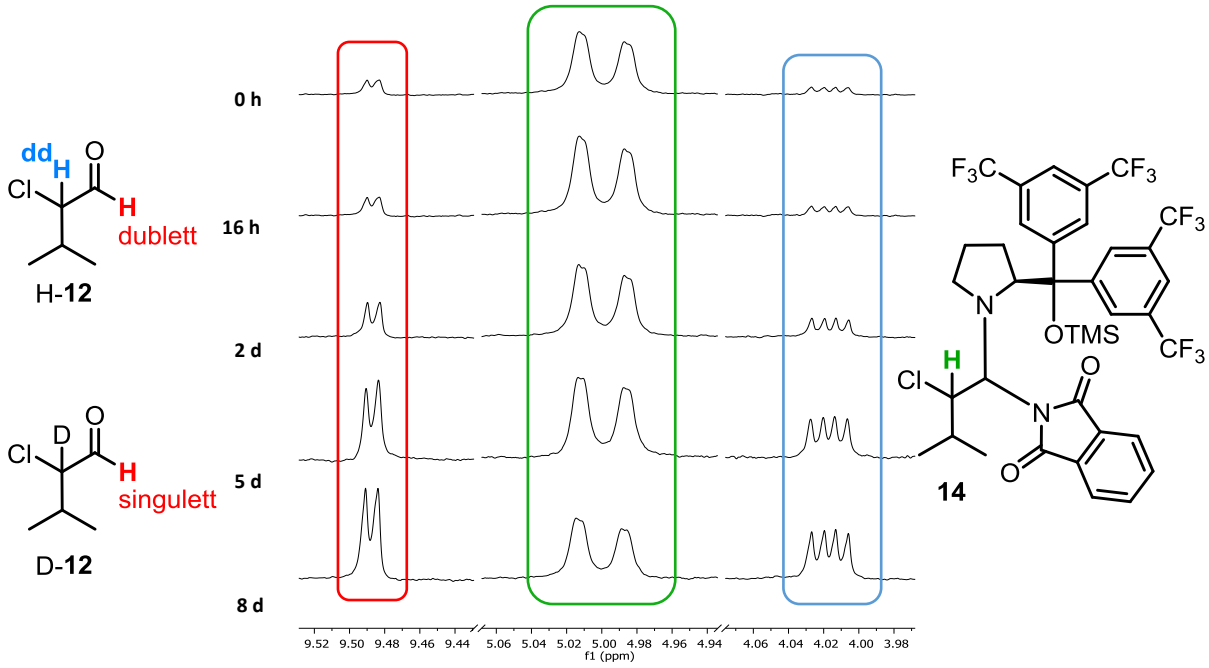

Figure SI-45. ^{1}H-NMR spectra of the ongoing decomposition reaction (5 equiv of D_2O) of aminal **14** allows a qualitative evaluation of the deuterium incorporation into the α-chloroaldehydes.

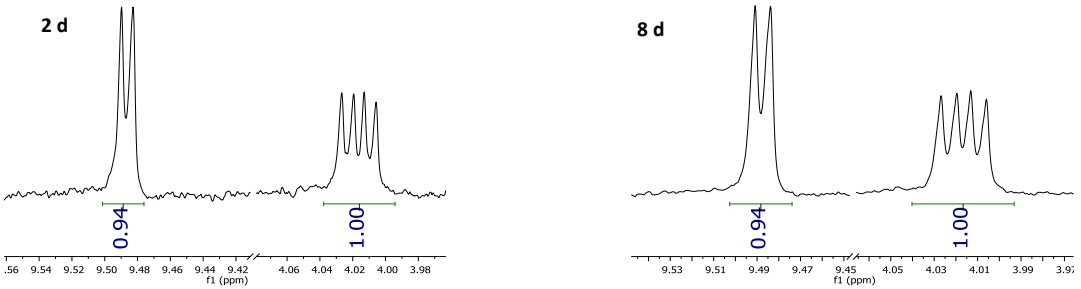

Figure SI-46. Exemplary ^{1}H-NMR spectra (after 2 d and 8 d) of the ongoing decomposition reaction (5 equiv of D_2O) of aminal **14** allows a quantification of the deuterium incorporation into the α-position.

Omitting acidic conditions further decreases the rate of aminal hydrolysis. Nevertheless, only D_2O can mediate the decomposition effectively. As shown in the figure above, aminal hydrolysis under non acidic conditions takes place without any detectable incorporation of deuterium in the α-position of the aldehyde over long term (8 days). The sharp doublet of the aldehyde proton (red) and the 1:1 ratio between the aldehyde proton (red) and the α-proton of the aldehyde (orange) prove this issue. E2-elimination of the aminal with generation of chloroenamines, as proposed for the Curtin-Hammett-scenario cannot explain the complete absence of deuterium incorporation. Whereas the “classical” hydrolysis pathway via chloroiminium ion with an intact α-position is in line with the absence of deuterium incorporation.

(*S*)-2-chloro-3-methylbutan-1-ol ((*S*)-SI5)

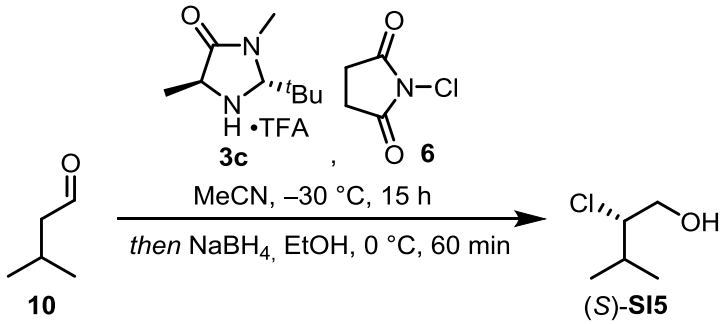

Isovaleraldehyde (0.215 mL, 2.00 mmol, 1.0 equiv) was dissolved in MeCN (8.0 mL) and cooled to –30 °C. Catalyst **3c** (0.114 g, 0.400 mmol, 20 mol%) and NCS (0.320 g, 2.40 mmol, 1.2 equiv) were added subsequently and the reaction mixture was stirred for 15 h at the same temperature. After the reaction was warmed to 0 °C, MeOH (3.0 mL) and $NaBH_4$ (0.189 g, 5.00 mmol, 2.5 equiv) were added and the mixture was stirred for 60 min at the same temperature. The reaction was quenched with aqueous saturated NH_4Cl (10 mL), the aqueous phase was extracted with dichloromethane (3x15 mL) and the combined organic phases were dried over $NaSO_4$. The solvent was removed under reduced pressure and the crude product was purified by column chromatography (Silica, pentane/EtOAc 10:1). Pure chloroalcohol (*S*)-**SI5** (0.111 g, 0.905 mmol, 45%, 89% ee) was obtained as a colorless oil.

^{1}H-NMR ($CDCl_3$, 400 MHz) δ = 3.92 (ddd, *J* = 7.8, 5.2, 3.8 Hz, 1H), 3.81 (dd, *J* = 12.0, 3.8 Hz, 1H), 3.73 (dd, *J* = 12.0, 7.8 Hz, 1H), 2.12 – 2.03 (m, 1H), 2.02 (s, 1H), 1.03 (d, *J* = 6.8 Hz, 3H), 1.01 (d, *J* = 6.7 Hz, 3H) ppm.

(*R*)-2-chloro-3-methylbutan-1-ol ((*R*)-SI5)

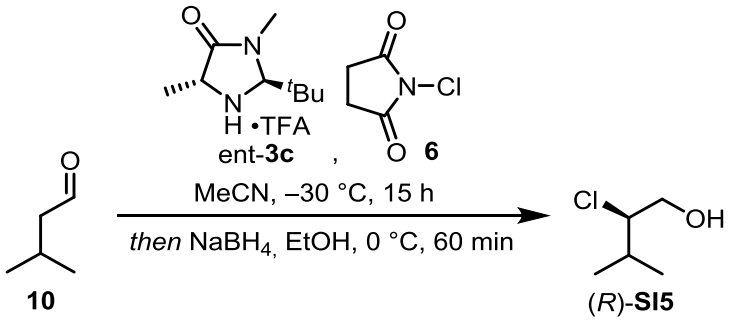

Isovaleraldehyde (0.215 mL, 2.00 mmol, 1.0 equiv) was dissolved in MeCN (8.0 mL) and cooled to –30 °C. Catalyst *ent*-**3c** (0.114 g, 0.400 mmol, 20 mol%) and NCS (0.320 g, 2.40 mmol, 1.2 equiv) were added subsequently and the reaction mixture was stirred for 15 h at the same temperature. After the reaction was warmed to 0 °C, MeOH (3.0 mL) and $NaBH_4$ (0.189 g, 5.00 mmol, 2.5 equiv) were added and the mixture was stirred for 60 min at the same temperature. The reaction was quenched with aqueous saturated NH_4Cl (10 mL), the aqueous phase was extracted with dichloromethane (3x15 mL) and the combined organic phases were dried over $NaSO_4$. The solvent was removed under reduced pressure and the crude product was purified by column chromatography (Silica, pentane/EtOAc 10:1). Pure chloroalcohol (*R*)-**SI5** (0.102 g, 0.832 mmol, 42%, 95% ee) was obtained as a colorless oil.

Spectroscopic data are in accordance with the previous experiment.

3.2. Aminals Derived from Propanal

3.2.1. Synthesis

When synthesizing aminal **14**, it was not possible to remove all impurities of isovaleraldehyde (**10**) and 2-chloro-3-methylbutanal (**12**) under reduced pressure. Due to the fact, that a pure and aldehyde-free aminal is crucial for some follow-up experiments we changed from isovaleraldehyde to the more volatile propanal. As a result, all aldehyde-impurities could be removed under reduced pressure.

2-(1-((*S*)-2-(bis(3,5-bis(trifluoromethyl)phenyl)((trimethylsilyl)oxy)methyl)pyrrolidin-1-yl)-2-chloropropyl)isoindoline-1,3-dione (SI6)

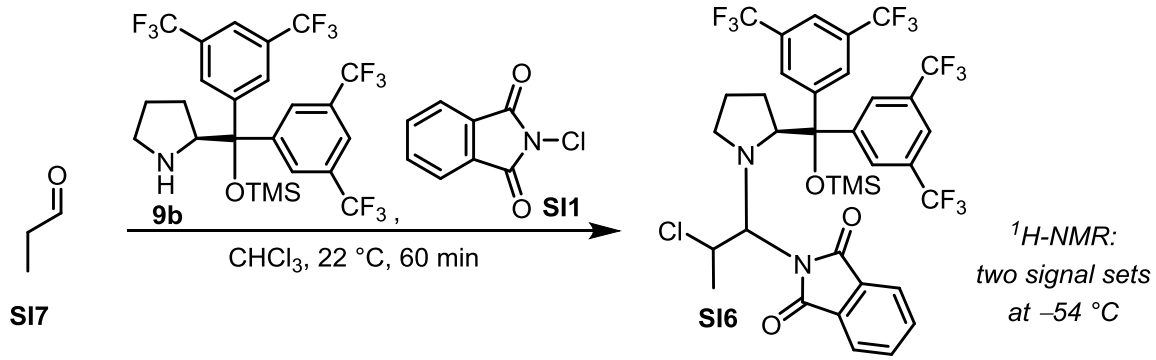

Catalysts **9b** (2.91 g, 4.87 mmol, 50 mol%) and NCP (0.884 g, 4.87 mmol, 0.5 equiv) were added successively to a solution of propanal (0.698 mL, 9.74 mmol, 1.0 equiv) in $CHCl_3$ (44 mL) at 22 °C. After 60 min the solvent and aldehydes were removed under reduced pressure. The crude product was dissolved in pentane (20 mL) and the precipitating solids were filtered off. Pentane was removed under reduced pressure and the aminal **SI6** was obtained as a foamy off-white solid (3.54 g, 4.32 mmol, 89%). ^{1}H-NMR spectroscopy at –54 °C shows two signal sets with a ratio of 68:32.

mp = 65 °C

IR (ATR): $\tilde{\nu}$ = 3055, 2988, 2307, 1713, 1280, 1264, 1176, 1139, 844, 733, 704 cm^{-1}.

HRMS (ESI, pos. mode): *m*/*z* calculated for $C_{35}H_{31}ClF_{12}N_2NaO_3Si$ $[M+Na]^+$: 841.1493, found 841.1487; *m*/*z* calculated for $C_{35}H_{31}ClF_{12}KN_2O_3Si$ $[M+K]^+$: 857.1233, found 857.1207.

major stereoisomer:

^{1}H-NMR ($CDCl_3$, 600 MHz, –54 °C) δ = 5.88 (d, *J* = 10.5 Hz, 1H), 5.19 (dq, *J* = 13.1, 6.7 Hz, 1H), 4.18 (dd, *J* = 10.2, 3.2 Hz, 1H), 3.00 (td, *J* = 9.5, 6.5 Hz, 1H), 2.46 (ddd, *J* = 9.9, 6.8, 3.4 Hz, 1H), 1.86 – 1.81 (m, 1H), 1.79 (d, *J* = 6.8 Hz, 3H), 1.40 – 1.34 (m, 1H), 1.32 – 1.26 (m, 1H), 0.41 – 0.31 (m, 1H), -0.18 (s, 9H) ppm.

^{13}C-NMR ($CDCl_3$, 151 MHz, –54 °C) δ = 171.0, 170.9, 83.7, 77.9, 66.8, 55.0, 47.6, 27.9, 23.8, 23.3, 1.5 ppm.

minor stereoisomer:

^{1}H-NMR ($CDCl_3$, 600 MHz, –54 °C) δ = 5.01 – 4.92 (m, 1H), 4.91 – 4.87 (m, 1H), 4.58 (d, *J* = 8.1 Hz, 1H), 3.12 (q, *J* = 8.3 Hz, 1H), 2.28 – 2.23 (m, 1H), 1.73 – 1.67 (m, 1H), 1.64 – 1.58 (m, 1H), 1.24 – 1.20 (m, 1H), 0.99 (d, *J* = 6.3 Hz, 3H), -0.15 (s, 9H) ppm.

^{13}C-NMR ($CDCl_3$, 151 MHz, –54 °C) δ = 171.1, 170.2, 78.5, 70.0, 53.8, 48.0, 27.4, 24.1, 22.3, 1.7 ppm.

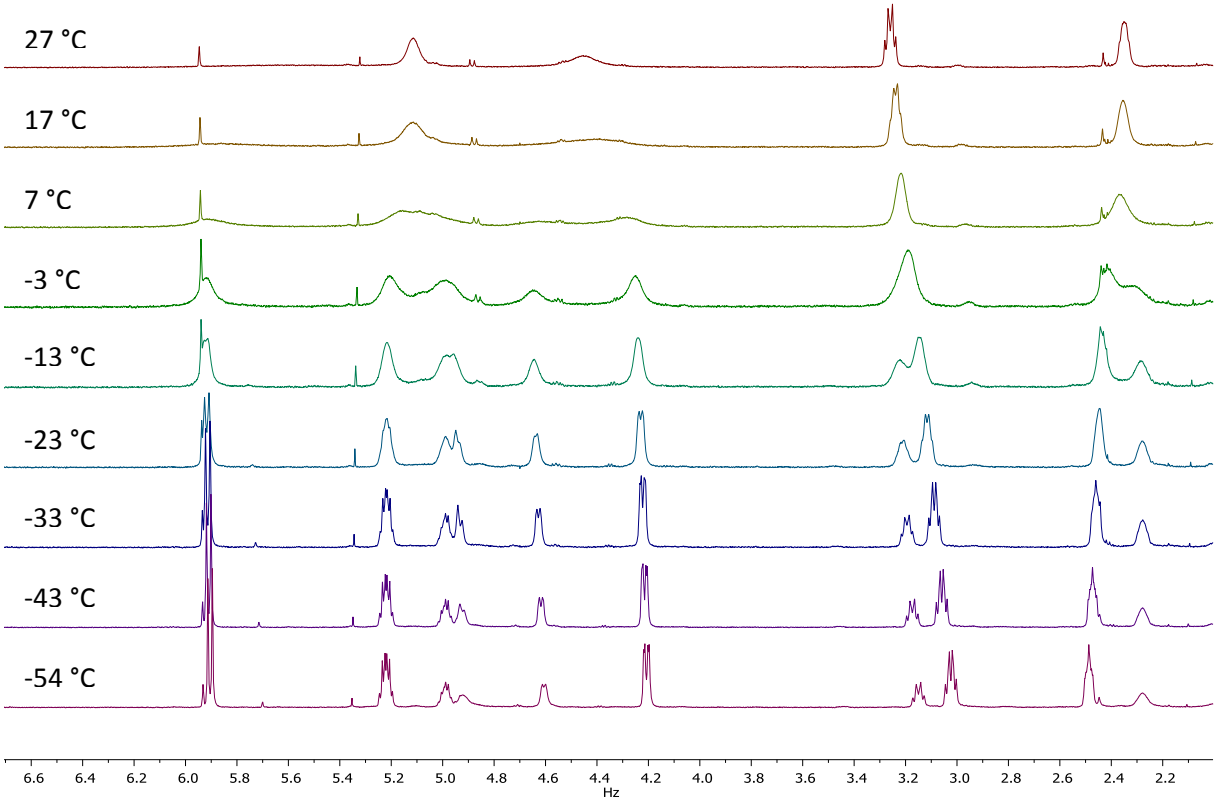

Figure SI-47. ^{1}H-NMR spectra of aminal **SI6** at different temperatures shows the emergence of two signal sets at low temperatures.

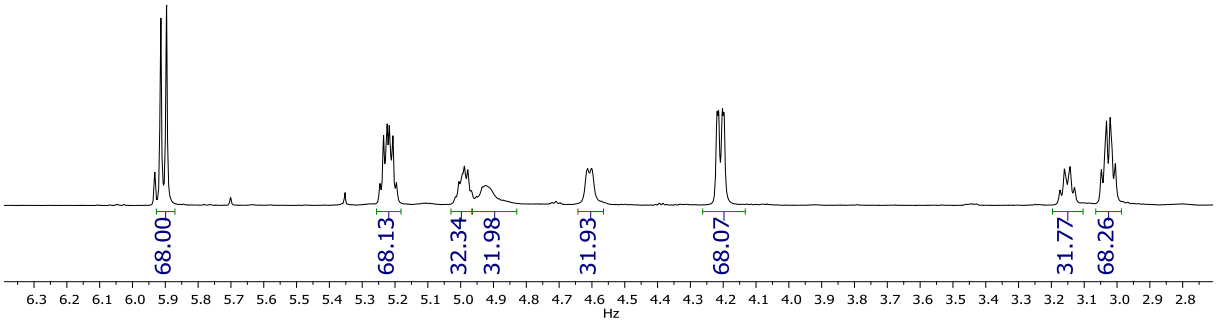

Figure SI-48. The isomeric ratio (68:32) was assigned at –54 °C.

The combination of aldehyde, Jørgensen-Hayashi-type catalyst **9b**, and NCP generates almost quantitatively the corresponding aminal species. As a consequence, the conversion of the aldehyde to the α-chloroaldehyde is always below 5%. The low conversion in combination with the high volatility of aldehyde **SI8** and alcohol **SI9** makes the isolation and purification difficult. To overcome these problems, the *in-situ* reduced chloroaldehyde **SI8** was directly transformed into the non-volatile 3,5-dinitrobenzoylester **SI10**.

Enantiomeric Excess (Propanal, Catalyst 9b and NCS/NCP)

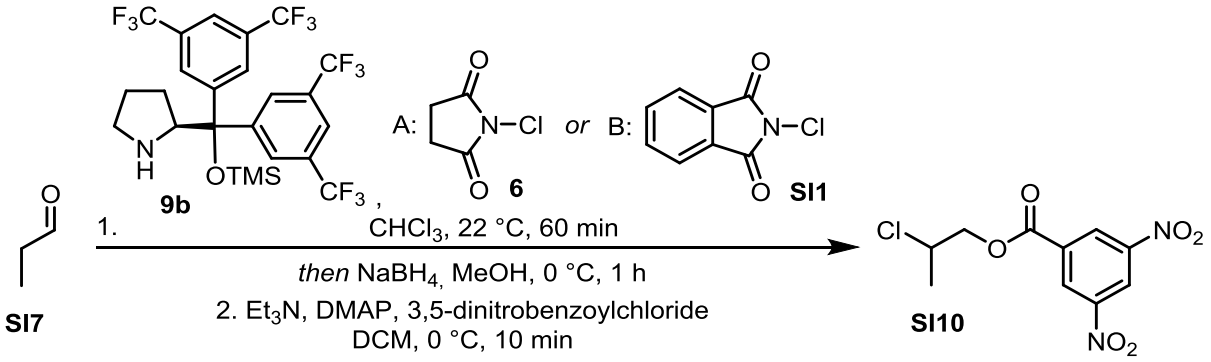

Propanal (0.359 mL, 5.00 mmol, 1.0 equiv) was dissolved in $CHCl_3$ (10.0 mL) at 22 °C. Catalyst **9b** (0.299 g, 0.500 mmol, 10 mol%) and A: NCS (0.734 g, 5.50 mmol, 1.1 equiv) or B: NCP (0.999 g, 5.50 mmol, 1.1 equiv) were added subsequently and the reaction mixture was stirred for 60 min at the same temperature. After the reaction was cooled to 0 °C, MeOH (3.3 mL) and $NaBH_4$ (0.473 g, 12.5 mmol, 2.5 equiv) were added and the mixture was stirred for 60 min at the same temperature. The reaction was quenched with aqueous saturated NH_4Cl (10 mL), the aqueous phase was extracted with dichloromethane (3x15 mL) and the combined organic phases were dried over $NaSO_4$. The solvent was removed under reduced pressure (product is volatile!) and the crude product was dissolved in dichloromethane (10 mL). The solution was cooled to 0 °C and DMAP (30.5 mg, 0.250 mmol, 0.1 equiv) and 3,5-dinitrobenzoylchloride (0.749 g, 3.25 mmol, 1.3 equiv) were added subsequently. Et_3N (0.589 mL, 4.25 mmol, 1.7 equiv) was added dropwise and the reaction mixture was stirred for 10 min at 0 °C. The reaction was quenched with aqueous saturated $NaHCO_3$ (10 mL), the aqueous phase was extracted with dichloromethane (3x15 mL) and the combined organic phases were dried over $NaSO_4$. The solvent was removed under reduced pressure and the crude product was purified by column chromatography (Silica, pentane/EtOAc 10:1).

A: Ester **SI10** (0.073 g, 0.253 mmol, 5%, 5% ee for the (*R*)-enantiomer) was obtained as a yellow oil.
B: Ester **SI10** (0.050 g, 0.173 mmol, 3%, 14% ee for the (*R*)-enantiomer) was obtained as a yellow oil.

^{1}H-NMR ($CDCl_3$, 600 MHz) δ = 9.23 (t, *J* = 2.1 Hz, 1H), 9.16 (d, *J* = 2.1 Hz, 2H), 4.57 (dd, *J* = 11.6, 5.1 Hz, 1H), 4.53 (dd, *J* = 11.6, 7.0 Hz, 1H), 4.44 – 4.31 (m, 1H), 1.64 (d, *J* = 6.7 Hz, 3) ppm.

^{13}C-NMR ($CDCl_3$, 151 MHz) δ = 162.2, 148.8, 133.4, 129.6, 122.8, 70.5, 53.6, 21.5.ppm.

HRMS (EI): *m/z* calculated for $C_{10}H_{10}ClN_2O_6$ $[M+H]^+$: 289.0222, found 289,0219.

The low ee and the inverted absolute configuration (compared to isovaleraldehyde) for propanal as a substrate may be due to the lower energy barrier for the rotation around the C-N-bond of the enamine compared to other substrates carrying more bulky alkyl-substituents (isovaleraldehyde).[52]

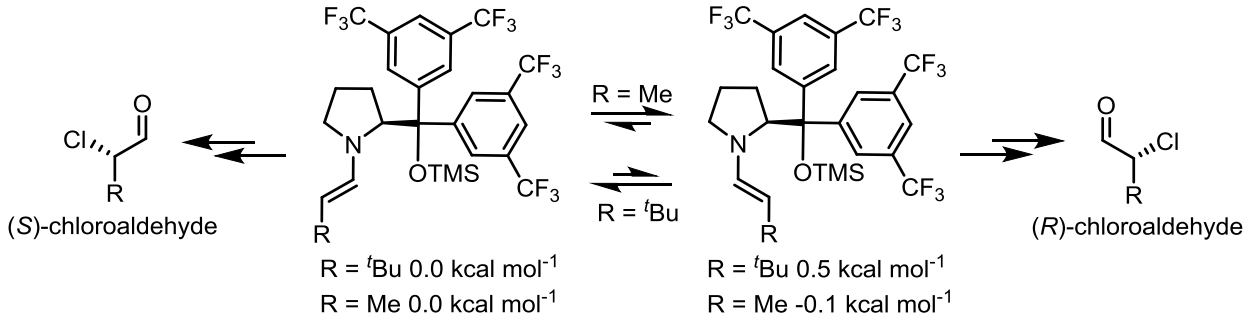

Figure SI-49. Relative free energies (ΔG) of isovaleralydehyde- and propanal-derived enamines according to Jørgensen et al.[52]

By simply replacing the substrate (isovaleraldehyde → propanal) we demonstrated that the correlation between the ratio of interconverting aminals (68:32; 36% excess) and the enantiomeric ratio of the chloroaldehyde product (57:43; 14% excess) is no longer present.

(*S*)-2-chloropropyl-3,5-dinitrobenzoate ((*S*)-SI10)

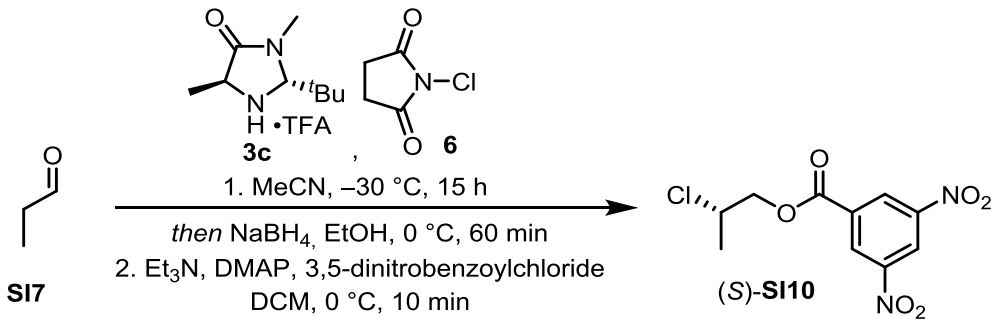

Propanal (0.143 mL, 2.00 mmol, 1.0 equiv) was dissolved in MeCN (8.0 mL) and cooled to –30 °C. Catalyst **3c**•TFA (0.114 g, 0.400 mmol, 20 mol%) and NCS (0.320 g, 2.40 mmol, 1.2 equiv) were added subsequently and the reaction mixture was stirred for 15 h at the same temperature. After the reaction was warmed to 0 °C, MeOH (3.0 mL) and $NaBH_4$ (0.189 g, 5.00 mmol, 2.5 equiv) were added and the mixture was stirred for 60 min at the same temperature. The reaction was quenched with aqueous saturated NH_4Cl (10 mL), the aqueous phase was extracted with dichloromethane (3x15 mL) and the combined organic phases were dried over $NaSO_4$. The solvent was removed under reduced pressure (product is volatile!) and the crude product was dissolved in dichloromethane (8 mL). The solution was cooled to 0 °C and DMAP (24.4 mg, 0.200 mmol, 0.1 equiv) and 3,5-dinitrobenzoylchloride (0.599 g, 2.60 mmol, 1.3 equiv) were added subsequently. Et_3N (0.474 mL, 3.40 mmol, 1.7 equiv) was added dropwise and the reaction mixture was stirred for 10 min at 0 °C. The reaction was quenched with aqueous saturated $NaHCO_3$ (10 mL), the aqueous phase was extracted with dichloromethane (3x10 mL) and the combined organic phases were dried over $NaSO_4$. The solvent was removed under reduced pressure and the crude product was purified by column chromatography (Silica, pentane/EtOAc 10:1). Ester (*S*)-**SI10** (0.108 g, 0.374 mmol, 19%, 94% ee) was obtained as a yellowish oil.

The ^{1}H-NMR spectrum is in accordance with the previous experiment.

(*R*)-2-chloropropyl-3,5-dinitrobenzoate ((*R*)-SI10)

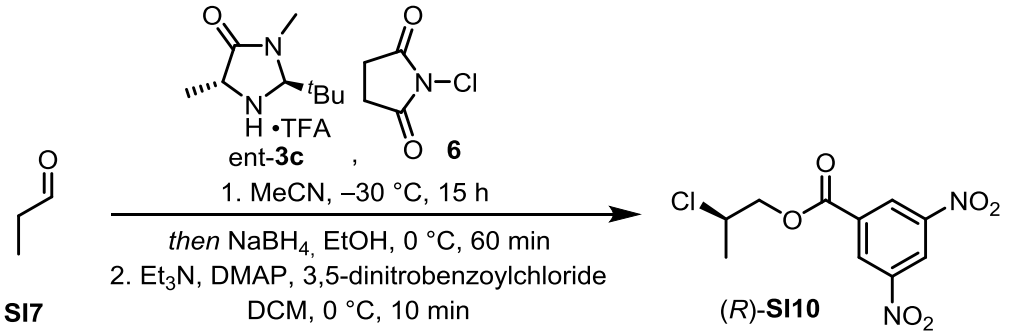

Propanal (0.143 mL, 2.00 mmol, 1.0 equiv) was dissolved in MeCN (8.0 mL) and cooled to –30 °C. Catalyst *ent*-**3c**•TFA (0.114 g, 0.400 mmol, 20 mol%) and NCS (0.320 g, 2.40 mmol, 1.2 equiv) were added subsequently and the reaction mixture was stirred for 15 h at the same temperature. After the reaction was warmed to 0 °C, MeOH (3.0 mL) and $NaBH_4$ (0.189 g, 5.00 mmol, 2.5 equiv) were added and the mixture was stirred for 60 min at the same temperature. The reaction was quenched with aqueous saturated NH_4Cl (10 mL), the aqueous phase was extracted with dichloromethane (3x15 mL) and the combined organic phases were dried over $NaSO_4$. The solvent was removed under reduced pressure (product is volatile!) and the crude product was redissolved in dichloromethane (8 mL). The solution was cooled to 0 °C and DMAP (24.4 mg, 0.200 mmol, 0.1 equiv) and 3,5-dinitrobenzoylchloride (0.599 g, 2.60 mmol, 1.3 equiv) were added subsequently. Et_3N (0.474 mL, 3.40 mmol, 1.7 equiv) was added dropwise and the reaction mixture was stirred for 10 min at 0 °C. The reaction was quenched with aqueous saturated $NaHCO_3$ (10 mL), the aqueous phase was extracted with dichloromethane (3x10 mL) and the combined organic phases were dried over $NaSO_4$. The solvent was removed under reduced pressure and the crude product was purified by column chromatography (Silica, pentane/EtOAc 10:1). Ester (*R*)-**SI10** (0.109 g, 0.378 mmol, 19%, 94% ee) was obtained as a yellowish oil.

The ^{1}H-NMR spectrum is in accordance with the previous experiment.

3.2.2. Decomposition and Deuterium Incorporation Studies

Decomposition of Aminal SI6 (1)

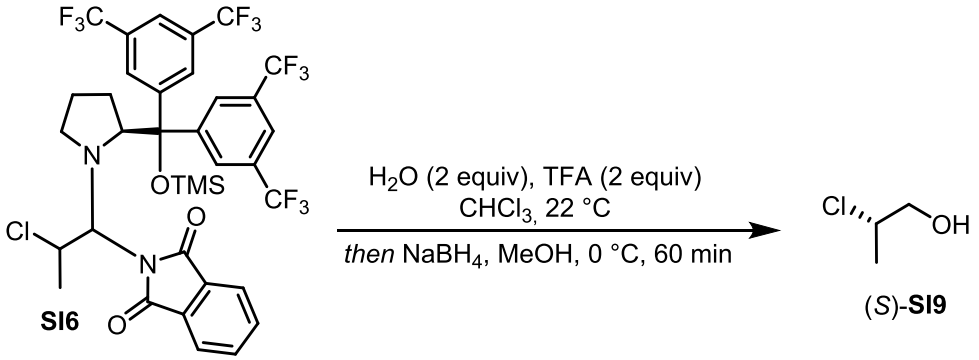

H_2O (72.1 µL, 4.00 mmol, 2.0 equiv) and TFA (308 µL, 4.00 mmol, 2.0 equiv) were added subsequently to a solution of aminal **SI6** (1.64 g, 2.00 mmol, 1.0 equiv) in $CHCl_3$ (100 mL) at 22 °C. Aliquots (10 mL) were taken from the reaction mixture after defined points of time (1 min, 5 min, 10 min, 20 min, 30 min, 60 min, 2 h, 98 h) and added to a solution of $NaBH_4$ (75.7 mg, 2.00 mmol, 10.0 equiv) in MeOH (4.0 mL). After 60 min the reactions were quenched with aqueous saturated NH_4Cl. The aqueous phase was extracted with dichloromethane (3x5 mL), the combined organic phases were dried over Na_2SO_4 and the solvent was partially removed under reduced pressure (product is volatile!). The enantiomeric excess of the crude products was determined by chiral GC.

1 min:	94% ee for the (*S*)-enantiomer
5 min:	94% ee
10 min:	94% ee
20 min:	95% ee
30 min:	94% ee
60 min:	93% ee
120 min:	93% ee
(98 h:	58% ee)

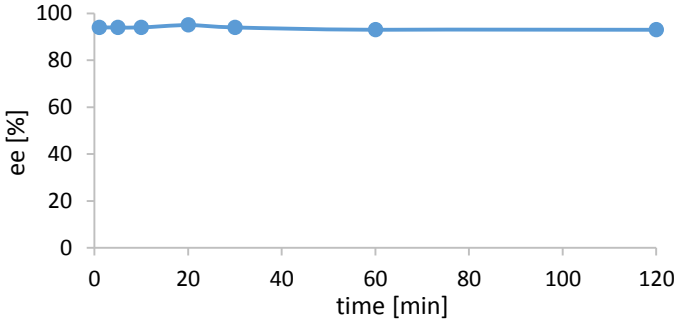

Figure SI-50. The acid-catalyzed decomposition of aminal **SI6** generates almost enantiopure (*S*)-chloroaldehyde product.

As mentioned before (decomposition of aminal **14**, synthesis of aminal **SI6**) it was possible to obtain aminal **SI6** without any detectable aldehyde or chloroaldehyde impurities. The decomposition experiment shows that aminal **SI6** decomposes to almost enantiopure chloroaldehyde (*S*)-**SI8**. In contrast, the mechanism of the Curtin-Hammett scenario predicts the existence of both enantiomers in the same ratio as the interconverting species (ratio of signal sets at –54 °C = 68:32 → 36% ee).

2-Chloropropan-1-ol (*rac*-SI9)

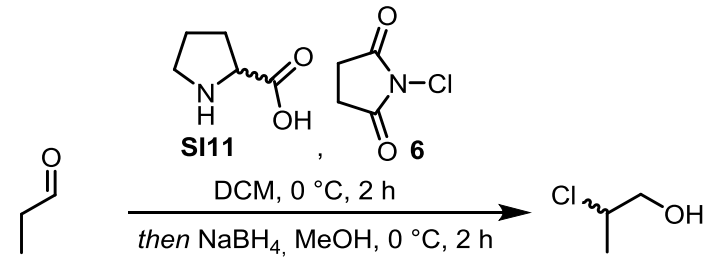

Racemic proline (**SI11**) (0.104 g, 0.900 mmol, 0.3 equiv) and NCS (0.401 g, 3.00 mmol, 1.0 equiv) were added successively to an ice-cold solution of propanal (0.215 mL, 3.00 mmol, 1.0 equiv) in dichloromethane (8.1 mL). After stirring for 2 h at 0 °C, MeOH (4.1 mL) and $NaBH_4$ (0.284 g, 7.50 mmol, 2.5 equiv) were added and the solution was stirred for another 2 h at 0 °C. The reaction was quenched with aqueous saturated NH_4Cl (5 mL), the aqueous phase was extracted with dichloromethane (3x10 mL) and the combined organic phases were dried over $NaSO_4$. The solvent was removed under reduced pressure (product is volatile!) and the crude product was purified by column chromatography (Silica, pentane/Et_2O 3:1). Alcohol *rac*-**SI9** (35.0 mg, 0.370 mmol, 12%; product is volatile!) was obtained as a colorless oil.

The ^{1}H-NMR spectrum is in accordance with the literature.[53]

^{1}H-NMR (CD_2Cl_2, 400 MHz) δ = 4.13 (pdd, *J* = 6.8, 4.2, 1.0 Hz, 1H), 3.71 (dd, *J* = 11.9, 4.0 Hz, 1H), 3.60 (dd, *J* = 12.0, 7.0 Hz, 1H), 2.29 (s, 1H), 1.48 (d, *J* = 6.7 Hz, 3H) ppm.

(*S*)-2-chloropropan-1-ol ((*S*)-SI9)

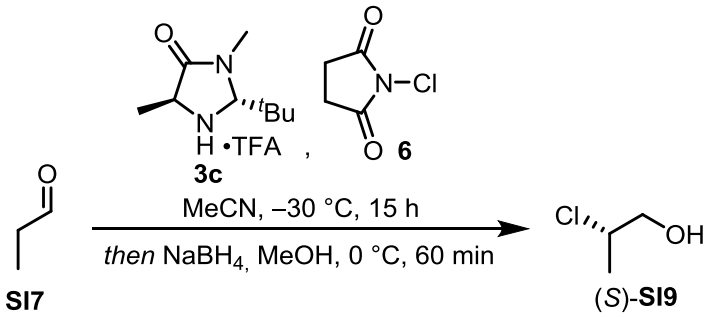

Propanal (0.143 mL, 2.00 mmol, 1.0 equiv) was dissolved in MeCN (8.0 mL) and cooled to –30 °C. Catalyst **3c**•TFA (0.114 g, 0.400 mmol, 20 mol%) and NCS (0.320 g, 2.40 mmol, 1.2 equiv) were added subsequently and the reaction mixture was stirred for 15 h at the same temperature. After the reaction was warmed to 0 °C, MeOH (3.0 mL) and $NaBH_4$ (0.189 g, 5.00 mmol, 2.5 equiv) were added and the mixture was stirred for 60 min at the same temperature. The reaction was quenched with aqueous saturated NH_4Cl (10 mL), the aqueous phase was extracted with dichloromethane (3x15 mL) and the combined organic phases were dried over $NaSO_4$. The solvent was removed under reduced pressure (product is volatile!) and the crude product (99% ee; determined by chiral GC) was used without further purification.

(*R*)-2-chloropropan-1-ol ((*R*)-SI9)

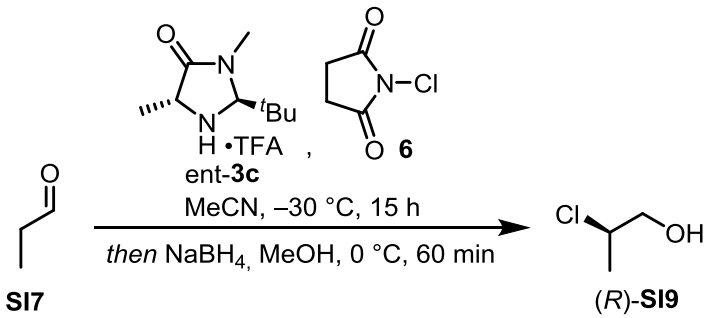

Propanal (0.143 mL, 2.00 mmol, 1.0 equiv) was dissolved in MeCN (8.0 mL) and cooled to –30 °C. Catalyst *ent*-**3c**•TFA (0.114 g, 0.400 mmol, 20 mol%) and NCS (0.320 g, 2.40 mmol, 1.2 equiv) were added subsequently and the reaction mixture was stirred for 15 h at the same temperature. After the reaction was warmed to 0 °C, MeOH (3.0 mL) and $NaBH_4$ (0.189 g, 5.00 mmol, 2.5 equiv) were added and the mixture was stirred for 60 min at the same temperature. The reaction was quenched with aqueous saturated NH_4Cl (10 mL), the aqueous phase was extracted with dichloromethane (3x15 mL) and the combined organic phases were dried over $NaSO_4$. The solvent was removed under reduced pressure (product is volatile!) and the crude product (>99% ee; determined by chiral GC) was used without further purification.

Decomposition of Aminal SI6 (2)

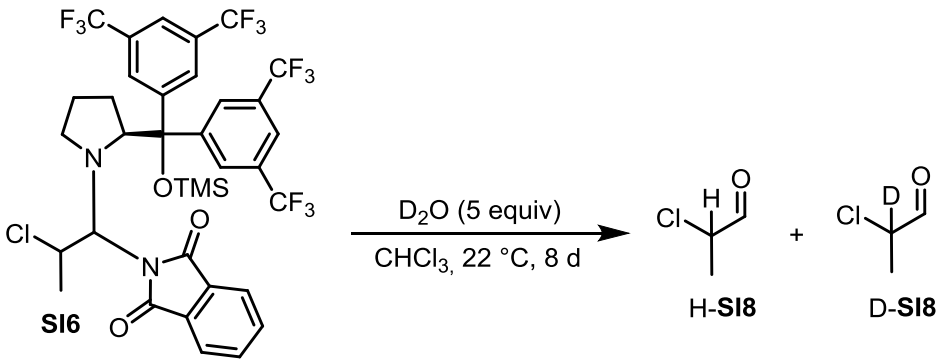

0.60 mL of a stock solution ($CDCl_3$ (6.0 mL), D_2O (11.8 µL) was added to a NMR-tube containing aminal **SI6** (9.67 mg, 11.8 µmol, 1.0 equiv). The NMR-tube was tightly sealed and ^{1}H-NMR spectra were recorded over a period of 8 days. Deuterium incorporation and conversion was qualitatively evaluated by ^{1}H-NMR spectroscopy.

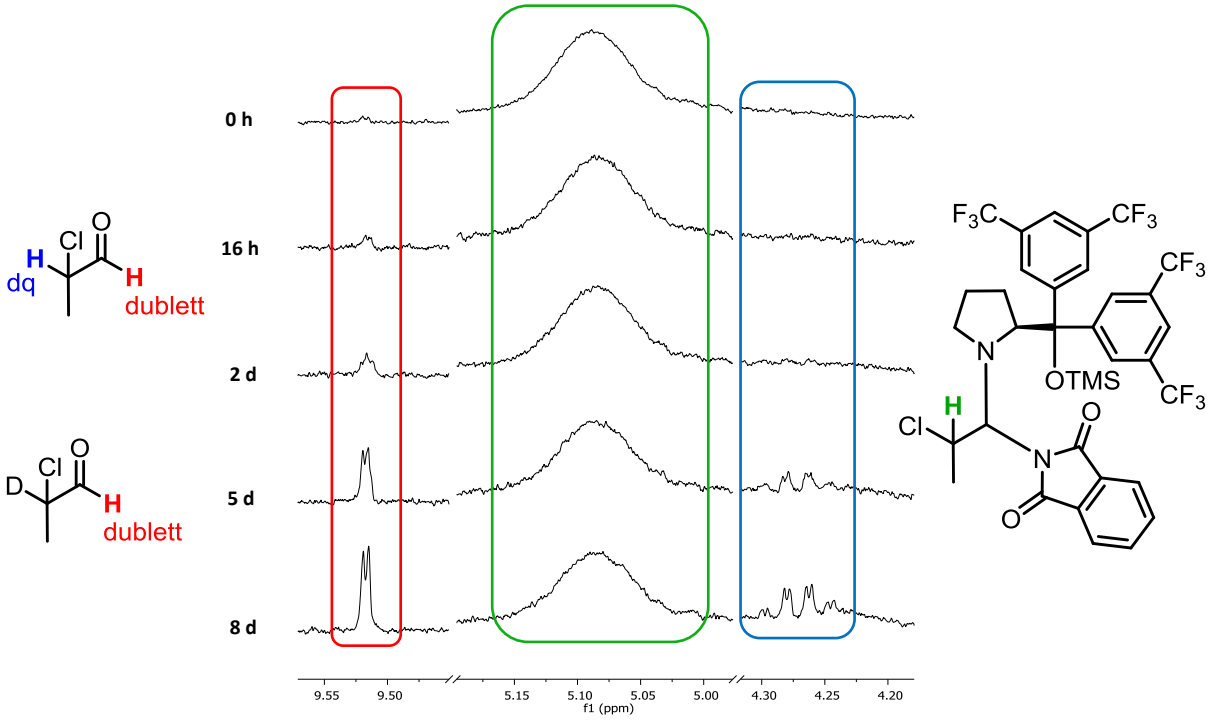

Figure SI-51. ^{1}H-NMR spectra of the ongoing decomposition reaction (5 equiv of D_2O) of aminal **SI6** allows a qualitative evaluation of the deuterium incorporation into the α-chloroaldehydes.

In accordance to the previous D_2O-mediated hydrolysis experiment of aminal **14**, significant deuterium incorporation cannot be detected.

4. FURTHER RESULTS

Deuterium incorporation experiment

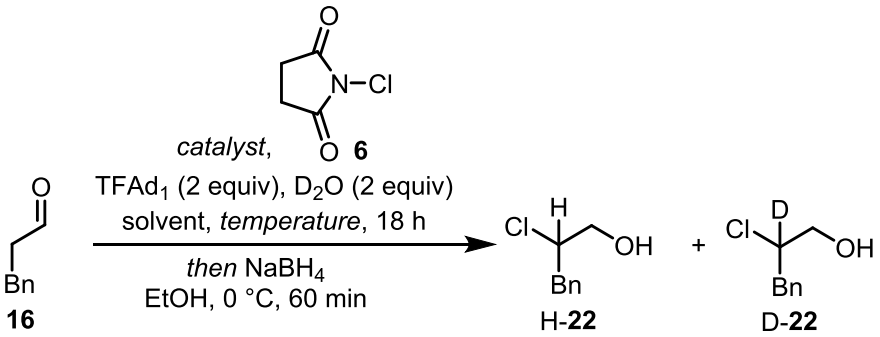

D_2O (98.0 µL, 6.02 mmol, 2 equiv), $TFAd_1$ (464 µL, 6.02 mmol, 2.0 equiv), the catalyst (0.602 mmol, 20 mol%) and NCS (0.442 g, 3.31 mmol, 1.1 equiv) were added subsequently to a solution of distilled hydrocinnamic aldehyde (0.400 mL, 3.01 mmol, 1.0 equiv) in MeCN (catalyst **3c** and *ent*-**3b**) or dichloromethane (catalyst **9c**) (12 mL) at 20 °C or –30 °C. After 18 h the reaction was adjusted to 0 °C. EtOH (4.00 mL) and $NaBH_4$ (0.569 g, 15.0 mmol, 5.0 equiv) were added and the reaction mixture was stirred for 60 min at the same temperature. The reaction was quenched with aqueous saturated NH_4Cl, extracted with EtOAc (3x10 mL) and the combined organic phases were dried over Na_2SO_4. The solvent was removed under reduced pressure and the crude product was purified by column chromatography (Silica, 10:1 to 5:1 pentane/EtOAc). Deuterium incorporation was qualitatively evaluated by comparison of the ^{13}C-NMR spectra and quantified by ^{1}H-NMR spectroscopy

Example:

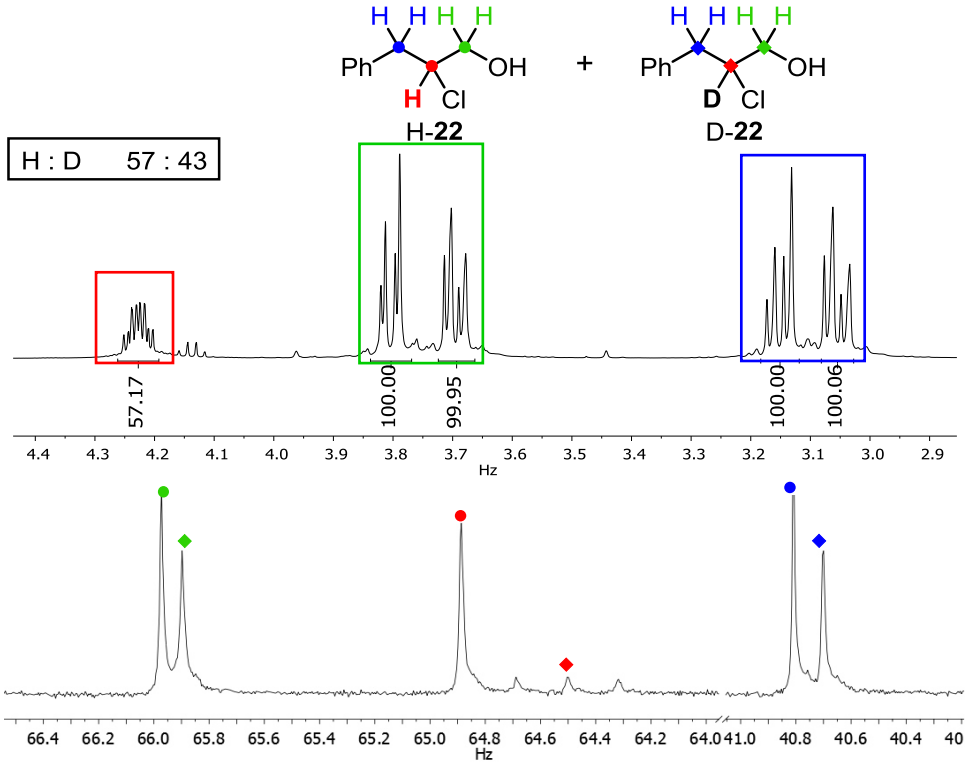

Figure SI-52. Exemplary ^{1}H- (top) and ^{13}C-NMR (bottom) spectrum for the evaluation of deuterium incorporation.

Table SI-41. Quantification of deuterium incorporation under various conditions

catalyst	solvent	T [°C]	H : D	t
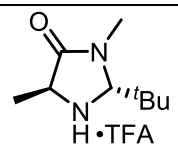 **3c**	MeCN	20	90 : 10	18 h
	MeCN	–30	100 : 0	18 h
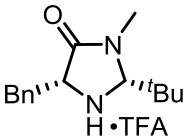 ent-**3b**	MeCN	20	57 : 43	18 h
	MeCN	–30	95 : 5	18 h
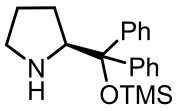 **9c**	dichloromethane	20	83 : 17	18 h
	dichloromethane	–30	89 : 11	18 h
	dichloromethane	20	97 : 3	5 min[a]

[a] no TFA-d_1, 12% conversion, 59% ee

Comparison of Different Catalysts

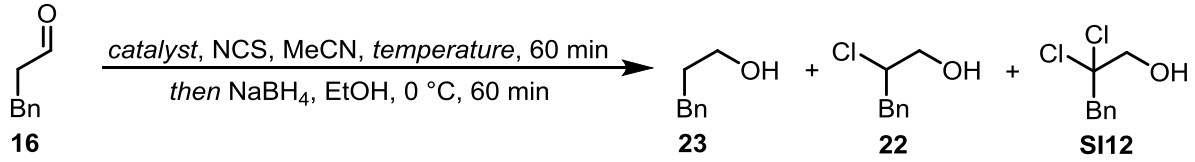

The catalyst (0.150 mmol, 20 mol%) and NCS (0.111 g, 0.828 mmol, 1.1 equiv) were added successively to a tempered (22 °C or 0 °C) solution of hydrocinnamic aldehyde (0.100 mL, 0.752 mmol, 1.0 equiv) and MeCN (3.0 mL). The reaction was stirred for 60 min at the indicated temperature and then cooled to 0 °C. EtOH (1.0 mL) and $NaBH_4$ (71.2 mg, 1.88 mmol, 2.5 equiv) were added and the reaction mixture was stirred for further 60 min at 0 °C. The reaction was quenched with aqueous saturated NH_4Cl, the aqueous phase was extracted with EtOAc (3x5 mL), the combined organic phases were dried over Na_2SO_4 and the solvent was removed under reduced pressure. The crude product was purified by column chromatography (SiO_2, pentane/EtOAc 10:1 to 5:1) and the pure alcohols **23**, **22** and **SI12** were obtained as colorless oils. The enantiomeric excesses of the chloroalcohols **22** were determined by chiral HPLC.

Table SI-42. Comparison of different pyrrolidine- and imidazolidinone-based organocatalysts in the α-chlorination of **16**

	temperature	**23** [%]	**22** [%]	**SI12** [%]	sum [%]	ee (**22**) [%]
pyrrolidine (**SI13**)	22 °C	26	17	19	62	0
	0 °C	42	16	10	68	0
L-proline ((*S*)-**SI11**)	22 °C	26	32	0	58	1
	0 °C	49	14	0	63	9
L-prolinamide (**SI14**)	22 °C	37	20	0	57	29
	0 °C	46	8	0	54	44
Jørgensen-Hayashi catalyst (**9c**)	22 °C	0	3	43	46	11
	0 °C	0	17	25	42	16
in dichloromethane	0 °C	0	33	13	46	69
diphenylyrrolidine catalyst (**SI15**)	22 °C	0	18	22	40	97
	0 °C	0	24	8	32	98
1st gen. *MacMillan* catalyst (**3a**)	22 °C	0	51	23	74	36
	0 °C	17	48	18	83	70
2nd gen. *MacMillan* catalyst (*ent*-**3b**)	22 °C	39	26	9	74	28
	0 °C	53	27	2	82	48
3rd gen. *MacMillan* catalyst (**3c**)	22 °C	2	64	0	66	91
	0 °C	24	54	0	78	96

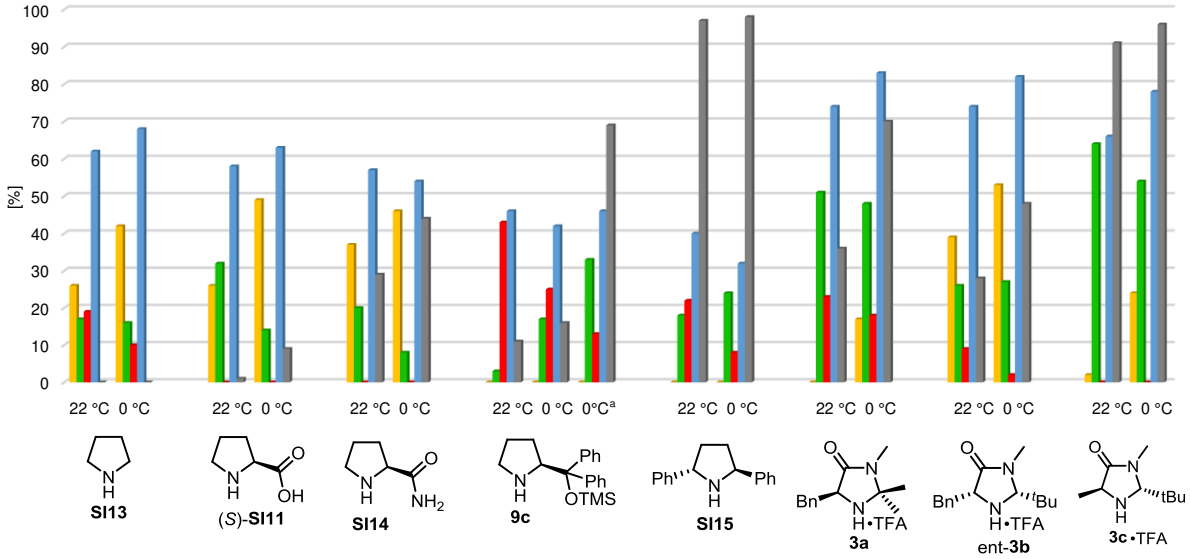

[a]: in dichloromethane

yellow: isolated yield reduced starting material **23**

green: isolated yield monochlorinated alcohol **22**

red: isolated yield dichlorinated alcohol **SI12**

blue: sum of **22**, **23** and **SI12**

grey: enantiomeric excess of **23**

Figure SI-53. Comparison of the catalytic performance between numerous pyrrolidine- and imidazolidinone-based organocatalysts.

The comparison of different pyrrolidine- and imidazolidinone-based organocatalysts reveals some major differences in the catalytic performance. Dichlorination can be completely suppressed when catalysts (*S*)-**SI11**, **SI14** and **3c** were used. Raising the temperature enhances the amount of dichlorinated byproduct for all other catalysts. Excellent enantioselectivities under these conditions were exclusively achieved with catalyst **SI15** and **3c**. The C2 or C2-like symmetry of both catalysts might play a role here. The sum of **23**, **22** and **SI12** can be considered as a parameter for the selectivity of the catalytic system. Low values are indicative for ongoing side-reactions, whereas high values reflect a “clean” reaction with less side products. Concerning the formation of side products, imidazolidinone-based catalysts perform better than pyrrolidine-based catalysts under these conditions.

5. REFERENCES

(1) Bodenhausen, G.; Ruben, D. J. *Chem. Phys. Lett.* **1980**, *69*, 185–189.

(2) Bax, A.; Summers, M. F. *J. Am. Chem. Soc.* **1986**, *108*, 2093–2094.

(3) Thiele, C. M.; Petzold, K.; Schleucher, J. *Chem. Eur. J.* **2009**, *15*, 585–588.

(4) Thrippleton, M. J.; Keeler, J. *Angew. Chem. Int. Ed.* **2003**, *42*, 3938–3941.

(5) Kupče, E.; Boyd, J.; Campbell, I. D. *J. Magn. Reson. B* **1995**, *106*, 300–303.

(6) Ilgen, J.; Nowag, J.; Kaltschnee, L.; Schmidts, V.; Thiele, C. M. *J. Magn. Reson.* **2021**, *324*, 106900.

(7) Foroozandeh, M.; Adams, R. W.; Meharry, N. J.; Jeannerat, D.; Nilsson, M.; Morris, G. A. *Angew. Chem. Int. Ed.* **2014**, *53*, 6990–6992.

(8) Hu, H.; Krishnamurthy, K. *J. Magn. Reson.* **2006**, *182*, 173–177.

(9) Kolmer, A.; Edwards, L. J.; Kuprov, I.; Thiele, C. M. *J. Magn. Reson.* **2015**, *261*, 101–109.

(10) Neuhaus, D.; Williamson, M. P. The Nuclear Overhauser Effect in Structural and Conformational Analysis, 2nd Ed., Wiley, Chichester, 2000.

(11) Kolmer, A.; Edwards, L. J.; Kuprov, I.; Thiele, C. M. *J. Magn. Reson.* **2015**, *261*, 101–109.

(12) Sinnaeve, D.; Foroozandeh, M.; Nilsson, M.; Morris, G. A. *Angew. Chem. Int. Ed.* **2016**, *55*, 1090–1093.

(13) a) https://gaussian.com/scrf/; b) Tomasi, J.; Mennucci, B.; Cammi, R. *Chem. Rev.* **2005**, *105*, 2999–3093; c) London, F. *J. Phys. Radium*, **1937**, *8*, 397–409; d) McWeeny, R. *Phys. Rev.* **1962**, *126*, 1028–1034; e) Ditchfield, R. *Mol. Phys.* **1974**, *27*, 789–807; f) Wolinski, K.; Hinton, J. F.; Pulay, P. *J. Am. Chem. Soc.* **1990**, *112*, 8251–8260; g) Cheeseman, J. R.; Trucks, G. W.; Keith, T. A.; Frisch, M. J. *J. Chem. Phys.* **1996**, *104,* 5497–5509; h) Towns, J.; Cockerill, T.; Dahan, M.; Foster, I.; Gaither, K.; Grimshaw, A.; Hazlewood, V.; Lathrop, S.; Lifka, D.; Peterson, G. D.; Roskies, R.; Scott, J. R.; Wilkins-Diehr, N. *Comput. Sci. Eng.* **2014**, *16*, 62–74; i) Grimme, S.; Antony, J.; Ehrlich, S.; Krieg, H. *J. Chem. Phys.* **2010**, *132*, 154104; j) Grimme, S.; Ehrlich, S.; Goerigk, L. *J. Comput. Chem.* **2011**, *32*, 1456–1465.

(14) Gaussian 16, Revision C.01: Frisch, M. J.; Trucks, G. W.; Schlegel, H. B.; Scuseria, G. E.; Robb, M. A.; Cheeseman, J. R.; Scalmani, G.; Barone, V.; Petersson, G. A.; Nakatsuji, H.; Li, X.; Caricato, M.; Marenich, A. V.; Bloino, J.; Janesko, B. G.; Gomperts, R.; Mennucci, B.; Hratchian, H. P.; Ortiz, J. V.; Izmaylov, A. F.; Sonnenberg, J. L.; Williams-Young, D.; Ding, F.; Lipparini, F.; Egidi, F.; Goings, J.; Peng, B.; Petrone, A.; Henderson, T.; Ranasinghe, D.; Zakrzewski, V. G.; Gao, J.; Rega, N.; Zheng, G.; Liang, W.; Hada, M.; Ehara, M.; Toyota, K.; Fukuda, R.; Hasegawa, J.; Ishida, M.; Nakajima, T.; Honda, Y.; Kitao, O.; Nakai, H.; Vreven, T.; Throssell, K.; Montgomery, J. A., Jr.; Peralta, J. E.; Ogliaro, F.; Bearpark, M. J.; Heyd, J. J.; Brothers, E. N.; Kudin, K. N.; Staroverov, V. N.; Keith, T. A.; Kobayashi, R.; Normand, J.; Raghavachari, K.; Rendell, A. P.; Burant, J. C.; Iyengar, S. S.; Tomasi, J.; Cossi, M.; Millam, J. M.; Klene, M.; Adamo, C.; Cammi, R.; Ochterski, J. W.; Martin, R. L.; Morokuma, K.; Farkas, O.; Foresman, J. B.; Fox, D. J. Gaussian, Inc., Wallingford CT, 2016.

(15) Pracht, P.; Bohle, F.; Grimme, S. *Phys. Chem. Chem. Phys.* **2020**, *22*, 7169–7192.

(16) Grimme, S. *J. Chem. Theory Comput.* **2019**, *15*, 2847–2862.

(17) Lodewyk, M. W.; Siebert, M. R.; Tantillo, D. J. *Chem. Rev.* **2012**, *112*, 1839–1862.

(18) CHESHIRE, Chemical Shift Repository with Coupling Constants Added Too. http://cheshirenmr.info

(19) a) Foster, J. P.; Weinhold, F. *J. Am. Chem. Soc.* **1980**,*102*, 7211–7218; b) Reed, A. E.; Weinhold, F. *J. Chem. Phys.* **1983**, *78*, 4066–4073; c) Reed, A. E.; Weinstock, R. B.; Weinhold, F. *J. Chem. Phys.* **1985***, 83*, 735–746; d) Reed, A. E.; Weinhold, F. *J. Chem. Phys.* **1985**, *83*, 1736–1740; e) J. E. Carpenter, *Extension of Lewis structure concepts to open-shell and excited-state molecular species*, Ph.D. thesis, University of Wisconsin, Madison, WI, 1987; f) Carpenter, J. E.; Weinhold, F. *J. Mol. Struct. (Theochem)* **1988**, *139*, 41–62; g) Reed, A. E.; Curtiss, L. A.; Weinhold, F. *Chem. Rev.* **1988**, *88*, 899–926; h) Weinhold, F. and Carpenter, J. E. in *The Structure of Small Molecules and Ions*, Naaman, E. R.; Vager, Z. *Plenum*, 1988, 227–236.

(20) Legault, C. Y. CYLview, 1.0b. *Université de Sherbrooke*. 2009.

(21) Álvarez-Moreno, M.; de Graaf, C.; López, N.; Maseras, F.; Poblet, J. M.; Bo, C. *J. Chem. Inf. Model.* **2015**, *55*, 95–103.

(22) Ponath, S.; Menger, M.; Grothues, L.; Weber, M.; Lentz, D.; Strohmann, C.; Christmann, M. *Angew. Chem. Int. Ed.* **2018**, *57*, 11683–11687.

(23) Burés, J.; Armstrong, A.; Blackmond, D. G. *Acc. Chem. Res.* **2016**, *49*, 214–222.

(24) Burés, J.; Dingwall, P.; Armstrong, A.; Blackmond, D. G. *Angew. Chem. Int. Ed.* **2014**, *53*, 8700–8704.

(25) Wiest, J. The Role of Charged and Uncharged Intermediates in Organocatalysis, MS Thesis, 2012, Universität Basel (conducted in the Blackmond group at The Scripps Research Institute)

(26) Brochu, M. P.; Brown, S. P.; MacMillan, D. W. C. *J. Am. Chem. Soc.* **2004**, *126*, 4108–4109.

(27) Amatore, M.; Beeson, T. D.; Brown, S. P.; MacMillan, D. W. C. *Angew. Chem. Int.* Ed. **2009**, *48*, 5121–5124.

(28) Burés, J.; Armstrong, A.; Blackmond, D. G. *J. Am. Chem. Soc.* **2012**, *134*, 6741–6750.

(29) Chen, G.; Fu, C.; Ma, S. *Tetrahedron* **2006**, *62*, 4444–4452.

(30) Warnke, S.; von Helden, G.; Pagel, K. *Proteomics* **2015,** *15*, 2804-2812.

(31) Hoffmann, W.; Langenhan, J.; Huhmann, S.; Moschner, J.; Chang, R.; Accorsi, M.; Seo, J.; Rademann, J.; Meijer, G.; Koksch, B.; Bowers, M. T.; von Helden, G.; Pagel, K. *Angew. Chem. Int. Ed.* **2019,** *58*, 8216–8220.

(32) Revercomb, H. E.; Mason, E. A. *Anal. Chem.* **1975,** *47*, 970–983.

(33) Gabelica, V.; Shvartsburg, A. A.; Afonso, C.; Barran, P.; Benesch, J. L. P.; Bleiholder, C.; Bowers, M. T.; Bilbao, A.; Bush, M. F.; Campbell, J. L.; Campuzano, I. D. G.; Causon, T.; Clowers, B. H.; Creaser, C. S.; De Pauw, E.; Far, J.; Fernandez-Lima, F.; Fjeldsted, J. C.; Giles, K.; Groessl, M.; Hogan, C. J., Jr.; Hann, S.; Kim, H. I.; Kurulugama, R. T.; May, J. C.; McLean, J. A.; Pagel, K.; Richardson, K.; Ridgeway, M. E.; Rosu, F.; Sobott, F.; Thalassinos, K.; Valentine, S. J.; Wyttenbach, T. *Mass Spectrom. Rev.* **2019,** *38*, 291–320.

(34) Supady, A.; Blum, V.; Baldauf, C. *J. Chem. Inf. Model.* **2015,** *55*, 2338–2348.

(35) Blum, V.; Gehrke, R.; Hanke, F.; Havu, P.; Havu, V.; Ren, X.; Reuter, K.; Scheffler, M. *Comput. Phys. Commun.* **2009,** *180*, 2175–2196.

(36) Perdew, J. P.; Burke, K.; Ernzerhof, M. *Phys. Rev. Lett.* **1996,** *77*, 3865–3868.

(37) Tkatchenko, A.; Scheffler, M. *Phys. Rev. Lett.* **2009,** *102*, 073005.

(38) Singh, U. C.; Kollman, P. A. *J. Comput. Chem.* **1984,** *5*, 129–145.

(39) Adamo, C.; Barone, V. *J. Chem. Phys.* **1999,** *110*, 6158–6170.

(40) Zanotto, L.; Heerdt, G.; Souza, P. C. T.; Araujo, G.; Skaf, M. S. *J. Comput. Chem.* **2018,** *39*, 1675–1681.

(41) Horii, Z-I.; Iwata, C.; Tamura, Y. *J. Org. Chem.* **1961**, *26*, 2273–2276.

(42) Thiele, C. M.; Kolmer A. *J. Magn. Reson.* **2016**, *266*, 69–72.

(43) a) Schmid, M. B.; Zeitler, K.; Gschwind, R. M. *Angew. Chemie. Int. Ed.* **2010**, *49*, 4997–5003; b) Schmid, M. B.; Zeitler, K.; Gschwind, R. M. *Chem. Sci.* **2011**, *2*, 1793–1803; c) Renzi, P.; Hioe, J.; Gschwind, R. M. *Acc. Chem. Res.* **2017**, *50*, 2936–2948.

(44) Iron, M. A. *J. Chem. Theory Comput.* **2017**, *13*, 5798–5819.

(45) Merrill, A.T.; Tantillo, D. J. *Magn. Reson. Chem.* **2020**, *58*, 576–583.

(46) Seebach, D.; Sun, X.; Sparr, C.; Ebert, M.-O.; Schweizer, W. B.; Beck, A. K. *Helv. Chim. Acta* **2012**, *95*, 1064–1078.

(47) Seebach, D.; Sun, X.; Ebert, M.-O.; W. Schweizer, W. B.; Purkayastha, N.; Beck, A. K.; Duschmalé, J.; Wennemers, H.; Mukaiyama, T.; Benohoud, M.; Hayashi, Y.; Reiher, M. *Helv. Chim. Acta* **2013**, *96*, 799–852.

(48) Cassani, C.; Melchiorre, P. *Org. Lett.* **2012**, *14*, 5590–5593.

(49) Weber, A. K.; Schachtner, J.; Fichtler, R.; Leermann, T. M.; Neudörfl, J. M.; von Wangelin, A. J. *Org. Biomol. Chem.* **2014**, *12*, 5267–5277.

(50) Gurubrahamam, R.; Chen, Y. M.; Huang, W.-Y.; Chan, Y.-T.; Chang, H.-K.; Tsai, M.-K.; Chen, K. *Org. Lett.* **2016**, *18*, 3046–3049.

(51) Boeckman Junior, R. K.; Wang, H.; Rugg, K. W.; Genung, N. E.; Chen, K.; Ryder, T. R. *Org. Lett.* **2016**, *18*, 6136–6139.

(52) Dinér, P.; Kjærsgaard, A.; Lie, M.; Jørgensen, K. *Chem. Eur. J.* **2008**, *14*, 122–127.

(53) Marathias, V. M.; Goljer, I.; Bach II, A. C. *Magn. Reson. Chem.* **2005**, *43*, 512–519.

6. APPENDIX

6.1. NMR-Spectra

1-((1*S*,2*R*)-1-((*R*)-5-benzyl-2,2,3-trimethyl-4-oxoimidazolidin-1-yl)-2-chloro-3-methylbutyl)pyrrolidine-2,5-dione (*syn*-20)

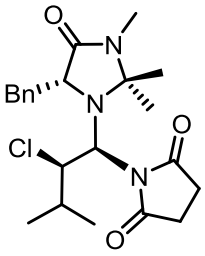

syn-**20**

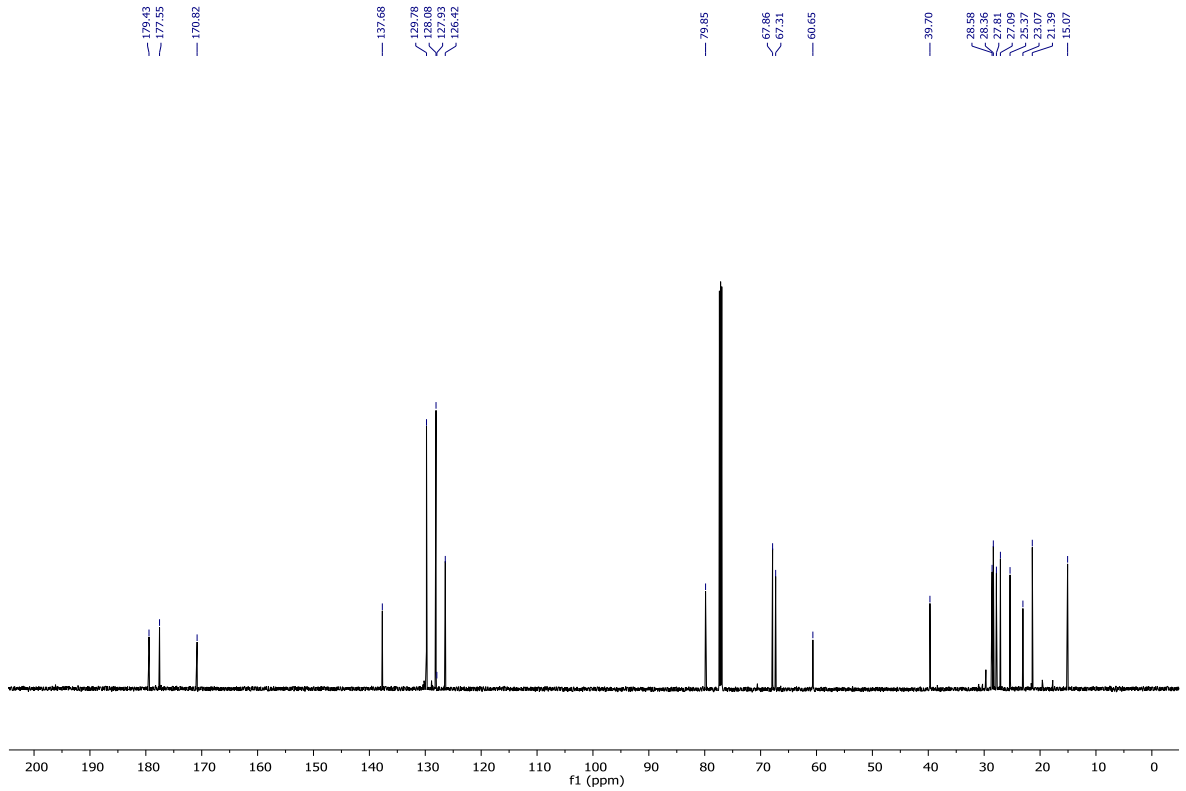

1-((*S*)-1-((*R*)-5-benzyl-2,2,3-trimethyl-4-oxoimidazolidin-1-yl)-2,2-dichloro-3-methylbutyl)pyrrolidine-2,5-dione (24a)

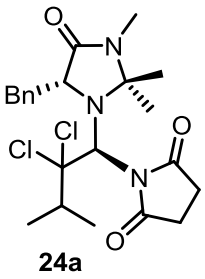

24a

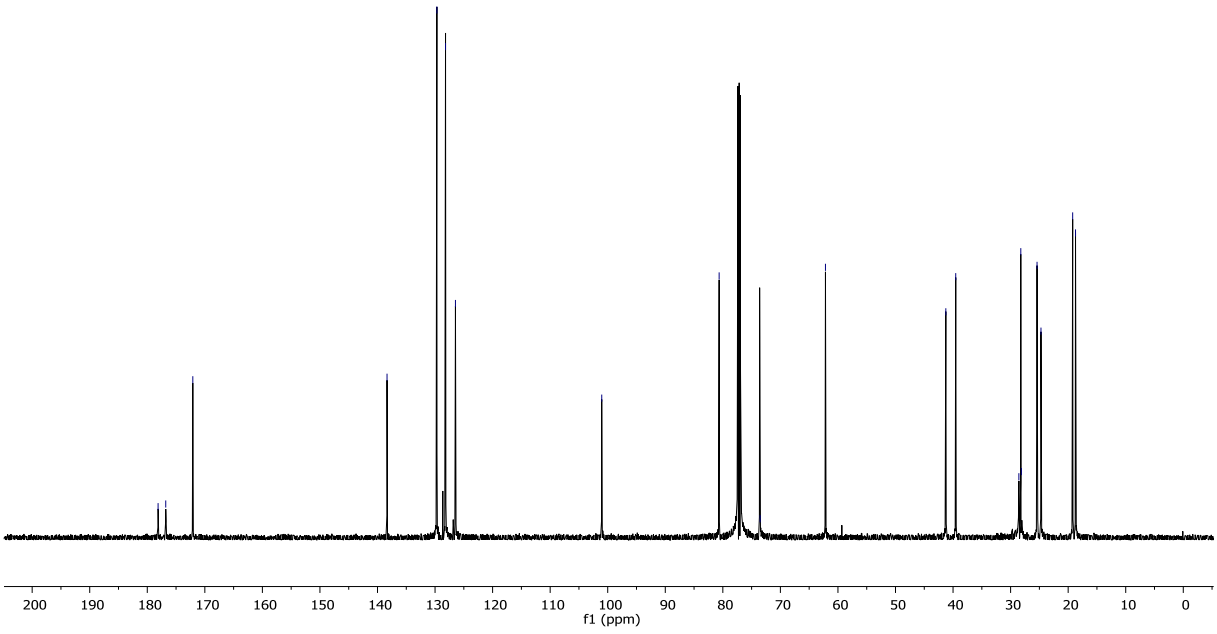

1-((1*S*,2*R*)-1-((2*R*,5*R*)-5-benzyl-2-(tert-butyl)-3-methyl-4-oxoimidazolidin-1-yl)-2-chloro-3-methylbutyl)pyrrolidine-2,5-dione ((1*S*,2*R*)-*syn*-21)

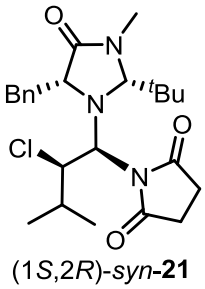

(1*S*,2*R*)-*syn*-**21**

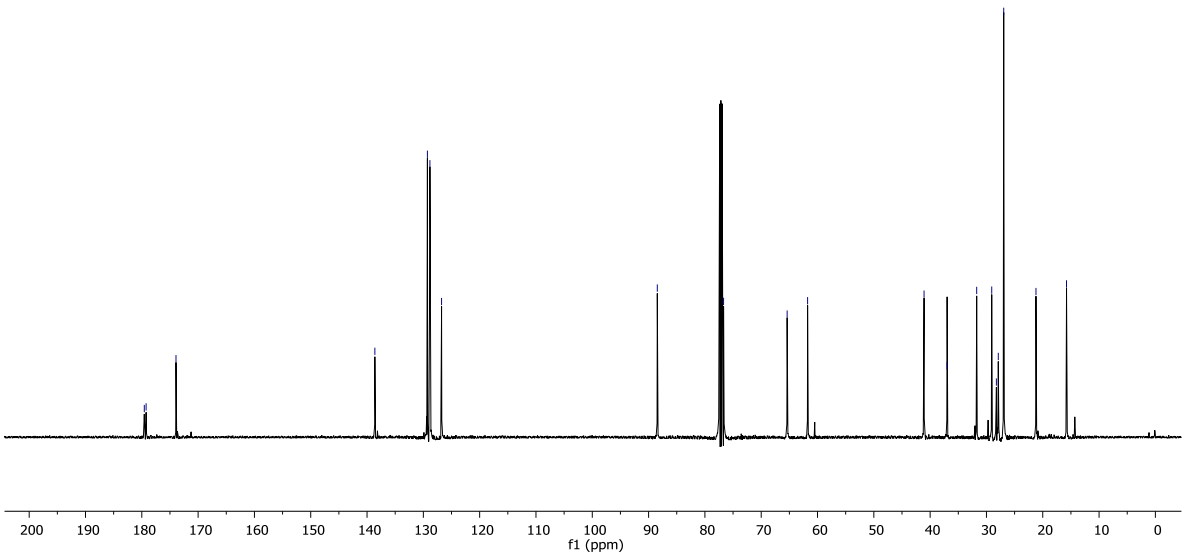

1-((1*S*,2*S*)-1-((2*R*,5*R*)-5-benzyl-2-(tert-butyl)-3-methyl-4-oxoimidazolidin-1-yl)-2-chloro-3-methylbutyl)pyrrolidine-2,5-dione ((1*S*,2*S*)-*anti*-21)

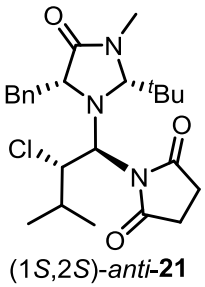

(1*S*,2*S*)-*anti*-**21**

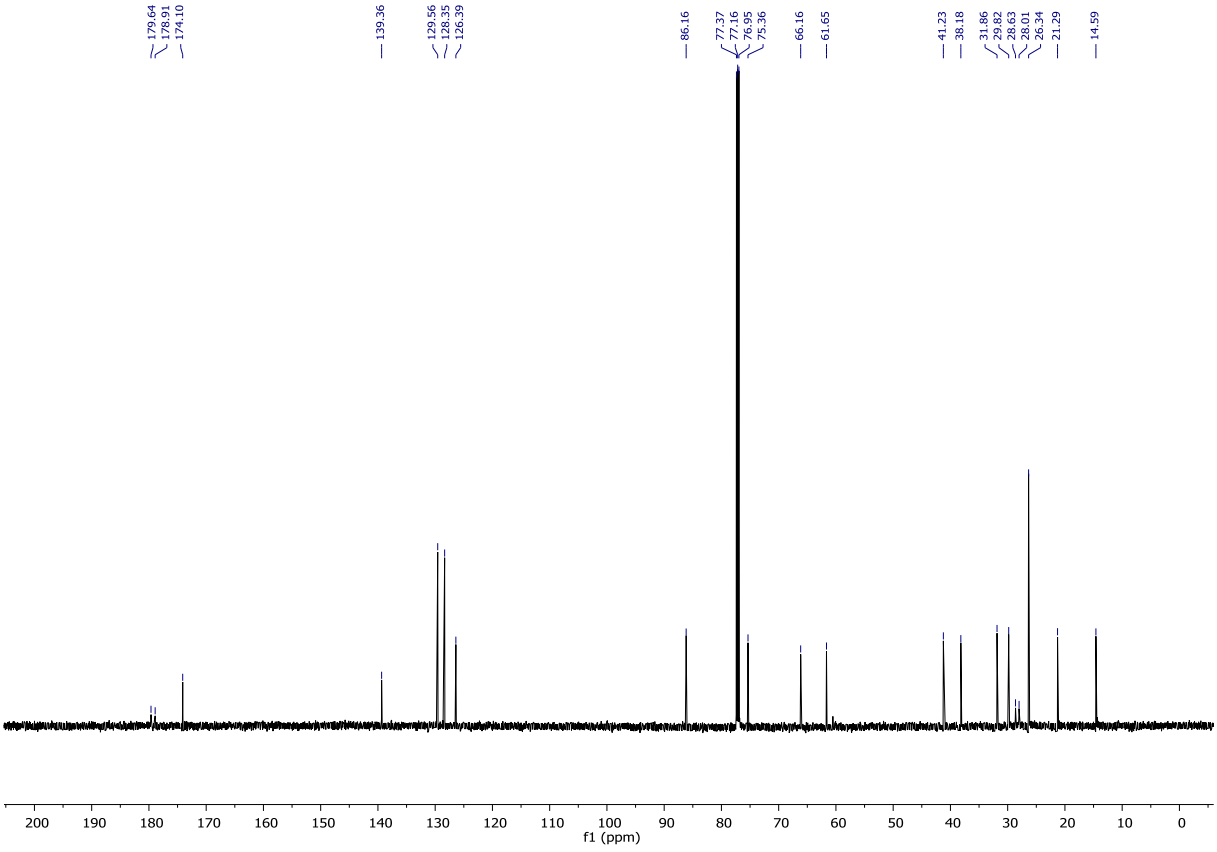

1-((1*R*,2*S*)-1-((2*R*,5*R*)-5-benzyl-2-(tert-butyl)-3-methyl-4-oxoimidazolidin-1-yl)-2-chloro-3-methylbutyl)pyrrolidine-2,5-dione ((1*R*,2*S*)-*syn*-21)

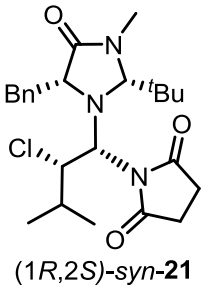

(1*R*,2*S*)-*syn*-**21**

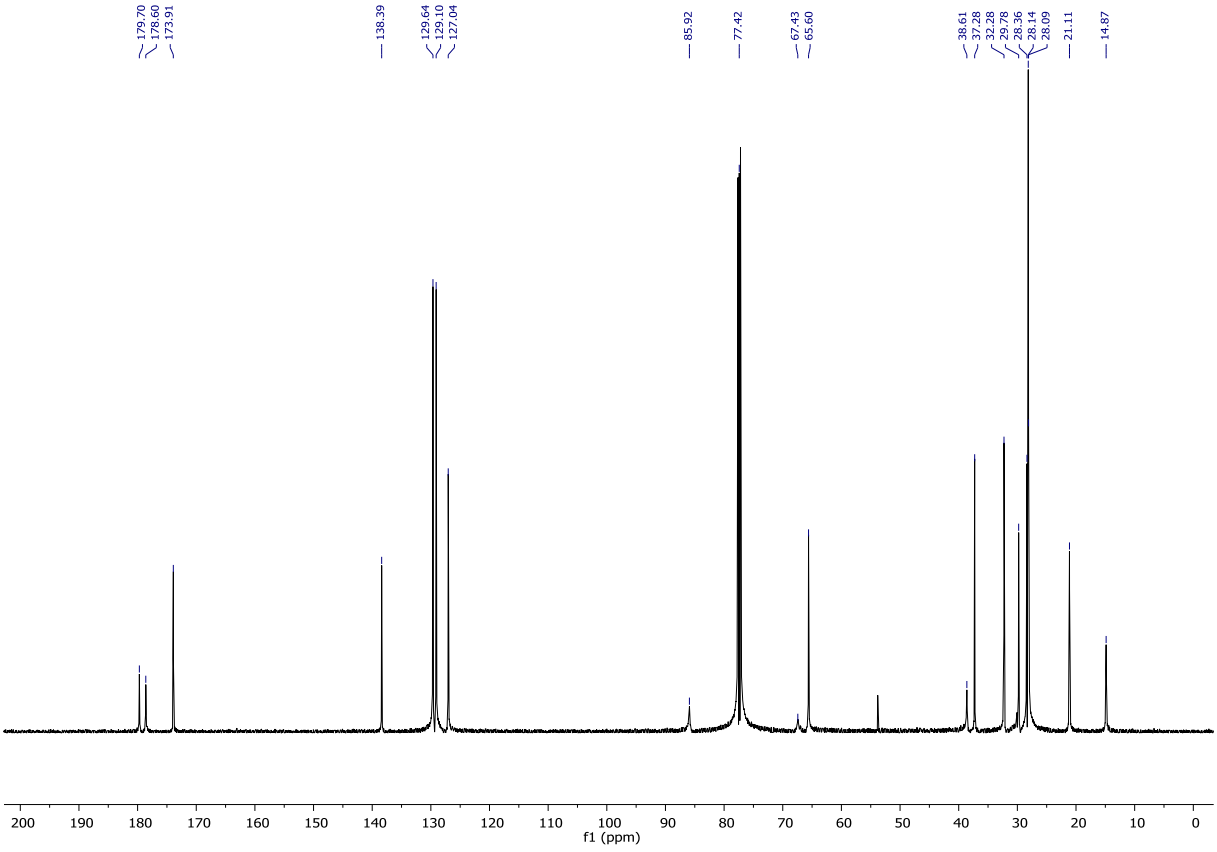

1-((1*S*,2*R*)-1-((2*R*,5*R*)-5-benzyl-2-(tert-butyl)-3-methyl-4-oxoimidazolidin-1-yl)-2-chloro-3-phenylpropyl)pyrrolidine-2,5-dione ((1*S*,2*R*)-*syn*-25)

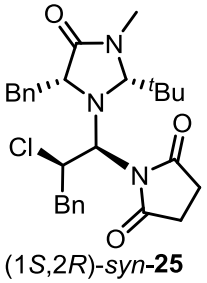

(1*S*,2*R*)-*syn*-**25**

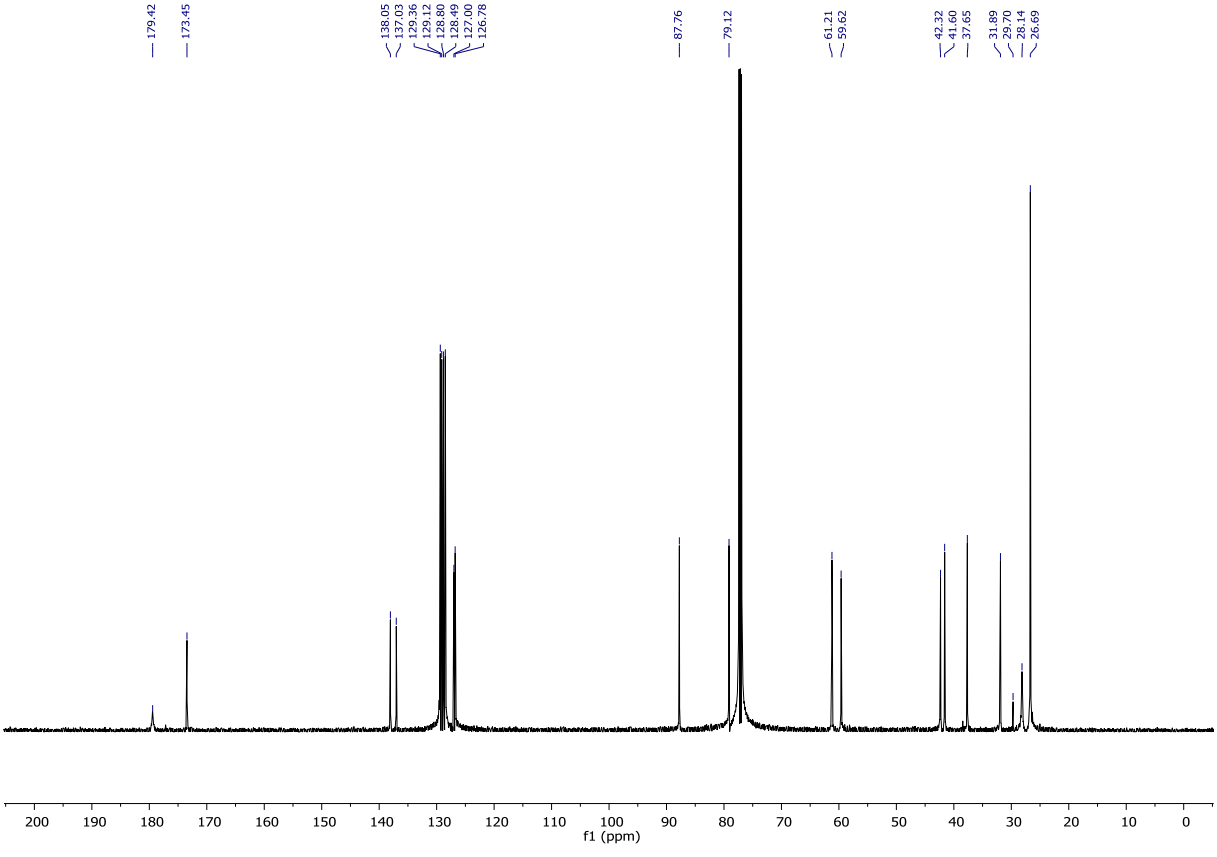

1-((1*S*,2*S*)-1-((2*R*,5*R*)-5-benzyl-2-(tert-butyl)-3-methyl-4-oxoimidazolidin-1-yl)-2-chloro-3-phenylpropyl)pyrrolidine-2,5-dione ((1*S*,2*S*)-*anti*-25)

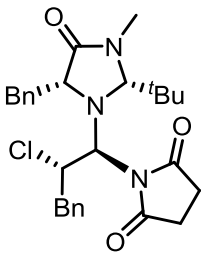

(1*S*,2*S*)-*anti*-**25**

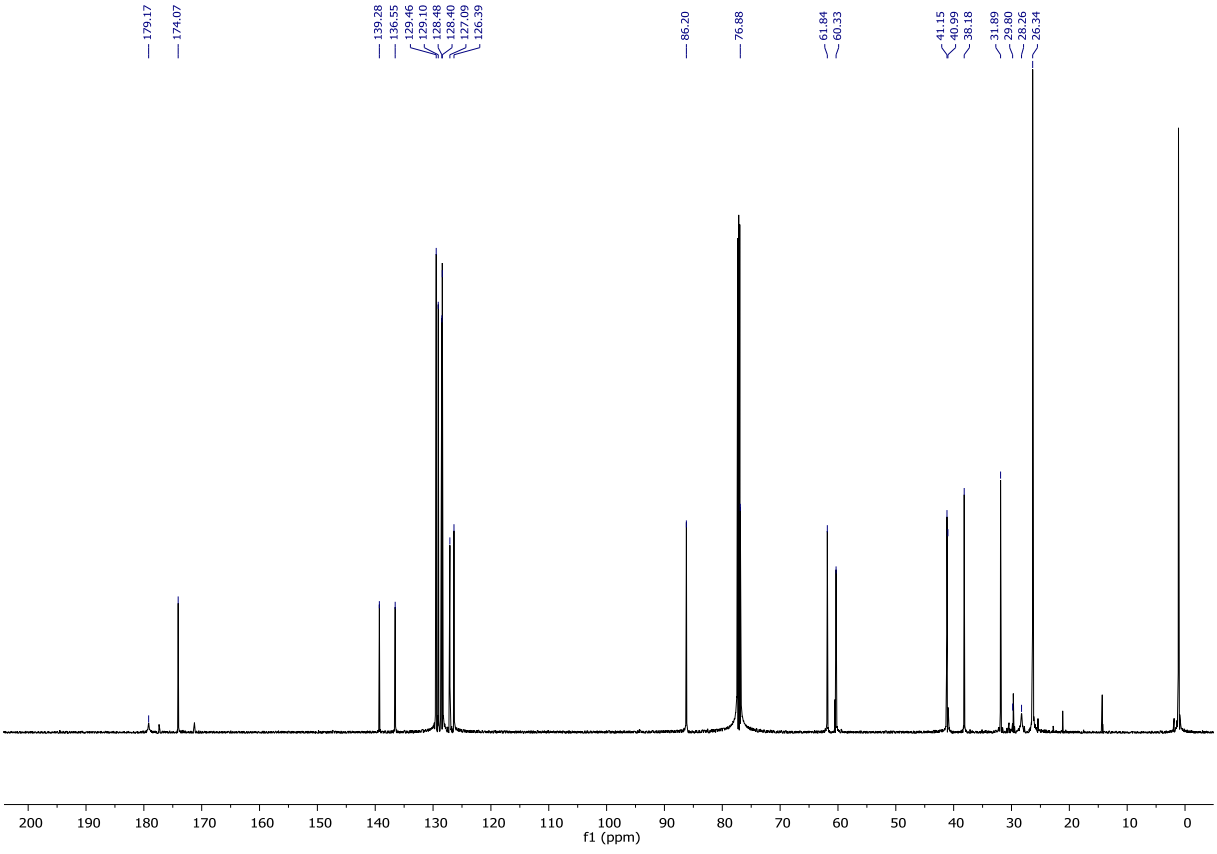

1-((1*R*,2*S*)-1-((2*R*,5*R*)-5-benzyl-2-(tert-butyl)-3-methyl-4-oxoimidazolidin-1-yl)-2-chloro-3-phenylpropyl)pyrrolidine-2,5-dione ((1*R*,2*S*)-*syn*-25)

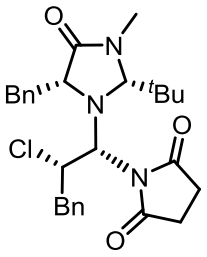

(1*R*,2*S*)-*syn*-**25**

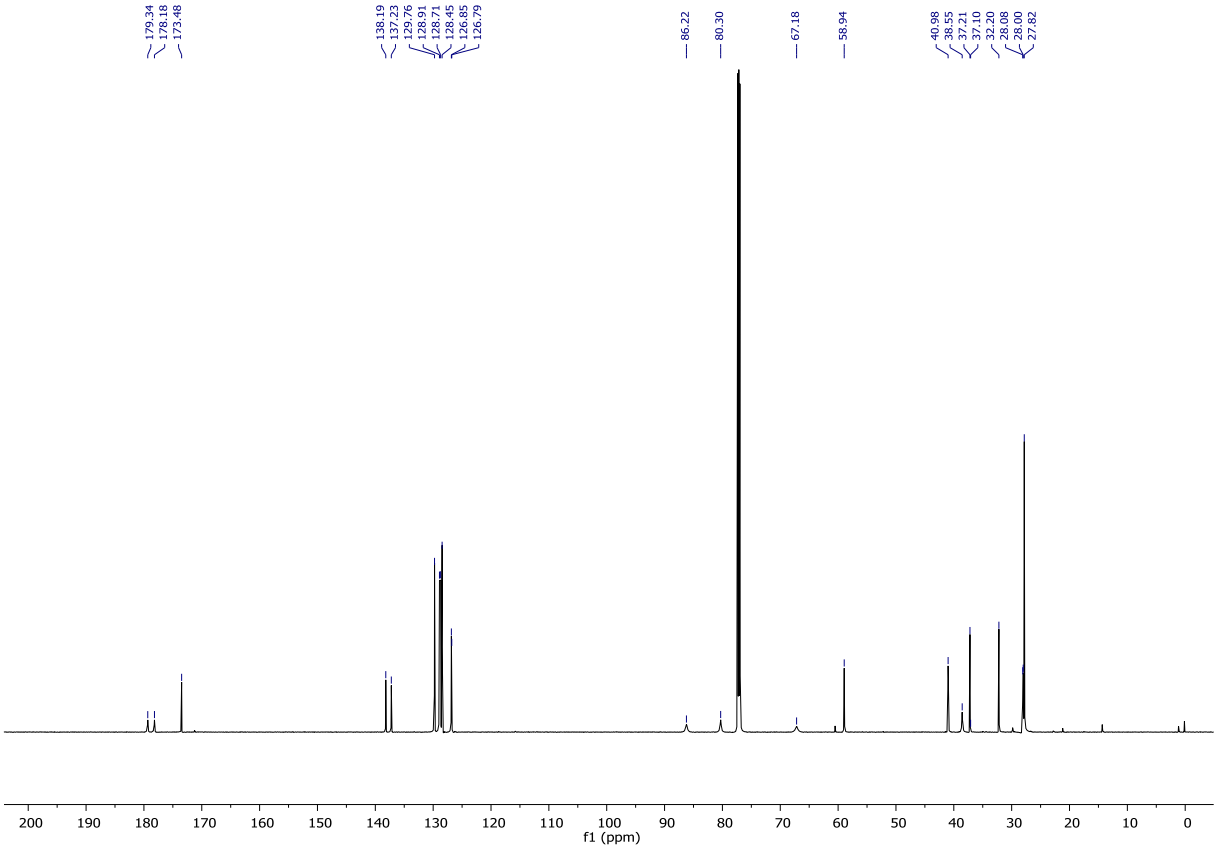

Decomposition of Aminal *syn*-18b

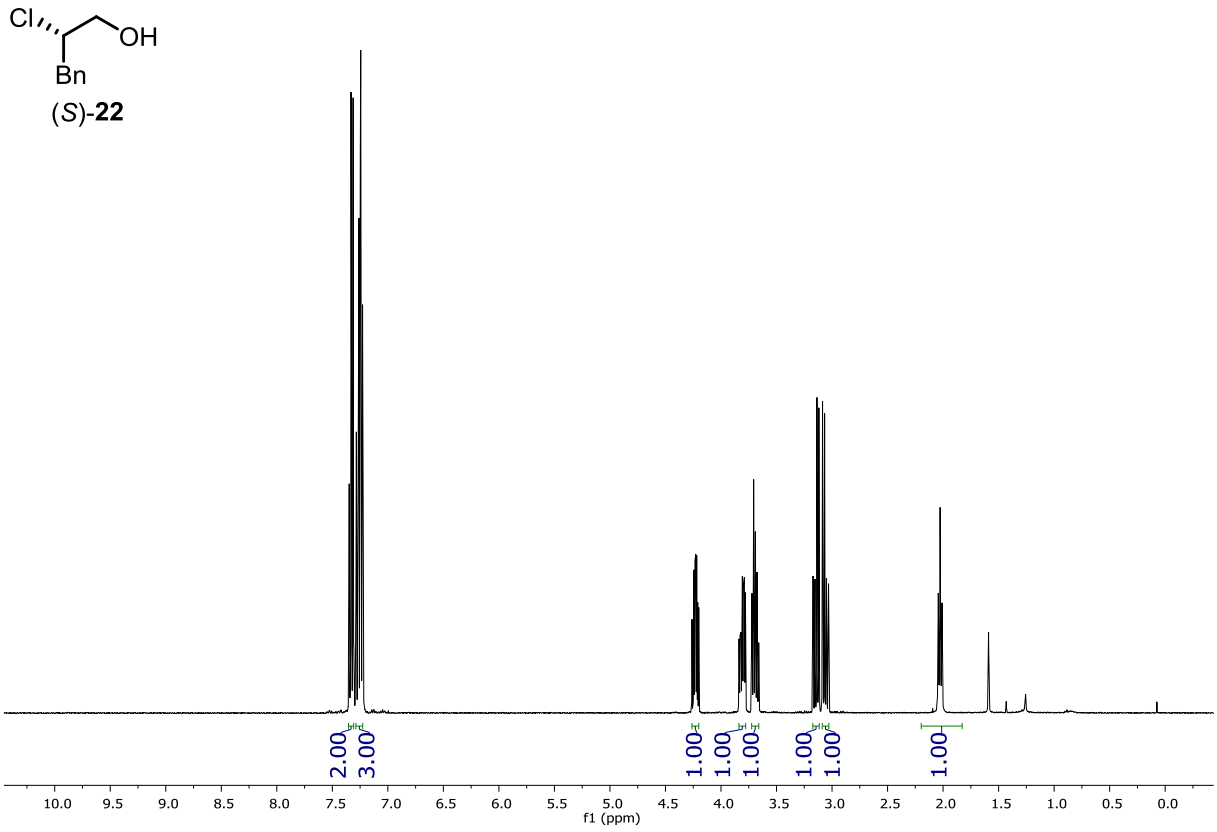

KIE-experiment (1)

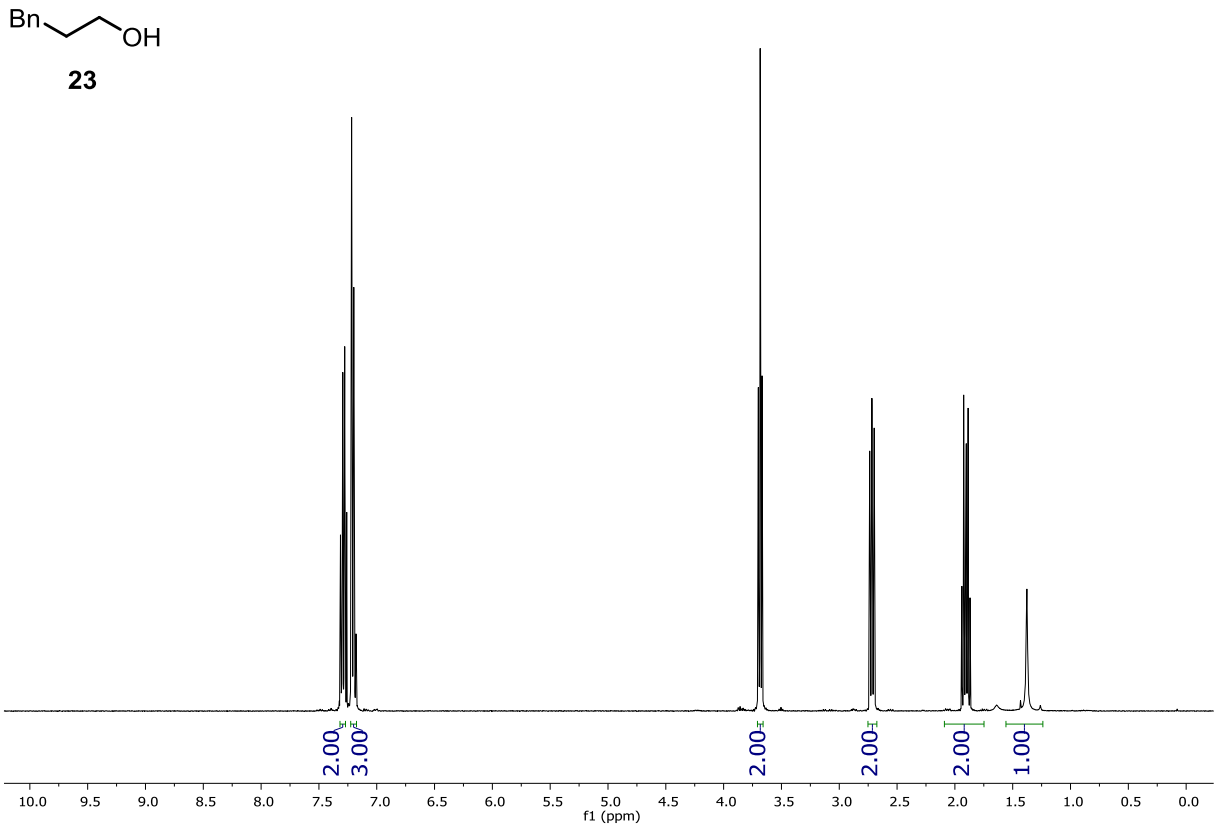

^{1}H-NMR (crude) after reductive work-up:

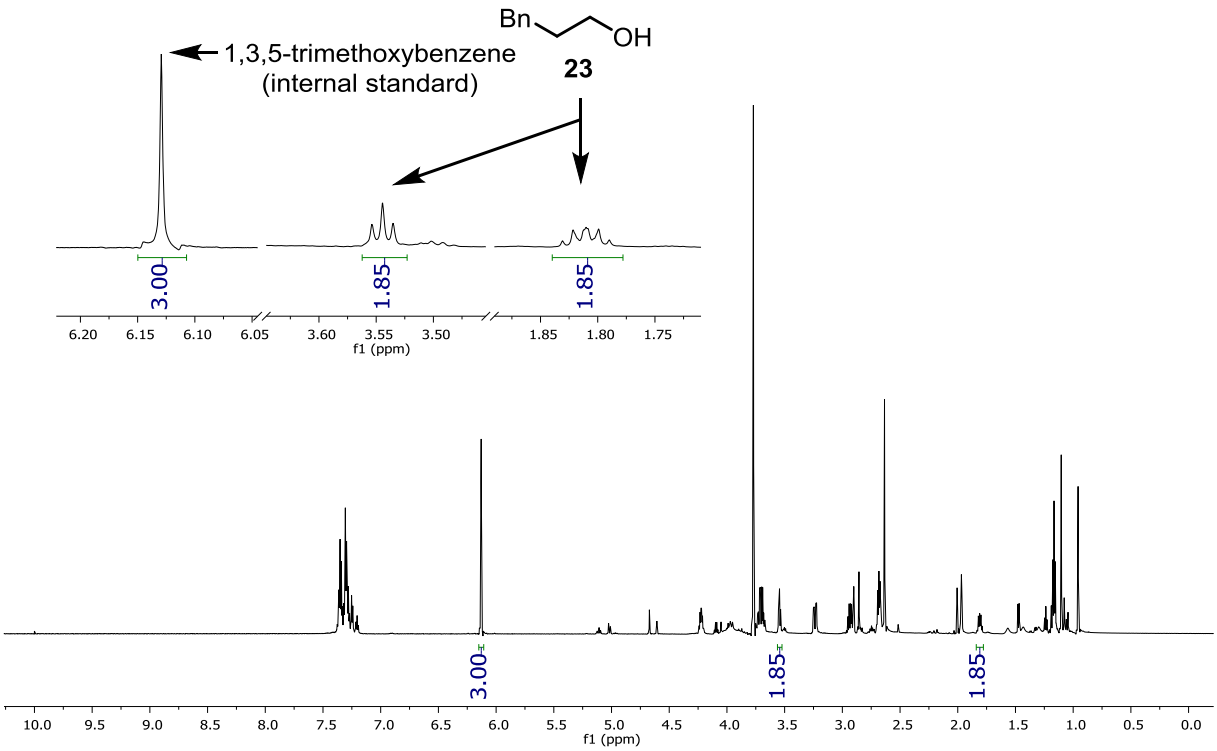

2-(1-((*S*)-2-(bis(3,5-bis(trifluoromethyl)phenyl)((trimethylsilyl)oxy)methyl)pyrrolidin-1-yl)-2-chloro-3-methylbutyl)isoindoline-1,3-dione (14)

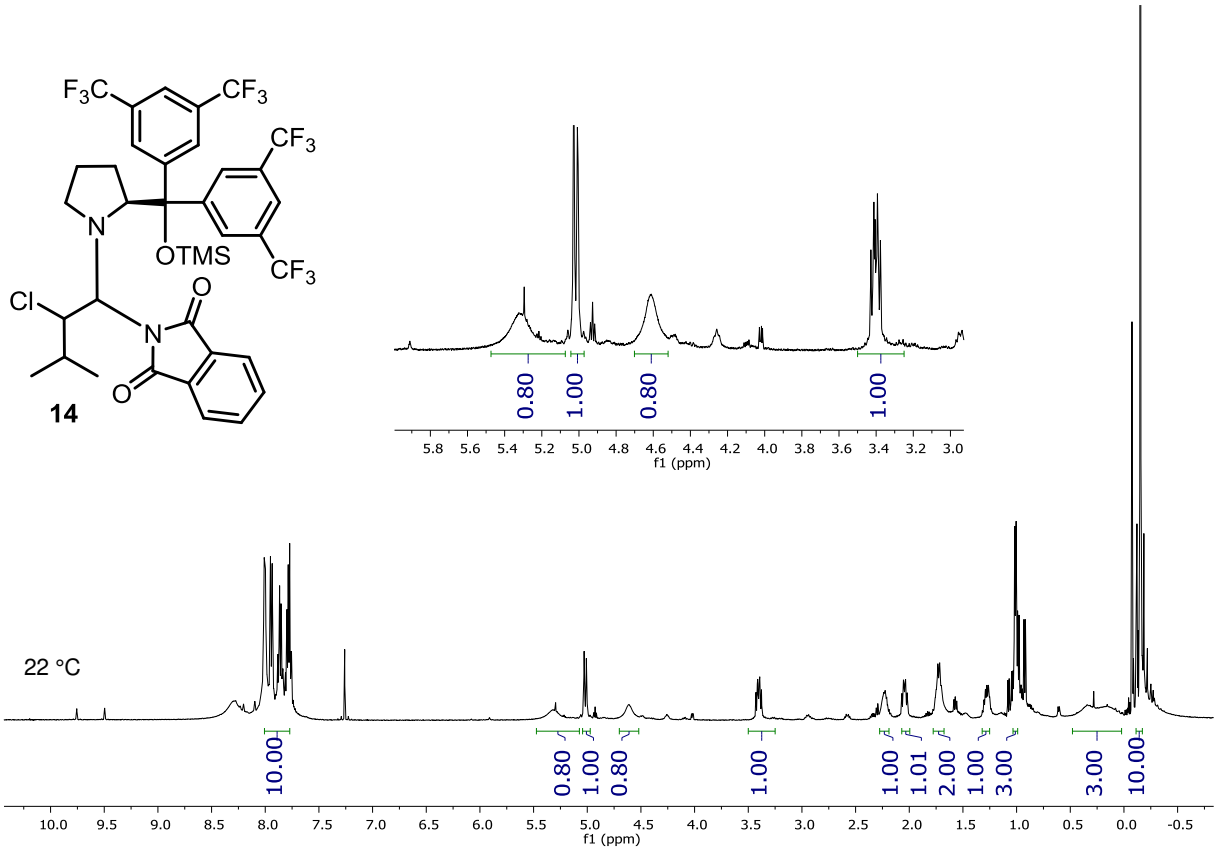

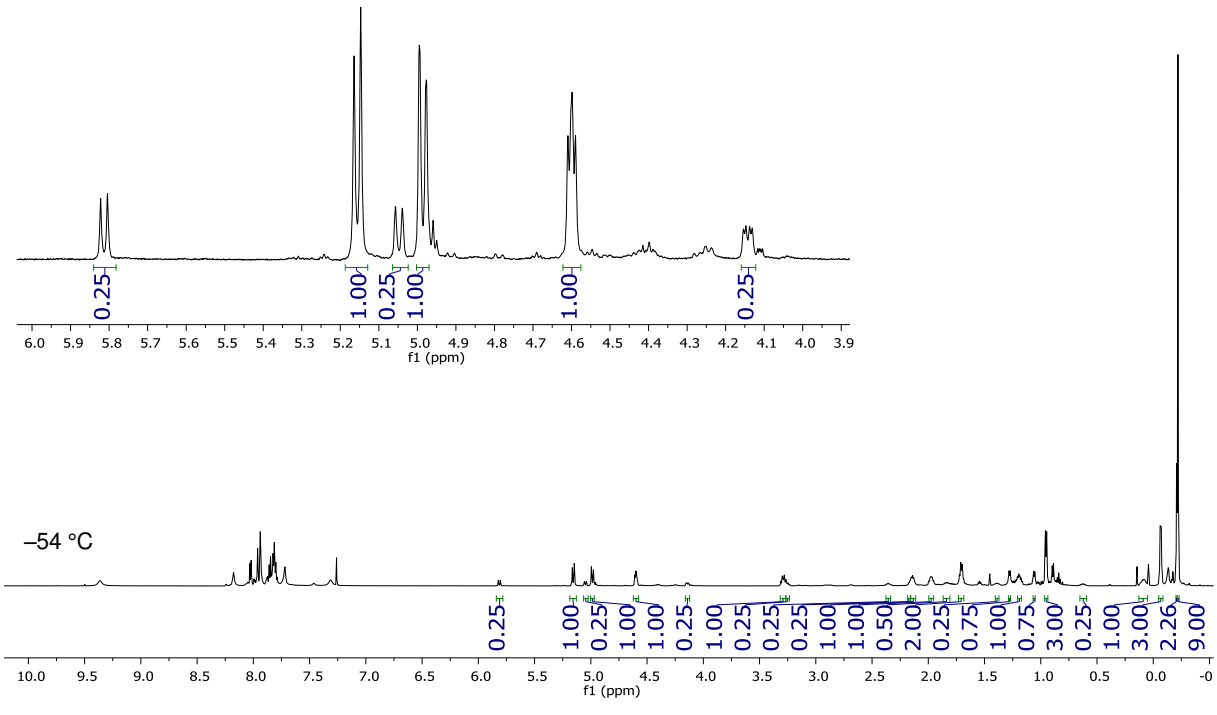

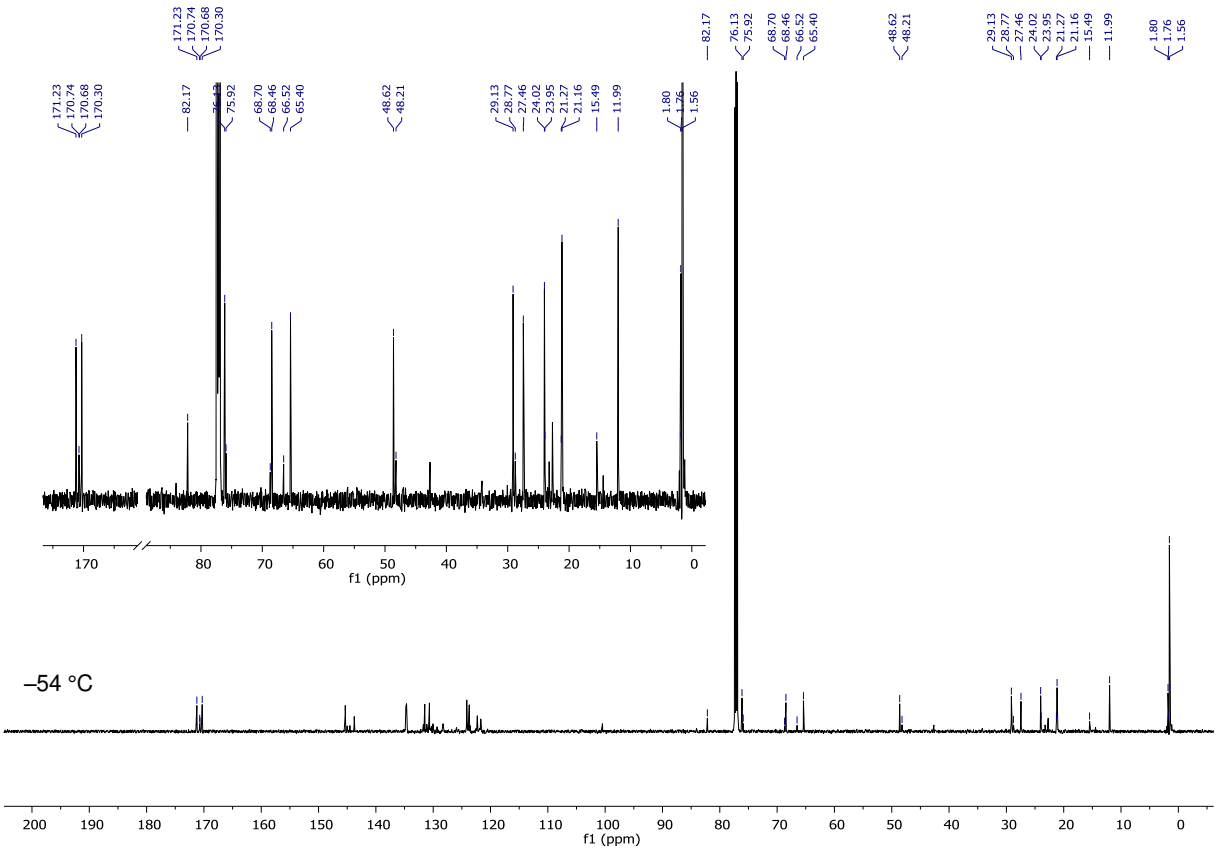
171.23
170.74
170.68
170.30
82.17
76.13
75.92
68.70
68.46
66.52
65.40
48.62
48.21
29.13
28.77
27.46
24.02
23.95
21.27
21.16
15.49
11.99
1.80
1.76
1.56
–54 °C
f1 (ppm)

(*S*)-2-chloro-3-methylbutyl 3,5-dinitrobenzoate ((*S*)-SI2)

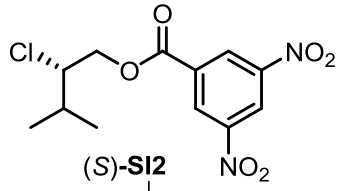

(*S*)-**SI2**

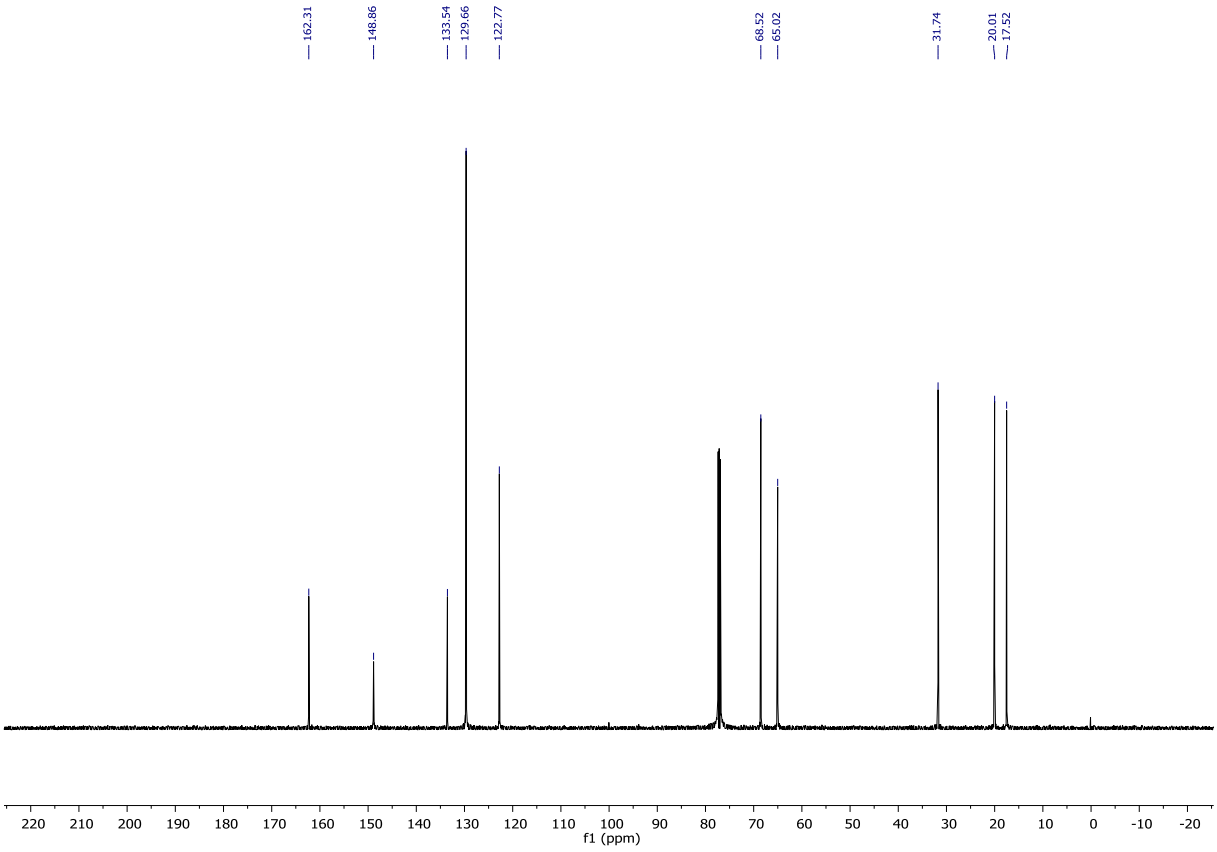

***N*-((1*S*,2*S*)-1-((*S*)-2-(bis(3,5-bis(trifluoromethyl)phenyl)((trimethylsilyl)oxy)methyl)pyrrolidin-1-yl)-2-chloro-3-methylbutyl)-2-(hydroxymethyl)benzamide (SI3)**

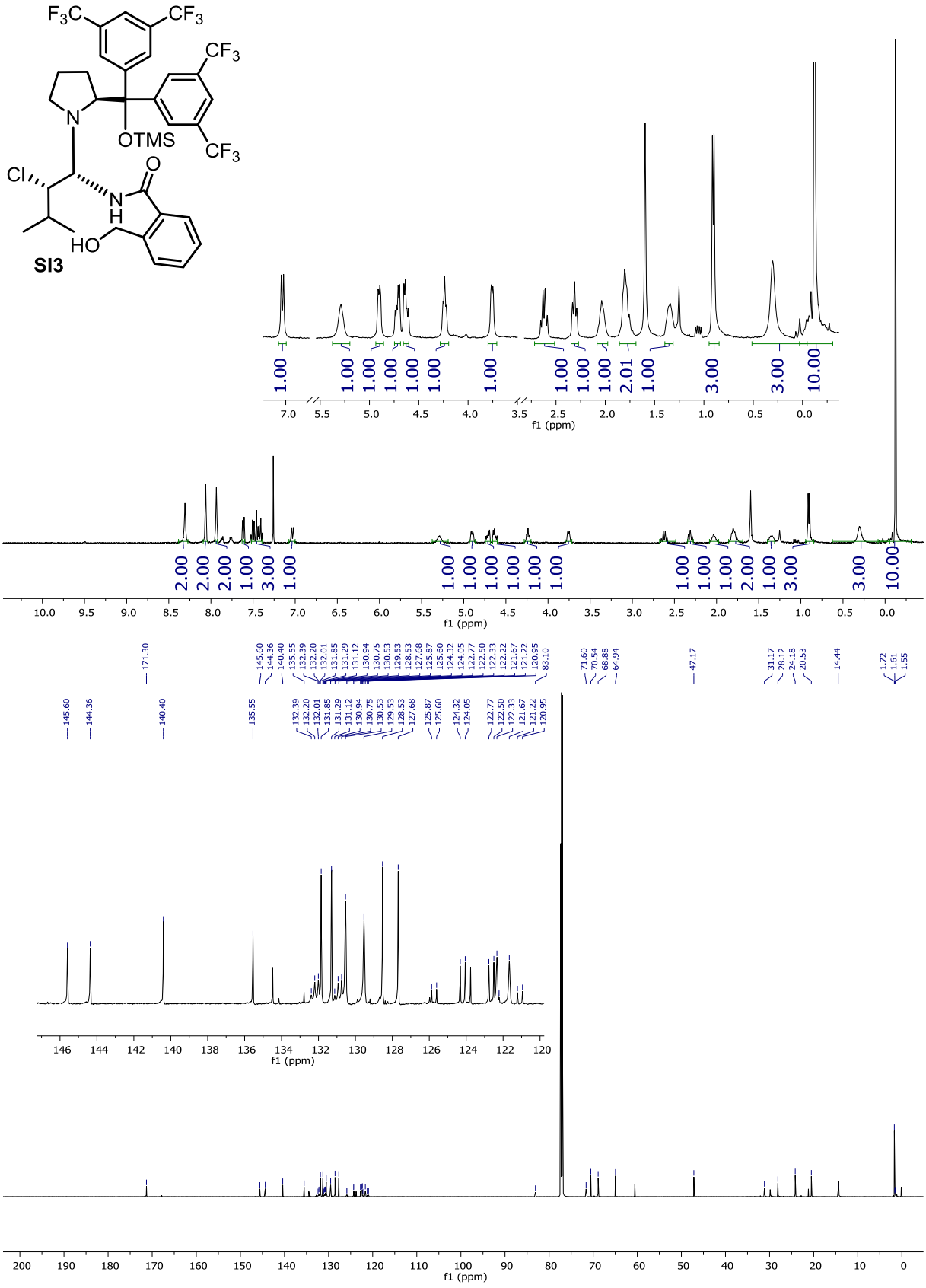

2-(((1*S*,2*S*)-1-((*S*)-2-(bis(3,5-bis(trifluoromethyl)phenyl)((trimethylsilyl)oxy)methyl)pyrrolidin-1-yl)-2-chloro-3-methylbutyl)carbamoyl)benzyl 3,5-dinitrobenzoate (15)

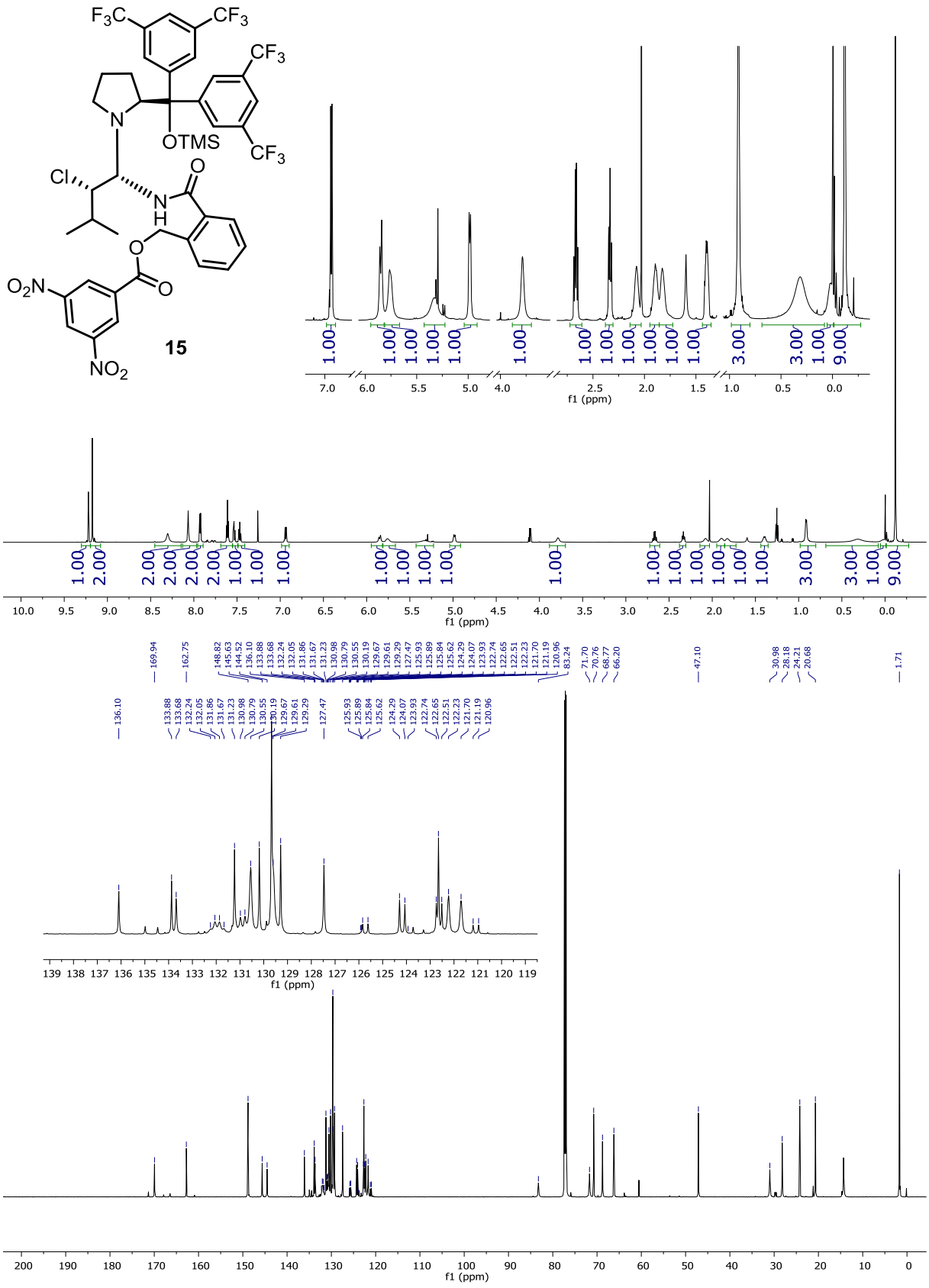

Decomposition of Aminal 14 (1) Last sample (70 h, EtOAc impurities)

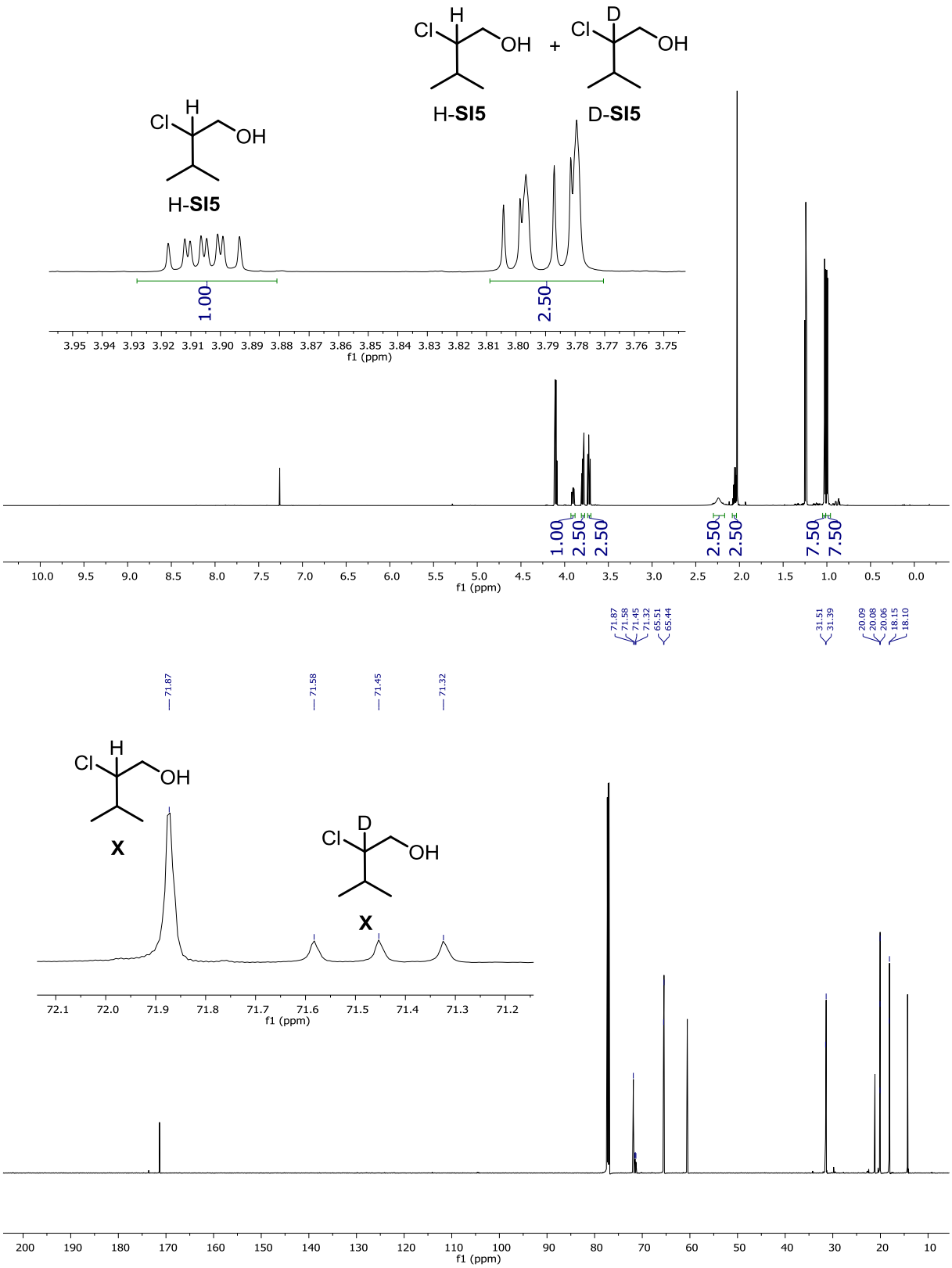

(*S*)-2-chloro-3-methylbutan-1-ol ((*S*)-SI5)

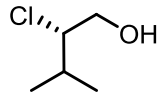

(*S*)-**SI5**

2-(1-((*S*)-2-(bis(3,5-bis(trifluoromethyl)phenyl)((trimethylsilyl)oxy)methyl)pyrrolidin-1-yl)-2-chloropropyl)isoindoline-1,3-dione (SI6)

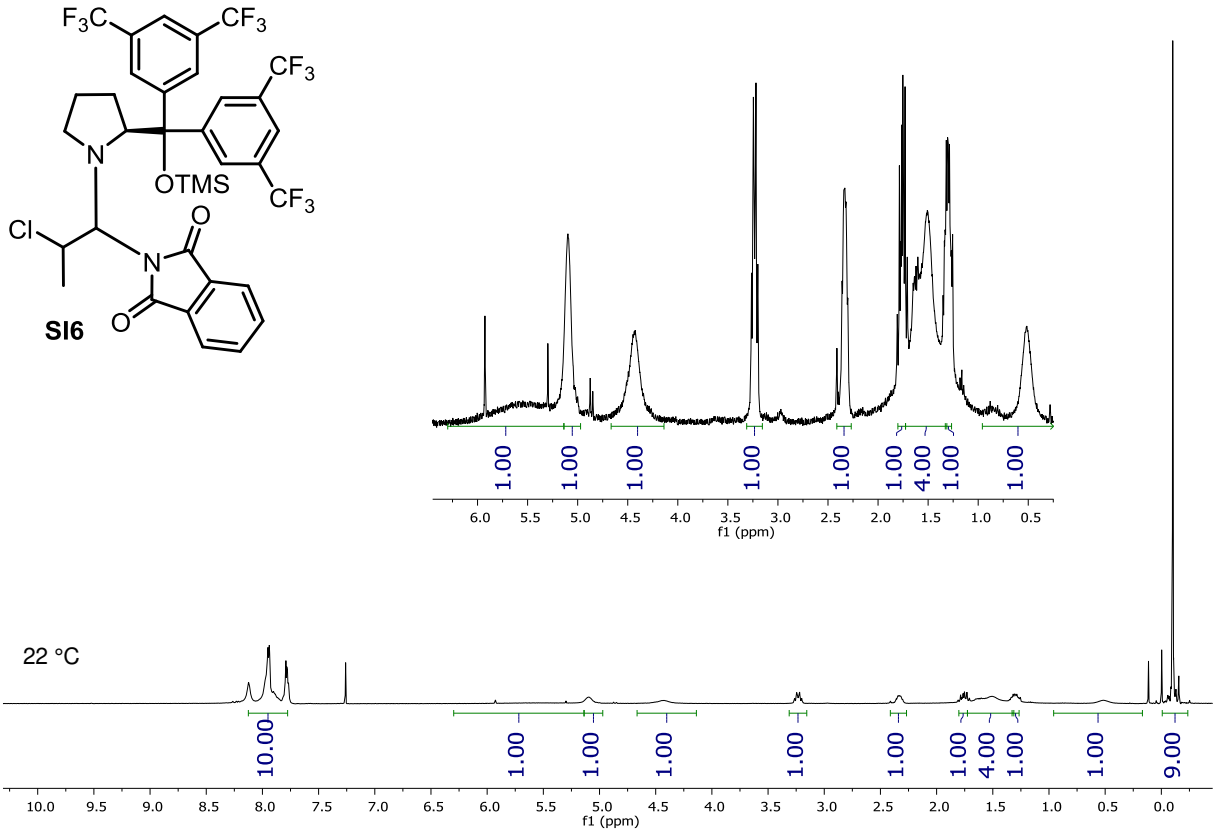

2-(1-((*S*)-2-(bis(3,5-bis(trifluoromethyl)phenyl)((trimethylsilyl)oxy)methyl)pyrrolidin-1-yl)-2-chloropropyl)isoindoline-1,3-dione (SI6)

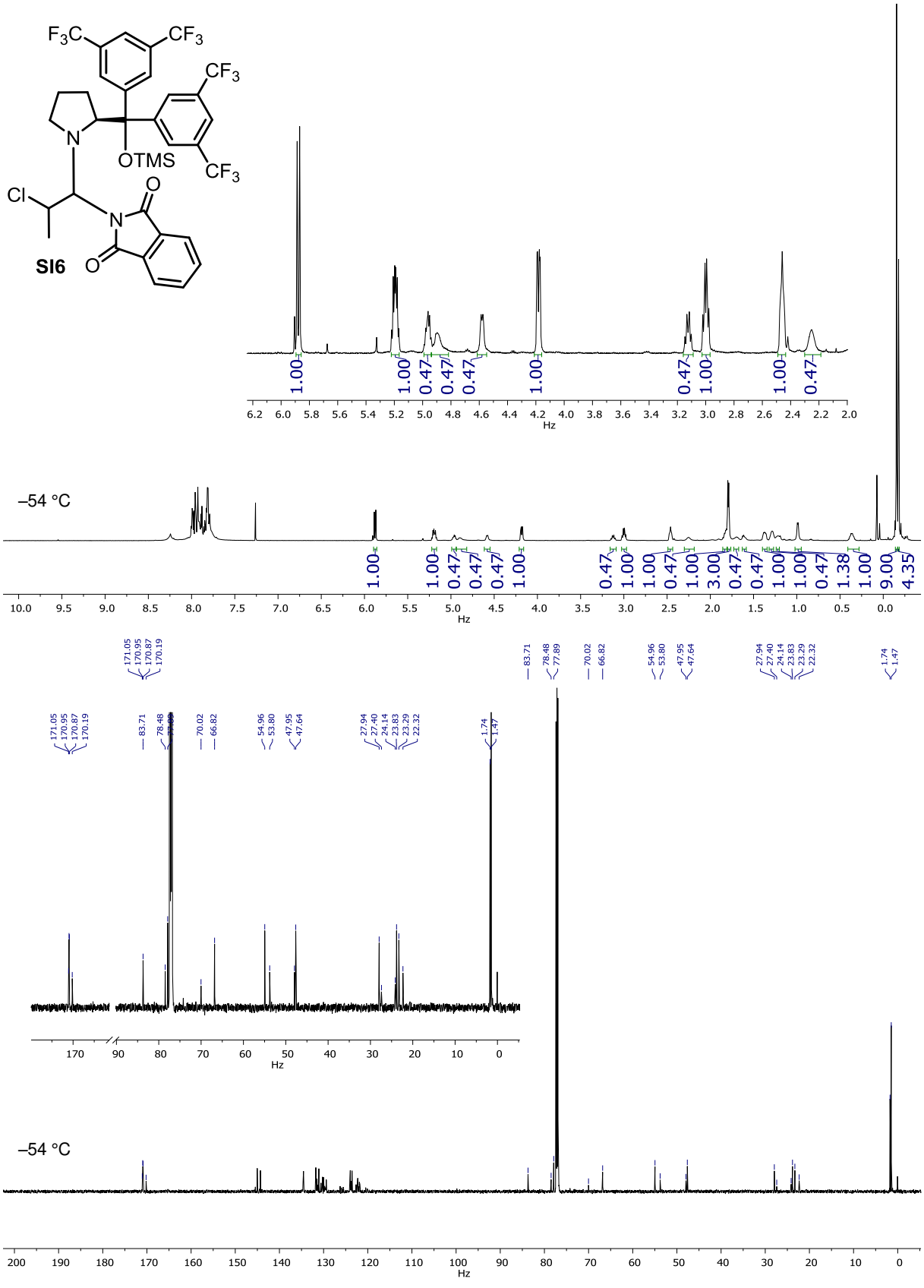

(*S*)-2-chloropropyl 3,5-dinitrobenzoate ((*S*)-SI10)

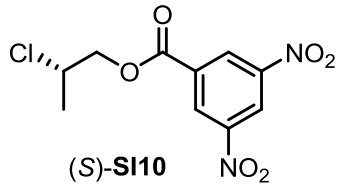

(*S*)-**SI10**

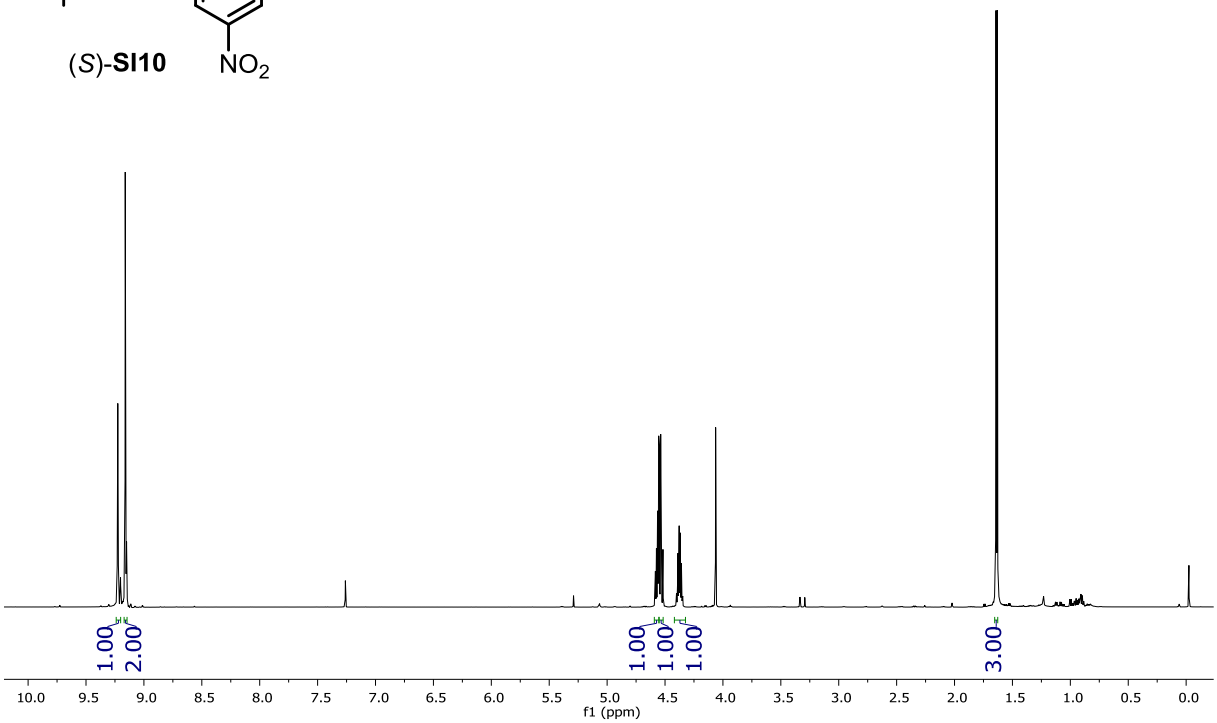

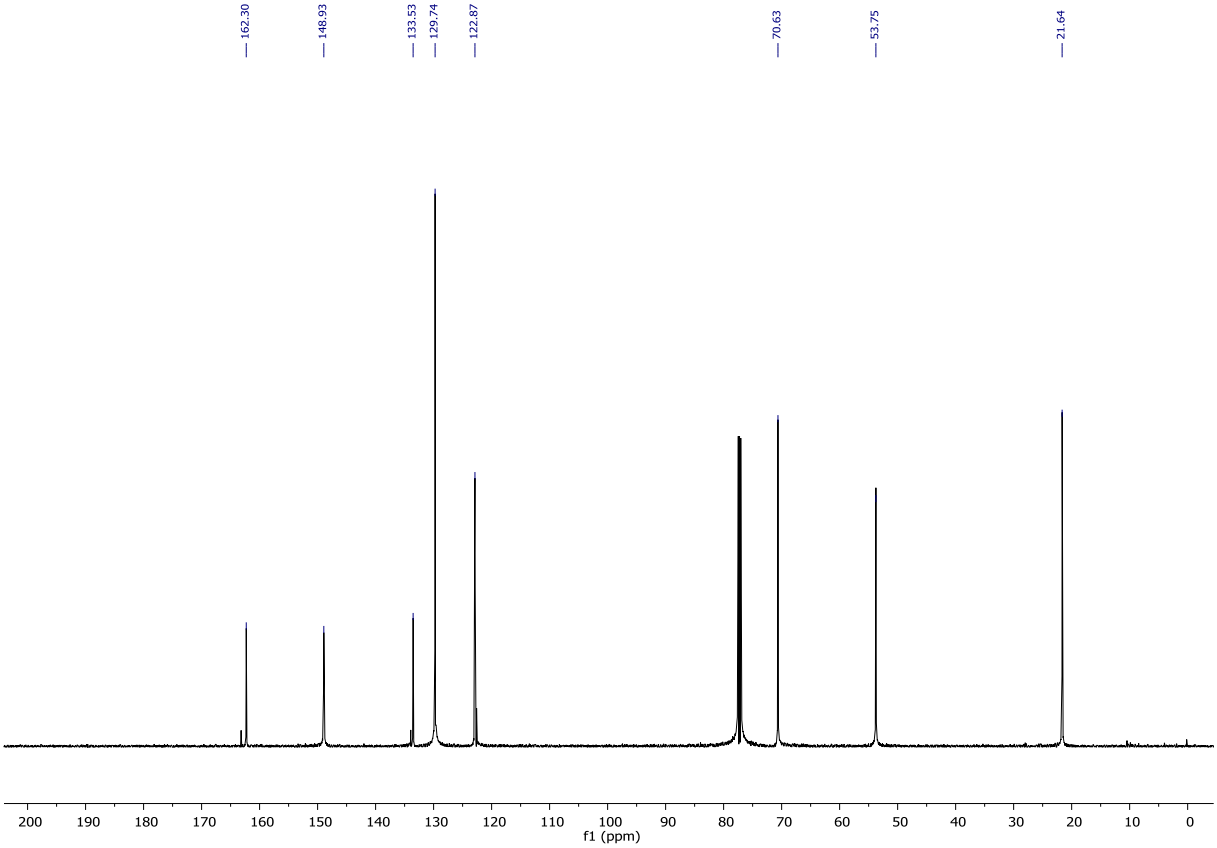

2-chloropropan-1-ol (rac-SI9)

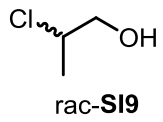

rac-**SI9**

Deuterium incorporation experiment

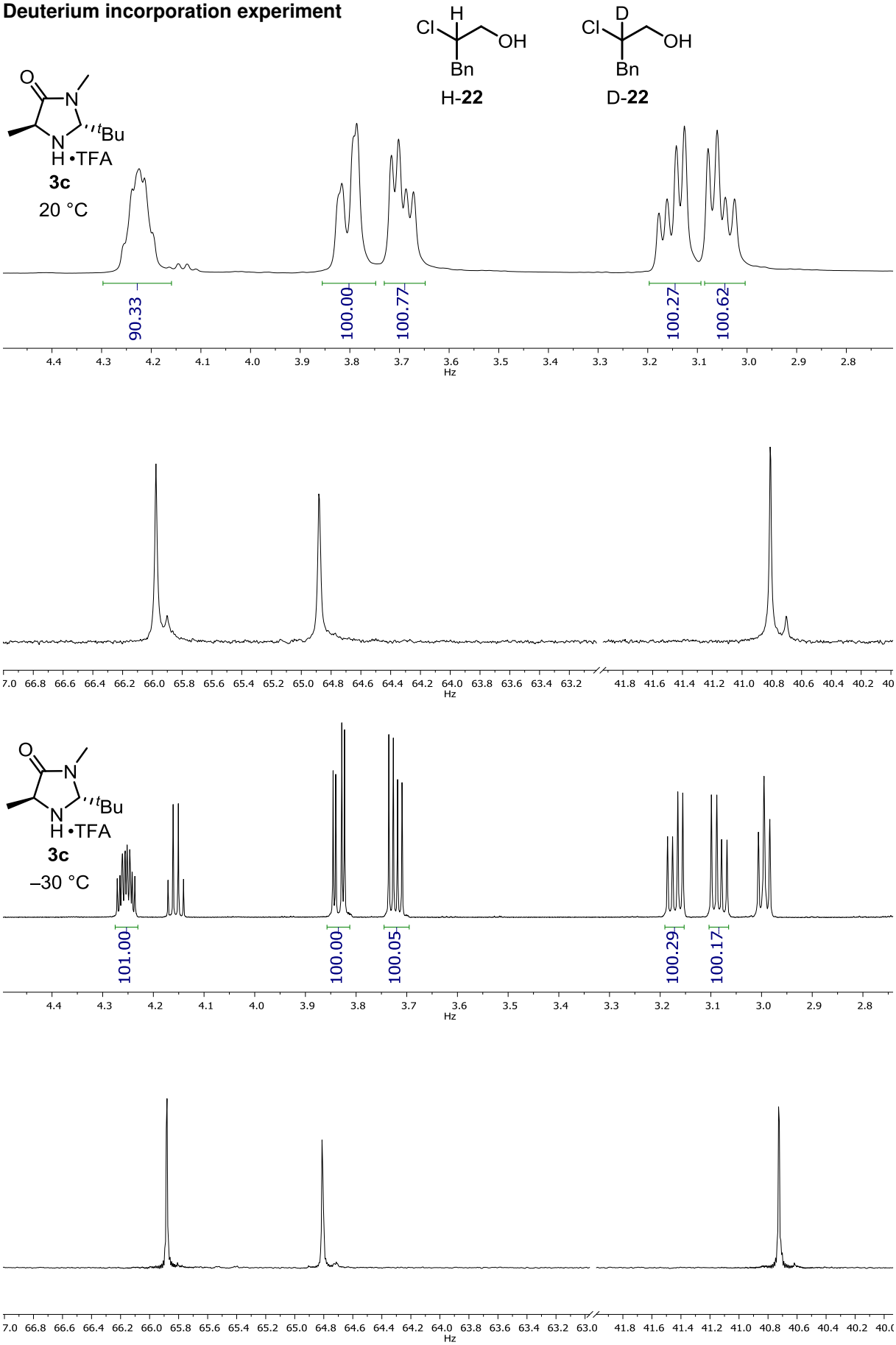

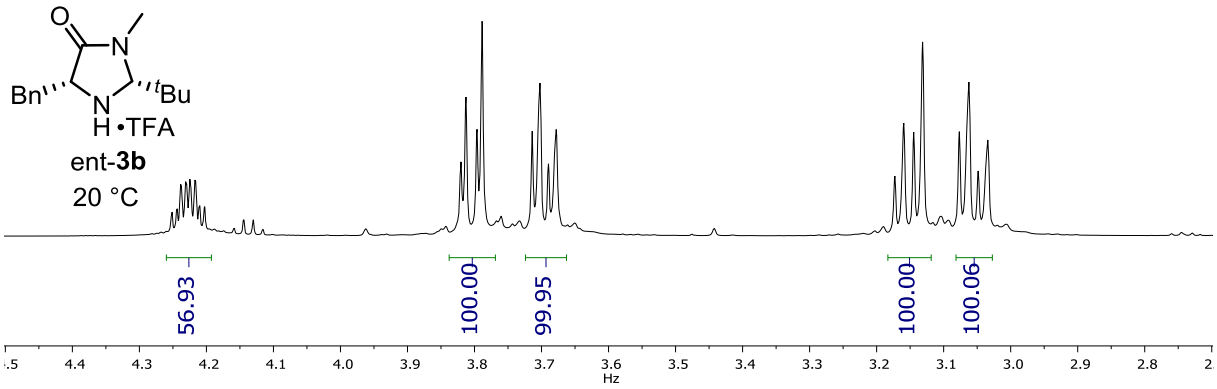
O
N
Bn
N
tBu
H •TFA
ent-3b
20 °C
56.93
100.00
99.95
100.00
100.06
4.5 4.4 4.3 4.2 4.1 4.0 3.9 3.8 3.7 3.6 3.5 3.4 3.3 3.2 3.1 3.0 2.9 2.8 2
Hz

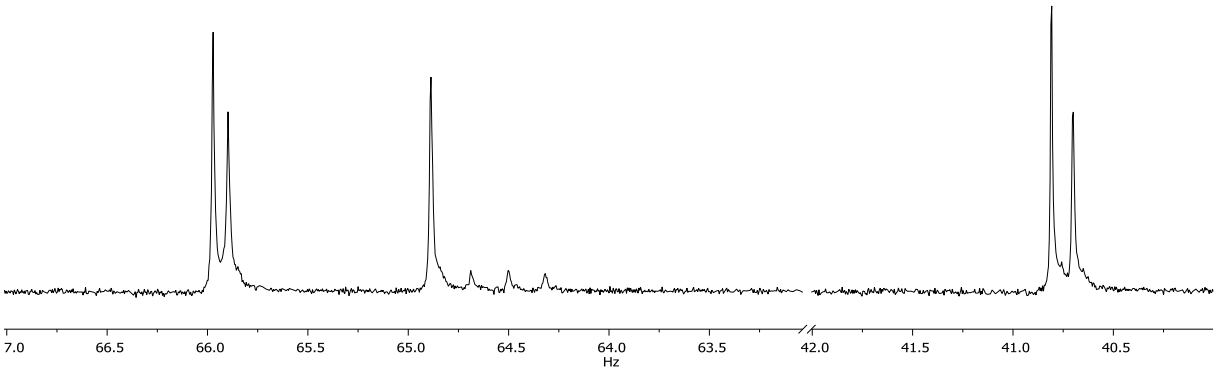
67.0 66.5 66.0 65.5 65.0 64.5 64.0 63.5 42.0 41.5 41.0 40.5
Hz

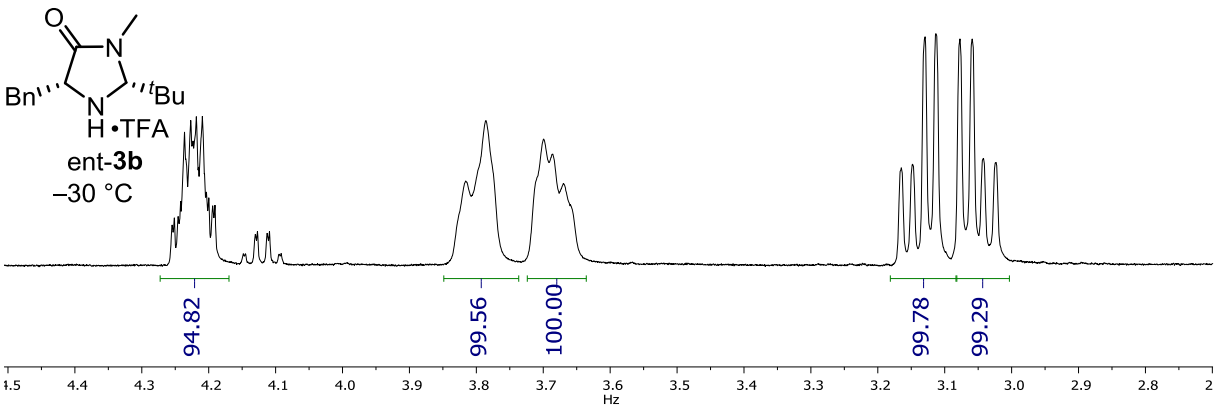
O
N
Bn
N
tBu
H •TFA
ent-3b
–30 °C
94.82
99.56
100.00
99.78
99.29
4.5 4.4 4.3 4.2 4.1 4.0 3.9 3.8 3.7 3.6 3.5 3.4 3.3 3.2 3.1 3.0 2.9 2.8 2
Hz

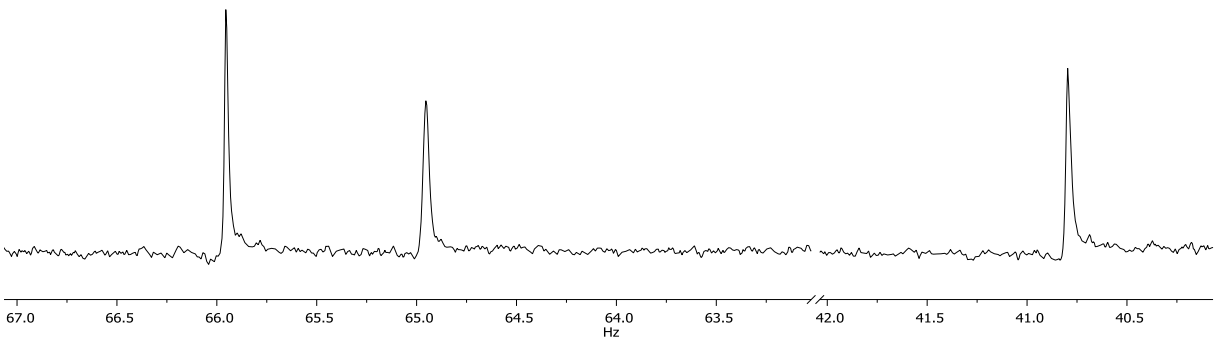
67.0 66.5 66.0 65.5 65.0 64.5 64.0 63.5 42.0 41.5 41.0 40.5
Hz

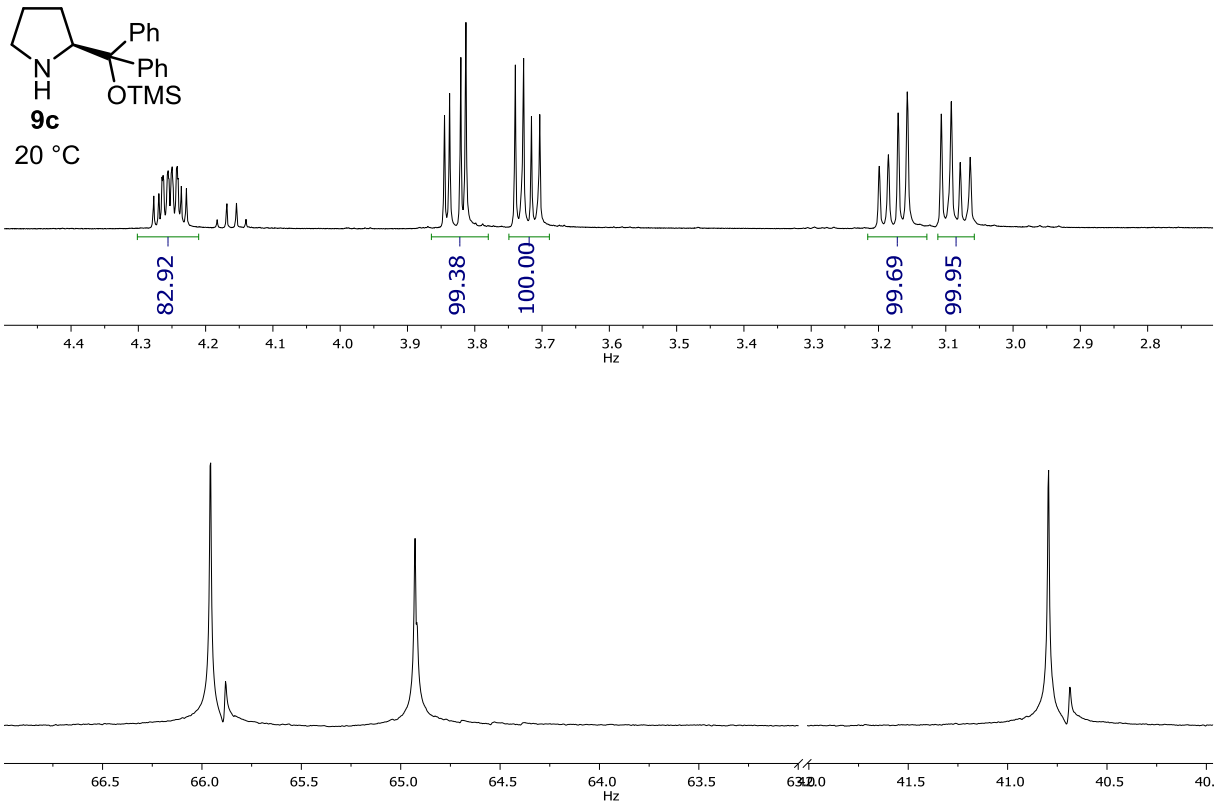
Ph
Ph
OTMS
N
H
9c
20 °C
82.92
99.38
100.00
99.69
99.95
4.4 4.3 4.2 4.1 4.0 3.9 3.8 3.7 3.6 3.5 3.4 3.3 3.2 3.1 3.0 2.9 2.8
Hz
66.5 66.0 65.5 65.0 64.5 64.0 63.5 41.5 41.0 40.5
Hz

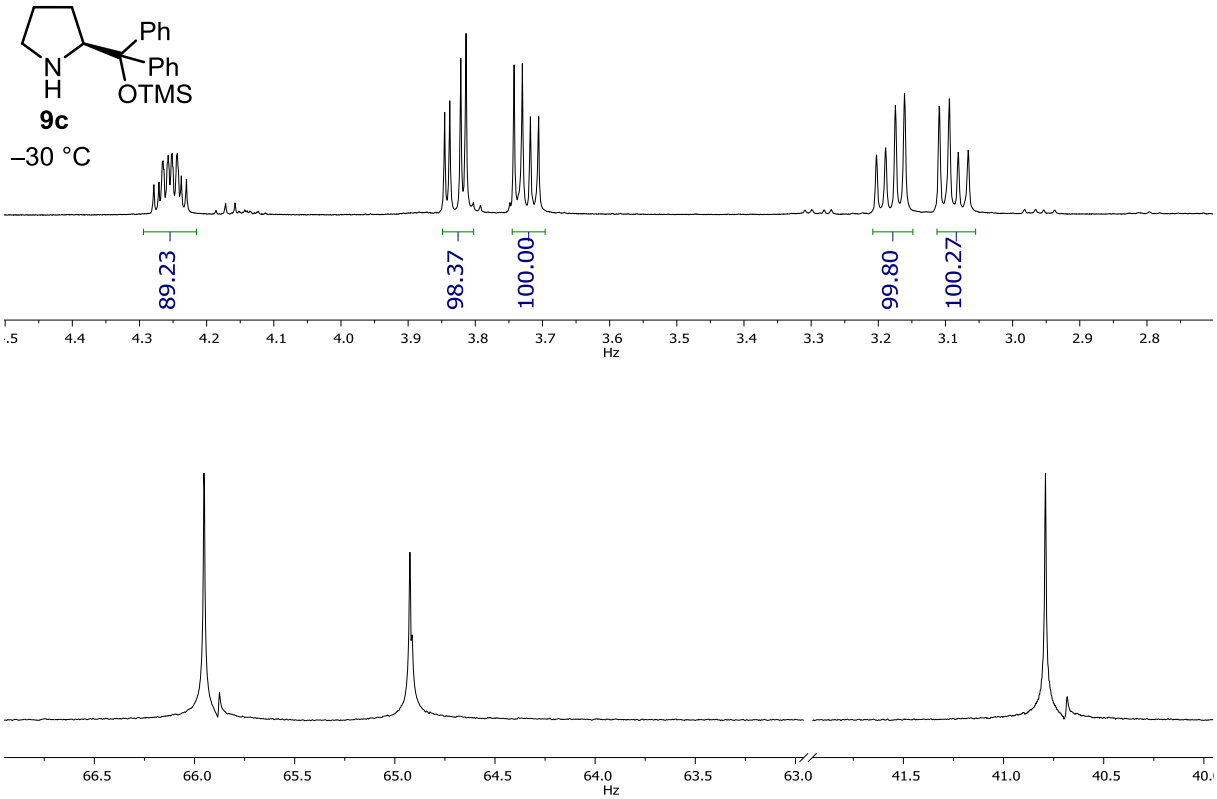
Ph
Ph
OTMS
N
H
9c
–30 °C
89.23
98.37
100.00
99.80
100.27
4.4 4.3 4.2 4.1 4.0 3.9 3.8 3.7 3.6 3.5 3.4 3.3 3.2 3.1 3.0 2.9 2.8
Hz
66.5 66.0 65.5 65.0 64.5 64.0 63.5 63.0 41.5 41.0 40.5
Hz

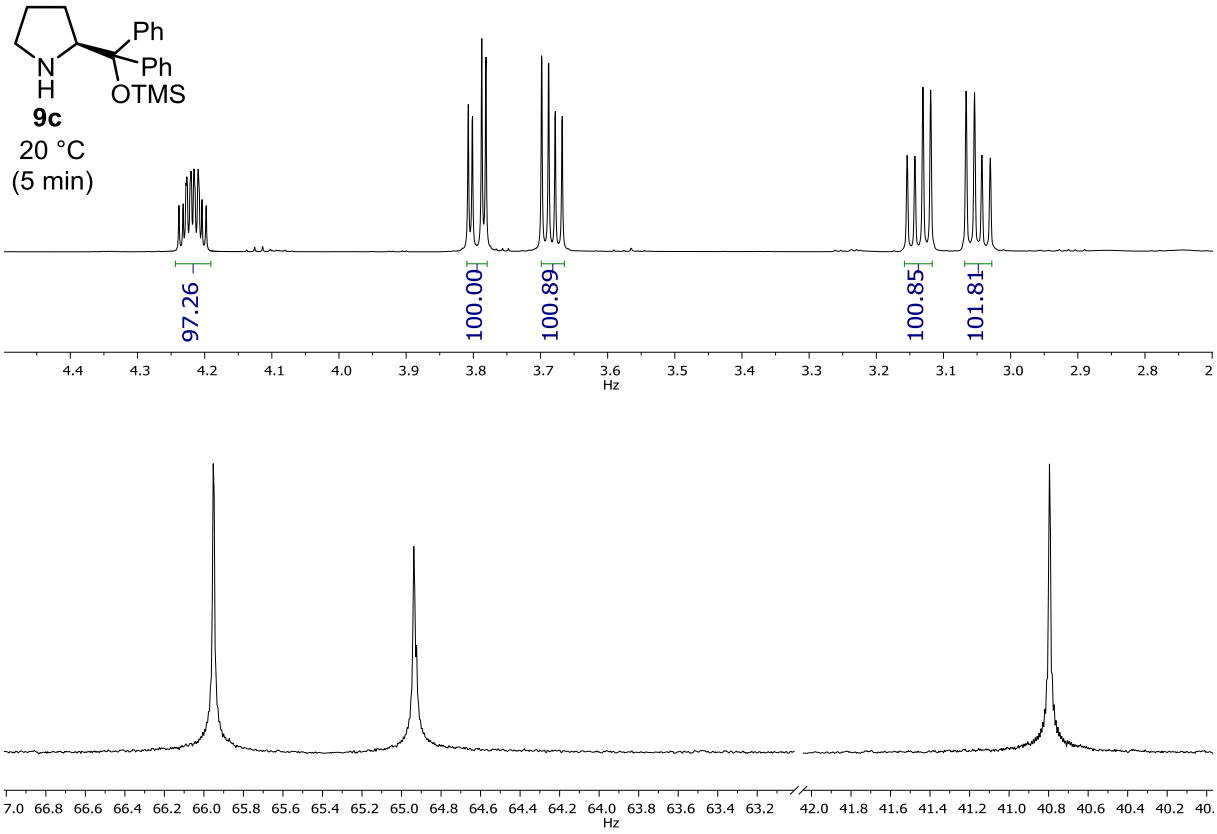
Ph
Ph
N
H
OTMS
9c
20 °C
(5 min)
97.26
100.00
100.89
100.85
101.81
Hz
Hz

2,2-dichloro-3-phenylpropan-1-ol (SI12)

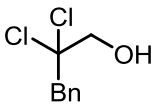

SI12

3-phenylpropanal-2,2-d_2 (D_2-16)

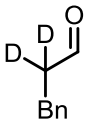

D_2-**16**

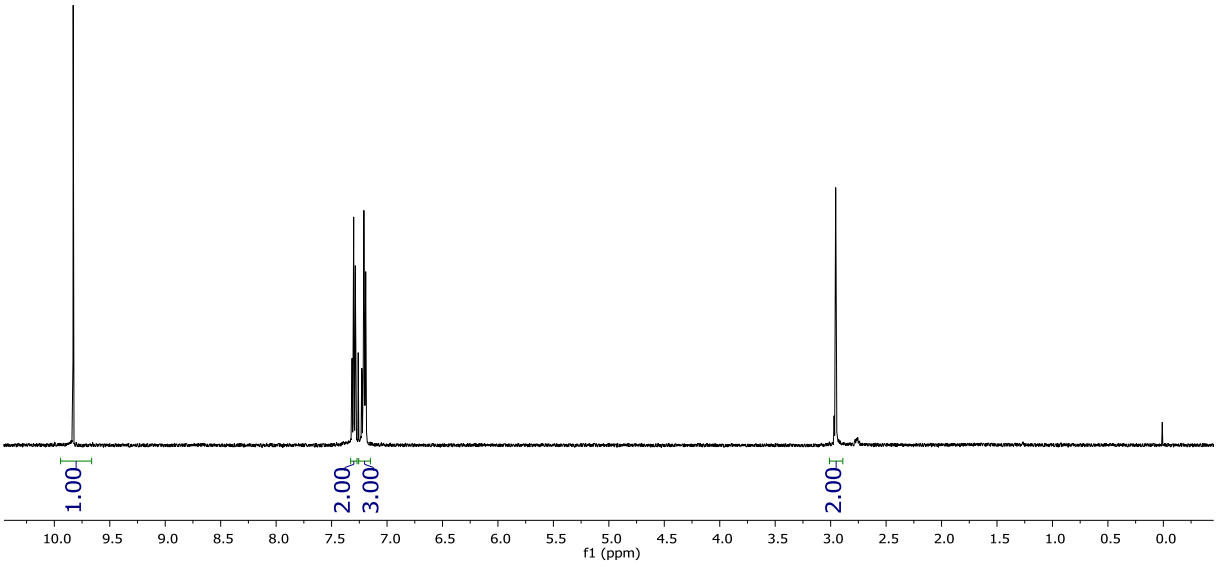

Isotopic competition experiment

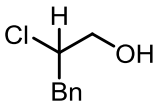

H-**22**

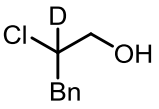

D-**22**

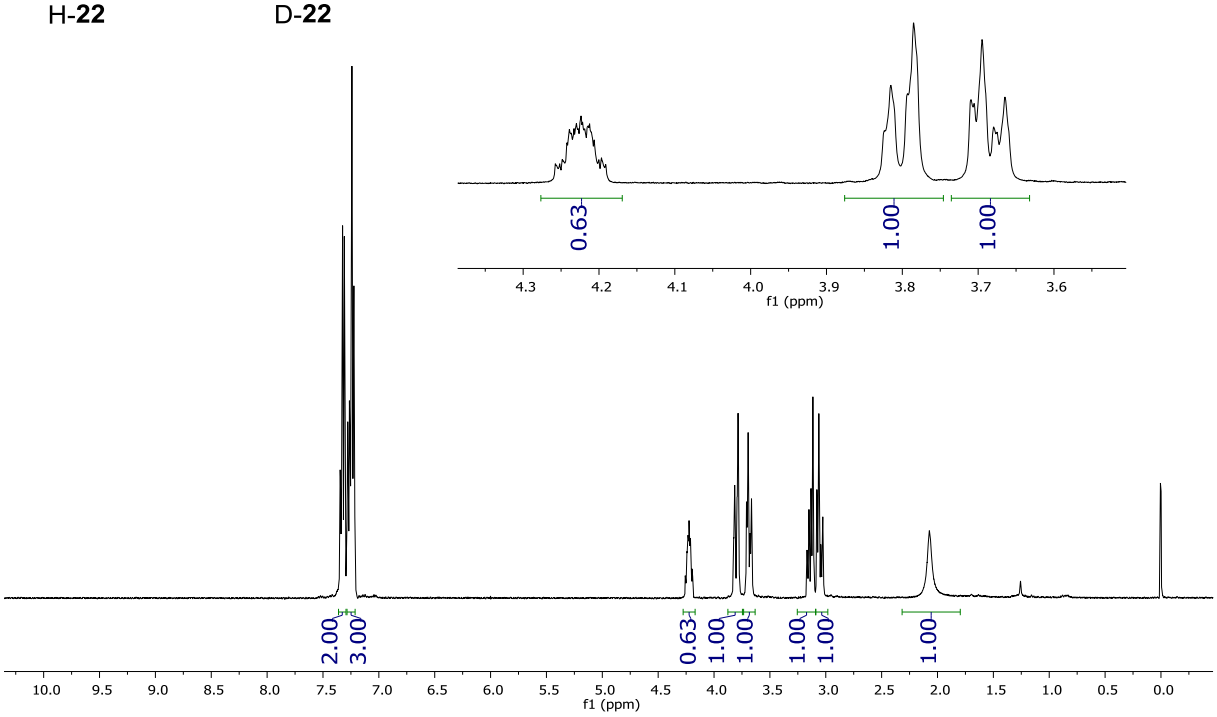

6.2. HPLC /GC Traces

1-((1*S*,2*R*)-1-((2*R*,5*R*)-5-benzyl-2-(tert-butyl)-3-methyl-4-oxoimidazolidin-1-yl)-2-chloro-3-methylbutyl)pyrrolidine-2,5-dione ((1*S*,2*R*)-*syn*-21), 1-((1*S*,2*S*)-1-((2*R*,5*R*)-5-benzyl-2-(tert-butyl)-3-methyl-4-oxoimidazolidin-1-yl)-2-chloro-3-methylbutyl)pyrrolidine-2,5-dione ((1*S*,2*S*)-*anti*-21), 1-((1*R*,2*S*)-1-((2*R*,5*R*)-5-benzyl-2-(tert-butyl)-3-methyl-4-oxoimidazolidin-1-yl)-2-chloro-3-methylbutyl)pyrrolidine-2,5-dione ((1*R*,2*S*)-*syn*-21)

HPLC: 1.0 ml/min, 25% ^{i}PrOH/hexane, Nucleosil 50-5 (0.4 x 25 cm)

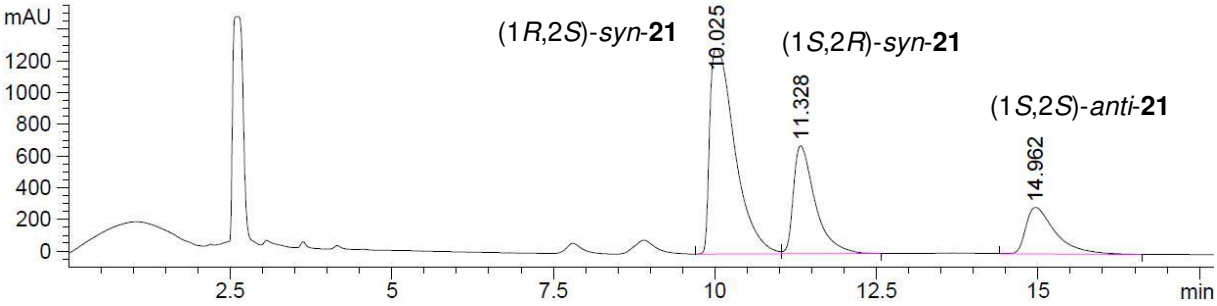

Peak #	RetTime [min]	Type	Width [min]	Area [mAU*s]	Height [mAU]	Area %
1	10.025	BV	0.4153	3.49800e4	1294.37756	57.9933
2	11.328	VB	0.3489	1.59431e4	681.62506	26.4321
3	14.962	VB	0.4726	9394.18164	294.14526	15.5746

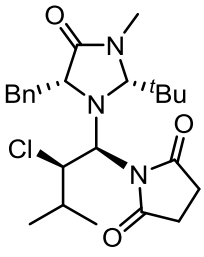

(1*S*,2*R*)-*syn*-**21**

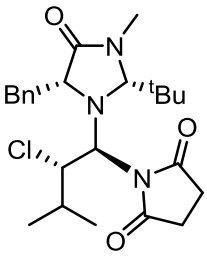

(1*S*,2*S*)-*anti*-**21**

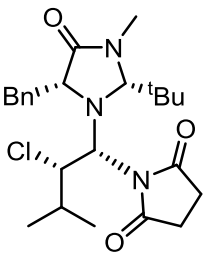

(1*R*,2*S*)-*syn*-**21**

1-((1*S*,2*R*)-1-((2*R*,5*R*)-5-benzyl-2-(tert-butyl)-3-methyl-4-oxoimidazolidin-1-yl)-2-chloro-3-phenylpropyl)pyrrolidine-2,5-dione ((1*S*,2*R*)-*syn*-25), 1-((1*S*,2*S*)-1-((2*R*,5*R*)-5-benzyl-2-(tert-butyl)-3-methyl-4-oxoimidazolidin-1-yl)-2-chloro-3-phenylpropyl)pyrrolidine-2,5-dione ((1*S*,2*S*)-*anti*-25), 1-((1*R*,2*S*)-1-((2*R*,5*R*)-5-benzyl-2-(tert-butyl)-3-methyl-4-oxoimidazolidin-1-yl)-2-chloro-3-phenylpropyl)pyrrolidine-2,5-dione ((1*R*,2*S*)-*syn*-25)

HPLC: 1.0 ml/min, 20% ^{i}PrOH/hexane, Nucleosil 50-5 (0.4 x 25 cm)

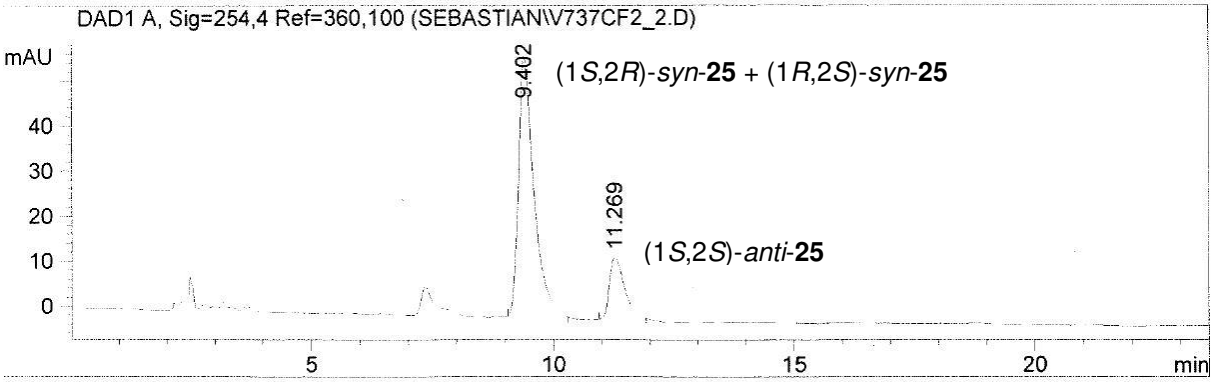

Peak #	RetTime [min]	Type	Width [min]	Area [mAU*s]	Height [mAU]	Area %
1	9.402	BB	0.3199	1263.66797	57.60223	80.3618
2	11.269	BB	0.3338	308.80560	13.97331	19.6382

HPLC: 20.0 ml/min, 5% EtOH/hexane, Nucleosil 50-5 (1.6 x 25 cm)

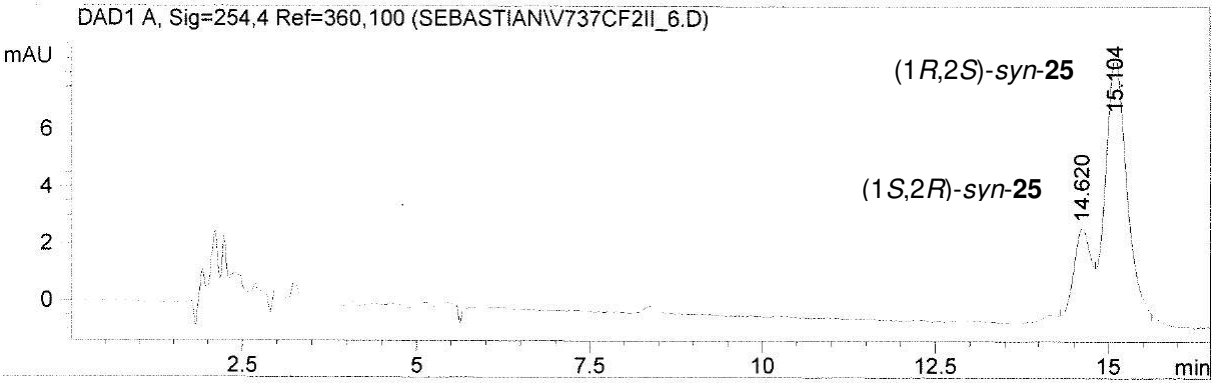

Peak #	RetTime [min]	Type	Width [min]	Area [mAU*s]	Height [mAU]	Area %
1	14.620	BV	0.2665	54.80790	3.12625	22.2573
2	15.104	VB	0.3160	191.43855	9.15442	77.7427

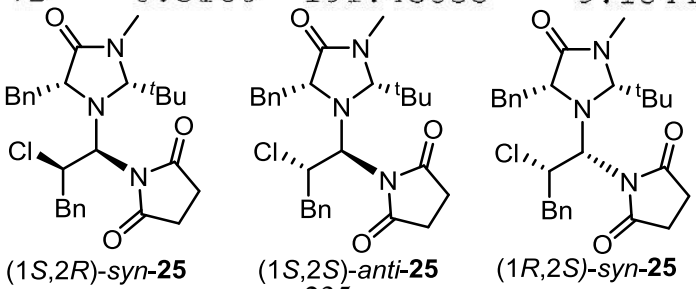

(1*S*,2*R*)-*syn*-**25** (1*S*,2*S*)-*anti*-**25** (1*R*,2*S*)-*syn*-**25**

Decomposition of Aminal *syn*-18b

HPLC: 0.8 ml/min, 5% EtOH/hexane, Chiralpak IA (0.46 x 25 cm)

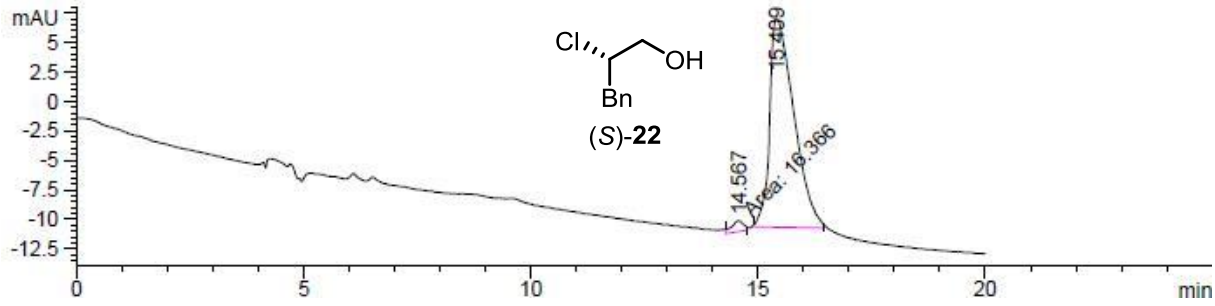

Peak #	RetTime [min]	Type	Width [min]	Area [mAU*s]	Height [mAU]	Area %
1	14.567	MM	0.2986	16.36597	9.13470e-1	2.4270
2	15.409	BB	0.5419	657.95312	17.69229	97.5730

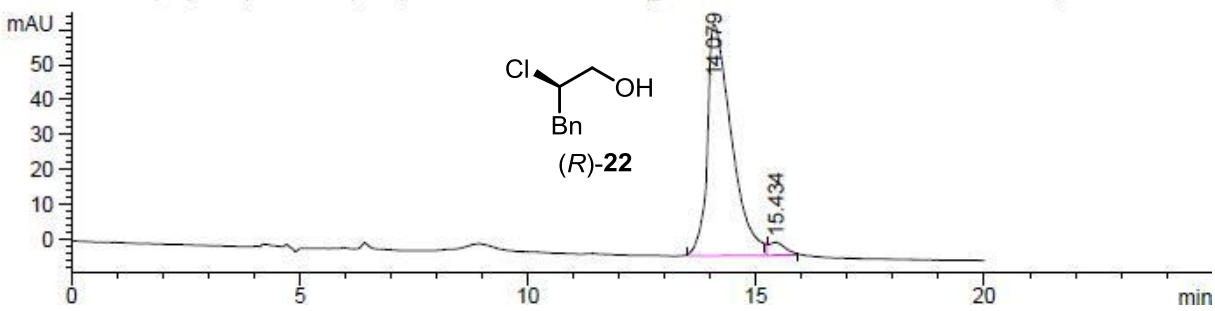

Peak #	RetTime [min]	Type	Width [min]	Area [mAU*s]	Height [mAU]	Area %
1	14.079	BB	0.5355	2435.25098	66.45875	96.2897
2	15.434	BB	0.3249	93.83700	3.63817	3.7103

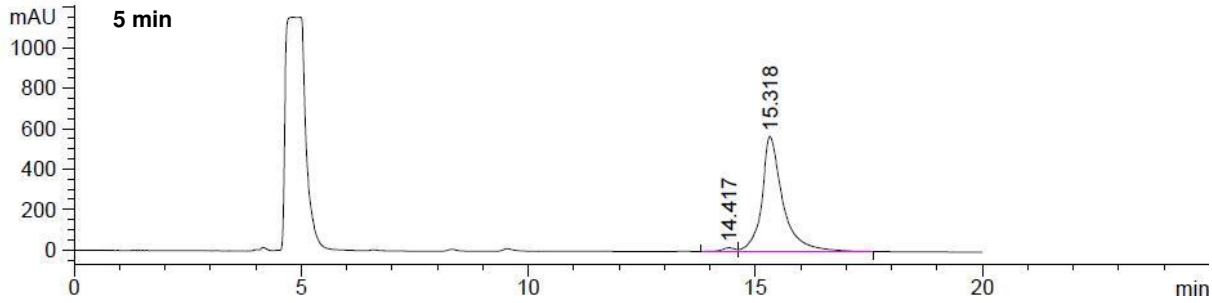

Peak #	RetTime [min]	Type	Width [min]	Area [mAU*s]	Height [mAU]	Area %
1	14.417	VV	0.3072	427.34329	20.00624	2.2579
2	15.318	VB	0.4600	1.84990e4	570.97870	97.7421

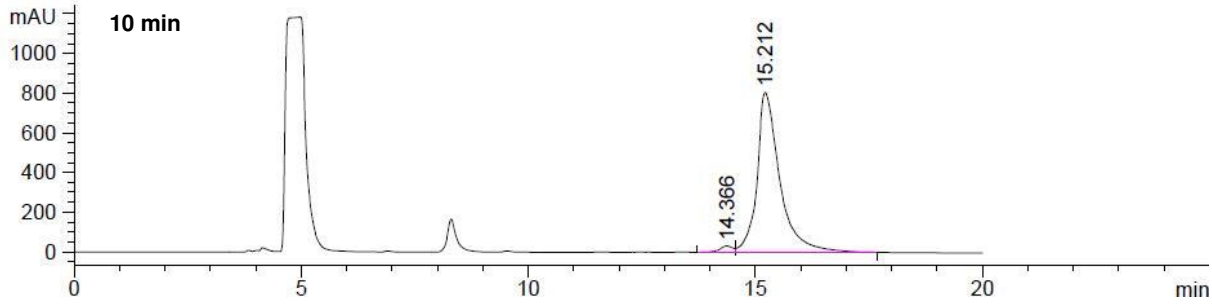

Peak #	RetTime [min]	Type	Width [min]	Area [mAU*s]	Height [mAU]	Area %
1	14.366	VV	0.2906	681.08905	33.29926	2.3432
2	15.212	VB	0.5104	2.83855e4	807.01697	97.6568

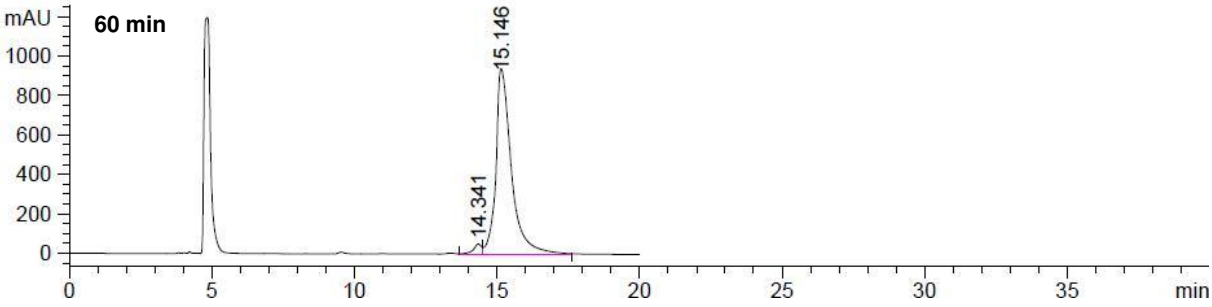

Peak #	RetTime [min]	Type	Width [min]	Area [mAU*s]	Height [mAU]	Area %
1	14.341	VV	0.2942	1034.41980	50.65568	2.8259
2	15.146	VB	0.5620	3.55711e4	938.95190	97.1741

Enantiomeric excess (Isovaleraldehyde, Catalyst 9b and NCS)

HPLC: 0.8 ml/min, 10% EtOH/hexane, Chiralpak IA (0.46 x 25 cm)

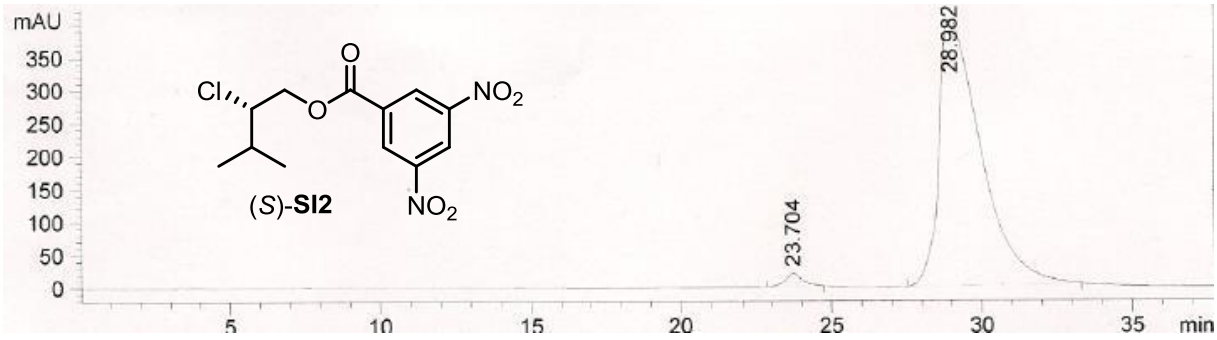

Peak #	RetTime [min]	Type	Width [min]	Area [mAU*s]	Height [mAU]	Area %
1	23.704	BB	0.5956	870.54803	20.91682	2.1585
2	28.982	BB	1.4286	3.94612e4	405.05087	97.8415

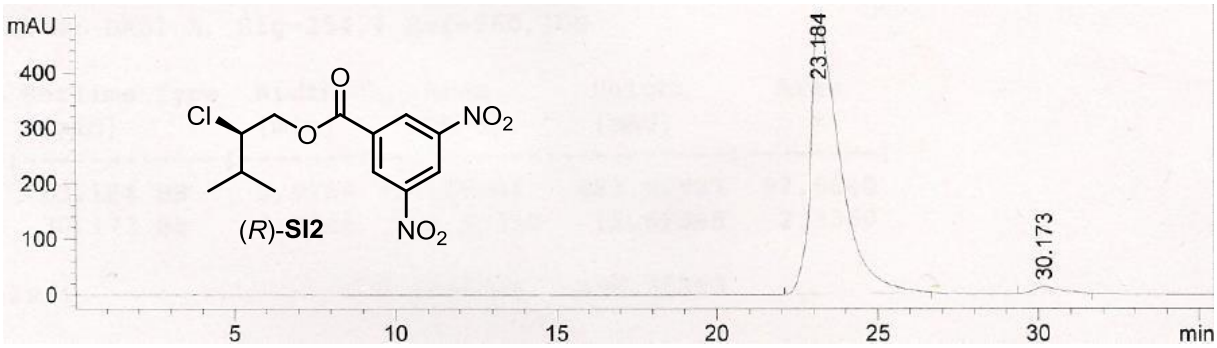

Peak #	RetTime [min]	Type	Width [min]	Area [mAU*s]	Height [mAU]	Area %
1	23.184	BB	0.9789	3.17069e4	483.62997	97.6640
2	30.173	BB	0.8069	758.40350	12.62385	2.3360

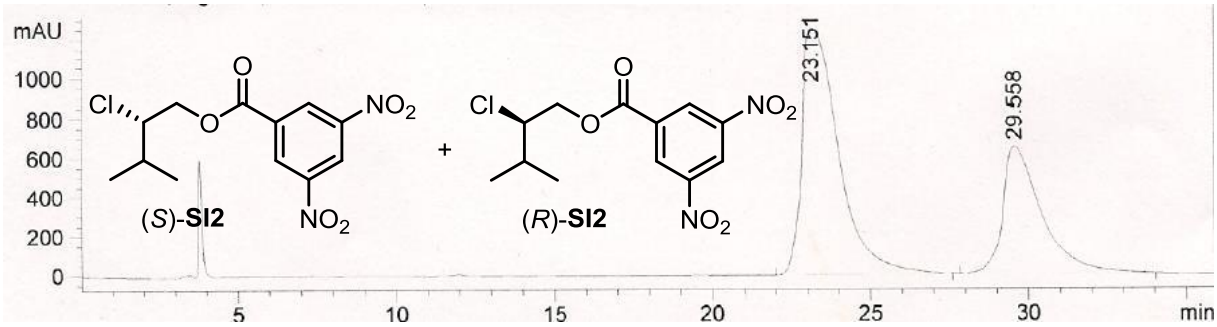

Peak #	RetTime [min]	Type	Width [min]	Area [mAU*s]	Height [mAU]	Area %
1	23.151	BB	1.0464	1.02246e5	1252.42908	64.8886
2	29.558	BB	1.2256	5.53255e4	648.32123	35.1114

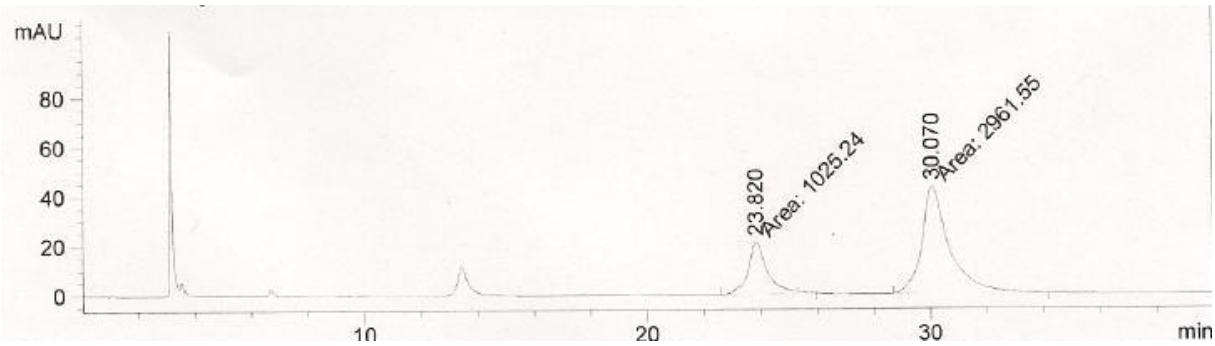

Peak #	RetTime [min]	Type	Width [min]	Area [mAU*s]	Height [mAU]	Area %
1	23.820	MM	0.8110	1025.23926	21.07000	25.7159
2	30.070	MM	1.1454	2961.54541	43.09299	74.2841

Enantiomeric Excess (Propanal, Catalyst 9b and NCP or NCS)

HPLC: 1.0 ml/min, 20% EtOH/hexane, Chiralpak IA (0.46 x 25 cm)

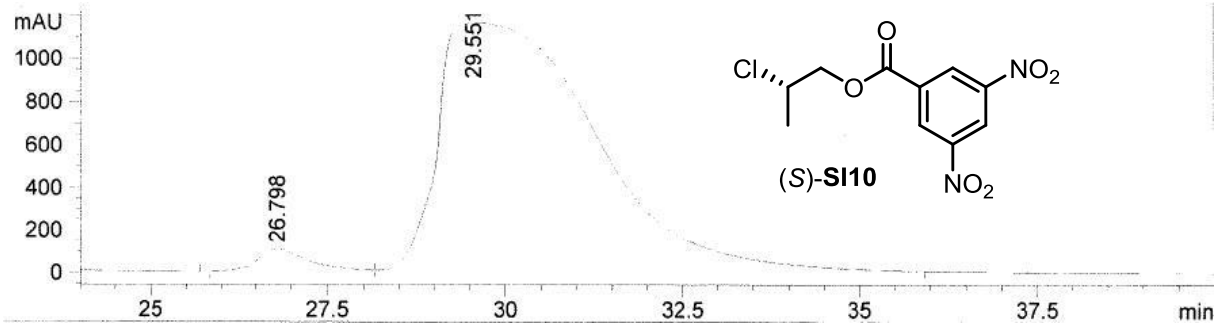

Peak #	RetTime [min]	Type	Width [min]	Area [mAU*s]	Height [mAU]	Area %
1	26.798	BV	0.7513	5542.09766	106.82458	3.0138
2	29.551	VB	1.8062	1.78352e5	1161.00269	96.9862

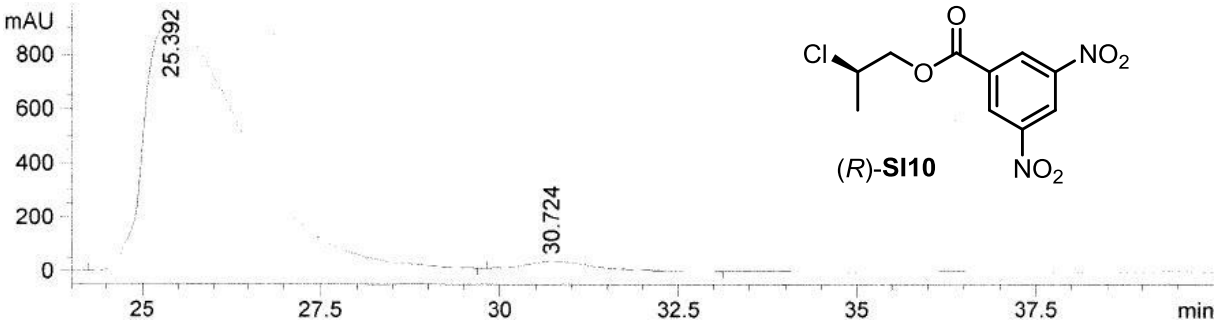

Peak #	RetTime [min]	Type	Width [min]	Area [mAU*s]	Height [mAU]	Area %
1	25.392	BB	1.4621	9.27877e4	923.58813	96.9844
2	30.724	BB	1.0172	2885.07446	39.63746	3.0156

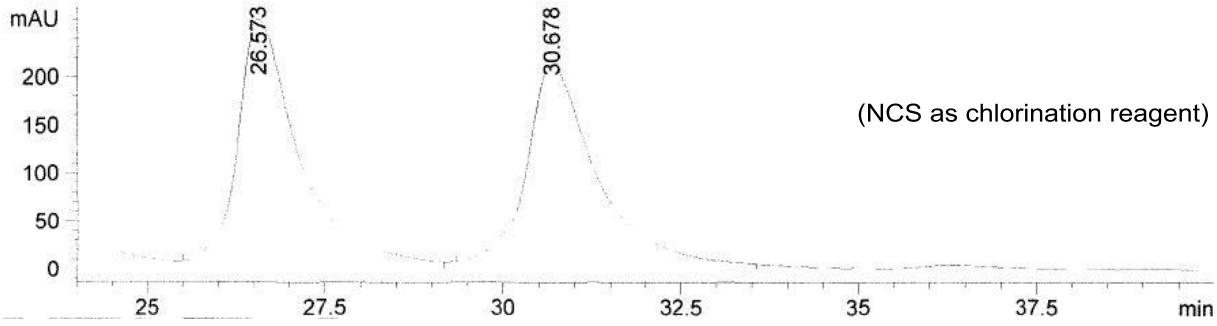

(NCS as chlorination reagent)

Peak #	RetTime [min]	Type	Width [min]	Area [mAU*s]	Height [mAU]	Area %
1	3.190	BV	0.1254	659.03363	71.59568	2.0853
2	3.342	VV	0.1079	514.15607	69.82114	1.6269
3	3.466	VV	0.0726	163.46495	33.66722	0.5172
4	26.573	BB	0.8810	1.58659e4	258.16086	50.2025
5	30.678	BB	0.9658	1.44013e4	209.03409	45.5681

corrected: t=26.573 area: 52.4195%; t=30.678 area: 47.5805%

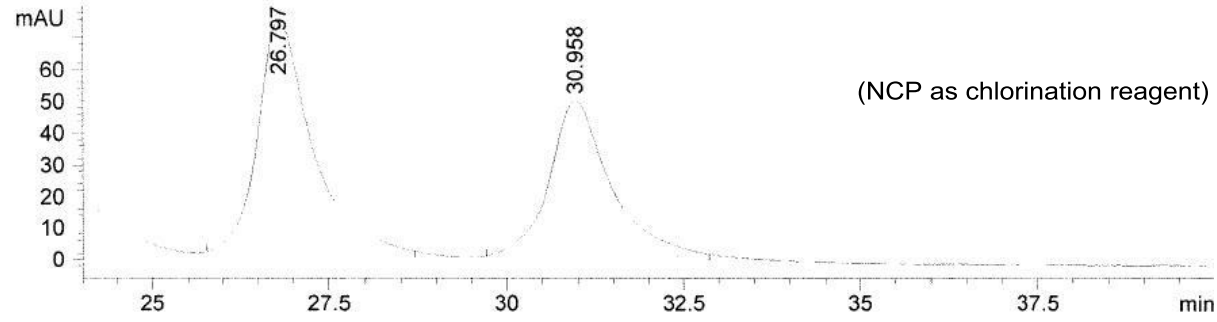

(NCP as chlorination reagent)

Peak #	RetTime [min]	Type	Width [min]	Area [mAU*s]	Height [mAU]	Area %
1	26.797	BB	0.7625	3951.39868	74.05814	57.1695
2	30.958	BB	0.8495	2960.32642	49.37291	42.8305

Decomposition of aminal 14 (1)

GC: Lipodex-E, 70°C, 1,1 ml/min He ; FID 300°C, Split 50:1

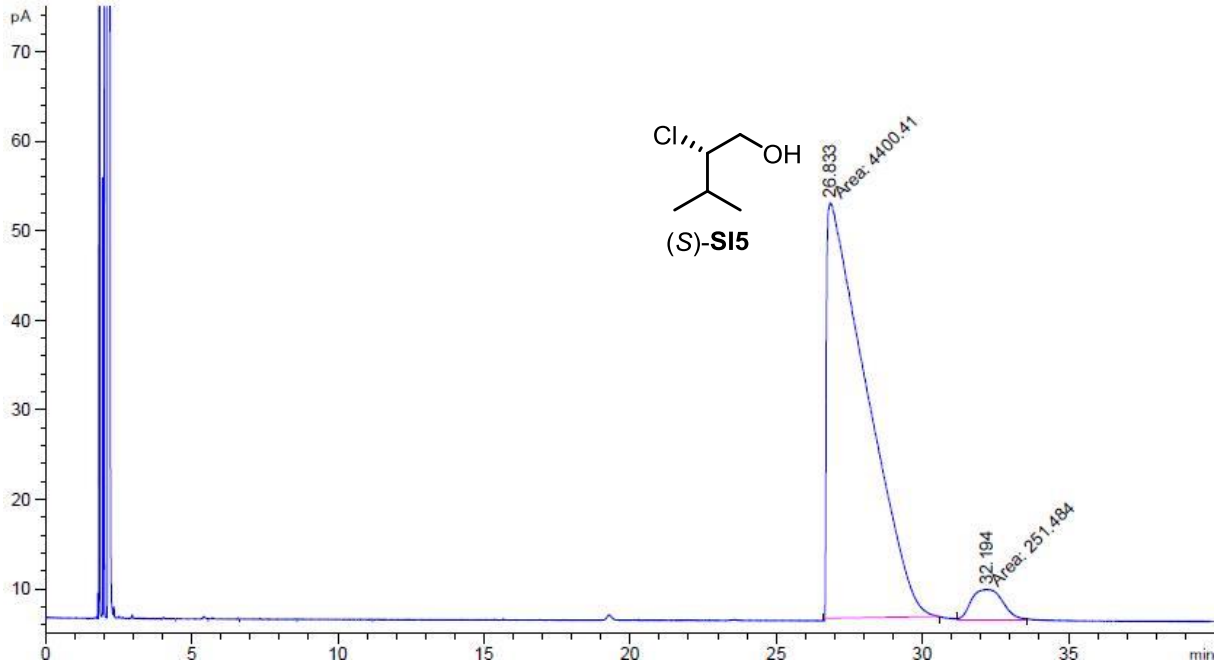

Peak #	RetTime [min]	Type	Width [min]	Area [pA*s]	Height [pA]	Area %
1	26.833	MM	1.5808	4400.40869	46.39410	94.59394
2	32.194	MM	1.2375	251.48433	3.38700	5.40606

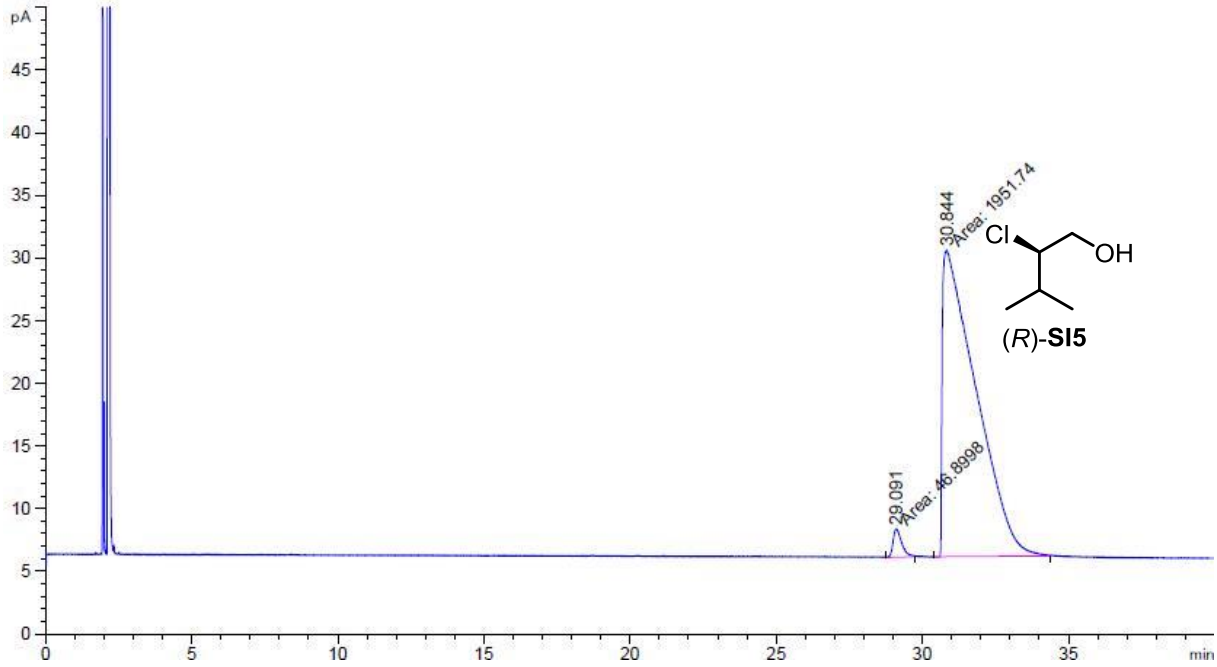

Peak #	RetTime [min]	Type	Width [min]	Area [pA*s]	Height [pA]	Area %
1	29.091	MM	0.3463	46.89983	2.25745	2.34659
2	30.844	MM	1.3296	1951.74133	24.46551	97.65341

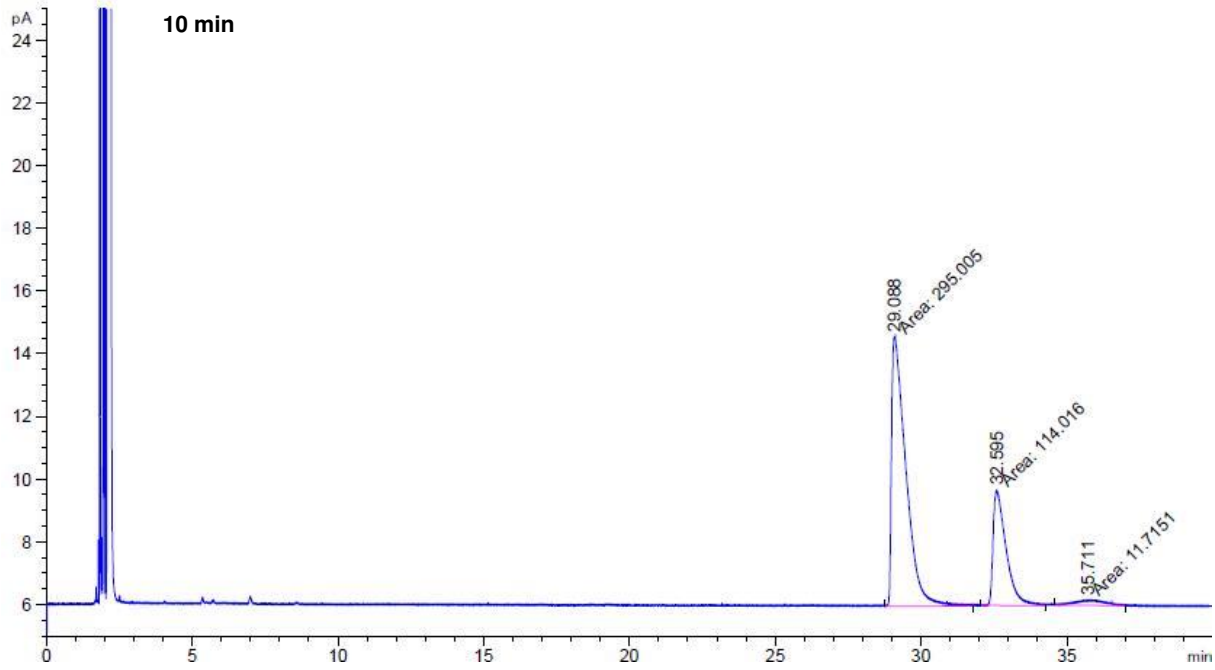

Peak #	RetTime [min]	Type	Width [min]	Area [pA*s]	Height [pA]	Area %
1	29.088	MM	0.5721	295.00470	8.59443	70.11639
2	32.595	MM	0.5154	114.01585	3.68689	27.09916
3	35.711	MM	1.0918	11.71514	1.78837e-1	2.78444

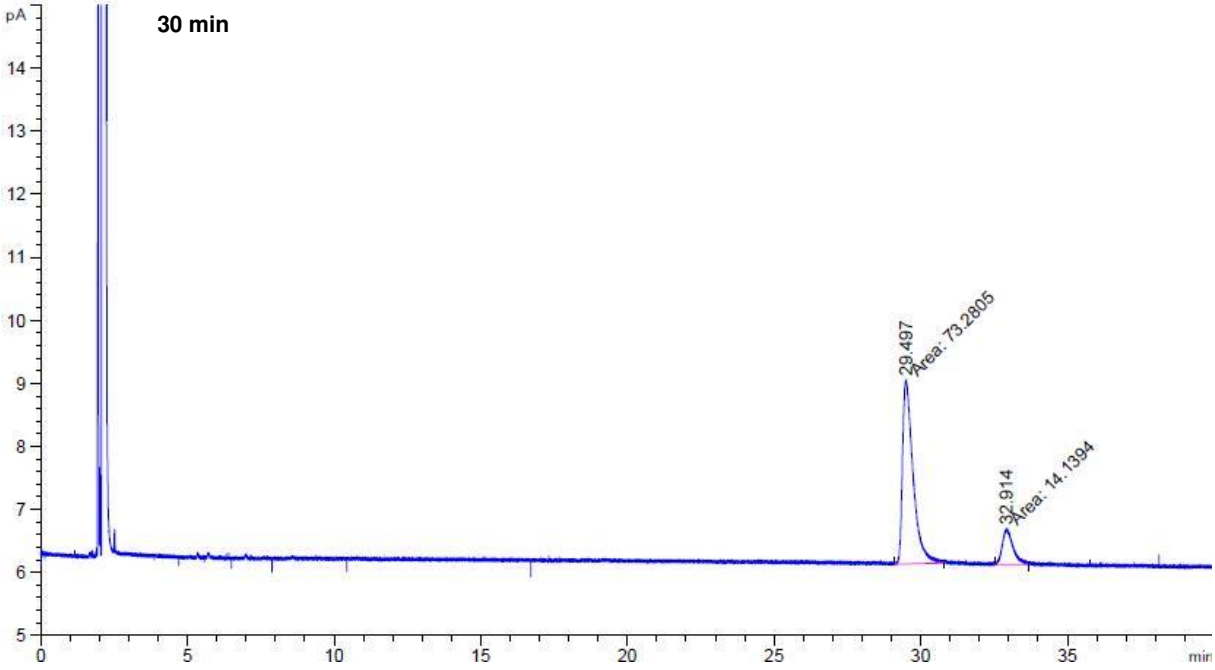

Peak #	RetTime [min]	Type	Width [min]	Area [pA*s]	Height [pA]	Area %
1	29.497	MM	0.4188	73.28048	2.91662	83.82590
2	32.914	MM	0.4191	14.13937	5.62286e-1	16.17410

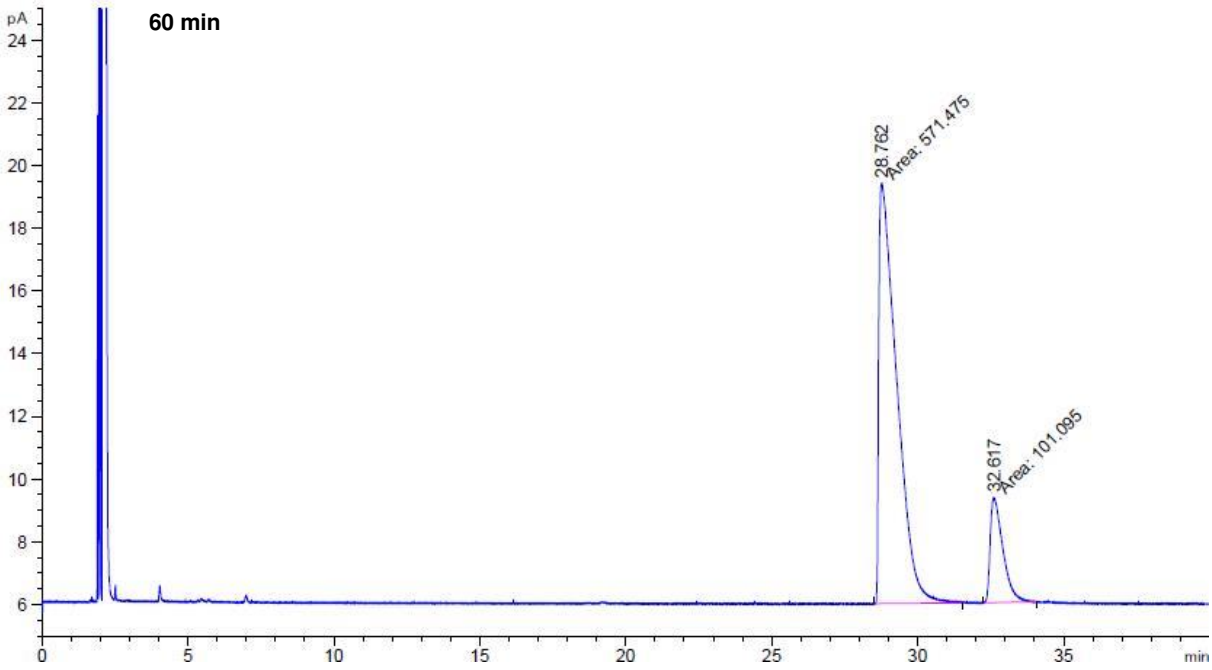

Peak #	RetTime [min]	Type	Width [min]	Area [pA*s]	Height [pA]	Area %
1	28.762	MM	0.7094	571.47546	13.42658	84.96886
2	32.617	MM	0.5011	101.09499	3.36233	15.03114

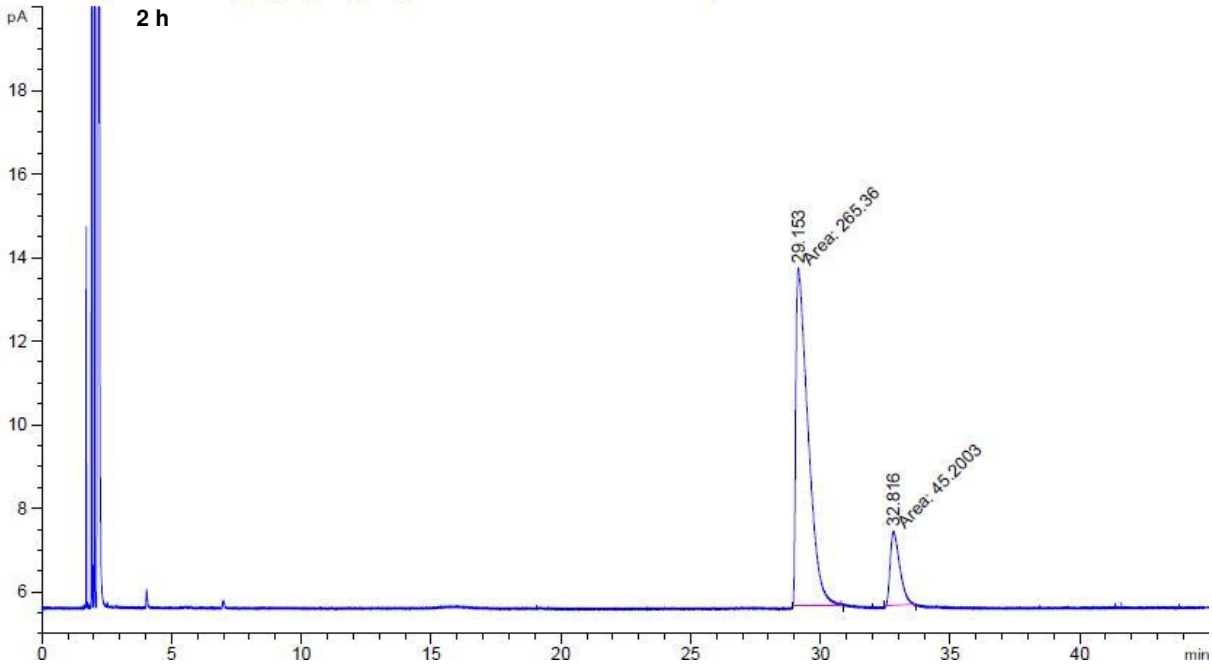

Peak #	RetTime [min]	Type	Width [min]	Area [pA*s]	Height [pA]	Area %
1	29.153	MM	0.5473	265.36035	8.08067	85.44559
2	32.816	MM	0.4243	45.20028	1.77552	14.55441

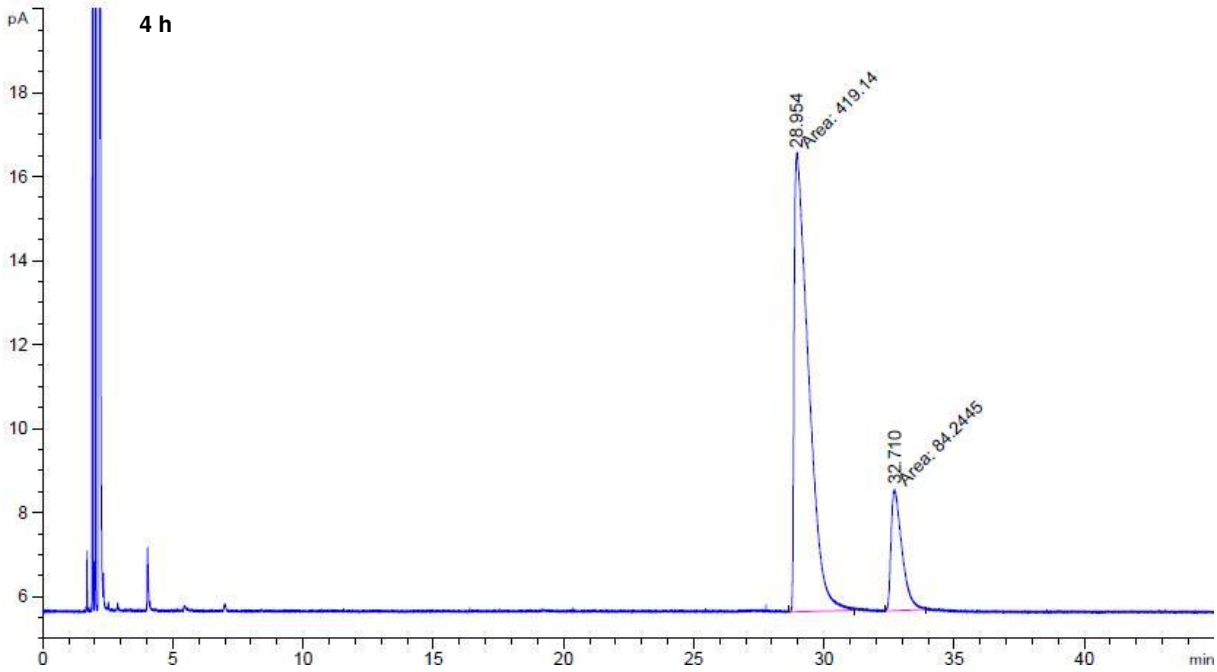

Peak #	RetTime [min]	Type	Width [min]	Area [pA*s]	Height [pA]	Area %
1	28.954	MM	0.6382	419.13995	10.94524	83.26438
2	32.710	MM	0.4847	84.24448	2.89672	16.73562

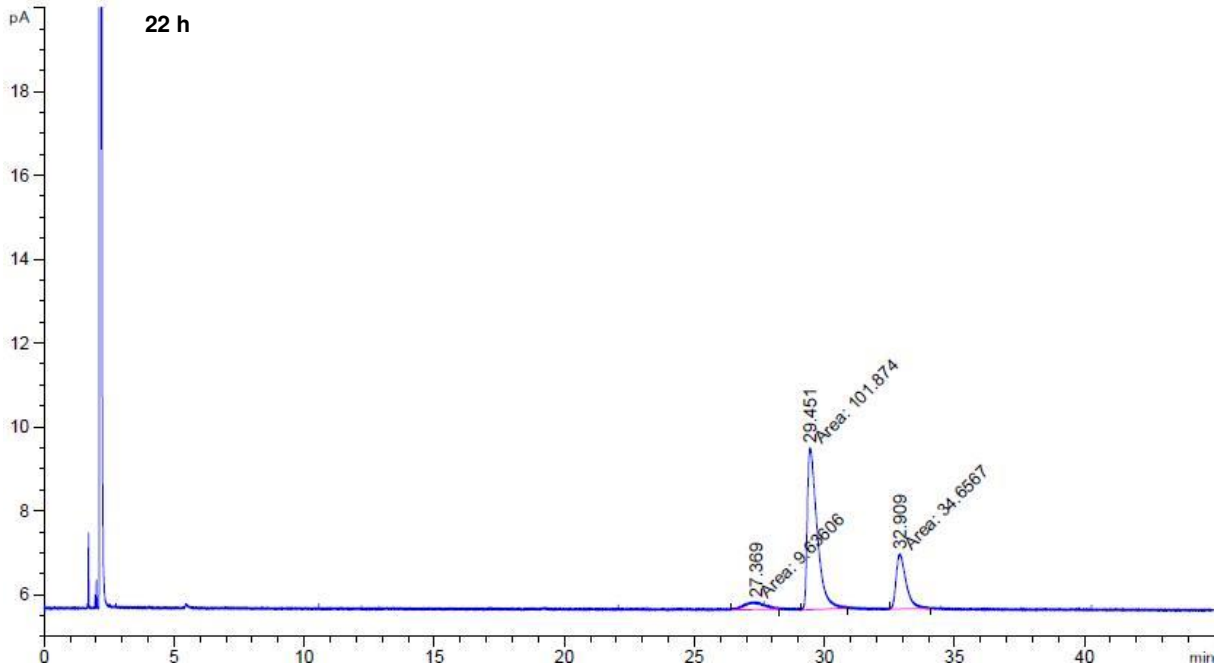

Peak #	RetTime [min]	Type	Width [min]	Area [pA*s]	Height [pA]	Area %
1	27.369	MM	0.8590	9.63606	1.86967e-1	6.59252
2	29.451	MM	0.4386	101.87379	3.87100	69.69704
3	32.909	MM	0.4375	34.65674	1.32032	23.71044

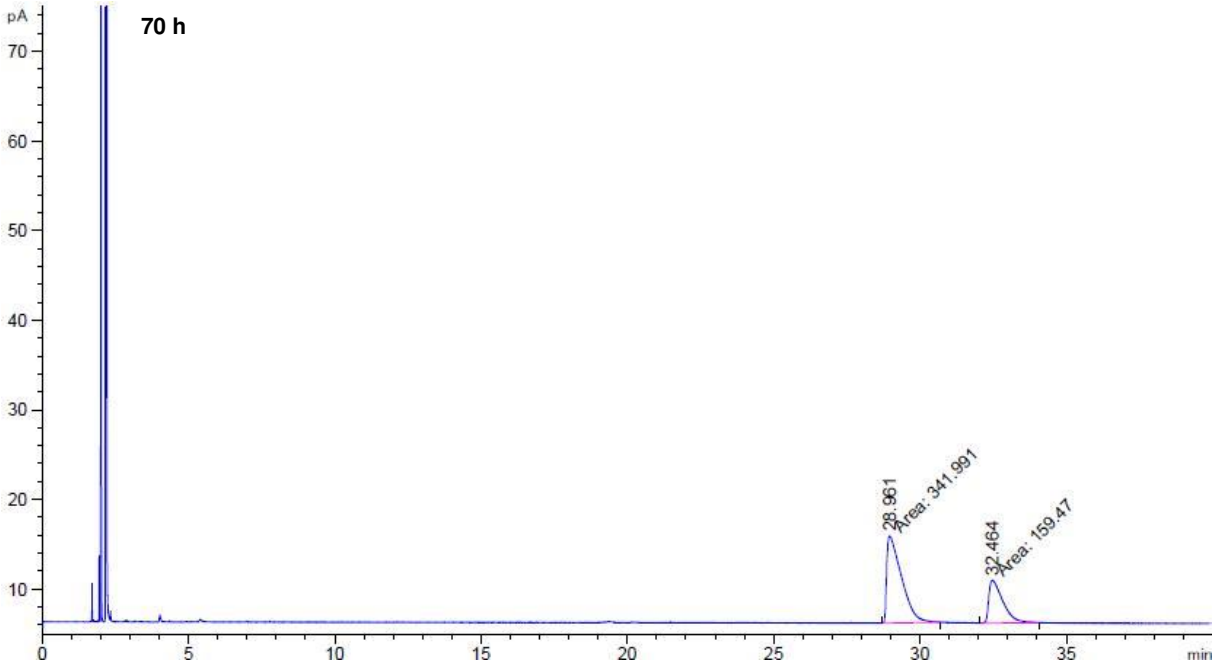

Peak #	RetTime [min]	Type	Width [min]	Area [pA*s]	Height [pA]	Area %
1	28.961	MM	0.5849	341.99069	9.74476	68.19890
2	32.464	MM	0.5527	159.47005	4.80860	31.80110

Decomposition of aminal SI6 (1)

GC: Lipodex-E, 40 – 70°C (1.5 °C / min), 1,1 ml/min He ; FID 300°C, Split 50:1

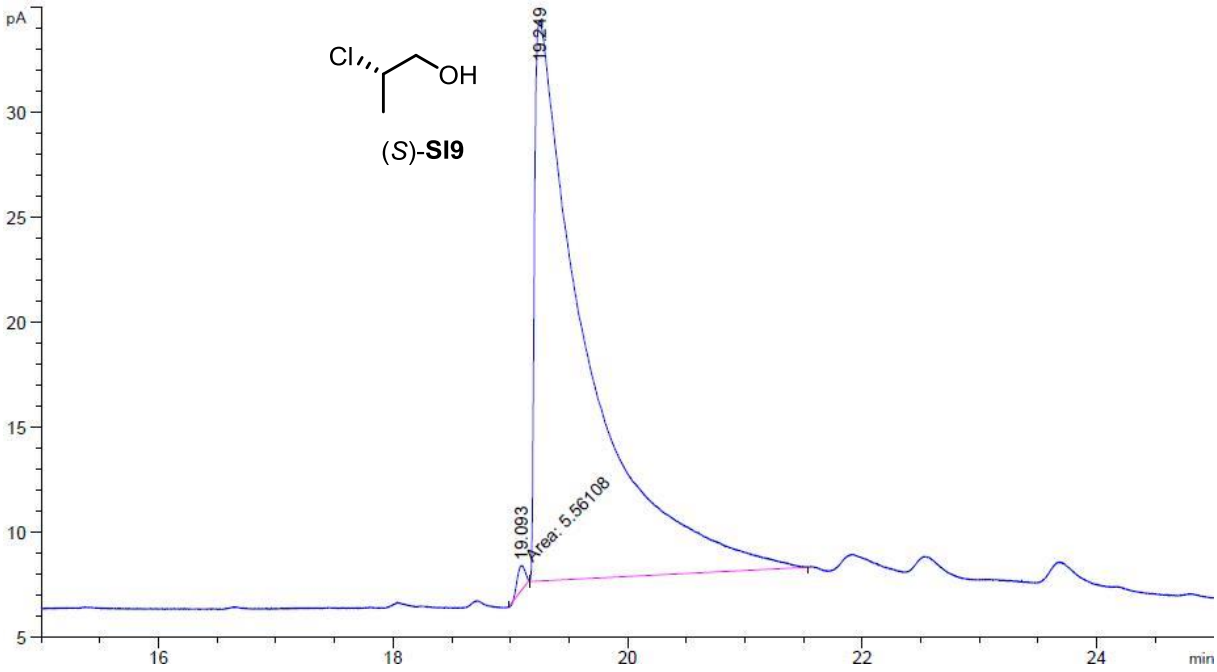

Peak #	RetTime [min]	Type	Width [min]	Area [pA*s]	Height [pA]	Area %
1	19.093	MM	0.0767	5.56108	1.20808	0.67186
2	19.249	BB	0.3803	822.15637	26.68312	99.32814

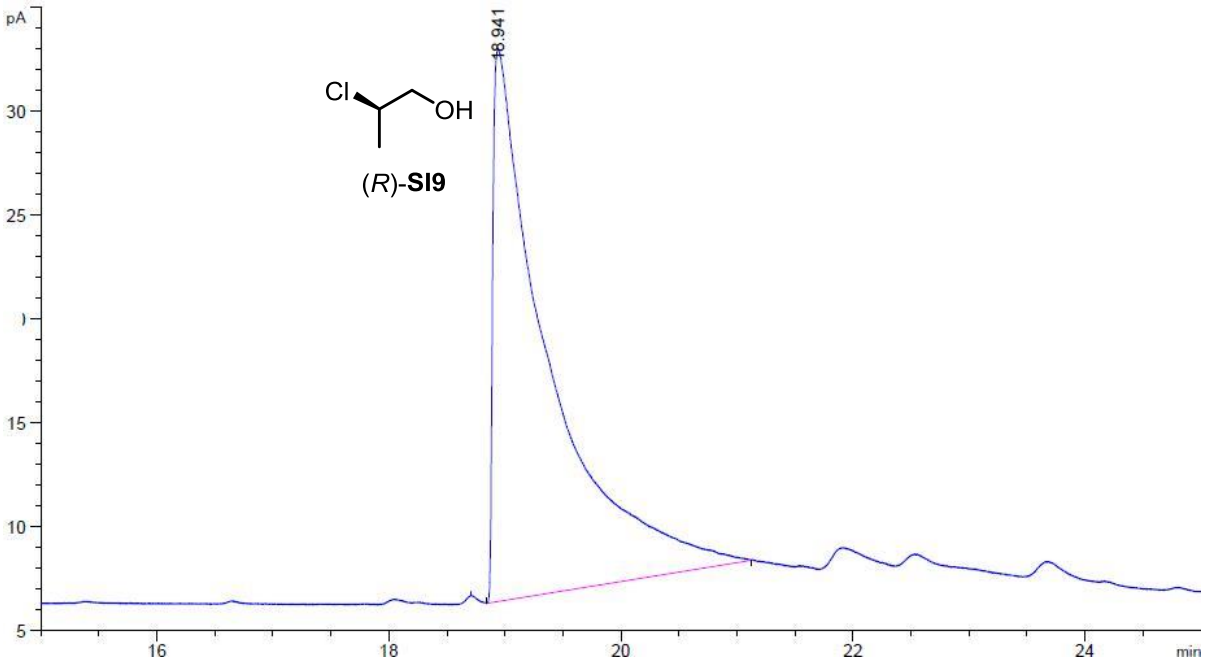

Peak #	RetTime [min]	Type	Width [min]	Area [pA*s]	Height [pA]	Area %
1	18.941	BB	0.4068	886.03485	26.61722	1.000e2

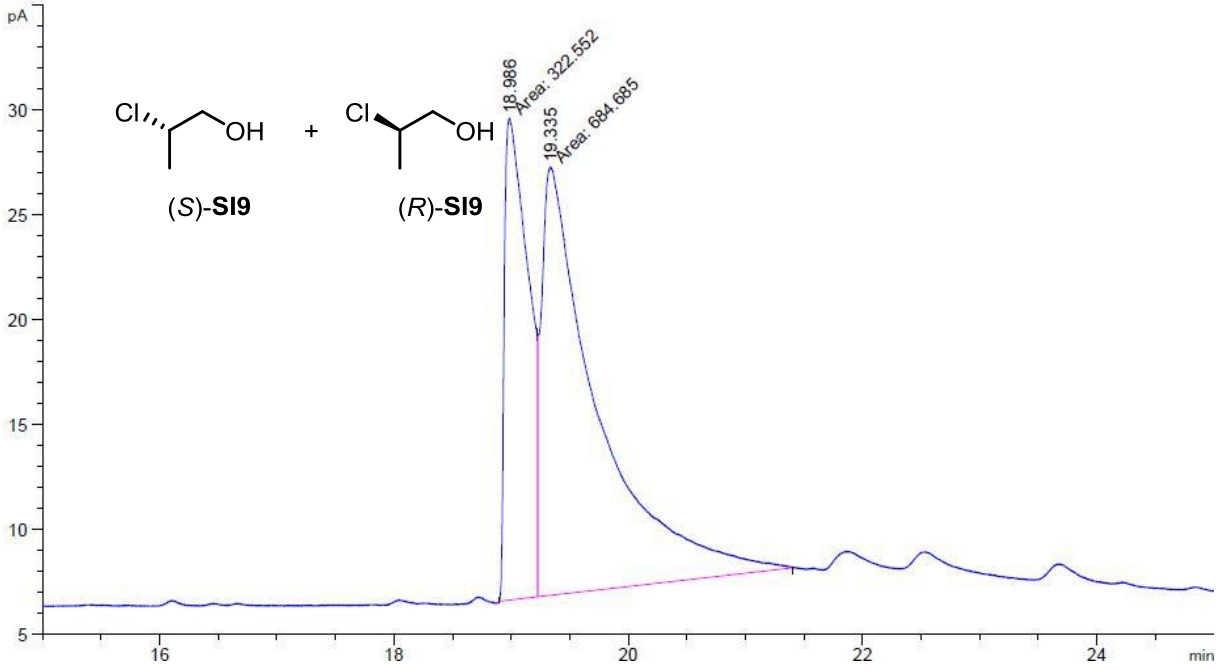
pA
30
25
20
15
10
5
16
18
20
22
24
min
Cl
OH
+
Cl
OH
(S)-SI9
(R)-SI9
18.986
Area: 322.552
19.335
Area: 684.685

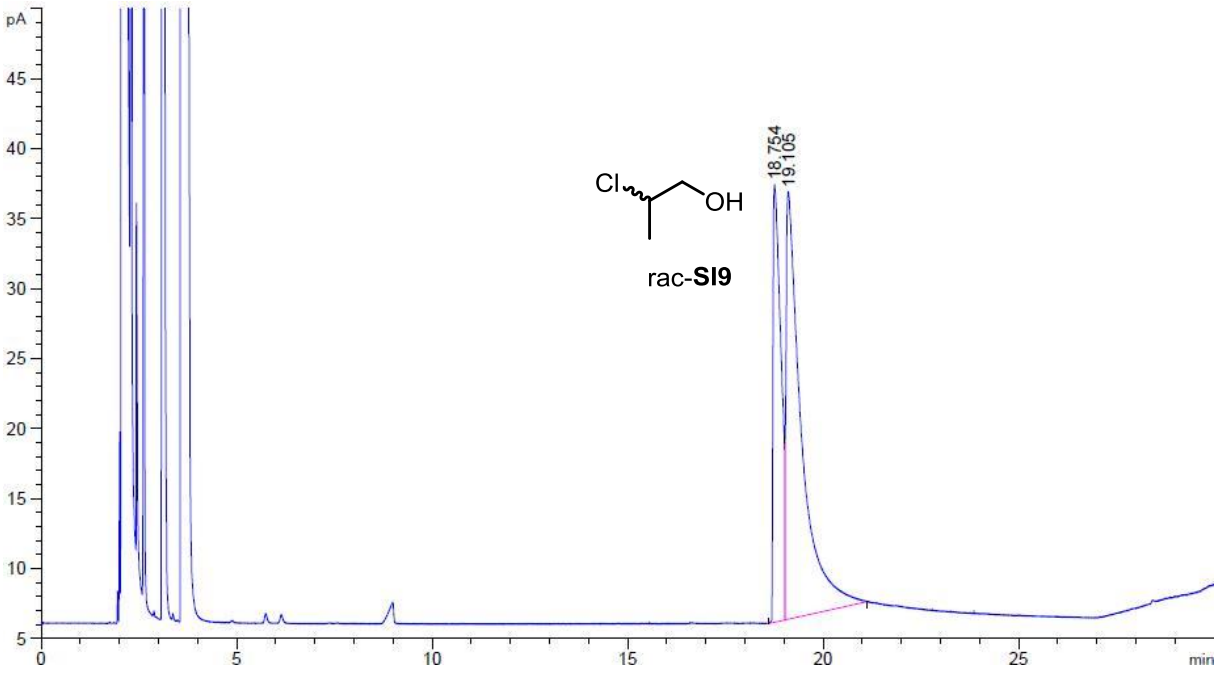
pA
45
40
35
30
25
20
15
10
5
0
5
10
15
20
25
min
Cl
OH
rac-SI9
18.754
19.105

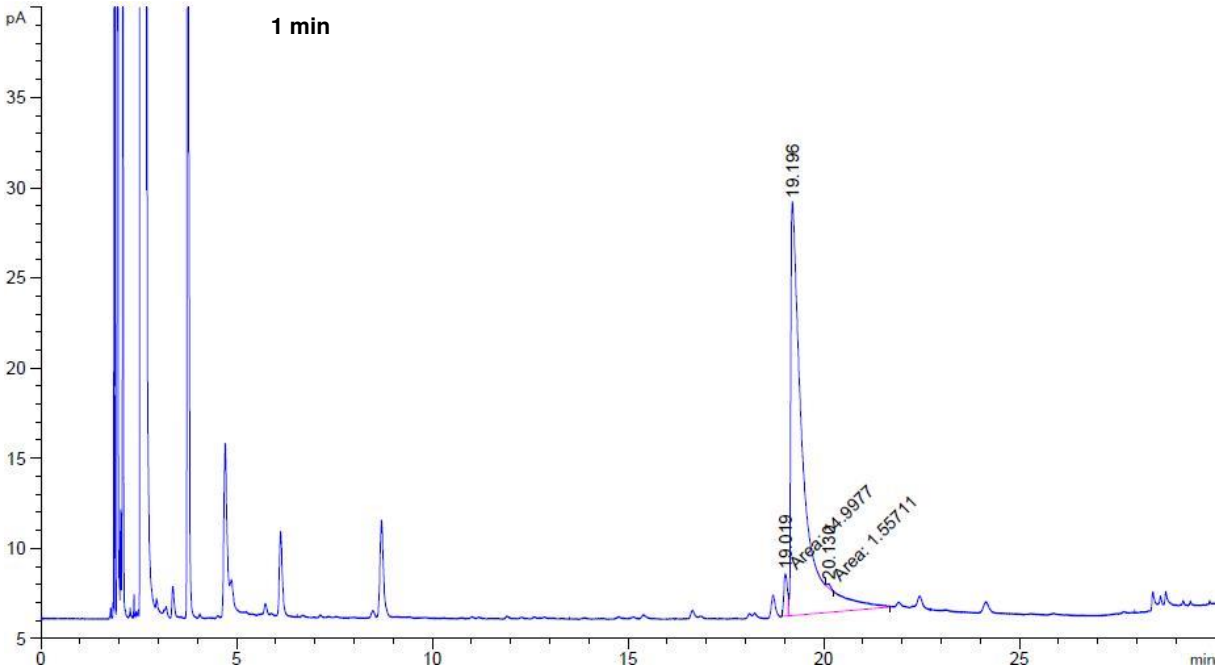

Peak #	RetTime [min]	Type	Width [min]	Area [pA*s]	Height [pA]	Area %
1	19.019	MF	0.1061	14.99774	2.35689	2.94455
2	19.196	FM R	0.3587	492.78448	22.89794	96.74974
3	20.130	MM T	0.1128	1.55711	2.30102e-1	0.30571

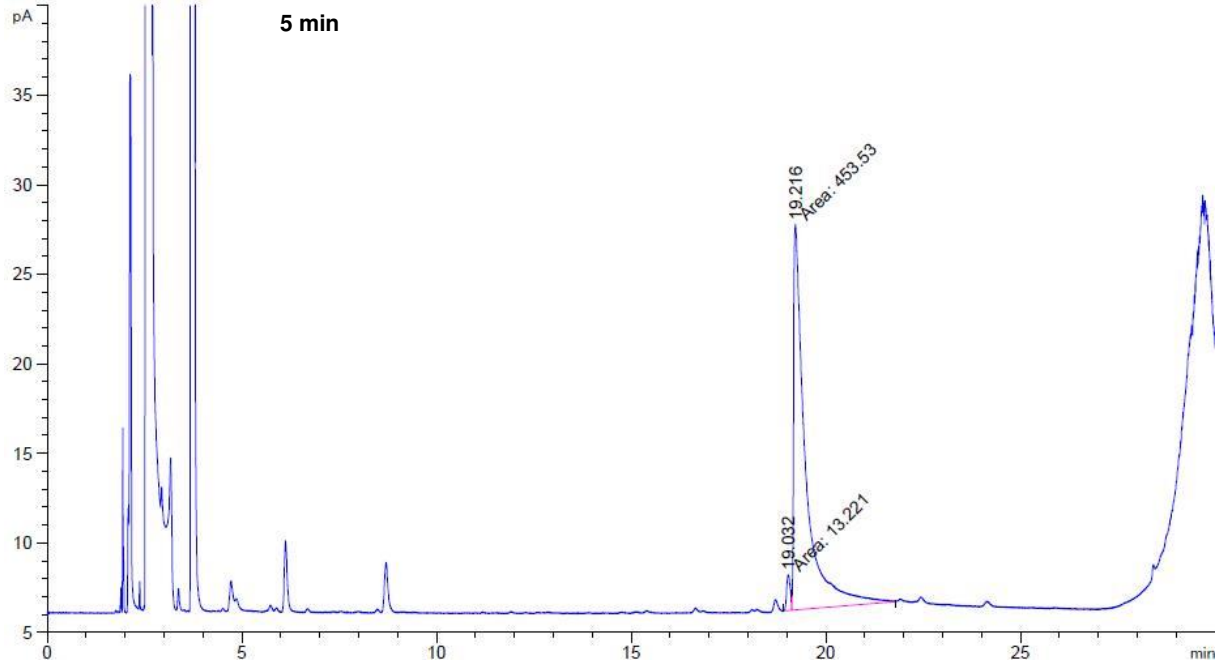

Peak #	RetTime [min]	Type	Width [min]	Area [pA*s]	Height [pA]	Area %
1	19.032	MF	0.1098	13.22100	2.00708	2.83256
2	19.216	FM	0.3513	453.52966	21.51792	97.16744

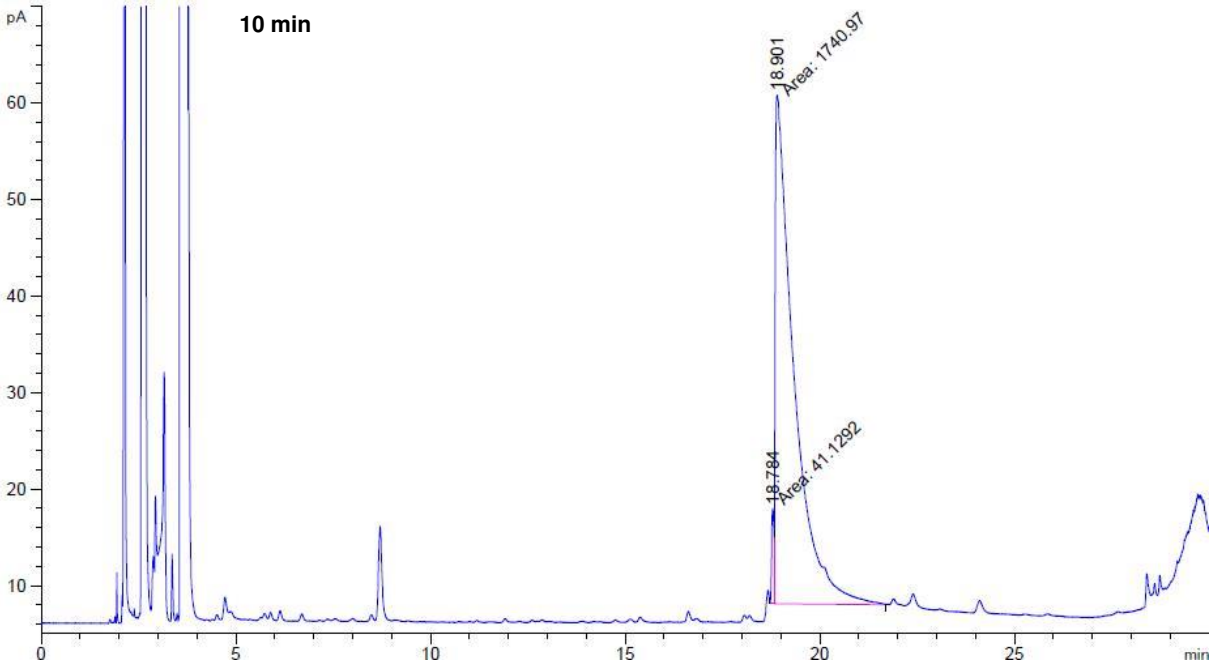

Peak #	RetTime [min]	Type	Width [min]	Area [pA*s]	Height [pA]	Area %
1	18.784	MF	0.0695	41.12918	9.85845	2.30791
2	18.901	FM	0.5504	1740.96619	52.72257	97.69209

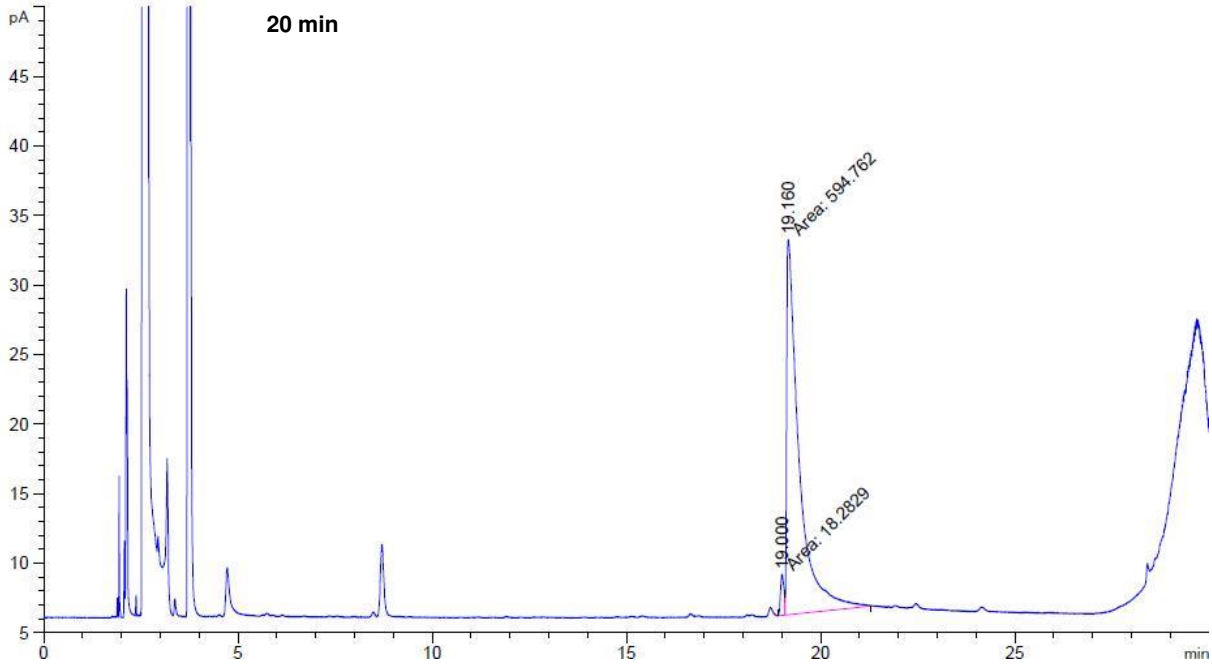

Peak #	RetTime [min]	Type	Width [min]	Area [pA*s]	Height [pA]	Area %
1	19.000	MF	0.1030	18.28292	2.95949	2.98231
2	19.160	FM	0.3671	594.76196	27.00425	97.01769

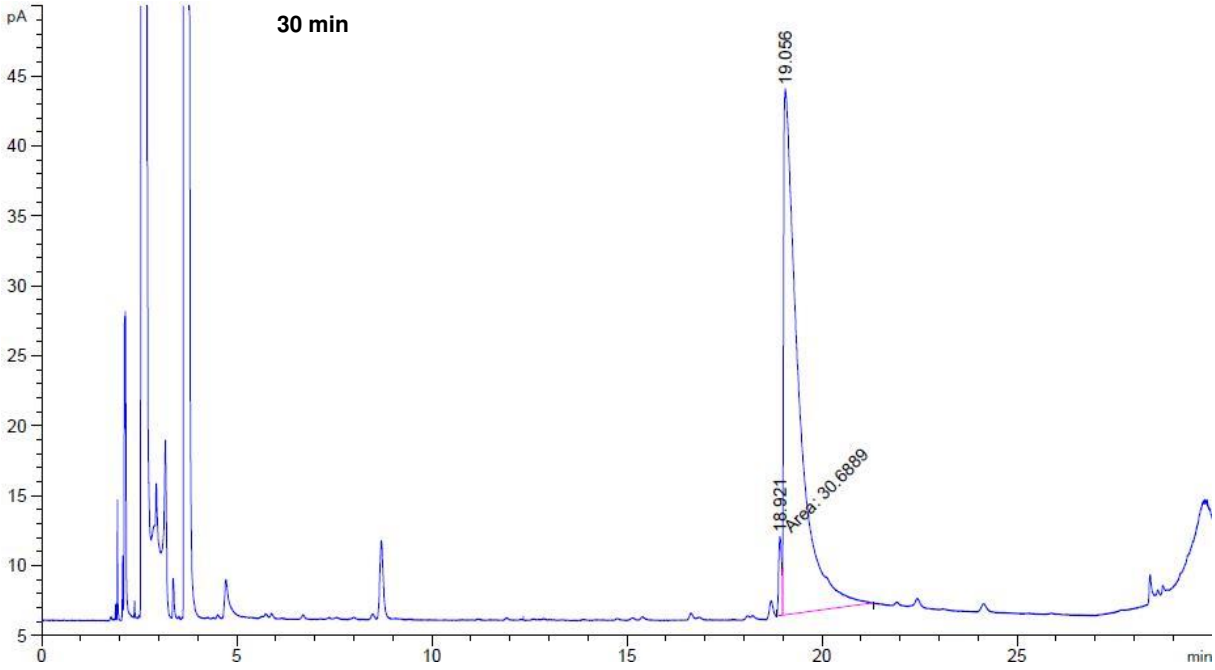

Peak #	RetTime [min]	Type	Width [min]	Area [pA*s]	Height [pA]	Area %
1	18.921	MF	0.0910	30.68887	5.61901	3.00003
2	19.056	FM R	0.4403	992.26202	37.56114	96.99997

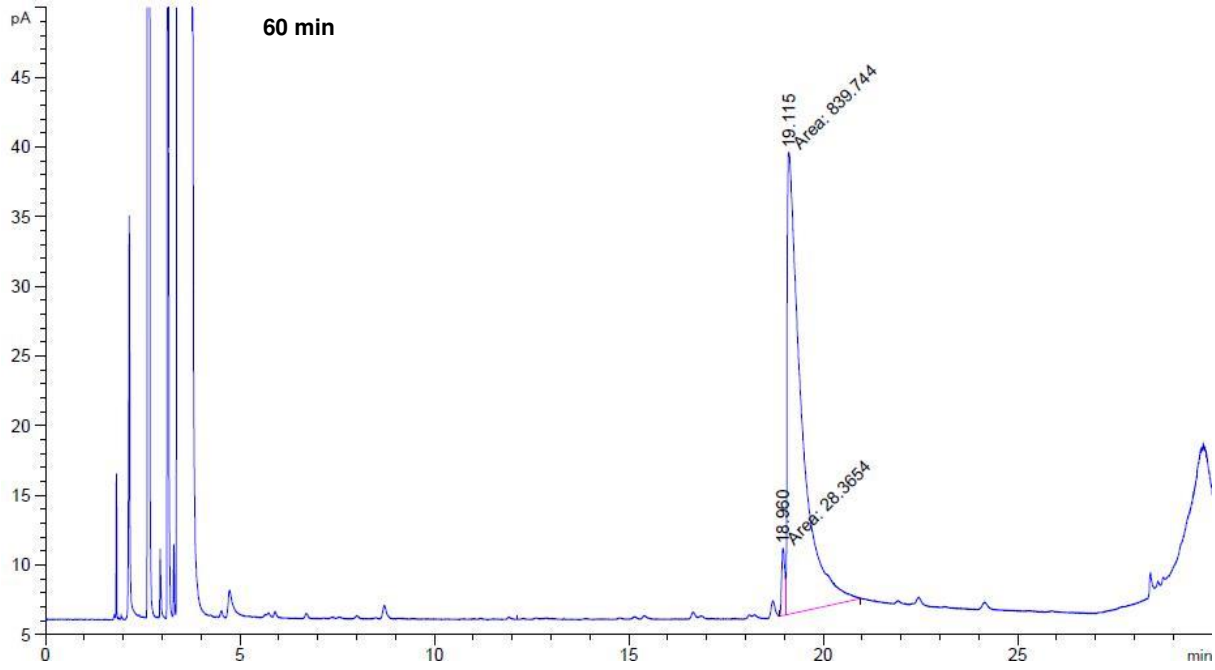

Peak #	RetTime [min]	Type	Width [min]	Area [pA*s]	Height [pA]	Area %
1	18.960	MF	0.0984	28.36537	4.80676	3.26749
2	19.115	FM	0.4226	839.74414	33.11969	96.73251

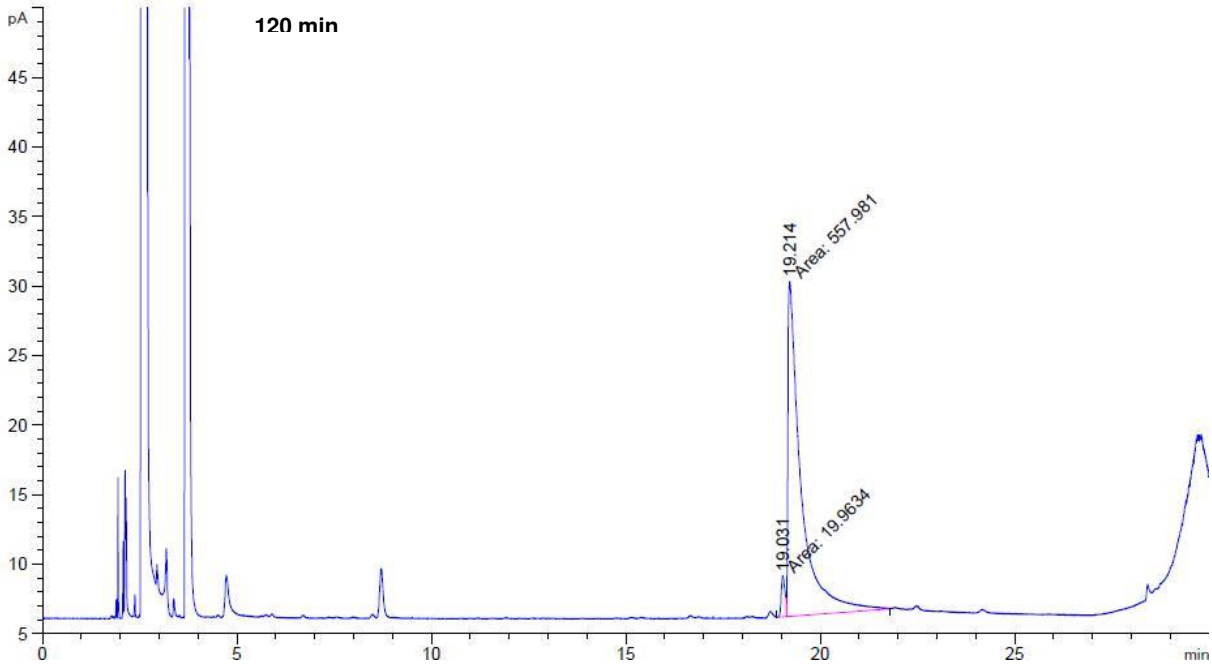

Peak #	RetTime [min]	Type	Width [min]	Area [pA*s]	Height [pA]	Area %
1	19.031	MF	0.1137	19.96338	2.92755	3.45421
2	19.214	FM	0.3861	557.98065	24.08886	96.54579

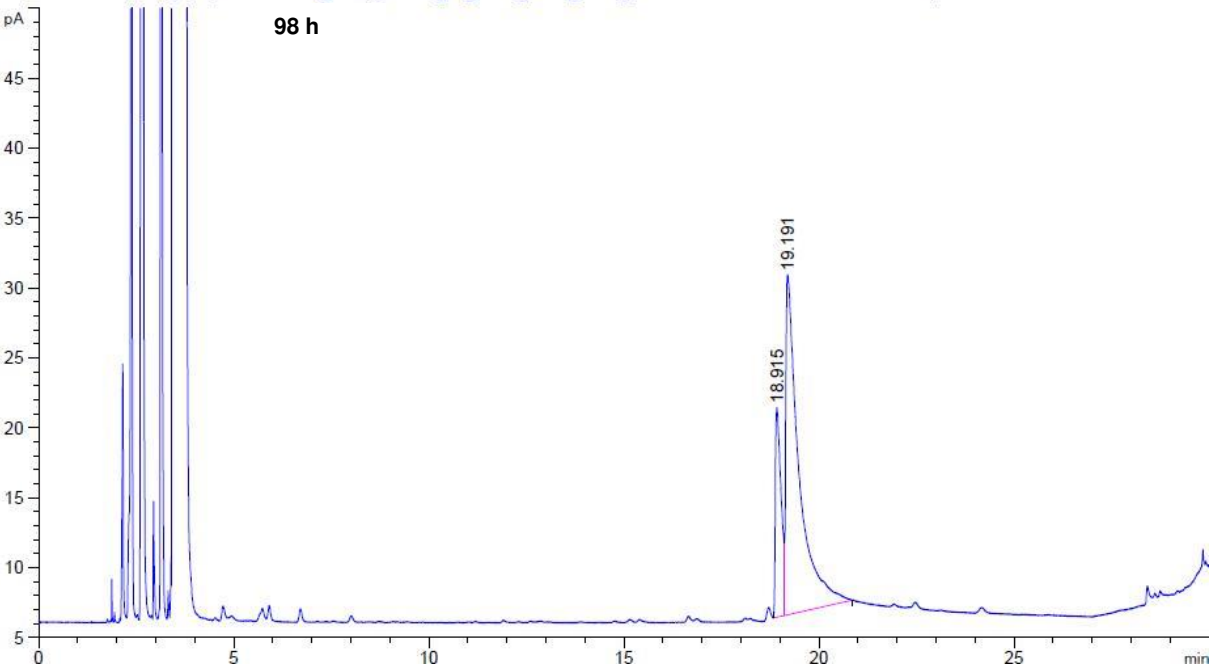

Peak #	RetTime [min]	Type	Width [min]	Area [pA*s]	Height [pA]	Area %
1	18.915	BV	0.1388	152.47072	14.96760	21.03967
2	19.191	VB	0.2948	572.21130	24.29045	78.96033

Deuterium incorporation experiment

HPLC: 0.8 ml/min, 5% EtOH/hexane, Chiralpak IA (0.46 x 25 cm)

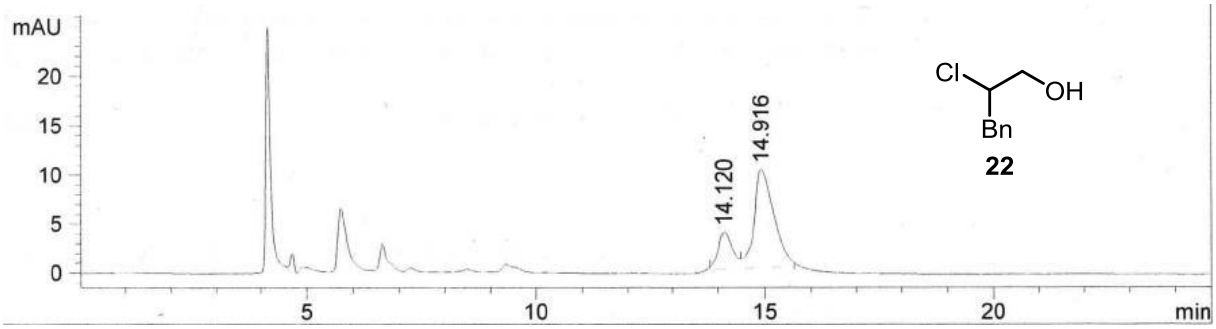

Peak #	RetTime [min]	Type	Width [min]	Area [mAU*s]	Height [mAU]	Area %
1	14.120	BV	0.3020	78.58987	3.78948	20.7408
2	14.916	VB	0.4263	300.32538	10.06108	79.2592

6.3. Crystallographic Data

1-((1*S*,2*R*)-1-((*R*)-5-benzyl-2,2,3-trimethyl-4-oxoimidazolidin-1-yl)-2-chloro-3-methylbutyl)pyrrolidine-2,5-dione (*syn*-20)

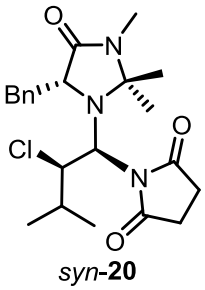

syn-**20**

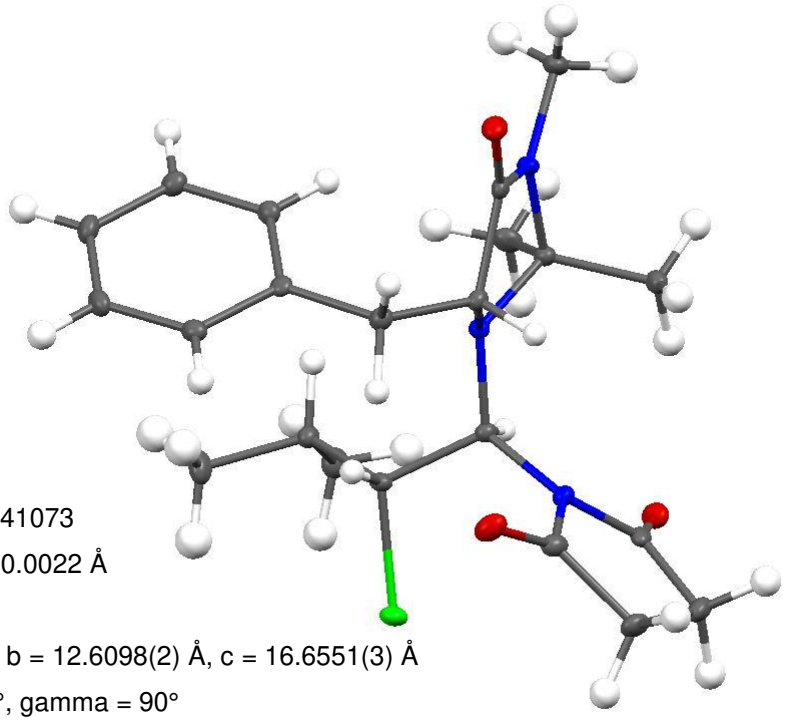

Deposition number: 2041073

Bond precision: C-C = 0.0022 Å

Wavelength = 1.54178

Cell: a = 10.1851(2) Å, b = 12.6098(2) Å, c = 16.6551(3) Å

alpha = 90°, beta = 90°, gamma = 90°

Temperature: 100 K

Volume: 2139.05(7) $Å^3$

Space group: P 21 21 21

Hall group: P 2ac 2ab

Dx,g cm-3: 1.304

Z: 4

Mu (mm-1): 1.808

F000: 896.0

F000': 899.88

h,k,lmax: 12, 15, 20

Nref: 3871

Tmin,Tmax: 0.588, 0.753

Tmin': 0.384

Reported T Limits: Tmin = 0.588, Tmax = 0.753

AbsCorr = MULTI-SCAN

Data completeness = 1.73/0.99

Theta(max) = 68.353

R(reflections) = 0.0214 (3831)

wR2(reflections) = 0.0556 (3871)

S = 1.045

Npar = 268

1-((*S*)-1-((*R*)-5-benzyl-2,2,3-trimethyl-4-oxoimidazolidin-1-yl)-2,2-dichloro-3-methylbutyl)pyrrolidine-2,5-dione (24a)

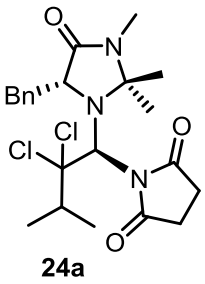

24a

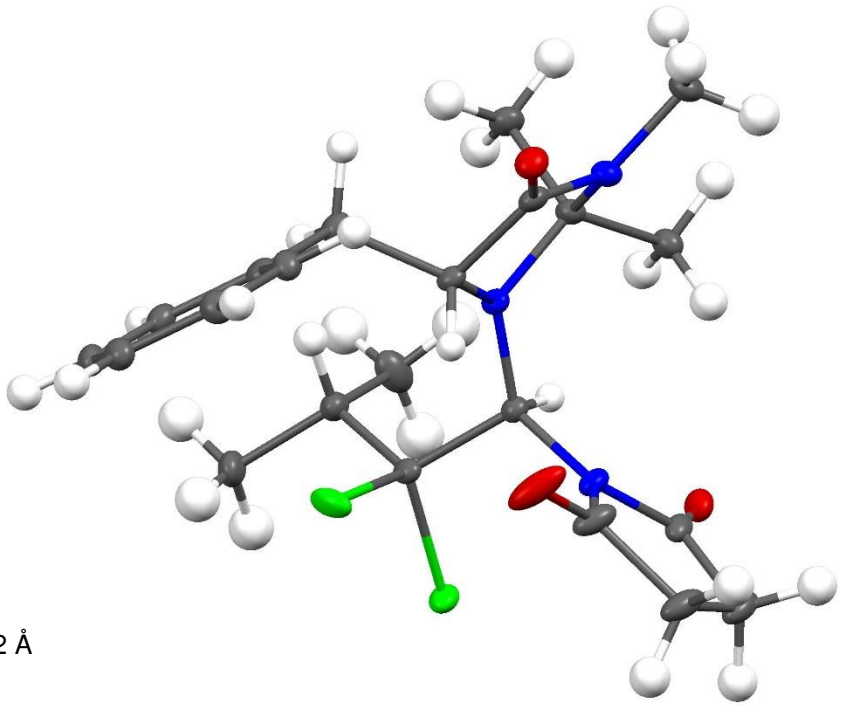

Deposition number: 2049431

Bond precision: C-C = 0.0032 Å

Wavelength = 1.54178

Cell: a = 10.72160(7) Å, b = 9.17122(6) Å, c = 22.72408(14) Å

alpha = 90°, beta = 91.1666(3)°, gamma = 90°

Temperature: 100 K

Volume: 2234.00(2) $Å^3$

Space group: P 21

Hall group: P 2yb

Dx,g cm-3: 1.351

Z: 4

Mu (mm-1): 2.848

F000: 960.0

F000': 965.35

h,k,lmax: 12, 11, 27

Nref: 8056

Tmin,Tmax: 0.540, 0.693

Tmin': 0.417

Reported T Limits: Tmin = 0.540, Tmax = 0.693

AbsCorr = MULTI-SCAN

Data completeness = 1.85/0.99

Theta(max) = 68.262

R(reflections) = 0.0231 (7929)

wR2(reflections) = 0.0615 (8056)

S = 1.040

Npar = 551

1-((1*S*,2*R*)-1-((2*R*,5*R*)-5-benzyl-2-(tert-butyl)-3-methyl-4-oxoimidazolidin-1-yl)-2-chloro-3-methylbutyl)pyrrolidine-2,5-dione ((1*S*,2*R*)-*syn*-21)

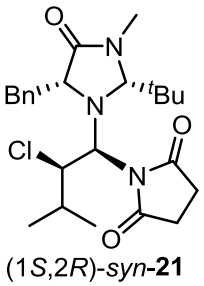

(1*S*,2*R*)-*syn*-**21**

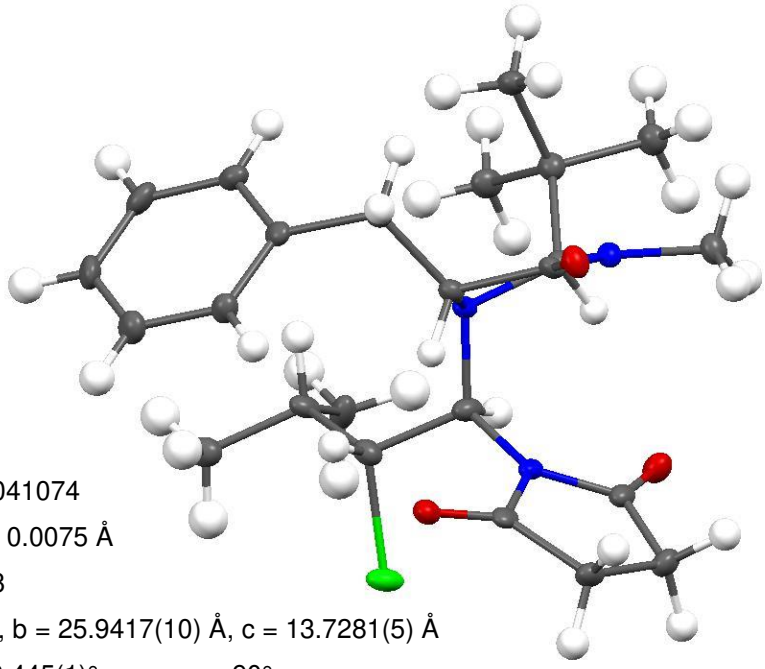

Deposition number: 2041074
Bond precision: C-C = 0.0075 Å
Wavelength = 1.54178
Cell: a = 10.4883(4) Å, b = 25.9417(10) Å, c = 13.7281(5) Å
Alpha = 90°, beta = 96.445(1)°, gamma = 90°
Temperature: 101 K
Volume: 3711.6(2) Å^3
Space group: P 21 P 1 21 1
Hall group: P 2yb P 2yb
Dx,g cm-3 = 1.203
Z: 6
Mu (mm-1): 1.592
F000: 1440.0
F000': 1446.02
h,k,lmax: 12, 31, 16
Nref: 13347
Tmin,Tmax: 0.638,0.728
Tmin': 0.548
Reported T Limits: Tmin = 0.638, Tmax = 0.728
AbsCorr = MULTI-SCAN
Data completeness = 1.89/0.97
Theta(max) = 68.874
R(reflections) = 0.0548 (13035)
wR2(reflections) = 0.1294 (13347)
S = 1.024
Npar = 857

1-((1*S*,2*S*)-1-((2*R*,5*R*)-5-benzyl-2-(tert-butyl)-3-methyl-4-oxoimidazolidin-1-yl)-2-chloro-3-methylbutyl)pyrrolidine-2,5-dione ((1*S*,2*S*)-*anti*-21)

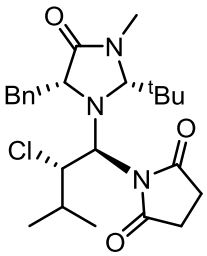

(1*S*,2*S*)-*anti*-**21**

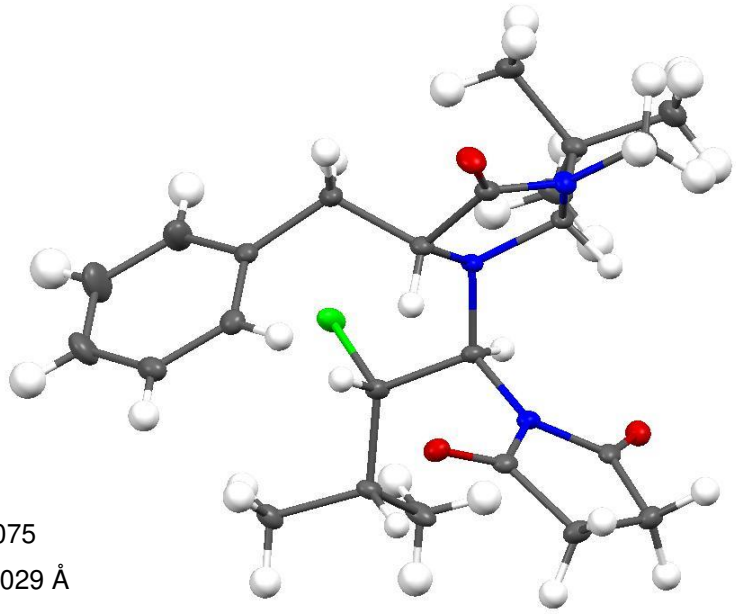

Deposition number: 2041075

Bond precision: C-C = 0.0029 Å

Wavelength = 1.54178

Cell: a = 24.00236(15) Å, b = 9.35451(6) Å, c = 10.74110(7) Å

alpha = 90°, beta = 93.6494(1)°, gamma = 90°

Temperature: 100 K

Volume: 2406.81(3) $Å^3$

Space group: C 2 C 2

Hall group: C 2y C 2y

Dx,g cm-3: 1.236

Z: 4

Mu (mm-1): 1.637

F000: 960.0

F000': 964.01

h,k,lmax: 28, 11, 12

Nref: 4089

Tmin,Tmax: 0.464, 0.563

Tmin': 0.365

Reported T Limits: Tmin = 0.464, Tmax = 0.563

AbsCorr = MULTI-SCAN

Data completeness = 1.74/0.93

Theta(max) = 68.276

R(reflections) = 0.0236 (4085)

wR2(reflections) = 0.0581 (4089)

S = 1.079

Npar = 287

1-((1*R*,2*S*)-1-((2*R*,5*R*)-5-benzyl-2-(tert-butyl)-3-methyl-4-oxoimidazolidin-1-yl)-2-chloro-3-methylbutyl)pyrrolidine-2,5-dione ((1*R*,2*S*)-*syn*-21)

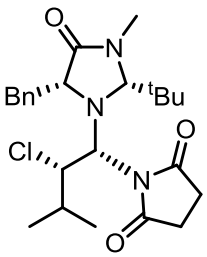

(1*R*,2*S*)-*syn*-**21**

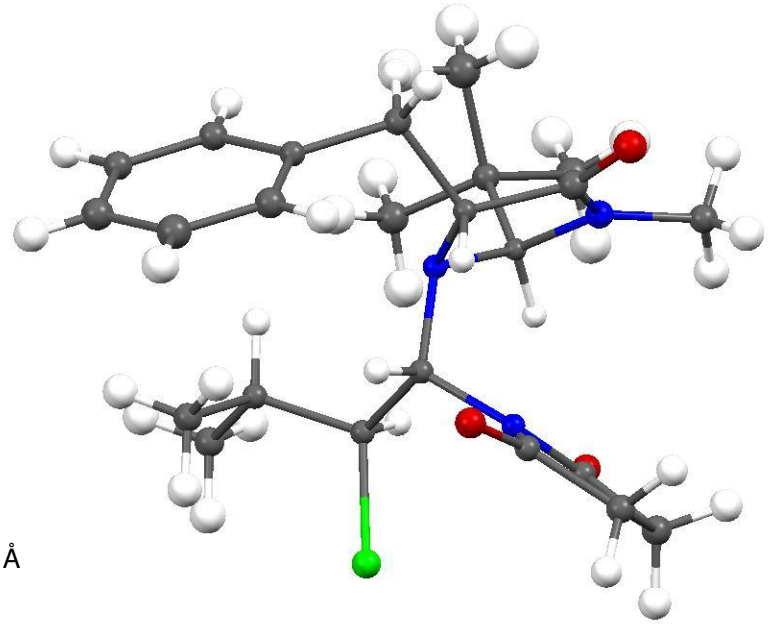

Deposition number: 2041077

Bond precision: C-C = 0.0320 Å

Wavelength =1.54178

Cell: a = 10.2163(4) Å, b = 25.1458(11) Å, c = 14.4592(6) Å

alpha = 90°, beta = 94.880(2)°, gamma = 90°

Temperature: 100 K

Volume: 3701.1(3) Å^3

Space group: P 21 P 1 21 1

Hall group: P 2yb P 2yb

Moiety formula

Dx,g cm-3: 1.207

Z: 6

Mu (mm-1): 1.597

F000: 1442.0

F000': 1448.02

h,k,lmax: 12, 30, 17

Nref: 11279

Tmin,Tmax: 0.557, 0.753

Tmin': 0.270

Reported T Limits: Tmin = 0.557, Tmax = 0.753

AbsCorr = MULTI-SCAN

Data completeness= 1.62/0.83

Theta(max) = 68.367

R(reflections) = 0.1344 (10576)

wR2(reflections) = 0.3992 (11279)

S = 1.382

Npar = 392

1-((1*S*,2*R*)-1-((2*R*,5*R*)-5-benzyl-2-(tert-butyl)-3-methyl-4-oxoimidazolidin-1-yl)-2-chloro-3-phenylpropyl)pyrrolidine-2,5-dione ((1*S*,2*R*)-*syn*-25)

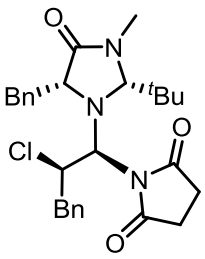

(1*S*,2*R*)-*syn*-**25**

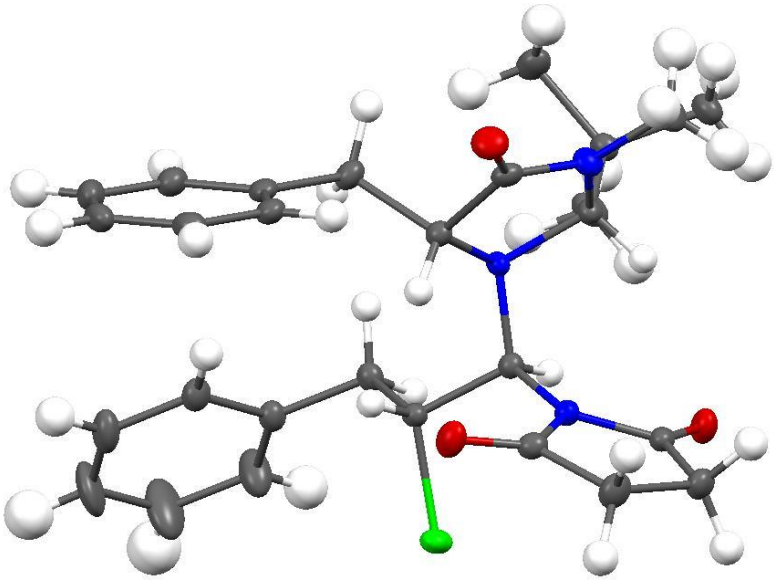

Deposition number: 2041078

Bond precision: C-C = 0.0024 Å

Wavelength = 1.54178

Cell: a = 10.52726(7) Å, b = 13.34540(9) Å, c = 18.82390(12) Å

alpha = 90°, beta = 90°, gamma = 90°

Temperature: 100 K

Volume: 2644.58(3) Å^3

Space group: P 21 21 21

Hall group: P 2ac 2ab

Dx,g cm-3: 1.246

Z: 4

Mu (mm-1): 1.544

F000: 1056.0

F000': 1060.29

h,k,lmax: 12, 16, 22

Nref: 4815

Tmin,Tmax: 0.480, 0.714

Tmin´: 0.420

Reported T Limits: Tmin = 0.480, Tmax = 0.714

AbsCorr = MULTI-SCAN

Data completeness = 1.75/0.99

Theta (max) = 68.453

R (reflections) = 0.0227 (4763)

wR2 (reflections) = 0.0586 (4815)

S = 1.046

Npar = 320

1-((1*S*,2*S*)-1-((2*R*,5*R*)-5-benzyl-2-(tert-butyl)-3-methyl-4-oxoimidazolidin-1-yl)-2-chloro-3-phenylpropyl)pyrrolidine-2,5-dione ((1*S*,2*S*)-*anti*-25)

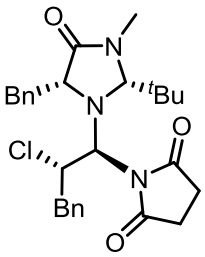

(1*S*,2*S*)-*anti*-**25**

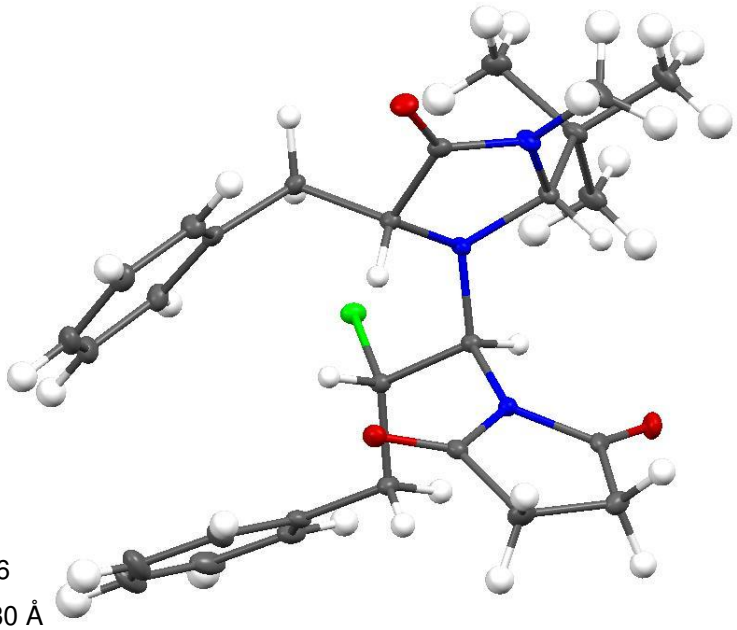

Deposition number: 2041076

Bond precision: C-C = 0.0030 Å

Wavelength = 1.54178

Cell: a = 9.0086(4) Å, b = 10.9058(6) Å, c = 13.4651(6) Å

alpha = 90°, beta = 97.426(2)°, gamma = 90°

Temperature: 100 K

Volume: 1311.80(11) Å^3

Space group: P 1 21 1

Hall group: P 2yb

Dx,g cm-3: 1.256

Z: 2

Mu (mm-1): 1.557

F000: 528.0

F000': 530.14

h,k,lmax: 10,13,16

Nref: 4722

Tmin,Tmax: 0.583, 0.753

Tmin': 0.388

Reported T Limits: Tmin = 0.583, Tmax = 0.753

AbsCorr = MULTI-SCAN

Data completeness = 1.85/0.98

Theta(max) = 68.467

R(reflections) = 0.0250 (4685)

wR2(reflections) = 0.0624 (4722)

S = 1.032

Npar = 321

1-((1*R*,2*S*)-1-((2*R*,5*R*)-5-benzyl-2-(tert-butyl)-3-methyl-4-oxoimidazolidin-1-yl)-2-chloro-3-phenylpropyl)pyrrolidine-2,5-dione ((1*R*,2*S*)-*syn*-25)

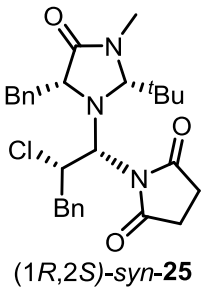

(1*R*,2*S*)-*syn*-**25**

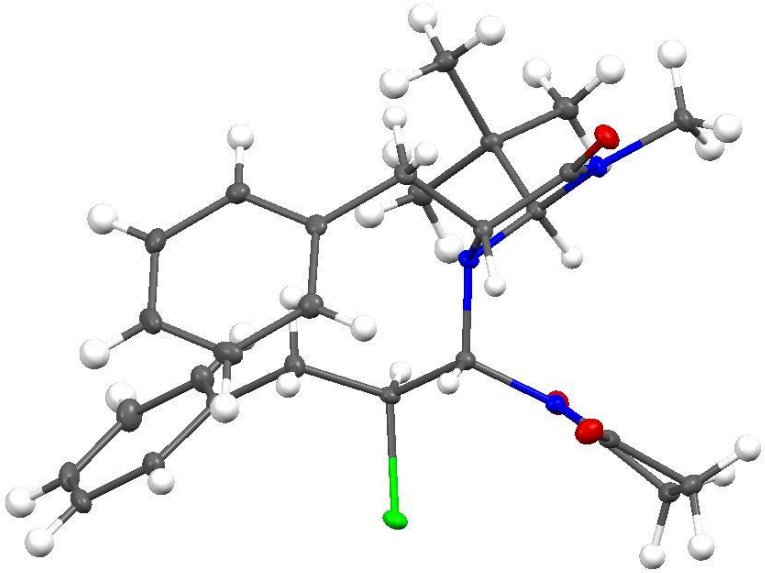

Deposition number: 2043370

Bond precision: C-C = 0.0028 Å

Wavelength = 0.71073

Cell: a = 8.9226(2) Å, b = 15.9789(3) Å, c = 17.9095(3) Å

alpha = 90°, beta = 90°, gamma = 90°

Temperature: 100 K

Volume: 2553.42(9) Å^3

Space group: P 21 21 21

Hall group: P 2ac 2ab

Dx,g cm-3: 1.290

Z: 4

Mu (mm-1): 0.184

F000: 1056.0

F000': 1057.00

h,k,lmax: 10,19,21

Nref: 4853

Tmin,Tmax: 0.780,0.836

Tmin': 0.941

Reported T Limits: Tmin = 0.780, Tmax = 0.836

AbsCorr = MULTI-SCAN

Data completeness = 1.76/1.00

Theta(max) = 25.702

R(reflections) = 0.0247 (4738)

wR2(reflections) = 0.0603 (4853)

S = 1.075

Npar = 320

2-(((1*S*,2*S*)-1-((*S*)-2-(bis(3,5-bis(trifluoromethyl)phenyl)((trimethylsilyl)oxy)methyl)pyrrolidin-1-yl)-2-chloro-3-methylbutyl)carbamoyl)benzyl 3,5-dinitrobenzoate (15)

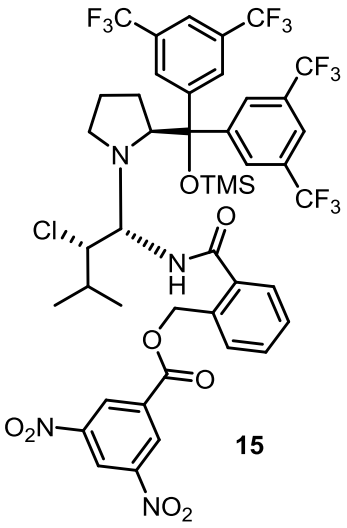

15

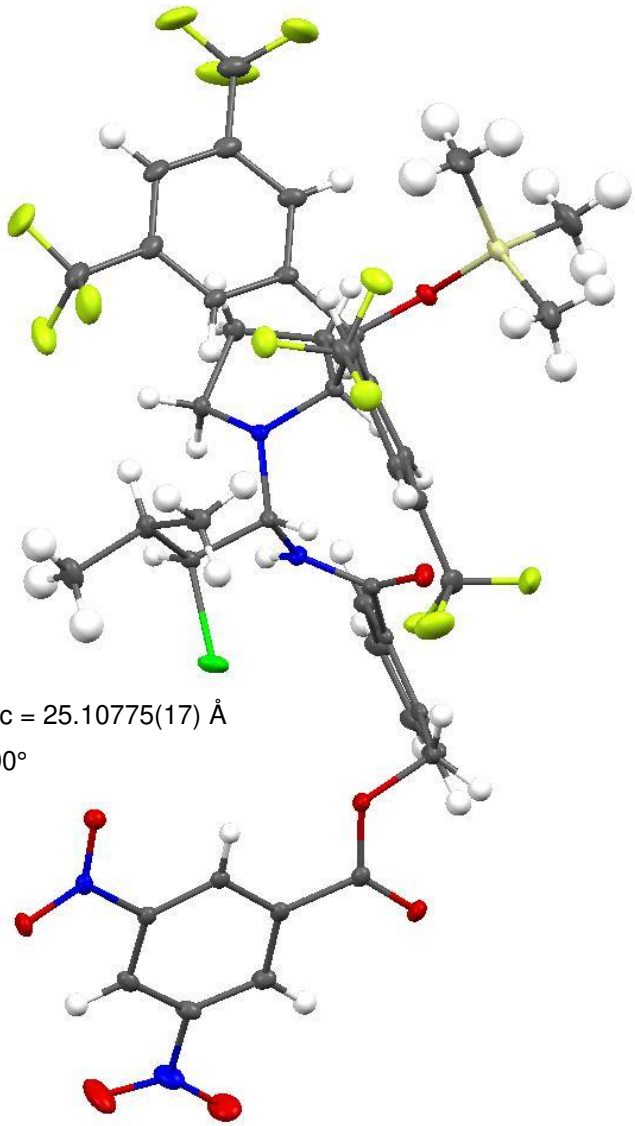

Deposition number: 2045387

Bond precision: C-C = 0.0060 Å

Wavelength = 1.54178

Cell: a = 9.87405(7) Å, b = 19.31855(13) Å, c = 25.10775(17) Å

alpha = 90°, beta = 96.9297(3)°, gamma = 90°

Temperature: 100 K

Volume: 4754.37(6) Å^3

Space group: P 21

Hall group: P 2yb

Dx,g cm-3: 1.460

Z: 4

Mu (mm-1): 1.876

F000: 2144.0

F000': 2154.95

h,k,lmax: 11,23,30

Nref: 16869

Tmin,Tmax: 0.502,0.705

Tmin': 0.394

Reported T Limits: Tmin = 0.502, Tmax = 0.705

AbsCorr = MULTI-SCAN

Data completeness = 1.88/0.97

Theta(max) = 68.297

R(reflections) = 0.0435 (16690)

wR2(reflections)= 0.1138 (16869)

S = 1.111

Npar = 1272

5.4. Supporting Information: In Situ Synthesis and Applications for Polyinterhalides based on BrCl

Chemistry–A European Journal

Supporting Information

In Situ Synthesis and Applications for Polyinterhalides Based on BrCl

Benjamin Schmidt,[a] Sebastian Ponath,[b] Johannes Hannemann,[a] Patrick Voßnacker,[a] Karsten Sonnenberg,[a] Mathias Christmann,[b] and Sebastian Riedel*[a]

Supporting Information

Table of Content

1. Results and Discussion

a. Crystal Data

Table S1. Crystal data of the synthesized compounds.

Empirical formula	$C_8H_{20}BrCl_2N$ (**1**)	$C_{16}H_{40}Br_3Cl_5N_2$ (**2**)	$C_8H_{20}Br_3Cl_4N$ (**3**)
Formula weight	281.06	677.48	511.78
Temperature/K	100.0	100.0	100.0
Crystal system	orthorhombic	monoclinic	monoclinic
Space group	*Pnma*	$P2_1/m$	$P2_1/c$
a/Å	11.9218(16)	7.7583(4)	12.0185(6)
b/Å	12.4514(15)	12.8611(7)	10.1733(5)
c/Å	17.4209(17)	14.2896(8)	14.5527(6)
α/°	90	90	90
β/°	90	103.750(2)	99.093(2)
γ/°	90	90	90
Volume/Å^3	2586.0(5)	1384.96(13)	1756.97(14)
Z	8	2	4
ρ_{calc}g/cm^3	1.444	1.625	1.935
μ/mm^{-1}	3.551	4.858	7.476
F(000)	1152.0	680.0	992.0
Crystal size/mm^3	0.3 × 0.2 × 0.11	0.458 × 0.453 × 0.28	0.58 × 0.31 × 0.24
Radiation	MoKα (λ = 0.71073)	MoKα (λ = 0.71073)	MoKα (λ = 0.71073)
2Θ range for data collection/°	4.676 to 56.61	5.406 to 56.634	4.906 to 56.68
Reflections collected	24805	65037	30162
Independent reflections	3364 [R_{int} = 0.0595, R_{sigma} = 0.0344]	3601 [R_{int} = 0.0524, R_{sigma} = 0.0176]	4370 [R_{int} = 0.0929, R_{sigma} = 0.0545]
Data/restraints/parameters	3364/0/122	3601/0/134	4370/0/149
Goodness-of-fit on F^2	1.054	1.048	1.079
Final R indexes [I>=2σ (I)]	R_1 = 0.0277, wR_2 = 0.0537	R_1 = 0.0200, wR_2 = 0.0434	R_1 = 0.0426, wR_2 = 0.1008
Final R indexes [all data]	R_1 = 0.0404, wR_2 = 0.0571	R_1 = 0.0259, wR_2 = 0.0456	R_1 = 0.0609, wR_2 = 0.1096
Largest diff. peak/hole / e Å^{-3}	0.39/-0.55	0.37/-0.52	0.87/-1.56
CCDC deposition numbers	1965315	1984581	1965317

Table S2. Crystal data of the synthesized compounds.

Empirical formula	$C_{12}H_{28}Br_4Cl_5N$ (**4**)	$C_8H_{20}Br_{5.6}Cl_{5.4}N$ (**5**)	$C_8H_{20}Br_{2.32}Cl_{2.68}N$	$C_{15}H_{12}BrClO$
Formula weight	683.24	769.17	410.47	323.61
Temperature/K	100.0	100.0	100.0	100.0
Crystal system	tetragonal	monoclinic	monoclinic	monoclinic
Space group	$I\bar{4}$	$P2_1/n$	$P2_1/n$	Cc
a/Å	11.8884(13)	14.6745(13)	8.4748(3)	5.7073(3)
b/Å	11.8884(13)	10.3054(8)	13.9985(5)	25.3888(13)
c/Å	8.5997(9)	16.5643(14)	12.9242(4)	9.0603(5)
α/°	90	90	90	90
β/°	90	114.001(3)	93.8220(10)	95.499(2)
γ/°	90	90	90	90
Volume/Å^3	1215.4(3)	2288.4(3)	1529.85(9)	1306.81(12)
Z	2	4	4	4
ρ_{calc}g/cm^3	1.867	2.233	17.820	1.645
μ/mm^{-1}	7.169	10.450	6.564	6.030
F(000)	664.0	1451.0	806.2	648.0
Crystal size/mm^3	0.26 × 0.21 × 0.21	0.403 × 0.339 × 0.298	0.319 × 0.303 × 0.206	0.322 × 0.075 × 0.033
Radiation	MoKα (λ = 0.71073)	MoKα (λ = 0.71073)	Mo Kα (λ = 0.71073)	CuKα (λ = 1.54178)
2Θ range for data collection/°	4.846 to 56.49	3.134 to 56.67	4.3 to 66.34	6.964 to 139.3
Reflections collected	9392	54685	38582	16304
Independent reflections	1516 [R_{int} = 0.0532, R_{sigma} = 0.0375]	5702 [R_{int} = 0.0893, R_{sigma} = 0.0448]	5755 [R_{int} = 0.0363, R_{sigma} = 0.0245]	2313 [R_{int} = 0.0538, R_{sigma} = 0.0345]
Data/restraints/parameters	1516/0/52	5702/7/195	5755/0/151	2313/2/163
Goodness-of-fit on F^2	1.098	1.047	1.059	1.080
Final R indexes [I>=2σ (I)]	R_1 = 0.0255, wR_2 = 0.0570	R_1 = 0.0333, wR_2 = 0.0794	R_1 = 0.0226, wR_2 = 0.0478	R_1 = 0.0343, wR_2 = 0.0832
Final R indexes [all data]	R_1 = 0.0286, wR_2 = 0.0580	R_1 = 0.0475, wR_2 = 0.0857	R_1 = 0.0354, wR_2 = 0.0547	R_1 = 0.0360, wR_2 = 0.0845
Largest diff. peak/hole / e Å^{-3}	0.53/-0.51	0.76/-1.07	0.60/-0.96	0.79/-0.82
CCDC deposition numbers	1965314	1965318	1971174	1984909

b. Solid State Structures

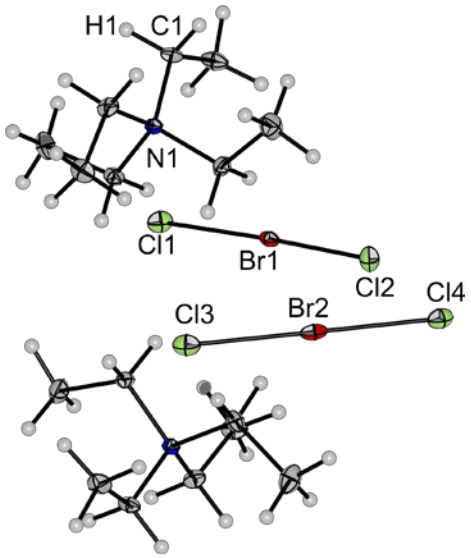

Figure S1. Molecular structure of $[NEt_4][Cl(BrCl)]$ in the solid state with thermal ellipsoids set at 50 % probability. Selected bond lengths [pm] and angles [°]: Cl1-Br1 241.8(1), Cl2-Br1 235.7(1), Cl3-Br2 240.4(1), Cl4-Br2 239.1(1); Cl1-Br1-Cl2 174.8(1), Cl3-Br2-Cl4 179.1(1).

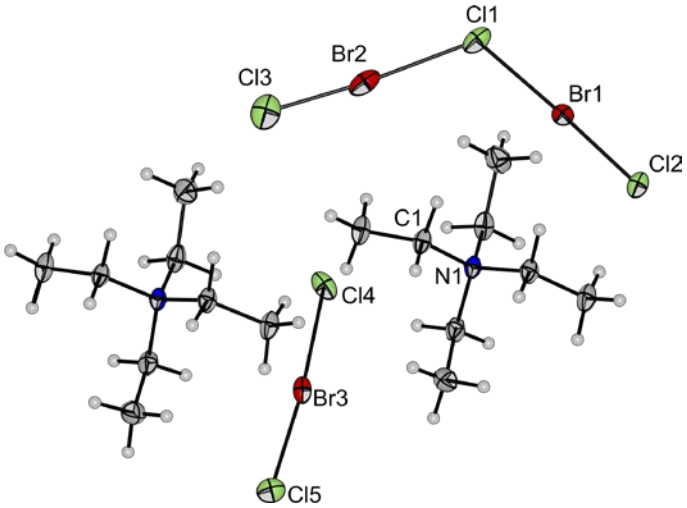

Figure S2. Molecular structure of $[NEt_4]_2[Cl(BrCl)_2][ClBrCl]$ in the solid state with thermal ellipsoids set at 50 % probability. Selected bond lengths [pm] and angles [°]: Cl1-Br1 251.7(1), Cl1-Br2 262.3(1), Br1-Cl2 227.8(1), Br2-Cl3 224.1(1), Cl4-Br3 239.8(1), Cl5-Br3 236.8(1); Cl1-Br1-Cl2 178.0(1), Cl1-Br2-Cl3 175.7(1), Br2-Cl1-Br1 116.6(1), Cl4-Br3-Cl5 174.7(1).

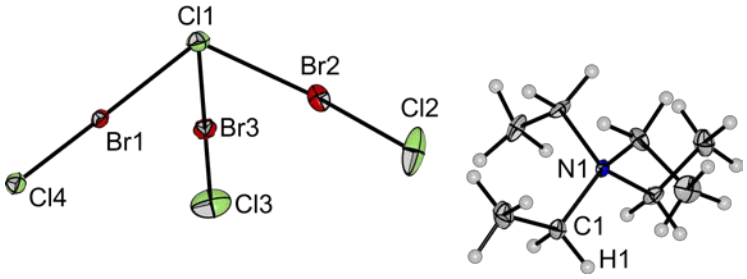

Figure S3. Molecular structure of $[NEt_4][Cl(BrCl)_3]$ in the solid state with thermal ellipsoids set at 50 % probability. Selected bond lengths [pm] and angles [°]: Cl1-Br1 266.4(2), Cl1-Br2 273.0(2), Cl1-Br3 269.2(2), Br1-Cl4 223.0(2), Br2-Cl2 220.1(2), Br3-Cl3 221.0(2); Cl1-Br1-Cl4 177.6(1), Cl1-Br3-Cl3 178.0(1), Cl1-Br2-Cl2 175.5(1), Br1-Cl1-Br3 90.5(1), Br3-Cl1-Br2 87.7(1), Br1-Cl1-Br2 104.2(1).

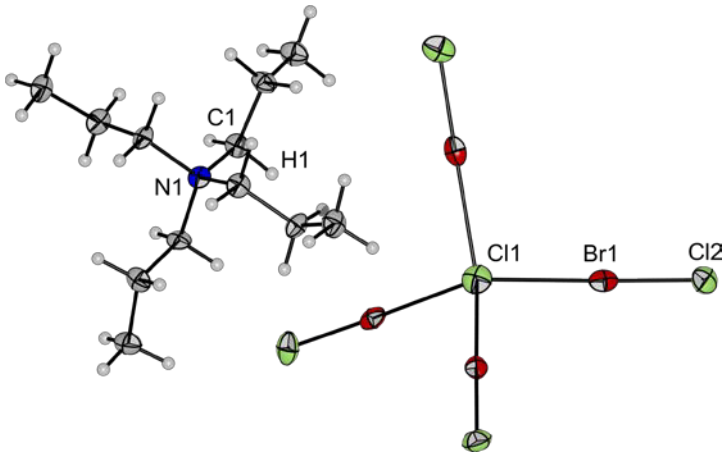

Figure S4. Molecular structure of $[NPr_4][Cl(BrCl)_4]$ in the solid state with thermal ellipsoids set at 50 % probability. Selected bond lengths [pm] and angles [°]: Cl1-Br1 278.6(1), Br1-Cl2 221.3(2); Cl1-Br1-Cl2 177.7(1), Br1-Cl1-Br1' 100.3(1), 130.1(1).

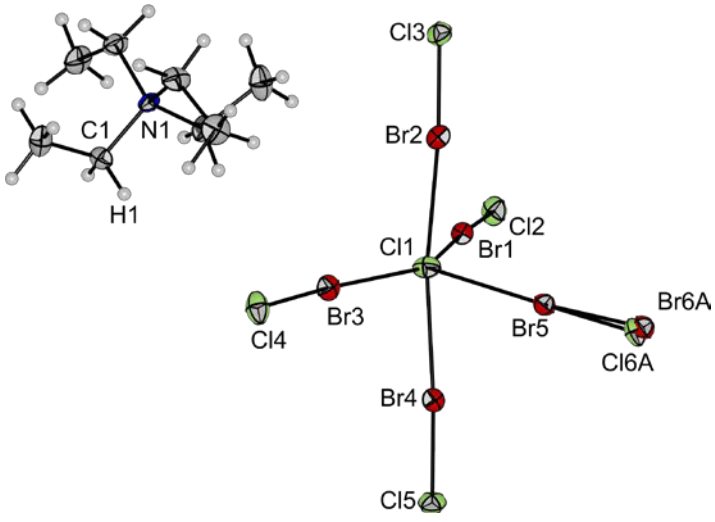

Figure S5. Molecular structure of $[NEt_4][Cl(BrCl)_5]$ in the solid state with thermal ellipsoids set at 50 % probability. Selected bond lengths [pm] and angles [°]: Cl1-Br1 286.4(2), Cl1-Br2 281.6(2), Cl1-Br3 281.4(2), Cl1-Br4 281.1(2), Cl1-Br5 298.6(2), Br1-Cl2 218.0(2), Br2-Cl3 219.4(2), Br3-Cl4 219.1(2), Br4-Cl5 218.9(2), Br5-Cl6A 218.4(16), Br5-Br6A 231.4(5); Cl1-Br1-Cl2 176.7(1), Cl1-Br2-Cl3 174.9(1), Cl1-Br3-Cl4 175.3(1), Cl1-Br4-Cl5 176.1(1), Cl1-Br5-Cl6A 174.8(8), Br3-Cl1-Br1 148.7(1), Br2-Cl1-Br4 171.5(1);); population of the disorders: Cl6A: 40 %, Br6A: 60 %.

c. Raman Spectra

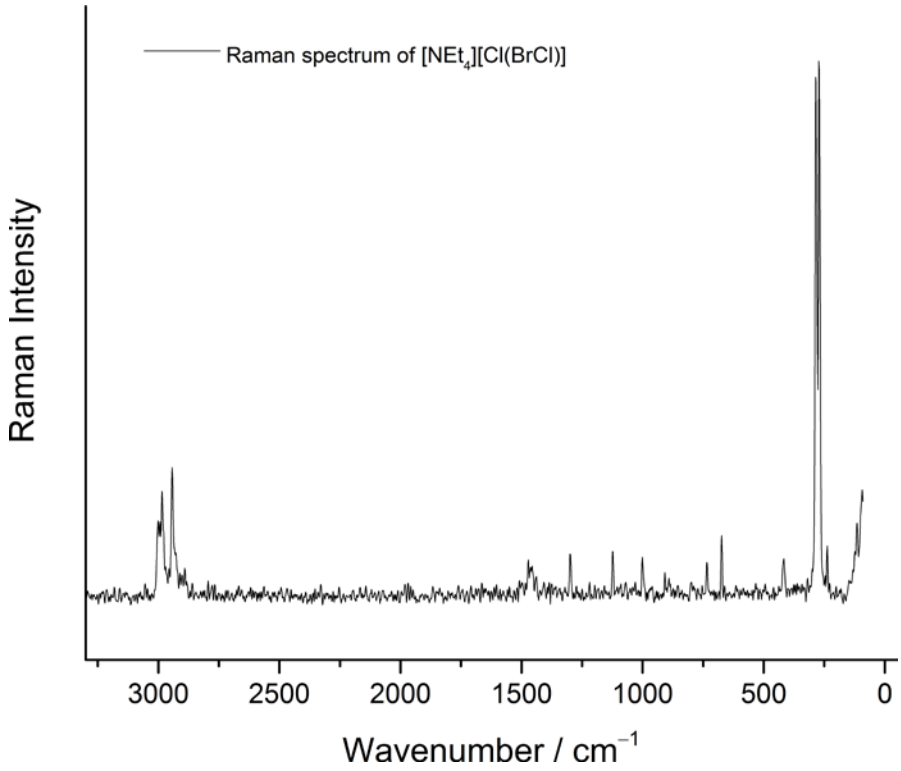

Figure S6. Raman spectrum of a single crystal of [NEt_4][Cl(BrCl)], taken at low temperature (–196 °C).

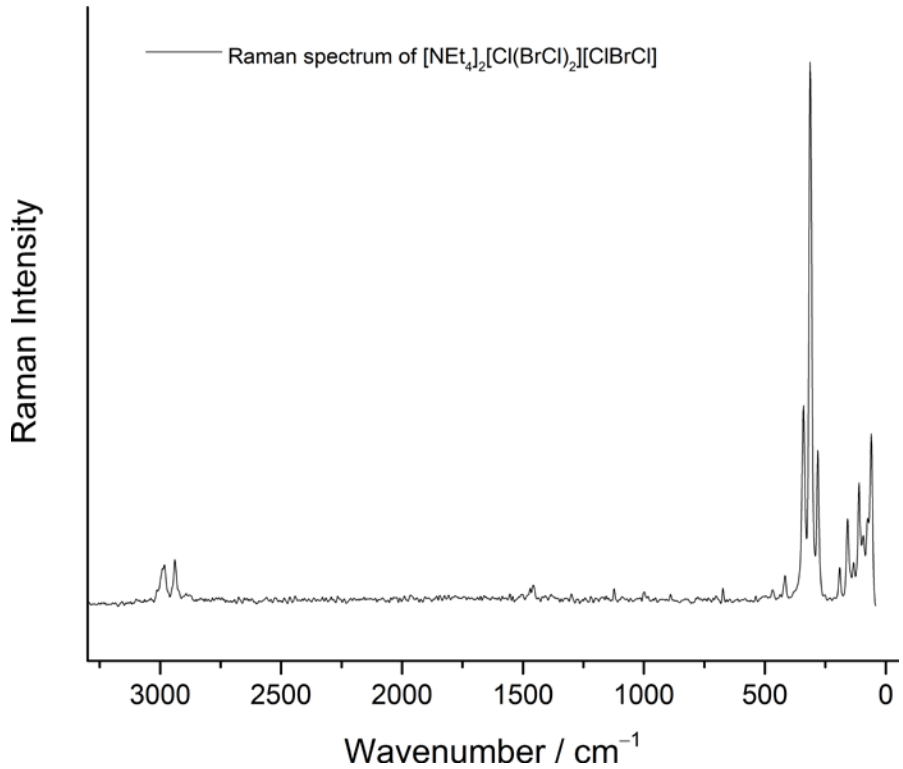

Figure S7. Raman spectrum of a single crystal of [NEt_4]$_2$[Cl($BrCl$)$_2$][ClBrCl], taken at low temperature (–196 °C).

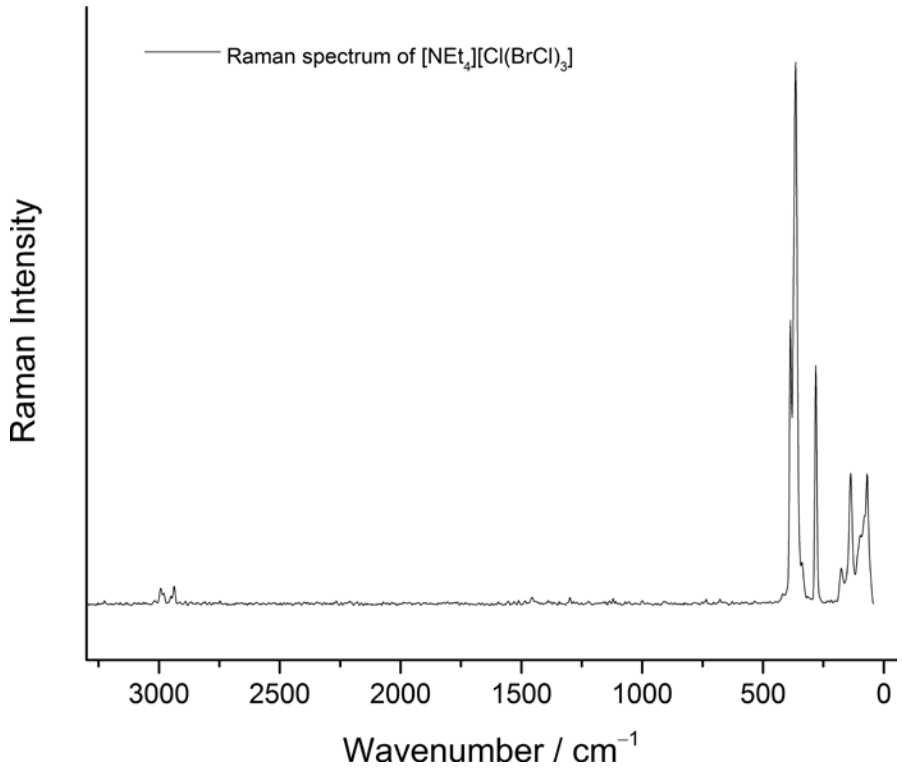

Figure S8. Raman spectrum of a single crystal of $[NEt_4][Cl(BrCl)_3]$, taken at low temperature (–196 °C).

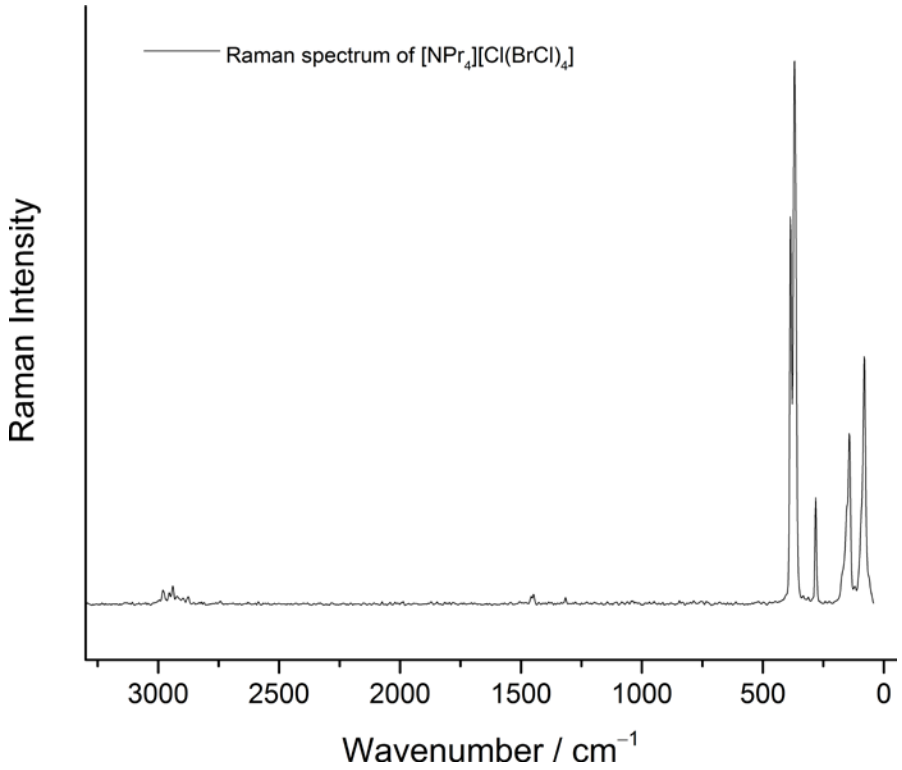

Figure S9. Raman spectrum of a single crystal of $[NPr_4][Cl(BrCl)_4]$, taken at low temperature (–196 °C).

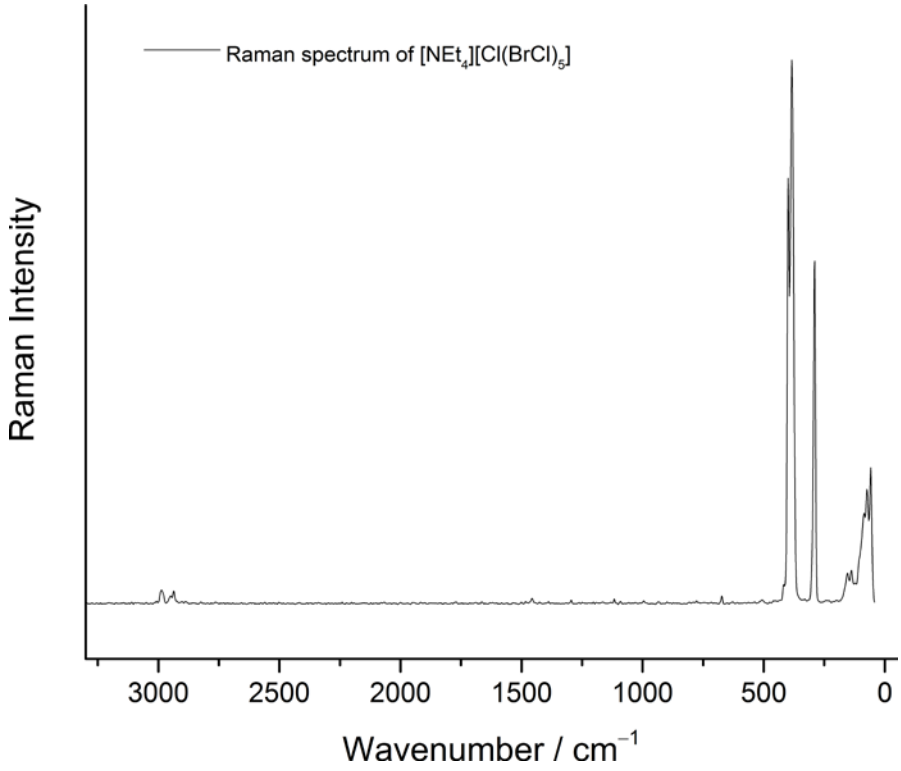

Figure S10. Raman spectrum of a single crystal of $[NEt_4][Cl(BrCl)_5]$, taken at low temperature (–196 °C).

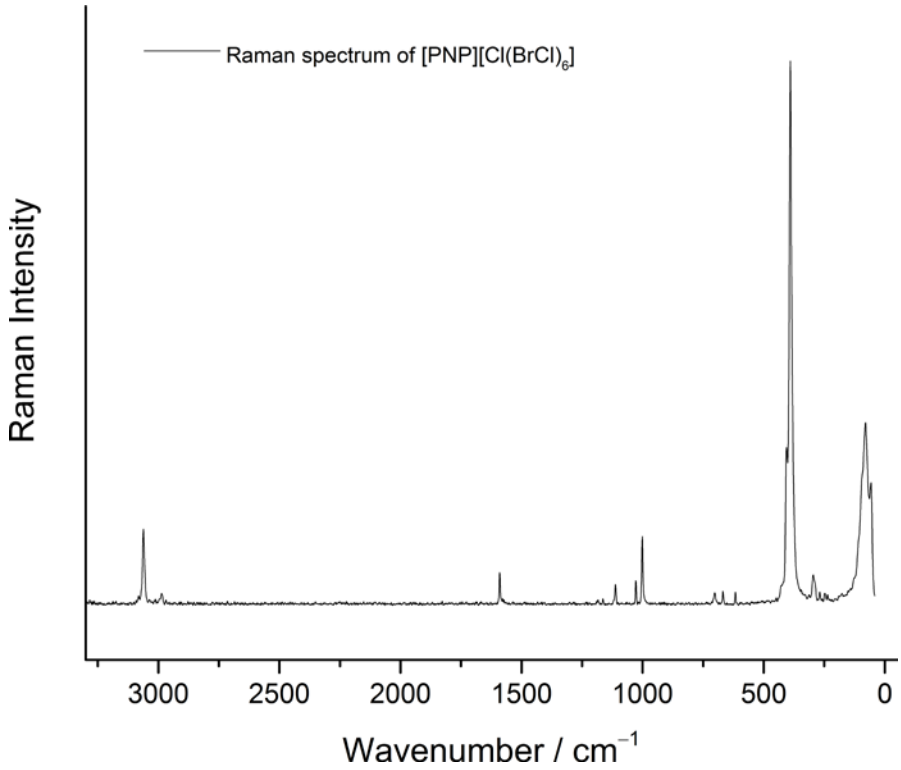

Figure S11. Raman spectrum of a single crystal of $[PNP][Cl(BrCl)_6]$, taken at low temperature (–196 °C).

d. IR Spectra

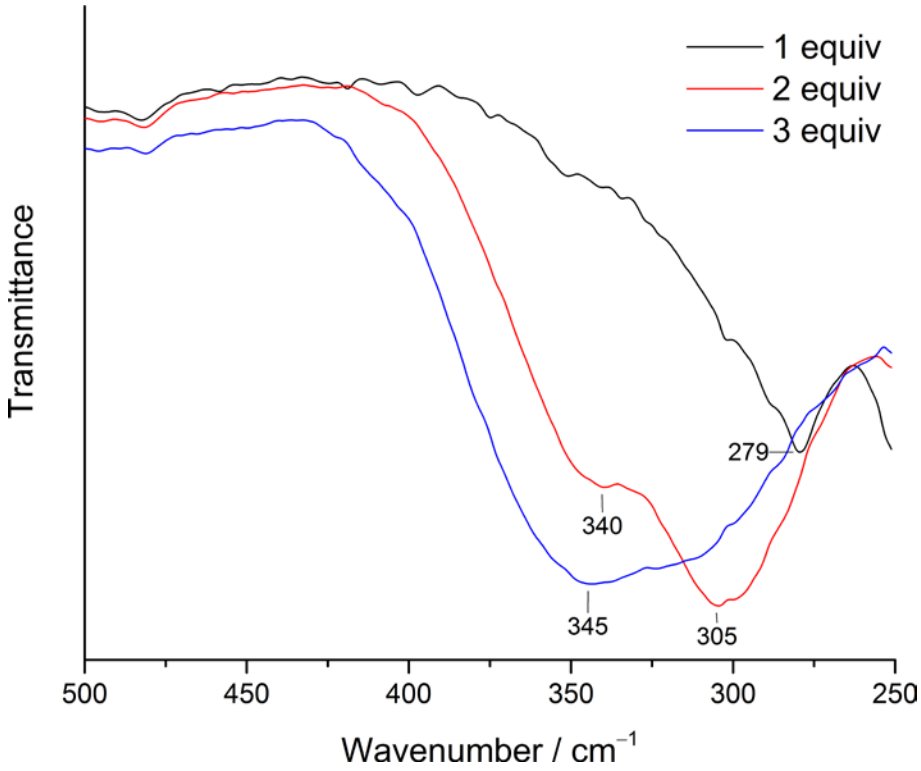

Figure S12. Selected bands of the ATR-IR spectra of RT-ILs obtained from $[N_{2221}]Cl$ and 1 – 3 equiv of BrCl.

e. Calculated Thermochemistry

Table S3. Calculated ΔG (298.15 K, 1 bar) and ΔE values for the formation of $[Cl(BrCl)_n]^-$ calculated at B3LYP-D3(BJ)/def2-TZVPP and SCS-MP2/def2-TZVPP levels.

	B3LYP-D3(BJ)		**SCS-MP2**	
	ΔG [kJ/mol]	**ΔE [kJ/mol]**	**ΔG [kJ/mol]**	**ΔE [kJ/mol]**
$[Cl(BrCl)]^- + BrCl \rightarrow [Cl(BrCl)_2]^-$ (C_{2v})	–48.8	–81.1	–30.4	–62.4
$[Cl(BrCl)_2]^- + BrCl \rightarrow [Cl(BrCl)_3]^-$ (C_{3v})	–19.0	–54.5	–11.1	–47.5
$[Cl(BrCl)_3]^- + BrCl \rightarrow [Cl(BrCl)_4]^-$ (T_d)	–9.2	–42.4	–8.1	–39.8
$[Cl(BrCl)_4]^- + BrCl \rightarrow [Cl(BrCl)_5]^-$ (D_{3h})	7.4	–29.9	12.8	–33.1
$[Cl(BrCl)_5]^- + BrCl \rightarrow [Cl(BrCl)_6]^-$ (O_h)	8.1	–32.2	9.1	–34.8
$2\ BrCl \rightarrow Cl_2 + Br_2$	5.2	1.7	5.9	2.4
$2\ [Cl(BrCl)_4]^- \rightarrow [Cl(Cl_2)_4]^- + [Cl(Br_2)_4]^-$	89.6	103.8	114.9	122.0
$2\ [Cl(BrCl)_2]^- \rightarrow [Cl(Cl_2)_2]^- + [Cl(Br_2)_2]^-$	65.9	67.6	78.3	81.4

f. Interhalogenation: Substrate Scope

Table S4. Substrate scope of the interhalogenation with the reactive IL $[NEt_3Me][Cl(BrCl)_2]$.

Nr.	substrate	product	yield
A		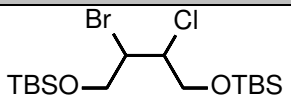	86%
B	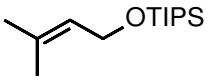	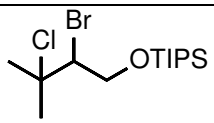	83%
C	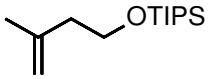	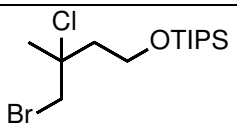	86%
D	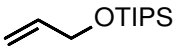	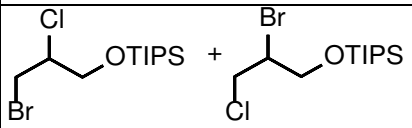 regioisomeric ratio = 1:1	87%
E	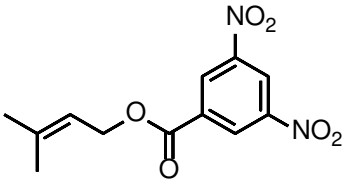	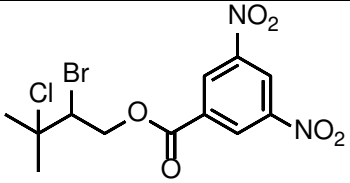	84%
F	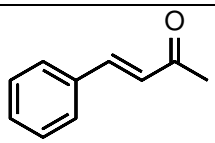	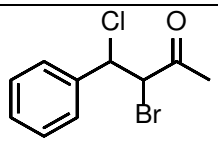	88%
G	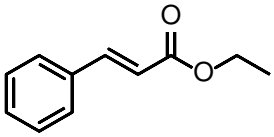	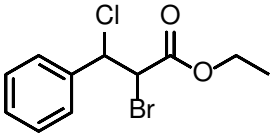	91%
H	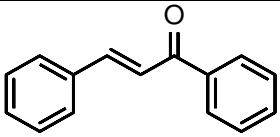	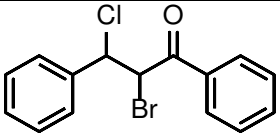	89%
I	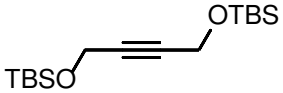	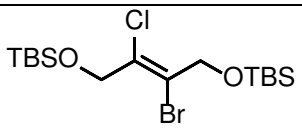	71%

The excellent regio- and diastereoselectivity (*cis*/*trans, E*/*Z*) of all compounds (beside **D**) is in accordance with the classical reactivity of unsaturated substrates with interhalides. The more electrophilic bromine atom forms a bromonium ion which is subsequently attacked by the remaining chloride. The nucleophilic attack on the bromonium ion is directed by the substitution pattern (tertiary>secondary>primary carbocation) of the participating carbon atoms. For Michael-systems the nucleophilic chloride exclusively attacks the benzylic β-position. The solid state structure of compound **H** confirms these considerations.

g. NMR Spectra

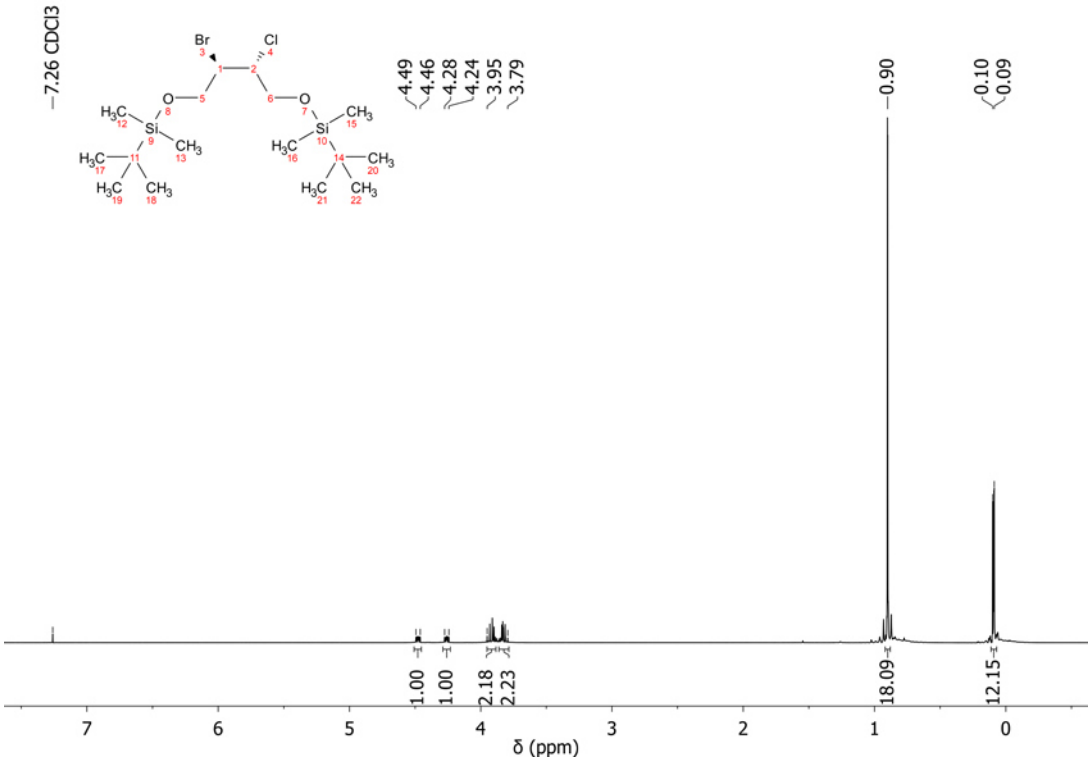

Figure S13. ^{1}H-NMR spectrum of the interhalogenation product **A**.

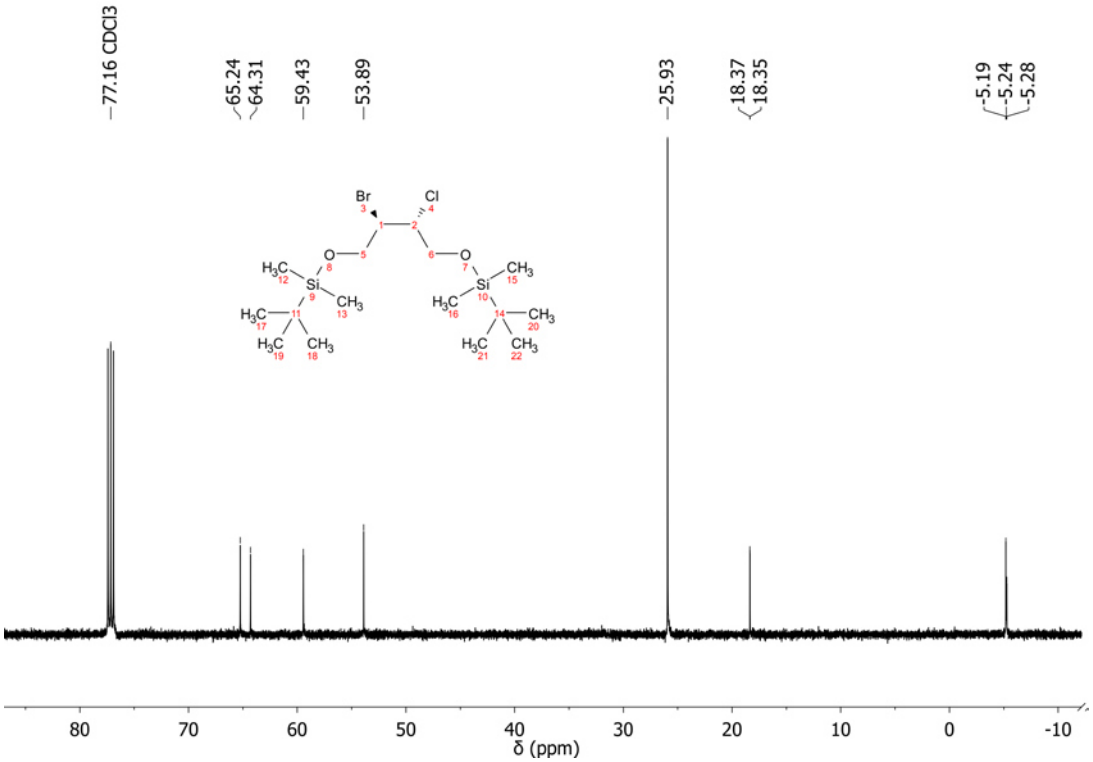

Figure S14. ^{13}C-NMR spectrum of the interhalogenation product **A**.

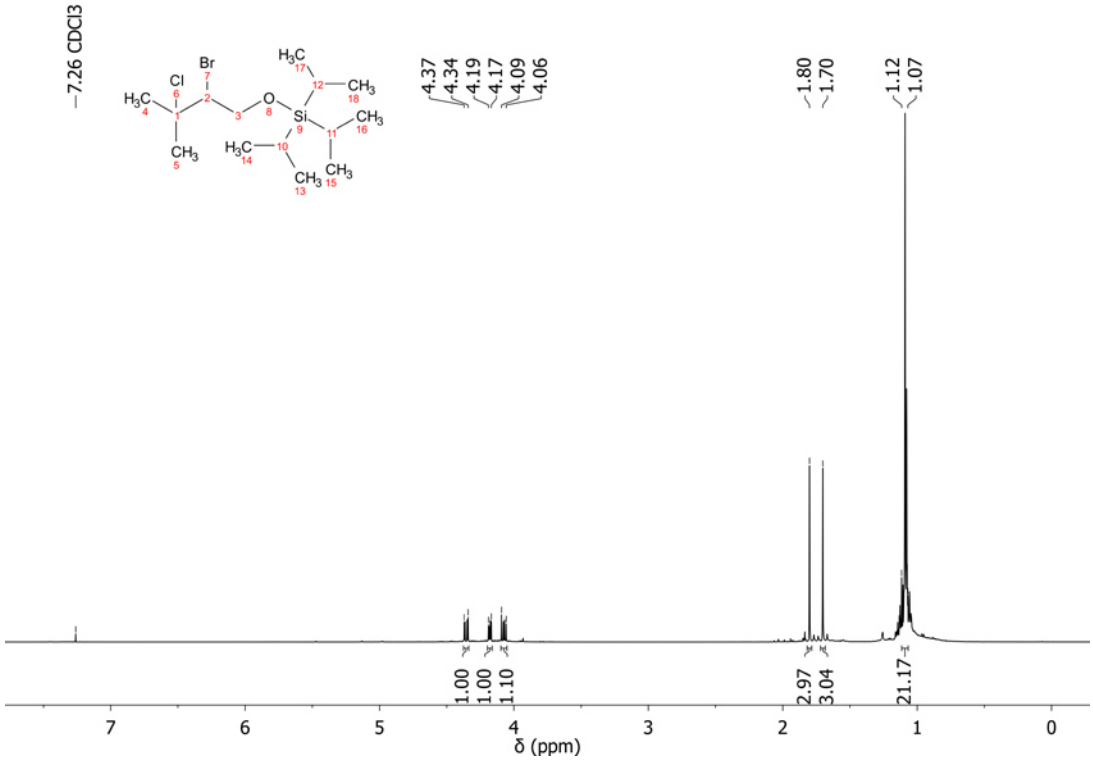

Figure S15. ^{1}H-NMR spectrum of the interhalogenation product **B**.

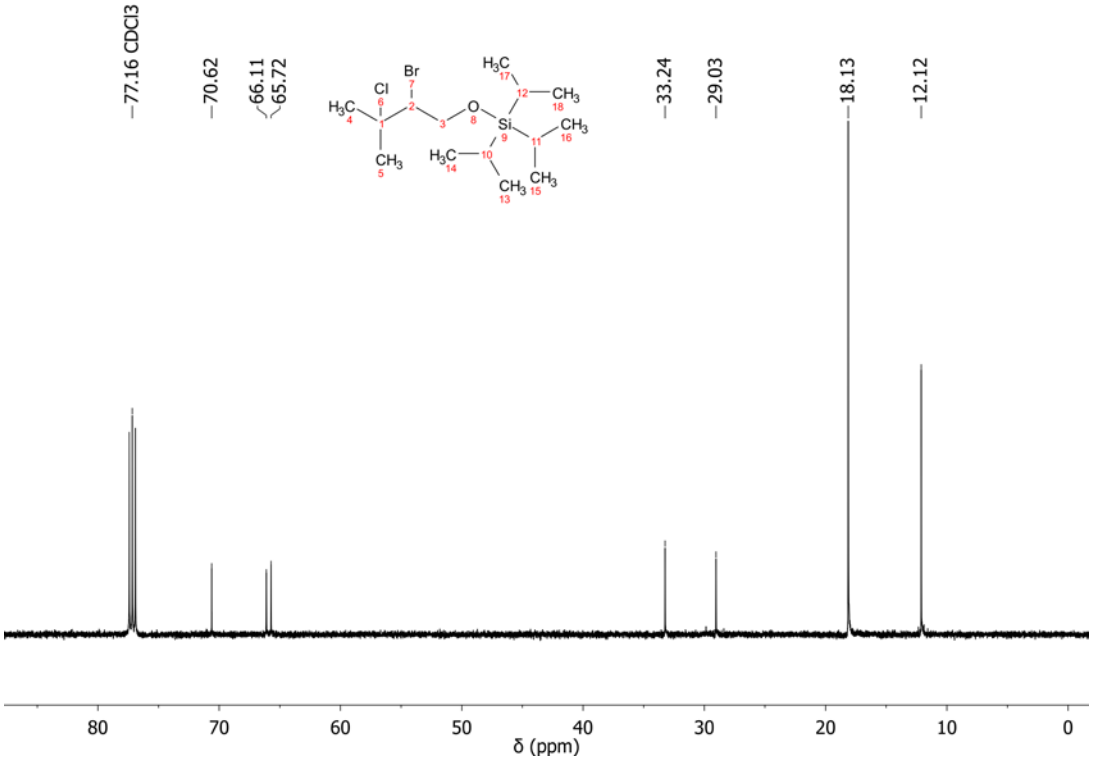

Figure S16. ^{13}C-NMR spectrum of the interhalogenation product **B**.

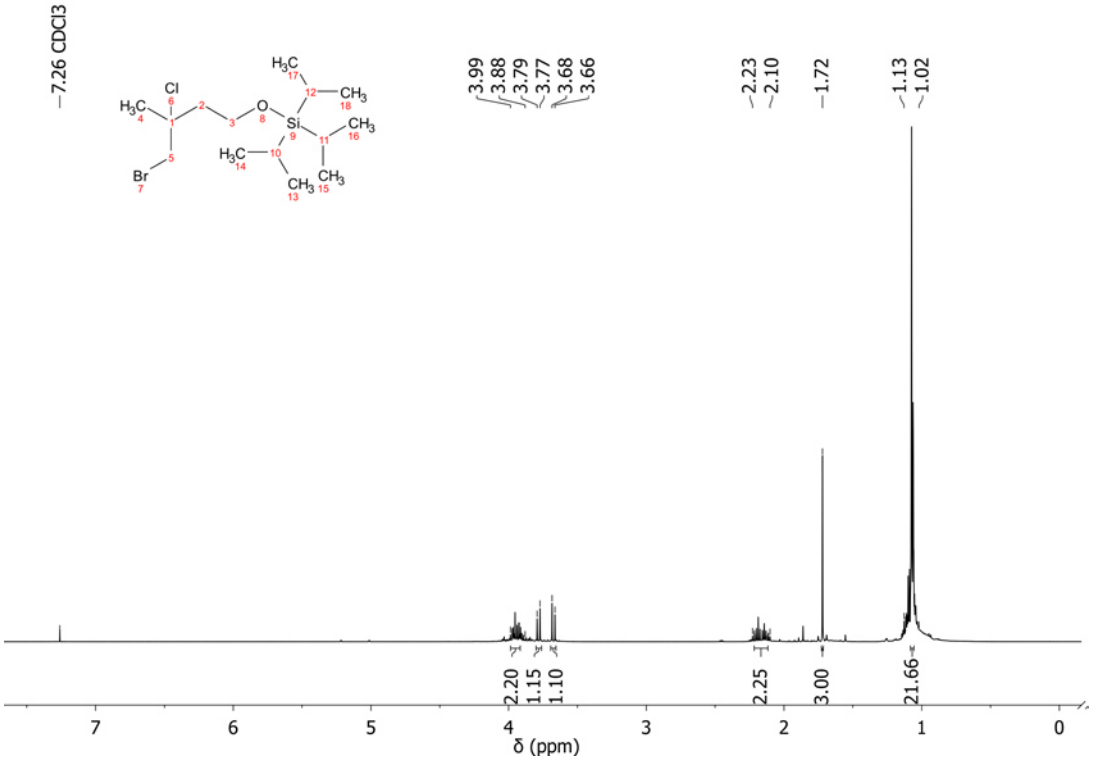

Figure S17. ^{1}H-NMR spectrum of the interhalogenation product **C**.

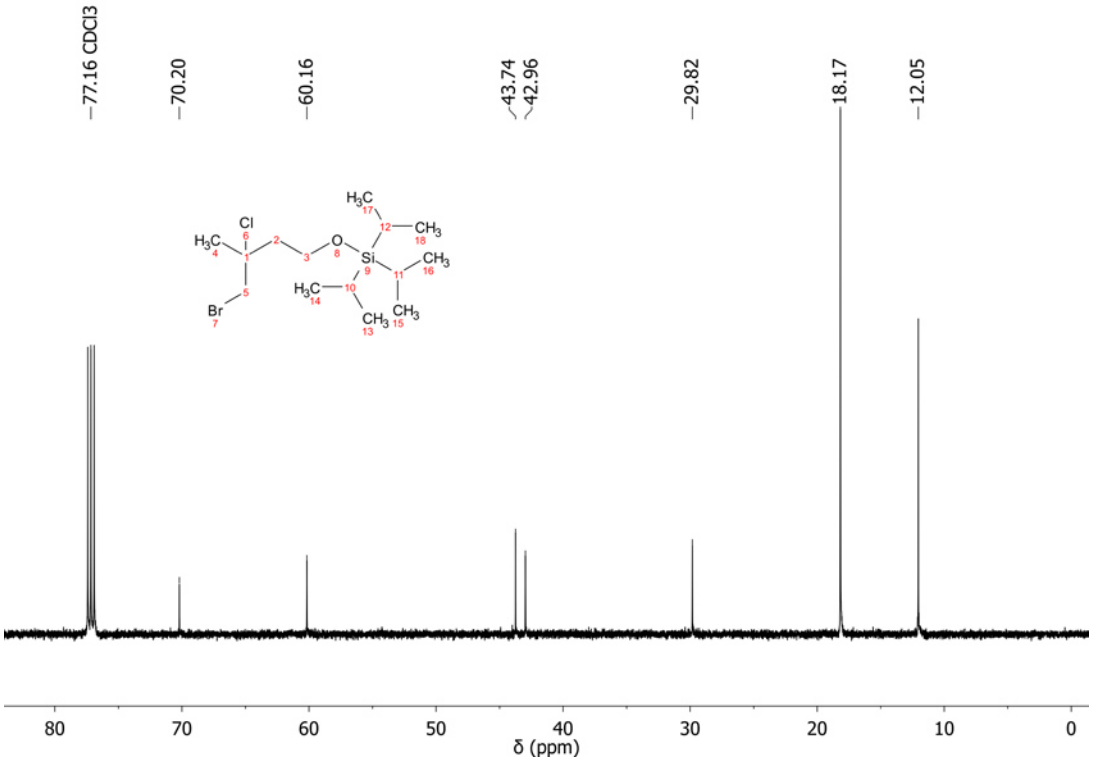

Figure S18. ^{13}C-NMR spectrum of the interhalogenation product **C**.

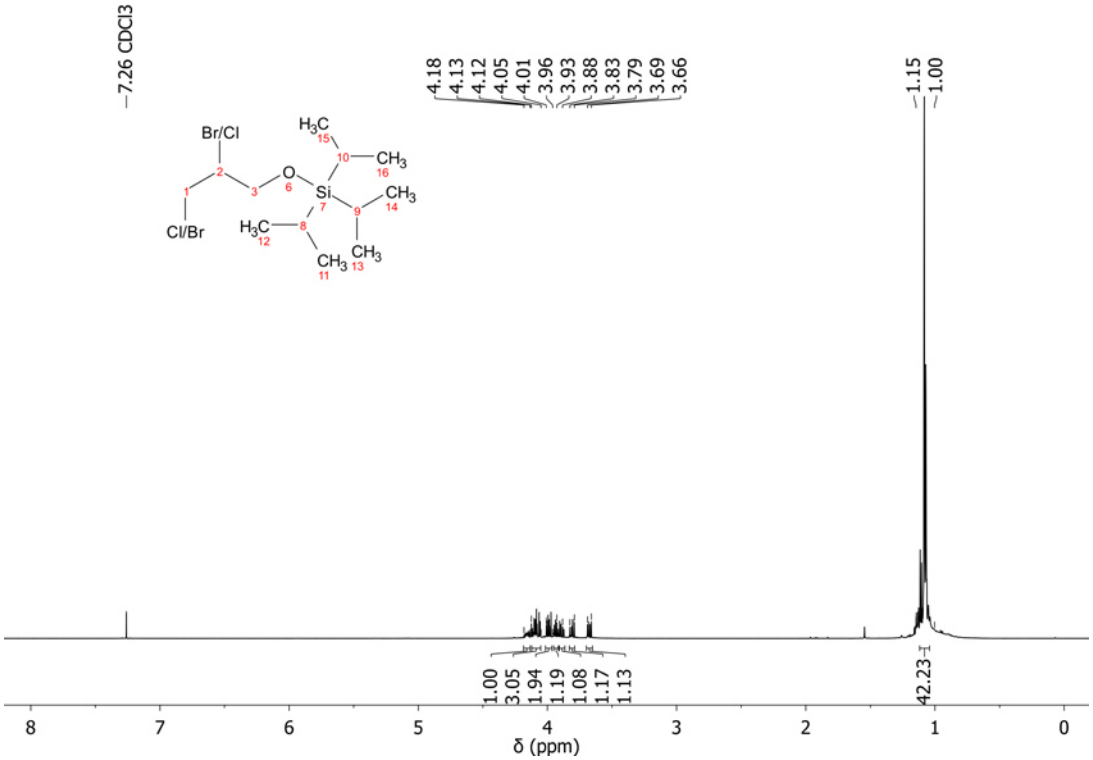

Figure S19. ^{1}H-NMR spectrum of the interhalogenation products **D**.

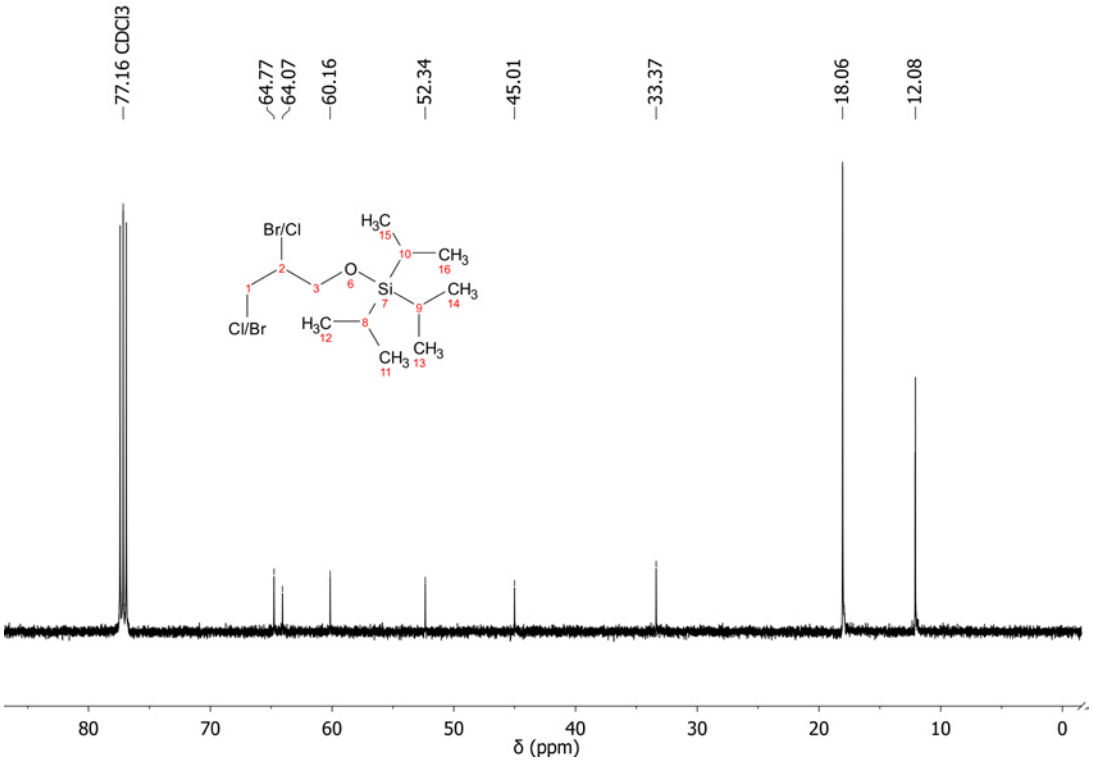

Figure S20. ^{13}C-NMR spectrum of the interhalogenation products **D**.

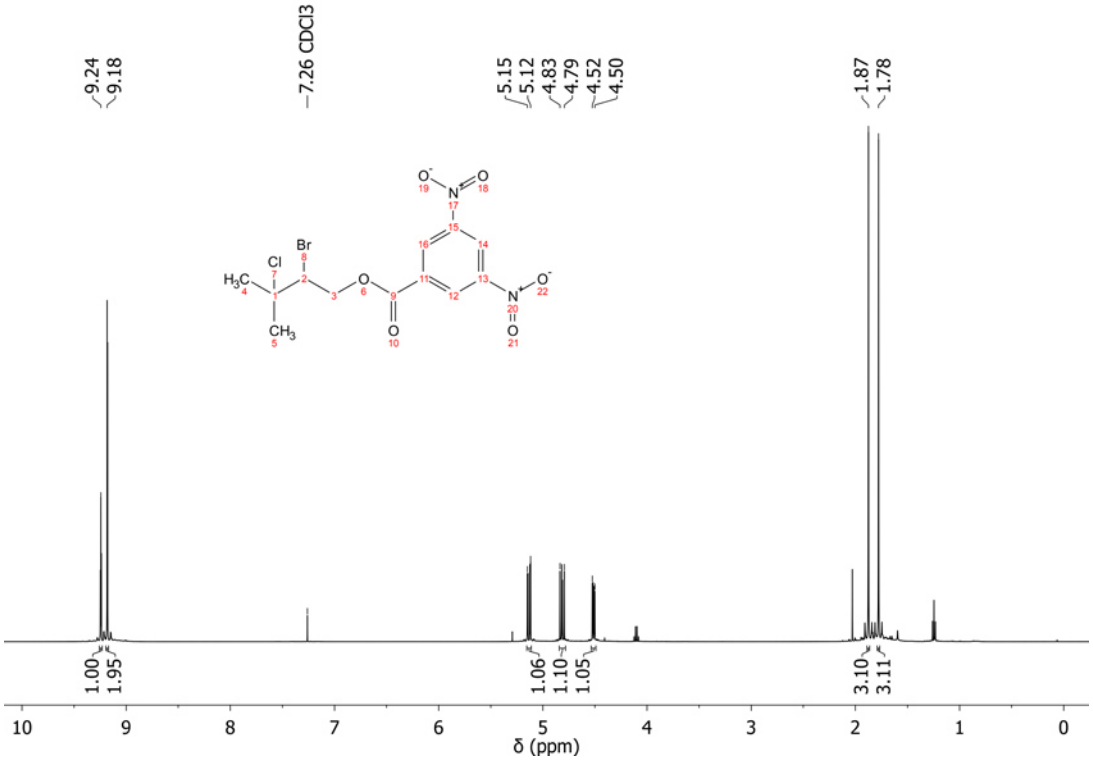

Figure S21. ^{1}H-NMR spectrum of the interhalogenation product **E**.

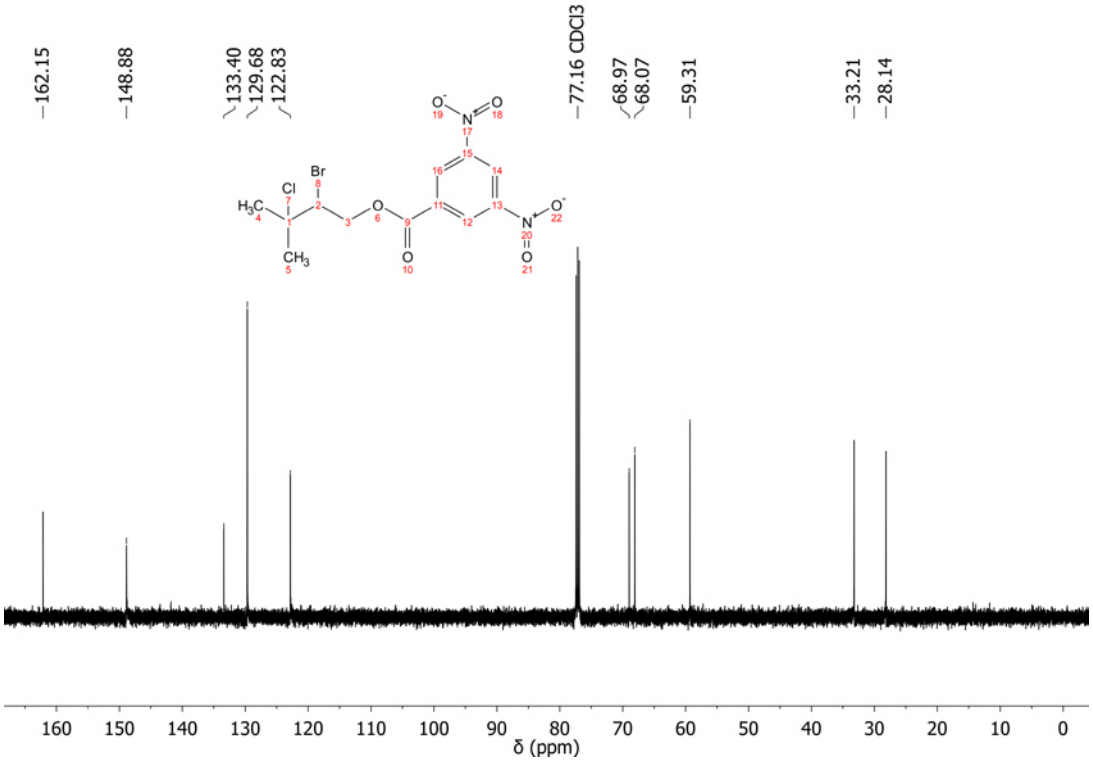

Figure S22. ^{13}C-NMR spectrum of the interhalogenation product **E**.

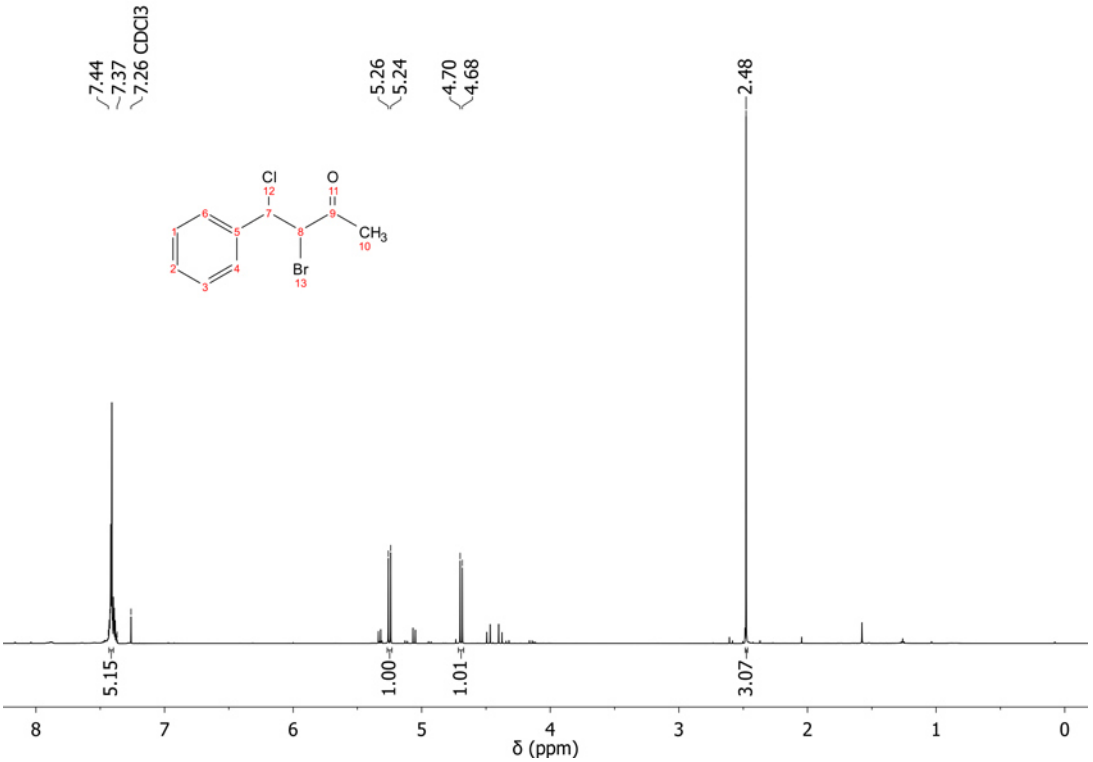

Figure S23. ^{1}H-NMR spectrum of the interhalogenation product **F**.

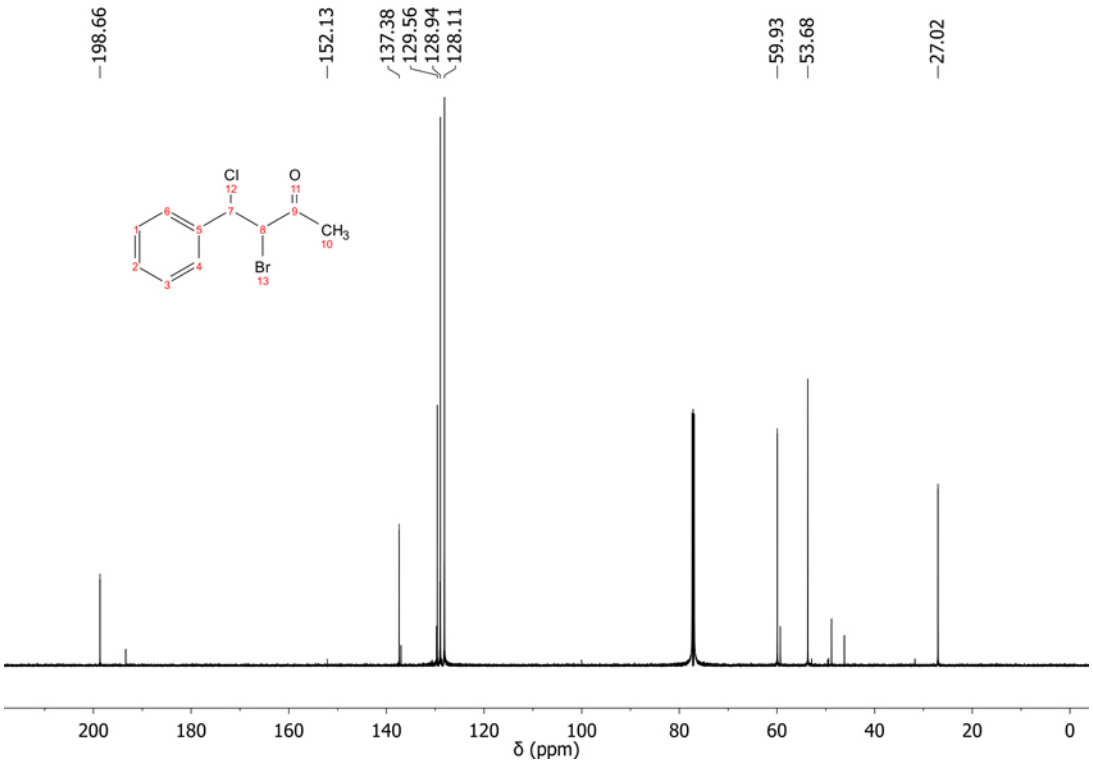

Figure S24. ^{13}C-NMR spectrum of the interhalogenation product **F**.

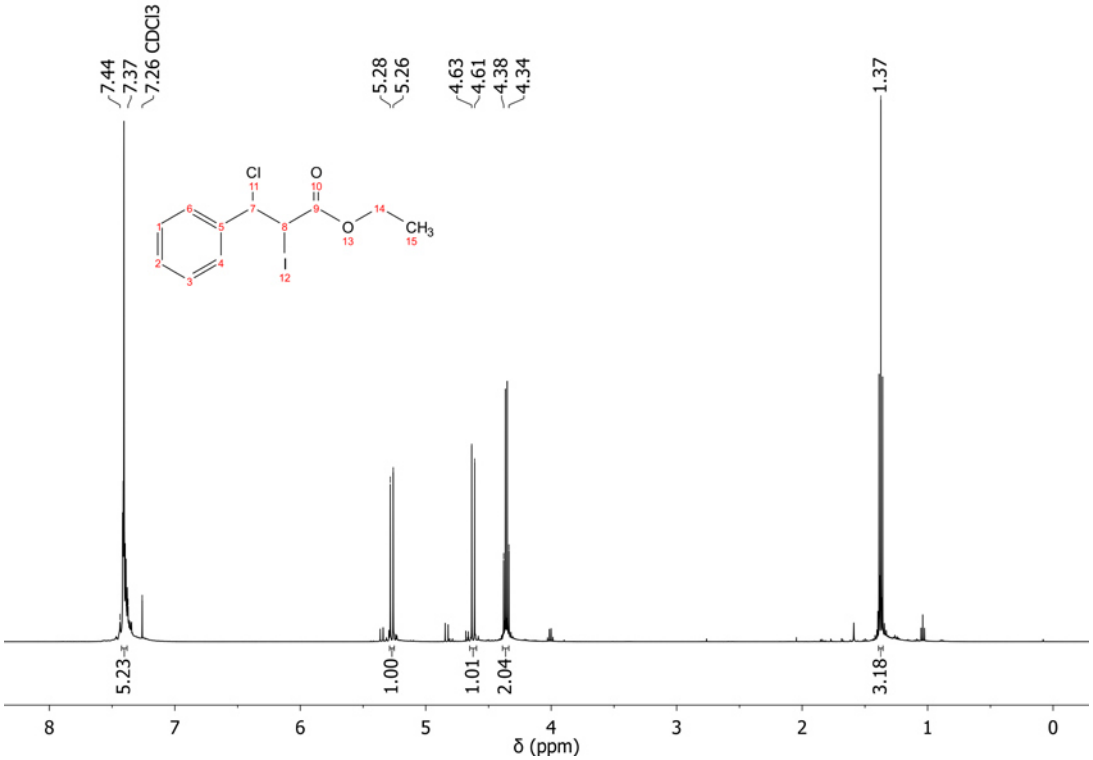

Figure S25. ^{1}H-NMR spectrum of the interhalogenation product **G**.

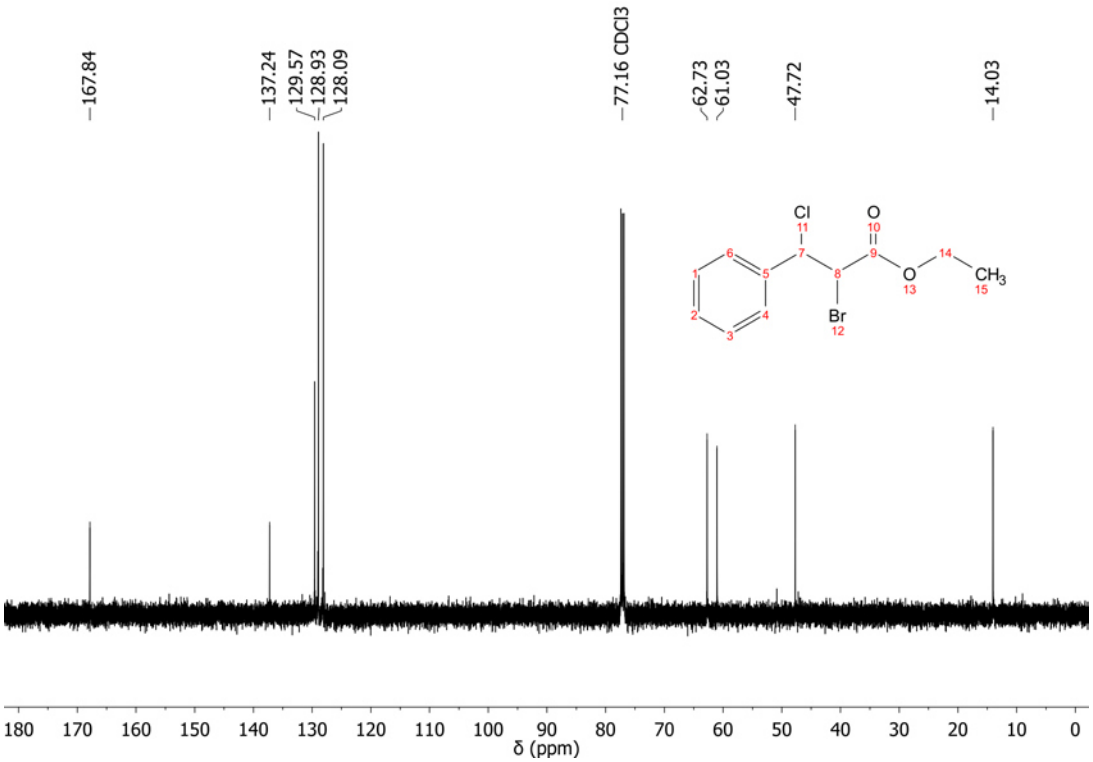

Figure S26. ^{13}C-NMR spectrum of the interhalogenation product **G**.

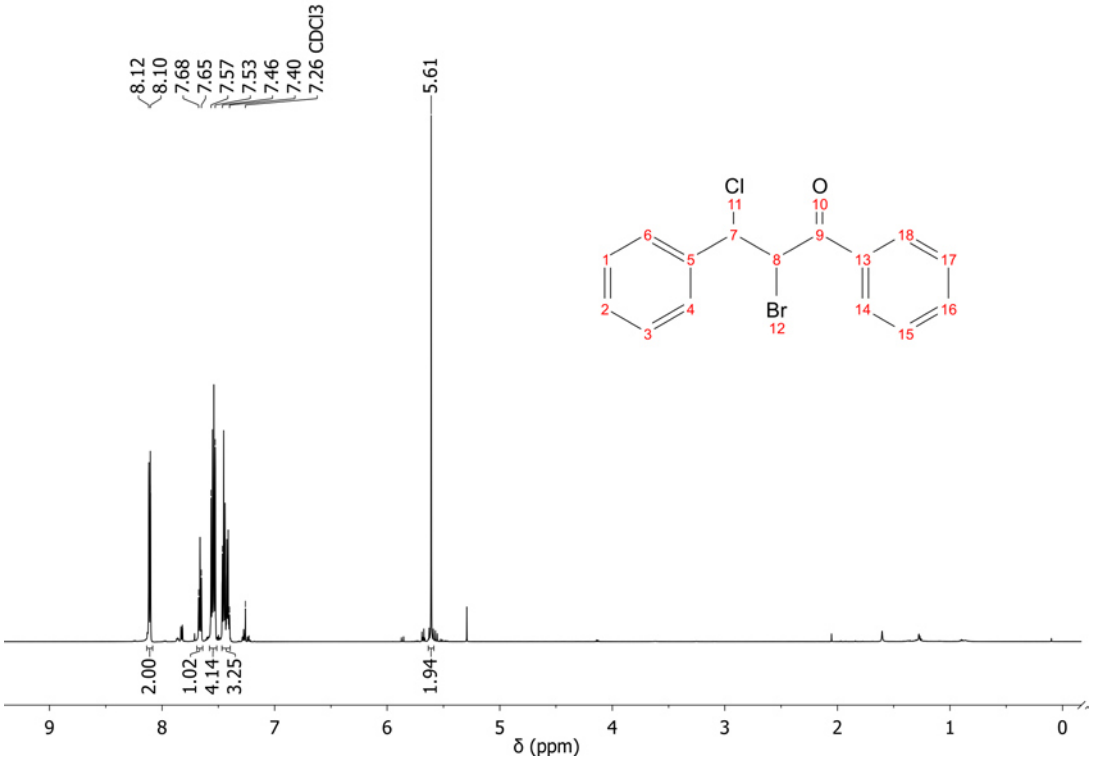

Figure S27. ^{1}H-NMR spectrum of the interhalogenation product **H**.

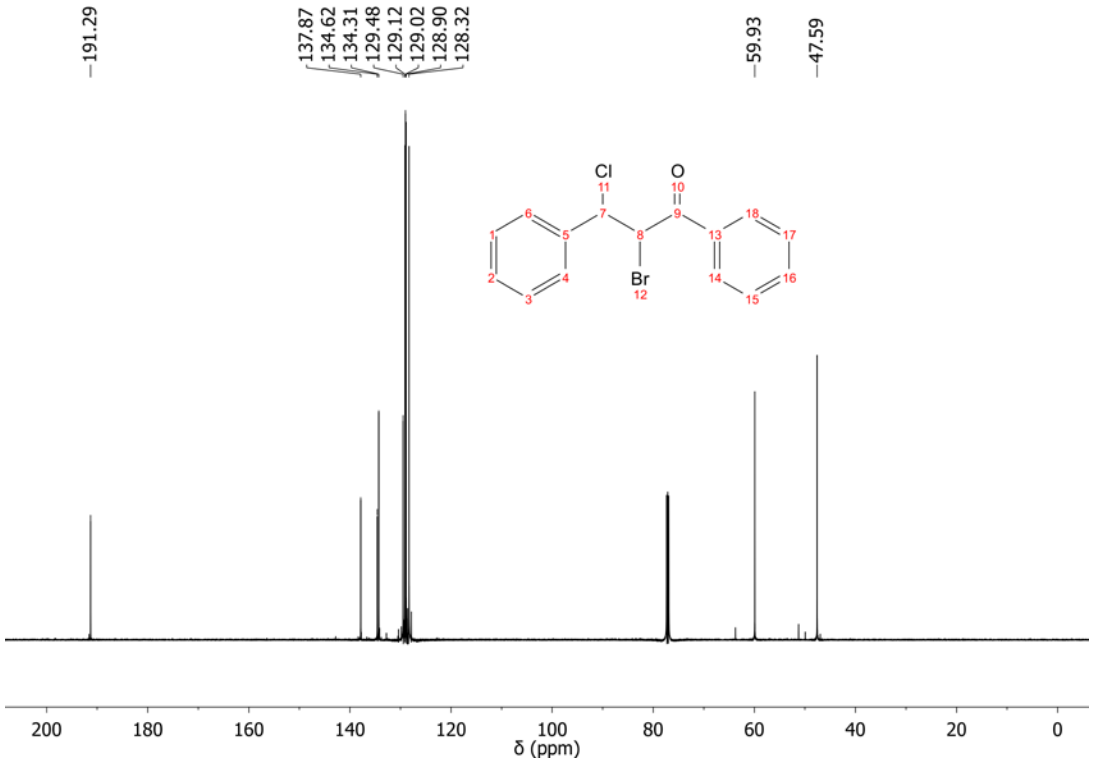

Figure S28. ^{13}C-NMR spectrum of the interhalogenation product **H**.

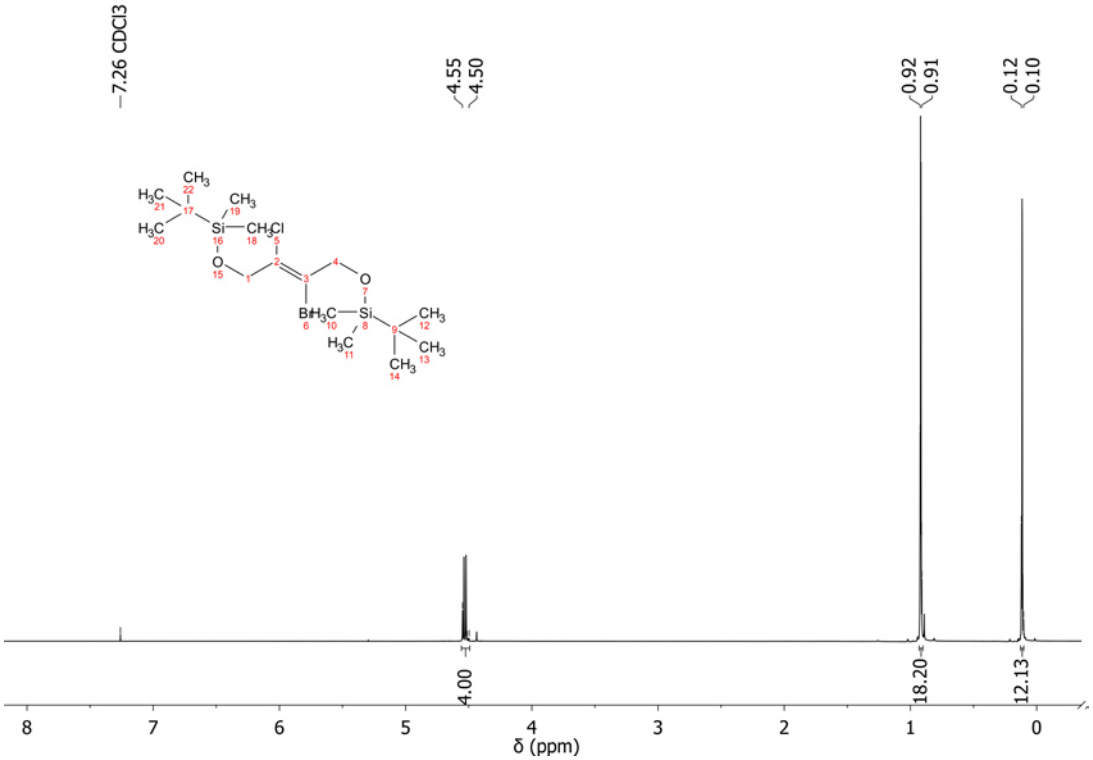

Figure S29. ^{1}H-NMR spectrum of the interhalogenation product **I**.

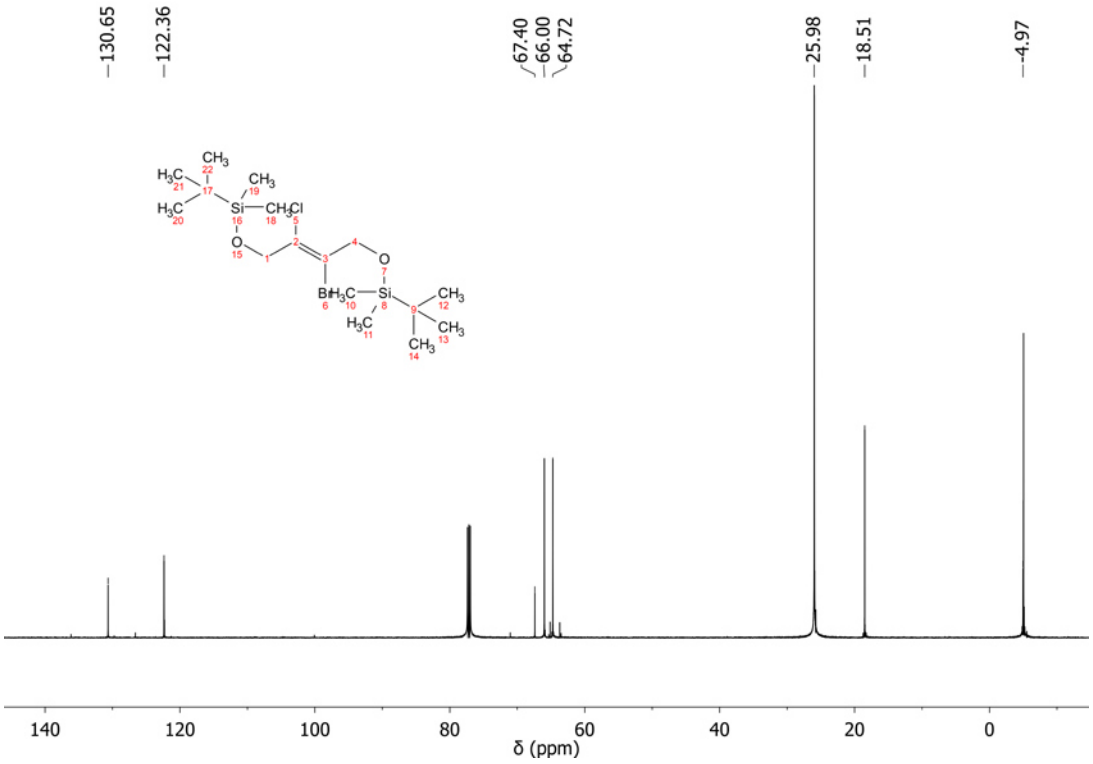

Figure S30. ^{13}C-NMR spectrum of the interhalogenation product **I**.

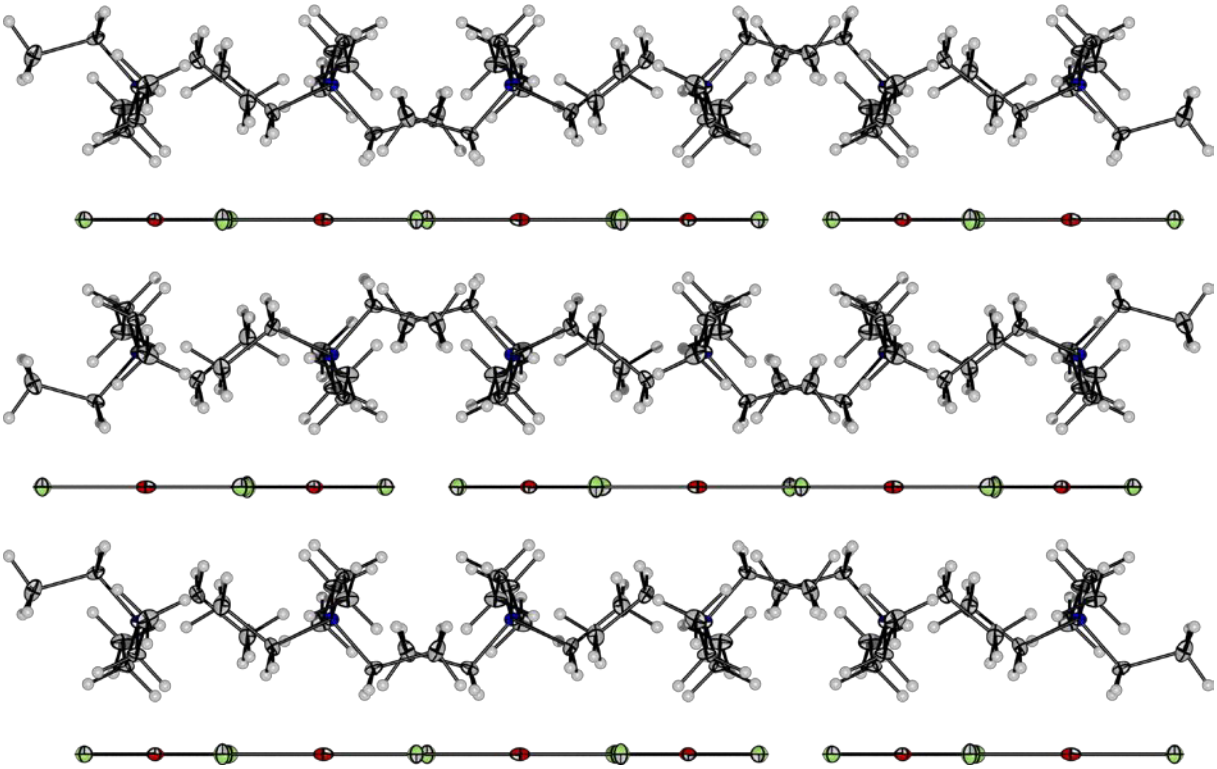

Figure S31. Crystal packing of $[NEt_4][Cl(BrCl)]$ viewing along the crystallographic *x*-axis; thermal ellipsoids are shown with 50 % probability. The anions and cations are arranged in layers. There are no significant interactions (distance shorter than the sum of the van der Waals radii) between the anions or anion and hydrogen atoms.

h. Crystal Packing / Intermolecular interactions

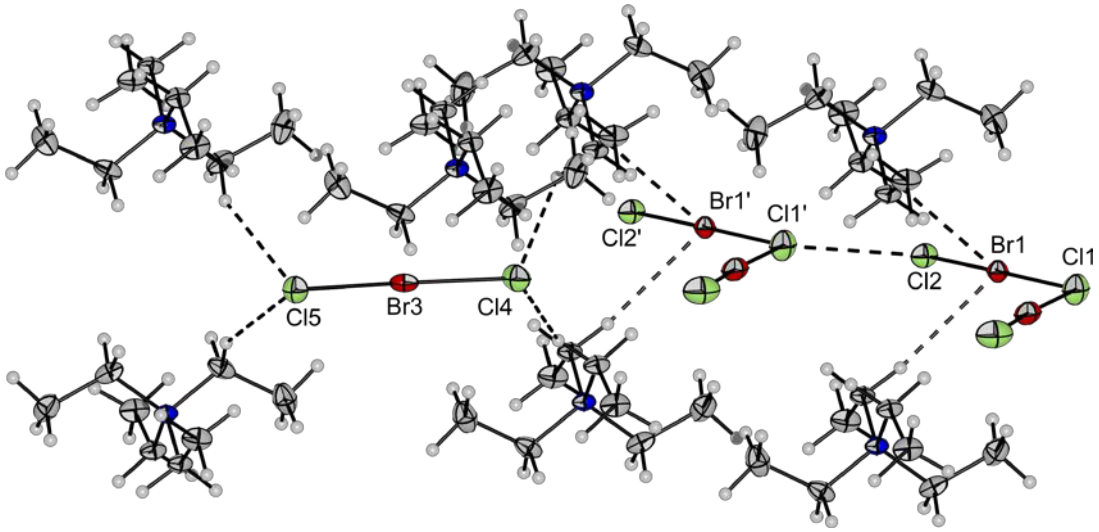

Figure S32. Crystal packing of $[NEt_4]_2[Cl(BrCl)_2][ClBrCl]$; thermal ellipsoids are shown with 50 % probability. The anions and cations are arranged in layers. There are weak hydrogen bond interactions to the anions (*d* H-Cl: 275 – 283 pm, *d* H-Br: 288 pm; depicted as dashed bonds) The $[Cl(BrCl)_2]^-$ units interact with each other, forming a chain (*d*. Cl2-Cl1' 318.1(1)).

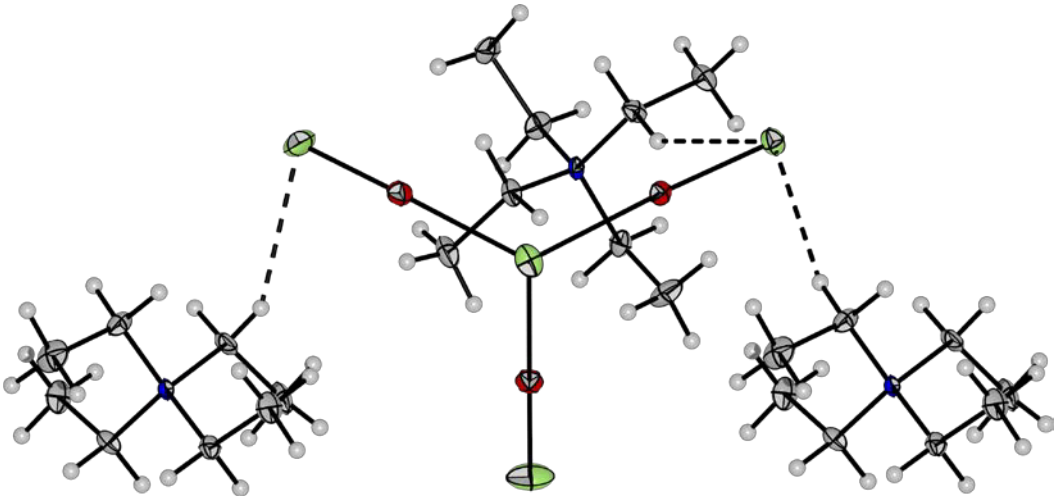

Figure S33. Hydrogen bonding between the $[Cl(BrCl)_3]^-$ anion and the surrounding $[NEt_4]^+$ cations; thermal ellipsoids are shown with 50 % probability. Three weak hydrogen bonds to the terminal chlorine atoms are observed (*d* H-Cl: 270 – 284 pm; depicted as dashed bonds). There are no interactions between the anions.

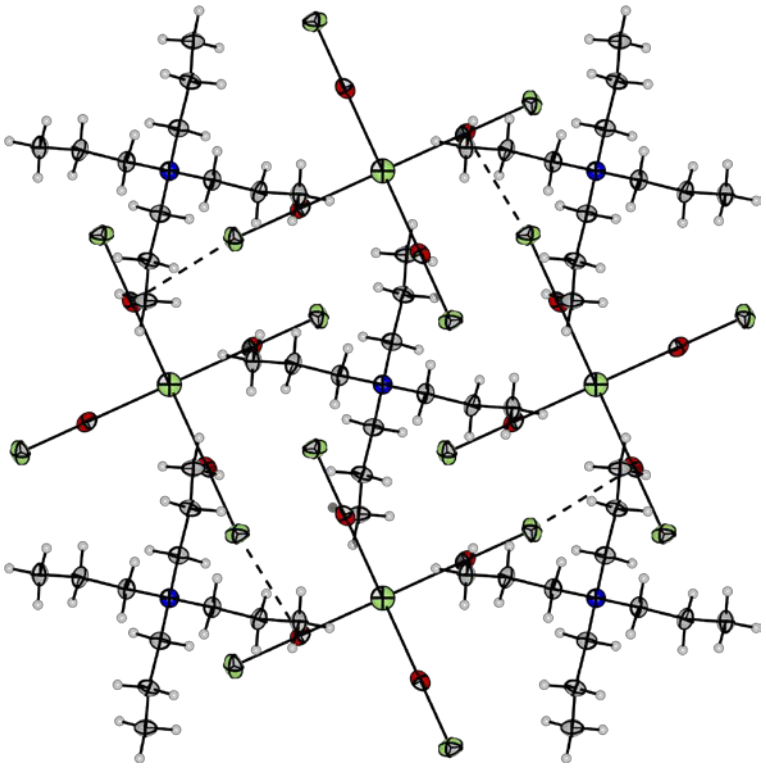

Figure S34. Crystal packing of $[NPr_4][Cl(BrCl)_4]$ viewing along the crystallographic *z*-axis; thermal ellipsoids are shown with 50 % probability. The anions and cations are arranged in columns. The intermolecular distances are depicted as dashed bonds (*d* Br-Cl: 350.8(2) pm). There are no interactions with the cations.

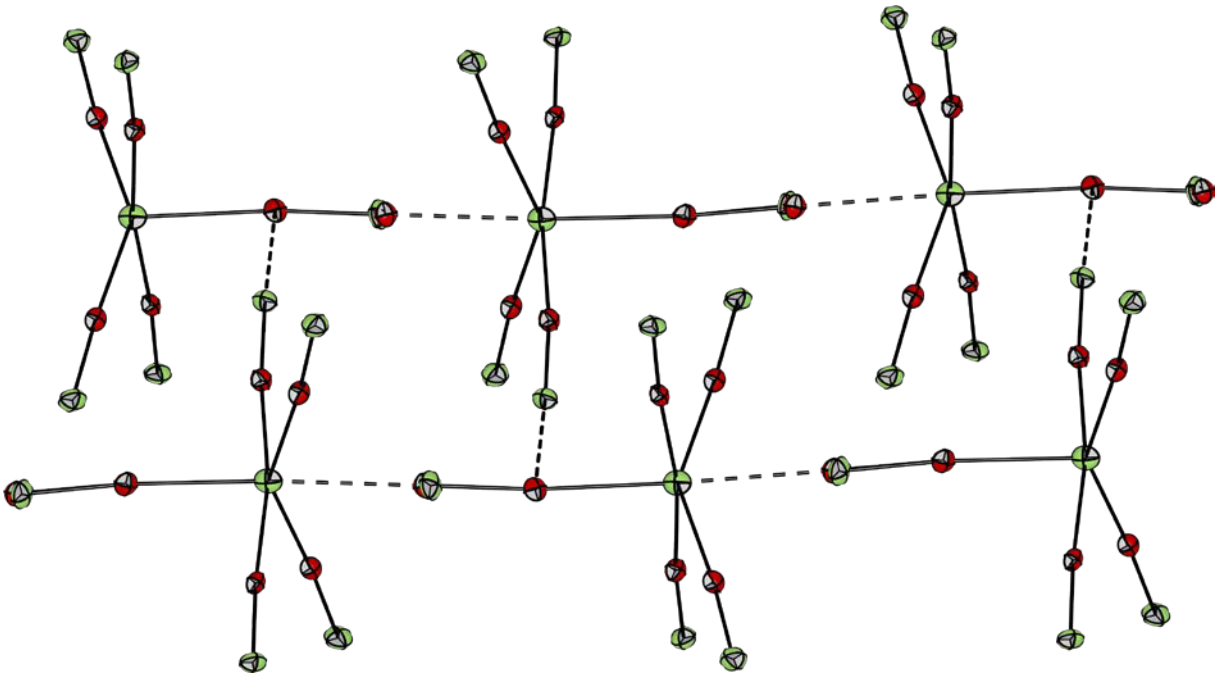

Figure S35. Anion-anion interactions of the $[Cl(BrCl)_5]^-$ units; thermal ellipsoids are shown with 50 % probability. A Br_2 molecule interacts with two central chlorides (*d* Br-Cl: 326.7(5), 298.6(2) pm) to form an infinite chain. The chains are very weakly interconnected to form an extended network (*d* Br-Cl: 336.9(1) pm). There are no interactions with the cations.

i. Long Term Stability Studies

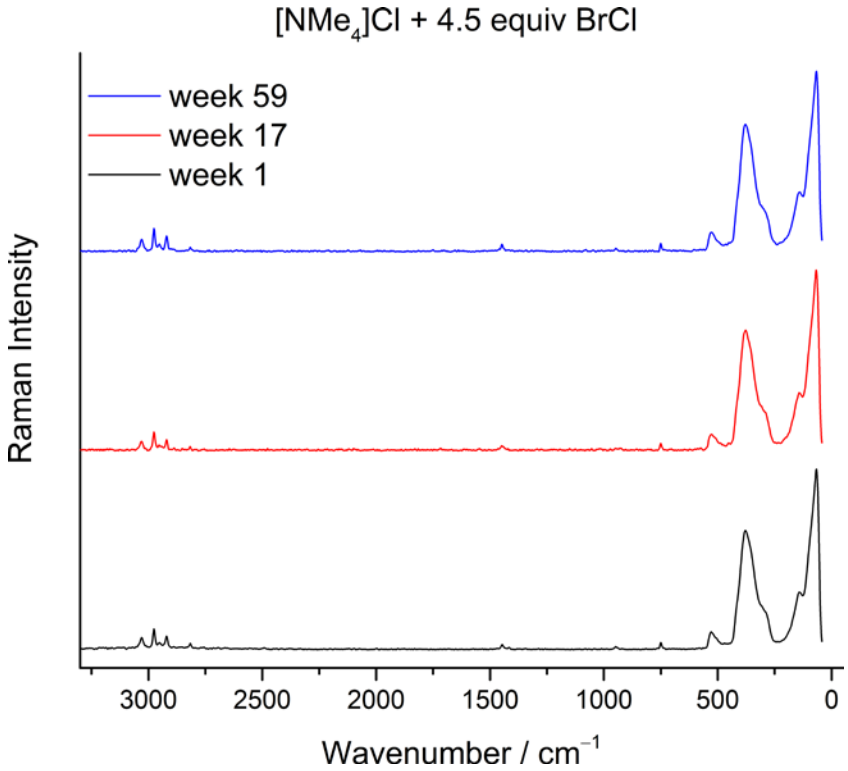

Figure S36. Long term stability studies of $[NMe_4]Cl$ and 4.5 equivalents of BrCl. After 59 weeks no new bands can be observed, which can be assigned to C-Br or C-Cl stretches. This indicates that the $[NMe_4]^+$ cation is stable against interhalogenation.

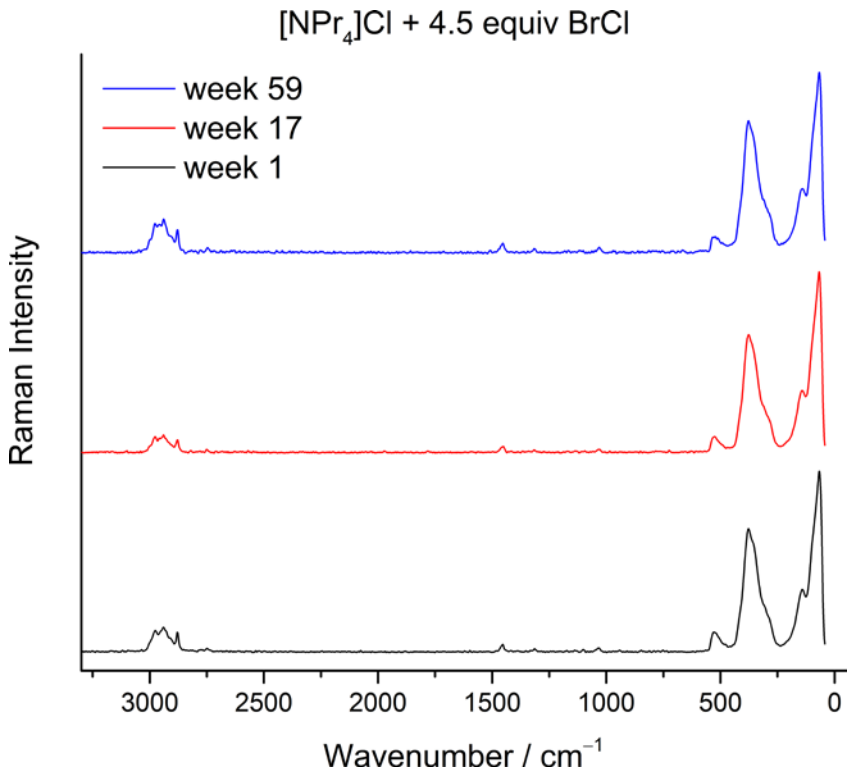

Figure S37. Long term stability studies of $[NPr_4]Cl$ and 4.5 equivalents of BrCl. After 59 weeks no new bands can be observed, which can be assigned to C-Br or C-Cl stretches. This indicates that the $[NPr_4]^+$ cation is stable against interhalogenation.

j. Computed Vibrational Frequencies

Table S5. Computed vibrational frequencies of $[Cl(BrCl)]^-$ in $D_{\infty h}$ symmetry.

B3LYP-D3(BJ)/def2-TZVPP					SCS-MP2/def2-TZVPP		
Nr.	Symmetry	Wavenumber [cm^{-1}]	IR Intensity [km mol^{-1}]	Nr.	Symmetry	Wavenumber [cm^{-1}]	IR Intensity [km mol^{-1}]
1	Π_u	117.0	3	1	Π_u	129.5	3
2	Π_u	117.0	3	2	Π_u	129.5	3
3	Σ_u^-	232.4	268	3	Σ_u^-	246.1	376
4	Σ_g^+	244.2	0	4	Σ_g^+	269.7	30

Table S6. Computed vibrational frequencies of $[Cl(BrCl)_2]^-$ in C_{2v} symmetry.

B3LYP-D3(BJ)/def2-TZVPP					SCS-MP2/def2-TZVPP		
Nr.	Symmetry	Wavenumber [cm^{-1}]	IR Intensity [km mol^{-1}]	Nr.	Symmetry	Wavenumber [cm^{-1}]	IR Intensity [km mol^{-1}]
1	A_1	20.3	0	1	A_1	18.7	0
2	B_1	95.5	4	2	B_1	99.7	24
3	A_2	98.5	0	3	A_2	107.8	0
4	A_1	105.2	1	4	A_1	109.3	2
5	B_2	120.2	2	5	B_2	131.7	3
6	A_1	187.6	25	6	B_1	167.0	502
7	B_1	190.6	346	7	A_1	193.7	48
8	B_1	283.7	165	8	B_1	313.9	142
9	A_1	305.7	50	9	A_1	335.0	63

Table S7. Computed vibrational frequencies of $[Cl(BrCl)_3]^-$ in C_{3v} symmetry.

B3LYP-D3(BJ)/def2-TZVPP					SCS-MP2/def2-TZVPP		
Nr.	Symmetry	Wavenumber [cm^{-1}]	IR Intensity [km mol^{-1}]	Nr.	Symmetry	Wavenumber [cm^{-1}]	IR Intensity [km mol^{-1}]
1	E	13.5	0	1	A_1	16.2	0
2	E	13.5	0	2	E	16.5	0
3	A_1	17.0	0	3	E	16.5	0
4	E	86.6	6	4	E	86.9	25
5	E	86.6	6	5	E	86.9	25
6	A_2	87.5	0	6	A_1	93.3	1
7	A_1	90.5	0	7	A_2	93.8	0
8	E	95.8	5	8	E	98.6	4
9	E	95.8	5	9	E	98.6	4
10	A_1	157.6	7	10	E	157.5	196
11	E	173.0	166	11	E	157.5	196
12	E	173.0	166	12	A_1	164.8	18
13	E	316.0	173	13	E	350.3	143
14	E	316.0	173	14	E	350.3	143
15	A_1	342.3	20	15	A_1	373.3	28

Table S8. Computed vibrational frequencies of $[Cl(BrCl)_4]^-$ in T_d symmetry.

B3LYP-D3(BJ)/def2-TZVPP					SCS-MP2/def2-TZVPP		
Nr.	Symmetry	Wavenumber [cm^{-1}]	IR Intensity [km mol^{-1}]	Nr.	Symmetry	Wavenumber [cm^{-1}]	IR Intensity [km mol^{-1}]
1	*E*	7.9	0	1	*E*	6.9	0
2	*E*	7.9	0	2	*E*	6.9	0
3	T_2	9.1	0	3	T_2	9.1	0
4	T_2	9.1	0	4	T_2	9.1	0
5	T_2	9.1	0	5	T_2	9.1	0
6	A_1	75.6	0	6	A_1	73.0	0
7	T_2	78.7	10	7	T_2	78.5	16
8	T_2	78.7	10	8	T_2	78.5	16
9	T_2	78.7	10	9	T_2	78.5	16
10	T_1	80.2	0	10	T_1	85.9	0
11	T_1	80.2	0	11	T_1	85.9	0
12	T_1	80.2	0	12	T_1	85.9	0
13	*E*	90.5	0	13	*E*	93.0	0
14	*E*	90.5	0	14	*E*	93.0	0
15	T_2	170.8	104	15	T_2	163.9	122
16	T_2	170.8	104	16	T_2	163.9	122
17	T_2	170.8	104	17	T_2	163.9	122
18	T_2	338.0	155	18	T_2	374.1	124
19	T_2	338.0	155	19	T_2	374.1	124
20	T_2	338.0	155	20	T_2	374.1	124
21	A_1	363.1	0	21	A_1	393.8	0

Table S9. Computed vibrational frequencies of $[Cl(BrCl)_5]^-$ in D_{3h} symmetry.

B3LYP-D3(BJ)/def2-TZVPP					SCS-MP2/def2-TZVPP		
Nr.	Symmetry	Wavenumber [cm^{-1}]	IR Intensity [km mol^{-1}]	Nr.	Symmetry	Wavenumber [cm^{-1}]	IR Intensity [km mol^{-1}]
1	*E'*	6.2	0	1	*E'*	14.6	0
2	*E'*	6.2	0	2	*E'*	14.6	0
3	*E'*	16.1	0	3	*E''*	15.5	0
4	*E'*	16.1	0	4	*E''*	15.5	0
5	*E''*	18.4	0	5	A_2''	22.5	0
6	*E''*	18.4	0	6	*E'*	25.5	0
7	A_2''	19.1	0	7	*E'*	25.5	0
8	A_1'	52.0	0	8	A_1'	51.0	0
9	*E'*	67.0	1	9	A_1'	68.9	0
10	*E'*	67.0	1	10	*E'*	76.1	9
11	*E''*	67.5	0	11	*E'*	76.1	9
12	*E''*	67.5	0	12	*E''*	81.7	0
13	A_1'	70.6	0	13	*E''*	81.7	0

14	A_2''	75.1	7	14	E'	82.5	0
15	E'	75.7	9	15	E'	82.5	2
16	E'	75.7	9	16	E'	82.5	2
17	A_2'	75.9	0	17	A_2'	83.3	10
18	E''	81.9	0	18	E''	92.1	0
19	E''	81.9	0	19	E''	92.1	0
20	A_2''	139.0	153	20	A_2''	150.5	153
21	E'	157.4	100	21	E'	155.6	105
22	E'	157.4	100	22	E'	155.6	105
23	E'	353.7	142	23	E'	390.3	104
24	E'	353.7	142	24	E'	390.3	104
25	A_1'	359.7	0	25	A_1'	394.0	0
26	A_2''	368.6	152	26	A_2''	399.4	115
27	A_1'	383.9	0	27	A_1'	411.2	0

Table S10. Computed vibrational frequencies of $[Cl(BrCl)_6]^-$ in O_h symmetry.

B3LYP-D3(BJ)/def2-TZVPP					SCS-MP2/def2-TZVPP		
Nr.	Symmetry	Wavenumber [cm^{-1}]	IR Intensity [km mol^{-1}]	Nr.	Symmetry	Wavenumber [cm^{-1}]	IR Intensity [km mol^{-1}]
1	T_{2u}	11.1	0	1	T_{2u}	15.3	0
2	T_{2u}	11.1	0	2	T_{2u}	15.3	0
3	T_{2u}	11.1	0	3	T_{2u}	15.3	0
4	T_{2g}	17.0	0	4	T_{2g}	20.6	0
5	T_{2g}	17.0	0	5	T_{2g}	20.6	0
6	T_{2g}	17.0	0	6	T_{2g}	20.6	0
7	T_{1u}	17.1	0	7	T_{1u}	27.4	0
8	T_{1u}	17.1	0	8	T_{1u}	27.4	0
9	T_{1u}	17.1	0	9	T_{1u}	27.4	0
10	E_g	51.8	0	10	E_g	53.3	0
11	E_g	51.8	0	11	E_g	53.3	0
12	T_{1g}	64.0	0	12	A_{1g}	67.5	0
13	T_{1g}	64.0	0	13	T_{1u}	77.3	5
14	T_{1g}	64.0	0	14	T_{1u}	77.3	5
15	T_{2u}	64.7	0	15	T_{1u}	77.3	5
16	T_{2u}	64.7	0	16	T_{1g}	79.2	0
17	T_{2u}	64.7	0	17	T_{1g}	79.2	0
18	T_{1u}	66.6	3	18	T_{1g}	79.2	0
19	T_{1u}	66.6	3	19	T_{2u}	80.2	0
20	T_{1u}	66.6	3	20	T_{2u}	80.2	0
21	A_{1g}	67.4	0	21	T_{2u}	80.2	0
22	T_{2g}	73.7	0	22	T_{2g}	86.3	0
23	T_{2g}	73.7	0	23	T_{2g}	86.3	0
24	T_{2g}	73.7	0	24	T_{2g}	86.3	0

25	T_{1u}	137.6	136	25	T_{1u}	151.6	125
26	T_{1u}	137.6	136	26	T_{1u}	151.6	125
27	T_{1u}	137.6	136	27	T_{1u}	151.6	125
28	T_{1u}	373.0	135	28	T_{1u}	405.6	95
29	T_{1u}	373.0	135	29	T_{1u}	405.6	95
30	T_{1u}	373.0	135	30	T_{1u}	405.6	95
31	E_g	373.3	0	31	E_g	405.8	0
32	E_g	373.3	0	32	E_g	405.8	0
33	A_{1g}	393.1	0	33	A_{1g}	419.7	0

k. Additional Information

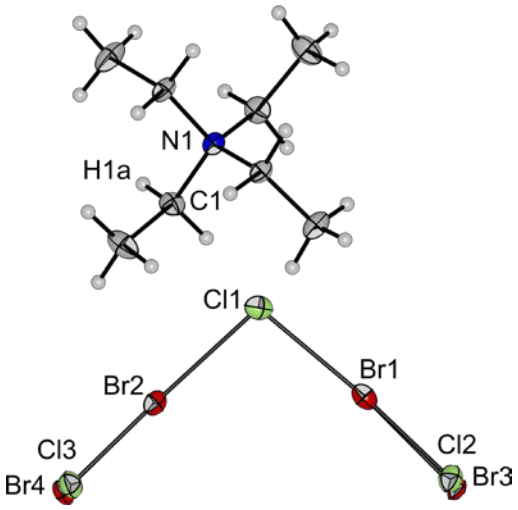

Figure S38. Molecular structure of $[NEt_4][Cl(BrCl)_2]$ in the solid state with thermal ellipsoids set at 50 % probability. Selected bond lengths [pm] and angles [°]: Cl1-Br1 259.6(1), Cl1-Br2 265.5(1), Br1-Cl2 224.4(3), Br2-Cl3 220.7(4), Br1-Br3 247.0(9), Br2-Br4 241.1(7); Cl1-Br1-Cl2 175.0(2), Cl1-Br2-Cl3 176.1(2), Br2-Cl1-Br1 97.1(1); population of the disorders: Cl2: 88%, Br3: 12 %, Cl3: 81 %, Br4: 19 %.

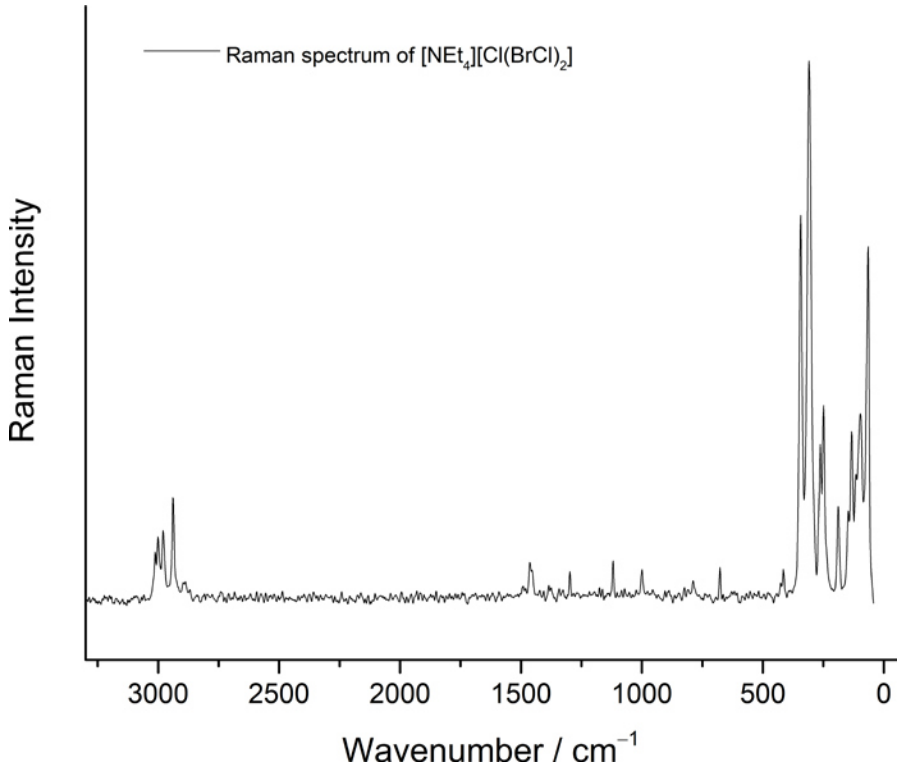

Figure S39. Raman spectrum of a single crystal of $[NEt_4][Cl(BrCl)_2]$, taken at low temperature (–196 °C).

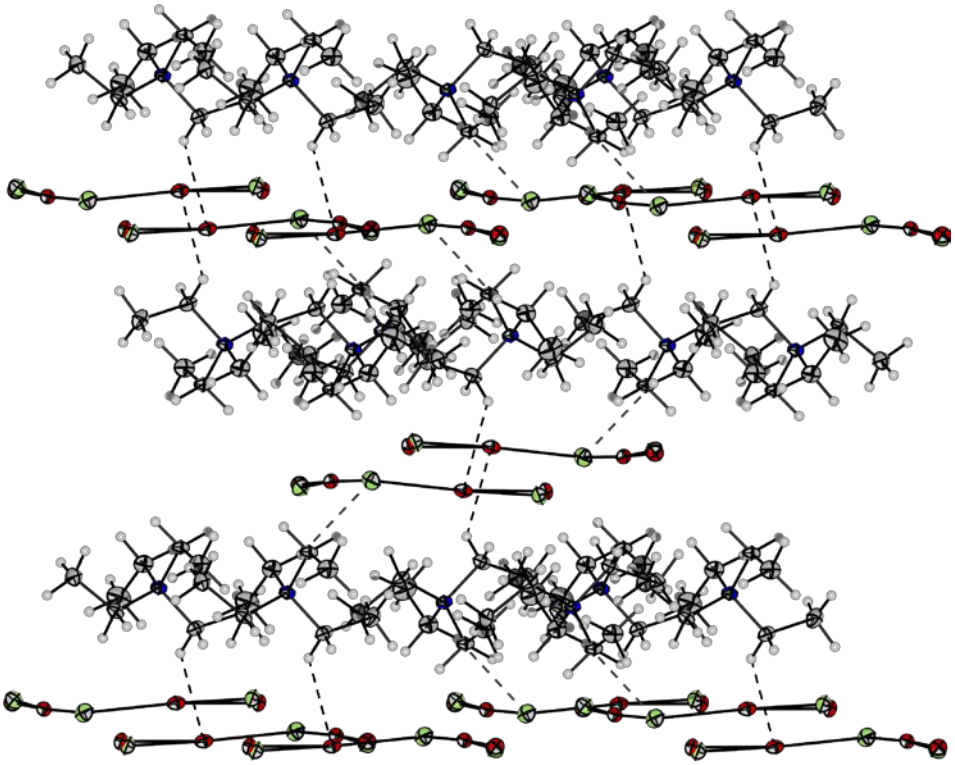

Figure S40. Crystal packing of $[NEt_4][Cl(BrCl)_2]$; thermal ellipsoids are shown with 50 % probability. The anions and cations are arranged in layers. There are very weak hydrogen bond interactions to the anions (*d* H-Cl: 279 pm, *d* H-Br: 286 pm; depicted as dashed bonds) Anion-anion interactions are depicted in Figure S41.

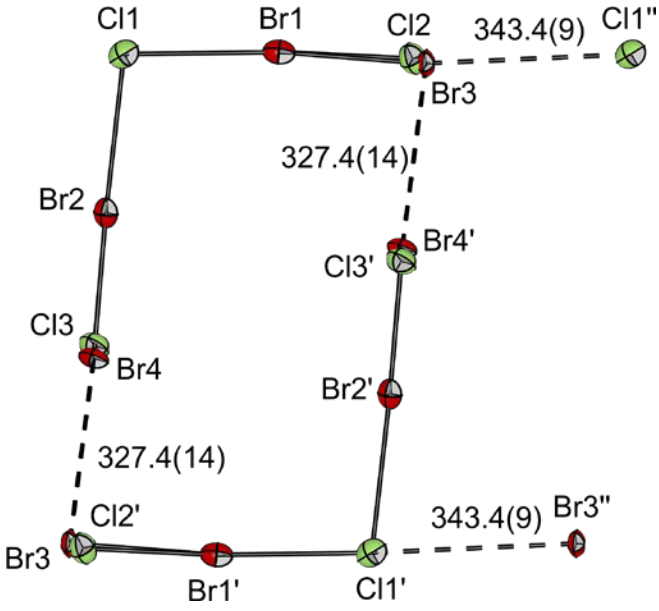

Figure S41. Anion-anion interactions of the $[Cl(BrCl)_2]^-$ units viewing along the crystallographic *y*-axis; thermal ellipsoids are shown with 50 % probability. Two pentahalide anions form a rectangle and are connected via the bromine atoms (*d* Br3-Br4: 327.4(14) pm). The connections between Br and Cl are less pronounced (*d* Cl2-Br4': 334.0(8) pm, *d* Cl3-Br3' 350.3(12)). The rectangles are interconnected via the Cl1'-Br3''' interaction (343.4(9) pm).

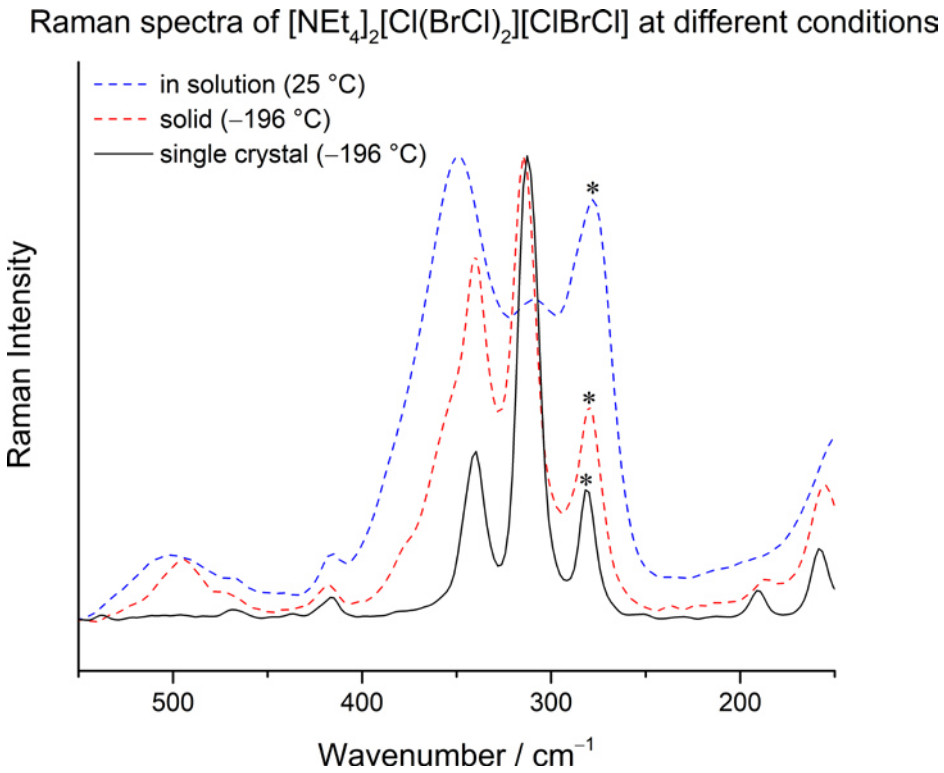

Figure S42. Raman spectra of $[NEt_4]_2[Cl(BrCl)_2][ClBrCl]$ at different conditions. The spectra were taken in a DCM solution at 25 °C, as solid (–196 °C) and as single crystal Raman scope spectrum (–196 °C). Gas phase calculations show that the symmetric stretching mode (A_1) of the coordinating BrCl molecules has a higher Raman intensity (see Figure 6) than the asymmetric stretch (B_1). In solution, these intensities are in agreement with the calculations. However, spectra of the solid state show, that the intensities change, resulting in a higher intensity for the asymmetric stretching mode. This can be explained by interactions in the solid state. The band at 281 cm^{-1} associated with $[ClBrCl]^-$ is indicated by asterisks.

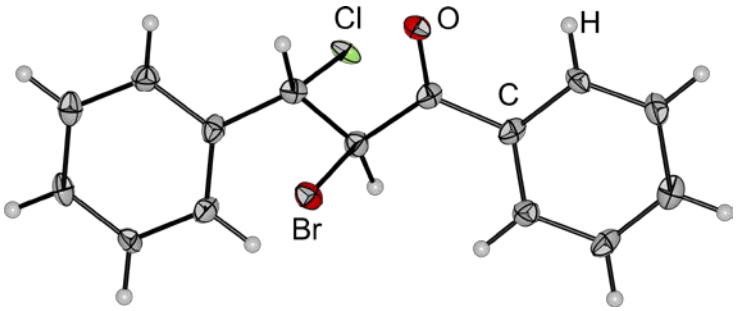

Figure S43. Solid state structure of the product **H** after interhalogenation with the BrCl based reactive ionic liquid; thermal ellipsoids are shown with 50 % probability. The halogens are arranged trans to each other.

I. xyz-Files of the Calculated Molecules

$[Cl(BrCl)]^-$

B3LYP-D3(BJ)/def2-TZVPP:

0.00000000000000	0.00000000000000	-4.65478608806984	cl
0.00000000000000	0.00000000000000	-0.00000000000000	br
0.00000000000000	0.00000000000000	4.65478608806984	cl

E_{tot} = -3494.476772972 H, *ZPE* = 4.214 kJ/mol, *H* = 19.25 kJ/mol, μ = -66.39 kJ/mol

SCS-MP2/def2-TZVPP:

0.00000000000000	0.00000000000000	-4.56717617284753	cl
0.00000000000000	0.00000000000000	0.00000000000000	br
0.00000000000000	0.00000000000000	4.56717617284753	cl

$E_{(SCF)}$ = -3491.495333171 H, $E_{(MP2)}$ = -1.026591420411 H, *ZPE* = 4.634 kJ/mol

H = 19.38 kJ/mol, μ = -65.25 kJ/mol

$[Cl(BrCl)_2]^-$

B3LYP-D3(BJ)/def2-TZVPP:

0.00000000000000	0.00000000000000	-3.21138772166569	cl
-4.03201490368139	0.00000000000000	-0.40108236354168	br
4.03201490368139	0.00000000000000	-0.40108236354168	br
7.71939332291606	0.00000000000000	2.00671238810105	cl
-7.71939332291606	0.00000000000000	2.00671238810105	cl

E_{tot} = -6528.696640102 H, *ZPE* = 8.345 kJ/mol, *H* = 33.57 kJ/mol, μ = -92.22 kJ/mol

SCS-MP2/def2-TZVPP:

0.00000000000000	0.00000000000000	-3.34336507817772	cl
-3.91977218528769	0.00000000000000	-0.41982630251125	br
3.91977218528769	0.00000000000000	-0.41982630251125	br
7.41698127141964	0.00000000000000	2.09144500532661	cl
-7.41698127141964	0.00000000000000	2.09144500532661	cl

$E_{(SCF)}$ = -6523.408663161 H, $E_{(MP2)}$ = -1.700585487184 H, *ZPE* = 8.851 kJ/mol

H = 33.76 kJ/mol, μ = -91.16 kJ/mol

$[Cl(BrCl)_3]^-$

B3LYP-D3(BJ)/def2-TZVPP:

-0.00000000000000	0.00000000000000	-2.38862142703802	cl
-2.34937161747260	4.06923100732284	-0.39846634525948	br
-2.34937161747260	-4.06923100732284	-0.39846634525948	br
4.69874323494525	0.00000000000000	-0.39846634525948	br
8.68845360089481	0.00000000000000	1.20131512417996	cl
-4.34422680044738	7.52442153797727	1.20131512417996	cl
-4.34422680044738	-7.52442153797727	1.20131512417996	cl

E_{tot} = -9562.906293914 H, *ZPE* = 12.24 kJ/mol, *H* = 49.17 kJ/mol, μ = -115.05 kJ/mol

SCS-MP2/def2-TZVPP:

-0.00000000000000	0.00000000000000	-2.71886913342799	cl
-2.29119276264963	3.96846227484326	-0.45817098245949	br
-2.29119276264963	-3.96846227484326	-0.45817098245949	br
4.58238552529929	0.00000000000000	-0.45817098245949	br
8.37584103748935	0.00000000000000	1.37110233017664	cl
-4.18792051874466	7.25369111652598	1.37110233017664	cl
-4.18792051874466	-7.25369111652598	1.37110233017664	cl

$E_{(SCF)}$ = -9555.321018629 H, $E_{(MP2)}$ = -2.369837219305 H, *ZPE* = 12.93 kJ/mol

H = 49.48 kJ/mol, μ = -112.71 kJ/mol

$[Cl(BrCl)_4]^-$

B3LYP-D3(BJ)/def2-TZVPP:

-0.00000000000000	0.00000000000000	-0.00000000000000	cl
-3.01884831384178	-3.01884831384178	3.01884831384178	br
3.01884831384178	-3.01884831384178	-3.01884831384178	br
-3.01884831384178	3.01884831384178	-3.01884831384178	br
3.01884831384178	3.01884831384178	3.01884831384178	br
-5.46944696218501	-5.46944696218501	5.46944696218501	cl
5.46944696218501	5.46944696218501	5.46944696218501	cl
-5.46944696218501	5.46944696218501	-5.46944696218501	cl
5.46944696218501	-5.46944696218501	-5.46944696218501	cl

E_{tot} = -12597.11120670 H, *ZPE* = 15.81 kJ/mol, *H* = 64.82 kJ/mol, μ = -140.55 kJ/mol

SCS-MP2/def2-TZVPP:

-0.00000000000000	0.00000000000000	0.00000000000000	cl
-3.03262051540363	-3.03262051540363	3.03262051540363	br
3.03262051540363	-3.03262051540363	-3.03262051540363	br
-3.03262051540363	3.03262051540363	-3.03262051540363	br
3.03262051540363	3.03262051540363	3.03262051540363	br
-5.43875660644968	-5.43875660644968	5.43875660644968	cl
5.43875660644968	5.43875660644968	5.43875660644968	cl
-5.43875660644968	5.43875660644968	-5.43875660644968	cl
5.43875660644968	-5.43875660644968	-5.43875660644968	cl

$E_{(SCF)}$ = -12587.23284961 H, $E_{(MP2)}$ = -3.036569955557 H, *ZPE* = 16.76 kJ/mol

H = 65.28 kJ/mol, μ = -139.27 kJ/mol

$[Cl(BrCl)_5]^-$

B3LYP-D3(BJ)/def2-TZVPP:

-0.00000000000000	0.00000000000000	-0.00000000000000	cl
-2.67580366236152	-4.63462789428903	0.00000000000000	br
-2.67580366236152	4.63462789428903	0.00000000000000	br
5.35160732472303	0.00000000000000	0.00000000000000	br
0.00000000000000	0.00000000000000	5.48805052183008	br
0.00000000000000	0.00000000000000	-5.48805052183008	br
9.56402041542057	0.00000000000000	0.00000000000000	cl
-4.78201020771027	-8.28268464206720	0.00000000000000	cl
-4.78201020771027	8.28268464206720	0.00000000000000	cl
0.00000000000000	0.00000000000000	9.67207751604432	cl
0.00000000000000	0.00000000000000	-9.67207751604432	cl

E_{tot} = -15631.31125760 H, *ZPE* = 19.16 kJ/mol, *H* = 80.46 kJ/mol, μ = -162.28 kJ/mol

SCS-MP2/def2-TZVPP:

0.00000000000000	0.00000000000000	0.00000000000000	cl
-2.68812454489377	-4.65596828882895	0.00000000000000	br
-2.68812454489377	4.65596828882895	0.00000000000000	br
5.37624908978751	0.00000000000000	0.00000000000000	br
0.00000000000000	0.00000000000000	5.45552697524794	br
0.00000000000000	0.00000000000000	-5.45552697524794	br
9.51781151670752	0.00000000000000	0.00000000000000	cl
-4.75890575835375	-8.24266656190080	0.00000000000000	cl
-4.75890575835375	8.24266656190080	0.00000000000000	cl
0.00000000000000	0.00000000000000	9.58271041987689	cl
0.00000000000000	0.00000000000000	-9.58271041987689	cl

$E_{(SCF)}$ = -15619.13933117 H, $E_{(MP2)}$ = -3.706321438418 H, *ZPE* = 21.12 kJ/mol

H = 81.14 kJ/mol, μ = -151.05 kJ/mol

$[Cl(BrCl)_6]^-$

B3LYP-D3(BJ)/def2-TZVPP:

-0.00000000000000	-0.00000000000000	0.00000000000000	cl
5.51151017729707	0.00000000000000	-0.00000000000000	br
-0.00000000000000	-0.00000000000000	-5.51151017729707	br
0.00000000000000	-5.51151017729707	0.00000000000000	br
0.00000000000000	0.00000000000000	5.51151017729707	br
-5.51151017729707	-0.00000000000000	0.00000000000000	br
-0.00000000000000	5.51151017729707	0.00000000000000	br
-0.00000000000000	9.68747412917864	0.00000000000000	cl
9.68747412917864	0.00000000000000	-0.00000000000000	cl
0.00000000000000	-0.00000000000000	-9.68747412917864	cl
-0.00000000000000	0.00000000000000	9.68747412917864	cl
-9.68747412917864	-0.00000000000000	0.00000000000000	cl
0.00000000000000	-9.68747412917864	-0.00000000000000	cl

E_{tot} = -18665.51215904 H, *ZPE* = 22.44 kJ/mol, *H* = 96.12 kJ/mol, μ = -181.05 kJ/mol

SCS-MP2/def2-TZVPP:

-0.00000000000000	-0.00000000000000	-0.00000000000000	cl
5.49514970038369	0.00000000000000	0.00000000000000	br
0.00000000000000	-0.00000000000000	-5.49514970038369	br
0.00000000000000	-5.49514970038369	-0.00000000000000	br
-0.00000000000000	0.00000000000000	5.49514970038369	br
-5.49514970038369	-0.00000000000000	-0.00000000000000	br
-0.00000000000000	5.49514970038369	0.00000000000000	br
-0.00000000000000	9.61346003715582	0.00000000000000	cl
9.61346003715582	0.00000000000000	-0.00000000000000	cl
0.00000000000000	-0.00000000000000	-9.61346003715582	cl
-0.00000000000000	0.00000000000000	9.61346003715582	cl
-9.61346003715582	-0.00000000000000	0.00000000000000	cl
0.00000000000000	-9.61346003715582	0.00000000000000	cl

$E_{(SCF)}$ = -18651.04434211 H, $E_{(MP2)}$ = -4.378111120132 H, *ZPE* = 25.33 kJ/mol

H = 97.01 kJ/mol, μ = -165.00 kJ/mol

5.5. Experimental Part

All reactions were carried out in standard glass apparatus. If necessary, work was carried out using *Schlenk* technique and inert gas atmosphere (argon). All chemicals were used without further purification unless otherwise noted. The solvents used for column chromatography were obtained from technical grade solvents by distillation under reduced pressure at 40 °C water bath temperature. IKA RV 10 and Heidolph Hei-Vap Advantage rotary evaporators were used for this purpose. All other solvents were used analytically pure and without further purification. Qualitative reaction control was carried out with the aid of silica gel-coated aluminum plates of the type Kieselgel 60 F254 from Merck. Subsequent indication was performed by irradiation under UV light (254 nm and 366 nm) and treatment with various staining reagents based on potassium permanganate, anisaldehyde or ninhydrin. The stationary phase of the column chromatography was silica gel with a pore size between 40 and 63 µm from Macherey-Nagel. The mobile phase consisted of solvent mixtures of distillatively purified *n*-pentane, ethyl acetate, diethyl ether, methanol, and dichloromethane. Melting points were measured on a Stuart SMP-30 instrument. All melting points in this work correspond to the uncorrected values. To measure the optical rotation value of chiral compounds, a polarimeter of the Jasco P-2000 type was used. ^{1}H and ^{13}C NMR spectra were recorded on a JEOL ECX 400 (400 MHz), JEOL ECP 500 (500 MHz), Bruker Avance 500 (500 MHz), JEOL ECZ600 S (600 MHz) and Bruker Avance 700 (700 MHz) spectrometers. Chemical shifts (δ) were expressed in parts per million (ppm) relative to tetramethylsilane. The internal standard is the respective deuterated solvent. Coupling constants (*J*) were given in Hertz (Hz). All IR spectra were recorded using a JASCO FT/IR-4100 spectrometer. Samples were measured in liquid or solid state and characteristic bands are reported as wavenumbers ($\tilde{\nu}$) in reciprocal cm. High-resolution mass spectrometry (HRMS) was performed on an Agilent 6210 ESI-TOF instrument from Agilent Technologies. For the determination of the enantiomeric excess (ee), a system consisting of a GC oven type 6850 Network GC System and an autosampler type 7683B Series Injector from Agilent Technologies were used. Detection of the compounds were performed using a flame ionization detector. Enantiomeric excesses (ee) were also determined using chiral HPLC methods. The Agilent Technologies 1200 Series system with DAD detector were used for this purpose.

5.5.1. Triazoles

(2*R*,4*R*)-2,4-Dichloropentane-1,5-diol (ent-57) ("classic" conditions)

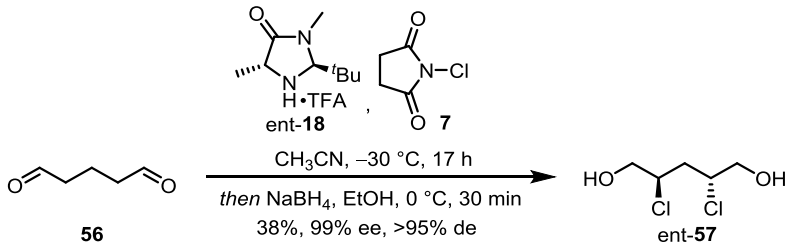

Catalyst ent-**18** (573 mg, 2.00 mmol, 40 mol%) and NCS (1.47 g, 11.0 mmol, 2.2 equiv.) were added at –30 °C to a solution of pentanedial **56** (500 mg, 4.99 mmol, 1.0 equiv.) and CH_3CN (35 mL) and stirred for 17 h at –30 °C. EtOH (35 ml) and $NaBH_4$ (944 mg, 25.0 mmol, 5.0 equiv.) were added subsequently to the reaction mixture and stirring was continued for 30 min at 0 °C. Saturated aqueous NH_4Cl solution (70 mL) was added to the reaction, the aqueous phase was extracted with Et_2O (4x100 mL), the combined organic phases were dried over Na_2SO_4, and the solvent was removed under reduced pressure. After purification by column chromatography (SiO_2, *n*-pentane/EtOAc 3:1 to 1:1) diol ent-**57** (328 mg, 1.90 mmol, 38%, >99% ee, >99% de) was obtained as a colorless solid. The absolute stereoconfiguration was determined by single crystal structure analysis.

^{1}H NMR (CD_3CN, 400 MHz): δ = 4.23 (dq, *J* = 8.0, 5.5 Hz, 2H), 3.74 – 3.63 (m, 4H), 3.21 (t, *J* = 6.3 Hz, 2H), 2.09 (dd, *J* = 8.0, 5.6 Hz, 2H) ppm.

^{13}C NMR ($CDCl_3$, 126 MHz): δ = 67.1, 62.2, 39.8 ppm.

IR (ATR): $\tilde{\nu}$ = 3551, 2262, 1193, 1037, 832 cm^{-1}.

HRMS (ESI, pos. mode): *m*/*z* calculated for $C_5H_{10}Cl_2NaO_2$ $[M+Na]^+$: 194.9950, found 194.9947.

(2*S*,4*S*)-2,4-Dichloropentane-1,5-diol (57) (modified conditions)

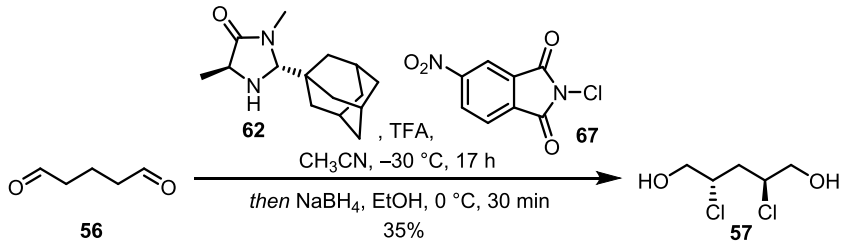

Catalyst **62** (248 mg, 998 µmol, 20 mol%), TFA (76.9 µL, 998 µmol, 20 mol%), and NO_2NCP (2.49 g, 11.0 mmol, 2.2 equiv.) were added at –30 °C to a solution of pentanedial **56** (500 mg, 4.99 mmol, 1.0 equiv.) and CH_3CN (35 ml) and stirred for 17 h at –30 °C. EtOH (35 mL) and $NaBH_4$ (944 mg, 25.0 mmol, 5.0 equiv.) were added and the reaction mixture was stirred for 30 min at 0 °C. Saturated aqueous NH_4Cl solution (70 mL) was added to the reaction, the aqueous phase was extracted with Et_2O (4x100 mL), the combined organic phases were dried over Na_2SO_4, and the solvent was removed under reduced pressure. After purification by column chromatography (SiO_2, *n*-pentane/EtOAc 3:1 to 1:1) diol **57** (298 mg, 1.72 mmol, 35%) was obtained as a pale yellow solid.

The spectroscopic data are in accordance with the previous experiment.

(2*R*,4*R*)-1,5-Diazidopentane-2,4-diol (58)

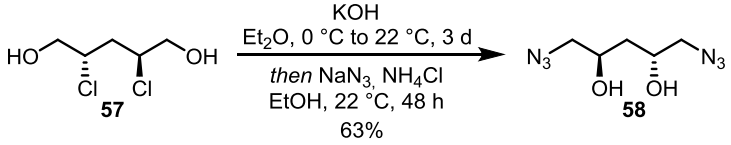

KOH (642 mg, 11.4 mmol, 6.6 equiv.) was added to a 0 °C cold solution of chlorohydrin **57** (300 mg, 1.73 mmol, 1.0 equiv.) and Et_2O (14 mL) and stirred for 3 days at 22 °C. The reaction mixture was filtered over a short plug of $MgSO_4$ and the solvent was removed under reduced pressure (950 mbar, 40 °C). The crude product was dissolved in EtOH (18 mL), NaN_3 (1.12 g, 17.3 mmol, 10.0 equiv.) and NH_4Cl (906 mg, 16.9 mmol, 9.8 equiv.) were added and stirring was continued for 48 h at 22 °C. The reaction mixture was diluted with EtOAc (10 mL) and the precipitated solid was filtered off. The solvent was removed under reduced pressure and EtOAc (20 mL) and H_2O (20 mL) were added to the crude product. The aqueous phase was extracted with EtOAc (3x20 mL), dried over Na_2SO_4, and the solvent was removed under reduced pressure. After purification by column chromatography (SiO_2, Et_2O/*n*-pentane 3:1) diol **58** (203 mg, 1.09 mmol, 63%) was obtained as a colorless oil.

^{1}H NMR ($CDCl_3$, 500 MHz): δ = 4.08 (tdd, *J* = 7.0, 5.5, 3.8 Hz, 2H), 3.43 (dd, *J* = 12.4, 3.9 Hz, 2H), 3.33 (dd, *J* = 12.4, 7.3 Hz, 2H), 2.48 (s, 2H), 1.65 (dd, *J* = 6.7, 5.4 Hz, 2H) ppm.

^{13}C NMR ($CDCl_3$, 126 MHz): δ = 67.7, 57.0, 37.2 ppm.

IR (ATR): $\tilde{\nu}$ = 3398, 2924, 2096, 1274, 1084 cm^{-1}.

HRMS (ESI, pos. mode): *m*/*z* calculated for $C_5H_{10}N_6NaO_2$ $[M+Na]^+$: 209.0757, found 209.0753; *m*/*z* calculated for $C_5H_{10}KN_6O_2$ $[M+K]^+$: 225.0497, found 225.0494.

(2*R*,4*R*)-1,5-Diazido-2,4-bis(prop-2-yn-1-yloxy)pentane (64)

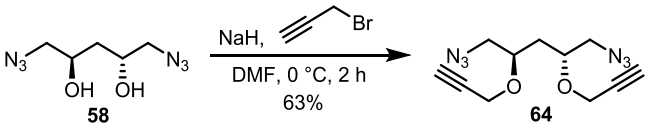

NaH (60% in mineral oil; 35.4 mg, 886 µmol, 3.0 equiv.) was added to a 0 °C cold solution of diol **58** (55.0 mg, 295 µmol, 1.0 equiv.) and DMF (2.4 mL) and stirred for 60 min at 0 °C. Propargyl bromide (80% in toluene; 82.3 µL, 739 µmol, 2.5 equiv.) was added and the reaction was stirred for additional 60 min at 0 °C. Saturated aqueous NH_4Cl solution (3 mL) was added subsequently, the aqueous phase was extracted with Et_2O (3x5 mL), the combined organic phases were dried over Na_2SO_4, and the solvent was removed under reduced pressure. After purification by column chromatography (SiO_2, *n*-pentane/EtOAc 10:1) propargyl ether **64** (49.0 mg, 187 µmol, 63%) was obtained as a pale yellow oil. Due to its instability the compound was immediately used in the next step.

^{1}H NMR ($CDCl_3$, 400 MHz): δ = 4.32 (dd, *J* = 5.5, 2.4 Hz, 4H), 3.91 (dddd, *J* = 7.1, 5.6, 4.8, 4.0 Hz, 2H), 3.58 (dd, *J* = 13.0, 4.0 Hz, 2H), 3.26 (dd, *J* = 13.0, 4.8 Hz, 2H), 2.50 (t, *J* = 2.4 Hz, 2H), 1.73 (dd, *J* = 7.0, 5.6 Hz, 2H) ppm.

Bis((*R*)-6,7-dihydro-4*H*-[1,2,3]triazolo[5,1-c][1,4]oxazin-6-yl)methane (60)

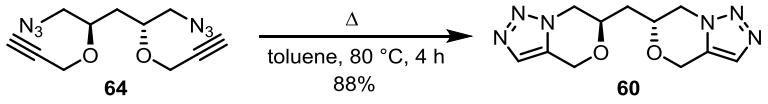

Propargyl ether **64** (40.0 mg, 153 µmol, 1.0 equiv.) was dissolved in toluene (1 mL) and stirred for 4 h at 80 °C. The precipitated solid was filtered through a suction filter (Por. 4) and dried under high vacuum overnight. Bistriazole **60** (35.0 mg, 134 µmol, 88%) was obtained as a colorless solid without further purification. The absolute stereoconfiguration was confirmed by single crystal structure analysis.

^{1}H NMR (DMSO-d_6, 500 MHz): δ = 7.58 (s, 2H), 5.11 (d, *J* = 15.2 Hz, 2H), 4.84 (d, *J* = 15.3 Hz, 2H), 4.19 – 4.12 (m, 2H), 4.05 (dd, *J* = 12.6, 10.5 Hz, 2H), 2.02 (t, *J* = 6.2 Hz, 2H) ppm.

^{13}C NMR (DMSO-d_6, 126 MHz): δ = 130.9, 127.8, 70.2, 61.2, 49.3, 35.5 ppm.

IR (ATR): $\tilde{\nu}$ = 2249, 2123, 1053, 1024 cm^{-1}.

HRMS (ESI, pos. mode): *m*/*z* calculated for $C_{11}H_{14}N_6NaO_2$ $[M+Na]^+$: 285.1070, found 285.1064; *m*/*z* calculated for $C_{11}H_{14}KN_6O_2$ $[M+K]^+$: 301.0810, found 301.0809.

(6*R*,8*R*)-6,8-Dichloro-2,2,3,3,11,11,12,12-octamethyl-4,10-dioxa-3,11-disilatridecane (65)

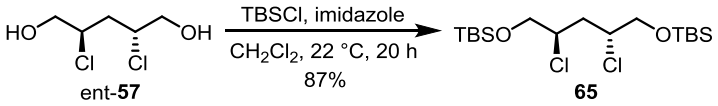

TBSCl (2.66 g, 12.5 mmol, 2.4 equiv.) and imidazole (850 mg, 12.5 mmol, 2.4 equiv.) were added to a solution of chlorohydrin ent-**57** (900 mg, 5.20 mmol, 1.0 equiv.) and CH_2Cl_2 (22 mL) and stirred for 20 h at 22 °C. H_2O (20 mL) was added to the reaction mixture, the aqueous phase was extracted with CH_2Cl_2 (3x20 mL), the combined organic phases were dried over Na_2SO_4, and the solvent was removed under reduced pressure. After purification by column chromatography (SiO_2, *n*-pentane/EtOAc 200:1) silyl ether **65** (1.81 g, 4.51 mmol, 87%) was obtained as a colorless solid.

^{1}H NMR ($CDCl_3$, 500 MHz): δ = 4.26 – 4.17 (m, 2H), 3.88 – 3.83 (dd, *J* = 10.6, 4.8 Hz, 2H), 3.75 – 3.70 (m, 2H), 2.13 (dd, *J* = 8.0, 5.5 Hz, 2H), 0.90 (s, 18H), 0.08 (s, 12H) ppm.

^{13}C NMR ($CDCl_3$, 126 MHz): δ = 67.5, 59.7, 39.8, 26.0, 18.4, –5.2 (2xC) ppm.

IR (ATR): $\tilde{\nu}$ = 2954, 2929, 2857, 1255, 1122, 835, 814 cm^{-1}.

HRMS (ESI, pos. mode): *m/z* calculated for $C_{17}H_{38}Cl_2NaO_2Si_2$ $[M+Na]^+$: 423.1679, found 423.1700.

(2*S*,4*S*)-2,4-Diazidopentane-1,5-diol (ent-59)

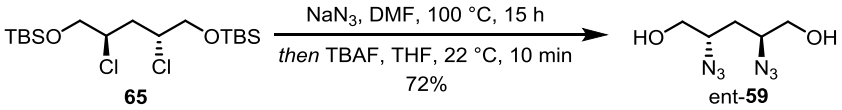

NaN_3 (3.52 g, 54.2 mmol, 15 equiv.) was added to a solution of silyl ether **65** (1.45 g, 3.61 mmol, 1.0 equiv.) and DMF (50 mL) and stirred in a pressure tube for 15 h at 100 °C. After cooling to 22 °C, TBAF (1M in THF; 21.7 mL, 21.7 mmol, 6 equiv.) was added and the reaction was stirred for additional 10 min at 22 °C. Saturated aqueous NH_4Cl solution (40 mL) was added, the aqueous phase was extracted with Et_2O (3x50 mL), the combined organic phases were dried over Na_2SO_4, and the solvent was removed under reduced pressure. After purification by column chromatography (SiO_2, CH_2Cl_2/MeOH 30:1 to 20:1) diol ent-**59** (481 mg, 2.58 mmol, 72%) was obtained as a colorless solid.

^{1}H NMR (CD_3CN, 500 MHz): δ = 3.67 (dd, *J* = 11.2, 3.8 Hz, 2H), 3.64 – 3.58 (m, 2H), 3.51 (dd, *J* = 11.2, 6.9 Hz, 2H), 3.20 (s, 2H), 1.44 (dd, *J* = 7.8, 6.0 Hz, 2H) ppm.

^{13}C NMR (CD_3CN, 126 MHz): δ = 65.8, 62.2, 32.3 ppm.

(2*S*,4*S*)-2,4-Diazido-1,5-bis(prop-2-yn-1-yloxy)pentane (66)

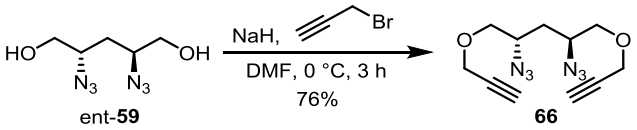

NaH (60% in mineral oil; 309 mg, 7.72 mmol, 3.0 equiv.) was added to a 0 °C cold solution of diol ent-**59** (479 mg, 2.57 mmol, 1.0 equiv.) and DMF (21 mL) and stirred for 60 min at 0 °C. Propargyl bromide (80% in toluene; 860 µL, 7.72 mmol, 3.0 equiv.) was added dropwise and the reaction mixture was stirred for additional 2 h at 0 °C. Aqueous saturated NH_4Cl solution (20 mL) was added to the reaction, the aqueous phase was extracted with Et_2O (3x40 mL), the combined organic phases were dried over Na_2SO_4, and the solvent was removed under reduced pressure. After purification by column chromatography (SiO_2, *n*-pentane/EtOAc 10:1) propargyl ether **66** (509 mg, 1.94 mmol, 76%) was obtained as a pale yellow oil. Due to its instability the compound was immediately used in the next step.

^{1}H NMR ($CDCl_3$, 400 MHz): δ = 4.22 (dt, *J* = 2.4, 1.2 Hz, 4H), 3.83 – 3.76 (m, 2H), 3.70 (dd, *J* = 9.9, 3.8 Hz, 2H), 3.59 (dd, *J* = 9.8, 6.8 Hz, 2H), 2.47 (t, *J* = 2.4 Hz, 2H), 1.59 – 1.49 (m, 2H) ppm.

Bis((*S*)-6,7-dihydro-4*H*-[1,2,3]triazolo[5,1-c][1,4]oxazin-7-yl)methane (ent-61)

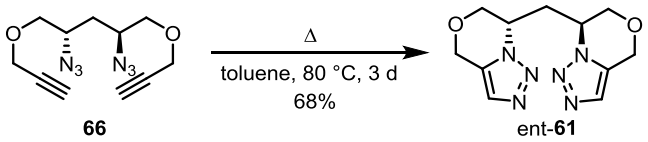

Propargyl ether **66** (500 mg, 1.91 mmol, 1.0 equiv.) was dissolved in toluene (13 mL) and stirred for 3 days at 80 °C. The precipitated solid was filtered through a suction filter (Por. 4) and dried under high vacuum overnight. Bistriazole ent-**61** (341 mg, 1.30 mmol, 68%) was obtained as a colorless solid without further purification. The absolute stereoconfiguration could be confirmed by single crystal structure analysis.

mp = 162 °C

$[\boldsymbol{\alpha}]_{\boldsymbol{D}}^{\boldsymbol{26}}$ = 14.1° (*c* = 1.00, CH_2Cl_2)

^{1}H NMR ($CDCl_3$, 700 MHz): δ = 7.52 (s, 2H), 5.38 – 5.34 (m, 2H), 4.97 – 4.90 (m, 4H), 4.06 (dd, *J* = 12.2, 3.9 Hz, 2H), 3.81 (dd, *J* = 12.2, 5.0 Hz, 2H), 2.38 (t, *J* = 6.1 Hz, 2H) ppm.

^{13}C NMR ($CDCl_3$, 126 MHz): δ = 130.6, 128.4, 68.5, 62.6, 54.1, 36.7 ppm.

IR (ATR): $\tilde{\nu}$ = 2953, 2930, 2881, 2864, 1551, 1464, 1446, 1430, 1384, 1333, 1189, 1160, 1088, 986, 880, 824, 775 cm^{-1}.

HRMS (ESI, pos. mode): *m*/*z* calculated for $C_{11}H_{15}N_6O_2$ $[M+H]^+$: 263.1251, found 263.1243; *m*/*z* calculated for $C_{11}H_{14}N_6NaO_2$ $[M+Na]^+$: 285.1070, found 285.1067; *m*/*z* calculated for $C_{11}H_{15}KN_6O_2$ $[M+K]^+$: 301.0810, found 301.0824.

(2*S*,4*S*)-2,4-Dichloropentane-1,5-diol (57)

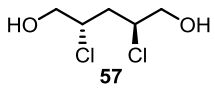

57

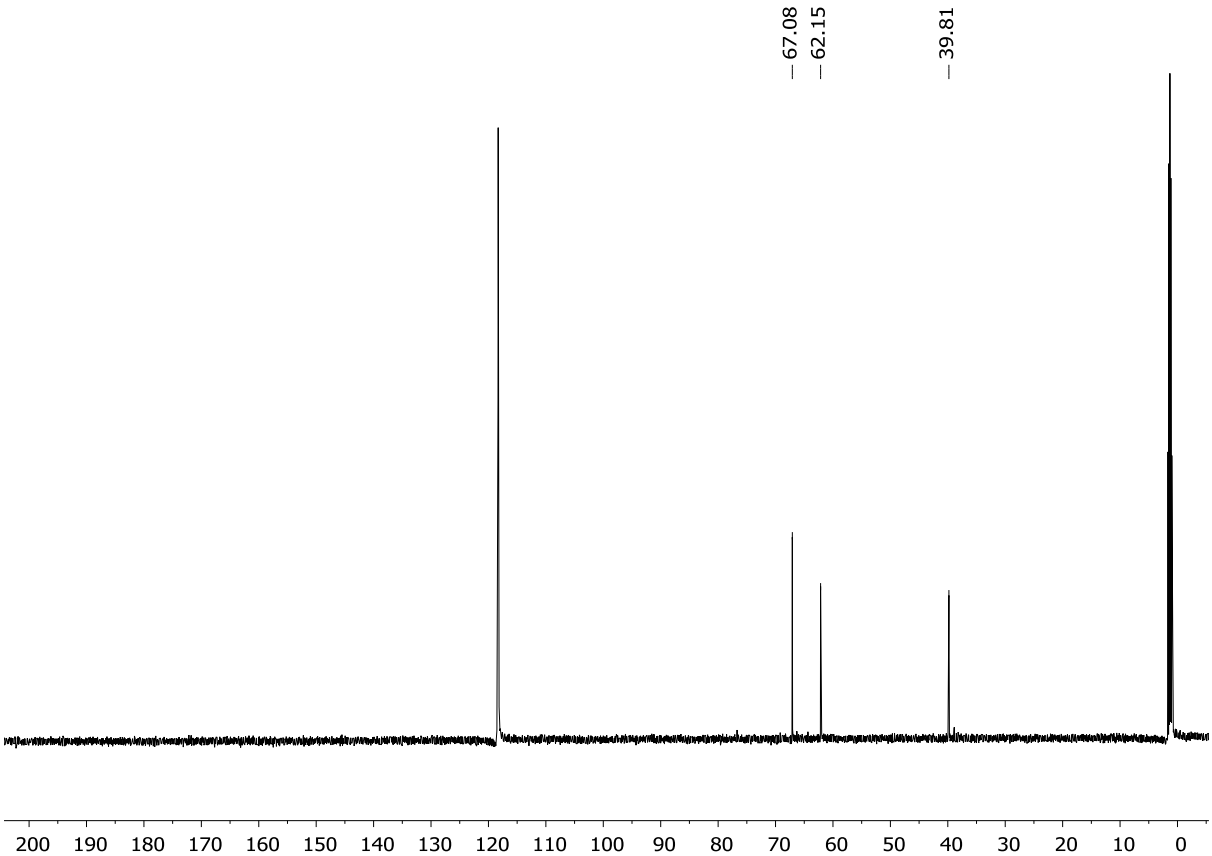

(2*R*,4*R*)-1,5-Diazidopentane-2,4-diol (58)

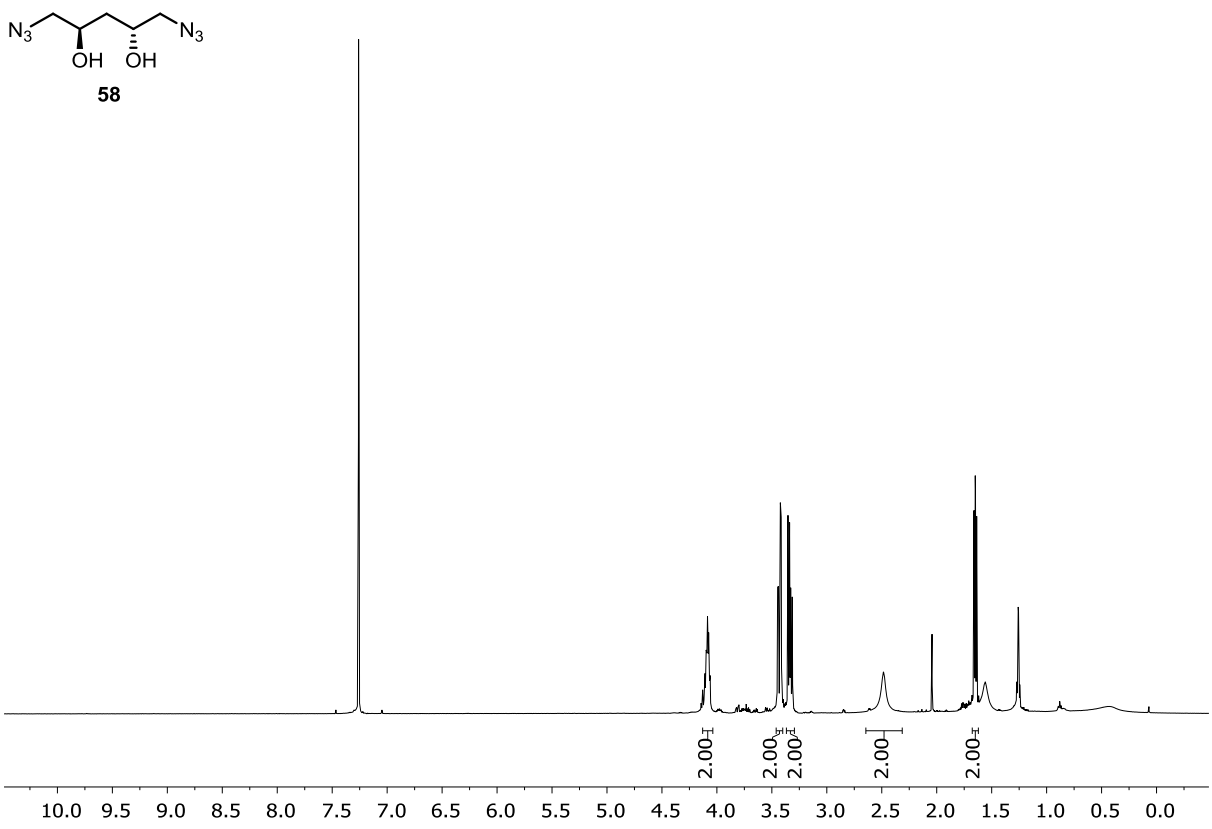

(2*R*,4*R*)-1,5-Diazido-2,4-bis(prop-2-yn-1-yloxy)pentane (64)

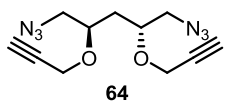

64

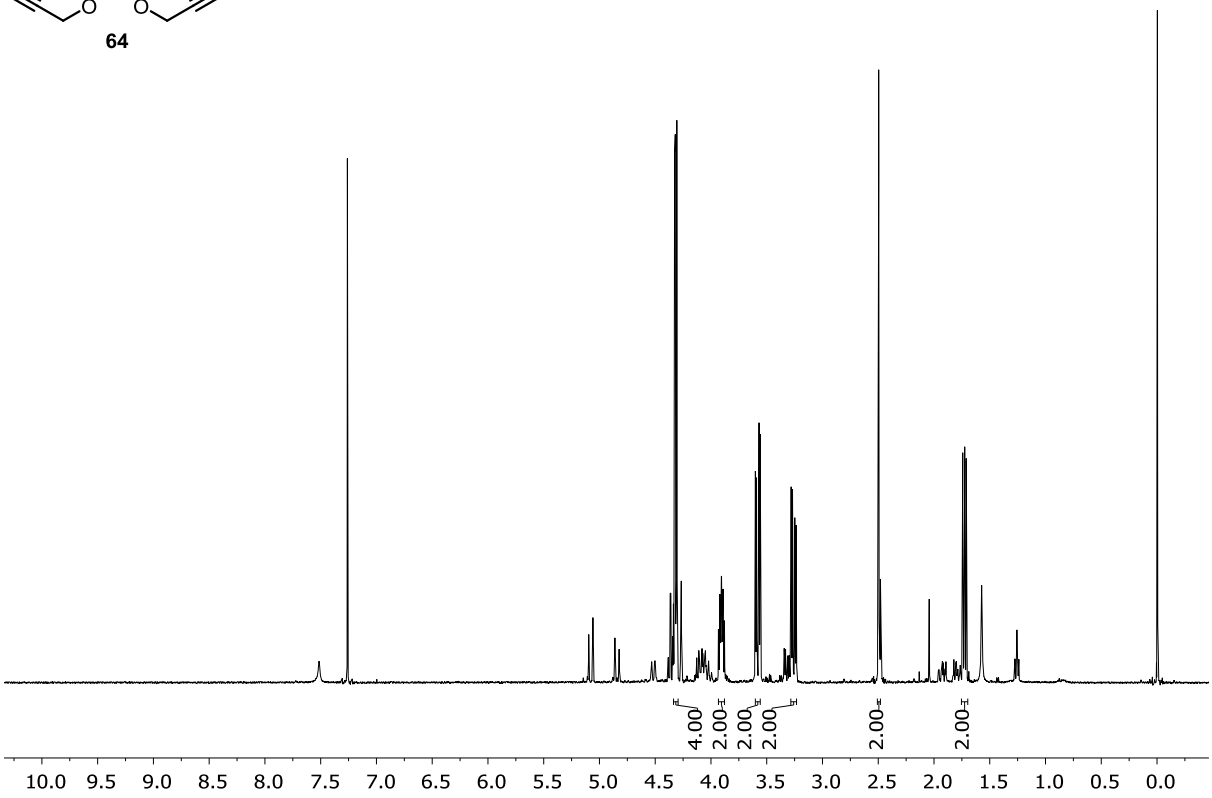

Bis((*R*)-6,7-dihydro-4*H*-[1,2,3]triazolo[5,1-c][1,4]oxazin-6-yl)methane (60)

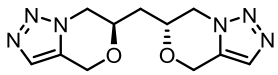

60

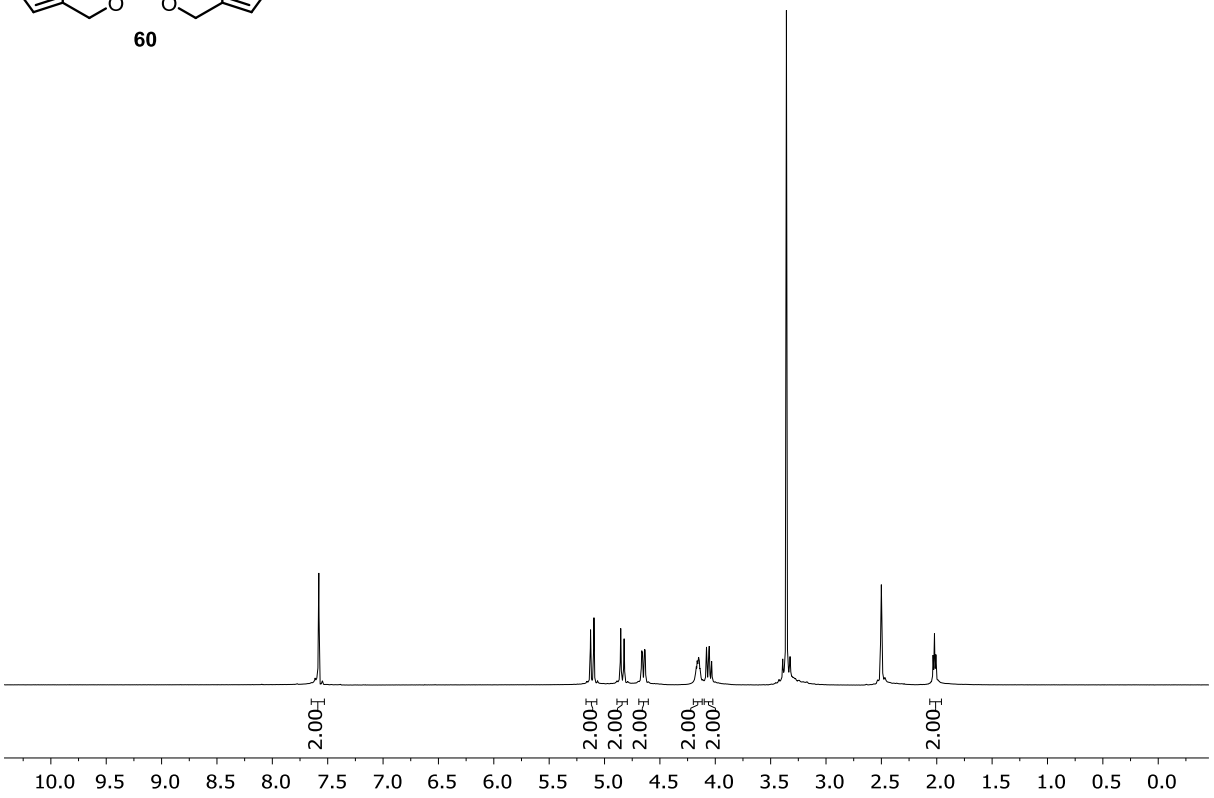

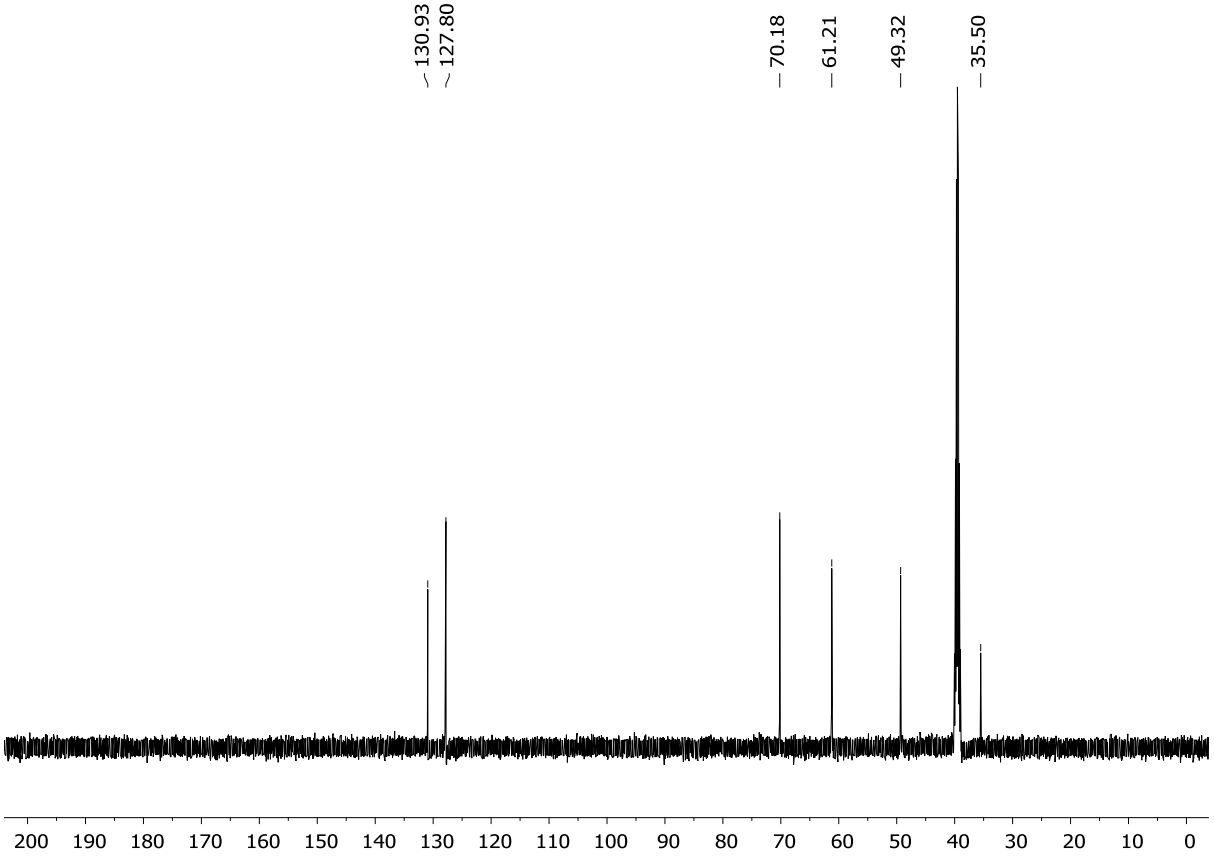

(6*R*,8*R*)-6,8-Dichloro-2,2,3,3,11,11,12,12-octamethyl-4,10-dioxa-3,11-disilatridecane (65)

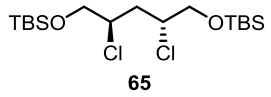

65

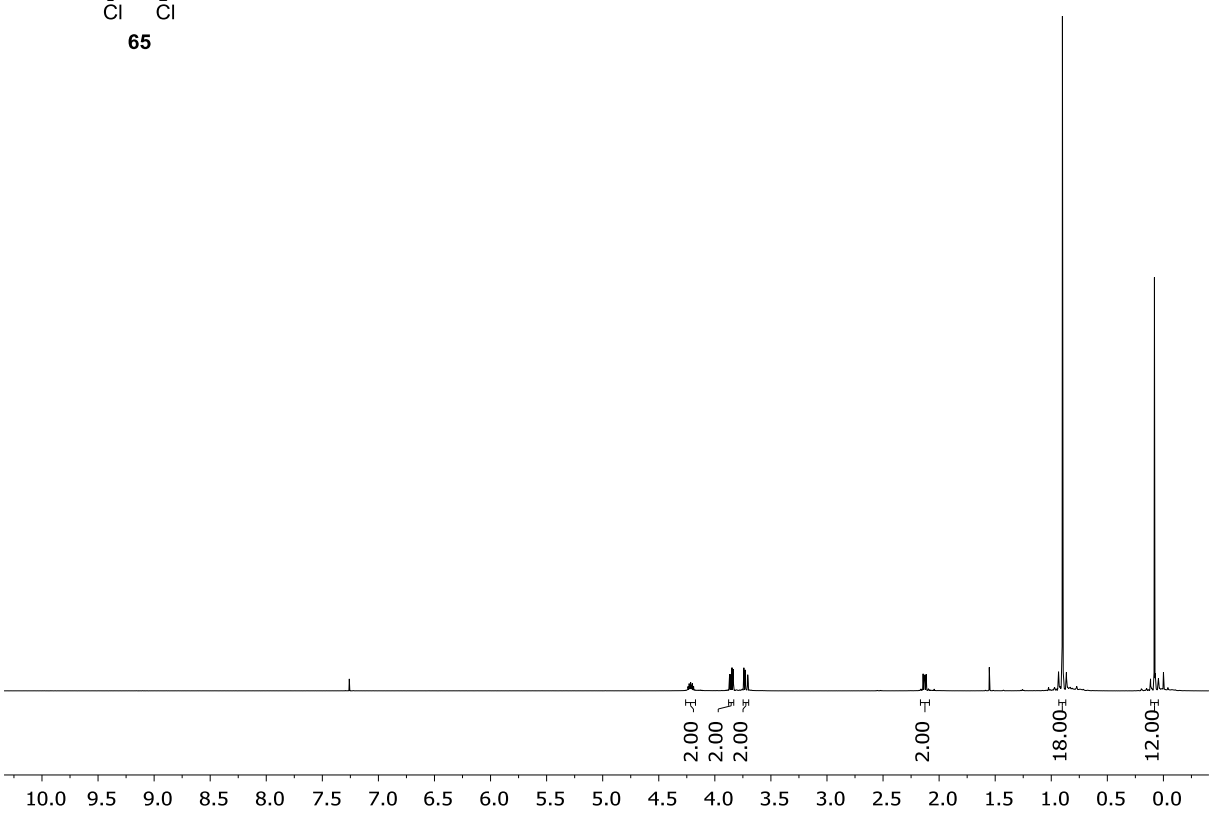

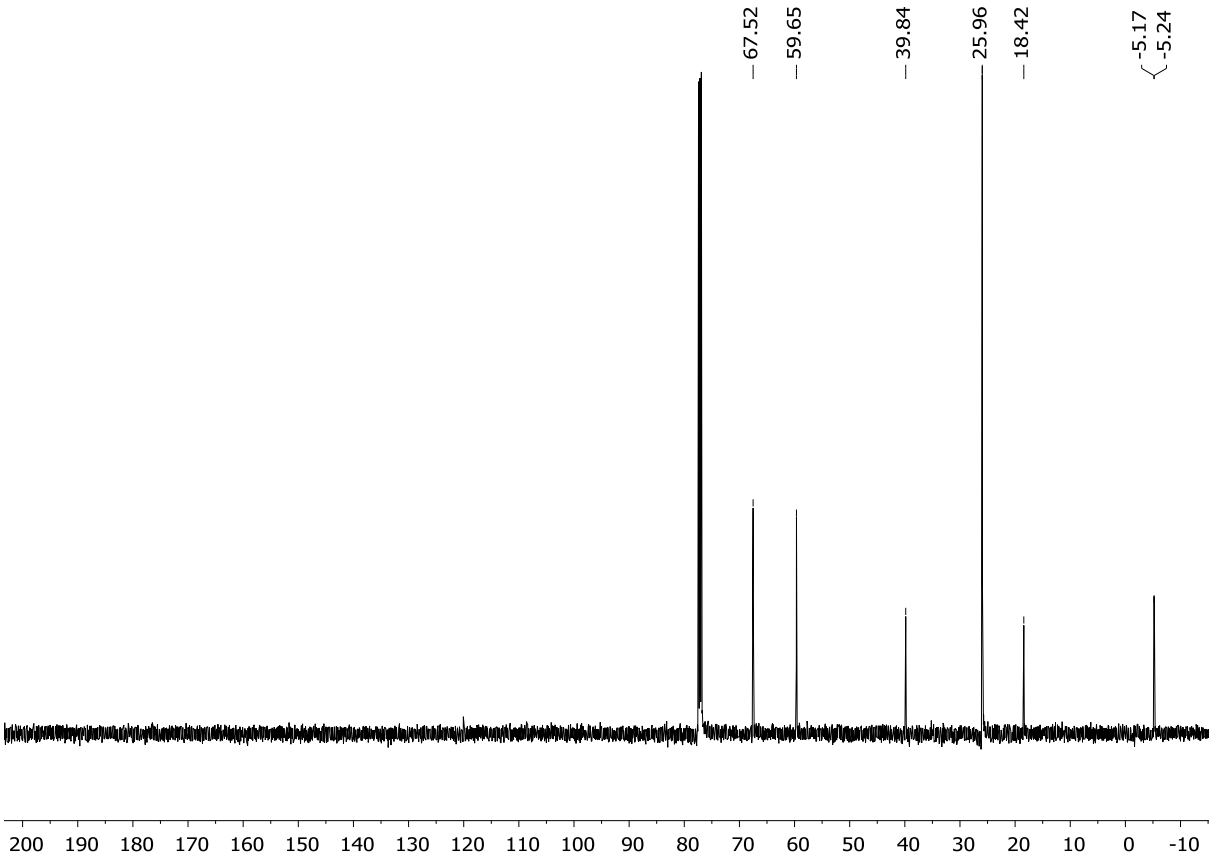

(2*S*,4*S*)-2,4-Diazidopentane-1,5-diol (ent-59)

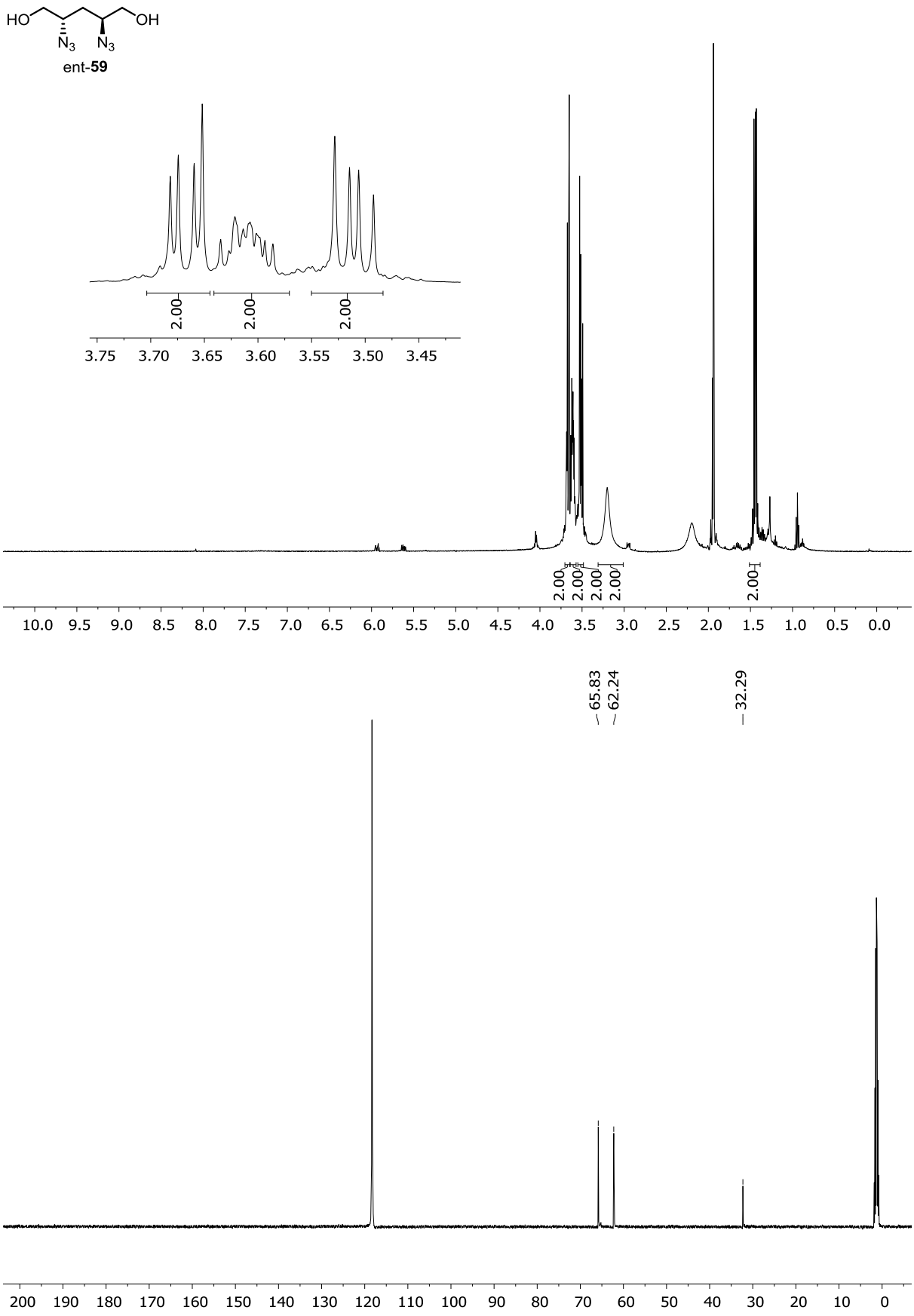

(2*S*,4*S*)-2,4-Diazido-1,5-bis(prop-2-yn-1-yloxy)pentane (66)

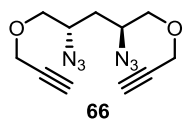

66

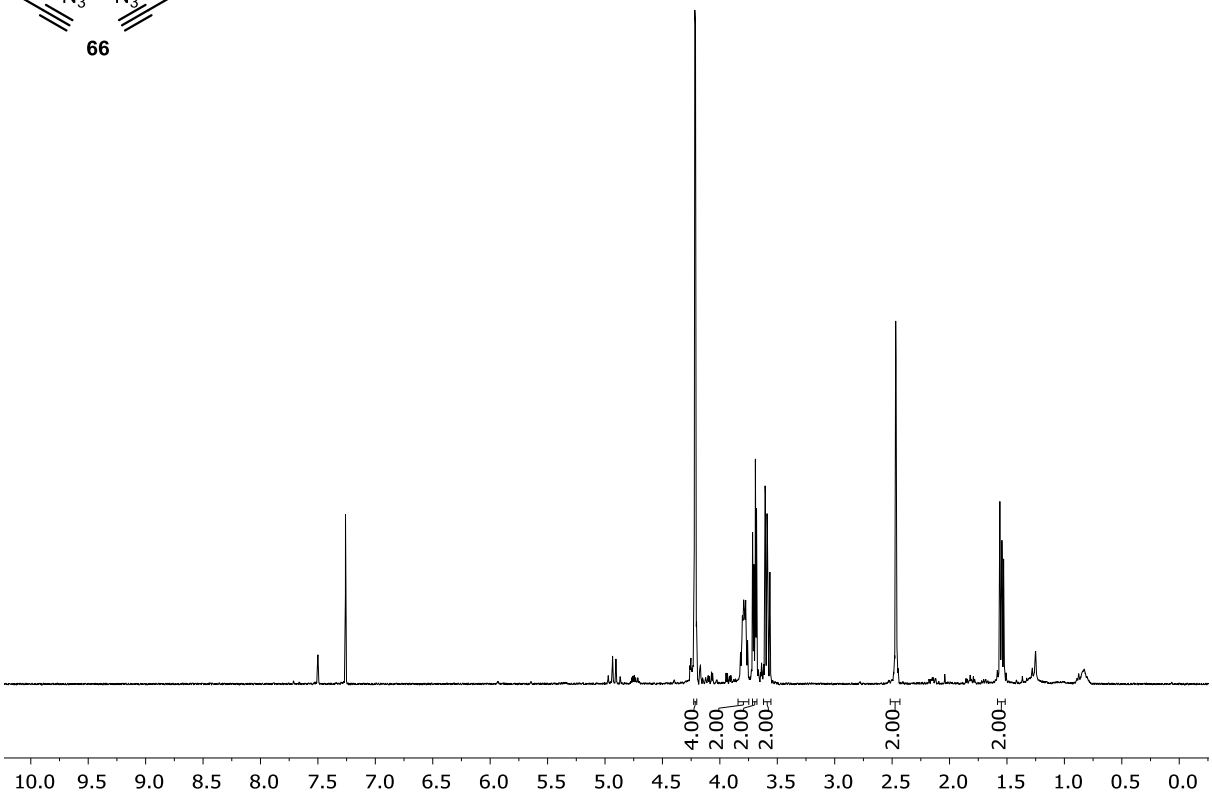

Bis((*S*)-6,7-dihydro-4*H*-[1,2,3]triazolo[5,1-c][1,4]oxazin-7-yl)methane (ent-61)

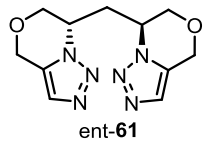

ent-**61**

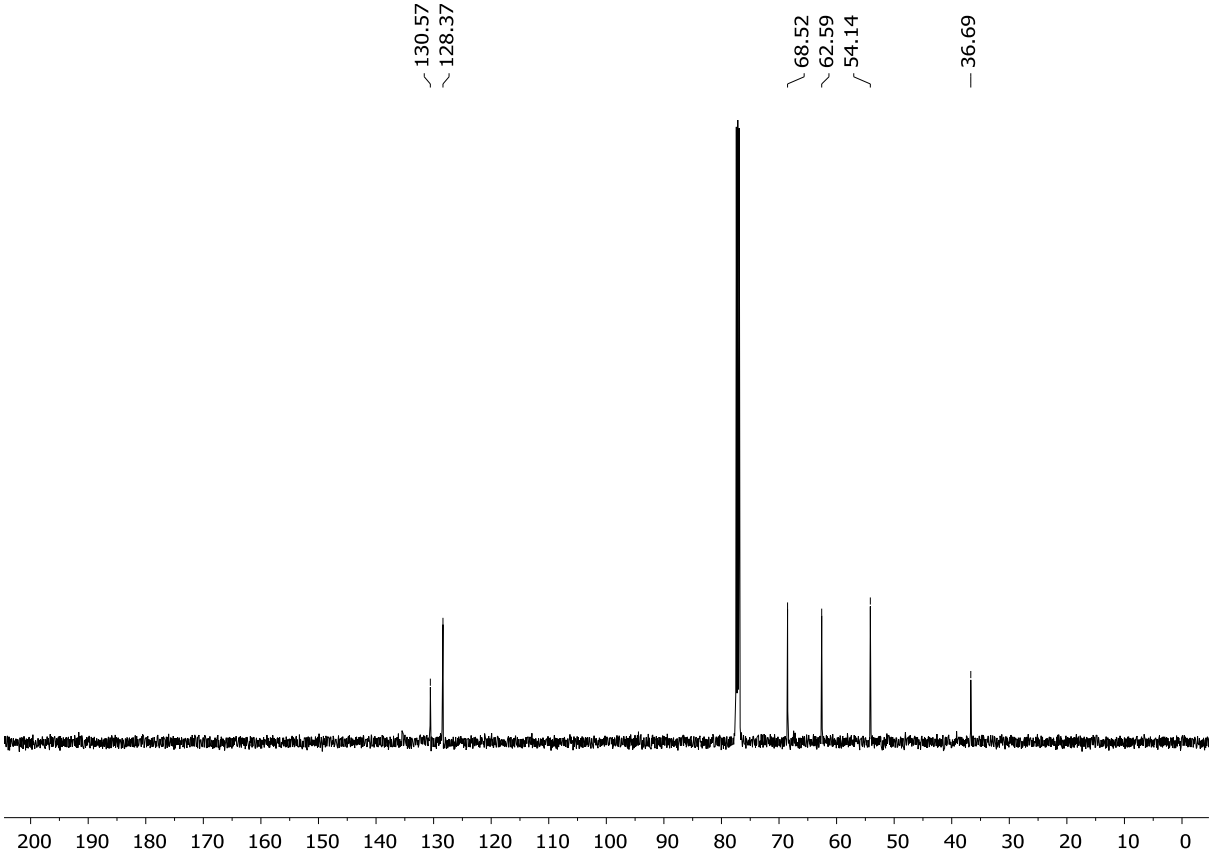

(2*R*,4*R*)-2,4-Dichloropentane-1,5-diol (ent-57)

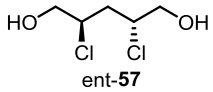

ent-**57**

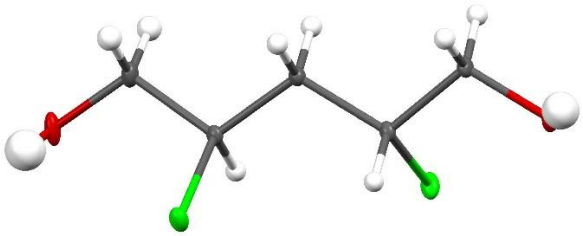

Cell: a = 5.0131(1) Å, b = 5.7783(1) Å, c = 7.1692(2) Å

α = 91.147(1)°, β = 102.993(1)°, γ = 107.702(1)°

Temperature: 100 K

Volume: 191.898(7) $Å^3$

Space group: P 1

Hall group: P 1

Mr: 173.03

Dx [g/cm^3]: 1.497

Z: 1

Mu [1/mm]: 0.774

F000: 90.0

F000’: 90.33

h,k,lmax: 6,7,8

Nref: 1310

Tmin,Tmax: 0.761, 0.875

Tmin’: 0.769

Data completeness = 1.78/0.89

Theta(max) = 25.749

R(reflections) = 0.0221 (1285)

wR2(reflections)= 0.0568 (1310)

S = 1.067

Npar = 90

Bis((*R*)-6,7-dihydro-4*H*-[1,2,3]triazolo[5,1-c][1,4]oxazin-6-yl)methane (60)

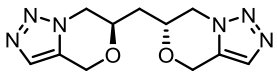

60

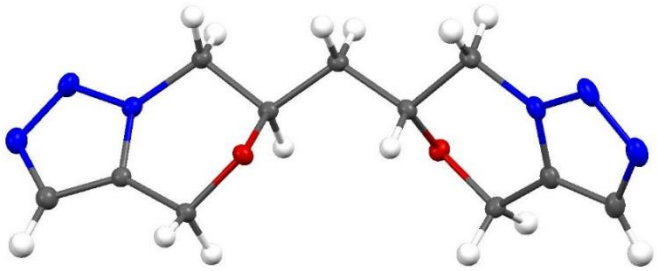

Temperature/K	100.0
Crystal system	monoclinic
Space group	$P2_1$
a/Å	4.46200(10)
b/Å	11.0166(3)
c/Å	12.2067(3)
α/°	90
β/°	98.6440(10)
γ/°	90
Volume/Å^3	593.22(3)
Z	2
ρ_{calc}g/cm^3	1.468
μ/mm^{-1}	0.891
F(000)	276.0
Crystal size/mm^3	0.32 × 0.147 × 0.117
Radiation	CuKα (λ = 1.54178)
2Θ range for data collection/°	7.324 to 144.436
Index ranges	-5 ≤ h ≤ 5, -13 ≤ k ≤ 13, -14 ≤ l ≤ 15
Reflections collected	24236
Independent reflections	2326 [R_{int} = 0.0434, R_{sigma} = 0.0211]
Data/restraints/parameters	2326/1/172
Goodness-of-fit on F^2	1.082
Final R indexes [I>=2σ (I)]	R_1 = 0.0275, wR_2 = 0.0693
Final R indexes [all data]	R_1 = 0.0280, wR_2 = 0.0699
Largest diff. peak/hole / e Å^{-3}	0.16/-0.23
Flack parameter	0.12(6)

Bis((*S*)-6,7-dihydro-4*H*-[1,2,3]triazolo[5,1-c][1,4]oxazin-7-yl)methane (ent-61)

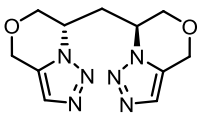

ent-**61**

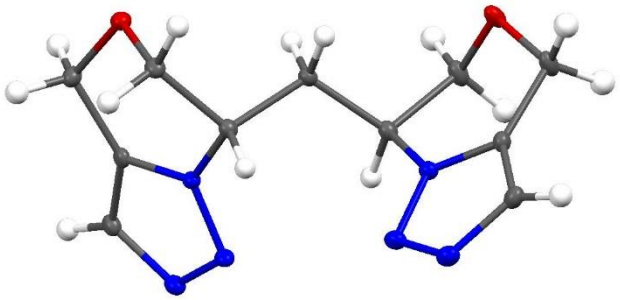

Temperature/K	100.0
Crystal system	orthorhombic
Space group	$P2_12_12_1$
a/Å	8.1095(6)
b/Å	11.6834(10)
c/Å	12.6166(9)
α/°	90
β/°	90
γ/°	90
Volume/Å^3	1195.38(16)
Z	4
ρ_{calc}g/cm^3	1.457
μ/mm^{-1}	0.885
F(000)	552.0
Crystal size/mm^3	0.306 × 0.165 × 0.157
Radiation	CuKα (λ = 1.54178)
2Θ range for data collection/°	10.318 to 144.36
Index ranges	-10 ≤ h ≤ 10, -14 ≤ k ≤ 12, -15 ≤ l ≤ 15
Reflections collected	20613
Independent reflections	2362 [R_{int} = 0.0473, R_{sigma} = 0.0202]
Data/restraints/parameters	2362/0/172
Goodness-of-fit on F^2	1.088
Final R indexes [I>=2σ (I)]	R_1 = 0.0264, wR_2 = 0.0651
Final R indexes [all data]	R_1 = 0.0278, wR_2 = 0.0663
Largest diff. peak/hole / e Å^{-3}	0.12/-0.19
Flack parameter	-0.07(8)

5.5.2 Studies on the Total Synthesis of Hypatulin A and B

2-Allyl-1,3,2-dioxaborinane (136)

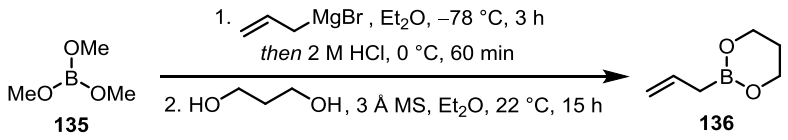

Borinane **136** was synthesized according to a procedure of *Brown et al*.[124] Allylmagnesium bromide (1 M in Et_2O; 100 mL, 100 mmol, 1.04 equiv.) was added to a –78 °C cold solution of boric acid ester **135** (10.0 g, 96.2 mmol, 1.0 equiv.) and dry Et_2O (300 mL) over a period of 60 min and stirring was continued for additional 2 h at –78 °C. The reaction was warmed to 0 °C, added slowly to 2 M HCl (100 mL), and stirred for 60 min at 0 °C. The aqueous phase was extracted with Et_2O (3x100 mL), the combined organic phases were dried over Na_2SO_4, and the solvent was reduced to a volume of 200 mL under reduced pressure (600 mbar, 25 °C). The solution was degassed in an argon stream and molar sieve (3 Å; 2.00 g) and 1,3-propanediol (6.96 mL, 96.2 mmol, 1.0 equiv.) were added. The reaction mixture was stirred at 22 °C for 15 h, then filtered and the volume of the solvent was halved under reduced pressure (600 mbar, 25 °C). *n*-Pentane (200 mL) was added and the resulting suspension was filtered over Celite®. The solvent of the filtrate was again removed under reduced pressure (80 mbar, 0 °C) and borinane **136** (10.2 g, 81.0 mmol, 84% over 2 steps) was obtained as a colorless liquid without further purification.

The spectroscopic data are in accordance with the literature.[124]

^{1}H NMR ($CDCl_3$, 400 MHz): δ = 5.86 (ddt, *J* = 17.5, 10.0, 7.7 Hz, 1H), 4.97 – 4.87 (m, 2H), 4.01 – 3.97 (m, 4H), 1.95 (p, *J* = 5.5 Hz, 2H), 1.65 (d, *J* = 7.6 Hz, 2H) ppm.

(*S*)-1-Allyl-2-iodocyclopent-2-en-1-ol (122)

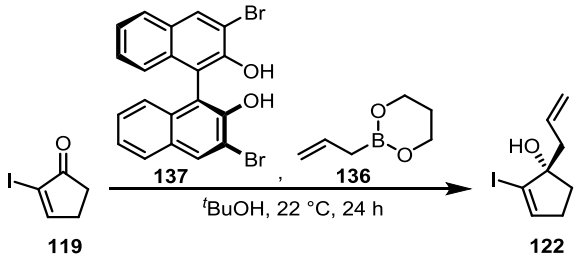

Alcohol **122** was synthesized according to a procedure of *Taber et al*.[116] (*S*)-3,3'-Dibromo-[1,1'-binaphthalene]-2,2'-diol (**137**) (2.74 g, 6.18 mmol, 5.0 mol%) was added to a solution of 2-allyl-1,3,2-dioxaborinane (**136**) (23.3 g, 185 mmol, 1.5 equiv.) and ^{t}BuOH (18.3 g, 247 mmol, 2.0 equiv.) and the mixture was stirred till complete homogeneity at 22 °C. Enone **119** (25.7 g, 124 mmol, 1.0 equiv.) was added and the stirring was continued for 24 h at 22 °C. Subsequently, the reaction was diluted with Et_2O (200 mL) and washed with 2N NaOH (3x100 mL). The organic phase was dried over Na_2SO_4 and the solvent was removed under reduced pressure. After purification by column chromatography (SiO_2, *n*-pentane/EtOAc 10:1) alcohol **122** (27.3 g, 109 mmol, 88%, 94% ee) was obtained as a pale yellow solid. The aqueous phase was adjusted to pH = 1 with 15% HCl, extracted with EtOAc (3x50 mL), and the solvent was removed under reduced pressure. BINOL derivative **137** (2.36 g, 5.31 mmol, 86%) could thus be recovered clean and almost quantitative without further purification.

The spectroscopic data are in accordance with the literature.[116]

^{1}H NMR ($CDCl_3$, 400 MHz): δ = 6.25 (t, *J* = 2.5 Hz, 1H), 5.74 (dddd, *J* = 16.8, 10.1, 7.9, 6.7 Hz, 1H), 5.24 – 5.12 (m, 1H), 5.18 – 5.09 (m, 1H), 2.50 – 2.41 (m, 1H), 2.41 – 2.29 (m, 2H), 2.29 – 2.19 (m, 2H), 1.97 – 1.90 (m, 1H), 1.89 (s, 1H) ppm.

1-Allyl-2-iodocyclopent-2-en-1-ol (rac-122)

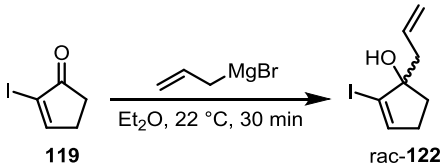

119 rac-**122**

Allylmagnesium bromide (1M in Et_2O; 96.2 µL, 96.2 µmol, 2.0 equiv.) was added dropwise to a solution of enone **119** (10.0 mg, 48.1 µmol, 1.0 equiv.) and dry Et_2O (1.0 mL) and stirred for 30 min at 22 °C. H_2O (0.5 mL) was added and the reaction mixture was extracted with Et_2O (3x1 mL). The combined organic phases were dried over Na_2SO_4 and the solvent was removed under reduced pressure. After purification by column chromatography (SiO_2, *n*-pentane/EtOAc 10:1) alcohol rac-**122** (8.9 mg, 35.6 µmol, 74%) was obtained as a pale yellow solid.

The spectroscopic data are in accordance with the literature.[116]

^{1}H NMR ($CDCl_3$, 400 MHz): δ = 6.25 (t, *J* = 2.5 Hz, 1H), 5.75 (dddd, *J* = 17.0, 10.1, 7.9, 6.7 Hz, 1H), 5.24 – 5.14 (m, 1H), 5.18 – 5.10 (m, 1H), 2.50 – 2.41 (m, 1H), 2.40 – 2.29 (m, 2H), 2.29 – 2.18 (m, 2H), 1.98 – 1.89 (m, 1H), 1.86 (s, 1H) ppm.

(*S*)-1-Allyl-2-methylcyclopent-2-en-1-ol (123)

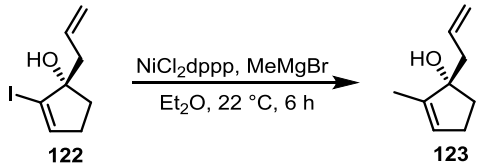

122 **123**

Alcohol **123** was synthesized according to a procedure of *Taber et al*.[117] Methylmagnesium bromide (3M in Et_2O; 21.5 mL, 64.5 mmol, 2.3 equiv.) was added dropwise to a suspension of $NiCl_2$dppp (75.9 mg, 140 µmol, 0.5 mol%) and dry Et_2O (120 mL) and stirred for 10 min. A solution of alcohol **122** (7.00 g, 28.0 mmol, 1.0 equiv.) and dry Et_2O (60 mL) was added and the reaction mixture was stirred for 6 h at 22 °C. Na_2SO_3 (14 g) and saturated aqueous $Na_2S_2O_3$ solution (50 mL) were added to the reaction and the aqueous phase was rapidly extracted with Et_2O (3x100 mL), the combined organic phases were dried over Na_2SO_4 and Na_2SO_3, and the solvent was removed under reduced pressure. After purification by column chromatography (SiO_2, *n*-pentane/Et_2O 5:1) alcohol **123** (3.72 g, 26.9 mmol, 96%) was obtained as a colorless oil.

The spectroscopic data are in accordance with the literature.[125]

^{1}H NMR (CD_2Cl_2, 400 MHz): δ = 5.78 (dddd, *J* = 17.1, 10.2, 7.8, 6.8 Hz, 1H), 5.49 – 5.46 (m, 1H), 5.15 – 5.05 (m, 2H), 2.39 (ddt, *J* = 13.7, 7.8, 1.2 Hz, 1H), 2.32 – 2.23 (m, 2H), 2.18 – 2.05 (m, 2H), 1.79 – 1.73 (m, 1H), 1.68 (q, *J* = 2.0 Hz, 3H), 1.59 (s, 1H) ppm.

Methyl (3*S*,4*R*)-4-allyl-3-methyl-2-oxocyclopentane-1-carboxylate (118)

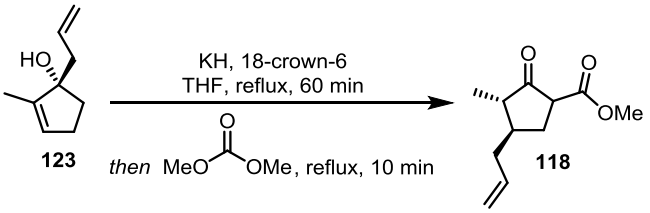

KH (30% in mineral oil; 21.5 g, 161 mmol, 2.5 equiv.) was washed with dry *n*-pentane (3x20 mL) and the remaining solvent was removed under reduced pressure. Dry THF (300 mL), 18-crown-6 (20.4 g, 77.3 mmol, 1.2 equiv.), and alcohol **123** (8.90 g, 64.4 mmol, 1.0 equiv.) were added subsequently and heated for 60 min under reflux. The reaction mixture was cooled to 0 °C, dimethyl carbonate (21.7 mL, 258 mmol, 4.0 equiv.) was added and heated for another 10 min under reflux. The reaction was again cooled to 0 °C and 2M HCl (100 mL) was added. The aqueous phase was extracted with Et_2O (3x200 mL), the combined organic phases were dried over Na_2SO_4, and the solvent was removed under reduced pressure. β-Keto ester **118** (12.3 g, 62.7 mmol, 97%) was obtained as a colorless oil without further purification. NMR spectroscopic evaluation reveals multiple isomers resulting from the interconversion of the stereocenter between the two carbonyl groups and keto/enol tautomerism. For the further synthesis, this behavior has no negative consequences.

$[\boldsymbol{\alpha}]_{\boldsymbol{D}}^{\mathbf{26}}$ = +17.0° (*c* = 0.45, CH_2Cl_2)

^{1}H NMR (mixture of isomers, $CDCl_3$, 500 MHz): δ = 5.87 – 5.69 (m, 1H), 5.15 – 5.01 (m, 2H), 3.75 – 3.65 (m, 3H), 3.37 – 3.12 (m, 1H), 2.52 – 1.63 (m, 6H), 1.16 – 1.01 (m, 3H) ppm.

^{13}C NMR (major isomer, $CDCl_3$, 126 MHz): δ = 212.7, 170.0, 135.3, 117.3, 54.4, 52.6, 49.8, 41.9, 37.9, 31.3, 12.6 ppm.

IR (ATR): $\tilde{\nu}$ = 2954, 2931, 1754, 1725, 1436, 1337, 1228, 1152, 993, 913, 730 cm^{-1}.

HRMS (ESI, pos. mode): *m*/*z* calculated for $C_{11}H_{16}NaO_3$ $[M+Na]^+$: 219.0991, found 219.0995.

Methyl (3*S*,4*R*)-4-allyl-2-(allyloxy)-3-methylcyclopent-1-en-1-carboxylate (124)

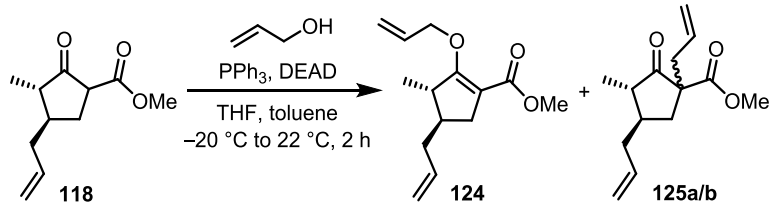

The *Mitsunobu*-like *O*-allylation was performed following a procedure by *Jacobsen et al*.[119] PPh_3 (24.7 g, 94.2 mmol, 1.5 equiv.) was dissolved in dry THF (125 mL) and cooled to –20 °C. DEAD (40% in toluene; 41.0 g, 94.2 mmol, 1.5 equiv.), allyl alcohol (5.13 mL, 75.4 mmol, 1.2 equiv.), and β-keto ester **118** (12.3 g, 62.8 mmol, 1.0 equiv.) were added subsequently, and the reaction mixture was warmed to 22 °C over 2 h. Hexane (1200 mL) was added, the precipitated solid was filtered over a short plug of Celite® and the solvent was removed under reduced pressure. After an initial purification by column chromatography (SiO_2, *n*-pentane/EtOAc 30:1) a mixture of *O*-allyl-β-keto ester **124** and diastereomeric *C*-allyl-β-keto esters **125a**/**b** (10.2 g, 43.2 mmol, 68%) was obtained. After a second purification by column chromatography (SiO_2, *n*-pentane/CH_2Cl_2 1:2) *O*-allyl-β-keto ester **124** (5.29 g, 22.4 mmol, 36%) and *C*-allyl-β-keto esters **125a**/**b** (4.51 g, 19.1 mmol, 30%) were obtained separately.

***O*-Allyl-β-keto ester 124:**

$[\alpha]_D^{26}$ = +6.8° (*c* = 0.7, CH_2Cl_2)

^{1}H NMR (CD_2Cl_2, 400 MHz): δ = 5.93 (ddt, *J* = 17.2, 10.4, 5.1 Hz, 1H), 5.75 (ddt, *J* = 17.2, 10.3, 6.9 Hz, 1H), 5.35 (dq, *J* = 17.2, 1.7 Hz, 1H), 5.20 (dq, *J* = 10.5, 1.5 Hz, 1H), 5.02 (ddt, *J* = 10.3, 2.3, 1.4 Hz, 1H), 4.99 – 4.97 (m, 1H), 4.61 (ddt, *J* = 13.5, 5.0, 1.7 Hz, 1H), 4.51 (ddt, *J* = 13.5, 5.3, 1.6 Hz, 1H), 3.63 (s, 3H), 2.69 (ddd, *J* = 15.0, 8.1, 1.9 Hz, 1H), 2.53 (dddd, *J* = 6.9, 4.1, 2.0, 0.9 Hz, 1H), 2.20 – 2.02 (m, 3H), 1.78 (ddq, *J* = 11.4, 7.7, 3.9 Hz, 1H), 1.11 (d, *J* = 7.0 Hz, 3H) ppm.

^{13}C NMR (CD_2Cl_2, 126 MHz): δ = 170.7, 166.0, 137.4, 134.3, 117.4, 116.5, 104.5, 71.9, 51.2, 45.1, 41.6, 40.2, 34.5, 18.3 ppm.

IR (ATR): $\tilde{\nu}$ = 3078, 2953, 2928, 1750, 1725, 1639, 1436, 1203, 1145, 1083, 994, 915, 773, 712 cm^{-1}.

HRMS (ESI, pos. mode): *m*/*z* calculated for $C_{14}H_{20}NaO_3$ $[M+Na]^+$: 259.1304, found 259.1310.

(*R*)-*N*-(2,6-Dimethylphenyl)piperidine-2-carboxamide (139)

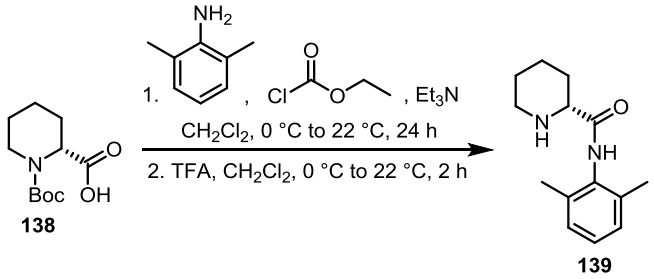

Amide **139** was synthesized according to a procedure of *Müller et al*.[126] Dry Et_3N (1.43 mL, 10.3 mmol, 1.1 equiv.) and ethyl chloroformate (982 µL, 10.3 mmol, 1.1 equiv.) were added subsequently to a 0 °C cold solution of pipecolic acid derivative **138** (2.15 g, 9.38 mmol, 1.0 equiv.) and dry CH_2Cl_2 (17 mL) and stirred at for 60 min 0 °C. 2,6-Dimethylaniline (1.56 mL, 12.7 mmol, 1.4 equiv.) was added and stirring was continued for 24 h at 22 °C. The reaction mixture was subsequently washed with 1 M H_2SO_4 (35 mL), aqueous saturated $NaHCO_3$ solution (20 mL), and aqueous saturated NaCl solution (20 mL). The organic phase was dried over Na_2SO_4 and the solvent was removed under reduced pressure. The residue was dissolved in CH_2Cl_2 (25 mL), cooled to 0 °C, and TFA (3.98 mL, 51.6 mmol, 5.5 equiv.) was added slowly. The reaction was stirred for 2 h at 22 °C, H_2O (10 mL) was added, and the pH was adjusted to 10 with 2N NaOH. The reaction mixture was extracted with CH_2Cl_2 (3x20 mL), the combined organic phases were dried over Na_2SO_4, and the solvent was removed under reduced pressure. Amide **139** (1.55 g, 6.67 mmol, 71% over 2 steps) was obtained as a colorless solid without further purification.

The spectroscopic data are in accordance with the literature.[126]

^{1}H NMR (CD_3CN, 400 MHz): δ = 8.35 (s, 1H), 7.12 – 7.04 (m, 3H), 3.35 (dd, *J* = 9.9, 3.3 Hz, 1H), 3.05 (dtd, *J* = 12.5, 3.8, 1.3 Hz, 1H), 2.71 (ddd, *J* = 12.2, 10.6, 3.1 Hz, 1H), 2.16 (s, 6H), 1.98 – 1.94 (m, 1H), 1.83 – 1.76 (m, 1H), 1.66 – 1.53 (m, 2H), 1.52 – 1.41 (m, 2H) ppm.

(2*R*,2'*R*)-1,1'-(Propane-1,3-diyl)bis(*N*-(2,6-dimethylphenyl)piperidine-2-carboxamide) (140)

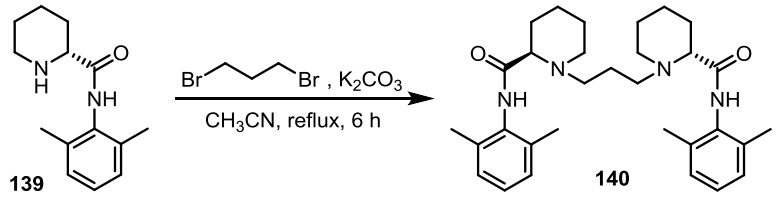

Diamine **140** was synthesized following a procedure of *Feng et al*.[127] K_2CO_3 (2.04 g, 14.8 mmol, 4.0 equiv.) and 1,3-dibromopropane (376 µL, 3.69 mmol, 1.0 equiv.) were added sequentially to a solution of amide **139** (1.71 g, 7.38 mmol, 2.0 equiv.) and CH_3CN (8 mL) and heated for 6 h under reflux. The reaction mixture was cooled to 22 °C, the solid was filtered off, and the solvent was removed under reduced pressure. After purification by column chromatography (SiO_2, CH_2Cl_2/MeOH 10:1) diamine **140** (1.50 g, 2.97 mmol, 81%) was obtained as a colorless solid.

^{1}H NMR ($CDCl_3$, 400 MHz): δ = 8.06 (s, 2H), 7.12 – 7.05 (m, 6H), 3.19 (d, *J* = 11.6 Hz, 2H), 2.90 – 2.83 (m, 2H), 2.84 – 2.77 (m, 2H), 2.30 – 2.16 (m, 14H), 2.12 – 2.07 (m, 2H), 2.06 – 1.99 (m, 2H), 1.93 – 1.86 (m, 2H), 1.77 (dt, *J* = 12.6, 3.8 Hz, 2H), 1.74 – 1.65 (m, 4H), 1.56 – 1.46 (m, 2H), 1.38 – 1.28 (m, 2H) ppm.

(1*S*,1'*S*,2*R*,2'*R*)-1,1'-(Propane-1,3-diyl)bis(2-((2,6-dimethylphenyl)carbamoyl)piperidine-1-oxide) (141)

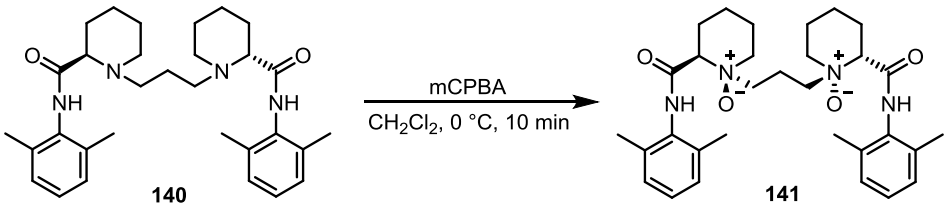

N,*N*'-dioxide **141** was synthesized following a procedure of *Feng et al*.[127] mCPBA (1.06 g, 6.12 mmol, 2.1 equiv.) was added to a 0 °C cold solution of diamine **140** (1.47 g, 2.91 mmol, 1.0 equiv.) and CH_2Cl_2 (15 mL) and stirred for 10 min at 0 °C. The solvent was removed under reduced pressure and after purification by column chromatography (SiO_2, CH_2Cl_2/MeOH 5:1 to 3:1) *N*,*N*'-dioxide **141** (1.18 g, 2.20 mmol, 76%) was obtained as a colorless solid.

mp = 91 °C

$[\boldsymbol{\alpha}]_{\boldsymbol{D}}^{\mathbf{24}}$ = +57.6° (*c* = 1.0, CH_2Cl_2)

^{1}H NMR ($CDCl_3$, 500 MHz): δ = 12.03 (s, 2H), 7.08 – 7.01 (m, 6H), 3.73 – 3.66 (m, 2H), 3.65 – 3.61 (m, 2H), 3.59 – 3.54 (m, 2H), 3.51 – 3.44 (m, 2H), 2.96 (td, *J* = 12.4, 2.9 Hz, 2H), 2.71 (p, *J* = 7.8 Hz, 2H), 2.61 (qd, *J* = 13.0, 3.8 Hz, 2H), 2.38 (qt, *J* = 13.0, 3.7 Hz, 2H), 2.20 (s, 12H), 2.14 – 2.11 (m, 2H), 1.90 (dt, *J* = 13.4, 3.8 Hz, 2H), 1.71 – 1.66 (m, 2H), 1.44 (qt, *J* = 13.2, 3.9 Hz, 2H) ppm.

^{13}C NMR ($CDCl_3$, 151 MHz): δ = 166.7, 134.3, 133.6, 128.4, 126.9, 76.3, 66.3, 64.7, 26.9, 22.4, 20.3, 19.1, 16.5 ppm.

IR (ATR): $\tilde{\nu}$ = 2926, 2857, 1673, 1520, 1471, 1440, 1376, 1266, 1212, 920, 770, 730 cm^{-1}.

HRMS (ESI, pos. mode): *m*/*z* calculated for $C_{31}H_{45}N_4O_4$ $[M+H]^+$: 537.3436, found 537.3456; *m*/*z* calculated for $C_{31}H_{44}N_4NaO_4$ $[M+Na]^+$: 559.3255, found 559.3246.

Methyl (1*R*,3*S*,4*R*)-1,4-diallyl-3-methyl-2-oxocyclopentane-1-carboxylate (125a)

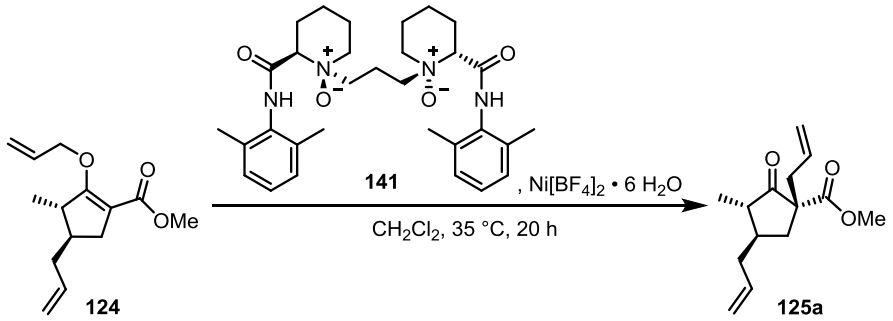

C-Allyl-β-keto ester **125a** was synthesized following a procedure of *Feng et al*.[120] $Ni[BF_4]_2$ (381 mg, 1.12 mmol, 5 mol%) was dissolved in THF (22 mL), added to a solution of ligand **141** (600 mg, 1.12 mmol, 5 mol%) and CH_2Cl_2 (22 mL), and stirred for 30 min at 35 °C. The solvent was removed under reduced pressure and the solid was added to a solution of *O*-allyl-β-keto ester **124** (5.28 g, 22.4 mmol, 1.0 equiv.) and CH_2Cl_2 (220 mL). The reaction mixture was stirred for 20 h at 35 °C and the solvent was subsequently removed under reduced pressure. After purification by column chromatography (SiO_2, CH_2Cl_2/*n*-pentane 4:1) *C*-allyl-β-keto ester **125a** (4.94 g, 20.9 mmol, 93%, dr = 10:1) was obtained as a colorless oil.

$[\boldsymbol{\alpha}]_{\boldsymbol{D}}^{\boldsymbol{26}}$ = +24.2° (*c* = 0.5, CH_2Cl_2)

^{1}H NMR ($CDCl_3$, 400 MHz): δ = 5.82 (ddt, *J* = 17.1, 10.2, 7.0 Hz, 1H), 5.69 – 5.54 (m, 1H), 5.14 – 5.03 (m, 4H), 3.68 (s, 3H), 2.67 (ddt, *J* = 13.9, 7.7, 1.1 Hz, 1H), 2.47 – 2.39 (m, 3H), 2.11 – 1.95 (m, 2H), 1.84 – 1.73 (m, 1H), 1.48 (dd, *J* = 13.4, 11.4 Hz, 1H), 1.12 (d, *J* = 6.9 Hz, 3H) ppm.

^{13}C NMR (CD_2Cl_2, 126 MHz): δ = 215.7, 171.6, 135.6, 133.0, 119.4, 117.0, 60.5, 52.7, 50.1, 41.4, 39.2, 38.3, 36.9, 13.5 ppm.

IR (ATR): $\tilde{\nu}$ = 3079, 2954, 2928, 1750, 1726, 1641, 1435, 1274, 1212, 1132, 994, 913, 731 cm^{-1}.

HRMS (ESI, pos. mode): *m*/*z* calculated for $C_{14}H_{20}NaO_3$ $[M+Na]^+$: 259.1304, found 259.1303.

Methyl (1*R*,6*R*,7*S*)-7-methyl-8-oxobicyclo[4.2.1]non-3-ene-1-carboxylate (126)

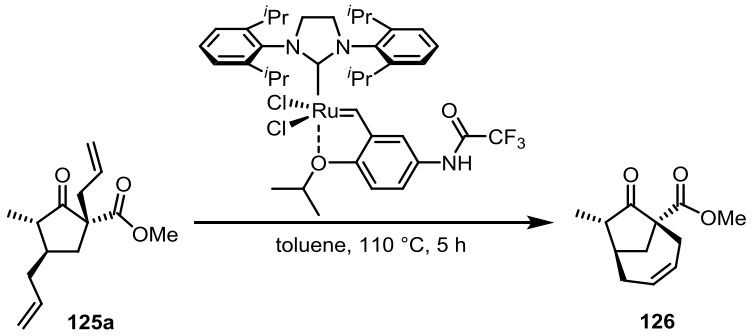

Umicore M71 SIPr (approximately 1 mg) was added to a solution of β-keto ester **125a** (20.0 mg, 84.6 µmol, dr = 10:1, 1.0 equiv.) and dry toluene (1.4 mL) and stirred in a pressure tube for 5 h at 110 °C. The solvent was removed under reduced pressure. After purification by column chromatography (SiO_2, *n*-pentane/EtOAc 30:1) bicycle **126** (12.0 mg, 57.6 µmol, 68%, 75% based on the main diastereomer) was obtained as a pale yellow solid.

mp = 66 °C

$[\boldsymbol{\alpha}]_{\boldsymbol{D}}^{\mathbf{24}}$ = +45.1° (*c* = 1.0, CH_2Cl_2)

^{1}H NMR ($CDCl_3$, 400 MHz): δ = 5.56 – 5.43 (m, 2H), 3.71 (s, 3H), 3.00 (dd, *J* = 12.8, 6.0 Hz, 1H), 2.85 (dd, *J* = 17.7, 5.0 Hz, 1H), 2.56 – 2.48 (m, 1H), 2.36 – 2.31 (m, 3H), 2.09 – 1.98 (m, 1H), 1.98 (dd, *J* = 13.4, 1.5 Hz, 1H), 1.22 (d, *J* = 7.8 Hz, 3H) ppm.

^{13}C NMR ($CDCl_3$, 151 MHz): δ = 220.0, 172.7, 126.9, 124.6, 58.7, 52.7, 49.4, 38.4, 38.1, 36.9, 36.6, 17.1 ppm.

IR (ATR): $\tilde{\nu}$ = 3011, 2953, 2919, 2875, 2832, 1747, 1727, 1456, 1432, 1263, 1237, 1202, 1070, 1027, 974, 867 cm^{-1}.

HRMS (ESI, pos. mode): *m*/*z* calculated for $C_{12}H_{16}NaO_3$ $[M+Na]^+$: 231.0991, found 231.0986.

Methyl (1*R*,4*R*)-1,4-diallyl-3-methyl-2-((trimethylsilyl)oxy)cyclopent-2-ene-1-carboxylate (117)

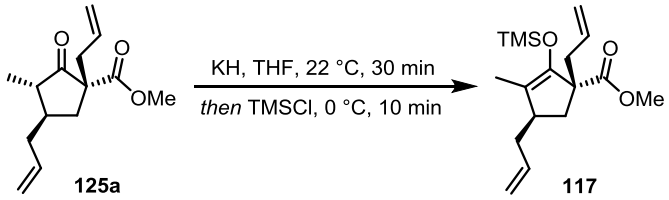

125a **117**

KH (30% in mineral oil; 638 mg, 4.77 mmol, 1.2 equiv.) was washed with dry *n*-pentane (3x5 mL) and the remaining solvent was removed under reduced pressure. A solution of ketone **125a** (940 mg, 3.98 mmol, 1.0 equiv.) and dry THF (25 mL) were added and the reaction mixture was stirred for 30 min at 22 °C. TMSCl (606 µL, 4.77 mmol, 1.2 equiv.) was added subsequently and stirring was continued for 10 min at 0 °C. Aqueous saturated $NaHCO_3$ solution (20 mL) was added to the reaction mixture, the aqueous phase was extracted with Et_2O (3x20 mL), the combined organic phases were dried over Na_2SO_4, and the solvent was removed under reduced pressure. Silyl enol ether **117** (1.16 g, 3.77 mmol, 95%) was obtained as a colorless oil without further purification.

^{1}H NMR (C_6D_6, 400 MHz): δ = 5.93 (dddd, *J* = 17.0, 10.2, 7.6, 6.7 Hz, 1H), 5.71 (ddt, *J* = 17.1, 10.2, 7.0 Hz, 1H), 5.12 – 4.99 (m, 4H), 3.33 (s, 3H), 2.91 (ddt, *J* = 13.8, 7.6, 1.2 Hz, 1H), 2.82 – 2.73 (m, 1H), 2.55 – 2.45 (m, 2H), 2.32 – 2.24 (m, 1H), 1.92 – 1.82 (m, 1H), 1.56 (dd, *J* = 13.2, 7.5 Hz, 1H), 1.49 (d, *J* = 1.2 Hz, 3H), 0.20 (s, 9H) ppm.

IR (ATR): $\tilde{\nu}$ = 3077, 2954, 2923, 2855, 1732, 1682, 1639, 1435, 1379, 1252, 1214, 1141, 991, 911, 844, 755 cm^{-1}.

HRMS (ESI, pos. mode): *m*/*z* calculated for $C_{17}H_{28}NaO_3Si$ $[M+Na]^+$: 331.1700, found 331,1704.

Ethyl 2-(2-phenyl-1,3-dioxolan-2-yl)-acetate (143)

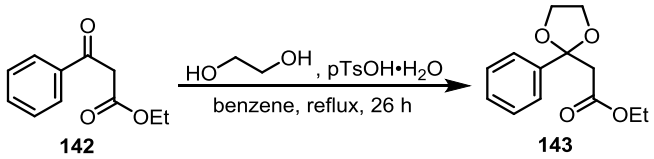

142 **143**

Acetal **143** was synthesized according to a procedure of *Kinoshita et al*.[128] β-Keto ester **143** (10.0 g, 52.0 mmol, 1.0 equiv.), ethylene glycol (7.56 mL, 135 mmol, 2.6 equiv.), and pTsOH•H_2O (108 mg, 624 µmol, 1.2 mol%) were dissolved in benzene (35 mL) and heated for 26 h under reflux. Water was continuously removed using a *Dean-Stark* trap. After cooling to 22 °C, the solution was washed with saturated aqueous $NaHCO_3$ solution (30 mL) and the aqueous phase was extracted with EtOAc (1x30 mL). The combined organic phases were washed with aqueous saturated NaCl solution (30 mL), the organic phase was dried over Na_2SO_4, and the solvent was removed under reduced pressure. After purification by column chromatography (SiO_2, *n*-pentane/EtOAc 10:1 to 3:1) acetal **143** (10.4 g, 44.0 mmol, 85%) was obtained as a colorless oil.

The spectroscopic data are in accordance with the literature.[128]

^{1}H NMR ($CDCl_3$, 400 MHz): δ = 7.52 – 7.48 (m, 2H), 7.37 – 7.27 (m, 3H), 4.11 – 4.04 (m, 4H), 3.90 – 3.74 (m, 2H), 2.97 (s, 2H), 1.15 (t, *J* = 7.1 Hz, 3H) ppm.

2-(2-Phenyl-1,3-dioxolan-2-yl)acetaldehyde (116)

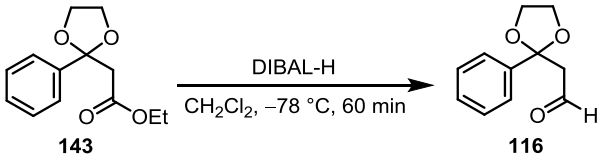

143 **116**

Aldehyde **116** was synthesized according to a procedure of *Davis et al.*[129] Acetal **143** (4.93 g, 20.9 mmol, 1.0 equiv.) was dissolved in dry CH_2Cl_2 (160 mL) and cooled to –78 °C. DIBAL-H (1M in CH_2Cl_2; 25.0 mL, 1.2 equiv.) was added while the temperature did not exceeded –70 °C throughout the procedure. After additional 60 min at –78 °C, 3M HCl (100 mL) was carefully added to the reaction and slowly warmed to 22 °C. The aqueous phase was extracted with CH_2Cl_2 (3x100 mL), the combined organic phases were dried over Na_2SO_4 and the solvent was removed under reduced pressure. Aldehyde **116** (3.86 g, 20.1 mmol, 96%) was obtained without further purification.

The spectroscopic data are in accordance to the literature.[129]

^{1}H NMR ($CDCl_3$, 400 MHz): δ = 9.77 (t, *J* = 2.9 Hz, 1H), 7.50 – 7.47 (m, 2H), 7.40 – 7.31 (m, 3H), 4.14 – 4.05 (m, 2H), 3.89 – 3.80 (m, 2H), 2.91 (d, *J* = 2.9 Hz, 2H) ppm.

Methyl (1*R*,3*R*,4*R*)-1,4-diallyl-3-((*S*)-1-hydroxy-3-oxo-3-phenylpropyl)-3-methyl-2-oxocyclopentane-1-carboxylate (127) and Methyl (1*R*,3*R*,4*R*)-1,4-diallyl-3-((*S*)-1-hydroxy-2-(2-phenyl-1,3-dioxolan-2-yl)ethyl)-3-methyl-2-oxocyclopentane-1-carboxylate (128)

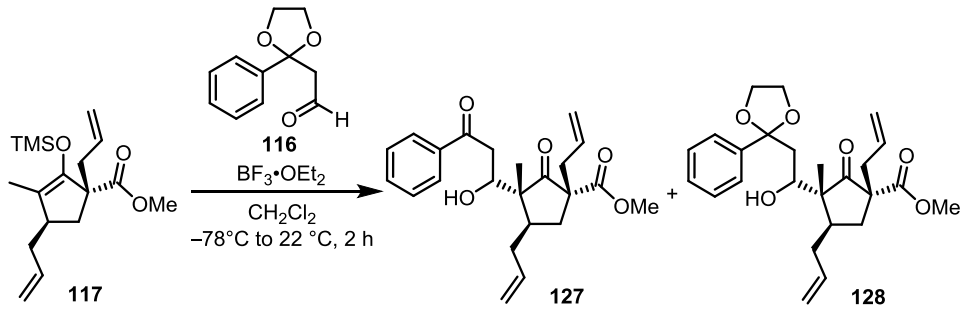

Aldehyde **116** (74.8 mg, 389 µmol, 1.0 equiv.) and silyl enol ether **117** (180 mg, 583 µmol, 1.5 equiv.) were dissolved in dry CH_2Cl_2 (15 mL) and cooled to –78 °C. BF_3•OEt_2 (247 µL, 1.95 mmol, 5.0 equiv.) was slowly added and the reaction mixture was warmed to 22 °C over 2 h. Aqueous saturated $NaHCO_3$ solution (10 mL) was added, the aqueous phase was extracted with CH_2Cl_2 (3x10 mL), the combined organic phases were dried over Na_2SO_4, and the solvent was removed under reduced pressure. After purification by column chromatography (SiO_2, *n*-pentane/EtOAc 10:1 to 5:1) ketone **127** (78.0 mg, 203 µmol, 52%) and acetal **128** (13.0 mg, 30.3 µmol, 8%) were obtained as colorless oils.

Ketone 127:

$[\boldsymbol{\alpha}]_{\boldsymbol{D}}^{\boldsymbol{26}}$ = +4.3° (*c* = 0.5, CH_2Cl_2)

^{1}H NMR ($CDCl_3$, 600 MHz): δ = 7.96 – 7.93 (m, 2H), 7.59 – 7.54 (m, 1H), 7.48 – 7.44 (m, 2H), 5.87 (ddt, *J* = 17.1, 10.1, 6.9 Hz, 1H), 5.60 (ddt, *J* = 17.2, 10.1, 7.3 Hz, 1H), 5.15 – 5.00 (m, 4H), 4.20 (d, *J* = 9.7 Hz, 1H), 3.67 (s, 3H), 3.52 (dd, *J* = 17.7, 10.3 Hz, 1H), 3.35 (s, 1H), 3.14 (dd, *J* = 17.7, 1.5 Hz, 1H), 2.84 – 2.77 (m, 1H), 2.75 (dd, *J* = 13.9, 7.9 Hz, 1H), 2.67 (dd, *J* = 13.1, 6.3 Hz, 1H), 2.44 – 2.36 (m, 1H), 2.33 (dd, *J* = 13.9, 6.9 Hz, 1H), 1.97 (dt, *J* = 14.1, 8.6 Hz, 1H), 1.35 (t, *J* = 12.9 Hz, 1H), 0.98 (s, 3H) ppm.

^{13}C NMR ($CDCl_3$, 151 MHz): δ = 217.1, 201.3, 169.8, 136.9, 136.8, 133.7, 133.0, 128.8, 128.2, 119.1, 116.3, 70.9, 62.4, 55.1, 52.9, 40.1, 40.0, 38.0, 35.0, 34.6, 15.3 ppm.

IR (ATR): $\tilde{\nu}$ = 3537, 3076, 2952, 2923, 2871, 1748, 1726, 1677, 1598, 1449, 1376, 1294, 1215, 993, 915, 754 cm^{-1}.

HRMS (ESI, pos. mode): *m*/*z* calculated for $C_{23}H_{29}O_5$ $[M+H]^+$: 385.1932, found 385.2002; *m*/*z* calculated for $C_{23}H_{28}NaO_5$ $[M+Na]^+$: 407.1829, found 407.1819; *m*/*z* calculated for $C_{23}H_{28}KO_5$ $[M+K]^+$: 423.1569, found 423.1557.

Acetal 128:

^{1}H NMR ($CDCl_3$, 400 MHz): δ = 7.43 – 7.40 (m, 2H), 7.36 – 7.29 (m, 3H), 5.91 – 5.76 (m, 1H), 5.56 (ddt, *J* = 17.3, 10.1, 7.4 Hz, 1H), 5.12 – 4.97 (m, 4H), 4.09 – 3.99 (m, 2H), 3.88 (dd, *J* = 10.6, 1.3 Hz, 1H), 3.83 (td, *J* = 7.4, 6.8, 5.1 Hz, 1H), 3.73 – 3.66 (m, 2H), 3.62 (s, 3H), 2.73 (dd, *J* = 13.9, 7.8 Hz, 1H), 2.69 – 2.60 (m, 2H), 2.39 – 2.28 (m, 2H), 2.30 – 2.19 (m, 1H), 2.00 (dd, *J* = 15.1, 1.3 Hz, 1H), 1.89 (dt, *J* = 14.1, 9.1 Hz, 1H), 1.25 – 1.24 (m, 1H), 0.85 (s, 3H) ppm.

HRMS (ESI, pos. mode): *m*/*z* calculated for $C_{25}H_{33}O_6$ $[M+H]^+$: 429.2272, found 429.2273; *m*/*z* calculated for $C_{25}H_{32}NaO_6$ $[M+Na]^+$: 451.2091, found 451.2095; *m*/*z* calculated for $C_{25}H_{32}KO_6$ $[M+K]^+$: 467.1831, found 467.1831.

Methyl (1*R*,3*R*,4*R*)-1,4-diallyl-3-methyl-2-oxo-3-((*E*)-3-oxo-3-phenylprop-1-en-1-yl)cyclopentan-1-carboxylate (115) (from ketone 127)

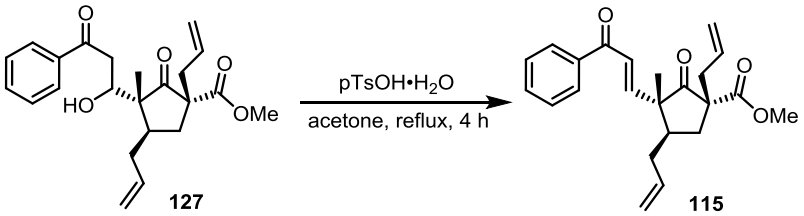

127 115

pTsOH•H_2O (4.95 mg, 26.0 µmol, 1.0 equiv.) was added to a solution of ketone **127** (10.0 mg, 26.0 µmol, 1.0 equiv.) and acetone (0.2 mL) and heated for 4 h under reflux. After cooling to 22 °C, the reaction was washed with aqueous saturated $NaHCO_3$ solution (0.5 mL), the aqueous phase was extracted with CH_2Cl_2 (3x0.5 mL), the combined organic phases were dried over Na_2SO_4, and the solvent was removed under reduced pressure. Enone **115** (10.0 mg, 27.3 µmol, quant.) was obtained as a colorless oil without further purification.

Methyl (1*R*,3*R*,4*R*)-1,4-diallyl-3-methyl-2-oxo-3-((*E*)-3-oxo-3-phenylprop-1-en-1-yl)cyclopentan-1-carboxylate (115) (from acetal 128)

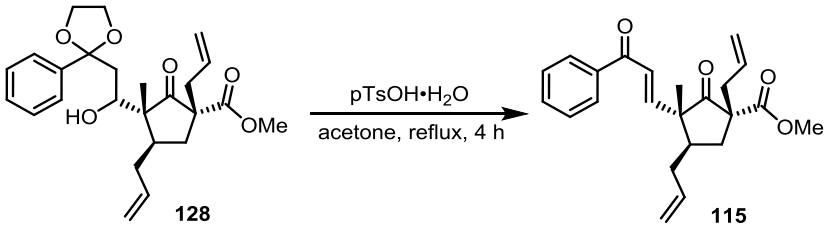

128 115

pTsOH•H_2O (9.77 mg, 51.3 µmol, 2.0 equiv.) was added to a solution of acetal **128** (11.0 mg, 25.7 µmol, 1.0 equiv.) and acetone (0.2 mL) and heated for 4 h under reflux. After cooling to 22 °C, the reaction was washed with aqueous saturated $NaHCO_3$ solution (0.5 mL), the aqueous phase was extracted with CH_2Cl_2 (3x0.5 mL), the combined organic phases were dried over Na_2SO_4, and the solvent was removed under reduced pressure. Enone **115** (10.0 mg, 27.3 µmol, quant.) was obtained as a colorless oil without further purification.

$[\boldsymbol{\alpha}]_{\boldsymbol{D}}^{\mathbf{24}}$ = –45.0° (*c* = 1.5, $CHCl_3$)

^{1}H NMR ($CDCl_3$, 400 MHz): δ = 7.95 – 7.90 (m, 2H), 7.59 – 7.54 (m, 1H), 7.50 – 7.44 (m, 2H), 6.97 (d, *J* = 15.7 Hz, 1H), 6.90 (d, *J* = 15.7 Hz, 1H), 5.78 (ddt, *J* = 17.1, 10.1, 6.9 Hz, 1H), 5.71 – 5.58 (m, 1H), 5.17 – 5.03 (m, 4H), 3.70 (s, 3H), 2.71 (ddt, *J* = 13.9, 7.9, 1.1 Hz, 1H), 2.57 – 2.46 (m, 3H), 2.33 – 2.24 (m, 1H), 2.08 – 1.98 (m, 1H), 1.67 – 1.57 (m, 1H), 1.14 (s, 3H) ppm.

^{13}C NMR ($CDCl_3$, 151 MHz): δ = 213.9, 190.6, 171.0, 150.1, 137.9, 135.9, 133.0, 132.8, 128.8, 128.7, 125.6, 119.8, 116.9, 61.4, 55.1, 53.0, 43.3, 39.0, 35.2, 34.5, 16.6 ppm.

IR (ATR): $\tilde{\nu}$ = 3077, 2977, 2952, 2840, 1750, 1730, 1670, 1616, 1447, 1295, 1219, 1178, 1017, 991, 917, 847 cm^{-1}.

HRMS (ESI, pos. mode): *m*/*z* calculated for $C_{23}H_{26}NaO_4$ $[M+Na]^+$: 389.1723, found 389.1741; *m*/*z* calculated for $C_{23}H_{26}KO_4$ $[M+K]^+$: 405.1463, found 405.1482.

Methyl (1*R*,3*R*,4*R*)-1,4-diallyl-3-methyl-2-oxo-3-((*R*)-1-oxo-1-phenylhex-5-en-3-yl)cyclopentane-1-carboxylate (129a; desired diastereomer) and Methyl (1*R*,3*R*,4*R*)-1,4-diallyl-3-methyl-2-oxo-3-((*S*)-1-oxo-1-phenylhex-5-en-3-yl)cyclopentane-1-carboxylate (129b; undesired diastereomer)

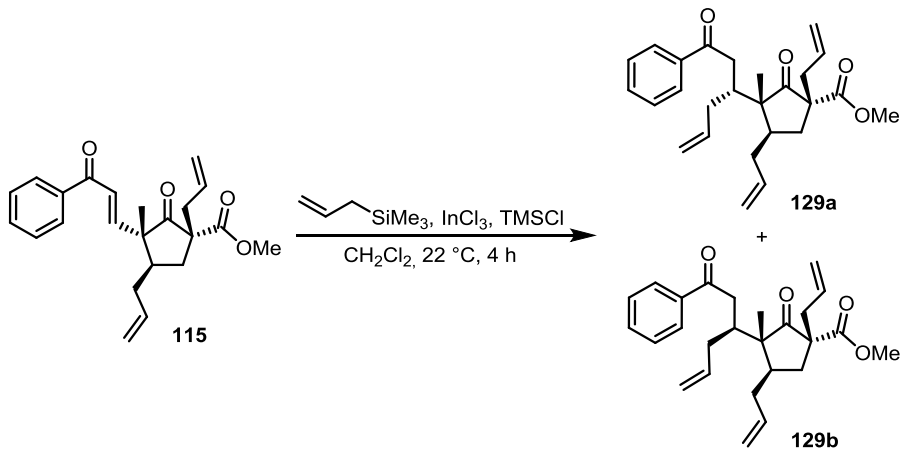

Triallyl **129a**/**b** was synthesized following a procedure of *Lee et al*.[122] Anhydrous $InCl_3$ (42.6 mg, 192 µmol, 15 mol%), TMSCl (814 µL, 6.41 mmol, 5.0 equiv.), and allyltrimethylsilane (306 µL, 1.92 mmol, 1.5 equiv.) were added sequentially to a solution of enone **115** (470 mg, 1.28 mmol, 1.0 equiv.) and dry CH_2Cl_2 (3.9 mL) and stirred for 4 h at 22 °C. The reaction was subsequently washed with saturated aqueous $NaHCO_3$ solution (4 mL) and the aqueous phase was extracted with CH_2Cl_2 (3x5 mL). The combined organic phases were dried over Na_2SO_4 and the solvent was removed under reduced pressure. After purification by column chromatography (SiO_2, *n*-pentane/EtOAc 30:1) triallyl **129a**/**b** (302 mg, 739 µmol, 58%, dr (**129a**:**129b**) = 1:2.4) was obtained as a colorless oil. The separation of the two diastereomers was performed by chiral HPLC. The stereoconfiguration of the two diastereomers was elucidated in the further course of the synthesis with the aid of X-ray crystal structure analysis.[121]

Mixture of the two diastereomers 129a and 129b:

IR (ATR): $\tilde{\nu}$ = 3075, 2952, 2925, 2868, 1723, 1686, 1639, 1447, 1375, 1293, 1222, 998, 911, 732 cm^{-1}.

HRMS (ESI, pos. mode): *m*/*z* calculated for $C_{26}H_{32}NaO_4$ $[M+Na]^+$: 431.2193, found 431.2208.

Desired diastereomer 129a:

^{1}H NMR ($CDCl_3$, 400 MHz): δ = 7.98 – 7.94 (m, 2H), 7.56 – 7.51 (m, 1H), 7.47 – 7.41 (m, 2H), 5.87 (dddd, *J* = 17.5, 10.1, 7.6, 6.0 Hz, 1H), 5.68 – 5.53 (m, 2H), 5.16 – 5.03 (m, 4H), 4.96 – 4.86 (m, 2H), 3.66 (s, 3H), 3.46 (dd, *J* = 18.2, 5.8 Hz, 1H), 2.94 (dd, *J* = 18.2, 5.4 Hz, 1H), 2.77 (ddt, *J* = 13.9, 7.5, 1.1 Hz, 1H), 2.68 – 2.59 (m, 2H), 2.53 – 2.38 (m, 2H), 2.31 – 2.24 (m, 2H), 1.99 – 1.84 (m, 1H), 1.75 (dt, *J* = 14.4, 9.7 Hz, 1H), 1.40 (dd, *J* = 13.3, 11.8 Hz, 1H), 0.89 (s, 3H) ppm.

Undesired diastereomer 129b:

^{1}H NMR ($CDCl_3$, 400 MHz): δ = 7.89 – 7.85 (m, 2H), 7.55 – 7.50 (m, 1H), 7.45 – 7.40 (m, 2H), 5.81 (dddd, *J* = 16.9, 10.1, 7.8, 6.0 Hz, 1H), 5.68 – 5.56 (m, 2H), 5.13 – 5.03 (m, 4H), 4.93 (dtd, *J* = 17.0, 1.9, 1.0 Hz, 1H), 4.82 (dddd, *J* = 10.1, 2.2, 1.6, 0.7 Hz, 1H), 3.64 (s, 3H), 2.98 (dd, *J* = 18.0, 4.4 Hz, 1H), 2.90 (dd, *J* = 18.0, 6.4 Hz, 1H), 2.76 (ddt, *J* = 13.9, 7.5, 1.1 Hz, 1H), 2.66 (ddt, *J* = 10.4, 6.4, 4.1 Hz, 1H), 2.58 (dd, *J* = 13.5, 6.6 Hz, 1H), 2.45 (dtd, *J* = 13.6, 3.8, 1.7 Hz, 1H), 2.38 – 2.10 (m, 4H), 1.94 – 1.83 (m, 1H), 1.39 (dd, *J* = 13.5, 11.9 Hz, 1H), 0.98 (s, 3H) ppm.

^{13}C NMR ($CDCl_3$, 176 MHz): δ = 217.5, 199.1, 170.3, 137.7, 137.4, 136.5, 133.1, 132.9, 128.6, 128.0, 119.1, 116.8, 116.5, 61.4, 54.7, 52.8, 40.5, 39.4, 38.0, 35.8, 35.5, 35.0, 16.6 ppm.

Methyl (1*R*,3*R*,4*R*)-1,4-diallyl-3-methyl-2-oxo-3-((*R*,*E*)-1-phenyl-1-((trimethylsilyl)oxy)-hexa-1,5-dien-3-yl)cyclopentane-1-carboxylate (130a; desired diastereomer) and Methyl (1*R*,3*R*,4*R*)-1,4-diallyl-3-methyl-2-oxo-3-((*S*,*E*)-1-phenyl-1-((trimethylsilyl)oxy)-hexa-1,5-dien-3-yl)cyclopentane-1-carboxylate (130b; undesired diastereomer)

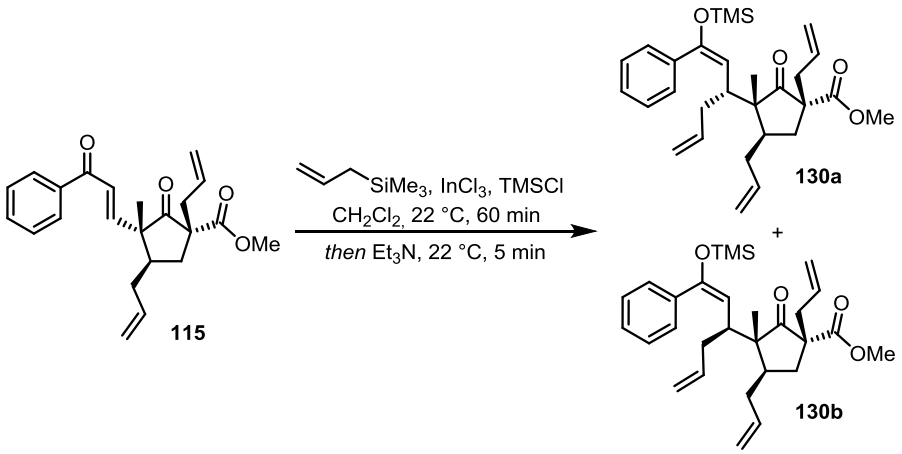

Anhydrous $InCl_3$ (60.4 mg, 273 µmol, 20 mol%), TMSCl (1.73 mL, 13.6 mmol, 10.0 equiv.), and allyltrimethylsilane (1.08 mL, 6.82 mmol, 5.0 equiv.) were added subsequently to a solution of enone **115** (500 mg, 1.36 mmol, 1.0 equiv.) and dry CH_2Cl_2 (4.0 mL) and stirred for 60 min at 22 °C. Dry Et_3N (1.90 mL, 13.6 mmol, 10.0 equiv.) was then added and stirring was continued for 5 min at 22 °C. *n*-Pentane (4 mL) was added and the precipitated solid was filtered over a short plug of Celite®. The filtrate was washed with aqueous saturated $NaHCO_3$ solution (8 mL), the aqueous phase was extracted with CH_2Cl_2 (3x8 mL), the combined organic phases were dried over Na_2SO_4, and the solvent was removed under reduced pressure. After purification by column chromatography (SiO_2, *n*-pentane/EtOAc 100:1 to 50:1) silyl enol ether **130a**/**b** (410 mg, 853 µmol, 63%, dr (**130a**:**130b**) = 1:2) was obtained as a colorless oil. The two diastereomers could be separated by column chromatography at a later stage of the synthesis.[121]

^{1}H NMR (CD_2Cl_2, 500 MHz): δ = 7.44 – 7.38 (m, 2H, major & minor), 7.32 – 7.22 (m, 3H, major &minor), 5.97 – 5.84 (m, 1H, major & minor), 5.82 – 5.70 (m, 1H, major & minor), 5.66 – 5.51 (m, 1H, major & minor), 5.11 (d, *J* = 10.4 Hz, 1H, minor), 5.10 – 4.92 (m, 6H, major & minor), 4.66 (d, *J* = 10.6 Hz, 1H, major), 3.56 (s, 3H, minor), 3.07 (s, 3H, major), 2.82 – 1.81 (m, 10H, major & minor), 1.37 (dd, *J* = 13.4, 11.5 Hz, 1H, minor), 1.30 (t, *J* = 12.7 Hz, 1H, major), 0.97 (s, 3H, major), 0.94 (s, 3H, minor), 0.09 (s, 9H, minor), 0.08 (s, 9H, major) ppm.

^{13}C NMR (CD_2Cl_2, 176 MHz): δ = 218.2 (major), 217.0 (minor), 170.5 (minor), 169.7 (major), 152.6 (major), 151.6 (minor), 140.2 (minor), 140.1 (major), 138.9 (major), 138.5 (minor), 138.0 (major), 137.6 (minor), 134.0 (minor), 133.9 (major), 128.6 (minor), 128.5 (major), 128.4 (major), 128.2 (minor), 126.6

(major), 126.6 (minor), 118.9 (minor), 118.8 (major), 116.3 (minor), 115.9 (major), 115.9 (minor), 115.8 (major), 112.5 (major), 111.9 (minor), 62.5 (major), 61.9 (minor), 56.2 (major), 55.8 (minor), 52.9 (minor), 52.5 (major), 42.1 (minor), 41.9 (major), 41.2 (major), 41.1 (minor), 40.4 (minor), 39.6 (major), 36.1 (minor), 35.6 (minor), 35.4 (major), 35.4 (major), 35.2 (minor), 34.8 (major), 17.9 (major), 16.7 (minor), 1.3 (minor), 1.2 (major) ppm.

IR (ATR): $\tilde{\nu}$ = 3076, 2953, 2925, 2870, 1726, 1641, 1445, 1346, 1252, 1210, 1082, 911, 887, 840, 758 cm^{-1}.

HRMS (ESI, pos. mode): *m/z* calculated for $C_{29}H_{40}NaO_4Si$ $[M+Na]^+$: 503.2588, found 503.2610.

Methyl (1*R*,3*R*,4*R*)-1,4-diallyl-3-methyl-2-oxo-3-((*E*)-3-oxo-3-phenylprop-1-en-1-yl)cyclopentane-1-carboxylate (115) (from enone 120)

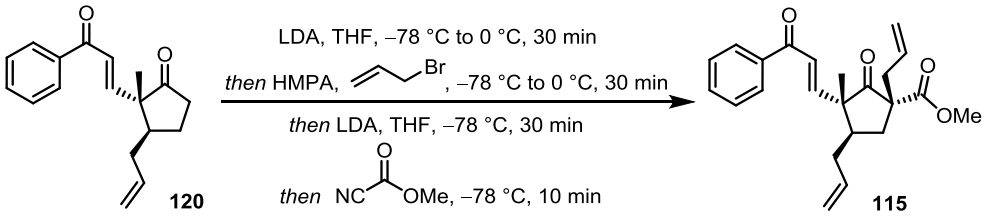

Freshly prepared LDA (0.52 M in THF; 790 µL, 410 µmol, 1.1 equiv.) was slowly added to a –78 °C cold solution of enone **120**[121] (100 mg, 373 µmol, 1.0 equiv.) and dry THF (4.2 mL) and stirred for 30 min at –78 °C. HMPA (700 µL) and allyl bromide (35.4 µL, 410 µmol, 1.1 equiv.) were added subsequently and the reaction was stirred for another 30 min at –78 °C. LDA (0.52 M in THF; 790 µL, 410 µmol, 1.1 equiv.) was added again and the reaction was stirred for 30 min at –78 °C. Methyl cyanoformate (59.2 µL, 745 µmol, 2.0 equiv.) was added and the reaction mixture was stirred for additional 10 min at –78 °C. H_2O (5 mL) was then added to the reaction, the aqueous phase was extracted with Et_2O (3x5 mL), the combined organic phases were dried over Na_2SO_4, and the solvent was removed under reduced pressure. After purification by column chromatography (SiO_2, *n*-pentane/EtOAc 10:1) enone **115** (62.0 mg, 169 µmol, 45%) was obtained as a colorless oil.

The spectroscopic data are in accordance with the previous synthesized enone **115**.

2-Allyl-1,3,2-dioxaborinane (136)

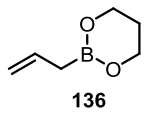

136

(*S*)-1-Allyl-2-iodocyclopent-2-en-1-ol (122)

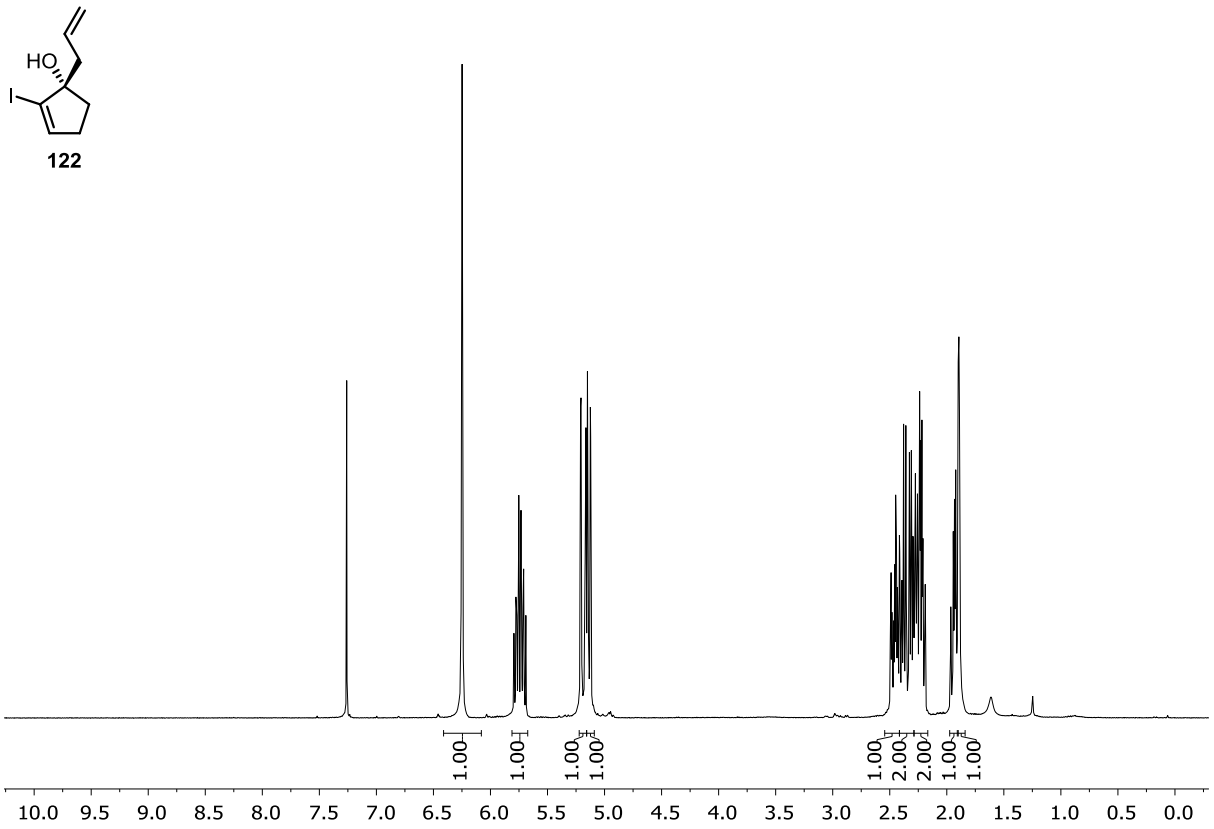

(*S*)-3,3'-Dibromo-[1,1'-binaphthalene]-2,2'-diol (137) (reisolated)

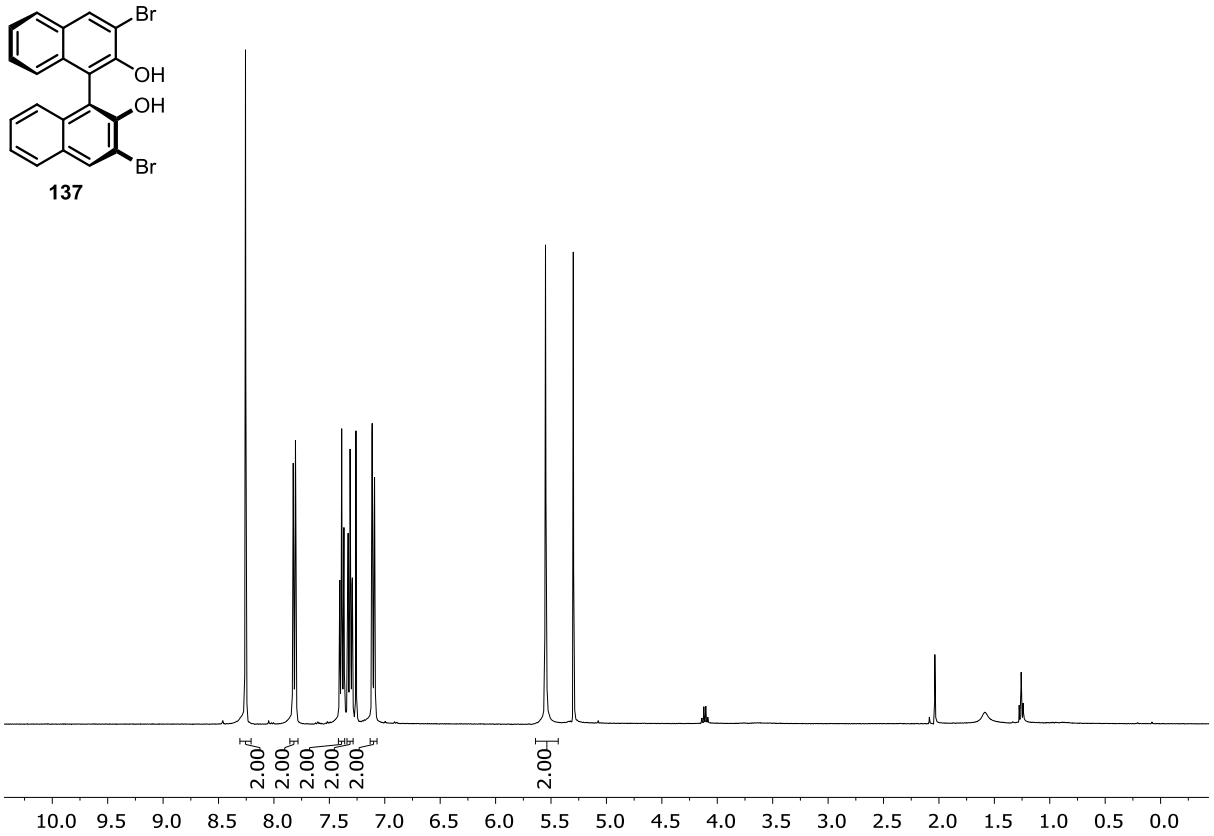

1-Allyl-2-iodocyclopent-2-en-1-ol (rac-122)

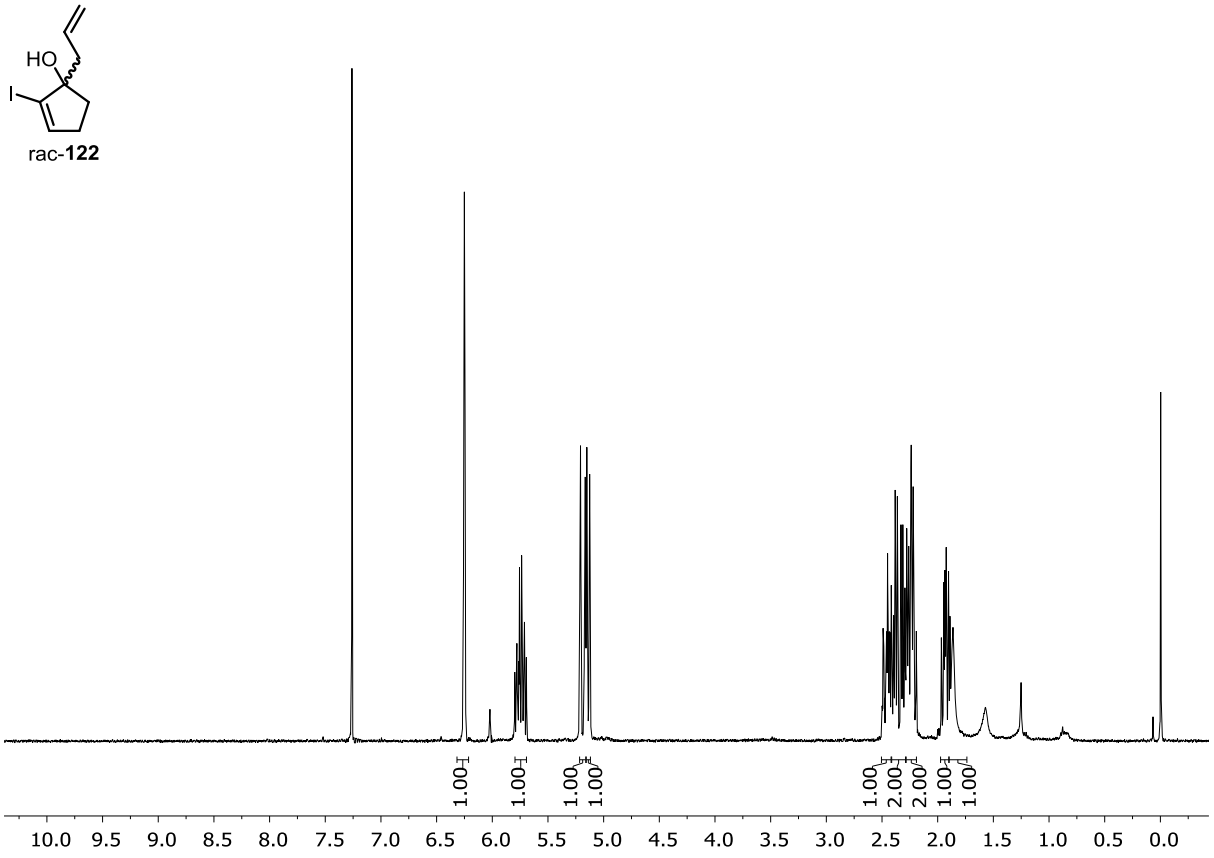

(*S*)-1-Allyl-2-methylcyclopent-2-en-1-ol (123)

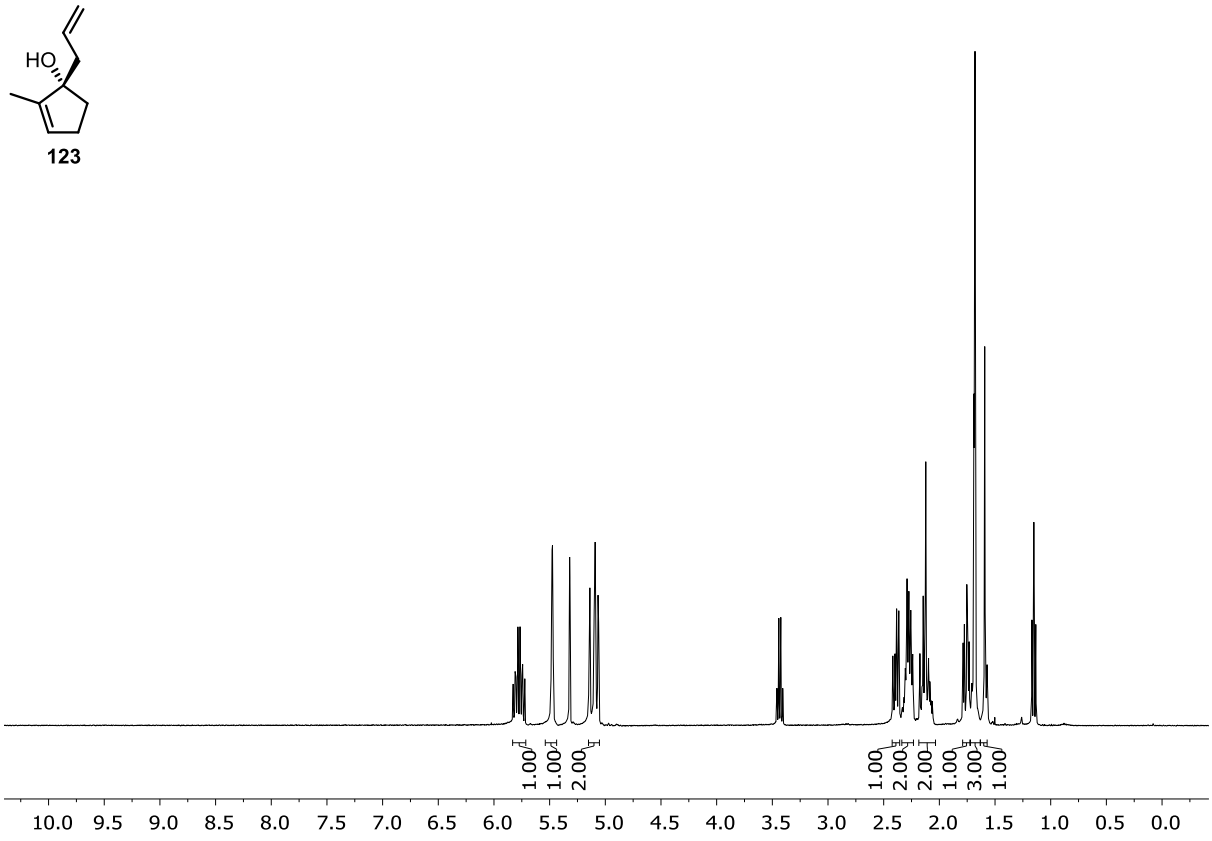

Methyl (3*S*,4*R*)-4-allyl-3-methyl-2-oxocyclopentane-1-carboxylate (118)

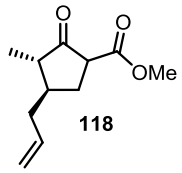

118

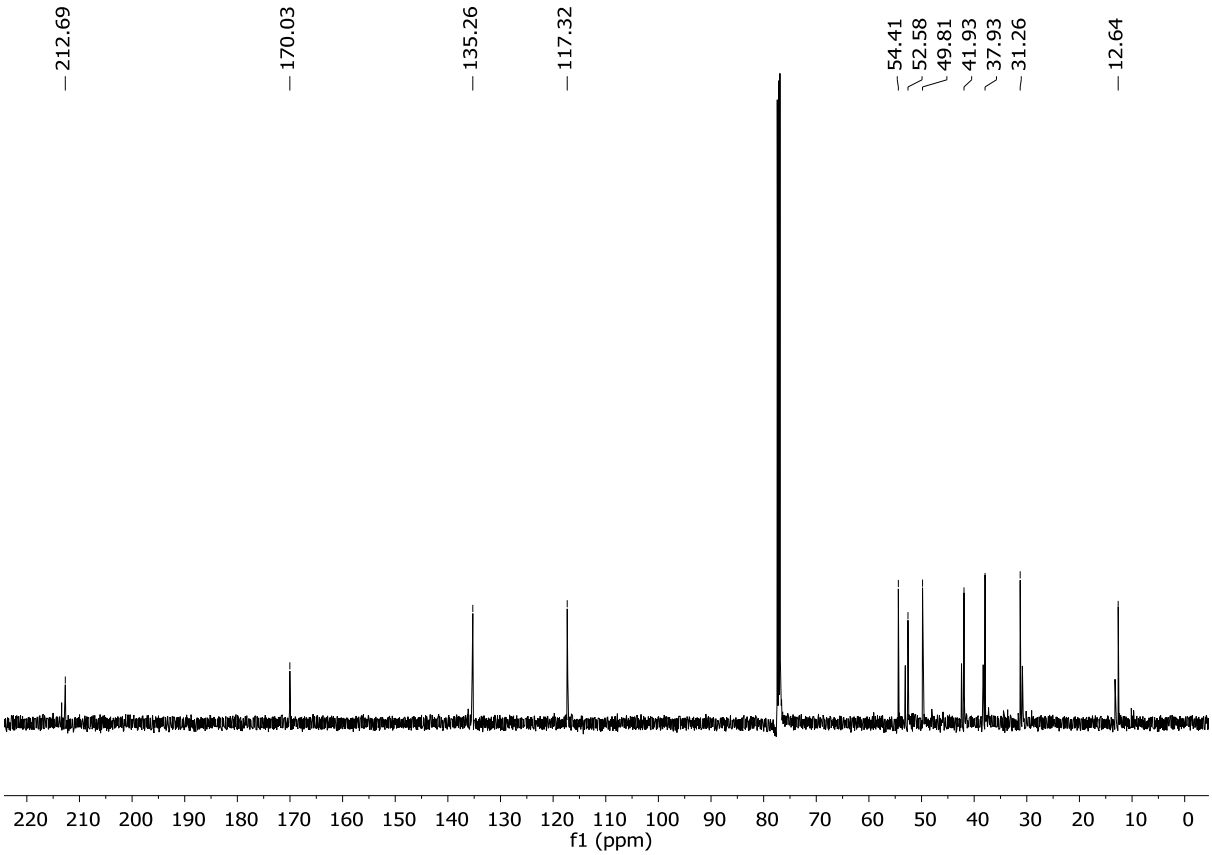

Mixture of *O*-Allyl-β-keto ester 124 and *C*-Allyl-β-keto ester 125a und 125b

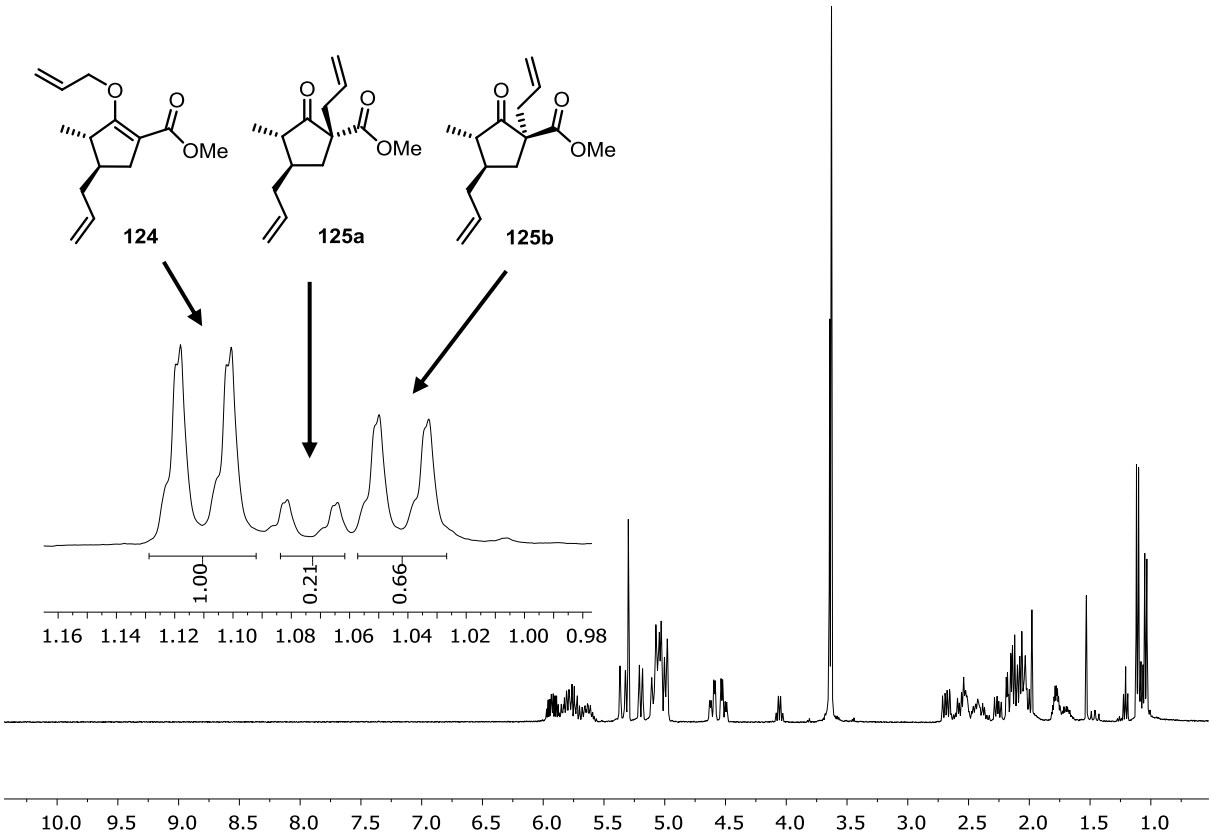

***C*-Allyl-β-ketoester 125a and 125b**

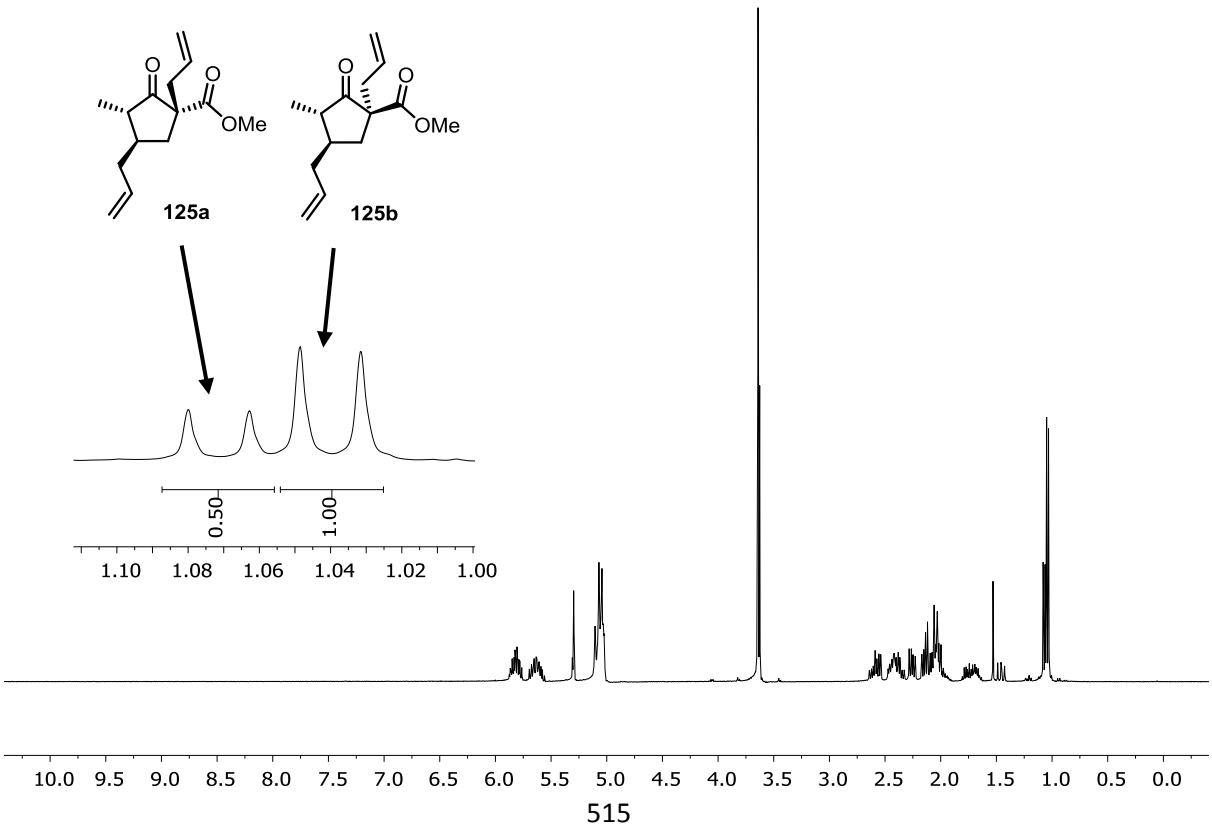

Methyl (3*S*,4*R*)-4-allyl-2-(allyloxy)-3-methylcyclopent-1-en-1-carboxylate (124)

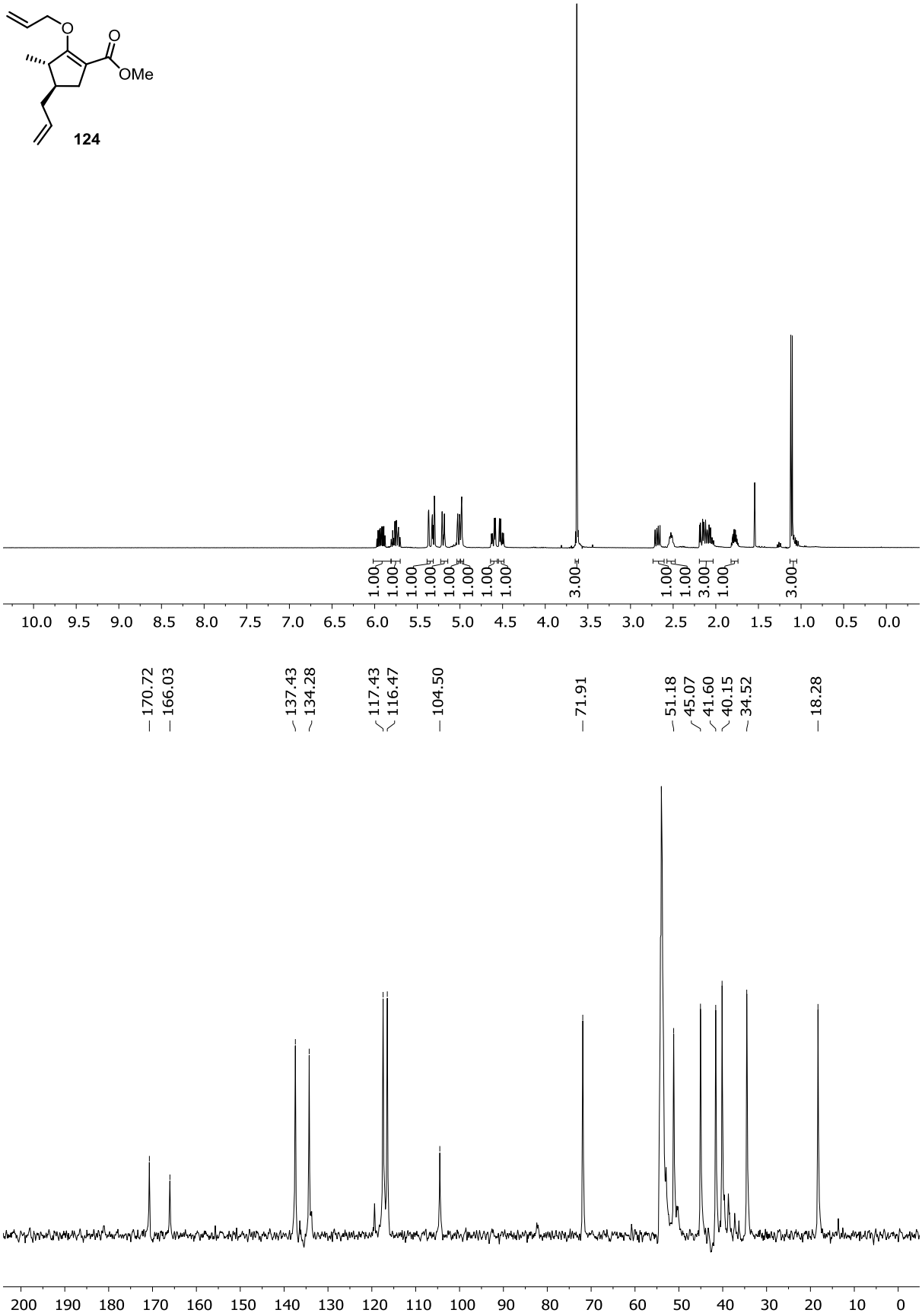

(*R*)-*N*-(2,6-Dimethylphenyl)-piperidine-2-carboxamide (139)

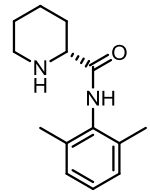

139

(2*R*,2'*R*)-1,1'-(Propane-1,3-diyl)bis(*N*-(2,6-dimethylphenyl)piperidine-2-carboxamide) (140)

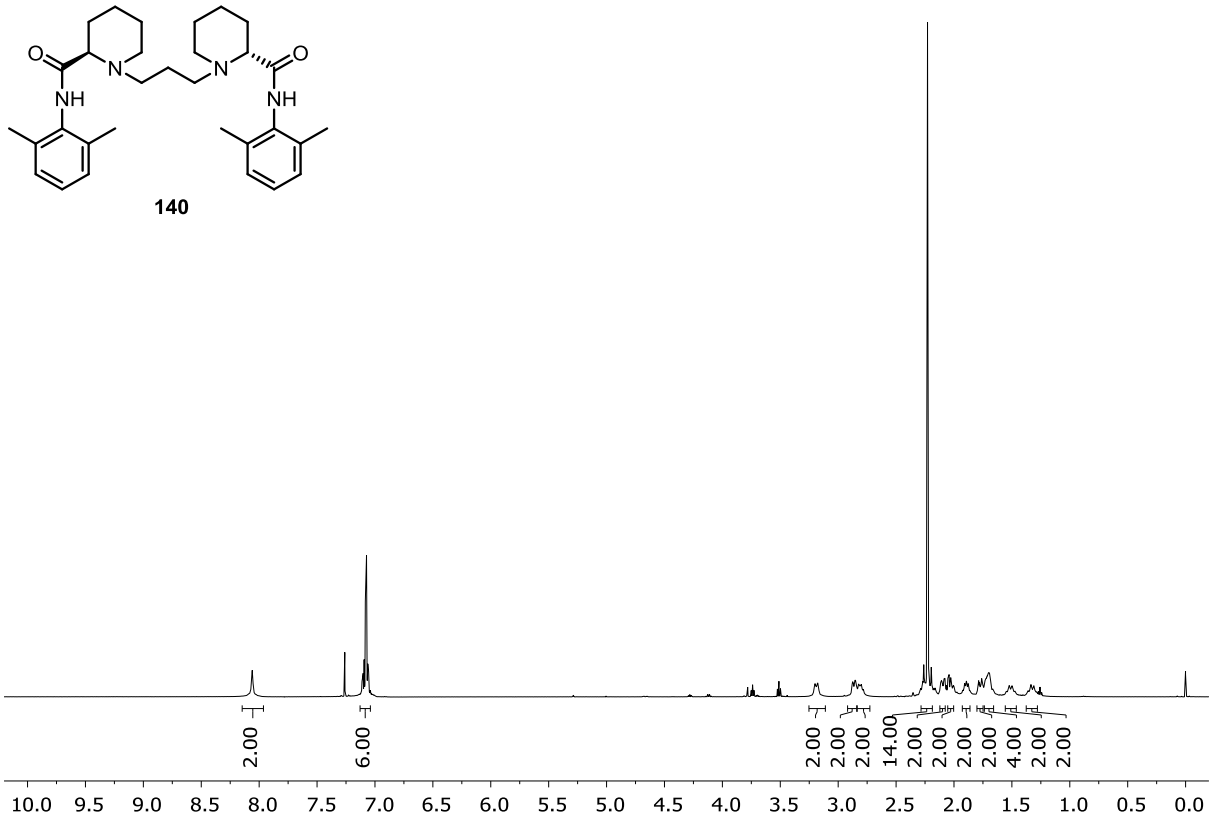

(1*S*,1'*S*,2*R*,2'*R*)-1,1'-(Propane-1,3-diyl)bis(2-((2,6-dimethylphenyl)carbamoyl)-piperidine 1-oxide) (141)

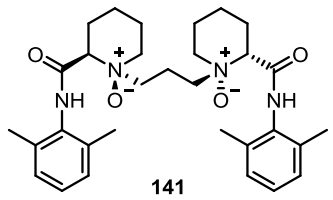

141

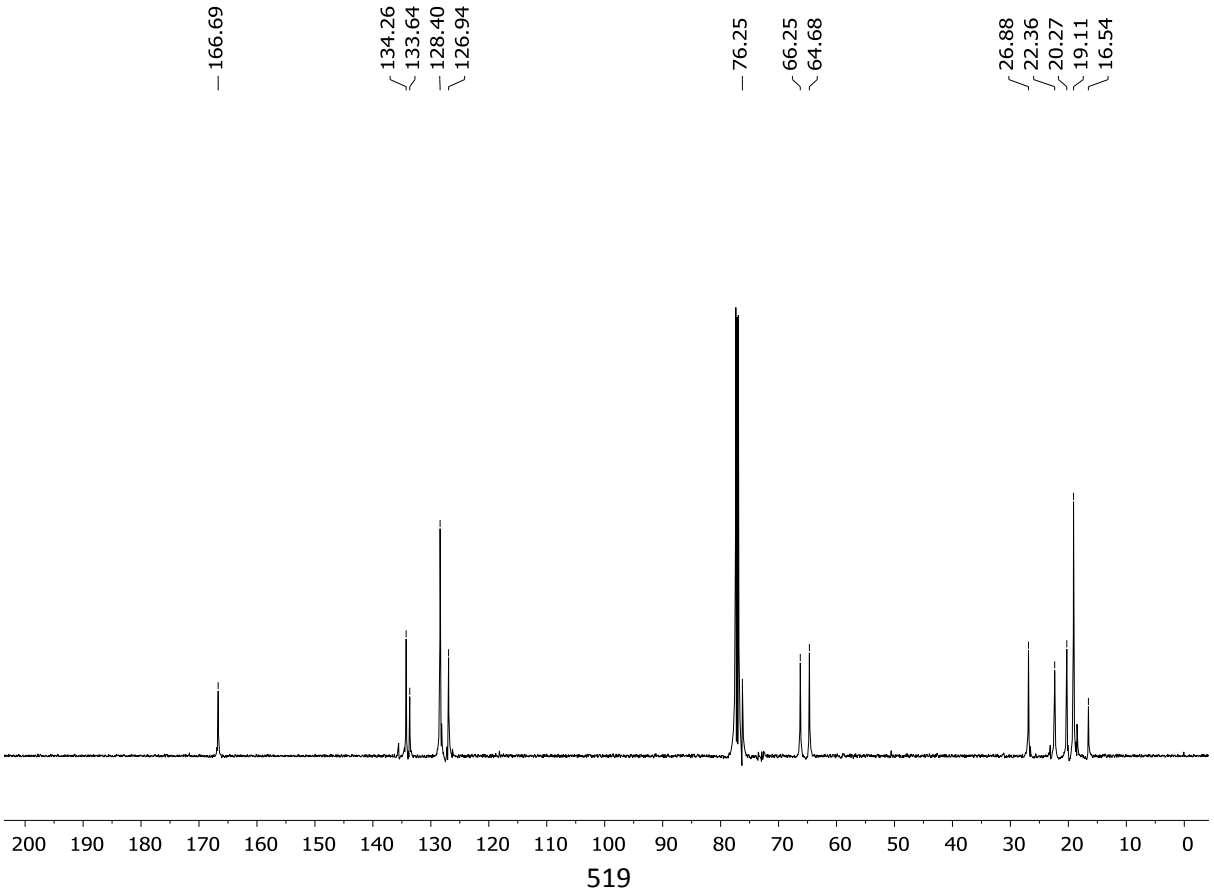

Methyl (1*R*,3*S*,4*R*)-1,4-diallyl-3-methyl-2-oxocyclopentane-1-carboxylate (125a)

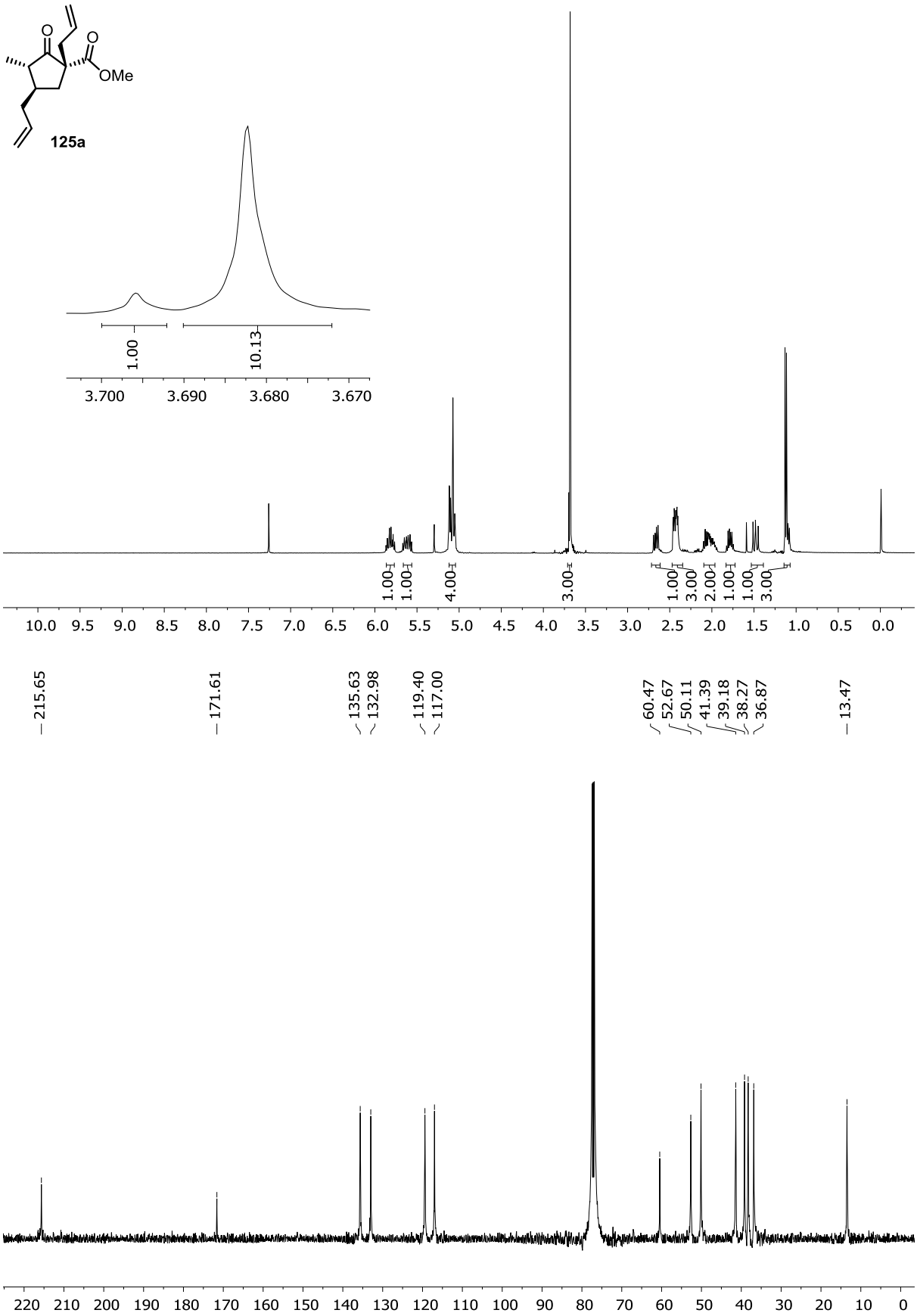

Methyl (1*R*,6*R*,7*S*)-7-methyl-8-oxobicyclo[4.2.1]non-3-ene-1-carboxylate (126)

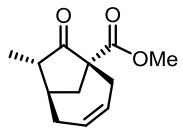

126

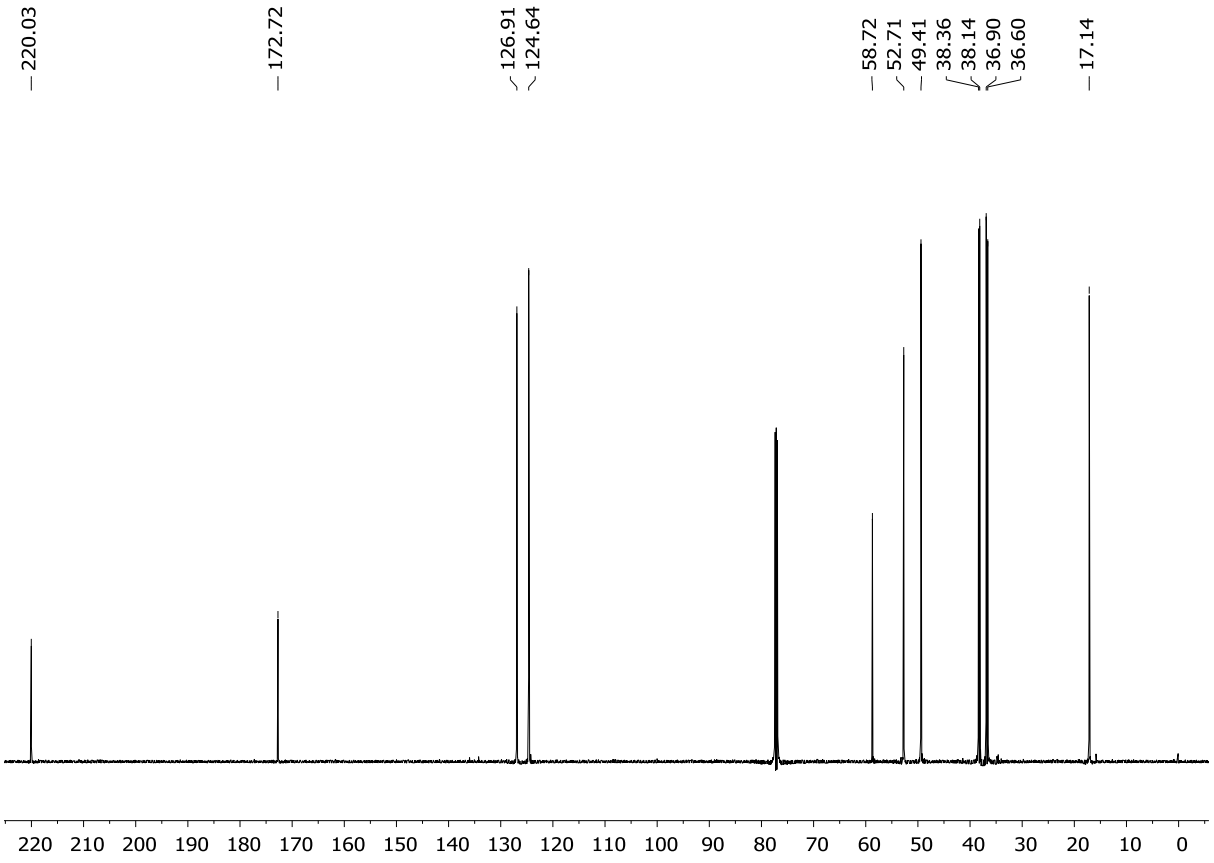

Methyl (1*R*,4*R*)-1,4-diallyl-3-methyl-2-((trimethylsilyl)oxy)cyclopent-2-ene-1-carboxylate (117)

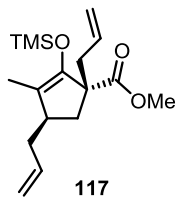

117

Ethyl 2-(2-phenyl-1,3-dioxolan-2-yl)acetate (143)

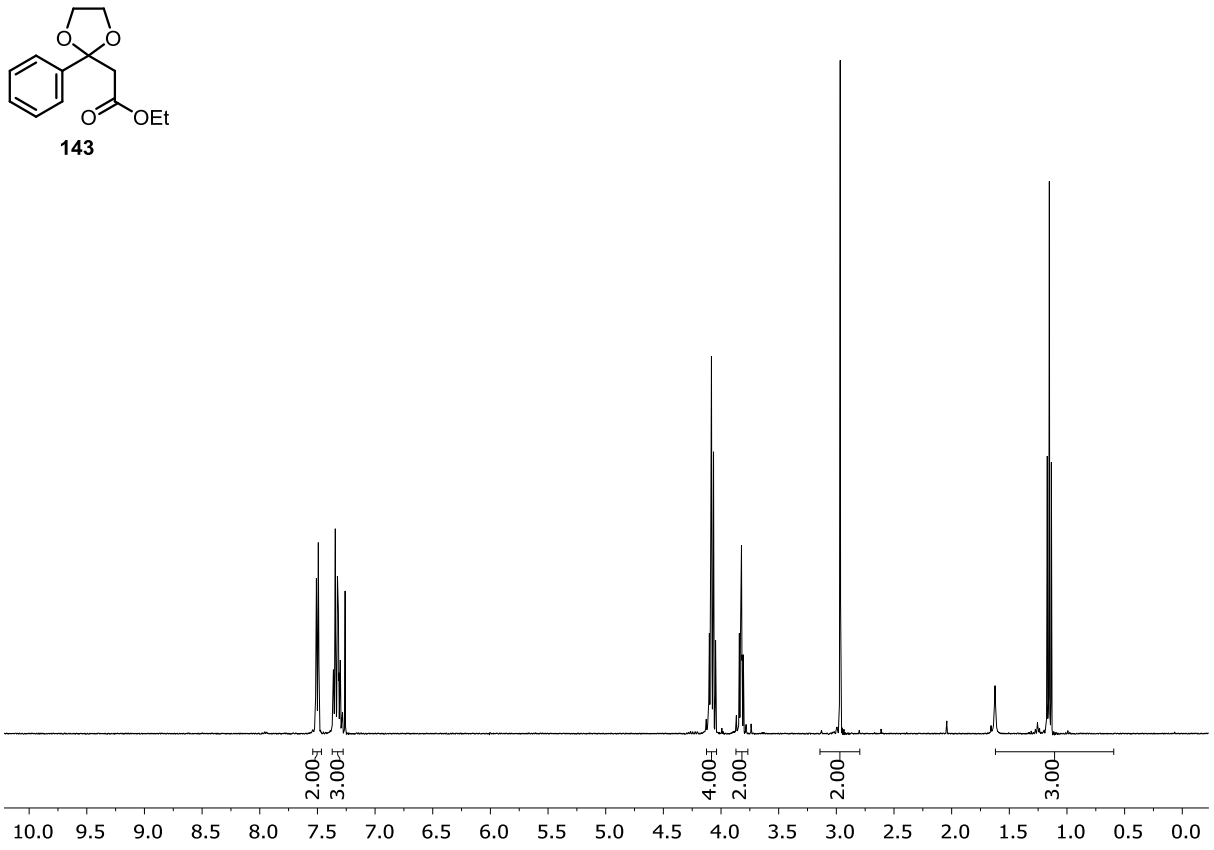

2-(2-Phenyl-1,3-dioxolan-2-yl)acetaldehyde (116)

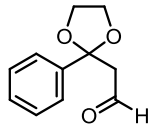

116

Methyl (1*R*,3*R*,4*R*)-1,4-diallyl-3-((*S*)-1-hydroxy-3-oxo-3-phenylpropyl)-3-methyl-2-oxocyclopentane-1-carboxylate (127)

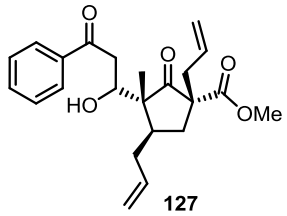

127

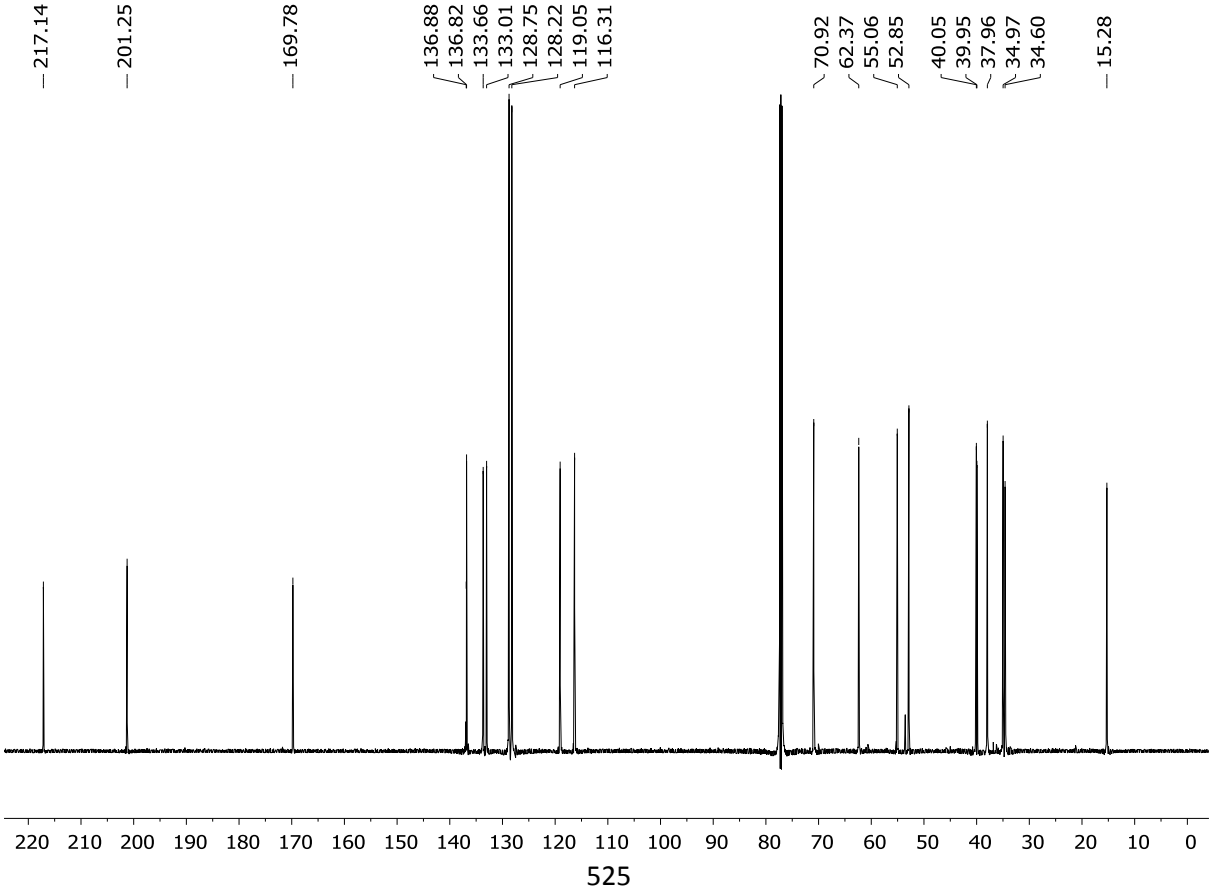

Methyl (1*R*,3*R*,4*R*)-1,4-diallyl-3-((*S*)-1-hydroxy-2-(2-phenyl-1,3-dioxolan-2-yl)ethyl)-3-methyl-2-oxocyclopentane-1-carboxylate (128)

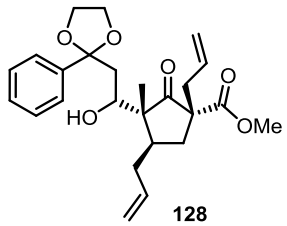

128

Methyl (1*R*,3*R*,4*R*)-1,4-diallyl-3-methyl-2-oxo-3-((*E*)-3-oxo-3-phenylprop-1-en-1-yl)cyclopentane-1-carboxylate (115)

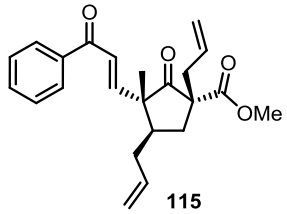

115

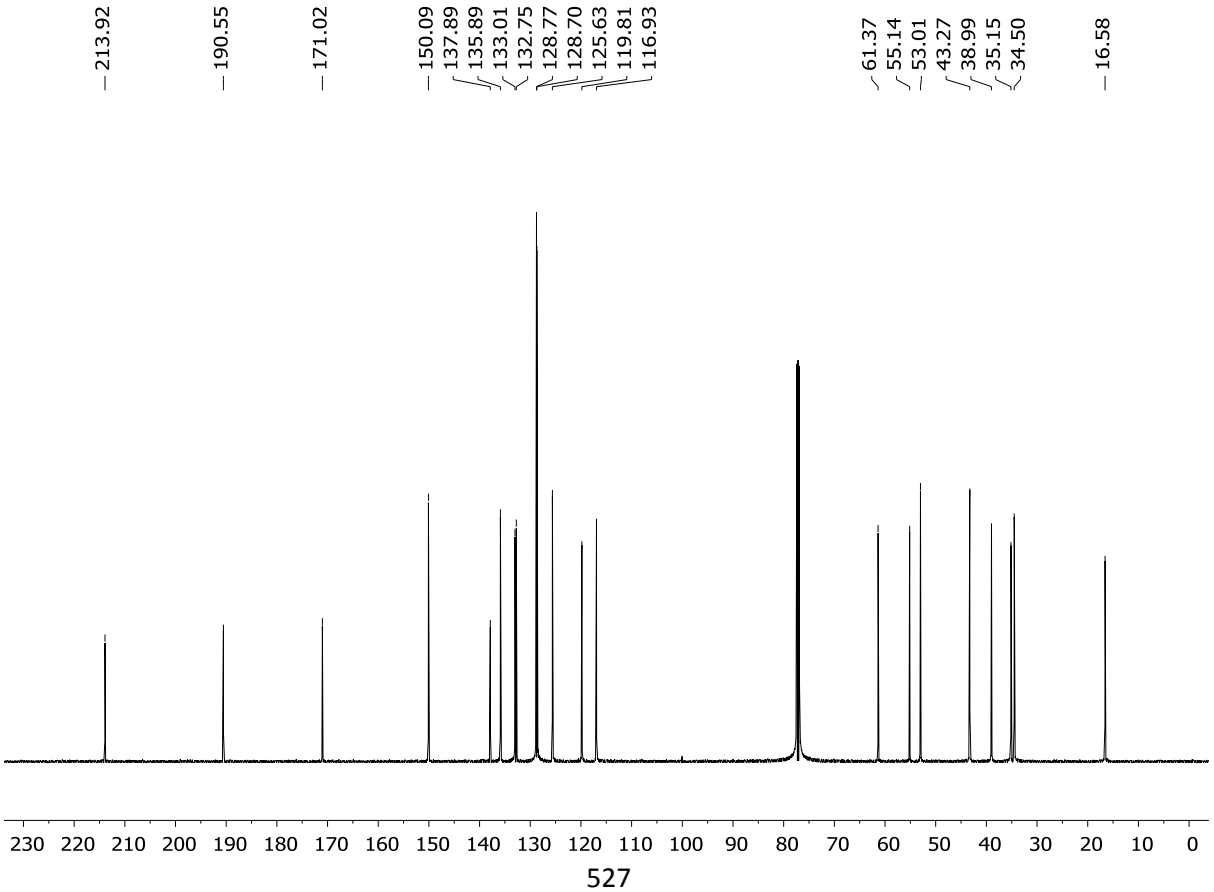

Mixture of the two diastereomers 129a and 129b

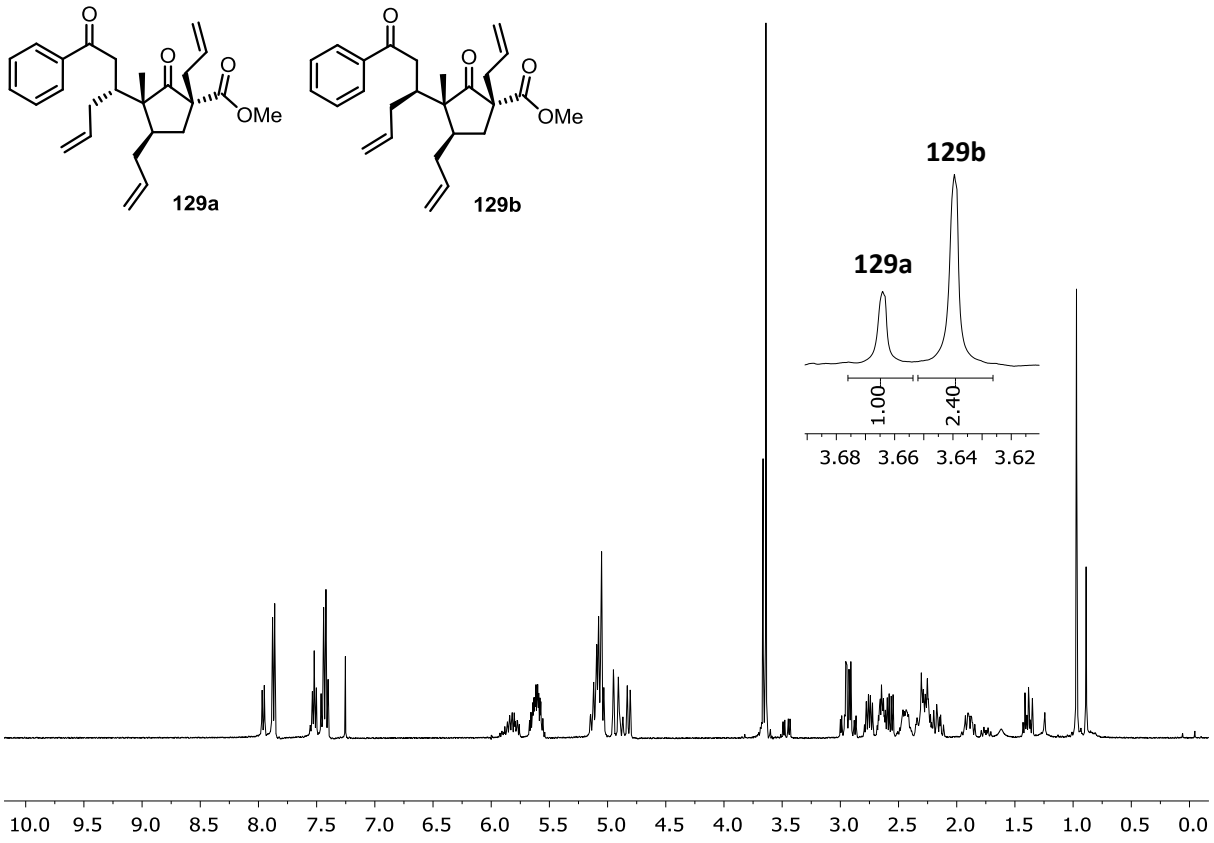

Methyl (1*R*,3*R*,4*R*)-1,4-diallyl-3-methyl-2-oxo-3-((*R*)-1-oxo-1-phenylhex-5-en-3-yl)cyclopentane-1-carboxylate (129a; desired diastereomer)

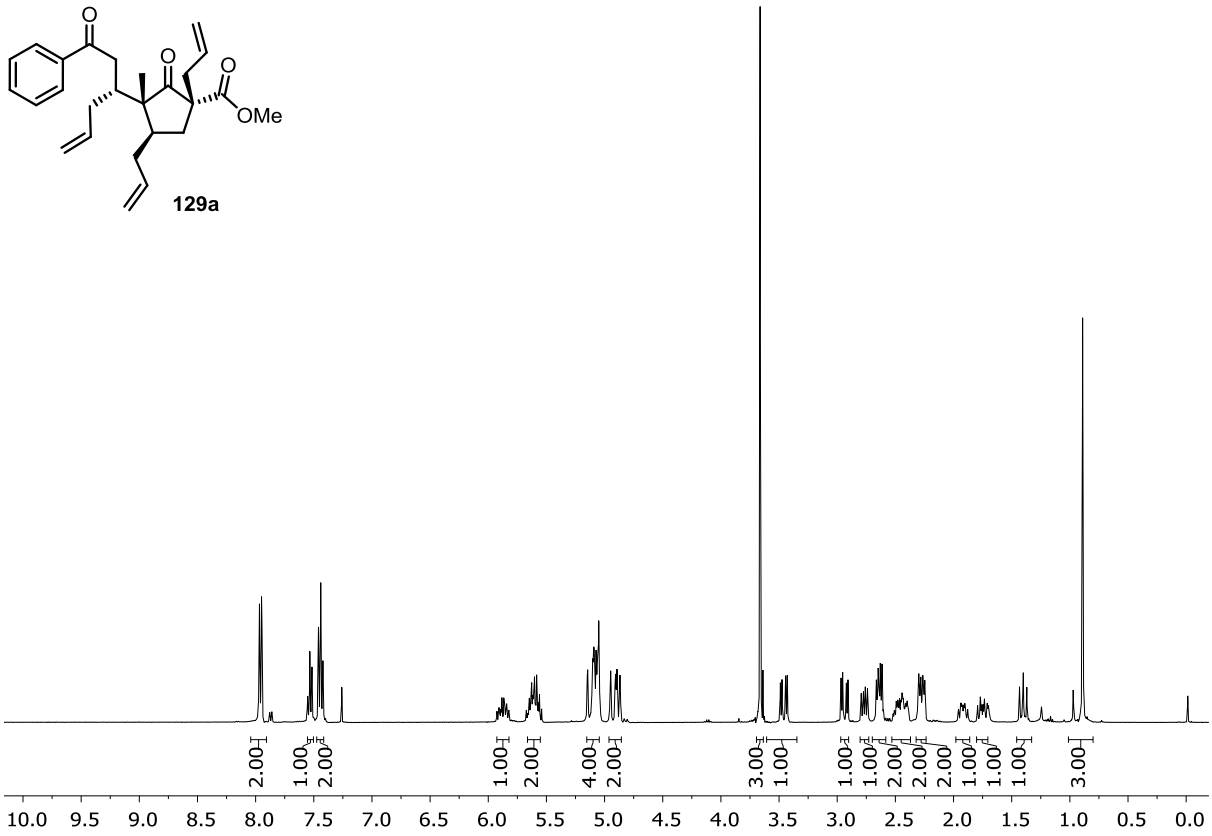

Methyl (1*R*,3*R*,4*R*)-1,4-diallyl-3-methyl-2-oxo-3-((*S*)-1-oxo-1-phenylhex-5-en-3-yl)cyclopentane-1-carboxylate (129b; undesired diastereomer)

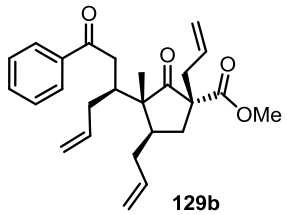

129b

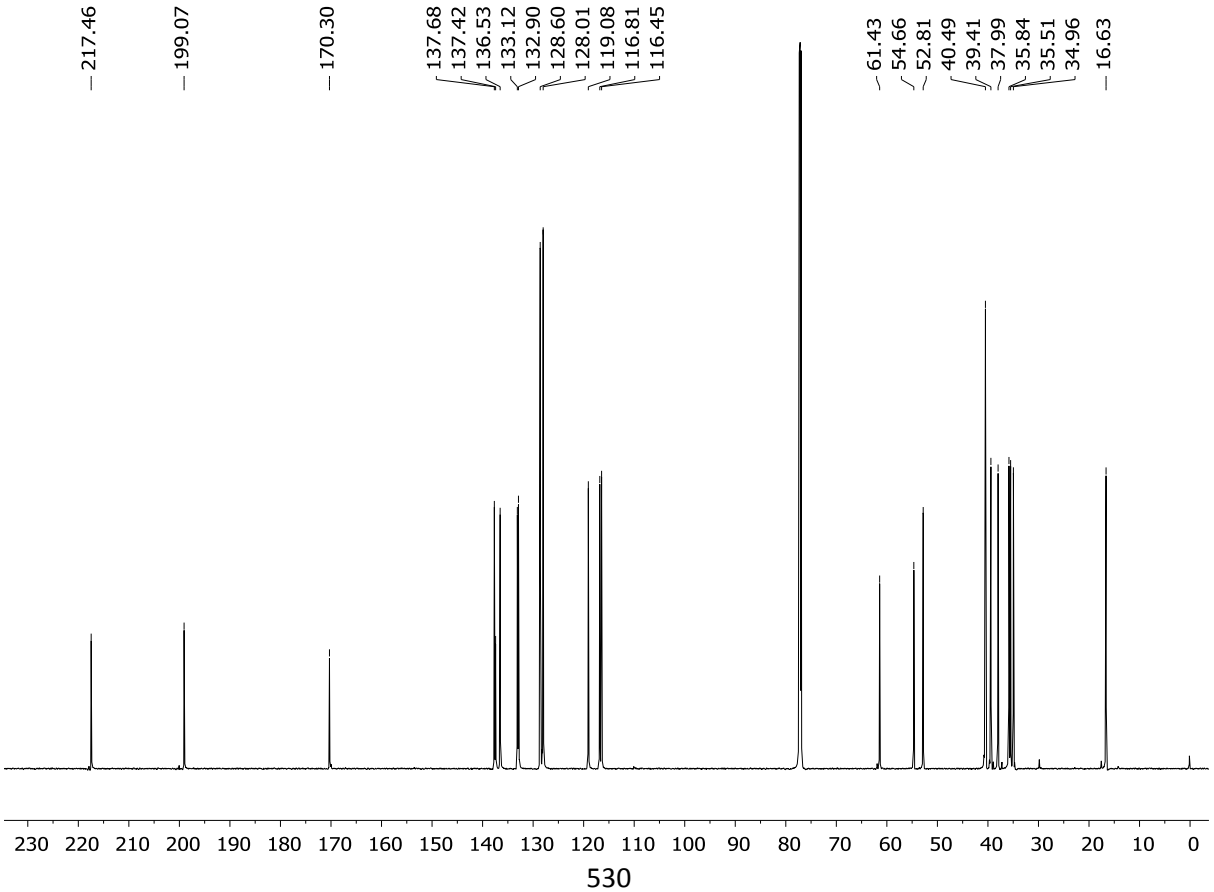

Methyl (1*R*,3*R*,4*R*)-1,4-diallyl-3-methyl-2-oxo-3-((*E*)-1-phenyl-1-((trimethylsilyl)oxy)hexa-1,5-dien-3-yl)cyclopentane-1-carboxylate (130a/b)

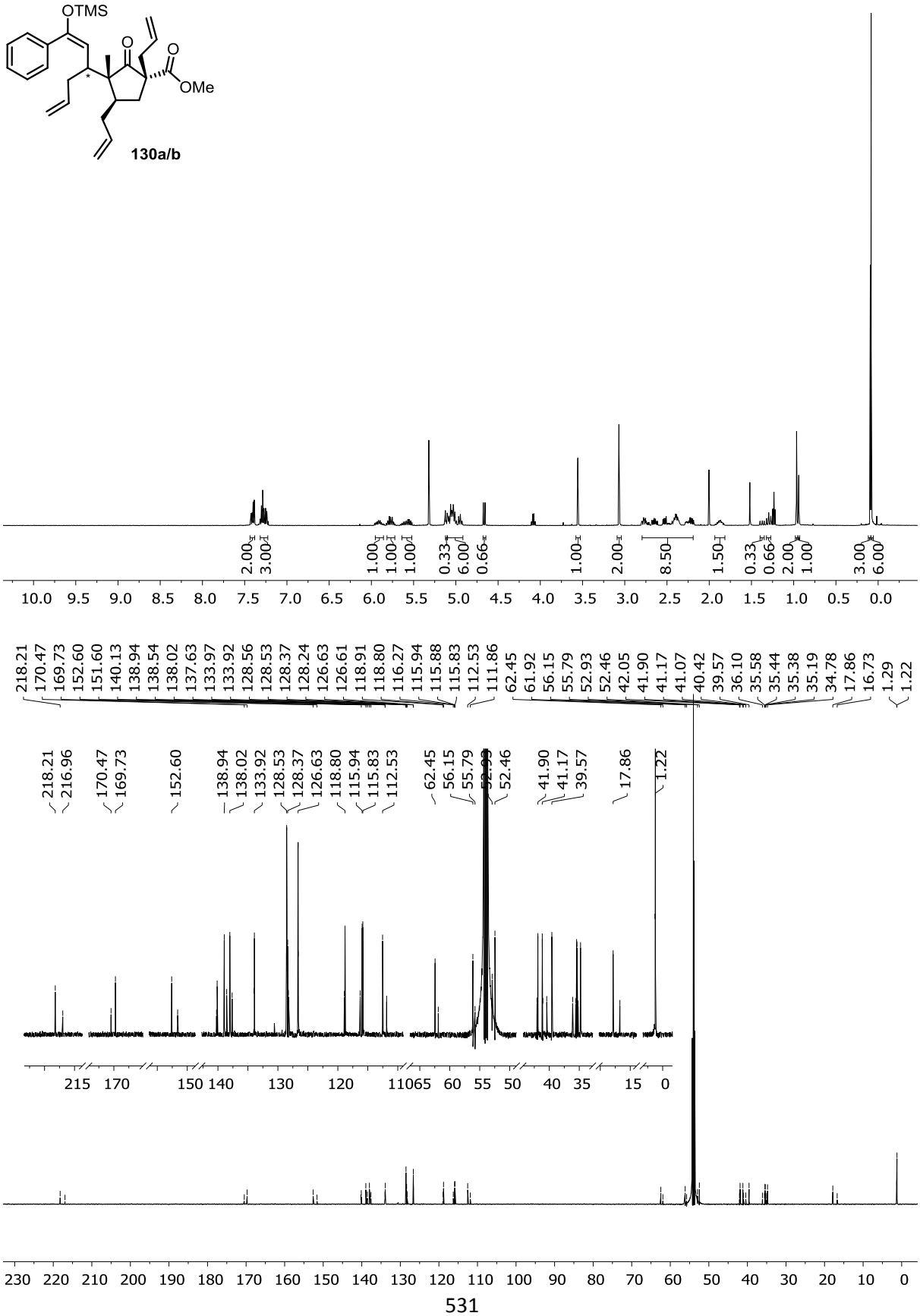

(*S*)-1-Allyl-2-iodocyclopent-2-en-1-ol (122)

GC: Lipodex-E, 50 – 190°C, 1,1 ml/min He ; FID 300°C, Split 50:1

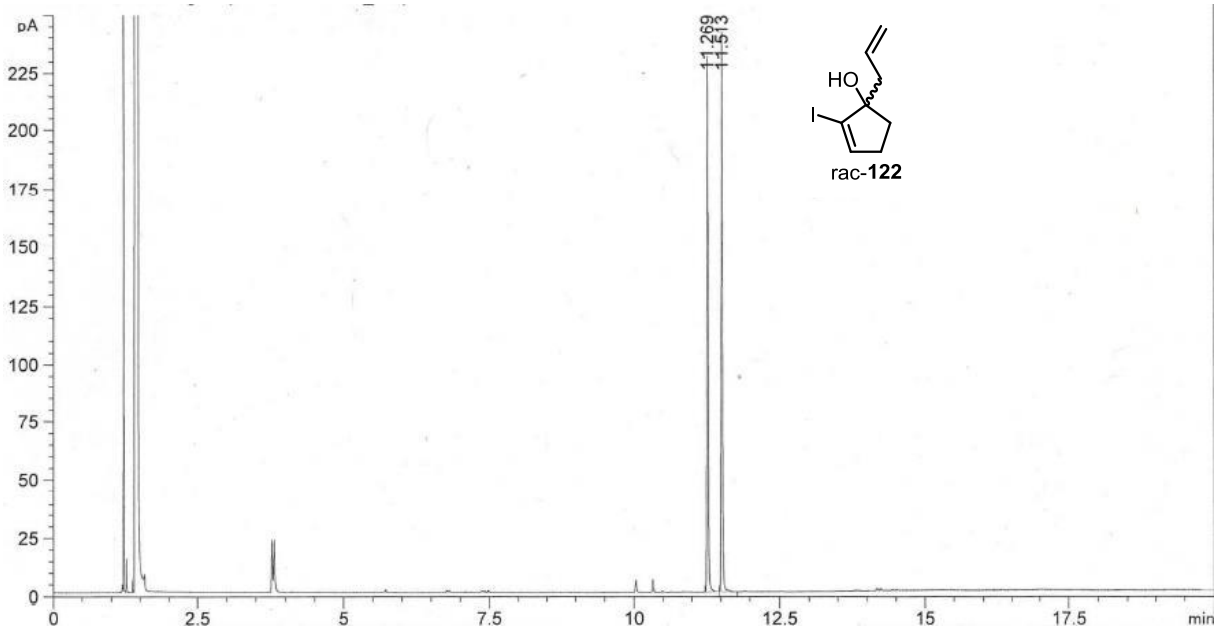

Peak #	RetTime [min]	Type	Width [min]	Area [pA*s]	Area %
4	5.556		0.0000	0.00000	0.00000
5	11.269	BB	0.0232	346.10767	48.60883
6	11.513	BB	0.0235	365.91870	51.39117

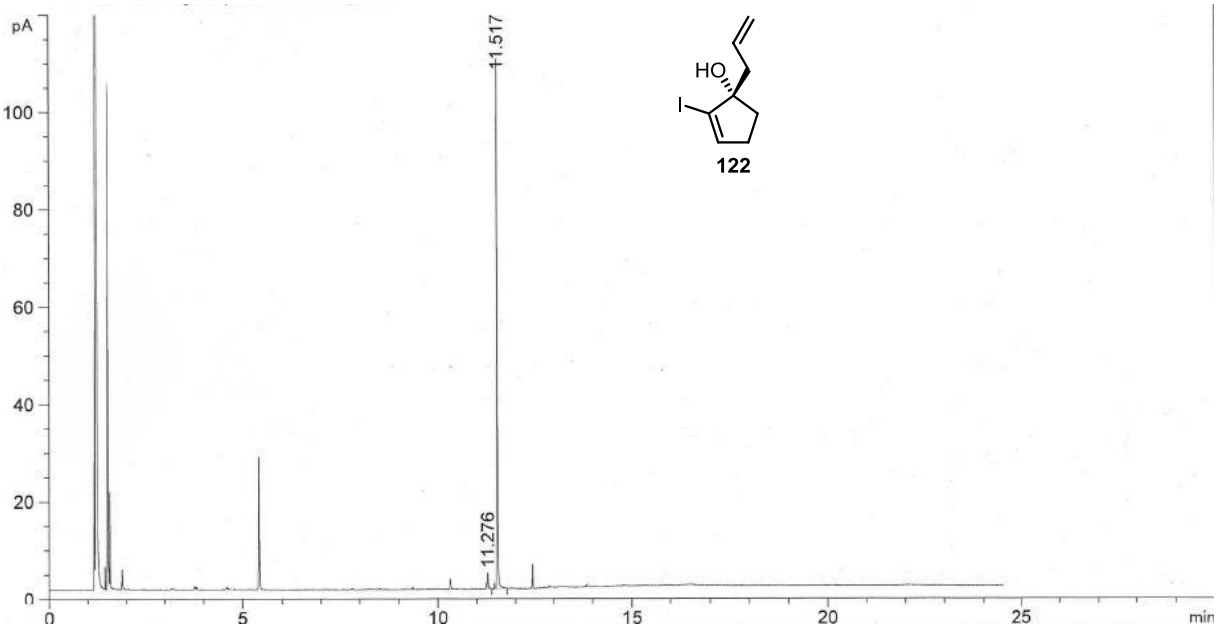

Peak #	RetTime [min]	Type	Width [min]	Area [pA*s]	Area %
4	5.556		0.0000	0.00000	0.00000
5	11.276	BB	0.0248	5.36454	3.07199
6	11.517	BB	0.0238	169.26268	96.92801